Use and Measurement of

Fully Softened Shear Strength

Bernardo A. Castellanos

Dissertation submitted to the faculty of the Virginia Polytechnic Institute and State University in partial fulfillment of the requirements for the degree of

Doctor of Philosophy
In
Civil Engineering

Thomas L. Brandon, Chair
J. Michael Duncan
George M. Filz
Adrian Rodriguez-Marek

February 20, 2014
Blacksburg, VA

Keywords: fully softened, shear strength, clays, embankments, stiff clays, cut slopes, drained strength, normally consolidated clays, laboratory tests

Use and Measurement of

Fully Softened Shear Strength

by Bernardo A. Castellanos

Dr. Thomas L. Brandon, Chairman
Charles E. Via, Jr. Department of Civil and Environmental Engineering

ABSTRACT

The fully softened shear strength was defined by Skempton (1970) as the peak drained shear strength of a clay in a normally consolidated state. All the experience available on the applicability of the fully softened shear strength for slopes is based on back-analyses. Back-analyses of first-time failures in cuts in stiff-fissured clays and embankments constructed of fat clays have shown that, over a long period of time, the shear strength gets reduced from what is measured in the laboratory using undisturbed samples to the fully softened shear strength. These back-analyses require knowledge or assumption of pore pressures in the slope, which will have a significant influence on the shear strength obtained.

Karl Terzaghi, in 1936, was the first person that qualitatively explained the behavior of cut slopes in stiff-fissured clays. According to Terzaghi (1936), a softening process is initiated by the water percolating into the fissures causing swelling and decreasing the overall shear strength of the clay mass. Investigations presented later by Skempton and his colleagues showed that the controlling shear strength for cuts in stiff-fissured clays was equal to the fully softened shear strength and recommended this shear strength to be used for design (Skempton 1970; Chandler and Skempton 1974; Chandler 1974; Skempton 1977). Skempton (1977) concluded that displacements caused by progressive failure decrease the shear strength of stiff clays toward the fully softened shear strength.

At first, it was believed that only stiff-fissured clays were subjected to softening and that intact clays should be designed using the peak shear strength measured using undisturbed samples (Skempton and Brown 1961; Skempton 1964, 1970). Recent publications have showed that the likelihood of a clay experiencing softening is more dependent on the plasticity of the clay rather than the fissures (Bjerrum 1967; Chandler 1984a; Mesri and Abdel-Ghaffar 1993). Fat clays, when compared to lean clays, tend to be more brittle. This means that fat clays have a more pronounced decrease in shear strength after the peak shear strength is achieved and for this reason are more susceptible to progressive failure.

First-time failures in stiff clays usually occur a long period of time after construction. For this reason, steady state seepage was used in the back-analyses of the case histories presented by Skempton and his colleagues. They found that a pore pressure ratio of 0.3 was applicable to first-

time failures in cuts in stiff-fissured clays (James 1970; Vaughan and Walbancke 1973; Chandler 1974; Skempton 1977).

Investigations presented by Professor Steve Wright and his colleagues of the University of Texas at Austin showed, based on back-analyses, that the fully softened shear strength is also the controlling shear strength of compacted embankments constructed of highly plastic clays (Green and Wright 1986; Kayyal and Wright 1991; Wright 2005; Wright et al. 2007). Steve Wright and his colleagues concluded that weathering, expressed in cycles of wetting and drying, was the main mechanism decreasing the shear strength of compacted clay embankments toward the fully softened shear strength. Failures in this type of projects were found to be shallow (less than 10 ft deep) and to occur numerous years after construction (USACE 1983; Stauffer and Wright 1984; Kayyal and Wright 1991; Wright et al. 2007). A pore pressure ratio ranging from 0.4 to 0.6 was found to be applicable for the case histories analyzed by Wright and his colleagues. Day and Axten (1989) recommended the use of the infinite slope method with seepage parallel to the slope face for slope stability analyses. This same recommendation was presented by Lade (2010). A seepage parallel to the slope face corresponds to a pore pressure ratio ranging from 0.4 to 0.5 for slopes with ratios of 2H:1V to 5H:1V. Failures on compacted clay embankments related to softening have been reported in Texas (Stauffer and Wright 1984; Kayyal and Wright 1991; Wright 2005; Wright et al. 2007), and Mississippi (USACE 1983). According to McCook (2012), softening of this type of structures also occur in Louisiana

To perform slope stability analyses using fully softened shear strength parameter, the type of soils, type of projects, and depths where this shear strength is applicable, and the pore pressures and factor of safety to be used in design should be determined. As stated above, the fully softened shear strength has been found to be the controlling shear strength of cuts in stiff clays and compacted embankments constructed of highly plastic clays. Steady state seepage conditions should be used to design cuts in stiff clays, and a pore pressure ratio ranging from 0.4 to 0.6 or a phreatic surface at the surface of the slope should be used to design compacted embankments made of fat clays.

In cuts in stiff clays, both shallow and deep failures related to fully softened shear strength have been observed. For this type of project, the recommended methodology for design is to assign a curved fully softened failure envelope to the whole slope, search for the critical failure surface, and obtain the factor of safety. This approach will provide the correct factor of safety but the critical surface obtained might not be what is expected to occur *in situ*. Pore pressures corresponding to steady state seepage should be used for design. It should be emphasized that the recommendation to use fully softened shear strength in first-time failures in stiff clays is based on the back-analyses of case histories. Research is required to better understand progressive failure and its influence on the shear strength mobilized *in situ.*

In compacted embankments constructed of fat clays, only shallow failures related to fully softened shear strength have been observed. For this type of projects, the recommended methodology for design is to assign a curved fully softened failure envelope to the whole

embankment, search for the critical failure surface, and obtain the factor of safety. If for any reason deep failures are to be considered in designing compacted embankments constructed of fat clays, based on the fact that failures in this type of projects are usually shallow, the first 10 ft below the surface of the slope should be assumed to have a shear strength equal to the fully softened shear strength. Pore pressures should be calculated based on a water table coincident with the slope face.

The fully softened shear strength should not be used in the foundation soil. If any softening occurred in the foundation soil, this should be reflected in the shear strength measured using undisturbed samples. Softening of the foundation soil is not expected to occur after the embankment is constructed.

The consequences of shallow and a deep failures are usually not the same. For this reason, is reasonable that the same factor of safety should not be required for both cases. A shallow failure may be considered by some agencies solely as a maintenance issue. The factor of safety should be based on the uncertainties in the parameters being used for design and the consequences of failure of the structure (Duncan and Wright 2005). The parameters that have more impact on the factor of safety obtained for slope stability are shear strength and pore pressures. The fully softened shear strength is the lowest shear strength expected to be mobilized in first-time slides. This shear strength, coupled with a conservative assumption of pore pressure gives a low uncertainty in the parameters that have the most influence in the factor of safety.

For shallow failures, the consequences of failure are very low. For this reason, if the fully softened shear strength is used, coupled with a water table corresponding to the worst case scenario possible, a factor of safety as low as 1.25 can be used. For deep failures, the consequences of failure will vary depending on the structure. The pore pressure for this type of analyses should be based on the worst seepage condition expected throughout the life of the project. In this case, for structures with low to mid consequences of failure, a factor of safety of 1.35 can be used. For structures with a high consequence of failure, a factor of safety of 1.50 can be used. These factors of safety are based on the recommendations presented by Duncan and Wright (2005) for factors of safety based on uncertainties in the parameters and consequences of failures.

The fully softened shear strength should be measured using normally consolidated remolded specimens as recommended by Skempton (1977). Soil samples should be hydrated for two days using distilled or site-specific water. The soil sample should then be washed or pushed through a No. 40 (425 μm) sieve. To achieve the desired water content, the soil sample cab be air-dried or more water should be added. Water contents equal to or higher than the liquid limit should be used to prepare test specimens for fully softened shear strength measurements.

The direct shear device is recommended for fully softened shear strength measurements. The Bromhead ring shear device does not provide accurate values of fully softened shear strength. The triaxial device requires more time and effort to measure the fully softened shear strength and provides about the same fully softened shear strength as the direct shear device.

The fully softened shear strength failure envelope can be estimated using the correlation presented in Figure 6.59 for the parameters required for Equation 4.1. This correlation is only intended to be used in preliminary design or if better information is not available. Laboratory determination of fully softened shear strength is always recommended for final designs. If this is not possible, the confidence limits presented in Figure 6.59 should be used to determine the fully softened shear strength parameters.

DEDICATION

I want to dedicate this dissertation to God, for the opportunities given and for being the guide of my life. To my family, for their unconditional support through all these years, for being the inspiration of my life, and for making me a better person with their examples. Last but not least, to all my friends and all others that supported me all these years, encouraging me to keep going, and for being a family away from home.

ACKNOWLEDGEMENTS

First and foremost, I want to express my gratitude and respect to my advisor, Prof. Thomas L. Brandon, for his guidance, dedication, patience, support, and inspiration throughout my graduate studies at Virginia Tech, and for offering his friendship. I was very fortunate to be able to work with and learn from him during these years. I know sometimes it was not easy.

I am very grateful to Prof. Mike Duncan, for his support, advice, and for making possible some of my presentations in different conferences. Also, to the rest of my committee members, Dr. George M. Filz and Dr. Adrian Rodriguez-Marek, for their time and assistance during this investigation.

I am indebted to the U. S. Army Corps of Engineers' (USACE) Engineer Research and Development Center (ERDC) and The Virginia Tech Center for Geotechnical Practice and Research (CGPR) for providing funding for this investigation.

Special thanks to Steve Trautwein and Hardik Mehta from Trautwein Soil Testing Equipment for their support with the laboratory equipment; to Lucas Walshire and Isaac Stephens for their collaboration during this research; and to Prof. Steve Wright for providing comments and suggestions during this investigation.

I also want to thank all the great friends I made during my time in Blacksburg. Specially, Lindy and Wes Cranwell for helping me and making me part of their family since the day I arrived to Blacksburg; Nancy Lopez for being my Dominican mother in Blacksburg; Dan VandenBerge for his valuable discussions and help in the laboratory; Alex Reeb for being a true friend and support throughout these years; and Ashly Cabas, Celso Castro, Ana Lisa Valenciano, Melisa Brenes, Kate Gunberg, and Craig and Shanna Morris for their valuable friendship.

Lastly, I would like to acknowledge my family for their unconditional support and love all these years.

Table of Contents

List of Figures

List of Tables

Chapter 1

Introduction

1.1 Background

Investigations performed by Alec Skempton and his colleagues between the 40s and the 70s on several failures in clay slopes revealed that the shear strength mobilized *in situ* for cut slopes in stiff-fissured clays was less than the shear strength measured using undisturbed samples and equal to the fully softened shear strength. The fully softened shear strength is commonly defined as the drained peak shear strength of a normally consolidated clay (Skempton 1970). Nowadays, this shear strength has been acknowledged to be the controlling shear strength for cuts in stiff-fissured clays, shales, and mudstones; and for slopes constructed of compacted high plasticity clays. The term *stiff-fissured clays* in this document is used as defined by Terzaghi (1936) and refers to clays that are highly overconsolidated[1], with a natural water content close to the plastic limit, unconfined compressive strength usually exceeding 4,000 psf, and characterized by the presence of a network of joints and fissures. The term stiff-fissured clays has been found in the literature both hyphenated and not, for this dissertation it will be hyphenated.

The fully softened shear strength has been linked to other shear strength concepts like the critical state concept presented by Roscoe et al. (1958) and this has caused some confusion. Different recommendations have been given for what type of test specimens should be used to measure fully softened shear strength parameters. Skempton (1977) recommended the use of remolded normally consolidated samples to measure the fully softened shear strength, while Terzaghi et al. (1996) suggested that undisturbed samples could be used to measure the fully softened shear strength in the triaxial device. The mechanisms causing the decrease in shear strength from peak undisturbed to fully softened, and the correct methods to measure and apply the fully softened shear strength are also not well defined. Various mechanisms have been proposed to explain this decrease in shear strength; however, no consensus has been reached. Specific guidelines for the use of fully softened shear strength are not readily available aside from the Virginia Tech Center for Geotechnical Practice and Research (CGPR) report by Duncan et al. (2011). The fully softened shear strength is usually applied to slope stability problems but the conditions regarding where it should be applied, the minimum required factor of safety required, and pore pressures that should be used for design are left to the discretion of the designer.

Various laboratory test apparatuses have been used to measure fully softened shear strength, but little research has been performed to assess the validity of the results obtained with these different devices.

[1] An overconsolidated clay is a clay that has been loaded in the past to a pressure higher than it is experiencing in the field at the present.

Historically, triaxial and direct shear devices have been the most common apparatuses used to measure the peak shear strength of soils; therefore, these have also been used for the measurement of fully softened strength. In recent years, the ring shear device was proposed as being capable of measuring the fully softened shear strength (Stark and Eid 1997; Stark et al. 2005; Stark and Hussain 2013). The most recent correlation proposed by Stark and Hussain (2013) for estimating fully softened shear strength parameters is based on results obtained using the ring shear device. No extensive comparison has been made with the results obtained with the ring shear apparatus and other devices that are normally used for measuring peak shear strength of soils.

Historically, different sample preparation techniques and initial conditions have been used to measure the fully softened shear strength. Test specimens have often been *blenderized* or *ball-milled* prior to testing. *Blenderizing* refers to a specimen preparation technique where the soil slurry is thoroughly mixed with water in a blender or milkshake mixer. *Ball-milling* is a process where air-dried soil is disaggregated by rotating the soil in a drum or other vessel along with special grinding media. The water content used to form the test specimens has ranged from below the liquid limit to considerably greater than the liquid limit (Kayyal and Wright 1991; Stark and Eid 1997; Stark et al. 2005; Wright et al. 2007). Little research has been conducted to examine the influence of the sample preparation techniques or the molding water content on the resulting fully softened shear strength parameters.

The topic of fully softened shear strength has recently captured the attention of many geotechnical engineering professionals and researchers. A workshop focusing on fully softened shear strength was held at the Virginia Tech campus on August 16 and 17, 2011. This workshop brought together more than 50 engineering practitioners, academics, and researchers who shared their experiences and opinions related to the use and measurement of fully softened shear strength. Also, during the American Society of Civil Engineers (ASCE) Geo-Congress 2013 in San Diego, a section of the proceedings and a panel discussion were dedicated to this subject and a new subcommittee on this subject was created in the ASCE. Also in 2013, a new subcommittee of the ASCE Embankments, Dams, and Slopes committee was formed to focus on fully softened shear strength parameters.

This dissertation summarizes the research conducted at Virginia Tech for the U.S. Army Corps of Engineers (USACE) and the CGPR investigating the measurement and use of fully softened shear strength parameters. The main focus of this research has been to clarify the uncertainties surrounding the use and measurement of fully softened shear strength. In this document, the term “the author” refers to the author of this document.

This research was conducted as a cooperative effort between the U. S. Army Corps of Engineers’ (USACE) Engineer Research and Development Center (ERDC) and the Virginia Tech CGPR.

1.2 Motivation

An important motivation for this study was the research conducted by S. Wright and his colleagues at the University of Texas at Austin (Abrams and Wright 1972; Gourlay and Wright 1984; Stauffer and Wright 1984; Green and Wright 1986; Rogers and Wright 1986; Kayyal and Wright 1991; Saleh and Wright 1997; Wright 2005; Wright et al. 2007). They found that the fully softened shear strength applies to highway

embankments constructed of compacted high plasticity clays. Heretofore, fully softened shear strength concepts had only been applied to cut slopes in stiff-fissured clays and highway embankments constructed of fat clays (Skempton 1970, 1977; Kayyal and Wright 1991; Wright 2005; Wright et al. 2007; Duncan et al. 2011). If the fully softened shear strength applies to embankments constructed of compacted high plasticity clays, it may also apply to levees, dams, and other flood control structures.

Recently, the U.S Army Corps of Engineers investigated the stability of the levees in the Dallas Floodway Project located on the Trinity River. Based on previous research by S. Wright and his colleagues, the Corps decided to use the fully softened shear strength to analyze the stability of the levees in this project. During this investigation, several direct shear tests on remolded samples were performed to measure the fully softened shear strength. When the results from these direct shear tests were compared to the correlation for fully softened shear strength parameters presented by Stark and Eid (1997) and Stark et al. (2005), it was found that the failure envelope obtained with the direct shear device was often higher than the failure envelope obtained from the correlations. This finding, and the fact that the ring shear device, as proposed by Stark and Eid (1997) and Stark et al. (2005), had seldom been used to measure peak shear strength of soils, led to the question: "How should the fully softened shear strength be measured?" The ring shear device was originally designed to measure the residual shear strength of soils. Aside from a very limited number of tests presented by Stark and Eid (1997), there was scant information available that assured that the ring shear device is a device capable of measuring reliable values of the fully softened shear strength parameters.

1.3 Research Objectives

This research focuses on providing guidelines for the use and measurement of fully softened shear strength. The main objectives of this research are:

1) To determine the mechanism responsible for causing softening: Softening of clay slopes in the field has been recognized since the 1930s (Terzaghi 1936); however, final conclusions about the mechanisms responsible for causing softening have not been presented. Various mechanisms have been proposed as being responsible for the softening process that occurs in cuts in stiff-fissured clays and mudstones, and embankments constructed of compacted high plasticity clays. In order to determine the mechanisms that better explain the softening process, the literature was searched to find case histories and theoretical explanations supporting or disregarding the proposed mechanisms.
2) To provide guidelines for the use of fully softened shear strength for design: Specific guidelines on the use of fully softened shear strength for slope stability analyses are required to help designers correctly apply this shear strength in their projects. Some of the questions that will be addressed in this research about the use of fully softened shear strength are listed below:
    - What type of soils can experience softening?
    - What depths do fully softened shear strength apply to in natural and compacted soils?
    - What values of pore pressure have been used or should be used with fully softened shear strength parameters?

- What factor of safety should be required for design with fully softened shear strength parameters?
- Does fully softened shear strength apply to other geotechnical structures besides slopes (e.g. braced excavations and other earth retaining structures)?
- Are there regional considerations for using the fully softened shear strength in design (e.g. climatic considerations)?

These questions were answered by documenting case histories where fully softened shear strength has been found to apply, by compiling case histories where fully softened has been used successfully, by contacting engineers and researchers that have a wide experience on the subject, and by assessing the available literature.

3) To provide guidelines for the measurement of fully softened shear strength: Reliable and repeatable values of the fully softened shear strength parameters need to be measured in order to successfully apply the fully softened shear strength in a project. Laboratory tests were performed in order to compare the fully softened shear strength parameters obtained with triaxial, direct shear, and ring shear devices. Different sample preparation procedures were evaluated to measure the effects of variations in the initial water content and sample preparation technique on the shear strength and soil index properties measured.

   The curvature of the fully softened failure envelope has been found to increase with decreasing normal effective stress (Kayyal and Wright 1991; Stark and Eid 1997; Stark et al. 2005; Wright et al. 2007). A curved failure envelope can be characterized by using secant friction angles corresponding to given normal stresses. The secant friction angle is defined as the inverse tangent of the shear stress divided by the normal effective stress The increase in curvature of the fully softened shear strength failure envelope is represented by an increase in the secant fully softened secant friction angle with decreasing effective normal stress on the failure plane as presented in Figure 1.1. This curvature can be an important factor in the evaluation of the slope stability of shallow surfaces where the normal stresses are often below 500 psf. Measuring the shear strength at these low consolidation stresses in the laboratory can be quite challenging. Modifications to existing devices and sample preparation procedures were performed in order to measure the fully softened shear strength at low stresses. Based on the acquired experience and the results obtained, guidelines are provided to perform tests at low stresses.

4) To provide guidelines for estimating fully softened shear strength parameters: Obtaining reliable estimations of the fully softened shear strength parameters from correlations is useful when doing preliminary designs for cost estimates in a project. A new correlation was developed using the data obtained from the laboratory testing program to obtain fully softened shear strength parameters.
5) To clarify the misconceptions surrounding the fully softened shear strength concept: The shear strength of normally consolidated soils has been investigated using different frameworks than just the fully softened shear strength concept. Literature regarding the critical state soil mechanics concepts presented by Roscoe et al. (1958) was compiled. This literature was analyzed in order to

reconcile this theory with the concept of fully softened shear strength and the results from the laboratory measurements. Skempton (1970) stated that the fully softened shear strength is a practical approximation of the critical state strength but no detailed discussion was presented.

The fully softened shear strength is usually measured on remolded normally consolidated test specimens. Undisturbed normally consolidated samples might have interparticle bonding and/or fabric differences that could influence the shear strength measured. The relationship between the fully softened and the undisturbed normally consolidated shear strengths was addressed by searching the literature for previous investigations performed on this subject.

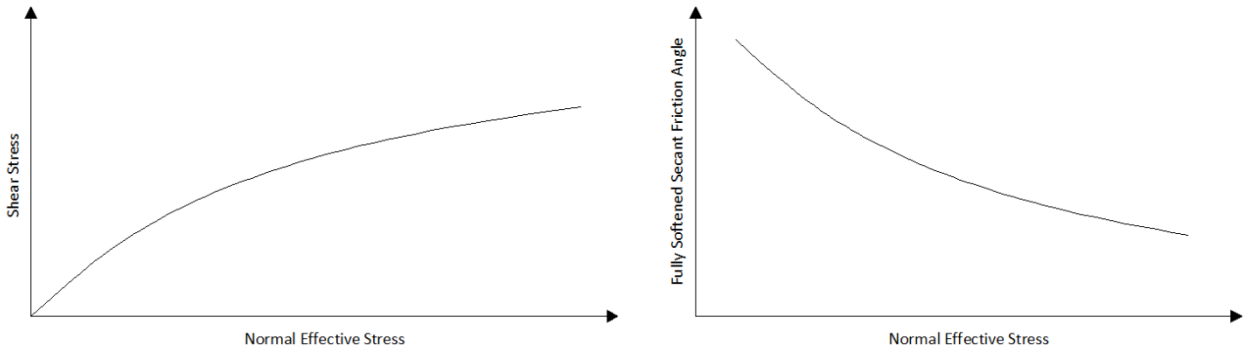

Figure 1.1 Curvature of the fully softened failure envelope

1.4 Research Outline

This research is organized in seven chapters and seven appendices.

Chapter 1 presents background information about the subject of this dissertation, the motivation for and the objectives of this study, and the outline of this document.

Chapter 2 presents a review of the literature available regarding the subject of fully softened shear strength. In this chapter, the history of fully softened shear strength is presented. The contribution of different researchers is summarized to provide a historical perspective about the investigations that led to the development of the fully softened shear strength concept throughout the years.

Chapter 3 presents a discussion about some misconceptions that surround the concept of fully softened shear strength. In this chapter, the relationship between the concept of critical state shear strength and fully softened shear strength and the use of undisturbed samples to measure the fully softened shear strength are addressed.

Chapter 4 summarizes the findings about the use of fully softened shear strength. This chapter addresses the mechanisms that have been used to explain the softening process, the cases when the fully softened shear strength should be used, the pore pressures that have been used in conjunction with fully softened shear strength parameters, the structures affected by a softening process, and the factor of safety that

should be used for design using fully softened shear strength parameters, among other subjects related to the use of fully softened shear strength.

Chapter 5 addresses the measurement of fully softened shear strength. In this chapter, the different devices used for fully softened shear strength measurement are described, a sample preparation technique to form test specimens is presented, and a comparison between all the devices is made.

Chapter 6 summarizes the results of the laboratory testing program undertaken to investigate the effect of the sample preparation technique and the device used to measure the fully softened shear strength on the results obtained. In this chapter, the results of a series of triaxial tests performed to investigate the effect of allowing compacted clay test specimens to swell under a low confining pressure in the triaxial cell are also presented. The results obtained from the laboratory testing program were used to develop a correlation, which is also included in this chapter, to obtain the fully softened shear strength failure envelope.

Chapter 7 presents a summary of the work performed in this research, the major findings, conclusions, and recommendations for future research.

Appendix A presents a proposed ASTM standard to measure the fully softened shear strength using a direct shear device.

Appendix B presents a manual to perform fully softened shear strength measurements using a GeoTac direct shear device.

Appendices C, D, and E present the laboratory reports of the direct shear, ring shear, and triaxial tests, respectively, performed for this investigation.

Appendix F presents a summary of the direct shear tests performed by ERDC.

Appendix G presents the results of the triaxial tests performed on compacted clay test specimens allowed to swell in the triaxial cell at a low confining pressure.

Chapter 2

History of Fully Softened Shear Strength

2.1 Introduction

The shear strength mobilized *in situ* in first-time failures of slopes in overconsolidated clays, compacted clay embankments, and slopes in mudstones has been found to be less than the shear strength measured in the laboratory using undisturbed samples. Several researchers have performed investigations to better understand this problem, and based on these studies, different theories have been proposed. Empirically, the fully softened shear strength have been found to be the controlling shear strength for slopes in overconsolidated fat clays, compacted fat clay embankments, and mudstones. This chapter presents a summary of the research available regarding fully softened shear strength. Also, a summary of the existing research concerning the measurement and use of fully softened shear strength is presented.

2.2 Early Research

The first paper, to the author's knowledge, that describes a long-term slope failure in a stiff-fissured clay was published in the "Minutes of the Proceedings" by Charles Gregory in 1844. Gregory (1844a) described a slide in an excavation in clay associated with the construction of the London and Croydon railway. The slope was stable for certain time and it was inferred that a new event disturbed the equilibrium. The profile of the cut consisted of a yellow clay that contained numerous "breaks" on top of a stiff, homogenous, and impermeable blue clay. The term *breaks* used by Gregory is synonymous with the term *fissures* that is commonly used now in geotechnical engineering. The yellow and blue clay described by Gregory are better known as Brown and Blue London Clay, respectively.

The cut made in 1838 for the construction of the New Cross train station failed in 1841, according to a re-evaluation of this failure performed by Skempton (1977). As shown in Figure 2.1, the profile of the cut consisted of 56 ft of the Brown London Clay and 19 ft of the stronger Blue London Clay for a total cut height of 75 ft. This figure also shows the profile before (using a dashed line) and after the failure. The vertical depth of the failure surface was 44 ft. As can be seen in Figure 2.1, the failure surface was confined to the Brown London Clay. The vertical depth of a slide as used in this dissertation is defined as the maximum vertical distance between the slope surface and the failure plane as shown in Figure 2.2.

To explain the failure, Gregory hypothesized that the water percolates through the "breaks" of the clay until the clay becomes saturated, causing swelling in the soil mass. During the summer, the clay dries out

and shrinks, but does not return to the original volume, leaving permanent deformation and generating new cracks in the soil mass. These new cracks will allow more water to percolate; therefore, the tendency to have a slope failure increases over time. Gregory mentioned that this clay is very strong when dry, but when wet, it behaves as a semi-fluid that is unable to support itself.

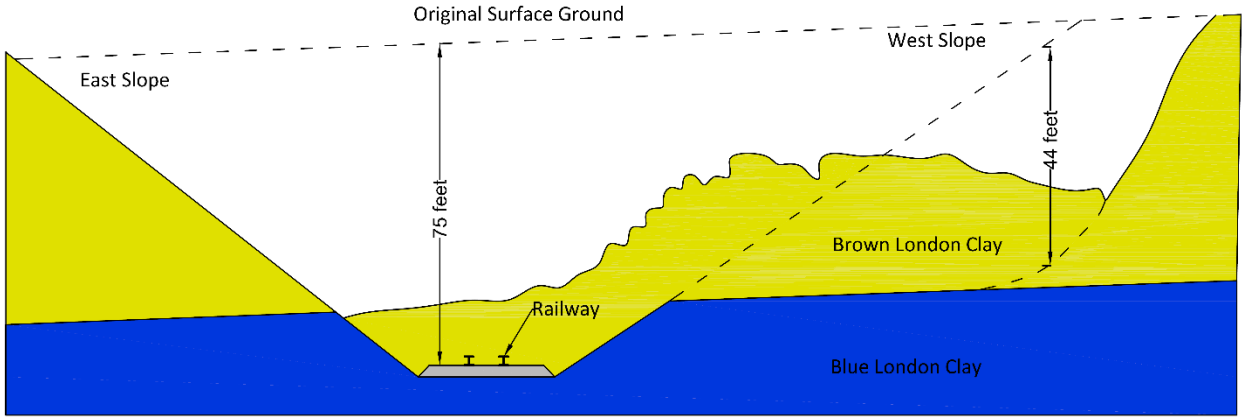

Figure 2.1 Position of the slip in the New Cross cutting, November 2, 1841 (After Gregory 1844a) (Used under fair use).

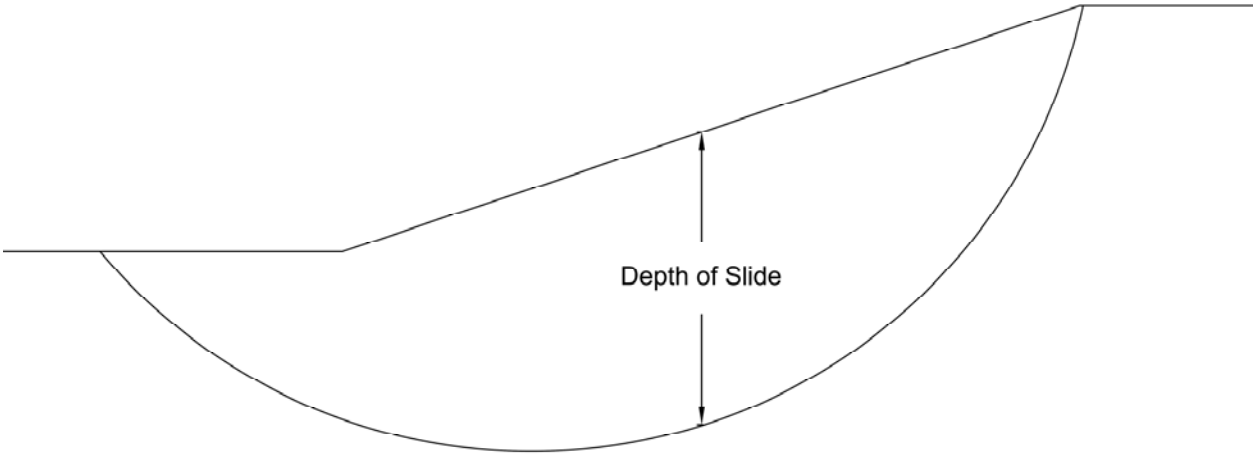

Figure 2.2 Vertical depth of slide.

In the discussion of the paper by Gregory (1844b), Mr. Hoof stated that his experience with slope failures associated with the Croydon Railway confirmed the process described by Gregory. Sir H. T. Delabeche explained that wherever a fissure enables the water to percolate into the soil, the substratum becomes "mud," which is squeezed out by the weight of the soil causing failure.

After 1844, no references were found related to the problem of slope stability in stiff-fissured clays until 1936, when Karl Terzaghi published a paper relating his experiences. Terzaghi (1936) classified clays into soft intact, stiff intact, and stiff-fissured clays. In his paper, Terzaghi discussed five first-time slope failures in stiff-fissured clays. From these case histories, Terzaghi pointed out that the mobilized shear strength in the field was less than the shear strength expected from laboratory tests. It was not specified whether he was referring to drained or undrained shear strength, although it seems likely that he was referring to undrained shear strength. No information about the index properties of the soils involved in the slides nor the depth of sliding were given.

To explain the difference in the shear strength expected from laboratory tests and the shear strength developed in the field, Terzaghi hypothesized that, as long as the stiff-fissured clay remains in the natural state, the joints would have no effect on the clay behavior because the large lateral pressures, usually encountered in heavily overconsolidated clays, close these fissures, as shown in Figure 2.3a. After a cut is made, the clay experiences lateral expansion in response to the decrease in stress in the soil mass and the fissures open as shown in Figure 2.3b. During rainstorms, water accumulates in the fissures and the clay swells under zero pressure along the open cracks. Swelling weakens the soil and new cracks open as shown by the dashed lines in Figure 2.3b. Once displacement begins to occur along these cracks, the excess water in the softened material cannot escape and the shear strength is reduced to the value it would have under zero pressure in the laboratory.

According to Terzaghi, the fissures, when dry, can remain open up to a depth equal to the compressive shear strength of the clay divided by the moist unit weight.

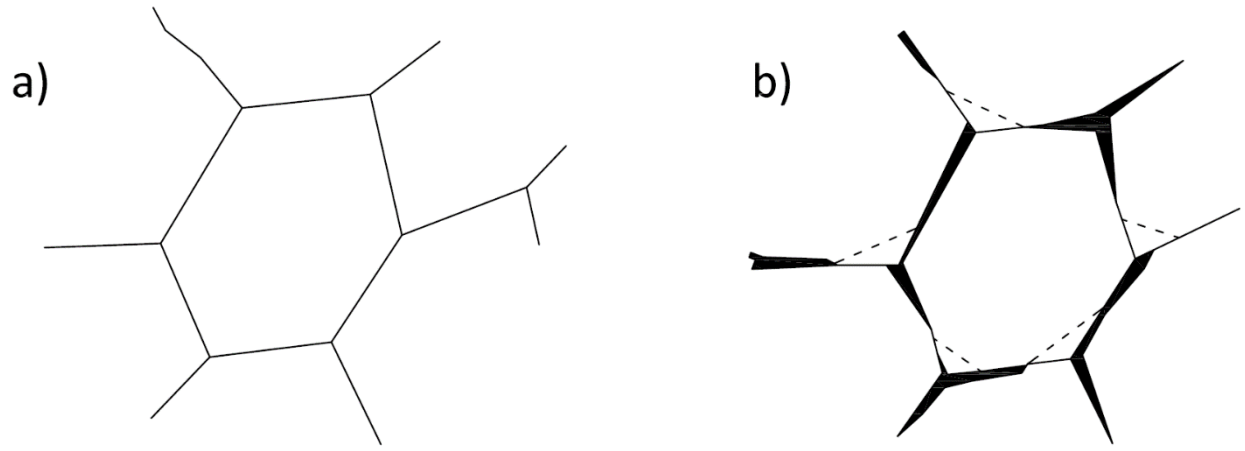

Figure 2.3 Crack propagation in stiff-fissured clays (After Terzaghi 1936) (Used under fair use).

Sir Alec Skempton dedicated a significant portion of his career to the behavior of stiff-fissured clays. In one of his earliest papers, Skempton (1948) analyzed the failures in Brown London Clay of the cut in the Watford by-pass and the retaining walls at Kensal Green, Walthamstow, Mill Lane, Park Village East, and

Wembley Hill. The Brown London Clay is a heavily overconsolidated stiff-fissured clay with a liquid limit of 82, a plastic limit of 30, and a clay-sized fraction[2] of 55% on average (Chandler and Skempton 1974).

The cut for the Watford by-pass was made in 1927 and numerous slips occurred between 5 years and 10 years later. The average back-calculated undrained shear strength was 220 psf and the measured undrained shear strength on undisturbed samples was 1,000 psf. The height of the cut was 15 ft with a slope of 2.5H:1V. The vertical depth of the failure plane was eight feet.

The Kensal Green failure occurred in 1941 beneath a 20-ft-tall retaining wall built in 1912. The failure surface was 19-ft-deep measured vertically and was forced by the retaining wall to go underneath the wall foundation. The back-calculated undrained shear strength along the failure plane was 340 psf and the undrained shear strength measured on undisturbed samples was 1,300 psf. Field investigations made by Skempton showed fissures with softened surfaces. Skempton stated that the undrained shear strength of the softened layer was around 250 psf and that the softening did not extend more than 0.25 inches from the fissures into the clay.

The Walthamstow failure occurred beneath a 15-ft-tall retaining wall built in 1895. The wall cracked in 1936 and by 1942, considerable movement had occurred. The back-calculated undrained shear strength was 390 psf and the undrained shear strength measured on undisturbed samples was 1,500 psf. The failure surface was 25-ft-deep measured vertically and was forced by the retaining wall to go underneath the wall foundation.

The Mill Lane failure occurred beneath a 32-ft-tall retaining wall built in 1902. The wall started to move in 1930 and failed in 1943. The undisturbed undrained shear strength was estimated to be around 2,300 psf while the shear strength measured on samples from the actual slip plane was between 500 psf to 800 psf. The failure surface was 42-ft-deep, measured vertically, and was forced by the retaining wall to go underneath the wall foundation.

The Park Village East failure occurred beneath a 34-ft-tall retaining wall built in 1901. In 1920, significant wall movements were observed and remedial measures were taken. In 1941, more movement occurred. The back-calculated undrained shear strength along the failure plane was 800 psf and the undrained shear strength measured on undisturbed samples was 2,700 psf. The failure surface was 42-ft-deep, measured vertically, and was forced by the retaining wall to go underneath the wall foundation.

The last case history presented by Skempton in this paper was the failure of the Wembley Hill retaining wall. The wall was built in 1905 and failure occurred in 1919. The wall was 22-ft-high with a 3H:1V backfill slope extending above it for a total height of 56 ft, including the wall. No subsurface investigation was made at this site. The mobilized and peak undrained shear strengths were estimated to be 880 psf and 2,500 psf, respectively. The estimated failure plane was 30-ft-deep, measured vertically, and passed underneath the foundation of the retaining wall.

[2] The clay-sized fraction of the soil is defined as the percentage of soil smaller than 7.9×10^{-5} inches (0.002 mm).

From these failures, it can be seen that the undrained shear strength mobilized in the field was lower than the undrained shear strength measured in the laboratory on undisturbed samples. No details were given on how the undrained shear strength was measured in the laboratory. According to Skempton, a softening process was occurring in the field. In this paper, Skempton first used the term *fully softened strength*. Although no clear definition was given, it appears that he was referring to the undrained shear strength that a clay will have after all the expected decrease in shear strength with time had occurred. Skempton presented the softening process of stiff-fissured clays as time dependent. A tentative relationship for the decrease in shear strength with time for the Brown London Clay was presented, and is reproduced in this dissertation as Figure 2.4. From this figure, it can be seen that the decrease in shear strength with time is non-linear and that the rate of decrease in shear strength decreases with increasing time.

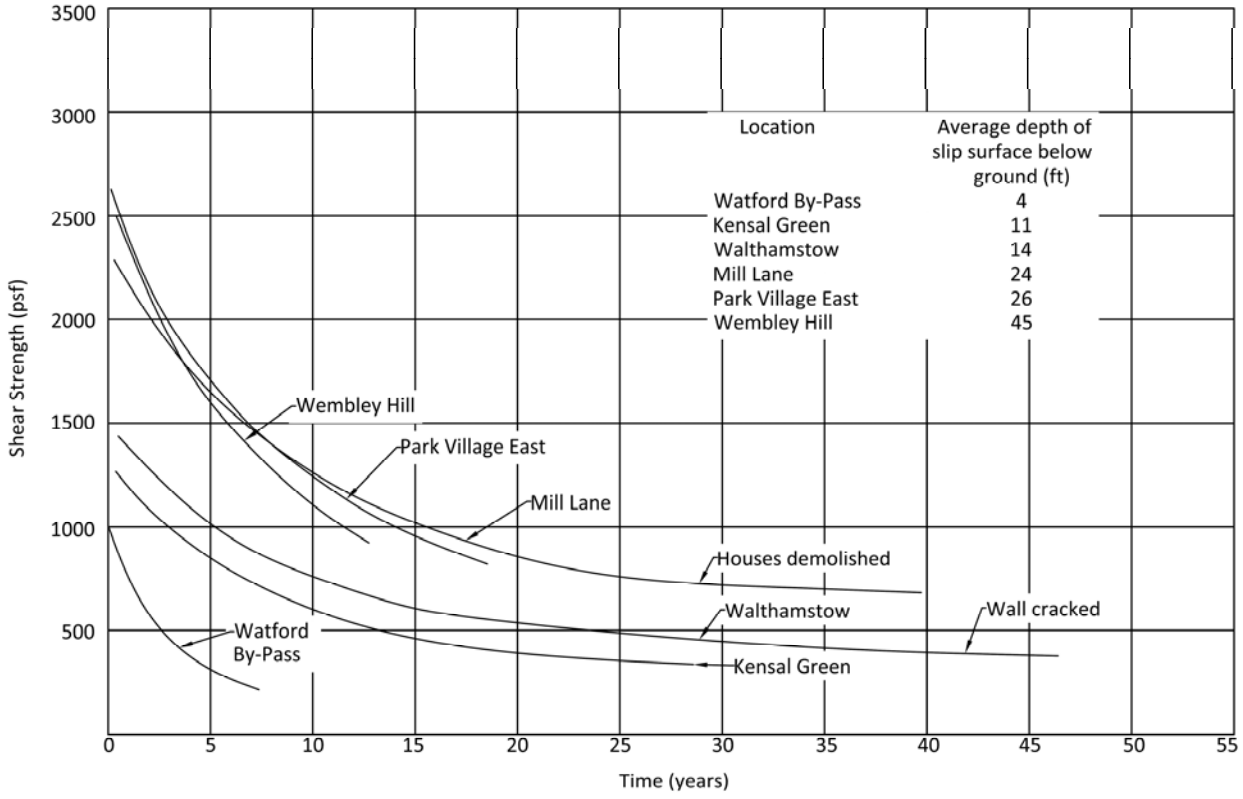

Figure 2.4 Proposed relationship between average undrained shear strength along the slip surface and time for cuttings and retaining walls in London Clay (After Skempton 1948) (Used under fair use).

During the winter of 1951-1952, a slide took place at Jackfield in Shropshire (Henkel and Skempton 1955). The vertical dimension of the failure zone in this slide was estimated to be about two inches thick and was located in a soft clay layer, having higher water content and lower shear strength, than the surrounding clay away from the failure plane. Drained direct shear and undrained triaxial tests, with pore water

pressure measurement on few specimens, were performed to characterize the drained and undrained shear strength of the soil involved in the slide.

Henkel and Skempton stated that the high undrained shear strength measured in stiff-fissured clays was due the tendency for dilation during shear which produces negative pore pressures. These negative pore pressures dissipate with time so a more appropriate factor of safety for slope stability would be calculated using an effective stress analysis and drained shear strengths. They also stated that during drained tests, because of the deformations during shear, the clay will dilate, causing an increase in water content and softening in the vicinity of the failure plane.

This slide was back-analyzed by Henkel and Skempton using the infinite slope method with seepage parallel to the face of the slope. The infinite slope solution was used owing to the relatively shallow depth of the slide, 17 ft measured vertically, compared to the 700 ft of length. Laboratory tests showed that the drained and undrained shear strengths of the softened clay, found in the failure zone, were lower than the drained and undrained shear strengths of the adjacent clay. No difference was found in the drained friction angle or the Atterberg limits. Based on these results, Henkel and Skempton inferred that the difference in the shear strength is due to a decrease in the effective stress cohesion intercept in the failure zone.

Total and effective stress slope stability analyses were performed by Henkel and Skempton to back-analyze this failure. The factor of safety obtained with the total stress analysis, using the undrained shear strength obtained from undisturbed samples away from the failure plane, was 4.0. The factor of safety using the undrained shear strength from samples in the failure zone was 1.12. Using an effective stress analysis with the drained shear strength parameters obtained from undisturbed samples ($c' = 150$ psf and $\phi' = 21$), the factor of safety was 1.45. Using the same effective stress friction angle, and assuming $c' = 0$, the factor of safety was 1.07. This finding was presented as field evidence that the effective stress cohesion intercept might largely disappear on an extended (years) time scale in clay slopes. The $c' = 0$ approach was presented as a lower bound of the shear strength expected in the field since any expected decrease in shear strength *in situ* could not take it below the normally consolidated shear strength.

Local movements, seasonal variation of the water table, and fissures were proposed by Henkel and Skempton as mechanisms that could potentially reduce the effective stress cohesion of the clay in the long-term. The concept of *local movement*, as defined by Henkel and Skempton, is better known as *progressive failure* in current geotechnical engineering parlance. Progressive failure is a condition where the shear strength is not fully mobilized at all points on the failure plane at the same time. This is caused by the strain-softening characteristics of the soil and the fact that the sliding mass is not rigid, but compressible. When certain points on the failure plane have mobilized the peak shear strength, other points having achieved less or more displacement have mobilized shear strengths less that the peak shear strength.

David Henkel analyzed slides that occurred in Brown London Clay slopes at Wood Green and Northolt (Henkel 1957). These slides were back-analyzed using an effective stress analysis, assuming an effective stress friction angle, ϕ', of 20° to obtain the value of effective stress cohesion required for stability. The

Wood Green train station was built in a cut in Brown London Clay supported by a 16-ft-tall retaining wall. Above the retaining wall, a 21-ft-tall slope was cut at 2.5H:1V. The retaining wall was built in 1893, and by November 1948, it began to move. The slide at Wood Green was 23-ft-deep measured vertically. Due to the presence of a retaining wall, the failure surface was forced to go deep underneath the foundation of the wall. During the subsurface investigation of this slide, very wet and soft soils were found in the vicinity of the failure plane.

The Northolt cut was made in London Clay in 1903. In 1936, the cut was widened to a vertical depth of 33 ft, on a 2.5H:1V slope. Twenty-three feet of the cut was in Brown London Clay and the rest was in the stronger Blue London Clay. Early in 1955, substantial movement occurred. The vertical depth of the failure surface was found to be 14 ft. Very soft clay with a high water content was found in the region of the slip plane. Henkel concluded that softening is normally confined to a relatively small volume of clay, usually limited only to the vicinity of the surface where sliding occurs.

Based on back-analysis of slope failures, Henkel postulated a relationship suggesting a decrease in effective stress cohesion with time after construction, and this is shown as Figure 2.5. As mentioned before, this proposed relationship assumed that the drained friction angle was the same for all sites.

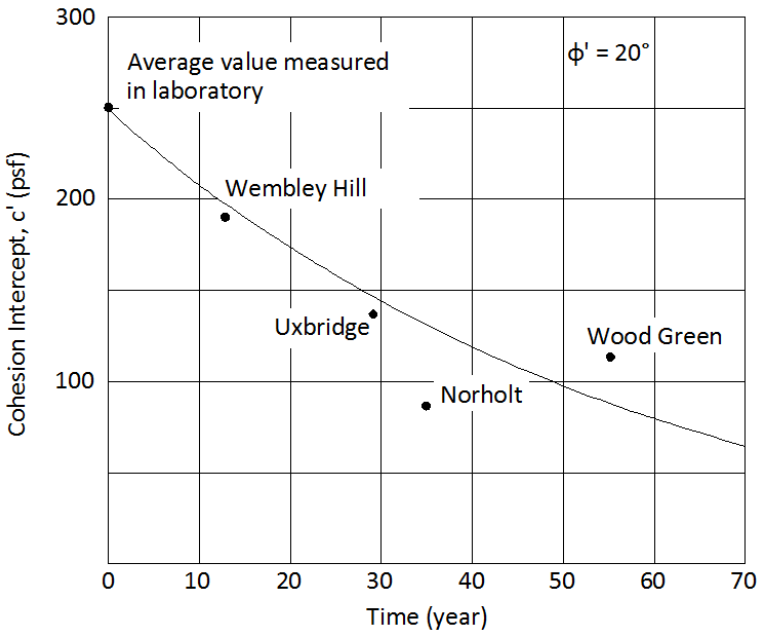

Figure 2.5 Relation between effective stress cohesion intercept and time between construction and failure (After Henkel 1957) (Used under fair use).

Skempton and DeLory (1957) measured the angles of stable and unstable natural slopes in Brown London Clay. Based on their survey, they concluded that 10° (6H:1V) is the critical angle for natural slopes in London Clay. This value agrees with the theoretical value of the slope angle, for a factor of safety of one,

obtained using the infinite slope method with the assumption that the water table is at the ground surface, seepage is parallel to the slope, ϕ' = 20°, and c'= 0. They found strong evidence suggesting that in an extended time scale (years or tens of years), stiff-fissured clays in natural slopes behave as if the effective stress cohesion intercept was equal to zero.

During the subsurface investigations for the design of Selset Dam, a slip was discovered in the boulder clay forming the valley side (Skempton and Brown 1961). The slope was 42 ft high with a 1.9H:1V inclination. The slip occurred entirely within a deposit of heavily overconsolidated intact boulder clay. The boulder clay is a lean clay (CL) with a liquid limit of 26, a plastic limit of 13, and a clay-sized fraction of 17%. With difficulty, undisturbed samples were obtained. In a few of the samples, large stones were present preventing the proper trimming of the test specimen. For these cases, samples were obtained by packing the soil, without the stones, into a brass tube at the field water content. Drained triaxial tests were performed to measure the shear strength of this soil. No significant difference was found in the shear strength measured in undisturbed and "packed" specimens. An effective stress friction angle of 32° and a cohesion intercept of 180 psf were measured. The test specimens did not exhibit significant strain softening.

Slope stability analyses, performed on circular slip surfaces using an effective stress method, showed that the full value of effective stress cohesion of 180 psf was required to obtain a factor of safety of unity. At shallow depths, where weathering degraded the shear strength of the clay, movements were also reported. Slope stability analyses suggested that in this zone, the effective stress cohesion intercept might be around 30% of the effective stress cohesion of the unweathered clay.

The case history presented by Skempton and Brown is very important because is a case history where a stiff clay mobilizes the undisturbed peak shear strength. It should be emphasizes, that this failure occurred in a cut in a lean clay and not a fat clay like the others presented in this section.

2.3 Research by A. W. Skempton and Colleagues

Skempton was selected in 1964 to present the fourth Rankine Lecture entitled "Long-term stability of clay slopes." The information presented in the previous section of this dissertation contains various research performed before 1964 on the slope stability of overconsolidated clays. This information served as the basis for Skempton's Rankine Lecture for which all this information was compiled and analyzed as a first attempt to approach the slope stability of clay slopes using a consistent framework. Skempton (1964) began his lecture stating that steady state pore pressures are already present in natural clay slopes, while in cuttings, this condition is not reached until several months or years after the excavation is made. The main focus of Skempton's lecture was the long-term stability of overconsolidated clay slopes.

Skempton explained that the shear resistance of a clay increases with increasing displacement until the peak shear strength is reached. After the peak, the clay experiences a strain-softening behavior until the residual shear strength is attained after large displacements, as shown by the idealized behavior illustrated in Figure 2.6. Based on laboratory test results, Skempton concluded that the effective stress cohesion intercept of the residual shear strength envelope is very small. He stated that the residual friction angle in some soils is sometimes only one degree or two degrees less than the peak effective

friction angle, while in others, this difference can be as much as 10°. Skempton also stated the shear strength can approach residual values in shear zones caused by tectonic movements.

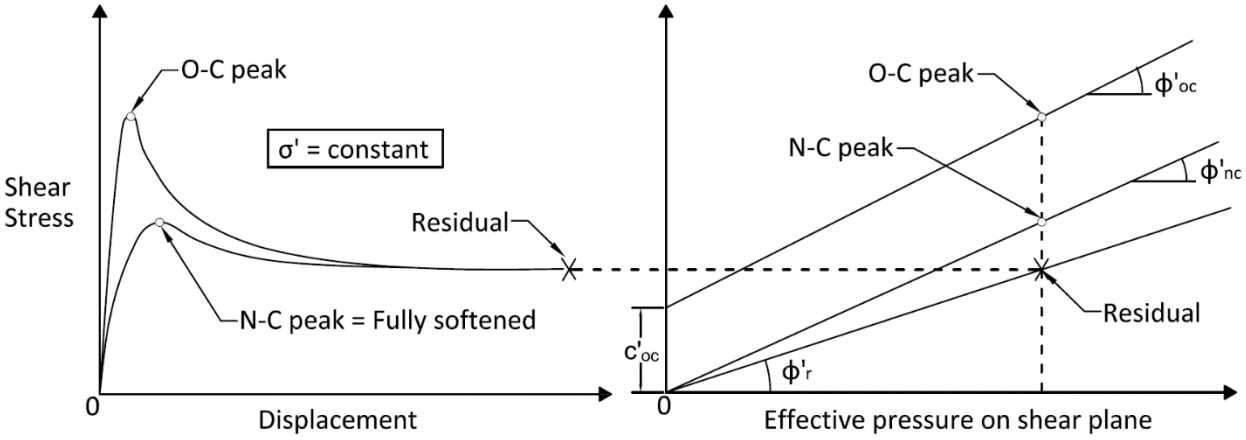

Figure 2.6 Shear strength of normally and overconsolidated clays (After Skempton 1964) (Used under fair use).

The residual shear strength was presented to be a characteristic of the soil, independent of the stress history. The residual shear strength measured from overconsolidated and normally consolidated test specimens taken to large displacements was found to be the same, as shown by the idealized behavior presented in Figure 2.6. From this figure it can be seen that a clay has three shear strength envelopes that can be used in slope stability analysis for different conditions: overconsolidated peak, normally consolidated peak or fully softened, and residual. The shear strength measured at large displacement in the laboratory, the residual shear strength, was also found to be approximately equal to the shear strength measured from natural sheared surfaces that had accumulated significant displacement.

A relationship that shows a decrease in the residual friction angle with increasing clay-sized fraction was presented by Skempton and is shown in Figure 2.7. The points in this figure represent the residual friction angle from numerous normally consolidated and overconsolidated clays. It was not clearly specified whether these friction angles were measured or back-calculated from failed slopes. The values of the mineral to mineral friction angle (ϕ_μ) shown for biotite, chlorite, quartz, and talc were measured by Horn and Deere (1962).

Skempton's opinion on the stability of clay slopes was that if the peak shear strength is passed at a particular point on the failure plane in the field, the shear strength at this point will decrease and will overstress a neighboring point so that it also passes the peak shear strength. In this way, a progressive failure can be initiated which eventually decreases the shear strength on the failure surface to the residual shear strength. According to Skempton, in fissured clays, the fissures will prevent the clay from developing the full shear strength over the complete length of the failure surface as a result of stress concentrations

in the fissures. Also, the low rate of loading in the field may also result in shear strength loss due to creep[3], so that the shear strength developed in the field will be smaller than the shear strength measured in the laboratory where creep is not significant. Scant data existed at that time to verify this hypothesis. Skempton also hypothesized that seasonal variation of water content and temperature could also decrease the shear strength of the clay, although this was believed to affect only shallow failures.

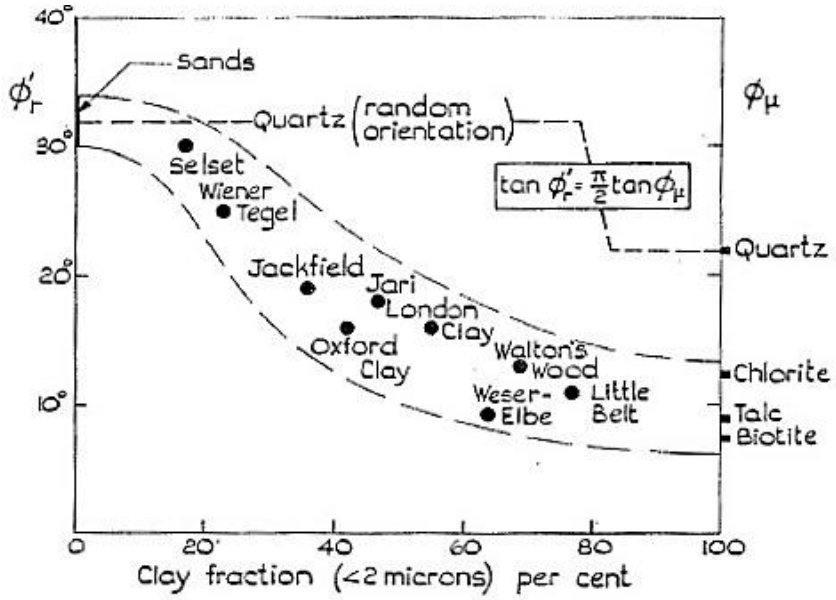

Figure 2.7 Relationship between the clay-sized fraction and residual friction angle (Skempton 1964) (Used under fair use).

The mobilized shear strength of slopes where failures had occurred was quantified by Skempton using the *residual factor.* This is shown as Equation 2.1. The residual factor was defined as the proportion of the total slip surface that has fallen to the residual shear strength. A residual factor of zero means that the peak shear strength is mobilized on the entire failure plane and a residual factor of one means that the residual shear strength is mobilized on the entire failure plane.

$$R = \frac{S_f - \bar{S}}{S_f - S_r} \tag{2.1}$$

[3] Creep is defined as the time-dependent shear deformation experienced by a soil element under constant shear stress.

Where:

R = Residual factor.
S_f = Peak shear strength at the average effective normal stress on the failure surface.
$\bar{S}$ = Average shear strength along the failure surface.
S_r = Residual shear strength at the average effective normal stress on the failure surface.

The case histories analyzed in Skempton's Rankine Lecture were the failure at Kensal Green, originally presented by Skempton (1948), the failure at Jackfield, originally presented by Henkel and Skempton (1955), the failure at Selset, first presented by Skempton and Brown (1961), the failure at Northolt, first presented by Henkel (1957), natural slopes, originally presented by Skempton and DeLory (1957), and the failure at Sudbury Hill. The failures at Kensal Green, Jackfield, Selset, and Northolt, and the natural slopes have already been described in this dissertation.

In this lecture, new details were presented about the failure at Kensal Green. At the time of failure, the wall was being monitored due to a slip that occurred in 1929 at the top of the slope. The first year of monitoring showed the rate of movement to be small, about 0.25 in/year. This rate gradually increased until failure occurred in 1941 at a total displacement of 18 inches. According to Skempton, this case history is an example of progressive failure.

The failure at Sudbury Hill, occurring in 1949, resulted from an excavation that was made in 1900 in Brown London Clay. The slope was 23-ft-tall, with a slope of 3H:1V. The failure surface was 14-ft-deep measured vertically.

A summary of the values of the residual factor for the slope failures analyzed by Skempton is presented in Table 2.1. It can be seen from this table that the shear strength mobilized in first-time slides in stiff-fissured clays is between peak and residual shear strength, which is indicated by an *R* value between zero and one. For non-fissured (intact) clays, the mobilized shear strength is close to the peak shear strength, which is reflected by the low value of the residual factor.

Table 2.1 Values of *Residual Factor* (After Skempton 1964) (Used under fair use).

Condition of the clay	Major soil unit	Location	Natural slopes = N Cutting = C (time to failure)	Residual factor *R*
No fissures or joints Unweathered	Boulder Clay	Selset	N	0.08
Fissures and joints Weathered	London Clay	Northolt	C (19 yrs.)	0.56
		Kensal Green	C (29 yrs.)	0.61
		Sudbury Hill	C (49 yrs.)	0.80
		Sudbury Hill	C (After slip)	1.04
		Varies	N	0.92-1.06
	Unknown	Jackfield	N	1.12

An increase in water content in the vicinity of the failure plane was found to be characteristic of slides in London Clay. Figure 2.8 shows the water content versus the distance from the failure plane for three slides reported by Skempton (1964).

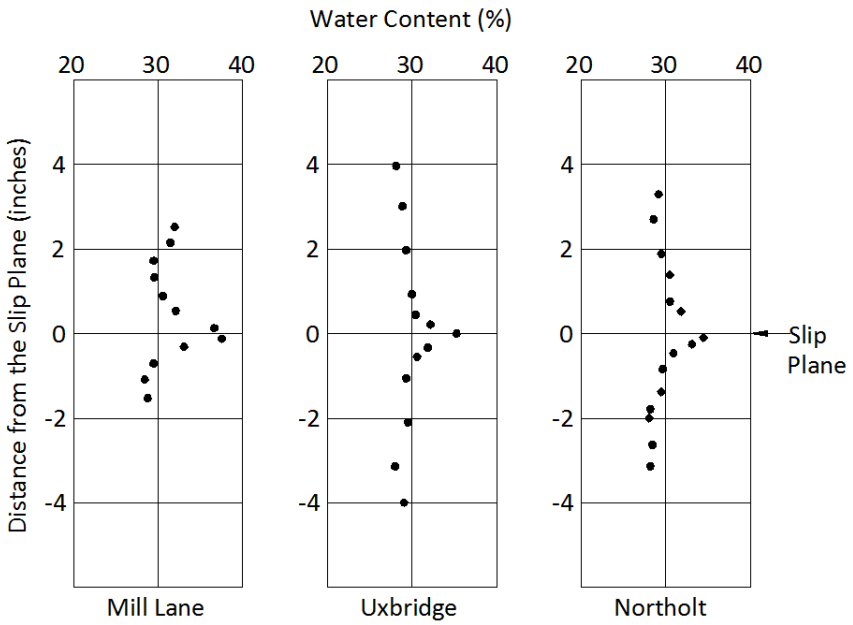

Figure 2.8 Distribution of water content near the slip surface (After Skempton 1964) (Used under fair use).

During the 1967 Geotechnical Conference at Oslo, Bishop (1967) presented the introduction to a session on progressive failure. During his introduction, Bishop defined a *brittleness index* for clays as follows:

$$I_B = \frac{\tau_f - \tau_r}{\tau_f} \cdot 100\% \tag{2.2}$$

Where:

I_B = Brittleness index.
τ_f = Drained peak shear strength at a specific effective normal stress.
τ_r = Residual shear strength at the same effective normal stress.

The brittleness index quantifies the relative value of the residual shear strength to the peak shear strength. The higher the brittleness index, the greater is the decrease from peak to residual shear strength, and the more "brittle" the soil is. According to Bishop, the brittleness index represents a measure of the

error that could be introduced by progressive failure if peak shear strengths are used to design a slope in a brittle soil. The brittleness index will vary with the effective normal stress on the failure plane and will range from a value of zero to less than one. A brittleness index of zero indicates that the soil is not strain-softening and the residual shear strength is equal to the peak shear strength. A brittleness index of one indicates that the residual shear strength is zero which is impossible.

A review of elements that play a role in a slope stability analysis was presented by Skempton and Hutchinson (1969). In this paper, Skempton and Hutchison addressed topics like clay formation, methods for slope stability analysis, case histories of slope failures, etc. They acknowledged that silty clays exhibit only a slight reduction in shear strength from peak to residual. The reduction in shear strength from peak to residual was recognized to increase with increasing clay-sized fraction even in normally consolidated soils. This paper appears to mark the first time that Skempton used the term *fully softened shear strength* referring to drained shear strength. Two of the case histories presented here were the Northolt failure, originally presented by Henkel (1957), and the Sudbury Hill failure, originally presented by Skempton (1964), both already described in this dissertation. While re-analyzing these case histories, Skempton mentioned "fully softened shear strength" and calculated a factor of safety using c' = 0, but no definition or details of the fully softened shear strength were given.

Chandler (1969) studied the effect of weathering on the properties of mudstones from England. Chandler stated that, when unweathered, these mudstones were composed mainly of silt-sized aggregations of clay-sized particles. Weathering was found to destroy these aggregations, decreasing the overall particle size of the soil. Consolidation and consolidated undrained (CU) and consolidated drained (CD) triaxial tests were performed on undisturbed samples representing different degrees of weathering. The results showed that weathering decreases the preconsolidation pressure and the effective stress shear strength parameters (ϕ' and c') of the mudstones. Chandler stated that an effective stress cohesion intercept is obtained because a straight line is fitted to a curved failure envelope. He also mentioned that the effective stress friction angle obtained from direct shear tests usually lies several degrees below that measured with the triaxial device. No results to support this statement were provided.

In 1970, Skempton reassessed his opinion on the limiting shear strength for first-time slides in overconsolidated clays. The idea that progressive failure reduces the shear strength to the residual shear strength conflicted with the theory of critical state soil mechanics presented by Roscoe et al. (1958) and did not take into account the relative small displacements that typically precede a first-time slide in overconsolidated clays. Roscoe et al. (1958) defined that a saturated clay reaches the critical state in a drained test when any further increment in shear distortion does not result in a change in water content (or void ratio or volume). This is shown diagrammatically in Figure 2.9. This figure shows an idealized behavior of normally consolidated and overconsolidated clays. Actual clay behavior can deviate significantly from this behavior. From this figure it can be seen that the critical state shear strength is the shear strength of an overconsolidated clay after it has dilated during shear. Based on this figure, there seems to be no distinction between residual, fully softened, and critical state shear strength since the normally consolidated clay exhibits no strain softening.

Skempton acknowledged that the critical state shear strength for an ideal clay is independent of the stress history. He also stated that the behavior of real clays that exhibit sensitivity, bonding, and preferred particle orientation is complex and the critical state shear strength parameters cannot be easily determined.

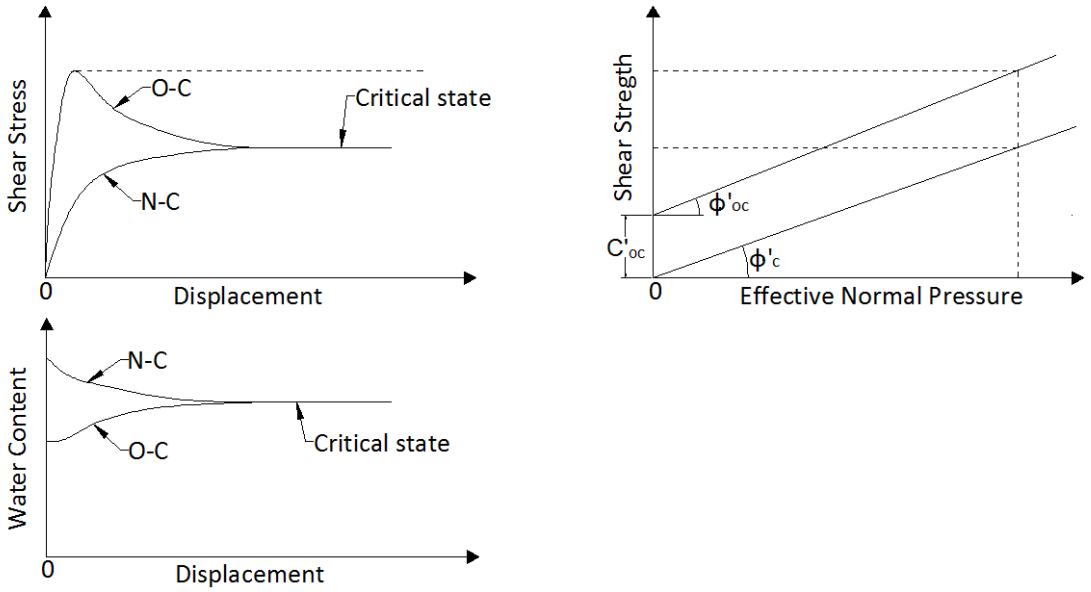

Figure 2.9 Idealized clay behavior (After Skempton 1970) (Used under fair use).

In this paper, the term *fully softened shear strength* was strictly defined for the first time. Skempton (1970) defined it as the drained peak shear strength of a clay in a normally consolidated state, as shown in Figure 2.10. Note that the stress-displacement relationships shown in this figure differ considerably from the idealized behavior shown in Figure 2.9, which were published in the same paper. Is important to note that, according to Skempton, Schofield and Wroth (1968) claim that the critical state condition will be attained at a higher displacement than the required to reach the fully softened condition as defined by Skempton.

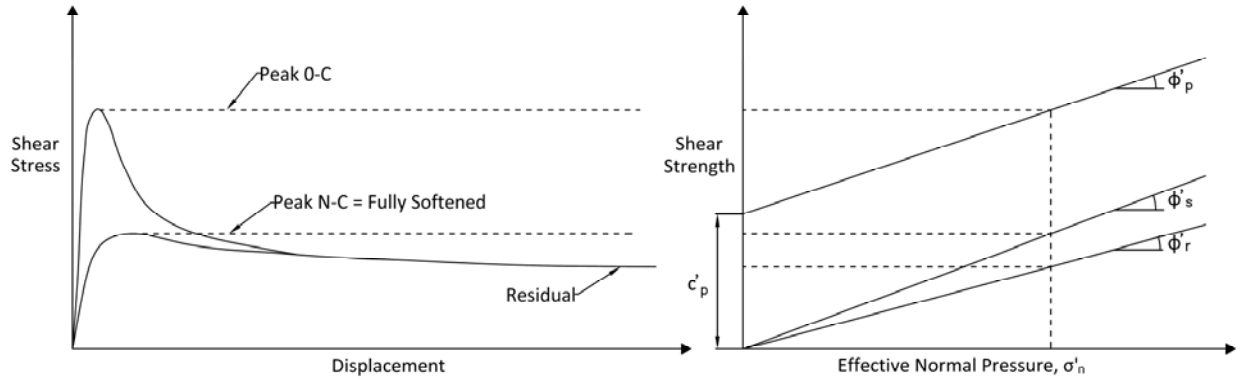

Figure 2.10 Shear characteristics of clays (After Skempton 1970) (Used under fair use).

The fully softened shear strength was considered by Skempton as a practical approximation of the critical state shear strength. He mentioned that, based on a diagram presented by Schofield (1967) (reproduced in this dissertation as Figure 2.11), Schofield seems to have agreed with this approximation. Figure 2.11 shows a sketch of the failure envelopes in a Cambridge stress path[4] space for the undisturbed peak, critical state, and residual strength on the left side and the strain-stress curves for these three conditions on the right side.

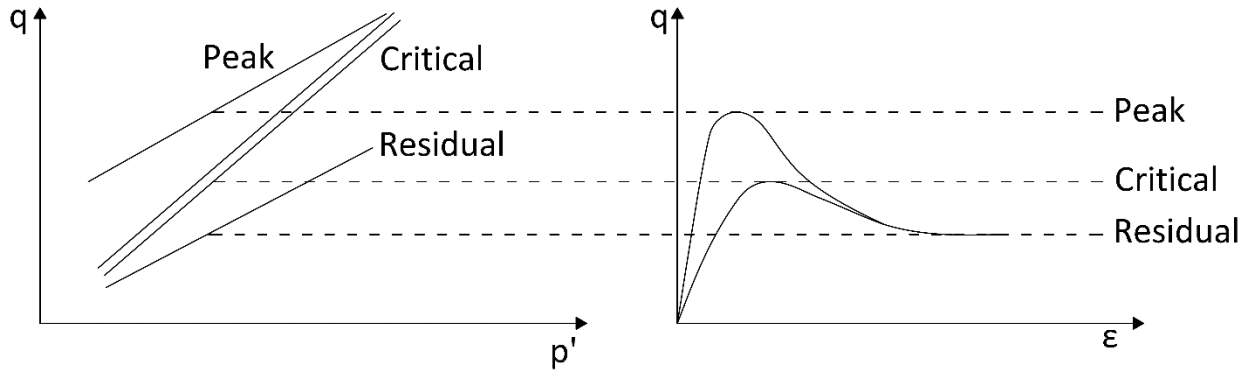

Figure 2.11 Peak, critical state, and residual strength clay behavior (After Schofield 1967) (Used under fair use).

As a simplification, Skempton divided the post-peak reduction in the shear strength of an overconsolidated clay in two stages: (1) increase in water content and decrease in the shear strength to the fully softened value caused by dilatancy and opening of the fissures, and (2) development of shear zones that will eventually link together and form a continuous shear zone, with a subsequent decrease in the shear strength to the residual shear strength along the entire failure surface after adequate displacement has occurred. Skempton stated that field evidence showed that the shear strength in first-time slides in London Clay approaches the fully softened shear strength and would normally not be less than that shear strength.

After analyzing various case histories, Skempton concluded that: (1) some clays will mobilize the peak shear strength as measured in the laboratory for first-time failures, (2) a mechanism of progressive failure and/or softening should exist to make the clay pass the peak shear strength, (3) some clays might experience a decrease in shear strength below the fully softened shear strength before a first-time slide occurs, and (4) the residual shear strength in a clay will be reached after a continuous shear plane is formed and this will be the controlling friction angle for ultimate stability (i.e. after a slide had occurred).

[4] In Cambridge stress paths, p' is defined as $\frac{\sigma'_1+\sigma'_2+\sigma'_3}{3}$ and q is defined as $\sigma'_1 - \sigma'_3$.

In 1970, P. M. James completed his Ph.D. dissertation at University of London entitled “Time effects and progressive failure in clay slopes.” In his dissertation, James (1970) analyzed several slope failures in different stiff-fissured clays. He explained the difference in the shear strength measured in undisturbed samples in the laboratory and the shear strength mobilized in the field by a decrease in the effective stress cohesion with time. Based on back-analysis of failures, he concluded that: (1) the failure surface in slopes in stiff-fissured clays usually does not pass below the toe of the slope and often follows the horizontal bedding planes, (2) in London Clay, the depth of weathering is about 20 ft to 30 ft, and (3) the residual shear strength could be mobilized along the horizontal bedding planes if they exist. Based on direct shear tests, James concluded that one shear reversal along the bedding plane causes more reduction in shear strength than seven reversals perpendicular to the bedding plane. He recommended that a factor of safety of 1.35 should be used with fully softened shear strength parameters for first-time slides in stiff-fissured clays.

A method to include the effect of progressive failure in limit equilibrium analysis was presented by Bishop (1971a). In his paper, Bishop proposed that a variation in the *residual factor* along the failure plane can be used in limit equilibrium analysis to account for the fact that uniform shear strength is not mobilized along the failure plane. Two different patterns of variation of the residual factor along the failure plane were proposed by Bishop as shown in Figure 2.12. The variation labeled as “Case 1” assumes that progressive failure starts at the toe and progresses towards the top of the slope and “Case 2” assumes that progressive failure starts at the toe and the top and progresses towards the center. According to Bishop, the pattern of this variation will depend on the shear-displacement characteristics, swelling characteristics, and shear modulus of the soil in the slope.

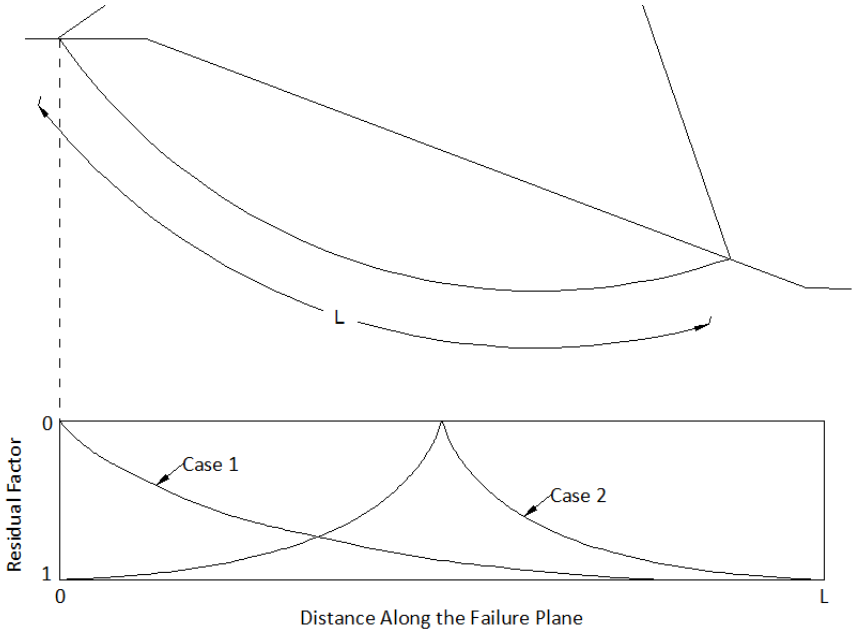

Figure 2.12 Variation of the residual factor along the failure plane (After Bishop 1971a) (Used under fair use).

Until 1973, the best explanation for the delay in failures in stiff-fissured clays was based on the assumption that the effective stress cohesion decreases with time after the cut was made (Henkel 1957; James 1970). This explanation was partially refuted after Vaughan and Walbancke (1973) measured values of pore pressures below steady state seepage values in a cut in Blue London Clay nine years after the cut was made. Observations showed a very slow rate of pore pressure equalization to the steady stage seepage condition from the low values that follow the stress reduction caused by the cut. Calculations showed that the coefficient of swelling obtained in the field was similar in magnitude to the value measured in the laboratory on small undisturbed samples. This would indicate that the fissures have little to no effect in the rate of dissipation of pore pressures after the excavation.

The pore pressures in a slope can be quantified by the use of the *pore pressure ratio*. The pore pressure ratio was defined by Bishop and Morgenstern (1960) as follows:

$$r_u = \frac{u}{\gamma H} \tag{2.3}$$

Where:

r_u = Pore pressure ratio.
u = Pore pressure at a given point.
γ = Unit weight of the soil.
H = Height of overburden above the point.

The slow equalization of pore pressures was suggested as the principal mechanism causing the delay in failures in stiff-fissured clays instead of the decrease in effective stress cohesion with time, as postulated by Henkel (1957) and James (1970). The case histories of first-time failures in stiff-fissured clays presented by James (1970) were re-analyzed by Vaughan and Walbancke (1973) assuming constant shear strength parameters of c' = 0 and ϕ' = 20° to calculate the average pore pressure ratio at the time of failure. The results are presented in Figure 2.13, where an increase in pore pressure ratio with time was determined from back-analyses. An equilibrium pore pressure ratio of about 0.25 to 0.30 was achieved after about 40 years. From this figure, it can also be seen that the rate of change in the pore pressure ratio decreases with increasing time after the cut was made.

Chandler (1974) analyzed 12 slope failures in cuts in overconsolidated Upper Lias Clay. The Upper Lias Clay is a heavily overconsolidated clay that was subjected in the past to equivalent overburden thicknesses in excess of 3,000 ft. The first 33 ft of the Upper Lias Clay is usually brecciated, consisting of a mass of clay lumps in a matrix of remolded clay. The natural water content for this clay is below the plastic limit in the un-weathered state and around the plastic limit when weathered. The liquid limit of this soil ranges from 57 to 68. The plastic limit ranges from 24 to 31, and the soil has a clay-sized fraction that ranges from 33% to 62%.

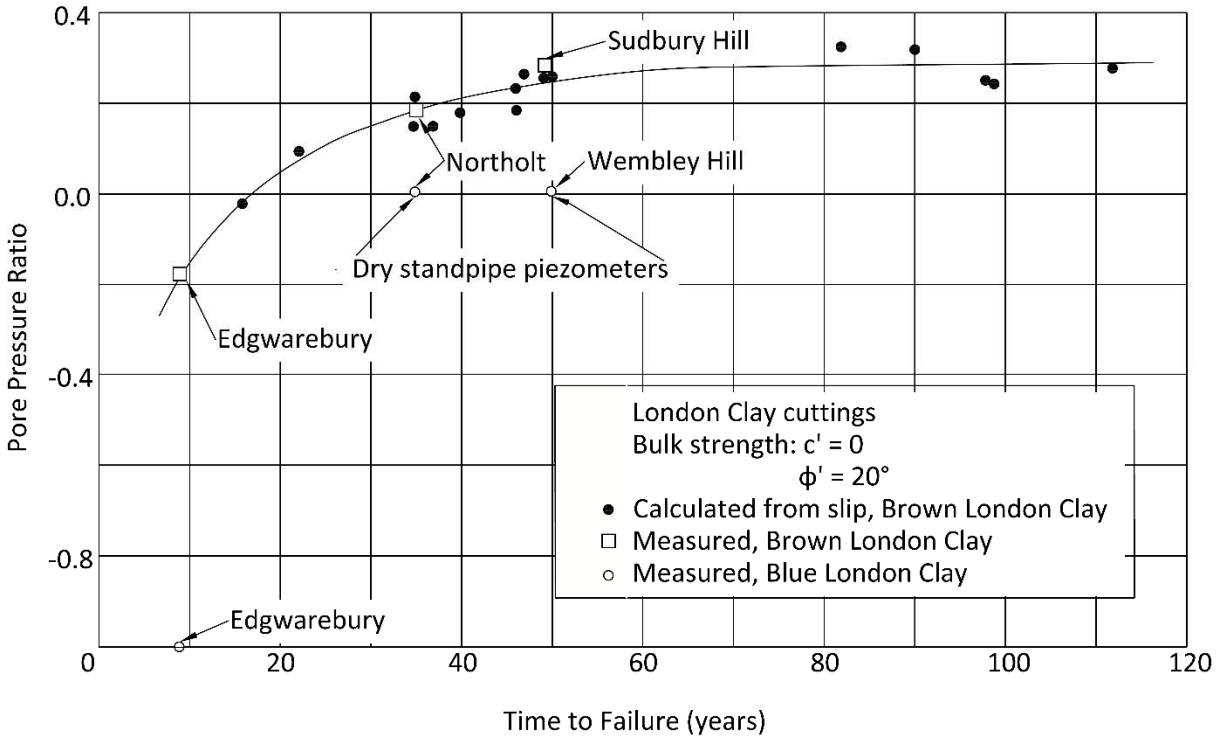

Figure 2.13 Variation of the pore pressure ratio with time (After Vaughan and Walbancke 1973) (Used under fair use).

Chandler's back-analyses of the slopes, using the limit equilibrium method developed by Morgenstern and Price (1965), showed a lower bound for the drained shear strength parameters of c' = 0 and ϕ' = 23° ± 1.5°. An average pore pressure ratio of 0.3 was found to be appropriate for the analysis of the slides. The cuts in brecciated Lias Clay were found to reach steady state pore pressures in less than 10 years, while cuts in weathered but unbrecciated Lias Clay took as long as 60 years to reach pore pressure equilibrium. Details for the slopes analyzed in this paper are summarized in Table 2.2. The slip surface in the slide at Culworth was identified by zones of high water content and the slides at Hunsbury Hill and Stowehill by localized zones of soft soil.

Chandler and Skempton (1974) stated that the assumption of c' = 0 is a very conservative lower bound and the practical significance of this has been overlooked. This assumption leads to the conclusion that the factor of safety of a slope is not dependent on the height of the slope, which contradicts practical experience. The fact that a small effective stress cohesion is sometimes measured in residual shear strength determinations, where the sample is subjected to large strains, was used by Chandler and Skempton to justify that the effective stress cohesion intercept cannot be zero for first-time slides.

Effective shear strength parameters of ϕ' = 20° and c' = 20 psf for the Brown London Clay, ϕ' = 21° and c' = 20 psf for the brecciated Upper Lias Clay, and ϕ' = 25° and c' = 30 psf for the unbrecciated but fissured and weathered Upper Lias Clay were obtained based on back-analyses of first-time failures. Chandler and Skempton offered progressive failure as a possible explanation for the difference in back-calculated

effective stress cohesion in first-time slides in stiff-fissured clays compared to laboratory results. They stated that progressive failure might cause strains sufficiently large to allow full dilatancy, which causes a water content increase in the vicinity of the failure surface, resulting in a critical state condition. They also stated that the residual shear strength does not play any role in first-time slides.

Table 2.2 Summary of the slopes analyzed by Chandler (1974).

Location of the slope	Height (ft)	Slope (H:V)	Time to Failure (yrs)	Vertical Depth of sliding (ft)
Ardley, Oxfordshire	52	2.5:1	52	10
Barrowden, Rutland	14	2:1	83	15
Culworth, Northamptonshire (2 slips)	30	2:1	57 and 61	-
Heyford, Northamptonshire	33	2:1	126	11
Hunsbury Hill, Northampton	54	2.25:1	44	21
Seaton, Rutland	30	2.5:1	68	10
Stowehill, Northamptonshire (2 slip)	30 and 20	-	65 and 122	-
Wellingborough, Northamptonshire	33	-	106	-
Wothorpe, Stamford, Lincolnshire (2 slips)	20 and N/A	3:1	5 and 9	5 and N/A

In 1977, a detailed summary of the investigations on first-time slides in cuttings in Brown London Clay was presented by Skempton (1977). The results of the back-analyses performed by Skempton showed that a pore pressure ratio of 0.3 is normally appropriate for stability analysis of cuts in Brown London Clay. Pore pressure measurements were taken in two cuts in Brown London Clay 19 years and 125 years after the cuts were made. These measurements showed pore pressure values that were about one-half of the steady state values in the younger cut. The older cut had already attained steady state conditions.

The conclusions arrived by Skempton from the investigations presented in this paper were:

1) Displacements caused by progressive failure decrease the shear strength of stiff-fissured clays towards the fully softened shear strength or the lower limit of the fissure shear strength. However, these displacements are not large enough to decrease the shear strength to the residual value.
2) A first-time slide in cuts in London Clay is a slow process that occurs many years after the excavation.
3) The principal reason for the delay in failures of cuts in stiff clays is the slow rate of pore pressure equilibration after the cut is made, which can take up to 50 years.
4) A displacement around three feet to seven feet is required in the field to reach residual conditions.

Chandler (1984a, 1984b) presented an analysis based on published research and case histories on slides in overconsolidated clays and soft rocks. Chandler concluded that the period of pore pressure

equilibration in excavations in saturated clay may vary from a few days to many years. Short drainage paths in the field, the capability of cemented clays to sustain open fissures after swelling, and high permeability can reduce the time required to achieve pore pressure equilibration. In the absence of these factors, pore pressure stabilization may require several decades.

After analyzing case histories of first-time slides, Chandler concluded that the shear strength developed in the field is a function of the plasticity index (PI) of the clay and that the presence of fissures has little influence on the shear strength mobilized. Clays of low plasticity generally tend to experience a small decrease in the shear strength after the peak, and accordingly, the peak shear strength may be used in the design of slopes in this material. Triaxial test results on low plasticity clays, compiled from existing literature by Chandler, showed that the shear strength of undisturbed and remolded samples was virtually the same, independent of the consolidation history. A similar statement was also presented by Bjerrum (1954) and Skempton and Hutchinson (1969). On the other hand, high plasticity clays, even when normally consolidated, can be quite brittle, showing a large decrease in shear strength after the peak, due to particle reorientation. Based on this shear strength characteristic, Chandler concluded that high plasticity clays are more susceptible to progressive failure than low plasticity clays.

The difference in the shear strength measured in the laboratory and the shear strength developed in the field in stiff-fissured clays has been attributed in the past to the fact that the small samples used in the laboratory are not representative of the fissured clay in the field. Triaxial tests performed by Chandler on 10-inch-diameter test specimens showed lower shear strengths than those measured on 1.4-inch-diameter specimens. Although the shear strength for the large diameter specimens was lower than that for the small diameter specimens, it was still higher than the shear strength mobilized in the field as determined from back-calculation.

Chandler provided three mechanisms to explain the discrepancy between the shear strength measured in the laboratory and the shear strength developed in the field: (1) softening, defined as a reduction in shear strength due to the increase in void ratio at constant normal effective stress, (2) a rheological, logarithmic rate of loss in available shear strength under constant shear stress (creep), and (3) progressive failure. Chandler felt that the time delay of failures in slopes of London Clay can be explained by the slow rate of swelling. He stated that, because of the slow rate, softening seems unlikely to be significant before swelling is completed (after 40 years to 50 years). Softening was presented to be an important mechanism decreasing the shear strength of the soil at shallow depths.

Chandler suggested that the agreement obtained between the shear strength mobilized in the field in failures of London and Upper Lias Clays, taking into account that these two clays are fat clays and show a brittle behavior, and the fully softened shear strength is surprising, yet perhaps fortuitous. In addition, due to the consistency of the results, he proposed that the fully softened shear strength might be used as an empirical method to design cuts in slopes having the same general dimensions as those where data is available. More study was acknowledged to be needed in order to arrive at firm conclusions on the importance of progressive failure in slope failures.

The residual shear strength was considered by Chandler to be the shear strength controlling slopes that were affected by either a previous slide or tectonic activity. Based on the case histories analyzed, he recognized the curvature of the residual shear strength failure envelope. A comparison between the residual shear strength measured in the laboratory, using a ring shear device of the type described by Bishop et al. (1971), and the residual shear strength obtained from back-analyses of failed slopes showed that the residual shear strength measured with the ring shear device is lower than that developed in the field. A difference in friction angle about two degrees to three degrees was found. Two reasons were offered by Chandler to explain this difference: (1) the simplified methods of stability analysis used do not exactly model the stresses and discontinuities in a landslide, and (2) in a landslide, the total movement is divided on a number of different shear surfaces that will not have movements comparable to that imposed on a single surface by the ring shear device.

In order to better understand the decrease in shear strength caused by weathering in clays, Chandler and Apted (1988) performed an investigation on undisturbed London Clay samples representing different degrees of weathering. A chemical analysis of the samples showed that the carbonate content decreased with increasing weathering. An insignificant variation was found in the presence and quantity of metallic elements, and no systematic variation was found in the mineralogy of the clay-sized fraction. A very small difference in index properties was measured for tests specimens representing different degrees of weathering.

Unconsolidated undrained triaxial tests with pore water pressure measurements were performed by Chandler and Apted. The pore water pressure was measured at the mid-height and the bottom of the sample. Generally, the values of pore pressure measured at the two locations were within 5% of each other, and the pore pressure parameter B, as defined by Skempton (1954), was always greater than 0.95. After analyzing the triaxial test results, assuming a constant effective friction angle of 20°, Chandler and Apted concluded that a decrease in the effective stress cohesion was caused by weathering. To explain this conclusion, they suggested that weathering decreases the value of the preconsolidation pressure of the clay. Figure 2.14 shows the normalized stress paths for three soils representing different degrees of weathering. The Roman numerals in the figure indicate the zone of weathering, with zone IV being the most weathered and zone I being the least weathered. It can be seen that the behavior of the most weathered clay did not approach the behavior of a normally consolidated clay.

2.4 Research by S. Wright and Colleagues

Professor Steve Wright and his colleagues at the University of Texas at Austin have performed extensive research on first-time failures in compacted clay embankments. In the 1960s, the Texas Highway Department, now called the Texas Department of Transportation, was experiencing problems with shallow slope failures in their highways embankments. A survey of these failures, performed by Abrams and Wright (1972), showed that the height of the slopes that failed ranged from 20 ft to 40 ft, with slopes inclination ranging from 2H:1V to 3H:1V. Abrams and Wright found that the majority of the failures were occurring in cuts in medium to highly plastic overconsolidated stiff-fissured clays and in compacted embankments of high plasticity clays. The failures tended to be shallow and semicircular, and usually developed numerous years after construction. The specific depths of the slides were not given. High

phreatic surfaces and evidence of saturation were found in all but few of the slides. A chart was developed to back-calculate the cohesion and friction angle in terms of total stresses for a given slope and slide geometry.

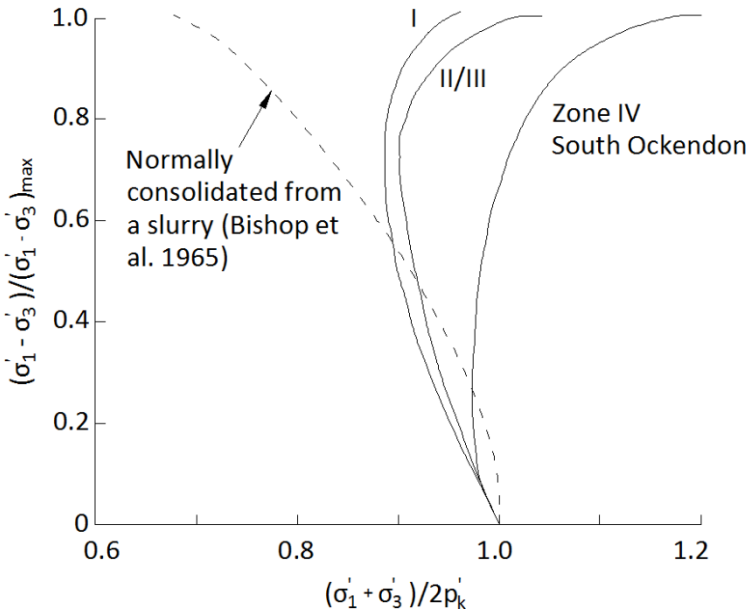

Figure 2.14 Normalized stress paths for London Clay (After Chandler and Apted 1988) (Used under fair use).

After the initial investigation of slope failures presented by Abrams and Wright (1972), no additional investigations were performed to explain the shallow failures of compacted clay embankments along the highways in Texas until 1984, when Gourlay and Wright presented the results obtained from laboratory tests performed on two soils involved in slides. One of the soils studied in that investigation was called "red clay," which had a liquid limit of 71, a plastic limit of 20, and a clay-sized fraction of 67%. The other soil was called "grey clay," which had a liquid limit of 54, a plastic limit of 18, and a clay-sized fraction of 47%.

The laboratory testing program consisted of several CU triaxial and unconfined compression tests. Test specimens of the "red clay" were compacted to a dry density of 96.3 pcf at a target moisture content of 24% and test specimens of the "grey clay" were compacted to a maximum dry density of 102.0 pcf at a target moisture content of 21%. Sometimes the compactive effort had to be modified due to variations in the water content to achieve the desired dry density. Slope stability analyses, using the shear strength parameters measured, showed that the slopes should have been very stable immediately after construction, with the long-term condition being the critical case.

Stauffer and Wright (1984) continued the investigation of slopes failures in embankments in Texas. They concluded that: (1) the slides usually occur 15 years to 25 years after construction, (2) the occurrence of the slides was not necessarily related to the embankment height, because the slides did not typically involve the full height of the slope, (3) the failures were shallow, from 2 ft to 10 ft deep, and were generally restricted to the face of the slope, and (4) the problematic soils were mostly fat clays, with liquid limits ranging from 42 to 97 and plasticity indices ranging from 30 to 71.

A series of charts were developed by Stauffer and Wright to back-calculate effective and total stress shear strength parameters from slope failures. The charts for the effective stress analysis were developed for different values of pore pressure ratio and different geometries.

A detailed analysis of two failures was presented by Stauffer and Wright. Back-analysis using shear strength parameters obtained by Gourlay and Wright (1984) showed factors of safety greater than one for slopes that had already failed. They concluded that the value of effective stress cohesion approaches zero in the long-term and should be ignored for design of slopes of compacted clays of high plasticity.

Green and Wright (1986) conducted a laboratory testing program to better understand the long-term behavior of highly plastic clay embankments in Texas, and to investigate the discrepancies between the laboratory-measured shear strength and the shear strength obtained from back-analyses of failed slopes. Four different sample preparation procedures were used: (1) specimens normally consolidated from a slurry, (2) "packed" specimens, formed by packing soil at a low water content by hand in a special cylindrical mold, (3) compacted specimens, and (4) undisturbed samples. Samples prepared using methods 1 and 2 were tested under consolidated undrained conditions in the triaxial device to obtain effective stress shear strength parameters. Compacted samples were used to obtain residual shear strength parameters in the direct shear device. CU and CD triaxial tests were performed on the undisturbed samples to measure peak shear strength parameters. According to Green and Wright, packed specimens and specimens normally consolidated from a slurry produced comparable peak shear strength parameters.

The factor of safety was calculated for a failed slope using the effective shear strength parameters obtained for the different sample preparations procedures and assuming that the pore water pressure was equal to zero. All the factors of safety obtained using peak shear strength parameters, from undisturbed and normally consolidated specimens, were found to be greater than one. The factor of safety calculated using residual shear strength was found to be less than one, but no justification was found to recommend the use of residual shear strengths for designing compacted slopes of high plasticity clays. Tests on undisturbed samples showed a lower effective stress cohesion when compared to soils compacted in the laboratory.

Green and Wright acknowledged that testing normally consolidated specimens in the triaxial device is problematic, particularly for low effective stresses. The specimen must be consolidated to a significant pressure outside of the triaxial cell in order to achieve the strength needed to be handled, trimmed, and mounted in the triaxial apparatus. The specimen must then be consolidated to a greater effective stress in the triaxial cell if a normally consolidated condition at failure is to be achieved. This procedure is time

consuming and imposes a limitation on the minimum effective stress that can be used for testing normally consolidated samples in the triaxial device.

In order to provide an explanation for the failures in compacted embankments of high plasticity clays, Rogers and Wright (1986) investigated the effects of cycles of wetting and drying on the effective shear strength parameters of compacted clays. The laboratory testing program consisted of direct shear and CU triaxial tests performed on samples subjected to 1 to 30 cycles of wetting and drying. The samples were first soaked in distilled water for 24 hours which represented a wetting cycle. A drying cycle consisted of 24 hours in an oven at 140 °F. A special mold was designed for each device to allow the samples to be wetted and dried while maintaining their shape. A substantial decrease in shear strength was measured in the samples tested in the direct shear apparatus after cycles of wetting and drying. No substantial variation in the friction angle was measured, and the decrease in shear strength was caused by a decrease in the effective stress cohesion intercept. No significant effect of the number of cycles of wetting and drying on the drained shear strength was found. Most of the decrease in shear strength happened after one cycle.

Specimens tested with the triaxial device did not exhibit a decrease in drained shear strength due to cycles of wetting and drying. According to Rogers and Wright, the reason for the difference between the triaxial and the direct shear results was attributed to the relative short period of time allowed for wetting and drying. The drainage path for the triaxial specimens is longer; therefore, it may not have had the same change in saturation as the direct shear test specimens. Also, the triaxial specimens were confined during cycles and free swelling was not allowed on these samples.

Back-analyses of failed slopes using the shear strength obtained after wetting and drying resulted in a factor of safety greater than one. Rogers and Wright suggested that more research was needed to adequately explain the failures.

In order to improve the procedure used by Rogers and Wright (1986) for testing specimens subjected to cycles of wetting and drying using the triaxial device, Kayyal and Wright (1991) designed a new specimen container and conducted additional tests on two fat clays from Texas. The laboratory testing program consisted of CU triaxial tests performed on compacted samples, compacted samples subjected to cycles of wetting and drying, and samples normally consolidated from a slurry. The new container allowed samples subjected to cycles of wetting and drying to free swell during the wetting stage while maintaining their shape. It was verified, using the triaxial device, that cycles of wetting and drying decreased the shear strength of compacted fat clays. The shear strength measured on this type of specimens was found to be similar to the shear strength obtained from specimens normally consolidated from a slurry. X-ray diffraction tests indicated that the particle orientation in samples subjected to wetting and drying was similar to the samples consolidated from a slurry.

Based on those results, Kayyal and Wright (1991) concluded that the long-term shear strength of high plasticity compacted clays can be measured in the laboratory using normally consolidated specimens. Slope stability analyses performed by Kayyal and Wright showed that the decrease in shear strength by wetting and drying can be one of the causes of slope failure. High pore water pressures must also be

present to explain many of the failures. A water table coinciding with the ground surface, corresponding to a pore pressure ratio ranging from 0.5 to 0.6, was recommended for design.

Saleh and Wright (1997) and Wright (2005) presented correlations, based on the data presented by Stark and Eid (1997) and Stark et al. (2005), respectively, to estimate the fully softened shear strength parameters using soil index properties. These correlations are now outdated since Stark and Hussain (2013) presented a new version of the correlation which includes more data.

Wright (2005) also presented a summary of the research performed for the Texas Department of Transportation by the Center of Transportation Research on the slope stability of compacted clay embankments in Texas. In this report, he stated that CU and CD triaxial tests yield essentially the same effective shear strength failure envelope.

More research on the failures of embankments constructed of compacted high plasticity clays in Texas was presented by Wright et al. (2007). Wright et al. presented the results of a laboratory testing program performed to characterize the shear strength of Eagle Ford Shale. This soil has also been involved in failures in compacted clay embankments. This soil has a liquid limit of 88, a plastic limit of 39, and a clay-sized fraction of 64%. Samples were prepared in three ways: (1) compacted, (2) compacted and subjected to cycles of wetting and drying, and (3) normally consolidated from a slurry. CU triaxial tests were performed to obtain the effective stress shear strength parameters for this soil. The results showed a curved failure envelope for all sample preparation techniques.

Cycles of wetting and drying did not reduce the shear strength envelope of Eagle Ford Shale to the normally consolidated state even after 20 cycles. The procedures used for wetting and drying cycles were similar to the ones used by Kayyal and Wright (1991). The results showed that the normally consolidated specimens had a higher void ratio than the specimens subjected to cycles of wetting and drying, and this was believed to be the reason for the difference in the shear strength measured. Based on a back-analysis of a failed slope in Eagle Ford Shale, Wright suggested that use of the fully softened shear strength in conjunction with a pore pressure ratio between 0.43 and 0.53 were applicable for field conditions.

2.5 Research by T. Stark and G. Mesri

Professors Tim Stark and Gholamreza Mesri, both from University of Illinois at Urbana-Champaign, have focused part of their research to the slope stability of overconsolidated clays. T. Stark has also performed research on the measurement of fully softened shear strength. This section summarizes their findings.

Stark and Duncan (1991) presented an investigation on a failure in the San Luis Dam located in Merced County, California. On September 4, 1981, a failure occurred in the upstream slope, after the reservoir was drawn down 180 ft in 120 days. This failure occurred after 14 years of normal operation of the dam. The slide was deep-seated and extended into the foundation beneath the upstream slope. The clay involved in this slide was a stiff-fissured clay with a liquid limit ranging from 35 to 45, and a plastic limit ranging from 18 to 24. The results from slope stability analyses showed that the residual shear strength should have been acting on the failure plane to explain the failure. This conclusion was in conflict with experience on previous first-time slides in stiff-fissured clays that showed that the fully softened shear

strength should have been the controlling shear strength (Skempton 1970; Chandler and Skempton 1974; Skempton 1977).

The condition of the upstream soil was different than the downstream soil. The downstream soil was dry, very stiff, with a natural water content around 8%, and a degree of saturation between 50% and 60%. The upstream soil was softer and wetter, with a water content around 19%. Consolidation and direct shear tests were performed on undisturbed samples obtained from the upstream and downstream slopes. A few of the specimens were soaked in water and allowed to swell prior to testing.

Results from consolidation tests showed that soaking the upstream specimens in water and allowing them to undergo free swell before testing did not influence the consolidation characteristics of the soil. The values of overconsolidation ratio (OCR)[5] for the upstream samples ranged from 1.0 to 1.8. Specimens from the downstream slope were soaked in water under an applied normal stress. Soaking the downstream specimens in water erased their memory for the preconsolidation pressure and the test specimens behaved as normally consolidated. This difference in the behavior after soaking in water was attributed to the elimination of the negative pore water pressures present in the desiccated and partially saturated clay found downstream.

Reversal direct shear tests were performed in order to measure the peak, fully softened, and residual shear strengths of the soil samples. Specimens from the upstream and downstream slopes were tested in the undisturbed, soaked, and remolded conditions. For the upstream samples, no difference was found in the drained peak shear strength measured using undisturbed and soaked specimens, and only a small difference was found in the shear strength measured using undisturbed and remolded samples. On the downstream side the results were different. The undisturbed samples were very strong, while the soaked and remolded downstream specimens had the same shear strength as the upstream soaked specimens.

Modified direct shear tests were also performed on undisturbed samples from the downstream area to simulate cycles of loading and unloading caused by the rise and fall of the reservoir level. The result from these tests showed that the shear strength decreased to the residual shear strength after enough displacement was accumulated from cycles of loading and unloading. It was concluded that the residual shear strength was the governing shear strength in cases were a stiff clay is subjected to cyclic loading from rising and lowering a reservoir.

Shewbridge and Schaffer (2013) stated that a loss in apparent cohesion due to saturation of the soil can be used to explain the failure in the San Luis Dam. A loss in apparent cohesion is not enough to explain why the residual shear strength was mobilized on the failure plane in this case history. The residual shear strength is achieved after enough strain to reduce the shear strength to this condition is accumulated on the failure plane. For this reason, the explanation presented by Shewbridge and Schaffer (2013) cannot explain the failure in the San Luis Dam.

[5] The overconsolidation ratio is defined as the ratio of the maximum effective stress experienced by the soil in the past to the actual effective vertical stress in the field.

Mesri and Abdel-Ghaffar (1993) described the importance of the effective stress cohesion intercept in slope stability analysis. Mesri and Abdel-Ghaffar stated that the effective stress cohesion intercept has a big influence on the factor of safety and the location of the critical failure surface for slope stability. According to them, the effective stress cohesion intercept is normally obtained from a linear approximation of a non-linear failure envelope over a defined range of normal stresses. Although they acknowledged the non-linearity of the failure envelope, they felt that the failure envelope for normally consolidated soils can be approximated as linear for practical purposes.

After analyzing numerous case histories of slope failures in soft and stiff clays, Mesri and Abdel-Ghaffar proposed a reduction factor for the peak shear strength to account for the difference in the mobilized shear strength in the field in certain soils. The reduction factor, η, was intended to be used in effective stress analyses, and is shown as a function of plasticity index in Figure 2.15. From this figure, it can be seen that for soft clays, and stiff clays with plasticity indices less than 20, the mobilized shear strength in the field is equal to the shear strength measured in the laboratory on undisturbed specimens. For soils with PI values greater than 20, the difference of the mobilized and measured shear strength increases until a PI of around 60. From that point, as PI increases, the reduction factor increases. It should be noted the bulk of the data shown are for PI values less than 60.

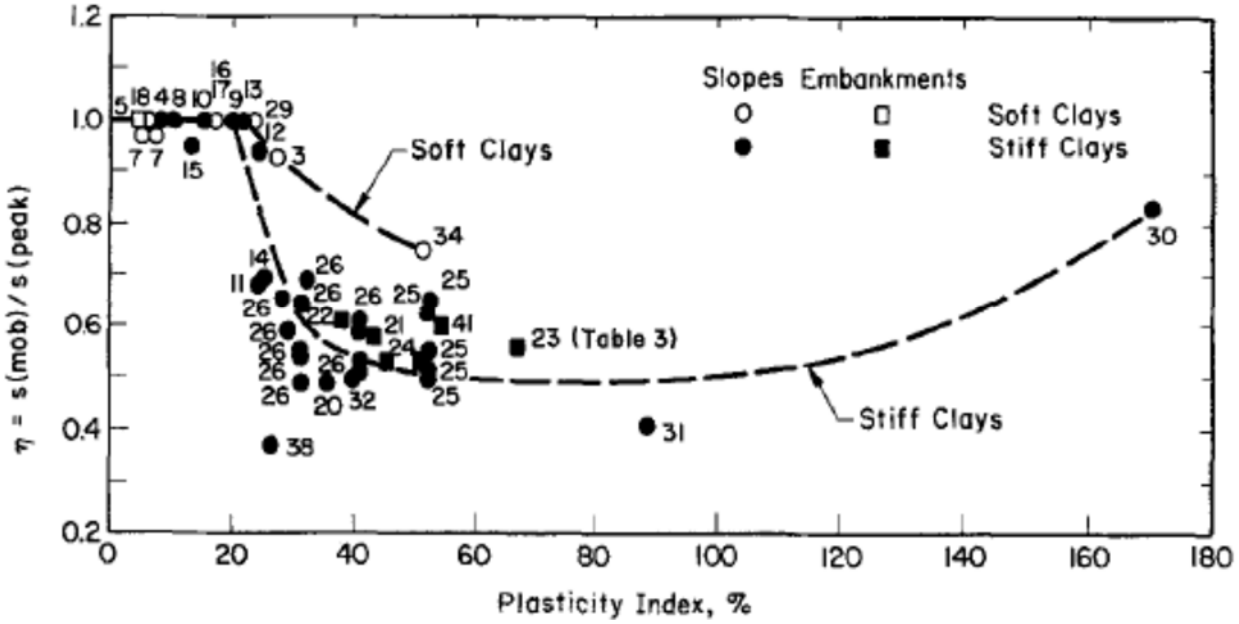

Figure 2.15 Correction factor for peak shear strength used in effective stress stability analysis (Mesri and Abdel-Ghaffar 1993) (Used under fair use).

To locate the critical failure surface in limit equilibrium analyses, Mesri and Abdel-Ghaffar recommended the use of peak shear strength parameters. This conclusion was reached after analyzing 40 case histories. These analyses showed that the observed slip surface in the field closely matched the critical failure surface when peak shear strength parameters were used for the soil. The use of peak shear strength

parameters was recommended to locate the critical failure surface. To compute the factor of safety, the adjusted shear strength should be used with the critical failure surface found.

Results from back-analyses performed by Mesri and Abdel-Ghaffar also showed that the mobilized shear strength in first-time slides can be less than the fully softened shear strength. This conclusion was based on the fact that, in certain cases, a reduction in the effective stress cohesion was not enough to explain the failure. A reduction in the effective stress friction angle was also required to obtain a factor of safety of unity. It should be noted that the Mesri and Abdel-Ghaffar assumed that the peak (undisturbed) friction angle was equal to the fully softened friction angle, therefore the only difference in strength between the two conditions could be attributed to the effective stress cohesion.

The measurement of fully softened shear strength using different devices was investigated by Stark and Eid (1997), who presented the results of torsional ring shear, direct shear, and triaxial compression tests on cohesive soils. The torsional ring shear device used for these tests was a ring shear device, as described by Bromhead (1979), with the modification to reduce side-wall friction presented by Stark and Eid (1993). Twenty-four different soils, including shales, mudstones, silts, and clays, were tested using the ring shear device. Air-dried mudstone and shale samples were disaggregated by ball-milling until they passed a No. 200 (75 μm) sieve. Remolded silts and clays were obtained by air-drying the samples, crushing them with a mortar and pestle, and processing them through a No. 40 (425 μm) sieve. These sample preparation techniques were used to prepare samples for soil index properties and shear strength measurements. Samples for shear testing were mixed with distilled water to obtain a liquidity index of 1.5 and then allowed to rehydrate for at least a week in a moist room. It is worth to emphasize that two different sieve sizes were used to process the soils, which may affect the shear strengths measured.

The liquidity index is defined as:

$$LI = \frac{w - PL}{LL - PL} \tag{2.4}$$

Where:

LI = Liquidity index.
w = Water content of the sample.
PL = Plastic limit.
LL = Liquid limit.

To compare the fully softened shear strength measured with the ring shear and direct shear devices, two tests were conducted on two soils by Stark and Eid. Both soils were tested at consolidation pressures of 2,089 psf and 8,354 psf using both devices. The complete set of results was presented by Eid (1996). The soils tested were the Panoche Shale with a liquid limit of 53, a plastic limit of 29, and a clay-sized fraction of 50% and the Lower Pepper Shale with a liquid limit of 94, a plastic limit of 26, and a clay-sized fraction

of 77%. According to Stark and Eid, the results showed that the difference in the fully softened friction angle measured with the direct shear and the torsional ring shear devices was very small, resulting in a difference of less than one degree. Stark and Eid did not specify how the shear strength parameters were determined. The results of the tests presented by Eid (1996) are summarized in Table 2.3. From this table, it can be seen that is likely that Stark and Eid used either the ϕ'_{secant} from each test or the c' = 0 interpretation to reach to their conclusion. Looking at the c'-ϕ' interpretation, greater differences between the fully softened shear strength parameters are obtained. For both soils, the fully softened shear strength obtained with the ring shear device was higher than that obtained with the direct shear device. More results comparing these two devices are presented in Chapter 6. It should be mentioned that at high normal stresses, a small difference in secant friction angle can represent a significant difference in shear strength.

Table 2.3 Direct shear and ring shear fully softened test results presented by Eid (1996).

						Shear Strength Interpretations		
Soil	Device	τ/σ'	σ' (psf)	τ (psf)	ϕ'_{secant} (deg)	c' & ϕ'		c' = 0 & ϕ'
						c' (psf)	ϕ' (deg)	ϕ' (deg)
Panoche Shale	RS	0.45	2089.0	937.0	24.2	167.7	20.2	21.4
		0.39	8354.0	3243.9	21.2			
	DS	0.47	2089.0	976.2	25.1	289.2	18.2	20.3
		0.36	8354.0	3036.3	20.0			
Lower Pepper Shale	RS	0.38	2089.0	794.0	20.8	247.5	14.7	16.5
		0.29	8354.0	2432.9	16.2			
	DS	0.36	2089.0	755.8	19.9	213.3	14.6	16.2
		0.29	8354.0	2382.7	15.9			

Eid (1996) also compared the direct shear and triaxial apparatuses using test results from five soils. The soils used for this comparison were the Panoche and Lower Pepper shales (described previously); a glacial till, with a liquid limit of 24, a plastic limit of 16, and a clay-sized fraction of 18%; Oahe Firm Shale, with a liquid limit of 138, a plastic limit of 41, and a clay-sized fraction of 78%; and Oahe Bentonitic Shale, with a liquid limit of 192, a plastic limit of 47, and a clay-sized fraction of 65%. Different liquidity indices were used to form the triaxial test specimen of each soil. A liquidity index of 1.0 was used for the glacial till, 0.9 for the Panoche Shale, 0.87 for the Lower Pepper Shale, 0.71 for the Oahe Firm Shale, and 0.62 for the Oahe Bentonitic Shale. No more details about the technique used to form test specimens for triaxial testing were giving. According to Stark and Eid, the results showed that the fully softened friction angle measured with the triaxial device was, on average, 2.5° higher than the friction angle measured with the torsional ring shear apparatus. The actual difference ranged from about 1.5° to about 3°, with the shear strength measured with the triaxial device being always higher. The complete dataset of the results used to reached this conclusion was not given by Eid (1996) nor Stark and Eid (1997), so it is not clear what shear strength interpretation was used to arrive at that conclusion. Eid (1996) stated that for samples that

presented a bulging failure (i.e. the deviator stress-strain did not peak), the shear strength corresponding to a 20% axial strain was chosen as the fully softened shear strength.

A correlation of the secant fully softened friction angle to the liquid limit and the clay-sized fraction obtained from ball-milled samples was first presented by Stark and Eid (1997), later updated by Stark et al. (2005), and the last version was presented in 2013 by Stark and Hussain (2013). The last version of this correlation is shown in Figure 2.16. This correlation was based on the results from torsional ring shear tests increased by 2.5°, according to Stark and his colleagues, to match the triaxial compression mode of shear. The soils were divided into three groups based on the ball-milled clay-sized fraction. Results showed that the fully softened friction angle was stress dependent. The decrease in fully softened friction angle with increased consolidation stress was attributed to the increase in face-to-face orientation of the clay particle as the normal pressure increases (Stark and Eid 1997).

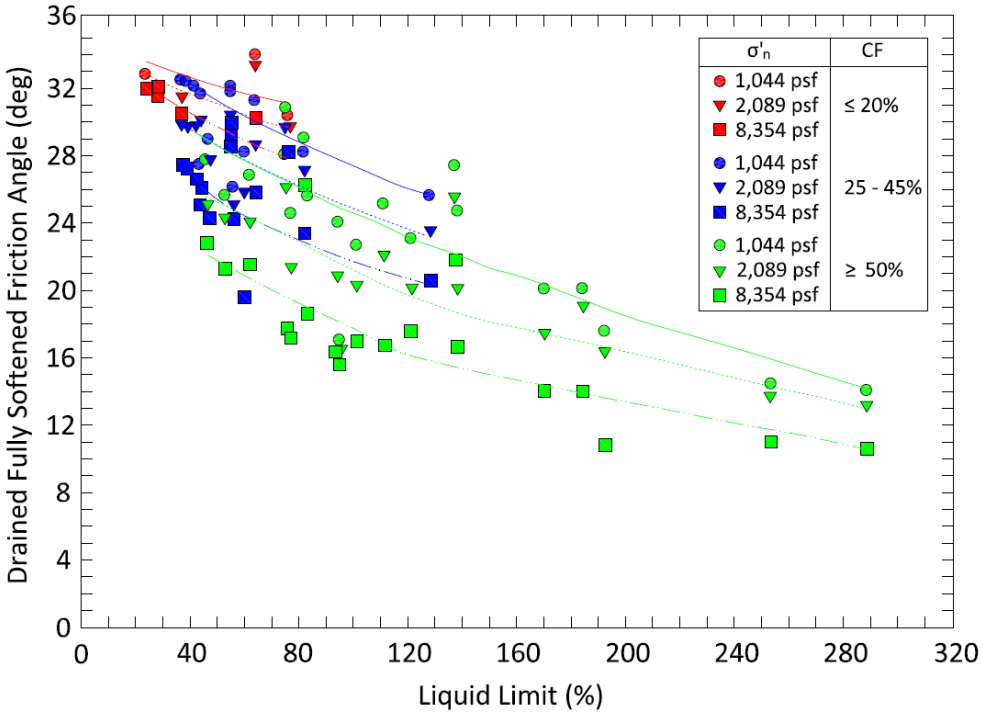

Figure 2.16 Relationship between drained fully softened friction angle and ball-milled liquid limit for triaxial compression mode of shear (After Stark and Hussain 2013) (Used under fair use).

Three sets of equations were presented by Stark and Hussain (2013) for the different trend lines presented in Figure 2.16. Also, a Microsoft Excel® spreadsheet with these equations built-in is available on Stark's website (http://tstark.net/geotechnical-software). The equations are presented below:

For soils with a ball-milled clay-sized fraction ≤ 20% and a ball-milled liquid limit between 30 and 80:

$$\left(\phi_{fs-secant}\right)_{\sigma'_n=1{,}044\ psf} = 34.85 - 0.0709LL + 2.35x10^{-4}LL^2 \quad (2.5)$$

$$\left(\phi_{fs-secant}\right)_{\sigma'_n=2{,}089\ psf} = 34.39 - 0.0863LL + 2.66x10^{-4}LL^2 \quad (2.6)$$

$$\left(\phi_{fs-secant}\right)_{\sigma'_n=8{,}354\ psf} = 34.76 - 0.13LL + 4.71x10^{-4}LL^2 \quad (2.7)$$

For soils with a ball-milled clay-sized fraction ranging from 25% to 45% and a ball-milled liquid limit ranging from 30 to 130:

$$\left(\phi_{fs-secant}\right)_{\sigma'_n=1{,}044\ psf} = 36.18 - 0.1143LL + 2.354x10^{-4}LL^2 \quad (2.8)$$

$$\left(\phi_{fs-secant}\right)_{\sigma'_n=2{,}089\ psf} = 33.11 - 0.107LL + 2.2x10^{-4}LL^2 \quad (2.9)$$

$$\left(\phi_{fs-secant}\right)_{\sigma'_n=8{,}354\ psf} = 30.7 - 0.1263LL + 3.44x10^{-4}LL^2 \quad (2.10)$$

For soils with a ball-milled clay-sized fraction ≥50% and a ball-milled liquid limit ranging from 30 to 300:

$$\left(\phi_{fs-secant}\right)_{\sigma'_n=1{,}044\ psf} = 33.37 - 0.11LL + 2.344x10^{-4}LL^2 - 2.96x10^{-7}LL^3 \quad (2.11)$$

$$\left(\phi_{fs-secant}\right)_{\sigma'_n=2{,}089\ psf} = 31.17 - 0.142LL + 4.678x10^{-4}LL^2 - 6.726x10^{-7}LL^3 \quad (2.12)$$

$$\left(\phi_{fs-secant}\right)_{\sigma'_n=8{,}354\ psf} = 28.0 - 0.1533LL + 5.64x10^{-4}LL^2 - 8.414x10^{-7}LL^3 \quad (2.13)$$

Where:

$\phi_{fs-secant}$ = Fully softened secant friction angle.
σ'_n = Normal stress corresponding to the secant fully softened friction angle.
LL = Ball-milled liquid limit of the soil.

Stark et al. (2005) remarked that, in a ring shear device with an inner diameter of 2.76 inches and an outer diameter of 3.94 inches, the fully softened shear strength is usually mobilized before a shear displacement of 0.40 inches.

They recognized that the ball-milling procedure changes the measured liquid limit and clay-sized fraction of the soils. Usually, higher liquid limit and clay-sized fraction were obtained with ball-milled samples when compared to samples that were not ball-milled prior to testing. According to Stark et al., ball-milling disaggregates the particles, increasing the specific surface, thus allowing more water to be absorbed. Figures 2.17 and 2.18 show the behavior of the ratio of the liquid limit and clay-sized fraction obtained with ball-milled samples to the ASTM-derived value as a function of the liquid limit, respectively. The correlations presented in these figures are outdated because Stark and Hussain (2013) used more data to update the equations to obtain these ratios. These figures are presented in this dissertation to show the general trend of the data since Stark and Hussain (2013) did not provide new plots. From these figures, it can be seen that the difference in the liquid limit increases with increasing ASTM liquid limit while the difference in the clay-sized fraction decreases with increasing ASTM clay-sized fraction. Equations 2.14 and 2.15 were proposed by Stark and Hussain (2013) to obtain these ratios. These equations should be used to obtain the value of the ball-milled liquid limit, if not measured, to be used with the correlation presented in Figure 2.16.

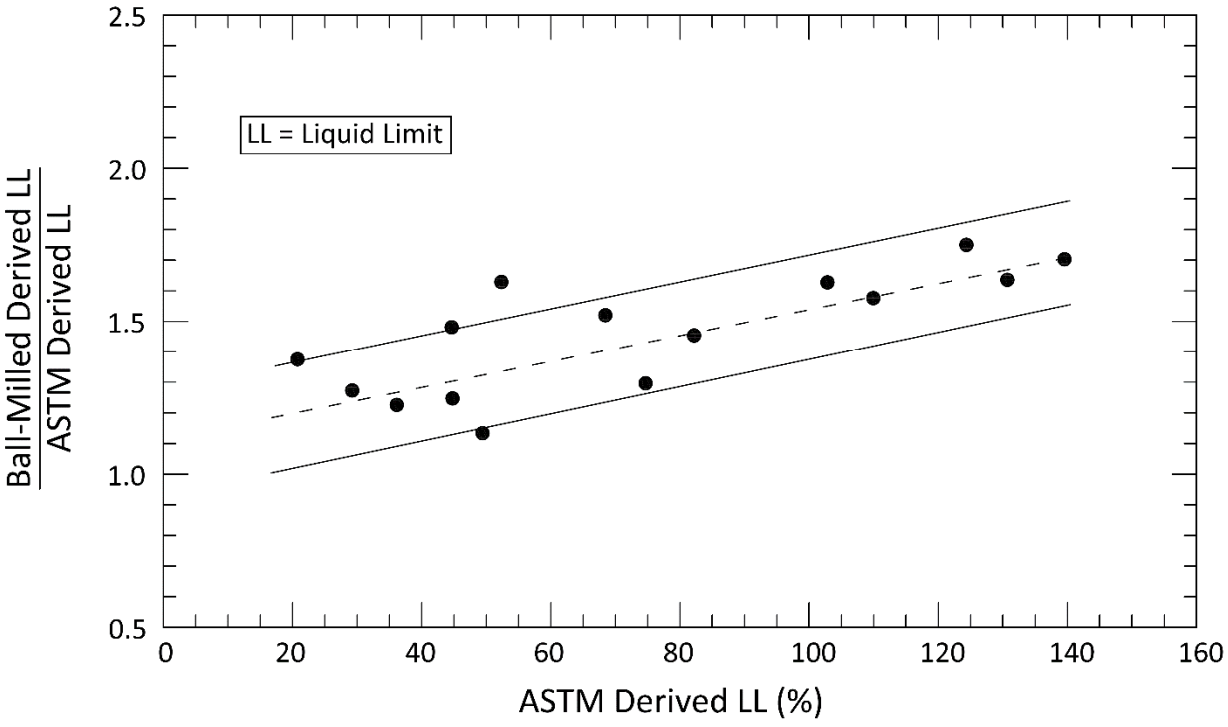

Figure 2.17 Ratio of ball-milled and ASTM values of liquid limit (After Stark et al. 2005) (Used under fair use).

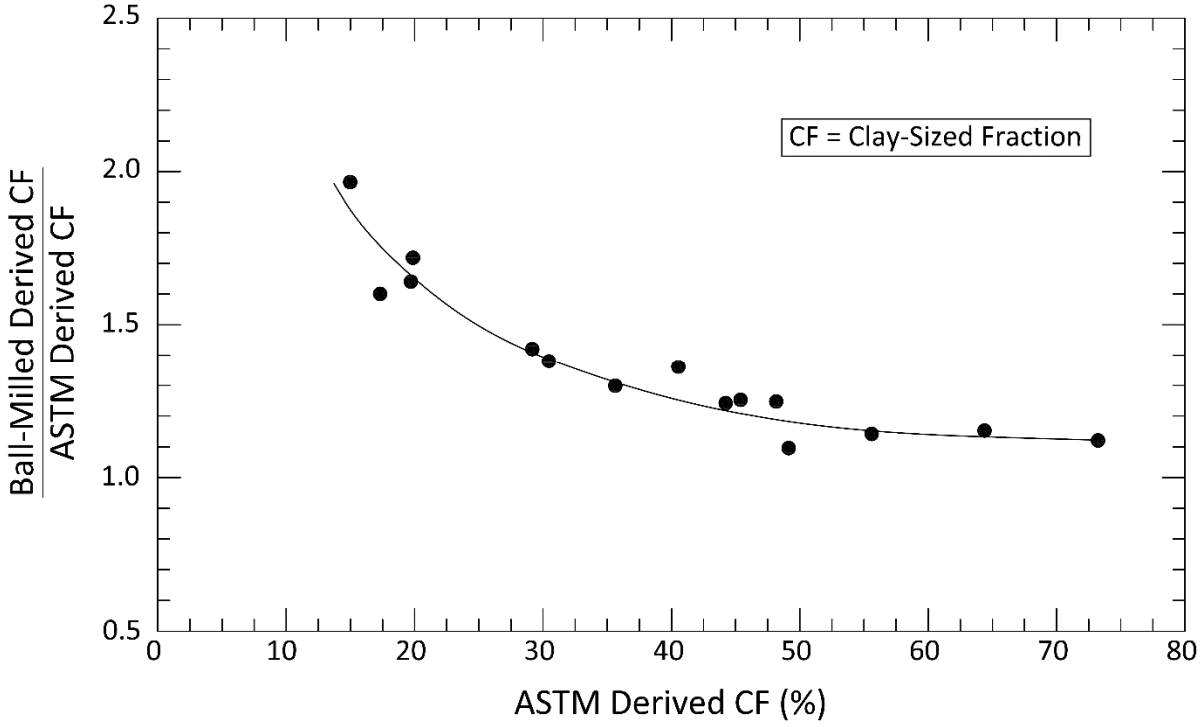

Figure 2.18 Ratio of ball-milled and ASTM values of clay-sized fraction (After Stark et al. 2005) (Used under fair use).

$$\frac{Ball\ milled\ derived\ LL}{ASTM\ derived\ LL} = 0.003(ASTM\ derived\ LL) + 1.23 \tag{2.14}$$

$$\frac{Ball\ milled\ CF}{ASTM\ derived\ CF} = 2E^{-4}(ASTM\ derived\ CF)^2 - 0.0278(ASTM\ derived\ CF) + 2.15 \tag{2.15}$$

To use the fully softened shear strength in slope stability analysis, Stark and Eid (1997) suggested that the location of the failure surface should be determined using peak shear strength parameters and then this same surface analyzed using fully softened shear strength. This follows the recommendation of Mesri and Abdel-Ghaffar (1993). According to Stark and Eid, the reason to use this approach is that progressive failure occurs on the critical surface and decreases the shear strength of the clay towards the fully softened shear strength.

The results of the analysis of 14 case histories of first-time slides in overconsolidated clays were presented by Stark and Eid. Most of the data for the slides were extracted from the Ph.D. dissertation of Abdel-Ghaffar (1990). A few of the case histories only reported undisturbed shear strengths parameters and did not report the fully softened shear strength parameters. For those cases, the fully softened friction angle

was estimated using the correlation presented by Stark and Eid (1997). Results showed that a decrease in the effective stress cohesion measured from undisturbed samples was needed to explain most of the failures; and in certain cases, a decrease in the effective stress friction angle was also needed to obtain FS = 1. For a few of these case histories, the mobilized effective stress friction angle was lower than the effective friction angle predicted using the correlation. Smaller values for the mobilized friction angle were only used if the condition of c' = 0 was not sufficient to explain the failures. Based on this discrepancy between the results obtained from back-analysis and the correlation presented by Stark and Eid, they concluded that the mobilized shear strength for first-time slides can be less than the fully softened shear strength.

It should be noted that it is likely that the values of liquid limit and clay-sized fraction from the case histories were not obtained from ball-milled samples; and in 1997, the correlation to estimate ball-milled liquid limits and clay-sized fractions from ASTM derived values were not available. As shown above, the liquid limits and clay-sized fraction are higher for ball-milled samples when compared to values obtained using ASTM standard procedures. Using ASTM derived values of liquid limit and clay-sized fraction with the correlation presented by Stark and Eid (1997) will cause an over-estimation of the fully softened friction angle. This over-estimation of the fully softened friction angles might explain why friction angles below the assumed fully softened friction angles were required to explain some of the failures.

Mesri and Shahien (2003) presented a review of the long-term stability of stiff clay and clay shale slopes and a re-evaluation of 99 case histories. Based on the case histories analyzed, they concluded that the fully softened shear strength is the lowest mobilized shear strength in first-time slides in homogeneous soft to stiff plastic clays, and on sections of the slip surface perpendicular to bedding planes and laminations in fissured clays. The residual shear strength was assumed to be mobilized in first-time slides on horizontal or near horizontal failure surfaces including stratigraphic discontinuities. In first-time slope failures in un-stratified stiff clays of low plasticity, the mobilized shear strength, according to them, is equal to the peak shear strength as measured in the laboratory using undisturbed test specimens.

Mesri and Shahien (2003) concluded that the shear strength envelope of stiff-fissured clays and shales is curved with no shear strength at zero normal stress for the peak, fully softened, and residual conditions. The reason given for the curvature of the fully softened shear strength envelope is that the high effective normal stresses promote face-to-face interaction of plate-shaped particles. This hypothesis was previously presented by Stark and Eid (1997). Mesri and Shahien stated that empirical correlations for residual and fully softened friction angle are not applicable to clays or shales that are composed of clay minerals that are not plate-shaped, such as attapulgite, and allophane, or are exceptionally aggregated.

The equation shown below was presented by Mesri and Shahien to represent the curvature of the fully softened failure envelope.

$$S(fs) = \sigma'_n \tan\left(\phi'_{fs}\right)_s^{100} \left(\frac{P_a}{\sigma'_n}\right)^{1-m_{fs}} \quad (2.16)$$

Where:

$S(fs)$ = Fully softened shear strength.

σ'_n = Effective normal stress at the failure plane.

$(\phi'_{fs})_s^{100}$ = Secant fully softened friction angle at σ_n' = 2,089 psf (100 kPa).

$1 - m_{fs}$ = Slope of a $\log\left[\tan(\phi'_{fs})_s / \tan\left(\phi'_{fs}\right)_s^{100}\right]$ versus $\log(P_a/\sigma'_n)$ plot.

P_a = Atmospheric pressure.

Mesri and Shahien recommended that the failure surface for stability analysis of natural and excavated slopes should be selected based on knowledge and experience with the geology of the area. The designer should be aware of features such as pre-sheared surfaces produced by old landslides, tectonic or glacial deformation, downslope creep, as well as horizontal or sub-horizontal bedding planes, laminations, and weak seams that will reach the residual condition after small displacements. For existing slopes, observations of movement can help to locate the position and shape of the critical slip surface. In the absence of well-defined weak surfaces, including preexisting shear surfaces, the base of the critical slip surface, in stiff clays and shales, should be parallel to the bedding and horizontal at the level of the base of the slope.

Stark et al. (2005) explained that the fully softened condition is achieved when an overconsolidated clay undergoes an increase in water content to a maximum equilibrium value. They showed that the effective stress cohesion intercept plays an important role in slope stability analysis and that even a small value of effective stress cohesion intercept can have a huge impact on the calculated factor of safety. An effective stress cohesion intercept equal to zero was recommended to analyze first-time slides in stiff-fissured clays.

2.6 Research Performed in Canada

Several research papers have been published in Canada regarding the problem of slope stability in overconsolidated clays. These papers are summarized in this section.

Eigenbrod and Morgenstern (1972) presented the details of a slide that occurred in 1965 in the Upper Cretaceous Edmonton formation in Devon, Alberta. The failure surface was non-circular. A horizontal portion of the failure plane was found in a layer of bentonitic clay with a liquid limit of 100, a plastic limit of 40, and a clay-sized fraction of 47%. An inclined portion of the failure plane, that day-lighted at the ground surface, occurred in a weathered clay having a liquid limit of 85, a plastic limit of 20, and a clay-sized fraction of 52%. The section of the failure surface in the bentonitic clay was found to be a reactivation of an old landslide, therefore it was assumed that the soil had mobilized the residual shear strength.

In the summer of 1965, before the failure occurred, the cut was reconstructed for a highway improvement at a slope of 2.75H:1V to a height of 60 ft. The vertical depth of the failure surface was 40 ft. The shear strength of the soils involved in the slide was characterized using drained triaxial tests on undisturbed samples. The residual shear strength of the bentonitic clay was measured in the triaxial device using

undisturbed samples containing the failure plane. For residual shear strength measurements, the failure plane in the test specimens was oriented to coincide with the expected failure plane in the triaxial device. A factor of safety of 1.01 was found using an average residual friction angle of 8° for the bentonitic clay and fully softened shear strength parameters of c' = 190 psf and ϕ' = 33° for the inclined section in the weathered clay. The main causes of this slide were the removal of the support at the toe of the slope by the construction and the reduction in shear strength caused by weathering of the material. Weathering was presented as an important mechanism that can increase the water content of the clay, thereby decreasing the shear strength.

A summary of the research and case histories on slopes and excavation in heavily overconsolidated clays available prior to 1977 was presented by Morgenstern (1977). Morgenstern concluded that most of the field evidence supports the softening hypothesis more than the progressive failure theory. Softening was presented as a mechanism that reduces the dilatancy characteristics of the soil. This paper was primarily an overview and summary of the research to the date, without providing significant additional details in any of the case histories presented.

In September 1974, a large landslide occurred near Wainwright, Alberta. On the south side of the site, a recently formed scarp was identified. The slope containing this scarp was investigated by Thomson and Tweedie (1978). This site is in the Belly River formation, which consists of layers of marine shales and deltaic sands. The predominant soil in the location of the slide was a grey bentonitic clay shale with a liquid limit between 102 and 149, a plastic limit between 20 and 30, and a clay-sized fraction of 76%. Reversal direct shear tests were performed on undisturbed samples to measure the peak and residual shear strength of the soils involved in the slide. Softening and weathering were found along the joints of the bentonitic clay shale.

Part of this slide was found to be the reactivation of an old landslide. The back-analysis was performed using the method developed by Morgenstern and Price (1965), using the residual shear strength for the section of the slide that corresponded to the reactivated slide and varying the shear strength in the other section until a factor of safety of unity was obtained. The analysis of this slope showed that the shear strength of the soils involved in the slide, aside from the section that was at residual shear strength already, had decreased from peak values to fully softened or residual values.

A first-time slide that occurred in a 23-ft-deep cut in overconsolidated glacial lake sediments five years after construction was analyzed by Thomson and Kjartanson (1985). The slide was triggered by heavy rains. The slope was composed of a dark gray silty clay with a liquid limit of 98, a plastic limit of 37, and a clay-sized fraction of 77%; and a lean clay[6] with a liquid limit of 44, a plastic limit of 23, and a clay-sized fraction of 25%. The failure surface of this slide was found to be 18-ft-deep, measured vertically. Remedial work for this slide allowed Thomson and Kjartanson to observe part of the failure surface. The top section of the scarp was highly fractured and fissured with a blocky structure. The lower zone did not possess the blocky structure, but contained a system of joints. Examination of the surface of the joints revealed no softening.

[6] Thomson and Kjartason (1985) described this soil as a clayey silt.

The testing program in this investigation consisted of CU and CD triaxial tests and direct shear tests on undisturbed samples. The results showed that at stresses below the *in situ* stress, the "nugget" structure of the soil made it behave as a cohesionless material with failure occurring around the nuggets. Slope stability analyses, using the method developed by Morgenstern and Price (1965), showed that the shear strength existing at the moment of the slide was greater than the fully softened shear strength but less than the peak shear strength of the soil.

A failure criterion for soils and rocks exhibiting softening was presented by Yoshida et al. (1990). The equation governing the shear strength can be developed in terms of total or effective stresses and was expressed as follows:

$$\sigma_1 = \sigma_3 + A\sigma_c \left(\frac{\sigma_3}{\sigma_c} - S\right)^{1/B} \tag{2.17}$$

Where:

$\sigma_1 \; and \; \sigma_3$ = Major and minor principal stresses.
σ_c = Uniaxial compressive strength.
$A, B \; and \; S$ = Empirical curve-fitting constants.

The effect of softening using this failure criterion can be represented by a reduction in the magnitude of the parameters *A*, *B*, and *S*. Details regarding the determination of *A*, *B*, and *S* were given in the appendix of the paper. For the fully softened condition, the parameters *B* and *S* were recommended to be equal to 1 and 0, respectively. As a byproduct of this recommendation, the resulting fully softened failure envelope is linear. Yoshida (1991) suggested using inverse hyperbolic functions to account for the reduction of strength parameters with time. This failure criterion, coupled with the equations relating the variation in the strength parameters with time, was presented as a useful tool to be used in finite element analysis to account for the softening process.

An example of the general shape of failure envelopes obtained using this failure criterion is presented in Figure 2.19. In this figure it can be seen how changes in the different parameters affect the shape of the failure envelope obtained. In this plot a failure envelope representing the fully softened conditions (i.e. *B* = 1 and *A* = 0) was also included. From Figure 2.19 it can be seen that as *S* increases, the basic shape of the failure envelope does not change but the shear strength decreases. As *B* decreases, the shear strength increases and the curvature of the failure envelope decreases. As *A* increases, the shear strength increases.

An implementation of the failure criterion proposed by Yoshida et al. (1990) for practical problems was presented by Yoshida et al. (1991a). This failure criterion was modified in order to be integrated into limit

equilibrium slope stability analyses using the infinite slope method, the method of slices, and the simplified method presented by Bishop (1955).

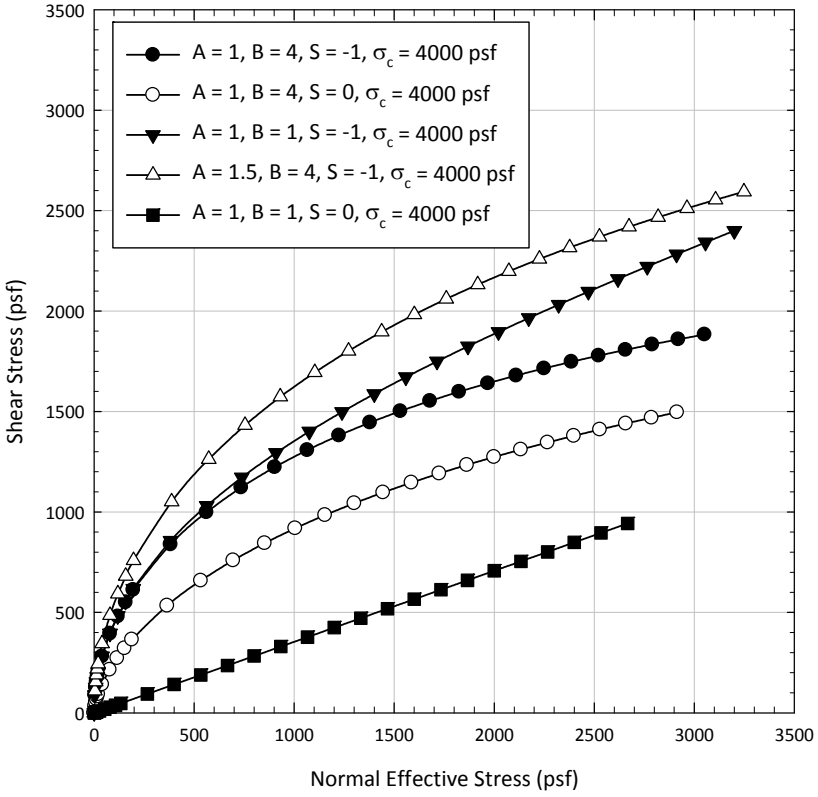

Figure 2.19 Failure envelopes obtained with the failure criterion proposed by Yoshida et al. (1990).

The modified failure criterion for the slope stability methods is presented below:

$$\tau = \frac{P\sigma_c}{F_s}\left(\frac{\sigma'_n}{\sigma_c} - Q\right)^{1/R} \tag{2.18}$$

Where:

τ	=	Shear strength.
$P, Q, and\ R$	=	Empirical curve-fitting constants.
σ'_n	=	Effective normal stress.
F_s	=	Factor of safety.
σ_c	=	Unconfined compressive strength.

The effect of softening with time in this failure criterion can be represented by a variation of the strength parameters *P*, *Q*, and *R*. No information was given on how to obtain the parameters *P*, *Q*, and *R*, although it can be assumed that it would be similar to the method for the parameters *A*, *B*, and *S* presented by Yoshida et al. (1990).

Yoshida et al. (1991b) classified the processes that can cause softening into internal and external processes. Internal processes were defined as the ones that can affect the structure of the soil similar to the mechanism described by Terzaghi (1936). External processes were defined as processes where the energy affecting the soil comes from an external agent. Weathering is considered an external process. Weathering causes the degradation of the soil fabric resulting in a decrease in shear strength. The main physical weathering processes are cyclic wetting and drying, and freezing and thawing. Oxidation, reduction, and hydrolysis were given as examples of chemical weathering. Yoshida et al. believed that weathering, because of its nature, only affects shallow depths.

Yoshida et al. (1991b) concluded that the effect of softening is to reduce the shear strength and the dilatant characteristics of the clay. They believed that the softening process starts only after the negative pore water pressure in the soil mass had dissipated.

A detailed paper summarizing research available up to the year 2000 on the shear strength and the behavior of natural slopes and cuts in clays was presented by Leroueil (2001). In a section describing the shear strength of soils using a critical state framework, Leroueil stated that the critical state condition corresponds to the drained peak shear strength of the clay in a normally consolidated state or the fully softened shear strength. After analyzing the information available, Leroueil concluded that the mechanisms that cause slope failure are poorly understood. These mechanisms are creep, fatigue, weathering, destructuring processes, influence of partial saturation, progressive failure, and the development of post-failure movements.

2.7 Research Performed in Italy

Failures of slopes in overconsolidated clays in Italy also led their researchers to perform studies on the shear strength of this material. These studies are presented in this section.

A first-time failure in an overconsolidated clay slope in northern Italy in 1978 was described by Cancelli (1981). This failure was triggered by an increase in the angle of the slope due to soil erosion caused by a river flowing next to the slope. The soil profile of the slope consisted of a fat clay with a liquid limit ranging from 40 to 60, a plasticity index ranging from 16 to 33, and a clay-sized fraction ranging from 23% to 47%. The vertical depth to the failure surface was 46 ft. Triaxial tests were performed on undisturbed samples to measure the peak shear strength and also on samples remolded at the liquid limit to measure the fully softened shear strength. No further details were given on the sample preparation technique used to prepare samples for fully softened shear strength measurements. Results from back-analysis showed that a friction angle about two degrees less than the lowest fully softened friction angle measured was required to explain the failure.

An investigation on the effect of swelling on the shear strength of Todi Clay was presented by Calabresi and Rampello (1987). Todi Clay is an overconsolidated fissured clay with a liquid limit ranging from 43 to 54, a plasticity index ranging from 20 to 28, and a clay-sized fraction ranging from 33% to 43%. The investigation consisted of consolidation and CU triaxial tests performed on samples prepared in three different ways: (1) intact blocks of soil which were allowed to undergo free swell submerged in distilled water surrounded by loose sand, (2) intact blocks of soil air-dried, at temperatures not specified, and then allowed to swell submerged in water at zero confining stress, and (3) remolded samples formed by mixing the soil with de-aired water and reconsolidated in a batch consolidometer to a pressure of 2,090 psf.

The results from the consolidation tests showed that allowing undisturbed samples to undergo free swell in water did not completely erase the memory for the preconsolidation pressure. The CU triaxial tests showed that the samples allowed to undergo free swell in water still behaved as an overconsolidated clay during shear. Swelling was found to decrease the effective stress cohesion intercept measured and sometimes even the effective stress friction angle. This decreased shear strength was still greater than the shear strength measured on remolded normally consolidated samples. Based on this finding, Calabresi and Rampello recommended the measurement of the shear strength on samples allowed to undergo free swell in water to assess the shear strength for cuts in overconsolidated clays.

The mechanical behavior of Todi clay was also studied by Rampello (1991). The Todi clay used in this research had a liquid limit of 48, a plastic limit of 20, and a clay-sized fraction of 39%. Rampello stated that the slides found in this material are usually between 13 ft to 33 ft deep and parallel to the slope face. Back-analysis of these slides usually showed a mobilized shear strength close to the fully softened shear strength. Consolidated undrained triaxial tests were performed on samples prepared in three different manners: (1) undisturbed samples allowed to undergo free swell in a large box filled with distilled water and loose sand for two to three months, (2) weathered samples, which were undisturbed samples that were desiccated at 68 °F for 11 days or subjected to 10 cycles of temperature changes between 68 °F and 23 °F prior to allowing them undergo free swell in water, and (3) undisturbed samples.

The results from consolidation tests showed that the value of preconsolidation pressure obtained in weathered samples and samples that were allowed to undergo free swell was about the same as the preconsolidation pressure obtained from undisturbed samples. Consolidated undrained triaxial tests showed that samples allowed to undergo free swell and weathered samples had a lower shear strength as compared to undisturbed samples. This decrease in shear strength was reflected in a significant reduction in the effective stress cohesion intercept and a small variation of the effective stress friction angle. Despite that, the effective stress cohesion intercept did not go to zero for any of the sample tested. Although the shear strength was lower on weathered and swollen samples, those still behaved as an overconsolidated clay during shear.

A summary of research available in the year 2001 about the role of pore pressures fluctuation in the failure of slopes in stiff clays and clay shales was presented by Picarelli et al. (2001). After a detailed review of the information available, Picarelli et al. concluded that these failures are preceded by factors like creep, fatigue, or weathering and that a decrease in the shear strength of the soil and an increase in pore pressure are just the triggering factors. They also concluded that classical rigid-plastic or elastic-plastic

models cannot explain first-time failures in slopes in stiff clays and clay shales and that these failures usually involve a progressive failure mechanism.

Picarelli et al. (2006) discussed the softening of natural slopes in plastic stiff-fissured clays and clay shales based on available publications up to the year 2005. They stated that weathering, slaking, and fatigue can cause accumulation of plastic strain, generally at shallow depths, decreasing the shear strength of the soil by destroying the inter-particle bonds. Picarelli et al. reported research by Cicolella and Picarelli (1990) (in Italian, therefore not reviewed for this dissertation) on the shear strength of undisturbed Bisaccia Clay that was allowed to swell prior to testing. This clay has a liquid limit ranging from 110 to 190 and a clay-sized fraction ranging from 60% to 70%. In these tests, undisturbed samples were allowed to swell in the direct shear box under a confining pressure of 209 psf before consolidation to the final desired pressure. The results showed that the clay behaved as normally consolidated and that the shear strength decreased. Tests performed at consolidation stresses lower than the preconsolidation stress also showed a decrease in shear strength when compared to the shear strength of undisturbed samples.

2.8 Others

2.8.1 Finite Element Modeling

The finite element method is a powerful computational tool that approximates the solution of the differential equations that govern different phenomena based on boundary conditions. This method can often be used to analyze several problems in a faster, more convenient, and more accurate way than using other methods. In this section, the investigations found in the literature that used this method to address the problem of slope stability in overconsolidated and compacted clays are summarized.

Duncan and Dunlop (1969) performed finite element analyses to investigate the effects of an excavation on the stress regime in normally consolidated and heavily overconsolidated clays. Heavily overconsolidated clays and shales are characterized by large horizontal stresses and thus have a greater tendency for lateral rebound than normally consolidated clays. The results presented by Duncan and Dunlop indicated that shear stresses large enough to cause local failure might develop at points in the slope. Shear stresses around excavated slopes in heavily overconsolidated clays were found to be much larger than for excavations in normally consolidated clays. Therefore, Duncan and Dunlop concluded that progressive failure is more likely to occur in heavily overconsolidated clays than in normally consolidated clays.

In a similar study, Dunlop and Duncan (1970) performed finite element analyses to investigate how the failure surface develops around excavated slopes. Results showed that the failure surface in normally consolidated clays begins beneath the midpoint of the slope. As the excavation continues, it extends upward toward the slope crest and downward towards the slope toe. The final shape of the failure surface approximated a circular arc. In overconsolidated clays, non-circular failure surfaces were obtained in this study.

An investigation using the finite element method to explain the failure of the upstream slope of Carsington Dam was performed by Potts et al. (1990). Details about the dam and the construction can be found in

the paper. A shear strength model that simulates the strain-softening behavior of the soils was used in the analyses. The results of the finite element model showed non-uniformity in the strain distribution along the failure plane causing local failures. Potts et al. found that the drained shear strength in specific sections of the failure plane had decreased significantly toward the residual shear strength. The resulting decrease in shear strength was equal to 80% of the difference between the peak and residual shear strengths. Just prior to failure, the failure plane was not fully developed and sections of the failure surface were mobilizing shear strengths lower than the peak shear strength, due to low strains. This failure was presented by Potts et al. as clear evidence of progressive failure.

In another paper, Potts et al. (1997) presented the results of a comprehensive study where the finite element method was used to explain failures of cut slopes in stiff clays. This study investigated the effects of slope inclination, height, coefficient of earth pressure at-rest (K_o), and boundary conditions on the development of the failure surface and the time to failure using a strain-softening and elastic-perfectly plastic models for the soil. Only the results of the strain-softening model will be discussed in this dissertation. For this investigation, Potts et al. assumed a pore pressure value equal to 210 psf at the ground surface.

The results presented by Potts et al. showed that the typical failure surface developed in slides in stiff clays begins as a horizontal surface at the toe of the slope and curves upward toward the ground surface as the time after the excavation increases. As the failure surface develops, the horizontal section accumulates enough displacement to reach the residual shear strength. The failure surface consisted of four sections: (1) a horizontal section, which forms first, and reaches the residual shear strength, (2) a short section that serves as a transition from residual to peak shear strength in the failure surface, (3) a curved section where the displacements are not large enough to initiate strain-softening behavior, and (4) an inclined section, when K_o is low, that is close to the ground surface and develops when the slope fails. These sections are shown in Figure 2.20. In all the cases, the section that is between peak and residual shear strength was found to be short in length.

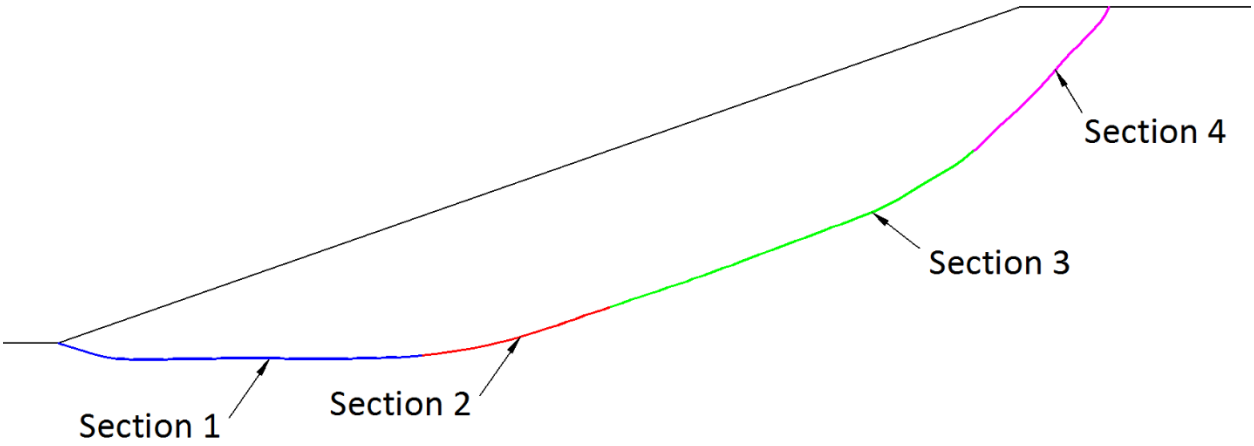

Figure 2.20 Sections in a failure surface as described by Potts et al. (1997).

Potts et al. also found that monitoring displacement and pore water pressure does not give useful information on the risk of slope failure. The pore pressures that were calculated in the finite element model exhibited only small changes in the years preceding the failure. The failure was found to be abrupt, sometimes without any appreciable warning from the displacements or pore pressures. The results also showed that the value of K_o influenced the shape of the failure surface, the time to failure, and the amount of progressive failure that occurs in the slope; but it did not influence the probability of collapse of the slope. As the value of K_o increased from 1.0 to 1.75, the failure surface became deeper. Further increase in K_o moved the scarp of the slip surface closer to the crest of the slope, as shown in Figure 2.21. Although the value of K_o was found to affect the time to failure for the softening model, no distinct trend was found in the results.

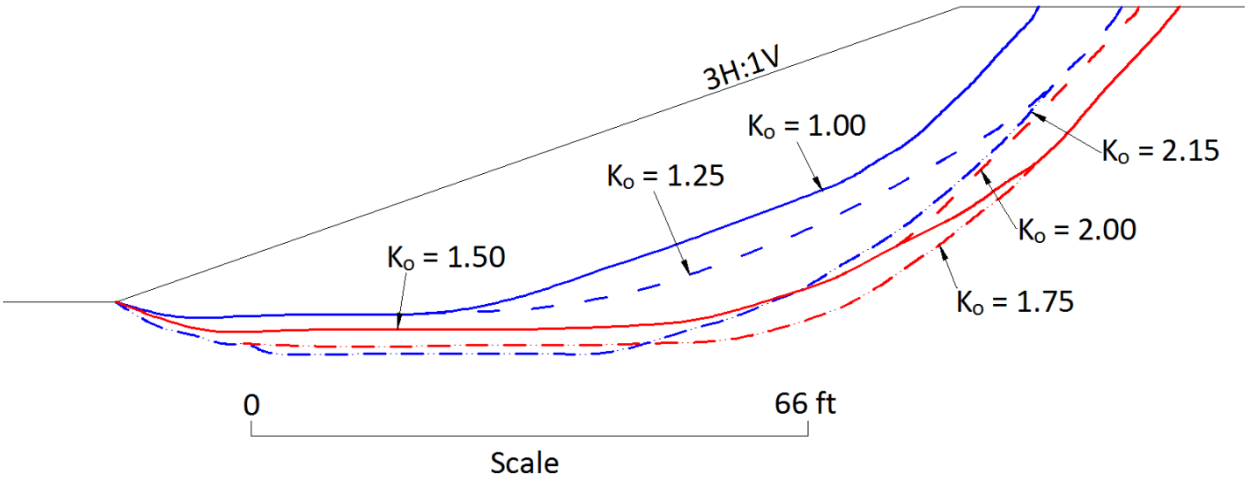

Figure 2.21 Failure surfaces for different values of K_o (After Potts et al. 1997) (Used under fair use).

Potts et al. made a comparison of the critical failure surface found by the finite element method with the critical failure surface found by the limit equilibrium analysis. This comparison showed that the deeper failure surface obtained using the finite element method, for high values of K_o, did not match the critical failure surface from the limit equilibrium analysis. A better agreement was found for low values of K_o.

The results from the finite element model also showed that progressive failure, represented by the residual factor, R, increased with increasing K_o up to 1.75, then decreased until K_o = 2.0, and then increased again as shown in Figure 2.22. In order to explain this phenomenon, a closer inspection of Figure 2.21 must be made. The length of the horizontal section of the failure surface, which reaches the residual strength, increased with increasing value of K_o up to 1.75. As the value of K_o increased beyond 1.75, the curved section of the failure plane moved closer to the slope, thereby decreasing the length of the horizontal section. The results also showed that the value of the negative pore pressure at the surface boundary also influenced the results. An increase in the value of suction at the surface increased the effect

of progressive failure but the stability improved due to a decrease in the pore pressures in the failure plane. In the field, this increase in suction can be caused by vegetation or surface drains.

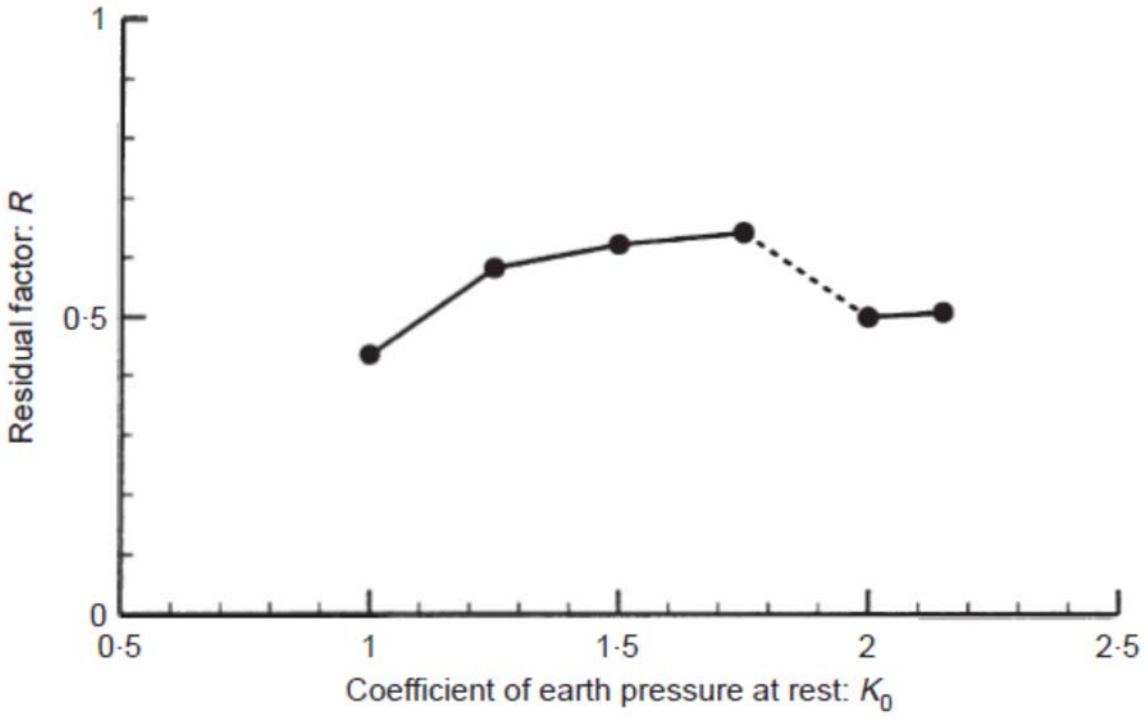

Figure 2.22 Change in the residual factor as a function of K_o (Potts et al. 1997) (Used under fair use).

Potts et al. concluded that progressive failure is the main mechanism causing the decrease in shear strength of stiff clays in the field. According to them, progressive failure is initiated by the strains caused when the soil swells as a response to the decrease in stress caused by the excavation. The finite element method was proposed as a viable way to investigate these failures due to the ability to reproduce observed field behavior assuming that the parameters of the soil are appropriate. In their investigation, no shallow slope failure was predicted, but they stated that this type of failure is only explained by the effects of weathering and seasonal pore pressure variation on the shear strength of the soil.

The results of an investigation on the development of progressive failure in a compacted clay embankment due to seasonal climate changes using the finite element method was presented by Kovacevic et al. (2001). They concluded that embankments of plastic clays can experience delayed failures due to progressive failure caused by seasonal weather variations. This variation causes the soil to shrink and swell causing cumulative plastic strains that eventually leads to the failure of the slope.

The Biological and Engineering Impacts of Climate Change on Slopes (BIONICS) project is being conducted in the United Kingdom (UK) to determine the effects of climate change on the embankments that form part of the transportation network of that country. This project involves the use of finite element

modeling, centrifuge modeling, and the construction of a test embankment. As part of this project, several papers have been published, some of which are included in this dissertation. The results of numerical modeling to evaluate the effect of climate on the stability of slopes was presented by Rouainia et al. (2009). A 23-ft-tall embankment with a 2.5H:1V slope made of London Clay was modeled. In order to predict the behavior of slopes in the UK, the finite element model was coupled with a weather model that can simulate current and future weather conditions in the UK. The results showed, using the weather data for Newbury, UK, that with current weather conditions the embankment will fail after the fifth year. Hypothetical future weather conditions, in comparison to the current weather conditions, include increased temperature and rainfall intensity, and decreased rainfall duration, while keeping the total amount of rainfall the same. Using these conditions, the embankment was found not to fail after 20 years, although, significant softening was predicted in the embankment, especially at the toe. According to Rouainia et al., this change in the rainfall will cause less infiltration in the embankments, causing an improvement in the stability.

2.8.2 Additional Lab Studies

Research has been conducted to investigate the effect of fissures on the drained shear strength of stiff-fissured clays, the effect of cycles of wetting and drying and cycles of freezing and thawing on the drained shear strength of overconsolidated clays, and the effect of the pore water chemistry on the fully softened shear strength measured. Some of this research has already been presented in this dissertation. This section summarizes the research which has not been presented previously related to laboratory testing of clays aimed to characterize the shear strength of fissured clays, the fully softened shear strength, or any softening mechanism.

Marsland and Butler (1967) and Marsland (1971) performed studies to investigate the effect of fissures on the measured drained shear strength of stiff-fissured clays. Drained triaxial tests were performed on 4-inch-diameter and 1.5-inch-diameter undisturbed samples of unweathered Blue London Clay with an average fissure spacing of about 1.6 inches. The results showed that at effective stresses lower than the *in situ* effective vertical stress, the soil behaved as a "granular material" and failure occurred along the fissures and not through the clay mass. As the confining pressure increased, portions of the failure plane started to go through the clay mass. At high pressures, the failure plane was not influenced by the presence of the fissures. A curved failure envelope going through the origin was obtained from these tests. The shear strength measured in drained triaxial tests on specimens with 4-inch diameters was found to be lower than the drained shear strength measured on 1.5-inch diameter samples for effective stresses below 2,000 psf. Above 2,000 psf, the difference in the shear strength measured was not significant.

Based on these results and the analysis of previous research, Marsland concluded that the drained shear strength measured in the laboratory on samples of stiff-fissured clays depends not only on the sampling techniques and disturbance, but also on the size of the sample and fissure spacing, orientation, surface roughness, and shape. For soils where the fissure spacing is not very large, a reasonable size specimen will give you the appropriate shear strength in the laboratory. If the fissure spacing is large, laboratory tests may provide unrepresentative results.

Moon (1984) performed direct shear and staged consolidated undrained triaxial tests on a reddish-brown silty clay with a liquid limit ranging from 46 to 124, a plastic limit ranging from 28 to 44, and a clay-sized fraction ranging from 30% to 65%. The fully softened shear strength parameters were defined by Moon as the peak drained friction angle obtained in laboratory tests on undisturbed samples coupled with the residual strength cohesion obtained in reversal direct shear strength tests. Tests on undisturbed samples were deemed superior to tests conducted using remolded samples because Moon felt that remolding destroys any diagenetic bonds or preferred particle orientation which might occur in natural soils.

Direct shear tests on samples remolded at a water content close to the liquid limit were also performed. The peak effective friction angle measured using a direct shear device on undisturbed samples was 3.3° higher than the peak effective friction angle obtained from remolded samples tested in the same device. For undisturbed samples, the effective stress friction angle obtained with the triaxial device was 0.9° higher for samples with a plasticity index of 50 or greater and 0.2° higher for samples with a plasticity index less than 40 when compared to the effective friction angle obtained from direct shear tests on undisturbed samples. The results also showed that the fully softened friction angle was dependent on the plasticity of the soil.

Graham and Au (1985) examined the effect of freezing and thawing on the consolidation properties and shear strength of clays. Undisturbed samples of a fat clay with a liquid limit ranging from 51 to 58, a plasticity index ranging from 49 to 52, and a clay-sized fraction ranging from 63% to 67% were used for this investigation. The effective shear strength parameters were measured by performing CD and CU triaxial tests on undisturbed samples, specimens that were subjected to five cycles of freezing and thawing, and specimens that were allowed to swell in a triaxial cell with major and minor principal stresses of 84 psf and 42 psf respectively until a constant volume was achieved. The freezing cycle consisted of subjecting the soil test specimen to temperatures of 23 °F or -13 °F. The cycles lasted between one day and four days, the sample was enclosed in a membrane, and access to water was not permitted.

The results of consolidation tests showed that the preconsolidation pressure is reduced by cycles of freezing and thawing and by allowing the sample to swell. This decrease in the preconsolidation pressure was found to be greater for samples subjected to cycles of freezing and thawing. The shear strength tests showed that the shear strength measured for samples allowed to swell and samples subjected to cycles of freezing and thawing is less than the shear strength measured on overconsolidated undisturbed samples. This effect was more significant for samples subjected to cycles of freezing and thawing. No comparison was made by Graham and Au of the shear strength obtained after cycles of freezing and thawing and the normally consolidated shear strength.

Another investigation on the effect of cycles of freezing and thawing on the mechanical properties of clays was performed by Leroueil et al. (1991). For this investigation, nine Champlain Sea clays, covering a wide range of plasticity indices, were obtained from different sites. The testing program consisted of CU and UU triaxial tests conducted on undisturbed samples and undisturbed samples subjected to one cycle of freezing and thawing. The freezing cycle consisted of subjecting the sample to a temperature of 23 °F for about 20 hours. The thawing cycle consisted of placing a frozen specimen in a triaxial cell, enclosing it in a membrane, filling the cell with water, and allowing the specimen to thaw with the drainage lines closed.

The results showed that one cycle of freezing and thawing had a significant impact on the shear strength of these clays. The undrained shear strength of samples subjected to cycles of freezing and thawing was found to be the same as the undrained shear strength of remolded normally consolidated samples. Again, no comparison was made of the shear strength measured after cycles of freezing and thawing with the fully softened shear strength.

Failures in cuts and compacted embankments of high plasticity clays have also been a problem in England (Crabb and Atkinson 1991). These failures usually occur at depths ranging from three feet to seven feet and are normally parallel to the slope face. To characterize the soils involved in these failures, stress path drained triaxial tests were performed on undisturbed samples, and conventional drained triaxial tests were performed on remolded samples. The stress path tests consisted of increasing the pore water pressure while keeping the total stress constant. Crabb and Atkinson stated that using this type of test allowed an easier characterization of the curvature of the peak shear strength failure envelope at low stresses. The remolded samples were fabricated by oven-drying, pulverizing, and mixing the soil with enough water to form a slurry, which was then reconsolidated. They made no distinction in the use of fully softened versus critical state shear strength to refer to the drained peak shear strength of normally consolidated specimens. Crabb and Atkinson stated that the critical state shear strength is usually reached at strains between 10% and 30% *in situ* while achieving the residual shear strength requires displacement in the order of several feet. However, they did not state how they were associating strains with displacements.

Back-analyses of slope failures in the material tested showed that using a curved undisturbed peak failure envelope could not fully explain the failures. Crabb and Atkinson concluded that the stability of the slopes analyzed was controlled by the fully softened shear strength.

Botts (1998) conducted a laboratory testing program to measure the effect of wetting and drying on the shear strength of Pierre Shale. He found that a 40% to 80% reduction in the peak shear strength can occur in clay shales in a period of 2 years to 70 years. According to him, fissures are plane of weakness that are prone to cause failure, can increase the permeability of the soil, and can increase the surface area exposed to weathering agents.

The laboratory testing program consisted on CD triaxial tests on undisturbed samples subjected to cycles of wetting and drying. Samples were first air-dried for a period ranging from zero to 28 days. After that, the samples were wetted for a period ranging from 1 day to 23 days under a confining pressure of 1,440 psf and then tested under confining pressures of 1440 psf, 4320 psf, and 7200 psf. The results showed that increasing the duration of the drying cycle, even by small amounts, caused a significant increase in the amount of swelling during the wetting stage. Also, increasing the drying time caused a greater decrease in the shear strength after swelling. The greatest loss in shear strength was found for the first cycle of wetting and drying.

The chemistry of the pore water in the soil has been found to affect the residual strength measured (Di Maio 1996; Di Maio and Onorati 2000; Di Maio et al. 2004). Scant research has been performed about the effect of the pore water chemistry on the fully softened shear strength. Di Maio and Onorati (2000)

performed CU triaxial and direct shear tests on remolded normally consolidated samples of Bisaccia clay mixed using distilled water or a 1M NaCl solution. The Bisaccia clay had a liquid limit of 110 when mixed with distilled water and 51 when mixed with the 1M NaCl solution. The clay-sized fraction of this soil was 65%. The results from CU triaxial and direct shear tests showed that the fully softened shear strength obtained from the samples mixed with the 1M NaCl solution was considerably higher than the fully softened shear strength obtained on samples mixed with distilled water. Based on this finding, Di Maio and Onorati concluded that the fully softened shear strength should be measured using water similar to that expected in the field.

The influence of the mineralogical composition of the clay-sized fraction on the fully softened friction angle was first investigated by Tiwari and Ajmera (2011). Thirty-six different mixtures of sodium montmorillonite, kaolinite, and quartz were tested using normal stresses of 1044 psf, 2089 psf, 3133 psf, and 5221 psf in a direct shear device. They did not feel that it was appropriate to use the ring shear device to measure the fully softened shear strength because of the phenomenon of progressive failure associated with this device. Four different mixtures were created: montmorillonite-kaolinite, montmorillonite-quartz, kaolinite-quartz, and montmorillonite-kaolinite-quartz. The minerals were mixed to the required proportions based on dry weight. The samples were prepared at a moisture content equal to the liquid limit, using distilled water, and hydrated for 72 hrs.

The results of the direct shear tests showed a linear fully softened failure envelope for most of the tests performed. Slightly curved failure envelopes were found only in a few of the soil mixtures. Therefore, Tiwari and Ajmera decided to use an average fully softened friction angle, obtained by doing a linear regression analysis of the shear strength measured for each soil, to develop correlations. Results showed that as the proportion of montmorillonite and kaolinite increased in the soil mixtures, the measured fully softened shear strength decreased.

Different correlations relating the average fully softened friction angle with parameters like the *clay content*, shown in Figure 2.23; the liquid limit, shown in Figure 2.24; and the plasticity index, shown in Figure 2.25, were presented. The term *clay content*, as used by Tiwari and Ajmera, is analogous to the term clay-sized fraction. From these correlations, it can be seen that the average fully softened friction angle decreases with increasing clay content, liquid limit, and plasticity index. The correlation using clay content shows a significant difference in the fully softened friction angle for samples with the same liquid limit and different clay minerals. The correlations that use the liquid limit and plasticity index show more gradual trends.

A three-axis plot relating the percentage of montmorillonite, kaolinite, and quartz to the fully softened friction angle was also presented and is shown in Figure 2.26. From this correlation it can be seen that percentages of montmorillonite below 30% and percentages of kaolinite greater than 70% have a big influence in the measured fully softened shear strength. The blue dots in this figure represent data points.

The presented correlations were verified using the results from 82 natural soils tested using a direct shear device. These soils were all ball-milled prior to the determination of the liquid limit. In a private communication, Tiwari (2013) acknowledged that the samples were ball-milled for shear strength

measurements, and Tiwari and Ajmera (2011) hypothesized that the peak shear strength measured on ball-milled specimens can be lower than the peak shear strength measured on soils that had not been ball-milled. Tiwari and Ajmera (2011) stated that the results presented show that using the correlation presented in Figure 2.25, the fully softened friction angle was estimated with an error of ±25% while using the correlation presented in Figure 2.26, the error was ±15% for the majority of the natural soils tested (Tiwari and Ajmera 2011).

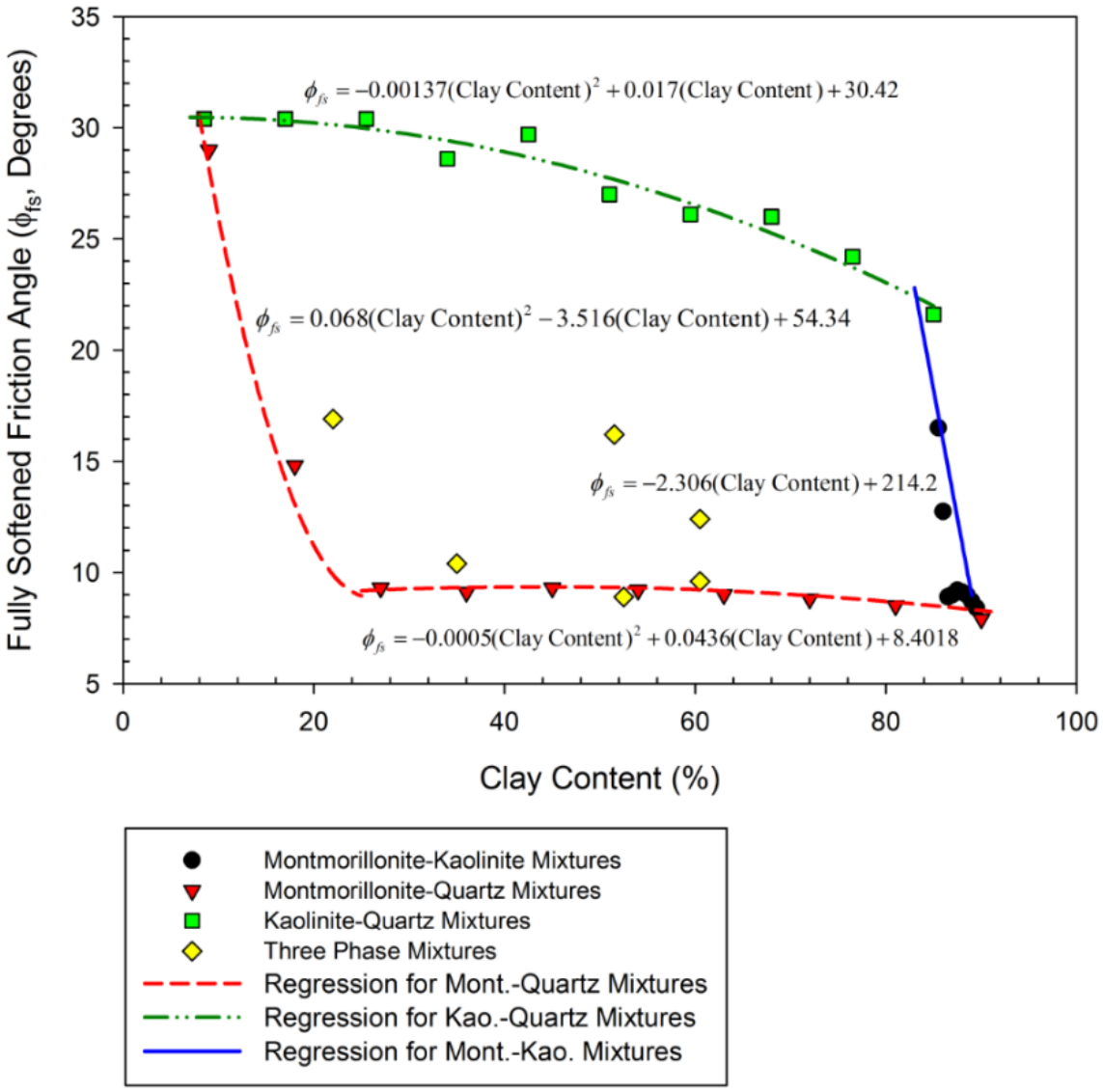

Figure 2.23 Variation of the fully softened friction angle with the clay content (Tiwari and Ajmera 2011) (Used under fair use).

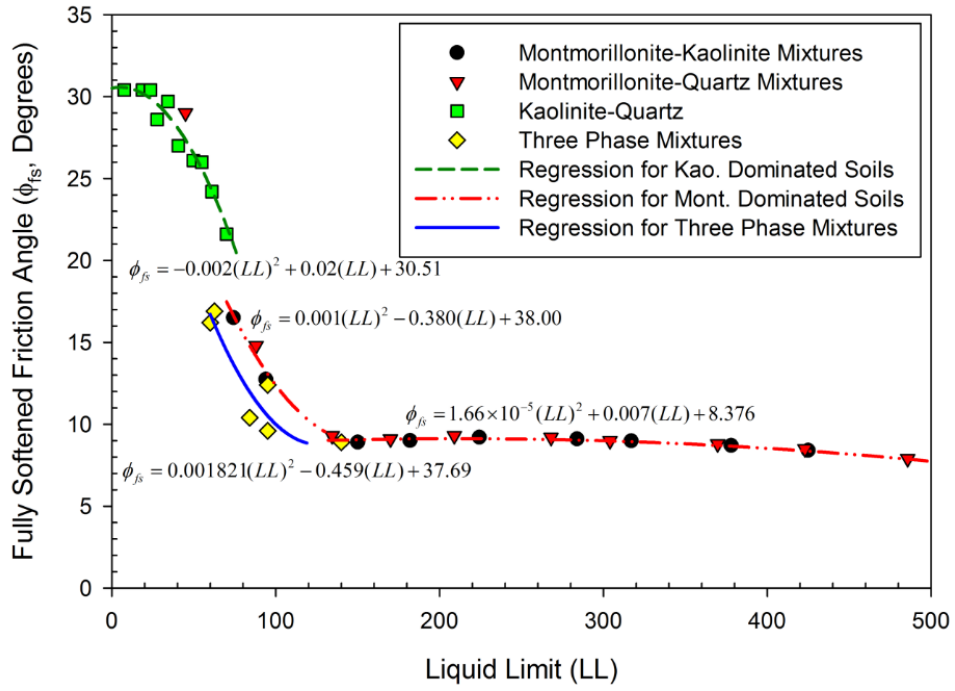

Figure 2.24 Variation of the fully softened friction angle with the liquid limit (Tiwari and Ajmera 2011) (Used under fair use).

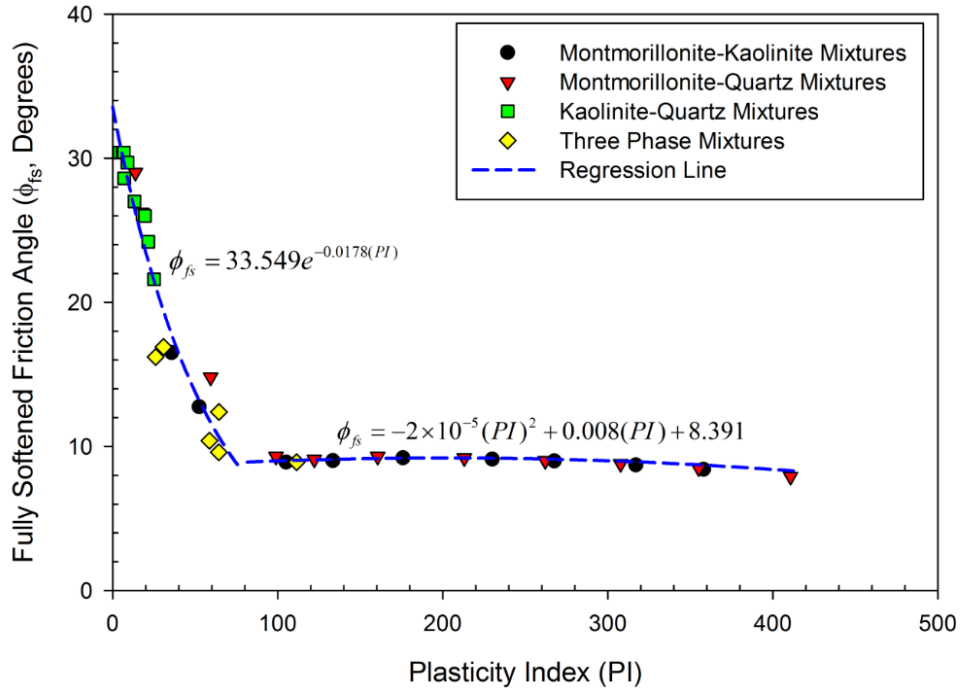

Figure 2.25 Variation of the fully softened friction angle with the plasticity index (Tiwari and Ajmera 2011) (Used under fair use).

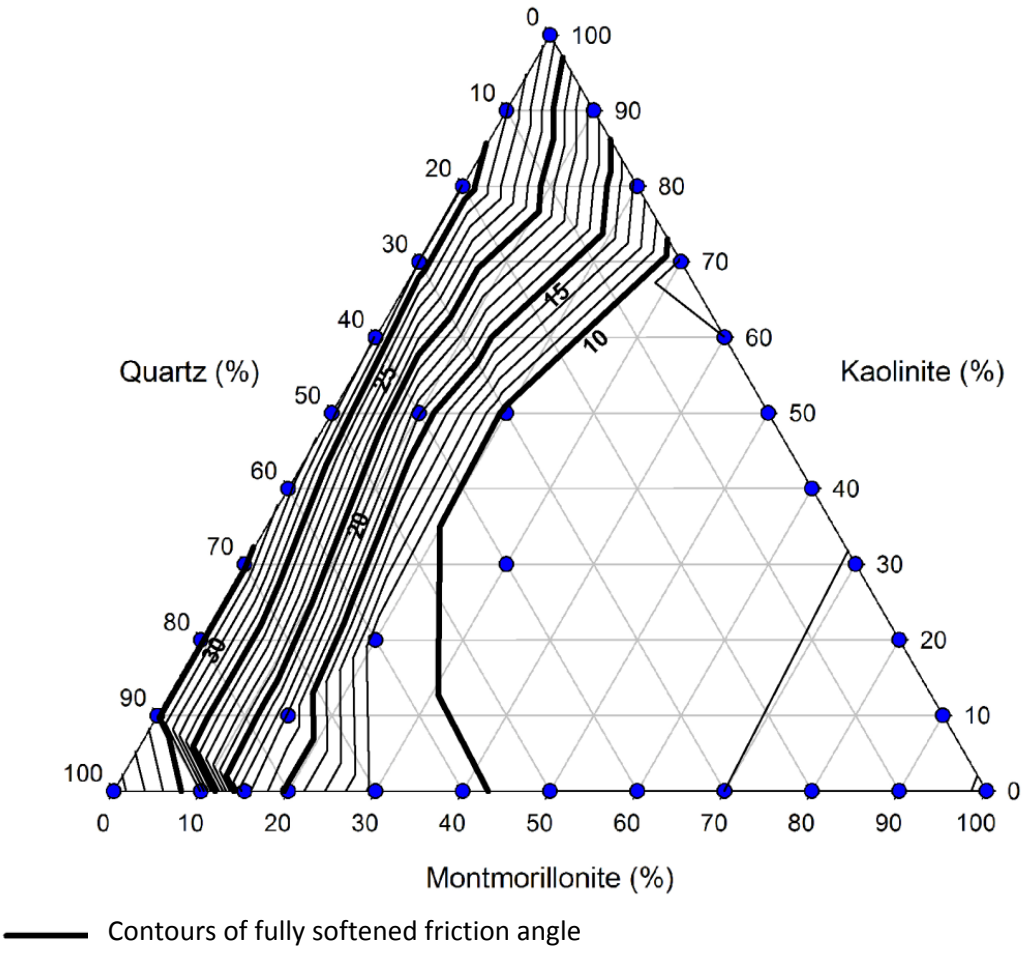

Figure 2.26 Correlation between the fully softened friction angle and the percentage of montmorillonite, kaolinite and quartz (After Tiwari and Ajmera 2011) (Used under fair use).

2.8.3 Centrifuge Modeling

Centrifuge modeling is a very powerful tool that can be used to create scaled models of physical structures and phenomena, reducing the amount of money, personnel, and time that is usually required for full-scale testing and monitoring real structures. Two independent research programs to investigate the effect of cycles of wetting and drying in clay slopes using centrifuge modeling were found in the literature. One was performed at Imperial College in London by M. D. Bolton and his colleagues, and the other one was performed as part of the BIONICS project. These two investigations are described in this section. In this dissertation, *real scale* refers to the actual measurements of the model and model scale refers to the dimensions modeled in the centrifuge test by applying a given acceleration.

A payload chamber that can be used in centrifuge testing to simulate seasonal moisture changes was developed by Take and Bolton (2002). The simulation of seasonal moisture changes was achieved by controlling the relative humidity of the air in the chamber that contains the model. The models used by

Bolton in all his publications were carved from a block of Speswhite Kaolin clay that was pre-consolidated to a pressure of 10,443 psf under K_o conditions from a slurry formed at twice the liquid limit of the soil. In their research, Take and Bolton wanted to study the effect of seasonal moisture changes in slopes of overconsolidated clays. The slopes were formed at an angle of 36° (1.4H:1V). The real height of the slope was 5.5 inches which corresponds to an equivalent height of 28 ft at an acceleration of 60 g. The pore pressures and displacements of the slope were measured in all the experiments.

In the paper by Take and Bolton (2002), the climate around the slope consisted of five months of a wet season, simulated by a relative humidity of 100%, and seven months of a dry season, simulated by a relative humidity of 40%. Pore pressure measurements showed an increase in pore pressure during the wet season followed by a decrease during the dry season. Most of the movement of the slope in response to the weather variation was measured to be perpendicular to the slope face. Movement in the downslope direction was also measured. According to the Take and Bolton, this movement can cause tensile stresses in the soil and could potentially lead to progressive failure.

In another paper, Take and Bolton (2004) presented a detailed study, using centrifuge modeling, on the behavior of slopes subjected to seasonal weather variation. In this case, the slope was subjected to different lengths of dry and wet cycles. From displacement measurements, Take and Bolton found that swelling was only confined to the near surface, and the depth of swelling was relatively uniform in the slope. The slope was found to swell most at the toe, where 0.47 inches of scaled movement were measured (purported 0.0079 inches real). The duration of the wet season did not influence the pore pressures generated very much but it did significantly increase the amount of swelling. The amount of swelling measured during the wet season was not recovered during the dry season, so plastic deformations occurred in the soil mass. The cumulative plastic deformations with increasing cycles in the slope eventually led to the development of progressive failure. Similar results were also presented by Take and Bolton (2011).

More results on centrifuge tests performed in overconsolidated clays were presented by Take and Bolton (2011). The model was subjected to five months of wet season and seven months of dry season. The dry and wet seasons were modeled as described previously. Measurements of pore pressures showed that the variation of pore pressures due to climate changes is greater at shallow depths and decreased with increasing depth.

Take and Bolton (2011) considered that critical state friction angle as being synonymous with the fully softened friction angle, defined as the drained peak shear strength of normally consolidated remolded clay samples. The shear strength mobilized at a given time was estimated by performing limit equilibrium analyses using the measured pore pressures to calculate the shear strength required to obtain a factor of safety of one. The results of the limit equilibrium analyses showed that during the dry season, the soil was mobilizing a friction angle less than the critical state friction angle. During the wet season, shear strengths between the peak and the critical state shear strength were mobilized to maintain equilibrium. Measurements of displacement showed that mobilizing shear strengths above the critical state friction angle produced plastic deformations in the soil that could lead to progressive failure. Shear displacement were found to be greater at the toe of the slope where residual shear strength might have been mobilized.

Take and Bolton recommended the use of fully softened shear strength to design slopes of overconsolidated high plasticity clays. Take and Bolton stated that it might be possible that if a slope is designed using fully softened shear strength, shear displacement large enough to decrease the shear strength of the soil towards the residual strength can develop. Although this statement was made, they also stated that they were not aware of any failure of a slope designed using limit equilibrium analysis, fully softened shear strength, and the highest expected pore pressures.

As part of the centrifuge modeling program included in the BIONICS project, Hudacsek and Bransby (2008) performed centrifuge tests on embankments subjected to seasonal moisture changes. In the apparatus used, the wet season was modeled using a set of fine misting nozzles capable of inserting "rain" into the system. The dry season was modeled by introducing dry air into the system. The pore pressures and displacements in the model were monitored.

The model used by Hudacsek and Bransby (2008) was 3.94-inch-tall in real scale, which represents a 20-ft-tall embankment at an acceleration of 60 g. The model was made of compacted till formed with a 2H:1V slope. The glacial till used had a liquid limit of 40 and a plastic limit of 20. The model was compacted using a variable static pressure to control the density of the embankment. The maximum pressure used was around 2,500 psf. After the block of soil was compacted, it was removed from the mold and the slope model was carved. For this experiment, the duration modeled was five years with wet and dry season lasting six months each in model scale (72 minutes real scale). The wet season consisted of six rainfall events with a duration of 60 hours and an intensity of 0.06 in/hr in model scale. After the fifth year, the maximum displacement measured was 0.20 inches in model scale (0.0031 inches in real scale). The results showed that the displacements are concentrated at a depth of 6.6 ft to 9.8 ft, model scale, below the surface.

More results of centrifuge testing, using the technique presented above, were published by Hudacsek et al. (2009). In this case, the same soil and geometry used by Hudacsek and Bransby (2008) was used but the static pressure used to compact the soil was varied. The center of the embankment was compacted using a pressure of 3,050 psf to simulate a high compaction effort, and the end sections were compacted using a pressure of 1,796 psf to simulate light compaction. In this case, the model was subjected to 20 years of seasonal variation with the wet season lasting five month and the dry season seven months in model scale. The wet season consisted of 10 events with a duration of 30 hours and a rainfall intensity of 0.06 in/hr in model scale.

The observed movement in the slope was mostly downslope and did not involve any shear localization. Surprisingly, the amount of movement decreased with increased number of cycles, which means that the performance of the embankment was improving with the number of cycles of wetting and drying. No failure or excessive movement was observed in the 20-year simulation. Hudacsek et al. concluded that a well-compacted embankment is unlikely to fail due to seasonal climate changes.

2.8.4 Field Experiments

In this section, field experiments that have been performed to understand the behavior of clay slopes are presented.

In order to better understand the behavior of stiff clays, Cooper et al. (1998) presented the results of a field experiment that was conducted on a 2H:1V 30-ft-tall cut in a heavily overconsolidated high plasticity clay with various degrees of weathering. The liquid limit of the soil in this cut ranged from 70 to 75 at the top to 60 to 65 at a depth of 52 ft. The plastic limit was more or less constant at a value of 22 and the clay-sized fraction ranged from 38% to 48%. The peak shear strength parameters were characterized by performing CU and CD triaxial tests using 3-inch and 4-inch diameter undisturbed samples and direct shear tests using 2.4-inch square samples. The results showed a reduction in the peak shear strength parameters with increasing weathering. The fully softened shear strength envelope was determined by running triaxial tests on 1.5-inch-diameter samples reconstituted by remolding the soil and mixing it at a water content equal to 1.5 times the plastic limit. The residual shear strength was determined by means of reversal direct shear tests and a ring shear device. The results of the ring shear device showed residual friction angles one degree less than the one obtained with reversal direct shear tests.

The cut was instrumented using surface wire extensometers, vibrating wire and pneumatic piezometers, and inclinometers to measure the pore pressures and movements in the cut. The cut was failed by increasing the pore pressure in the slope. As the pore pressure was increased, the failure surface was found to develop beginning at the toe and progressing into the slope. Pore pressure measurements showed that in the vicinity of the failure plane, the pore pressure was decreasing due to dilation during shear, even though the rate of movement of the slope continued to increase. Cooper et al. used this observation to explain that a decrease in shear strength had to be occurring at the failure plane to explain the increase in rate of movement although the effective stress was increasing in the failure plane. Slope stability analyses performed using the method developed by Morgenstern and Price (1965), showed that the average mobilized shear strength was equal to the fully softened shear strength.

2.8.5 Assorted Additional Research

In this section, papers associated with the stability of first-time failures related to fully softened shear strength are presented. The information presented in these papers does not fall within the other sections presented in this chapter but the content is important to the subject of this dissertation.

Bjerrum (1967) presented a new theory to explain the behavior of overconsolidated clays and shales in slope failures in the third Terzaghi lecture entitled “Progressive failure in slopes of overconsolidated plastic clays and shales.” To begin his lecture, Dr. Bjerrum explained the process of progressive failure, how it is initiated, and how it progresses in the clay mass. According to the Bjerrum, three conditions are necessary for progressive failure to occur: (1) internal lateral stresses should be high enough to stress a point in the clay mass past the peak shear strength, (2) sufficient amount of recoverable strain energy should be available to cause failure, and (3) the soil in the slope should have a substantial and rapid decrease from peak to residual shear strength (brittle behavior).

The recoverable strain energy was defined by Bjerrum as the energy available to cause a rebound in the soil when unloaded. The amount of strain recovered is a function of the amount of pressure removed from the soil and properties of the clay. According to Bjerrum, the amount of recoverable energy increases

with increasing plasticity of the clay. He believed that the recoverable strain was caused by the rebound of the flexible clay particles that recover their original shape when unloaded.

According to Bjerrum, the amount of recoverable strain at the moment of unloading is also a function of the strength of the diagenetic bonds. The diagenetic bonds are inter-particle bonds generated with time by physical and chemical agents in the clay. The effect of the diagenetic bonds in the unloading response of the overconsolidated clay is to reduce the horizontal stresses caused by the expansion of the clay by keeping part of the recoverable strain from being released. The weaker the bonds, the less stored strain energy will remain in the clay after unloading. Weathering will destroy the diagenetic bonds causing the clay to swell, increasing the water content, and decreasing the shear strength. Bjerrum stated that weathering effects would be confined to shallow depths.

A new classification for overconsolidated plastic clays was presented by Bjerrum:

a) *Overconsolidated plastic clays with weak or no diagenetic bonds.* This type of clay dissipates most of the recoverable strain energy during unloading. These clays will have larger horizontal stresses than the same clay in a normally consolidated state. Weathering of these clays does not have a big impact in the shear strength.
b) *Clay shales*. These are overconsolidated plastic clays with strong diagenetic bonds. This type of clay will keep stored some of the recoverable strain energy after unloading. The horizontal stresses will be lower and the clay will be stronger as compared to an overconsolidated plastic clay with weak bonds. Weathering will have a medium impact on the shear strength on these clays.
c) *Shale*. These are overconsolidated plastic clays with very strong diagenetic bonds. This type of clay will barely swell when unloaded. Most of the recoverable strain energy will stay stored in the diagenetic bonds. These clays will have low horizontal stresses and high shear strength. Weathering will have the biggest impact on the shear strength of these clays, transforming them eventually into overconsolidated plastic clays.

The more overconsolidated the clay, the more susceptible it is to developing progressive failure because of the increased amount of recoverable strain energy that will stay in the soil after unloading. According to Bjerrum, overconsolidated clays with low plasticity have a low probability of developing progressive failure because of the low content of active clay minerals and the small amount of recoverable strain energy this type of clay can store. Among the plastic clays, the probability of developing progressive failure was rated as follows: Very high for weathered shales and clay shales, high for unweathered and weathered overconsolidated plastic clays with weak bonds, and low for unweathered shales and clay shales.

Consolidation and slaking tests were performed by Brooker (1967) in order to investigate the validity of the energy theory presented by Bjerrum (1967). The results presented by Brooker tend to confirm the hypothesis presented by Bjerrum that the behavior of overconsolidated clay soils can be explained by the amount of energy that the soil can store.

Clemente (1992) stated that in the Washington D.C. area the fully softened shear strength is often measured from remolded samples formed at the natural water content in the direct shear device. Clemente also presented a correlation for the fully softened friction angle. His correlation is not reliable since he incorrectly mixed fully softened friction angles with residual friction angles.

Kaya (2009) utilized a back-propagation artificial neural network (ANN) model to predict the secant fully softened, and residual friction angles of soils. An ANN is a computational model that looks for linear and non-linear relationship between input and output variables. The model was developed using three quarters of the data presented by Stark et al. (2005), while the remaining quarter was used to validate the model. A sensitivity analysis was performed to evaluate the influence of the liquid limit, plastic limit, clay-sized fraction, activity[7], and effective normal stress on the secant fully softened friction angle measured. The results showed that the plastic limit and activity have almost no influence on the fully softened secant friction angle.

The validation of the ANN model, using the data not used for the calibration, showed that the model has potential to be a valuable tool, with a coefficient of determination (R^2) of 0.88 for predicting the fully softened friction angle of soils. The ANN model was also compared with the fully softened secant friction angle obtained using the Stark et al. (2005) curves and the Wright (2005) equation. It was found that the ANN model and the curves proposed by Stark et al. (2005) predicted the measured fully softened friction angle with good accuracy (R^2 = 0.80). The equation proposed by Wright (2005) was not as accurate at predicting the measured data (R^2 = 0.45) and was not recommended by Kaya (2009) to be used to estimate the fully softened secant friction angle.

A workshop focusing on fully softened shear strength was held on August 16 and 17, 2011, at the Virginia Tech campus. This workshop brought together more than 50 engineering practitioners, academics, and researchers who shared their experiences and opinions related to the use and measurement of fully softened shear strength. A summary of this workshop was presented by Duncan et al. (2011) and VandenBerge et al. (2013). From this workshop, it was concluded that the fully softened shear strength should be used for slope stability analyses of cuts in highly plastic stiff-fissured clays, and in compacted embankments constructed of highly plasticity clays subjected to extreme weathering conditions. Direct shear tests were recommended as the best method to measure the fully softened shear strength using a range of normal stresses applicable to the critical failure surface of the slope analyzed. The use of curved failure envelopes was found to be more appropriate than linear envelopes to represent the fully softened shear strength.

McCook (2012) presented a summary on the use of fully softened shear strength for levee design based on a literature review and his experience. He stated that the softening process caused by cycles of wetting and drying in compacted embankments of high plasticity clays is more severe in climates like the ones in Texas, Mississippi, and Louisiana. The slides in compacted fat clays were found to be characterized by a blocky structure in the clay mass, usually triggered by intense precipitation preceded by a long period of hot and dry weather, and occurring at shallow depths. In order to represent the fully softened failure

[7] The activity is defined as the ratio of the plasticity index to the clay-sized fraction.

envelope, McCook recommended the use of the built-in Excel® power function regression instead of the linear regression normally used. He reported a fully softened shear strength failure envelope obtained using a ring shear device that agreed well with the equation for the fully softened shear strength failure envelope proposed by Wright (2005). Also, he stated that the ring shear and direct shear devices will not always measure the same fully softened shear strength, but provided no details.

Slope stability analyses performed by McCook for clay embankments showed that in order to obtain a factor of safety of 1.5 using fully softened shear strength in the whole embankment, the slope required would be 6H:1V to 7H:1V. A factor of safety of 1.1 was recommended for shallow failure surfaces analyzed with fully softened shear strengths. McCook also investigated the effect of the shape of the assumed failure envelope, depth of softening, and the geometry of the slope on the calculated factor of safety for slope stability. The results showed that:

1) The use of a fully softened linear failure envelope instead of a curved envelope increased the calculated factor of safety.
2) Increasing the depth of softening decreased the factor of safety until the depth of softening matched the depth of the critical failure surface obtained using fully softened shear strength in the whole embankment. Increasing the depth of softening beyond this depth did not affect the factor of safety calculated for slope stability.

Chapter 3

Misconceptions about Fully Softened Shear Strength

Different ideas and hypotheses have been postulated involving the concept of fully softened shear strength. In this chapter, these postulations are discussed in order to clarify what can be regarded as fully softened shear strength and to explain other models that are related to or can be used in conjunction with the fully softened shear strength theory.

As a starting point, it is useful to define the drained peak shear strength measured using overconsolidated samples, the drained peak shear strength obtained from normally consolidated samples, and the residual shear strength. These three shear strengths are represented in stress-displacement diagrams and failure envelopes in Figure 3.1. The drained peak shear strength obtained using overconsolidated samples is the largest, followed by the normally consolidated drained peak shear strength, and then the residual shear strength. The main reasons for the differences in drained shear strengths between overconsolidated and normally consolidated samples are that the former has a lower void ratio than the latter at a given effective stress and that there are differences in structure between the two states. From this figure, it can also be seen that overconsolidated samples tend to be more brittle than normally consolidated samples. The residual shear strength is the drained shear strength obtained at large displacements, when the displacement on the failure plane is large enough to cause a face-to-face alignment of the clay particles, and when further increase in shear displacement does not cause a change in volume or shear strength. The residual shear strength is an intrinsic property of the soil that mostly depends on the mineralogy of the clay-sized fraction and is independent of the stress history of the soil (Skempton 1964), as can be seen in Figure 3.1. The residual shear strength is applicable to cases where significant displacement has already occurred.

In the literature, there is often a poor distinction between the concepts of fully softened shear strength, critical state shear strength, and ultimate shear strength. As stated before, the fully softened shear strength was defined by Skempton (1970) as the drained peak shear strength of a normally consolidated clay, as represented in Figure 3.1. Although in his 1970 paper, Skempton did not specify whether the fully softened shear strength is equal to the drained peak shear strength obtained from undisturbed or remolded normally consolidated specimens, in a later paper Skempton (1977) stated: "…the most appropriate laboratory parameters are those for the 'fully softened' or 'critical state' condition, which can be determined by measuring the strengths of remoulded, normally consolidated clay."

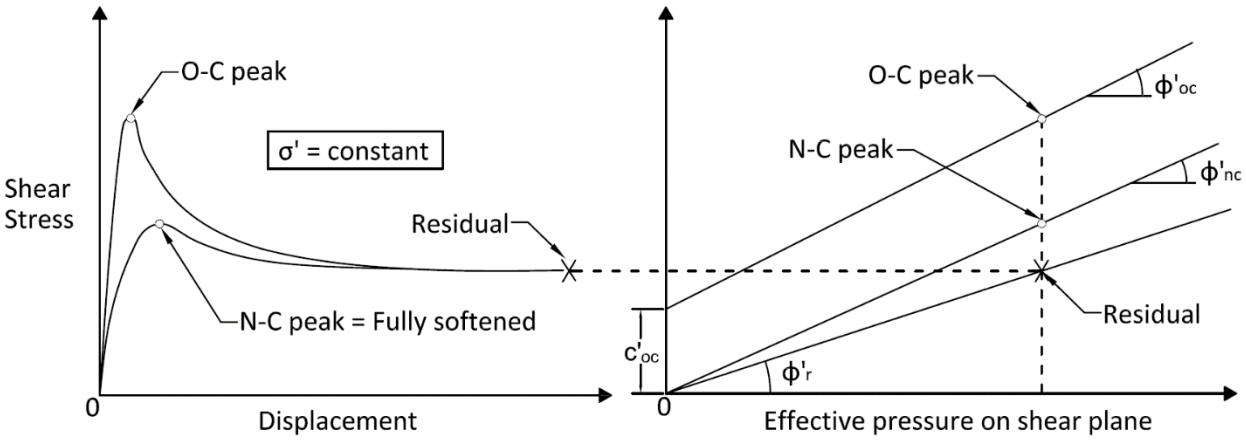

Figure 3.1 Simplified relation between normally and overconsolidated clays (After Skempton 1964) (Used under fair use).

Historically, the fully softened shear strength has been measured using remolded normally consolidated samples (Gibson 1953; Bishop et al. 1965; Petley 1966; Cancelli 1981; Mesri and Cepeda-Diaz 1986; Kayyal and Wright 1991; Stark and Eid 1997; Stark et al. 2005; Wright et al. 2007). Scant information is available showing a comparison of the drained shear strength measured using normally consolidated undisturbed and remolded samples. Kenney (1959) stated, based on unpublished data, that the effective stress friction angle is the same for normally consolidated remolded and undisturbed samples. Ball (1977) presented the results of CU triaxial tests performed using undisturbed and remolded normally consolidated clay samples from Ecuador. The results presented by Ball (1977) showed no significant difference in the effective stress shear strength parameters obtained from remolded and undisturbed normally consolidated samples. More data is required in order to reach to a conclusion of whether the drained shear strength measured from normally consolidated remolded and undisturbed samples is the same. *In situ*, the soil is subjected to a constant stress for a long period of time. During this period, diagenetic bonds will be formed in the clay and secondary compression will reduce the void ratio. These two phenomena are expected to influence the shear strength of the undisturbed clay. More research needs to be performed to see if the effect of these phenomena are measurable in the laboratory or if these effects are destroyed by reconsolidating undisturbed samples to the virgin compression line in the laboratory.

In clays, the mechanisms that are believed to be responsible for decreasing the intact shear strength to the fully softened shear strength are swelling, progressive failure, creep, and weathering. These mechanisms could potentially break the bonds in the clay causing remolding. For this reason, it seems appropriate to measure the fully softened shear strength using remolded samples.

The critical state soil mechanics theory was first postulated in a paper by Roscoe et al. (1958) and later more details were given in a book by Schofield and Wroth (1968). Critical state soil mechanics is an idealized behavior of saturated remolded clays based on continuum mechanics using plasticity and elasticity theory, and is not largely based on the behavior of real soils. A continuum is a body that can be subsequently subdivided into smaller particles that will retain the same properties of the original body.

Based on these definitions, it can be inferred that the concepts of critical state soil mechanics may not be applicable to soils that contain fissures and other types of non-homogenous soils.

Schofield and Wroth (1968) and Schofield (2005) described stiff-fissured clays as a body of rubble with the critical state shear strength being the shear strength along the contact area between the blocks of dense soil. Schofield (2005) stated:

> "When a large body of stiff fissured clay breaks up into a body of rubble it interlocks or slips. The ultimate strength will depend on the CS strength in layers of gouge material on contact surfaces between blocks of dense soil with interlocked grains sucking water into the gouge material."

This assumption does not comply with the definition of a continuum, which is the foundation of the critical state theory, because the properties of the soil mass is not represented by the properties of the dense blocks of soil.

The fact that soils do not purely agree with the theories of elasticity and plasticity was acknowledged by Professor Peter Wroth. He stated: "No soil is either linearly plastic or perfectly plastic, yet such idealizations are essential for the quantitative predictions of real soil behavior to be made"(Wroth 1971). From this statement, it is clear that even Professor Wroth, which was one of the proponents of the critical state theory, admitted that this is an idealization.

Roscoe et al. (1958) stated that a soil is in a critical state in a drained test when further increase in shear distortion will not result in a change in void ratio. In an undrained test, the critical state is reached when an additional increment of shear distortion does not cause a change in the effective stress in the sample (i.e. the pore pressure remains constant). The critical state strength is always expressed in terms of effective stress shear strength parameters. A stress-strain diagram illustrating the definition of critical state shear strength was not found in the original paper by Roscoe et al. (1958), the book *Critical State Soils Mechanics* by Schofield and Wroth (1968), or the book *Disturbed Soil Properties and Geotechnical Design* by Schofield (2005). A stress-displacement diagram illustrating the concept of critical state shear strength was presented by Skempton (1970) and is reproduced here as Figure 3.2. From this figure, it appears that normally consolidated clays were assumed not to experience strain softening and that the residual, fully softened, and the critical state shear strengths are the same.

The critical state soil mechanics concepts were inspired by the work performed by Taylor (1948) using cohesionless soils. These concepts were then applied to cohesive soils by Roscoe et al. (1958). The main cohesive soil used to validate the critical state soil mechanics concepts was the Weald Clay. This lean clay has a liquid limit of 43, a plastic limit of 18, and a clay-sized fraction of 40%. From the results presented by Henkel (1956) and Parry (1960) it can be seen that this soil, when normally consolidated, does not have a pronounced strain-softening behavior. All normally consolidated clays do not exhibit this plastic behavior. The direct shear, ring shear, and CU triaxial tests results presented in Appendices D, E, and F, respectively, show that many clays, even when normally consolidated, can exhibit a strain-softening behavior after the peak shear stress is reached. This has also been acknowledged by several researchers (Bjerrum 1967; Chandler 1984a; Gregory and Bumpas 2013).

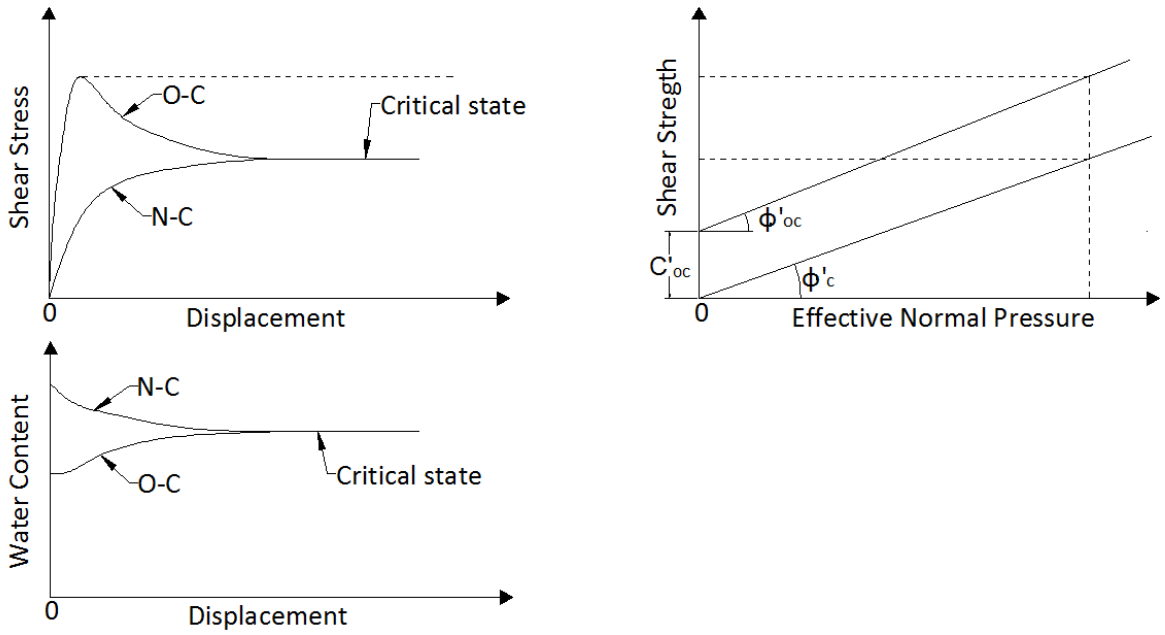

Figure 3.2 Idealized clay behavior (After Skempton 1970) (Used under fair use).

Henkel (1958) presented a discussion on the paper by Roscoe et al. (1958). In this discussion, Henkel stated:

> "The Writer has been concerned with the testing of saturated clays for a number of years and in his opinion the conclusions drawn from the test results by the Authors are in some instances misleading and present an over-simplified picture of the actual behaviour of clay."

In that same discussion Henkel also stated that Roscoe et al. (1958) only used a subset of all the data available for Weald Clay and that all the data for heavily overconsolidated clays was excluded.

The apparent similarity in the concepts of residual and critical state shear strengths should be clarified. During a workshop on critical state soil mechanics offered by Professor C. P. Wroth in Raleigh, NC on March 20, 1977, summarized by Jain (2000b), a question about this relationship was raised. Professor Wroth responded that the difference between critical state and residual shear strength is that the former is characterized by a random particle orientation in the test specimen and is obtained when the soil is sheared *without* allowing the specimen to develop a failure plane. In this case, the test specimen is considered to be a continuum. The residual shear strength is obtained after very large displacements. In this case, a failure plane is already formed in the soil and the tests specimen cannot be considered a continuum, and therefore, it does not comply with the critical state theory. A similar explanation of the difference between critical state strength and residual shear strength was presented by Atkinson and Bransby (1978), Atkinson (1981), Wood (1990), Crabb and Atkinson (1991), and Ortigao (1995).

Several researchers have used the term fully softened shear strength and critical state shear strength as synonyms, or they have defined the critical state shear strength as the drained peak shear strength of a normally consolidated clay (Tavenas and Leroueil 1981; Crabb and Atkinson 1991; Clemente 1992; Leroueil and Marques 1996; Leroueil 2001; Take and Bolton 2011). Regarding this subject, Schofield (1967) stated that the critical state strength corresponds to: "the strength *near the peak* of the drained tests of a lightly compressed samples."(Emphasis added).

Furthermore, Skempton (1970) stated that:

> "Schofield and Wroth (1968) consider that the peak strength of a normally consolidated remoulded clay occurs just before the critical state is reached and suggests a value of ϕ'_c= 22½° for London Clay. This may be compared with ϕ'_s = 20° for the normally consolidated peak. Since the latter strength can readily be determined it may be taken as a practical approximation to the critical state, and hence to the fully softened strength of an over-consolidated clay,"

No experimental data have been found in the literature to support this comparison. From a diagram presented by Skempton (1985), reproduced here as Figure 3.3, it can be seen that Skempton believed that this approximation only applies to normally consolidated soils with a clay-sized fraction less than 20%. For normally consolidated soils with a clay-sized fraction more than 20% or normally consolidated soils that experience strain-softening behavior after the peak, the approximation of the critical state shear strength as the peak shear strength does not comply with the definition of critical state shear strength presented above because the shear strength decreases with increasing displacement. This conclusion was also reached by Bishop (1971b) based on the results of remolded normally consolidated Blue London Clay tested using a ring shear device. Professor Wroth, in his discussion on the paper by Bishop (1971b), seems to agree that calling the peak shear strength of a normally consolidated clay that experiences strain-softening behavior after the peak the critical state strength is not consistent with the critical state definition (Wroth 1971). Professor Wroth said:

> "We are faced then with the situation that if we accept the accuracy of the experimental data (in spite of the knowledge that at large strains the values are suspect) then some remoulded clays may not reach a critical state condition which satisfies precisely Hvorslev's definition, such as the case of the remoulded blue London Clay…" (Wroth 1971)

Hvorslev defined the critical state condition as follows:

> "Eventually a condition is reached under which a continued flow does not cause further changes in the shearing resistance and void ratio. These ultimate values of the shearing resistance as well as the ultimate values of the void ratio are equal in both cases and therefore independent of the initial state of consolidation of the soil." (Hvorslev 1969)

In the author's opinion, Hvorslev's definition of critical state is the same definition presented by Roscoe et al. (1958). It is unclear why Professor Wroth made such a distinction in his comment.

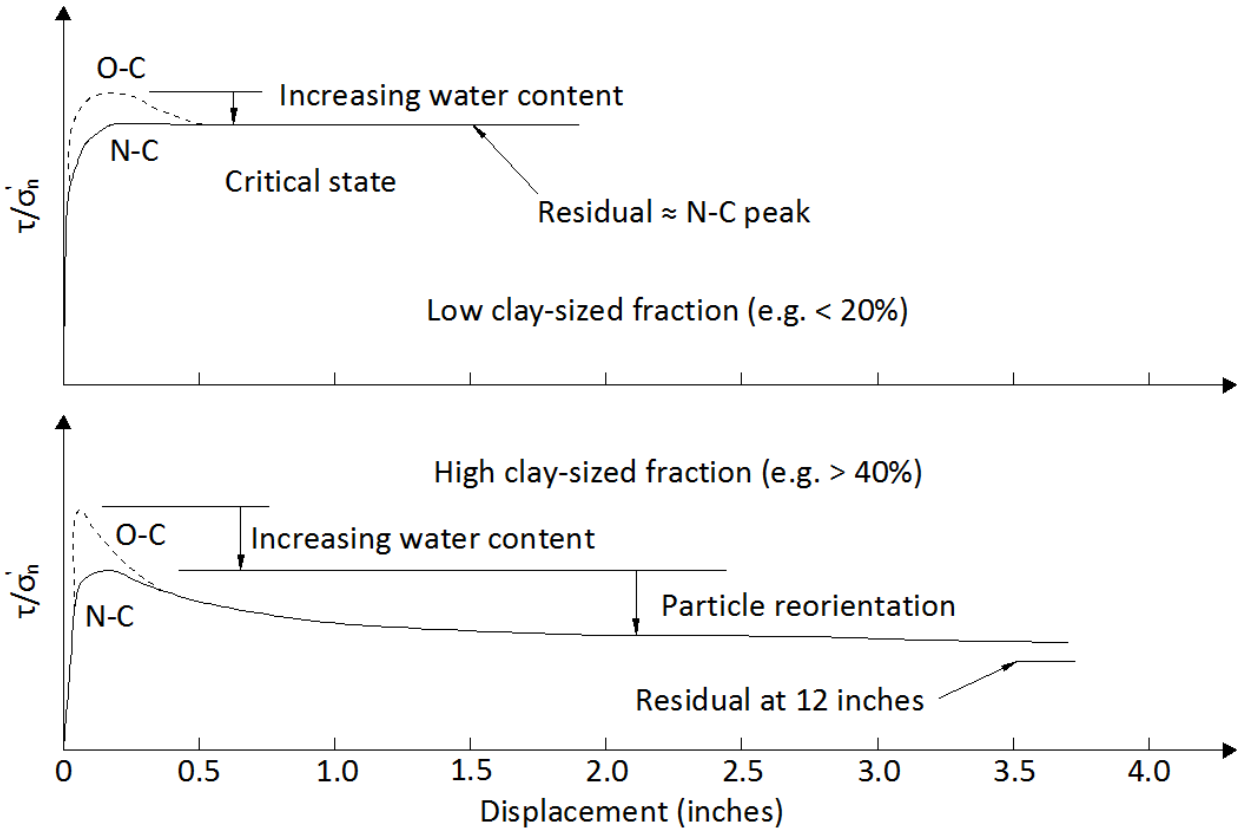

Figure 3.3 Comparison of critical state strengths with residual strengths for a constant value of σ'_n (After Skempton 1985) (Used under fair use).

Triaxial tests results on normally consolidated San Francisco Bay Mud presented by Jain (2000a) showed strain-softening behavior after the peak shear strength. This soil has a liquid limit of 88 and a plasticity index of 40. Jain (2000a) stated that for this soil, the critical state condition was never achieved. San Francisco Bay Mud is a soil with a plasticity comparable with the soils tested in this research which also showed a strain-softening behavior after the peak.

Even Professor Wroth admitted that the critical state condition is not attained in every soil. He stated: "… although some soils may not display a unique critical state under certain tests conditions, it does not mean that the concept of critical states is either valueless or irrelevant" (Wroth 1971).

According to the definitions presented above, the critical state shear strength should be measured in a device that prevents the test specimen from forming a defined failure plane. The direct simple shear device is the only device available in geotechnical engineering practice that is normally not associated with forming a distinct failure plane. The orientation of shear planes can be determined from the assumed state of stress at failure, but it is not possible to observe the failure plane within the test specimen. The direct simple shear test, as conducted to ASTM D6528-07 guidelines, is a constant volume test with a complex state of stress in the sample that is not readily suitable for the determination of drained or

effective stress shear strength parameters. This limitation is stated in ASTM D6528-07 "Standard Test Method for Consolidated Undrained Direct Simple Shear Testing of Cohesive Soils" and was also admitted by Schofield (2005). ASTM D6528-07 states:

> "The state of stress within the simple shear specimen is not sufficiently defined nor uniform enough to allow rigorous interpretation of the results. Expressing the data in terms of the shear stress and normal effective stress on the horizontal plane is useful for engineering purposes, but should not be confused with the effective stress parameters derived from other shear tests having better defined states of stress."

The *ultimate shear strength* is defined in the U.S. Army Corps of Engineers (USACE) Engineering Manual (EM) 1110-2-1906 "Laboratory Soils Testing" (USACE 1970) as the minimum post-peak shear stress measured in the direct shear box before or at 0.50 inches of displacement or the minimum post-peak deviator stress obtained in the triaxial device before or at 15% axial strain. This definition is represented in Figure 3.4.

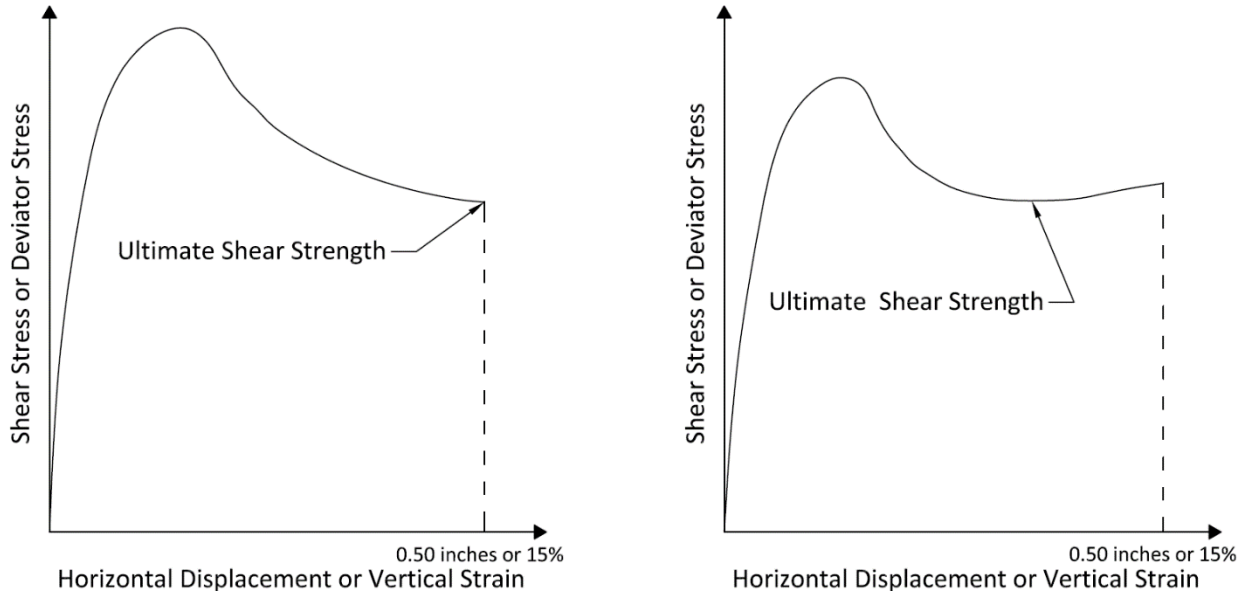

Figure 3.4 Definition of ultimate shear strength (After USACE 1970) (Used under fair use).

Terzaghi et al. (1996) stated that "The fully softened failure envelope for an overconsolidated clay can be determined by using intact specimens, intact specimens containing a distinct fissure or joint, or reconstituted normally consolidated specimens," and that "When intact specimens are used, or when specimens are remolded at water contents less than the liquid limit, the fully softened strength corresponds to the postpeak shear stress at which the increase in water content during shear levels off." They also stated that "… specimens remolded at a water content higher than the liquid limit or specimens

normally consolidated from slurry are preferred for the measurement of fully softened shear strength," (Terzaghi et al. 1996).

These definitions do not seem consistent with previous definitions of fully softened shear strength. If a soil specimen is remolded at a water content of about 80% of the liquid limit, it is not clear if the fully softened strength corresponds to the peak deviatoric stress or the stress at high strain (15%). As part of the literature review conducted for this project, the author found no laboratory test data indicating that the fully softened shear strength is equal to strength at high strains as measured in a drained or undrained triaxial test. More information regarding the influence of the molding water content on the fully softened strength is presented in Section 6.6.

Even though Terzaghi et al. (1996) suggested that undisturbed samples could be used to measure the fully softened shear strength, they also acknowledged the problems with this procedure:

> "Special care must be exercised on intact specimens to achieve, in the shear zone at the fully softened condition, complete porewater pressure equilibration and softening in drained tests, or complete porewater pressure equalization in undrained tests. Moreover, for intact samples, it may be difficult to define the area of the shear zone and to control axial loads after the formation of distinct shear planes."

Regarding the use of heavily overconsolidated clays to measure the fully softened shear strength, Roscoe et al. (1958) admitted that very high strains are required to reach the critical state in undisturbed specimens in a triaxial device and acknowledged that at this point, the errors incurred by assuming that the triaxial test specimen remains cylindrical when calculating the value of the principal stresses might be significant. Henkel (1958) was also opposed to the use of undisturbed specimens to measure the critical state strength in the triaxial device due to errors introduced at large strains by the necessary assumptions and corrections required for the triaxial test. Olson (1962) stated that the strain required to achieve a critical state condition in the triaxial device can seldom be attained. Skempton (1970) commented that defining the critical state shear strength in real soils with bonding, sensitivity, etc., is very difficult. Atkinson and Bransby (1978) acknowledged that triaxial tests results are unreliable at large strains and that overconsolidated samples often do not reach the critical state in the triaxial device. Crabb and Atkinson (1991) stated that triaxial tests on undisturbed samples are not suitable to determine the critical state strength due to the development of a failure plane in the test specimen.

Banks (1978) presented fully softened shear strength failure envelopes obtained using the direct shear and triaxial devices and ultimate shear strength failures envelopes obtained using undisturbed samples in the direct shear device for three soil. In all cases, the ultimate shear strength failure envelopes were higher than the fully softened failure envelopes.

In a recent engineering report made available to the author through the USACE, fully softened shear strengths were determined using the approach presented by Terzaghi et al. (1996). Undisturbed samples were used to measure the fully softened shear strength using the triaxial device, and the fully softened shear strength was defined as the ultimate shear strength at an axial strain value of 15%. It is clear that the definition of fully softened shear strength based on an arbitrary value of strain and not based on a

condition attained by the test specimen can be problematic. The results of a series of CU triaxial tests from the report are presented in Figure 3.5. From this figure it can be seen that at 15% strain both the deviator stress and the pore pressure were still decreasing. This means that neither the critical state nor the fully softened shear strength condition was achieved.

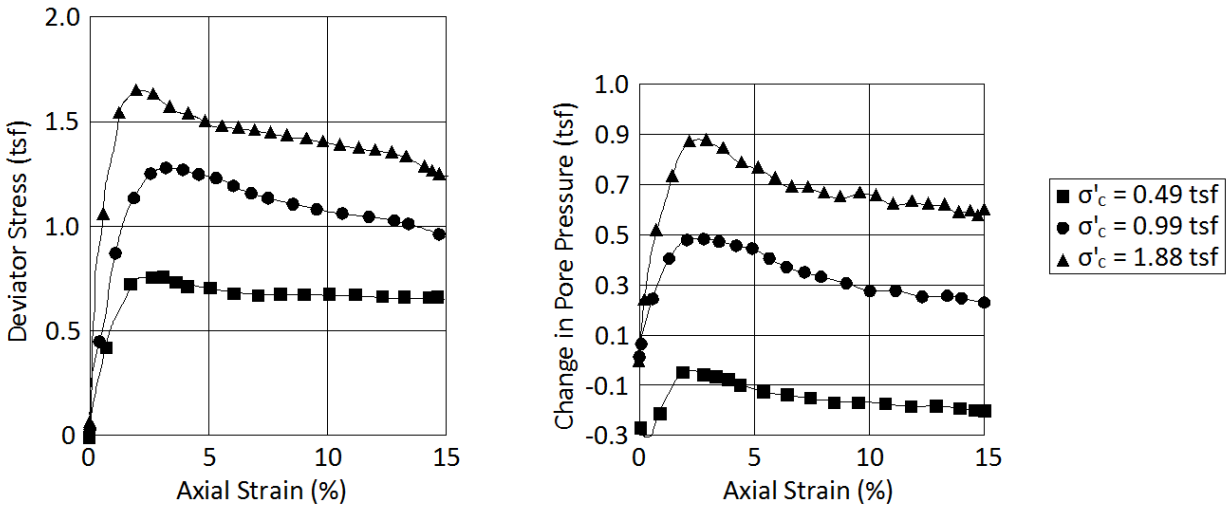

Figure 3.5 CU triaxial tests on sample from a flood risk management project report (Used under fair use).

Based on the discussions presented above, it can be concluded that:

1) The critical state strength is based on an idealized soil behavior which does not correspond to the actual behavior of some soils.
2) The critical state shear strength and residual shear strength are usually are not the same, although their definitions might sound similar. The critical state shear strength is obtained by shearing a test specimen without a failure plane forming and the residual shear strength requires a failure plane to be formed and enough displacement on that failure plane to cause a face-to-face orientation of the clay-sized particles.
3) The concept of residual shear strength is not fully compatible with critical state theory. However, under certain idealized behavior conditions for soil exhibiting no strain-softening, the residual shear strength would be equal to the fully softened shear strength.
4) In soils that experience a strain-softening behavior after the peak shear strength, the necessary conditions to define the critical state strength are not attained in the direct shear, ring shear, or triaxial devices. For this reason, is not technically correct to say that the critical state strength is equal to the peak shear strength of the normally consolidated clay measured using these devices.
5) For clays that do not exhibit strain-softening behavior, the critical state shear strength is perhaps equal to the peak shear strength of a normally consolidated test specimen and is also approximately

the same as the residual shear strength. Clays that exhibit this behavior normally have low clay-sized fractions.

6) The direct simple shear apparatus is not suitable for determining neither the critical state shear strength, the fully softened shear strength, nor the residual shear strength of clays.
7) Undisturbed samples have not proven to be useful for determining critical state shear strengths or fully softened shear strengths.
8) Remolded normally consolidated samples are normally necessary to measure the fully softened shear strength.
9) There is not a well-defined or industry-accepted test procedure using any apparatus to measure the critical state shear strength of soils, even after more than 50 years since the theory was developed.

Chapter 4

Use of Fully Softened Shear Strength

4.1 Introduction

In this chapter, the topics related to the use of fully softened shear strength in geotechnical practice are discussed and assessed based on information found in the literature. Case histories of first-time failures involving softening were examined to provide information on: (1) the soils that can experience softening, (2) the depths at which the fully softened shear strength applies, (3) the pore water pressures that have been used in conjunction with fully softened shear strength parameters, (4) the type of project where softening is an issue, and (5) the time after construction at which these failures usually occur. The effect of climatic conditions on the likelihood of a soil experiencing softening is addressed based on information available in the literature. The minimum factors of safety specified by different agencies and researchers are evaluated to provide recommendations for factors of safety that should be applied to the design of slopes and embankments using fully softened shear strength parameters.

4.2 Mechanisms Causing a Decrease in Shear Strength *In Situ*

The main factor causing a decrease in shear strength with time in slopes in stiff clays, compacted clays embankments, and mudstones, is an increase in void ratio which causes softening of the soil mass. Different mechanisms have been proposed to explain the difference in the shear strength mobilized *in situ* in first-time failures and the undisturbed peak shear strength measured in the laboratory. In this section, these mechanisms are discussed.

4.2.1 Fissures

The presence of fissures in overconsolidated clays has been used to explain the difference in the drained shear strength measured in the laboratory and the drained shear strength developed in the field in first-time failures in stiff-fissured clays. Fissures have been identified as a feature that can promote softening of the soil mass, and also as a feature that will influence the shear strength measured using undisturbed samples in the laboratory (Terzaghi 1936; Marsland and Butler 1967; Marsland 1971; Chandler 1984a; b).

Terzaghi (1936) provided an explanation for the decrease in shear strength with time experienced by stiff-fissured clays. His idea was that water percolates into the fissures, and the clay along the walls of the fissures would swell under zero confining pressure. This process will weaken the soil and more cracks will

form. This explanation might not fully explain the low shear strength mobilized *in situ* in first-time failures in stiff-fissured clays. The investigation performed by Skempton (1948) on the failure at Kensal Green showed that softening did not progress more than 0.25 inches from the fissures into the clay mass. Henkel (1957) stated that the softening process and the increase in water content might be limited to a small volume of the clay, and in some cases, only to the vicinity of the sliding surface. Skempton (1964) found a localized increase in water content and softening in the failure plane in first-time failures in stiff-fissured clays, as can be seen in Figure 4.1. This finding implies that swelling is mainly occurring in the failure plane of stiff-fissured clays and not in the whole clay mass as would be expected if the mechanism proposed by Terzaghi (1936) was acting. Thomson and Kjartanson (1985) found no softening along the fissures in a first-time slide in a stiff-fissured clay where the fully softened shear strength was found to be the controlling shear strength. In a different study, Thomson and Tweedie (1978) found softening in the fissures in a first-time failure in a stiff-fissured clay, but it was not specified how deep into the clay mass the softening extended.

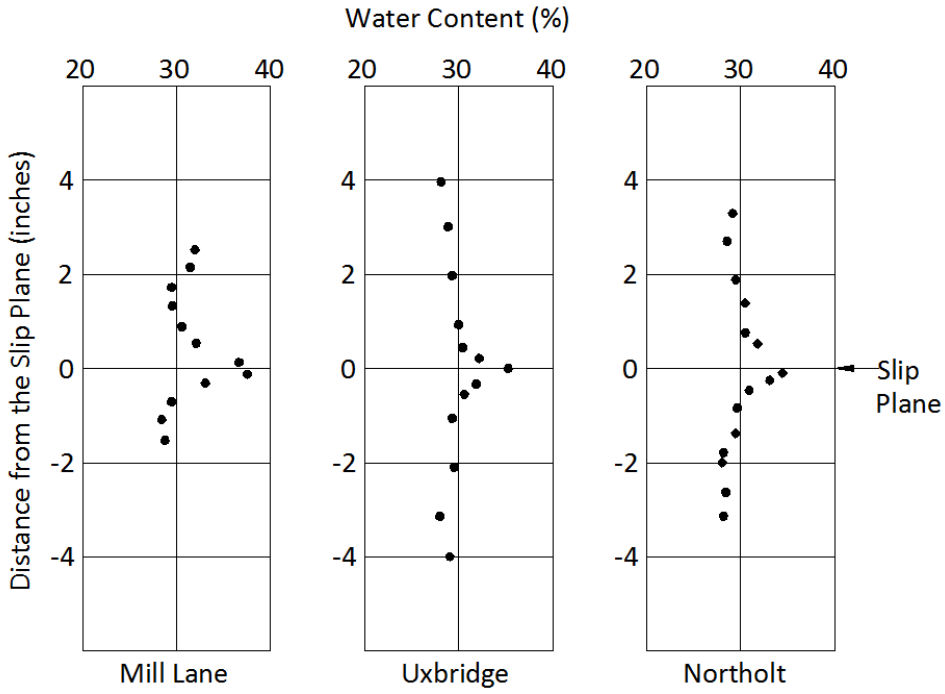

Figure 4.1 Distribution of water content near the slip surface (After Skempton 1964) (Used under fair use).

Some researchers have indicated that progressive failure is part of the mechanism for the reduction in shear strength (Henkel and Skempton 1955; Skempton 1964; James 1970; Skempton 1970; Bishop 1971a; Chandler and Skempton 1974; Skempton 1977; Chandler 1984a, b; Potts et al. 1990, 1997; Kovacevic et al. 2001; Picarelli et al. 2001; Take and Bolton 2004, 2011). However, Morgenstern (1977) stated that field evidence obtained from case histories of first-time failures in stiff-fissured clays tend to support more

the hypothesis of softening presented by Terzaghi (1936) more than the progressive failure hypothesis. He stated that a case history showing that the mobilized effective stress friction angle *in situ* was less that the peak drained friction angle measured using undisturbed samples would be a good evidence of progressive failure. More recently, several case histories have been documented that have shown that the effective stress friction angle mobilized *in situ* in first-time failures in stiff-fissured clays could be less than the undisturbed peak drained friction angle measured in the laboratory (e.g. Cancelli 1981; Stark and Eid 1997; Mesri and Shahien 2003). In later publications, Morgenstern acknowledged that progressive failure could be acting along with other softening mechanisms in first-time failures in stiff clays (Chan and Morgenstern 1987; Morgenstern 1990). More details about progressive failure is presented in Section 4.2.3.

The amount of fissures contained in a soil sample has also been found to influence the shear strength measured in the laboratory (Marsland and Butler 1967; Marsland 1971; Skempton 1977; Chandler 1984a; b; Contreras et al. 2012). The drained shear strength measured in the laboratory decreases with increasing number of fissures in the test specimen. Several researchers have found that the effect of the fissures on the drained peak shear strength measured using undisturbed test specimens is not sufficient to explain the low drained shear strength mobilized in first-time failures in stiff-fissured clays (Chandler 1984a; b; Skempton 1977b). Even using 10-inch diameter test specimens, triaxial tests performed by Chandler (1984a; b) and by Sandroni (1977), as cited by Skempton (1977), on Upper Lias Clay and London Clay showed that the drained shear strength measured in the laboratory was still greater than the drained shear strength back-calculated from first-time slides in these materials.

4.2.2 Weathering

Weathering is another mechanism that has been proposed to explain the difference in the drained peak shear strength measured using undisturbed samples and the drained shear strength mobilized *in situ* in first-time failures in overconsolidated clays, compacted clays, and mudstones. Weathering can be divided into physical and chemical weathering. Physical weathering is caused by processes like cyclic wetting and drying, and freezing and thawing. Chandler (1969) performed an investigation on the effect of weathering in mudstones, and found that weathering decreases the preconsolidation pressure and the effective stress shear strength parameters of mudstones. Other research performed by Chandler (1972) and Chandler and Apted (1988) showed that weathering also decreases the preconsolidation pressure and effective stress shear strength parameters of overconsolidated clays. Chandler and Apted (1988) concluded that, assuming that the drained friction angle of the soil is constant, increased weathering decreases the effective stress cohesion intercept of overconsolidated clays.

The effect of wetting and drying cycles in compacted high plasticity clays has been investigated in detail by Professor Steve Wright and his colleagues at the University of Texas at Austin (Rogers and Wright 1986; Kayyal and Wright 1991; Wright 2005; Wright et al. 2007). They found that cycles of wetting and drying decrease the drained shear strength of compacted high plasticity clays toward values equal to the fully softened shear strength. Most of the shear strength loss in the clays tested occurred in the first cycle of wetting and drying (Rogers and Wright 1986). Kayyal and Wright (1991) found that the failure plane observed in the field in compacted clay embankments matched the critical surface obtained using limit

equilibrium analyses and fully softened shear strength parameters. In addition, the back-calculated shear strength parameters approximated the laboratory-determined fully softened shear strength parameters. This finding implies that weathering might be an important mechanism decreasing the drained shear strength of compacted clay embankments toward the fully softened shear strength. Bishop and Henkel (1962) stated that due to changes in water content in compacted clay embankments, the effective stress cohesion intercept will decrease to zero with time. Chandler et al. (1973) acknowledged that in compacted clay embankments, water can percolate into the soil decreasing its shear strength. A similar statement was also made by Day and Axten (1989). The finite element method was used by Kovacevic et al. (2001) to investigate the effect of cycles of wetting and drying in a compacted embankment constructed of high plasticity clay. The results showed that cycles of wetting and drying can cause progressive failure to develop in embankments, thereby decreasing the shear strength mobilized *in situ*. Wright et al. (2007) found that although cycles of wetting and drying decrease the shear strength, it is not always decreased to the fully softened shear strength.

Similar results were found for the overconsolidated clays studied by Crawford (1964). Crawford performed triaxial tests using undisturbed samples of an overconsolidated fat clay that were allowed to undergo free swell in water for hours. The results presented by Crawford show a significant decrease in drained shear strength caused by allowing the samples to undergo free swell prior to testing when compared to undisturbed samples that were not allowed to swell. Similar results were found by Calabresi and Rampello (1987), and Rampello (1991). Stark and Duncan (1991) found that desiccated samples of the clay located in the downstream slope of San Luis Dam had the consolidation and shear strength characteristics of a normally consolidated clay after allowed to undergo free swell submerged in water. Botts (1998) presented triaxial test results on undisturbed samples and samples subjected to cycles of wetting and drying of Pierre Shale. Botts found that the duration of the drying stage greatly influenced the amount of swelling and the loss in drained shear strength during the wetting stage. Most of the shear strength loss was also found to occur in the first cycle of wetting and drying. According to the results presented by Botts, the drained shear strength after wetting and drying was coincidentally very close to the ultimate shear strength (defined at 20% strain) as obtained in the triaxial device using undisturbed samples.

James (1970) reported a shallow slide (5-ft-deep) in a stiff-fissured clay where the soil from the failure surface to the ground surface was found to be soft. James believed that some of this softening was caused by freezing and thawing but no proof was presented. Graham and Au (1985) showed that the undisturbed drained peak shear strength of a high plasticity clay from Canada is decreased by cycles of freezing and thawing or by allowing tests specimens to undergo free swell under water prior to testing. They also found that the decrease in drained shear strength was more pronounced for samples that were subjected to freeze and thaw cycles than for samples that were allowed to undergo free swell in water. It was not specified whether or not the drained shear strength after cycles of freezing and thawing was equal to the fully softened shear strength. Leroueil et al. (1991) presented the results obtained from triaxial tests on undisturbed samples and samples subjected to one cycle of freezing and thawing of clays from the Champlain Sea. Leroueil et al. found that freezing and thawing destroys the bonds in the clay, increasing the coefficient of consolidation, and decreasing the shear strength. The undrained shear strength after

cycles of freezing and thawing was found to be equal to the remolded normally consolidated undrained shear strength of the clay. No comparison was made with the remolded drained shear strength. Take and Bolton (2002, 2004, 2011) investigated the effect of changes in moisture content in the stability of slopes in overconsolidated high plasticity clays using centrifuge simulations. The results presented by Take and Bolton showed that variations in the moisture contents in this type of projects can decrease the shear strength toward the fully softened shear strength. The depth of the failure observed in the simulations was not reported by Take and Bolton, although, from pictures and diagrams presented in the paper, the failure observed seems to be shallow.

Cycles of wetting and drying have also been found to decrease the drained shear strength of mudstones towards the fully softened shear strength (Bhattarai et al. 2006). Bhattarai et al. concluded that physical weathering is the main agent causing the decrease in the drained shear strength of mudstones and that chemical weathering does not play an important role in the softening process. Other authors have described chemical weathering processes but it has not been concluded that it will substantially decrease the shear strength of soils (Chigira 1990; Wetzel and Einsele 1991; Chigira and Oyama 1999; Bhattarai et al. 2006).

4.2.3 Progressive failure

Progressive failure has also been proposed to explain the difference in the peak drained shear strength measured using undisturbed samples and that mobilized *in situ* in first-time failures in overconsolidated clays (Henkel and Skempton 1955; Skempton 1964; James 1970; Skempton 1970; Bishop 1971a; Chandler and Skempton 1974; Skempton 1977; Chandler 1984a, b; Potts et al. 1990, 1997; Kovacevic et al. 2001; Picarelli et al. 2001; Take and Bolton 2004, 2011). Progressive failure is not a mechanism causing softening, but a mechanism that decreases the average shear strength mobilized by causing different shear strains along the failure plane. Strains large enough to make the soil pass the peak shear strength have been found in slopes of overconsolidated clays (Duncan and Dunlop 1969; Dunlop and Duncan 1970; Potts et al. 1997). Back-analyses of slope failures in stiff-fissured clays have shown that the critical surface obtained in limit equilibrium analysis more closely match the observed failure surface when undisturbed drained peak shear strength parameters are used to search instead of mobilized drained shear strength parameters (Abdel-Ghaffar 1990; Mesri and Abdel-Ghaffar 1993). Abdel-Ghaffar reached this conclusion by analyzing several first-time failures in this type of material. This finding implies that progressive failure could be a controlling mechanism for first-time failures in stiff clays. As explained by Abdel-Ghaffar, the peak shear strength of the soil is available before the failure starts. At this moment, the critical failure surface is governed by the undisturbed peak effective shear strength parameters. This surface, being critical, will have larger stresses and strains which will make it to be the most susceptible to develop progressive failure. More details about this procedure are presented in Section 4.4.

Bromhead (1978) and Chandler (1984b), after reviewing case histories of slope failures, felt that the fully softened shear is an empirical method to take into account progressive failure for slopes that can be used to analyze slopes similar to the case histories where the fully softened shear strength has been found to apply. Cooper et al. (1998) performed a field experiment to fail a cut in a heavily overconsolidated plastic clay. From this experiment, they found that the failure surface developed progressively from the toe into

the slope. Using limit equilibrium analysis, they concluded that the fully softened shear strength parameters in conjunction with the measured pore pressures could have predicted the failure. Picarelli et al. (2001) stated that first-time failures in stiff-fissures clays are usually caused by progressive failure.

A method to include the effect of progressive failure in limit equilibrium analyses was proposed by Bishop (1971). In his paper, Bishop suggested that a variation in the residual factor proposed by Skempton (1964), defined in Equation 2.1, along the failure surface could successfully account for progressive failure. No references were found on the use of this method to analyze real slopes, but it is believed that it could prove to be a very useful tool to include the effect of progressive failure into limit equilibrium analyses. Other methods to take into account progressive failure in limit equilibrium analyses have been presented by different researchers (e.g. Chirapuntu and Duncan 1977; Law and Lumb 1978; Cooper 1988; Chang 1992; Rodriguez-Marek 1992). The finite element method has also been suggested as a viable method to investigate progressive failure in slopes and cuts (Bromhead 1978; Potts et al. 1990, 1997).

4.2.4 Creep

Creep is another mechanism that has been proposed to explain the difference in the shear strength mobilized *in situ* and that measured in the laboratory where creep effects are not expected to be significant (Skempton 1964; Tavenas and Leroueil 1981; Chandler 1984a; b; Leroueil 2001; Picarelli et al. 2001; Mitchell and Soga 2005). According to Mitchell and Soga (2005), the decrease in shear strength caused by creep is important in soft clays sheared under undrained conditions and heavily overconsolidated clays sheared under drained conditions. Creep causes higher pore pressures to be developed during undrained shearing of soft clays and a greater increase in the water content of overconsolidated clays during drained shearing, causing, in both cases, a decrease in shear strength (Mitchell and Soga 2005).

Mitchell and Soga (2005) offered creep as the possible explanation for the failures presented by Skempton (1977). This was explained using Figure 4.2. In this figure, the total and effective stress path of an overconsolidated clay in a CU triaxial test are represented by the lines AC and AB respectively. According to Mitchell and Soga, if a deviator stress DE is applied to an overconsolidated sample, a negative pore pressure EF will be developed in the sample. After creep, the effective stress in the sample will be represented by point E. If the sample is sheared undrained, the shear strength will be represented by point G which is lower than the shear strength of the sample that was not subjected to creep, which is represented by point B. As can be seen from this figure, the drained failure envelope for the sample before and after creep is assumed to be the same. The failures presented by Skempton (1977) occurred several decades after construction and no increase in the deviator stress was reported after the slope was formed for any of the slides analyzed. For this reason, the pore pressures on the failure plane were calculated using steady state seepage conditions which seems to be an appropriate assumption. If the effective stress failure envelope before and after creep is the same, the factor of safety obtained in drained analyses, if the effective stresses are calculated using correct pore pressures, should not change.

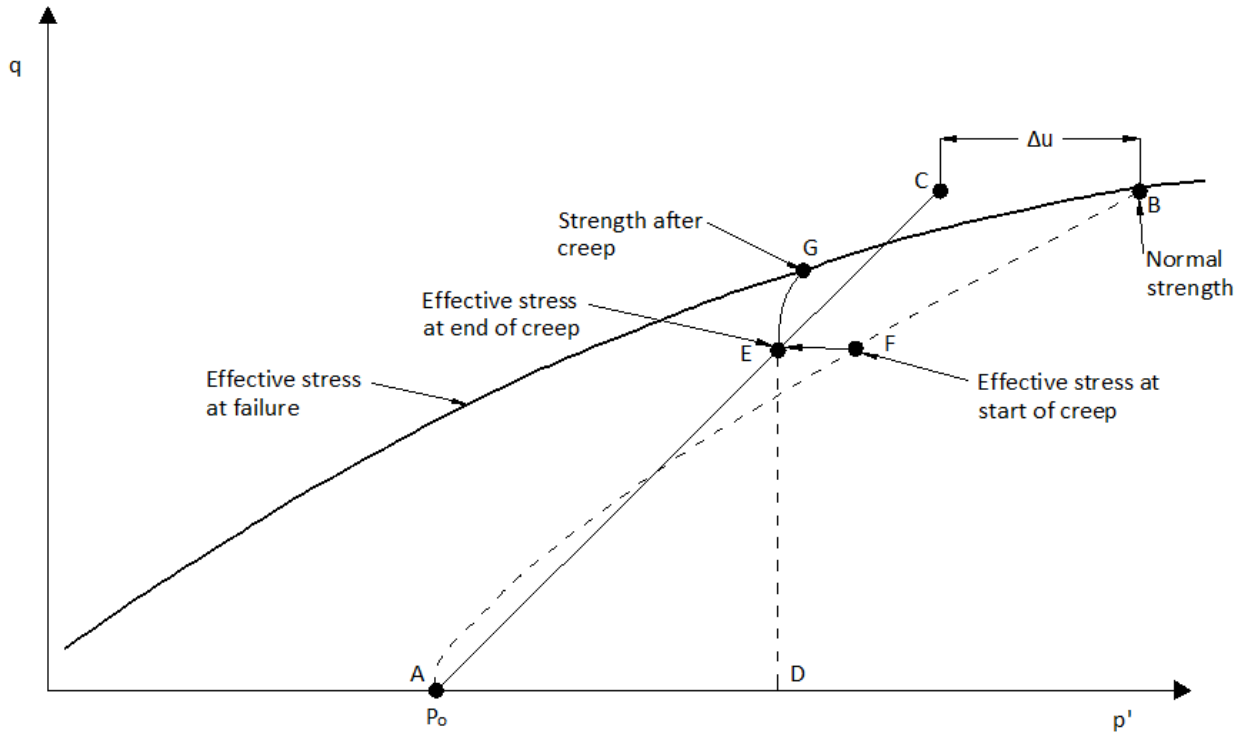

Figure 4.2 Stress paths plot for normal undrained shear tests and drained creep tests in heavily overconsolidated clays (After Mitchell and Soga 2005) (Used under fair use).

Other researchers have found that the effective stress failure envelope for overconsolidated clays is not a function of the strain rate used for testing (Bishop and Lovenbury 1969; Vaid 1979; Sheahan et al. 1996). Bishop and Lovenbury (1969) presented the results of creep tests performed on undisturbed samples of Brown London Clay with a duration of up to 3.5 years. Based on the results obtained, Bishop and Lovenbury concluded that, in an engineering time scale, only a small portion of the decrease in shear strength can be attributed to creep. These results imply that creep does not play a major role on the effective stress failure envelope obtained from overconsolidated clays.

For structured soft clays from Canada, Lefebvre (1981), after analyzing several case histories of first-time failures in slopes, laboratory tests results, and literature available on the subject, concluded that the drained shear strength is decreased by creep. Structured soft clays from Canada are characterized by bonds and cementation that are easily broken during shear (Lefebvre 1981). This structure causes these soils to be very brittle. According to Lefebvre (1981), bonds and cementations are easily broken when the soil is subjected to sustained loads higher than the ultimate shear strength.

4.3 Soils Subjected to Softening

An important step in performing slope stability analyses is to decide whether the peak, fully softened, or residual shear strength is the correct shear strength for the case being analyzed. For this reason, it is imperative to develop some guidelines on which shear strength should be applied for the different cases

and soils involved in slope stability analyses. It has been commonly accepted that the residual shear strength applies to reactivated landslides and failure surfaces subjected to tectonic movements (Skempton 1964, 1970; Eigenbrod and Morgenstern 1972; Chandler and Skempton 1974; Skempton 1977; Thomson and Tweedie 1978; Chandler 1984a, b; Crabb and Atkinson 1991). This dissertation focuses on the cases where the fully softened shear strength versus the peak shear strength should be applied.

Different theories have been proposed to explain which soils can mobilize a lower shear strength *in situ* when compared to that measured using undisturbed samples in the laboratory. These theories are discussed in this section along with case histories of first-time failures involving soils that have mobilized a lower shear strength.

When researchers first realized that the drained shear strength developed in the field in some clays was different that the drained shear strength measured in the laboratory using undisturbed samples, it was believed that this was only a problem in stiff-fissured clays and that non-fissured clays would not suffer this decrease in shear strength (Skempton and Brown 1961; Skempton 1964, 1970). Recent findings suggest that fat clays, as compared to lean clays, are more likely to mobilize a lower drained shear strength *in situ* than that measured using undisturbed samples in the laboratory (Chandler 1984a). According to Bjerrum (1967), fat clays experience a more pronounced strain-softening behavior than lean clays. In other words, the difference between the drained peak and residual shear strengths is greater for fat clays than for lean clays. For this reason, progressive failure will have a greater effect on the mobilized drained shear strength *in situ* for high plasticity soils.

Similarly, Chandler (1984a) stated that the difference in the behavior of stiff-fissured clays and non-fissured clays is more dependent on the plasticity of the clay than on the fissures themselves. Chandler agreed with Bjerrum (1967) that fat clays tend to be more brittle, even when normally consolidated, than lean clays. That means that fat clays can develop stronger bonds between the soil particles and so the decrease in shear strength after the peak is greater for fat clays than for lean clays. Also, weathering and progressive failure will have a bigger impact in the shear strength of fat clays when compared to lean clays because of the stronger bonds that the former will develop. Skempton and Hutchinson (1969) also acknowledged that the difference between the undisturbed drained peak and residual shear strength increases with increasing clay-sized fraction even for normally consolidated soils. Higher clay-sized fraction usually means higher plasticity.

Laboratory test results found in the literature tend to support these statements. A relationship presented by Stark et al. (2005) between the difference in the secant fully softened and residual friction angles and the liquid limit is reproduced here as Figure 4.3. In this figure, it can be seen that for a given pressure, the difference in the fully softened and residual secant friction angle increases with increasing liquid limit up to a liquid limit of about 100 to 140 where it starts to decrease.

Abdel-Ghaffar (1990) and Mesri and Abdel-Ghaffar (1993) analyzed first-time slides in overconsolidated clays and quantified the ratio of the mobilized drained shear strength in the field and the measured undisturbed drained peak shear strength in the laboratory. These results are plotted in Figure 4.4. In this figure, the ratio is plotted against the plasticity index of the soil. From this figure, it can be seen that for

most of the soils with plasticity indices less than 20, the mobilized drained shear strength in the field is very close to the measured undisturbed drained peak shear strength in the laboratory. For soils with a plasticity index greater than 20, the difference in the mobilized and measured shear strength starts to decrease with increasing plasticity. For plasticity indices above 80, an increase in the ratio of mobilized to peak shear strength occurs. The trend after a plasticity index above 80 is driven by only one case history. More data is needed in order to prove the validity of the shape of this trend for plasticity indices greater than 80.The numbers next to each data point are from a numbering system used by Mesri and Abdel-Ghaffar (1993) for the case histories.

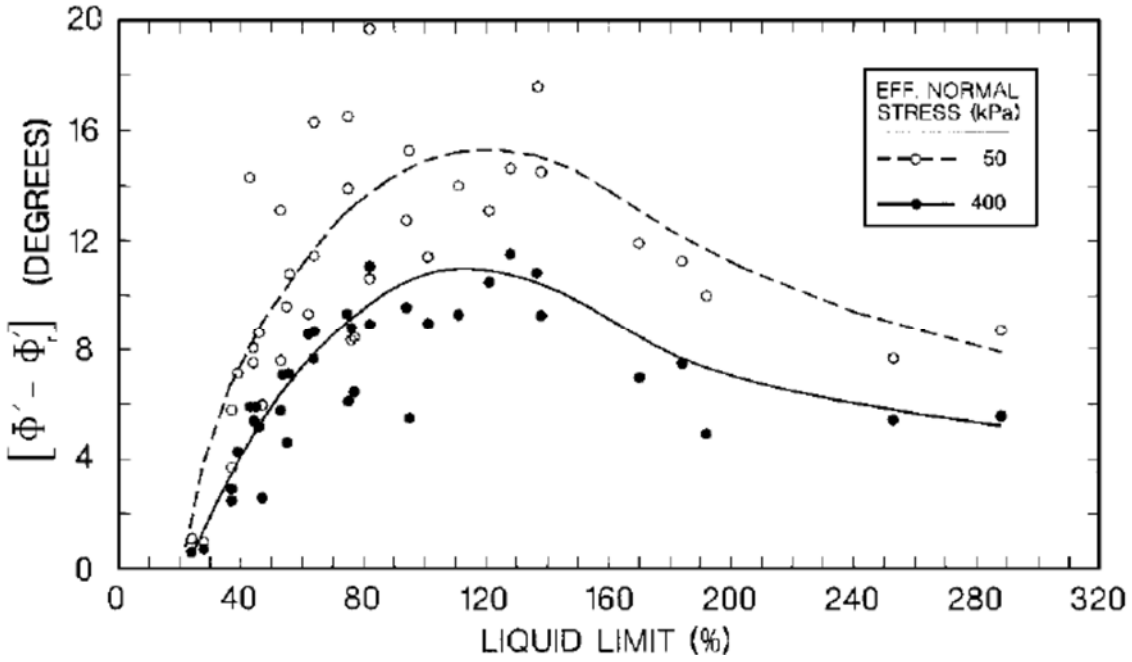

Figure 4.3 Difference in the fully softened and residual secant friction angle as a function of the liquid limit (Stark et al. 2005) (Used under fair use).

Mesri and Shahien (2003) analyzed 99 case histories of slope failures and concluded that the undisturbed peak shear strength as measured in the laboratory is the governing shear strength for first-time slides in unstratified lean clays. Mesri and Shahien also concluded that the fully softened shear strength is the controlling shear strength for first-time slides in homogeneous slopes of fat clays and on the portion of the slip surface cutting across the bedding planes in stiff-fissured clays.

A literature review was performed to collect case histories of failures where the fully softened shear strength was found to be the controlling shear strength. Sixty eight failures in stiff-fissured clays and 74 failures in compacted clay embankments related to fully softened shear strength were collected. The liquid limits and plasticity indices of the soils involved in these slides are plotted in Figure 4.5. From this figure it can be seen that most of the failures are located in slopes and embankments formed of fat clays.

Some exceptions are found but no case history was found where softening was reported in clays with a liquid limit below 40 or a plasticity index below 20. From this discussion, it can be concluded that fat clays are more likely to experience a decrease in shear strength *in situ* than lean clays.

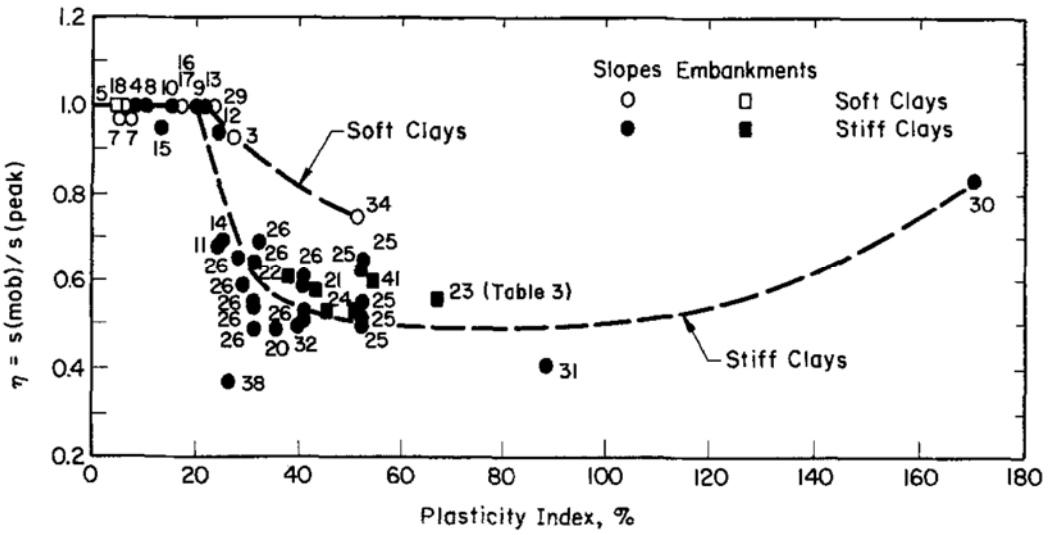

Figure 4.4 Mobilized shear strength for first-time slides in clays (Mesri and Abdel-Ghaffar 1993).

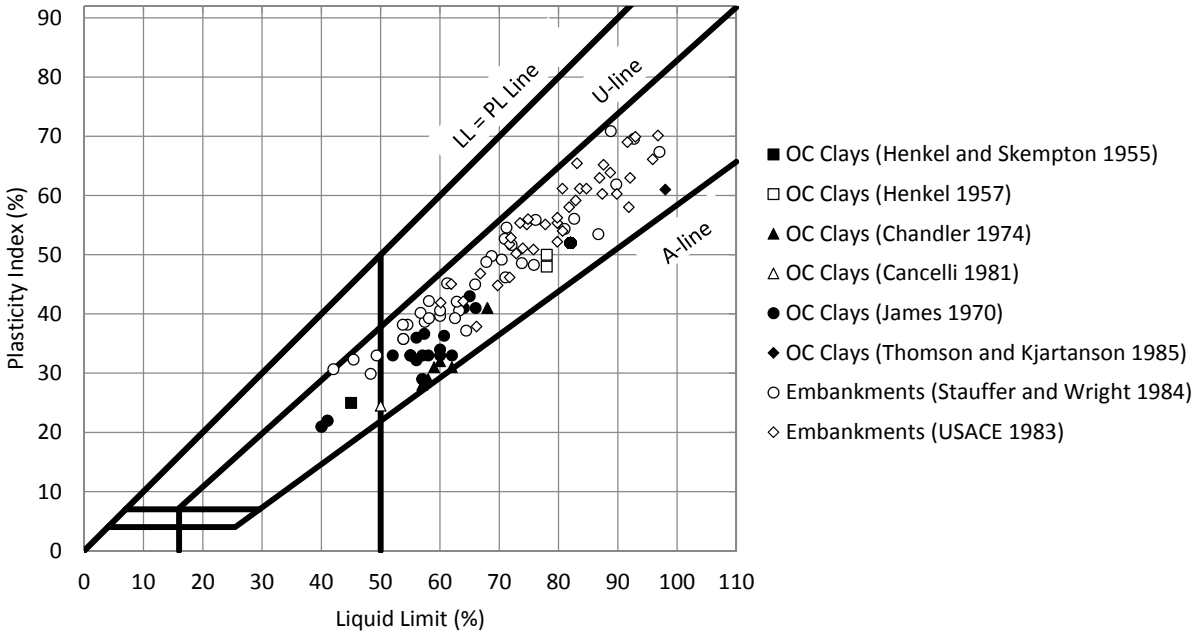

Figure 4.5 Plasticity chart showing the liquid limits and plasticity indices for soils involved in failures where the fully softened shear strength was the controlling shear strength.

The history and the structure of the clay also play and important role in this decrease in shear strength. Overconsolidated clays, in general, tend to be more brittle than normally consolidated clays. This brittleness increases with increasing OCR. Also, overconsolidated clays tend to have more diagenetic bonds that contribute to the shear strength. For these reasons, the shear strength of overconsolidated clays will be more likely to be affected by processes like progressive failure that will decrease the average mobilized shear strength on the failure plane, and weathering that will break the bonds in the clay.

Highly structured soft clays can also have a pronounced brittle behavior. A mobilized shear strength lower than the peak shear strength measured using undisturbed samples has also been reported for some soft structured Canadian clays (Lefebvre 1981). According to Lefebvre (1981), the shear strength mobilized *in situ* in this type of formation is equal to the post-peak (ultimate) shear strength measured in the triaxial device. Lefebvre acknowledged that the shear strength mobilized in this type of formation is higher than the fully softened shear strength.

The shear strength of mudstones has also been found to be decreased by weathering processes. Research performed by Chandler (1969), Nakano (1979), Yoshida (1991), Yoshida et al. (1991a), and Bhattarai et al. (2006) showed that weathering decrease the shear strength of mudstones with the lower bound of this decreased shear strength being the fully softened shear strength.

4.4 Depth of Softening

In order to establish the depths for which the fully softened shear strength should be used, case histories of first-time slides in compacted clay embankments and cuts in overconsolidated clays where the fully softened shear strength was reported as the controlling shear strength were analyzed. The vertical depth of the slides as defined in Figure 2.2 was used for this assessment.

A summary of the measured vertical depths of the failure surface is presented in Figure 4.6. From this figure it can be seen that slides in stiff clays can occur over a wide range of depths. Some of the reported deep failures were forced to go deep by the presence of a retaining wall. In compacted clay embankments, the failures tend to be shallower, as can be seen in Figure 4.6. With only one exception, all the reported slides for compacted clay embankments are less than 10-ft-deep.

The case histories used for Figure 4.6 were presented by Skempton (1948), Henkel and Skempton (1955), Henkel (1957), James (1970), Chandler (1974), Skempton (1977), Cancelli (1981), Stauffer and Wright (1984), and Thomson and Kjartanson (1985). Only first-time failures were considered.

Based on the information provided in this dissertation, it can be recommended that a method to estimate the location of the critical surface and obtain the factor of safety for the stability of shallow surfaces in compacted clay embankments is to assign the shear strength of the entire slope to the fully softened shear strength. For shallow failures, the location of the critical surface and the factor of safety will not change if the depth of softening is extended below the location of the critical surface (McCook 2012). Results presented by Kayyal and Wright (1991) showed that the observed failure surface *in situ* for shallow failures in compacted clay embankments matched the critical surface obtained from slope stability analysis using fully softened shear strength parameters. Hudacsek and Bransby (2008) performed centrifuge tests to

evaluate the effect of cycles of wetting and drying in compacted clay embankments. They found that wetting and drying cycles can cause volumetric strains that are confined in the upper 6 feet to 10 ft below the surface of the slope. These volumetric strains can break the structure created by compaction decreasing the shear strength of the soil.

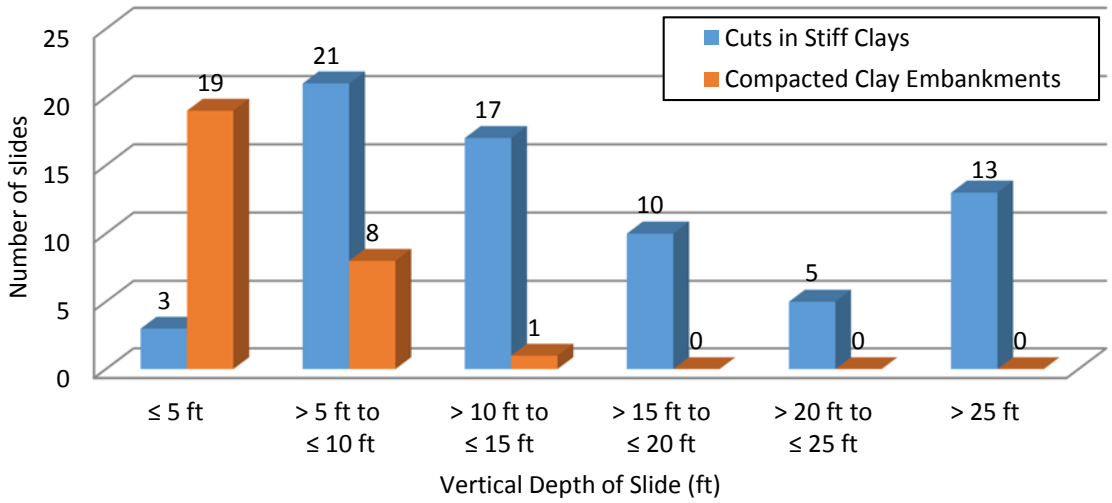

Figure 4.6 Vertical depths of slides in failures in cuts in overconsolidated clays and compacted clay embankments where the fully softened shear strength has been found to apply.

Deep-seated slides related to fully softened shear strengths appear to occur only in stiff clays. Abdel-Ghaffar (1990), Mesri and Abdel-Ghaffar (1993), and Stark and Eid (1997) recommended that the depth of this type of failures can be found by searching for the critical surface using undisturbed peak effective stress shear strength parameters. Then, this critical failure surface should be analyzed with the shear strength parameters required to account for the decrease in shear strength. In stiff clays, the location of the failure plane can be influenced by features like pre-existing landslides, bedding planes, and weak planes (James 1970; Mesri and Shahien 2003). James (1970) found that the slip surface in failures in stiff-fissured clays usually does not pass below the base of the cut and usually go along the horizontal bedding planes in the bottom part of the failure plane.

Two first-time failures of cuts in stiff clays with enough details about the shear strength of the soils involved in the slides, pore pressures at failure, and the location of the failure plane were analyzed to verify this recommendation. These were the failure at Northolt, presented by Henkel (1957), and the failure at Selborne, presented by Cooper et al. (1998).

The failure at Northolt occurred in a cut in Brown London Clay around 35 years after the cut was made. For this analysis, the shear strength of the Brown London Clay was characterized using the effective stress

shear strength parameters recommended by Chandler and Skempton (1974) and Skempton (1977). Skempton (1977) recommended a c' = 292 psf and a ϕ' = 20° for the undisturbed shear strength and Chandler and Skempton (1974) recommended a c' = 31 psf and a ϕ' = 20° for the fully softened shear strength. Using these parameters and the cross-section presented in Figure 4.7, the critical failure surfaces and factors of safety were obtained using the undisturbed peak failure envelope and the fully softened failure envelope. These failure surfaces are compared to the observed failure surface *in situ* in Figure 4.8. From this figure, it can be seen that the observed failure surface *in situ* better matches the critical failure surface obtained with undisturbed peak shear strength parameters. The factor of safety calculated using fully softened shear strength parameters for the critical failure surface obtained using peak strength parameters was equal to 1.05. This factor of safety is in close agreement with the factor of safety obtained using the fully softened failure envelope to do the entire analysis.

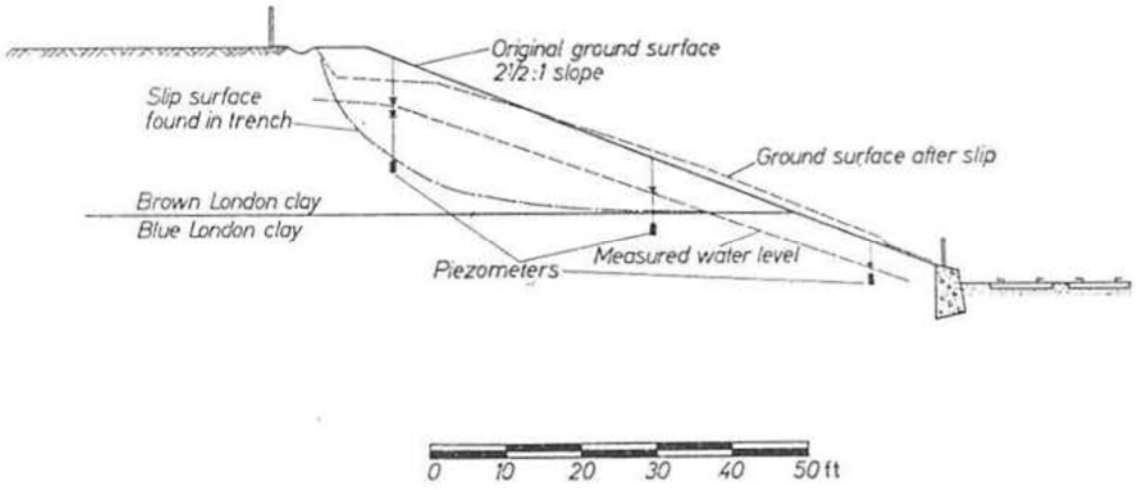

Figure 4.7 Cross-section of the cut at Northolt (Henkel 1957) (Used under fair use).

The cut at Selborne was a field experiment performed to better understand the behavior of cuts in stiff clays. The shear strength parameters used for the analysis are summarized in Table 4.1. These shear strength parameters were provided by Cooper et al. (1998). Failure was caused by increasing the pore water pressure in the cut and the pore pressures were measured using piezometers. According to Cooper et al. (1998), pore pressures corresponding to an average pore pressure ratio of 0.12 were acting on the failure plane at the moment of failure. This value was used in the analysis. The failure surfaces obtained using undisturbed peak shear strength and the fully softened shear strength are compared to the observed failure surface *in situ* in Figure 4.9. From this figure it can be seen that the critical failure surface obtained using peak shear strength parameters better matches the failure surface observed *in situ*. Also shown in this figure are the factors of safety obtained with the different shear strength parameters. The factor of safety obtained using fully softened shear strength parameters for the critical surface obtained

using peak shear strength parameters was equal to 1.05. This factor of safety is equal to that obtained using the fully softened shear strength to perform the entire analysis.

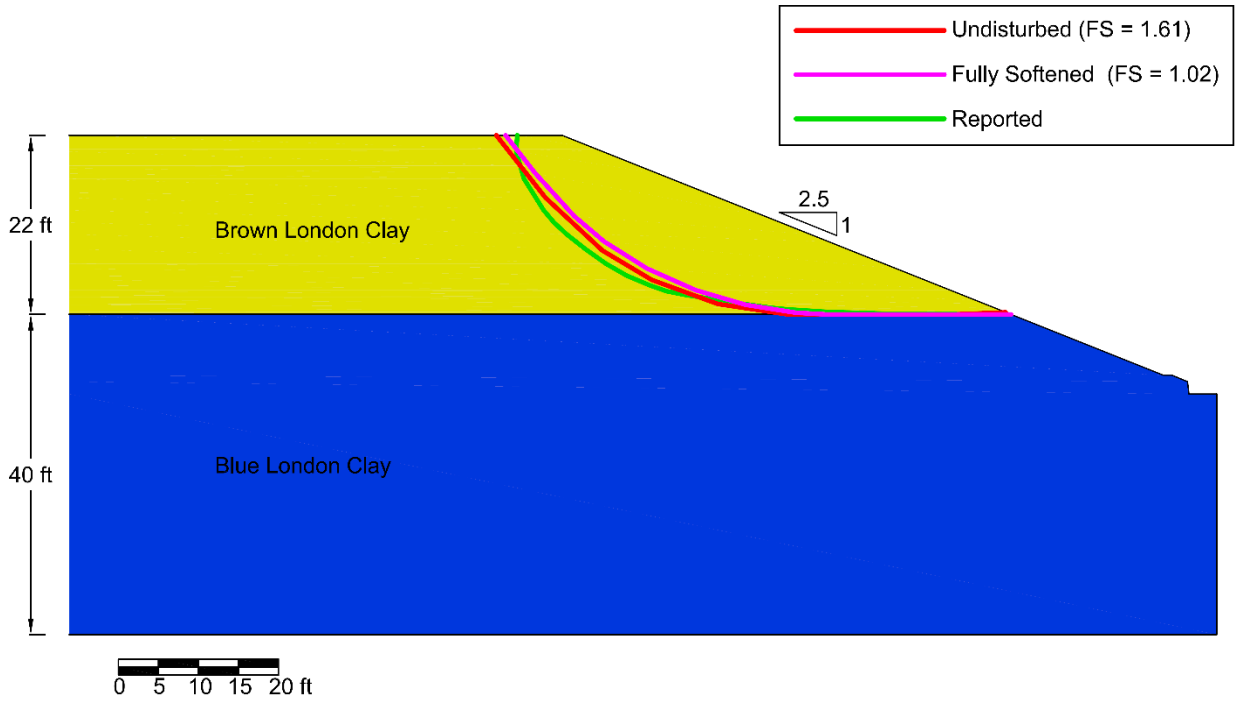

Figure 4.8 Critical and observed failure surfaces for the failure at Northolt.

Table 4.1 Shear strength properties of the soils involved in the Selborne cut (After Cooper et al. 1998) (Used under fair use).

Soil	Undisturbed Peak Shear Strength		Fully Softened Shear Strength	
	ϕ' (deg)	c' (psf)	ϕ' (deg)	c' (psf)
Soliflucted Clay	21	104	21	0
Weathered Gault Clay	24	251	22	84
Gault Clay	26	522	23	104

4.5 Effect of Climatic Conditions on the Development of Fully Softened Shear Strength

Climatic weather conditions can decrease the shear strength of overconsolidated and compacted clays. These weather conditions, represented by cycles of wetting and drying or freezing and thawing, have been found to decrease the shear strength of overconsolidated and compacted clays with the lower bound of this decreased shear strength being the fully softened shear strength (Graham and Au 1985; Botts 1986; Kayyal and Wright 1991; Leroueil et al. 1991; Wright 2005; Wright et al. 2007). Cycles of wetting and drying

in situ are caused by dry and wet seasons. In this section, the effects of the duration of the dry and wet seasons and the intensity of the rainfall event in the decrease in shear strength are evaluated based on information found in the literature. The research performed to investigate the effect of freeze and thaw cycles was already described in Section 4.2.2. Details of the effect of the duration and temperature of the freeze and thaw cycles were not found in the literature.

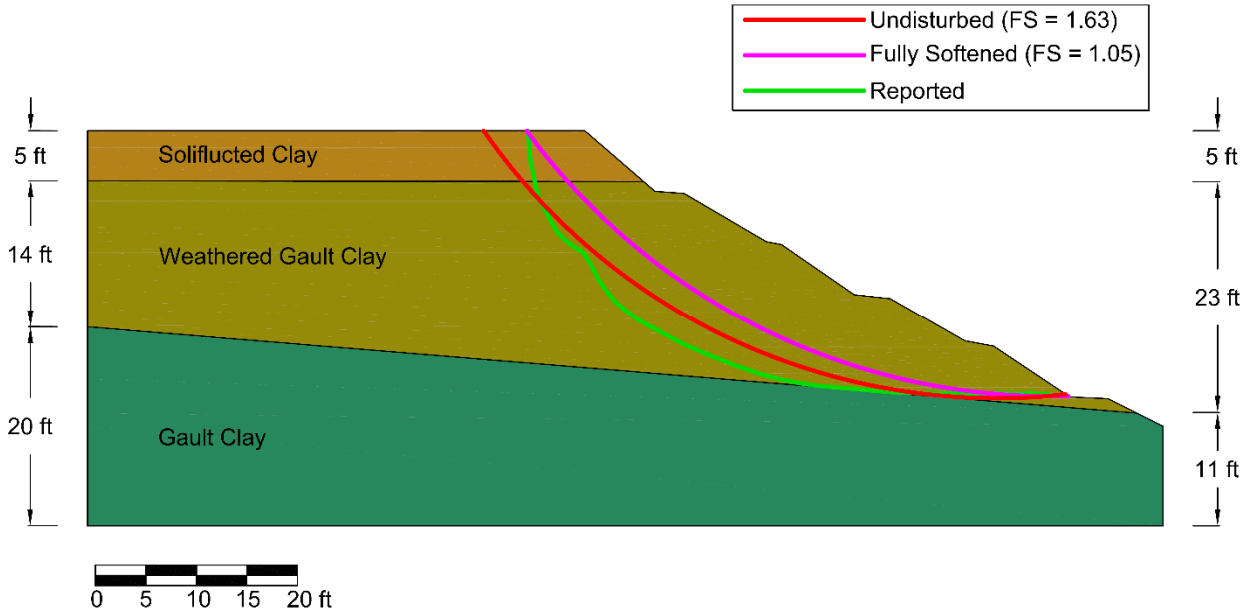

Figure 4.9 Critical and observed failure surfaces for the Selborne cut.

Botts (1998) performed CU triaxial tests on undisturbed samples and samples subjected to cycles of wetting and drying of an overconsolidated clay. The results obtained by Botts showed that increasing the duration of the drying cycle increased the swelling and the amount of shear strength lost during the wetting cycle. Rouainia et al. (2009) performed finite element analysis to investigate the effects of weather conditions on the stability of compacted clay embankments. They found that the intensity and duration of the rainfall event influence the amount of softening experience by the compacted clay embankment. If the amount of rain is kept constant, increasing rainfall intensity was found to decrease the amount of softening experience by the embankment. According to Rouainia et al., increasing the rainfall intensity will cause less infiltration in the embankments, causing an improvement on the stability. Take and Bolton (2011), using centrifuge modeling, found that the duration of the wet season does not influence the amount of pore pressure generated in the slope but it does significantly increase the amount of swelling.

The information found in the literature regarding the effect of climatic conditions on the likelihood of a soil experiencing softening is limited. The information provided above shows that softening of compacted

clay embankments will be more likely to occur in climatic conditions characterized by a long and hot dry season followed by a very wet season. So far, softening of compacted clay embankments have been found to be a problem in Texas, Mississippi and Louisiana in the U.S. and certain areas in England (USACE 1983; Kayyal and Wright 1991; Wright 2005; Wright et al. 2007; Hudacsek and Bransby 2008; Rouainia et al. 2009; McCook 2012).

4.6 Time to Failure

First-time failures in cuts in overconsolidated clays and compacted clay embankments have been found to be a time-dependent process (Henkel 1957; Skempton 1964, 1970; Vaughan and Walbancke 1973; Chandler 1974; Skempton 1977; Chandler 1984a, b; Stauffer and Wright 1984; Kayyal and Wright 1991; Leroueil 2001). The first approach to quantify the time component of failures in stiff-fissured clays was presented by Skempton (1948). Using the results of back analyses to back-calculate the shear strength required for stability, Skempton proposed the relationship presented in Figure 2.4, that shows a decrease in undrained shear strength with time.

After it was realized that the failures in stiff-fissured clays were controlled by the drained shear strength, Henkel (1957), following Skempton's approach, postulated a relationship showing a decrease in the effective stress cohesion intercept with time presented in Figure 4.10. The values of effective stress cohesion intercept were calculated assuming a constant effective stress friction angle of 20°.

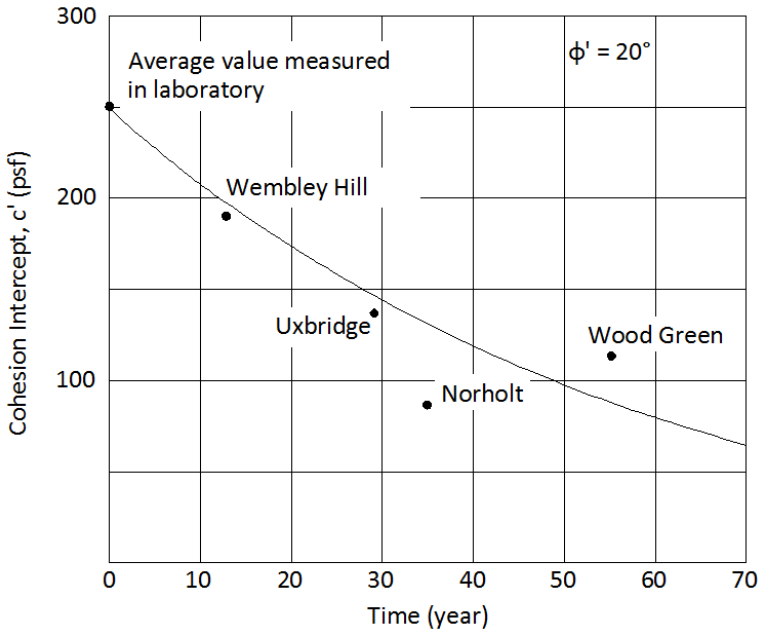

Figure 4.10 Relation between effective stress cohesion intercept and time between construction and failure (After Henkel 1957) (Used under fair use).

Another point of view was presented by Vaughan and Walbancke (1973). Observations presented by Vaughan and Walbancke showed a very slow rate of pore pressure equalization to the steady stage seepage condition from the low values following the stress reduction. This observation was used to explain the time component of the failures in cuts in stiff-fissured clays and to partially refute the theory presented by Henkel (1957). A relationship for the value of pore pressure ratio as a function of time was presented by Vaughan and Walbancke and is reproduced here in Figure 4.11. From this relationship it can be seen that after about 60 years pore pressures get equilibrated.

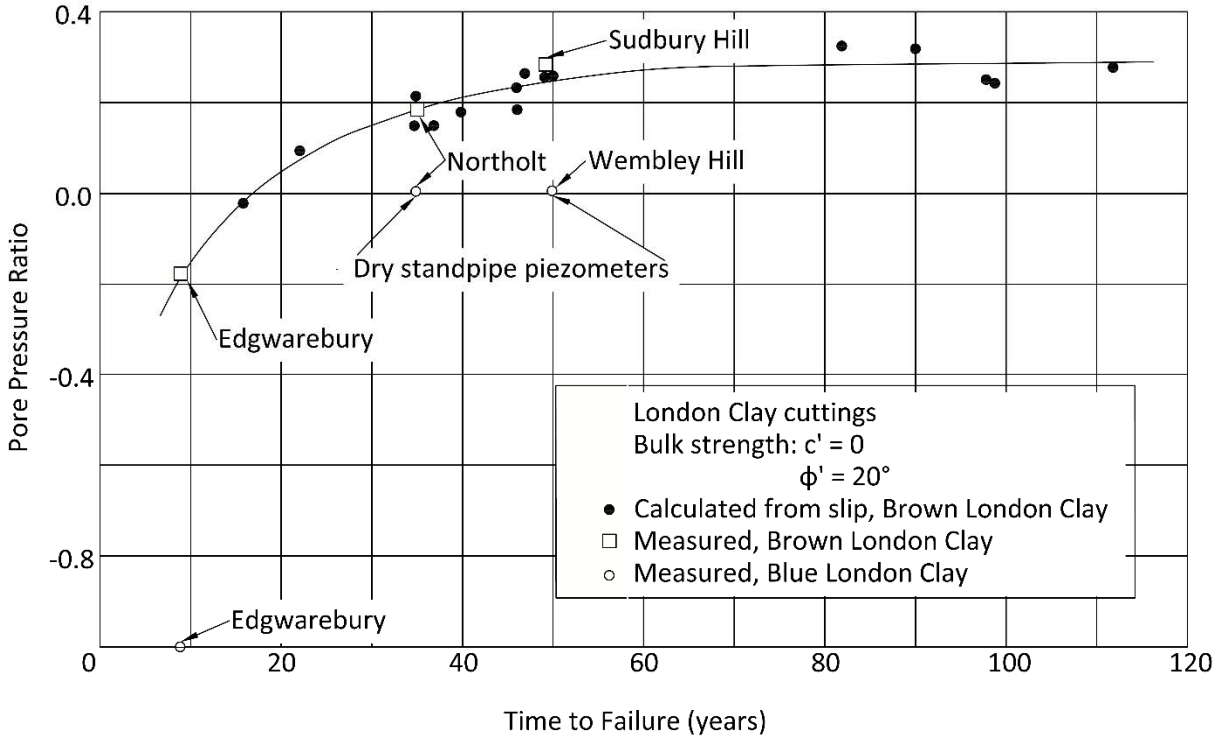

Figure 4.11 Variation of the pore pressure ratio with time (After Vaughan and Walbancke 1973) (Used under fair use).

Chandler (1974) also found that cuts in brecciated Lias Clay reached steady state seepage conditions after less than 10 years and cuts in unbrecciated Lias Clay reached steady state conditions after as much as 60 years. Skempton (1977) reported that pore pressures measured in a cut in Brown London Clay 19 years after the cut was made were half of the steady state values. Skempton also stated that the principal reason for the delay in failures in London Clay was the slow rate of pore pressure dissipation that can last 40 years to 50 years after the excavations is made.

A potential reason for the delay in first-time failures in compacted clay embankments is that the decrease in shear strength *in situ* takes time to occur. A very wet season is also usually required for failure to occur.

A model based on surface cracking, water diffusion into compacted clay embankments, and unsaturated soil mechanics was presented by Aubeny and Lytton (2002, 2003, 2004) to explain the delay in failures in compacted clay embankments.

Sixty three case histories of first-time failures in cuts in stiff-fissured clay and 28 case histories of first-time failures in compacted clay embankments, where the time to failure was reported, were collected from the literature. The times to failure are presented in Figure 4.12. From this figure, it can be seen that first-time failures in compacted clay embankments occur sooner after construction than first-time failures in cuts in stiff-fissured clays. First-time failures in compacted clay embankments usually occurs in the first 20 years after construction, while cuts in stiff-fissured clays can fail after more than 100 years after construction. The case histories used for Figure 4.12 were presented by Skempton (1948), Henkel and Skempton (1955), Henkel (1957), James (1970), Chandler (1974), Skempton (1977), Cancelli (1981), and Stauffer and Wright (1984). Only first-time slides were considered.

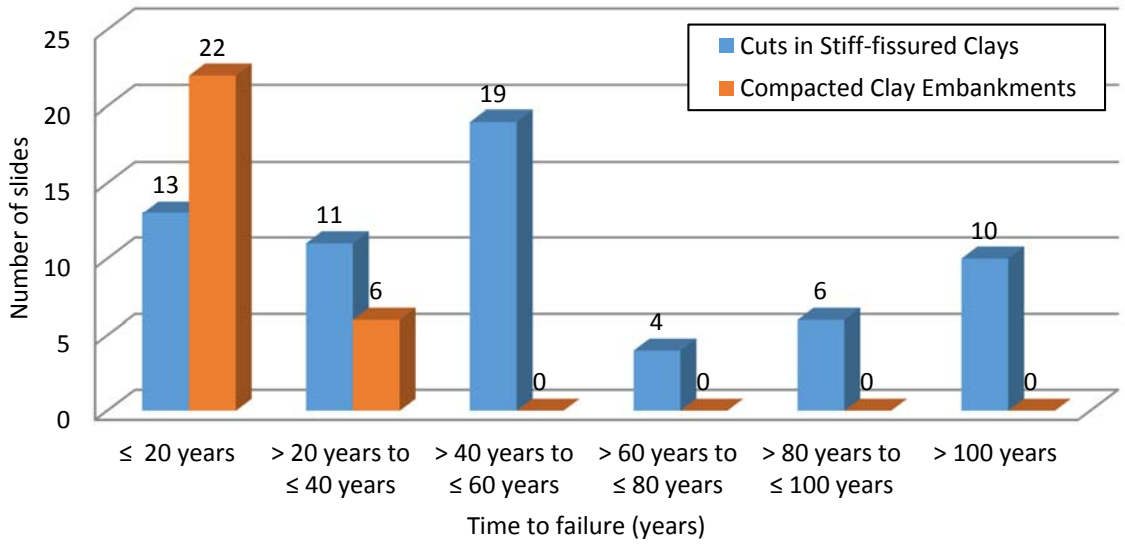

Figure 4.12 Time to failure for cuts in overconsolidated clays and compacted clay embankments where the fully softened shear strength has been found to apply.

4.7 Geotechnical Projects Affected by a Decrease in Shear Strength with Time

The use and applicability of the fully softened shear strength concept has been well documented in the literature for cut slopes in and compacted embankments constructed of clayey materials. These type of projects have already been covered in details in this dissertation. Scant information was found in the literature about the applicability of this concept to other geotechnical structures. As presented in previous sections, failures associated with the fully softened shear strength in clays occur years or tens of years

after construction. For this reason, the fully softened shear strength is not expected to be the controlling shear strength for structures of short permanency (e.g. temporary excavations).

Nakano (1979) presented a detailed investigation on the behavior of tunnels in mudstones in Japan. Based on a literature review and the analysis of case histories, Nakano concluded that if a tunnel is excavated in mudstones and the tunnel is not rock-bolted and gunnited right after the excavation is made, swelling and progressive failure can be initiated, decreasing the shear strength of the mudstone towards the fully softened shear strength. Nakano provided strong evidence to support his conclusion. More research is required to clarify and obtain more details about this phenomenon.

4.8 Pore Water Pressures

Pore water pressures are an important component of a slope stability analysis using effective stress shear strength parameters that have a significant influence on the factor of safety. The pore water pressure required in a slope stability analysis is very specific to the project and the conditions being analyzed and its selection requires geotechnical engineering judgment. For this reason, no global recommendations for pore pressure ratios to be used in final designs are given in this dissertation. Instead, the findings of different researchers are presented in order to give the reader an idea of what has been used, what has worked in the past, and what can be used for preliminary design of cuts in stiff-fissured clays and compacted clay embankments.

James (1970), after analyzing several case histories of first-time slides in stiff-fissured clays, found that the value of the pore pressure ratio obtained from slopes where piezometric readings were available usually ranged from 0.25 to 0.35. According to James, the lower bound of this range usually applies to steeper slopes and the upper bound to flatter slopes. James (1970) used a pore pressure ratio of 0.30 for the case histories he analyzed, when reliable information was not available.

Vaughan and Walbancke (1973), after analyzing case histories of first-time slides in London Clay, presented the variation of the pore pressure ratio with time for London Clay shown in Figure 4.11. From this proposed variation, it can be seen that the pore pressure ratio trends to a value of about 0.30 after 60 years. Chandler (1974) also found that a pore pressure ratio of 0.30 was in agreement with analyses performed on first-time slides in Lias Clay. A value of 0.30 for the pore pressure ratio was also recommended by Skempton (1977) for analyses of first-time slides in London Clay.

For compacted clay embankments, Day and Axten (1989) recommended the use of the infinite slope method with seepage parallel to the slope face for slope stability analyses. This same recommendation was presented by Lade (2010). A seepage parallel to the slope face corresponds to a pore pressure ratio ranging from 0.4 to 0.5 for slopes with ratios of 2H:1V to 5H:1V. Kayyal and Wright (1991) found that, in order to explain the failures that they analyzed, the fully softened shear strength should be coupled with a pore pressure ratio ranging from 0.5 to 0.6, and they recommended these values for design. In another study on compacted embankments constructed of a different fat clay, Wright et al. (2007) found that a pore pressure ratio between 0.43 and 0.53 should have existed in those embankments at the time of failure. According to Kayyal and Wright (1991) and Wright et al. (2007), these high pore pressure ratios are more or less equivalent to steady-state horizontal seepage near the face of the slope. Pore pressure

measurements in a compacted clay embankments after a rainfall even were presented by Hughes et al. (2009). These measurements show that pore pressures close to hydrostatic can exist in the upper six feet of the embankment after prolonged rainfalls. Water content measurements presented by Hughes et al. showed that the wetting front can go as deep as 20 ft.

A pore pressure ratio of 0.3 can be used for preliminary design of cuts in in stiff clays if better information is not available. For final designs, pore water pressures corresponding to steady state seepage conditions representing the worst case scenario should be used. For compacted clay embankments, pore water pressures corresponding to a water table coincident with the slope surface should be used for design if better information is not available.

4.9 Factor of Safety

The factor of safety in slope stability analysis has been commonly defined as the ratio of the shear strength of the soil to the shear stress required for equilibrium. Alternative definitions of the factor of safety have been used in the past but the definition presented previously is the most common used in slope stability analyses. The factor of safety provides a deterministic evaluation on whether the slope will be stable or not during the conditions being analyzed. A factor of safety of one represents that the slope is in the border line between stability and failure. Less than one means that the slope will not be stable for the conditions being analyzed.

The required factor of safety for a given project should be selected based on the uncertainties associated with the parameters involved in the analysis (e.g. shear strength and pore pressures) and the consequences of failure associated with the structure being analyzed. Different agencies have dissimilar requirements for the factor of safety for slope stability. The USACE, in their EM 1110-2-1902 “Slope Stability” (USACE 2003), requires a factor of safety of 1.5 for long-term conditions with steady state seepage conditions for their dams. According to Duncan and Wright (2005), the factors of safety presented in EM 1110-2-1902 are based on experience and are adequate for USACE projects, where more or less the same exploration techniques, testing procedure, and analysis methods are used in every project. For projects where the conditions are different, these factors of safety might not be appropriate (Duncan and Wright 2005). The same factor of safety is also required by The United States Department of Agriculture (USDA) in their Technical Release (TR) 60 “Earth Dams and Reservoirs” (USDA 2005). The U.S. Department of the Interior Bureau of Reclamation (USDIBR) in their Design Standards No. 13 “Embankment Dams” (USDIBR 2011) requires a factor of safety of 1.5 for steady state seepage conditions under the active conservation pool and 1.2 under the maximum reservoir level (during a probable maximum flood). These factors of safety, like the factors of safety presented by the USACE, are expected to apply to projects of the agency that proposed them, where the protocols for subsurface investigation, laboratory testing, and methods of analysis should be standardized.

The factors of safety presented above are for earth dams and levees. Different factors of safety are required for highway embankments. For example, the Texas Department of Transportation (TXDOT), in their “Geotechnical Manual,” requires a minimum factor of safety of 1.3 for both long and short term

conditions, except for slopes that support abutments, buildings, or any other structure with a low tolerance for failure, for which a factor of safety of 1.5 is required (TXDOT 2012).

As stated before, the minimum factor of safety required should be based on the uncertainties with the parameters used for design and the consequences of failure. Based on these parameters, Duncan and Wright (2005) proposed the factors of safety presented in Table 4.2. These factors of safety can be applied to any project, but require some engineering judgment to quantify the degree of uncertainty with the parameters involved in the analysis.

Table 4.2 Recommended minimum values of factor of safety (Duncan and Wright 2005) (Used under fair use).

Cost and Consequences of Slope Failure	Uncertainty of Analysis Conditions	
	Small[1]	Large[2]
Cost of repair comparable to incremental cost to construct more conservatively designed slope	1.25	1.50
Cost of repair much greater than incremental cost to construct more conservatively designed slope	1.50	2.00 or greater

[1] The uncertainty regarding analysis conditions is smallest when the geologic setting is well understood, the soil conditions are uniform, and thorough investigations provide a consistent, complete, and logical picture of conditions at the site.

[2] The uncertainty regarding analysis conditions is largest when the geologic setting is complex and poorly understood, soil conditions vary sharply from one location to another, and investigations do not provide a consistent and reliable picture of conditions at the site.

From the previous discussion, it can be seen that recommendations for the factor of safety that should be used in conjunction with fully softened shear strength parameters are not available for earth dams, levees, and highway embankments in the guidelines of major agencies. Based on back-analyses of first-time failures in London Clay, James (1970) presented a graph showing a decrease in factor of safety with time, reproduced here as Figure 4.13. The factor of safety for first-time slides were calculated using fully softened shear strength parameters. James (1970) recommended that a factor of safety of 1.35 could be used in conjunction with fully softened shear strength parameters. James stated that this factor of safety would assure that the overall factor of safety in the slope will be just above one even if the residual shear strength is being mobilized or if progressive failure is acting on the failure plane.

From Figure 4.13, it can be inferred that, although a factor of safety of 1.35 covers most of the failures presented, it does not cover all the failures. Four case histories are presented that had a factor of safety above 1.35 and failed. These case histories are the two slides at Bradwell (FS = 2.53 and 1.68 and failed right after construction), the slide at Isle of Sheppey (FS = 2.4 and time to failure of seven years), and the slide at Kingsbury (FS = 1.52 and time to failure of 15 years). The slide at Bradwell is a short-time failure that occurred five days after construction. This case history is an undrained failure and should not be analyzed using drained strength parameters because the pore pressures are not known. More details about this failure are presented by Skempton and LaRochelle (1965). The slide at the Isle of Sheppey is presented by James (1970). For this case history, James was not sure if this slide was in London Clay or

some other formation which means that the shear strength parameters used might not be appropriate. The slide at Kingsbury is presented by James (1970). In this case history, the location of the failure plane and the value of pore pressure ratio were assumed. These assumptions will have a significant influence in the factor of safety obtained.

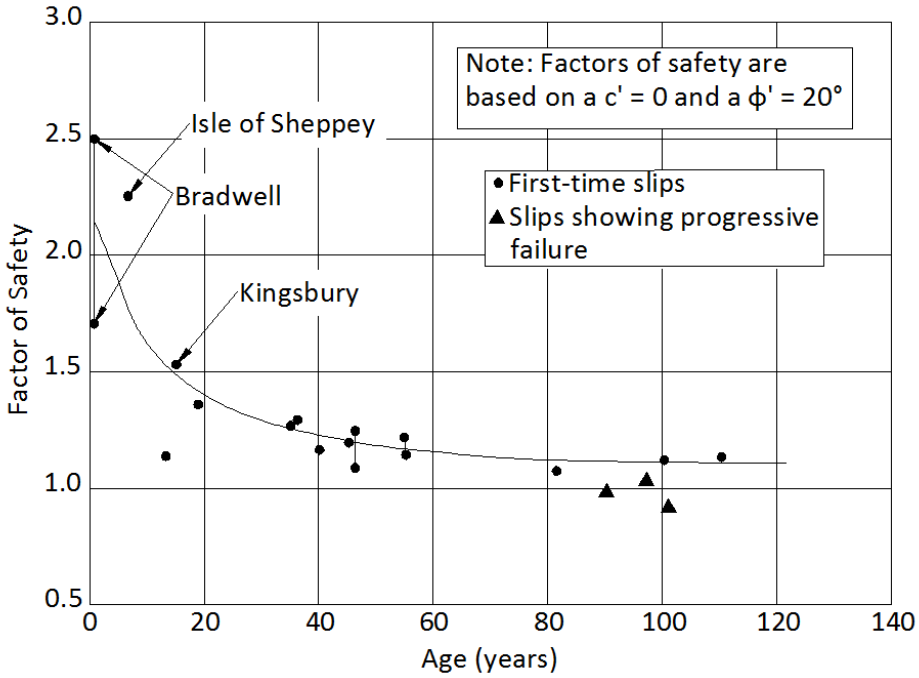

Figure 4.13 Decay in factor of safety with time (After James 1970) (Used under fair use).

The factors of safety above unity presented in Figure 4.13 for slopes that already failed imply, except for the cases explained above, either that higher pore pressures than estimated were acting on the failure plane or that the shear strength mobilized was lower than the fully softened shear strength.

Atkinson and Bransby (1978), and Atkinson (1981) suggested that a lower factor of safety than usually required for design using undisturbed drained peak shear strength could be used if critical state strengths are used, although a specific value was not given. Swanson and Jones (1984) presented design recommendations for slopes in overconsolidated fat clays in the Potomac formation. For slopes in this formation, Swanson and Jones recommended the use of a factor of safety of 1.25 for small project where the probability of loss of life and property is small, a factor of safety of 1.5 for projects where the probability of loss of life and properties is large, and a factor of safety of 2.0 for high risk situations. Schofield (2005, 2006) recommended that a factor of safety of 1.25 was safe and not over-conservative to be used with critical state shear strength parameters. McCook (2012) recommended to use a factor of safety of 1.1 for shallow failures and 1.5 for deep-seated failures.

Based on the discussion presented above, the factors of safety proposed by Duncan and Wright (2005), presented in Table 4.2 are recommended to be used in conjunction with fully softened shear strength parameters. To be more specific, for shallow failures, the consequences of failure are often very low. For this reason, if the fully softened shear strength is used coupled with a water table corresponding to the worst case scenario possible, a factor of safety as low as 1.25 can be used. For deep failures, the consequences of failure will vary depending on the structure. The pore pressure for this type of analyses should be based on the worst seepage condition expected throughout the life of the project. In this case, for structures with low to mid consequences of failure, a factor of safety of 1.35 can be used. For structures with a high consequence of failure, a factor of safety of 1.50 can be used.

4.10 Curvature of the Fully Softened Shear Strength Envelope

The curvature of the fully softened failure envelope has been acknowledged by many researchers (e. g., Mesri and Cepeda-Diaz 1986; Kayyal and Wright 1991; Stark and Eid 1997; Mesri and Shahien 2003; Stark et al. 2005; Wright 2005; Duncan et al. 2011). The downward curvature of the fully softened failure envelope implies that the fully softened secant friction angle decreases with increasing consolidation stress. This decrease in secant friction angle has been attributed to the tendency of the clay particles to a more face-to-face orientation with increasing consolidating pressure (Stark and Eid 1997; Mesri and Shahien 2003).

There have been numerous attempts to develop an equation to characterize the curvature of the Mohr-Coulomb failure envelope (De Mello 1977; Charles and Watts 1980; Atkinson and Farrar 1985; Maksimovic 1989; Crabb and Atkinson 1991; Mesri and Shahien 2003; Noor and Anderson 2006; Lade 2010; McCook 2012). Some of these equations are very complex and do not offer extra benefits when compared to simpler equations like the one presented by Lade (2010). In his paper, Lade suggested to characterize the curvature of the failure envelope using the power function presented in Equation 4.1. It should be mentioned that although other authors have suggested the use of power functions to characterize the curvature of the failure envelope (De Mello 1977; Charles and Watts 1980; Atkinson and Farrar 1985; Maksimovic 1989; Crabb and Atkinson 1991; McCook 2012), Lade was the one that suggested to normalize the stresses in the equation so that the fitting parameters become unitless.

$$\tau = aP_a \left(\frac{\sigma'}{P_a}\right)^b \tag{4.1}$$

Where:

- τ = Shear strength of the soil.
- a, b = Curve fitting parameters.
- P_a = Atmospheric pressure.
- σ' = Effective normal stress on the failure plane in the same units as atmospheric pressure.

The curvature of the failure envelope, using the equation presented above, is controlled by the parameter b and the shear strength is controlled by both *a* and *b*. As *b* increases, the curvature of the failure envelope decreases until *b* is equal to one, and the failure envelope becomes linear. The above representation of the curvature of the failure envelope was used to characterize the failure envelopes of the soils tested in this investigation presented in Chapter 6. Details on how to obtain the parameters *a* and *b* from shear strength tests are presented in Section 6.2.4. For linear envelopes (i.e. *b* = 1), the parameter *a* is equal to $\tan \phi'$.

The calculated factor of safety for slope stability and the location of the critical failure surface are influenced by whether a curved or linear failure envelope is used. To illustrate this, a hypothetical 20-ft-tall embankment with a 3H:1V slope constructed of Vicksburg Buckshot Clay was analyzed using the slope stability software SLIDE by Rocscience Inc. The slope was analyzed using Spencer's method. The cross-section of the slope analyzed is shown in Figure 4.14. The linear and nonlinear shear strength parameters used in this example were obtained from the direct shear test results shown in Figure 4.15. From these results, the parameters obtained for the linear failure envelope were a c' = 214 psf and a ϕ' = 16.7°, and a = 0.4266 and b = 0.7292 for the curved failure envelope.

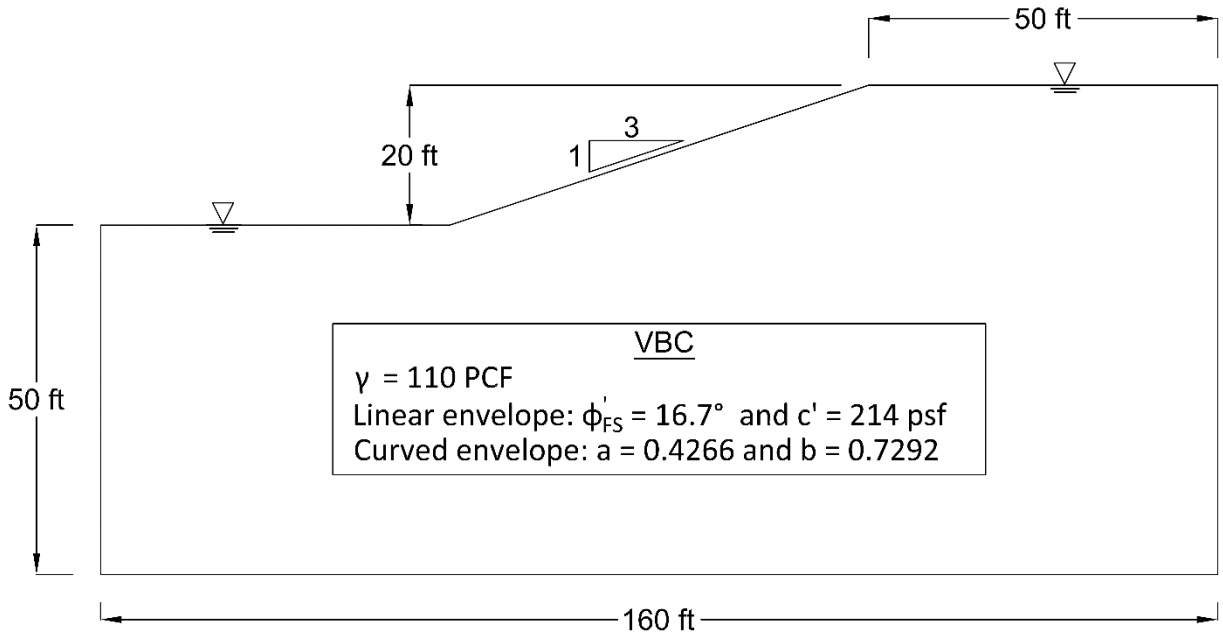

Figure 4.14 Hypothetical slope.

The results of the slope stability analyses performed are presented in Figure 4.16. From this figure it can be seen that using a linear fully softened failure envelope increases the factor of safety and the depth of the failure surface obtained. Similar results have been presented by Duncan et al. (2011) and McCook (2012). The reason for the increase in factor of safety is that the shear strength at low effective stresses

is overestimated by fitting a line to an envelope that is curved. Enough data have been presented in the literature (Kayyal and Wright 1991; Terzaghi et al. 1996; Stark and Eid 1997; Stark et al. 2005; Wright 2005; Wright et al. 2007; Stark and Hussain 2013) and in Chapter 6 of this dissertation that shows that the fully softened failure envelope is curved. For this reason, a curved interpretation of the fully softened failure envelope is required to obtain the correct factor of safety.

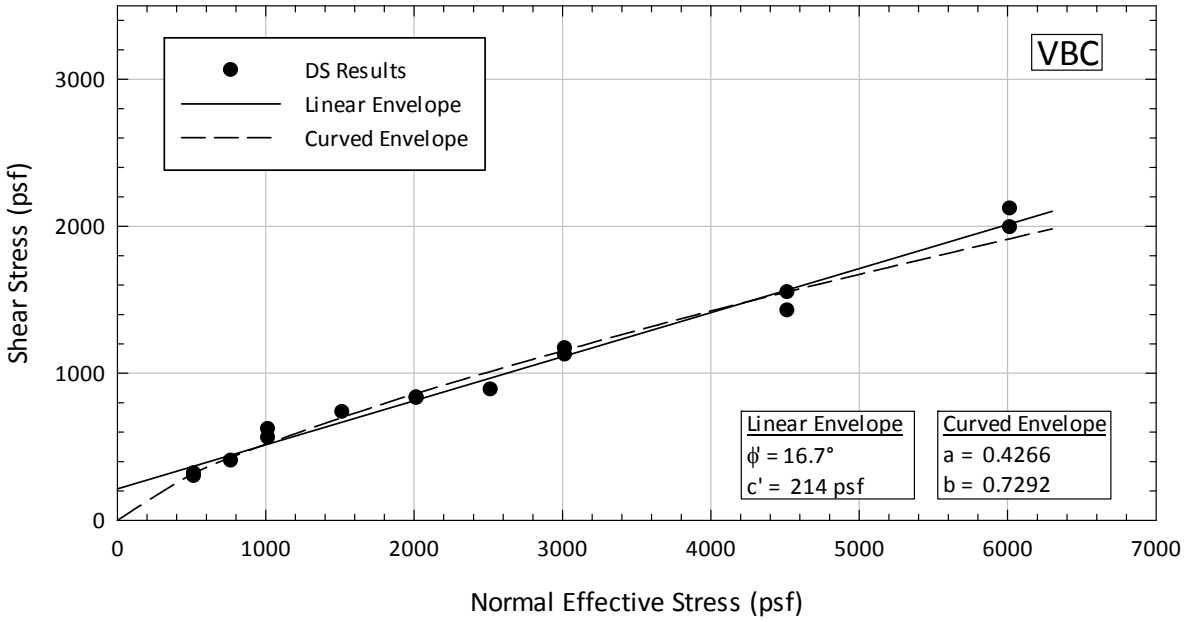

Figure 4.15 Linear and curved failure envelopes from direct shear test results from VBC.

4.11 Conclusions

Based on the literature reviewed and the case histories analyzed, it can be concluded that softening is only a problem in clays with a liquid limit above 40 and a plasticity index above 20, mudstones, and structured soft clays. Among clays, overconsolidated clays are more likely to experience a decrease in shear strength *in situ* than normally consolidated clays.

For cuts in stiff clays, the fact that (1) softening and increased water content are just observed in the vicinity of the failure plane, and (2) the observed failure plane *in situ* better matches the critical failure plane found in slope stability analysis using undisturbed peak effective stress shear strength parameters tend to support progressive failure above the other proposed mechanisms. The presence of fissures will also decrease the shear strength of the clay mass, but this is not believed to be the factor causing a decrease in drained shear strength towards the fully softened shear strength of cuts in stiff clays. Weathering, represented by cycles of wetting and drying or freezing and thawing, will also have an influence on the shear strength of this type of material, although this will only affect shallow depths (less than 10 ft deep).

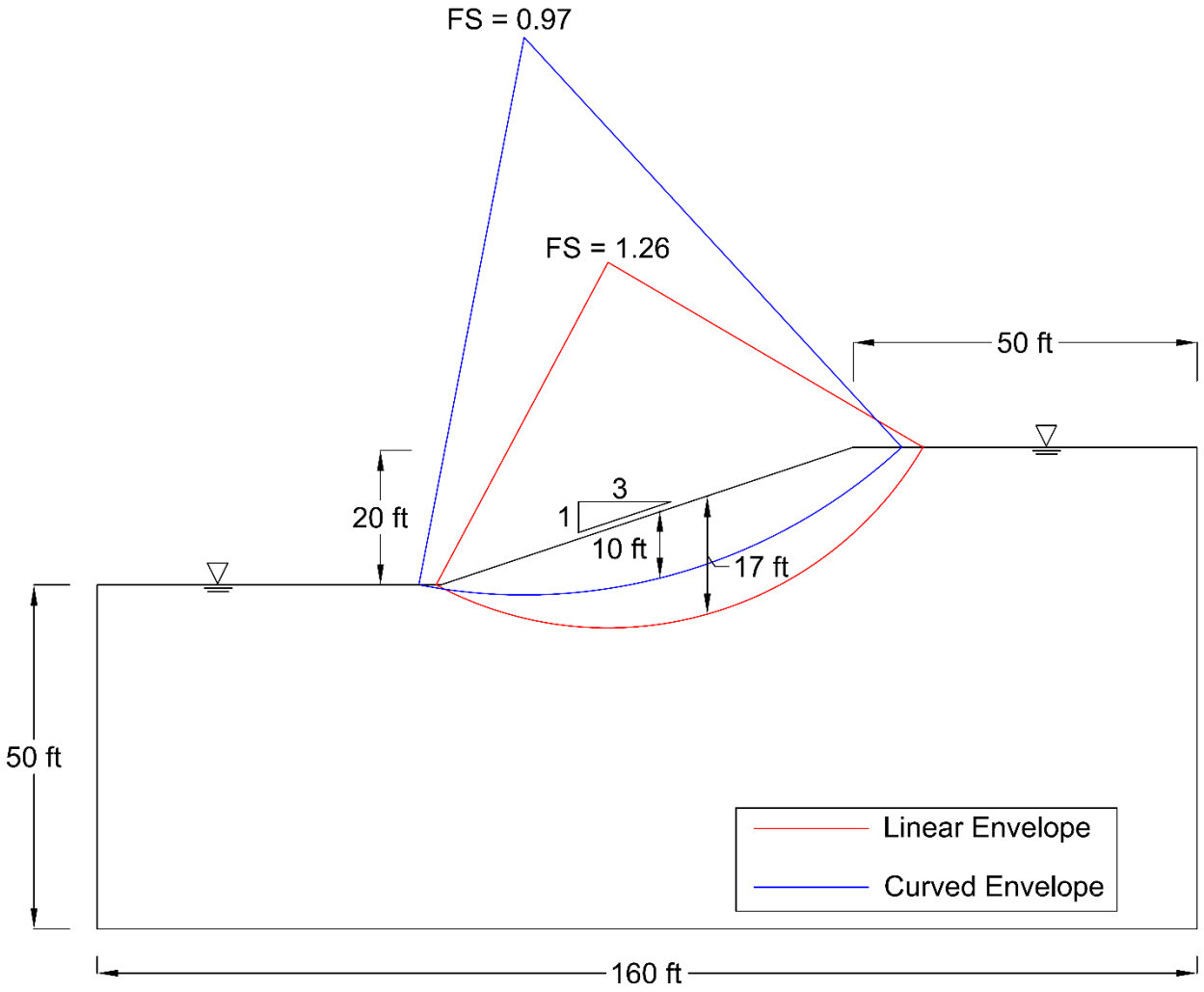

Figure 4.16 Effect of curvature of the failure envelope in the results obtained from slope stability analyses.

For first-time slides in cuts in stiff clays, the depth of the failure plane varies within a wide range. Abdel-Ghaffar (1990) and Mesri and Abdel-Ghaffar (1993) suggested that to obtain the critical failure surface, drained undisturbed peak shear strength parameters should be used in limit equilibrium analyses. Then, the obtained failure surface should be analyzed using the fully softened shear strength. This method was investigated in this dissertation and compared to just using the fully softened shear strength to analyze the cut. The method suggested by Abdel-Ghaffar and Mesri provided a better match of the critical failure surface and the failure surface observed *in situ* when compared to using the fully softened shear strength in the entire cross-section. However, the factor of safety obtained with Abdel-Ghaffar and Mesri's method was about the same as that obtained by analyzing the entire cut with the fully softened shear strength. Using the fully softened shear strength to analyze the entire cut is a simpler method to implement, requires less laboratory testing, and will give you the correct factor of safety. For this reason, this method should be used to design cuts in stiff clays. A pore pressure ratio of 0.3 seems to be appropriate

preliminary design or if better information is not available for cuts in stiff clays. For final designs, pore pressures corresponding to steady state seepage conditions should be used.

For compacted clay embankments, the main mechanism causing the decrease in shear strength appears to be weathering. Both cycles of wetting and drying or freezing and thawing will decrease the drained shear strength of compacted clays towards the fully softened shear strength. This mechanism is supported, above the others mechanisms, by the fact that first-time failures related to fully softened shear strength are usually shallow and that the observed failure plane *in situ* better matches the critical surface obtained performing slope stability analyses using fully softened shear strength parameters. Even though weathering seems to be the main mechanism decreasing the shear strength, it cannot explain the phenomenon in every case. This is reflected in the laboratory test results presented by Wright et al. (2007), where cycles of wetting and drying did not reduce the shear strength of the soil studied to the fully softened shear strength. Despite this fact, the fully softened shear strength was necessary to obtain a factor of safety of one in the case histories analyzed by Wright et al. (2007). From the results presented by Kovacevic et al. (2001), it seems that progressive failure also influences the shear strength mobilized *in situ* in this type of project.

For analysis of shallow slides in compacted clay embankments, the shear used in the analysis should be the fully softened strength. For slope stability analysis of these embankments, pore pressures corresponding to a water table coincident with the slope surface should be used for design, if better information is not available. To analyze deep failures, not related to fully softened shear strength, the shear strength of the first 10 ft below the face of the embankment should be assumed as the fully softened shear strength. This recommendation is based on the fact that all the first-time slides related to softening in this type of construction are below 10 ft deep. The shear strength of the soil in the foundation of the embankment should be based on shear strength tests performed using undisturbed samples. Softening of the foundation soil is not expected to occur after the embankment is in place.

For failures in soft structured clays, like the ones often encountered in Canada, creep seems to be the mechanism behind the decrease in shear strength. For slopes in this type of soil, the ultimate shear strength measured in a CU triaxial test may be useful for design. More research is required to better characterize the behavior of these soils involved in first-time failures of slopes.

Although the use of fully softened strengths may empirically account for progressive failure effects, more information and research is also needed to better understand the phenomenon of progressive failure and how to incorporate it into slope stability analyses.

First-time failures in compacted clay embankments and stiff clays related to fully softened shear strength are more likely to occur in climates characterized by a long and hot dry season followed by a long wet season. Also, in climates with wet summers and cold winters.

First-time failures related to fully softened shear strength are a time-dependent process. Failures in compacted clay embankment occur sooner after construction than cuts in stiff clays. The reason for the time component in cuts in stiff clays is the slow dissipation of pore pressures from the low values after the cut to return to the steady state seepage conditions. In compacted clay embankments, the time

component is caused by the time required for the drained shear strength to be decreased to the fully softened shear strength and the time required for a heavy rain to cause elevated pore pressures.

Different factors of safety for stability have been proposed by various agencies to design earth dams, levees, and compacted clay embankments. The factors of safety proposed by Duncan and Wright (2005), presented in Table 4.2 are recommended by the author to be used in conjunction with fully softened shear strength parameters. The reasons for this recommendation are that the factors of safety proposed by the different agencies do not include a recommendation for fully softened shear strength parameters, that the recommendations by Duncan and Wright (2005) are independent of any agency protocols, and that these recommendations take into account the two of the most important aspects required to define a factor of safety, which are uncertainties in the parameters used in the analyses and consequences of failure. To be more specific, for shallow failures, the consequences of failure are very low. For this reason, if the fully softened shear strength is coupled with a water table corresponding to the worst case scenario possible, a factor of safety as low as 1.25 can be used. For deep failures, the consequences of failure will vary depending on the structure. The pore pressure for this type of analyses should be based on the worst seepage condition expected throughout the life of the project. In this case, for structures with low to mid consequences of failure, a factor of safety of 1.35 can be used. For structures with a high consequence of failure, a factor of safety of 1.50 can be used.

The curvature of the fully softened failure envelope was found to have a significant influence on the factor of safety for slope stability and the location of the critical failure plane obtained. Deeper failure surfaces and higher factors of safety are obtained if a linear interpretation is made to fully softened shear strength measurements and this interpretation results in a cohesion intercept. For this reason, it is recommended that a curved failure envelope should be used for design. A practical representation of the curvature of the failure envelope can be done using Equation 4.1.

Chapter 5

Measuring Fully Softened Shear Strength

5.1 Introduction

The value of the results obtained from testing remolded samples begins with the quality of the sample preparation technique used. Proper sample preparation allows the creation of repeatable and homogenous test specimens that could represent the soil that needs to be characterized. After a soil sample is prepared, a device that can measure the desired soil property is required. The most common devices available in geotechnical engineering to measure drained shear strength of soils are the direct shear, ring shear, and triaxial devices. There are not many published research results comparing the peak shear strength measured with these three devices. Historically, the fully softened shear strength has been measured using the direct shear and triaxial devices (Gibson 1953; Bishop et al. 1965; Skempton 1977; Cancelli 1981; Stark and Eid 1997; Stark et al. 2005; Bhattarai et al. 2006; Wright et al. 2007). Recently, the ring shear device has also been used for this purpose (Stark and Eid 1997; Stark et al. 2005). The triaxial and direct shear devices have been used successfully in the past to measure peak shear strength and their results verified using back-analyses. The ring shear device was designed mainly to investigate the residual shear strength of soils because an infinite displacement can be applied in one direction to a shear surface. This device has not often been used to measure the peak shear strength of soils. Thus, its ability to measure the correct peak shear strength is not yet proven.

The objectives of this chapter are (1) to describe the soils used in this investigation, (2) to present a method to prepare soil samples for fully softened shear strength measurements, (3) to describe the equipment used, (4) to present procedures to form test specimens to measure the fully softened shear strength in the direct shear, ring shear, and triaxial devices, and (5) to compare these different shear devices.

5.2 Soils

In order to provide a thorough assessment of the effects of the device and sample preparation techniques used on the measured fully softened shear strength, 15 different clays were used in this research. These clays covered a wide range of geographic locations, liquid limits, liquidity indices, and clay-sized fractions. The clays used were six soils from Dallas, Texas, which were processed and sent to Virginia Tech by ERDC; clays from projects in Cullman, Alabama; Silverstone, Colorado; Northern Virginia (NOVA Clay); the Oahe

Dam foundation in South Dakota; and Oak Harbor clay from Ohio, and Vicksburg Buckshot Clay (VBC) from Mississippi that were available at Virginia Tech. NOVA Clay and VBC have been used in other research projects at Virginia Tech (Geiman 2005; Rafalko 2006). Also, the VBC has been used in research projects of the USACE (Ladd and Preston 1965; Mitchell et al. 1965; Al-Hussaini and Townsend 1974). The soil index properties of these soils are presented in Table 5.1 and in the plasticity chart presented in Figure 5.1. The soil index properties were measured following the testing procedure outlined in the ASTM corresponding to the property being measured.

Table 5.1 Soil index properties

Sample	Specific Gravity (ASTM D854-10)	USCS (ASTM D2487-11)		Atterberg Limits (ASTM D4318-10)			Clay-sized Fraction (< 2µm) (ASTM D422-63 (2007))
		Symbol	Group Name	LL	PL	PI	
Texas 1	2.78	CH	Fat Clay	68	25	43	63
Texas 2	2.78	CH	Fat Clay	66	23	43	58
Texas 3	2.82	CH	Fat Clay	65	21	44	55
Texas 4	2.81	CH	Fat Clay	66	24	42	67
Texas 5	2.86	CH	Fat Clay	76	28	48	59
Texas 6	2.85	CH	Fat Clay	73	26	47	51
Alabama 1	2.73	CL	Lean Clay	42	23	19	33
Alabama 2	2.72	CH	Sandy Fat Clay	51	26	25	40
Alabama 3	2.79	ML	Silt	47	29	18	29
Alabama 4	2.71	CL	Lean Clay	43	23	20	37
Colorado Clay	2.78	CL	Lean Clay	42	22	20	24
NOVA Clay	2.80	CH	Fat Clay	66	28	38	17
Oahe Dam	2.88	CH	Fat Clay	74	24	50	50
Oak Harbor	2.82	CL	Lean Clay	47	22	25	47
VBC	2.79	CH	Fat Clay	78	26	52	69

5.3 Sample Preparation

Soil samples should be first soaked in water for at least two days, as shown in Figure 5.2. Even though distilled water was used for this project, site-specific water is preferred if available. Some of the soil samples were blenderized after the soaking stage and prior to sieving. For this purpose, a conventional household blender, shown in Figure 5.3, was used. During blenderizing, water was added in order to create a homogenous mass. Then, the soil was pushed or washed through a No. 40 (425 µm) sieve.

After sieving, the test soil was at a water content greatly in excess of that acceptable for forming test specimens. Test specimens were normally molded at water contents equivalent to liquidity indices ranging from about 0.6 to 2.0. To reduce the water content, the soil samples were air-dried in funnels or

bowls with filter paper, as shown in Figures 5.4 and 5.5. A fan directed on the soil sample was sometimes used to help speed up the drying process. For samples with a target water content equal to the liquid limit, a Casagrande liquid limit cup was used to infer the moisture content. The liquid limit test specimen was prepared in the usual fashion, as described in ASTM D4318-10, and the water content was assumed to be correct when the number of blows required to close the gap cut in the soil was in the range of 23 blows to 25 blows. Other values of target water content were verified by standard water content measurements, either using a microwave oven (ASTM D4643-08) or a convection oven (ASTM D2216-10).

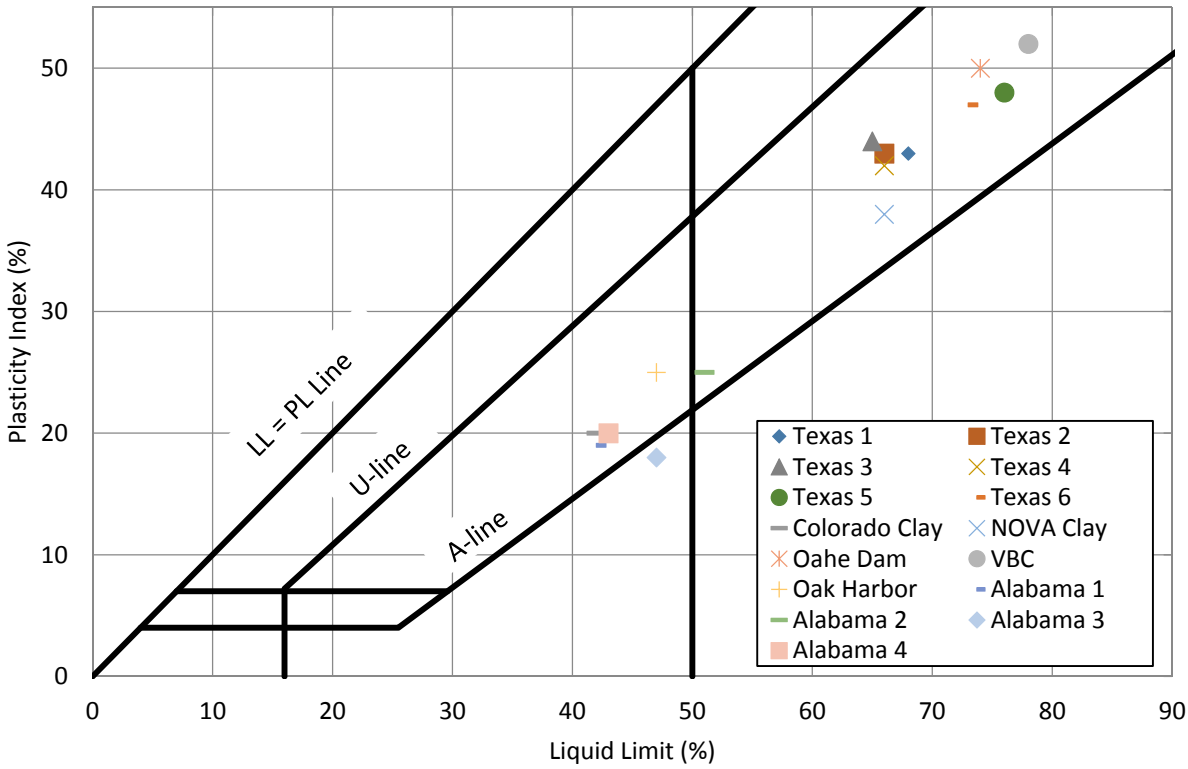

Figure 5.1 Plasticity chart showing the soils tested.

5.4 Shear Testing Equipment

The laboratory testing program of this research was performed using ring shear, direct shear, and triaxial devices to measure the fully softened shear strength. These three devices are described in this section.

Figure 5.2 Soil samples allowed to soak in water.

Figure 5.3 Soil sample ready to be blenderized.

Figure 5.4 Soil sample being air-dried in funnels with filter paper.

Figure 5.5 Soil sample being air-dried in a bowl with filter paper.

5.4.1 Direct shear device

The direct shear apparatuses used in this investigation were GeoTac devices fabricated by Trautwein Soil Testing Equipment and an example is shown in Figure 5.6. This device can test circular and square test specimens, although mainly circular test specimens were used in this research. The circular test specimens had a diameter of 2.5 inches. The average initial height of the test specimens was around 1.4 inches instead of the normal 1.0 inches. This was done to accommodate the large amount of vertical strain that occurs during consolidation of the test specimen. The test specimens were formed directly in the shear box as described in Section 5.5. The direct shear box and top platen assembly for this device can be seen in Figure 5.7. In this device, tests specimens are prevented from expanding laterally by the specimen container during the consolidation stage (K_o conditions) and are compressed between two porous stones to allow drainage.

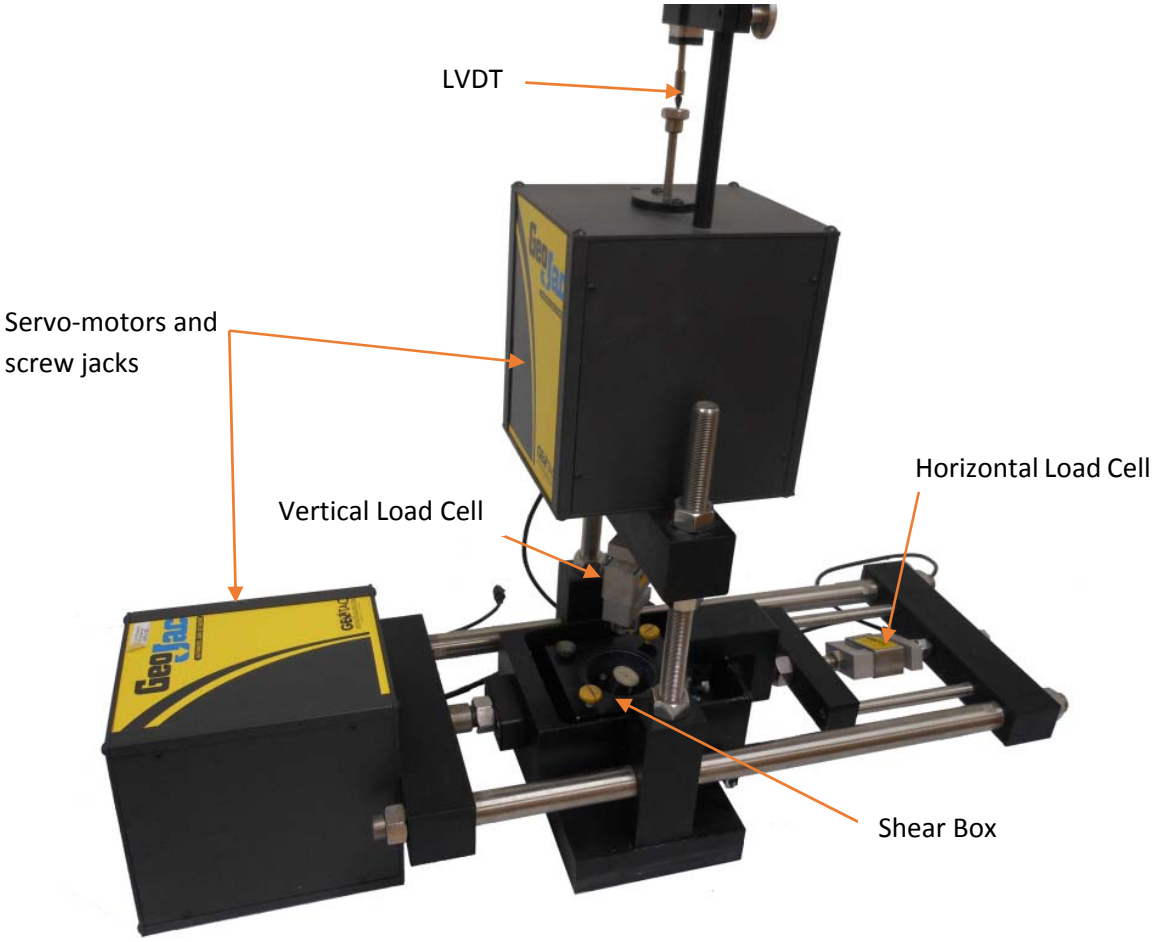

Figure 5.6 Direct shear device fabricated by Trautwein Soil Testing Equipment.

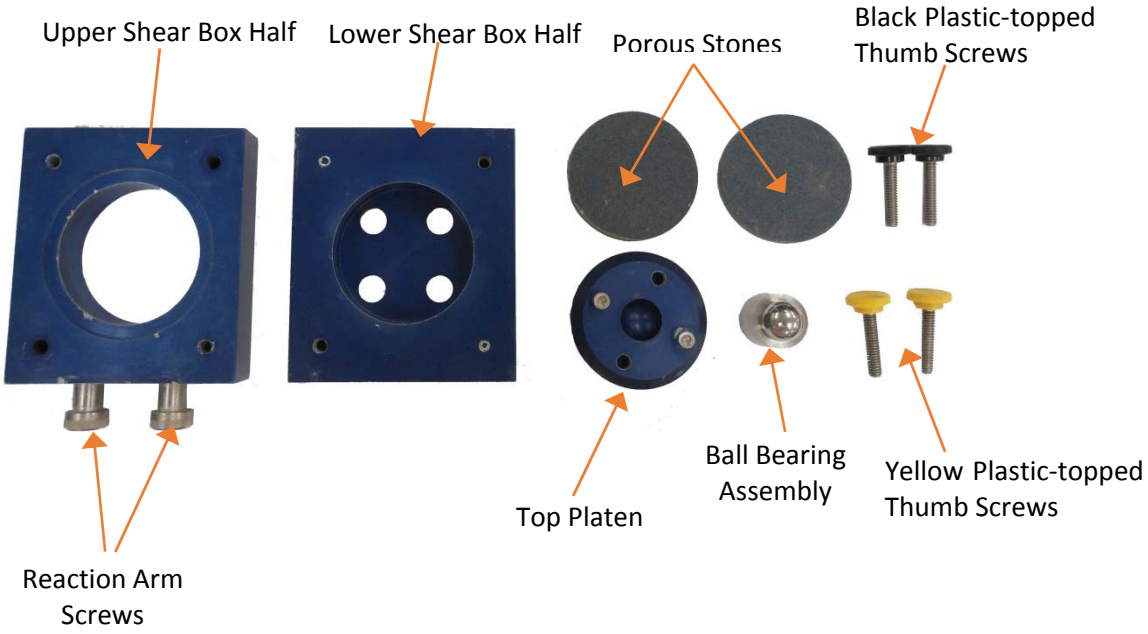

Figure 5.7 Direct shear box and top platen assembly.

For this research, four direct shear devices were used to perform tests at vertical stresses higher than 500 psf, and two were equipped with load cells of lower capacity to perform the tests at 500 psf. This direct shear device uses a 2,000 lb capacity servo-motor that turns jack to apply the normal force to the test specimen which is measured by means of a load cell. The devices with lower capacity used a 500 lb load cell to measure the normal force while the others used a 1,000 lb load cell. This device is equipped with a linear variable differential transformer (LVDT) to measure the vertical displacement of the test specimen. The shear box allows the test specimen to be submerged in water during the test to prevent drying. To shear the test specimen, this device uses a servo-motor that turns a jack similar to the one used to apply the vertical load. This motor can shear the sample at a constant rate of displacement, ranging from $2x10^{-6}$ inches/min to 2 inches/min. During shear, the bottom half of the direct shear box is moved relative to the top half. The horizontal load required to prevent the top half from moving was measured using 300 lb and 500 lb load cells for the low and high capacity devices, respectively. The horizontal displacement in this device is calculated using a calibration factor to convert the "steps" of the horizontal servo-motor into units of displacement.

To perform tests at consolidation stresses below 500 psf, special fixtures were fabricated and lower capacity horizontal and vertical load cells were used. During shear in this device, the top half of the direct shear box rides on the test specimen increasing the normal stress on the failure plane. To reduce this effect, a smaller and lighter top half was constructed out of cast acrylic as can be seen in Figure 5.8. Also, a smaller and lighter yoke constructed out of aluminum was used and is also shown in Figure 5.8. No fixed connection was used between the yoke and the top half of the direct shear box to prevent the yoke from

applying a vertical load to the sample. The connection can be seen in Figure 5.9. The direct shear box with the modified top half appeared as shown in Figure 5.10.

Figure 5.8 Modified direct shear box top half and yoke.

Figure 5.9 Connection between the yoke and the direct shear box.

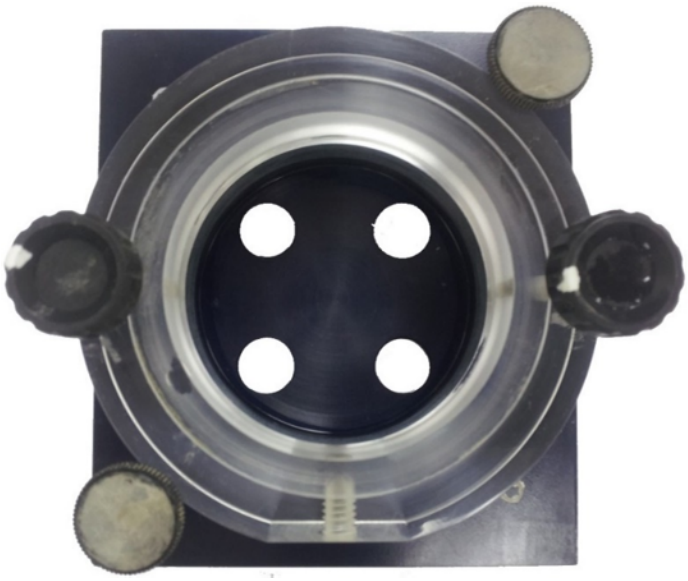

Figure 5.10 Direct shear box with the modified top half.

The high capacity load cell that is commonly included with the Geotac direct shear device and the low capacity load cell used for tests at consolidation stresses below 500 psf are shown in Figure 5.11. The horizontal load cell was moved closer to the direct shear box to eliminate the friction that could exist in the bearings located between the original horizontal load cell and the direct shear box. For tests performed at consolidation stresses below 500 psf, 100 lb load cells were used to measure the horizontal and vertical forces.

This apparatus is controlled by the DigiShear software developed by Trautwein Soil Testing Equipment. This software runs the test and records the data from the sensors to a file that can be accessed later.

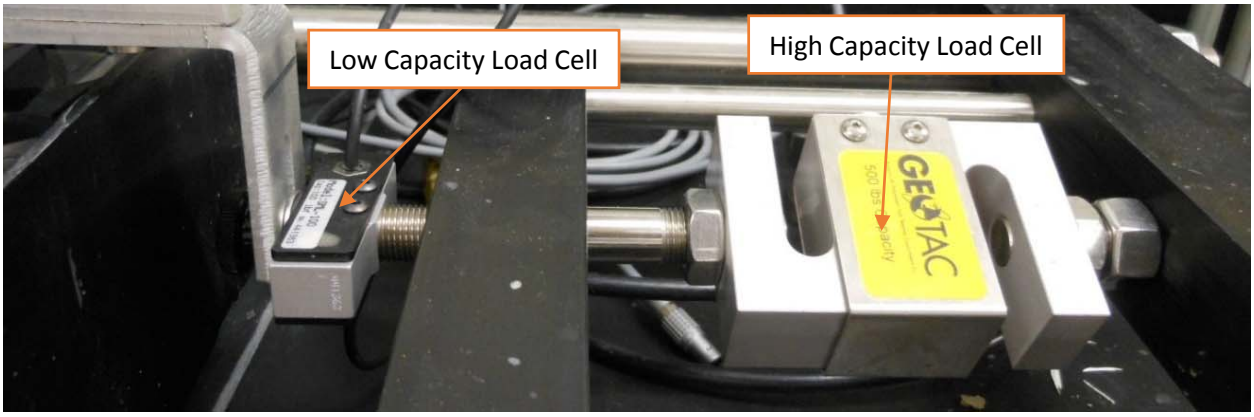

Figure 5.11 Location of the horizontal load cell for direct shear tests at consolidation stresses below 500 psf.

5.4.2 Ring shear device

The ring shear devices used in this research were of the type designed by Bromhead (1979), fabricated by Wykeham-Farrance, and modified with the modifications to reduce side-wall friction presented by Meehan et al. (2007). This device is shown in Figure 5.12. This ring shear device uses an annular test specimen of 0.20 inches of thickness with inner and outer diameters of 2.76 inches and 3.94 inches, respectively. This device allows test specimens to be formed inside the specimen container using a spatula as described in Section 5.6. The test specimen container and the top platen of this device can be seen in Figure 5.13.

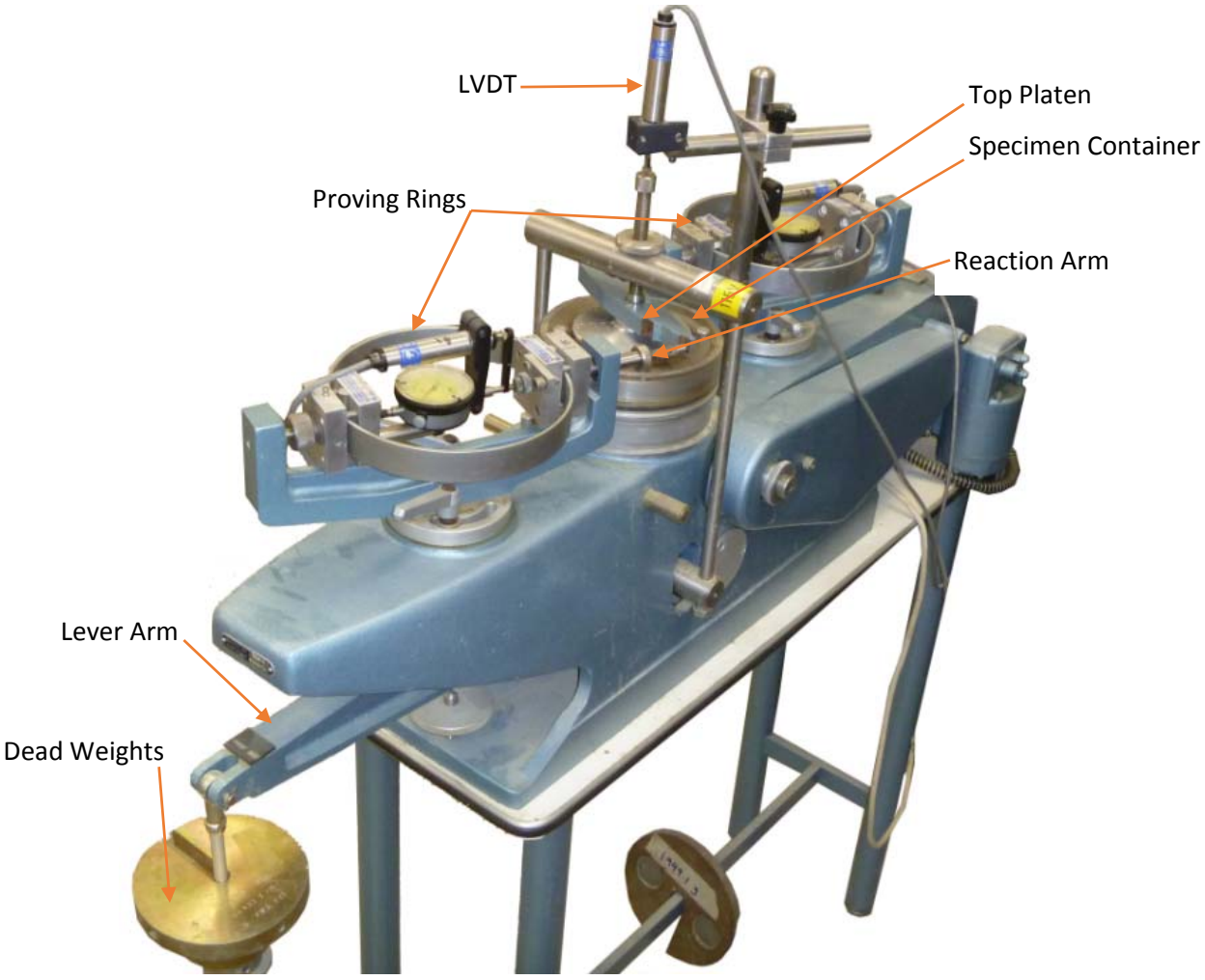

Figure 5.12 Bromhead ring shear device.

During consolidation, the test specimen is subjected to K_o conditions and is compressed in between two sintered bronze end platens to allow drainage. The normal stress is applied by means of dead weights

using a 10:1 ratio lever arm. The axial displacements are measured using an LVDT located above the top platen.

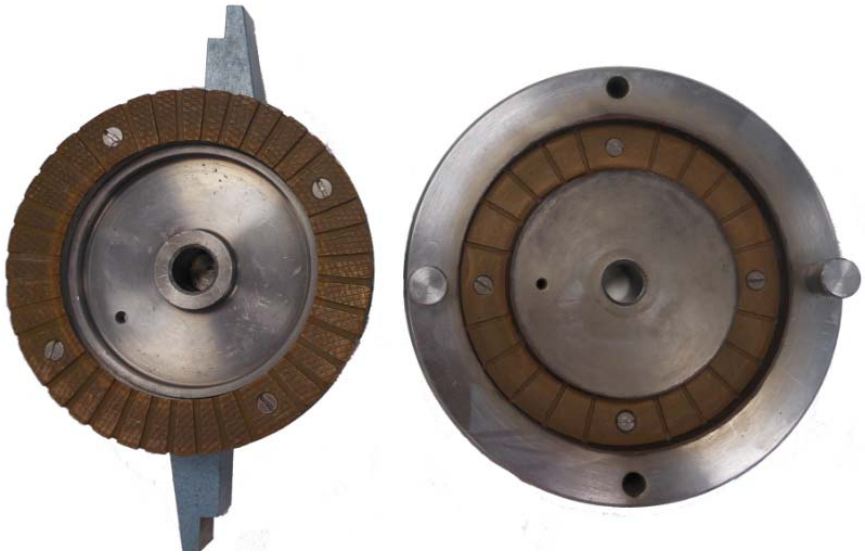

Figure 5.13 Bromhead ring shear device test specimen container.

This device allows the test specimen to be submerged in water to prevent drying during the test. To shear the test specimen, the test specimen container rotates and the top platen reacts against two proving rings that measure the force required to prevent movement. The proving rings are positioned in opposite directions forming a 90° angle with the reaction arm from the top platen. The sintered bronze end platens attached to the bottom of the test specimen container and top platen are serrated to prevent slippage from occurring at the soil-end-platen interface. It is difficult to discern, but appears that the failure surface in this device occurs near the top of the test specimen, very close to the top platen. The rate of displacement is controlled by a set of gears that allows the test specimen to be sheared at a constant rate of displacement from $7x10^{-4}$ inches/min to 1.75 inches/min. The proving rings and LVDT are connected to a Keithley 2000 multimeter data acquisition system that records the change in voltage of these devices in response to the change in load and vertical displacement of the test specimen. This information is processed and converted to engineering units using a computer program developed by the author and some colleagues.

5.4.3 Triaxial device

Two types of triaxial devices were used in this investigation. A fully-automated test apparatus was used to perform triaxial tests at consolidation stresses higher than 800 psf and a manual apparatus was mainly used to perform triaxial tests for consolidation stresses below 800 psf. The equipment was manufactured by Trautwein Soil Testing Equipment.

The fully-automated test system is shown in Figure 5.14. This setup is capable of performing CU, CD, and CK_oU triaxial compression and extension tests. Most triaxial test specimens used in this research had diameters of about 1.4 inches and heights of about 3.0 inches with the exception of the "packed" specimens, described in Section 5.7, that had diameters of about 1.30 inches and heights of about 2.80 inches. In this device, the cell pressure and backpressure are applied to the sample by means of two flow pumps of 300 psi capacity. Mounted on these pumps are transducers that measures the pressure applied by the pump. The vertical load is applied by means of a servo-motor driving a screw jack, similar to the one used in the direct shear device, that can shear the sample at a constant rate of strain.

Figure 5.14 Triaxial setup manufactured by Trautwein Soil Testing Equipment.

The vertical force is measured by means of a load cell mounted on the system. For this research, load cells of 100 lb and 300 lb have were used, depending on the confining pressure of the tests being performed. The pore pressures generated during shear are measured by a transducer, similar to the ones connected to the pumps. This system is controlled by the TruePath software also developed by Trautwein Soil Testing Equipment. In this setup, the backpressure saturation stage is automatically controlled by the software to prevent the test specimen from being overconsolidated. The software is used to run the test and to record measurements from the transducers in a file that can be accessed later.

Test specimens for triaxial testing were trimmed from a cylinder of soil preconsolidated in a batch consolidometer, shown in Figure 5.15, to a pressure of 800 psf under K_o conditions. The specimen container of the batch consolidometer has a diameter and height of six inches. The batch of soil was consolidated from a water content close to the liquid limit. Details about forming test specimens for triaxial tests are presented in Section 5.7.

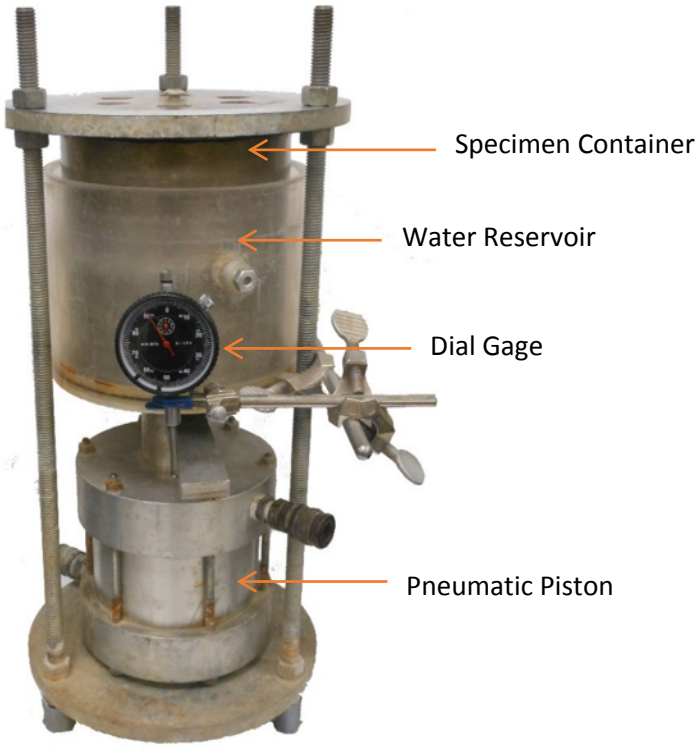

Figure 5.15 Batch consolidometer

The manual triaxial device is shown in Figure 5.16. This apparatus consists of a pressure panel board that can be used to apply cell pressure and backpressure and a load frame similar to the one used in the fully-automated device. In this apparatus, two different pressure transducer are used to measure the cell and pore pressures. To perform test at consolidation stresses below 800 psf, a Valydine P305D effective stress transducer was used to obtain more resolution in the pore pressures generated during shear. This

transducer is shown in Figure 5.17. An effective stress transducer has two connections, one for the backpressure and one for the cell pressure. This type of transducer measures the difference between these two pressures. For this investigation, the effective stress transducer had a capacity of 20 psi. The backpressure saturation and consolidation stages are performed manually using the pressure board. The shearing stage is controlled by the Sigma-CU software developed by Trautwein Soil Testing Equipment. This program controls the loading frame and records the load and pressures in the sample during shear.

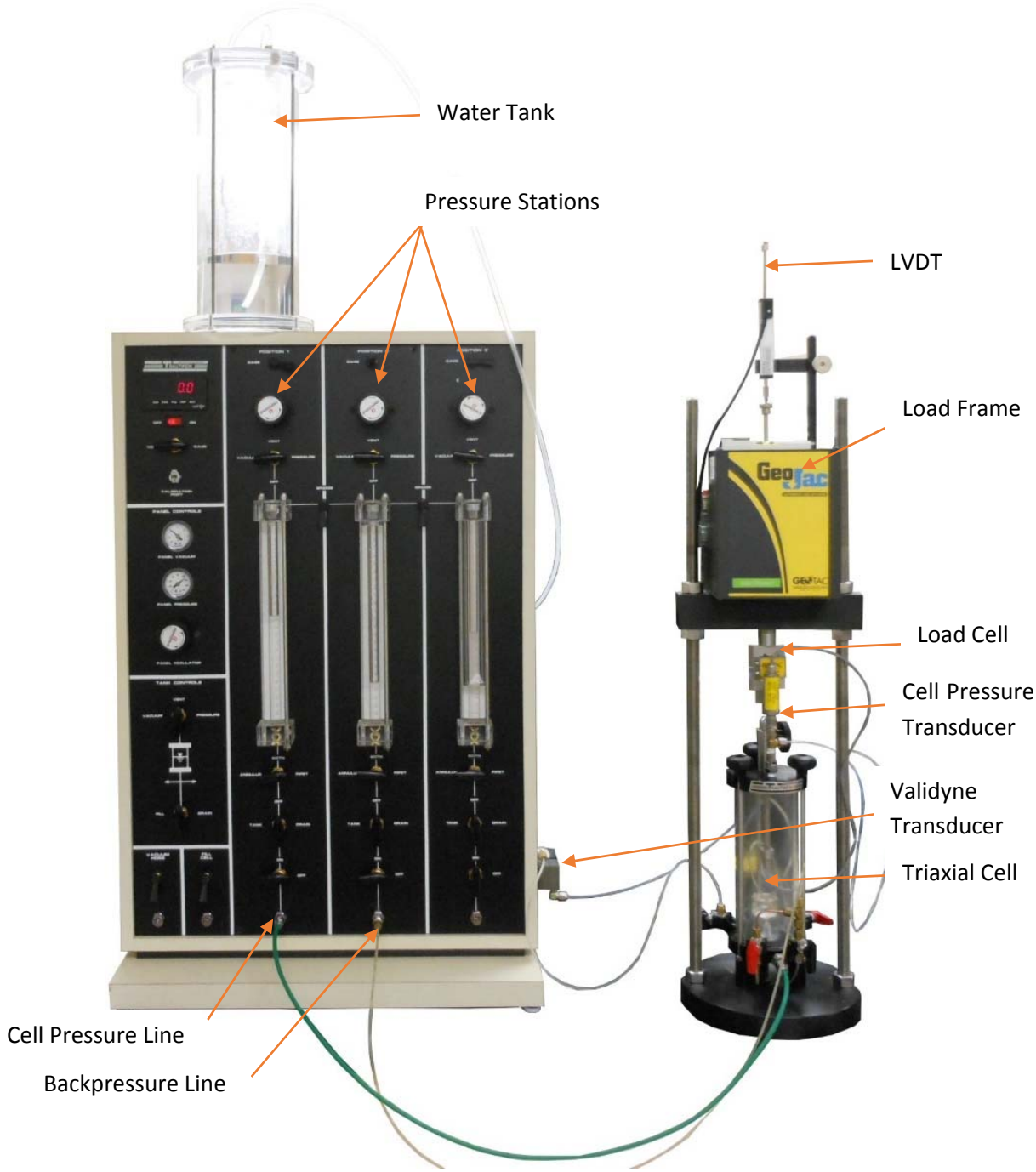

Figure 5.16 Manual triaxial apparatus.

Figure 5.17 Effective stress transducer.

5.5 Direct Shear Test Specimen Fabrication and Testing Procedure

Below is a summary of the procedure used to fabricate test specimens for direct shear testing. A proposed new ASTM standard to measure the fully softened shear strength using a direct shear device is presented in Appendix A, and a complete step-by-step manual for the test using a GeoTac device is given in Appendix B.

The sample fabrication procedure starts with the shear box divided into its upper and lower halves. After the porous stone and the filter paper are placed in the bottom section, the bottom half of the shear box is filled with soil from the edges to the center. The box is filled using a spatula, as shown in Figure 5.18, or "piped" using a pastry bag. Care should be taken to eliminate the occurrence of air bubbles during the sample fabrication procedure. After the bottom half is filled, the extra soil outside the specimen container is removed and the top surface of the box is cleaned, as shown in Figure 5.19.

The top half of the shear box is then physically connected to the bottom half using the black plastic-topped thumb screws as can be seen in Figure 5.20. After that, the top half of the shear box is filled with soil, using the same procedure as the bottom half, from the edges to the center, as shown in Figure 5.20. The soil is again placed in small amounts applying pressure to eliminate the air bubbles in the soil mass.

After the top half is completed, the top of the test specimen is leveled flush with the top of the shear box using a wood utensil, as shown in Figure 5.21. It is important that the top of the test specimen be as level as possible to prevent tilting of the top platen during the consolidation stage. The outside of the specimen container is then cleaned, and the final test specimen should appear as shown in Figure 5.22. After the specimen container is weighed, it is ready to be placed in the direct shear device. For test specimens formed at a water content corresponding to a liquidity index of 1.5 and above, it is recommended that the test specimen is formed around 0.1 inches short of the height of the direct shear box to prevent excessive extrusion upon application of the first consolidation load. At this high water content, the soil behaves more like a liquid and the wood utensil might not be needed to level the specimen.

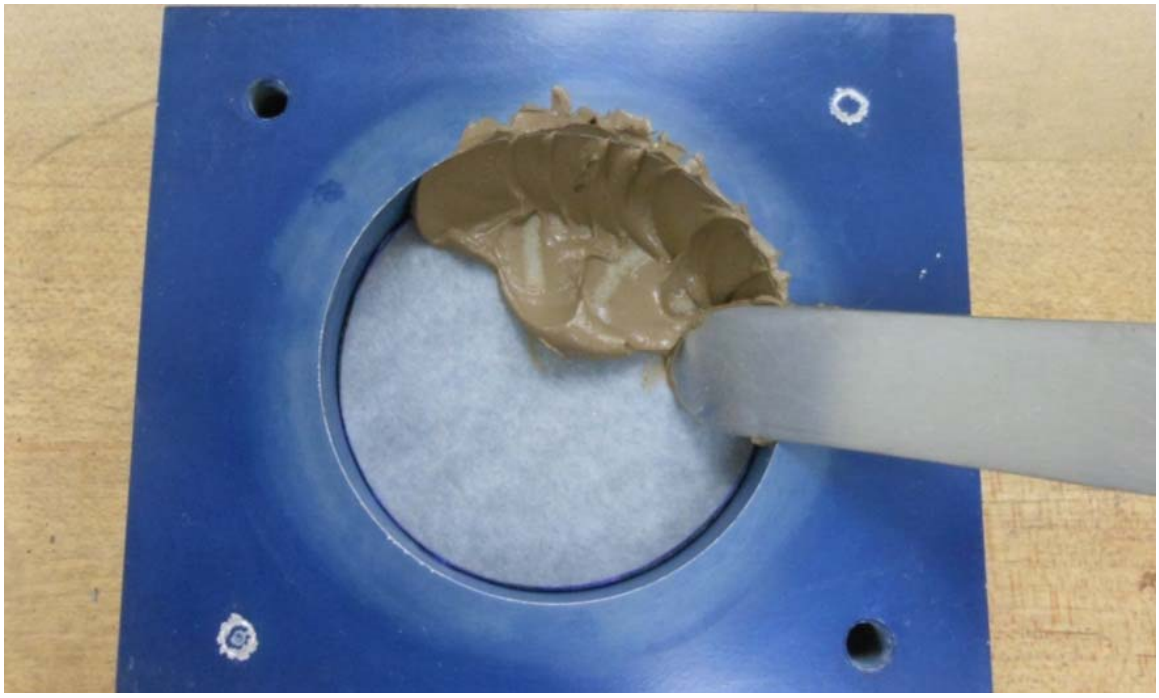

Figure 5.18 Bottom half of the direct shear box being filled.

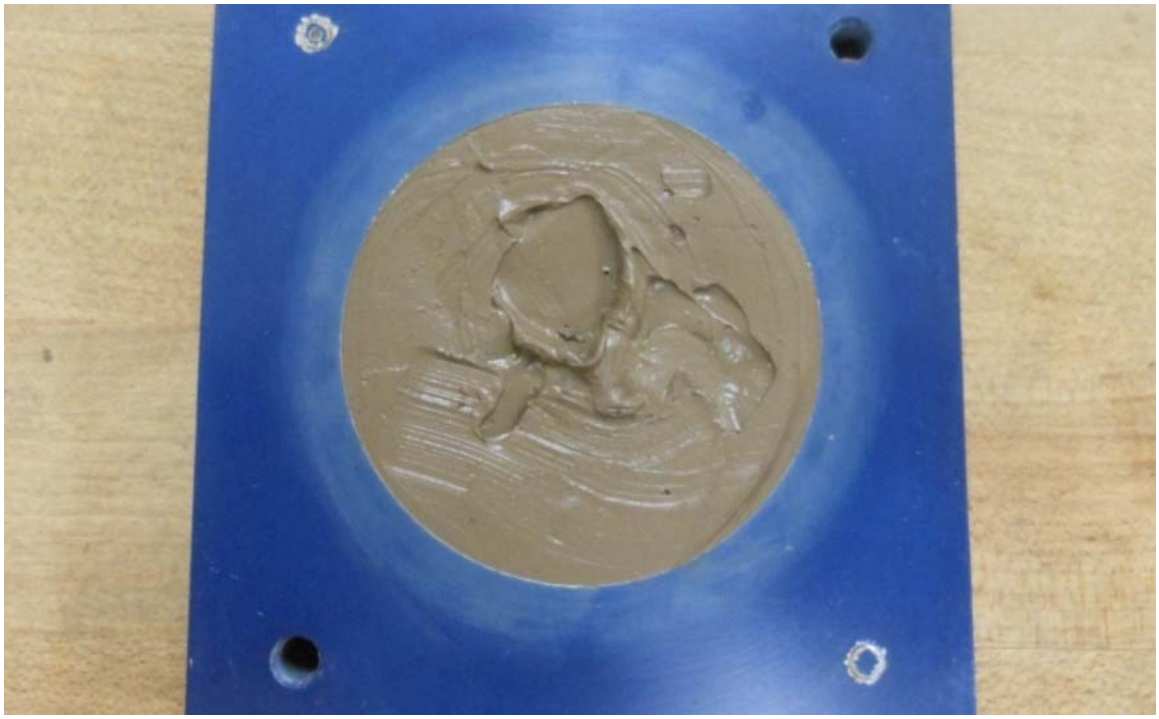

Figure 5.19 Bottom half of the direct shear box after being filled and cleaned.

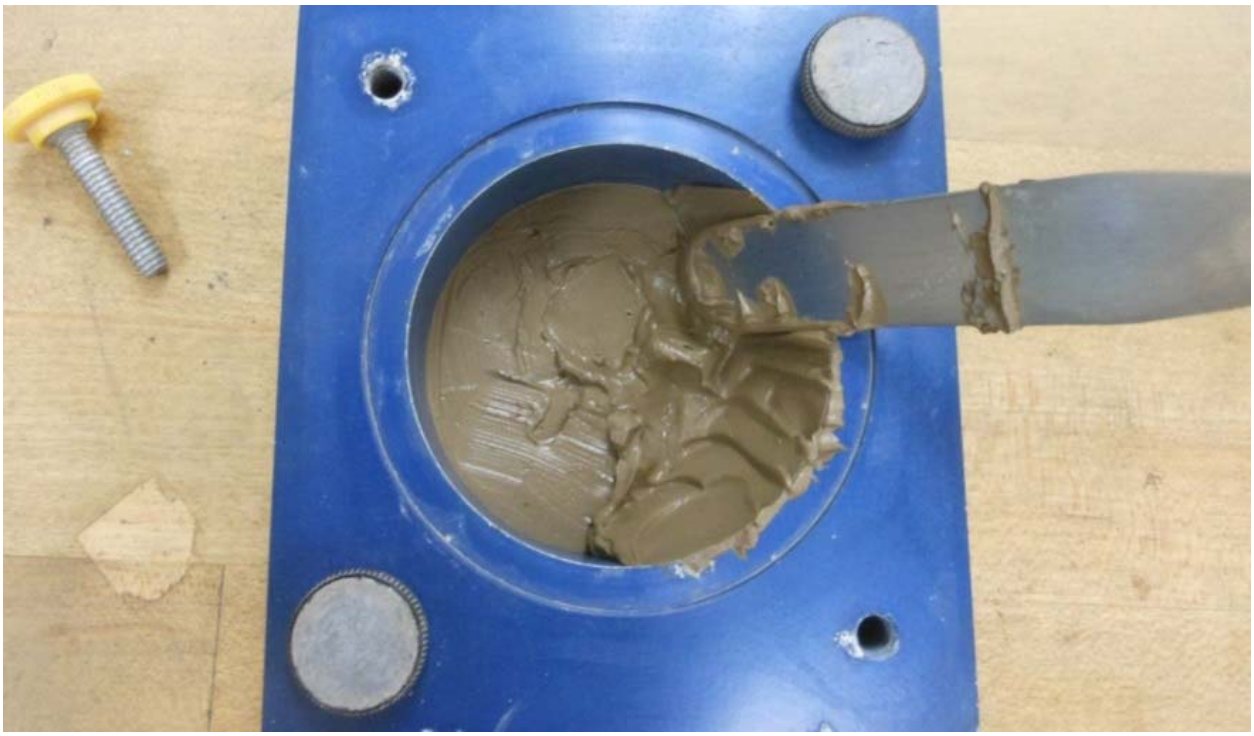

Figure 5.20 Top half of the direct shear box put being filled

Figure 5.21 Test specimen being leveled with the top of the shear box.

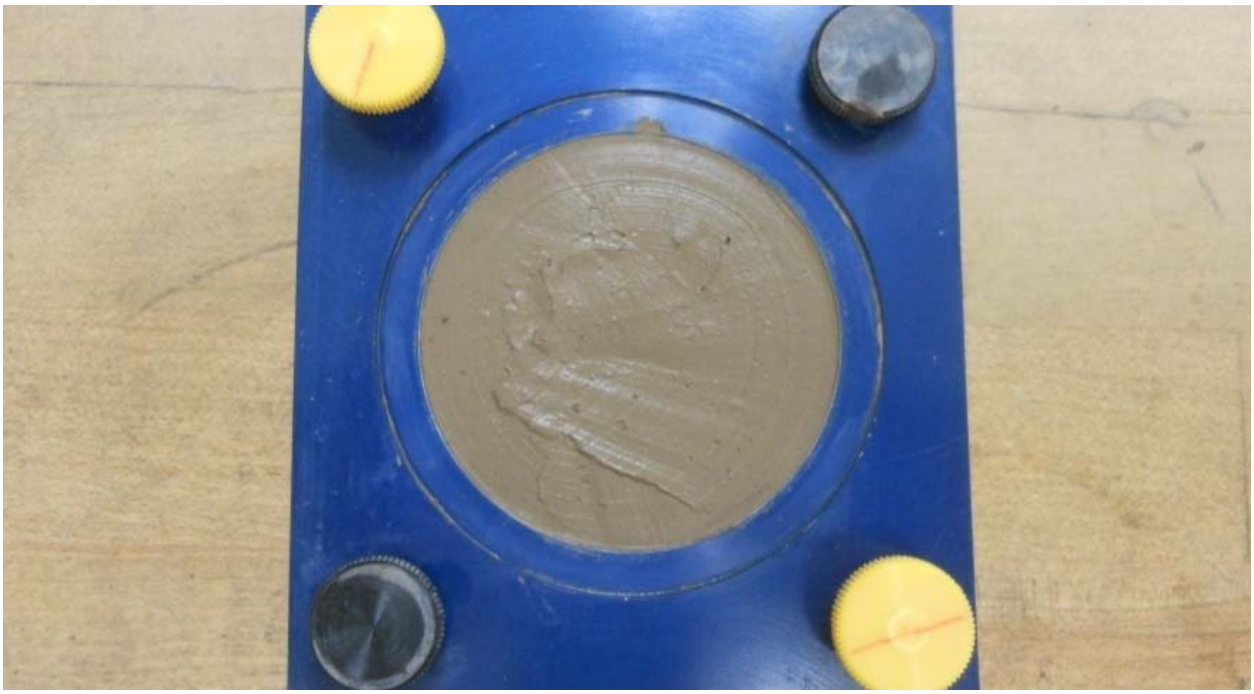

Figure 5.22 Specimen container ready to be weighed and placed in the direct shear device.

The specimen container is then placed in the direct shear device, the top porous stone (including a filter paper) and the top platen assembly are placed on top of the test specimen, and the appropriate zero readings are obtained. The test specimen is then ready to be consolidated. The first stress applied to the test specimen should be low enough to avoid extrusion of the soil upon application of the load. This is normally about 100 psf. For test specimens formed at a water content equivalent to a liquidity index of 1.5 and above, an initial consolidation stress of 50 psf is recommended to avoid soil extrusion upon application of the first load. The next consolidation loads are applied using a load increment ratio of one (i.e. the load is doubled). Each load is maintained on the test specimen until the end of primary consolidation is achieved or at least 24 hours. The last consolidation load should be kept on the sample as long as necessary to reach the end of primary consolidation. Immediately after the consolidation process begins, distilled water is added to the sample reservoir to keep the test specimen from drying, as shown in Figure 5.23. Water is added frequently to replace evaporated water.

When the end of primary consolidation is verified for the final stress, the test specimen is ready to be sheared. The test specimen should be sheared slow enough to allow dissipation of pore water pressures generated during shear. The displacement rate (R_d) required should be selected based on the criterion presented in ASTM D3080-11 which is represented by Equations 5.1 and 5.2:

$$t_f = 50\ x\ t_{50} \tag{5.1}$$

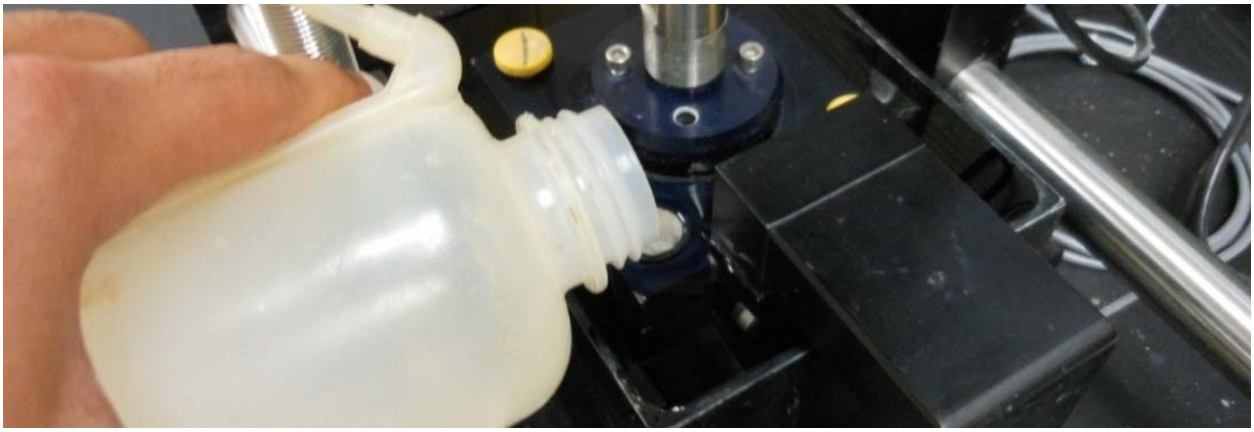

Figure 5.23 Distilled water being added to the water bath in the direct shear device.

$$R_d = \frac{d_f}{t_f} \tag{5.2}$$

Where:

t_f = Time required to failure.
t_{50} = Time required to achieve 50% consolidation.
R_d = Displacement rate.
d_f = Expected displacement at failure. ASTM D3080-11 recommends using 0.5 inches (12.7 mm) for normally or lightly overconsolidated fine-grained soils and 0.2 inches (5 mm) otherwise, if better information is not available.

To calculate the displacement rate using the equation presented above, an expected displacement to failure of 0.1 inches was used for all soils in this investigation. This assumed displacement at failures was appropriate for all the soils tests in this investigation. After the displacement rate is calculated, a gap is created for the shear plane by separating the top half of the direct shear box from the bottom half using the gap screws. In this investigation, a gap of 0.0625 inches was used as recommended in EM 1110-2-1906 “Laboratory Soil Testing” (USACE 1970). After the gap is created, the test specimen should be left to rest for about five minutes before removing the gap screws to allow the development of the shear stresses supporting the top half of the direct shear box. After that, the gap screws are removed and the shearing stage can be initiated. For tests performed at consolidation stresses below 500 psf, using the modified top half of the direct shear box, the gap screws were left in place to prevent the gap from closing during shear.

The test specimen is sheared until a defined peak is observed in the shear stress or a displacement of 0.40 inches is achieved.

5.6 Ring Shear Test Specimen Fabrication and Testing Procedure

The ring shear device is the only device with an approved ASTM standard to measure the fully softened shear strength (ASTM D7608-10). The procedure presented in this section complies with the requirements of ASTM D7608-10.

In the ring shear device, the test specimen can be formed in the annular space of the test specimen container using a spatula. The soil is placed in small amounts applying pressure to eliminate the air bubbles in the soil mass, as shown in Figure 5.24. After the annular space is filled with soil, it is leveled with the top of the container. A long razor blade can be used for this purpose, and this process is shown in Figure 5.25. After the top of the test specimen is leveled, the outside of the specimen container is cleaned, as shown in Figure 5.26. The specimen container is then weighed and placed in the ring shear device.

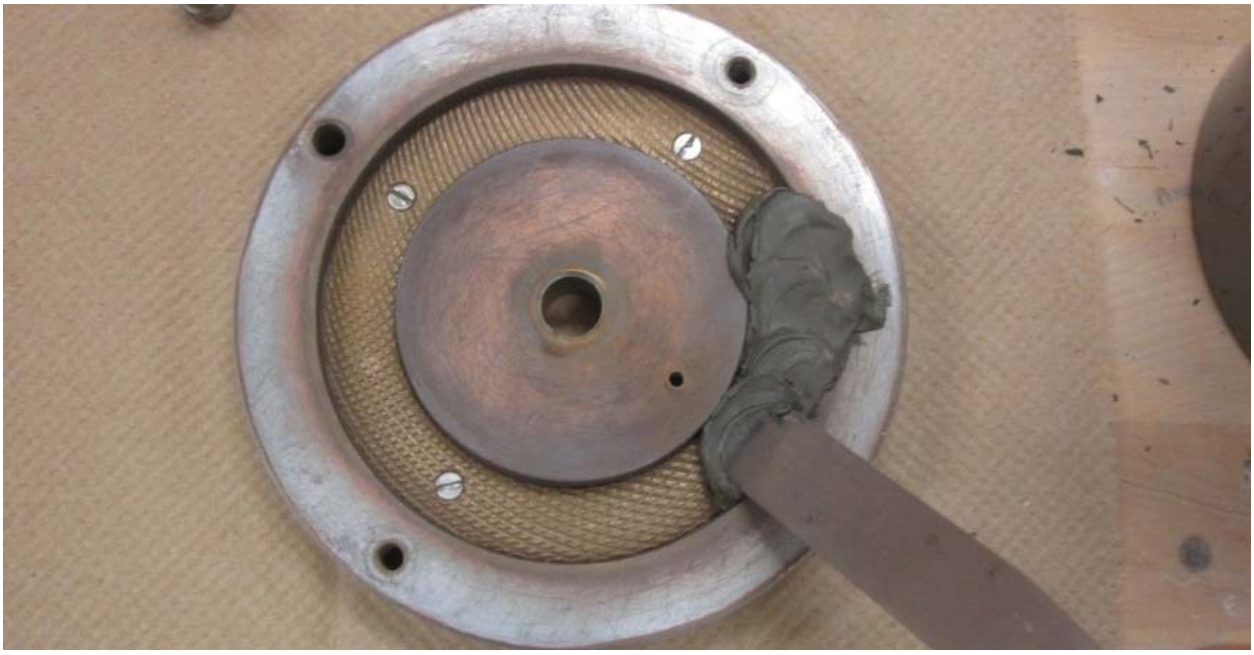

Figure 5.24 Ring shear specimen container being filled.

After the specimen container is placed in the ring shear device and the nuts are tightened, grease should be applied to the rod that serves as the center of rotation to the top platten to reduce the friction, as shown in Figure 5.27. The top platen is then placed at a right angle with the proving rings, as shown in Figure 5.28.

Figure 5.25 Ring shear test specimen being leveled with the top of the specimen container.

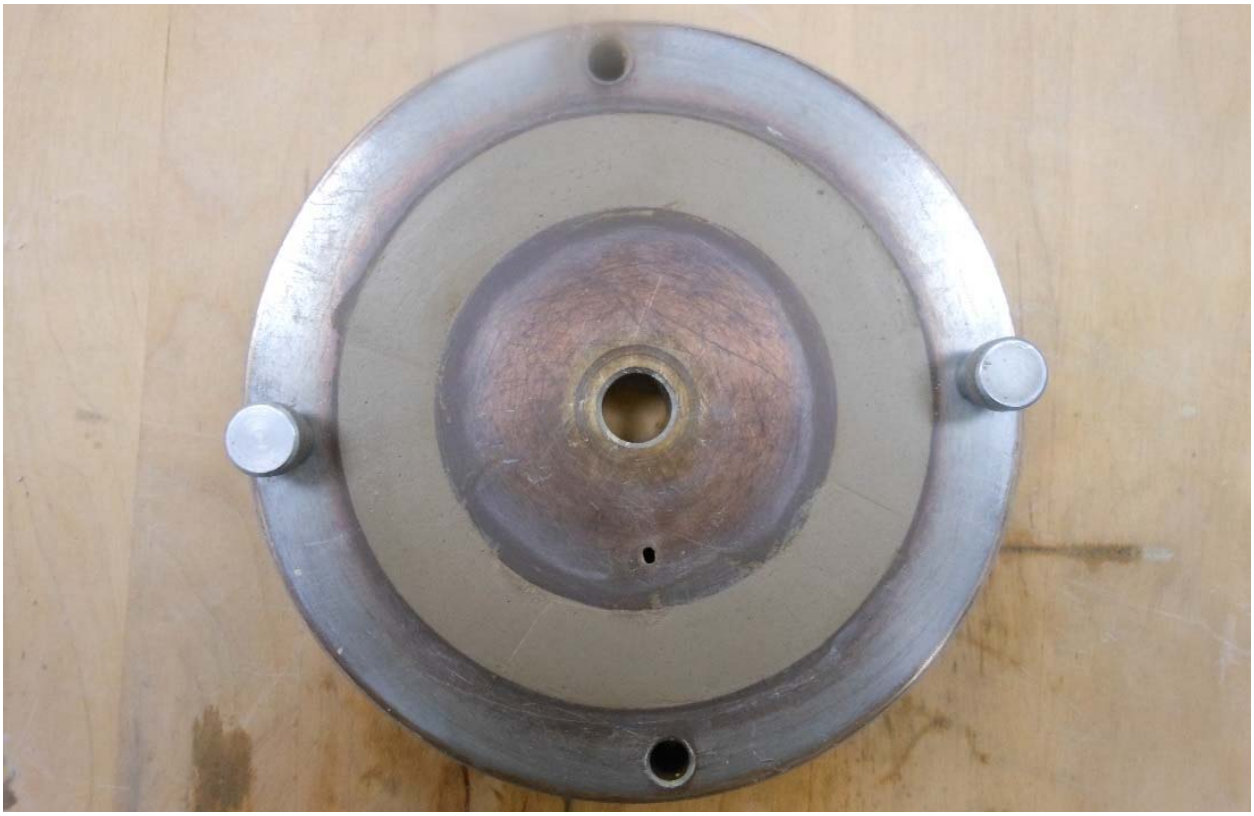

Figure 5.26 Final test specimen.

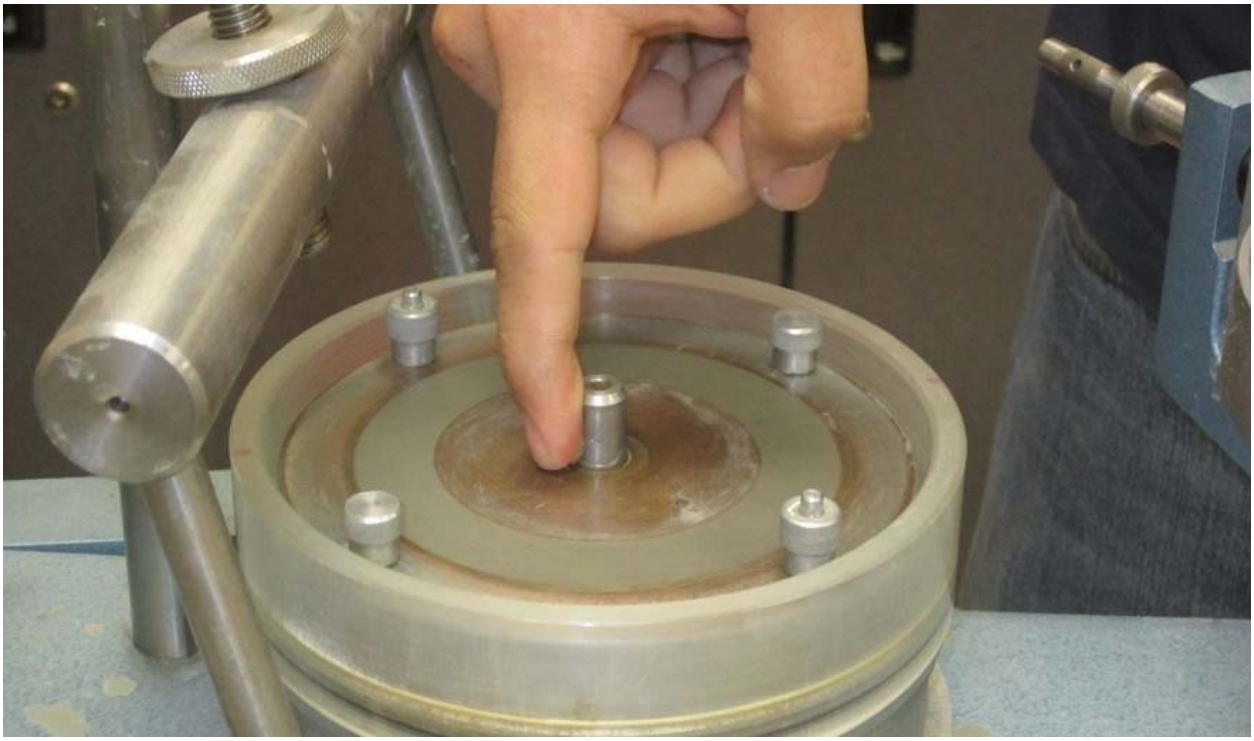

Figure 5.27 Vacuum grease being applied to the center of rotation of the specimen container.

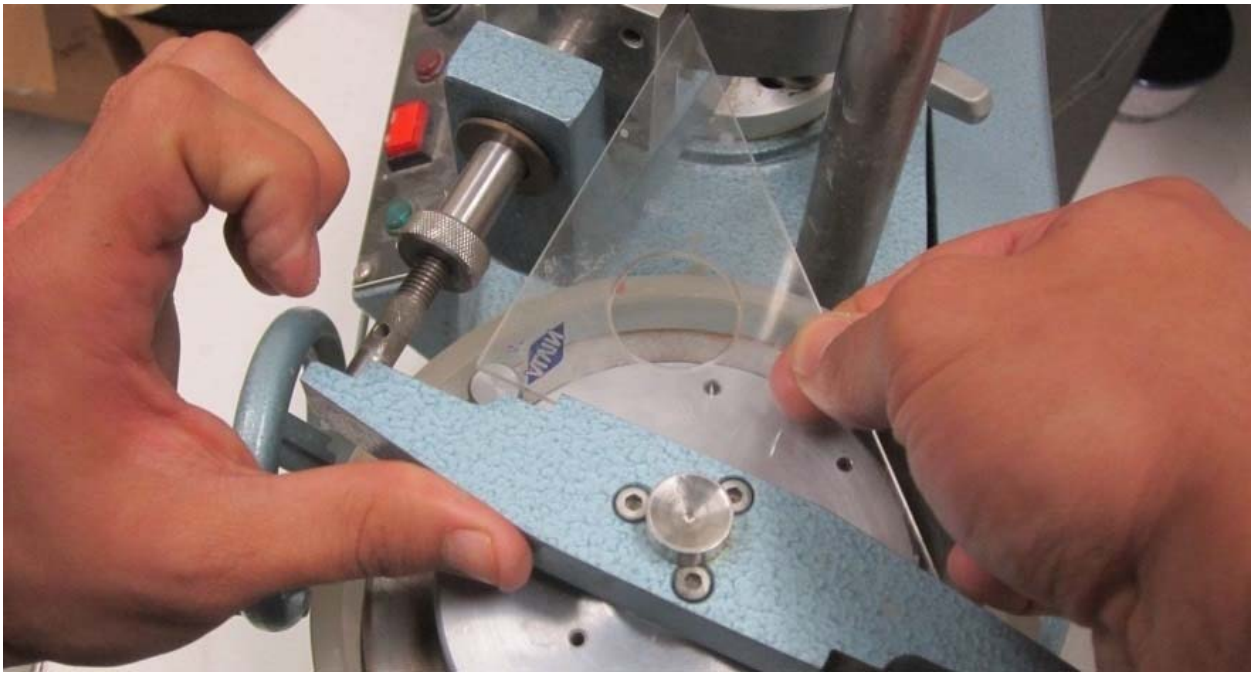

Figure 5.28 Verification of the orthogonality between the top platen and the proving rings.

After the weight hanger is installed and the zero measurements are recorded, the first consolidation load is applied to the test specimen. An initial stress low enough to avoid extrusion of the soil should be applied. This is normally a dead weight of 0.43 lb, which produces a normal stress of around 150 psf on the sample (taking into account the weight of the top platen). Immediately after the consolidation load is placed and the consolidation process started, distilled water is added to the bath of the ring shear device to keep the sample from drying, as shown in Figure 5.29. Water is added frequently to replace evaporated water.

Figure 5.29 Distilled water being added to the water bath of the ring shear device.

Subsequent consolidation loads are applied using a load increment ratio of one. Each load should be maintained on the test specimen until the end of primary consolidation is achieved. Owing to the thin test specimen (0.2 inches), it is possible to apply many consolidation loads in a 24-hour period.

After the end of primary consolidation is reached under the final desired consolidation stress, the test specimen is ready to be sheared. The test specimen should be sheared slow enough to allow dissipation of the pore water pressures generated during shear. The criterion presented in ASTM D7608-10 to select the maximum shearing rate that can be used is presented in Equations 5.1 and 5.2. For this research, the test specimens were sheared using the slowest speed allowed by the ring shear device, which is $7x10^{-4}$ inches/min. A discussion about the required shearing speed and the available shearing speeds in this device is presented in Section 5.8.2.

5.7 Triaxial Test Specimen Fabrication and Testing Procedure

Preparing test specimens for triaxial tests requires more effort than for the other devices. Since the triaxial device does not use a test specimen container, soil samples have to be, (a) formed in a separate container and consolidated to a pressure that allows triaxial test specimens to be trimmed and handled without being damaged, or (b) packed in a special mold at a low liquidity index .

For samples formed in a separate container, a batch of soil is prepared to the desired water content following the instructions presented in Section 5.3. The soil is then placed in the specimen container of a batch consolidometer in a similar fashion as the direct shear test specimens are formed. The specimen container of the batch consolidometer used in this research is shown in Figure 5.30. Spacers were used to subdivide the total height of the container to facilitate the placement of the soil in the container and prevent air bubbles from being entrapped in the soil specimen. For this research, the batch of soil was prepared to a liquidity index of one.

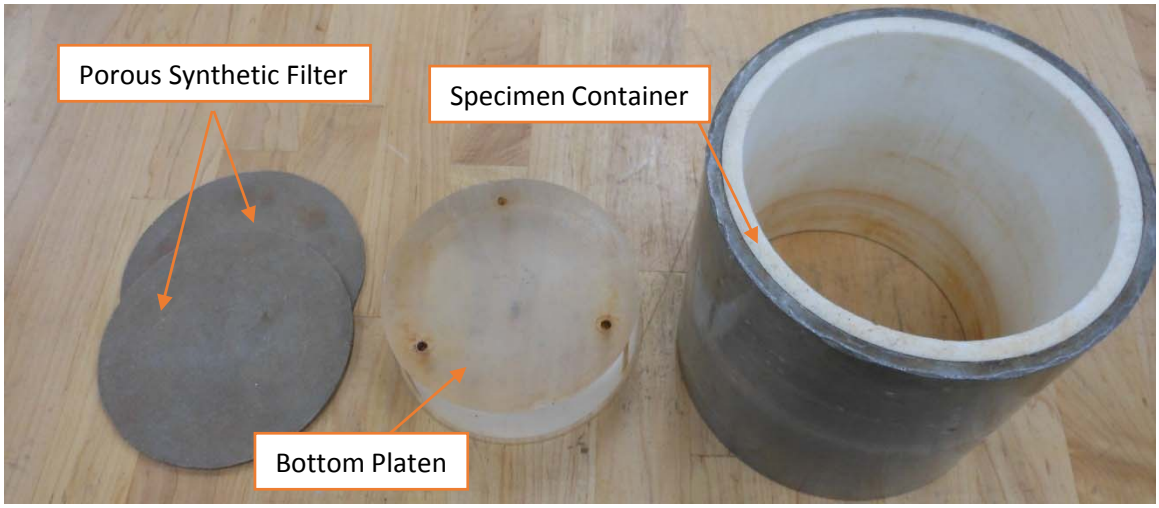

Figure 5.30 Batch consolidometer specimen container.

A porous synthetic filter is then placed on top of the bottom platen and the spacers, leaving a section of about one inch thick to be filled with soil. The soil is placed using a big spatula as shown in Figure 5.31, making sure no air-bubbles are incorporated in the specimen. After a layer is completed, a spacer is removed from the bottom, and more soil is placed in the specimen container until it is full or reaches the desired height.

Once the specimen container is filled, as shown in Figure 5.32, a porous synthetic filter is placed on top and the container positioned in the batch consolidometer. For this research, a pressure of 800 psf was then applied in one step to the soil, and the soil was allowed to consolidate until the end of primary consolidation was reached. This pressure was determined empirically as providing a test specimen having adequate strength for trimming and handling. During consolidation, a dial gage that measures the change in height of the specimen is read. With this information, a plot of displacement as a function of time is made and a Casagrande's construction is used to assess the end of primary consolidation. After primary consolidation is reached, the soil sample is extruded from the specimen container and triaxial test specimens can be trimmed.

Figure 5.31 Batch consolidometer's sample container being filled.

Figure 5.32 Batch consolidometer's specimen container full with soil.

For the batch consolidometer used in this investigation, usually five to six test specimens were obtained from each batch. Tests specimens were trimmed to about 1.4-inch diameter and three-inch height.

After a test specimen is trimmed, the diameter, height, and weight are measured. Then, the test specimen is placed in a conventional triaxial cell using standard procedures. In this research, two latex membranes were used around the test specimens. To place the membranes, a membrane expander is used to prevent damaging the test specimens. No filter paper drainage strips are used.

To perform triaxial tests at consolidation stresses below 800 psf, "packed" triaxial test specimens were used. "Packed" specimens are formed in a Harvard miniature compactor mold, at a liquidity index ranging from 0.5 to 0.8, using a spatula. For this purpose, the total height of the mold was subdivided using wood spacers of 0.25 inches of height. Eleven layers were used to form the test specimens. The Harvard miniature compactor mold, the wood spacers, and the extruders are shown in Figure 5.33. A similar procedure to form "packed" specimens was presented by Green and Wright (1986).

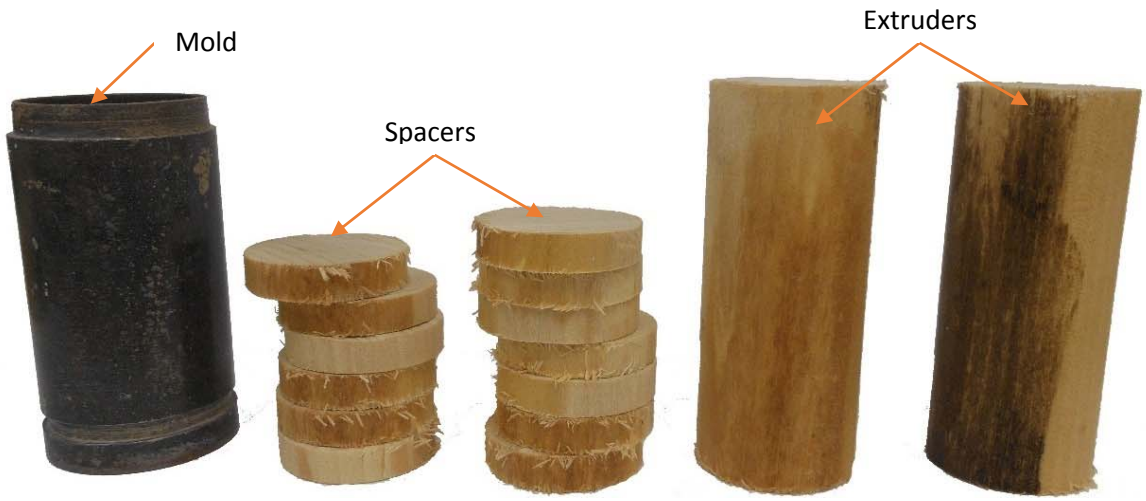

Figure 5.33 Tools used to form packed triaxial test specimens.

To form packed specimens, ten wood spacers are placed inside the mold. Then, the first layer is filled with soil using a spatula, making sure air bubbles are not entrapped in the specimen (Figure 5.34). After one layer is filled, the mold is raised to extract one of the spacers from the bottom. Then, the extruder is used to push down the layer of soil already finished (Figure 5.35a). Only the pressure required to push the layer down is applied, preventing the soil from getting over compacted. Since the soil is essentially saturated, the void ratio should not decrease during the sample fabrication procedure. This process is repeated until the total desired height of the test specimen is achieved. After that, the ends are trimmed flush with the ends of the mold. The test specimen is then slowly extruded using the extruder as can be seen in Figure 5.35b. A final packed specimen is shown in Figure 5.35c. After the test specimen is extruded, it is placed

in a conventional triaxial cell using standard procedures. Two latex membranes were also used in this case. To place the membranes, a membrane expander is used to prevent damaging the test specimens.

Figure 5.34 Packed specimen being formed.

Figure 5.35 Layer being pushed down.

After the test specimen is placed in the triaxial cell, the cell is filled with water. In the automated triaxial setup, the hydraulic pumps are then emptied and filled with de-aired water. The backpressure pump, being the most critical, is emptied and filled twice to reduce the possibility of having air in the system. The sample is then saturated using the backpressure saturation feature of the TruePath software. The test specimens are always close to 100% saturation before applying the backpressure, so a backpressure of 50 psi was normally sufficient to obtain a *B* value, as described by Skempton (1954), in excess of 0.95 as required by ASTM D4767-11.

For the manual triaxial device, after the specimen is installed in the cell, the burettes are filled with de-aired water, the cell is connected, the air in the lines and sensors is flushed out, and the backpressure saturation stage is initiated. The backpressure saturation stage is performed manually. Small increments of cell pressure and backpressure should be used during saturation. Each stress increment is left on the sample until the pore pressures are equilibrated. Since this setup was mostly used to perform tests at consolidation stresses below 800 psf, the cell pressure and backpressure were increased in increments of 72 psf. This increment was increased as the *B* value increased but never exceeded half of the final consolidation stress.

After the test specimen is backpressure saturated, it is consolidated to the desired pressure. Most of test specimens were consolidated to pressures ranging from 1,000 psf to 10,000 psf. Some low stress tests were also performed at consolidation stresses ranging from 144 psf to 432 psf. During consolidation, the change in volume in the sample was monitored with time. This information was used to create a plot of the change in volume with time. With this plot, a Casagrande's type of construction was made to assess the end of primary consolidation. After the end of primary consolidation is verified, the sample is ready to be sheared. To calculate the required strain rate to allow equilibration of the pore pressures generated during shear, the equation derived by Head (1986) was used and is presented below:

$$\dot{\varepsilon} = \frac{\varepsilon_f}{t_f} = \frac{\varepsilon_f}{0.51 \cdot t_{100}} \tag{5.3}$$

Where:

$\dot{\varepsilon}$ = Strain rate.
ε_f = Expected strain at failure. A value of 4% was used as recommended in ASTM D4767-11.
t_f = Expected time to failure.
t_{100} = Time required to achieve 100% primary consolidation.

ASTM D4767-11 has a different criterion to select the time to failure based on the time required to achieve 50% consolidation (t_{50}). This criterion and the one presented in Equation 5.3 produce similar shearing rates. The criterion presented in Equation 5.3 is more convenient because the time required to achieve

100% consolidation can be easily approximated by visual inspection of the strain vs. log of time plot on the computer screen. To obtain t_{50}, the data has to be extracted from the computer and plotted.

To shear the sample, the drainage lines are closed and the sample is sheared using the strain rate calculated until a minimum axial strain of 15%, as required by ASTM D4767-11.

5.8 Comparison of Features of the Triaxial, Direct Shear, and Ring Shear Devices

In this section, a comparison of the strengths and weaknesses of the direct shear, ring shear, and triaxial devices related to fully softened shear strength measurements and their influence on the results and duration of the tests are presented. The direct shear device is one of the oldest devices available to measure the shear strength of soils. Although there are several criticisms of this device, these issues have not been significant enough to remove it from geotechnical engineering practice. The ring shear apparatus has most often been used to measure residual shear strength parameters. In recent years, this device was presented as a viable option to measure the fully softened shear strength (Stark and Eid 1997; Stark et al. 2005). The triaxial device is the most versatile device in common geotechnical laboratories (Saada and Townsend 1981), and according to Hvorslev (1939), is the best device available for peak shear strength measurements.

5.8.1 Duration of the test

The duration of the test includes the time required to process the soil sample, and to form, consolidate, and shear the test specimen. The duration of a test can be an important factor on deciding which test to run when time is a constraint in a project. The duration of the consolidation and shearing stages in these devices is controlled by the coefficient of volumetric compressibility, the permeability, and the thickness of the test specimen. The data used in this discussion are from the test results presented in Appendices C, D, and E for the direct shear, ring shear, and triaxial devices, respectively.

- *Direct shear device:* Direct shear test specimens prepared for this investigation had an initial height of about 1.4 inches. The first consolidation stress applied to most of the direct shear test specimens was 100 psf. The consolidation stress was then increased using a load increment ratio of one until the desired shearing consolidation stress was reached. Each consolidation stress was left on the sample until the end of primary consolidation was achieved, which in this device required about one day per load. Using this procedure, the consolidation stage in the direct shear device lasted between three days and eight days for final consolidation stresses ranging from 500 psf to 14,400 psf. Assuming a displacement at failure of 0.10 inches to calculate the displacement rate, the time to failure for the various soils used in this research ranged from less than a day to 18 days, with five days being the average. Based on this information, the duration of each direct shear test performed in this investigation ranged from 4 days to 26 days.

- *Ring shear device:* Test specimens used in the ring shear device had an initial height of 0.20 inches. The first consolidation stress applied in this test was around 150 psf. The load was increased until the final shearing consolidation stress was achieved using a load increment ratio of one. Due to

the small thickness of the test specimen in this device, more than one consolidation load increase was possible during a 24-hour period. For the soils tested in this investigation, the time to achieve primary consolidation ranged from less than 1 min to 500 min, with 120 min being the average for consolidation pressures ranging from around 154 psf to around 14,500 psf. All soils were sheared at $7x10^{-4}$ inches/min, which is the slowest speed allowed in this device. For the soils tested, the displacements at failure ranged from 0.05 inches to 0.31 inches, with 0.13 inches being the average. With these displacements at failure, the duration of the shearing stage ranged from around one hour to a little over seven hours. Based on this information, the ring shear tests performed in this investigation lasted between one day and two days.

- *Triaxial device:* As described in Section 5.7, the triaxial device was the only device that required the test specimen to be preconsolidated outside of the device. In the batch consolidometer, the time required to reach the end of primary consolidation ranged from 1.15 days and 14 days. As the plasticity of the soil increases, the permeability usually decreases and the time required to reach the end of primary consolidation increases. At the beginning of backpressure saturation, the samples were very close to 100% saturation. For the tests performed using the automated triaxial equipment, the time require to increase the backpressure to the desired value was determined by the software, which calculates the increase in pore pressure based on the pore stiffness. The time required to increase the backpressure to the required value ranged from 1.5 hours to 20 hours with an average of nine hours. Usually the backpressure was left overnight. For tests performed at consolidation stresses below 800 psf with the manual triaxial equipment, the backpressure saturation stage lasted between 10 days and 20 days. In this test, the consolidation pressure was applied isotropically in only one step. The duration of the consolidation stage for the soil tested ranged from 1 hour to 64 hours. The strain rate used for shearing the samples was calculated using Equation 5.3 with an assumed strain at failure of 4%. The shear strain rates used ranged from 0.12 %/hr to 1 %/hr. For all soils tested, the axial strain at failure ranged from 7.8% to 15.1%, with 10.5% being the average. Based on this displacement rates and the measured displacement at failure, the duration of the shearing stage ranged from around 6 hours to 104 hours with an average duration of 39 hours. Based on the information presented above, 2 days to 22 days were required to perform a CU triaxial test using the automated apparatus and 14 days to 25 days were required using the manual apparatus.

The information presented above does not include the time required to prepare test specimens. Preparing test specimens for triaxial tests was the most time consuming, followed by direct shear test specimens, and then ring shear test specimens. Based on the information presented above, the ring shear device required less time to run a test, followed by the direct shear device, and then the triaxial device.

5.8.2 Available shearing speeds

Another aspect that needs to be consider is if the devices allow for the slow shearing rates required to achieve the conditions simulated in the tests. Shearing speeds slow enough to allow the dissipation of the pore water pressures generated during shear are required when performing drained tests. Speeds slow enough to allow the equilibration of the pore water pressures generated during shear are required when

undrained tests with pore water pressures measurements are performed. For the direct shear test, guidelines to choose the required shearing speed are presented in ASTM D3080-11 and are given in this dissertation in Equation 5.2. For the ring shear test, guidelines are presented in ASTM D7608-10 and are the same as given in Equation 5.2. For CU triaxial tests, guidelines used are given in this dissertation in Equation 5.3.

- *Direct shear device:* The direct shear devices used in this research allowed a minimum shearing speed of $2x10^{-6}$ inches/min. For the soil tested, the required shearing speed ranged from low shearing rates $8.49x10^{-6}$ inches/min to $5.06x10^{-3}$ inches/min, with an average required speed of $7.52x10^{-4}$ inches/min. These shearing speeds were calculated using the measured displacement at failure. The direct shear device did provide an adequate range of speeds to perform drained tests according to ASTM D3080-11 criteria represented here as Equation 5.2.

- *Ring shear device:* The ring shear devices used in this research permitted a minimum shearing speed of $7x10^{-4}$ inches/min. For the soil tested, the required shearing speed ranged from $1.37x10^{-5}$ inches/min to $1.59x10^{-2}$ inches/min, with an average required speed of $5.80x10^{-4}$ inches/min. These shearing speeds were calculated using the measured displacement at failure. For 96 out of 115 of the tests performed at consolidation stresses ranging from around 250 psf to 14,500 psf, the available speeds were not slow enough to comply with the ASTM D7608-10 required shearing rate represented by Equation 5.2. The available shearing speeds were only adequate for soils Alabama 1 through 4 and Colorado Clay.

- *Triaxial device:* The triaxial devices used in this research uses the same motor design as the direct shear device, which means that the minimum speed allowed is also $2x10^{-6}$ inches/min. The specification for the shearing rate in triaxial tests is usually given in %/hr. The height of the triaxial test specimens usually ranges from about 2.8 inches to 3.0 inches prior to consolidation. Using the minimum expected value for the height, the minimum shearing speed allowed by this device is $4.29x10^{-3}$ %/hr. The soils tested in this investigation required shearing speeds from 0.30 %/hr to 26.26 %/hr, with an average required speed of 4.79 %/hr. These shearing rates were calculated using the actual vertical strain at failure. The strain rates actually used to test the samples did not exceed 1.0 %/hr, following the recommendations of the SHANSEP procedure by Ladd and Foott (1974) and Ladd and DeGroot (2003). According to this information, the triaxial device did provide an adequate range of shearing speeds to perform CU triaxial tests according to the criterion presented in Equation 5.3.

Based on the information above, the ring shear device used in this research does not provide a range of shearing speeds that can always comply with the requirements of ASTM D7608-10 to measure fully softened shear strength parameters. A newer version of this device is available from Controls SRL. This new version allows shearing speeds as low as $2.9x10^{-5}$ inches/min which is better, but lower speeds are still needed. The direct shear and triaxial devices did comply with the required speeds for fully softened shear strength measurements.

5.8.3 Sample size

In the ring shear device, the initial thickness of the sample is 0.20 inches. During the consolidation stage, this thickness is reduced. The grove in the sintered bronze discs will also reduce this thickness as shown in Figure 5.36. The thickness of the sample before shearing depends on the consolidation stress applied and the characteristics of the soil being tested. The test specimen used in this device is very thin as compared to the test specimens used in devices that have been acknowledged to provide suitable peak shear strength results like the triaxial device, where the test specimen is around 3-inch thick and the direct shear device, where the test specimen thickness is in excess of one inch prior to consolidation, as shown in Figure 5.37. Also, the volume of the test specimen used in the ring shear device (1.24 inches^3) is about 25% of that used in the triaxial device (<4.31 inches^3) and the direct shear device (<4.91 inches^3).

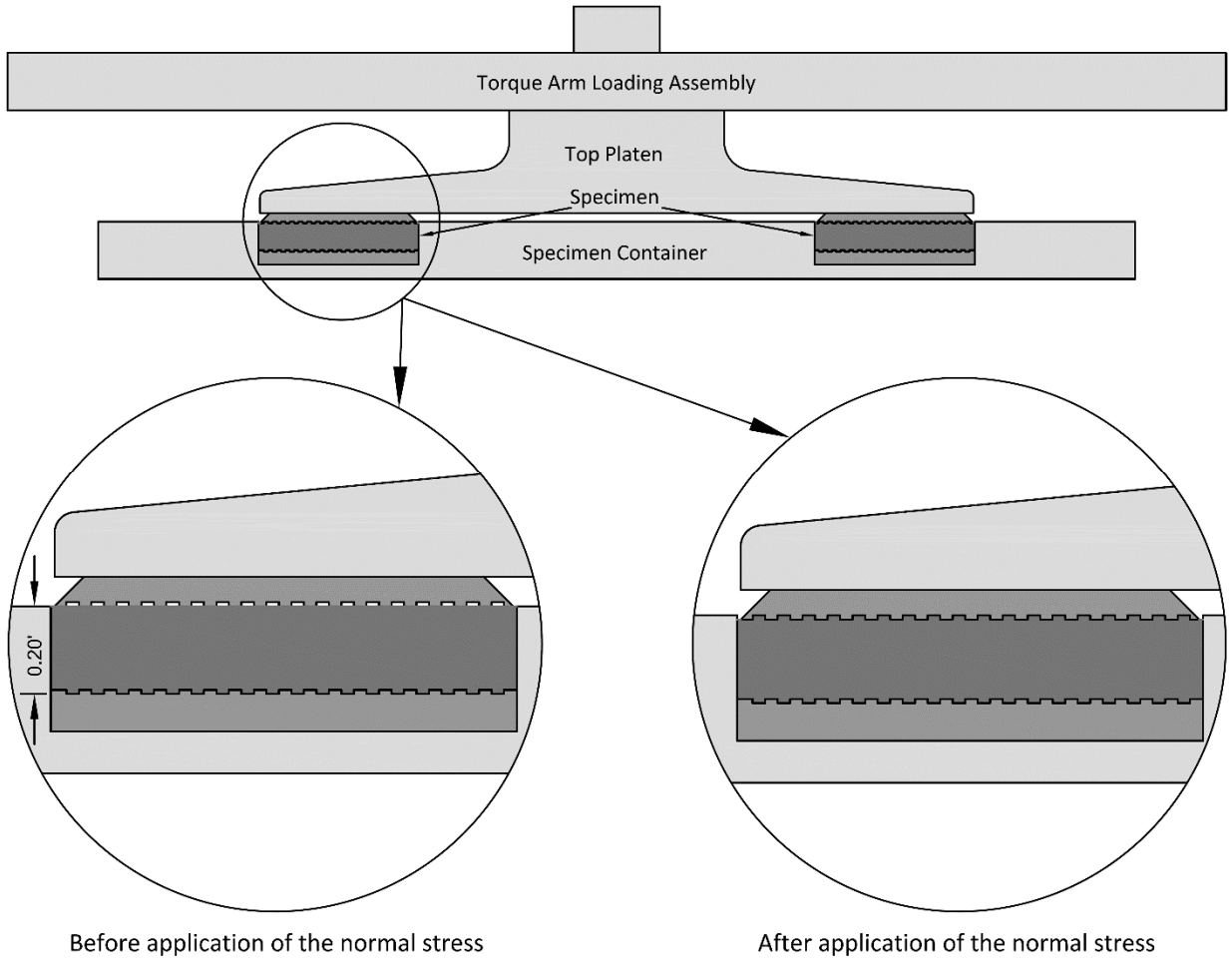

Figure 5.36 Details of the groves in the ring shear device.

5.8.4 Location and orientation of the failure plane

The predetermination of the location of the failure plane in a shear device can be a problem for natural soils because the soil is not necessarily failing on its weakest plane. However, in the case of the remolded test specimens used in this research, it would be expected that the shear strength would be less dependent on the failure plane orientation (Castellanos and Brandon 2013). In the direct shear and ring shear devices, the failure plane is forced by the configuration of the apparatus. In the ring shear device the failure plane is horizontal, thin, and located in close proximity to the top platen. Hvorslev (1960) recognized that the proximity of the failure plane to the end platens, as well as the end platen roughness, could influence test results. In the direct shear device, the failure plane is also horizontal but is located in the center of the test specimen where a gap is opened before shearing. In the triaxial device, the failure plane is not strictly predetermined and failure usually occurs at an angle of about 60° from horizontal. The failure plane in the test specimens for all three devices is shown in Figure 5.37. Based on this information the triaxial device should be the one that better characterizes the peak shear strength of undisturbed samples. For remolded samples, the direct shear and triaxial tests are expected to provide comparable results (Castellanos and Brandon 2013).

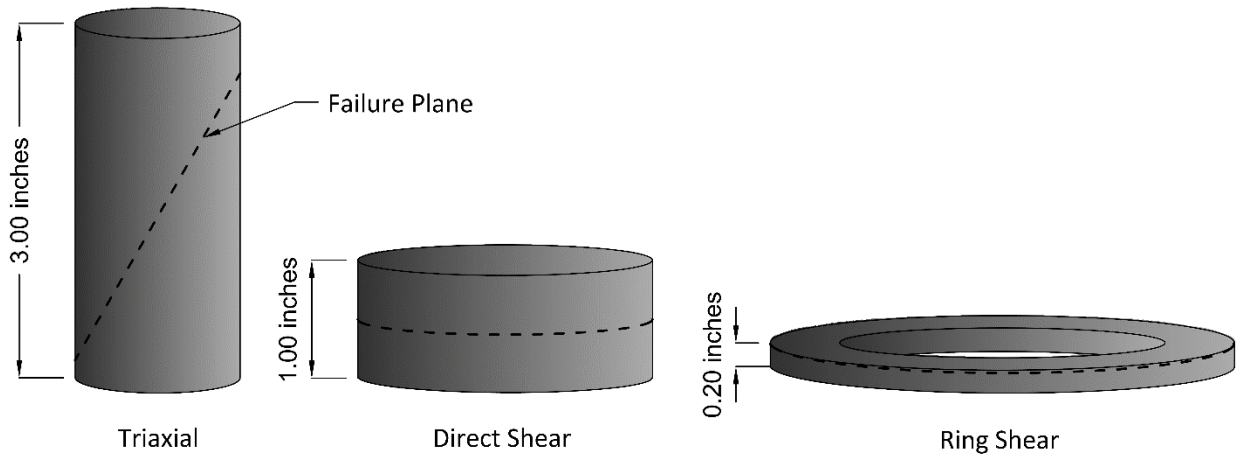

Figure 5.37 Test specimens for the triaxial, direct shear, and ring shear devices.

5.8.5 Stress concentration and progressive failure

One of the biggest criticisms of the direct shear and ring shear devices is that stress concentration within the test specimen can cause progressive failure, which will decrease the shear strength measured (Hvorslev 1939; Bromhead 1979; Saada and Townsend 1981). Hvorslev (1939) stated that although progressive failure is an issue in the direct shear device, reliable peak shear strength measurements can be obtained in remolded cohesive soils because the strain-softening behavior of these soils is not as pronounced as in undisturbed soils. In another study, Hvorslev (1969) observed that in the direct shear device, at the moment of failure, the displacement on the failure plane are fairly uniform. He estimated

that the error in the measured peak shear strength in the direct shear device is around 3% to 5%. The observations presented by Hvorslev were later confirmed by Potts et al. (1987). Potts et al. performed a finite element model of the direct shear test and found that, although stress concentration exists in the direct shear box, at the moment of failure, the stresses on the failure plane are more or less uniform. Thus, progressive failure is unlikely to affect the peak shear strength measured with the direct shear device to a large degree. In their analysis they modeled the strain-softening behavior of soils using a soil constitutive model.

For the ring shear device, no similar study was found. Bromhead (1979) believed that progressive failure could be an issue in ring shear devices providing unreliable results for peak shear strength measurements. According to Hvorslev (1939), the triaxial device does not develop stress concentration in the zone of failure before the failure occurs if long enough samples are used. Hvorslev also stated that right before and after failure, irregular changes in the cross-section of the test specimen occur causing a non-uniform distribution of stresses in the triaxial device. Research performed by Taylor (1941) and summarized by Rutledge (1947) showed that if test specimens in the triaxial device have a length to diameter ratio in between 1.5 and 3, reliable results can be obtained. Current ASTM D4767-11 recommends the use of length to diameter ratios between 2.0 and 2.5 for triaxial testing.

5.8.6 Soil extrusion

Soil extrusion occurs when soil is squeezed out of the test specimen. Soil extrusion can be a problem in the direct shear and ring shear devices. It normally cannot occur in the triaxial device. In the ring shear device and direct shear devices, soil extrusion can be a problem during the consolidation and shearing stages. In order to reduce extrusion during consolidation, the test specimen needs to be consolidated from a very low stress and/or formed using a relative low water content. In this research, an initial normal stress of 100 psf and a load increment ratio of one have been used successfully with test specimens prepared at liquidity indices below 1.5. For specimens prepared at a liquidity index above 1.5, an initial normal stress of 50 psf is recommended. More information about the effect of the initial molding water content in the measured fully softened shear strength is presented in Section 6.6.

During shear in the ring shear device, an excessive amount of extrusion can occur. Extrusion during shear has been found to reduce the normal stress on the failure plane, which also reduces the shear strength measured (La Gatta 1970). Extrusion also causes unreliable vertical displacements to be measured during shear in the ring shear device. As a consequence, these displacements should not be used to determine final unit weights, void ratio, or any other parameter associated with them.

5.8.7 Tilt of the top platen

Tilting of the top platen can be an issue in the triaxial and direct shear devices. In the triaxial device this is not considered to be much of a problem because of the fixity of the rod provided by the top platen. In the direct shear device, during the consolidation process, the top platen can rotate if the top of the test specimen is not leveled during specimen setup or if the load is not concentric. If this occurs, the porous stone can get wedged in the shear box causing a reduction in the normal stress felt by the test specimen.

If this problem is detected during the early stages of the consolidation process, the top platen can be re-leveled, and the test can be salvaged.

5.9 Conclusions

In this chapter, the devices that were used in the laboratory testing program presented in this research were described. A soil processing method and techniques to prepare test specimens for fully softened shear strength measurement in the direct shear, ring shear, and triaxial devices were presented. Also a comparison between these devices focusing on fully softened shear strength measurement was presented. From this comparison, it can be seen that the triaxial device is expected to more accurately measure the peak shear strength of soils, although, difficulties with preparing test specimens and the time required for testing make this device not very practical for fully softened shear strength measurements. The direct shear device, although having some issues, seems to be the most convenient device. The ring shear device had seldom been used for peak shear strength measurements. Some issues, like the available shearing speeds in commercially available ring shear devices, sample size, location of the failure plane, and soil extrusion during shear in this device might influence the fully softened shear strength measured. The difference of the fully softened shear strength measured with these devices is evaluated in the next chapter, where a comparison between the fully softened shear strength measured with all three devices is presented.

Chapter 6

Test Results

6.1 Introduction

The effect of the device used on the measured fully softened shear strength was investigated by comparing the results obtained with the direct shear, ring shear, and triaxial devices. Because of issues like progressive failure with the direct shear and ring shear devices and unproven capabilities of measuring correct values of peak drained shear strength of the ring shear device, the triaxial device was assumed to provide the most accurate measurement of fully softened shear strength. The validity of the other devices is assessed based on the results obtained from this device.

The research described in this dissertation also investigated forming test specimens using blenderized and non-blenderized techniques and their effect on the fully softened shear strength and index properties measured. Also, the effect of using different molding water contents to form test specimens on the fully softened shear strength measured was addressed by testing samples prepared at liquidity indices ranging from around 0.6 to 1.5 using the direct shear device.

The shear strength of compacted samples and undisturbed overconsolidated samples subjected to cycles of wetting and drying have been found to be approximately equal to the fully softened shear strength (Crawford 1964; Calabresi and Rampello 1987; Kayyal and Wright 1991; Stark and Duncan 1991; Botts 1998; Wright et al. 2007). Some authors have also found that most of the loss in shear strength happens in the first cycle of wetting (Calabresi and Rampello 1987; Botts 1998). In order to provide more insight on whether one cycle of swelling is enough to reduce the shear strength of compacted clay samples to the fully softened shear strength, the effect on the peak drained shear strength of allowing compacted clay samples to swell in the triaxial device was investigated. For this purpose, compacted triaxial samples were allowed to swell under 432 psf in the triaxial device prior to consolidation.

In this chapter, the results of the laboratory testing program performed to evaluate the effect of the technique used to measure the fully softened shear strength are presented.

The laboratory testing program was performed in five stages. The first stage included direct shear and ring shear tests to compare the fully softened shear strength measured with these devices. The second stage consisted of conducting direct shear tests to evaluate the effect of the sample preparation technique and molding water contents on the measured fully softened shear strength. The third stage consisted of performing CU triaxial tests using non-blenderized test specimens trimmed from soil samples pre-consolidated in a batch consolidometer. The fourth stage entailed performing direct shear and CU triaxial

tests at consolidation stresses below 500 psf. The fifth and last stage consisted in performing CU triaxial test on compacted clay test specimens allowed to swell prior to consolidation.

The test reports of the results presented in this chapter are presented in Appendices C thru G. Soil samples were processed in the non-blenderized fashion and mixed to an initial water content equal to the liquid limit unless specified otherwise.

6.2 Processing the Results

This section presents a detailed explanation on how the results of each test were interpreted and the assumptions behind these interpretations.

6.2.1 Direct shear device

In the direct shear test the normal and shear stress on the failure plane can be easily calculated based on the forces measured. The interpretation of the results from this device is based on the assumption that, although the cross-sectional area of the test specimens changes during shear, the ratio of the normal to shear stress is equal to the ratio of the normal to shear force (ASTM D3080-11). The equations provided in ASTM D3080-11 to calculate the effective normal stress and the shear stress on the failure plane were used. These equations are shown below:

$$\sigma'_n = \frac{N}{A} \tag{6.1}$$

$$\tau = \frac{F}{A} \tag{6.2}$$

Where:

σ'_n = Effective normal stress on the failure plane.
N = Applied normal force on the failure plane.
A = Cross-sectional area of the test specimen.
τ = Shear stress on the failure plane.
F = Measured shear force on the failure plane.

ASTM D3080-11 allows, but does not require, the use of correction factors to take into account the change in cross-sectional area during shear. As is represented in Figure 6.1, the cross-sectional area decreases as the horizontal displacement increases causing an increase in normal and shear stresses on the failure plane. The contact area of circular test specimens during shear can be calculated using Equations 6.3 and 6.4 presented by Sadrekarimi and Olson (2008) and Ölmez (2008).

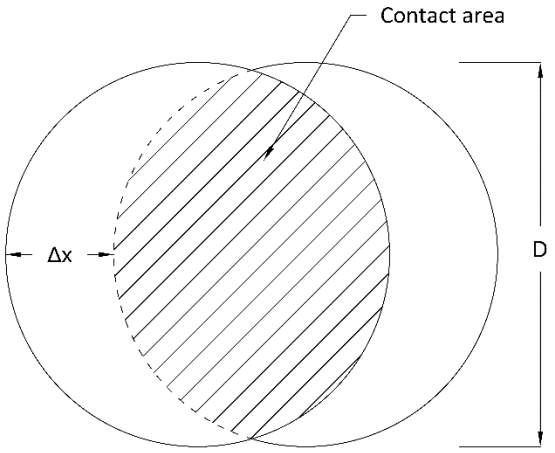

Figure 6.1 Change in cross-sectional area in circular test specimens during shear in the direct shear device.

$$A_c = A_o F \tag{6.3}$$

$$F = \frac{2}{\pi}\left[\cos^{-1}\left(\frac{\Delta x}{D}\right) - \frac{\Delta x}{D}\sqrt{1-\left(\frac{\Delta x}{D}\right)^2}\right] \tag{6.4}$$

Where:

A_c = Contact area.
A_o = Initial cross-sectional area.
F = Correction factor.
Δx = Horizontal displacement.
D = Diameter of the test specimen.

The results of the direct shear performed to NOVA Clay and VBC were analyzed using the initial cross-sectional area (uncorrected area) and the corrected area to assess the effect of correcting the cross-sectional area on the failure envelope obtained. From the results presented in Figures 6.2 and 6.3, it can be seen that the area correction does not have a significant effect on the failure envelope obtained. For this reason, area correction was not used to analyze the results of direct shear tests presented in this dissertation.

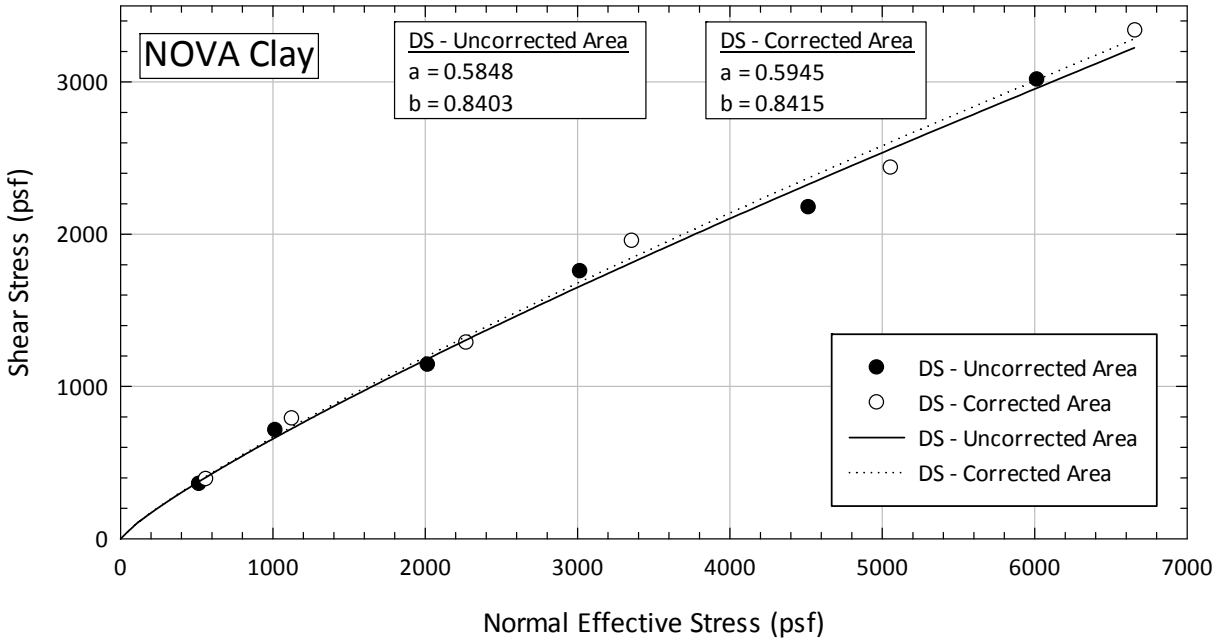

Figure 6.2 Effect of area correction on the direct shear test results of NOVA Clay.

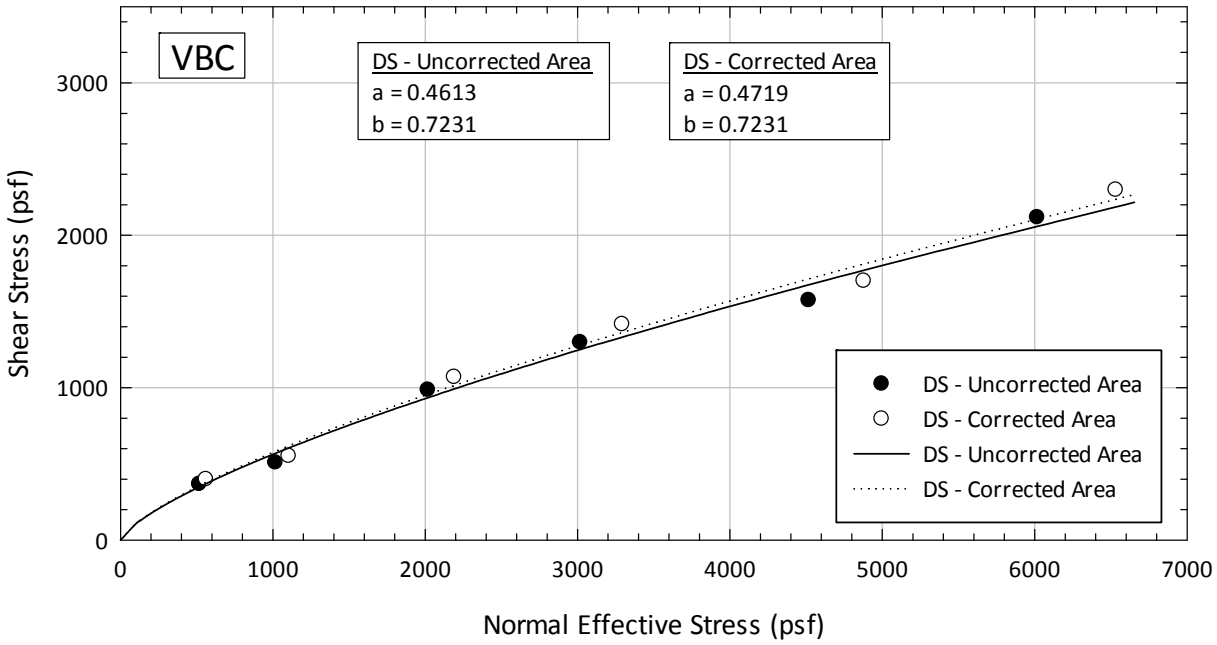

Figure 6.3 Effect of area correction on the direct shear test results of VBC.

6.2.2 Ring shear device

For the ring shear device, different distributions of the normal stress on the failure plane can be assumed. Each distribution of normal stress is represented by a different equation to calculate the average normal and shear stresses on the failure plane. A detailed explanation of these distributions along with the equations used for each case is presented by Bishop et al. (1971). They stated that the assumed distribution of normal stresses does not greatly influence the results. A variation of ±3° in the effective friction angle was reported by Bishop et al. for soils with ϕ'<40°, assuming different variations of the normal stress. For this research, the assumption that the normal and shear stresses are uniformly distributed on the failure plane, as recommended by Bishop et al. (1971), Bromhead (1979), and ASTM D7608-10, was used. The equations used are presented in Equations 6.5 and 6.6:

$$\sigma'_n = \frac{N}{\pi({R_2}^2 - {R_1}^2)} \tag{6.5}$$

$$\tau = \frac{3(F_1 + F_2)L}{4\pi({R_2}^3 - {R_1}^3)} \tag{6.6}$$

Where:

σ'_n	=	Effective normal stress on the failure plane.
N	=	Applied normal force on the failure plane.
$R_1,\ R_2$	=	Inner and outer radii.
τ	=	Shear stress on the failure plane.
$F_1,\ F_2$	=	Measured forces on the proving rings.
L	=	Torque arm length.

6.2.3 Triaxial device

The results from the triaxial device are the most difficult to interpret. In the triaxial test, as opposed to the direct shear and ring shear tests, normally, principal stresses are specified instead of stresses on the failure plane. For this reason, some assumptions have to be made in order to present the data in a similar fashion as the direct shear and ring shear results. First, the cross-sectional area and height of the test specimens change during consolidation. Different methods have been proposed to calculate the height and cross-sectional area of the test specimen after consolidation. For this research, the equations presented by Head (1986) were used. According to Head, these equations are based on the elastic theory for small volume change presented by Case and Chilver (1959) assuming a Poisson's ratio of 0.5. These

equations should be particularly valid for the test specimens since they were remolded and homogenous. These equations are presented below.

$$L_c = L_o\left(1 - \frac{1}{3}\frac{\varepsilon_v}{100}\right) \tag{6.7}$$

$$A_c = A_o\left(1 - \frac{2}{3}\frac{\varepsilon_v}{100}\right) \tag{6.8}$$

Where:

L_c = Length of the test specimen after consolidation.
L_o = Length of the test specimen before consolidation.
ε_v = Volumetric strain occurred during consolidation expressed as a percentage.
A_c = Cross-sectional area of the test specimen after consolidation.
A_o = Cross-sectional area of the test specimen before consolidation.

For the triaxial test, different failure criteria can be used, which in some cases, will influence the effective stress friction angle obtained. The failure criterion used in this research was the maximum principal stress ratio (PSR). For the soils tested, it was verified that using the maximum deviator stress as the failure criterion provides about the same failure envelope.

Because of the curvature observed in the fully softened failure envelope, the power function presented in Equation 4.1 was used to describe the failure envelopes of the soils tested. To fit a curved failure envelope to the triaxial tests results, a secant effective stress friction angle was calculated for each test using the relationship presented in Equation 6.9. This secant friction angle was then used to calculate the normal effective and shear stresses acting on the failure plane using Equations 6.10 and 6.11, respectively.

$$\left(\frac{\sigma'_1}{\sigma'_3}\right)_{peak} = \tan^2\left(45 + \frac{\phi'_{secant}}{2}\right) \tag{6.9}$$

$$\sigma'_f = \frac{\sigma'_{1-fail} + \sigma'_{3-fail}}{2} - \left(\frac{\sigma'_{1-fail} - \sigma'_{3-fail}}{2}\right) \cdot \sin(\phi'_{secant}) \tag{6.10}$$

$$\tau_f = \sigma'_f \cdot \tan(\phi'_{secant}) = \left(\frac{\sigma'_{1-fail} - \sigma'_{3-fail}}{2}\right) \cdot \cos(\phi'_{secant}) \quad (6.11)$$

Where:

$\sigma'_{1-fail}, \sigma'_{3-fail}$	=	Major and minor principal effective stresses at failure.
ϕ'_{secant}	=	Secant effective stress friction angle.
σ'_f	=	Effective normal stress on the failure plane at failure.
τ_f	=	Shear stress on the failure plane at failure.

6.2.4 Obtaining the parameters for the power function

After the shear and normal effective stresses on the failure plane at failure are obtained, a plot as shown in Figure 6.4 should be constructed to obtain the parameters *a* and *b* required for Equation 4.1. From this plot, a line is fit to the data points. The y-intercept of this line is equal to the logarithm of the parameter *a* in Equation 4.1 and the slope of this line is equal to the parameter *b* in that same equation.

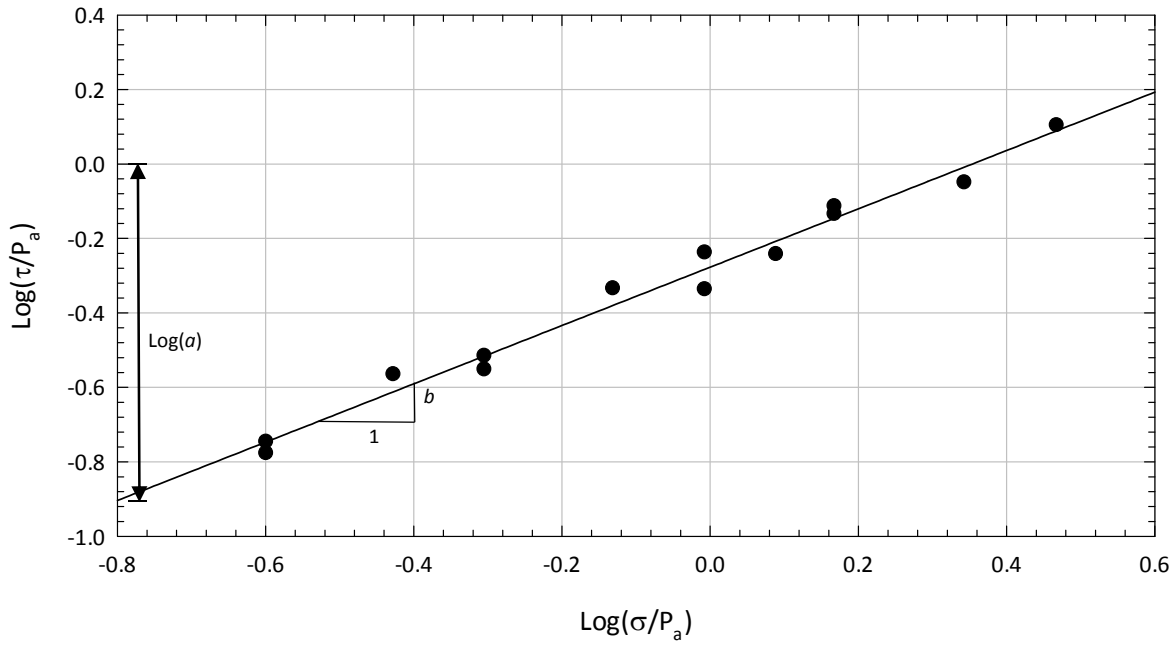

Figure 6.4 Plot to obtain Lade's power function shear strength parameters.

6.3 Ring Shear and Direct Shear Devices Comparison

The results of the tests performed to compare the fully softened shear strength measured with the direct shear and ring shear devices described in Section 5.4 are presented in this section. Ring shear tests were performed at Virginia Tech and direct shear tests were performed both at Virginia Tech and ERDC. Close agreement was found with the results of the direct shear tests performed by ERDC and Virginia Tech as can be seen from the results presented in this section.

Fourteen soils were tested using both devices. Samples Texas 1 through 6, Colorado Clay, NOVA Clay, Oahe Dam, and VBC were blenderized prior to testing in these two devices. Samples Alabama 1 through 4 were prepared in the non-blenderized fashion. The sample preparation procedure is described in Section 5.3. The results from the shear strength tests performed are presented in Figures 6.5 to 6.18 and summarized in Table 6.1.

The results show that the ring shear device provides a very conservative measurement of the fully softened shear strength. The fully softened failure envelope obtained with the direct shear device plotted above that obtained with the ring shear apparatus for every soil tested. In addition, the direct shear envelope exhibited more curvature than the ring shear envelope. The difference in the fully softened shear strength obtained with these devices was found to decrease with increasing consolidation pressure, as can be seen from the results presented in Figures 6.19 and 6.20.

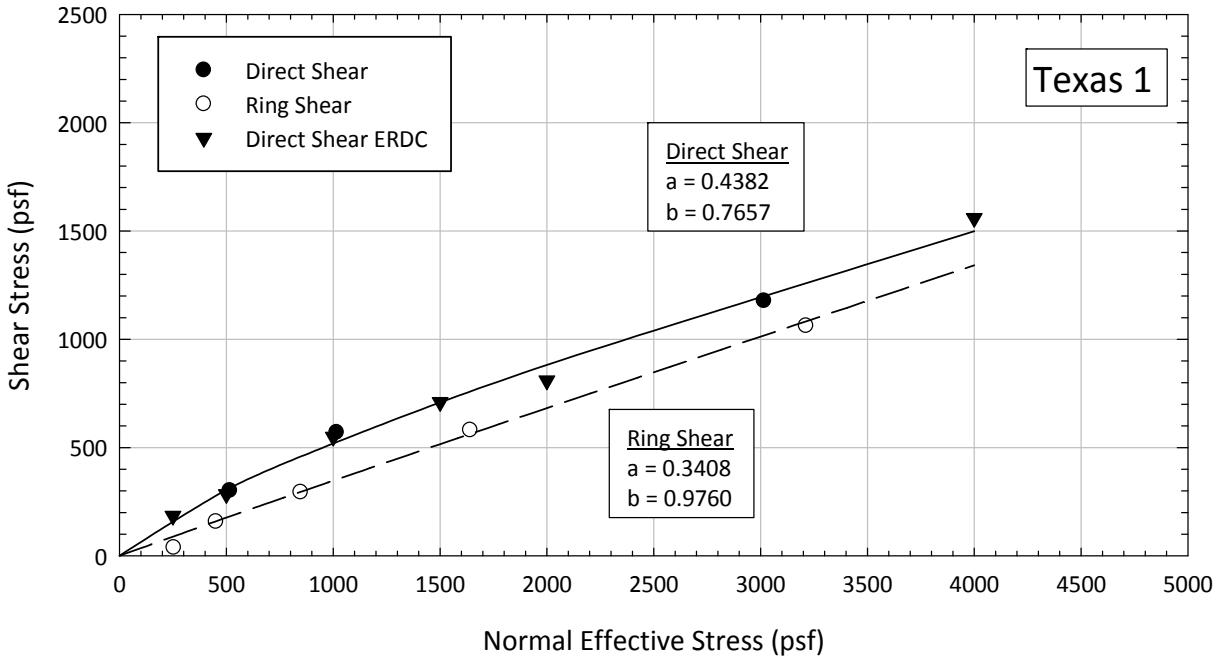

Figure 6.5 Direct shear and ring shear results for blenderized Texas 1 sample.

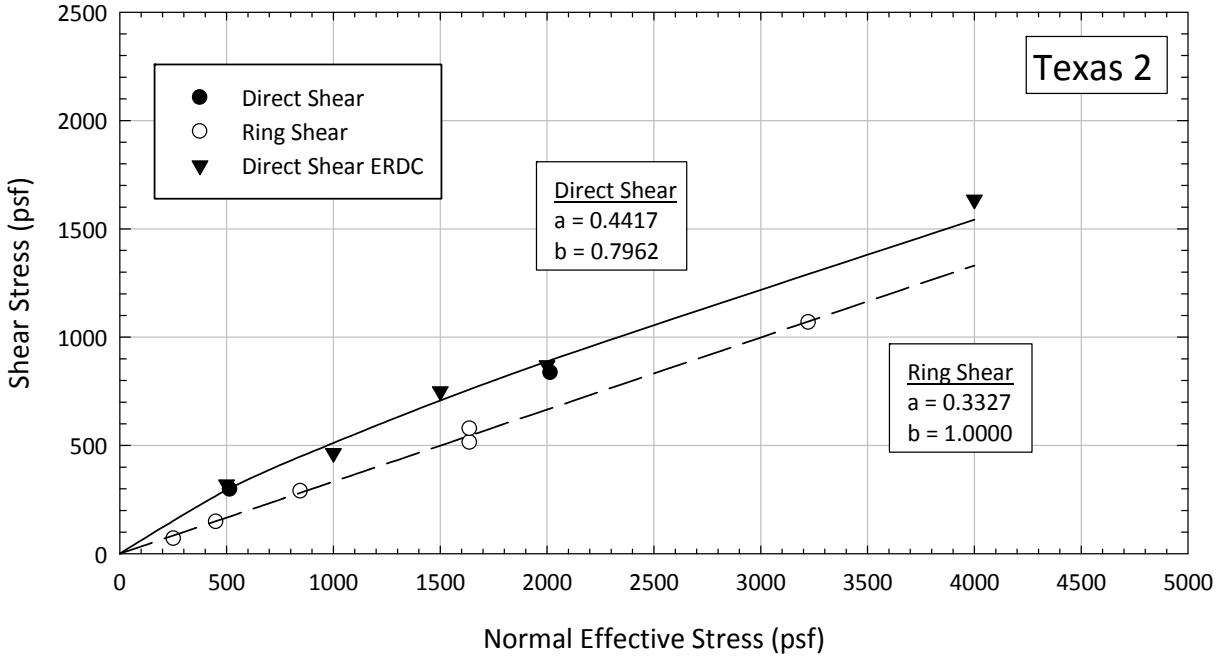

Figure 6.6 Direct shear and ring shear results for blenderized Texas 2 sample.

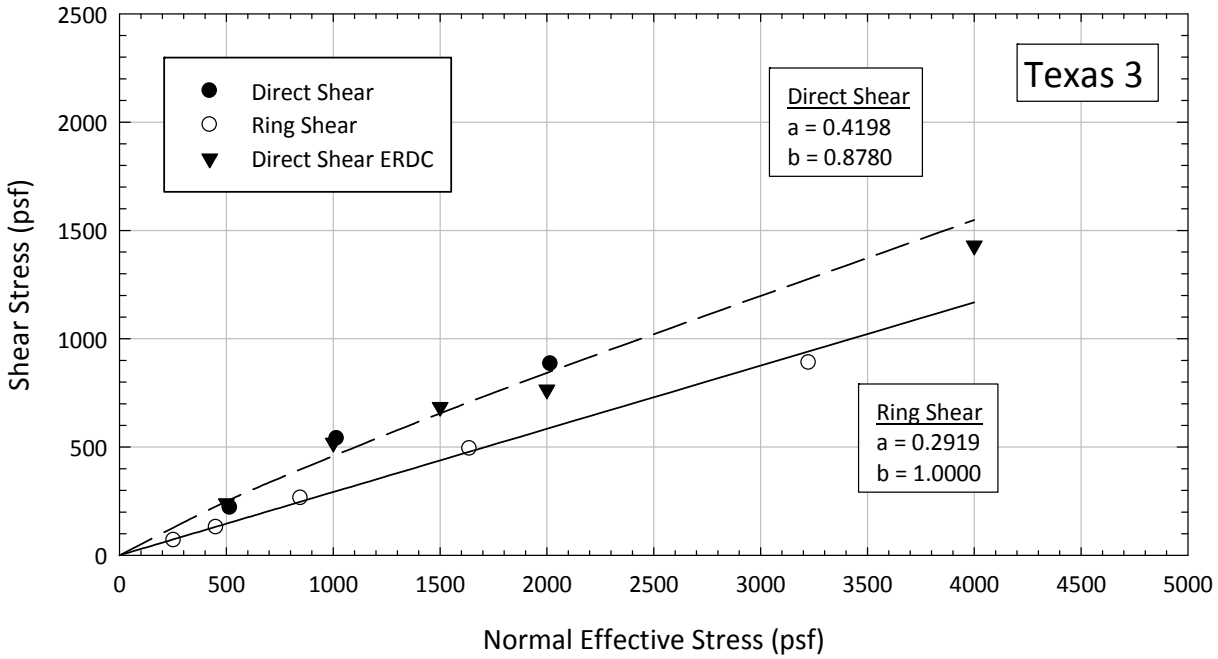

Figure 6.7 Direct shear and ring shear results for blenderized Texas 3 sample.

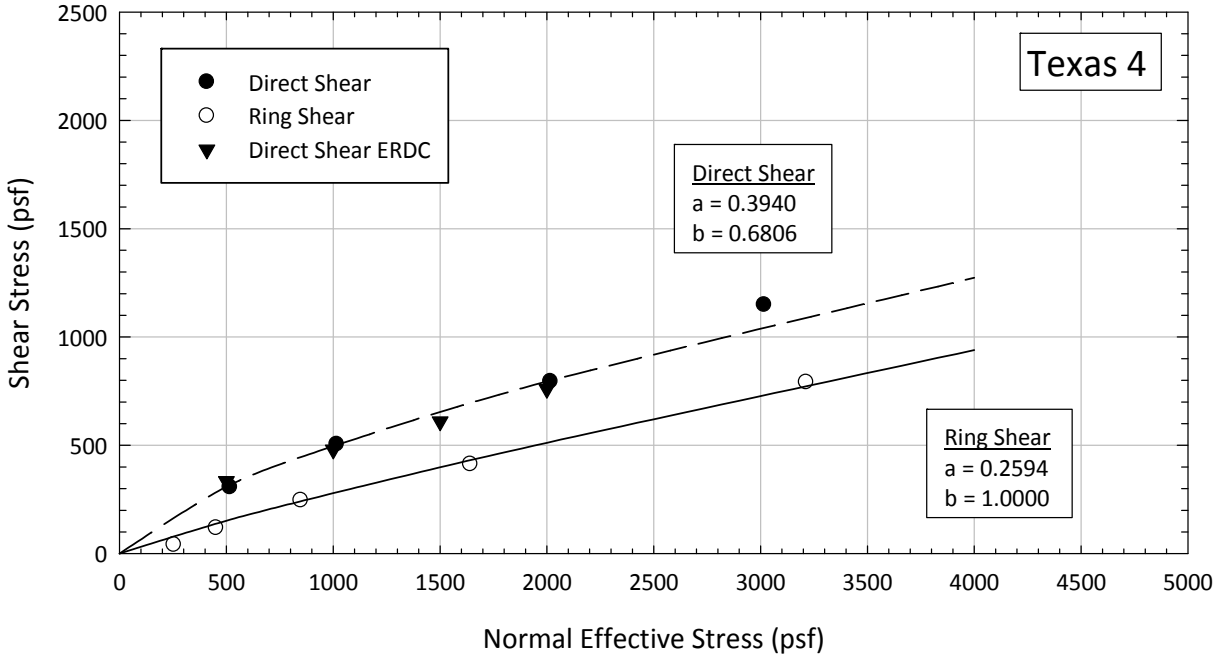

Figure 6.8 Direct shear and ring shear results for blenderized Texas 4 sample.

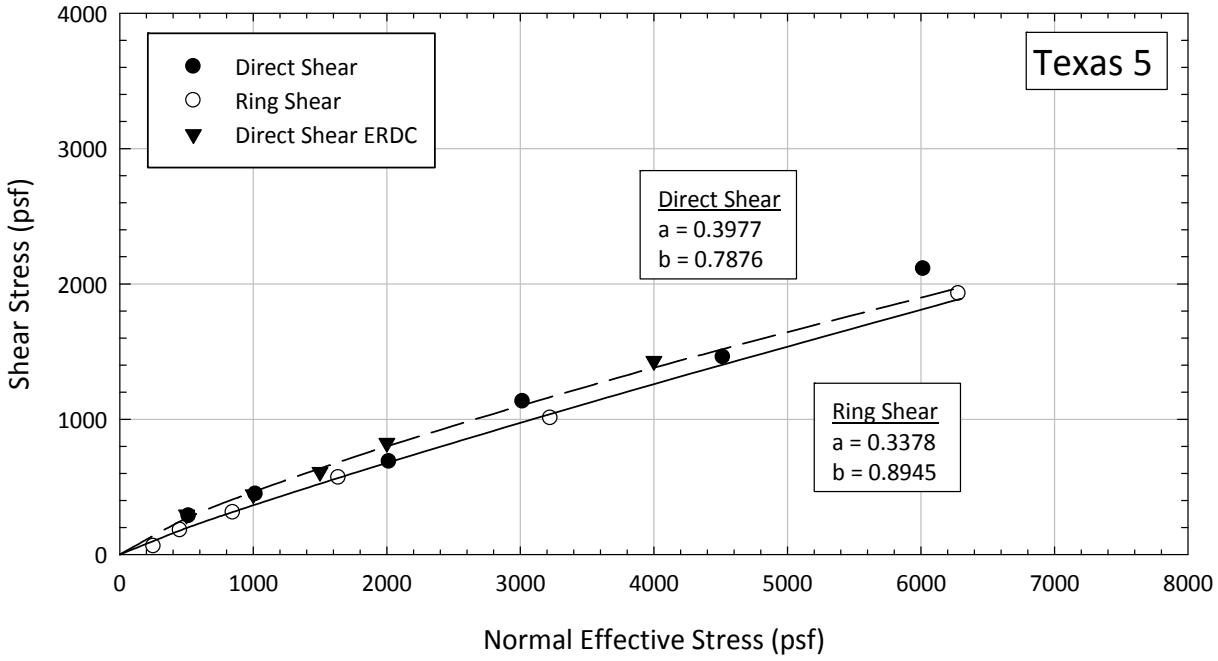

Figure 6.9 Direct shear and ring shear results for blenderized Texas 5 sample.

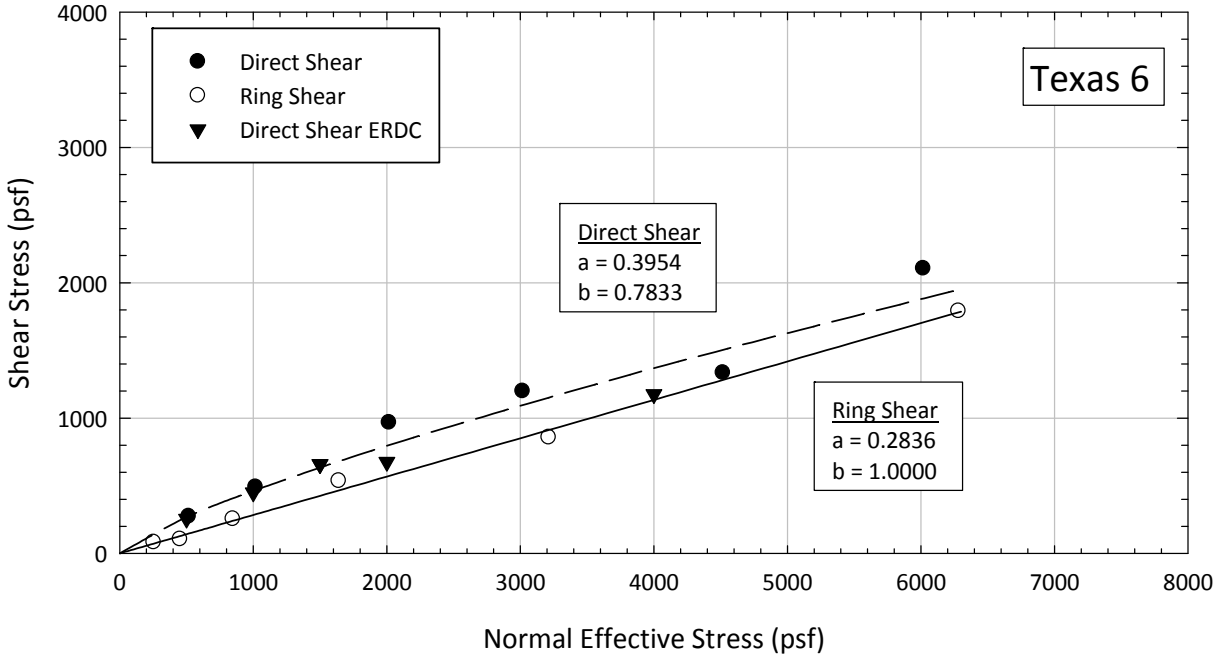

Figure 6.10 Direct shear and ring shear results for blenderized Texas 6 sample.

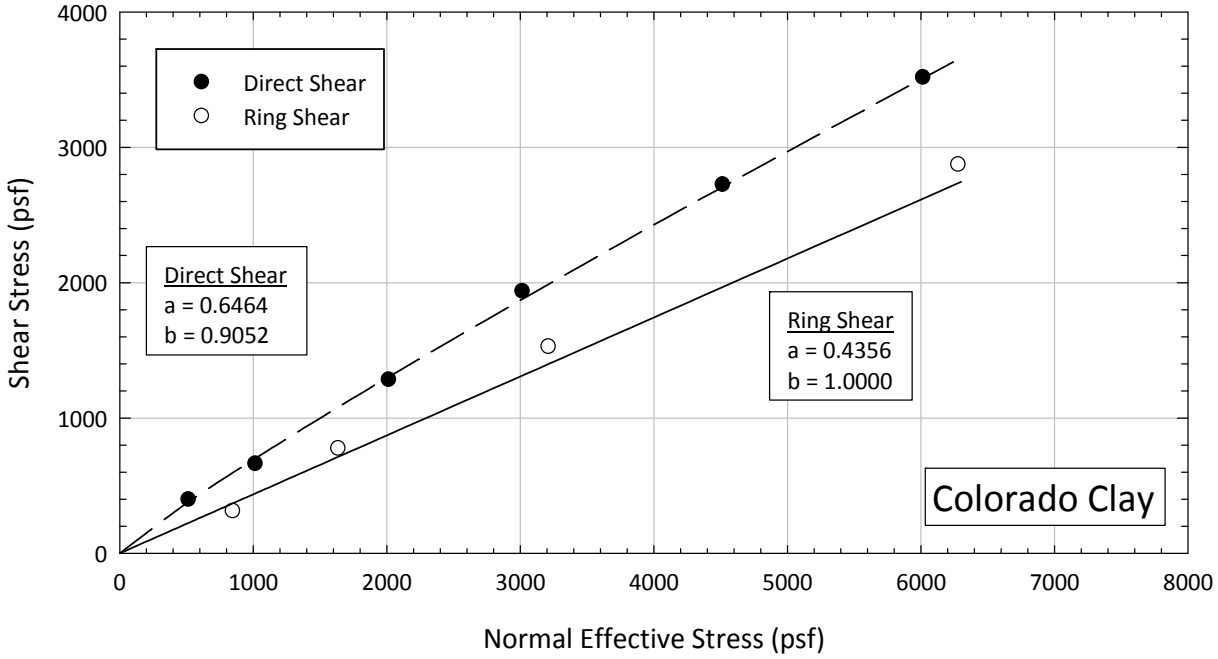

Figure 6.11 Direct shear and ring shear results for blenderized Colorado Clay sample.

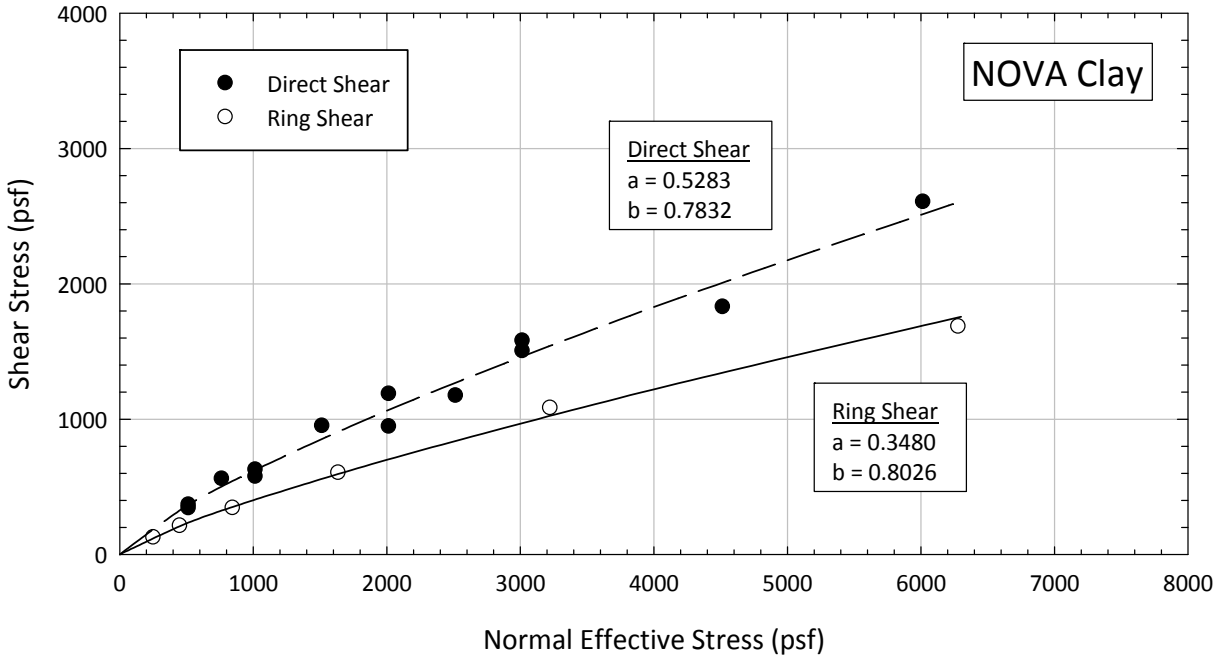

Figure 6.12 Direct shear and ring shear results for blenderized NOVA Clay sample.

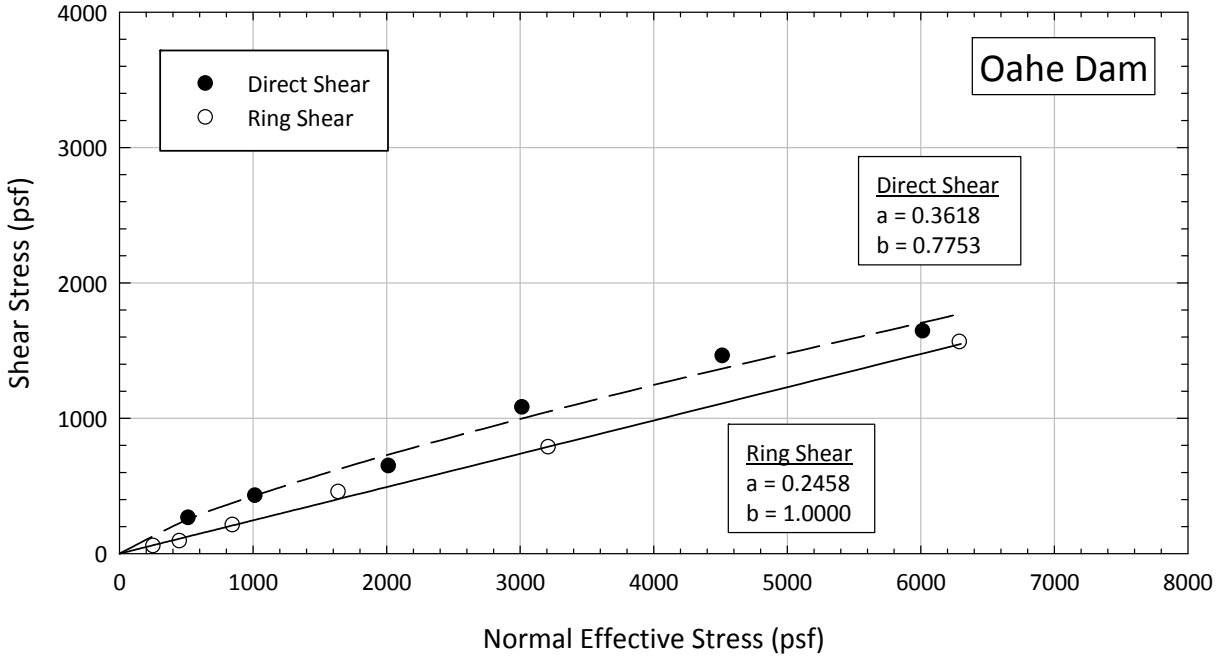

Figure 6.13 Direct shear and ring shear results for blenderized Oahe Dam sample.

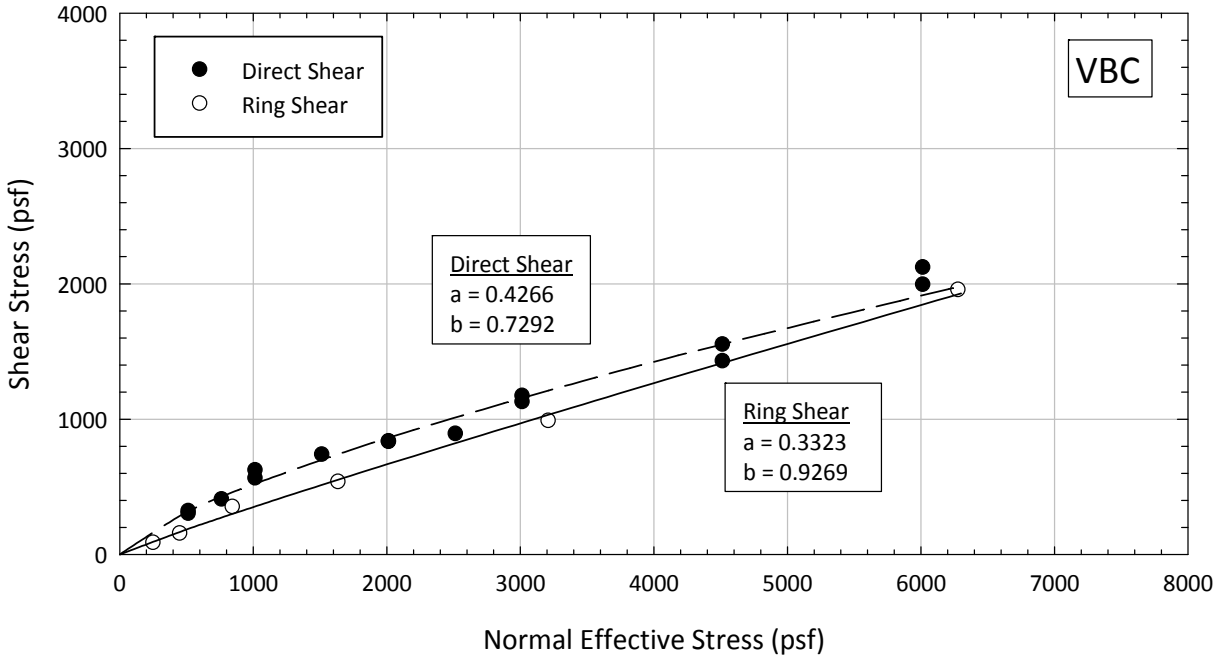

Figure 6.14 Direct shear and ring shear results for blenderized VBC sample.

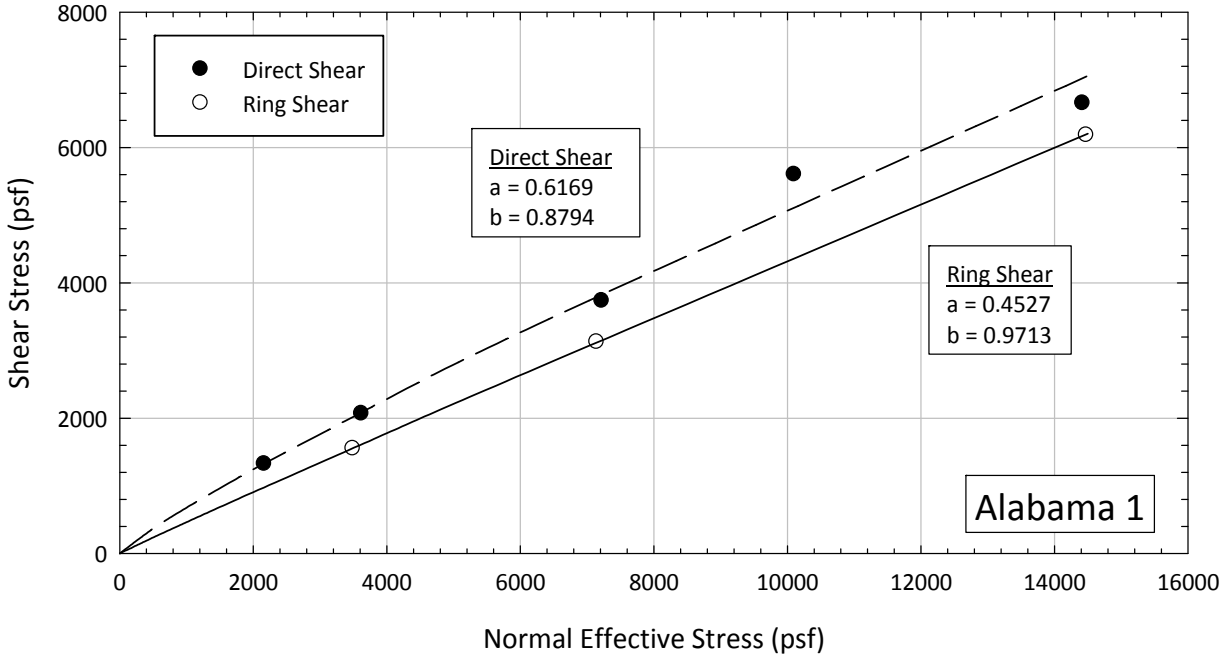

Figure 6.15 Direct shear and ring shear results for Alabama 1 sample.

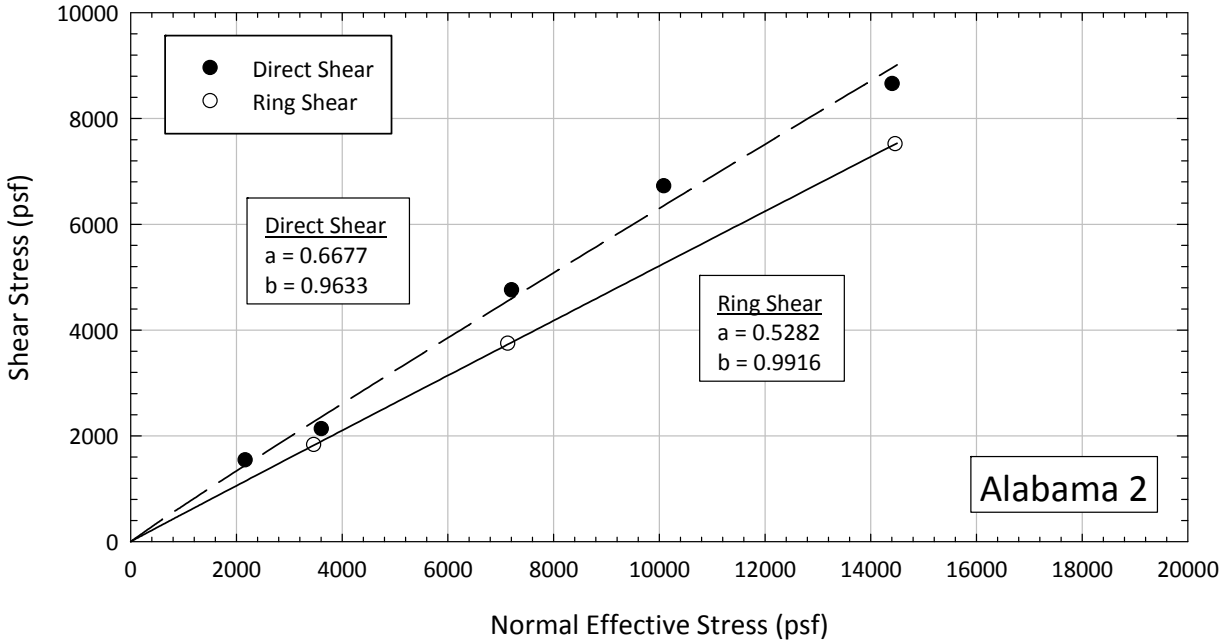

Figure 6.16 Direct shear and ring shear results for Alabama 2 sample.

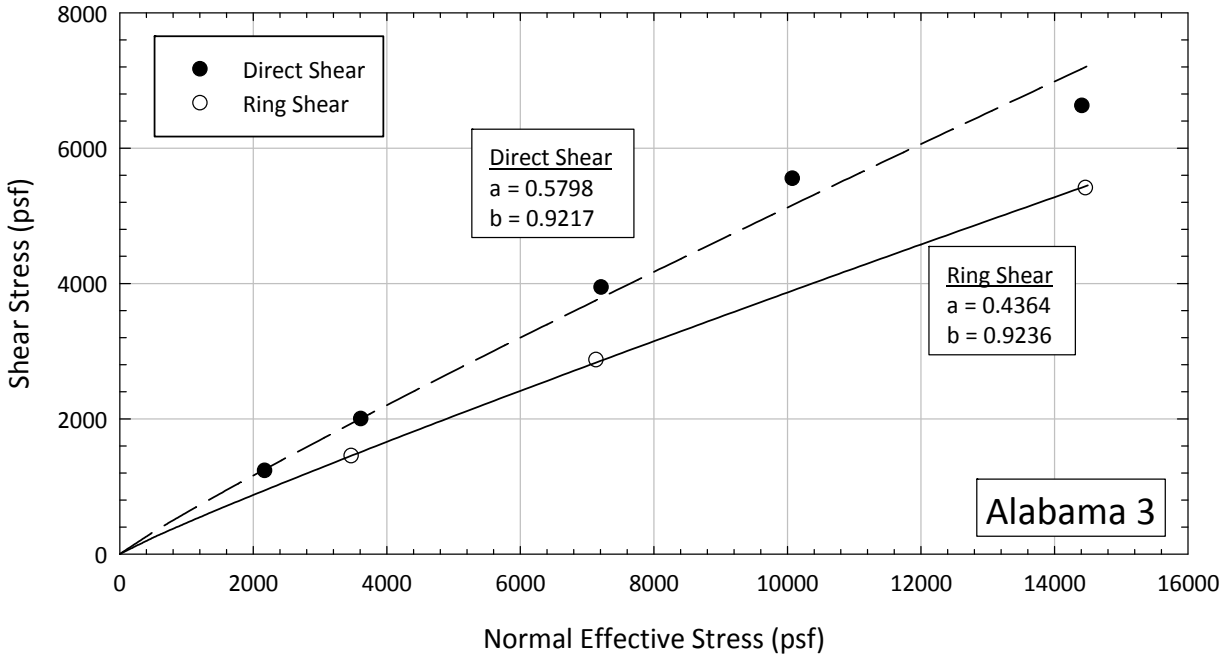

Figure 6.17 Direct shear and ring shear results for Alabama 3 sample.

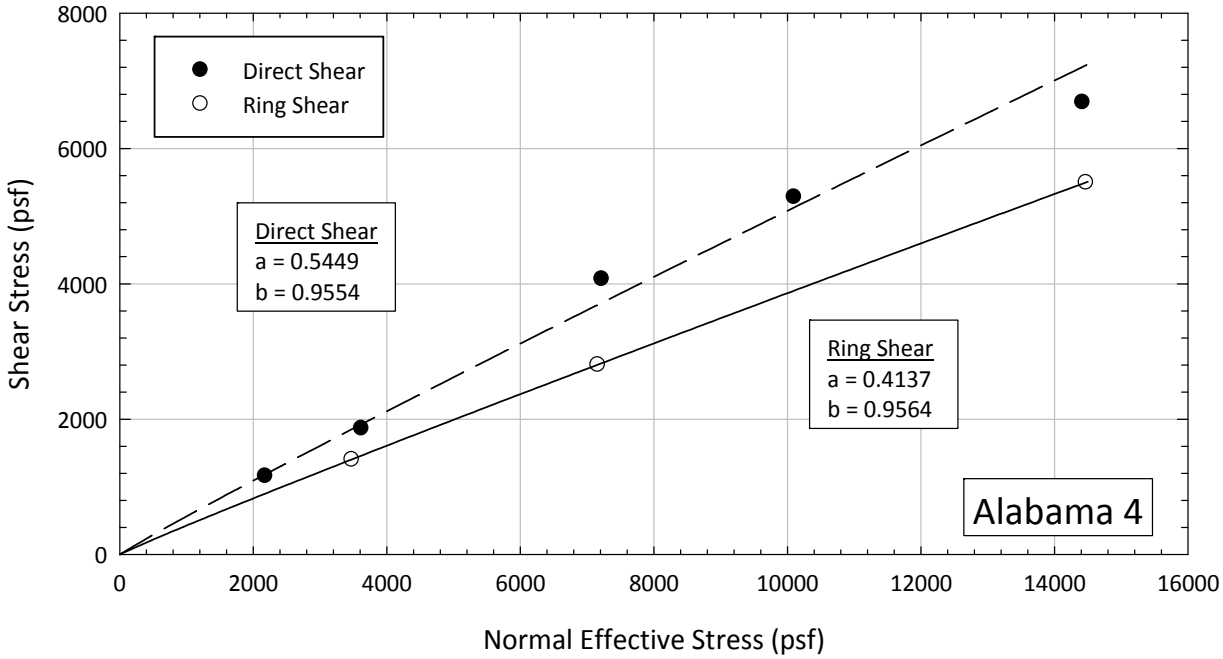

Figure 6.18 Direct shear and ring shear results for Alabama 4 sample.

Table 6.1 Summary of the values of *a* and *b* obtained from direct shear and ring shear tests

Soil	Direct Shear		Ring Shear	
	a	*b*	*a*	*b*
Texas 1	0.4382	0.7657	0.3408	0.9760
Texas 2	0.4417	0.7962	0.3327	1.0000
Texas 3	0.4198	0.8780	0.2919	1.0000
Texas 4	0.3940	0.6806	0.2594	1.0000
Texas 5	0.3977	0.7876	0.3378	0.8945
Texas 6	0.3954	0.7833	0.2836	1.0000
Colorado Clay	0.6464	0.9052	0.4356	1.0000
NOVA Clay	0.5283	0.7832	0.3480	0.8026
Oahe Dam	0.3618	0.7753	0.2458	1.0000
VBC	0.4266	0.7292	0.3323	0.9269
Alabama 1	0.6169	0.8794	0.4527	0.9713
Alabama 2	0.6677	0.9633	0.5282	0.9916
Alabama 3	0.5798	0.9217	0.4364	0.9236
Alabama 4	0.5449	0.9554	0.4137	0.9564

Other researchers have found smaller differences in the shear strength measured with these two devices (e.g. Hvorslev 1936, Tiedemann 1937 as reported by Hvorslev 1939; Stark and Eid 1997). Hvorslev (1936) found differences from 1% to 4% in the shear strength measured with a direct shear device and his version

of the torsional ring shear device on normally consolidated soils. For overconsolidated soils he found that the shear strength measured with his torsional ring shear device was 10% to 12% lower than the shear strength measured with a direct shear device. The consolidation stresses used by Hvorslev to test the normally consolidated specimens were 4,090 psf and 10,240 psf. From Figures 6.19 and 6.20, it can be inferred that the consolidation pressures used by Hvorslev were in a range where the difference between the shear strength measured in these two devices may be small.

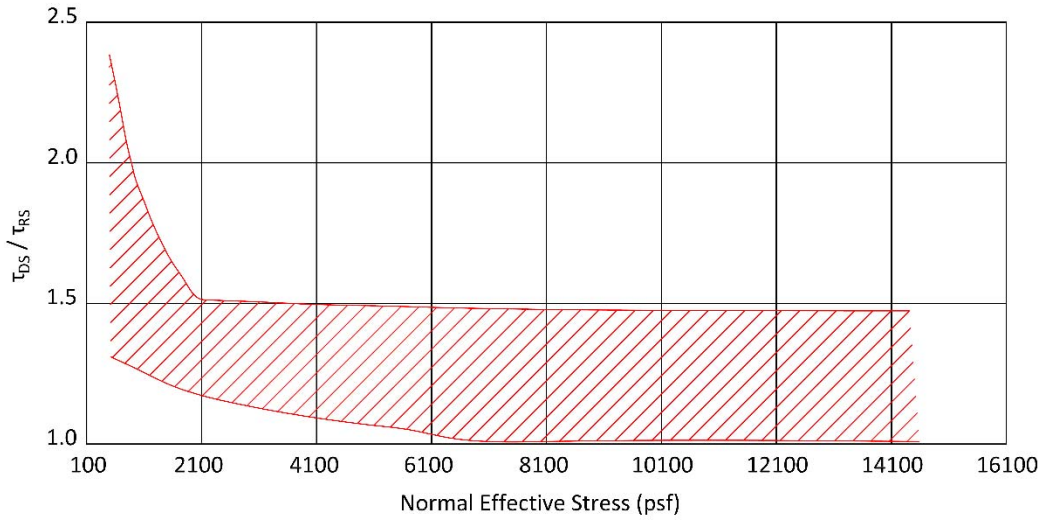

Figure 6.19 Measured range of the ratio of the fully softened shear strength measured with the direct shear and ring shear devices.

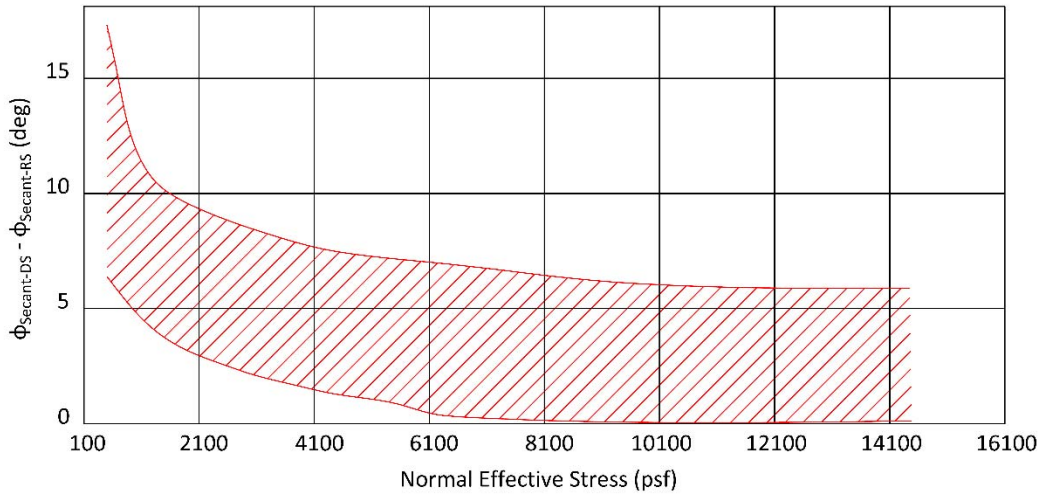

Figure 6.20 Range of the measured difference in direct shear and ring shear secant friction angle.

Hvorslev (1939) reported that Tiedemann (1937) found close agreement between the peak shear strength measured with Tiedemann's ring shear apparatus and a direct shear device. A review of Tiedemann's paper did not reveal if the agreement found between these two devices was in peak or residual shear strength, although it seems that he is referring to peak shear strength. In the paper by Tiedemann, the consolidation stresses used for the tests were not specified. Tiedemann did not present the test results, but stated that similar results were found with these two devices.

Stark and Eid (1997) compared the results of two different soils tested using only two different consolidation stresses with the direct shear and ring shear devices. The results showed that the difference in the fully softened friction angle measured with the direct shear and the torsional ring shear devices was very small, resulting in a difference of less than one degree. High pressures were selected for this comparison (2090 psf and 8350 psf). From the data presented in Figure 6.20, it can be inferred that for the range of pressures tested by Stark and Eid (1997), the difference in the fully softened secant friction angle measured with these two devices can be less than one degree. The conclusion by Stark and Eid was based on two tests using only two soils. It should be noted that, at high stresses a small difference in secant friction angle can result in a significant difference in shear strength.

The difference in the shear strength measured with both apparatuses may be due to the differences in specimen thicknesses, and the proximity of the failure plane to the end platens as shown in Figure 5.37. The thickness of the direct shear test specimen is about one inch after consolidation. In the ring shear device, the specimen thickness ranges from slightly less than 0.2 inches to 0.1 inches for consolidation pressures ranging from 150 psf to 14,400 psf. For this device, the failure plane has been observed to be in close proximity to the top platen. For the direct shear apparatus, the failure plane is normally about 0.5 inches from the end platen. Hvorslev (1960, 1969) recognized that the proximity of the failure plane to the end platens, as well as the end platen roughness, could influence test results. When addressing the use of the ring shear device to measure peak shear strength, Bromhead (1979) stated: "It should be noted that the non-uniform strain distribution greatly encourages progressive failure in brittle soils and it is therefore unlikely that any ring shear apparatus will give a reliable peak shear strength".

6.4 Direct Shear and Triaxial Devices Comparison

The fully softened shear strengths measured with the direct shear and the triaxial devices were compared using non-blenderized samples of Alabama 1, Colorado Clay, NOVA Clay, Oak Harbor, and VBC. The results of these tests are presented in Figures 6.21 to 6.25 and summarized in Table 6.2. The results show no significant difference in the fully softened shear strength measured with both devices. This finding is in agreement with the results presented by De Mello (1946), Skempton (1964), Moon (1984), Thomson and Kjartanson (1985), Abdel-Ghaffar (1990), and Maccarini (1993).

Skempton (1964) stated that the same effective stress shear strength parameters were obtained from eight test specimens of Boulder Clay using the direct shear and triaxial devices. Moon (1984) performed direct shear and CU triaxial tests on undisturbed samples of a high plasticity clay and found comparable results for the effective stress cohesion intercept and friction angle obtained from these two tests. Thomson and Kjartanson (1985) performed direct shear tests and CD and CU triaxial tests on undisturbed

samples of two different soils and found good agreement in the failure envelope obtained from all three tests. Abdel-Ghaffar (1990) compiled results from the literature where direct shear and triaxial tests were performed on the same soil. Based on that compilation, Abdel-Ghaffar concluded that the direct shear and triaxial devices provide comparable values for the effective stress friction angle and cohesion intercept. Maccarini (1993) performed direct shear and CD triaxial tests on a residual soil from Rio de Janeiro. For these tests, the tests specimens were oriented so that the failure plane in both devices coincided with the direction of stratification of the soil. Based on the results obtained, Maccarini concluded that similar values of effective stress cohesion and friction angle are obtained from both tests if the stratification is taken into account. As stated by Maccarini (1993), the stratification of the natural soil needs to be taken into account when comparing the results obtained from these two devices. The results presented by Castellanos and Brandon (2013), reproduced in Figure 6.26, tend to confirm the statement made by Maccarini. Castellanos and Brandon showed that that the horizontal layering encountered in natural soils could influence the shear strength parameters measured in the direct shear device.

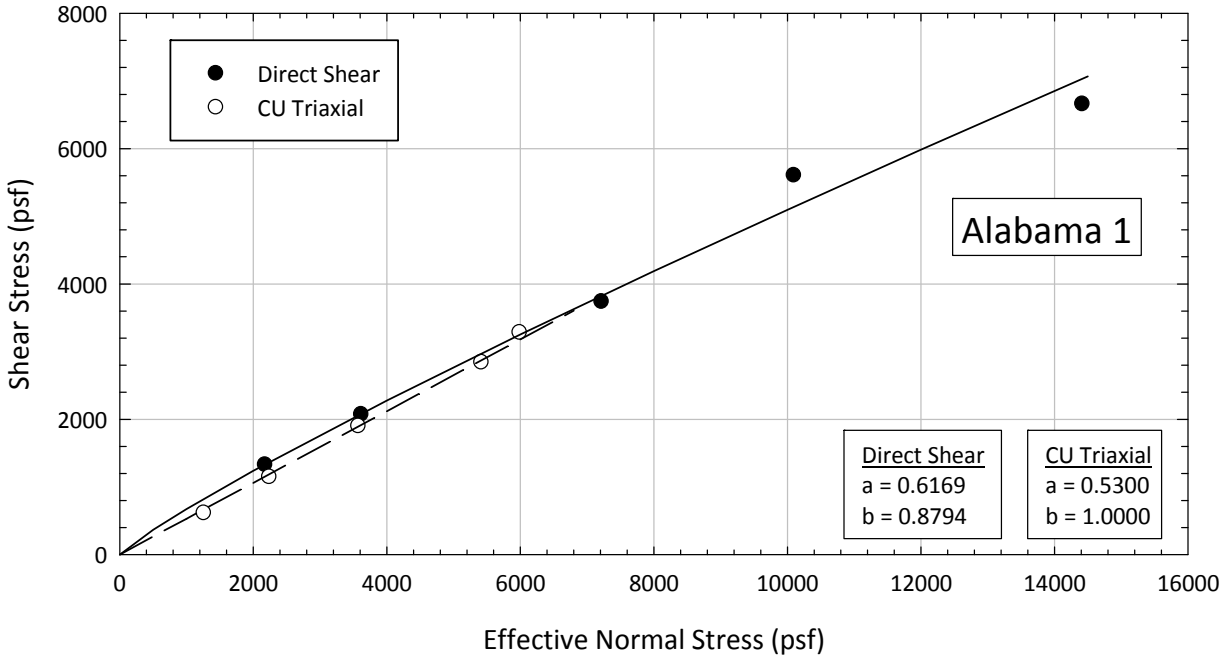

Figure 6.21 Direct shear and triaxial tests results for Alabama 1.

6.5 Effect of Blenderizing

Although disaggregating or blenderizing soils have been used for many years for soil preparation, no research was found to evaluate the influence of the sample preparation technique on the fully softened shear strength measured. The effect of blenderizing on the soil index properties was investigated by testing 10 different soils. The effect of blenderizing on the shear strength measured was investigated by direct shear testing blenderized and non-blenderized samples of Colorado Clay, NOVA Clay, and VBC,

mixed at a water content close to the liquid limit. Results are summarized in Table 6.3 and Figures 6.27 to 6.34.

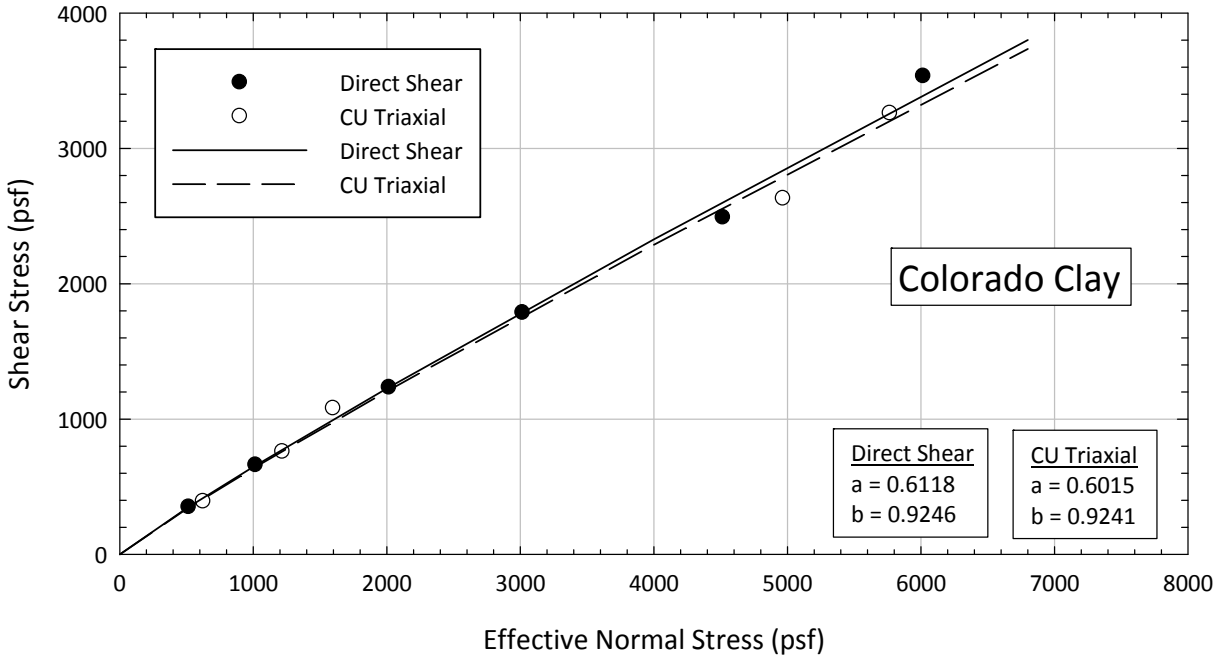

Figure 6.22 Direct shear and triaxial tests results for Colorado Clay.

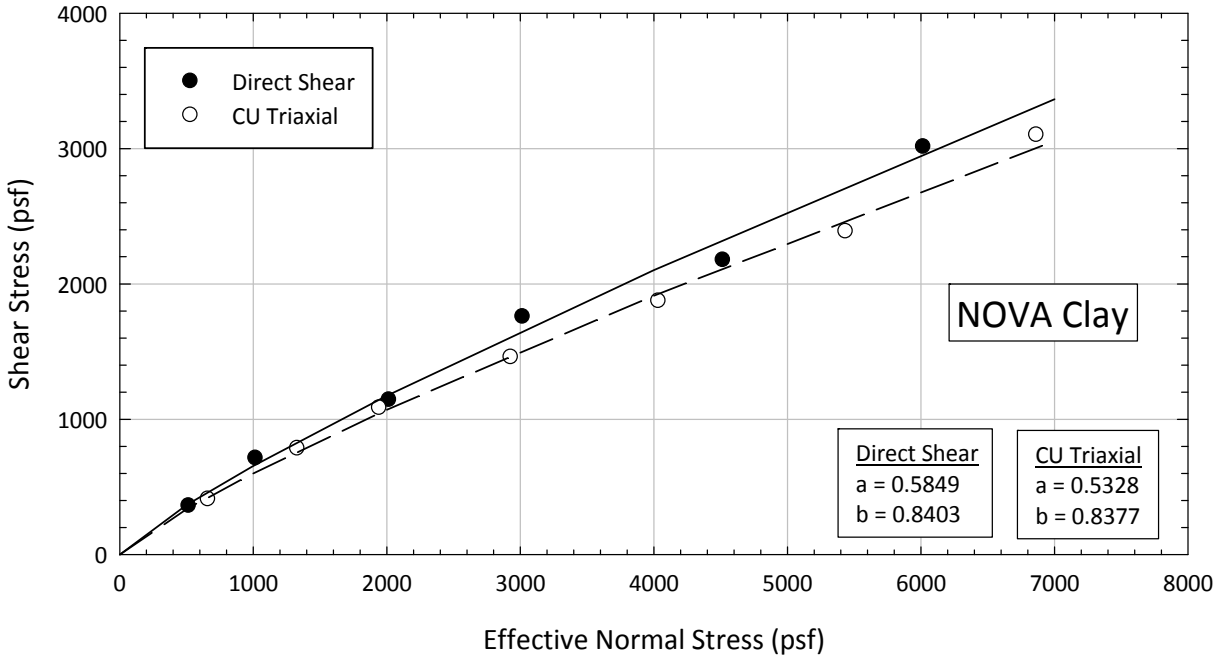

Figure 6.23 Direct shear and triaxial tests results for NOVA Clay.

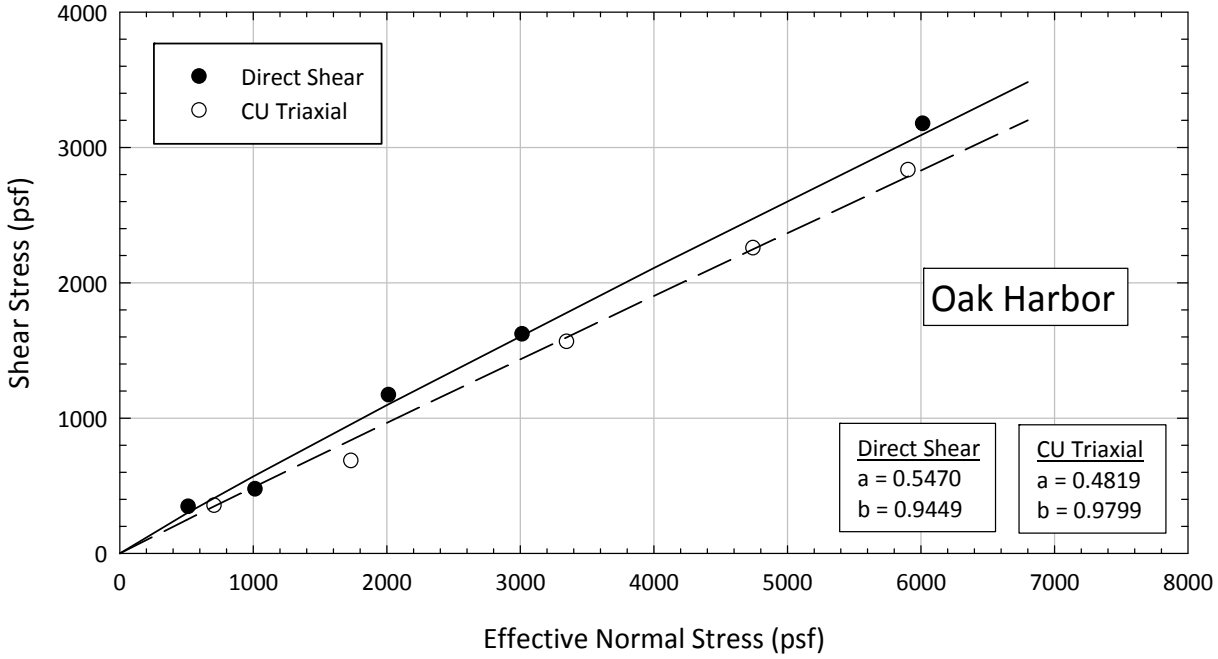

Figure 6.24 Direct shear and triaxial test results for Oak Harbor.

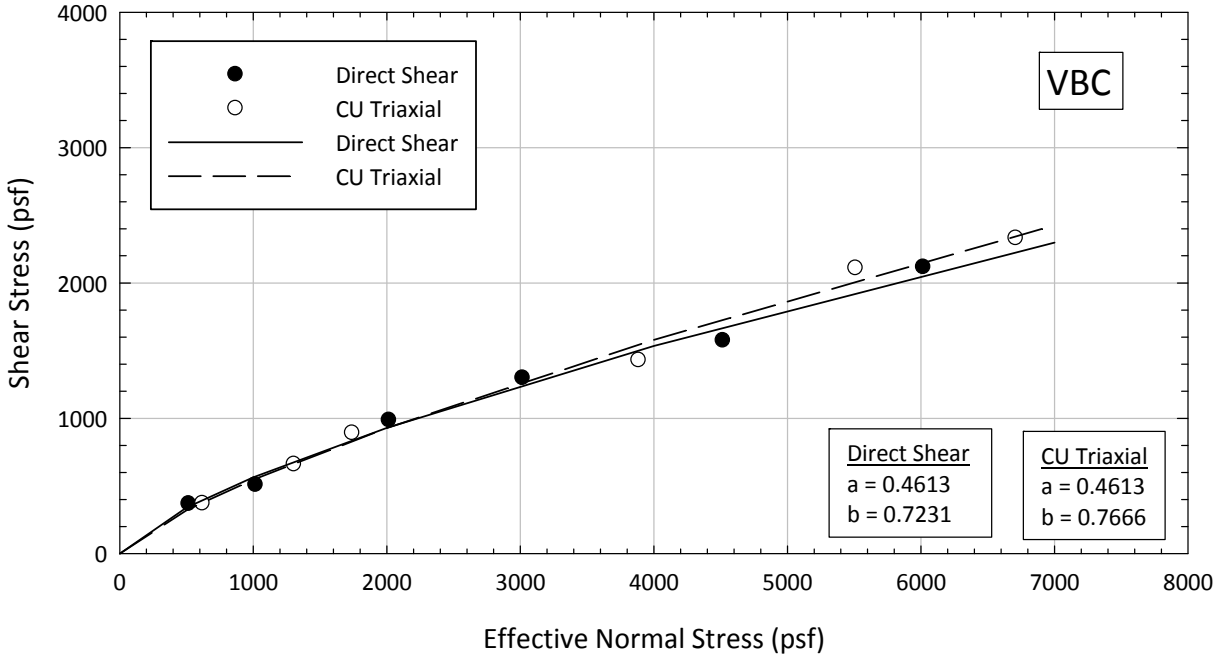

Figure 6.25 Direct shear and triaxial tests results for VBC.

Table 6.2 Summary of the values of *a* and *b* obtained from direct shear and CU triaxial tests

Soil	Direct Shear		CU Triaxial	
	a	*b*	*a*	*b*
Alabama 1	0.6169	0.8794	0.5300	1.0000
Colorado Clay	0.6118	0.9246	0.6015	0.9241
NOVA Clay	0.5849	0.8403	0.5328	0.8377
Oak Harbor	0.5470	0.9449	0.4819	0.9799
VBC	0.4613	0.7231	0.4613	0.7666

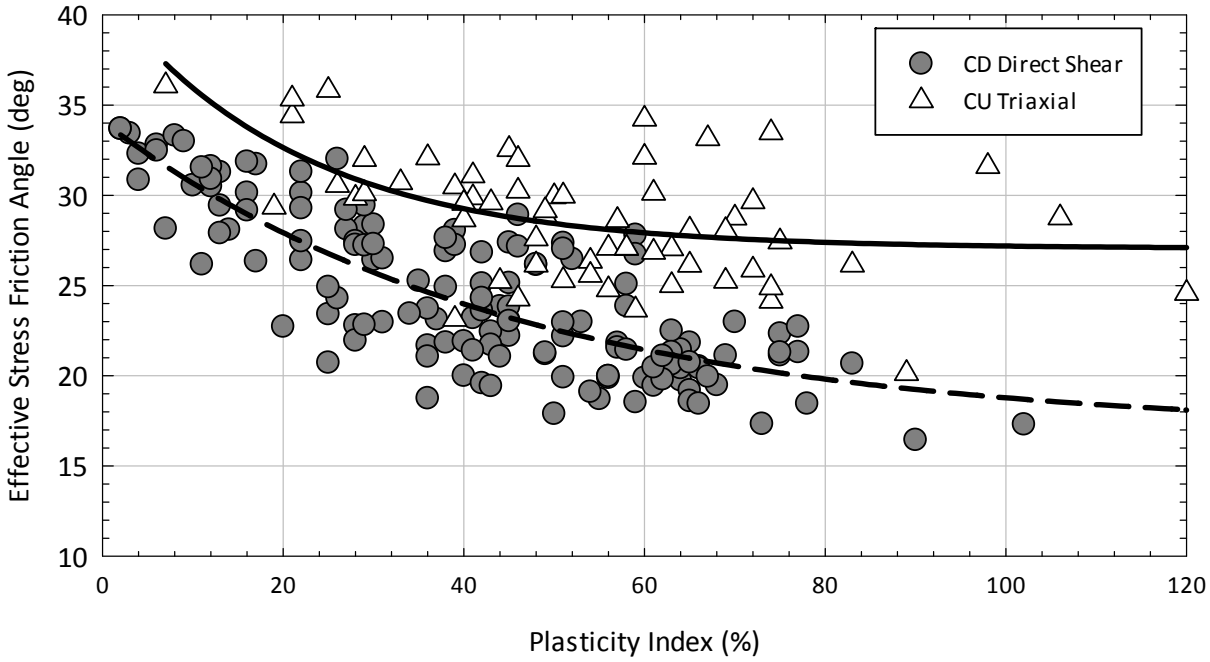

Figure 6.26 Relationship between effective stress friction angle and plasticity index for CD direct shear tests and CU triaxial tests on undisturbed samples (Castellanos and Brandon 2013).

Soil index properties measured from samples prepared using both techniques showed that blenderizing increases the liquid limit, but does not generally affect the plastic limit of the soil, as can be seen from the results presented in Table 6.3 and Figures 6.27 and 6.28. Similar results were found by Heley and MacIver (1971) and Banks (1978). The terms *ASTM clay-sized fraction* and *ASTM liquid limit* will be used to describe the clay-sized fraction and liquid limit, respectively, of non-blenderized samples. The clay-sized fraction of clays with an ASTM clay-sized fraction below 50 seems to be affected by the blenderizing procedure. For clays with an ASTM clay-sized fraction greater than 50, the clay-sized fraction does not seem to be affected by the blenderizing procedure. These results are consistent with the results from ball-milled samples presented by Stark et al. (2005), reproduced here in Figures 6.29 and 6.30. The processing is presumed to cause a decrease in the soil particle size, causing an increase in the specific surface, thus allowing more

water to be absorbed on the clay particle surfaces thereby increasing the liquid limit. The decrease in the soil particle size is reflected on the increase in the clay-sized fraction in blenderized samples as can be seen in Table 6.3. It is unclear why the liquid limit of clays with a high ASTM clay-sized fraction increases with blenderizing but the clay-sized fraction is not affected. Stark et al. (2005) hypothesized that the decrease in the ratio of blenderized clay-sized fraction to ASTM clay-sized fraction with increasing ASTM clay-sized fraction might be attributed to the dispersant being more effective in fat clays than in lean clays.

Table 6.3 Index properties for blenderized and non-blenderized samples.

Sample	Non-blenderized				Blenderized			
	LL	PL	PI	Clay-sized Fraction	LL	PL	PI	Clay-sized Fraction
Texas 1	68	25	43	63	76	25	51	58
Texas 2	66	23	43	58	74	21	53	56
Texas 3	65	21	44	55	71	22	49	52
Texas 4	66	24	42	67	76	23	53	62
Texas 5	76	28	48	59	84	27	57	53
Texas 6	73	26	47	51	77	25	52	52
Colorado Clay	42	22	20	24	42	22	20	55
NOVA Clay	66	28	38	17	79	28	51	35
Oahe Dam	74	24	50	50	126	26	100	75
VBC	78	26	52	69	94	26	68	65

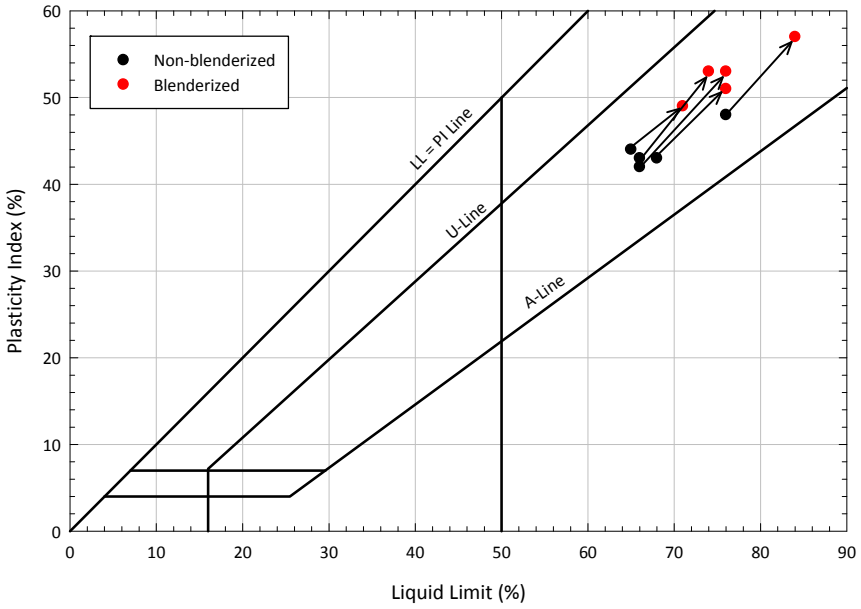

Figure 6.27 Plasticity chart showing the effect of blenderizing on the index properties.

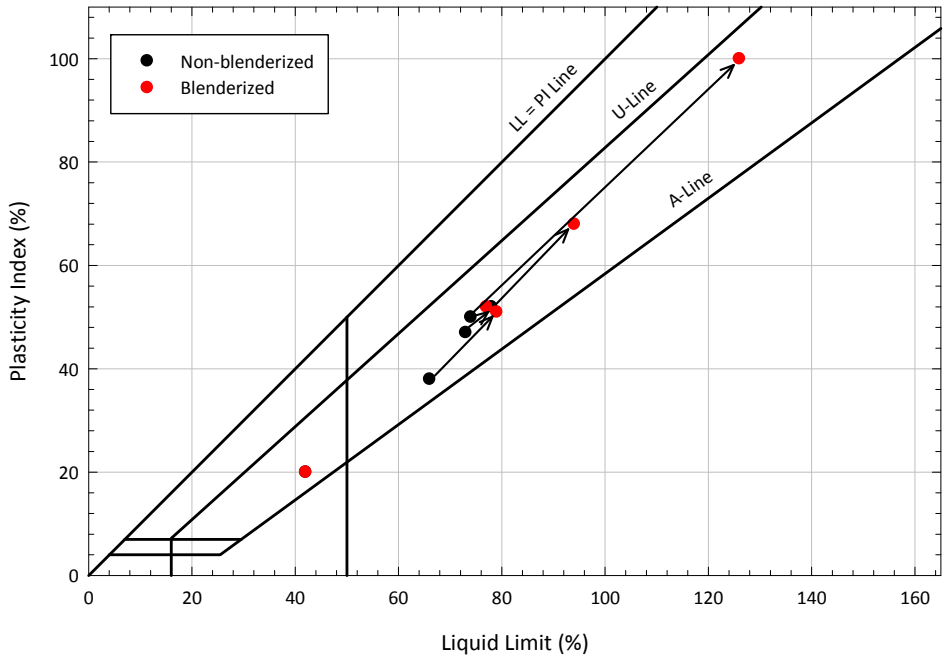

Figure 6.28 Plasticity chart showing the effect of blenderizing on the index properties.

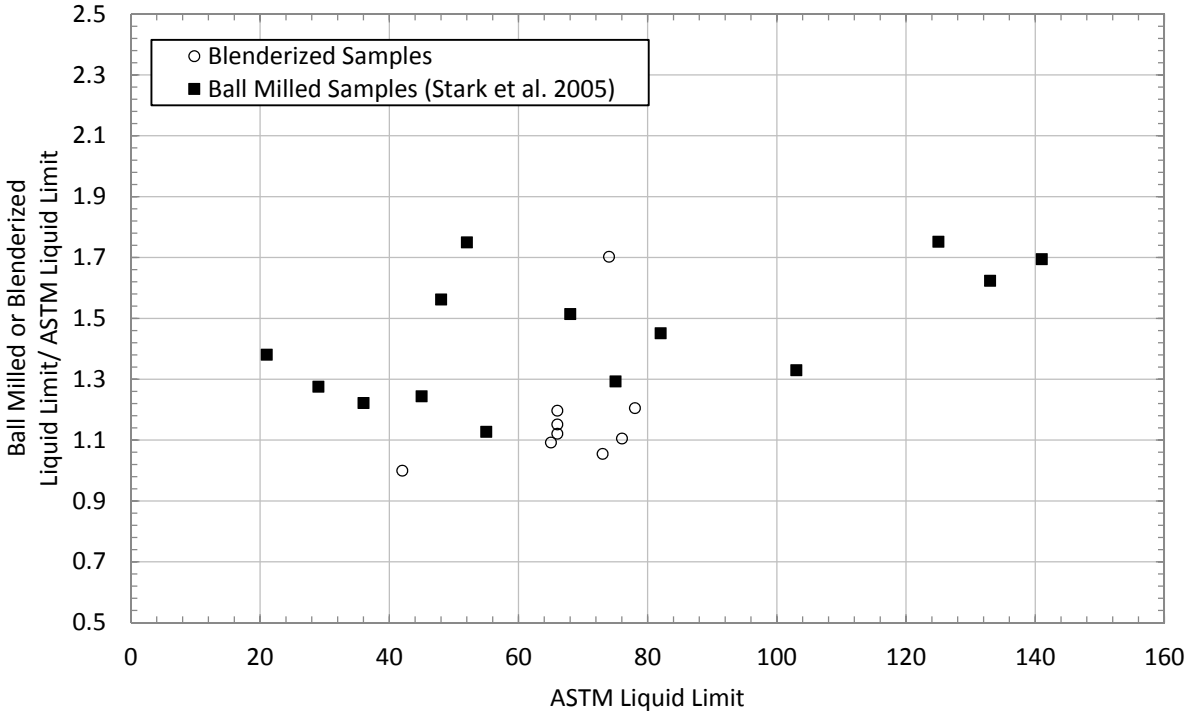

Figure 6.29 Effect of sample preparation procedure on the measured liquid limit.

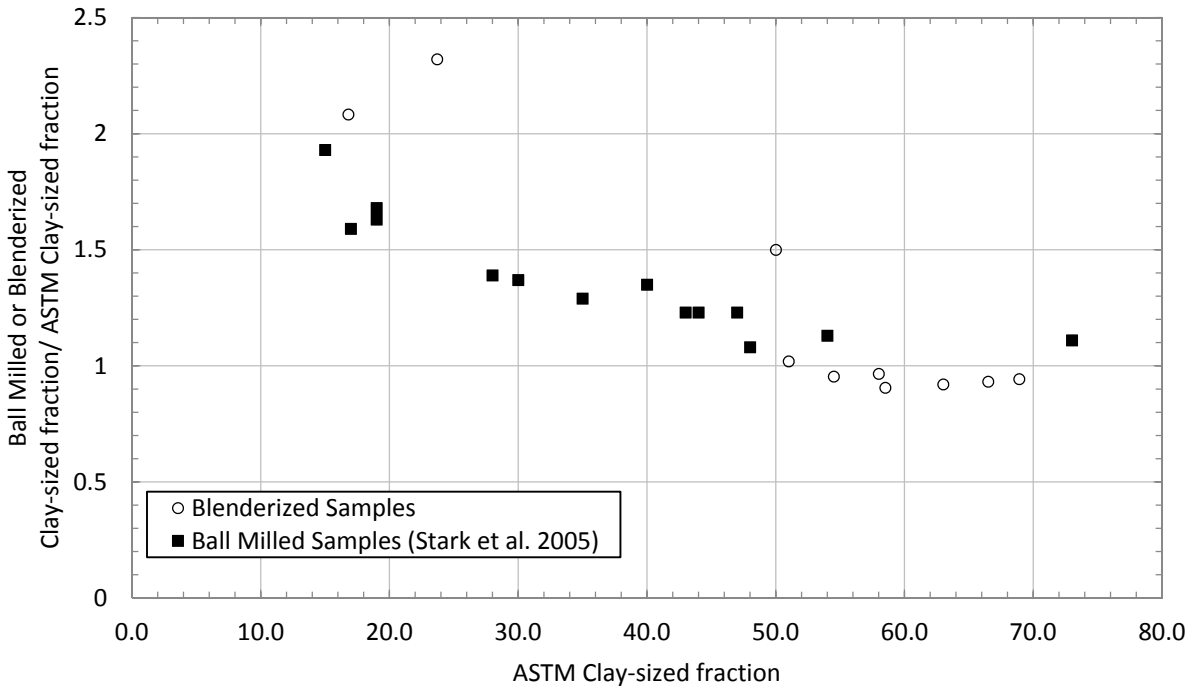

Figure 6.30 Effect of sample preparation procedure on the measured clay-sized fraction.

Blenderizing was also found to affect the coefficient of consolidation (c_v) of the soil, measured during the consolidation stage of the direct shear tests, as can be seen in Figure 6.31. A greater coefficient of consolidation was found in non-blenderized samples, compared to blenderized samples, for two of the three soil tested. The coefficient of consolidation is proportional to the permeability of the soil, and as the particles sizes decrease, the permeability of the soil decreases.

For the NOVA Clay, the coefficient of consolidation of non-blenderized samples was found to be two to five times the coefficient of consolidation of blenderized samples. For VBC, the ratio of the non-blenderized to the blenderized coefficient of consolidation was found to be about 1.5 on average. This decrease in the coefficient of consolidation for blenderized samples will cause an increase in the time required for testing, since the time required to reach end of primary consolidation will increase, and the strain rate is determined based on the coefficient of consolidation for consolidated undrained and consolidated drained tests. Also, the coefficients of consolidation obtained from blenderized samples may not be representative of the values in the field. For Colorado Clay different, results were obtained. Colorado Clay is a lean clay and NOVA Clay and VBC are fat clays

The results of the shear strength tests performed to assess the effect of blenderizing on the fully softened shear strength measured showed that blenderizing slightly influenced the fully softened shear strength measured, as can be seen from the results presented in Figures 6.32 to 6.34. From these figures it can be seen that the shear strength measured on test specimens of Colorado clay and VBC was about the same whether the soil was blenderized or not. The results for NOVA Clay show a difference in the fully softened

shear strength measured, with the non-blenderized test specimens being a little stronger than the blenderized test specimens. It is expected that ball-milling the test soils would have similar effects as blenderizing.

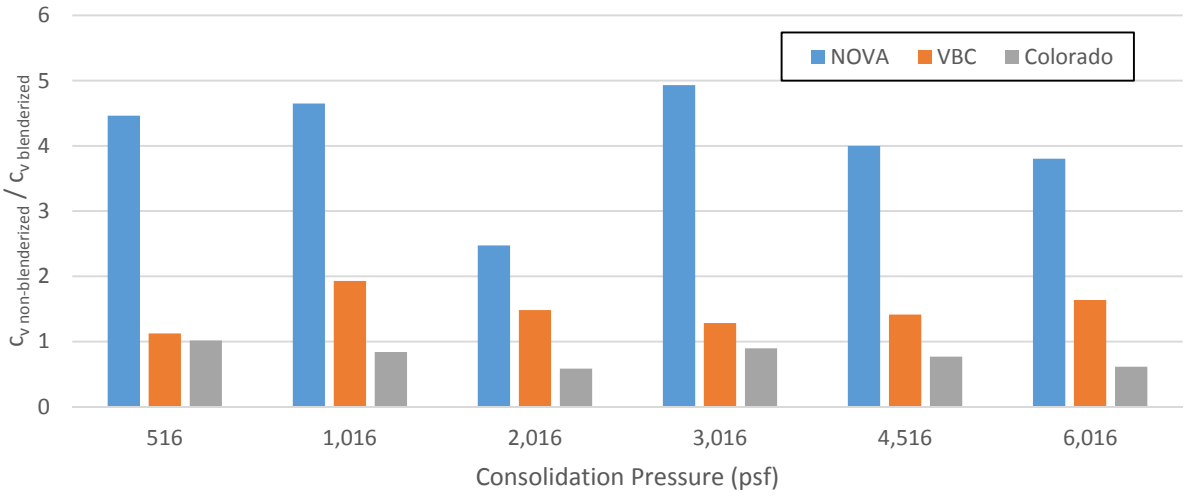

Figure 6.31 Effect of sample preparation procedure in the coefficient of consolidation.

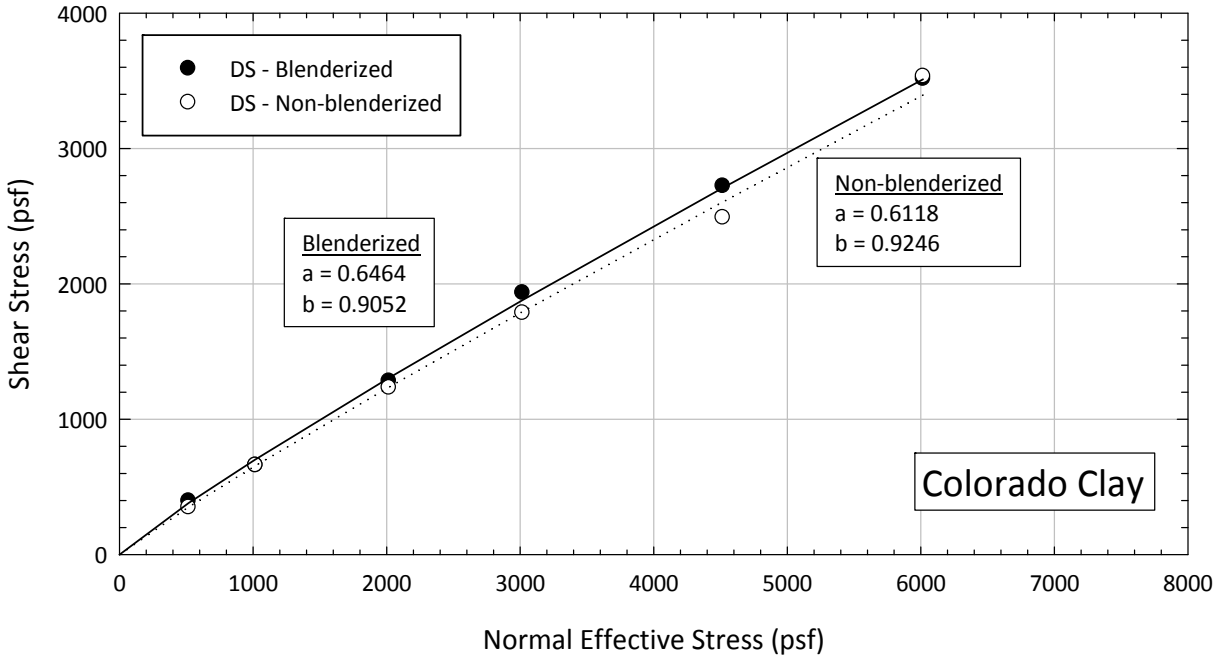

Figure 6.32: Colorado Clay blenderized vs. non-blenderized direct shear failure envelope.

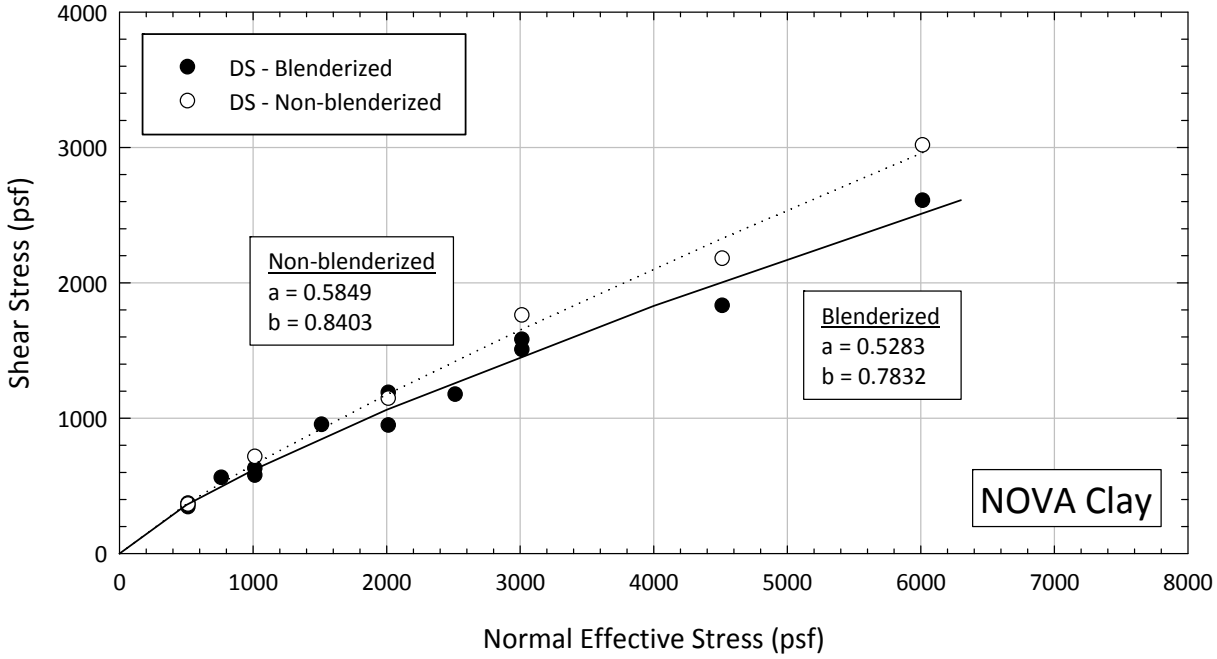

Figure 6.33 NOVA Clay blenderized vs. non-blenderized direct shear failure envelope.

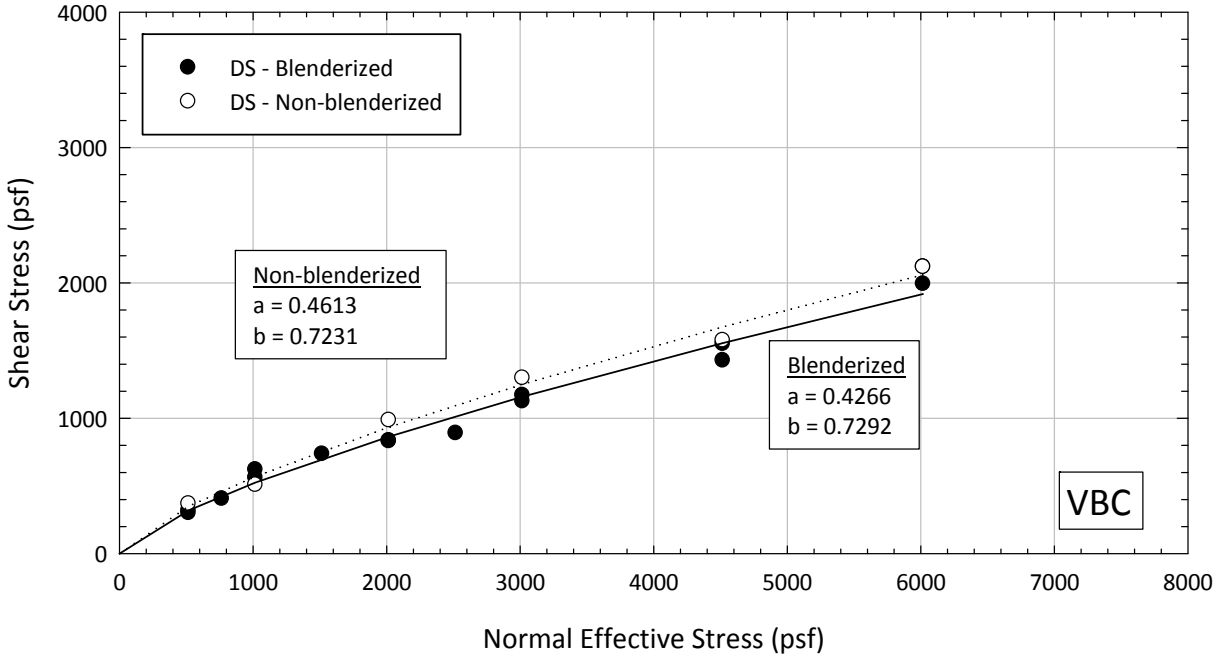

Figure 6.34 VBC blenderized vs. non-blenderized direct shear failure envelope.

6.6 Effect of Molding Water Content

Molding water contents ranging from the below the liquid limit to water contents corresponding to a liquidity index of 1.5 have been used in the past to measure the fully softened shear strength (Gibson 1953; Bishop et al. 1965; Cancelli 1981; Stark and Eid 1997; Stark et al. 2005; Bhattarai et al. 2006; Wright et al. 2007). The effect of the molding water content on the void ratio after consolidation and the fully softened shear strength measured was investigated by conducting direct shear tests using NOVA Clay and VBC samples mixed at initial water contents corresponding to liquidity indices ranging from 0.6 to 2.0. The results of the direct shear tests are presented in Figures 6.35 to 6.38 for the void ratio after consolidation and in Figures 6.39 to 6.42 for the shear strength envelopes.

In the direct shear device, the consolidation stage is performed in stages to avoid extrusion of the soil, as described in Section 5.5. During each stage, the compression of the test specimen is recorded. Using this information, the amount of strain and void ratio can be calculated for the end of primary consolidation for each stage. This means that, for one test, more than one point can be obtained in a consolidation plot. The amount of points obtained from each test will depend in the number of increments used to achieve the final desired consolidation pressure. This information was used to create the plots shown in Figures 6.35 to 6.38.

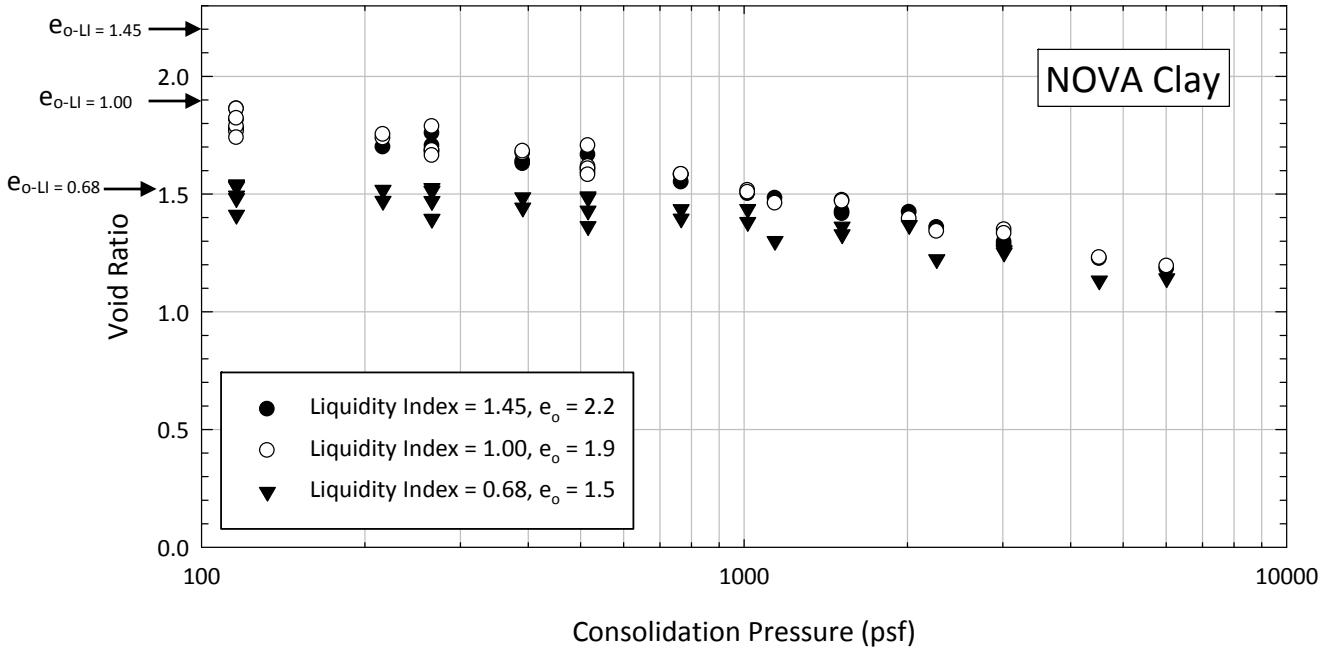

Figure 6.35 Void ratio vs. consolidation pressure plot for NOVA Clay at different molding water contents.

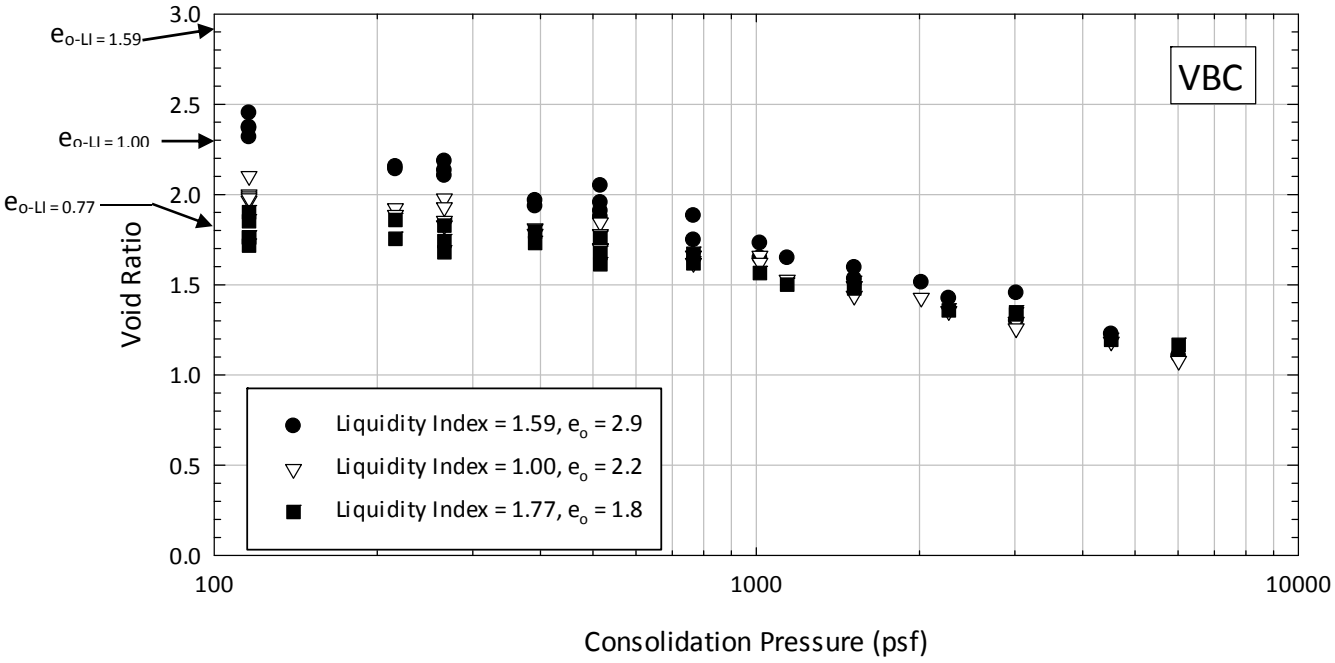

Figure 6.36 Void ratio vs. consolidation pressure plot for VBC at different molding water contents.

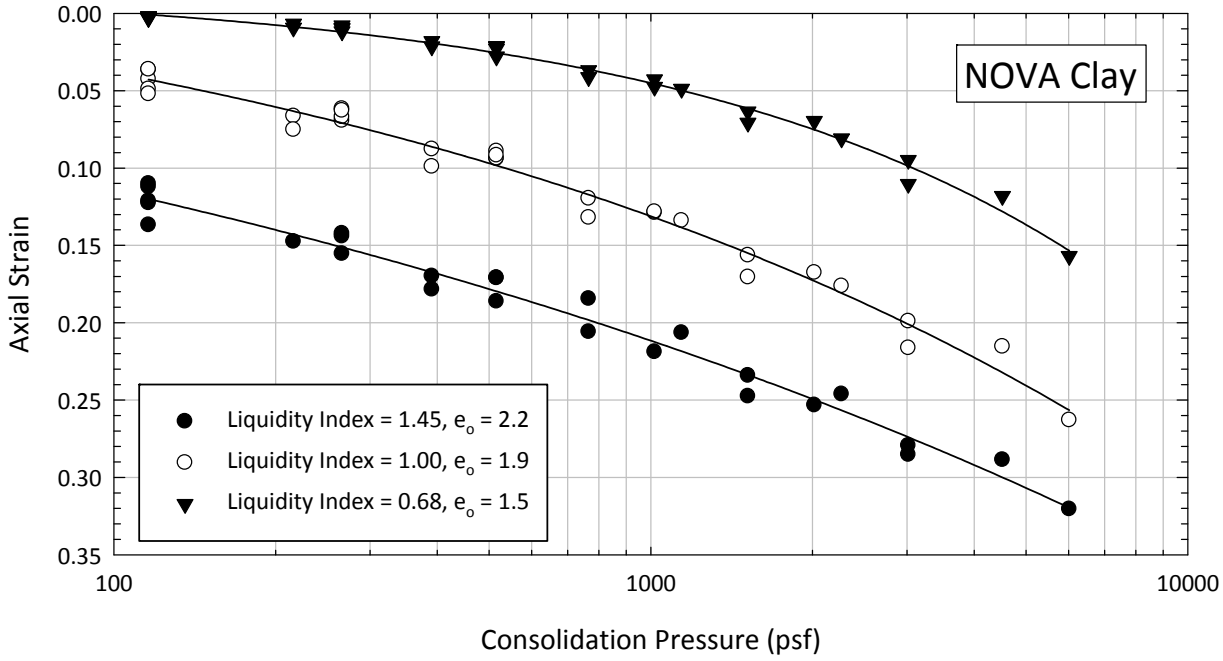

Figure 6.37 Axial strain vs. consolidation pressure plot for NOVA Clay at different molding water contents.

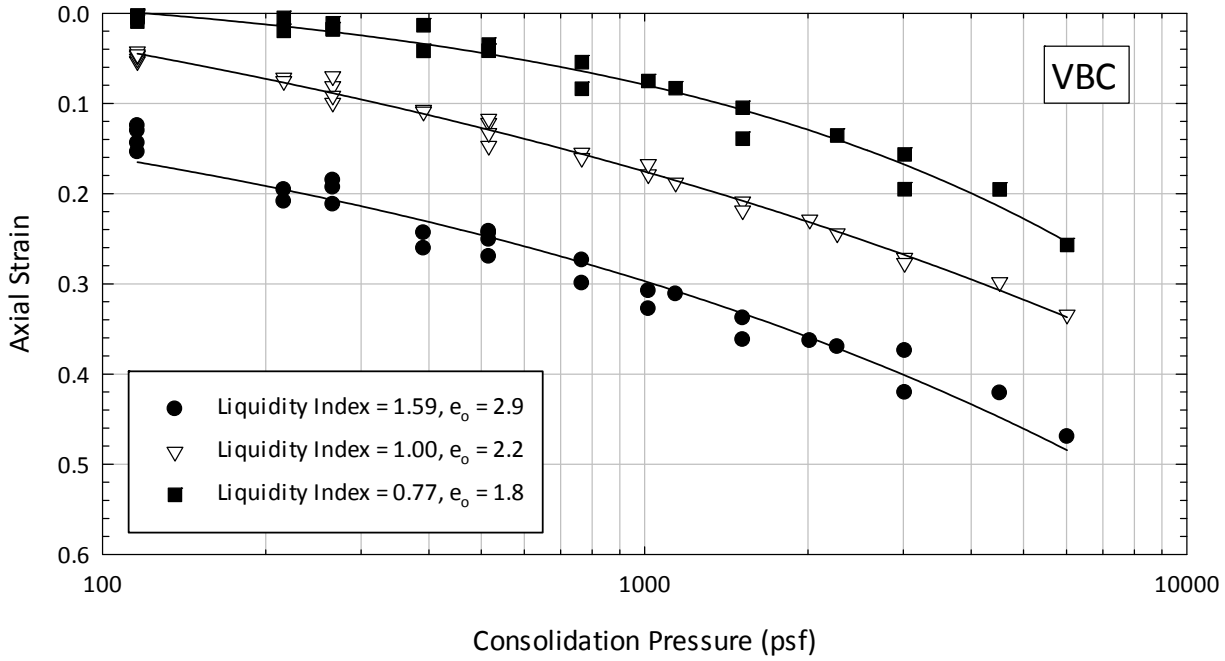

Figure 6.38 Axial strain vs. consolidation pressure plot for VBC at different molding water contents.

From the behavior during the consolidation stage, shown in Figures 6.35 and 6.36, it can be seen that a different void ratio is obtained at low pressures for the different liquidity indices. As the consolidation pressure increases, the void ratios tend to merge to the same line, removing the effects of the initial water content. Similar results were also obtained by Bjerrum (1951, 1954) and Hvorslev (1960). From Figures 6.37 and 6.38, it can be seen that more compression is experienced by the soil as the liquidity index increases. Some of the compression of samples with a high liquidity index during the first consolidation load can be attributed to extrusion. The data presented in these figures shows a more or less parallel trend in the strain behavior during consolidation for all three series of tests in both soils. A small curvature at low stresses was found for the tests performed at a low liquidity index, showing small compressions at low stresses. From these results, it can be inferred that, although the compression experienced during consolidation varies with liquidity index, the value of the virgin compression ratio ($C_{c\varepsilon}$) practically does not change.

No significant difference was found in the failure envelope measured for test specimens prepared at different molding water content. Figure 6.39 shows that for NOVA Clay, some differences were observed, especially at high stresses. The results of VBC, presented in Figure 6.40, showed practically no difference in the failure envelope obtained at different molding water contents. In Figures 6.41 and 6.42, the void ratios at failure for the two soils tested are plotted against the consolidation pressures used in the tests. The void ratios at failure were calculated from the initial void ratio and the vertical displacements experienced by the test specimen during consolidation and shear until failure. From these figures, it can be seen that no significant difference was observed in the void ratio at failure for samples tested above

1000 psf. For samples tested below 1000 psf, a greater difference in the void ratio at failure was observed, but no significant difference in the overall failure envelope was measured.

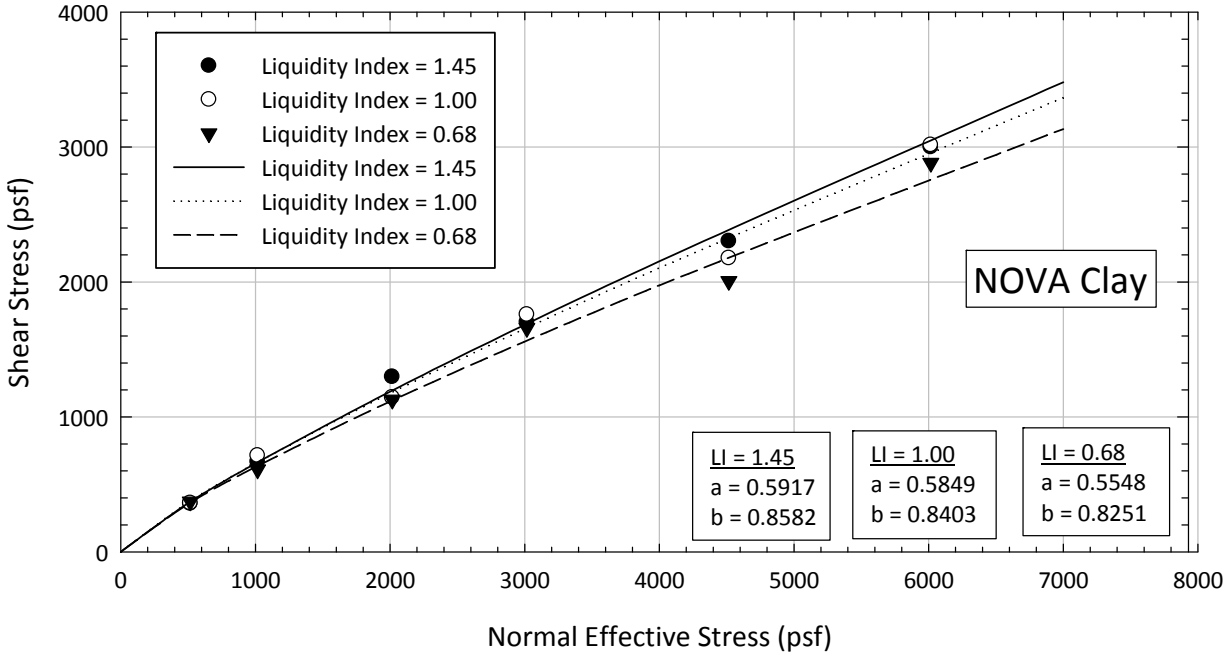

Figure 6.39 Direct shear failure envelope for NOVA Clay mixed at different molding water contents.

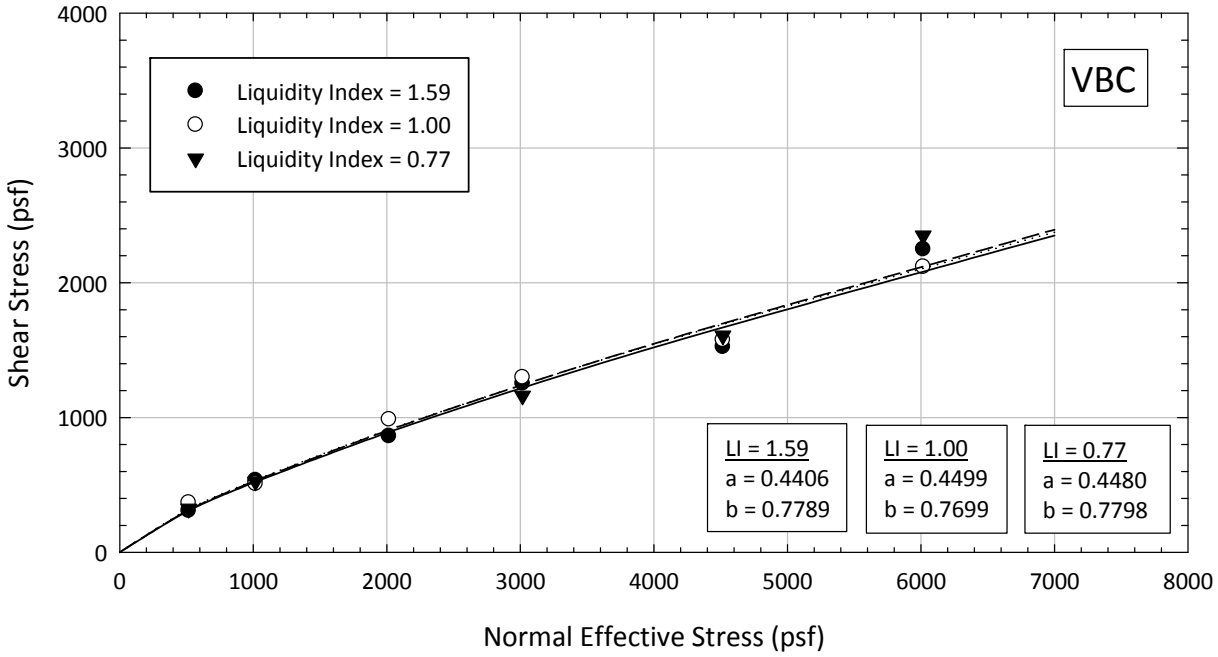

Figure 6.40 Direct shear failure envelope for VBC mixed at different molding water contents.

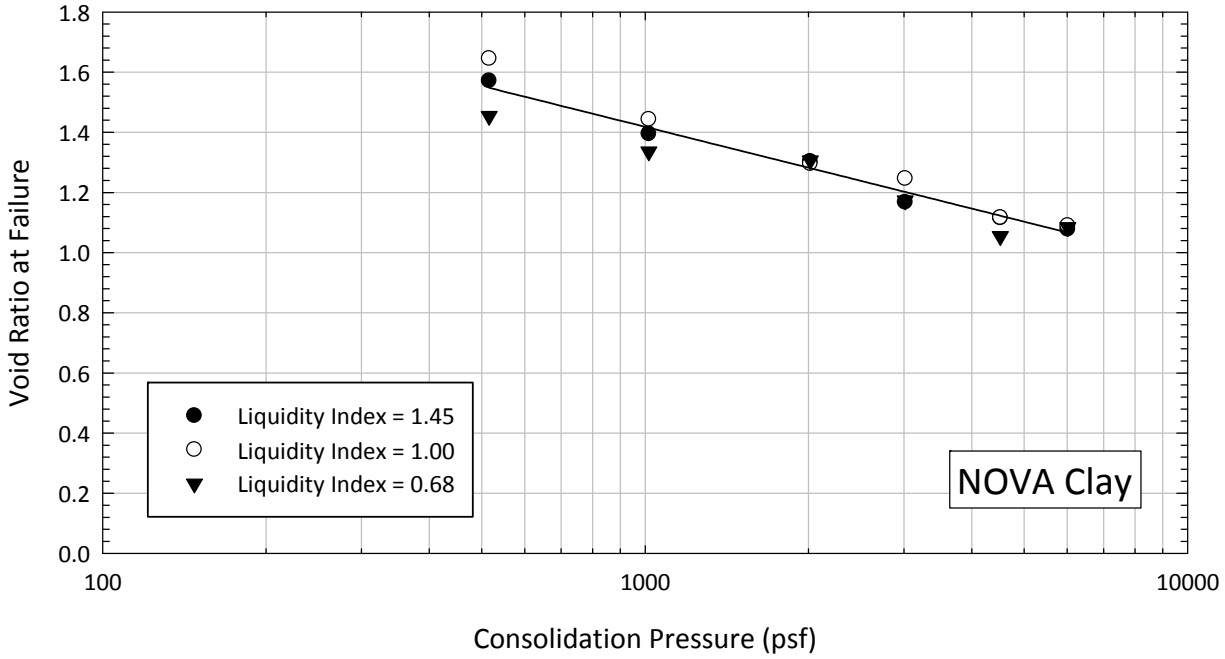

Figure 6.41 Void ratio at failure vs. consolidation pressure for NOVA Clay mixed at different molding water contents.

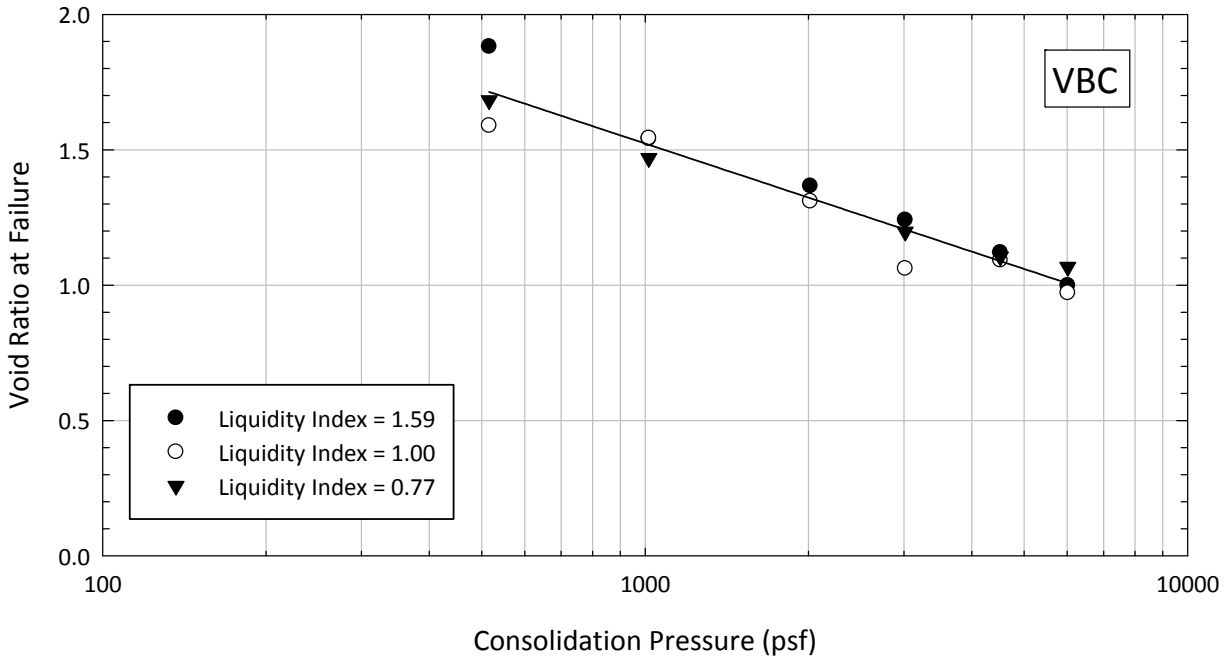

Figure 6.42 Void ratio at failure vs. consolidation pressure for VBC mixed at different molding water contents.

Because of the difference in void ratio after consolidation observed, especially at stresses below 1000 psf, more tests were performed at a consolidation pressure around 270 psf with samples formed at different liquidity indices using NOVA Clay. These tests were performed using the modifications for the direct shear device described in Section 5.4.1. The test specimens were formed at water contents corresponding a liquidity index of 1.0, 1.5, and 2.0. These liquidity indices correspond to initial void ratios of 1.87, 2.21, and 2.64, respectively. As can be seen in the results presented in Figure 6.43, the shear strength measured in all three test specimens was about the same. Test specimens formed at a liquidity index of 1.5 and 2.0 had about the same ductile behavior during shear while the test specimen formed at the liquid limit exhibited a more brittle behavior. From the results presented in Figure 6.44 it can be seen that the void ratio after consolidation was the same for all three test specimens. From these results, it can be concluded that the measured fully softened shear strength of NOVA Clay is the same for test specimens formed above the liquid limit and consolidated to stresses in excess of 250 psf. The results presented in Figure 6.45 show that fitting a failure envelope to tests consolidated to stresses only above 500 psf can over predict the shear strength at low stresses. This can be very important when dealing with shallow failures like the ones usually encountered in compacted clay embankments. More research is required in order to verify if this is actual soil behavior or just the result of scatter in the measurements, and to provide definite conclusions on the effect of the molding water content on the fully softened shear strength measured at low stresses.

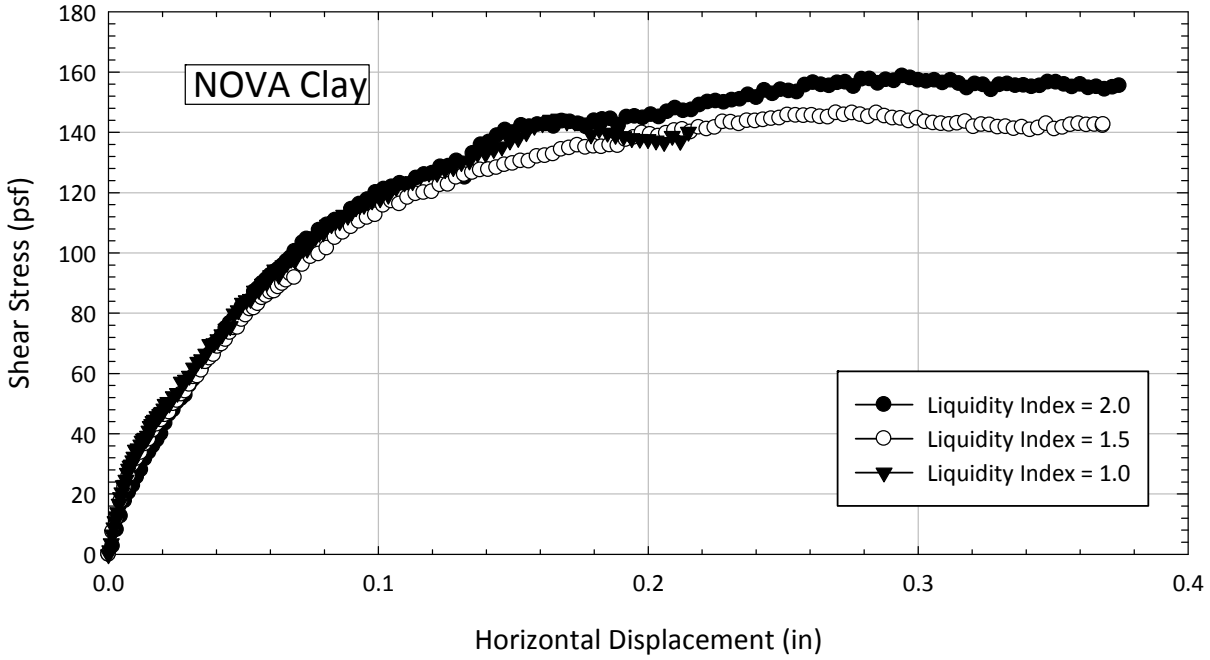

Figure 6.43 Stress-displacement behavior of NOVA clay samples formed at different liquidity indices and consolidated to 266 psf.

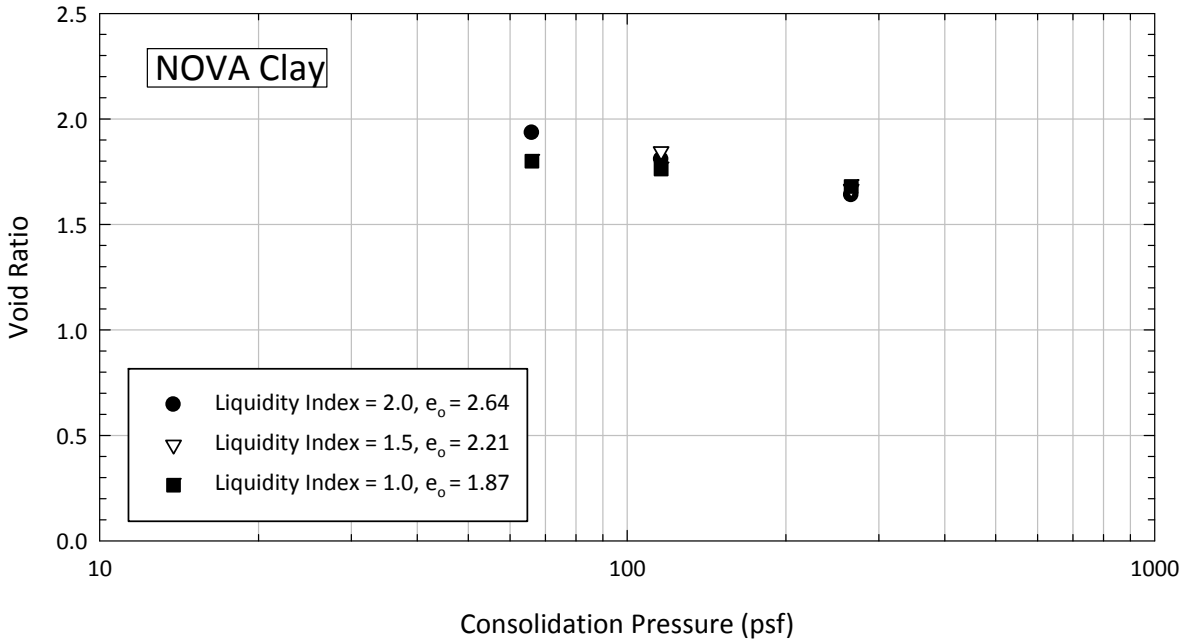

Figure 6.44 Void ratio after consolidation of NOVA clay samples formed at different liquidity indices and consolidated to 266 psf.

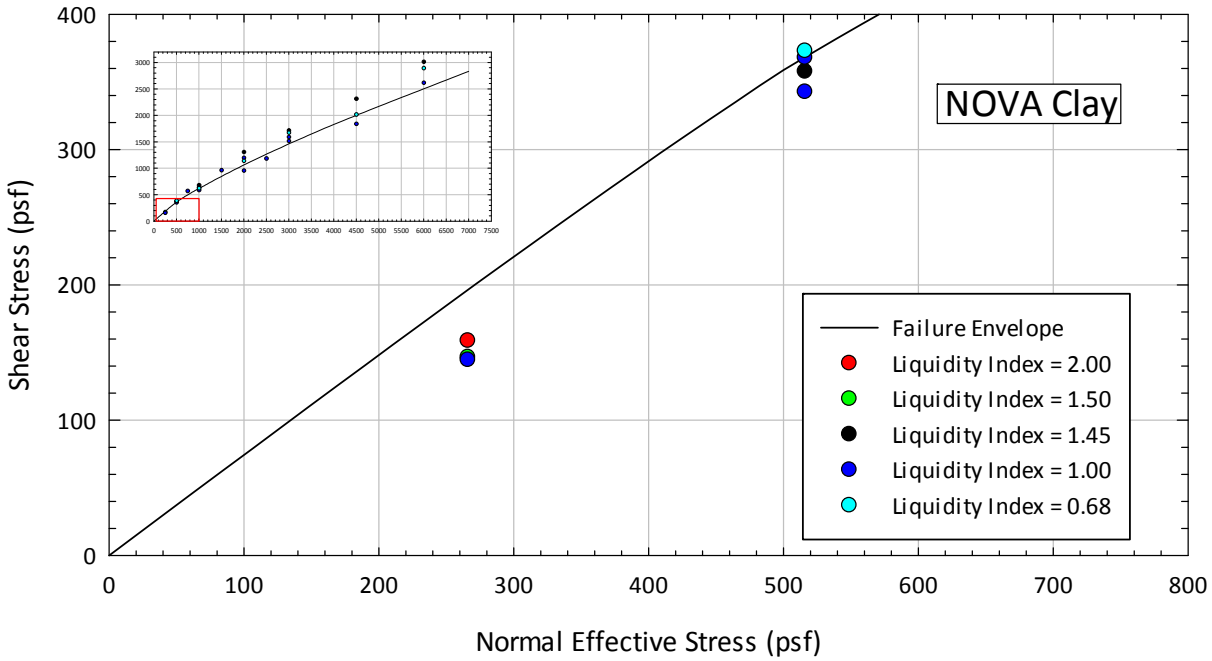

Figure 6.45 NOVA Clay Failure envelope obtained from DS test performed at high stresses compared with the results of tests performed at low stresses.

There are practical advantages and disadvantages to using different liquidity indices to form test specimens. A high molding liquidity index makes it easier to form test specimens, but increases the chances of the top platen getting tilted and wedged in the shear box. Also, care has to be taken when using a high liquidity index to form test specimens so that the compression during consolidation and shear does not compress the sample past the center of the shear box. If this happens, the porous stone or top platen can get in the location of the failure plane and the device can be damaged during shear. Using a low liquidity index has the benefits that the compression experienced by the sample during consolidation is reduced and higher pressures can be tested without compressing the sample past the center of the shear box. Also, using low liquidity indices reduces the chances of the top platen getting tilted and wedged. On the other side, using a low liquidity index increases the difficulty of forming the test specimen without air bubbles.

6.7 Packed Specimens for Fully Softened Shear Strength Measurements Using the Triaxial Device.

As explained in Section 5.7, triaxial test specimens were either (1) trimmed from a batch of soil consolidated in a special consolidometer from an initial water content equal to the liquid limit or (2) packed in a mold at a water content below the liquid limit. Packed specimens have been used in the past by Green and Wright (1986) to measure the shear strength of normally consolidated soils. The viability of using packed specimens for fully softened shear strength measurements was investigated because this is an easier and faster method to form triaxial test specimens, as compared to having to preconsolidate a batch of soil. Also, this method allows test specimens to be tested at lower stresses. The undrained shear strength of a test specimen increases as the water content decrease. For this reason, specimens formed at a low water content have the necessary shear strength to be formed and handled without having to preconsolidate the soil.

First, a series of CU triaxial tests were performed at consolidation pressures ranging from 2016 psf to 4464 psf using NOVA Clay. These tests were performed in a range of stresses that overlap the results obtained from test specimens trimmed from a batch of soil preconsolidated from a water content equal to the liquid limit. In this way, the use of packed specimens to measure the fully softened shear strength could be validated. For this purpose, packed specimens were formed at water contents equivalent to a liquidity index of around 0.65. The results of this series of tests are presented in Figure 6.46. From this figure it can be seen that for the consolidation pressures used, these two methods provide comparable fully softened shear strengths.

Additional tests were performed at stresses below 800 psf using the manual triaxial equipment described in Section 5.4.3 and the procedure described in Section 5.7. Two test specimens of NOVA Clay were tested in the triaxial device under consolidated undrained conditions using a consolidation stress of 432 psf. These specimens were packed at a water content producing liquidity indices of 0.68 and 0.80. From the pore pressure response of these tests (Figure 6.47), it can be seen that as the liquidity index decreases, the test specimen tend to be more dilative. From the results presented in Figures 6.48 and 6.49, it can be inferred that as the liquidity index decreases, the shear strength of the sample increases. From these results, it can be concluded that as the liquidity index decreases, the sample tend to behave more as an overconsolidated clay at low confining stresses. The void ratio after consolidation for the specimen

prepared at an initial liquidity index of 0.68 was 1.52 and 1.63 for the specimen formed at an initial liquidity index of 0.80. These void ratios are low when compared to the expected void ratio of 1.68 from samples formed at an initial water content equal to the liquid limit (Figure 6.35). The shear strength obtained from these two samples is compared to the failure envelope obtained from samples preconsolidated from the liquid limit in a batch consolidometer in Figure 6.50. From this figure it can be seen that the shear strength obtained from packed specimens tested at low stresses increases with decreasing molding liquidity index. At low stresses, even a small increase in shear strength, can represent a significant deviation in the actual shear strength and have an influence in the factor of safety obtained for shallow failure surfaces.

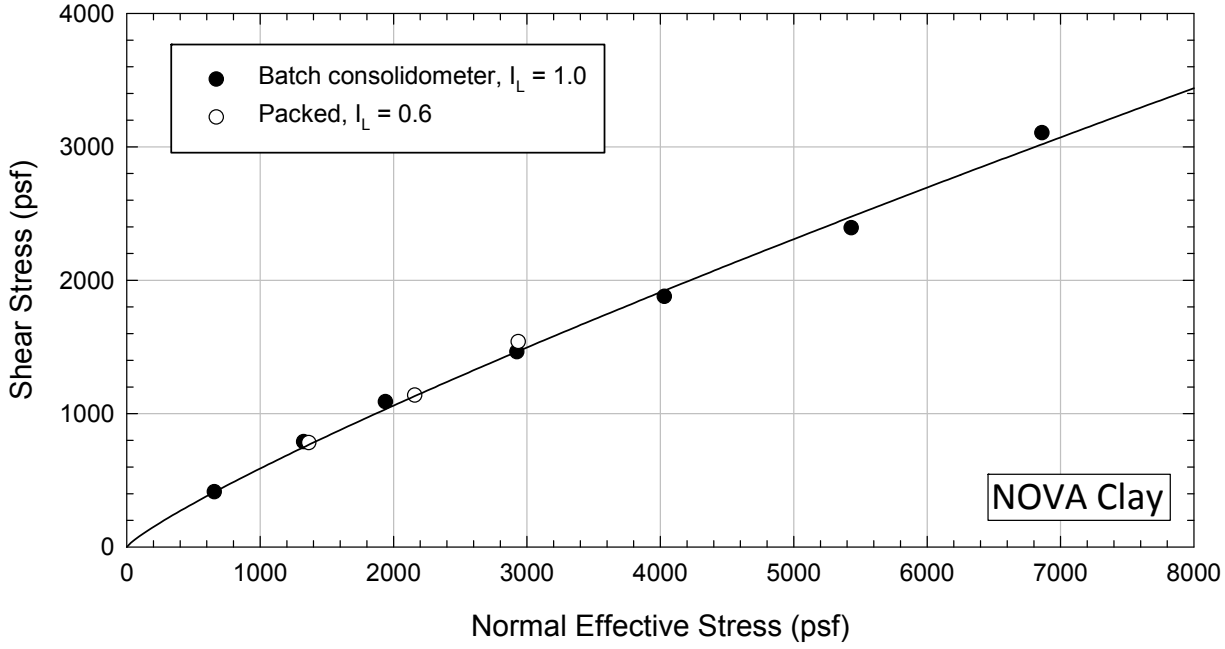

Figure 6.46 CU triaxial test results from preconsolidated and packed specimens.

Packed specimens of Oak Harbor Clay were also tested at confining stresses of 144 psf and 432 psf. These specimens were formed at a water content corresponding to a liquidity index of around 0.55. The results of these tests presented in Figures 6.51 to 6.54, also show that these samples showed a dilative behavior and over predicted the fully softened shear strength. More tests are required to provide final conclusions on the use of packed specimens to measure the fully softened shear strength at consolidation stresses below 800 psf in the triaxial device.

From the results presented in this section it can be seen that packed triaxial test specimens can be used to measure the fully softened shear strength at consolidation stresses higher than 2000 psf. At stresses of around 500 psf, packed specimens may provide a fully softened shear strength that is too high because the samples tend to behave more as overconsolidated clays. The measured shear strength at stresses around 500 psf appears to increase with decreasing molding water content. No tests were performed at

consolidation stresses between 500 psf and 2000 psf. Therefore, comments about the expected results in this range of stresses cannot be provided.

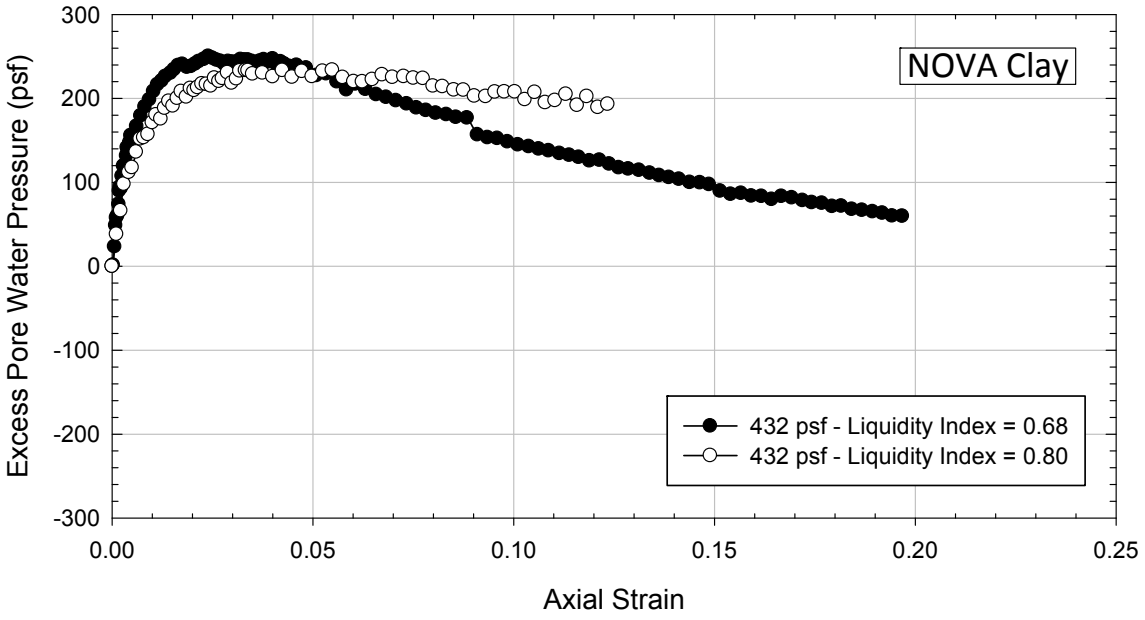

Figure 6.47 Excess pore pressures developed during shear in packed NOVA Clay specimens.

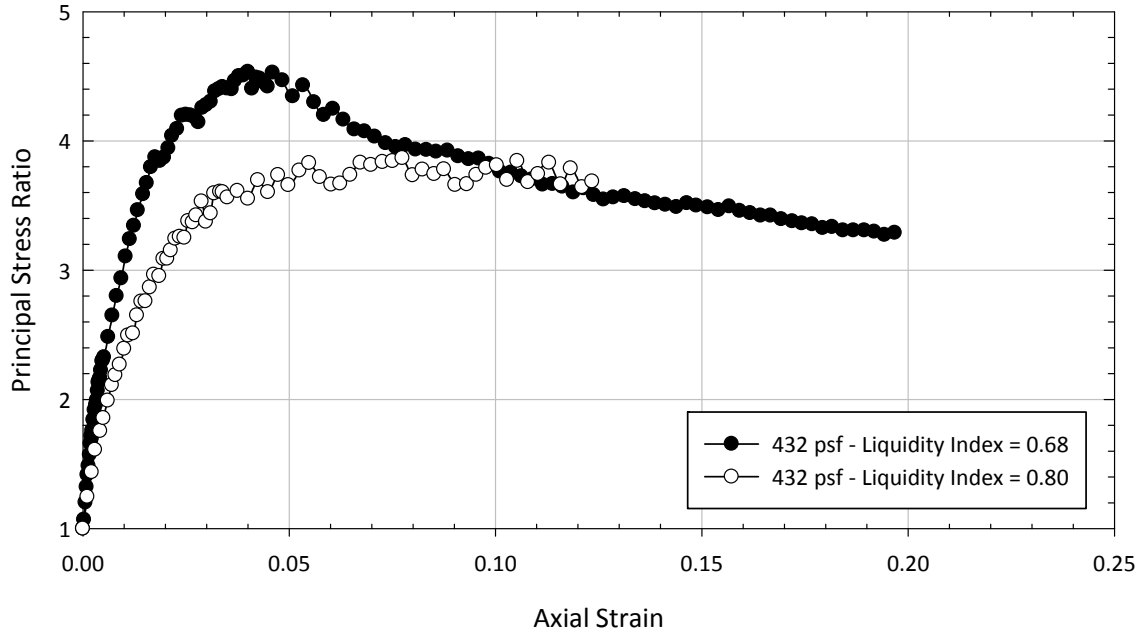

Figure 6.48 Principal stress ratio from packed NOVA Clay specimens molded at different liquidity indices.

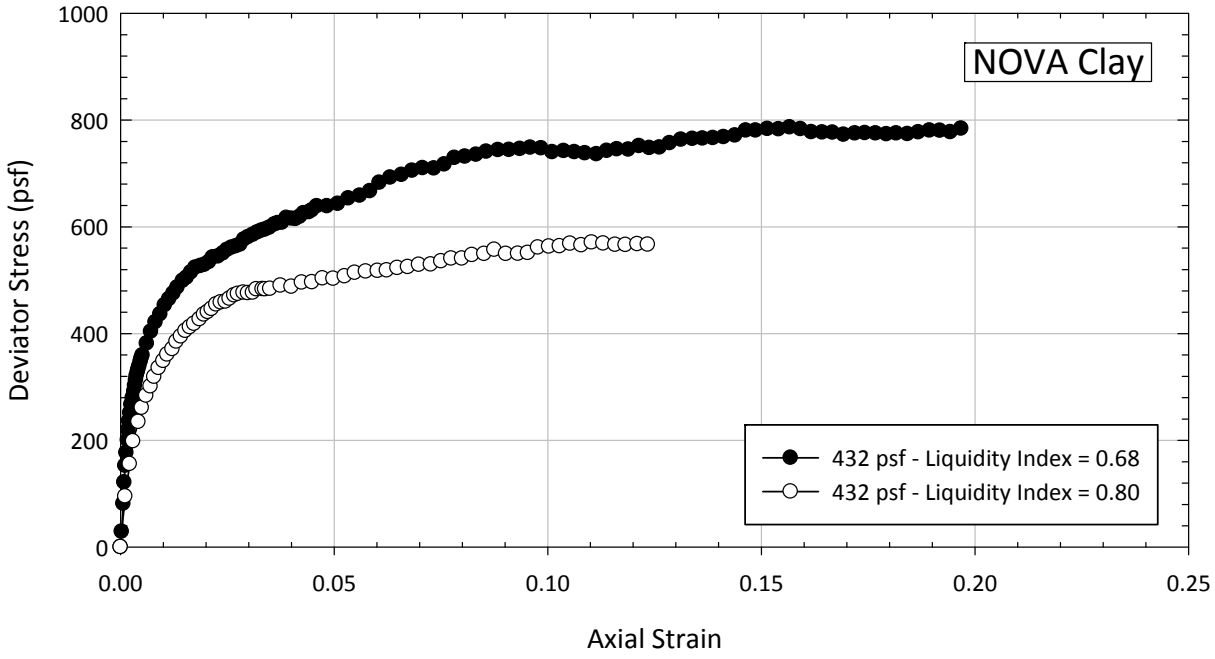

Figure 6.49 Deviator stress from packed NOVA Clay specimens molded at different liquidity indices.

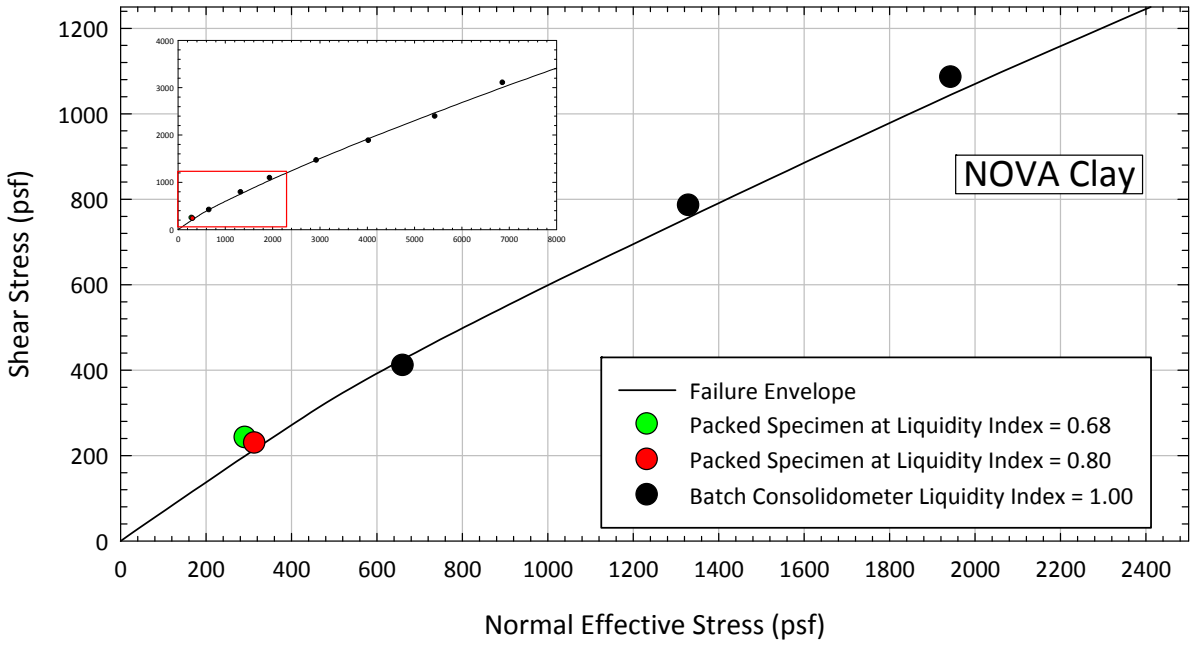

Figure 6.50 Shear strength obtained from packed NOVA Clay specimens molded at different liquidity indices compared to specimens preconsolidated from the liquid limit.

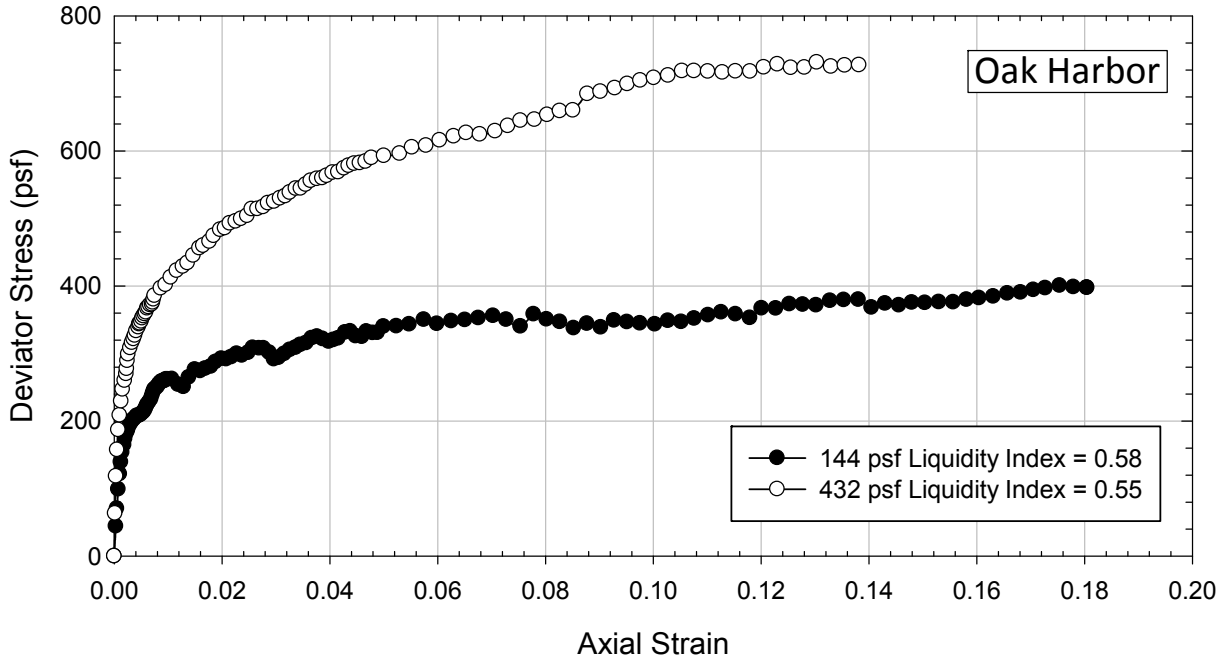

Figure 6.51 Deviator stress from packed Oak Harbor specimens.

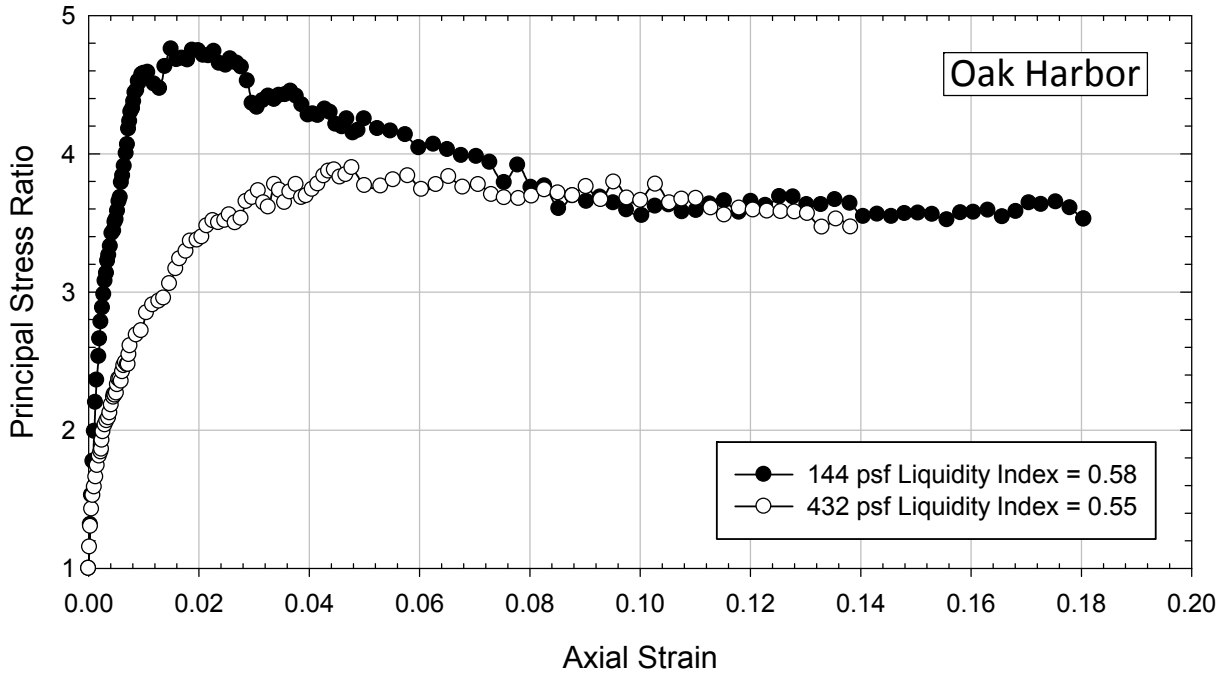

Figure 6.52 Principal stress ratio from packed Oak Harbor specimens.

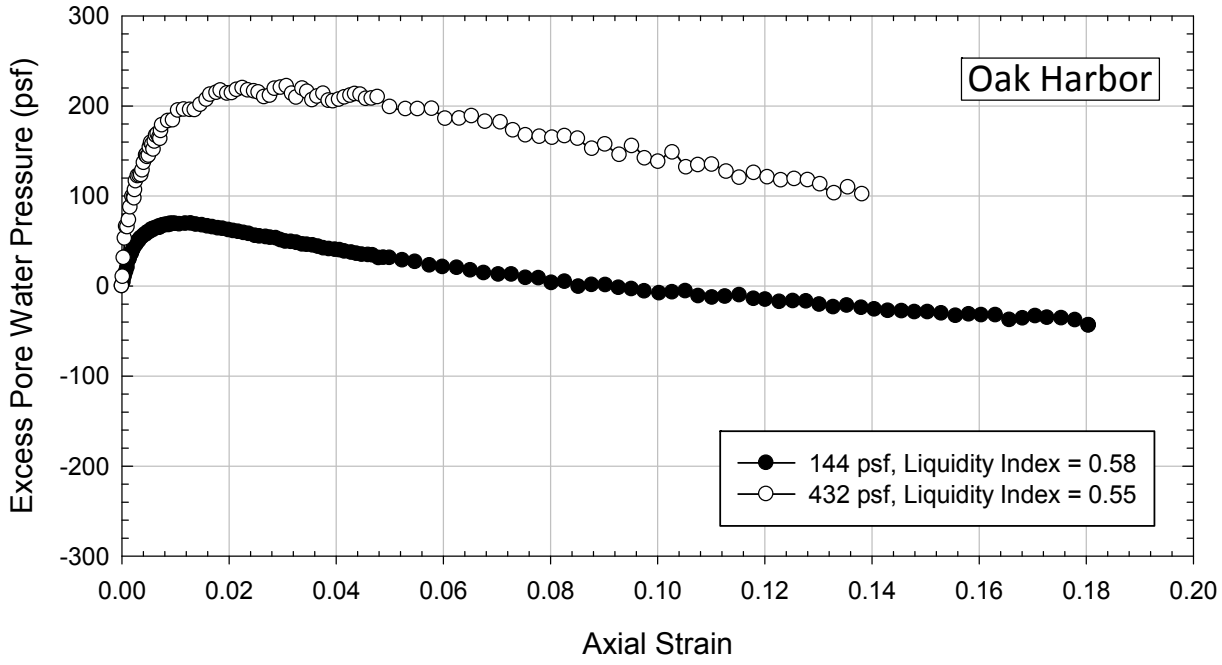

Figure 6.53 Excess pore pressures developed during shear in packed Oak Harbor specimens.

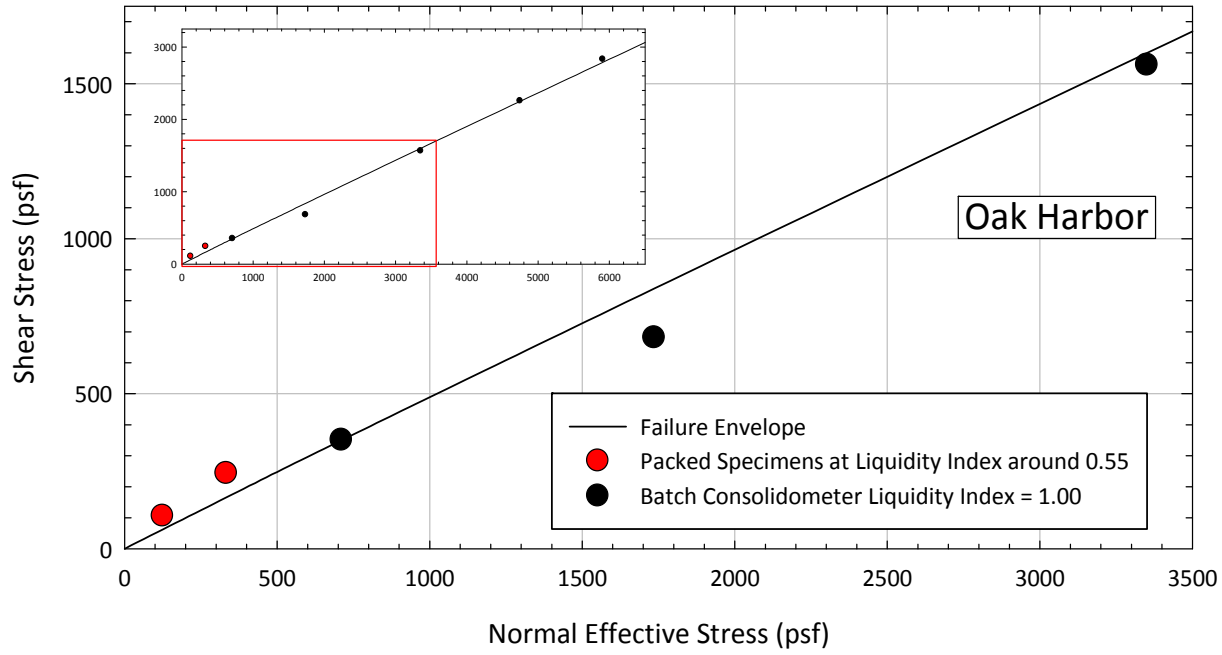

Figure 6.54 Shear strength obtained from packed Oak Harbor Clay specimens molded at a low liquidity index compared to specimens preconsolidated from the liquid limit.

6.8 Triaxial Tests on Compacted Samples Allowed to Swell Prior to Shearing

Several researchers have found that allowing samples of compacted and overconsolidated clays to swell prior to testing decreases the drained shear strength of these soils, with the lower bound of this decreased shear strength being equal to the fully softened shear strength (Graham and Au 1985; Rogers and Wright 1986; Calabresi and Rampello 1987; Kayyal and Wright 1991; Rampello 1991; Stark and Duncan 1991; Botts 1998; Picarelli et al. 2006; Wright et al. 2007). Swelling is believed to break the soil structure and bonds created by the compaction and consolidation procedure, thereby decreasing the shear strength of the clay.

As part of this investigation, ICU and ACU triaxial tests were performed on compacted test specimens of Oak Harbor and VBC that were allowed to swell prior to the consolidation stage inside the triaxial cell. This method was investigated to provide more insight on the effect of one swelling cycle on the shear strength of compacted clays and also to see if it could be a useful method to measure the fully softened shear strength in the triaxial device. A test on a VBC sample that was not allowed to swell during the backpressure saturation was also performed. For this test, the effective stress on the sample during backpressure saturation was maintained equal to the swelling pressure. This test was performed to compare the shear strength measure on a sample that was allowed to swell and one that was not allowed to swell. Both samples were consolidated to the same pressure.

The samples were compacted using a Harvard miniature compactor device equipped with a 20 lb spring. Ten layers of approximately equal mass and 22 tamps per layer were used to form the tests specimens at a water content of 2% above optimum to 100% relative compaction referred to standard Proctor (ASTM D698-12). The surface of each layer was scarified after compaction to assure better adhesion between the layers. ACU tests were performed using a ratio of major to minor principal stresses during consolidation equal to two. The samples were compacted one day or less before the start of the triaxial testing.

The samples were allowed to swell at effective stresses generally below 432 psf during and after the backpressure saturation stage. For most of the samples, the consolidation stage was started once swelling had ceased. The samples were consolidated after swelling to pressures ranging from 540 psf to 8300 psf.

The results of the shear tests performed are presented in Figures 6.55 and 6.56 for Oak Harbor Clay and VBC respectively. In these figures, the results of the direct shear and ICU triaxial tests performed on normally consolidated remolded specimens are also included. From Figure 6.55 it can be seen that the drained strength of the compacted Oak Harbor clay is only slightly higher than the fully softened shear strength after swelling at low pressures. Different results were obtained for the VBC. From Figure 6.56 it can be seen that the shear strength of VBC is not reduced to the fully softened shear strength after swelling at low pressures. Also, the shear strength of the sample not allowed to swell and tested at the swelling pressure was about the same as the shear strength of the samples allowed to swell.

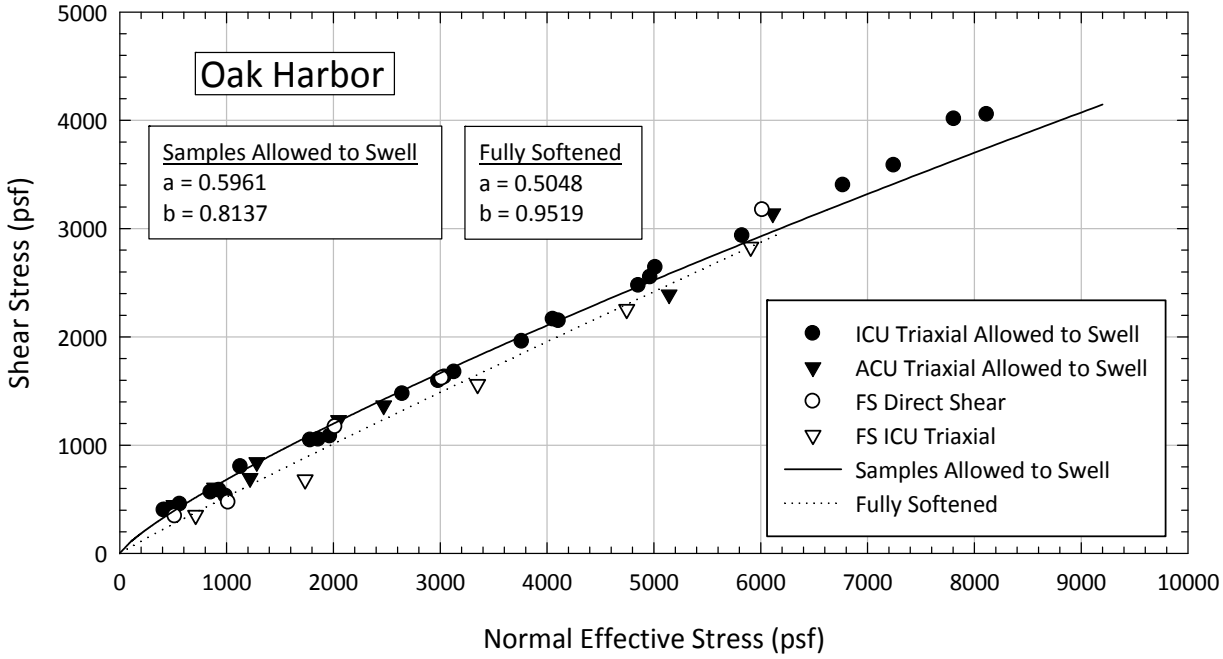

Figure 6.55 Results of ACU and ICU triaxial and direct shear tests on compacted specimens allowed to swell and normally consolidated specimens of Oak Harbor clay.

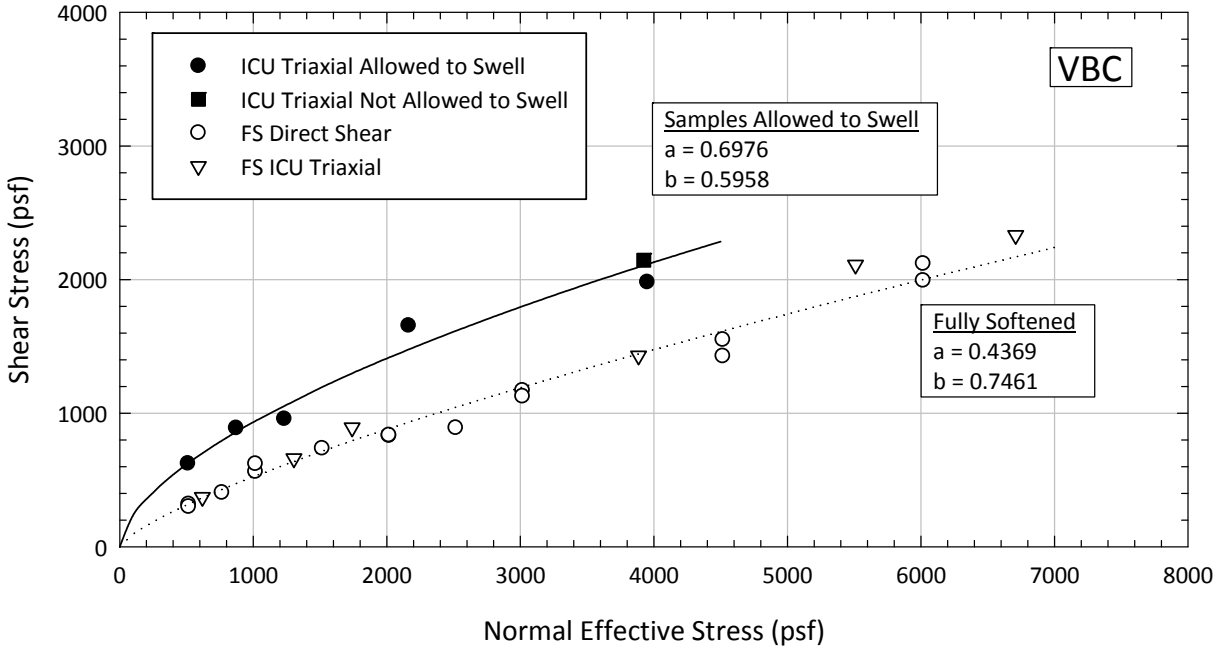

Figure 6.56 Results of ICU triaxial and direct shear tests on compacted samples allowed and not allowed to swell and normally consolidated samples of VBC.

6.9 Water Content in the Vicinity of the Failure Plane

The measurement of the final water content of the test specimen is usually performed using big slices of the specimen or the whole specimen itself. In order to assess the difference in the water content measured in the failure plane versus the remainder of the test specimen, the water contents using two methods were obtained from direct shear test samples. After the test was dismantled, the test specimen was separated into the upper and lower half by sliding the upper section of the box relative to the bottom section, thereby separating the test specimen on the existing failure plane. The surface of the failure plane was then scraped in both sections using a spatula to obtain the soil for the water content determination. Only the center section of the failure plane was used as shown in the sketch presented in Figure 6.57.

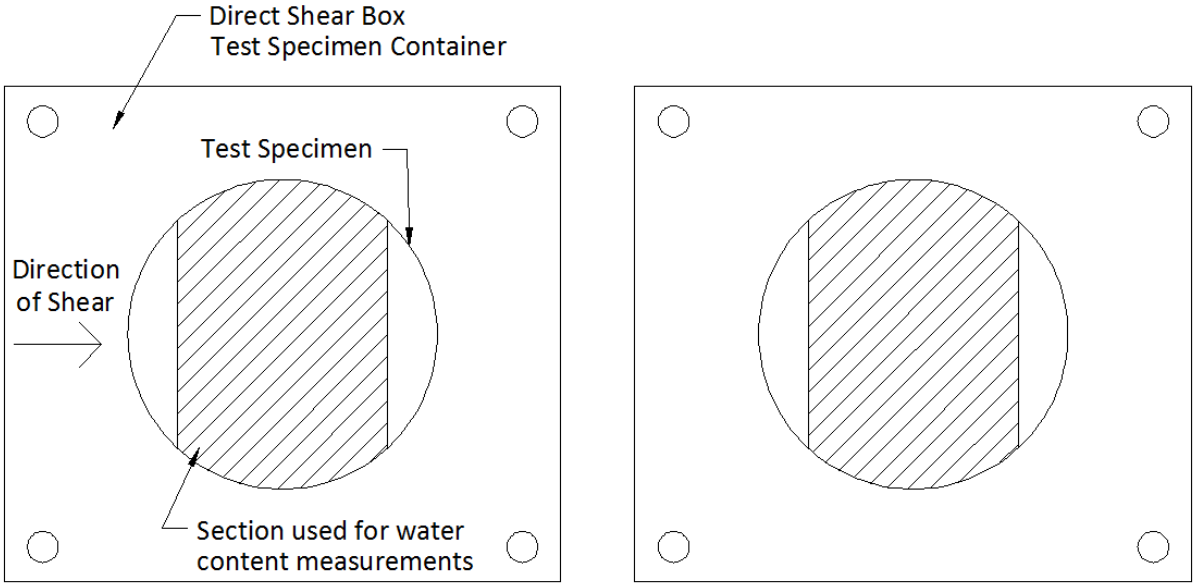

Figure 6.57 Sketch of the section used for water content determination in the failure plane from the two halves of the direct shear box.

The results of the water contents measured on the failure plane were compared to the water contents measured using one-inch square samples taken from the center of the test specimens. The one-inch square samples were taken from both the top and the bottom sections using the entire thickness of the test specimens after failure. The sections used for water contents measurements are shown in Figure 6.58. Similar water contents were obtained using both methods. The measurement of the water contents using both methods was performed for 38 tests. Usually, slightly higher water contents were obtained from the soil taken from the failure plane. Is possible that this was caused by the water ponded on the exposed surface due to the dismantling procedure.

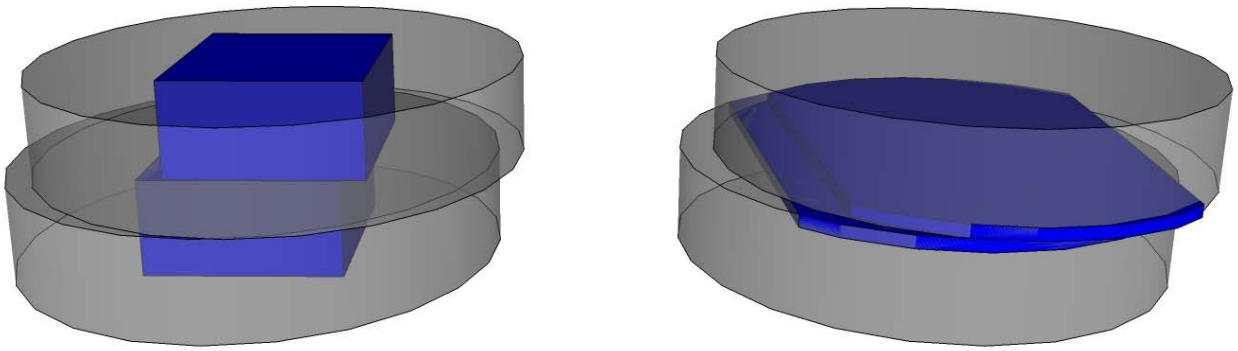

Figure 6.58 Perspective view of the sections used for water content measurement

6.10 Correlation to Represent the Curvature of the Failure Envelope

Two different correlations were found in the literature to estimate the fully softened shear strength failure envelope. These correlations were presented by T. Stark and his colleagues (Stark and Eid 1997; Stark et al. 2005; Stark and Hussain 2013) and by Professor S. Wright (Wright 2005). The correlation presented by Stark and his colleagues (Figure 2.16) is based on liquid limits and clay-sized fractions obtained from ball-milled samples. As was presented in Section 6.5, ball-milling and blenderizing increase the measured liquid limit and clay-sized fraction of soils. These procedures are commonly not performed in practice and this is a limitation for the use of this correlation. Equations haven been proposed by Stark and Hussain (2013) to estimate the liquid limit and clay-sized fraction of ball-milled samples based on these values measured using non-ball-milled samples. These equations are presented in Section 2.5. Using one correlation to estimate parameters to be input into another correlation to estimate the fully softened shear strength failure envelope can add a lot of uncertainty to the envelope obtained. Another limitation of this correlation is that a continuous failure envelope cannot be obtained. This correlation predicts the fully softened shear strength only at three normal stresses. The correlation presented by Wright (2005) is based on the results presented by Stark et al. (2005). This correlation is now outdated because Stark and Hussain (2013) have updated their correlation using additional test results. The correlation presented by Wright (2005) has the same limitations as the one presented by Stark and Hussain (2013), exept that it can predict a continous failure envelope.

Based on the limitations presented above, a correlation that uses index properties based on common procedures and that can provide a continuous failure envelope is needed. For this reason, a correlation for the *a* and *b* parameters, to be used with the power function presented in Equation 4.1, was developed. For this purpose, the *a* and b parameters obtained from the results of over 300 direct shear tests performed by the author and ERDC on 38 different clays were plotted as a function of the plasticity index in Figure 6.59. A second-degree polynomial was then fitted to this data to obtain the correlations. The plasticity index was used for this correlation because it showed a stronger relationship with the parameters *a* and *b* than the liquid limit, which is commonly used in fully softened shear strength correlations. In this figure, confidence limits obtained by increasing or decreasing the values obtained

from the correlation by one or two standard deviations are also included. The use of these confidence limits that is explained later in this section. Using Equation 4.1 and this correlation, a continuous failure envelope can be obtained and the possible errors due to a linear approximation of the failure envelope are eliminated.

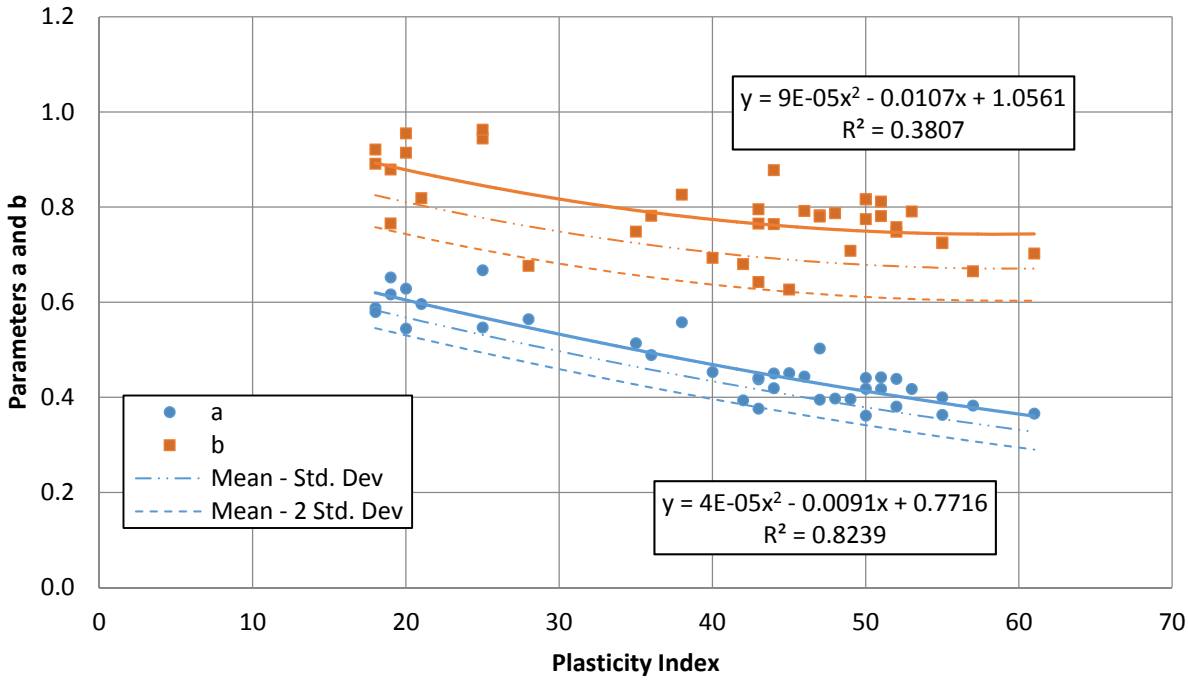

Figure 6.59 Correlation between the parameters *a* and *b* and plasticity index.

For this correlation, all the results obtained for a given soil (blenderized, non-blenderized, and different water contents) were used to obtain the *a* and *b* parameters because a significant difference was not obtained in the results from the different sample preparation methods. The results obtained from ERDC are presented in Appendix F.

The plasticity indices used in this correlation were obtained using non-blenderized samples prepared by standard procedures as specified in ASTM D4318-10. From this figure, it can be inferred that as the plasticity index of the soil increases, the shear strength of the soil decreases, as reflected by the decrease in parameters *a* and *b*. Also, as the plasticity index of the soil increases, the curvature of the failure envelope increases, as shown by a decrease in the parameter *b*.

Equation 4.1 is commonly not included in commercial slope stability software in that same form. The program Slide 6.0 by Rocscience inc. has a similar version built-in, and is shown in Equation 6.12.

$$\tau = c + a_{slide}(\sigma'_n + d)^{b_{slide}} + \sigma'_n \tan W \quad (6.12)$$

Where:

a_{slide}, b_{slide}, c = Fitting parameters.
d = Tensile strength of the soil.
W = Waviness angle.

To use the parameters obtained from the correlation presented in Figure 6.59 in Slide, the parameters *c*, *d*, and *W* have to be set equal to zero and the a_{slide} and b_{slide} parameters can be calculated using the equations below:

$$a_{slide} = a{P_a}^{(1-b)} \quad (6.13)$$

$$b_{slide} = b \quad (6.14)$$

For programs that do not include a power function to describe the failure envelope, the envelope can usually be entered using discrete points. For this purpose, a program like Microsoft Excel® can be used to generate any desired number of shear strength points in the range of effective stresses required for the slope being analyzed.

The proposed correlation and the correlation presented by Stark and Hussain (2013) were compared with the results of the shear tests performed in this investigation. Blenderized index properties were used to estimate the fully softened shear strength using the correlation presented by Stark and Hussain (2013).The results are presented in Figures 6.60 to 6.63. Since Stark's correlation does not provide a continuous failure envelope, the three data points obtained from this correlation were used to fit a power function. The power function obtained is what is plotted in Figures 6.60 to 6.63. From these figures it can be seen that the fully softened shear strength envelope predicted with Stark's correlation in most cases agreed well with the measured shear strength. These figures also show that the proposed correlation has a good agreement with the measured shear strength and in most of the cases also with the correlation presented by Stark and Hussain (2013).

The quality of a correlation can also be assessed by looking at the values of the standard deviation of the data from the proposed trend line. All the statistical descriptors of the data and the correlation are presented in Table 6.4. In this table, the mean values and standard deviations are provided for the proposed correlations.

For reliability analysis, the proposed correlations have to include an error term with a mean and a standard deviation. The complete forms of the correlation are as shown in Equations 6.15 and 6.16.

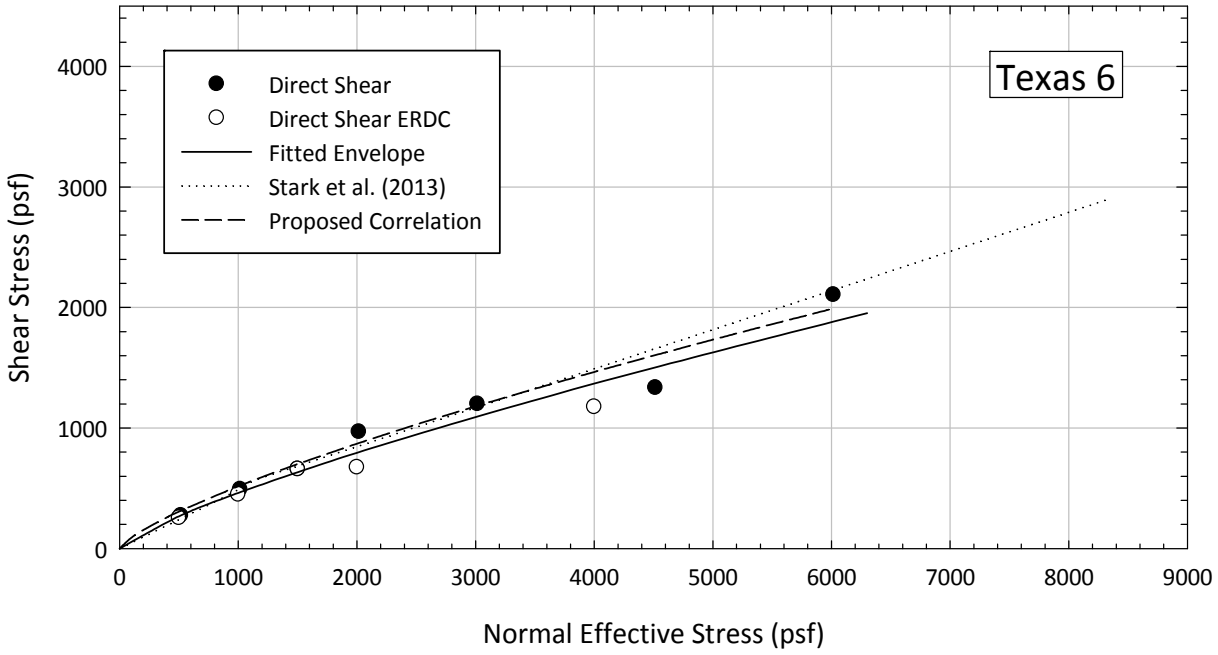

Figure 6.60 Comparison of Stark's correlation and the proposed correlation with the measured data for Texas 6.

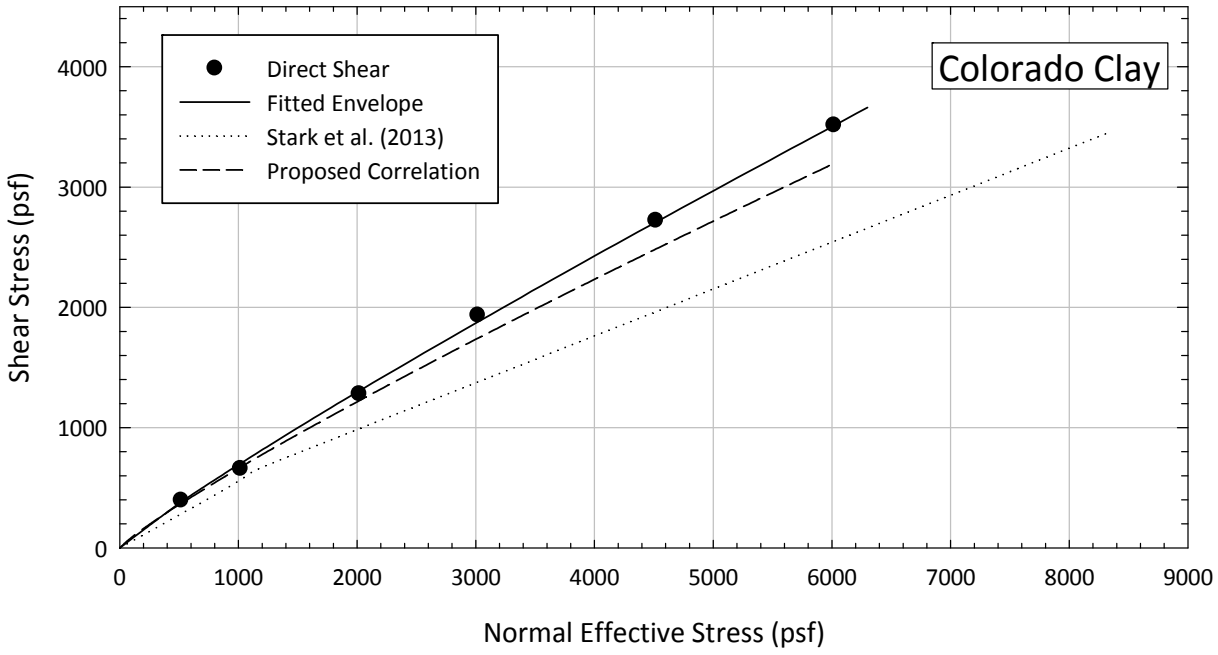

Figure 6.61 Comparison of Stark's correlation and the proposed correlation with the measured data for Colorado Clay.

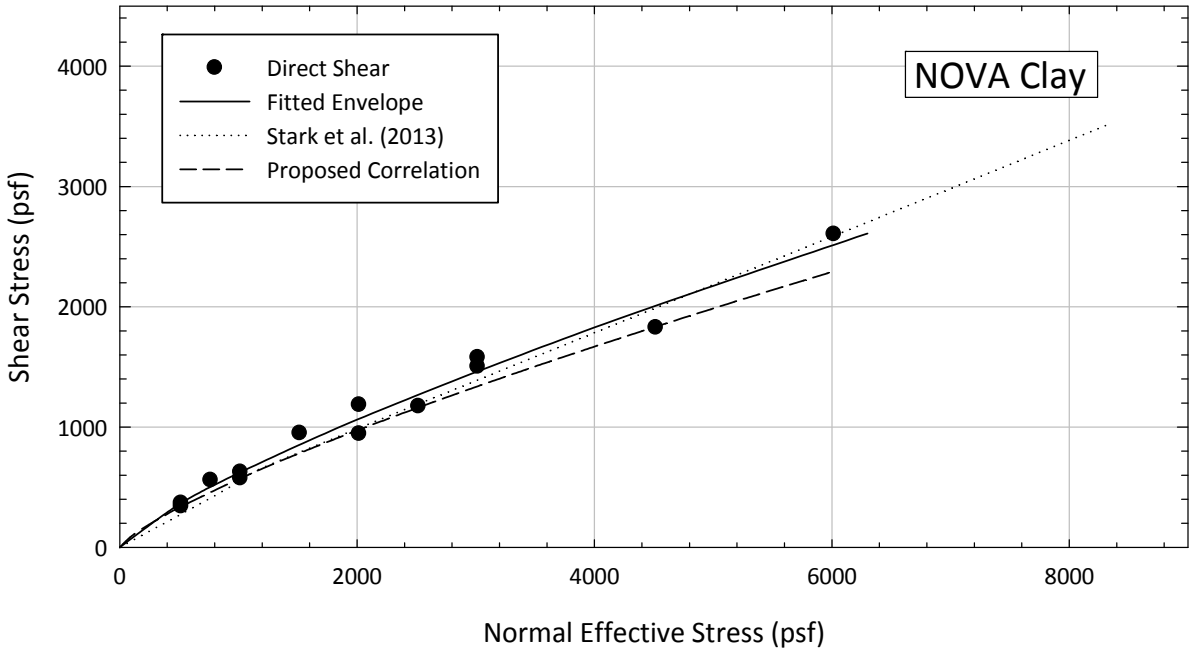

Figure 6.62 Comparison of Stark's correlation and the proposed correlation with the measured data for NOVA Clay.

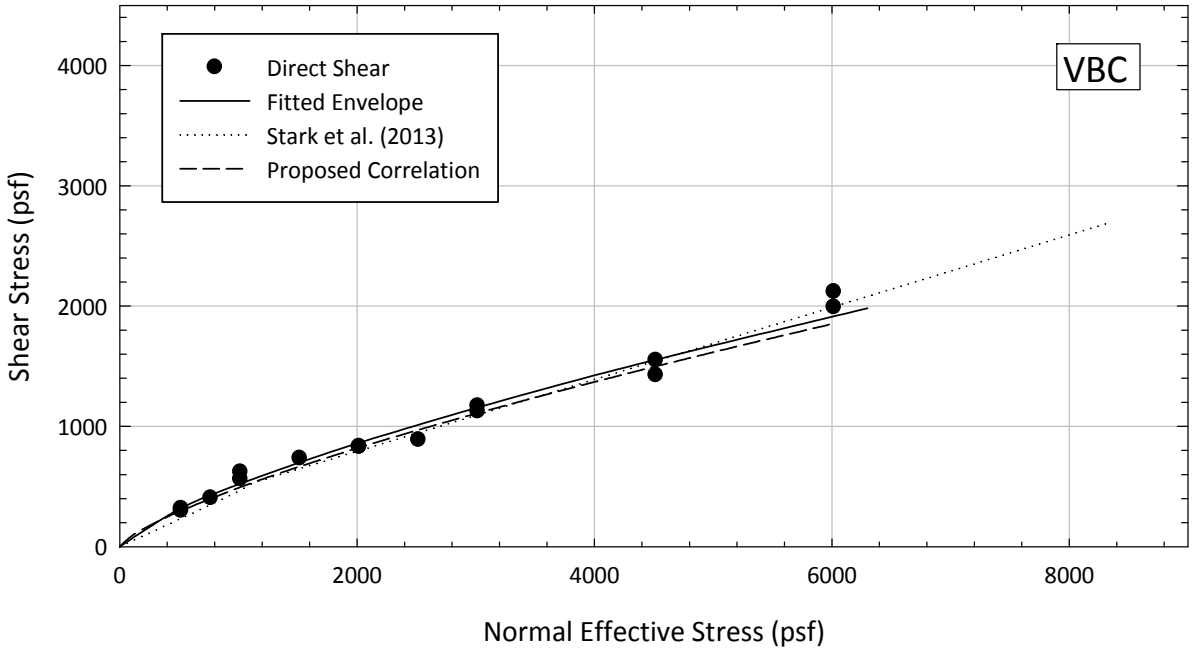

Figure 6.63 Comparison of Stark's correlation and the proposed correlation with the measured data for VBC.

Table 6.4 Statistical descriptors of the proposed correlations and errors.

Function	Mean	Std. Dev.
Predictive equation for *a*	$a = 0.00004PI^2 - 0.0091PI + 0.7716$	0.0247
Predictive equation for *b*	$b = 0.00009PI^2 - 0.0107PI + 1.0561$	0.0407

$$a = 0.00004PI^2 - 0.0091PI + 0.7716 + \xi_a(\mu_{\varepsilon_a}, \lambda_{\varepsilon_a}) \quad (6.15)$$

$$b = 0.00009PI^2 - 0.0107PI + 1.0561 + \xi_b(\mu_{\varepsilon_b}, \lambda_{\varepsilon_b}) \quad (6.16)$$

Where:

a, b = Shear strength parameters.
PI = Plasticity index.
ξ_a, ξ_b = Error term for parameters *a* and *b*.
$\mu_{\varepsilon_a}, \mu_{\varepsilon_b}$ = Mean values of the error of the parameters *a* and *b* ≈ 0.
$\lambda_{\varepsilon_a}, \lambda_{\varepsilon_b}$ = Standard deviation values presented in Table 6.4.

When the proposed correlation is used to estimate the strength parameters of a given soil, there is a 50% chance that one of the actual shear parameters will be above or below the value obtained from the correlation. In order to improve the reliability of a correlation, confidence limits can be established. Confidence limits are obtained by adding or subtracting a number of standard deviations from the mean to increase the confidence on the value obtained from a correlation. For example, as can be seen in Table 6.5, if we choose values for the shear strength parameters that are equal to the mean value minus one standard deviation, the likelihood of one of shear strength parameters being smaller than the value calculated is reduced to 16% (Duncan and Bursey 2013). If the mean minus two standard deviations is used to estimate the values of the shear strength parameters, the chances of one of them being smaller that the values calculated is reduced to 2%. The information presented in Table 6.5 is only valid if the distribution of the parameters is normal or log-normal. As can be seen from Figures 6.64 and 6.65 the distribution of the measured values of *a* approaches a log-normal distribution and the distribution of the measured values of *b* approaches a normal distribution. Different criteria were used to validate the assumed distributions:

1) The probability density function (PDF)[8] and cumulative density function (CDF)[9] from the measured data and proposed distribution agreed visually.
2) The proposed distribution did not predict negative values for *a* or *b*.

[8] The probability density function is a continuous function that describes the probability of a random variable to take a given value.
[9] The cumulative density function is a continuous function that describes the probability of a random variable to take a value less than or equal to a given value.

3) The assumed distribution was verified using the Kolmogorov-Smirnov criteria and the null hypothesis was not rejected for a 5% significance level.

Table 6.5 Relationship between standard deviation and confidence limits (Duncan and Bursey 2013) (Used under fair use).

Numbers of standard deviations above or below the trend line	Corresponding confidence limit
±1	84%
±2	98%
±3	99.9%

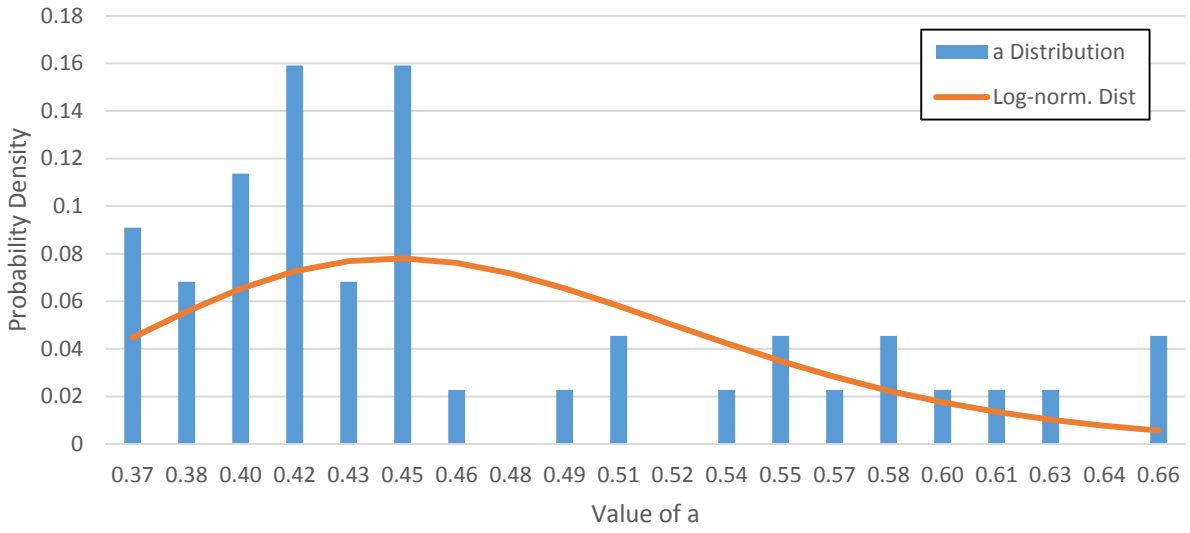

Figure 6.64 Probability density function of the measured values of *a*.

Using the correlation factors of the errors ($\delta\xi_a$, ξ_b) presented in Table 6.6, the probably of both values, *a* and *b*, being smaller than a given value can be evaluated by obtaining the joint distribution of these two parameters (i.e. the probability of the shear strength being lower than that calculated using the parameters chosen). Using this joint distribution, if the mean values are used, the probability of both parameters being lower than the mean is 34%, the probability of both parameters being smaller than the mean minus one standard deviation is 6.5%, and the probability of both parameters being smaller than the mean minus two standard deviations gets reduced to 0.43%.

This correlation is intended to be used for preliminary design estimates if better information cannot be obtained. It is always recommended that laboratory tests are performed to measure the actual shear strength of soils and the correlation can be used to validate the results obtained. If this correlation will be

used to estimate shear strength parameters for final designs, it is recommended to use the confidence limits proposed. The selection of one versus two standard deviations should be left to the discretion of the engineer.

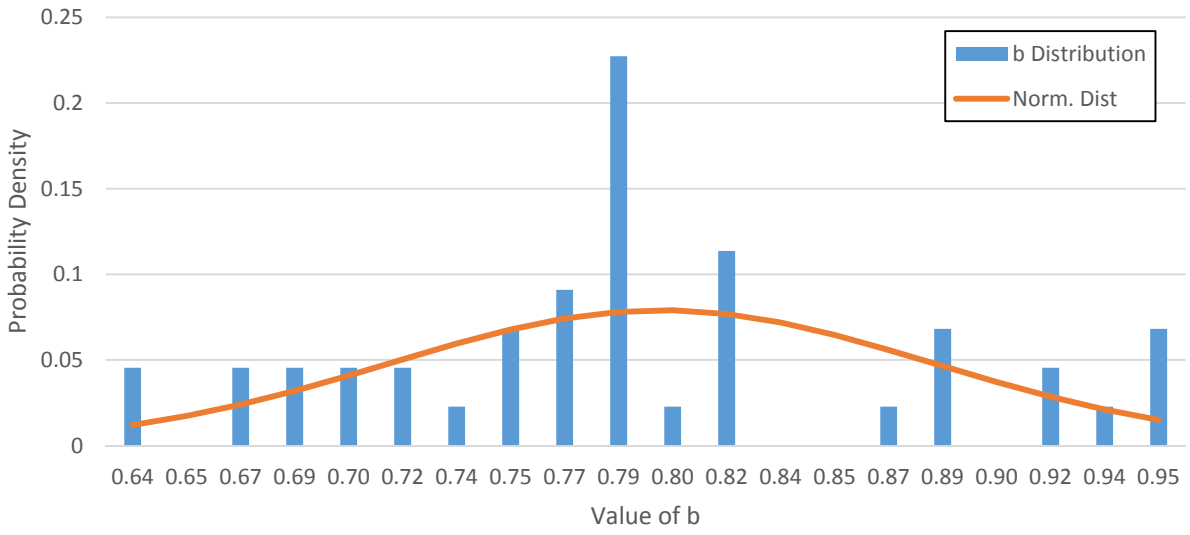

Figure 6.65 Probability density function of the measured values of *b*.

Table 6.6 Correlations for the measured data

Covariance (*a*,*b*)	**$\delta_{a,b}$**	**Covariance (ξ_a, ξ_b)**	**$\delta\xi_a$, ξ_b**
0.00383	0.53014	0.00028	0.27640

6.11 Conclusions

In this chapter, the results of the laboratory testing program were presented. From these results, it can be concluded that the ring shear device provides very conservative values for the fully softened shear strength parameters, and for this reason, it is generally not recommended for this purpose. The reasons for this may be associated with the proximity of the failure plane to the top platen in the ring shear device, effects of progressive failure, sample size effects, and extrusion during shear. The direct shear and triaxial devices have been historically used for measuring the fully softened shear strength and their results have been validated by several researchers based on back-analyses of case histories (Skempton 1977; Cancelli 1981; Kayyal and Wright 1991; Wright et al. 2007). From the results presented, it can be seen that similar fully softened shear strength parameters are obtained with the direct shear and triaxial devices.

The effect of blenderizing and mixing the soil at different water contents was also investigated. The results show that blenderizing increases the liquid limit but it does not affect the plastic limit of soils. The clay-

sized fraction of soils with an ASTM derived clay-sized fraction less than 50 increases with the blenderizing procedure. The clay-sized fraction for soils with an ASTM derived clay-sized fraction greater than 50 does not seem to be affected by the blenderizing procedure. The reason for the increase in liquid limit may be that blenderizing causes more disaggregation of the soil particles which increases the specific surface, thus more water can be absorbed by the soil particles. This increase in disaggregation is reflected in the increase in clay-sized fraction measured in blenderized samples. These findings are in agreement with the results for ball-milled samples presented by Stark et al. (2005). The blenderizing procedure was also found to slightly influence the fully softened shear strength measured. The procedure presented in Section 5.3 for non-blenderized samples is recommended to prepare samples for fully softened shear strength measurements.

Using different water contents to form test specimens to measure the fully softened shear strength was found not to influence the shear strength measured in the direct shear device for consolidation stresses above 500 psf. The fully softened shear strength failure envelope was found to be independent of the molding liquidity index. The value of $C_{\varepsilon c}$ was also found to be independent of the initial molding water content although a small curvature was observed at low stresses in samples formed at a low liquidity index. The void ratio after consolidation and at failure during shear was found to trend to the same line in tests consolidated to a pressure in excess of 1000 psf.

Packed specimens were found to provide a fast and easy way to measure the fully softened shear strength using the triaxial device at consolidation stresses above 2000 psf. At consolidation pressures below 500 psf, packed specimens seem to behave more as an overconsolidated clay, and for this reason, appear to overestimate the fully softened shear strength. More research is required to provide final conclusions. No tests were performed at consolidation stresses between 500 psf and 2000 psf, therefore, comments about the expected results in this range of stresses cannot be provided.

CU triaxial tests performed on compacted clay samples showed that allowing the specimen to swell in the triaxial cell at a low confining stress does not always decrease the shear strength to the fully softened shear strength. The peak drained shear strength of compacted Oak Harbor clay specimens that were allowed to swell prior to testing was found to be close to the fully softened shear strength. For VBC, the drained peak shear strength of samples allowed to swell was considerably higher than the fully softened shear strength. More research is required to isolate the reasons for this difference in behavior.

The water content measured using soil in the vicinity of the failure plane of a direct shear sample or using a one-inch square specimen from the center of the direct shear test specimen was found to be about the same. Usually, marginally higher water contents were obtained from the soil taken from the failure plane. Is possible that this was caused by the water ponded on the exposed surface due to the dismantling procedure. Measuring the water content using a representative sample from the interior of the test specimen is recommended because is simpler and less prone to errors.

A correlation was presented for the coefficients of the power function presented in Equation 4.1 to estimate the fully softened failure envelope. The results show that with increasing plasticity of the soil, the curvature of the fully softened failure envelope increases and the fully softened shear strength

decreases. The statistical descriptors of the proposed correlation were also presented. Confidence limits were proposed to increase the reliability of the parameters obtained using this correlation. This correlation is not intended to be used to obtain values to be used for design.

Chapter 7

Summary of Conclusions and Recommendations for Future Research

7.1 Introduction

The main objectives of this research are to compile the literature available on fully softened shear strength, to clarify the concepts involved with fully softened shear strength, and to provide guidelines for the use and measurement of fully softened shear strength. The history of fully softened shear strength was developed using the information obtained in the literature. An attempt was made to clarify certain misconceptions. Guidelines were provided for the use and measurement of fully softened shear strength based on literature review, analysis of case histories, and an extensive laboratory testing program. This chapter summarizes the main conclusions resulting from this research and provides recommendation for future research in this area.

7.2 Summary of Work Accomplished

A summary of the work accomplished during this investigation is given below:

1) An extensive literature review was conducted to compile theories proposed to explain the difference in the shear strength measured in the laboratory using undisturbed samples and that developed in the field for first-time failures in overconsolidated clays, compacted clays, and mudstones; to collect case histories related to softening; and to gather the opinion of researchers on items related to fully softened shear strength, its use, measurement, etc.
2) Evidence that could prove or disprove any of the proposed softening mechanism was compiled to reach to conclusions regarding the mechanism that can better explain the difference in the shear strength measured in the laboratory and that developed in the field.
3) One hundred and forty two case histories of first-time failures related to softening were compiled to provide guidelines regarding the soils that are more prone to softening, the depth to which the fully softened shear strength applies, the time to failure, and the pore water pressures that should be used in conjunction with fully softened shear strength parameters.

4) The effect of climatic condition on the likelihood of a soil being affected by a softening mechanism was addressed.
5) Recommendations for the factor of safety that should be used in conjunction with fully softened shear strength parameters were given.
6) A soil sample preparation technique than can provide consistent and repeatable values of fully softened shear strength parameters was presented.
7) Procedures to obtain test specimens for fully softened shear strength measurements using a direct shear, ring shear, and triaxial devices were presented.
8) The pros and cons of the ring shear, direct shear, and triaxial devices for fully softened shear strength measurements were assessed.
9) Fifteen different clays were tested as part of the laboratory testing program.
10) The difference in the fully softened shear strength measured using a ring shear, direct shear, and triaxial devices was investigated.
11) The effect of blenderizing on the index properties and fully softened shear strength measured was studied.
12) The advantages and disadvantages of using different molding water contents to prepare samples for fully softened shear strength measurements were analyzed.
13) The effect of the initial molding water content on the fully softened shear strength measured was investigated.
14) The viability of using packed specimens for fully softened shear strength determination using the triaxial device was addressed.
15) Over 130 direct shear tests on 15 soils, 67 ring shear tests on 14 soils, and 28 CU triaxial tests on five soils were performed at Virginia Tech.
16) One hundred and seventy one direct shear tests on 33 soils performed by ERDC were collected.
17) A series of CU triaxial tests was performed on compacted samples of Oak Harbor Clay and VBC allowed to swell prior to testing.
18) A correlation to obtain fully softened shear strength parameters for a power function using the plasticity index was presented.
19) A draft of an ASTM standard to measure the fully softened shear strength using the direct shear device was proposed.
20) A manual to measure the fully softened shear strength using a GeoTac direct shear device manufactured by Trautwein Soil Testing Equipment was presented.

7.3 Conclusions

7.3.1 Clarifications on various opinions about fully softened shear strength

The critical state soil mechanics theory and the “ultimate” shear strength concept have usually been related to the fully softened shear strength. An extensive literature review was performed in order to obtain information to clarify the relationship between these concepts. Also, the difference between the critical state strength and the residual shear strength and the use of undisturbed samples to measure the fully softened shear strength were clarified. Below are the conclusion obtained:

1) Critical state behavior is based on an idealized soil behavior which does not correspond to the actual behavior of some soils.
2) The critical state shear strength and residual shear strength usually are not the same, although their definitions are often described similarly. The critical state shear strength is obtained by shearing a test specimen *without a failure plane forming*. The residual shear strength requires a failure plane to be formed and enough displacement on that failure plane to cause a face-to-face orientation of the clay-sized particles.
3) The concept of residual shear strength is not fully compatible with critical state theory. However, under certain idealized behavior conditions for soil exhibiting no strain-softening, the residual shear strength would be equal to the fully softened shear strength.
4) In soils that experience a strain-softening behavior after the peak shear strength, the necessary conditions to define the critical state strength are not obtained in the direct shear, ring shear, or triaxial devices. For this reason, is not technically correct to say that the critical state strength is equal to the peak shear strength of the normally consolidated clay measured using these devices.
5) For clays that do not exhibit strain-softening behavior, the critical state shear strength is equal to the peak shear strength of a normally consolidated test specimen and is also approximately the same as the residual shear strength. Clays that exhibit this behavior normally have low clay-sized fractions.
6) The direct simple shear apparatus is not suitable for determining neither the critical state shear strength, the fully softened shear strength, nor the residual shear strength of clays.
7) Undisturbed samples have not proven to be useful for determining critical state shear strengths or fully softened shear strengths.
8) Remolded normally consolidated samples are normally necessary to measure the fully softened shear strength.
9) There is not a well-defined or industry-accepted test procedure using any apparatus to measure the critical state shear strength of soils, even after more than 50 years since the theory was developed.

7.3.2 Use of fully softened shear strength

The mechanisms that have been presented in the literature to explain the difference in the drained shear strength mobilized *in situ* and that measured in the laboratory on undisturbed samples were presented. For cuts in stiff clays, the fact that (1) softening and increased water content are just observed in the vicinity of the failure plane, and (2) the observed failure plane *in situ* better matches the critical failure plane found in slope stability analysis using undisturbed peak effective stress shear strength parameters tend to support progressive failure above the other proposed mechanisms. The presence of fissures will also decrease the shear strength of the clay mass, but this is not believed to be the factor causing a decrease in drained shear strength towards the fully softened shear strength of cuts in stiff clays. Weathering, represented by cycles of wetting and drying or freezing and thawing, will also have an influence on the shear strength of this type of material, although this will only affect shallow depths (less than 10 ft deep).

For compacted clay embankments, the main mechanism causing the decrease in shear strength appears to be weathering. Both cycles of wetting and drying or freezing and thawing will decrease the drained shear strength of compacted clays towards the fully softened shear strength. This mechanism is

supported, above the others mechanisms, by the fact that first-time failures related to fully softened shear strength are usually shallow and that the observed failure plane *in situ* better matches the critical surface obtained performing slope stability analyses using fully softened shear strength parameters. Even though weathering seems to be the main mechanism decreasing the shear strength, it cannot explain the phenomenon in every case. This is reflected in the laboratory test results presented by Wright et al. (2007), where cycles of wetting and drying did not reduce the shear strength of the soil studied to the fully softened shear strength. Despite this fact, the fully softened shear strength was necessary to obtain a factor of safety of one in the case histories analyzed by Wright et al. (2007). From the results presented by Kovacevic et al. (2001), it seems that progressive failure also influences the shear strength mobilized *in situ* in this type of project.

For failures in soft structured clays, like the ones often encountered in Canada, creep seems to be the mechanism behind the decrease in shear strength. For slopes in this type of soil, the ultimate shear strength measured in a CU triaxial test may be useful for design. More research is required to better characterize the behavior of these soils involved in first-time failures of slopes.

Based on the literature reviewed and the case histories analyzed, it can be concluded that softening is only a problem in clays with a liquid limit above 40 and a plasticity index above 20, mudstones, and structured soft clays. Among clays, overconsolidated clays are more likely to experience a decrease in shear strength *in situ* than normally consolidated clays.

For analysis of shallow slides in compacted clay embankments, the shear used in the analysis should be the fully softened strength. For slope stability analysis of these embankments, pore pressures corresponding to a water table coincident with the slope surface should be used for design, if better information is not available. To analyze deep failures, not related to fully softened shear strength, the shear strength of the first 10 ft below the face of the embankment should be assumed as the fully softened shear strength. This recommendation is based on the fact that all the first-time slides related to softening in this type of construction are below 10 ft deep. The shear strength of the soil in the foundation of the embankment should be based on shear strength tests performed using undisturbed samples. Softening of the foundation soil is not expected to occur after the embankment is in place.

For first-time slides in cuts in stiff clays, the depth of the failure plane varies within a wide range. Abdel-Ghaffar (1990) and Mesri and Abdel-Ghaffar (1993) suggested that to obtain the critical failure surface, drained undisturbed peak shear strength parameters should be used in limit equilibrium analyses. Then, the obtained failure surface should be analyzed using the fully softened shear strength. This method was investigated in this dissertation and compared to just using the fully softened shear strength to analyze the cut. The method suggested by Abdel-Ghaffar and Mesri provided a better match of the critical failure surface and the failure surface observed *in situ* when compared to using the fully softened shear strength in the entire cross-section. However, the factor of safety obtained with Abdel-Ghaffar and Mesri's method was about the same as that obtained by analyzing the entire cut with the fully softened shear strength. Using the fully softened shear strength to analyze the entire cut is a simpler method to implement, requires less laboratory testing, and will give you the correct factor of safety. For this reason, this method should be used to design cuts in stiff clays. A pore pressure ratio of 0.3 seems to be appropriate

preliminary design or if better information is not available for cuts in stiff clays. For final designs, pore pressures corresponding to steady state seepage conditions should be used.

Although the use of fully softened strengths may empirically account for progressive failure effects, more information and research is also needed to better understand the phenomenon of progressive failure and how to incorporate it into slope stability analyses.

First-time failures in compacted clay embankments and stiff clays related to fully softened shear strength are more likely to occur in climates characterized by a long and hot dry season followed by a long wet season. Also, in climates with wet summers and cold winters.

First-time failures related to fully softened shear strength are a time-dependent process. Failures in compacted clay embankment occur sooner after construction than cuts in stiff clays. The reason for the time component in cuts in stiff clays is the slow dissipation of pore pressures from the low values after the cut to return to the steady state seepage conditions. In compacted clay embankments, the time component is caused by the time required for the drained shear strength to be decreased to the fully softened shear strength and the time required for a heavy rain to cause elevated pore pressures.

Different factors of safety for stability have been proposed by various agencies to design earth dams, levees, and compacted clay embankments. The factors of safety proposed by Duncan and Wright (2005), presented in Table 4.2 are recommended by the author to be used in conjunction with fully softened shear strength parameters. The reasons for this recommendation are that the factors of safety proposed by the different agencies do not include a recommendation for fully softened shear strength parameters, that the recommendations by Duncan and Wright (2005) are independent of any agency protocols, and that these recommendations take into account the two of the most important aspects required to define a factor of safety, which are uncertainties in the parameters used in the analyses and consequences of failure. To be more specific, for shallow failures, the consequences of failure are very low. For this reason, if the fully softened shear strength is coupled with a water table corresponding to the worst case scenario possible, a factor of safety as low as 1.25 can be used. For deep failures, the consequences of failure will vary depending on the structure. The pore pressure for this type of analyses should be based on the worst seepage condition expected throughout the life of the project. In this case, for structures with low to mid consequences of failure, a factor of safety of 1.35 can be used. For structures with a high consequence of failure, a factor of safety of 1.50 can be used.

The curvature of the fully softened failure envelope was found to have a significant influence on the factor of safety for slope stability and the location of the critical failure plane obtained. Deeper failure surfaces and higher factors of safety are obtained if a linear interpretation is made to fully softened shear strength measurements and this interpretation results in a cohesion intercept. For this reason, it is recommended that a curved failure envelope should be used for design. A practical representation of the curvature of the failure envelope can be done using Equation 4.1.

7.3.3 Measurement of fully softened shear strength

The quality of the fully softened shear strength measured depends initially on the quality of the prepared sample. A sample preparation technique that proved able to provide repeatable and reliable values of fully softened shear strength was presented in Section 5.3. This sample preparation technique is recommended to be used to prepare samples for fully softened shear strength measurements.

Results presented in this dissertation show that the ring shear device is not suitable for determining the fully softened shear strength. Results obtained from 14 different soils showed that the peak shear strength measured with the ring shear device is always less than the peak shear strength measured with the direct shear device. This difference may be due to the location and thickness of the failure plane in the ring shear device relative to the end platens, extrusion during shear, progressive failure, by some other unidentified reason, or a combination of more than one of these previous reasons. Although the ring shear device is the only device that has an ASTM specification to measure fully softened shear strength, it has been shown that this device provides a very conservative measurement of fully softened shear strength.

The direct shear and triaxial devices were found to be useful for measuring the fully softened shear strength. The results of five soils tested using these two devices showed no significant difference in the fully softened shear strength measured. This finding is consistent with what others have reported in the geotechnical engineering literature. The direct shear device, except for the lengthy time required to perform test series, does not present major issues or limitations. Problems of extrusion can be avoided by using a low stress for the initial consolidation stress and a load increment ratio of one or by using a low molding water content to form the tests specimens for consolidation stresses above 500 psf. Tilting of the top platen can be reduced if the surface of the test specimen is leveled at the beginning of the test or if a low molding water content is used. If the top platen becomes tilted during early stages of the test, it can be corrected without any influence on the shear strength measured. A draft of an ASTM standard to be used to measure fully softened shear strength using the direct shear device and a complete manual to measure the fully softened shear strength using a GeoTac direct shear device have been included in Appendices A and B, respectively. The triaxial device can also be used to measure the fully softened shear strength, although conducting this type of test in this device is more labor intensive and time consuming when compared to the direct shear test, and little extra benefits are gained from using the triaxial device instead of the direct shear device.

Packed specimens were found to be a practical method to prepare samples for fully softened shear strength measurement for consolidation stresses above 2000 psf in the triaxial device. For consolidation stresses around 500 psf, packed specimens tend to overestimate the fully softened shear strength measured. No tests were performed at consolidation stresses between 500 psf and 2000 psf. So, comments about the expected results in this range of stresses cannot be provided.

The correlation to obtain the fully softened failure envelope presented by Stark and Hussain (2013) is based on fully softened shear strength tests performed with a ring shear device. Although the results presented in this dissertation showed that the ring shear device provides a very conservative measurement of the fully softened shear strength, this correlation is based on fully softened friction

angles increased by 2.5° and appear to provide reasonable results. One problem with this correlation is that it is based on ball-milled index properties which are usually not measured in practice. For this reason, it is recommended that the correlation presented in Section 6.10 for the parameters *a* and *b* and the power function presented in Section 4.10 be used to estimate the fully softened failure envelope.

The sample preparation techniques have been found to have a significant effect on the measured liquid limit, and sometimes on the clay-sized fraction of soils. The liquid limit of blenderized samples was found to be higher than the liquid limit of non-blenderized samples. The clay-sized fraction of soils with a low clay-sized fraction (less than 50%) was found to be increased by the blenderizing procedure. This difference in the liquid limit exists because the blenderizing procedure may help in the dispersion of the clay particles, decreasing the particles size, which then increases the specific surface. Thus, more water can be absorbed.

A decrease in the coefficient of consolidation was also found in blenderized samples. This decrease is attributed to a reduction in the permeability of the soil caused by a decrease in the size of the soil particles produced by the blenderizing process. The consequence of this increase in the coefficient of consolidation is a longer duration of the test for blenderized samples as compared to tests in non-blenderized samples. In blenderized samples, consolidation loads have to remain longer to achieve primary consolidation and the rate of shear has to be slower to allow dissipation of pore pressures. Another problem with blenderized samples is that the coefficient of consolidation measured will not be representative of that expected in the field. Although no significant differences were found in the fully softened shear strength measured on blenderized samples when compared to non-blenderized samples, it is recommended that samples are neither blenderized nor ball-milled for fully softened shear strength measurements.

CU triaxial tests performed on compacted clay samples showed that allowing the specimen to swell during the backpressure saturation process does not always decrease the shear strength to the fully softened shear strength. The peak drained shear strength of compacted Oak Harbor clay allowed to swell prior to testing was found to be equal to the fully softened shear strength. For VBC, the peak drained shear strength of compacted samples allowed to swell was considerable higher than the fully softened shear strength.

The molding water content used to prepare test specimens to measure the fully softened shear strength was found not to influence the results obtained in the direct shear device at consolidation stresses above 500 psf. In this investigation, samples were prepared using water contents equivalent to liquidity indices ranging from around 0.6 to around 1.5 and no significant difference was found in the fully softened shear strength measured. The value of $C_{\varepsilon c}$ was also found not to be affected by the molding liquidity index although a small curvature was observed at low stresses in samples formed at a low liquidity index. The void ratio after consolidation was found to trend to a single line after a pressure of about 1,000 psf. The same behavior was observed in the void ratio at failure.

7.4 Recommendations for Future Research

In the course of performing this investigations it was clear that more research was required in specific areas of this subject. Below is a list of areas on which future research is needed:

1) Different methods have been proposed to take into account progressive failure in slope stability analysis (e.g. Bishop 1971a; Chirapuntu and Duncan 1977; Law and Lumb 1978; Cooper 1988; Chang 1992; Rodriguez-Marek 1992). These methods should be evaluated further and could provide a viable and easy way to take progressive failure into account.
2) Some researchers have proposed that the residual shear strength can be mobilized in first-time failures. More detailed research is required to better understand this subject. The finite element method could be useful for this purpose.
3) The Bromhead ring shear device, although the most common and simple, is not the only ring shear device that has been designed. It would be useful to see if the Bishop- or Hvorslev-style ring shear apparatuses provide a better measure of fully softened shear strength.
4) Additional fully softened tests results will be useful to increase the reliability of the proposed correlation and to assess the effect of clay-sized fraction on the shear strength parameters.
5) Scant research was found that shows that the pore water chemistry influences the fully softened shear strength measured. More research is required to get a deeper understanding of this effect and to provide recommendations.
6) More tests should be performed to investigate the effect of the molding water content on the fully softened shear strength measured at consolidation stresses below 500 psf using a direct shear device.

Chapter 8

References

Abdel-Ghaffar, M. E. M. (1990). “The Meaning and Practical Significance of the Cohesion Intercept in Soil Mechanics.” Thesis presented to University of Illinois, Urbana-Champaign, IL in partial fulfillment of the requirements for the degree of Doctor of Philosophy, 262.

Abrams, T. G., and Wright, S. G. (1972). *A survey of earth slope failures and remedial measures in Texas*. Center for Transportation Research, University of Texas at Austin, 109.

Al-Hussaini, M. M., and Townsend, F. C. (1974). *Investigation of Tensile Testing of Compacted Soils*. Vicksburg, MS, 76.

Atkinson, J. H. (1981). *Foundations and Slopes: An Introduction to Applications of Critical State Soil Mechanics*. John Wiley & Sons, 382.

Atkinson, J. H., and Bransby, P. L. (1978). *The Mechanics of Soils: An Introduction to Critical State Soil Mechanics*. Mcgraw Hill Book Co Ltd, 375.

Atkinson, J. H., and Farrar, D. M. (1985). “Stress path tests to measure soil strength parameters for shallow landslips.” *Proceedings of the 11th International Conference on Soil Mechanics and Foundation Engineering*, 4, 983–986.

Aubeny, C. P., and Lytton, R. L. (2002). *Properties of High-Plasticity Clays*. Texas Transportation Institute, The Texas A&M University System, 42.

Aubeny, C. P., and Lytton, R. L. (2003). *Long-Term Strength of Compacted High-PI Clays*. Texas Transportation Institute, The Texas A&M University System, 90.

Aubeny, C. P., and Lytton, R. L. (2004). “Shallow slides in compacted high plasticity clay slopes.” *Journal of Geotechnical and Geoenvironmental Engineering*, 130(7), 717–727.

Ball, J. A. (1977). “A Study of the Shear Strength of Normally Consolidated Ecuadorian Varved Clay and its Sensitivity to Remolding.” A thesis submitted to the graduate faculty of Auburn University in partial fulfillment of the requirements for the degree of Master of Science, 89.

Banks, D. C. (1978). *Study of the Clay Shale Along the Panama Canal. Sumplemental Report: A Reanalysis of the East Culebra Slide Panama Canal*. U.S. Army Engineers Waterways Experiment Station, Vicksburg, MS, 249.

Bhattarai, P., Marui, H., Tiwari, B., Watanabe, N., and Tuladhar, G. R. (2006). “Influence of weathering on physical and mechanical properties of mudstone.” *Proceedings of the International Symposium on Disaster Mitigation of Debris Flows, Slope Failures and Landslides*, 467–479.

Bishop, A. W. (1955). “The use of the slip circle in the stability analysis of slopes.” *Géotechnique*, 5(1), 7–17.

Bishop, A. W. (1967). “Progressive failure with special reference to the mechanism causing it.” *Proceedings of the Geotechnical Conference Oslo 1967 on Shear Strength Properties of Natural Soils and Rocks*, 2, 142–150.

Bishop, A. W. (1971a). “The influence of progressive failure on the choice of the method of stability analysis.” *Géotechnique*, 21(2), 168–172.

Bishop, A. W. (1971b). “Shear strength parameters for undisturbed and remoulded soil specimens.” *Stress-strain Behavior of Soils. Roscoe Memorial Symposium*, 3–58.

Bishop, A. W., Green, G. E., Garga, V. K., Andresen, A., and Brown, J. D. (1971). “A new ring shear apparatus and its application to the measurement of residual strength.” *Géotechnique*, 21(4), 273–328.

Bishop, A. W., and Henkel, D. J. (1962). *The Measurement of Soil Properties in the Triaxial Test*. Edward Armold, London, 228.

Bishop, A. W., and Lovenbury, H. T. (1969). “Creep characteristics of two undisturbed clays.” *Proceedings of the 7th International Conference on Soil Mechanics and Foundation Engineering*, 1, 29–37.

Bishop, A. W., and Morgenstern, N. R. (1960). “Stability coefficients for earth slopes.” *Géotechnique*, 10(4), 129–153.

Bishop, A. W., Webb, D. L., and Lewin, P. I. (1965). “Undisturbed samples of London Clay from the Ashford Common Shaft: Strength–effective stress relationships.” *Géotechnique*, 15(1), 1–31.

Bjerrum, L. (1951). “Fundamental considerations on the shear strength of soil.” *Géotechnique*, 2(3), 209–218.

Bjerrum, L. (1954). *Theoretical and Experimental Investigations on the Shear Strength of Soils*. Norwegian Geotechnical Institute, Oslo, 113.

Bjerrum, L. (1967). “Progressive failure in slopes of overconsolidated plastic clay and clay shales.” *Journal of Soil Mechanics and Foundations Division*, 93(SM5), 3–49.

Botts, M. E. (1986). “The effects of slaking on the engineering behavior of clay shales.” Ph.D. Thesis, University of Colorado.

Botts, M. E. (1998). “Effects of slaking on the strength of clay shales: A critical state approach.” *Proceedings of the 2nd International Symposium on the Geotechnics of Hard Soils/Soft Rocks*, 1, 447–458.

Bromhead, E. N. (1978). “Large landslides in London Clay at Herne Bay, Kent.” *Quarterly Journal of Engineering Geology*, 11, 291–304.

Bromhead, E. N. (1979). “A simple ring shear apparatus.” *Ground Engineering*, 12(5), 40–44.

Brooker, E. (1967). “Strain energy and behaviour of overconsolidated soils.” *Canadian Geotechnical Journal*, 4(3), 326–333.

Calabresi, G., and Rampello, S. (1987). “Swelling of overconsolidated clays in excavations.” *Proceedings of the 9th European Conference on Soil Mechanics and Foundation Engineering on Groundwater Effects in Geotechnical Engineering*, 1, 11–15.

Cancelli, A. (1981). “Evolution of slopes in over-consolidated clays.” *Proceedings of the 10th International Conference on Soil Mechanics and Foundation Engineering*, 3, 377–380.

Case, J., and Chilver, A. H. (1959). *Strength of Materials: An Introduction to the Analysis of Stress and Strain*. Edward Armold, 389.

Castellanos, B., and Brandon, T. L. (2013). “A comparison between the shear strength measured with direct shear and triaxial devices on undisturbed and remolded Soils.” *Proceedings of the 18th International Conference on Soil Mechanics and Geotechnical Engineering*, (In Press).

Chan, D. H., and Morgenstern, N. R. (1987). “Analysis of progressive deformation of the Edmonton Convention Centre excavation.” *Canadian Geotechnical Journal*, 24(3), 430–440.

Chandler, R. J. (1969). “The effect of weathering on the shear strength properties of Keuper Marl.” *Géotechnique*, 19(3), 321–334.

Chandler, R. J. (1972). “Lias clay: Weathering process and their effect on shear strength.” *Géotechnique*, 22(4), 403–431.

Chandler, R. J. (1974). “Lias clay: The long-term stability of cutting slopes.” *Géotechnique*, 24(1), 21–38.

Chandler, R. J. (1984a). “Recent European experience of landslides in overconsolidated clays and soft rocks.” *Proceedings of the 4th International Symposium on Landslides*, Toronto, 1, 61–81.

Chandler, R. J. (1984b). “Delayed failure and observed strengths of first- time slides in stiff clays.” *Proceedings of the 4th International Symposium on Landslides*, Toronto, 2, 19–26.

Chandler, R. J., and Apted, J. P. (1988). “The effect of weathering on the strength of London Clay.” *Quarterly Journal of Engineering Geology*, 21(1), 59–68.

Chandler, R. J., Pachakis, M., Mercer, J., and Wrightman, J. (1973). “Four long-term failures of embankments founded on areas of landslip.” *Quarterly Journal of Engineering Geology*, 6(3-4), 405–422.

Chandler, R. J., and Skempton, A. W. (1974). “The design of permanent cutting slopes in stiff fissured clays.” *Géotechnique*, 24(4), 457–466.

Chang, C. (1992). “Discrete element method for slope stability analysis.” *Journal of Geotechnical Engineering*, 118(12), 1889–1905.

Charles, J. A., and Watts, K. S. (1980). “The influence of confining pressure on the shear strength of compacted rockfill.” *Géotechnique*, 30(4), 353–367.

Chigira, M. (1990). “A mechanism of chemical weathering of mudstone in a mountainous area.” *Engineering Geology*, 29(2), 119–138.

Chigira, M., and Oyama, T. (1999). “Mechanism and effect of chemical weathering of sedimentary rocks.” *Engineering Geology*, 55(1-2), 3–14.

Chirapuntu, S., and Duncan, J. M. (1977). “Cracking and progressive failure on embankment on soft clay foundation.” *Proceedings of the International Symposium on Soft Clay*, 453–470.

Cicolella, A., and Picarelli, L. (1990). “Decadimento meccanico di una tipica argilla a scaglie di elevata plasticita.” *Rivista Italiana di Geotecnica*, XXIV(1), 5–23.

Clemente, J. L. M. (1992). “Strength parameters for cut slope stability in ‘marine’ sediments.” *Proceedings of the Stability and Performance of Slopes and Embankments - II*, American Society of Civil Engineers, Berkeley, CA, 865–875.

Contreras, I. A., Greenwood, J. D., and Grosser, A. T. (2012). “The shear strength of Lake Agassiz clays and its role in slope stability.” *Proceedings of the University of Minnesota 60th Annual Geotechnical Engineering Conference*.

Cooper, M. R. (1988). “A displacement based analysis of progressive failure by the Reserve Capacity method.” *Proceedings of the 5th International Symposium on Landslides*, 1, 583–588.

Cooper, M. R., Bromhead, E. N., Petley, D. J., and Grant, D. I. (1998). “The Selborne cutting stability experiment.” *Géotechnique*, 48(1), 83–101.

Crabb, G. I., and Atkinson, J. H. (1991). “Determination of soil strength parameters for the analysis of highway slope failures.” *Proceeding of the International Conference on Slope Stability Engineering*, 13–18.

Crawford, C. B. (1964). “Some characteristics of Winnipeg Clay.” *Canadian Geotechnical Journal*, 1(4), 227–235.

Day, R. W., and Axten, G. W. (1989). “Surficial stability of compacted clay slopes.” *Journal of Geotechnical Engineering*, 115(4), 577–580.

Duncan, J. M., Brandon, T. L., and VandenBerge, D. R. (2011). *Report of the workshop on shear strength for stability of slopes in highly plastic clays*. Center for Geotechnical Practice and Research, Blacksburg, 79.

Duncan, J. M., and Bursey, A. (2013). “Soil modulus correlations.” *Foundation Engineering in the Face of Uncertainty*, American Society of Civil Engineers, 321–336.

Duncan, J. M., and Dunlop, P. (1969). “Slopes in stiff-fissured clays and shales.” *Journal of Soil Mechanics and Foundations Division*, 95(SM2), 467–491.

Duncan, J. M., and Wright, S. G. (2005). *Soil Strength and Slope Stability*. John Wiley & Sons, Hoboken, NJ, 309.

Dunlop, P., and Duncan, J. M. (1970). “Development of failure around excavated slopes.” *Journal of the Soil Mechanics and Foundations Division*, 96(2), 471–493.

Eid, H. T. (1996). “Drained shear strength of stiff clays for slope stability analyses.” Thesis presented to University of Illinois, Urbana-Champaign, IL in partial fulfillment of the requirements for the degree of Doctor of Philosophy, 242.

Eigenbrod, K. D., and Morgenstern, N. R. (1972). “A slide in cretaceous bedrock, Devon, Alberta.” *Geotechnical Practice for Stability in Open Pit Mining*, 223–238.

La Gatta, D. P. (1970). “Residual Strength of Clays and Clay-Shales by Rotation Shear Tests.” *Harvard Soil Mechanics Series No. 86*, Harvard University, Cambridge, Massachusetts.

Geiman, C. M. (2005). “Stabilization of Soft Clay Subgrades in Virginia: Phase I Laboratory Study.” Thesis presented to Virginia Polytechnic Institute and State University, at Blacksburg, VA in partial fulfillment of the requirements for the degree of Master of Science, 97.

Gibson, R. E. (1953). “Experimental determination of the true cohesion and true angle of internal friction in clays.” *Proceedings of the 3rd International Conference in Soil Mechanics*, 1, 126–130.

Gourlay, A. W., and Wright, S. G. (1984). *Initial laboratory study of the shear strength properties of compacted, highly plastic clays used for highway embankment construction in the area of Houston, Texas*. Center for Transportation Research, University of Texas at Austin, 224.

Graham, J., and Au, V. C. S. (1985). “Effects of freeze–thaw and softening on a natural clay at low stresses.” *Canadian Geotechnical Journal*, 22(1), 69–78.

Green, R., and Wright, S. G. (1986). *Factors affecting the long term strength of compacted Beaumont Clay*. Center for Transportation Research, University of Texas at Austin, 222.

Gregory, C. H. (1844a). “On railway cuttings and embankments: with an account of some slips in the London Clay, on the line of the London and Croydon railway.” *Minutes of the Proceedings*, 3, 135–145.

Gregory, C. H. (1844b). “Discussion on railway cuttings and embankments: with an account of some slips in the London Clay, on the line of the London and Croydon railway.” *Minutes of the Proceedings*, 3, 145–173.

Gregory, G. H., and Bumpas, K. K. (2013). “Post-peak fully-softened strength and curved strength envelope in shallow slope failure analysis.” *Proceedings of the Geo-Congress 2013: Stability and Performance of Slopes and Embankments III*, American Society of Civil Engineers, Reston, VA, 255–268.

Head, K. H. (1986). *Manual of Soil Laboratory Testing. Vol. 3: Effective Stress Tests*. John Wiley & Sons, 1238.

Heley, W., and Maclver, B. N. (1971). *Engineering Properties of Clay Shales. Report 1. Development of Classification Indexes for Clay Shales*. U.S. Army Engineer Waterways Experiment Station, Vicksburg, MS, 93.

Henkel, D. J. (1956). “The effect of overconsolidation on the behaviour of clays during shear.” *Géotechnique*, 6(4), 139–150.

Henkel, D. J. (1957). “Investigations of two long-term failures in London Clay slopes at Wood Green and Northolt.” *Proceedings of the 4th International Conference on Soil Mechanics and Foundation Engineering*, 2, 315–320.

Henkel, D. J. (1958). “Discussion: On the yielding of soils.” *Géotechnique*, 8(3), 134–136.

Henkel, D. J., and Skempton, A. W. (1955). “A landslide at Jackfield, Shropshire, in a heavily over-consolidated clay.” *Géotechnique*, 5(2), 131–137.

Horn, H. M., and Deere, D. U. (1962). “Frictional Characteristics of Minerals.” *Géotechnique*, 12(4), 319–335.

Hudacsek, P., and Bransby, M. F. (2008). “Centrifuge modelling of embankments subject to seasonal moisture changes.” *Advances in Transportation Geotechnics*, Taylor & Francis Group, London, 487–494.

Hudacsek, P., Bransby, M. F., Hallett, P. D., and Bengough, A. G. (2009). “Centrifuge modelling of climatic effects on clay embankments.” *Proceedings of the Institution of Civil Engineers - Engineering Sustainability*, 162(2), 91–100.

Hughes, P. N., Glendinning, S., Mendes, J., Parkin, G., Toll, D. G., Gallipoli, D., and Miller, P. E. (2009). “Full-scale testing to assess climate effects on embankments.” *Proceedings of the Institution of Civil Engineers - Engineering Sustainability*, 162(2), 67–79.

Hvorslev, M. J. (1936). “A ring shear apparatus for the determination of the shearing resistance and plastic flow of soils.” *Proceedings of the 1st International Conference on Soil Mechanics and Foundation Engineering*, 2, 125–129.

Hvorslev, M. J. (1939). “Torsion shear tests and their place in the determination of the shearing resistance of soils.” *Proceedings of the American Society Testing Material*, 39, 999–1022.

Hvorslev, M. J. (1960). “Physical components of the shear strength of saturated clays.” *Research Conference on Shear Strength of Cohesive Soils*, Boulder, Colorado, 169–273.

Hvorslev, M. J. (1969). *Physical Properties of Remolded Cohesive Soils*. *Translation 69-5*, U.S. Army Engineer Waterways Experiment Station, Vicksburg, 165.

Jain, S. K. (2000a). *Elementary Critical State Soil Mechanics: Worked Examples*. Engineering Publications, Blacksburg, VA, 60.

Jain, S. K. (2000b). *Elementary Critical State Soil Mechanics: A Prelude to Zienkiewicz et al.’s Computational Geomechanics*. Engineering Publications, Blacksburg, VA, 154.

James, P. M. (1970). “Time effects and progressive failure in clay slopes.” Thesis presented to University of London in partial fulfillment of the requirements for the degree of Doctor of Philosophy, 210.

Kaya, A. (2009). “Residual and fully softened strength evaluation of soils using Artificial Neural Networks.” *Geotechnical and Geological Engineering*, 27(2), 281–288.

Kayyal, M. K., and Wright, S. G. (1991). *Investigation of long-term properties of Paris and Beaumont Clays in earth embankments*. Center for Transportation Research, University of Texas at Austin, Austin, 134.

Kenney, T. C. (1959). “Discussion of geotechnical properties of glacial lake clays.” *Journal of the Soil Mechanics and Foundations Division*, 85(SM1), 67–79.

Kovacevic, N., Potts, D. M., and Vaughan, P. R. (2001). “Progressive failure in clay embankments due to seasonal climate changes.” *Proceedings of the 15th International Conference on Soil Mechanics and Geotechnical Engineering*, 3, 2127–2130.

Ladd, C. C., and DeGroot, D. J. (2003). “Recommended practice for soft ground site characterization: Arthur Casagrande Lecture.” *Proceedings of the 12th Panamerican Conference on Soil Mechanics and Geotechnical Engineering*, 3–57.

Ladd, C. C., and Foott, R. (1974). “New design procedure for stability of soft clays.” *Journal of the Geotechnical Engineering Division*, 100(GT7), 763–786.

Ladd, C. C., and Preston, W. B. (1965). *On the Secondary Compression of Saturated Clays*. Vicksburg, MS, 116.

Lade, P. V. (2010). “The mechanics of surficial failure in soil slopes.” *Engineering Geology*, 114(1-2), 57–64.

Law, K. T., and Lumb, P. (1978). “A limit equilibrium analysis of progressive failure in the stability of slopes.” *Canadian Geotechnical Journal*, 15(1), 113–122.

Lefebvre, G. (1981). “Fourth Canadian Geotechnical Colloquium: Strength and slope stability in Canadian soft clay deposits.” *Canadian Geotechnical Journal*, 18(3), 420–442.

Leroueil, S. (2001). “Natural slopes and cuts: movement and failure mechanisms.” *Géotechnique*, 51(3), 197–243.

Leroueil, S., and Marques, M. E. S. (1996). “Importance of strain rate and temperature effects in geotechnical engineering.” *Measuring and Modeling Time Dependent Soil Behavior*, T. C. Sheajan and V. N. Kaliakin, eds., American Society of Civil Engineers, 1–60.

Leroueil, S., Tardif, J., Roy, M., La Rochelle, P., and Konrad, J. M. (1991). “Effects of frost on the mechanical behaviour of Champlain Sea clays.” *Canadian Geotechnical*, 28(5), 690–697.

Lo, K. Y., and Morin, J. P. (1972). “Strength anisotropy and time effects of two sensitive clays.” *Canadian Geotechnical Journal*, 9(3), 261–277.

Maccarini, M. (1993). “A comparison of direct shear box tests with triaxial compression tests for a residual soil.” *Geotechnical and Geological Engineering*, 11(2), 69–80.

Di Maio, C. (1996). “Exposure of bentonite to salt solution: osmotic and mechanical effects.” *Géotechnique*, 46(4), 695–707.

Di Maio, C., and Onorati, R. (2000). “Influence of pore liquid composition on the shear strength of an active clay.” *Proceedings of 8th International Symposium on Landslides*, 463–468.

Di Maio, C., Santoli, L., and Schiavone, P. (2004). “Volume change behaviour of clays: the influence of mineral composition, pore fluid composition and stress state.” *Mechanics of Materials*, 36(5-6), 435–451.

Maksimovic, M. (1989). “Nonlinear failure envelope for soils.” *Journal of Geotechnical Engineering*, 115(4), 581–586.

Marsland, A. (1971). “The shear strength of stiff fissured clays.” *Stress-strain Behavior of Soils. Roscoe Memorial Symposium*, Foulis, Henley-on-Thames, UK, 59–68.

Marsland, A., and Butler, M. E. (1967). “Strength measurements on stiff fissured Barton Clay from Fawley (Hampshire).” *Proceedings of the Geotechnical Conference Oslo 1967 on Shear Strength Properties of Natural Soils and Rocks*, Building Research Station, Ministry of Public Building and Works, Oslo, 1, 139–145.

McCook, D. K. (2012). “Discussion of Modeling for Analyses of Fully Softened Levees.” *Innovative Dam and Levee Design and Construction for Sustainable Water Management*, New Orleans, 483–523.

Meehan, C. L., Brandon, T. L., and Duncan, J. M. (2007). “Measuring drained residual strengths in the Bromhead ring shear.” *Geotechnical Testing Journal*, 30(6), 466–473.

De Mello, V. F. B. (1946). “Laboratory Investigation of Shearing Resistance of Clays.” Thesis presented to the Massachusets Institute of Technology in partial fulfillment of the requirements for the degree of Doctor of Philosophy, 262.

De Mello, V. F. B. (1977). “Reflections on design decisions of practical significance to embankment dams.” *Géotechnique*, 27(3), 281–355.

Mesri, G., and Abdel-Ghaffar, M. E. M. (1993). “Cohesion intercept in effective stress-stability analysis.” *Journal of Geotechnical Engineering*, 119(8), 1229–1249.

Mesri, G., and Cepeda-Diaz, F. (1986). “Residual shear strength of clays and shales.” *Géotechnique*, 36(2), 269–274.

Mesri, G., and Shahien, M. (2003). “Residual shear strength mobilized in first-time slope failures.” *Journal of Geotechnical and Geoenvironmental Engineering*, 129(1), 12–31.

Mitchell, J. K., Shen, C., and Monismith, C. L. (1965). *Behavior of Stabilized Soils Under Repeated Loading. Report I. Background, Equipment, Preliminary Investigations, Repeated Compression and Flexure Tests on Cement-Treated Silty Clay.* Vicksburg, MS, 136.

Mitchell, J. K., and Soga, K. (2005). *Fundamentals of Soil Behavior*. John Wiley & Sons, Hoboken, NJ, 577.

Moon, A. T. (1984). “Effective shear strength parameters for stiff fissured clays.” *4th Australia-New Zealand Conference on Geomechanics*, 107–111.

Morgenstern, N. R. (1977). “Slopes and excavations in heavily over-consolidated clays.” *Proceedings of the 9th International Conference on Soil Mechanics and Foundation Engineering*, Tokyo, 2, 567–581.

Morgenstern, N. R. (1990). “Instability of mechanisms in stiff soils and weak rocks.” *Proc 10th Southeast Asian Geotechnical Conference*, 1, 27–36.

Morgenstern, N. R., and Price, V. E. (1965). “The analysis of the stability of general slip surfaces.” *Géotechnique*, 15(1), 79–93.

Nakano, R. (1979). “Geotechnical properties of mudstone of neogene tertiary in Japan.” *Proceedings of the Interntional Symposium on Soil Mechanics*, 1, 75 –92.

Noor, M. J. M., and Anderson, W. F. (2006). “A comprehensive shear strength model for saturated and unsaturated soils.” *Unsaturated Soils 2006 (GSP 147)*, ASCE, 1993–2003.

Ölmez, M. H. (2008). “Shear Strength Behaviour of Sand-Clay Mixtures.” Thesis presented to the Middle East Technical University in partial fulfillment of the requirements for the degree of Master of Science, 106.

Olson, R. E. (1962). “Correspondence.” *Géotechnique*, 12(4), 355–358.

Ortigao, J. A. R. (1995). *Soil Mechanics in the Light of Critical State Theories: An Introduction*. A. A. Balkema, 299.

Parry, R. H. G. (1960). “Triaxial compression and extension tests on remoulded saturated clay.” *Géotechnique*, 10(4), 166–180.

Picarelli, L., Urciuoli, G., Mandolini, A., and Ramondini, M. (2006). “Softening and instability of natural slopes in highly fissured plastic clay shales.” *Natural Hazards and Earth System Sciences*, 6, 529–539.

Picarelli, L., Urciuoli, G., and Russo, C. (2001). “Mechanics of slope deformation and failure in stiff clays and clay shales as a consequence of pore pressure fluctuation.” *Proceedings of the 8th International Symposium on Landslides*, 2, 1–34.

Potts, D. M., Dounias, G. T., and Vaughan, P. R. (1987). “Finite element analysis of the direct shear box test.” *Géotechnique*, 37(1), 11–23.

Potts, D. M., Dounias, G. T., and Vaughan, P. R. (1990). “Finite element analysis of progressive failure of Carsington embankment.” *Géotechnique*, 40(1), 79–101.

Potts, D. M., Kovacevic, N., and Vaughan, P. R. (1997). “Delayed collapse of cut slopes in stiff clay.” *Géotechnique*, 47(5), 953–982.

Rafalko, S. (2006). “Rapid Soil Stabilization of Soft Clay Soils for Contingency Airfields Rapid Soil Stabilization of Soft Clay Soils for Contingency Airfields.”

Rampello, S. (1991). “Some remarks on the mechanical behaviour of stiff clays: the example of Todi Clay.” *Proceedings of the Worshop on Experimental Characterization and Modelling of Soils and Soft Rocks*.

Rodriguez-Marek, A. (1992). “Discrete element method for slope stability analysis.” Thesis presented to Washington State University in partial fulfillment of the requirements for the degree of Masters of Science, 215.

Rogers, L. E., and Wright, S. G. (1986). *The effects of wetting and drying on the long-term shear strength parameters for compacted Beaumont Clay*. Center for Transportation Research, University of Texas at Austin, 146.

Roscoe, K. H., Schofield, A. N., and Wroth, C. P. (1958). “On the yielding of soils.” *Géotechnique*, 8(1), 22–53.

Rouainia, M., Davies, O., O'Brien, T., and Glendinning, S. (2009). "Numerical modelling of climate effects on slope stability." *Proceedings of the Institution of Civil Engineers - Engineering Sustainability*, 162(June), 81–89.

Rutledge, P. C. (1947). *Cooperative Triaxial Shear Research Program of the Corps of Engineers. Progress Report of the Soil Mechanics Fact Finding Survey*. Vicksburg, MS, 332.

Saada, A. S., and Townsend, F. C. (1981). "State of the art: laboratory strength testing of soils." *Laboratory shear strength of soil. ASTM STP 740*, R. N. Yong and F. C. Towsend, eds., American Society for Testing and Materials, 7–77.

Sadrekarimi, A., and Olson, S. M. (2008). "Investigating the Critical State Using Laboratory Ring Shear Tests." *Geotechnical Earthquake Engineering and Soil Dynamics IV GSP*, ASCE, 1–10.

Saleh, A. A., and Wright, S. G. (1997). *Shear strength correlations and remedial measure guidelines for long-term stability of slopes constructed of highly plastic clay soils*. Center for Transportation Research, The University of Texas at Austin, 154.

Sandroni, S. S. (1977). "The Strength of London Clay in Total and Effective Stress." Thesis presented to University of London in partial fulfillment of the requirements for the degree of Doctor of Philosophy.

Schofield, A. N. (1967). "Discussion on shear strength of stiff clays." *Proceedings of the Geotechnical Conference Oslo 1967 on Shear Strength Properties of Natural Soils and Rocks*, Oslo, 2, 180.

Schofield, A. N. (2005). *Disturbed Soil Properties and Geotechnical Design*. Thomas Telford, London, 142.

Schofield, A. N. (2006). "Interlocking, and peak and design strengths." *Géotechnique*, 56(5), 357–358.

Schofield, A. N., and Wroth, C. P. (1968). *Critical State Soil Mechanics*. Mcgraw Hill Book Co Ltd, 218.

Sheahan, T. C., Ladd, C. C., and Germaine, J. T. (1996). "Rate-dependent undrained shear behavior of saturated clay." *Journal of Geotechnical Engineering*, 122(2), 99–108.

Shewbridge, S., and Schaffer, J. (2013). "Some Unexpected 'Modern' Complications in Seepage and Slope Stability Analysis: Modeling Seepage and Strength for Flood-Loaded Structures." *Proccedings of the Dam Safety 2013 Conference*.

Skempton, A. W. (1948). "The rate of softening in stiff fissured clays, with special reference to London Clay." *Proceedings of the 2nd International Conference on Soil Mechanics and Foundation Engineering*, 2, 50–53.

Skempton, A. W. (1954). "The pore-pressure coefficients A and B." *Géotechnique*, 4(4), 143–147.

Skempton, A. W. (1964). "Long-term stability of clay slopes." *Géotechnique*, 14(2), 77–102.

Skempton, A. W. (1970). "First-time slides in over-consolidated clays." *Géotechnique*, 20(3), 320–324.

Skempton, A. W. (1977a). “Slope stability of cuttings in brown London clay.” *Proceedings of the 9th International Conference on Soil Mechanics and Foundation Engineering*, 3, 261–270.

Skempton, A. W. (1977b). “Slope stability of cuttings in Brown London Clay.” *Proceedings of the 9th International Conference on Soil Mechanics and Foundation Engineering*, 3, 261–270.

Skempton, A. W. (1985). “Residual strength of clays in landslides, folded strata and the laboratory.” *Géotechnique*, 35(1), 3–18.

Skempton, A. W., and Brown, J. D. (1961). “A landslide in Boulder Clay at Selset, Yorkshire.” *Géotechnique*, 11(4), 280–293.

Skempton, A. W., and DeLory, F. A. (1957). “Stability of natural slopes in London Clay.” *Proceedings of the 4th International Conference on Soil Mechanics and Foundation Engineering*, 2, 378–381.

Skempton, A. W., and Hutchinson, J. N. (1969). “Stability of natural slopes and embankment foundations.” *Proceedings of the 7th International Conference on Soil Mechanics and Foundation Engineering*, 4(State of the Art), 291–340.

Skempton, A. W., and LaRochelle, P. (1965). “The Bradwell Slip: A short-term failure in London Clay.” *Géotechnique*, 15(2), 221–242.

Stark, T. D., Choi, H., and McCone, S. (2005). “Drained shear strength parameters for analysis of landslides.” *Journal of Geotechnical and Geoenvironmental Engineering*, 131(5), 575–588.

Stark, T. D., and Duncan, J. M. (1991). “Mechanisms of strength loss in stiff clays.” *Journal of Geotechnical Engineering*, 117(1), 139–154.

Stark, T. D., and Eid, H. T. (1993). “Modified Bromhead ring shear apparatus.” *Geotechnical Testing Journal*, 16(1), 100–107.

Stark, T. D., and Eid, H. T. (1997). “Slope stability analyses in stiff fissured clays.” *Journal of Geotechnical and Geoenvironmental Engineering*, 123(4), 335–343.

Stark, T. D., and Hussain, M. (2013). “Empirical Correlations: Drained Shear Strength for Slope Stability Analyses.” *Journal of Geotechnical and Geoenvironmental Engineering*, 139(6), 853–862.

Stauffer, P. A., and Wright, S. G. (1984). *An examination of earth slope failures in Texas*. Center for Transportation Research, University of Texas at Austin, 273.

Swanson, P. G., and Jones, J. S. (1984). “Design and construction of slopes in Potomac formation deposits.” *Engineering Geology and Design of Slopes for Cretaceous Potomac Deposits in Fairfax County, Virginia, and Vicinity*, Geological Survey Bulletin 1556, U.S. Department of the Interior, Washington, DC, 49–62.

Take, W. A., and Bolton, M. D. (2002). “An atmospheric chamber for the investigation of the effect of seasonal moisture changes on clay slopes.” *Proceedings of the International Conference on Physical Modelling in Geotechnics, St. John’s*, Rotterdam: Balkema, 765–770.

Take, W. A., and Bolton, M. D. (2004). “Identification of seasonal slope behaviour mechanisms from centrifuge case studies.” *Proceedings of the Skempton Memorial Conference*, 2, 992–1004.

Take, W. A., and Bolton, M. D. (2011). “Seasonal ratcheting and softening in clay slopes, leading to first-time failure.” *Géotechnique*, 61(9), 757–769.

Tavenas, F., and Leroueil, S. (1981). “Creep and failure of slopes in clays.” *Canadian Geotechnical Journal*, 18(1), 106–120.

Taylor, D. W. (1941). *Cylindrical Compression Research Program on Stress-deformation and Strength Characteristics of Soils*. Cambridge, MA, 90.

Taylor, D. W. (1948). *Fundamentals of Soil Mechanics*. John Wiley, New York, 700.

Terzaghi, K. (1936). “Stability of slopes of natural clay.” *Proceedings of the 1st International Conference on Soil Mechanics and Foundation Engineering*, 1, 161–165.

Terzaghi, K., Peck, R. B., and Mesri, G. (1996). *Soil mechanics in engineering practice*. Wiley-Interscience, 547.

Thomson, S., and Kjartanson, B. H. (1985). “Study of delayed failure in a cut slope in stiff clay.” *Canadian Geotechnical Journal*, 22(2), 286–297.

Thomson, S., and Tweedie, R. W. (1978). “The Edgerton Landslide.” *Canadian Geotechnical Journal*, 15(4), 510–521.

Tiedemann, B. (1937). “Uber die Schubfestigkeit bindiger Boden.” *Bautechnik*, 15(30 and 33), 400 – 403 and 433 – 435.

Tiwari, B. (2013). “Personal communication.”

Tiwari, B., and Ajmera, B. (2011). “A new correlation relating the shear strength of reconstituted soil to the proportions of clay minerals and plasticity characteristics.” *Applied Clay Science*, 53(1), 48–57.

TXDOT. (2012). *Geotechnical Manual*. Texas Department of Transportation, Austin, TX, 60.

USACE. (1970). *Laboratory Soils Testing, Engineering Manual 1110-2-1906*. U.S. Army Corps of Engineers, Washington, DC, 407.

USACE. (1983). *Long-Term Reduction and Slough Slides in Mississippi River Levees*. Vicksburg, 147.

USACE. (2003). *Slope Stability, Engineering Manual 1110-2-1902*. U.S. Army Corps of Engineers, Washington, DC, 205.

USDA. (2005). *Earth Dams and Reservoirs (TR-60)*. United States Department of Agriculture, Washington, DC, 48.

USDIBR. (2011). *Design Standards No. 13: Embankments Dams*. U.S. Department of the Interior Bureau of Reclamation, Denver, CO.

Vaid, Y. (1979). "Strain rate behaviour of Saint-Jean-Vianney clay." *Canadian Geotechnical Journal*, 16(1), 34–42.

VandenBerge, D. R., Duncan, J. M., and Brandon, T. L. (2013). "Fully softened strength of natural and compacted clays for slope stability." *Proceedings of Geo-Congress 2013: Stability and Performance of Slopes and Embankments III*, 221–233.

Vaughan, P. R., and Walbancke, H. J. (1973). "Pore pressure changes and the delayed failure of cutting slopes in overconsolidated clay." *Géotechnique*, 23(4), 531–539.

Wetzel, A., and Einsele, G. (1991). "On the physical weathering of various mudrocks." *Bulletin of Engineering Geology and the Environment*, 44(1), 89–100.

Wood, D. M. (1990). *Soil Behaviour and Critical State Soil Mechanics*. Cambridge University Press, 462.

Wright, S. G. (2005). *Evaluation of soil shear strengths for slope and retaining wall stability analyses with emphasis on high plasticity clays*. Center for Transportation Research, University of Texas at Austin, 100.

Wright, S. G., Zornberg, J. G., and Aguettant, J. E. (2007). "The fully softened shear strength of high plasticity clays." Center for Transportation Research, University of Texas at Austin, 132.

Wroth, C. P. (1971). "Discussion on session 1: The meaning and measurement of basic soil parameters." *Stress-strain Behavior of Soils. Roscoe Memorial Symposium*, 122–124.

Yoshida, N. (1991). "Time-dependent instability in fissured, over-consolidated clays and mudstones." Thesis presented to University of Alberta, Edmonton in partial fulfillment of the requirements for the degree of Doctor of Philosophy, 293.

Yoshida, N., Morgenstern, N. R., and Chan, D. H. (1990). "A failure criterion for stiff soils and rocks exhibiting softening." *Canadian Geotechnical Journal*, 27(2), 195–202.

Yoshida, N., Morgenstern, N. R., and Chan, D. H. (1991a). "Analysis of softening effects in mudstone and over-consolidated clays." *Soils and Foundations*, 31(1), 121–130.

Yoshida, N., Morgenstern, N. R., and Chan, D. H. (1991b). "Finite-element analysis of softening effects in fissured, overconsolidated clays and mudstones." *Canadian Geotechnical Journal*, 28(1), 51–61.

Appendix A

Proposed Standard Test Method for Direct Shear Test to Determine Drained Fully Softened Shear Strength of Cohesive Soils

A.1. Introduction

An ASTM standard to measure the fully softened shear strength is only available for the ring shear device. As was presented in this dissertation, this device does not provide an accurate measurement of this shear strength. For this reason, an ASTM standard to measure the fully softened shear strength using a direct shear device is proposed in this section.

This section is formatted in format similar to that required for ASTM for submission of new standards. This new proposed standard has used both ASTM D3080-11 and ASTM D7608-10 as a skeleton.

A.2. Scope

A.2.1 This test method covers the determination of the fully softened shear strength of cohesive soils using the direct shear device. The fully softened shear strength is defined as the drained peak shear strength of a normally consolidated clay specimen. This test method focuses on the use of a reconstituted specimen to measure the fully softened shear strength. The test is performed by shearing a normally consolidated reconstituted specimen at a controlled rate on or near a single shear plane determined by the configuration of the apparatus until the peak shear resistance has been obtained.

A.2.2 The direct shear apparatus allows a reconstituted test specimen to be normally consolidated at the desired normal stress prior to drained shearing.

A.2.3 Shear stresses and displacements are non-uniformly distributed within the test specimen. An appropriate height cannot be defined for calculation of shear strains. Therefore, stress-strain relationships or any associated quantity, such as the shear modulus, cannot be determined from this test.

A.2.4 The selection of normal stresses and final determination of the shear strength failure envelope for design analysis and the criteria to interpret and evaluate the test results are the responsibility of the engineer or office requesting the test.

A.2.5 The results of the test may be affected by the presence of coarse-grained soil, rock particles, or both (see Section A.7.2).

A.2.6 Normal stresses are selected to represent the field conditions being investigated. The rate of shearing should be slow enough to ensure drained conditions (see Section A.10.13).

A.2.7 Generally, four or more tests are performed on specimens from one soil sample, each specimen under a different normal load, to determine the effects upon shear resistance. Results from a test series are combined to determine strength properties such as Mohr strength envelopes. Interpretation of multiple tests requires engineering judgment and is beyond the scope of this test method. This test method pertains to the requirements for a single test.

A.2.8 Units: The values stated in either inch-pound units or SI units [given in brackets] are to be regarded separately as standard. The values stated in each system may not be exact equivalents; therefore, each system shall be used independently of the other. Combining values from the two systems may result in non-conformance with the standard.

A.2.8.1 The gravitational system of inch-pound units is used. In this system, the pound (lbf) represents a unit of force (weight), while the unit for mass is slugs. The slug unit is not given, unless dynamic (F = ma) calculations are involved.

A.2.9 All observed and calculated values shall conform to the guidelines for significant digits and rounding established in Practice D6026.

A.2.9.1 The method used to specify how data are collected, calculated, or recorded in this standard is not directly related to the accuracy to which the data can be applied in design, other uses, or both. How one applies the results obtained using this standard is beyond its scope.

A.2.10 This standard does not purport to address all of the safety concerns, if any, associated with its use. It is the responsibility of the user of this standard to establish appropriate safety and health practices and determine the applicability of regulatory limitations prior to use.

A.3. Referenced Documents

A.3.1 ASTM Standards:

D422 Test Method for Particle-Size Analysis of Soils.

D653 Terminology Relating to Soil, Rock, and Contained Fluids.

D854 Test Methods for Specific Gravity of Soil Solids by Water Pycnometer.

D2216 Test Methods for Laboratory Determination of Water (Moisture) Content of Soil and Rock by Mass.

D2435 Test Methods for One-Dimensional Consolidation Properties of Soils Using Incremental Loading.

D2487 Practice for Classification of Soils for Engineering Purposes (Unified Soil Classification System).

D2488 Practice for Description and Identification of Soils (Visual-Manual Procedure).

D3080 Standard Test Method for Direct Shear Test of Soils Under Consolidated Drained Conditions.

D3740 Practice for Minimum Requirements for Agencies Engaged in Testing and/or Inspection of Soil and Rock as Used in Engineering Design and Construction.

D4318 Test Methods for Liquid Limit, Plastic Limit, and Plasticity Index of Soils.

D4753 Guide for Evaluating, Selecting, and Specifying Balances and Standard Masses for Use in Soil, Rock, and Construction Materials Testing.

D6026 Practice for Using Significant Digits in Geotechnical Data.

D6027 Practice for Calibrating Linear Displacement Transducers for Geotechnical Purposes.

D7608 Standard Test Method for Torsional Ring Shear Test to Determine Drained Fully Softened Shear Strength and Nonlinear Strength Envelope of Cohesive Soils (Using Normally Consolidated Specimen) for Slopes with No Preexisting Shear Surfaces.

A.4. Terminology

A.4.1 Definitions: For definitions of common technical terms used in this test method, refer to Terminology D653.

A.4.2 Definitions of Terms Specific to This Standard:

A.4.2.1 Consolidated: Soil specimen condition after primary consolidation under a specific normal stress.

A.4.2.2 Failure: The stress condition at failure for a test specimen. Failure is often taken as the maximum shear stress attained, or in the absence of a peak condition, the shear stress at 16% relative lateral displacement.

A.4.2.3 Nominal Normal Stress: In the direct shear test, the applied normal (vertical) force divided by the area of the shear box. The contact area of the specimen on the imposed shear plane decreases during shear and hence the true normal stress is unknown.

A.4.2.4 Fully softened shear force: The shear force being applied to the normally consolidated specimen when the shear resistance begins to decrease with continued shear displacement.

A.4.2.5 Fully softened shear strength: The peak shear resistance of a normally consolidated and not pre-sheared test specimen, which is equal to the fully softened shear force divided by the cross-sectional area of the test specimen.

A.4.2.6 Relative Lateral Displacement: The displacement between the top and bottom shear box halves.

A.4.2.7 Percent Relative Lateral Displacement: The ratio, in percent, of the relative lateral displacement to the diameter or lateral dimension of the specimen in the direction of shear.

A.5. Summary of Test Method

A.5.1 This test method consists of: forming a reconstituted test specimen in the direct shear box, applying a predetermined normal stress, providing for wetting or draining of the test specimen, or both, consolidating the test specimen under the normal stress, unlocking the shear box halves that hold the test specimen, and shearing the test specimen by displacing one shear box half laterally with respect to the other at a constant rate of shearing deformation while measuring the shearing force, relative lateral displacement, and normal displacement until the fully softened shear strength is reached. The shearing rate must be slow enough to allow nearly complete dissipation of excess pore pressure. A sketch of the device is presented in Figure A.1.

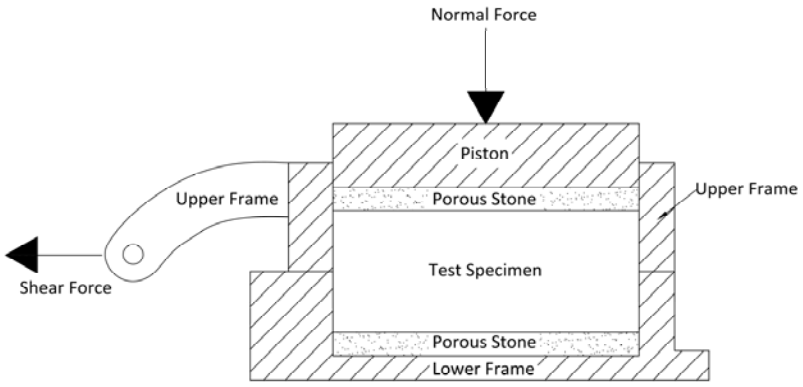

Figure A.1 Sketch of the direct shear device.

A.6. Significance and Use

A.6.1 The direct shear test is suited to the relatively rapid determination of fully softened strength properties because the drainage paths through the test specimen are short, allowing excess pore pressure to be dissipated more rapidly than other drained stress tests. There is, however, a limitation on maximum particle size (see A.7.2).

A.6.2 The direct shear apparatus allows for a reconstituted test specimen to be consolidated at the desired normal stress prior to drained shearing.

A.6.3 During the direct shear test, there is rotation of principal stresses, which may or may not model field conditions.

A.6.4 Shear stresses and displacements are non-uniformly distributed within the specimen, and an appropriate height is not defined for calculating shear strains or any associated engineering quantity. The slow rate of displacement provides for dissipation of excess pore pressures, but it also permits plastic flow of soft cohesive soils.

A.6.5 The range of normal stresses, rate of shearing, and general test conditions should be selected to approximate the specific soil conditions being investigated.

A.6.6 The area of the shear surface decreases during the test. This area reduction creates uncertainty in the actual value of the shear and normal stress on the shear plane but should not affect the ratio of these stresses.

Note 1: Notwithstanding the statement on precision and bias contained in this standard: The precision of this test method is dependent on the competence of the personnel performing the test and the suitability of the equipment and facilities used. Agencies which meet the criteria of Practice D3740 are generally considered capable of competent and objective testing. Users of this test method are cautioned that compliance with Practice D3740 does not in itself assure reliable testing. Reliable testing depends on several factors. Practice D3740 provides a means of evaluating some of these factors.

A.7. Apparatus

A.7.1 Shear Device: A device to hold the test specimen securely between two porous inserts in such a way that torque is not applied to the test specimen. The shear device shall provide a means for applying a normal stress to the faces of the test specimen, for measuring change in thickness of the test specimen, for permitting drainage of water through the porous inserts at the top and bottom boundaries of the test specimen, and for submerging the test specimen in water. The device shall be capable of applying a shear force to the test specimen in water along a predetermined shear plane (single shear) parallel to the faces of the test specimen. The frames that hold the test specimen shall be sufficiently rigid to prevent their distortion during shearing. The various parts of the shear device shall be made of material not subject to corrosion by moisture or substances within the soil (e.g., stainless steel, bronze, or aluminum). Dissimilar metals that may cause galvanic action are not permitted.

A.7.2 Shear Box*:* A shear box, either circular or square, made of stainless steel, bronze, or aluminum, with provisions for drainage through the top and bottom. The box is divided by a straight plane into two halves of equal thickness which are fitted together with alignment screws. The shear box is also fitted with gap screws, which create the space (gap) between the top and bottom halves of the shear box prior to shear. The two halves should provide a bearing surface for the specimen along the shear plane during relative lateral displacement.

A.7.2.1 The minimum diameter for circular test specimens, or width for square test specimens, shall be 2.0 inches [50 mm].

A.7.2.2 The minimum initial specimen thickness shall be 0.5 inches [13 mm].

A.7.2.3 The minimum specimen diameter to thickness or width to thickness ratio shall be 2:1.

Note 2: A light coating of grease applied to the inside of the shear box may be used to reduce friction between the test specimen and shear box. However, the upper ring in some shear devices requires friction to support the ring after the shear plates have been gapped. TFE-fluorocarbon coating may also be used instead of grease to reduce friction.

A.7.3 Porous Inserts*:* Porous inserts function to allow drainage from the test specimen along the top and bottom boundaries. They also function to transfer horizontal shear stress from the insert to the top and bottom boundaries of the test specimen. Porous inserts shall consist of silicon carbide, aluminum oxide, or metal that is not subject to corrosion by soil substances or soil moisture. The proper grade of insert depends on the soil being tested. The hydraulic conductivity of the insert should be substantially greater than that of the soil, but should be textured fine enough to prevent excessive intrusion of the soil into the pores of the insert. The diameter or width of the top porous insert or plate shall be 0.01 inches to 0.02 inches [0.2 mm to 0.5 mm] less than that of the inside of the shear box. Sandblasting or tooling the insert may help, but the surface of the insert should not be so irregular as to cause substantial stress concentrations in the test specimen. Porous inserts should be checked for clogging on a regular basis.

Note 3: Exact criteria for insert texture and hydraulic conductivity have not been established. For normal soil testing, medium grade inserts with a permeability of about $0.5x10^{3}$ ft/yr to $1.0x10^{3}$ ft/yr [$5.0x10^{-4}$ cm/s to $1.0x10^{-3}$ cm/s] are appropriate for testing clays. It is important that the permeability of the porous insert is not reduced by the collection of soil particles in the pores of the insert. Storing the porous inserts in a water filled container between uses will slow clogging. The inserts can be cleaned by flushing, boiling, or ultrasonic agitation.

A.7.4 *Loading Devices*:

A.7.4.1 Device for Applying the Normal Force: The normal force is typically applied by dead weights, a lever loading yoke activated by dead weights (masses), a pneumatic force cylinder, or a screw driven actuator. The device shall be capable of maintaining the normal force to within $\pm$1% of the specified force. It should apply the load quickly without significantly exceeding the steady value. Dead weight systems should be checked on a regular schedule. All systems with adjustable force application (e.g. pneumatic regulator or motor driven screw) require a force indicating device such as a proving ring, load cell, or pressure sensor.

A.7.4.2 Device for Shearing the Specimen: The device shall be capable of shearing the specimen at a uniform rate of displacement, with less than $\pm$5% deviation. The rate to be applied depends upon the consolidation characteristics of the test material as specified in A.10.13. The rate is usually maintained with an electric motor and gear box arrangement and the shear force is determined by a force indicating device such as a proving ring or load cell.

Note 4: In order to tests a wide range of soils, the apparatus should permit adjustment of the rate of displacement from 0.000002 inches/min to 0.04 inches/min [0.00005 mm/min to 1.0 mm/min].

Note 5: Shearing the test specimen at a rate greater than specified may produce partially drained shear results that will be smaller than the fully softened shear strength of the material. The specimen must be sheared slowly enough to allow pore pressures to dissipate.

A.7.5 Normal Force Measurement Device: A proving ring or load cell (or calibrated pressure sensor when using a pneumatic loading system) accurate to 0.5 lbf [2.5 N], or 1% of the normal force during shear, whichever is greater, is required when using anything but dead weights to apply the normal force.

A.7.6 Shear Force Measurement Device: A proving ring or load cell accurate to 0.5 lbf [2.5 N], or 1% of the shear force at failure, whichever is greater.

A.7.7 Deformation Indicators: Either dial gauges or displacement transducers capable of measuring the change in thickness (normal displacement) of the specimen, with a readability of at least 0.0001 inches [0.002 mm] and to measure relative lateral displacement with readability of at least 0.001 inches [0.02 mm]. D6027 provides details on the evaluation of displacement transducers.

A.7.8 Shear Box Bowl: A metallic box that supports the shear box and provides either a reaction against which one half of the shear box is restrained, or a solid base with provisions for aligning the half of the shear box which is free to move coincident with applied shear force along a plane. The bowl also serves as the container for the test water used to submerge the test specimen.

A.7.9 Controlled High Humidity Environment: If required, for preparing test specimens, such that water content gain or loss during specimen preparation is minimized.

A.7.10 Test Water: Water is necessary to saturate the porous stones and fill the submersion reservoir. Ideally, this water would be similar in composition to the specimen pore fluid. Options include extracted pore water from the field, potable tap water, distilled water, or saline water. The requesting agency should specify the water option. In the absence of a specification, the test should be performed with distilled water.

A.7.11 Balances: A balance or scale conforming to the requirements of Specification D4753, readable (with no estimate) to 0.1% or better.

A.7.12 Apparatus for Determination of Water Content: As specified in Test Method D2216.

A.7.13 Equipment for Remolding the Sample.

A.7.14 Miscellaneous Equipment: Including timing device with a second hand, distilled or demineralized water, spatulas, knives, straightedge, wire saws, etc., used in preparing the test specimen.

A.8. Test Specimen Preparation

A.8.1 The sample used for test specimen preparation should be sufficiently large so that a minimum of four similar test specimens can be prepared and the index properties of the sample can be determined. While this standard test method applies to the measurements on one specimen, the requesting agency will typically specify a series of tests which cover a range of stress levels. The series should be performed on similar material.

A.8.2. Assemble the shear box halves and determine the mass of the empty box with a porous insert. Also, determine the mass of a saturated porous stone and anything that will sit on top of the test specimen during consolidation.

A.8.3 Specimen Preparation:

A.8.3.1 A reconstituted specimen can be obtained by pushing a representative sample, at the as-received water content, through a No. 40 sieve. Soil with more than 25% organic content is to be reconstituted without drying.

A.8.3.2 Reconstituted clay specimens may be prepared by crushing an air-dried representative sample and passing it through a No. 40 sieve. The air dried method should not be used for highly plastic soils, tropical soils, and organic soils.

A.8.3.3 Reconstituted clay specimens may be prepared by allowing the sample to soak distilled or site-specific water for one or two days. The use of blenderizing or ball-milling to process the soil sample is left to the discretion of the agency performing the tests, although, these procedures are not recommended.

A.8.3.4 After sieving, the processed sample is mixed with site specific water/fluid or distilled water or air-dried until a water content near the liquid limit or higher is obtained. The water content can be verified using a Casagrande liquid limit cup. The liquid limit sample is prepared as described in ASTM D4318 and the water contents is acceptable when the number of blows required to close the groove cut in the sample is between 23 blows to 25 blows. Using this water content minimizes the amount of air trapped during placement of the soil paste into the test specimen container. The processed sample should be allowed to rehydrate for at least 24 hours in a high-humidity room before forming the test specimen if this was not already done before sieving.

A.8.3.5 Care is to be taken during crushing and mixing operations to avoid introducing impurities into the sample.

A.8.3.6 Place a saturated porous insert at the bottom of the shear box

Note 6: Filter papers located in between the test specimen and the porous stones are recommended to reduce the amount of soil going into the porous stones and assure better drainage.

A.8.3.7 Fill the test specimen container with soil using a spatula or piped using a pastry bag, making sure that no voids are created within the test specimen. Flush the top of the test specimen plane with the top of the test specimen container.

Note 7: If large particles are found during the sample preparation, these should be taken out of the test specimen.

Note 8: A controlled high-humidity room or laboratory glove box provides an appropriate atmosphere for preparing the test specimen.

A.8.3.8 The liquid limit, plastic limit, and clay-size fraction of the test specimens are measured using the soil used to create the test specimen.

A.8.4 Determine and record the initial mass of the box plus specimen and height of the wet specimen for use in calculating the initial water content and total mass density of the material.

A.8.5 Place a saturated porous insert on top of the specimen.

A.9. Calibration

A.9.1 Calibration is required to determine the deformation of the apparatus when subject to the consolidation loads, so that for each normal consolidation load, the apparatus deflection may be subtracted from the observed deformations. Therefore, only deformation due to test specimen consolidation will be reported for completed tests. Calibration for the equipment load-deformation characteristics need to be performed on the apparatus when first placed in service, or when apparatus parts are changed. Some devices might require the calibration to be performed with every new loading schedule. The following series of steps provide one method of calibrating the apparatus. Other methods of proven accuracy for calibrating the apparatus are acceptable.

A.9.2 Assemble the direct-shear device with a metal calibration disk or plate of a thickness approximately equal to the typical test specimen and a diameter or width that is slightly less than the direct shear box.

A.9.3 Assemble the normal force loading yoke and apply a small normal load equivalent to about 1 lbf/inches^2 [5 kPa].

A.9.4 Position the normal displacement indicator. Adjust this indicator so that it can be used to measure either consolidation or swell from the calibration disk or plate reading. Record the zero or “no load” reading.

A.9.5 Apply increments of normal force up to the equipment limitations or apply the loading schedule that is going to be used, and record the normal displacement indicator reading and normal force. Remove the applied normal force in reverse sequence of the applied force, and record the normal displacement indicator readings and normal force. Average the values and plot the load deformation of the apparatus as a function of normal load. Retain the results for future reference in determining the thickness of the test specimen and compression within the test apparatus itself.

A.9.6 Remove the calibration disk or plate.

A.9.7 If the apparatus deformation correction exceeds 0.1% of the initial specimen thickness at any load level during a test, the correction must be applied to every measurement of the test.

A.10. Procedures

A.10.1 Assemble the shear box and shear box bowl in the load frame.

A.10.2 Place the shear box containing the test specimen and porous inserts into the shear box bowl and attach the shear box.

Note 9: For some apparatus, the top half of the shear box is held in place by a notched rod which fits into a receptacle in the top half of the shear box. The bottom half of the shear box is held in place in the shear box bowl retaining bolts. For some apparatus, the top half of the shear box is held in placed by an anchor plate.

A.10.3 Connect and adjust the normal and shear forces loading systems so that no force is imposed on the load measuring devices. Record the zero values of the load measuring devices.

A.10.4 Position and adjust the shear displacement measurement device. Obtain an initial reading or set the measurement device to indicate zero displacement.

A.10.5 Place the load transfer plate and moment break on top of the porous insert.

A.10.6 Place the normal force loading yoke into position and adjust it so the loading bar is aligned. For dead weight lever loading systems, level the lever. For pneumatic or motor driven loading systems, adjust the yoke until it sits snugly against the recess in the load transfer plate, or place a ball bearing on the load transfer plate and adjust the yoke until the contact is snug.

A.10.7 Apply a small seating normal load to the specimen. Verify that the components of the loading system are seated and aligned. The top porous insert and load transfer plate must be aligned so that the movement of the load transfer plate into the shear box is not inhibited. The specimen should not undergo significant compression under this seating load.

Note 10: The seating normal load applied to the specimen should be sufficient to assure all the components are in contact and alignment but not so large as to cause compression of the specimen. For most applications, a load resulting in approximately 1 lbf/inches^2 [7 kPa] will be adequate but other values meeting the objective are acceptable.

A.10.8 Attach and adjust the normal displacement measurement device. Obtain an initial reading for the normal displacement measurement device along with a reading of the normal load (either weights or measurement device).

A.10.9 Consolidation: Calculate and record the normal force required to achieve the desired normal stress or increment thereof. Apply the desired normal stress by adding the appropriate mass to the lever arm hanger, or by increasing the pneumatic pressure.

Note 11: The normal force used for the test specimen will depend upon the data required. Application of the normal force in several increments may be necessary to prevent damage to the test specimen.

A.10.10 Apply the first load increment, begin recording the normal deformation readings against elapsed time, and fill the shear box bowl with test water and keep it full for the duration of the test. In the absence of specification, the bowl should be filled with distilled water.

Note 12: An initial load producing a normal stress of around 100 lbf/ft^2 (5 kPa) is recommended to avoid extrusion of soil during the first consolidation load. After that, a load increment ratio of one (i.e. the load is doubled) is recommended until the desire consolidation stress is reached. Test specimens prepared at a liquidity index of 1.5 or above might require an initial normal stress of around 50 lbf/ft^2 (2.5 kPa) to prevent extrusion.

A.10.11 For each intermediate stress level, apply the load as quickly as practical and record the normal deformation readings against elapsed time. For all load increments, verify completion of primary consolidation before proceeding (see Test Method D2435) or use a default value of 24 hours. For the last consolidation load, the end of primary consolidation must be verified by interpreting either the plot of normal displacement versus log of time or square root of time (in min). Test Method D2435 provides interpretation details of both methods.A.10.12 After primary consolidation is completed, remove the alignment screws or pins from the shear box. Use the gap screws to separate the shear box halves to approximately 0.025 inches [0.64 mm]. Let the sample sit for about five minutes to develop the shear stresses along the sides to support the top half of the shear box. Back out the gap screws.

Note 13: The gap screws in most equipment raise the upper box half relative to the lower box half by prying apart the halves. Creating the gap in this manner will apply a tensile stress increment along the potential failure surface. This can unintentionally weaken the material. The top cap should not move upwards while creating the gap.

A.10.13 Determine Shearing Rate: The specimen must be sheared at a relatively slow rate so that insignificant excess pore pressure exists at failure. Determination of the appropriate rate of displacement requires an estimate of the time required for pore pressure dissipation and amount of deformation required to reach failure. These two factors depend on the type of material and the stress history. The following procedures should be used to compute the required shear rate.

A.10.13.1 When data for the maximum consolidation increment yield a well-defined normal deformation versus log time curve which extends into secondary compression, the curve should be interpreted as in Test Method D2435 and the time to failure should be computed using the following equation:

$$t_f = 50\ x\ t_{50}$$

Where:

t_f = Total estimated elapsed time to failure (min).

t_{50} = Time required for the specimen to achieve 50% consolidation under the maximum normal stress (min).

A.10.13.2 When data for the maximum consolidation increment do not satisfy the requirements of A.10.13.1 but yield a well-defined normal deformation versus root time curve, the curve should be interpreted as in Test Method D2435 and the time to failure should be computed using the following equation:

$$t_f = 11.6\ x\ t_{90}$$

Where:

t_{90} = Time required for the specimen to achieve 90% consolidation under the specified normal stress (or increment thereof) (min).

Note 14: t_f should be obtained using both methods presented above. The highest t_f should be used.

A.10.14 Estimate the relative lateral displacement required to fail the specimen. This displacement will depend on many factors including the type of material and the stress history. In the absence of specific experience relative to the test conditions, as a guide, use d_f = 0.1 inches [2.5 mm] for fat and lean clays.

A.10.15 Determine the appropriate displacement rate from the following equation:

$$d_r = \frac{d_f}{t_f}$$

Where:

d_r = Displacement rate (inches/min, mm/min).
d_f = Estimated horizontal displacement at failure (inches, mm).
t_f = Total estimate elapsed time to failure (min).

A.10.16 Drained Shearing: For some types of apparatus, the displacement rate is achieved using combinations of gear wheels and gear lever positions. For other types the displacement rate is achieved by adjusting the motor speed. Select and record a displacement rate that is equal to or slower than the value computed in A.10.13.

A.10.16.1 Record the initial time, vertical and horizontal displacements, and normal and shear forces.

A.10.16.2 Start the apparatus and initiate shear.

A.10.16.3 Obtain data readings of time, vertical and horizontal displacement, and shear force at desired interval of displacement. Data readings should be taken often enough to accurately define a shear stress-displacement curve. At a minimum, data should be recorded at relative lateral displacements of about 0.1%, 0.2%, 0.3%, 0.4%, 0.5%, 1%, 1.5%, 2%, 2.5%, 3%, and then every 2% relative lateral displacement until test completion.

Note 15: Additional readings may be helpful especially at the beginning of the test in identifying trends in behavior and the value of the peak shear stress.

A.10.16.4 It may be necessary to stop the test and re-gap the shear box halves to maintain clearance between the shear box halves. The test should be checked periodically to confirm that a gap persists throughout the shearing phase of the test.

A.10.16.5 After the soil has exhibited a well-defined maximum or peak shear resistance or to at least 16% relative lateral displacement, stop the apparatus. The fully softened strength state has been achieved when the peak shear stress has been reached and the shear resistance begins to decrease, which usually requires a shear displacement of at least 0.1 inches (2.5 mm). This can be verified using the plotting technique in accordance with A.12.2.14.

A.10.16.6 Remove the normal force from the specimen by removing the mass from the lever and hanger, or by releasing the pressure.

A.10.17 Separate the shear box halves with a sliding motion along the failure plane. Do not pull the shear box halves apart perpendicularly to the failure surface, since it would damage the test specimen. Photograph, sketch, or describe in writing the failure surface.

A.10.18 Remove the test specimen from the shear box and determine its water content according to Test Method D2216.

Note 16: If large particles are found in the soil after testing, a particle size analysis should be performed in accordance with Method D422 to confirm the visual observations, and the result should be provided with the test report

A.11. Calculation

A.11.1 General: Typical units are shown for both IP and SI systems and SD stands for significant digits. Furthermore, the prefix used for each variable has been chosen based on current practice. Other prefixes are permissible and will require different numerical values for the Unit Conversion Factors. Other units are permissible, provided consistency of units is maintained throughout the calculations. See A.2.8 for additional comments on the use of inch-pound units.

A.11.2 Calculate the following for each reading during shear:

A.11.2.1 Nominal shear stress, acting on the specimen is:

$$\tau = \frac{F}{A}$$

Where:

τ = Nominal shear stress, lbf/inches^2 [kPa] (3 SD).
F = Shear force, lbf [N] (3 SD).
A = Cross-sectional area of the test specimen, inches^2 [m^2] (3 SD).

A.11.2.2 Nominal normal stress acting on the specimen is:

$$\sigma_n = \frac{N}{A}$$

Where:

σ_n = Nominal normal stress, lbf/inches^2 [kPa] (3 SD).
N = Normal vertical force acting on the test specimen, lbf [N] (3 SD).

Note 17: Factors which incorporate assumptions regarding the actual test specimen surface area over which the shear and normal forces are measured can be applied to the calculated values of shear or normal stress, or both. If a correction(s) is made, the factor(s) and rationale for using the correction shall be explained with the test results.

A.11.2.3 Displacement Rate: The average displacement rate along the shear surface is:

$$d_r = \frac{d_h}{t_e}$$

Where:

d_r = Displacement rate, inches/min [mm/min] (3 SD).
d_h = Relative lateral displacement, inches [mm] (3 SD).
t_e = Elapsed time of test, min (3 SD).

A.11.2.4 Percent Relative Lateral Displacement: The percent relative lateral displacement along the shear surface is:

$$d_p = \frac{d_h}{D} x\ 100\%$$

Where:

d_p = Percent relative lateral displacement, % (3 SD).
D = Specimen diameter or lateral dimension in direction of shear, inches [mm] (3 SD).

A.11.3 Compute the initial void ratio, initial dry density, and degree of saturation based on the specific gravity, initial water content, mass, and volume of the total test specimen. Test specimen volume is determined by measurements of the shear box lengths or diameter and the measured thickness of the test specimen.

A.11.4 Compute the preshear void ratio, dry density, and water content based on the values used in A.11.3 plus the measured normal deformation.

A.12. Report: Test Data Sheet(s)/Form(s)

A.12.1 The methodology used to specify how data are recorded on the data sheet(s)/form(s), as given below is covered in A.2.9 and Guide D6026.

A.12.2 Record as a minimum the following general information (data):

A.12.2.1 Sample identification, project, and location.

A.12.2.2 Test number, date, apparatus identification, and technician.

A.12.2.3 Description of type of shear device used in test.

A.12.2.4 Description of appearance of the test specimen, based on Practice D2488 (Test Method D2487 may be used as an alternative), Atterberg limits (Test Method D4318), and grain size data (Method D422), if obtained (see A.8).

A.12.2.5 Sample preparation procedure used to reconstitute the test specimen.

A.12.2.6 Liquid limit, plastic limit, and clay-sized fraction of the test specimen.

A.12.2.7 Initial and final water content.

A.12.2.8 Initial and pre-shear wet density.

A.12.2.9 Initial and pre-shear dry density and void ratio.

A.12.2.10 Initial and pre-shear degree of saturation.

A.12.2.11 Initial thickness and diameter (width for square shear boxes).

A.12.2.12 Loading schedule during consolidation, final normal stress, rate of deformation, shear displacement at failure, and corresponding nominal shear stress values and specimen thickness changes.

A.12.2.13 Plot of deformation versus log of time or square root of time for those load increments used to determine the shear rate.

A.12.2.14 Plot of nominal shear stress versus lateral displacement or percent relative lateral displacement.

A.12.2.15 Plot of normal displacement versus lateral displacement or percent relative lateral displacement.

A.12.2.15 Departure from the procedure outlines, such as special loading sequences or special wetting requirements.

A.13. Precision and Bias

A.13.1 Precision: Test data on precision are not presented due to the nature of the soil tested by this standard. It is either not feasible or too costly at this time to have ten or more laboratories participate in a round-robin testing program. In addition, it is either not feasible or too costly to produce multiple specimens that have uniform physical properties. Any variation observed in the data is just as likely to be due to specimen variation as to operator or laboratory testing variation.

A.13.2 Bias: There is no accepted reference value for this test method, therefore, bias cannot be determined.

A.14. Keywords

A.14.1 consolidated; drained test conditions; fully softened shear strength; reconstituted specimens; direct shear test; strength envelope.

Appendix B [10]

Direct Shear Manual for Fully Softened Shear Strength Using a GeoTac Direct Shear Apparatus and DigiShear Software

[10] This manual started as a yearly assignment for the Advance Soil Testing Class (CE5524) at Virginia Tech. As part of my dissertation, I took upon the existing manual and edited to its final form.

DIRECT SHEAR TEST

FOR

FULLY SOFTENED SHEAR STRENGTH

OF CLAYS

USING GEOTAC LOAD FRAME AND DIGISHEAR SOFTWARE

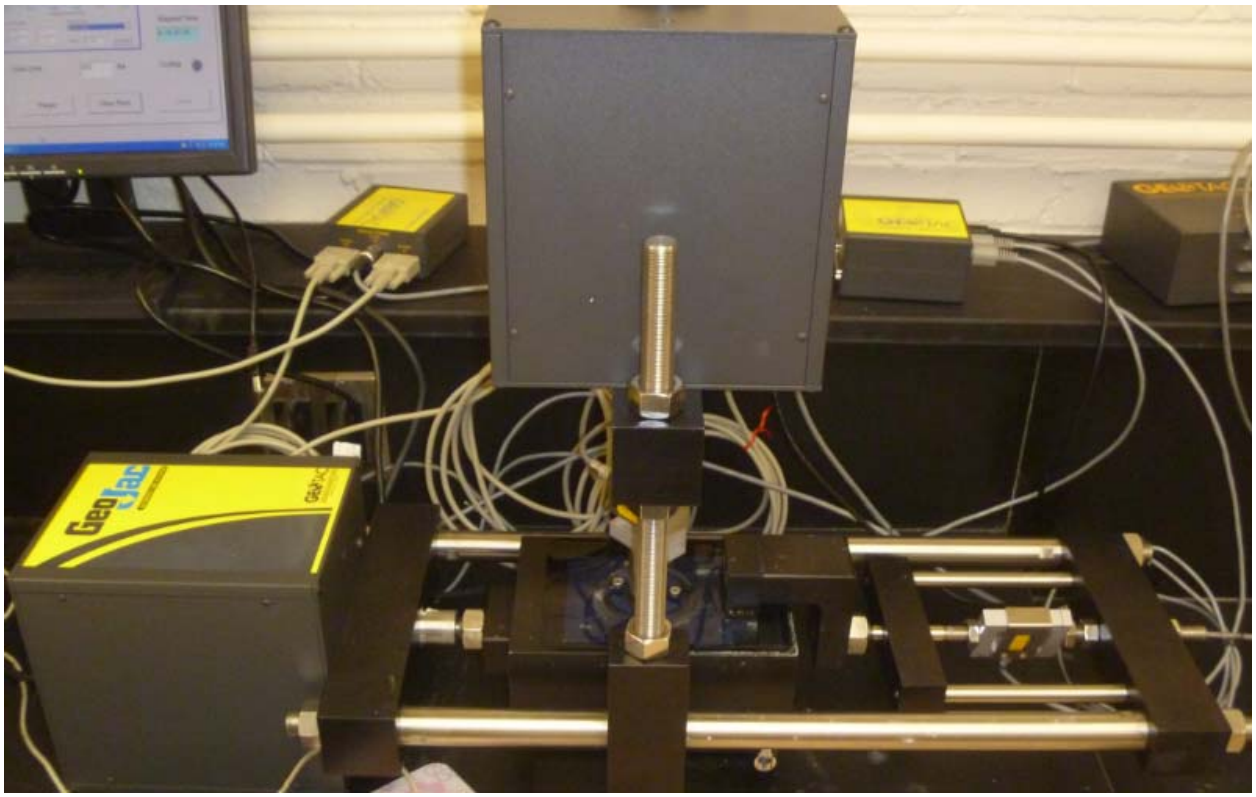

VIRGINIA POLYTECHNIC INSTITUTE AND STATE UNIVERSITY

TABLE OF CONTENTS

LIST OF FIGURES

B.1. Introduction

The direct shear test is a drained test that can be performed on undisturbed, remolded, or compacted test specimens. This manual describes the process of performing a direct shear test on a clay remolded at a water content close to the liquid limit using a GeoTac direct shear device. This manual also provides a procedure to prepare soil specimens for fully softened shear strength measurements.

This manual should be referenced in conjunction with the ASTM D3080, "Standard Test Method for Direct Shear Test of Soils Under Consolidated Drained Conditions." The ASTM standard also describes how to perform a direct shear test on test specimens other than remolded samples.

B.2. Equipment

The primary components of the GeoTac direct shear apparatus are shown in Figures B.1 and B.2. Figure B.1 shows the direct shear box assembly. This assembly consists of a specimen container, that can be divided into two halves, two porous stones to allow drainage at the top and bottom of the test specimen, a top platen and ball bearing assembly that transmit the load uniformly to the test specimen, two black plastic-topped thumb screws to fix the two halves of the direct shear box, and two yellow plastic-topped thumb screws to create a gap between the upper and lower half of the direct shear box during shearing (See Section B.5.2).

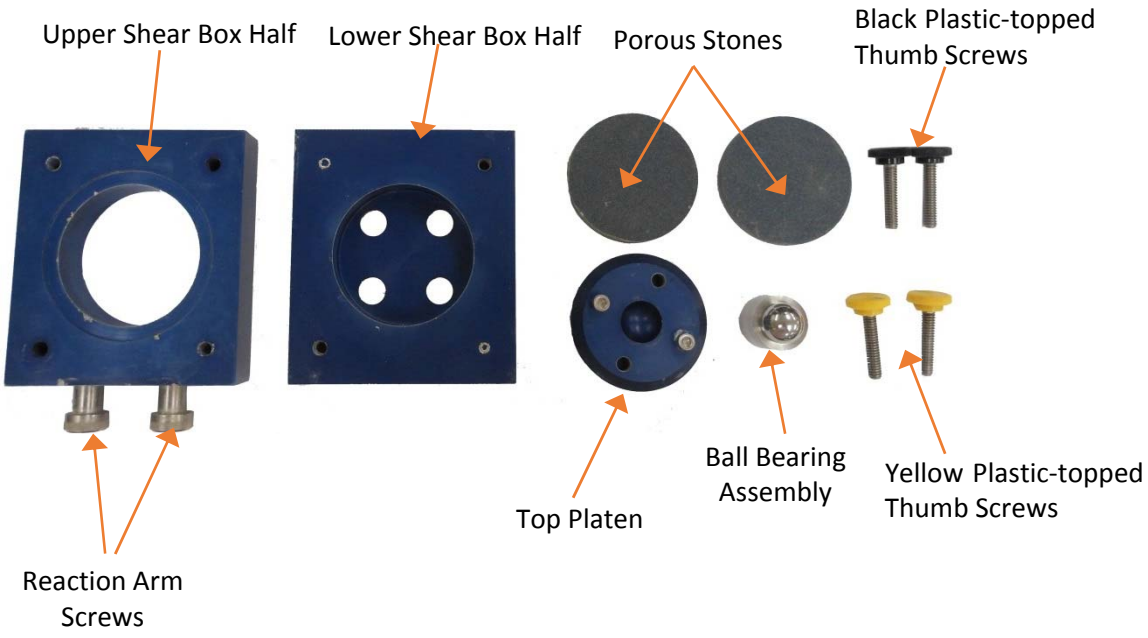

Figure B.1 Direct shear box assembly.

The direct shear box presented in Figure B.1 is to perform tests on circular test specimen. Square test specimens can also be used in the direct shear test. For this purpose, a different shear box is needed.

The direct shear device presented in Figure B.2 consists of two load cells to measure the normal and shear forces applied to the test specimen, a horizontal reaction arm to transmit the shear load to the test specimen, a reservoir to keep the test specimen under water to prevent it from drying, a load frame that serves as a reaction for the shear load, and nuts to fix the components of the direct shear device during the shearing stage (See Section B.5.2).

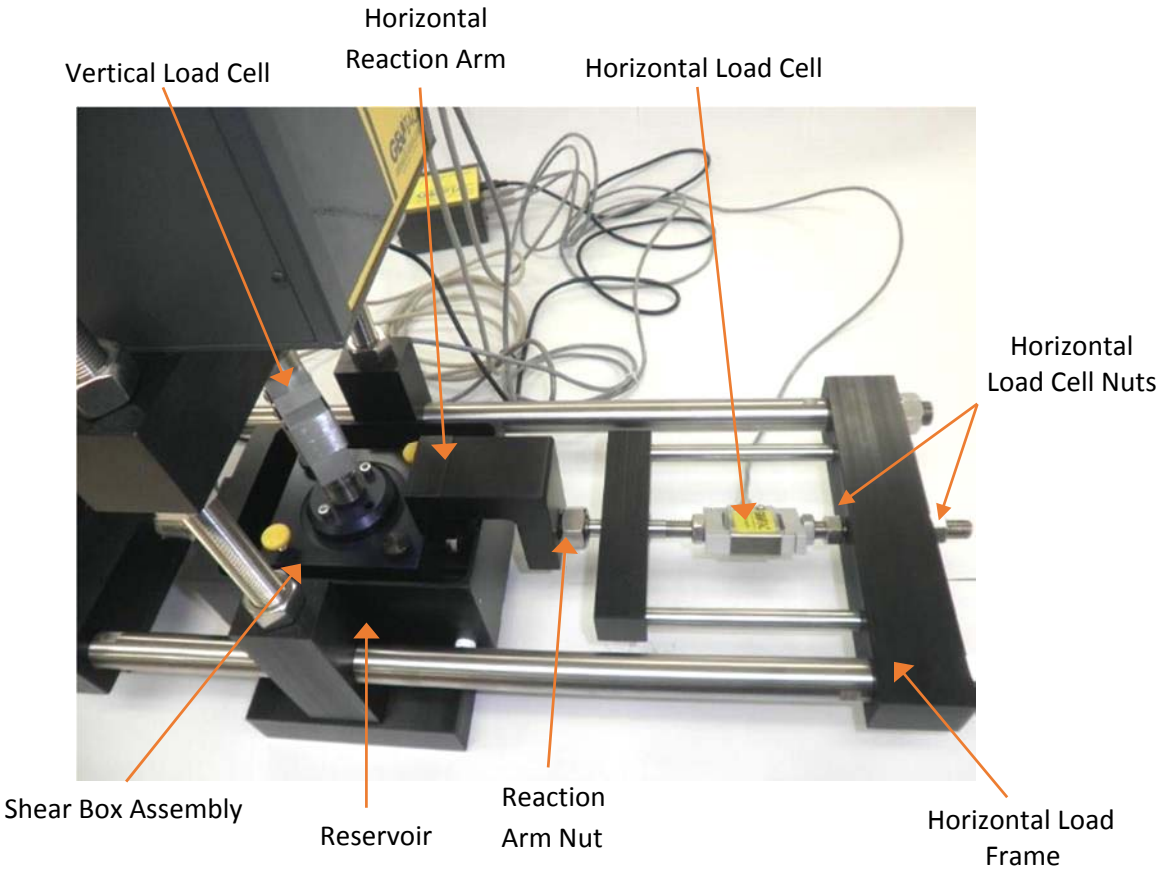

Figure B.2 Direct shear apparatus.

B.3. Sample Preparation

The materials necessary to process the soil sample are: clay material, a liquid limit device with a grooving tool, a spatula, a No. 40 (425 µm) sieve, a bowl, and distilled or site-specific water. Before starting, it may be helpful to review the procedure in Sections 11 and 12 of ASTM D4318-10 on performing the liquid limit test. In addition, the brass Casagrande cup needs to be calibrated according to ASTM D4318-10.

The goal of the sample preparation procedure is to remove any particle greater than 0.0167 inches (425 µm) and bring the clay sample close to the liquid limit or the desired water content. To accomplish this, follow these steps:

1) The as-received soil needs to be soaked in distilled or site specific water for at least two days.

2) After soaked, it needs to be pushed or washed using distilled water or site specific water through a No. 40 sieve.

3) At this point, if the soil is wetter than the liquid limit or the desired water content it has to be air-dried to reduce the water content. If the soil is dryer than the desired water content, distilled or site-specific waster has to be added until the water content is close to the required water content. When adding water, mix thoroughly to remove all clumps as shown in Figure B.3.

Figure B.3 Preparing the soil sample.

4) If the desired water content is the equal to the liquid limit, go to Step 5. If a different water content is desired, go to Step 6.

5) Place a portion of the soil sample in a Casagrande cup and perform the liquid limit test in accordance with ASTM D4318. If, 23 blows to 25 blows are required to close the gap cut in the soil, then the water content of the soil is acceptable. If more than 25 blows are required to close the gap cut in the soil, add more water and repeat Step 5. If less than 23 blows are required to close the gap, the soil sample needs to continue air-drying and Step 5 needs to be repeated.

6) Take a water content measurement. If the soil is wetter than the desired water content, air-dry the soil until it achieves the desired water content. A good way to do this is to calculate how much the total weight of the soil should be, based on the initial weight and water content of the soil, to get the desired water content. If the soil is drier than the desired water content, add distilled or site-specific water until the soil is at the desired water content. A good way to do this is to calculate how much water is needed, based on the initial weight and water content of the soil, to get the desired water content.

B.4. Test Assembly

The test assembly has two major steps: assembly of the shear box and setup of equipment and software. However, before these steps can be completed, there are minor steps that need to be performed. These minors and major steps are described in this section.

B.4.1 Zeroing the Vertical DCDT

The DCDT must be zeroed before beginning the test assembly to be able to obtain an accurate measurement of the height of the test specimen. Before zeroing, ensure that the DCDT is approximately at the center of its travel.

1) Assemble the two halves of the shear box.
2) Place a saturated porous stone and a wet filter paper in the bottom of the test specimen container.
3) Place a one-inch-high aluminum cylinder inside the test specimen container. The aluminum cylinder should comply with the requirements of ASTM D3080-11.
4) Place a wet filter paper on top of a porous stone.
5) Place the porous stone on top of the aluminum cylinder, with the filter paper facing down, followed by the top platen assembly (consisting of load platen and ball bearing assembly).
6) Manually lower the vertical load cell until it is just barely in contact with the top platen assembly (*Tools → Manual Mode → Vertical Axis*). After that, use the load control with a load of one pound to two pounds to close the final gap.
7) Zero the vertical DCDT (*Setup → Sensors →* [select desired DCDT] *→ Test → Take Zero → Ok*).
8) If the machine deflection is not going to be measured, close any dialog box that is still open, raise the load cell (*Tools → Manual Mode → Vertical Axis*), and disassemble the shear box. If the machine deflection is going to be measured, leave the equipment as it is and go to Sections B.4.2 and B.4.3.

A reference value has now been set for the vertical DCDT, in which a reading of zero will correspond to a specimen height of one inch. Once the test specimen has been prepared, its initial height can be determined from this reference value. To determine the actual height of the test specimen subtract from one inch the reading of the DCDT when the load cell is in contact with the top platen assembly. If the reading of the DCDT is less than zero, it means that the actual height of the test specimen is greater than one inch.

B.4.2 Create the Loading Schedule

A loading schedule has to be created to apply the final stress in increments to avoid extrusion of the soil sample during the consolidation stage. To setup a loading schedule the subsequent steps should be followed:

1) Open the loading schedule dialog box (*Setup → Loading Schedules → Add).*

2) Enter the schedule name and check the box that says "filter paper used." See Figure B.4 for reference.

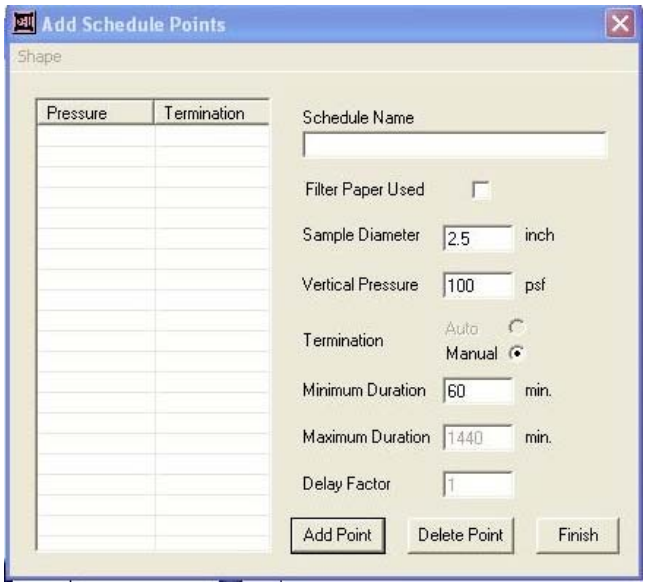

Figure B.4 New loading schedule dialog box.

3) Change the minimum duration to 1440 minutes, make sure the sample diameter is 2.5 inches, and the termination is set to manual.

4) Enter each load increment and press "Add Point" to include this increment in the schedule. It is recommended to use a maximum of 100 psf as the first stress increment to prevent soil extrusion. For test specimens formed at a water content equal to a liquidity index of 1.5 or above, use 50 psf as the first stress increment. Then, a load increment ratio of one (i.e. the load is doubled) is recommended until the desired consolidation stress is obtained. If a load increment different than one is required to achieve the desired final stress, it is recommended to do it as early as possible in the loading schedule. For the last load increment change the minimum duration of 2880 minutes.

B.4.3 Measuring Machine Deflection

When a normal load is applied to the test specimen, the machine will deform as a reaction to the load applied. The deformation of the device to the applied load needs to be measured so it can be subtracted from the measured deflection during consolidation to report only the deformation of the test specimen. The machine deflection has to be measured for every new loading schedule created. To measure the machine deflection, follow the steps below:

1) The machine has to be assembled as is if the LVDT is going to be zeroed (See Section B.4.1)
2) Make sure a gap not greater than 0.1 inches is between the piston and the top platen assembly.
3) Open the machine deflection dialog box (*Tools → Machine Deflection).*
4) Select the loading schedule for which the machine deflection is going to be measured. See Figure B.5 for reference.

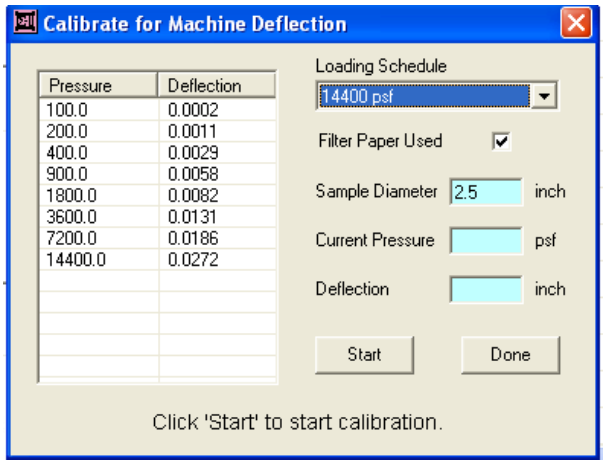

Figure B.5 Machine deflection dialog box.

5) Click “Start” and wait for the software to finish measuring the deflections.
6) Once finished, close any dialog box that is still open, raise the load cell (*Tools → Manual Mode → Vertical Axis*), and disassemble the shear box.

B.4.4 Shear Box Assembly and Test Specimen Formation

The following steps should be followed to assemble the direct shear box and form the test specimen:

1) Weigh and record the weight of one saturated porous stone, a wet filter paper, and the top platen assembly. Separately, record the weight of the top and bottom halves of the shear box with the four screws, a saturated porous stone, and a wet filter paper.

2) Trace the inside circular dimension of the shear box onto two pieces of filter paper and cut to produce two trimmed pieces of filter paper. **The filter paper should not be larger than the perimeter of a porous stone.**

3) Place one piece of wet filter paper on top of a saturated porous stone. Make sure that the filter paper does not hang outside the edges of the porous stone.

4) Place the saturated porous stone inside the bottom half of the shear box with the filter paper facing up.

5) Form the test specimen inside the direct shear box. This can be accomplished using either a spatula or a pastry bag. This manual only illustrates the use of a spatula for the sake of clarity. This process is illustrated in Figure B.6.

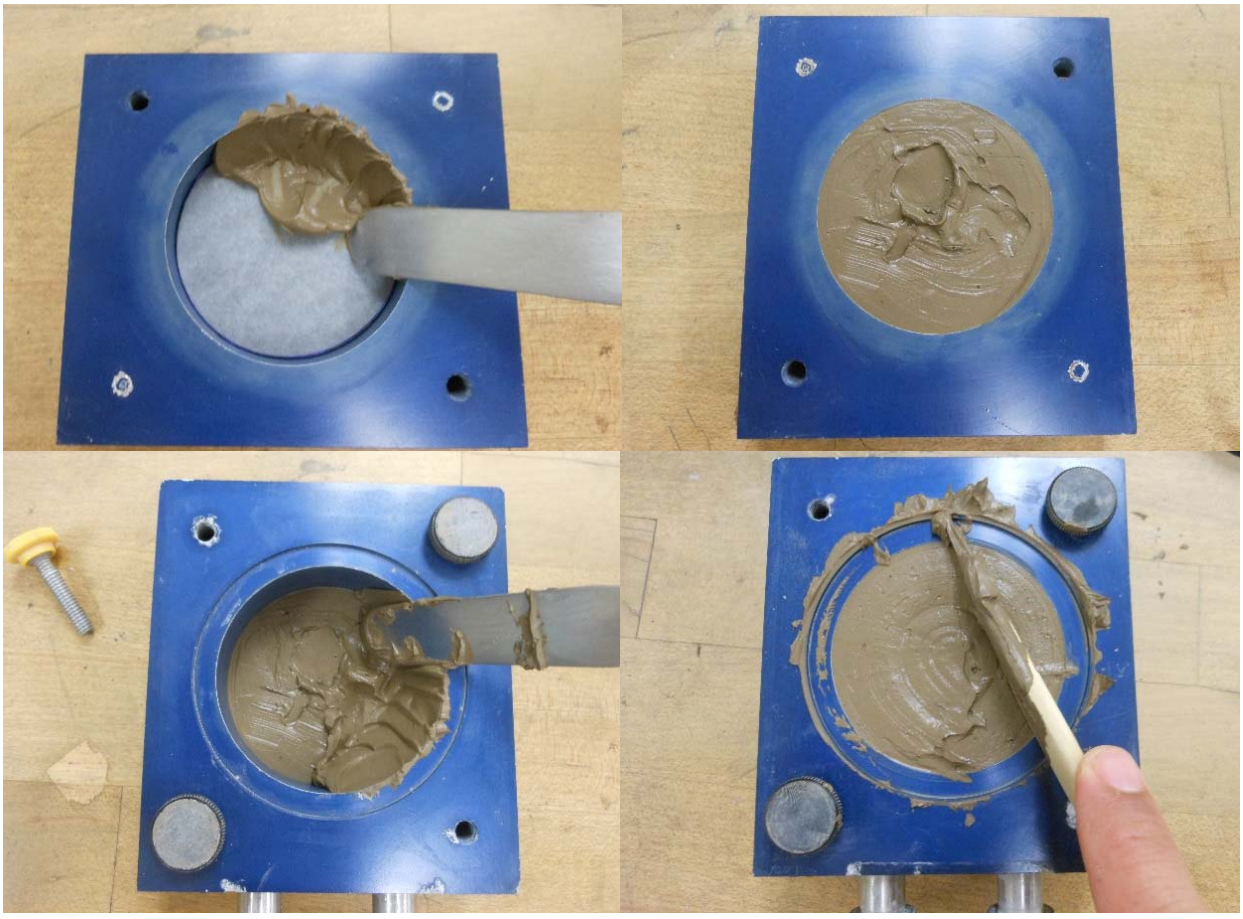

Figure B.6 Forming the test specimen into the shear box.

From top left: (a) Filling the bottom half from the outside inward; (b) bottom half of the shear box cleaned; (c) filling the top half; (d) smoothing the top and cleaning the lip of the shear box.

(a) Start with only the bottom half of the direct shear box with a saturated porous stone and filter paper inside. Using a spatula, place small scoops of the remolded sample into the direct shear box, **beginning at the outside and working inward,** making sure no air bubbles stay in the test specimen. Once the bottom half of the box is full, smooth the surface and clean any excess material from the top face of the lower box.

(b) Attach the top to the bottom of the shear box with the two black plastic-topped thumb screws. The black plastic-topped thumb screws thread into the bottom half of the shear box to hold the halves together.

(c) Fill the top half of the shear box in the same way as the bottom. Again, start at the outside and work inward making sure to remove the air bubbles from the test specimen.

(d) Level the top and clean any excess material from the lip of the shear box.

(e) Snug the yellow plastic-topped thumb screws into contact with the upper face of the bottom half of the shear box. These screws will be used later to create a small gap between the top and bottom halves of the box before shearing.

(f) Weigh the shear box to determine the weight of soil. The direct shear box should look as presented in Figure B.7.

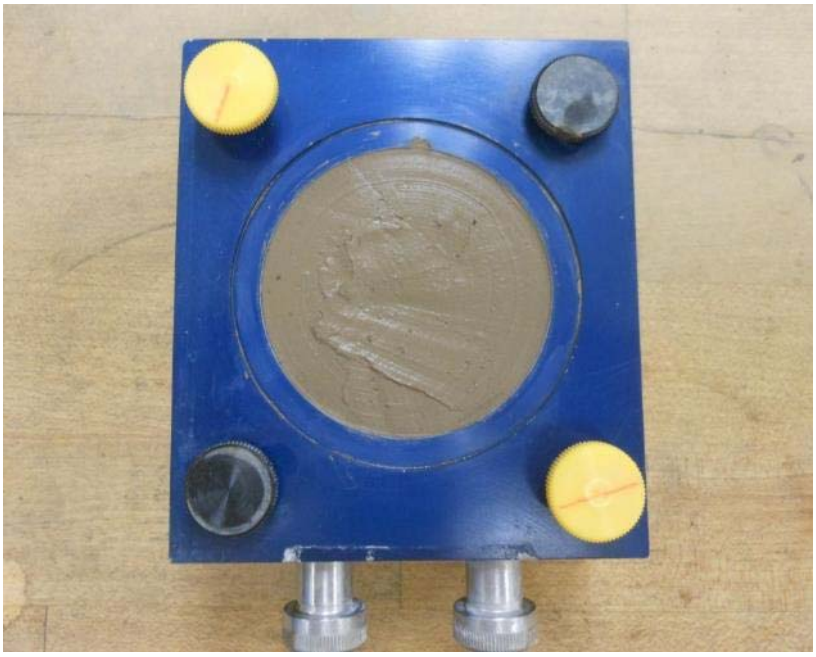

Figure B.7 Prepared soil sample.

6) Moisten a second piece of trimmed filter paper. Center the filter paper on a porous stone. Trim the excess paper that may overhang the porous stone.

7) Place the porous stone and filter paper centered on top of the sample. The filter paper should be between the test specimen and the porous stone.

8) Take a sample of the “trimmings” to determine the water content.

B.4.5 Equipment Setup

The procedure below outlines the equipment setup:

1) Place the assembled shear box with porous stone into the reservoir. Place the load platen, with steel ball, and ball seat adapter, centered on top of the porous stone. To avoid potential interference, assure that the porous stone and load platen are centered precisely over the test specimen.

2) Level the ball seat adapter and manually lower the vertical load cell so that only a small gap (around 0.1 inches) remains between the top of the adapter and the load cell (*Tools → Manual Mode → Vertical Axis*). A displacement rate of 0.1 inches per min is recommended to move down the piston. See Figure B.8 for reference.

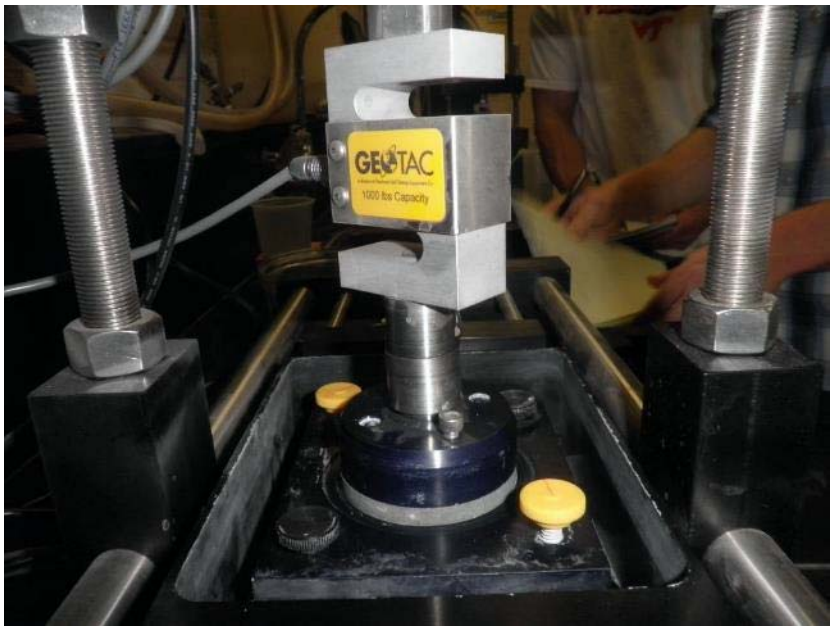

Figure B.8 Small gap between the ball seat adapter and load cell.

3) Prior to placing the specimen in the shear box, the vertical DCDT should have been zeroed with a one-inch-thick aluminum specimen, two porous stones, two filter papers, and the top platen assembly in the direct shear box (see Section B.4.1).

4) **Make sure the two horizontal load cell nuts are loose.** Then, place the horizontal reaction arm on the two reaction arm screws located on the side of the direct shear box. Connect the reaction

arm to the horizontal load frame and finger-tighten the reaction arm nut. Figure B.9 shows the placement of the horizontal reaction arm.

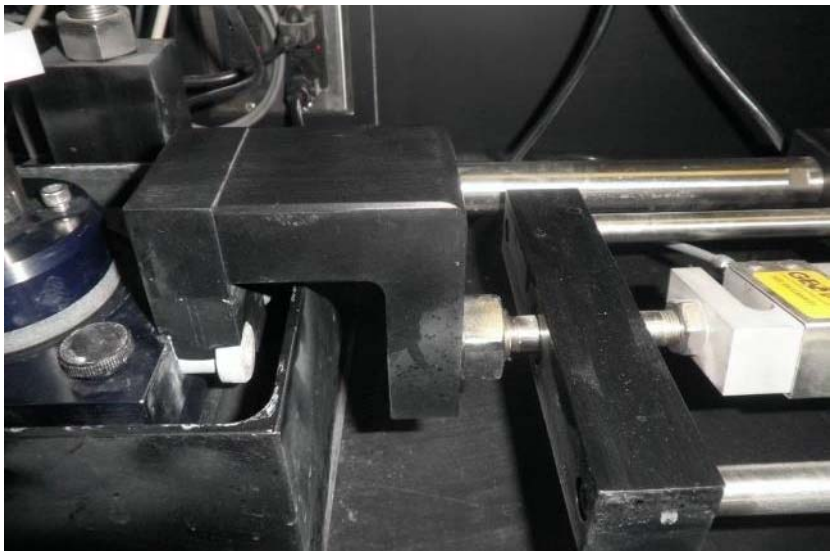

Figure B.9 Placement of the horizontal reaction arm.

B.4.6 Software Setup

This manual uses DigiShear software. The procedure below outlines the software setup:

1) Make sure there is zero load on the load cells (i.e., assure there is a gap between the vertical load cell and the ball seat adapter and that the horizontal load cell nuts are loose).

2) Zero horizontal and vertical load cells (*Setup* → *Sensors* → [select desired load cell] → *Test* → *Take Zero* → *Ok*). See Figure B.10 for reference.

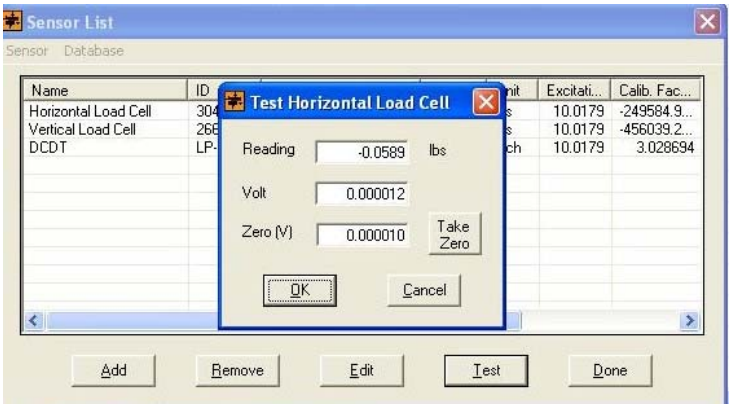

Figure B.10 Zeroing the horizontal and vertical load cell.

3) Input specimen data (*File* → *Specimen Data*). Enter all specimen information and save the file. **Make sure the diameter for the test specimen is set to 2.5 inches.**
4) Input test data (*File* → *Test Data).* In the consolidation section, select a loading schedule, select consolidation as the reading schedule, and select the options to "Maintain Seating Load" and "Constant Vertical Load." See Figure B.11 for reference. Figure B.12 shows the software when it is set up to begin the test.
5) Press "Save" to save the data file.

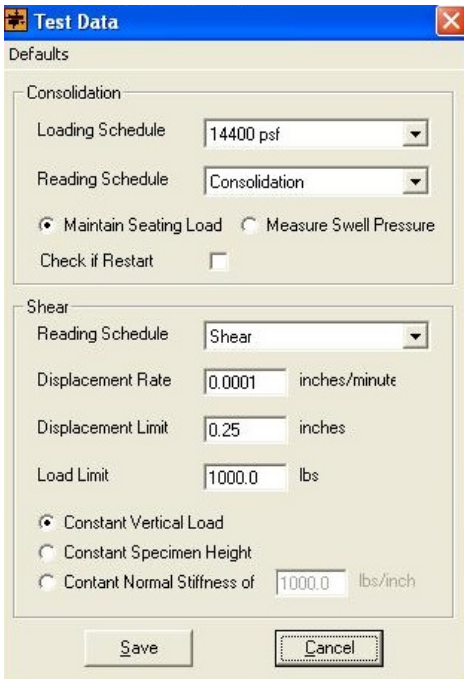

Figure B.11 Entering the consolidation test data in the "Test Data" tab.

B.5. Running the Test

The direct shear test consist of two parts. The first one is the consolidation stage. In this stage, a normal stress is applied to the sample until the end of primary consolidation is reached. After that, the next stress increment is applied and this process is repeated until the final stress is attained. After the test specimen has been consolidated to the last consolidation pressure, the sample is ready to be sheared. During the shearing stage, a gap is created in the middle of the shear box and the sample is sheared by moving the bottom half of the direct shear box while the top half is fixed. The shearing stage has to be performed slow enough to allow the dissipation of the pore pressures generated during shear. The shear stage is continued until a peak is observed in the shear stress vs displacement graph. How to perform the consolidation and shearing stages is described in this section.

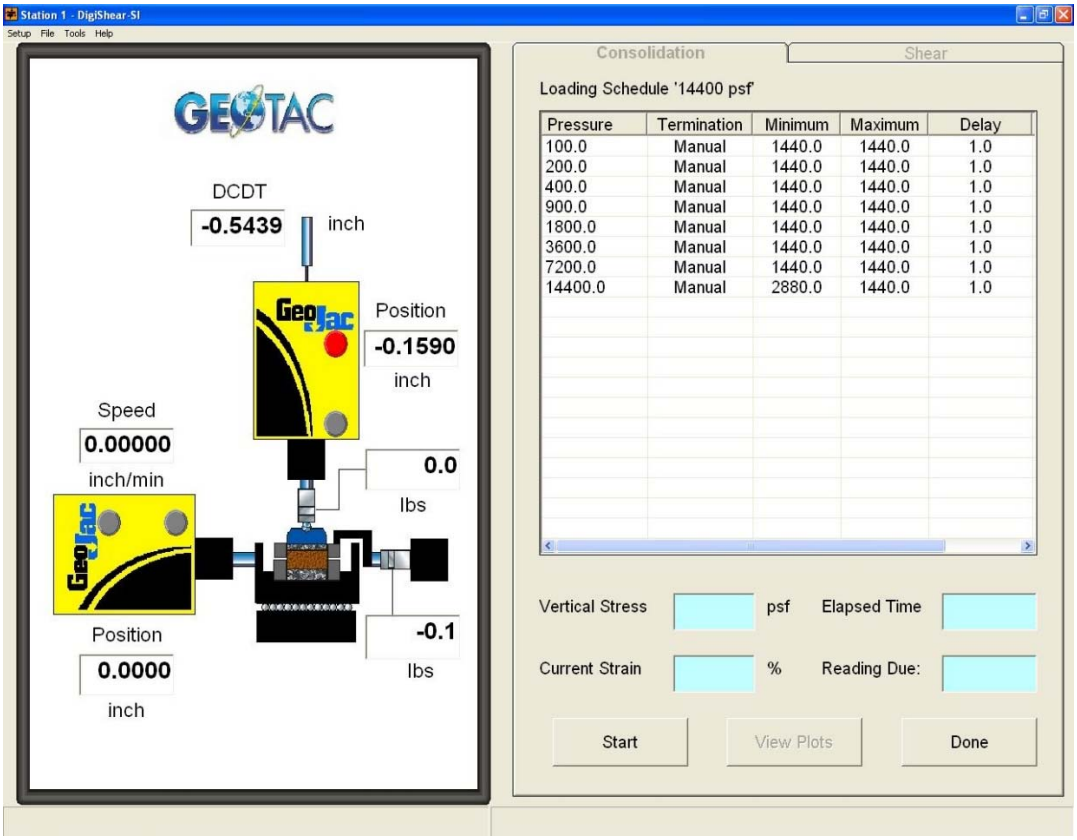

Figure B.12 Setup complete prior to starting consolidation.

B.5.1 Consolidation

The consolidation stage should be performed as follows:

1) Start consolidation (click "Start"). **Immediately fill the reservoir with distilled or site-specific water**. The machine will automatically perform the seating procedure. The consolidation portion of the test will require a few days depending on the loading schedule. Ensure that the water level does not drop below the top of the sample during this time.

2) At the end of the final load step, examine the consolidation curve to make sure the sample has reached the end of primary consolidation (click "View Plots").

3) Before proceeding further, check that the sample height is at least one inch (i.e. the DCDT displacement reads less than or equal to zero). If the test specimen is contained fully within the bottom half of the shear box, it is possible that the porous stone or load platen could be located partially between the bottom and upper shear box halves. **In this case, the sample should not be sheared. Shearing the "test specimen" may, in actuality, attempt to shear the porous stone or load platen, which could lead to significant damage of the test apparatus!**

4) If the test specimen height is adequate, calculate t_{50} from the final consolidation curve.

5) Estimate the minimum time to failure as $t_f = 50 \times t_{50}$ (see discussion in Appendix B.III: Why do we use $50t_{50}$? for the reasons that this value is used).

6) Estimate the displacement at failure, d_f. A value of 0.1 inches can be assumed.

7) Determine the displacement rate in inches/minute to use during shear by $d_r = \frac{d_f}{t_f}$

8) Click "Done" in DigiShear and "Yes" on the End Consolidation window.

B.5.2 Shear

The shearing stage should be performed as follows:

1) Remove the two black plastic-topped thumb screws completely from shear box.

2) Create a small gap between the two halves of the shear box by tightening the two yellow plastic-topped thumb screws (turn clockwise). Both screws should be tightened simultaneously. A ¼ turn of the screws corresponds to 0.0125 inches gap between the two shear box halves. ASTM D3080-11 recommends a minimum gap of 0.025 inches (0.5 rotation of screws). U.S. Army Corps of Engineers (USACE) Engineering Manual (EM) 1110-2-1906 "Laboratory Soils Testing" recommends a gap of 0.0625 inches (1.25 rotations of screws). This manual recommends the USACE gap suggestion.

3) Allow the sample to sit for a few minutes as shear stresses develop between shear box walls and the test specimen. Remove the two yellow plastic-topped thumb screws completely. Shear stress should maintain the gap between the two shear box halves.

4) Ensure there is contact between all elements of horizontal loading frame and load sensors so that no gaps are present in the assembly. For this purpose, finger-tighten the horizontal load cell nuts until in contact with the horizontal load frame. **Make sure that no excessive load is measured by the horizontal load cell in DigiShear.** Adjust the nuts until the measured horizontal load is nearly zero. One of the nuts will increase the load while the other will reduce it.

5) Ensure that the LVDT does not display a value greater than zero (See Section B.5.1 Step 3).

6) In DigiShear, enter the previously determined displacement rate, maximum displacement value, and maximum load value. The recommended value for maximum displacement is 0.4 inches. The maximum load allowed by the program should be the maximum load that the horizontal load cell can withstand.

7) Start shear (click "Start").

B.6. Disassembly

Follow these steps to disassemble the direct shear test.

1) Before ending the test, be sure the peak shear force or maximum displacement has been reached (Click “View Plots”).

2) If the test specimen is done shearing, click “Pause” then click “Done” in DigiShear.

3) Use a drainage line to drain water from the reservoir.

4) Raise the vertical load cell to remove the load on the sample (*Tools* → *Manual Mode* → *Vertical Axis*). Move the piston “up” for this purpose.

5) Loosen the horizontal load cell and reaction arm nuts. Remove the horizontal reaction arm, load platen, ball seat adaptor, and the ball bearing.

6) Return the horizontal axis to the home position (*Tools* → *Manual Mode* → *Horizontal Axis* → Return Home → Start).

7) Remove the shear box assembly from the reservoir.

8) Per ASTM D3080-11, separate the top and bottom shear box by sliding the two in opposite directions, being sure not to pull apart the shear box halves perpendicular. Photograph the failure surface. The Army Corps of Engineers Manual (EM 1110-2-1906) does not require this removal procedure.

9) Extract a one inch square from the center of the top and bottom halves of the test specimen. Weigh and record the sample wet weight. Place the sheared sample in the drying oven and determine its water content according to ASTM D2216-10.

10) Clean and dry the reservoir, direct shear box, top platen apparatus, and reaction arm.

11) Put the porous stones in the ultrasonic cleaner for about 10 minutes.

Appendix B.I: Reduction of Data

Data reduction is needed in order to convert the output file from the DigiShear Software to engineering units. The following steps demonstrate this process:

1) Import the file data to Microsoft Excel® (or other similar spreadsheet software). To import the data in Excel follow these steps:

    a. Click on the “Data” tab.

    b. In the section of “External Data”, click the button labeled “From Text”.

    c. Choose the dialog box to show all files.

    d. Locate your file and click “Open”.

Once your file is imported in Excel, your screen will look as Figure B.I.1.

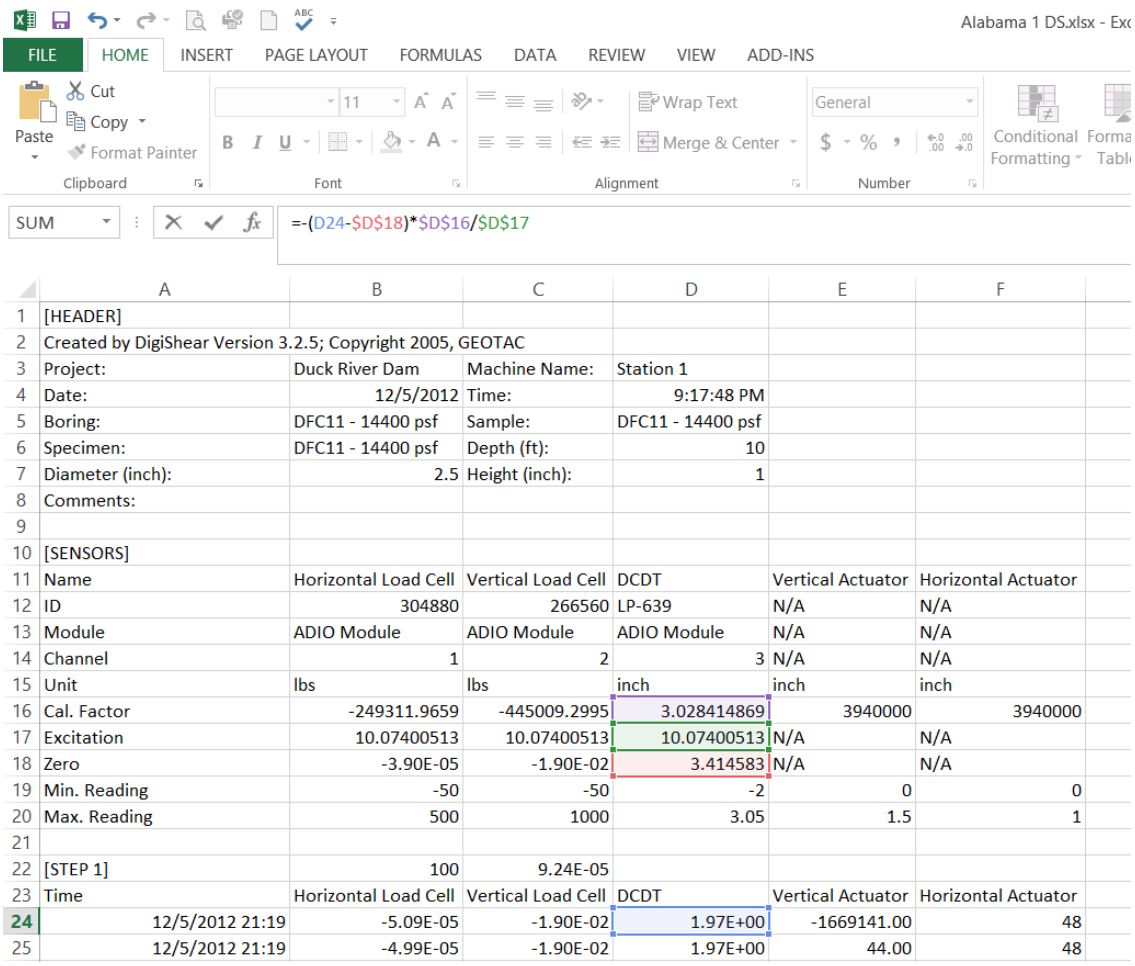

	A	B	C	D	E	F
1	[HEADER]					
2	Created by DigiShear Version 3.2.5; Copyright 2005, GEOTAC					
3	Project:	Duck River Dam	Machine Name:	Station 1		
4	Date:	12/5/2012	Time:	9:17:48 PM		
5	Boring:	DFC11 - 14400 psf	Sample:	DFC11 - 14400 psf		
6	Specimen:	DFC11 - 14400 psf	Depth (ft):	10		
7	Diameter (inch):	2.5	Height (inch):	1		
8	Comments:					
9						
10	[SENSORS]					
11	Name	Horizontal Load Cell	Vertical Load Cell	DCDT	Vertical Actuator	Horizontal Actuator
12	ID	304880	266560	LP-639	N/A	N/A
13	Module	ADIO Module	ADIO Module	ADIO Module	N/A	N/A
14	Channel	1	2	3	N/A	N/A
15	Unit	lbs	lbs	inch	inch	inch
16	Cal. Factor	-249311.9659	-445009.2995	3.028414869	3940000	3940000
17	Excitation	10.07400513	10.07400513	10.07400513	N/A	N/A
18	Zero	-3.90E-05	-1.90E-02	3.414583	N/A	N/A
19	Min. Reading	-50	-50	-2	0	0
20	Max. Reading	500	1000	3.05	1.5	1
21						
22	[STEP 1]	100	9.24E-05			
23	Time	Horizontal Load Cell	Vertical Load Cell	DCDT	Vertical Actuator	Horizontal Actuator
24	12/5/2012 21:19	-5.09E-05	-1.90E-02	1.97E+00	-1669141.00	48
25	12/5/2012 21:19	-4.99E-05	-1.90E-02	1.97E+00	44.00	48

Figure B.I.1 Screenshot of imported direct shear data file.

2) In order to convert the data to engineering units, use the following formula:

$P = CF\ [(V_s - V_0)/V_e]$

Where:

P	=	Magnitude of physical input.
CF	=	Calibration factor.
V_s	=	Sensor signal or output voltage (volts).
V_0	=	Zero reading.
V_e	=	Sensor excitation voltage (volts).

The values of CF, V_0 , and V_e for each sensor are listed under the heading [SENSORS] (Figure B.I.1). The values of V_s are also provided with respect to time for each sensor. For example, in Row 24 of Figure B.I.1, the displacement of the LVDT can be calculated using the formula:

$$\text{Displacement (inches)} = 3.028414869\left\{\frac{[(1.97) - (3.414583)]}{10.0740051269531}\right\} = -0.4346$$

In the calculation presented above, the negative sign in the displacement just means direction. In this case it means that the LVDT move down. It should be noted that the value for the zero reading might be taken differently depending on the parameter needed.

3) To convert the counts of the horizontal and vertical actuators to engineering units, apply the equation below:

$$P = \frac{V_S}{CF}$$

4) Calculate the total vertical force on the specimen during shear:

$$W_{Total} = L + W_{Porous\ Stone} + W_{Load\ Platen} + W_{Ball\ Bearing} + W_{Ball\ Seat\ Adaptor} + W_{DS\ Box}$$

Where:

W_{Total}	=	Total normal weight on the sample.
L	=	Force of the vertical load frame.
$W_{Porous\ Stone}$	=	Weight of the porous stone.

$W_{Load\ Platen}$ = Weight of the load platen.
$W_{Ball\ Bearing}$ = Weight of the ball bearing.
$W_{BB\ Adaptor}$ = Weight of ball seat adaptor.
$W_{DS\ Box}$ = Weight of top half of the direct shear box.

For additional guidance in calculating parameters such as shear stress and normal stress from this data, please refer to Section 10 of ASTM D3080-11.

Appendix B.II: Data Sheet

Direct Shear Test

Virginia Polytechnic Institute
W. C. English Geotechnical Research Laboratory

Project		Date	
Boring		Sample No.	
Visual Description			
Data File		Depth	

Constant Stress Increment ❑		Swell Pressure Measurement ❑	
Final Consolidation Stress, tsf		Backpressure, psi	

Apparatus No.		Height of specimen		Diameter of ring	
Weight of ring		Specific Gravity, G_s		Area of specimen, in^2	
Weight of plate		Measured ❑ Assumed ❑		Station No.	

	Before Test		After Test
	Specimen	Trimmings	Specimen
Tare No.			
Tare + Wet Soil, g			
Tare + Dry Soil, g			
Water, g			
Tare, g			
Dry Soil, g			
Water Content, w%			

Initial Void Ratio, e_0		Final Void Ratio, e_f	
Initial Degree of Saturation, S_i		Final Degree of Saturation, S_f	
Initial Dry Unit Weight, γ_{di}		Final Dry Unit Weight, γ_{df}	

Remarks: _____

Appendix B.III: Why do we use $50t_{50}$?

Direct shear tests are intended to measure drained strength parameters. However, it is very difficult to obtain fully drained conditions for soils (especially clays) in laboratory tests, and some excess pore water pressure remains even during drained testing conditions. Consequently, soils must be sheared at a rate slow enough to closely approximate fully drained conditions on the failure plane.

Gibson and Henkel (1954) considered that pore pressures which develop along the failure plane during shear dissipate in accordance with Terzaghi's theory of one-dimensional consolidation. The degree of excess pore pressures can then be expressed in terms of the degree of consolidation, *U*. The degree of consolidation at failure is expressed as:

$$U_f = 1 - \frac{\bar{u}_f}{\bar{u}_0}$$

Where $\bar{u}_f$ is the excess pore pressure at failure, and $\bar{u}_o$ is the pore water pressure that would have existed in the absence of drainage. If the test were truly drained, $\bar{u}_f$ would equal zero, and U_f would equal one. Therefore, the above equation indicates the efficiency of the drained laboratory test and shows how closely laboratory shear approximates fully drained conditions.

Gibson and Henkel then derived an equation for the direct shear test based on the consolidation equation. The following assumptions were made by Gibson and Henkel to derive this equation:

1. The pore water pressure that is present at any point in the specimen depends only upon the magnitude of the changes in principal stress and is not affected by the rotation of the planes.

2. The entire thickness of the sample is assumed to participate in the homogeneous simple shear, since the ratio of the thickness of the failure zone to the sample is unknown.

3. The failure zone is subjected to a uniformly distributed shear stress.

Direct shear tests are conducted at a constant rate of displacement. In order to determine the proper rate of displacement to allow drained conditions, an estimate must be made of the time to failure which will allow for sufficient dissipation of the pore water pressures in the soil. Using the above assumptions, Gibson and Henkel derived the following equation:

$$t_f = \frac{H^2}{2c_v(1 - U_f)}$$

Where *H* is the length of the drainage path, or half of the specimen height, and c_v is Terzaghi's coefficient of consolidation, defined as

$$c_v = \frac{T_v H^2}{t}$$

Where T_v is a time factor and t is equal to time.

Combining these equations gives

$$t_f = \frac{H^2}{2\left(\frac{T_v H^2}{t}\right)\left(1 - U_f\right)} = \frac{1}{2T_v\left(1 - U_f\right)} \cdot t$$

Tests by Gibson and Henkel demonstrated that a degree of consolidation of 95% permits sufficient drainage to approximate drained behavior. Therefore, slower rates of shear permitting additional dissipation of excess pore pressures will not result in any increase in strength. Substituting the value of 0.95 for U_f,

$$t_f = \frac{1}{2T_v(1 - 0.95)} \cdot t = \frac{1}{0.10T_v} \cdot t$$

In this equation, t represents any time in the consolidation process, and T_v is the corresponding time factor. Engineers in the U.S. have traditionally used t_{50}, or the time for 50% consolidation, which can be determined using Casagrande's method. Using the corresponding time factor of 0.197,

$$t_f = \frac{1}{0.10 \cdot 0.197} \cdot t_{50} \approx 50t_{50}$$

If the consolidation curve is plotted using Taylor's method, t_{90} may be used (T_v=0.848)

$$t_f = \frac{1}{0.10 \cdot 0.848} \cdot t_{90} \approx 12t_{90}$$

References:

Gibson, R. E., and Henkel, D. J. (1954). "Influence of duration of tests at constant rate of strain on measured 'drained' strength." Géotechnique, 4(1), 6-15.

Appendix C

Direct Shear Tests Results

Table of Contents

C.1. Alabama 1

C.1.1 Non-blenderized

Virginia Polytechnic Institute and State University
Geotechnical Engineering Laboratory
Direct Shear Data Sheet

Project:	Fully Softened Shear Strength
Sample I.D./Loc.:	Alabama 1 - Non-blenderized
Classification:	Lean clay (CL)

Sample Preparation	Remolded at LL		Specific Gravity	2.73

Test Number	1	2	3	4	5	6	7	8
Start Date (m/d/y)	12/15/2012	12/5/2012	12/5/2012	12/15/2012	12/5/2012			
End Date (m/d/y)	12/17/2012	12/8/2012	12/8/2012	12/17/2012	12/8/2012			
Consolidation Pressure (psf)	2176	3616	7216	10096	14416			
Initial Values								
Initial Height (in)	1.41	1.42	1.40	1.44	1.41			
Initial Diameter (in)	2.50	2.50	2.50	2.50	2.50			
Initial Sample Weight (g)	206	208	207	204	210			
Water Content (%)	42.06	41.62	41.71	42.28	42.03			
Dry Unit Weight (pcf)	79.7	80.4	80.9	77.4	81.4			
Wet Unit Weight (pcf)	113.3	113.8	114.6	110.2	115.7			
Consolidation Pressures								
Load 1 (psf)	116	116	116	116	116			
Load 2 (psf)	266	216	216	331	216			
Load 3 (psf)	556	416	416	646	416			
Load 4 (psf)	1096	916	916	1276	916			
Load 5 (psf)	2176	1816	1816	2536	1816			
Load 6 (psf)		3616	3616	5056	3616			
Load 7 (psf)			7216	10096	7216			
Load 8 (psf)					14416			
t_{50}								
Max. t_{50} for Load 1 (min)								
Max. t_{50} for Load 2 (min)								
Max. t_{50} for Load 3 (min)								
Max. t_{50} for Load 4 (min)								
Max. t_{50} for Load 5 (min)	1.45							
Max. t_{50} for Load 6 (min)		1.32						
Max. t_{50} for Load 7 (min)			0.88	0.79				
Max. t_{50} for Load 8 (min)					0.96			
Final Values								
Water Content (%)	28.88	27.23	24.30	22.88	22.29			
Dry Unit Weight (pcf)	98.0	101.1	105.8	106.2	110.2			
Wet Unit Weight (pcf)	126.3	128.6	131.5	130.4	134.8			
Failure								
Test Performed at Shear Rate (in/min)	5.00E-05	5.00E-05	5.00E-05	5.00E-05	5.00E-05			
Required Shear Rate (in/min)	2.24E-03	2.73E-03	4.21E-03	4.84E-03	3.80E-03			
Displacement at Failure (in)	0.16	0.18	0.19	0.19	0.18			
Peak Shear Stress (psf)	1327	2072	3737	5604	6656			
Total Change in Height at Failure (in)	0.26	0.29	0.33	0.39	0.37			
Secant Effective Friction Angle (deg)	31.4	29.8	27.4	29.0	24.8			

Comments:

Alabama 1 - Non-blenderized - 2176 psf

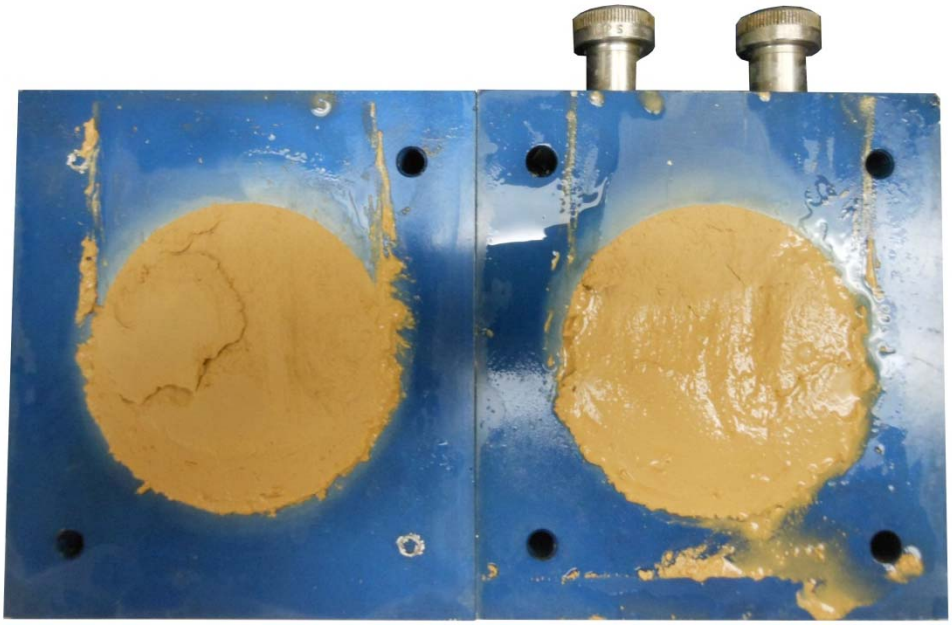

Alabama 1 - Non-blenderized - 3616 psf

Alabama 1 - Non-blenderized - 7216 psf

Alabama 1 - Non-blenderized - 10096 psf

Alabama 1 - Non-blenderized - 14416 psf

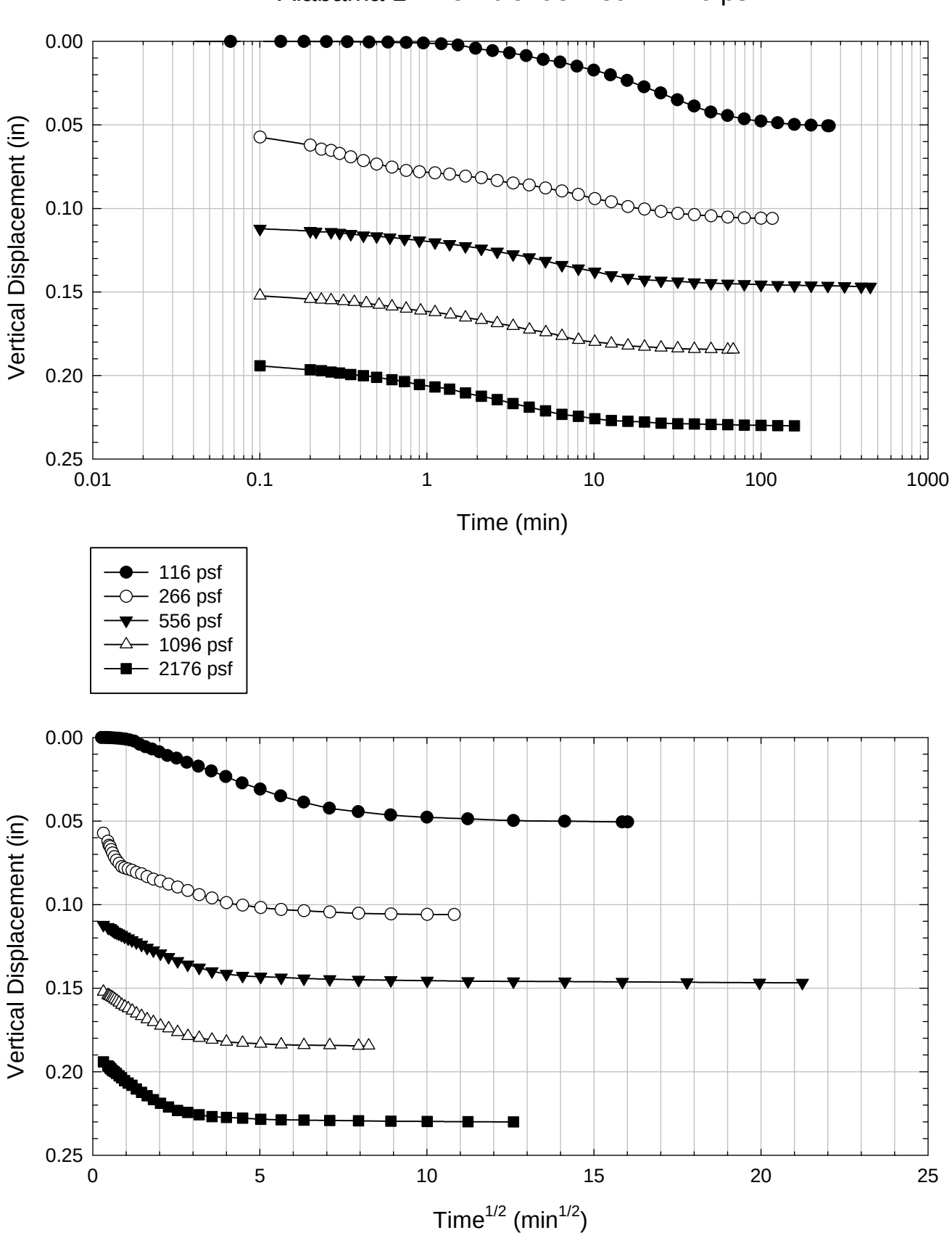
Alabama 1 - Non-blenderized - 2176 psf
Vertical Displacement (in)
0.00
0.05
0.10
0.15
0.20
0.25
0.01
0.1
1
10
100
1000
Time (min)
116 psf
266 psf
556 psf
1096 psf
2176 psf
Vertical Displacement (in)
0.00
0.05
0.10
0.15
0.20
0.25
0
5
10
15
20
25
Time1/2 (min1/2)

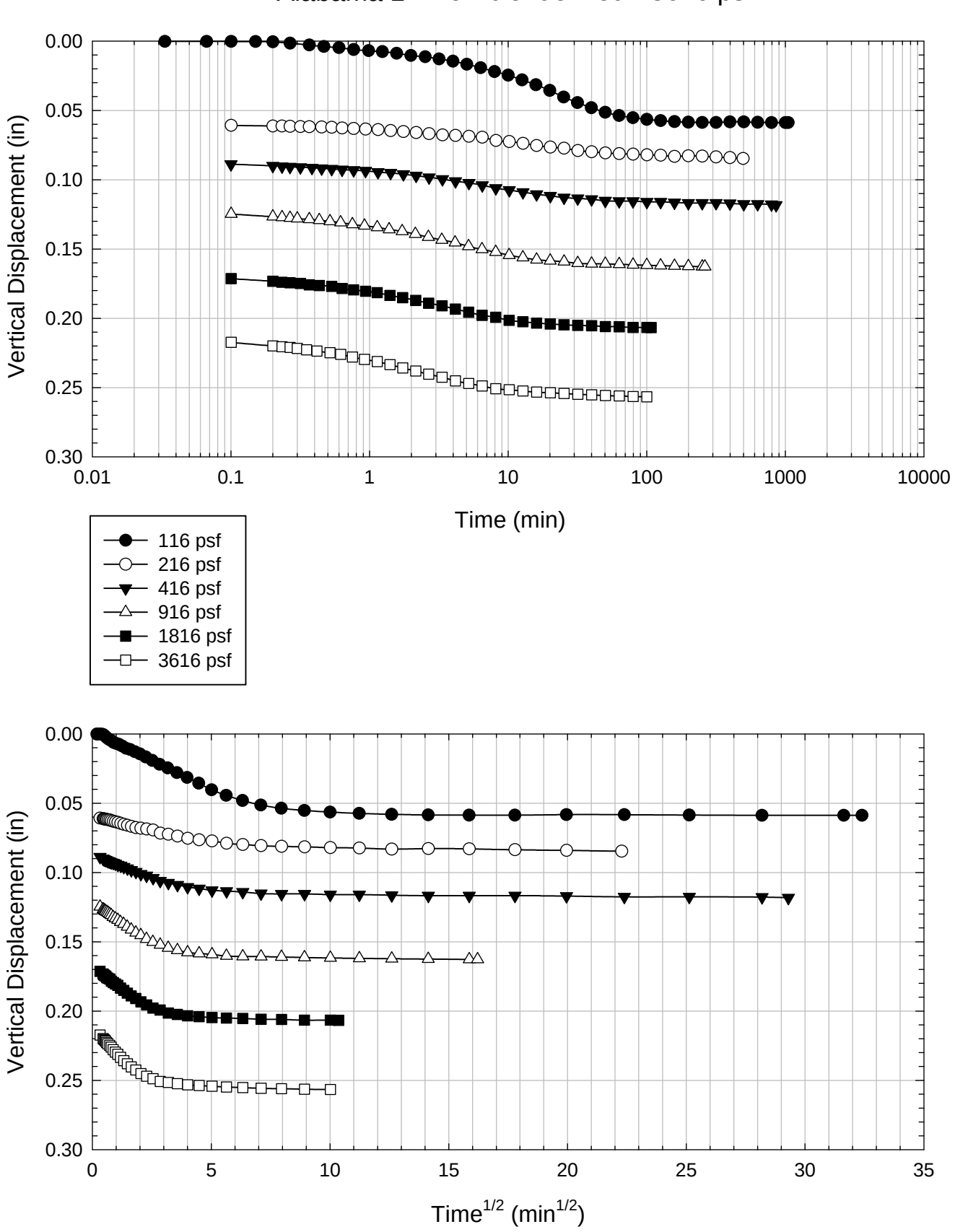
Alabama 1 - Non-blenderized - 3616 psf
Vertical Displacement (in)
0.00
0.05
0.10
0.15
0.20
0.25
0.30
0.01
0.1
1
10
100
1000
10000
Time (min)
116 psf
216 psf
416 psf
916 psf
1816 psf
3616 psf
Vertical Displacement (in)
0.00
0.05
0.10
0.15
0.20
0.25
0.30
0
5
10
15
20
25
30
35
Time^1/2 (min^1/2)

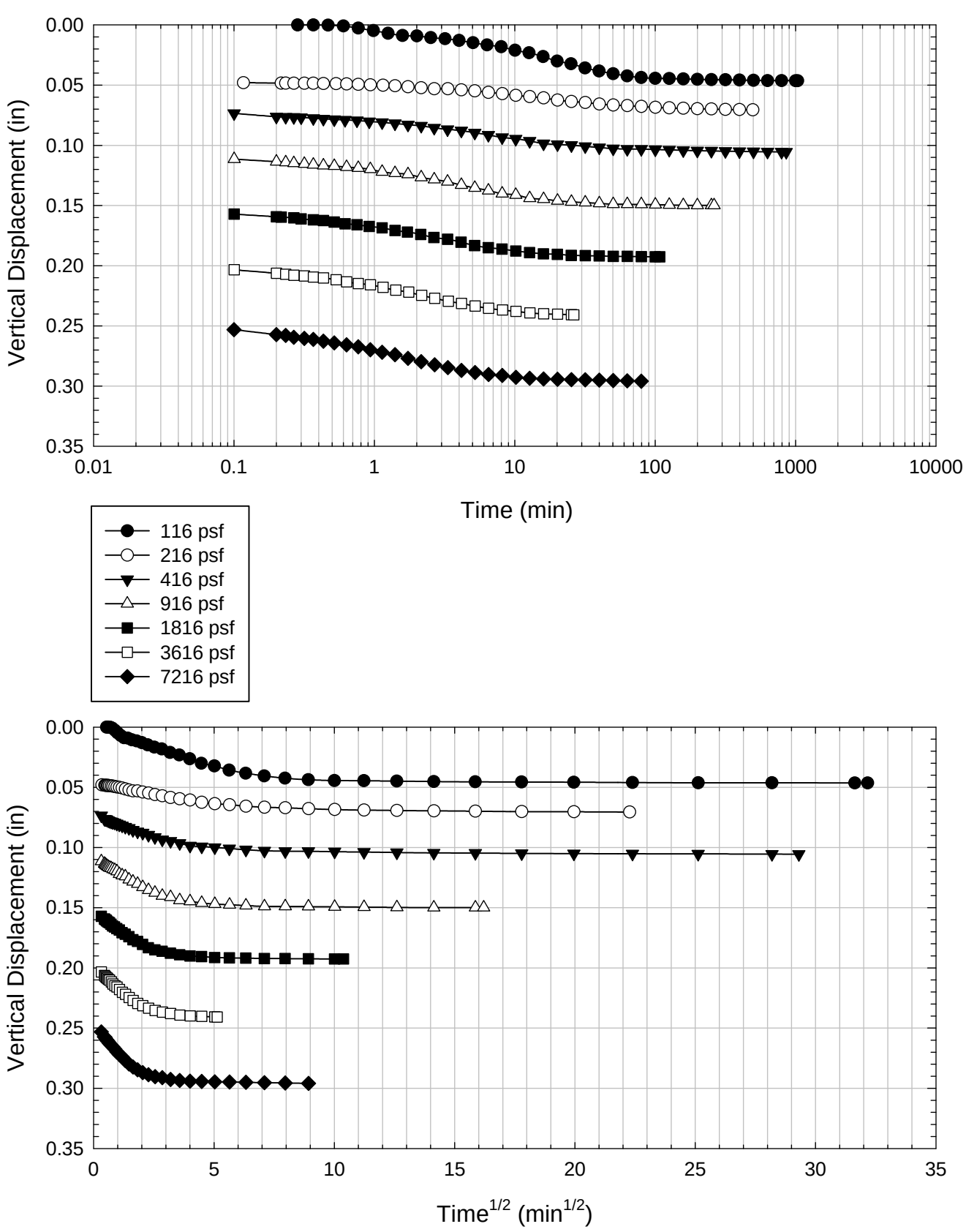
Alabama 1 - Non-blenderized - 7216 psf
Vertical Displacement (in)
0.00
0.05
0.10
0.15
0.20
0.25
0.30
0.35
0.01
0.1
1
10
100
1000
10000
Time (min)
116 psf
216 psf
416 psf
916 psf
1816 psf
3616 psf
7216 psf
Vertical Displacement (in)
0
5
10
15
20
25
30
35
Time1/2 (min1/2)

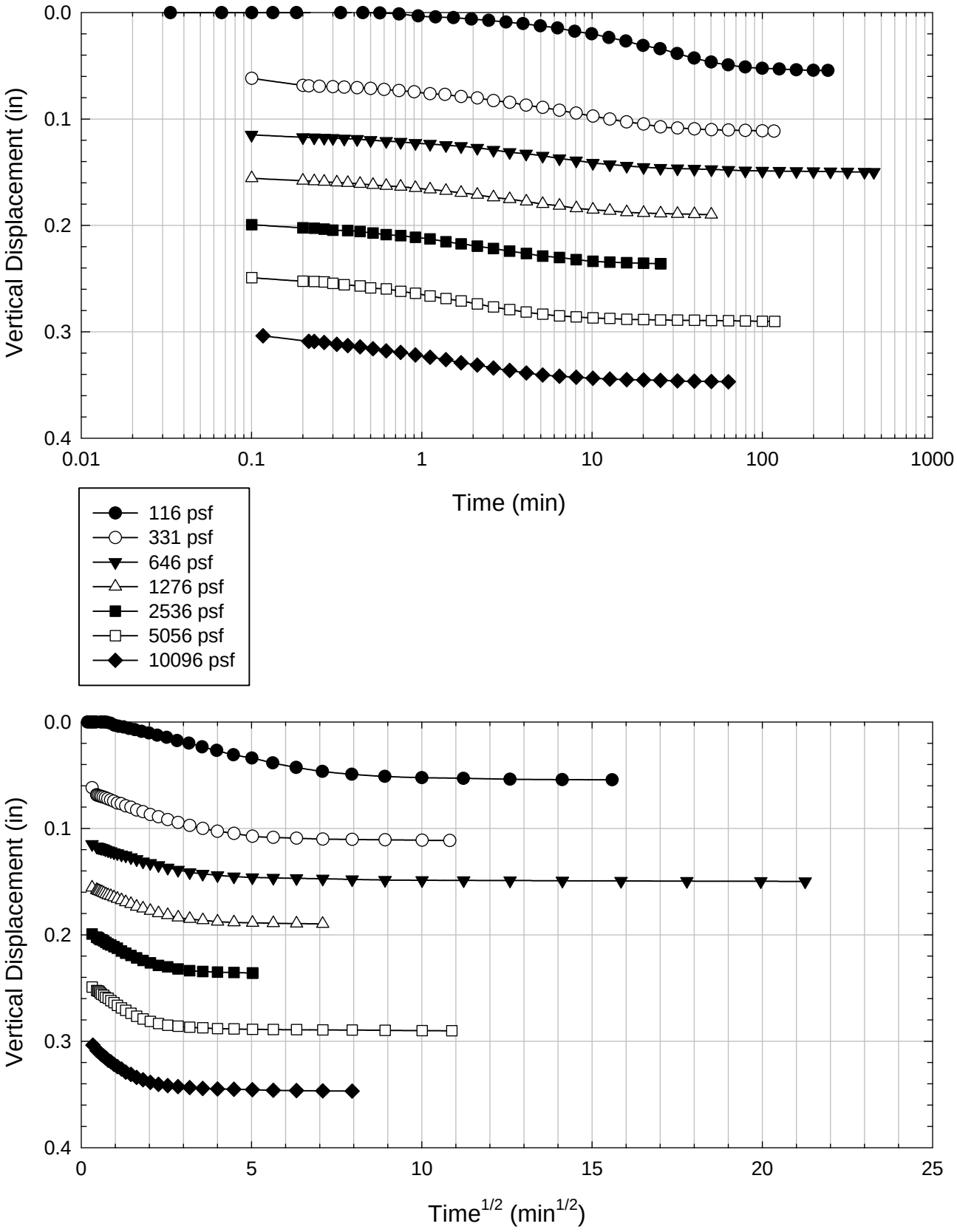
Alabama 1 - Non-blenderized - 10096 psf
Vertical Displacement (in)
0.0
0.1
0.2
0.3
0.4
0.01
0.1
1
10
100
1000
Time (min)
116 psf
331 psf
646 psf
1276 psf
2536 psf
5056 psf
10096 psf
Vertical Displacement (in)
0.0
0.1
0.2
0.3
0.4
0
5
10
15
20
25
Time^1/2 (min^1/2)

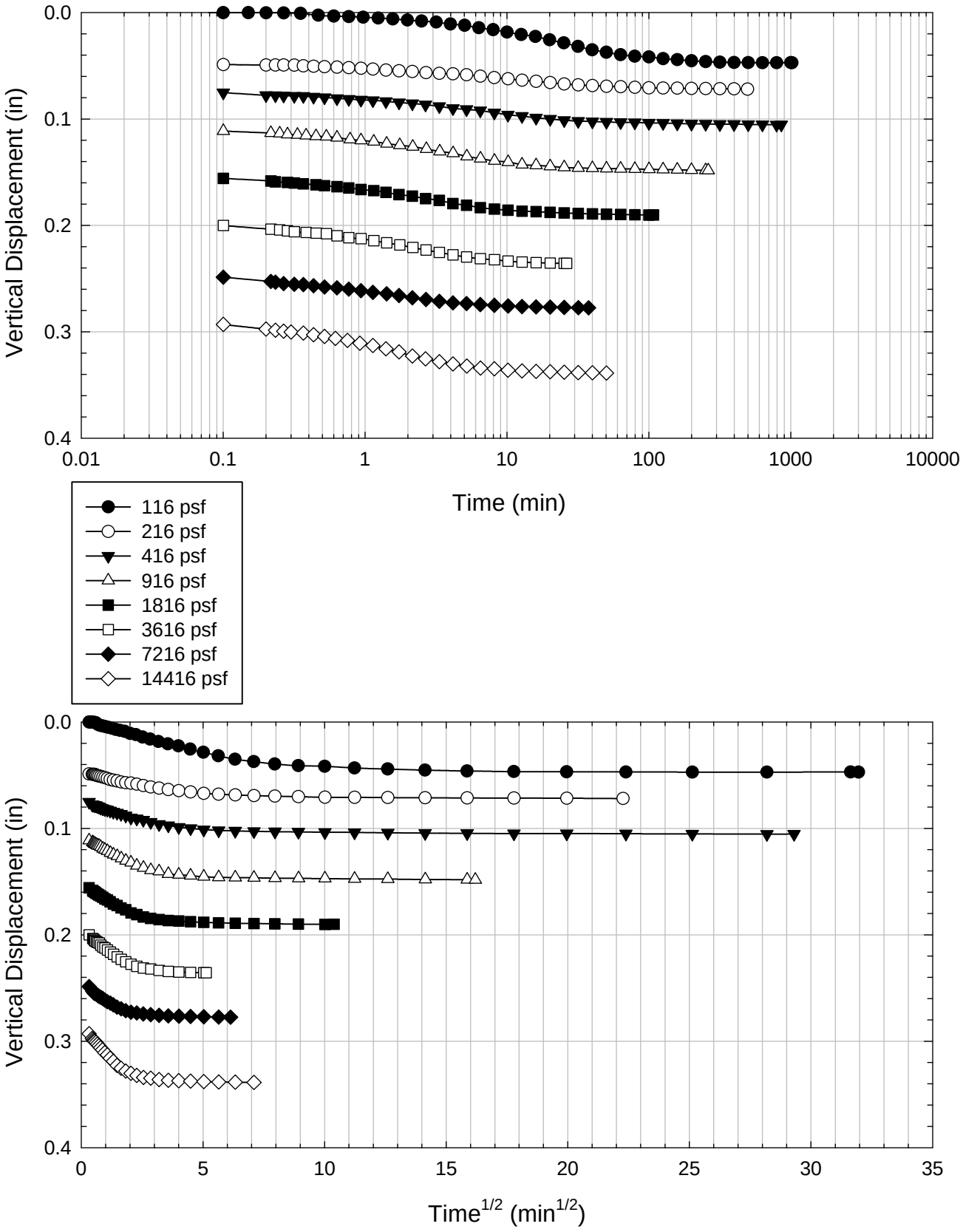
Alabama 1 - Non-blenderized - 14416 psf
Vertical Displacement (in)
0.0
0.1
0.2
0.3
0.4
0.01
0.1
1
10
100
1000
10000
Time (min)
116 psf
216 psf
416 psf
916 psf
1816 psf
3616 psf
7216 psf
14416 psf
Vertical Displacement (in)
0.0
0.1
0.2
0.3
0.4
0
5
10
15
20
25
30
35
Time^1/2 (min^1/2)

Alabama 1 - Non-blenderized

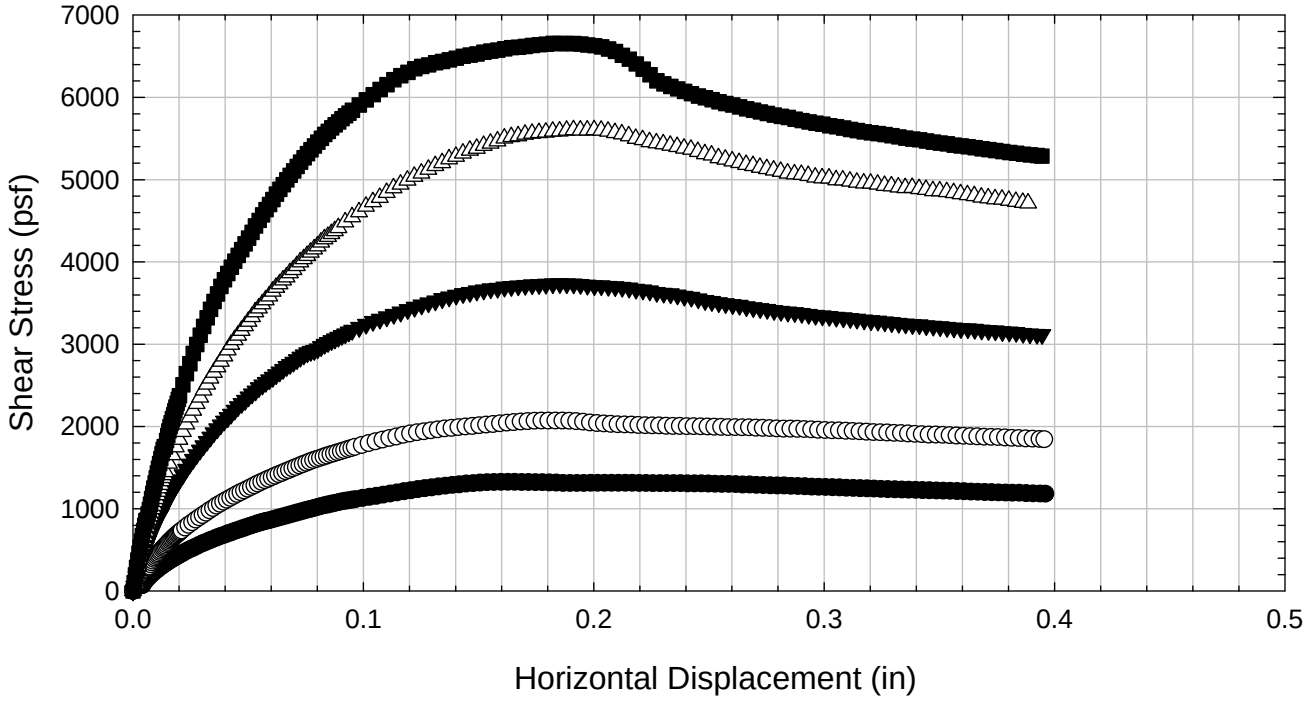

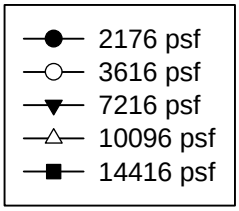

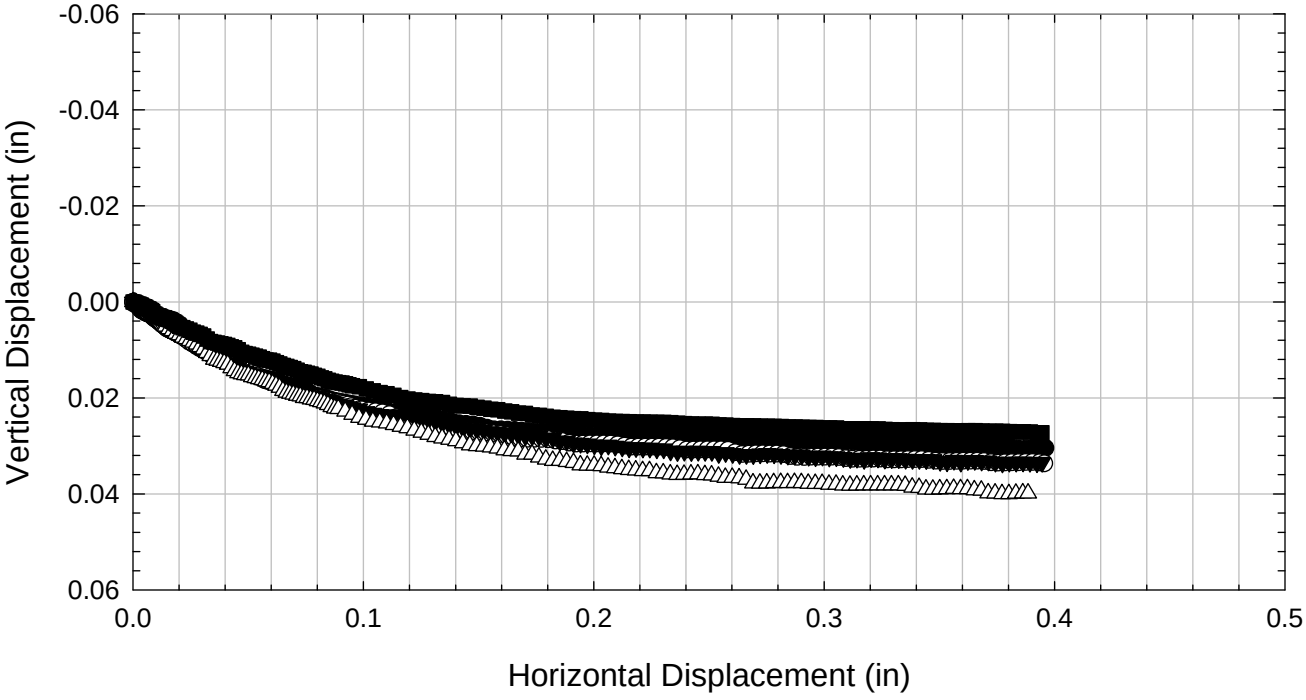

C.2. Alabama 2

C.2.1 Non-blenderized

Virginia Polytechnic Institute and State University
Geotechnical Engineering Laboratory
Direct Shear Data Sheet

Project:	Fully Softened Shear Strength
Sample I.D./Loc.:	Alabama 2 - Non-blenderized
Classification:	Sandy fat clay (CH)

Sample Preparation	Remolded at LL

Specific Gravity	2.72	Assumed

Test Number	1	2	3	4	5	6	7	8
Start Date (m/d/y)	12/14/2012	12/5/2012	12/5/2012	12/14/2012	12/14/2012			
End Date (m/d/y)	12/19/2012	12/11/2012	12/11/2012	12/19/2012	12/19/2012			
Consolidation Pressure (psf)	2176	3616	7216	10096	14416			
Initial Values								
Initial Height (in)	1.44	1.43	1.39	1.41	1.41			
Initial Diameter (in)	2.50	2.50	2.50	2.50	2.50			
Initial Sample Weight (g)	200	196	192	195	198			
Water Content (%)	48.65	52.55	51.58	49.25	50.16			
Dry Unit Weight (pcf)	72.7	69.7	70.9	72.0	72.6			
Wet Unit Weight (pcf)	108.0	106.4	107.4	107.5	109.1			
Consolidation Pressures								
Load 1 (psf)	116	116	116	116	116			
Load 2 (psf)	266	216	216	331	216			
Load 3 (psf)	556	416	416	646	416			
Load 4 (psf)	1096	916	916	1276	916			
Load 5 (psf)	2176	1816	1816	2536	1816			
Load 6 (psf)		3616	3616	5056	3616			
Load 7 (psf)			7216	10096	7216			
Load 8 (psf)					14416			
t_{50}								
Max. t_{50} for Load 1 (min)								
Max. t_{50} for Load 2 (min)								
Max. t_{50} for Load 3 (min)								
Max. t_{50} for Load 4 (min)								
Max. t_{50} for Load 5 (min)	11.62							
Max. t_{50} for Load 6 (min)		12.72						
Max. t_{50} for Load 7 (min)			7.15	5.88				
Max. t_{50} for Load 8 (min)					0.96			
Final Values								
Water Content (%)	33.38	32.20	30.09	28.26	25.64			
Dry Unit Weight (pcf)	90.1	91.3	101.5	97.8	98.3			
Wet Unit Weight (pcf)	120.2	120.8	132.0	125.4	123.5			
Failure								
Test Performed at Shear Rate (in/min)	1.00E-04	1.00E-04	1.00E-04	1.00E-04	1.00E-04			
Required Shear Rate (in/min)	4.25E-04	2.66E-04	1.02E-03	1.20E-03	3.80E-03			
Displacement at Failure (in)	0.25	0.17	0.36	0.35	0.18			
Peak Shear Stress (psf)	1535	2123	4748	6714	6656			
Total Change in Height at Failure (in)	0.28	0.34	0.42	0.37	0.37			
Secant Effective Friction Angle (deg)	35.2	30.4	33.3	33.6	24.8			

Comments:

Alabama 2 - Non-blenderized - 2176 psf

Alabama 2 - Non-blenderized - 3616 psf

Alabama 2 - Non-blenderized - 7216 psf

Alabama 2 - Non-blenderized - 10096 psf

Alabama 2 - Non-blenderized - 14416 psf

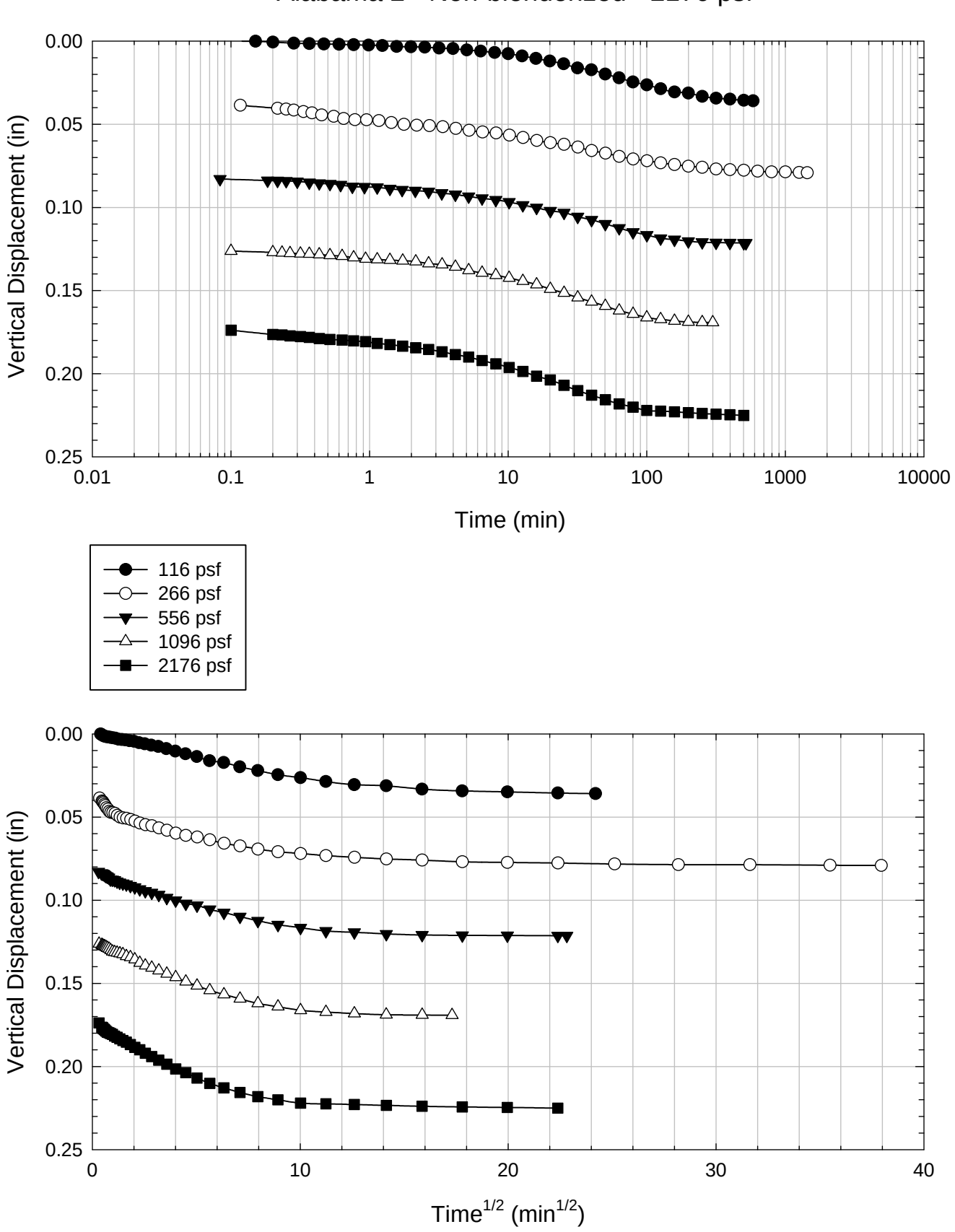
Alabama 2 - Non-blenderized - 2176 psf
Vertical Displacement (in)
0.00
0.05
0.10
0.15
0.20
0.25
0.01
0.1
1
10
100
1000
10000
Time (min)
116 psf
266 psf
556 psf
1096 psf
2176 psf
Vertical Displacement (in)
0.00
0.05
0.10
0.15
0.20
0.25
0
10
20
30
40
Time1/2 (min1/2)

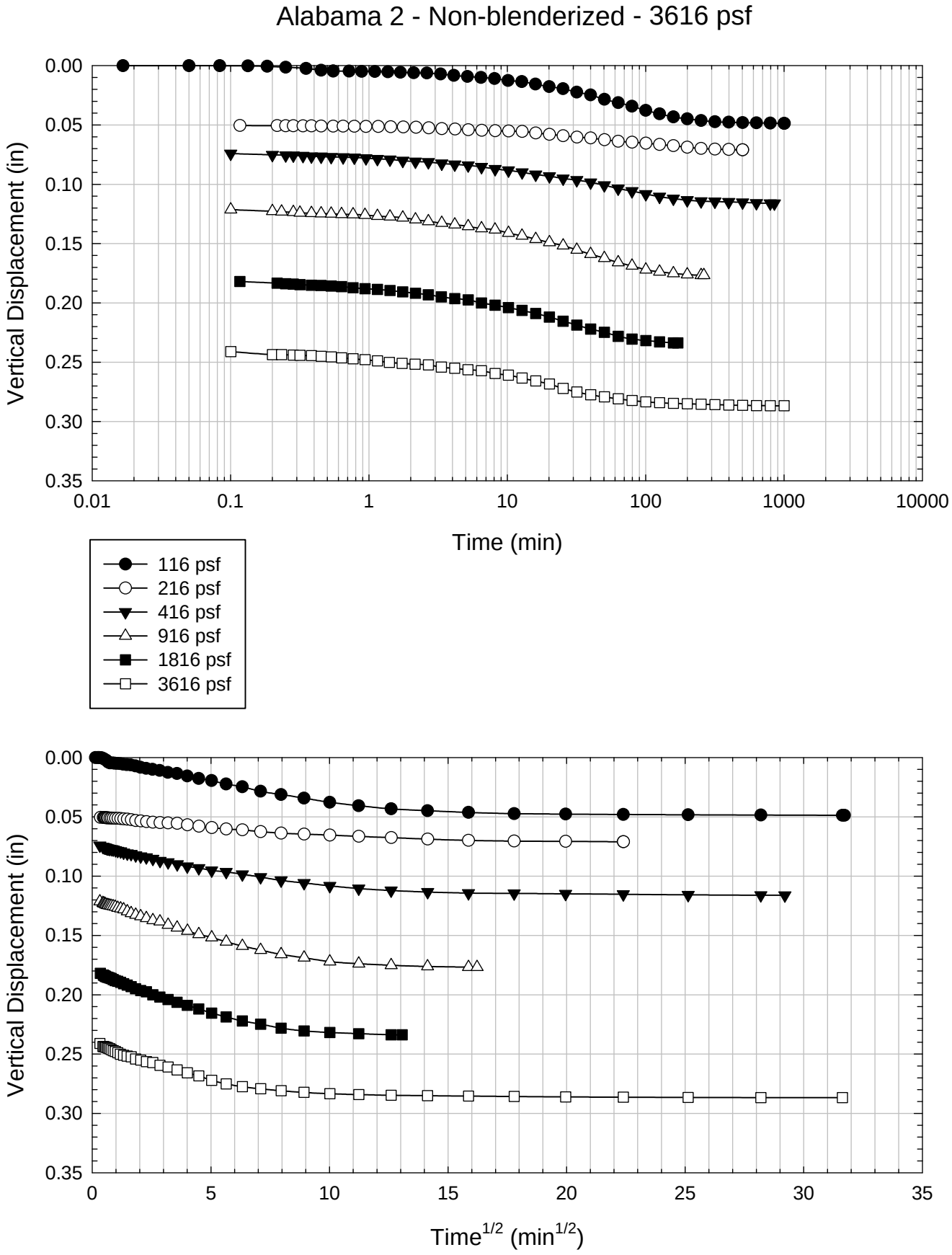
Alabama 2 - Non-blenderized - 3616 psf
Vertical Displacement (in)
0.00
0.05
0.10
0.15
0.20
0.25
0.30
0.35
0.01
0.1
1
10
100
1000
10000
Time (min)
116 psf
216 psf
416 psf
916 psf
1816 psf
3616 psf
Vertical Displacement (in)
0.00
0.05
0.10
0.15
0.20
0.25
0.30
0.35
0
5
10
15
20
25
30
35
Time1/2 (min1/2)

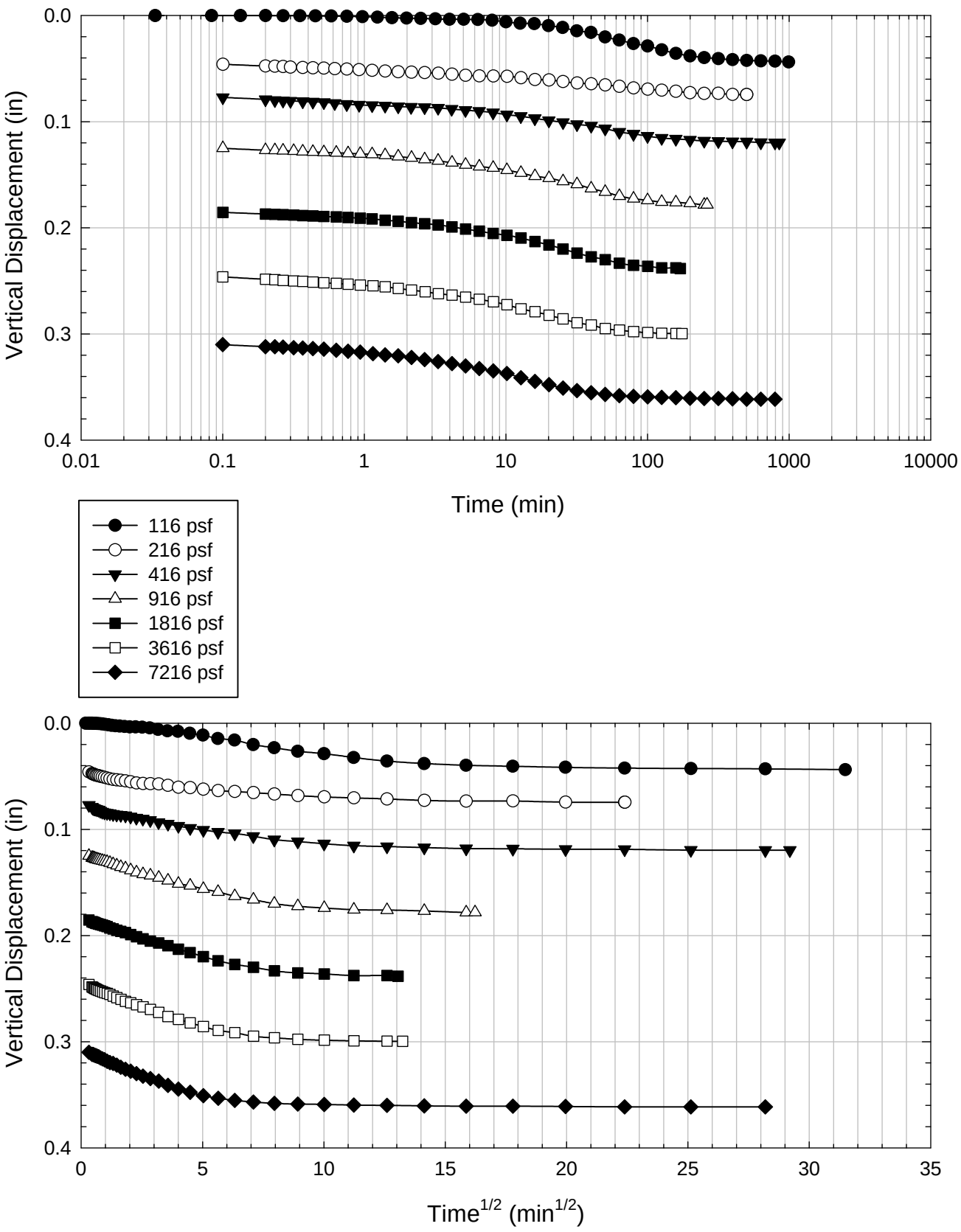
Alabama 2 - Non-blenderized - 7216 psf
Vertical Displacement (in)
0.0
0.1
0.2
0.3
0.4
0.01
0.1
1
10
100
1000
10000
Time (min)
116 psf
216 psf
416 psf
916 psf
1816 psf
3616 psf
7216 psf
Vertical Displacement (in)
0.0
0.1
0.2
0.3
0.4
0
5
10
15
20
25
30
35
Time^1/2 (min^1/2)

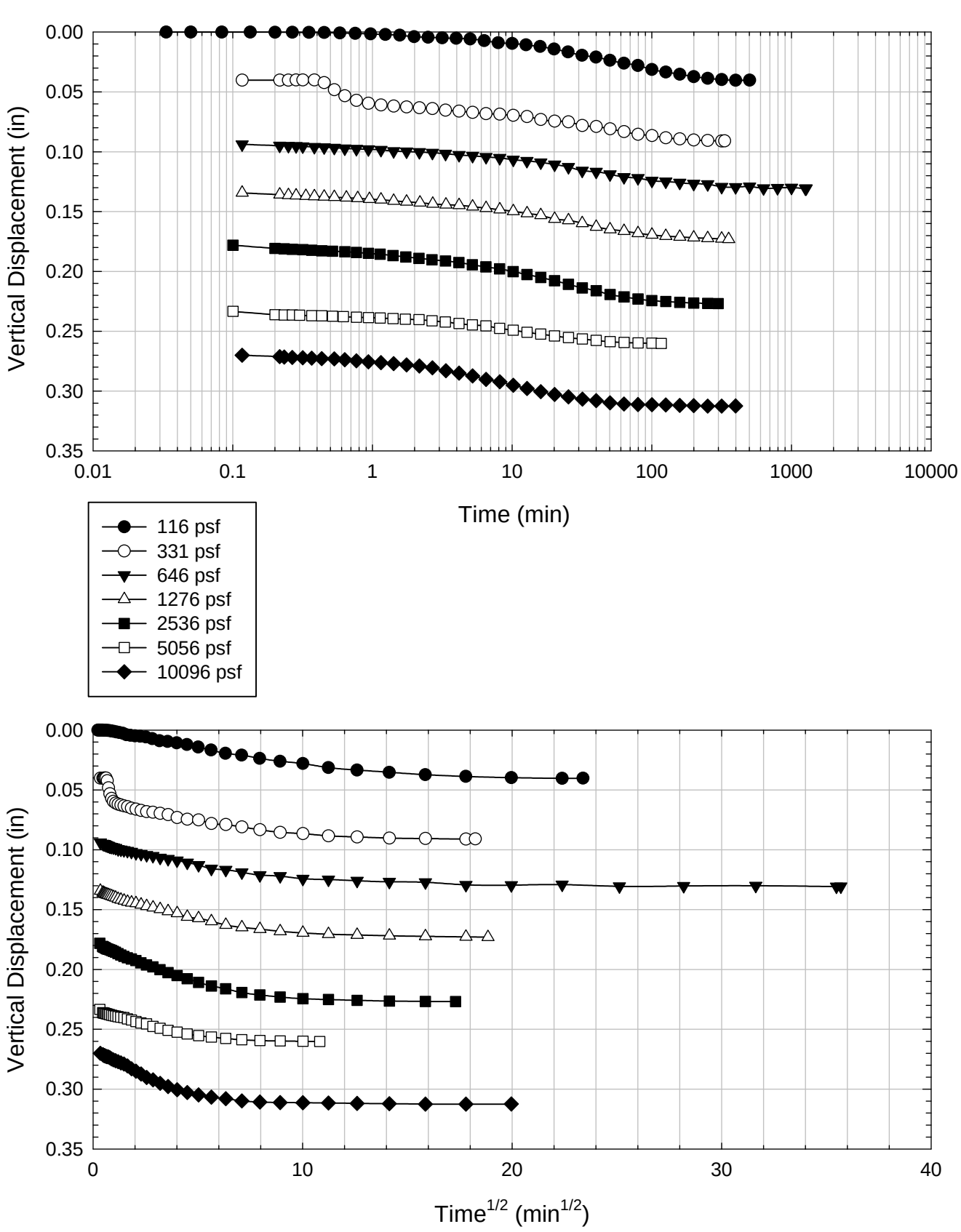
Alabama 2 - Non-blenderized - 10096 psf
Vertical Displacement (in)
0.00
0.05
0.10
0.15
0.20
0.25
0.30
0.35
0.01
0.1
1
10
100
1000
10000
Time (min)
116 psf
331 psf
646 psf
1276 psf
2536 psf
5056 psf
10096 psf
Vertical Displacement (in)
0
10
20
30
40
Time^1/2 (min^1/2)

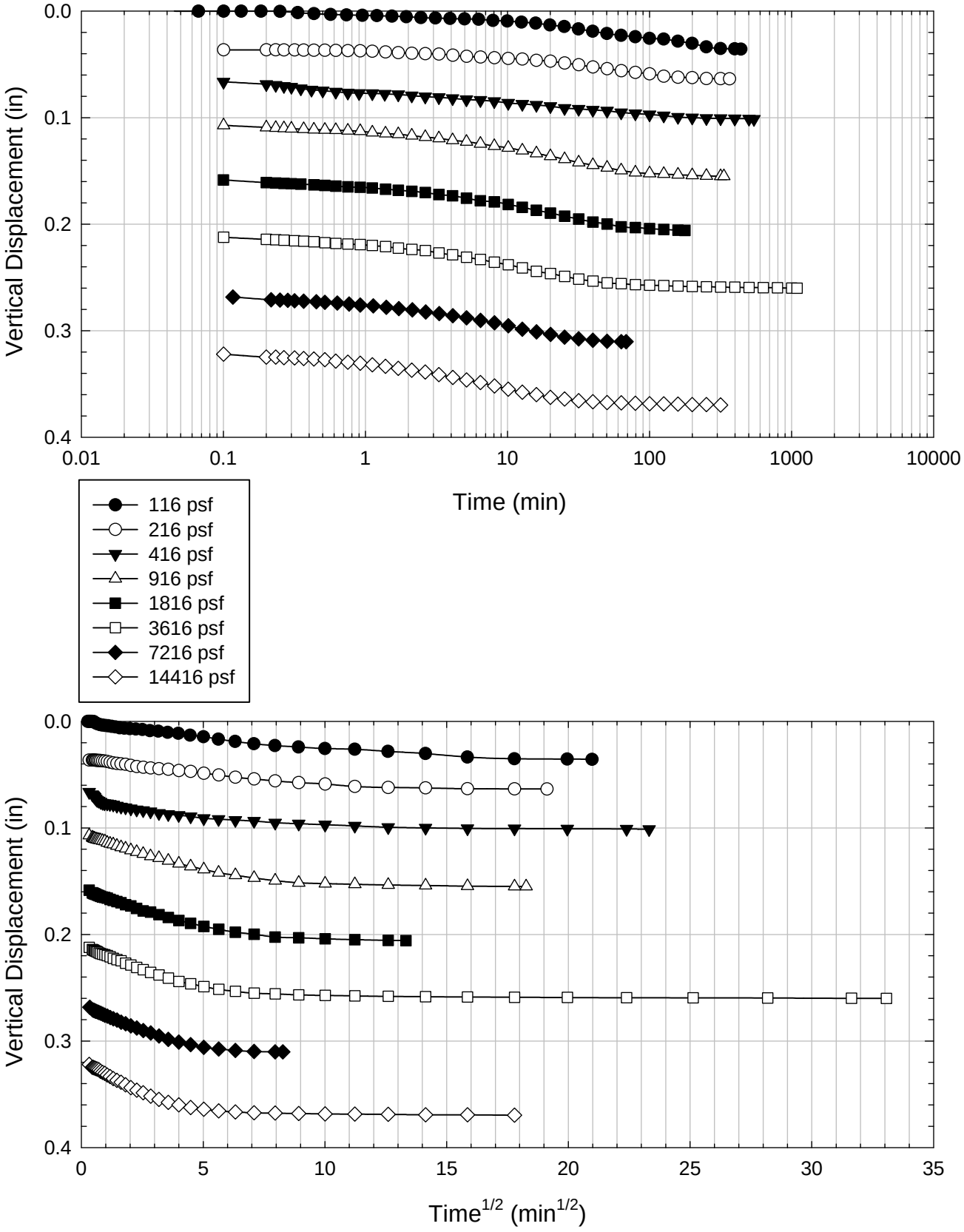
Alabama 2 - Non-blenderized - 14416 psf
Vertical Displacement (in)
0.0
0.1
0.2
0.3
0.4
0.01
0.1
1
10
100
1000
10000
Time (min)
116 psf
216 psf
416 psf
916 psf
1816 psf
3616 psf
7216 psf
14416 psf
Vertical Displacement (in)
0
5
10
15
20
25
30
35
Time^1/2 (min^1/2)

Alabama 2 - Non-blenderized

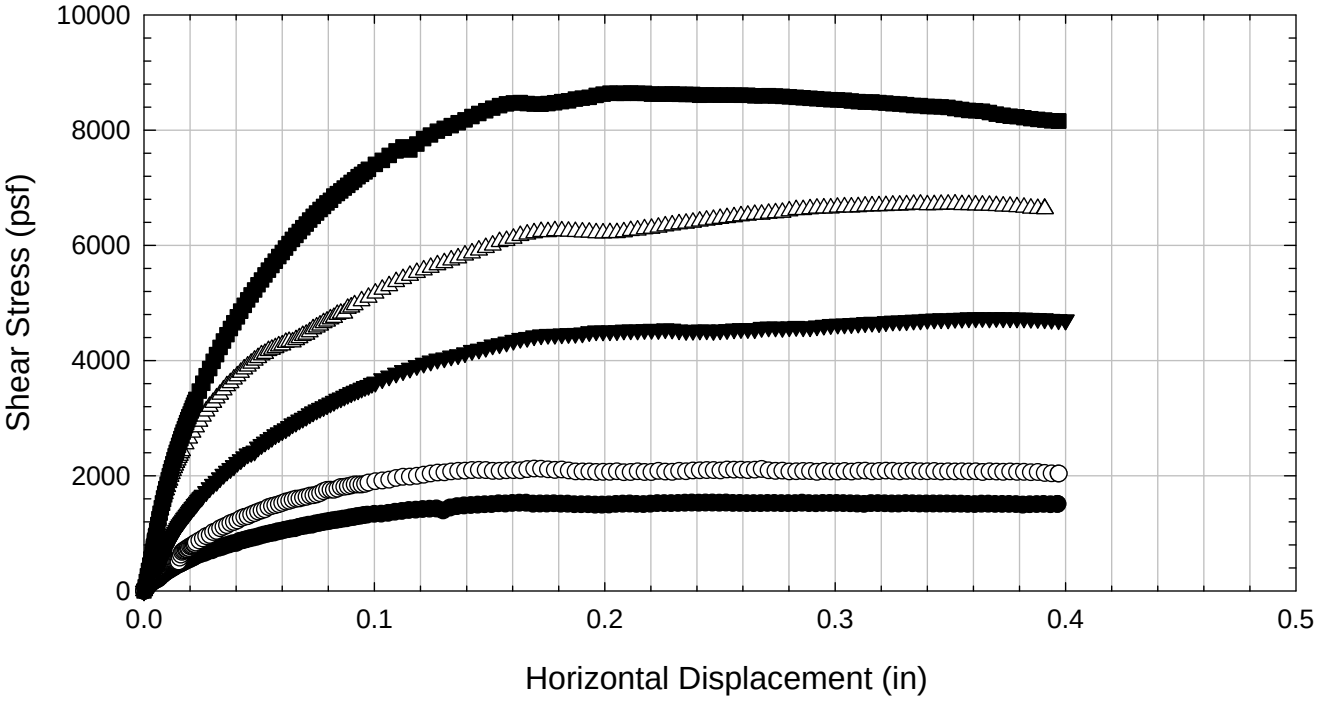

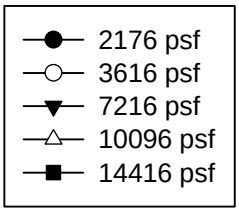

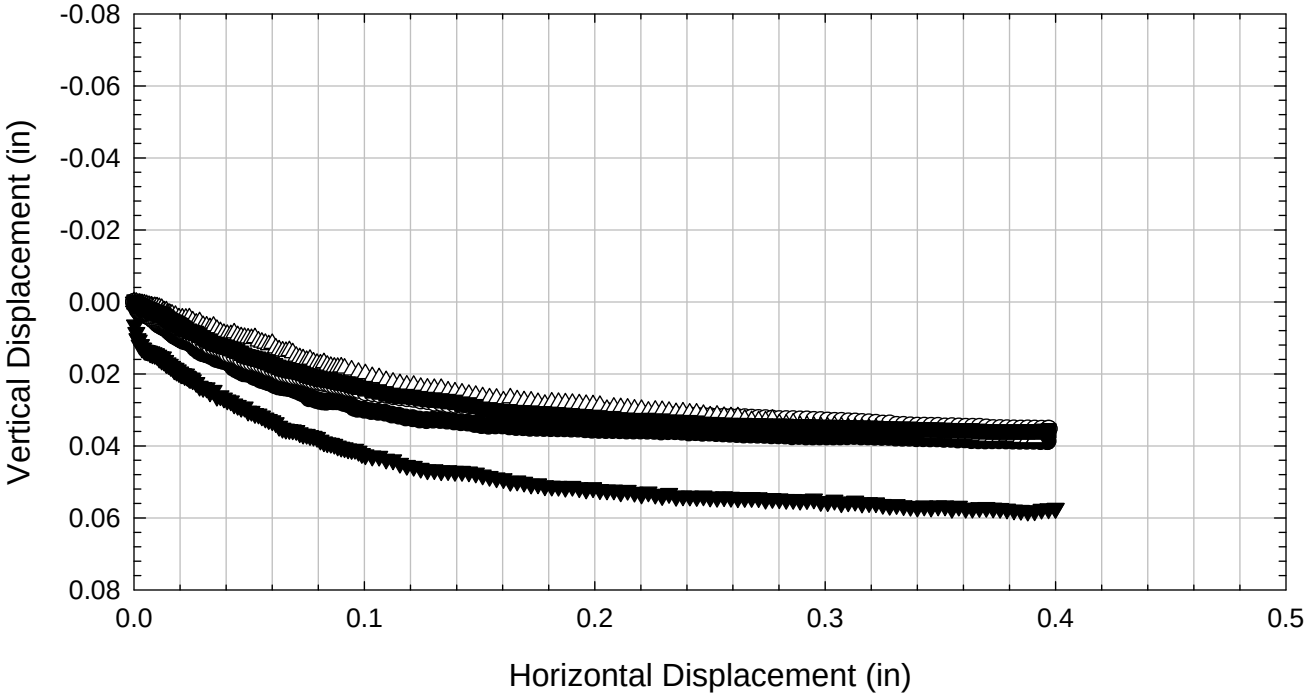

C.3. Alabama 3

C.3.1 Non-blenderized

Virginia Polytechnic Institute and State University
Geotechnical Engineering Laboratory
Direct Shear Data Sheet

Project:	Fully Softened Shear Strength
Sample I.D./Loc.:	Alabama 3 - Non-blenderized
Classification:	Low plasticity silt (ML)

Sample Preparation	Remolded at LL		Specific Gravity	2.79

Test Number	1	2	3	4	5	6	7	8
Start Date (m/d/y)	12/13/2013	12/11/2012	12/11/2012	12/14/2012	12/13/2012			
End Date (m/d/y)	12/15/2012	12/13/2012	12/13/2012	12/15/2012	12/14/2012			
Consolidation Pressure (psf)	2176	3616	7216	10096	14416			
Initial Values								
Initial Height (in)	1.42	1.44	1.40	1.41	1.39			
Initial Diameter (in)	2.50	2.50	2.50	2.50	2.50			
Initial Sample Weight (g)	202	205	200	204	200			
Water Content (%)	48.47	47.45	46.59	47.03	46.40			
Dry Unit Weight (pcf)	74.5	74.7	75.7	76.6	76.5			
Wet Unit Weight (pcf)	110.6	110.2	111.0	112.6	112.0			
Consolidation Pressures								
Load 1 (psf)	116	116	116	116	116			
Load 2 (psf)	266	216	216	331	216			
Load 3 (psf)	556	416	416	646	416			
Load 4 (psf)	1096	916	916	1276	916			
Load 5 (psf)	2176	1816	1816	2536	1816			
Load 6 (psf)		3616	3616	5056	3616			
Load 7 (psf)			7216	10096	7216			
Load 8 (psf)					14416			
t_{50}								
Max. t_{50} for Load 1 (min)								
Max. t_{50} for Load 2 (min)								
Max. t_{50} for Load 3 (min)								
Max. t_{50} for Load 4 (min)								
Max. t_{50} for Load 5 (min)	1.35							
Max. t_{50} for Load 6 (min)		1.65						
Max. t_{50} for Load 7 (min)			1.35	0.76				
Max. t_{50} for Load 8 (min)					0.77			
Final Values								
Water Content (%)	33.03	31.20	28.86	27.45	25.83			
Dry Unit Weight (pcf)	91.0	93.6	99.7	104.6	107.9			
Wet Unit Weight (pcf)	121.1	122.8	128.5	133.4	135.8			
Failure								
Test Performed at Shear Rate (in/min)	5.00E-05	5.00E-05	5.00E-05	5.00E-05	5.00E-05			
Required Shear Rate (in/min)	2.60E-03	2.29E-03	3.00E-03	4.73E-03	5.06E-03			
Displacement at Failure (in)	0.18	0.19	0.20	0.18	0.19			
Peak Shear Stress (psf)	1227	1994	3938	5544	6619			
Total Change in Height at Failure (in)	0.26	0.29	0.34	0.38	0.40			
Secant Effective Friction Angle (deg)	29.4	28.9	28.6	28.8	24.7			

Comments:

Alabama 3 - Non-blenderized - 2176 psf

Alabama 3 - Non-blenderized - 3616 psf

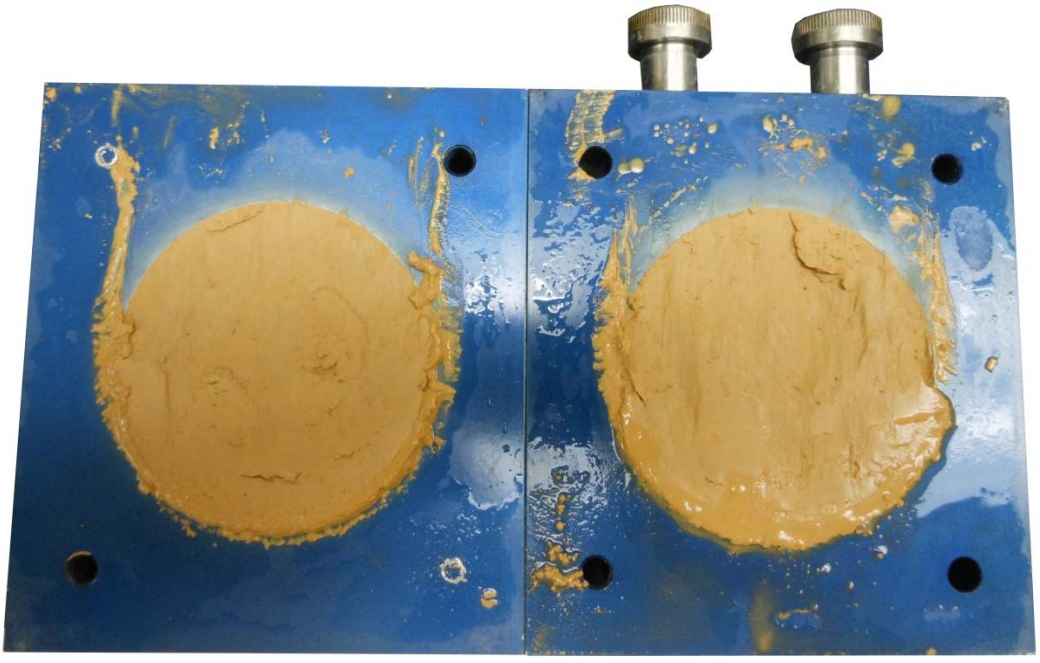

Alabama 3 - Non-blenderized - 7216 psf

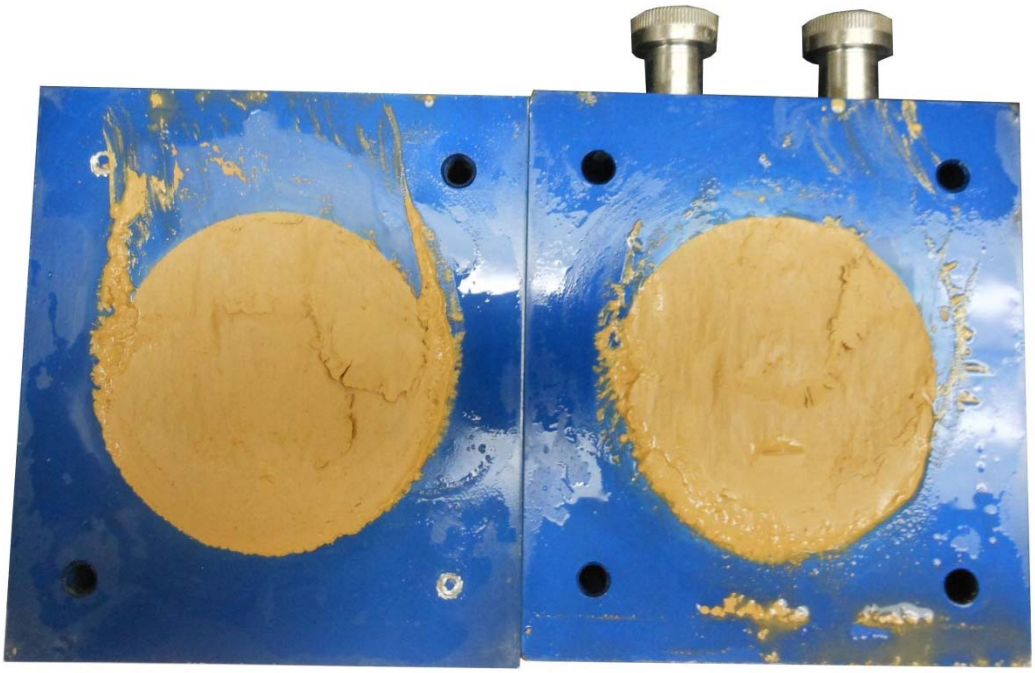

Alabama 3 - Non-blenderized - 10096 psf

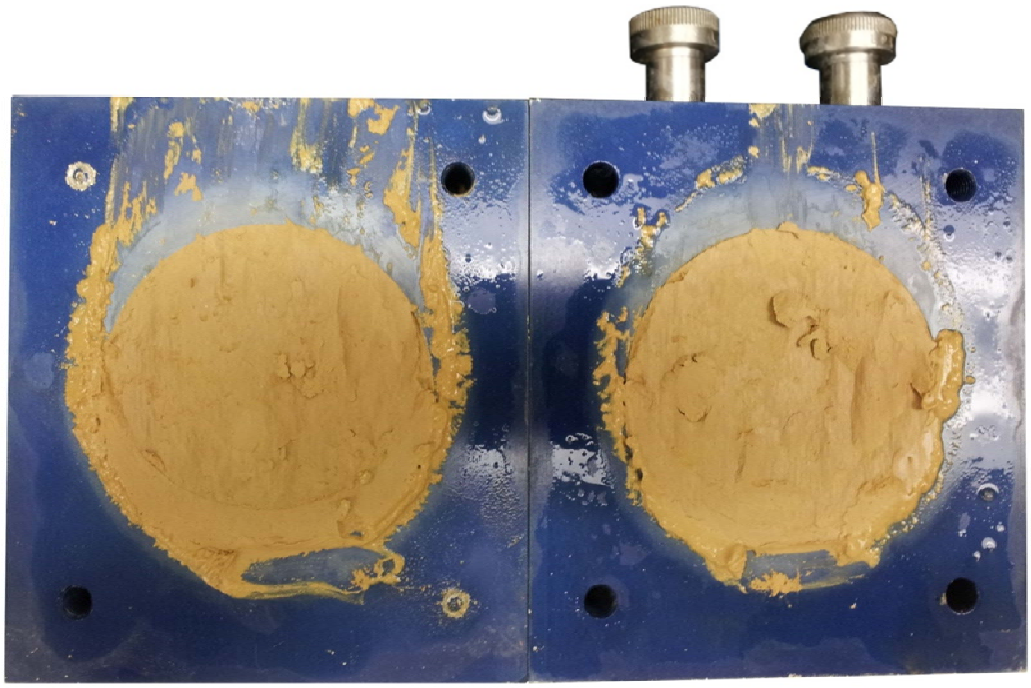

Alabama 3 - Non-blenderized - 14416 psf

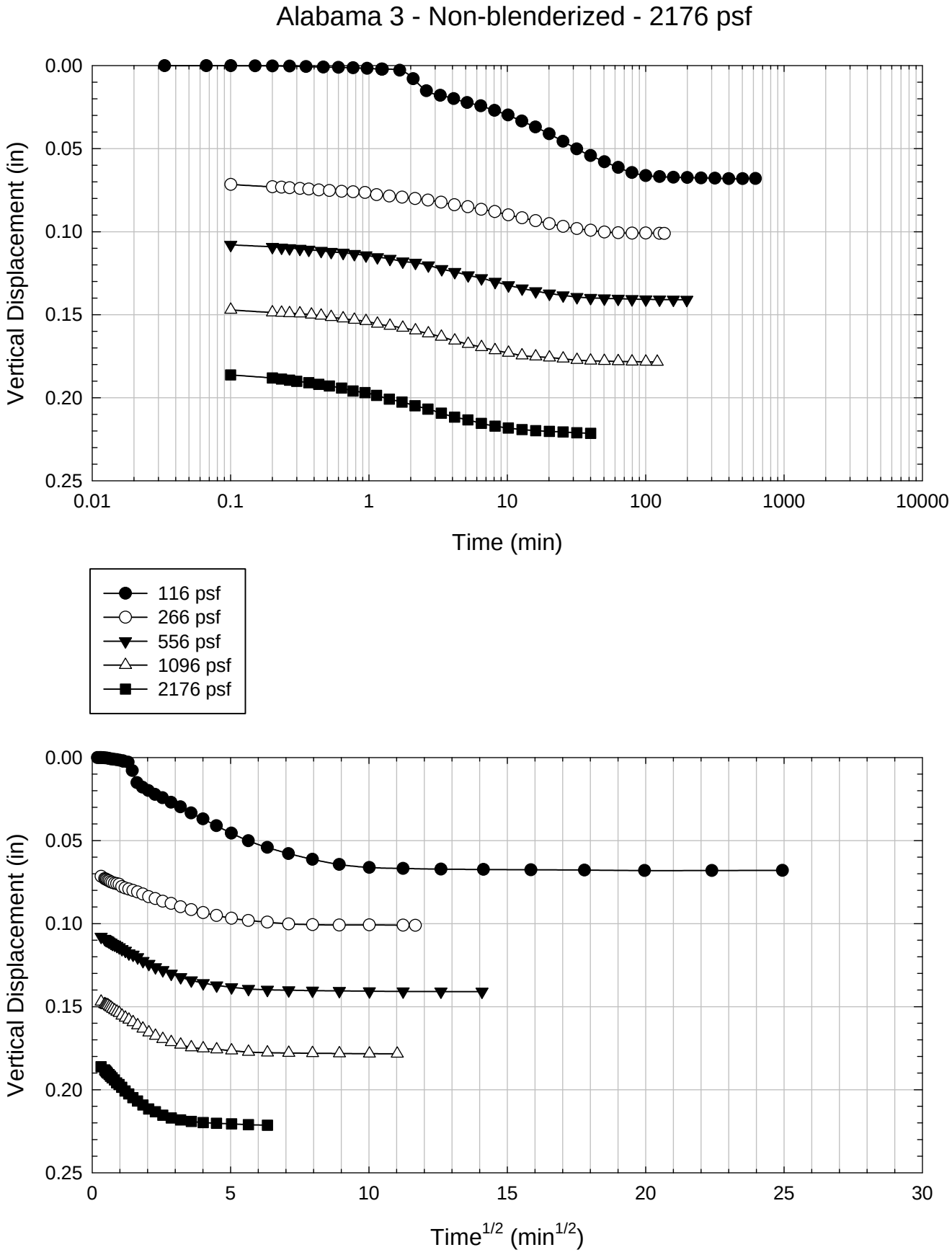
Alabama 3 - Non-blenderized - 2176 psf
Vertical Displacement (in)
0.00
0.05
0.10
0.15
0.20
0.25
0.01
0.1
1
10
100
1000
10000
Time (min)
116 psf
266 psf
556 psf
1096 psf
2176 psf
Vertical Displacement (in)
0.00
0.05
0.10
0.15
0.20
0.25
0
5
10
15
20
25
30
Time^1/2 (min^1/2)

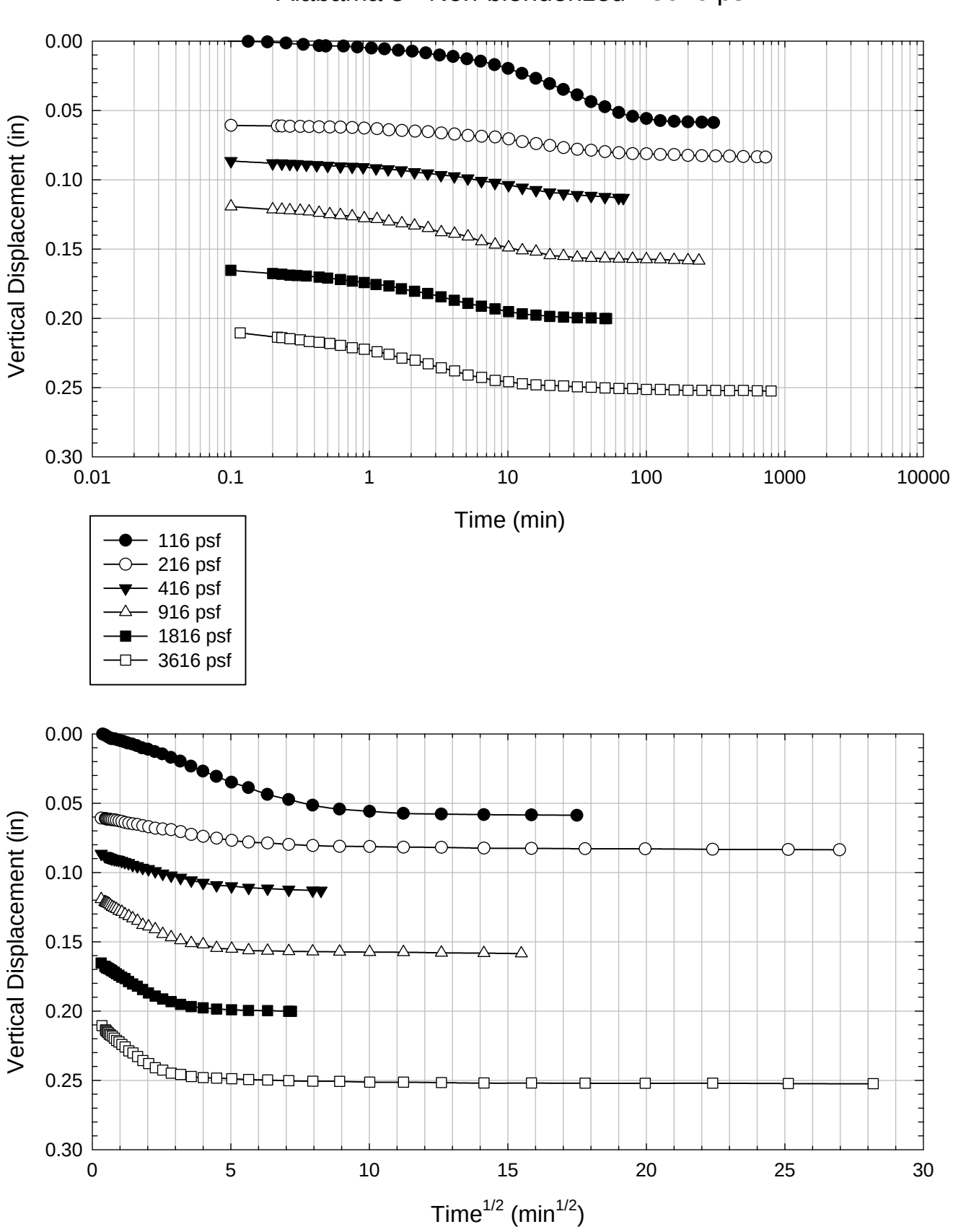
Alabama 3 - Non-blenderized - 3616 psf
Vertical Displacement (in)
0.00
0.05
0.10
0.15
0.20
0.25
0.30
0.01
0.1
1
10
100
1000
10000
Time (min)
116 psf
216 psf
416 psf
916 psf
1816 psf
3616 psf
Vertical Displacement (in)
0.00
0.05
0.10
0.15
0.20
0.25
0.30
0
5
10
15
20
25
30
Time1/2 (min1/2)

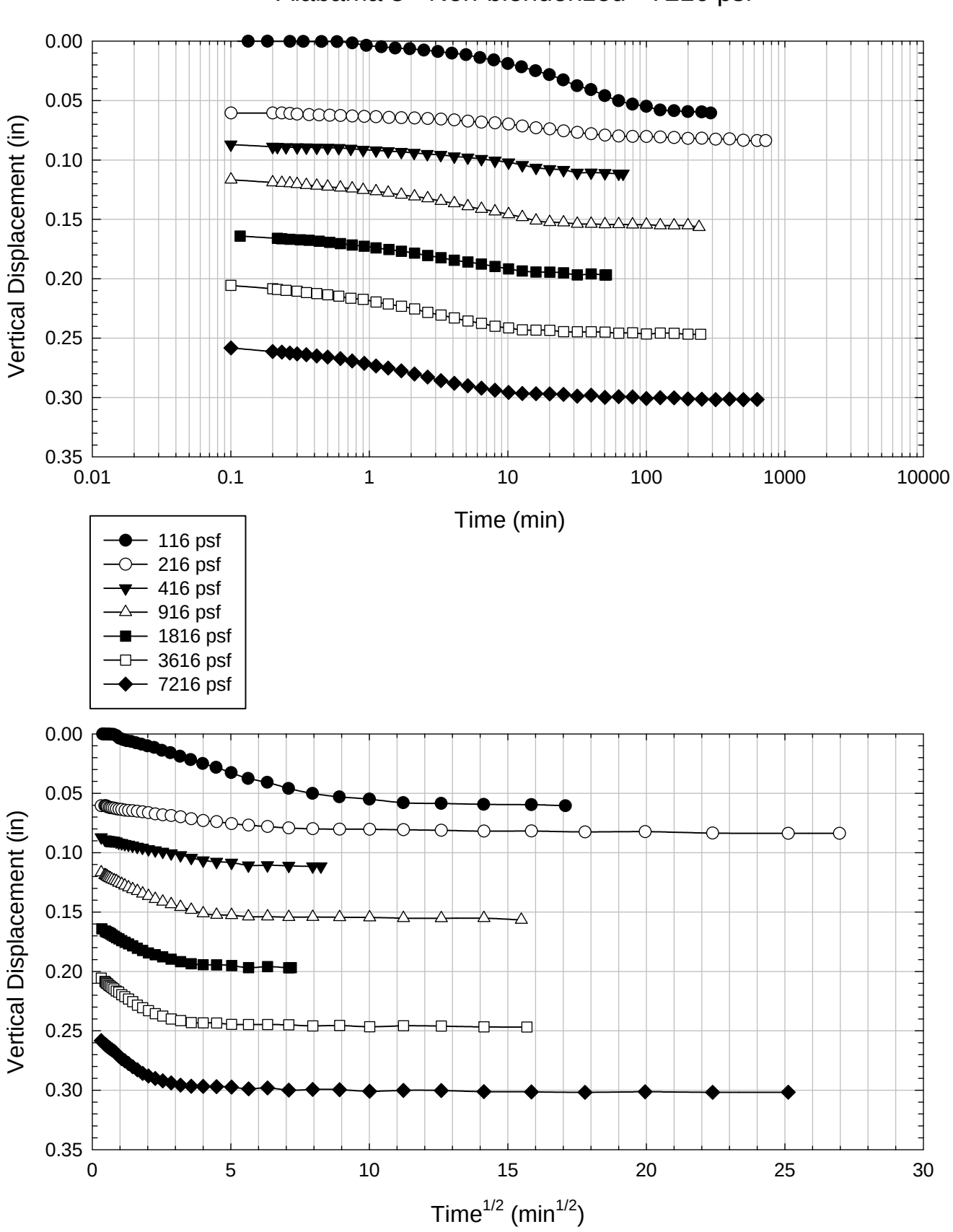
Alabama 3 - Non-blenderized - 7216 psf
Vertical Displacement (in)
0.00
0.05
0.10
0.15
0.20
0.25
0.30
0.35
0.01
0.1
1
10
100
1000
10000
Time (min)
116 psf
216 psf
416 psf
916 psf
1816 psf
3616 psf
7216 psf
Vertical Displacement (in)
0
5
10
15
20
25
30
Time^1/2 (min^1/2)

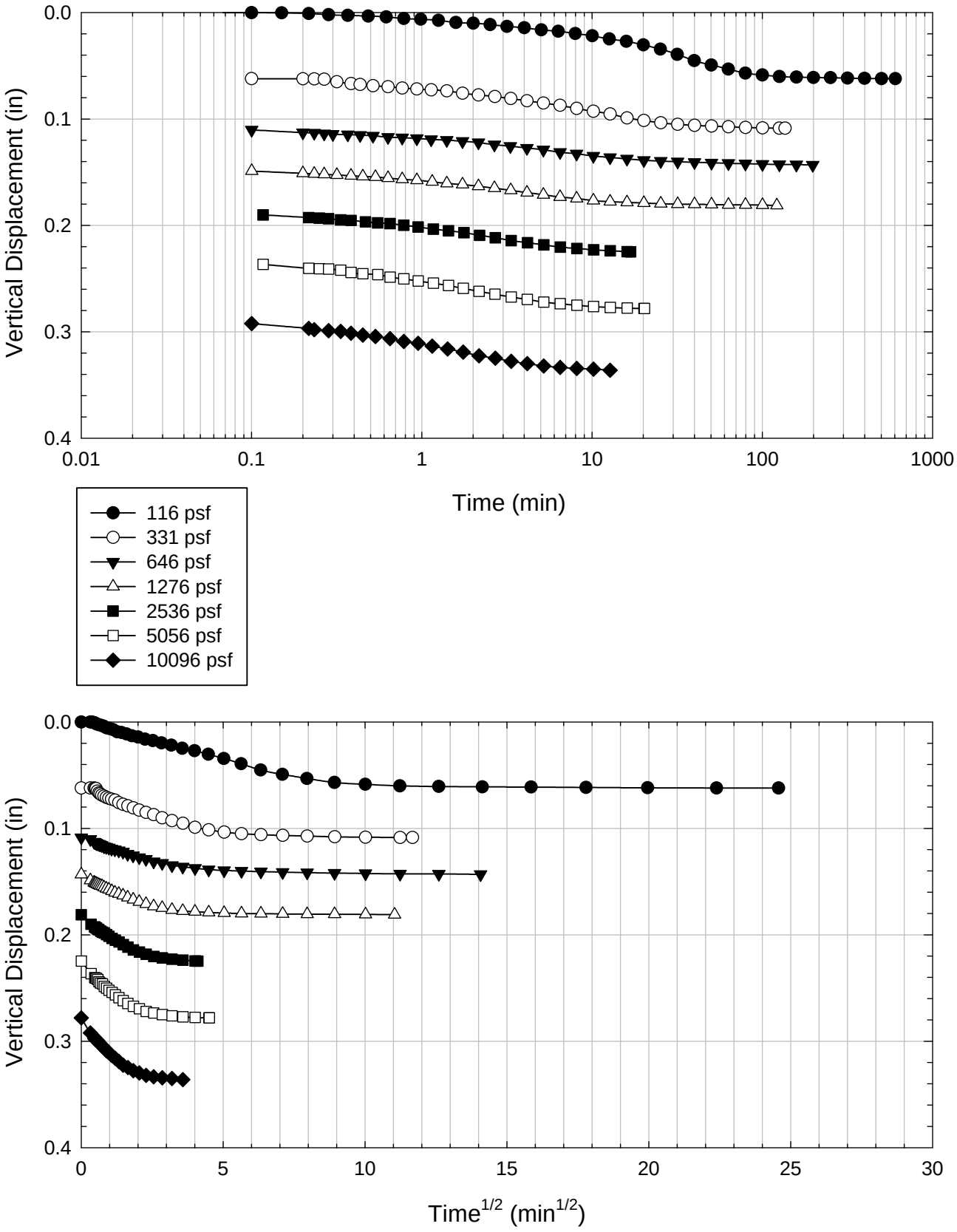
Alabama 3 - Non-blenderized - 10096 psf
Vertical Displacement (in)
0.0
0.1
0.2
0.3
0.4
0.01
0.1
1
10
100
1000
Time (min)
116 psf
331 psf
646 psf
1276 psf
2536 psf
5056 psf
10096 psf
Vertical Displacement (in)
0.0
0.1
0.2
0.3
0.4
0
5
10
15
20
25
30
Time^1/2 (min^1/2)

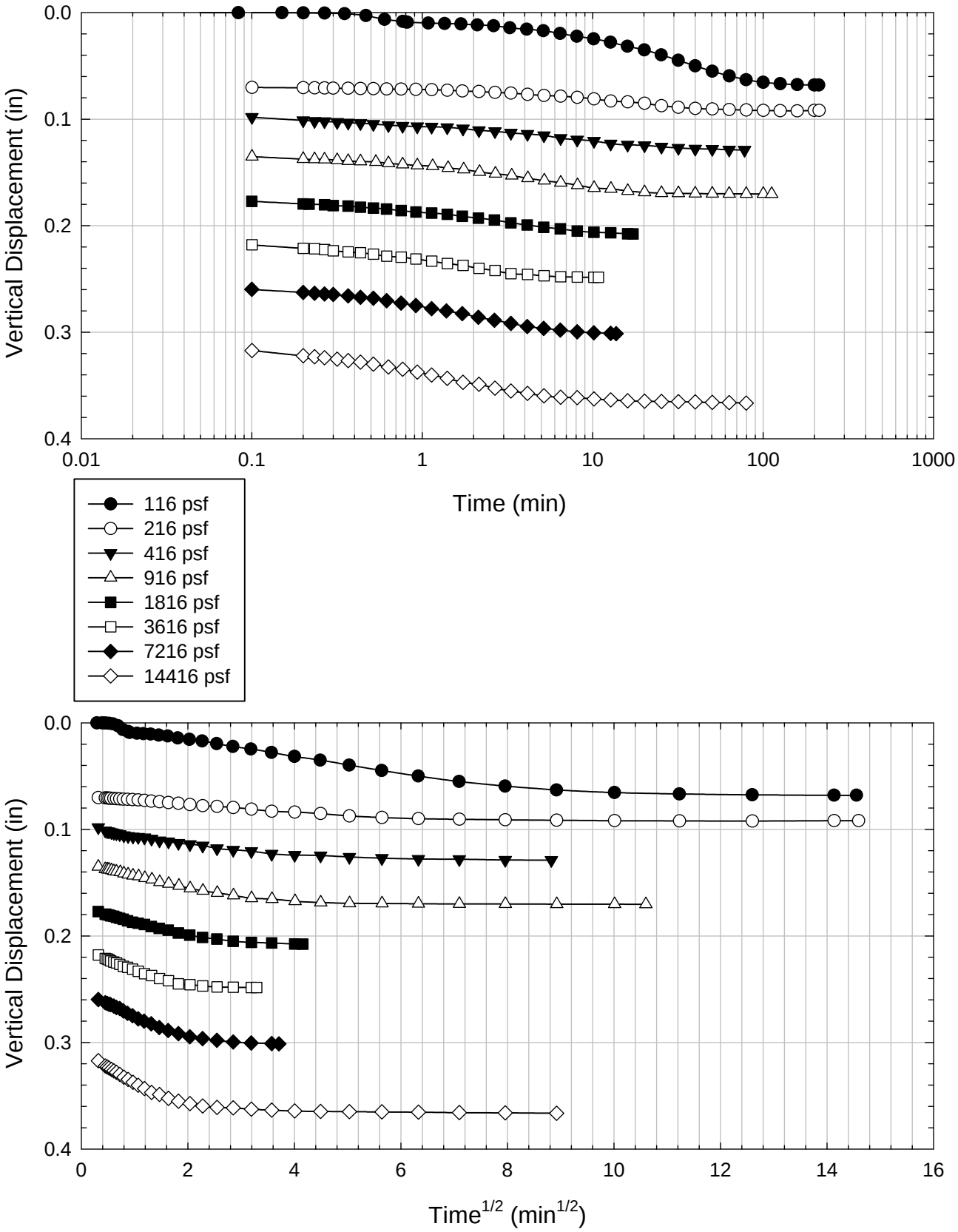
Alabama 3 - Non-blenderized - 14416 psf
Vertical Displacement (in)
0.0
0.1
0.2
0.3
0.4
0.01
0.1
1
10
100
1000
Time (min)
116 psf
216 psf
416 psf
916 psf
1816 psf
3616 psf
7216 psf
14416 psf
Vertical Displacement (in)
0.0
0.1
0.2
0.3
0.4
0
2
4
6
8
10
12
14
16
Time1/2 (min1/2)

Alabama 3 - Non-blenderized

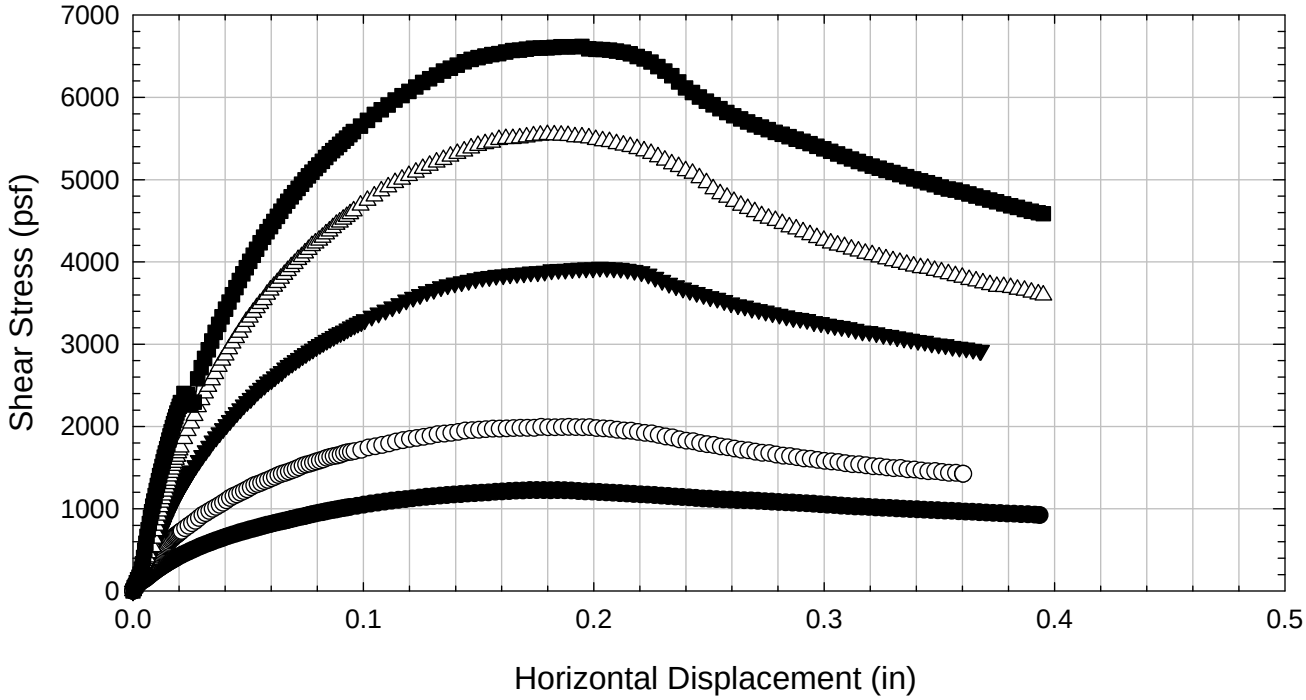

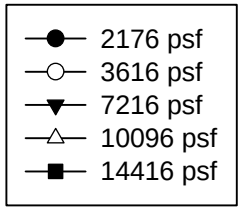

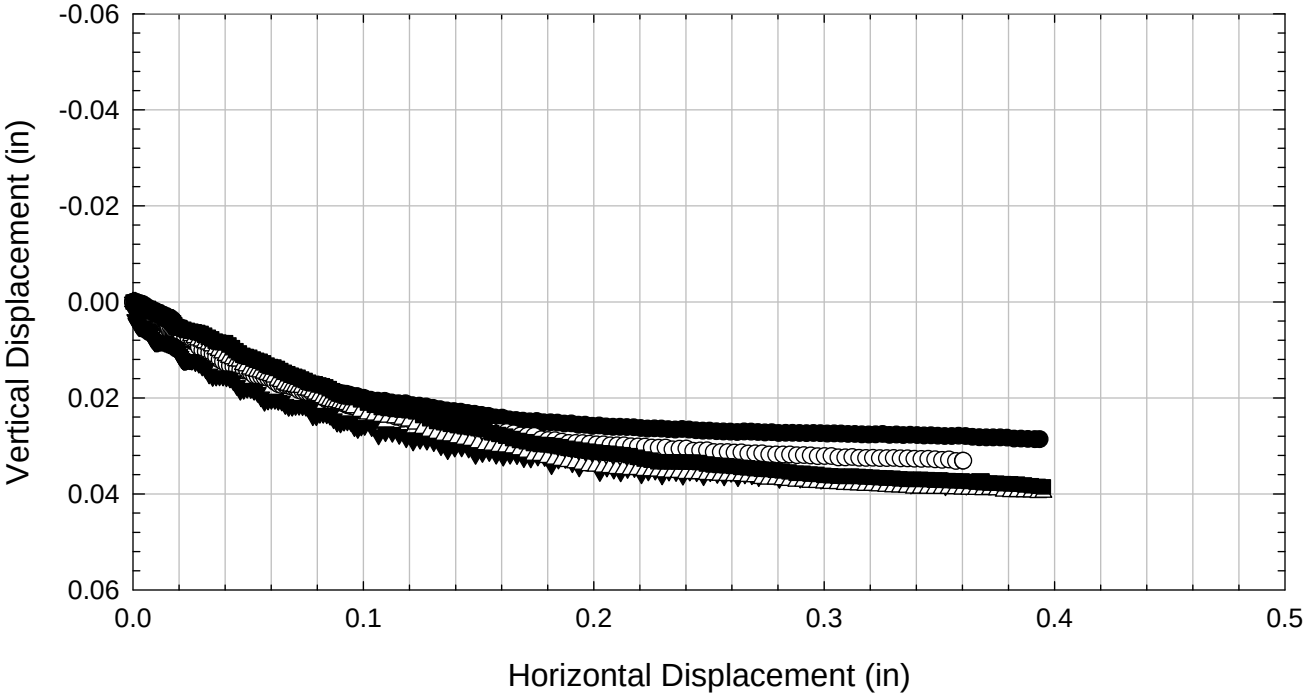

C.4. Alabama 4

C.4.1 Non-blenderized

Virginia Polytechnic Institute and State University
Geotechnical Engineering Laboratory
Direct Shear Data Sheet

Project:	Fully Softened Shear Strength
Sample I.D./Loc.:	Alabama 4 - Non-blenderized
Classification:	Lean clay (CL)

Sample Preparation	Remolded at LL		Specific Gravity	2.71

Test Number	1	2	3	4	5	6	7	8
Start Date (m/d/y)	12/17/2012	12/10/2012	12/10/2012	12/17/2012	12/10/2012			
End Date (m/d/y)	12/19/2012	12/13/2012	12/12/2012	12/19/2012	12/13/2012			
Consolidation Pressure (psf)	2176	3616	7216	10096	14416			
Initial Values								
Initial Height (in)	1.40	1.43	1.41	1.42	1.40			
Initial Diameter (in)	2.50	2.50	2.50	2.50	2.50			
Initial Sample Weight (g)	205	208	205	204	208			
Water Content (%)	43.24	43.00	42.67	43.54	42.75			
Dry Unit Weight (pcf)	79.3	79.1	79.1	77.6	80.9			
Wet Unit Weight (pcf)	113.6	113.2	112.9	111.3	115.6			
Consolidation Pressures								
Load 1 (psf)	116	116	116	116	116			
Load 2 (psf)	266	216	216	331	216			
Load 3 (psf)	556	416	416	646	416			
Load 4 (psf)	1096	916	916	1276	916			
Load 5 (psf)	2176	1816	1816	2536	1816			
Load 6 (psf)		3616	3616	5056	3616			
Load 7 (psf)			7216	10096	7216			
Load 8 (psf)					14416			
t_{50}								
Max. t_{50} for Load 1 (min)								
Max. t_{50} for Load 2 (min)								
Max. t_{50} for Load 3 (min)								
Max. t_{50} for Load 4 (min)								
Max. t_{50} for Load 5 (min)	3.00							
Max. t_{50} for Load 6 (min)		1.90						
Max. t_{50} for Load 7 (min)			1.41	1.55				
Max. t_{50} for Load 8 (min)					1.23			
Final Values								
Water Content (%)	31.04	29.55	25.77	24.84	24.83			
Dry Unit Weight (pcf)	95.0	97.8	104.3	103.9	109.0			
Wet Unit Weight (pcf)	124.4	126.7	131.2	129.7	136.1			
Failure								
Test Performed at Shear Rate (in/min)	5.00E-05	5.00E-05	5.00E-05	5.00E-05	5.00E-05			
Required Shear Rate (in/min)	1.03E-03	1.74E-03	2.38E-03	2.16E-03	2.56E-03			
Displacement at Failure (in)	0.16	0.17	0.17	0.17	0.16			
Peak Shear Stress (psf)	1162	1866	4072	5284	6648			
Total Change in Height at Failure (in)	0.23	0.27	0.34	0.36	0.36			
Secant Effective Friction Angle (deg)	28.1	27.3	29.4	27.6	24.8			

Comments:

Alabama 4 - Non-blenderized - 2176 psf

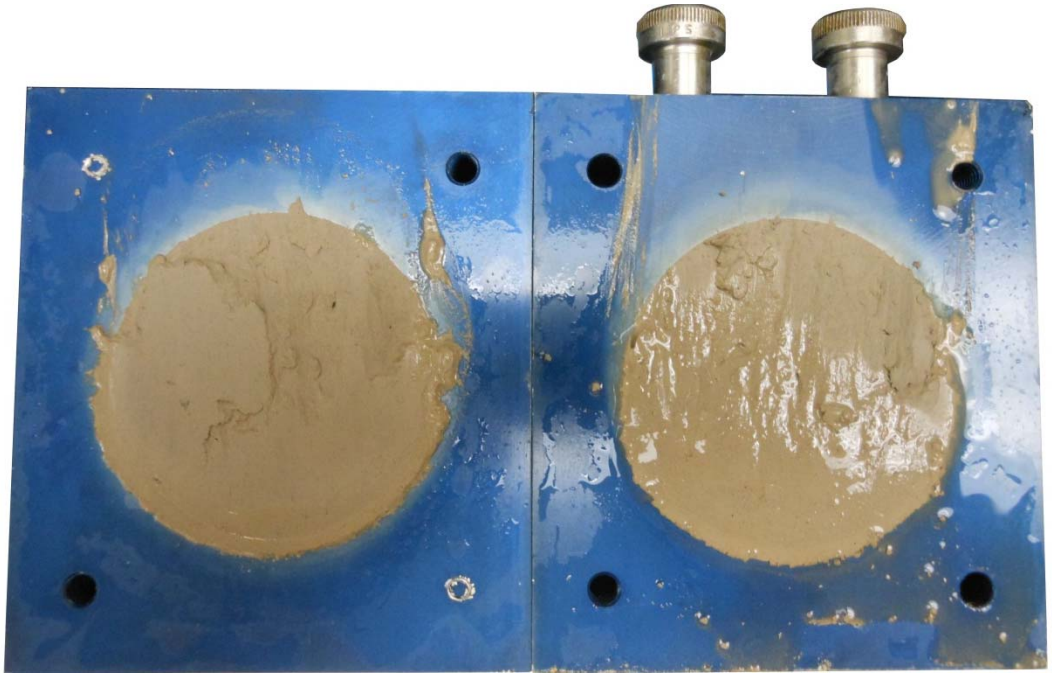

Alabama 4 - Non-blenderized - 3616 psf

Alabama 4 - Non-blenderized - 7216 psf

Alabama 4 - Non-blenderized - 10096 psf

Alabama 4 - Non-blenderized - 14416 psf

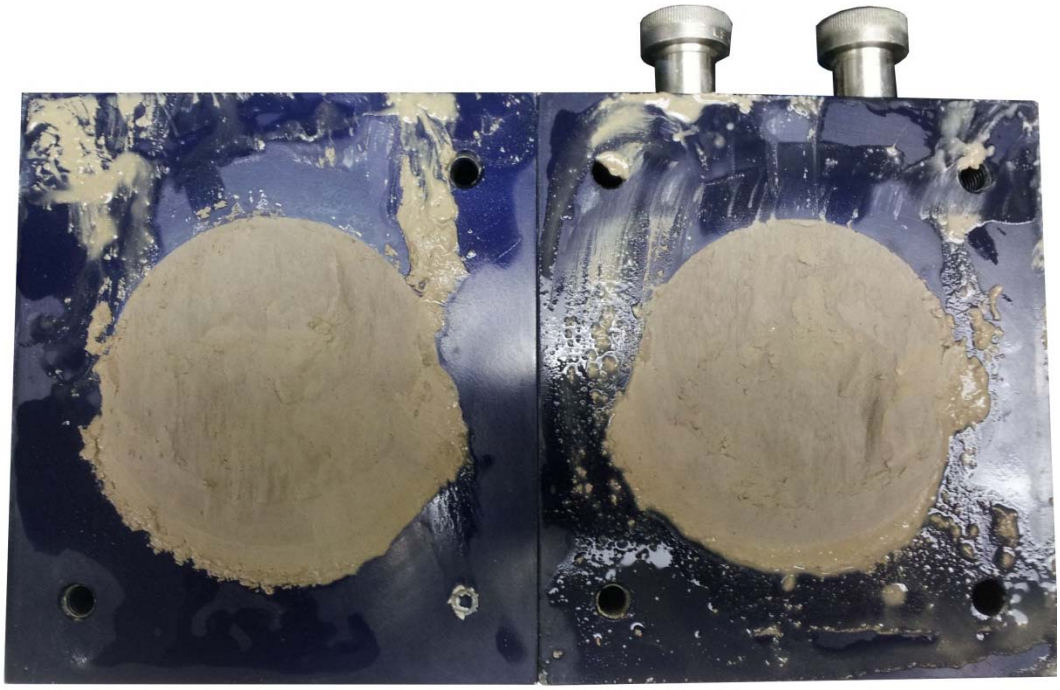

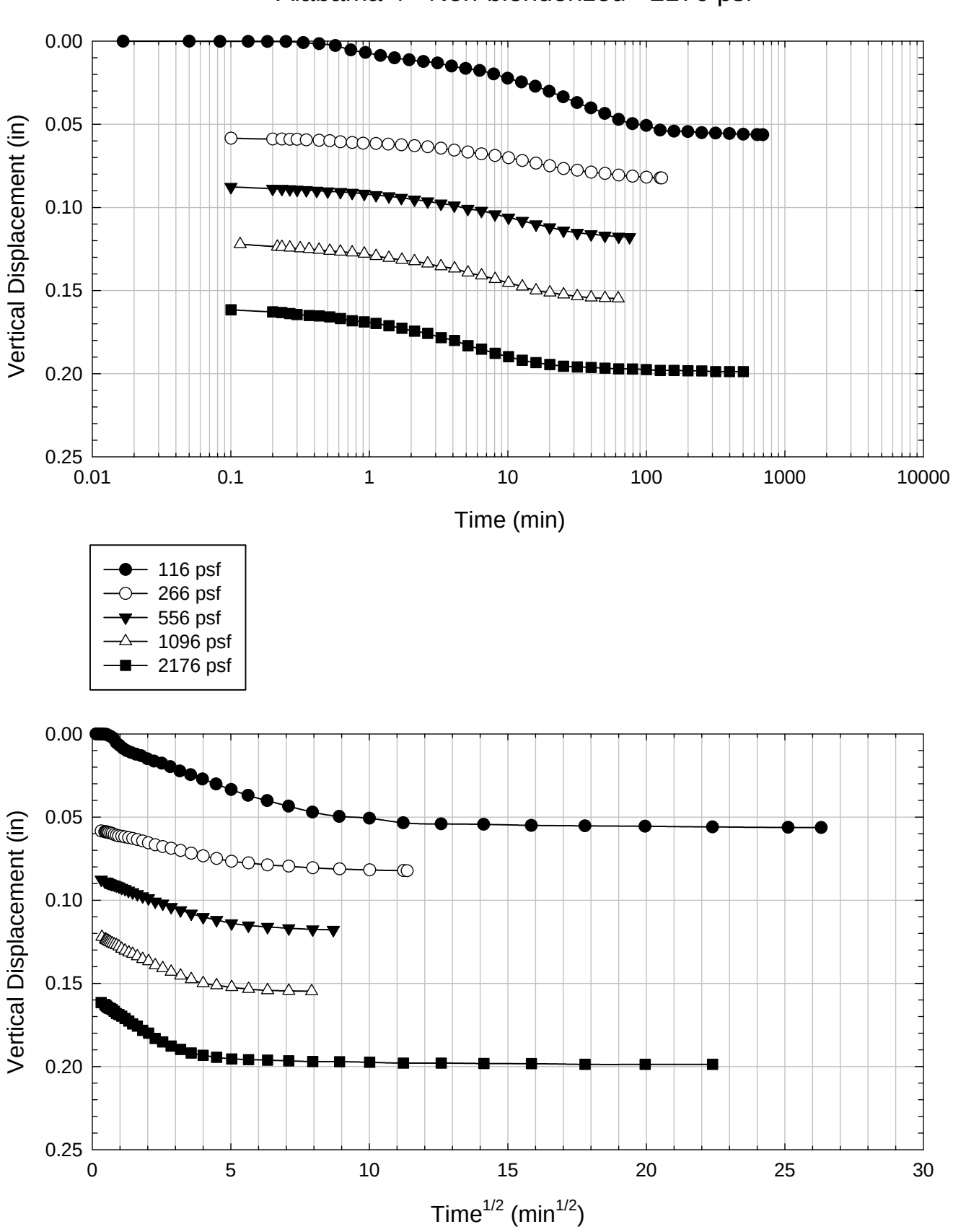
Alabama 4 - Non-blenderized - 2176 psf
Vertical Displacement (in)
0.00
0.05
0.10
0.15
0.20
0.25
0.01
0.1
1
10
100
1000
10000
Time (min)
116 psf
266 psf
556 psf
1096 psf
2176 psf
Vertical Displacement (in)
0.00
0.05
0.10
0.15
0.20
0.25
0
5
10
15
20
25
30
Time^1/2 (min^1/2)

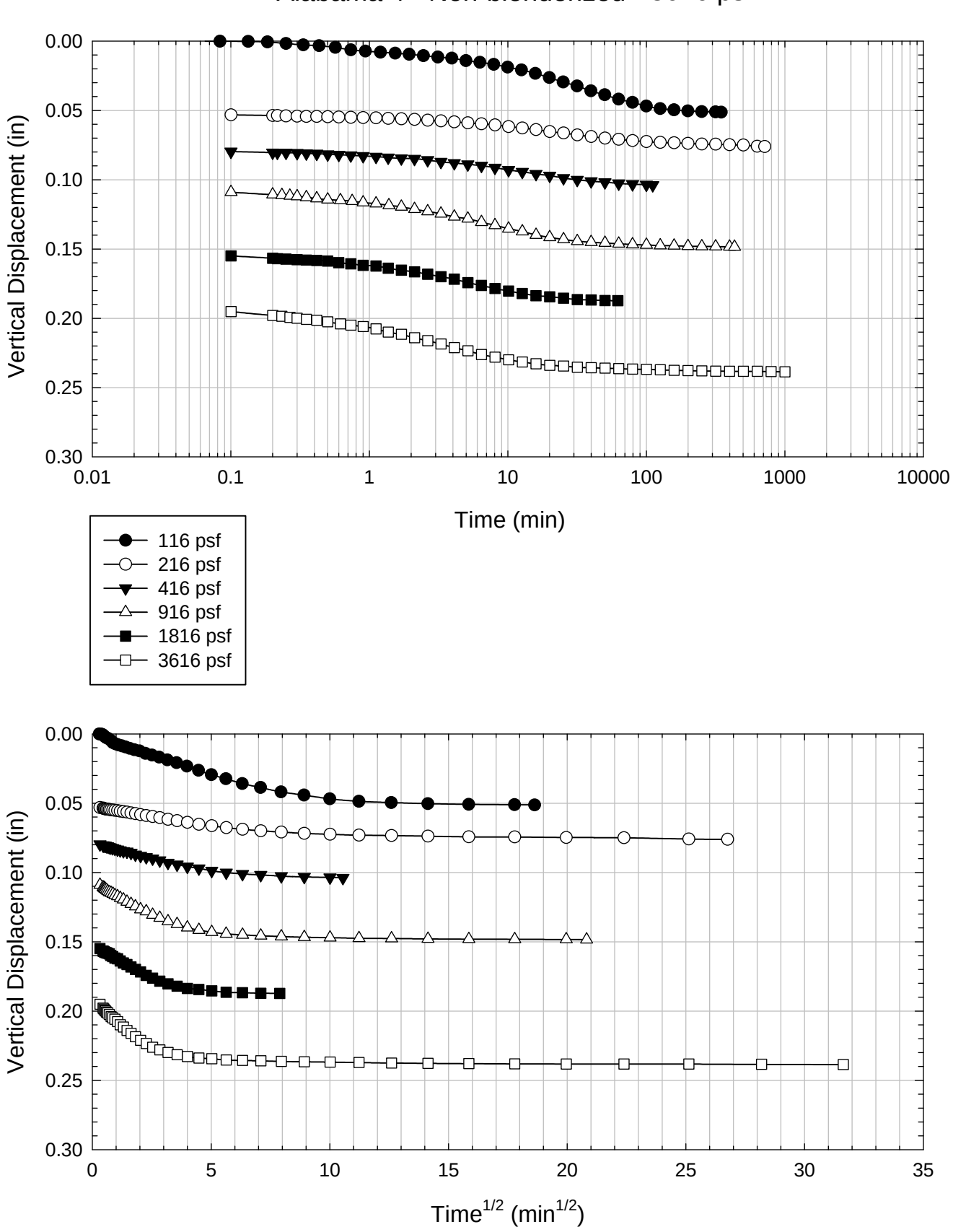
Alabama 4 - Non-blenderized - 3616 psf
Vertical Displacement (in)
0.00
0.05
0.10
0.15
0.20
0.25
0.30
0.01
0.1
1
10
100
1000
10000
Time (min)
116 psf
216 psf
416 psf
916 psf
1816 psf
3616 psf
Vertical Displacement (in)
0.00
0.05
0.10
0.15
0.20
0.25
0.30
0
5
10
15
20
25
30
35
Time^1/2 (min^1/2)

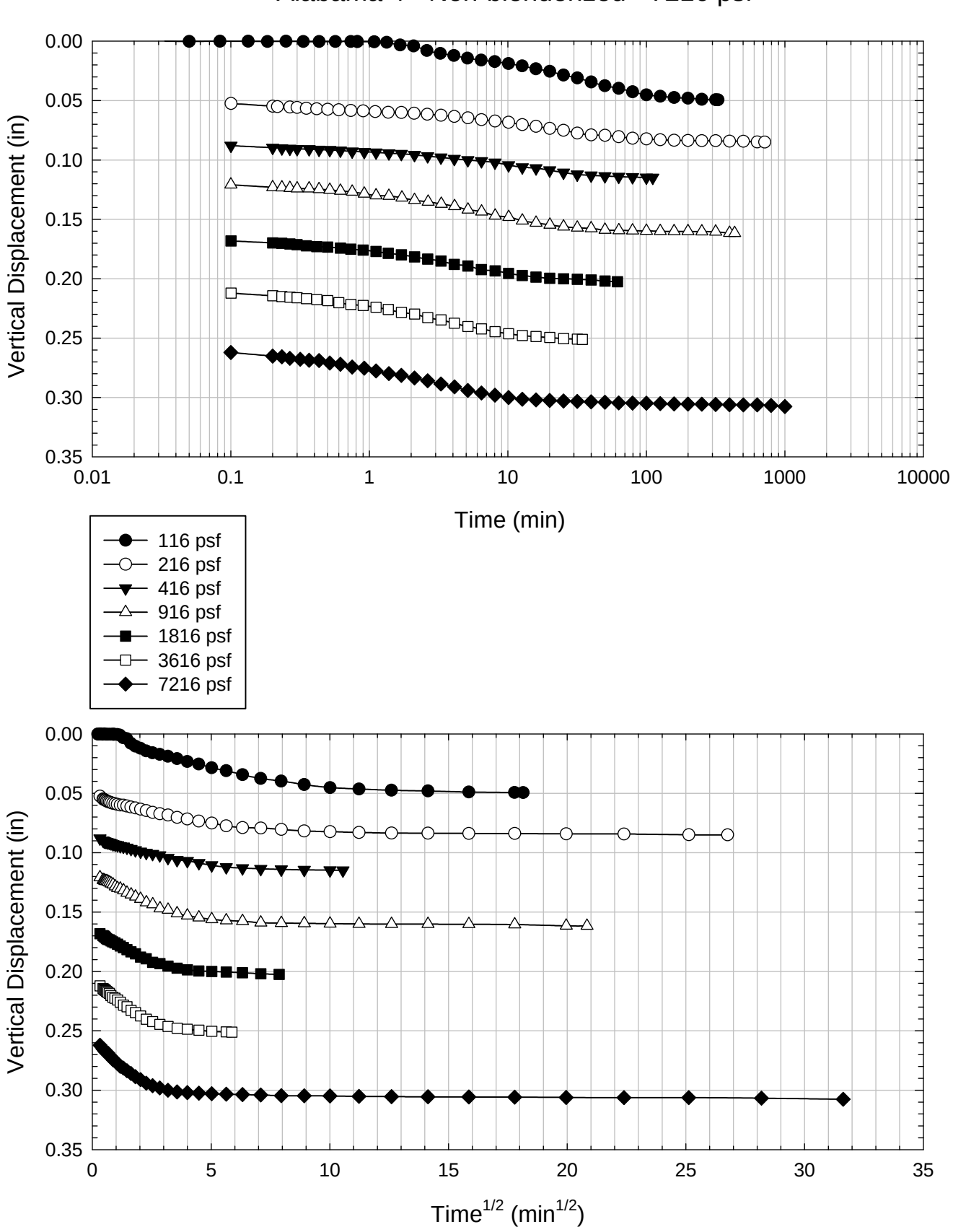
Alabama 4 - Non-blenderized - 7216 psf
Vertical Displacement (in)
0.00
0.05
0.10
0.15
0.20
0.25
0.30
0.35
0.01
0.1
1
10
100
1000
10000
Time (min)
116 psf
216 psf
416 psf
916 psf
1816 psf
3616 psf
7216 psf
Vertical Displacement (in)
0
5
10
15
20
25
30
35
Time1/2 (min1/2)

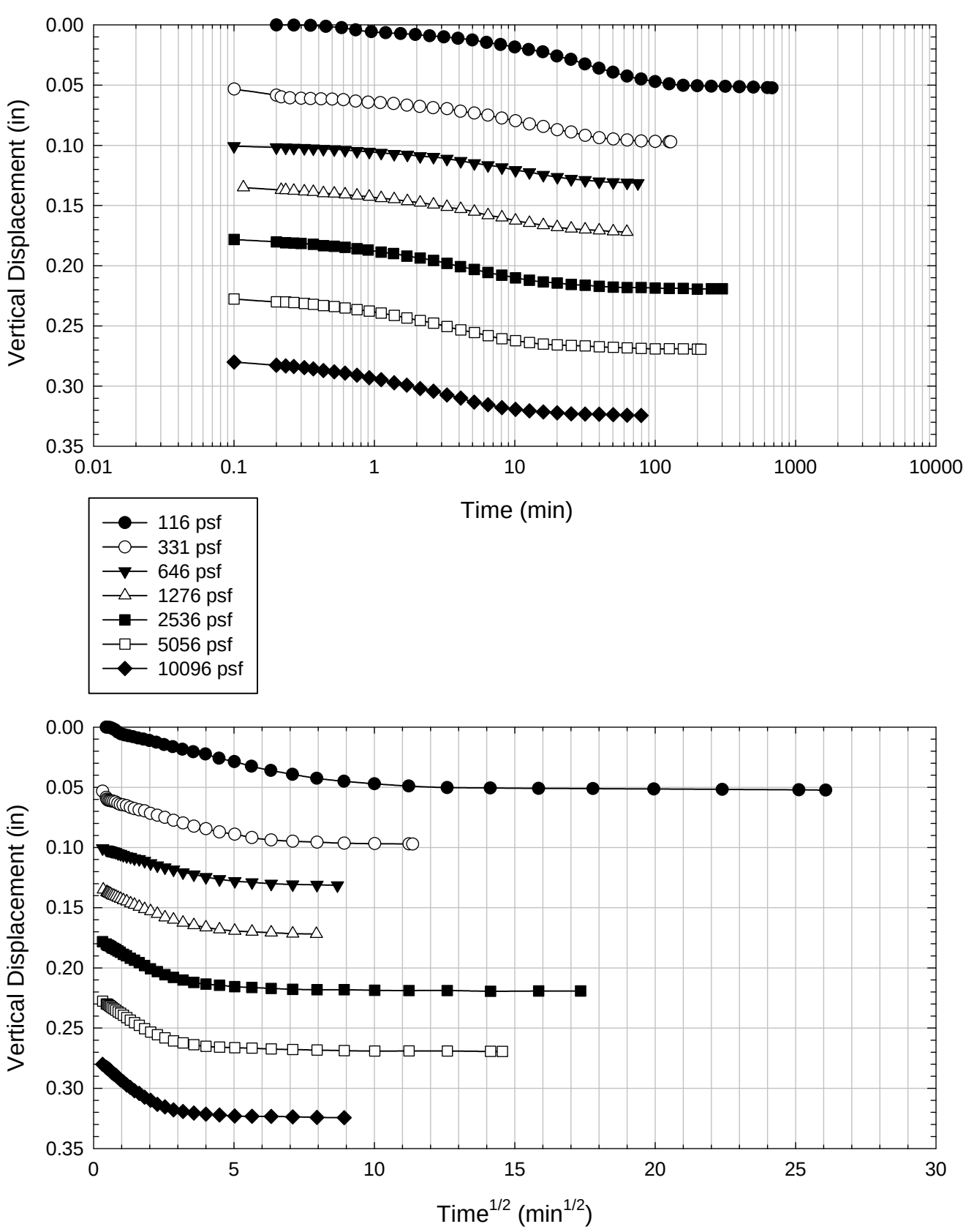
Alabama 4 - Non-blenderized - 10096 psf
Vertical Displacement (in)
0.00
0.05
0.10
0.15
0.20
0.25
0.30
0.35
0.01
0.1
1
10
100
1000
10000
Time (min)
116 psf
331 psf
646 psf
1276 psf
2536 psf
5056 psf
10096 psf
Vertical Displacement (in)
0
5
10
15
20
25
30
Time^1/2 (min^1/2)

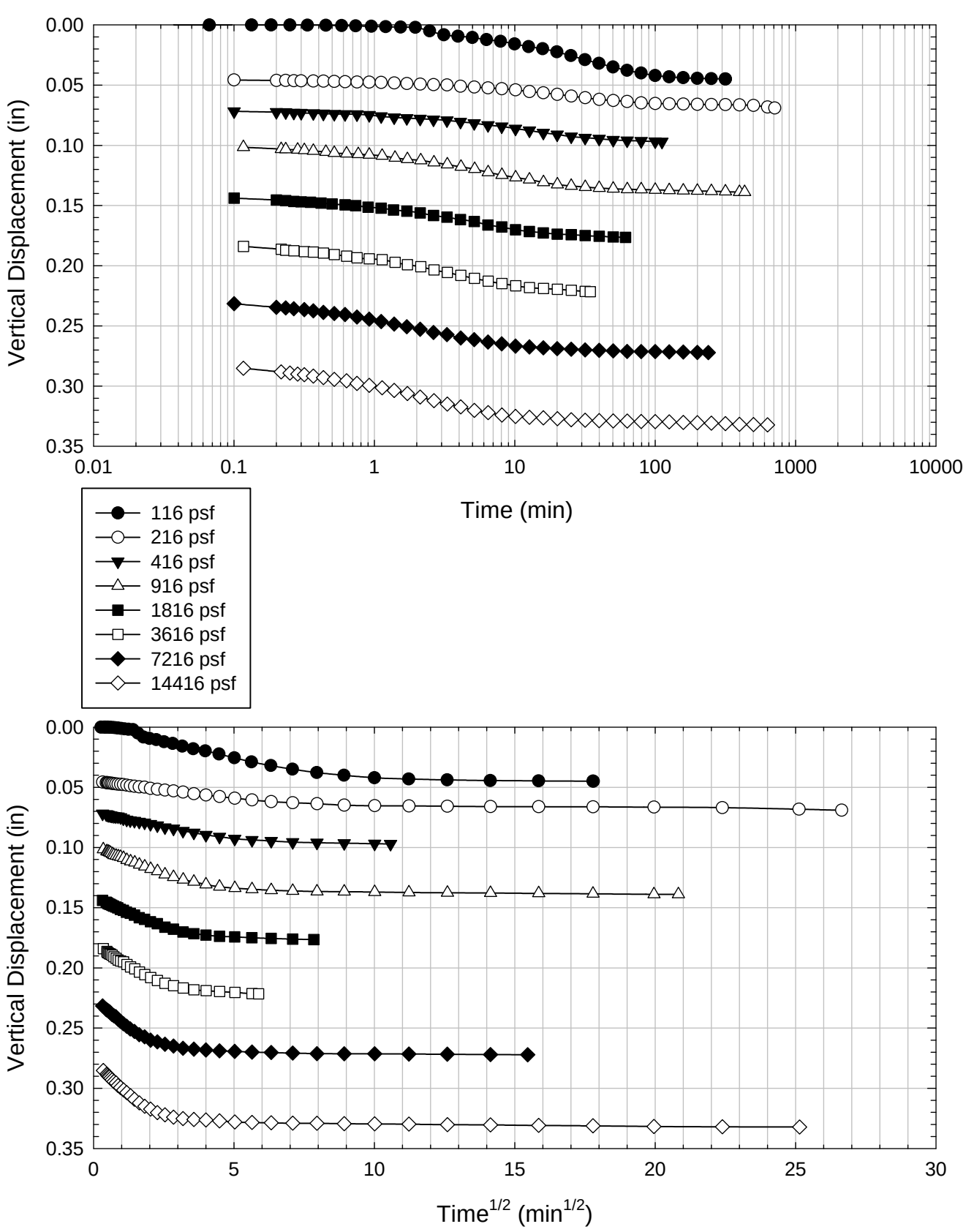
Alabama 4 - Non-blenderized - 14416 psf
Vertical Displacement (in)
0.00
0.05
0.10
0.15
0.20
0.25
0.30
0.35
0.01
0.1
1
10
100
1000
10000
Time (min)
116 psf
216 psf
416 psf
916 psf
1816 psf
3616 psf
7216 psf
14416 psf
Vertical Displacement (in)
0
5
10
15
20
25
30
Time^1/2 (min^1/2)

Alabama 4 - Non-blenderized

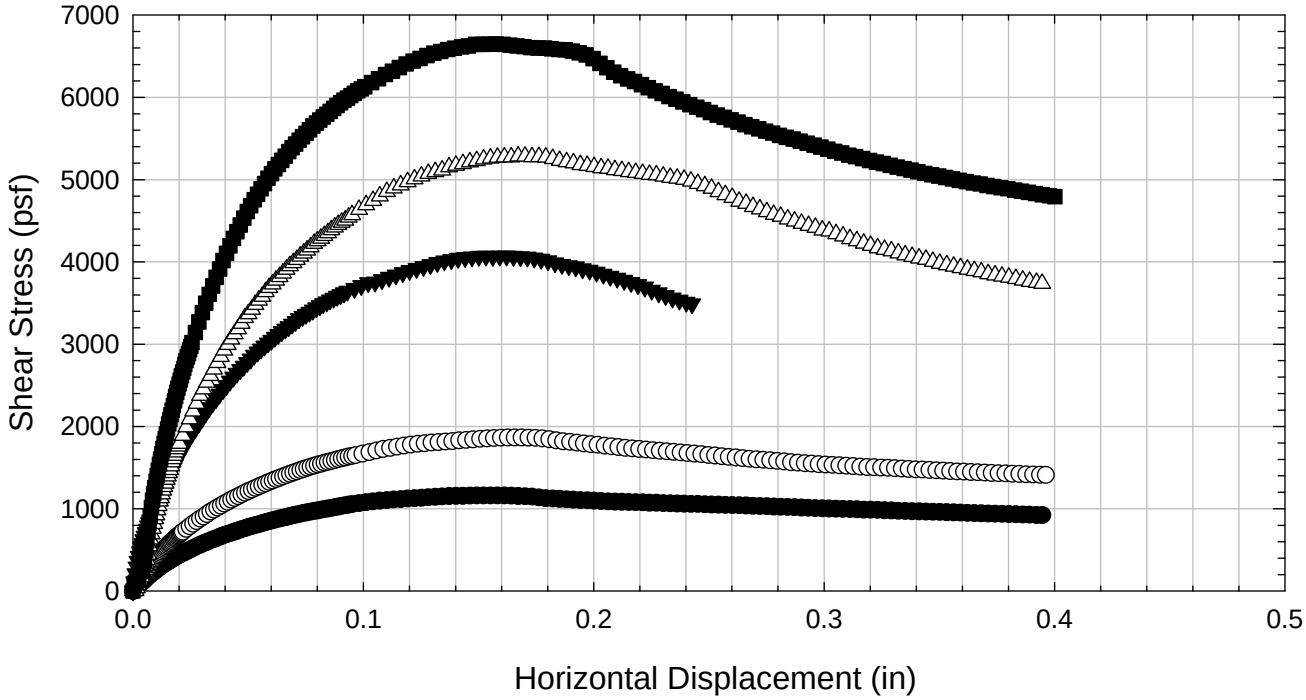

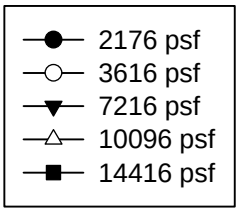

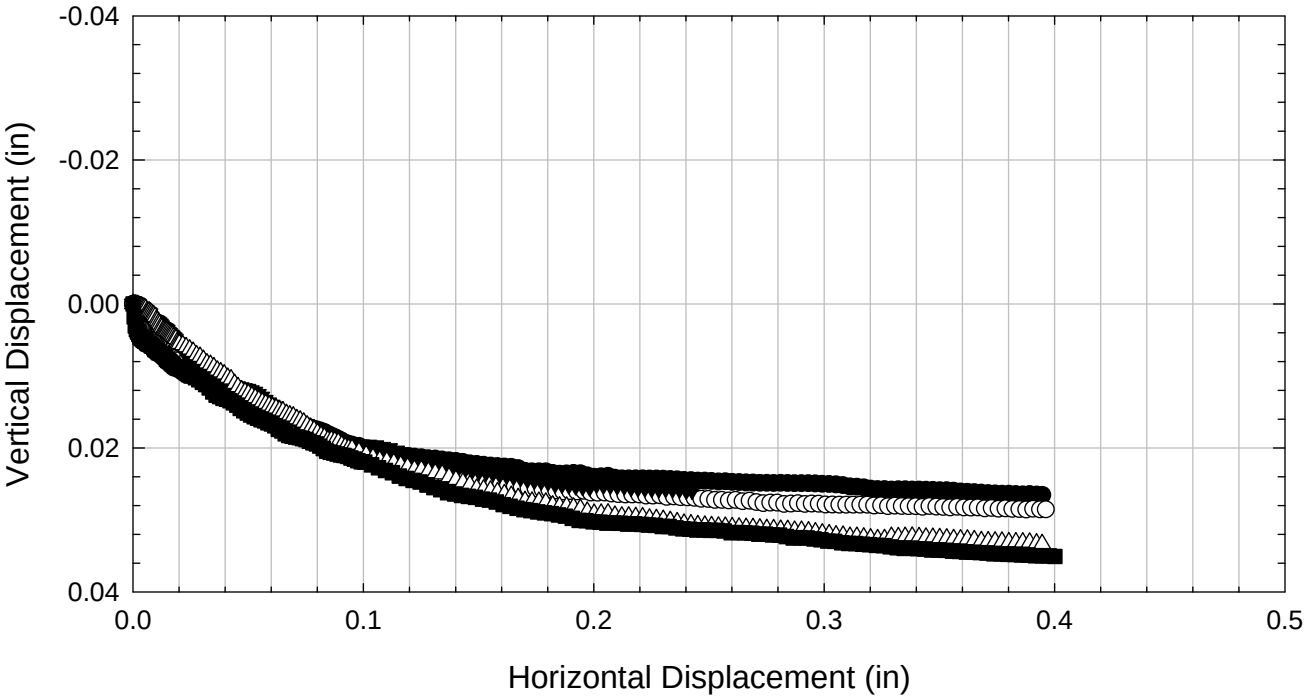

C.5. Colorado Clay

C.5.1 Blenderized

Virginia Polytechnic Institute and State University
Geotechnical Engineering Laboratory
Direct Shear Data Sheet

Project:	Fully Softened Shear Strength
Sample I.D./Loc.:	Colorado Clay - Blenderized
Classification:	Lean Clay (CL)

Sample Preparation	Remolded at LL		Specific Gravity	2.78

Test Number	1	2	3	4	5	6	7	
Start Date (m/d/y)	9/19/2011	9/14/2011	9/14/2011	9/14/2011	9/23/2011	9/12/2011		
End Date (m/d/y)	9/26/2011	9/22/2011	9/23/2011	9/23/2011	10/1/2011	9/21/2011		
Consolidation Pressure (psf)	516	1016	2016	3016	4516	6016		
Initial Values								
Initial Height (in)	1.43	1.42	1.44	1.44	1.43	1.42		
Initial Diameter (in)	2.50	2.50	2.50	2.50	2.50	2.50		
Initial Sample Weight (g)	206	209	211	211	212	206		
Water Content (%)	39.99	41.62	41.95	41.70	39.59	42.27		
Dry Unit Weight (pcf)	80.1	80.6	79.9	80.5	82.3	78.9		
Wet Unit Weight (pcf)	112.2	114.2	113.4	114.1	114.9	112.3		
Consolidation Pressures								
Load 1 (psf)	116	116	116	116	116	116		
Load 2 (psf)	266	266	266	216	266	216		
Load 3 (psf)	516	516	516	391	516	391		
Load 4 (psf)		1016	1016	766	1141	766		
Load 5 (psf)			2016	1516	2266	1516		
Load 6 (psf)				3016	4516	3016		
Load 7 (psf)						6016		
t_{50}								
Max. t_{50} for Load 1 (min)								
Max. t_{50} for Load 2 (min)								
Max. t_{50} for Load 3 (min)	44.56							
Max. t_{50} for Load 4 (min)		26.43						
Max. t_{50} for Load 5 (min)			14.83					
Max. t_{50} for Load 6 (min)				18.85	16.74			
Max. t_{50} for Load 7 (min)						11.22		
Final Values								
Water Content (%)	31.72	30.62	28.52	26.79	25.55	24.30		
Dry Unit Weight (pcf)	89.9	94.6	97.7	100.6	104.5	106.55		
Wet Unit Weight (pcf)	118.4	123.6	125.5	127.5	131.2	132.44		
Failure								
Test Performed at Shear Rate (in/min)	4.55E-05	8.70E-05	1.07E-04	1.11E-04	1.19E-04	1.80E-04		
Required Shear Rate (in/min)	6.73E-05	1.89E-04	3.37E-04	1.91E-04	2.27E-04	3.39E-04		
Displacement at Failure (in)	0.15	0.25	0.25	0.18	0.19	0.19		
Peak Shear Stress (psf)	397	661	1281	1935	2723	3516		
Total Change in Height at Failure (in)	0.15	0.21	0.26	0.28	0.30	0.37		
Secant Effective Friction Angle (deg)	37.6	33.0	32.4	32.7	31.1	30.3		

Comments:

Colorado Clay - Blenderized - 516 psf

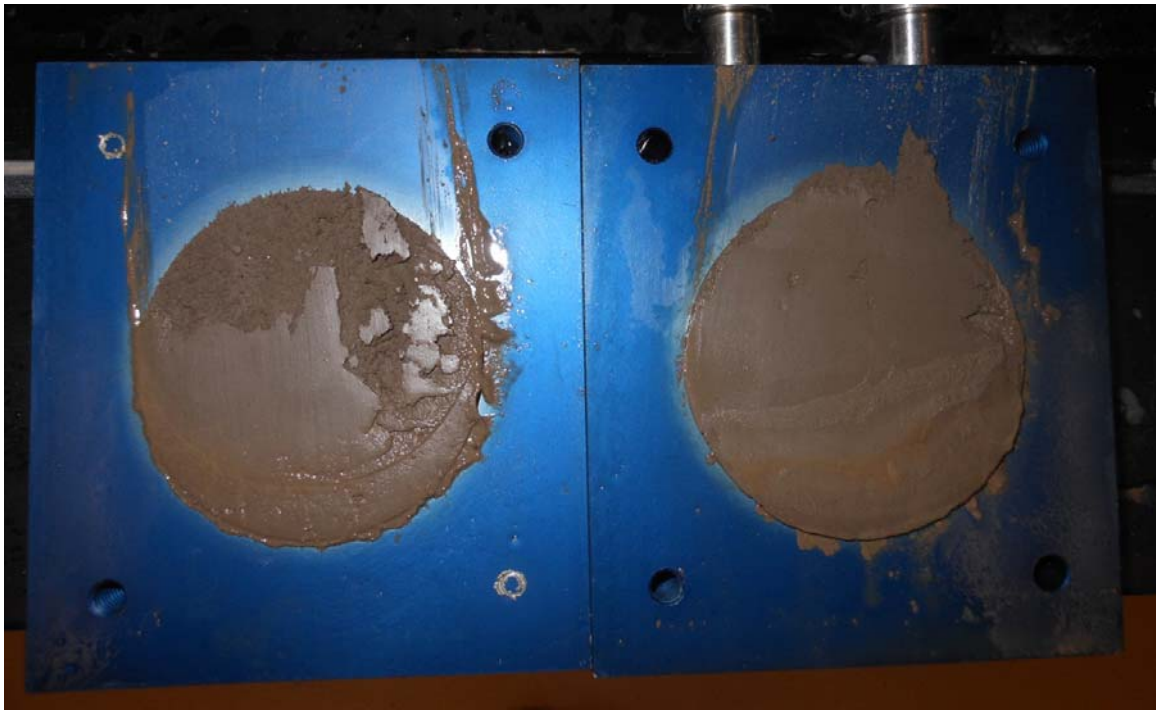

Colorado Clay - Blenderized - 1016 psf

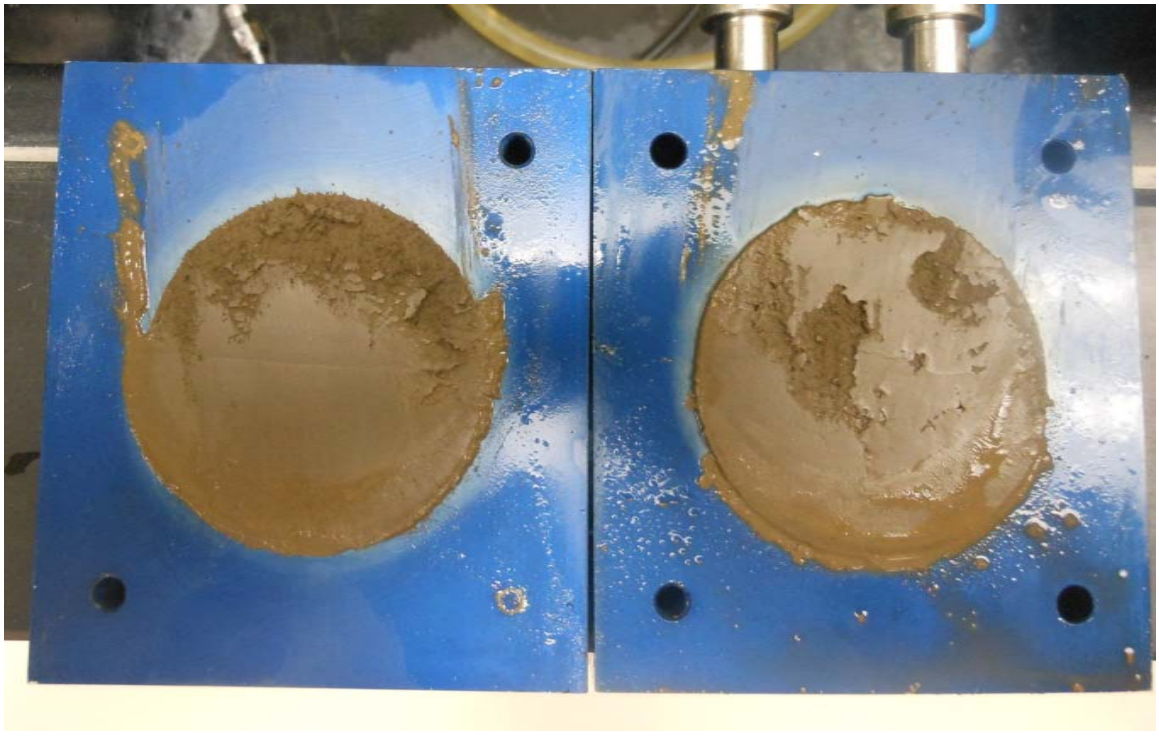

Colorado Clay - Blenderized - 2016 psf

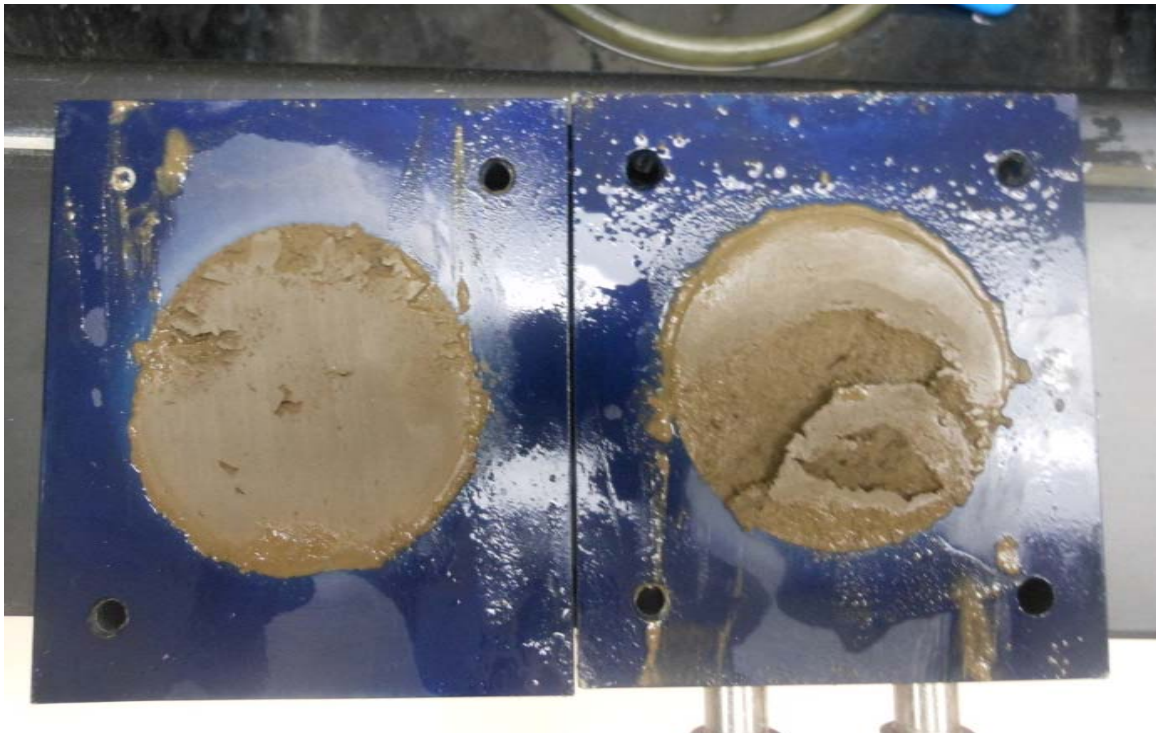

Colorado Clay - Blenderized - 3016 psf

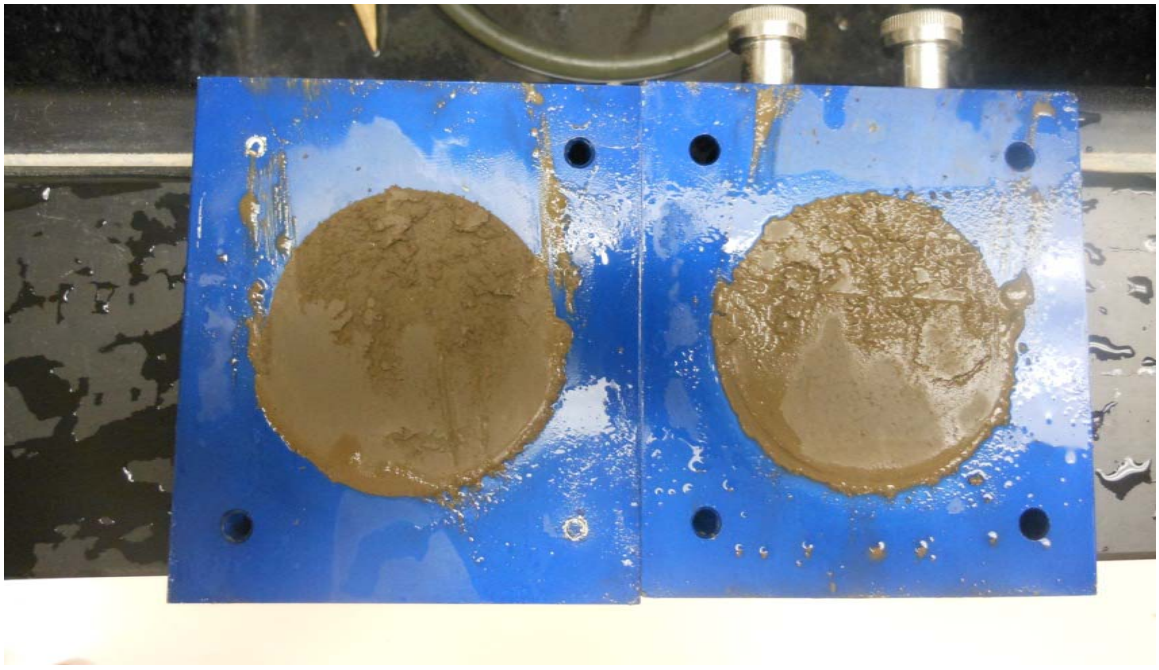

Colorado Clay - Blenderized - 4516 psf

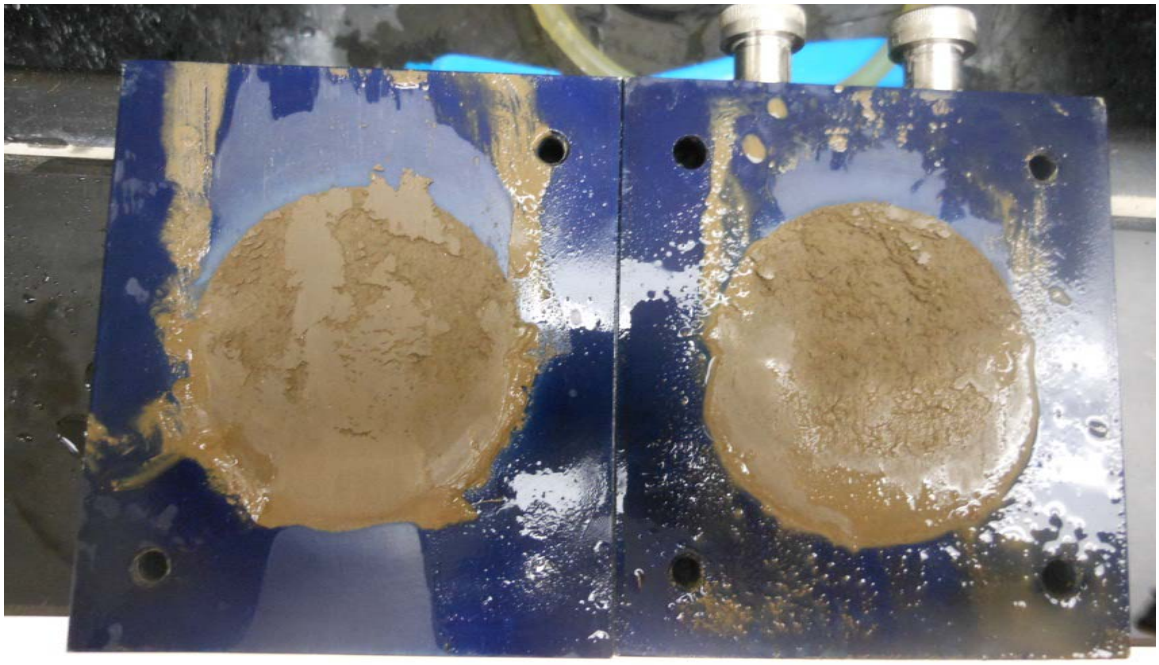

Colorado Clay - Blenderized - 6016 psf

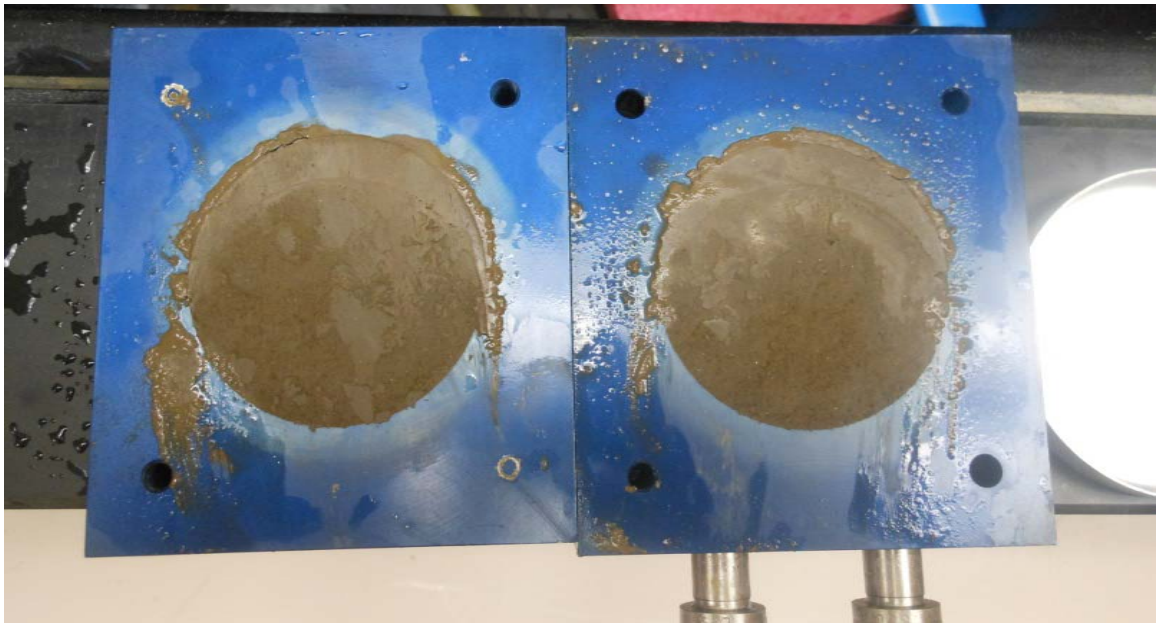

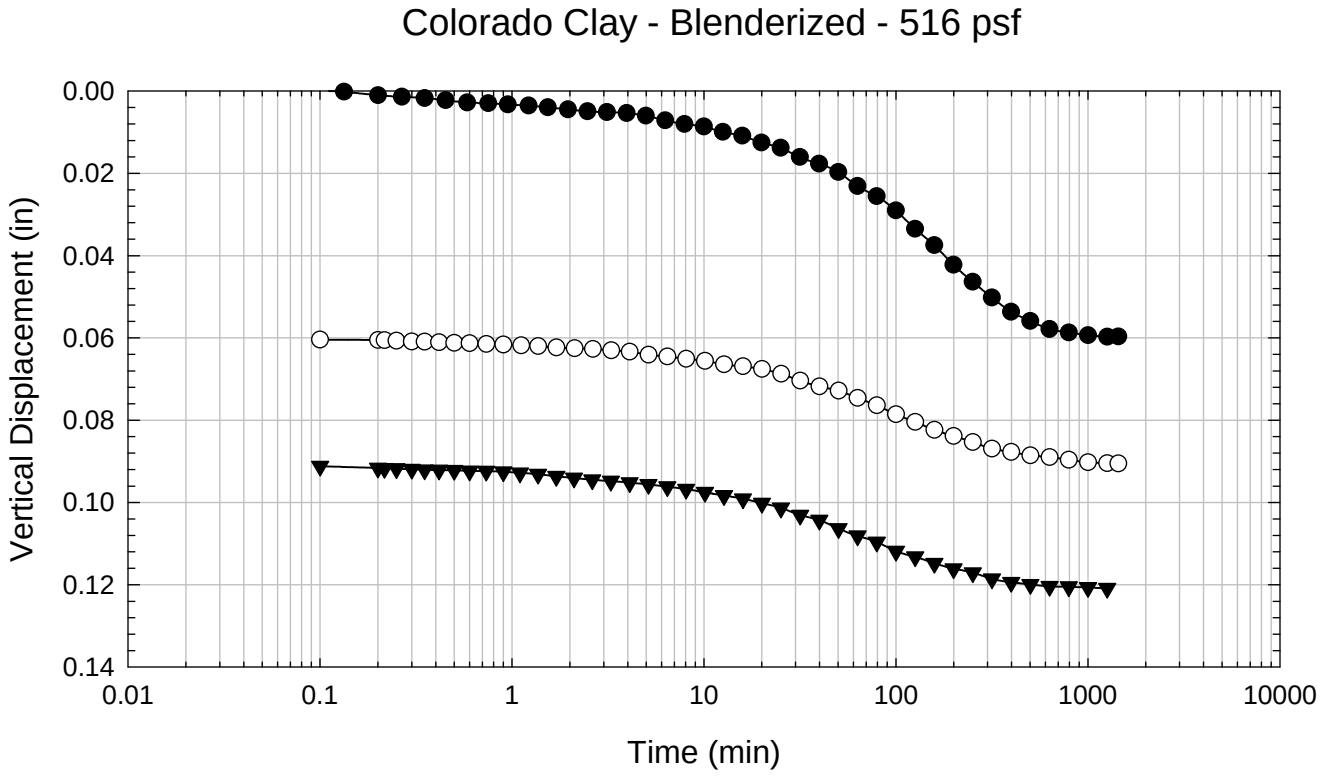
Colorado Clay - Blenderized - 516 psf
Vertical Displacement (in)
0.00
0.02
0.04
0.06
0.08
0.10
0.12
0.14
0.01
0.1
1
10
100
1000
10000
Time (min)

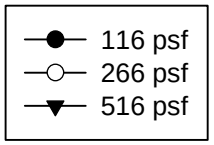
116 psf
266 psf
516 psf

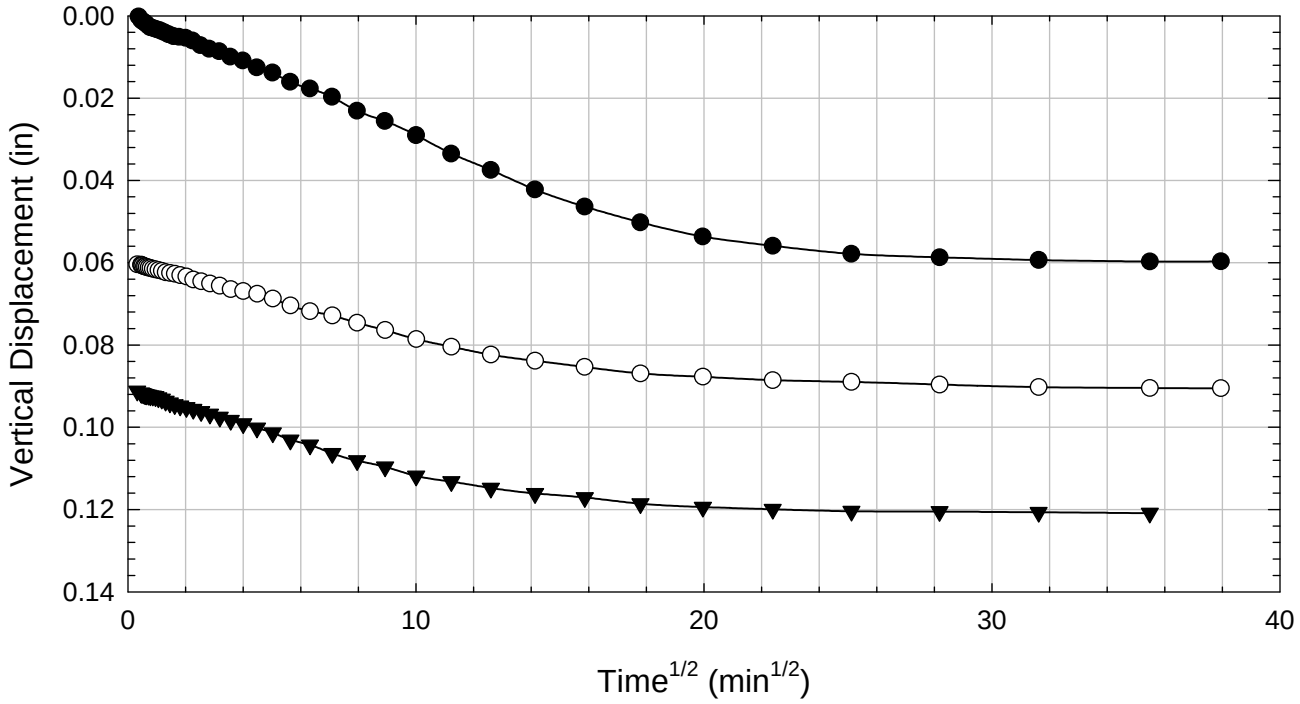
Vertical Displacement (in)
0.00
0.02
0.04
0.06
0.08
0.10
0.12
0.14
0
10
20
30
40
Time1/2 (min1/2)

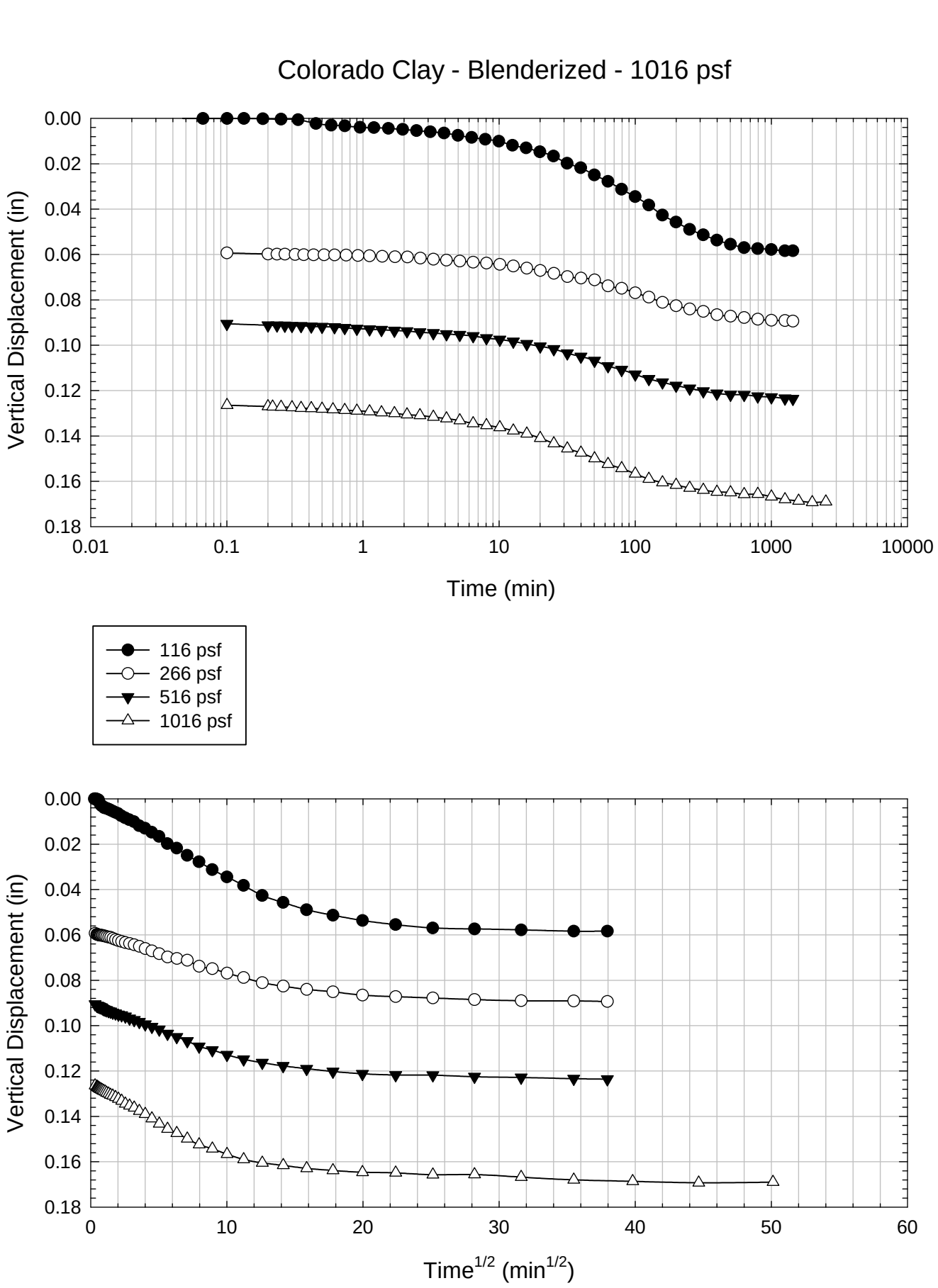
Colorado Clay - Blenderized - 1016 psf
Vertical Displacement (in)
0.00
0.02
0.04
0.06
0.08
0.10
0.12
0.14
0.16
0.18
0.01
0.1
1
10
100
1000
10000
Time (min)
116 psf
266 psf
516 psf
1016 psf
Vertical Displacement (in)
0
10
20
30
40
50
60
Time^1/2 (min^1/2)

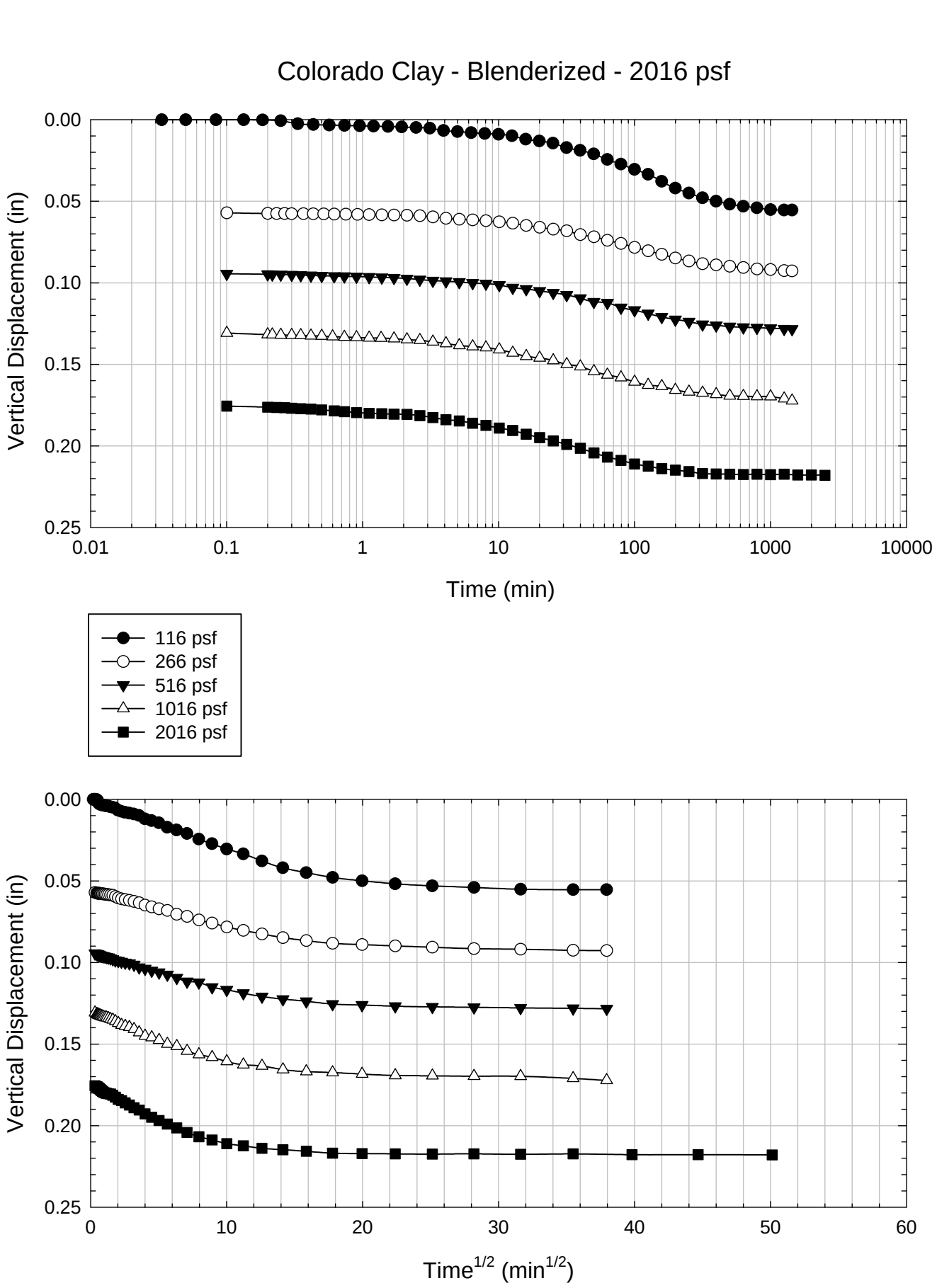
Colorado Clay - Blenderized - 2016 psf
Vertical Displacement (in)
0.00
0.05
0.10
0.15
0.20
0.25
0.01
0.1
1
10
100
1000
10000
Time (min)
116 psf
266 psf
516 psf
1016 psf
2016 psf
Vertical Displacement (in)
0.00
0.05
0.10
0.15
0.20
0.25
0
10
20
30
40
50
60
Time1/2 (min1/2)

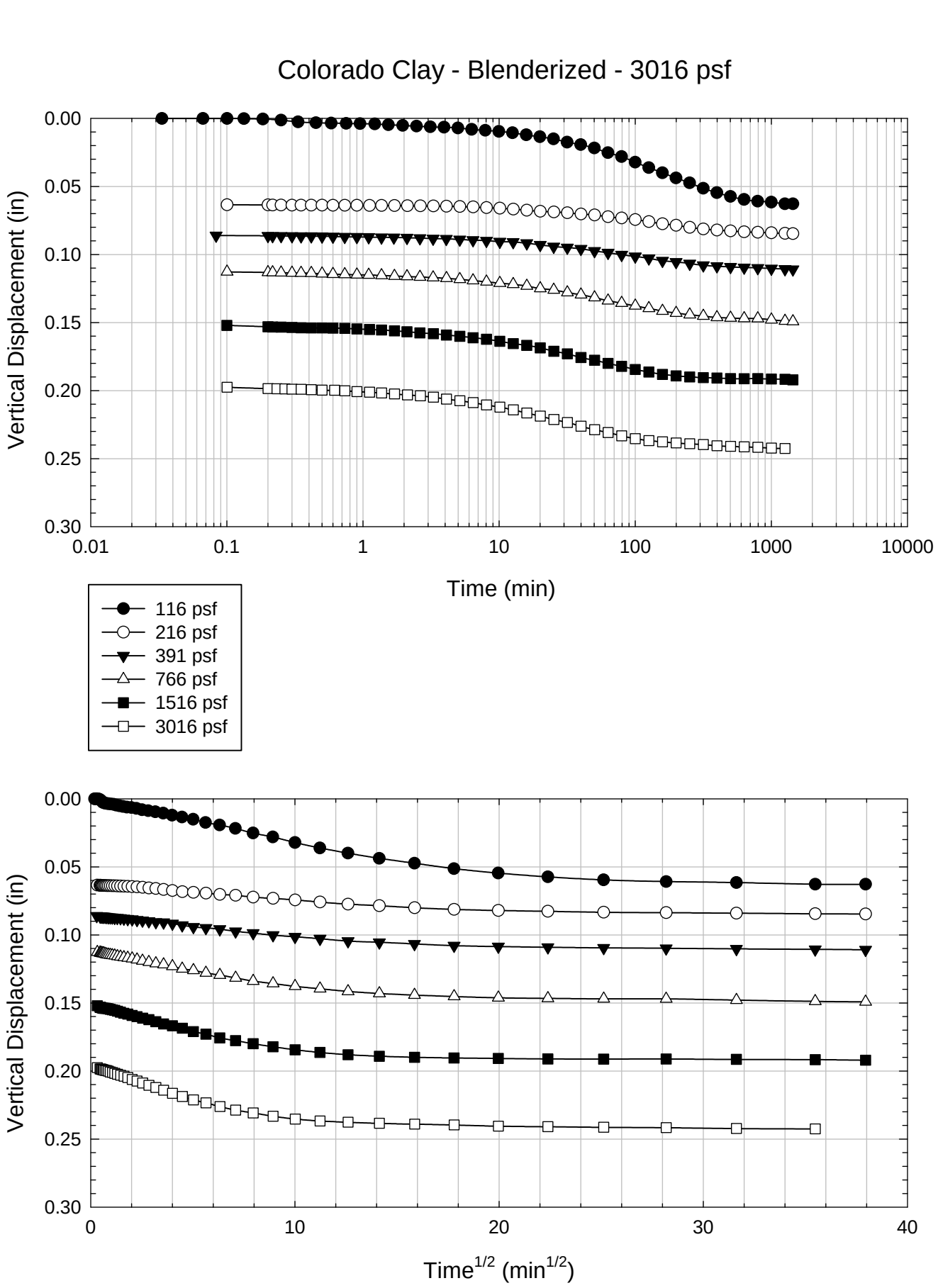
Colorado Clay - Blenderized - 3016 psf
Vertical Displacement (in)
0.00
0.05
0.10
0.15
0.20
0.25
0.30
0.01
0.1
1
10
100
1000
10000
Time (min)
116 psf
216 psf
391 psf
766 psf
1516 psf
3016 psf
Vertical Displacement (in)
0.00
0.05
0.10
0.15
0.20
0.25
0.30
0
10
20
30
40
Time^1/2 (min^1/2)

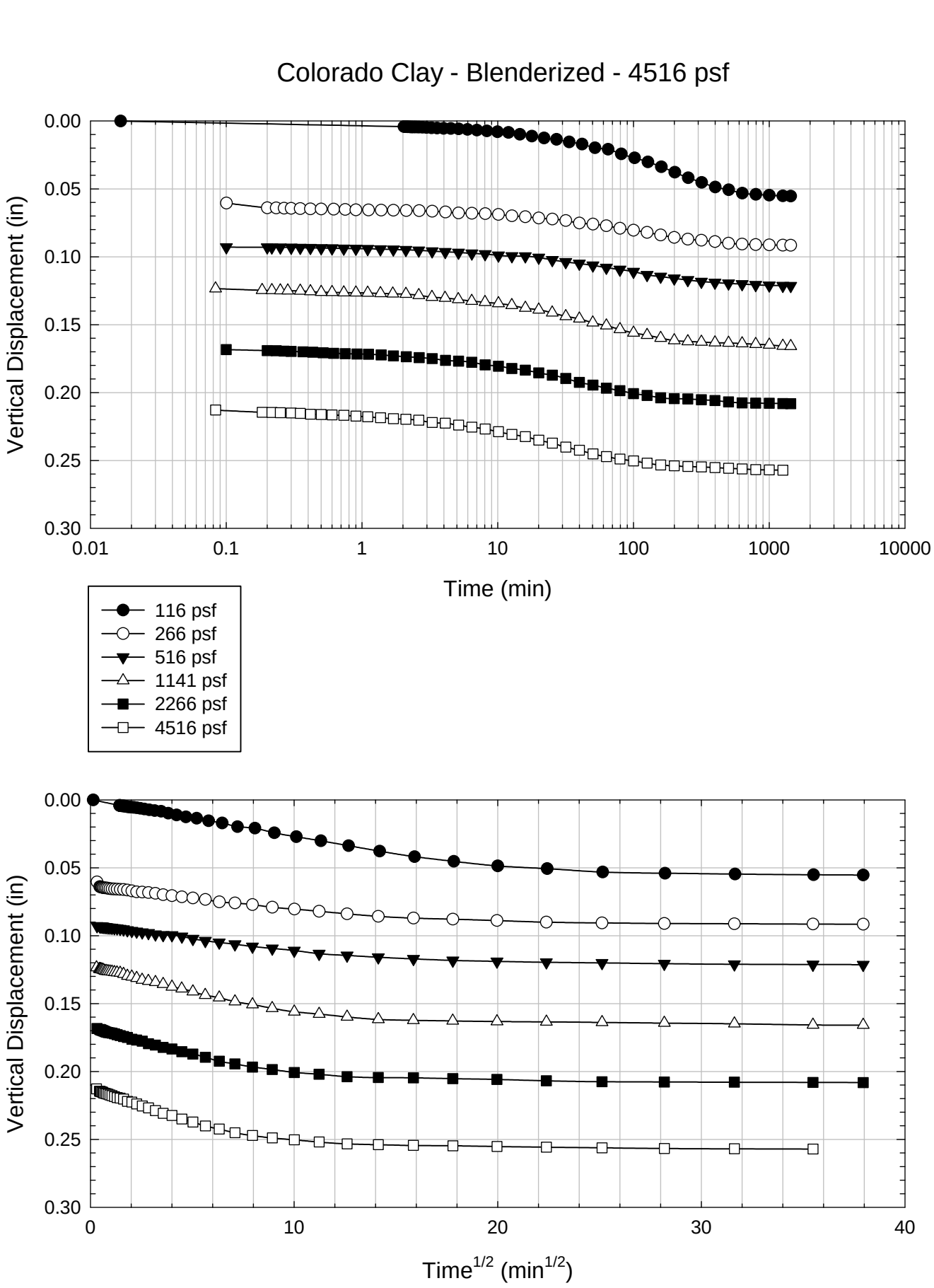
Colorado Clay - Blenderized - 4516 psf
Vertical Displacement (in)
0.00
0.05
0.10
0.15
0.20
0.25
0.30
0.01
0.1
1
10
100
1000
10000
Time (min)
116 psf
266 psf
516 psf
1141 psf
2266 psf
4516 psf
Vertical Displacement (in)
0.00
0.05
0.10
0.15
0.20
0.25
0.30
0
10
20
30
40
Time1/2 (min1/2)

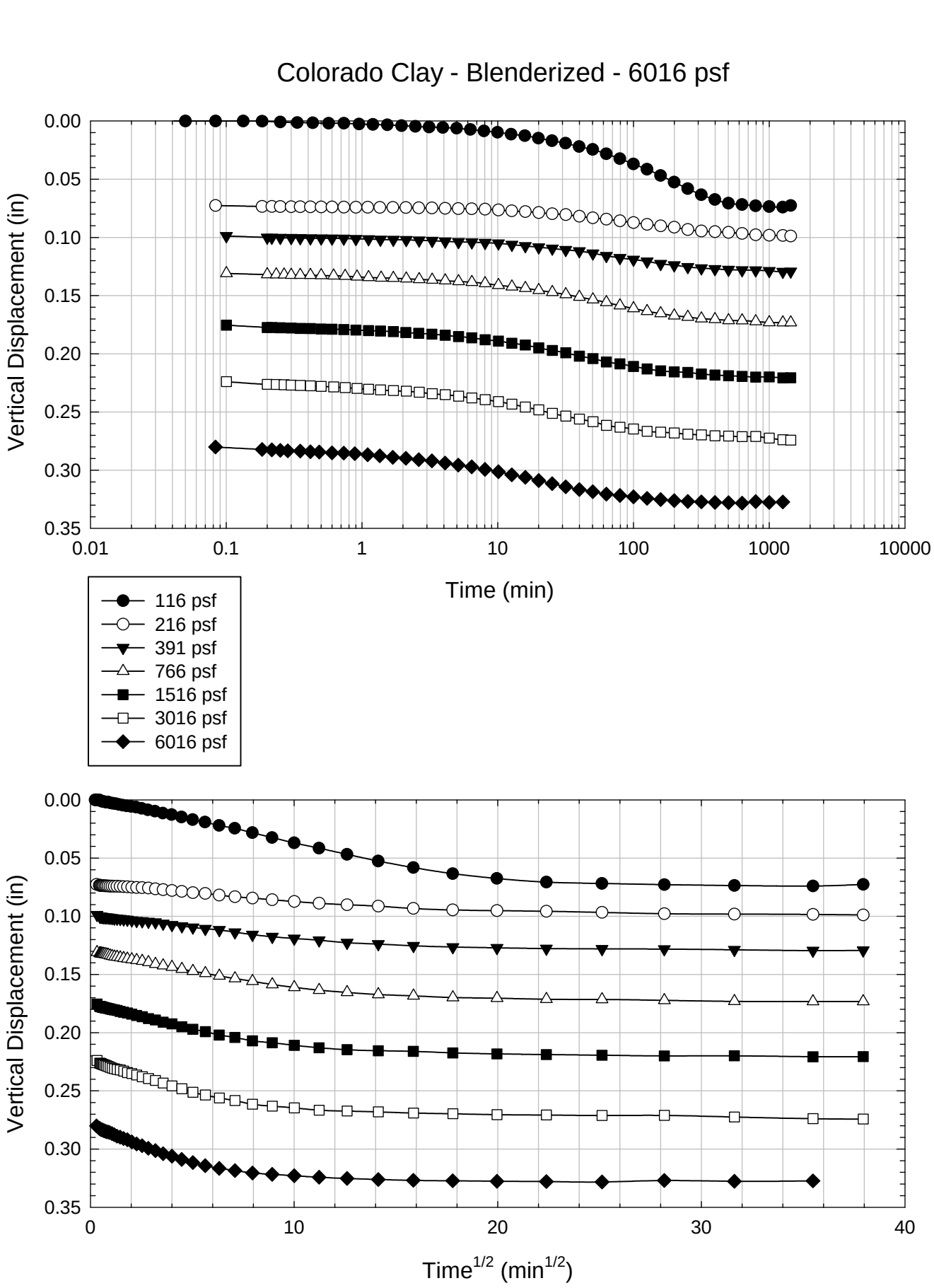
Colorado Clay - Blenderized - 6016 psf
Vertical Displacement (in)
0.00
0.05
0.10
0.15
0.20
0.25
0.30
0.35
0.01
0.1
1
10
100
1000
10000
Time (min)
116 psf
216 psf
391 psf
766 psf
1516 psf
3016 psf
6016 psf
Vertical Displacement (in)
0
10
20
30
40
Time^1/2 (min^1/2)

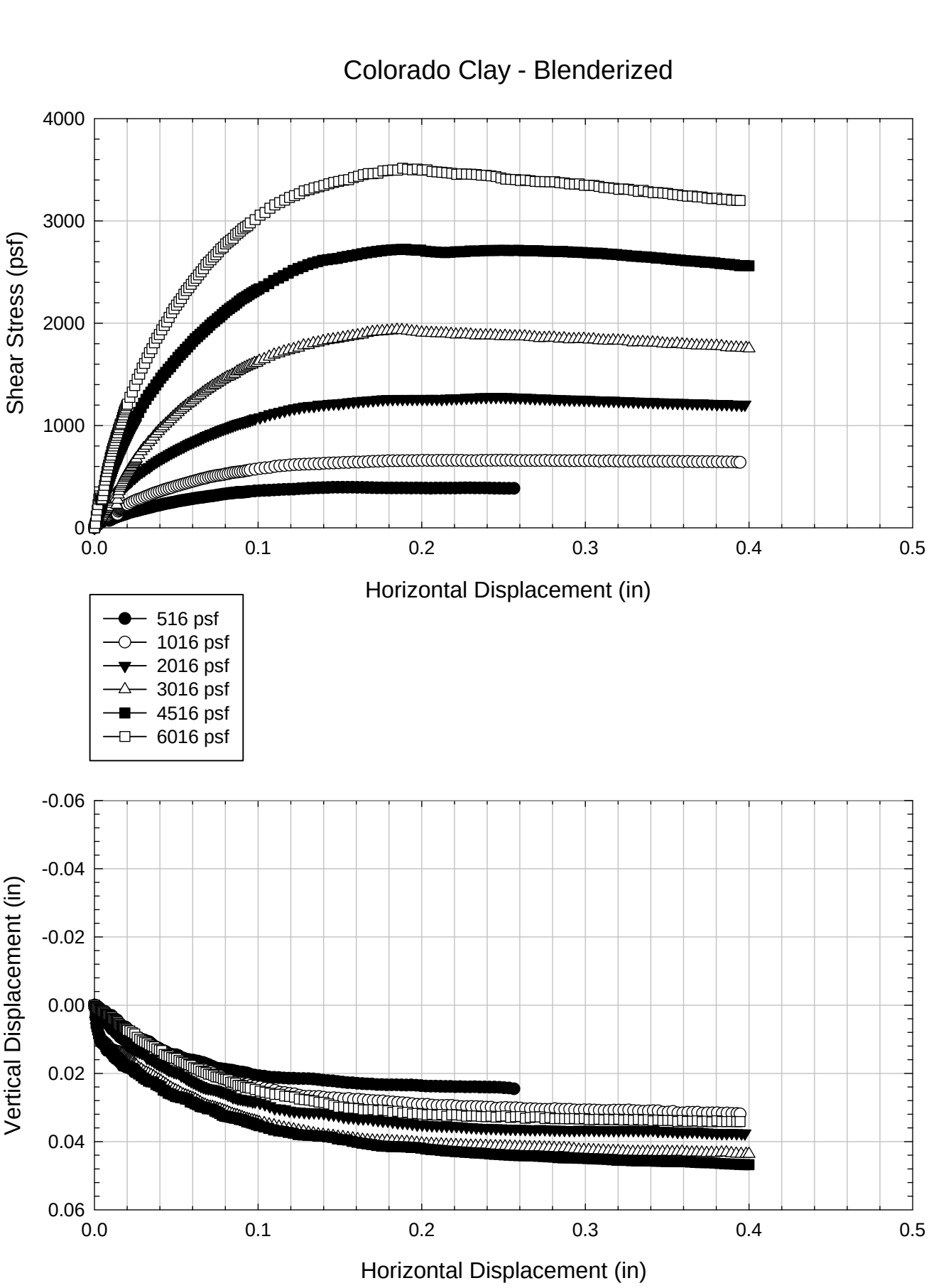
Colorado Clay - Blenderized
Shear Stress (psf)
4000
3000
2000
1000
0
0.0
0.1
0.2
0.3
0.4
0.5
Horizontal Displacement (in)
516 psf
1016 psf
2016 psf
3016 psf
4516 psf
6016 psf
Vertical Displacement (in)
-0.06
-0.04
-0.02
0.00
0.02
0.04
0.06
0.0
0.1
0.2
0.3
0.4
0.5
Horizontal Displacement (in)

C.5.2 Non-blenderized

Virginia Polytechnic Institute and State University
Geotechnical Engineering Laboratory
Direct Shear Data Sheet

Project:	Fully Softened Shear Strength
Sample I.D./Loc.:	Colorado Clay - Non-blenderized
Classification:	Lean Clay (CL)

Sample Preparation	Remolded at LL		Specific Gravity	2.78

Test Number	1	2	3	4	5	6	7	
Start Date (m/d/y)	4/9/2012	4/9/2012	4/9/2012	4/9/2012	4/9/2012	4/9/2012		
End Date (m/d/y)	4/18/2012	4/18/2012	4/18/2012	4/18/2012	4/18/2012	4/19/2012		
Consolidation Pressure (psf)	516	1016	2016	3016	4516	6016		
Initial Values								
Initial Height (in)	1.43	1.43	1.41	1.39	1.39	1.42		
Initial Diameter (in)	2.50	2.50	2.50	2.50	2.50	2.50		
Initial Sample Weight (g)	205	207	202	203	208	207		
Water Content (%)	44.34	44.00	43.72	43.91	43.32	43.17		
Dry Unit Weight (pcf)	77.1	78.2	77.3	78.9	80.8	79.0		
Wet Unit Weight (pcf)	111.3	112.6	111.1	113.6	115.8	113.0		
Consolidation Pressures								
Load 1 (psf)	116	116	116	116	116	116		
Load 2 (psf)	266	266	266	216	266	216		
Load 3 (psf)	516	516	516	391	516	391		
Load 4 (psf)		1016	1016	766	1141	766		
Load 5 (psf)			2016	1516	2266	1516		
Load 6 (psf)				3016	4516	3016		
Load 7 (psf)						6016		
t_{50}								
Max. t_{50} for Load 1 (min)								
Max. t_{50} for Load 2 (min)								
Max. t_{50} for Load 3 (min)	42.01							
Max. t_{50} for Load 4 (min)		32.46						
Max. t_{50} for Load 5 (min)			23.60					
Max. t_{50} for Load 6 (min)				18.66	19.54			
Max. t_{50} for Load 7 (min)						18.23		
Final Values								
Water Content (%)	33.63	31.00	28.71	26.69	25.37	24.28		
Dry Unit Weight (pcf)	89.1	93.3	96.0	102.1	105.6	106.95		
Wet Unit Weight (pcf)	119.0	122.3	123.6	129.4	132.4	132.92		
Failure								
Test Performed at Shear Rate (in/min)	4.76E-05	6.16E-05	8.47E-05	1.07E-04	1.02E-04	1.10E-04		
Required Shear Rate (in/min)	1.14E-04	1.42E-04	1.69E-04	2.79E-04	2.25E-04	2.08E-04		
Displacement at Failure (in)	0.24	0.23	0.20	0.26	0.22	0.19		
Peak Shear Stress (psf)	348	661	1234	1786	2490	3533		
Total Change in Height at Failure (in)	0.19	0.23	0.27	0.31	0.32	0.37		
Secant Effective Friction Angle (deg)	34.0	33.0	31.5	30.6	28.9	30.4		

Comments:

Colorado Clay – Non-blenderized - 516 psf

Colorado Clay - Non-blenderized - 1016 psf

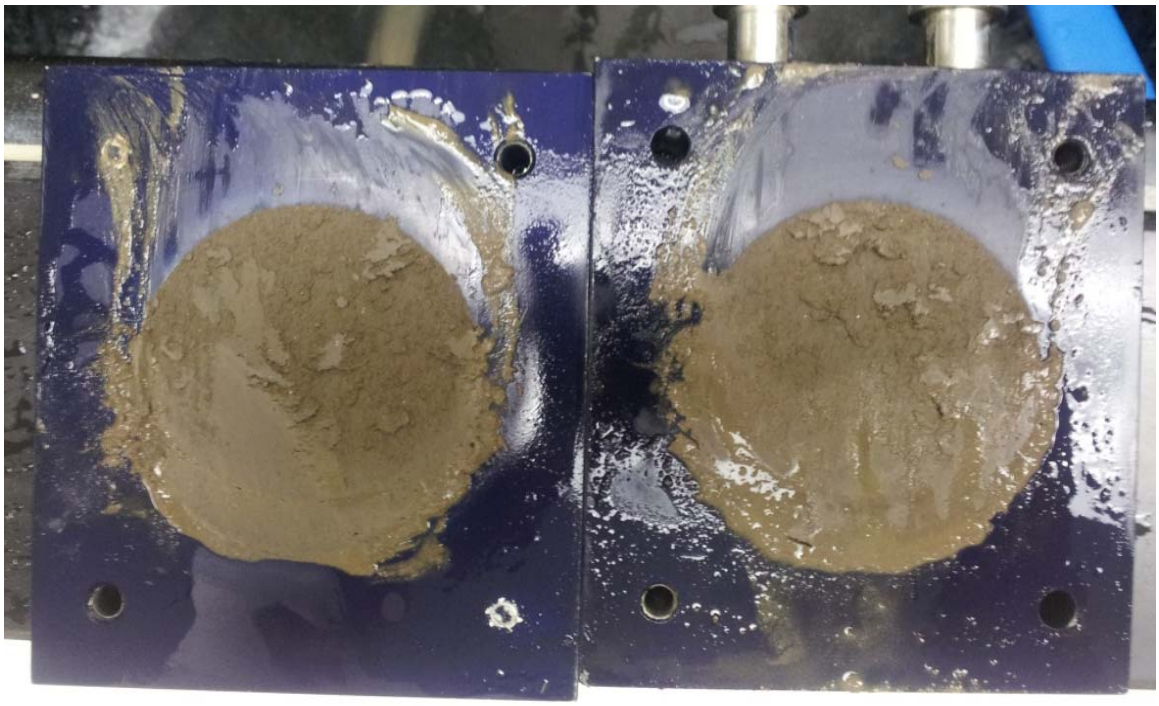

Colorado Clay - Non-blenderized - 2016 psf

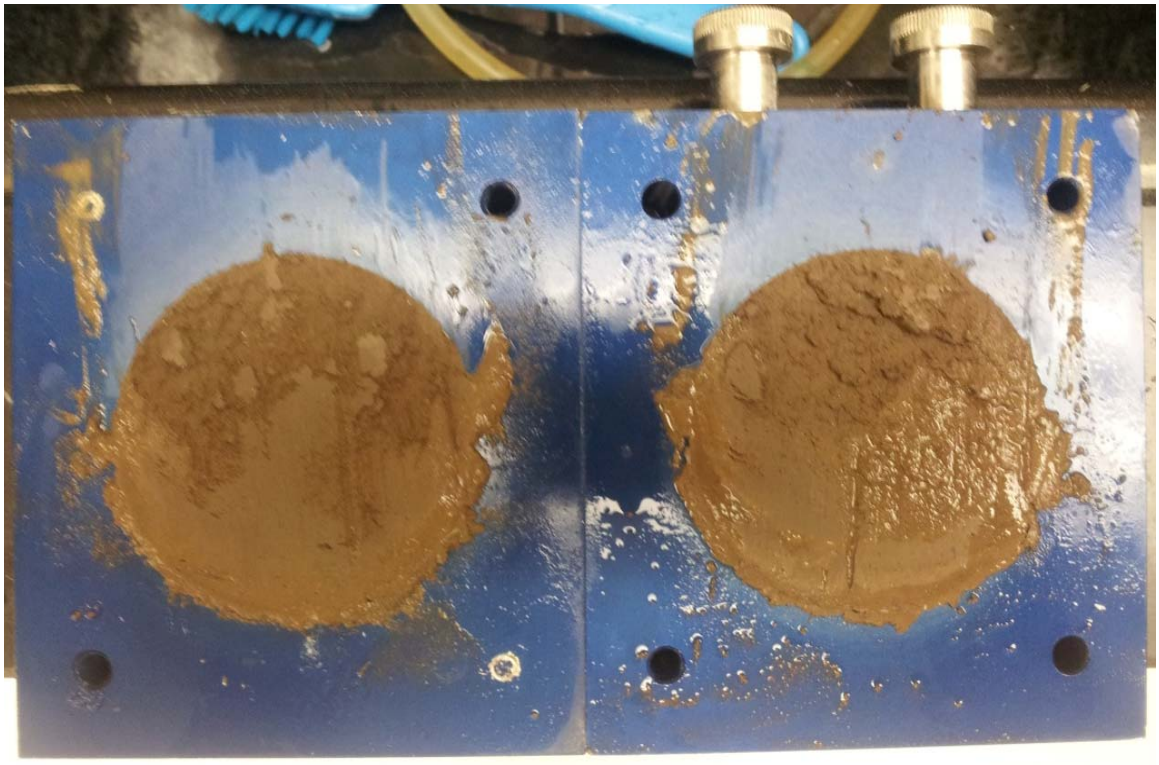

Colorado Clay - Non-blenderized - 3016 psf

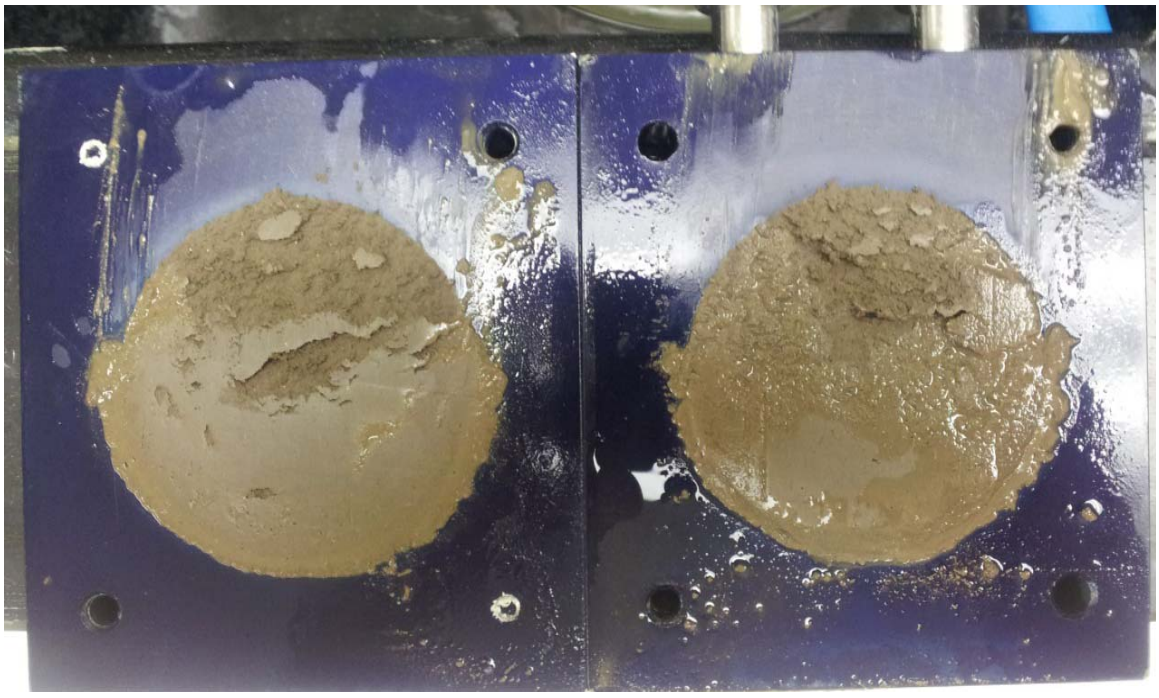

Colorado Clay - Non-blenderized - 4516 psf

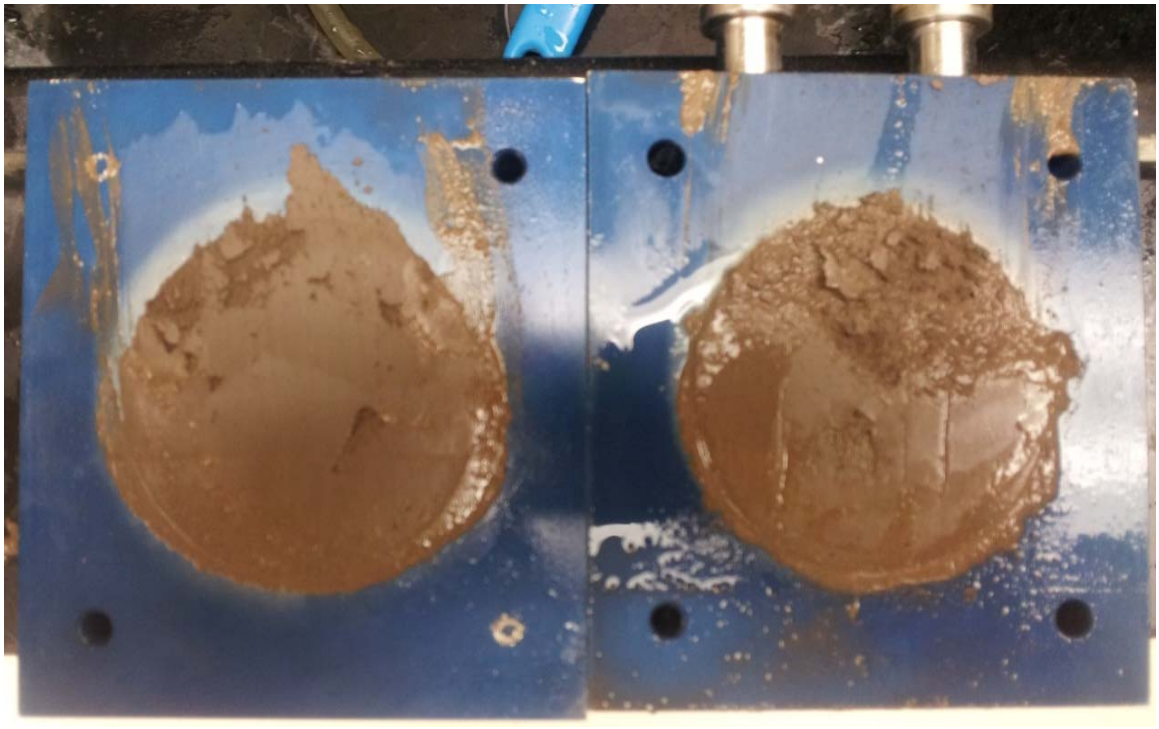

Colorado Clay – Non-blenderized - 6016 psf

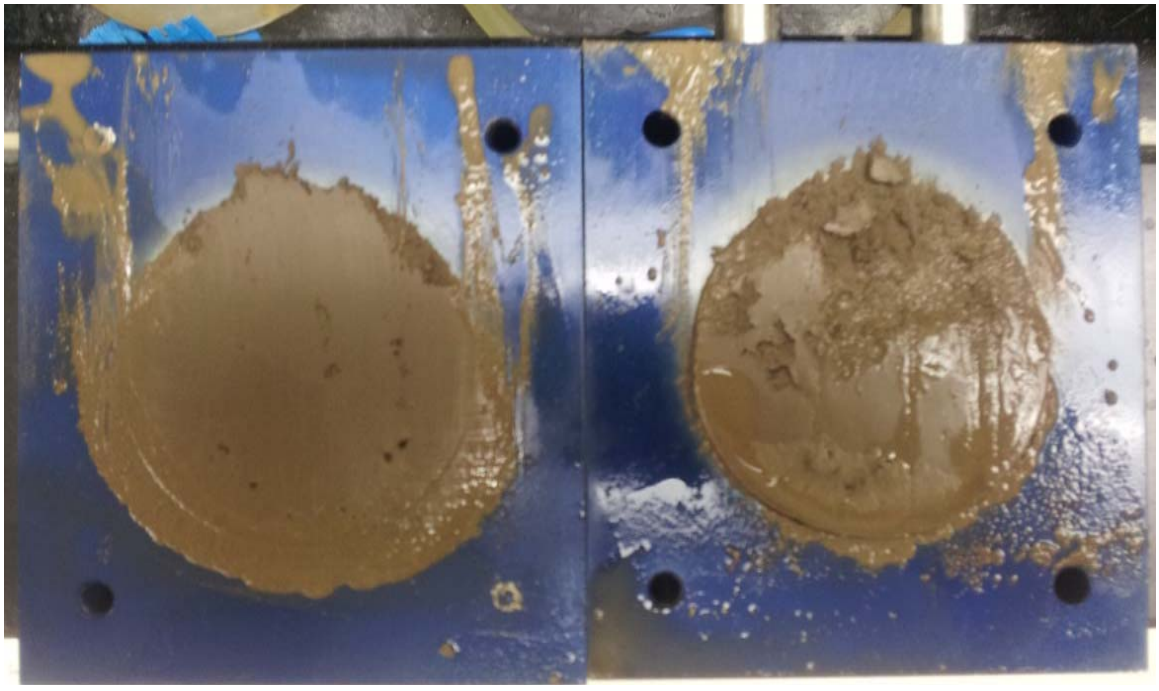

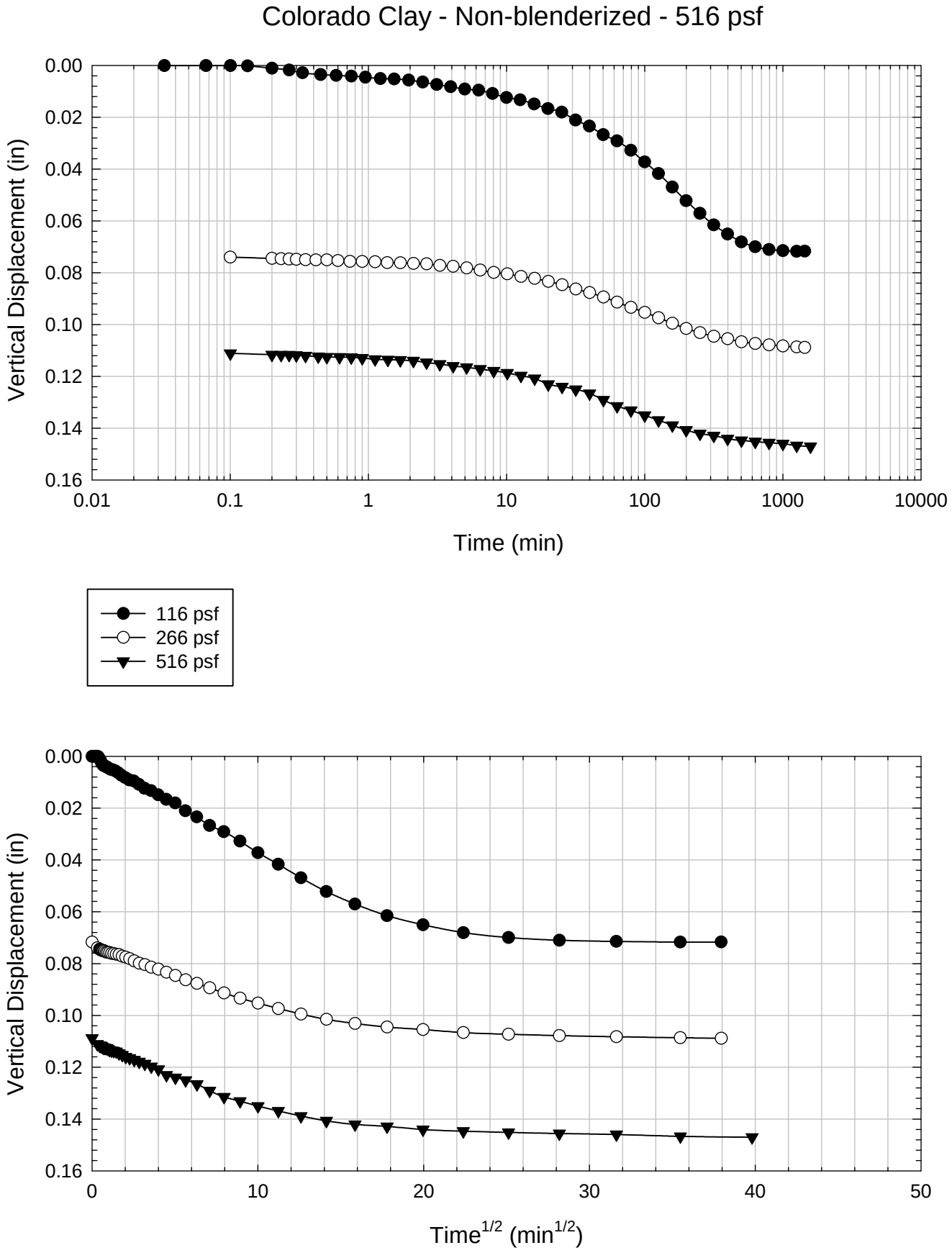
Colorado Clay - Non-blenderized - 516 psf
Vertical Displacement (in)
0.00
0.02
0.04
0.06
0.08
0.10
0.12
0.14
0.16
0.01
0.1
1
10
100
1000
10000
Time (min)
116 psf
266 psf
516 psf
Vertical Displacement (in)
0
10
20
30
40
50
Time^1/2 (min^1/2)

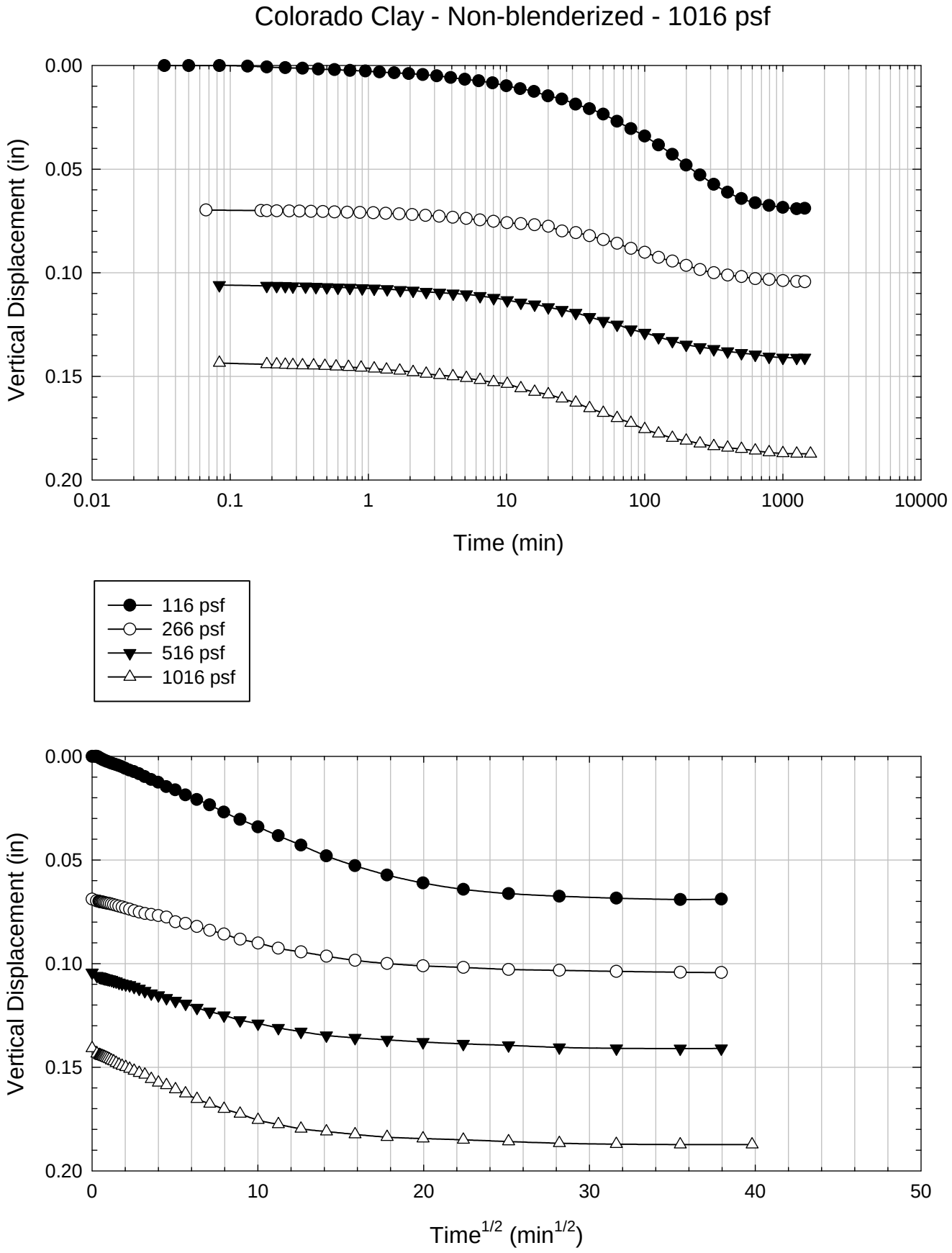
Colorado Clay - Non-blenderized - 1016 psf
Vertical Displacement (in)
0.00
0.05
0.10
0.15
0.20
0.01
0.1
1
10
100
1000
10000
Time (min)
116 psf
266 psf
516 psf
1016 psf
Vertical Displacement (in)
0.00
0.05
0.10
0.15
0.20
0
10
20
30
40
50
Time1/2 (min1/2)

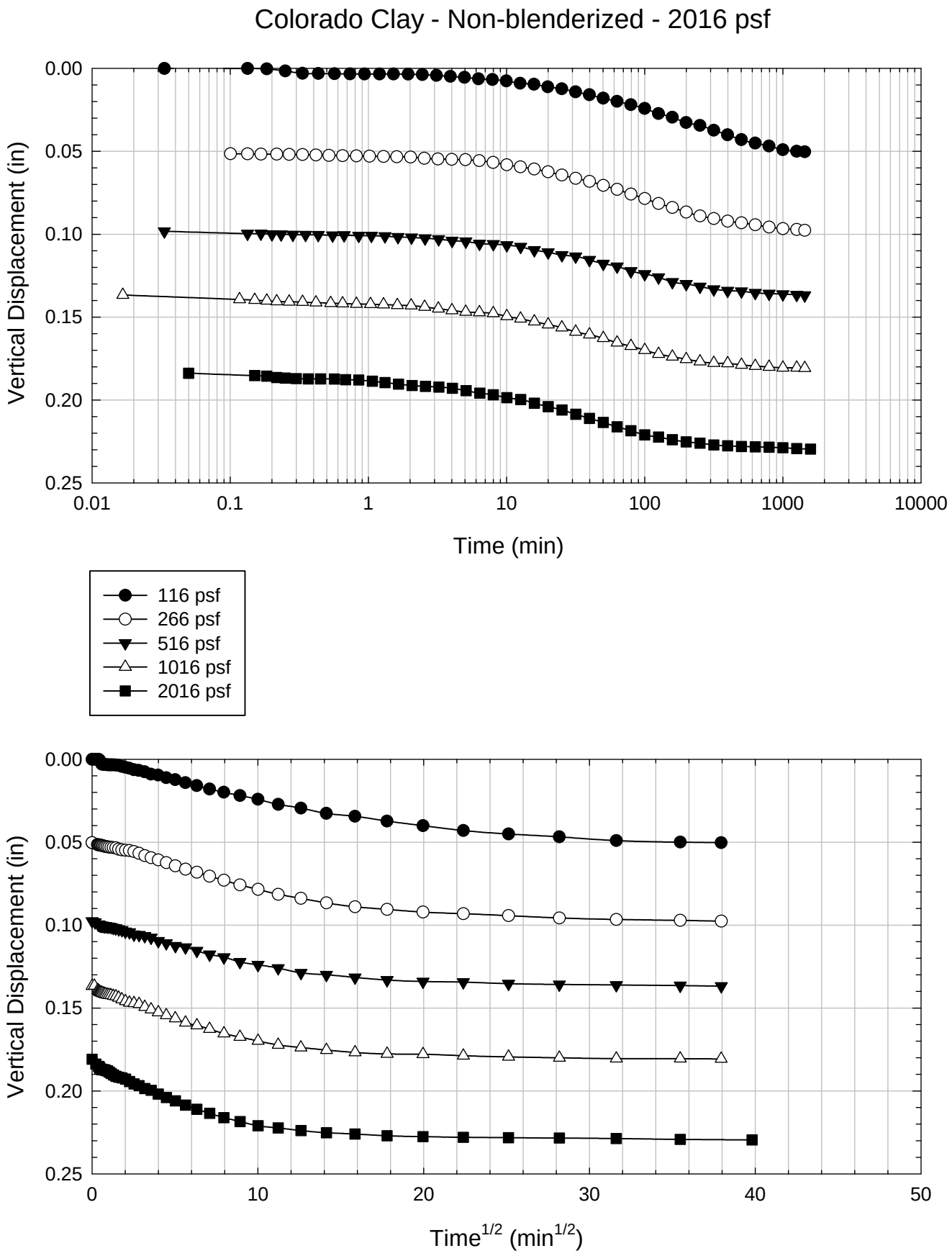
Colorado Clay - Non-blenderized - 2016 psf
Vertical Displacement (in)
0.00
0.05
0.10
0.15
0.20
0.25
0.01
0.1
1
10
100
1000
10000
Time (min)
116 psf
266 psf
516 psf
1016 psf
2016 psf
Vertical Displacement (in)
0.00
0.05
0.10
0.15
0.20
0.25
0
10
20
30
40
50
Time1/2 (min1/2)

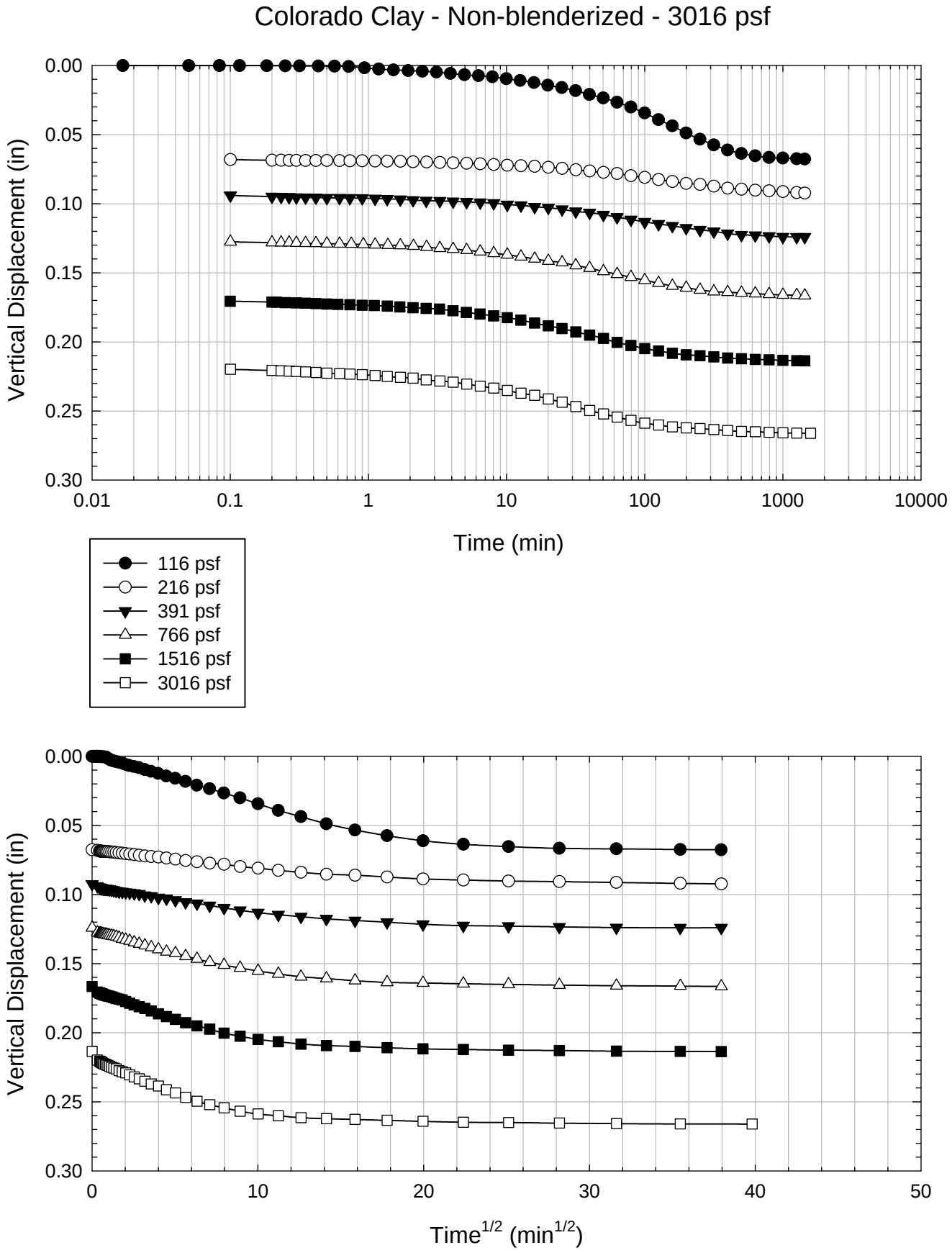
Colorado Clay - Non-blenderized - 3016 psf
Vertical Displacement (in)
0.00
0.05
0.10
0.15
0.20
0.25
0.30
0.01
0.1
1
10
100
1000
10000
Time (min)
116 psf
216 psf
391 psf
766 psf
1516 psf
3016 psf
Vertical Displacement (in)
0.00
0.05
0.10
0.15
0.20
0.25
0.30
0
10
20
30
40
50
Time^1/2 (min^1/2)

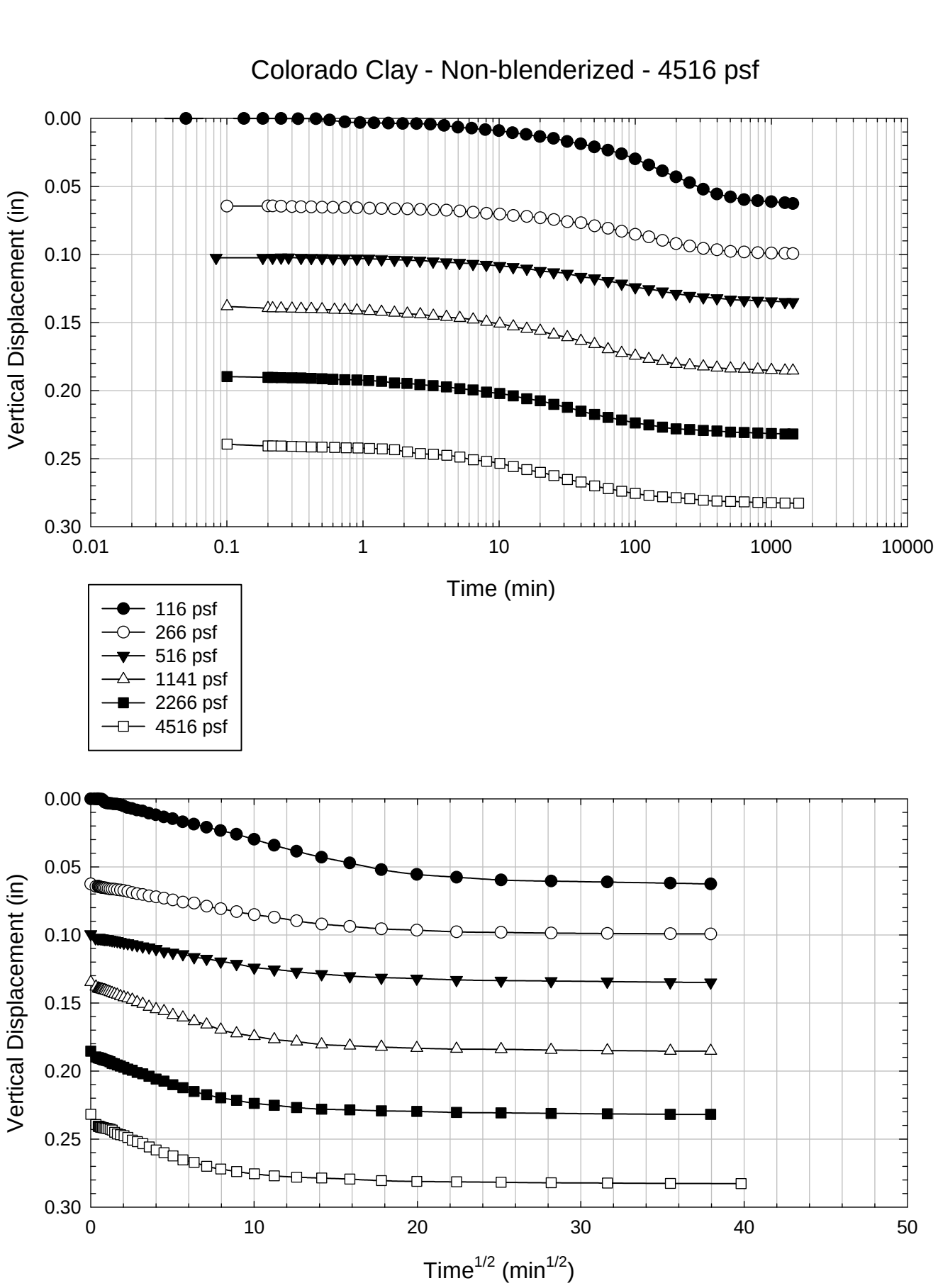
Colorado Clay - Non-blenderized - 4516 psf
Vertical Displacement (in)
0.00
0.05
0.10
0.15
0.20
0.25
0.30
0.01
0.1
1
10
100
1000
10000
Time (min)
116 psf
266 psf
516 psf
1141 psf
2266 psf
4516 psf
Vertical Displacement (in)
0.00
0.05
0.10
0.15
0.20
0.25
0.30
0
10
20
30
40
50
Time1/2 (min1/2)

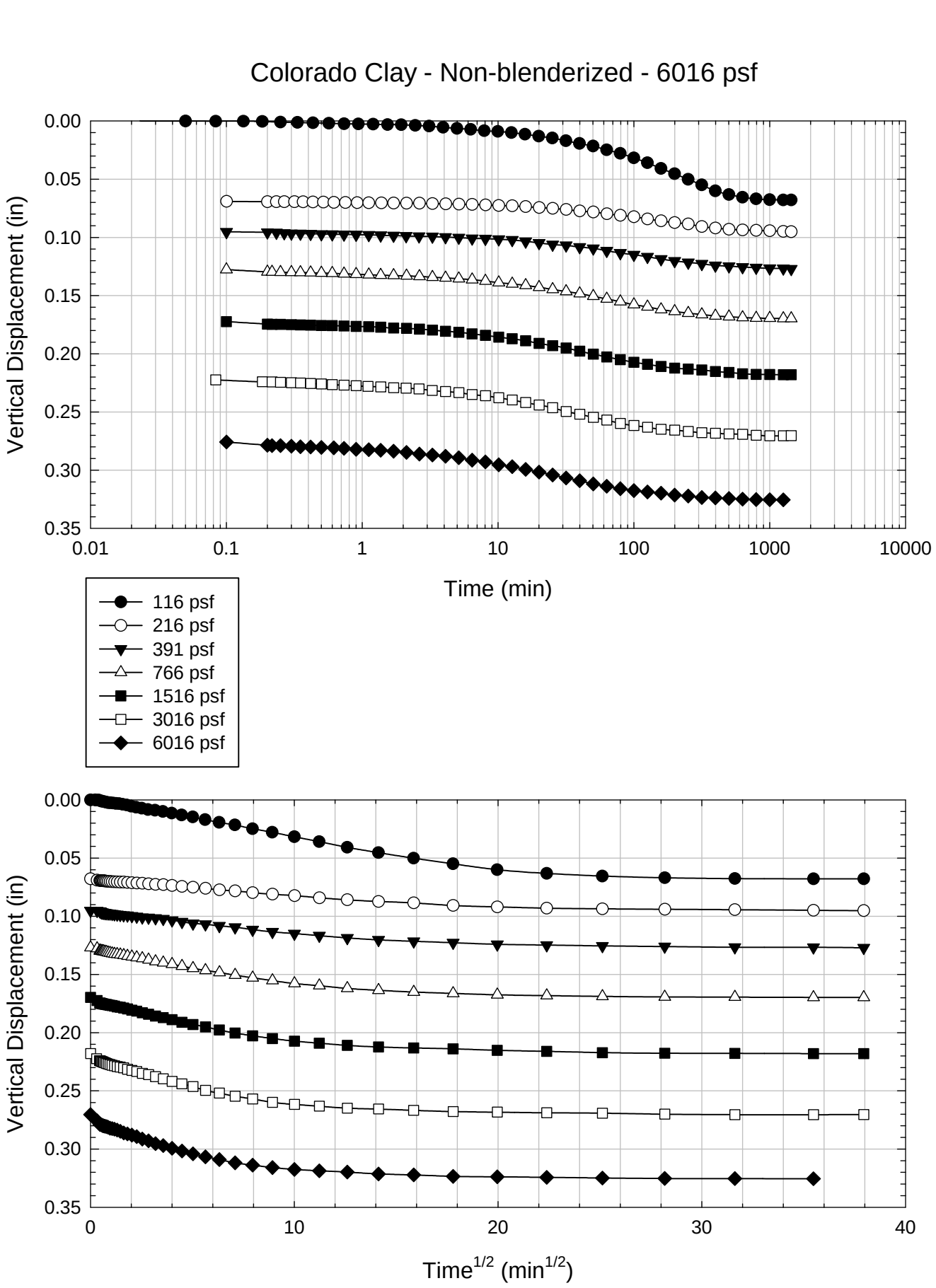
Colorado Clay - Non-blenderized - 6016 psf
Vertical Displacement (in)
0.00
0.05
0.10
0.15
0.20
0.25
0.30
0.35
0.01
0.1
1
10
100
1000
10000
Time (min)
116 psf
216 psf
391 psf
766 psf
1516 psf
3016 psf
6016 psf
Vertical Displacement (in)
0
10
20
30
40
Time^1/2 (min^1/2)

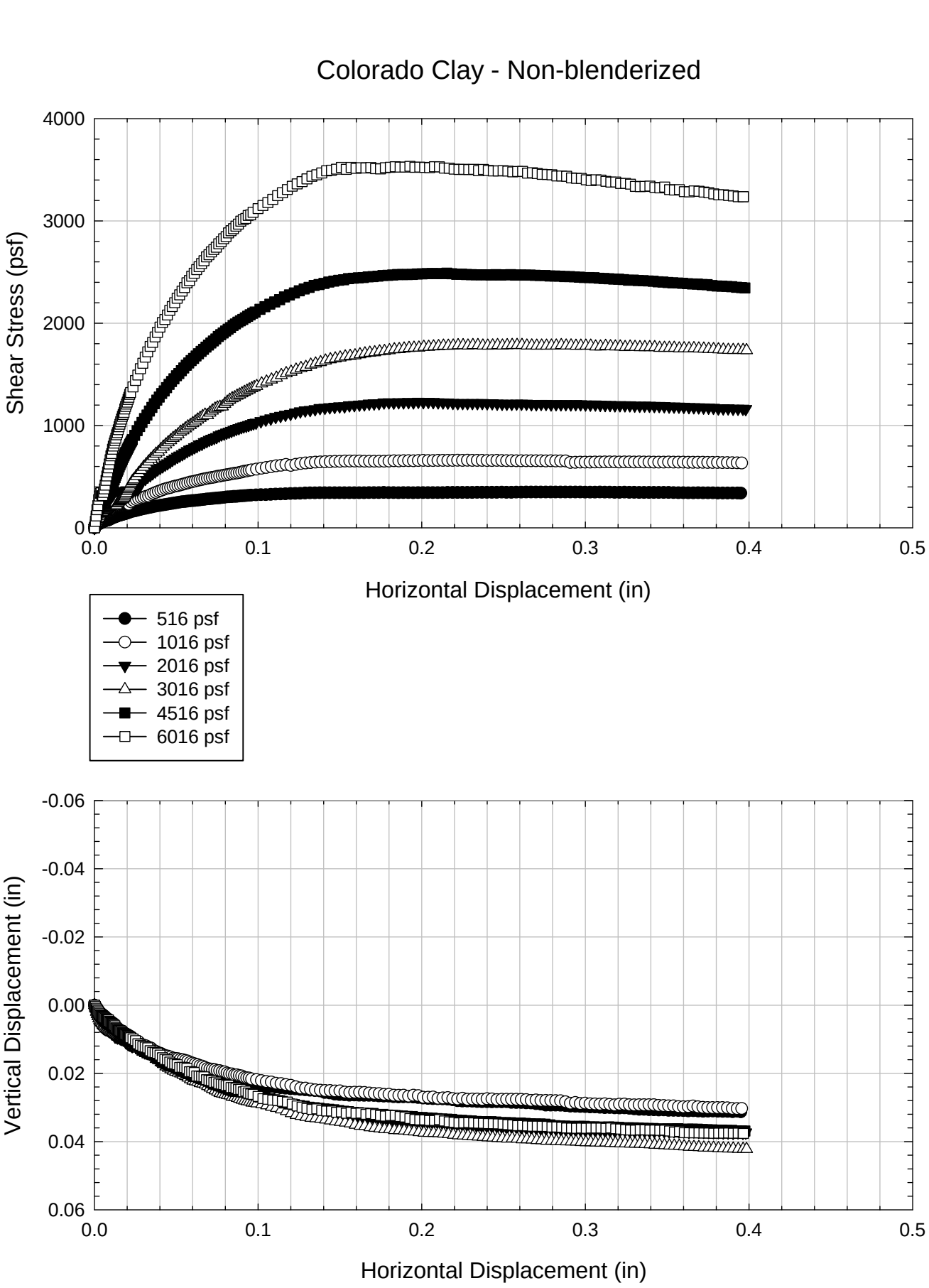
Colorado Clay - Non-blenderized
Shear Stress (psf)
4000
3000
2000
1000
0
0.0
0.1
0.2
0.3
0.4
0.5
Horizontal Displacement (in)
516 psf
1016 psf
2016 psf
3016 psf
4516 psf
6016 psf
Vertical Displacement (in)
-0.06
-0.04
-0.02
0.00
0.02
0.04
0.06
0.0
0.1
0.2
0.3
0.4
0.5
Horizontal Displacement (in)

C.6. NOVA

C.6.1 Blenderized

Virginia Polytechnic Institute and State University
Geotechnical Engineering Laboratory
Direct Shear Data Sheet

Project:	Fully Softened Shear Strength
Sample I.D./Loc.:	NOVA - Blenderized A
Classification:	Fat Clay (CH)

Sample Preparation	Remolded at LL		Specific Gravity	2.80

Test Number	1	2	3	4	5	6	7	8
Start Date (m/d/y)	9/28/2011	9/27/2011	10/2/2011	9/28/2011	9/28/2011	9/28/2011		
End Date (m/d/y)	10/10/2011	10/6/2011	10/15/2011	10/10/2011	10/10/2011	10/10/2011		
Consolidation Pressure (psf)	516	1016	2016	3016	4516	6016		
Initial Values								
Initial Height (in)	1.45	1.44	1.44	1.39	1.39	1.43		
Initial Diameter (in)	2.50	2.50	2.50	2.50	2.50	2.50		
Initial Sample Weight (g)	182	183	179	178	184	181		
Water Content (%)	81.43	79.08	78.32	81.59	79.29	79.41		
Dry Unit Weight (pcf)	53.54	55.3	54.3	54.7	57.2	54.7		
Wet Unit Weight (pcf)	97.13	99.0	96.8	99.4	102.5	98.1		
Consolidation Pressures								
Load 1 (psf)	116	116	116	116	116	116		
Load 2 (psf)	266	266	266	216	266	216		
Load 3 (psf)	516	516	516	391	516	391		
Load 4 (psf)		1016	1016	766	1141	766		
Load 5 (psf)			2016	1516	2266	1516		
Load 6 (psf)				3016	4516	3016		
Load 7 (psf)						6016		
t_{50}								
Max. t_{50} for Load 1 (min)								
Max. t_{50} for Load 2 (min)								
Max. t_{50} for Load 3 (min)	73.86							
Max. t_{50} for Load 4 (min)		76.17						
Max. t_{50} for Load 5 (min)			63.85					
Max. t_{50} for Load 6 (min)				60.42	47.90			
Max. t_{50} for Load 7 (min)						52.93		
Final Values								
Water Content (%)	61.76	62.88	53.15	49.83	48.04	42.57		
Dry Unit Weight (pcf)	76.0	67.6	72.4	80.4	85.4	87.88		
Wet Unit Weight (pcf)	123.0	110.0	110.8	120.5	126.4	125.29		
Failure								
Test Performed at Shear Rate (in/min)	2.71E-05	2.63E-05	2.63E-05	3.31E-05	3.87E-05	3.78E-05		
Required Shear Rate (in/min)	5.42E-05	4.20E-05	5.95E-05	6.62E-05	5.85E-05	6.42E-05		
Displacement at Failure (in)	0.20	0.16	0.19	0.20	0.14	0.17		
Peak Shear Stress (psf)	368	575	1186	1503	1828	2604		
Total Change in Height at Failure (in)	0.22	0.26	0.36	0.37	0.39	0.48		
Secant Effective Friction Angle (deg)	35.5	29.5	30.5	26.5	22.0	23.4		

Comments: In the test consolidated to 1016 psf, the computer crashed during shear but it was continued.

NOVA - Blenderized A - 516 psf

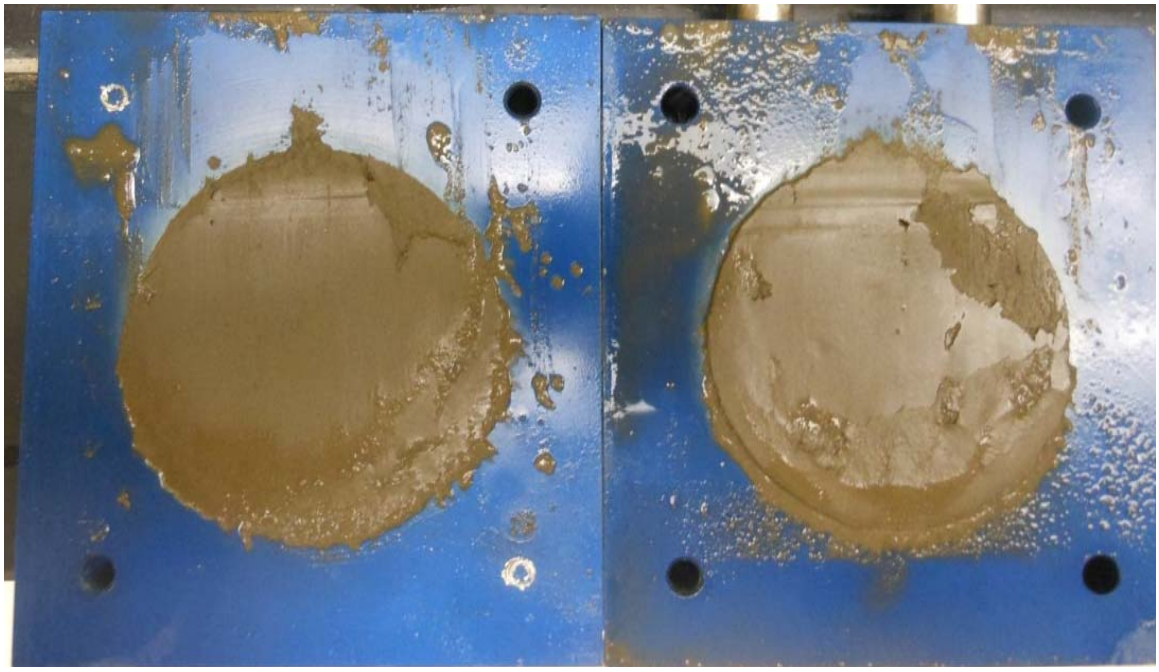

NOVA - Blenderized A - 1016 psf

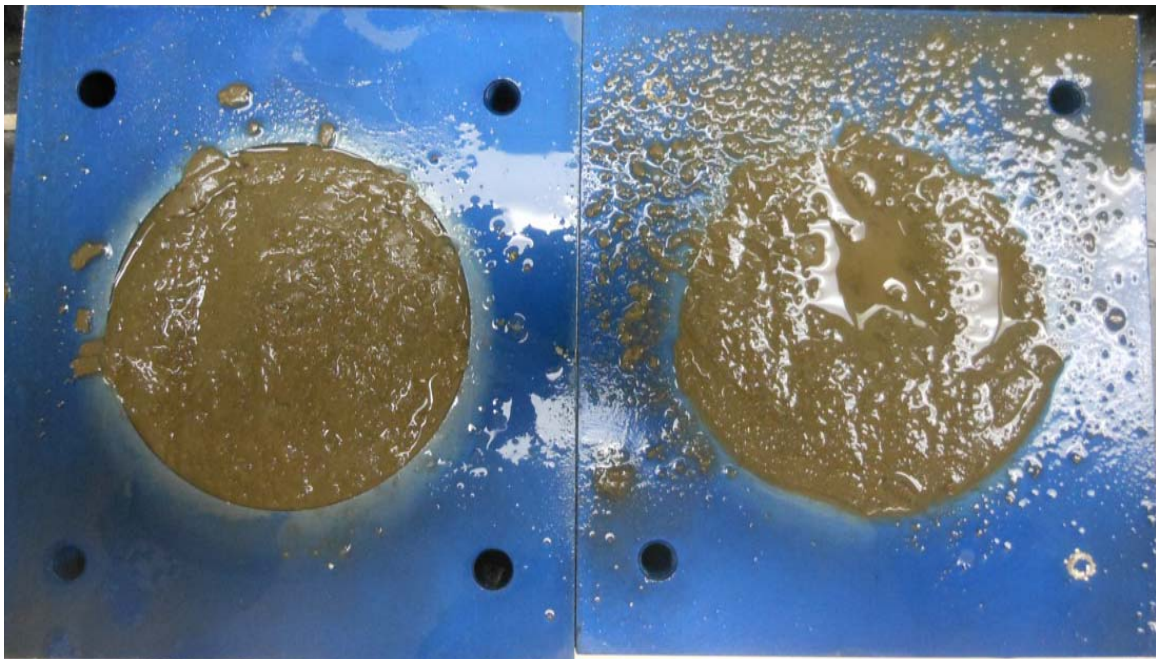

NOVA - Blenderized A - 2016 psf

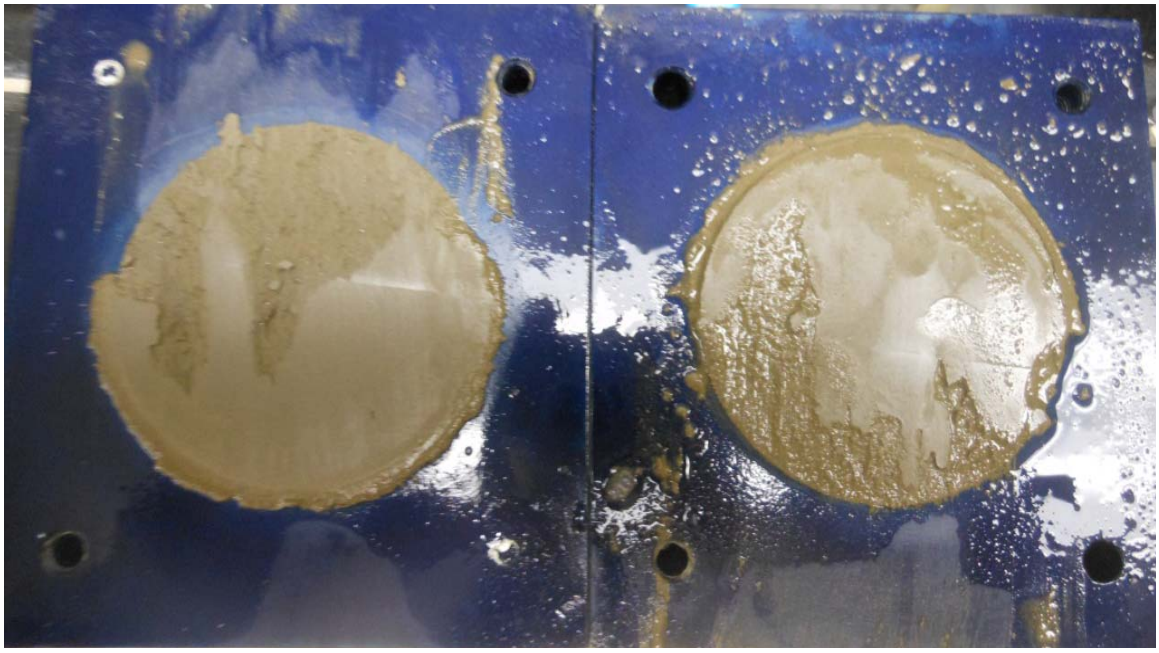

NOVA - Blenderized A - 3016 psf

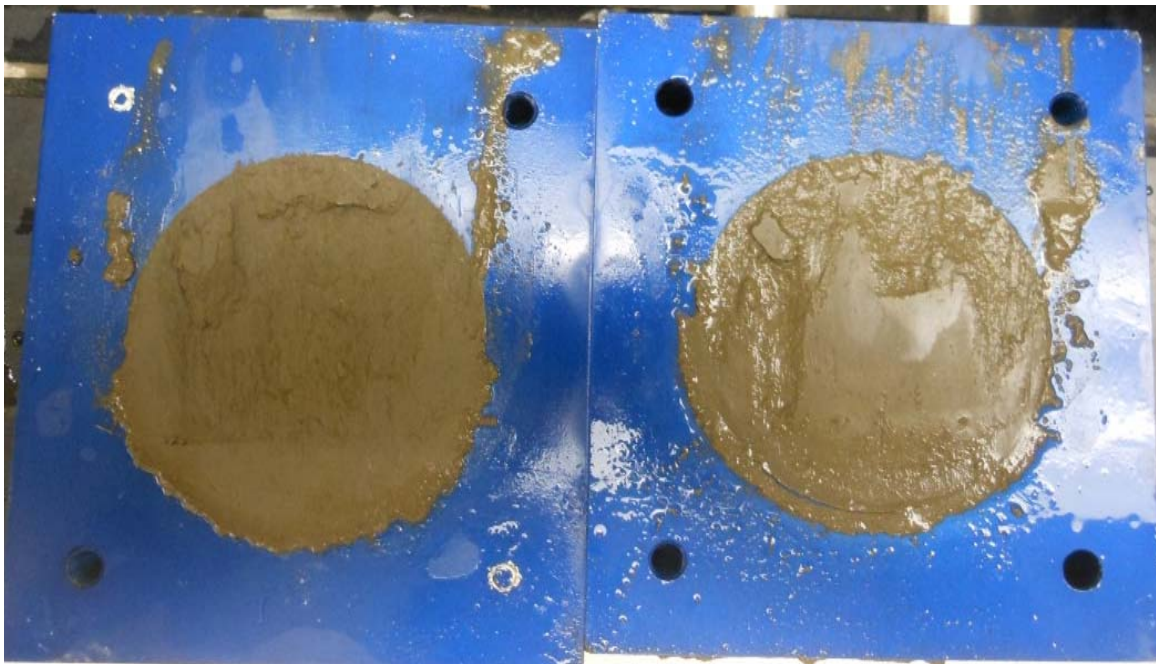

NOVA - Blenderized A - 4516 psf

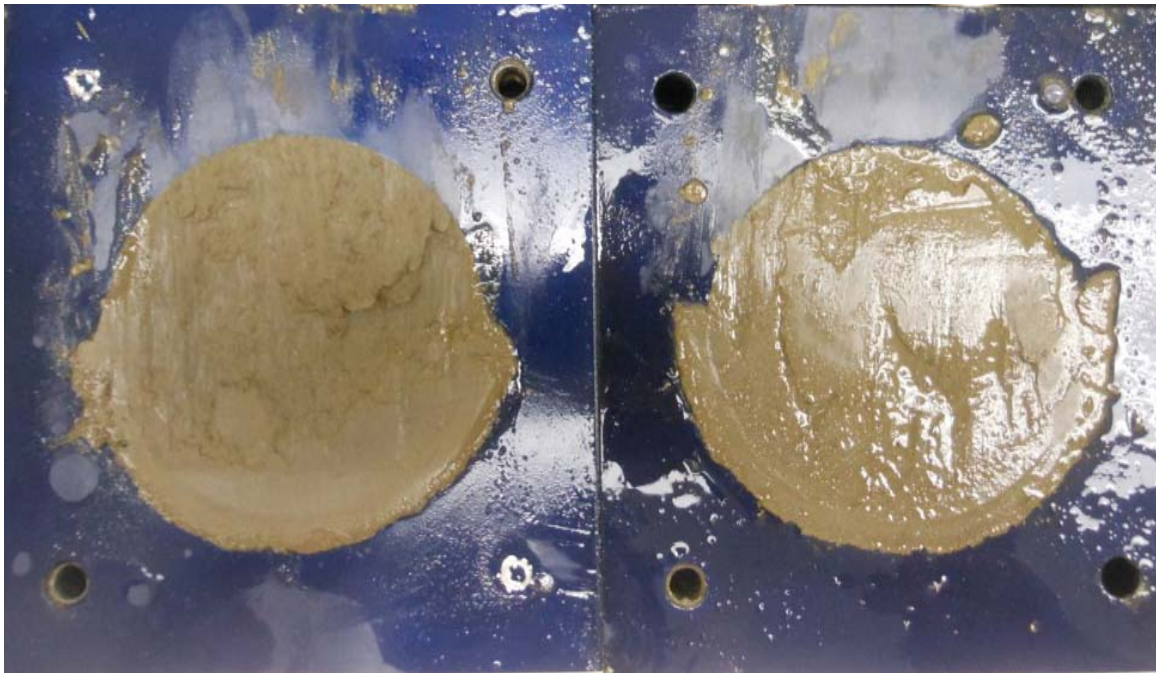

NOVA - Blenderized A - 6016 psf

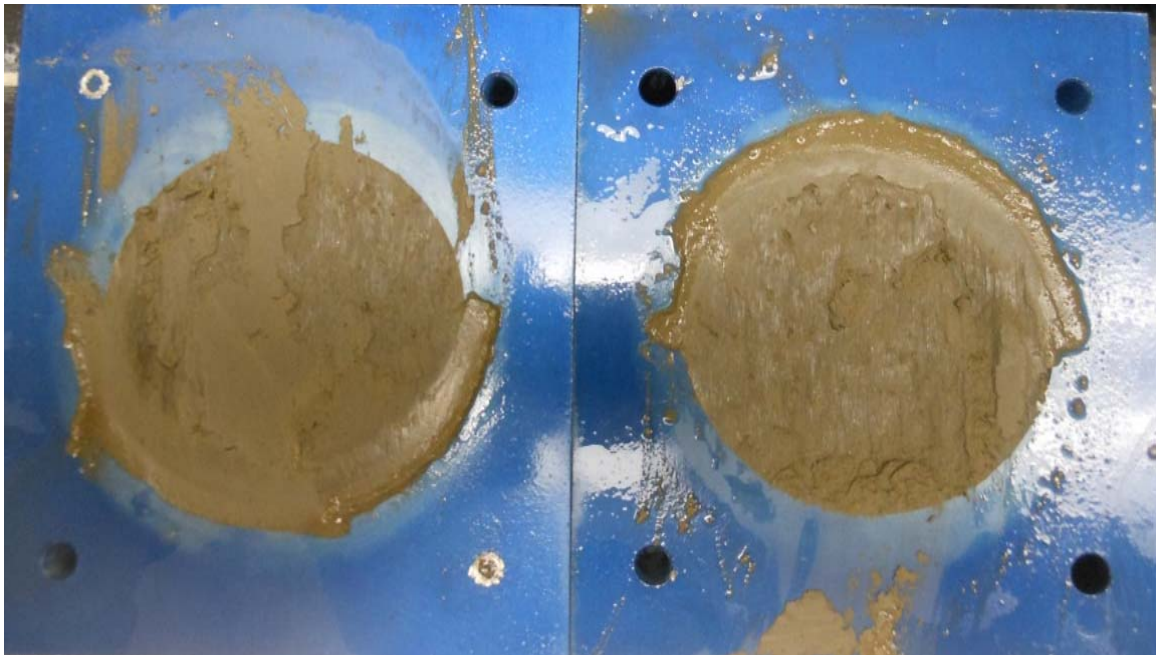

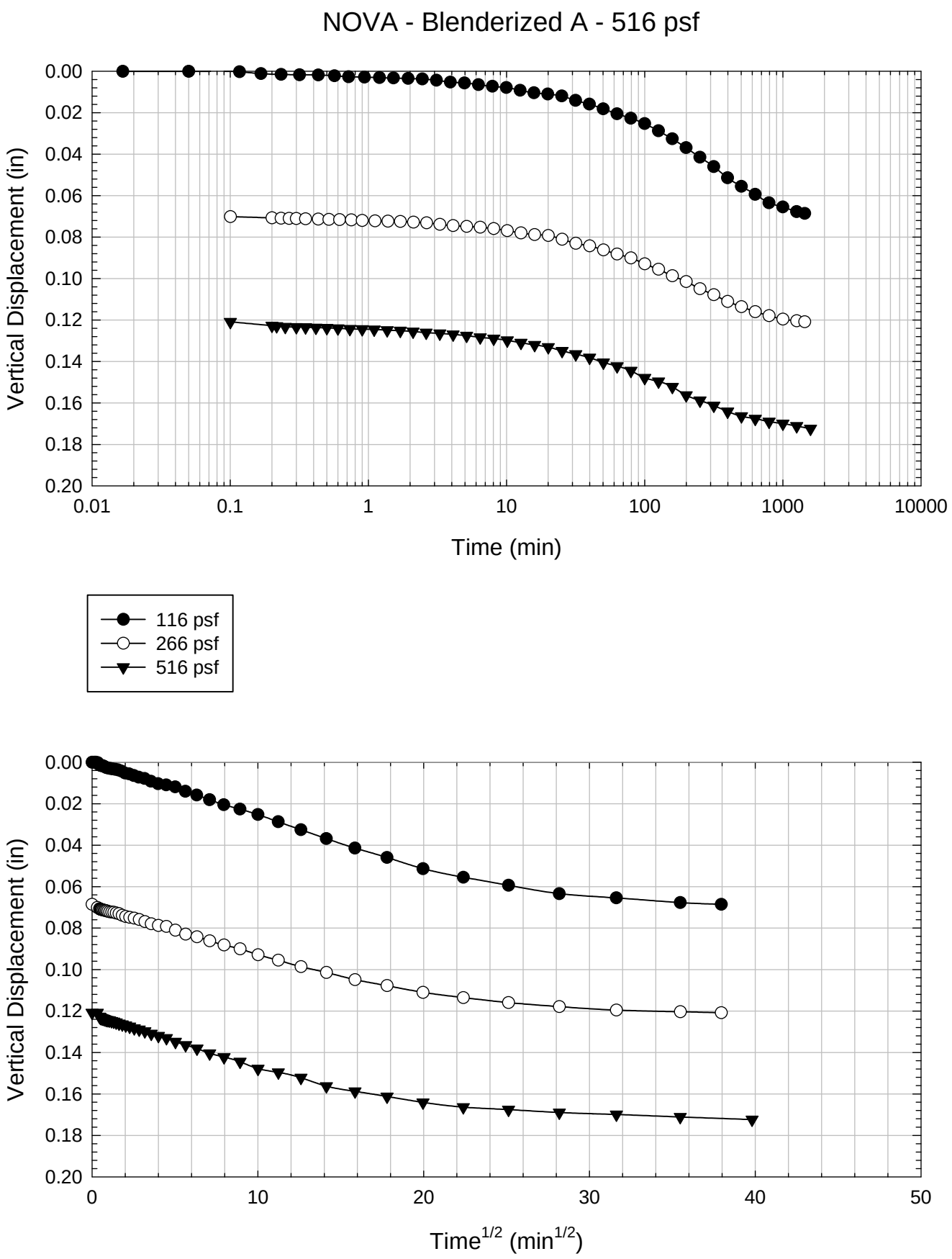
NOVA - Blenderized A - 516 psf
Vertical Displacement (in)
0.00
0.02
0.04
0.06
0.08
0.10
0.12
0.14
0.16
0.18
0.20
0.01
0.1
1
10
100
1000
10000
Time (min)
116 psf
266 psf
516 psf
Vertical Displacement (in)
0
10
20
30
40
50
Time^1/2 (min^1/2)

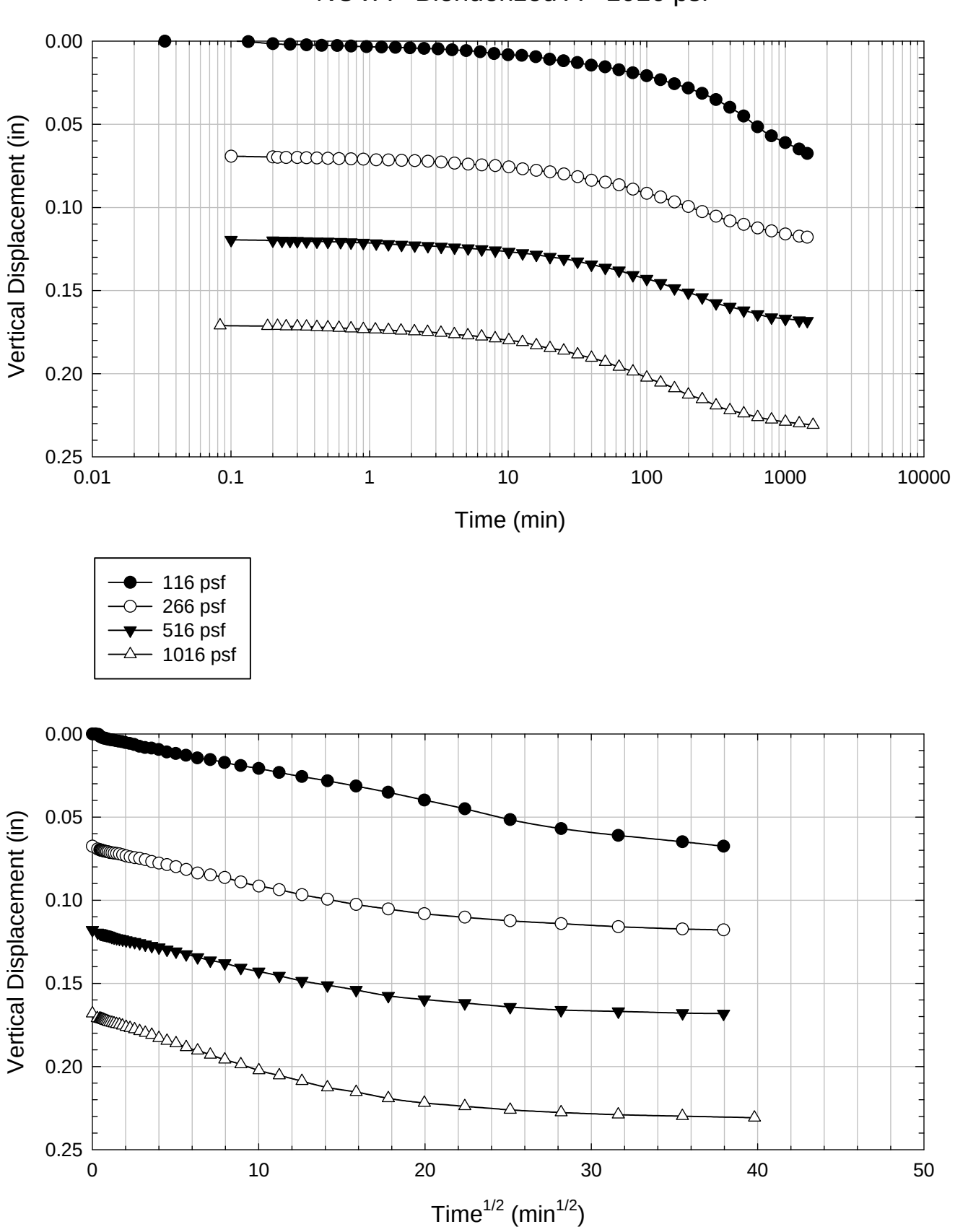
NOVA - Blenderized A - 1016 psf
Vertical Displacement (in)
0.00
0.05
0.10
0.15
0.20
0.25
0.01
0.1
1
10
100
1000
10000
Time (min)
116 psf
266 psf
516 psf
1016 psf
Vertical Displacement (in)
0.00
0.05
0.10
0.15
0.20
0.25
0
10
20
30
40
50
Time1/2 (min1/2)

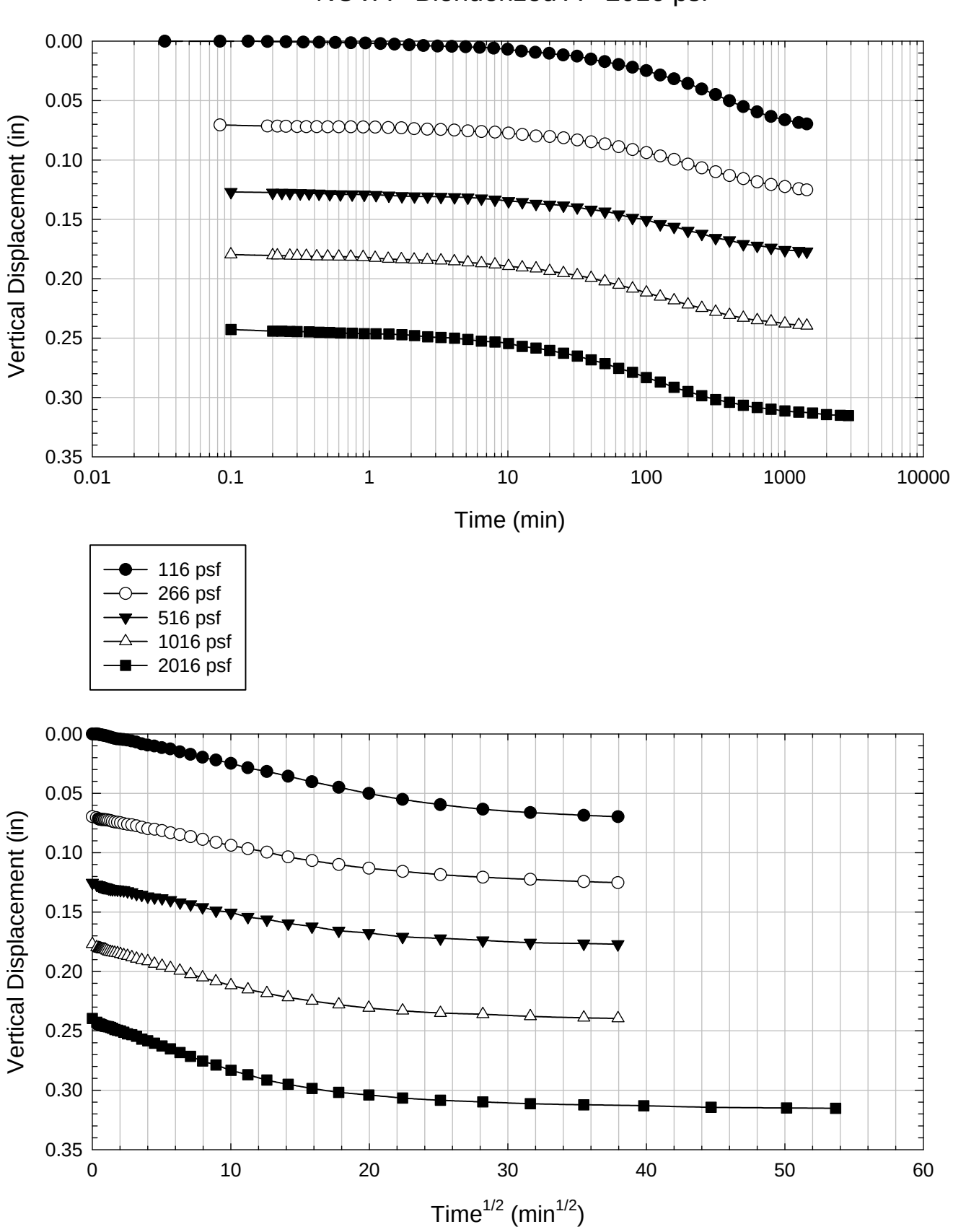
NOVA - Blenderized A - 2016 psf
Vertical Displacement (in)
0.00
0.05
0.10
0.15
0.20
0.25
0.30
0.35
0.01
0.1
1
10
100
1000
10000
Time (min)
116 psf
266 psf
516 psf
1016 psf
2016 psf
Vertical Displacement (in)
0
10
20
30
40
50
60
Time^1/2 (min^1/2)

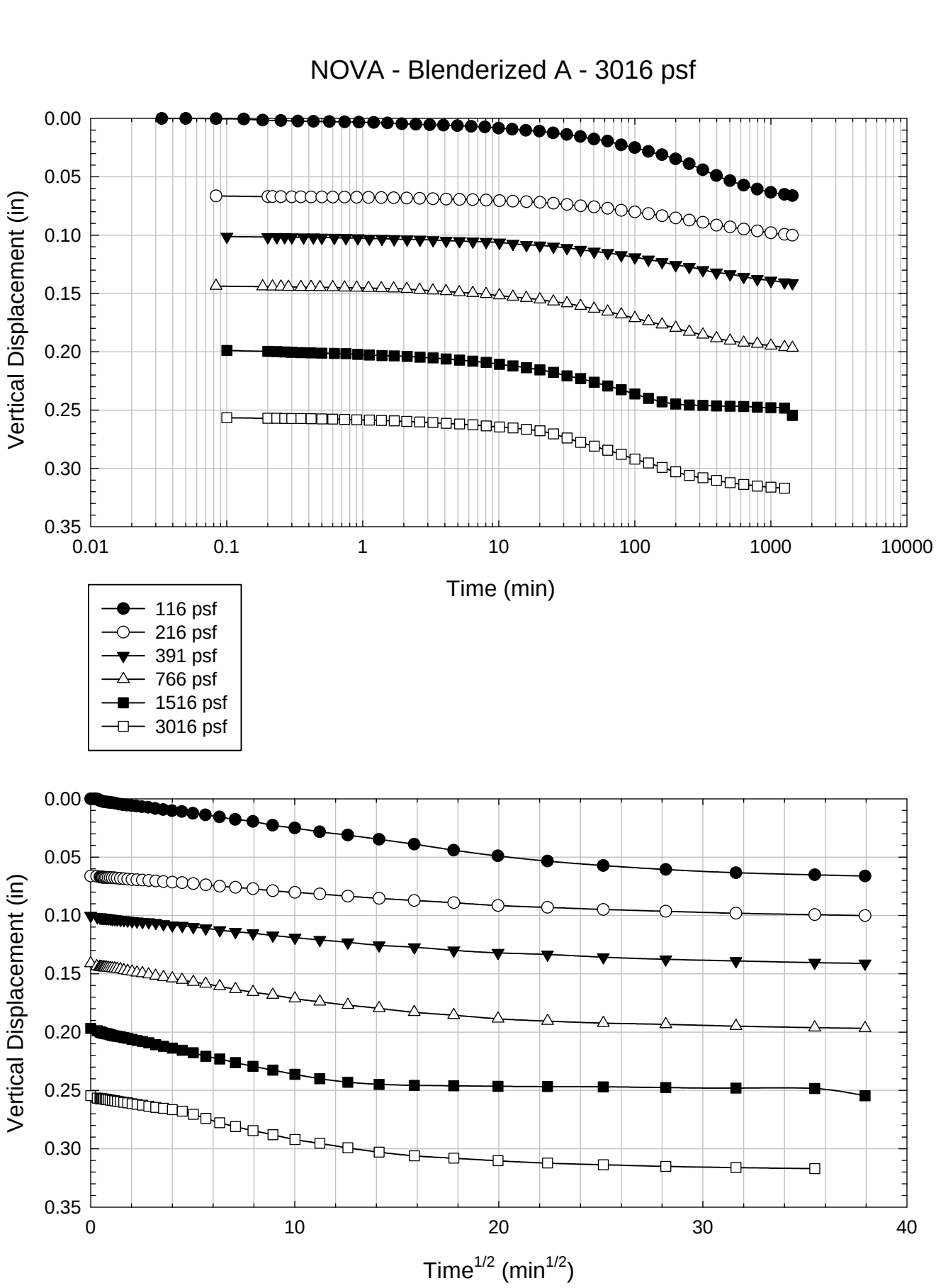
NOVA - Blenderized A - 3016 psf
Vertical Displacement (in)
0.00
0.05
0.10
0.15
0.20
0.25
0.30
0.35
0.01
0.1
1
10
100
1000
10000
Time (min)
116 psf
216 psf
391 psf
766 psf
1516 psf
3016 psf
Vertical Displacement (in)
0
10
20
30
40
Time^1/2 (min^1/2)

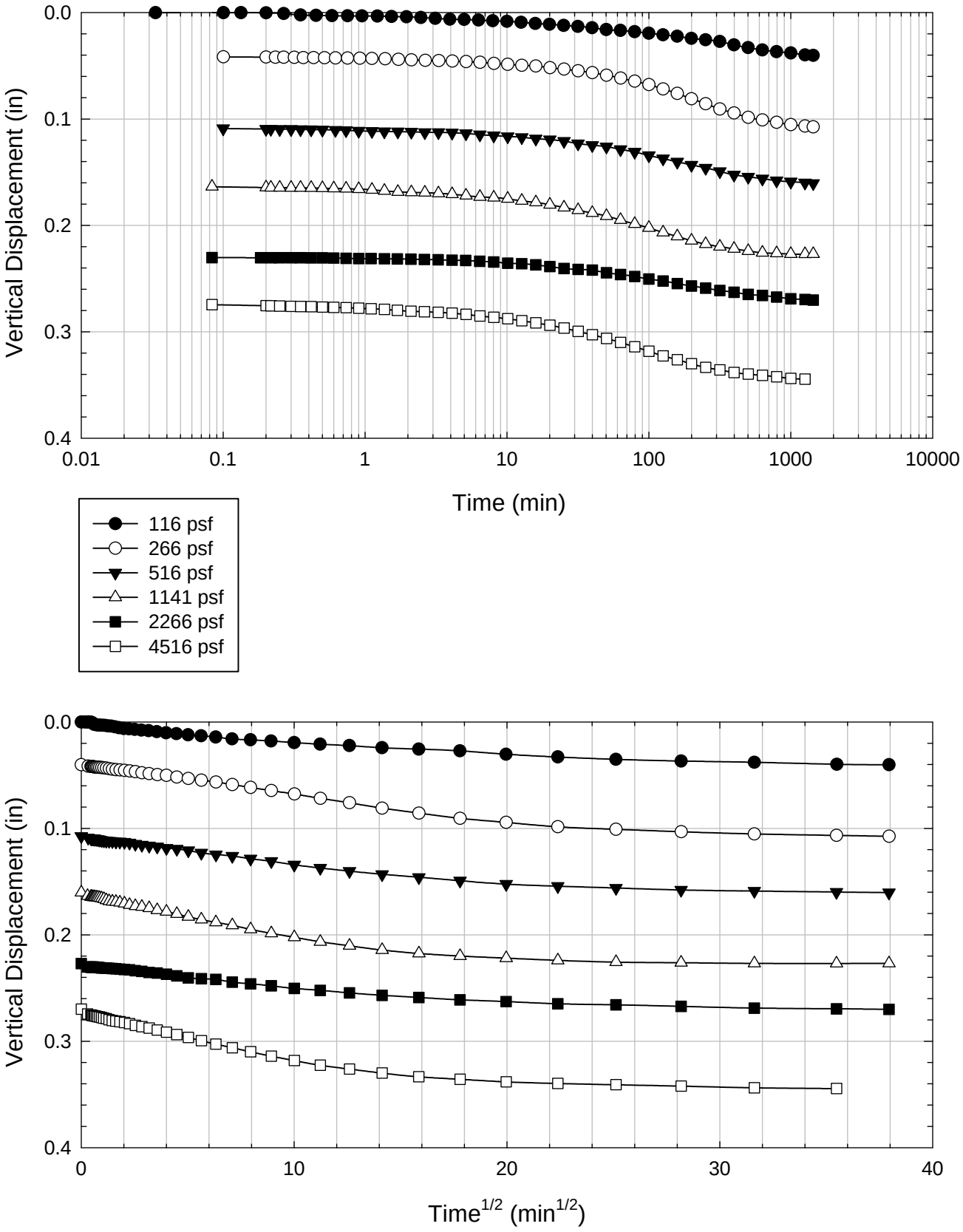
NOVA - Blenderized A - 4516 psf
Vertical Displacement (in)
0.0
0.1
0.2
0.3
0.4
0.01
0.1
1
10
100
1000
10000
Time (min)
116 psf
266 psf
516 psf
1141 psf
2266 psf
4516 psf
Vertical Displacement (in)
0.0
0.1
0.2
0.3
0.4
0
10
20
30
40
Time^1/2 (min^1/2)

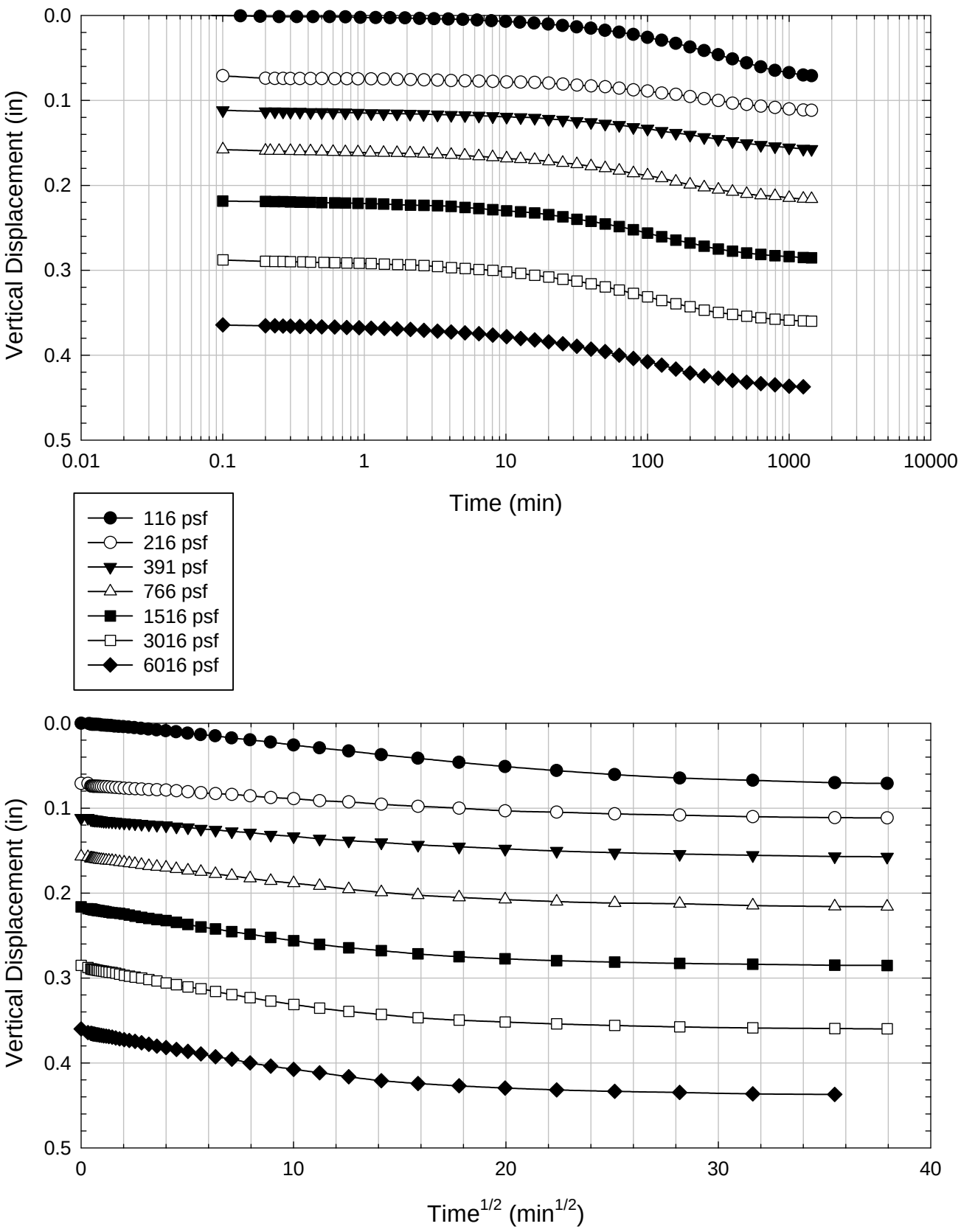
NOVA - Blenderized A - 6016 psf
Vertical Displacement (in)
0.0
0.1
0.2
0.3
0.4
0.5
0.01
0.1
1
10
100
1000
10000
Time (min)
116 psf
216 psf
391 psf
766 psf
1516 psf
3016 psf
6016 psf
Vertical Displacement (in)
0.0
0.1
0.2
0.3
0.4
0.5
0
10
20
30
40
Time^1/2 (min^1/2)

NOVA - A Blenderized

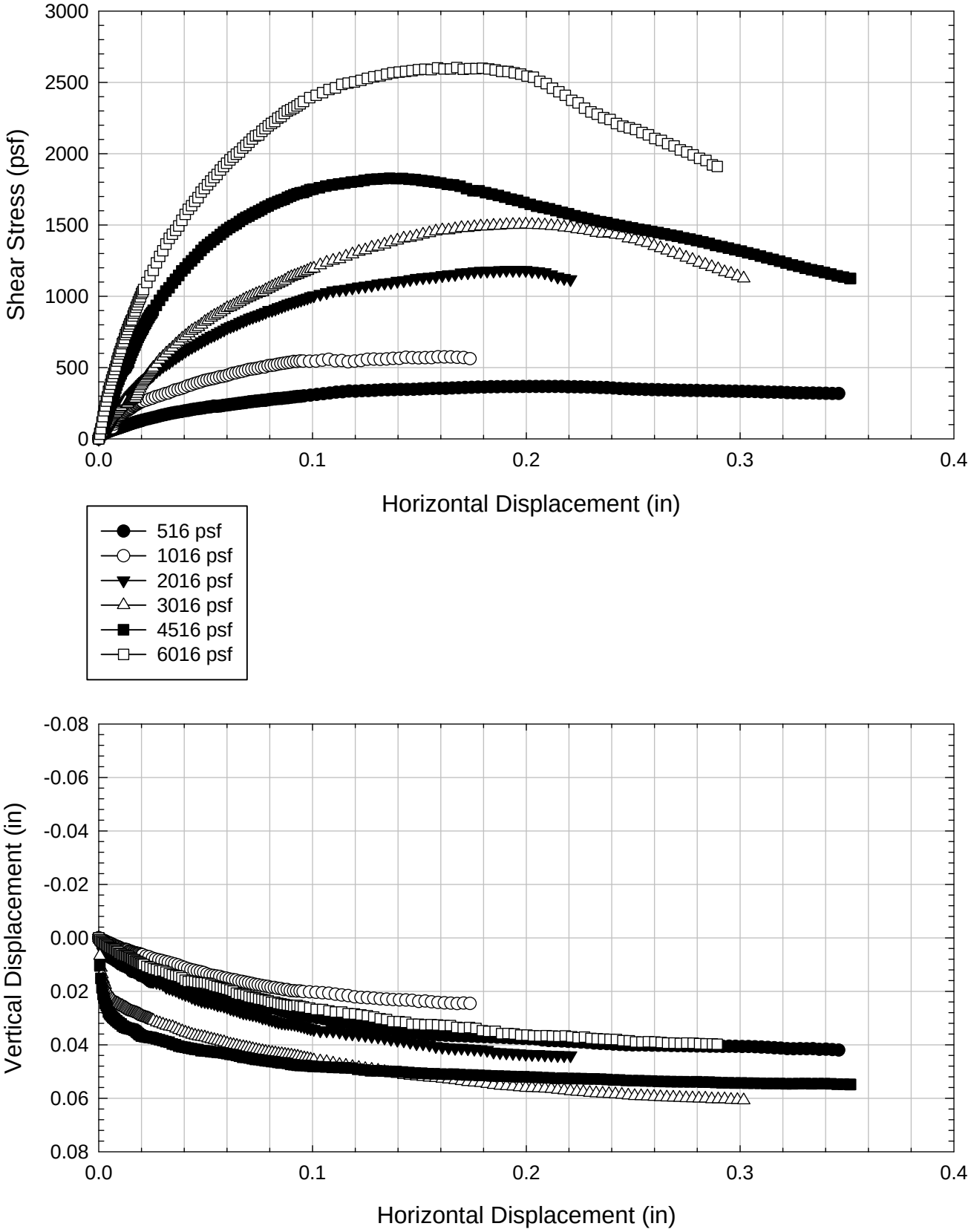

Virginia Polytechnic Institute and State University
Geotechnical Engineering Laboratory
Direct Shear Data Sheet

Project:	Fully Softened Shear Strength
Sample I.D./Loc.:	NOVA - Blenderized
Classification:	Fat Clay (CH)

Sample Preparation	Remolded at LL		Specific Gravity	2.80

Test Number	1	2	3	4	5	6	7	8
Start Date (m/d/y)	2/25/2011	7/9/2011	2/25/2011	7/9/2011	2/28/2011	7/9/2011	3/5/2011	
End Date (m/d/y)	3/7/2011	7/21/2011	3/7/2011	7/21/2011	3/11/2011	7/21/2011	3/18/2011	
Consolidation Pressure (psf)	516	766	1016	1516	2016	2516	3016	
Initial Values								
Initial Height (in) (Assumed if = 1.44)	1.44	1.42	1.44	1.39	1.44	1.39	1.44	
Initial Diameter (in)	2.50	2.50	2.50	2.50	2.50	2.50	2.50	
Initial Sample Weight (g)	180	185	175	183	181	188	164	
Water Content (%)	73.83	65.04	73.90	67.60	72.74	65.31	70.62	
Dry Unit Weight (pcf)	55.8	61.4	54.2	60.9	56.5	63.6	51.8	
Wet Unit Weight (pcf)	97.0	101.4	94.3	102.0	97.6	105.1	88.4	
Consolidation Pressures								
Load 1 (psf)	116	116	116	116	116	116	116	
Load 2 (psf)	266	216	216	216	266	266	216	
Load 3 (psf)	516	391	566	416	516	516	391	
Load 4 (psf)		766	1016	766	1016	1266	766	
Load 5 (psf)				1516	2016	2516	1516	
Load 6 (psf)							3016	
Load 7 (psf)								
t_{50}								
Max. t_{50} for Load 1 (min)	43.75				49.38			
Max. t_{50} for Load 2 (min)	50.39		31.75		61.41		10.87	
Max. t_{50} for Load 3 (min)	49.11		37.07		44.81		40.57	
Max. t_{50} for Load 4 (min)		59.86	43.20		41.05		7.41	
Max. t_{50} for Load 5 (min)				55.28	38.98	48.08	23.02	
Max. t_{50} for Load 6 (min)							29.67	
Max. t_{50} for Load 7 (min)								
Final Values								
Water Content (%)	62.14	55.43	56.27	52.65	51.56	48.36	46.44	
Dry Unit Weight (pcf)	64.1	72.0	67.3	73.0	72.9	78.67	64.08	
Wet Unit Weight (pcf)	103.9	111.9	105.2	111.5	110.5	116.71	93.85	
Failure								
Test Performed at Shear Rate (in/min)	4.00E-05	3.34E-05	4.60E-05	3.62E-05	3.00E-05	3.62E-05	3.00E-05	
Required Shear Rate (in/min)	6.11E-05	5.01E-05	8.80E-05	5.79E-05	9.75E-05	6.66E-05	1.21E-04	
Displacement at Failure (in)	0.15	0.15	0.19	0.16	0.19	0.16	0.18	
Peak Shear Stress (psf)	343	558	626	950	945	1173	1578	
Total Change in Height at Failure (in)	0.19	0.16	0.28	0.23	0.33	0.26	0.39	
Secant Effective Friction Angle (deg)	33.6	36.1	31.6	32.1	25.1	25.0	27.6	

Comments:

NOVA - Blenderized - 516 psf

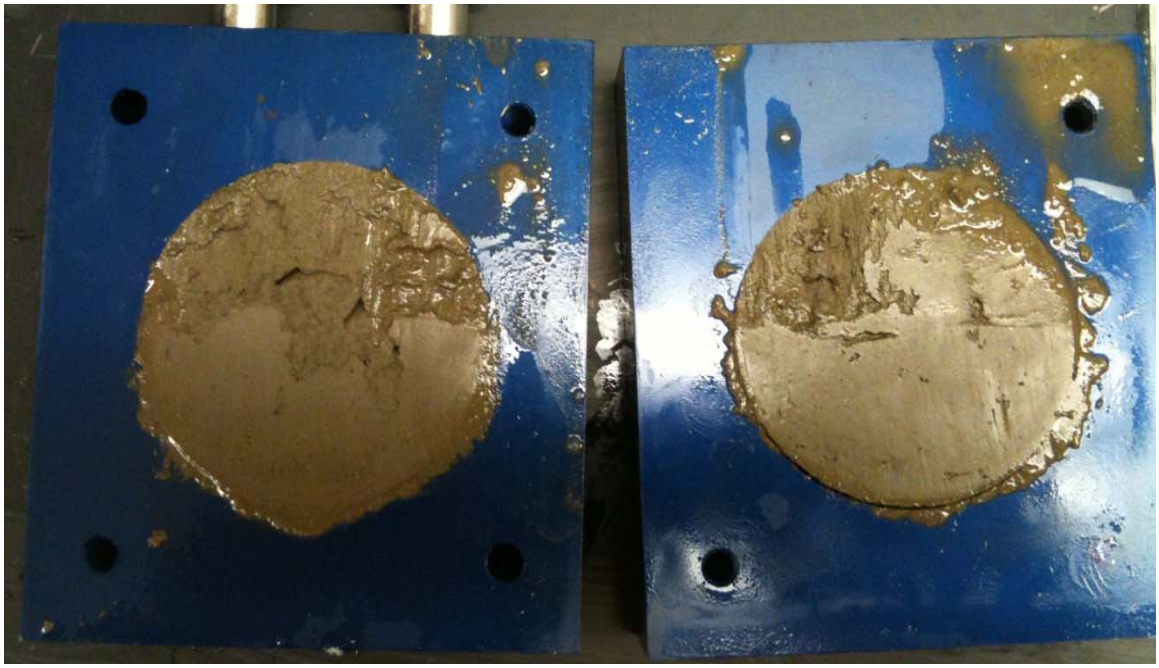

NOVA - Blenderized - 766 psf

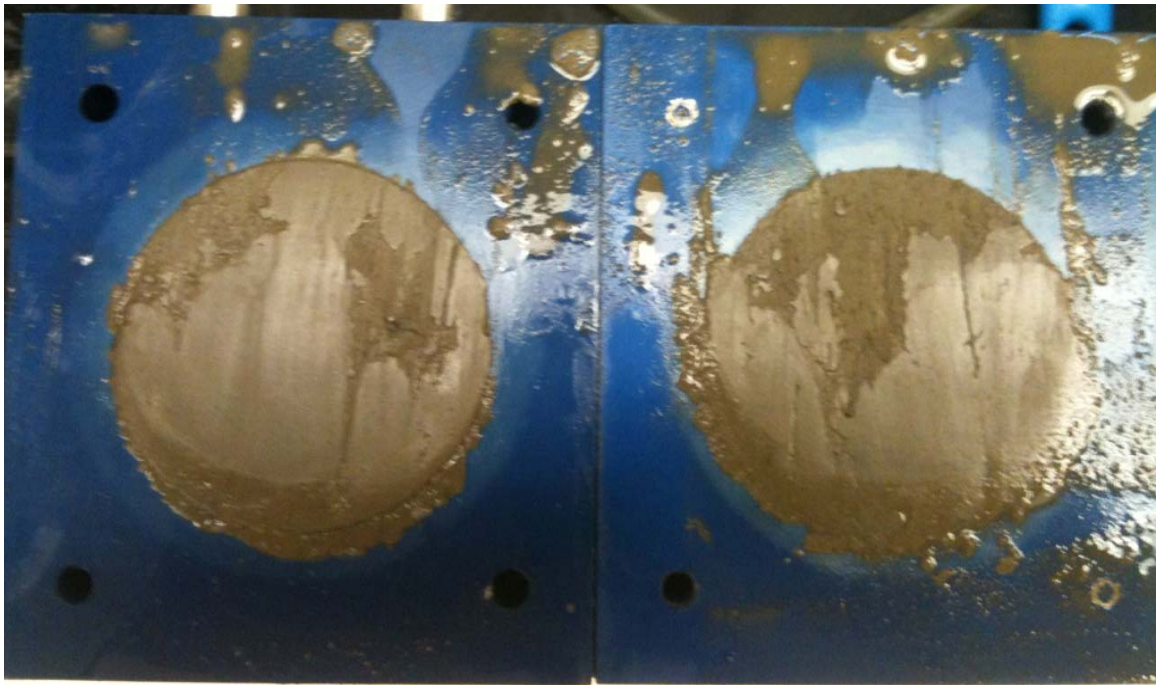

NOVA - Blenderized - 1016 psf

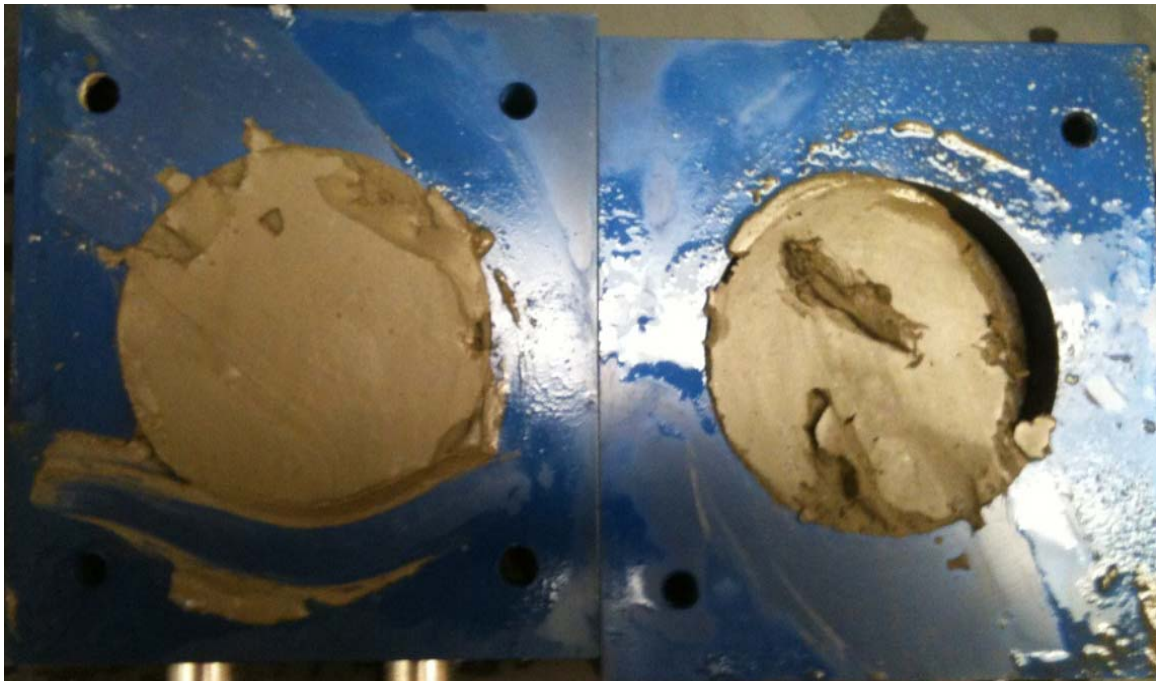

NOVA - Blenderized - 1516 psf

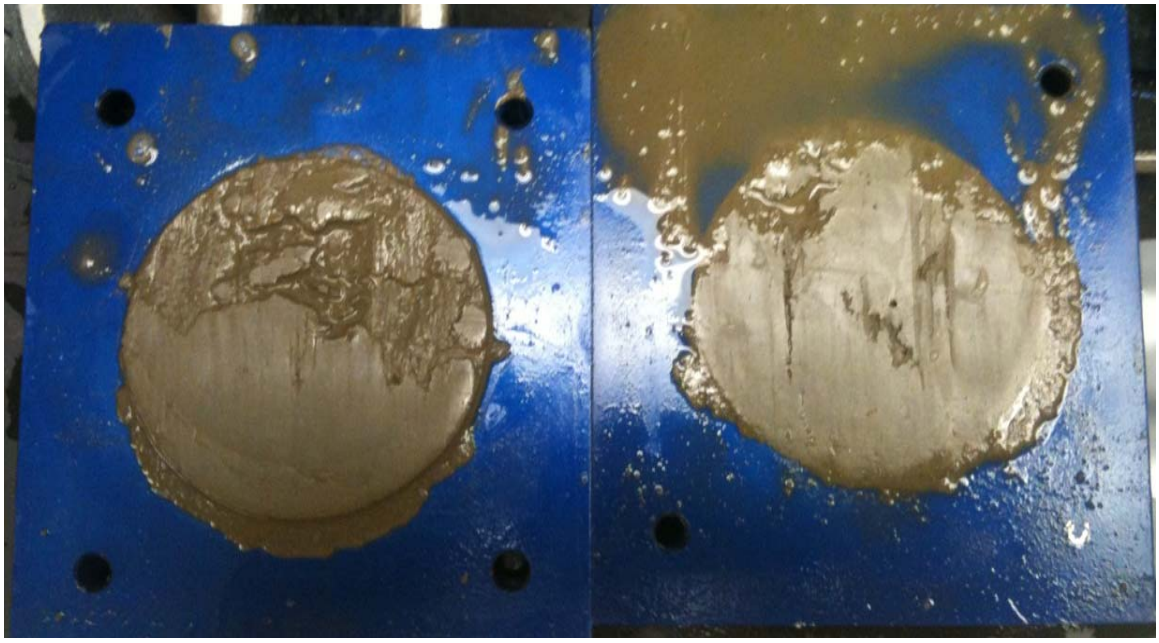

NOVA - Blenderized - 2016 psf

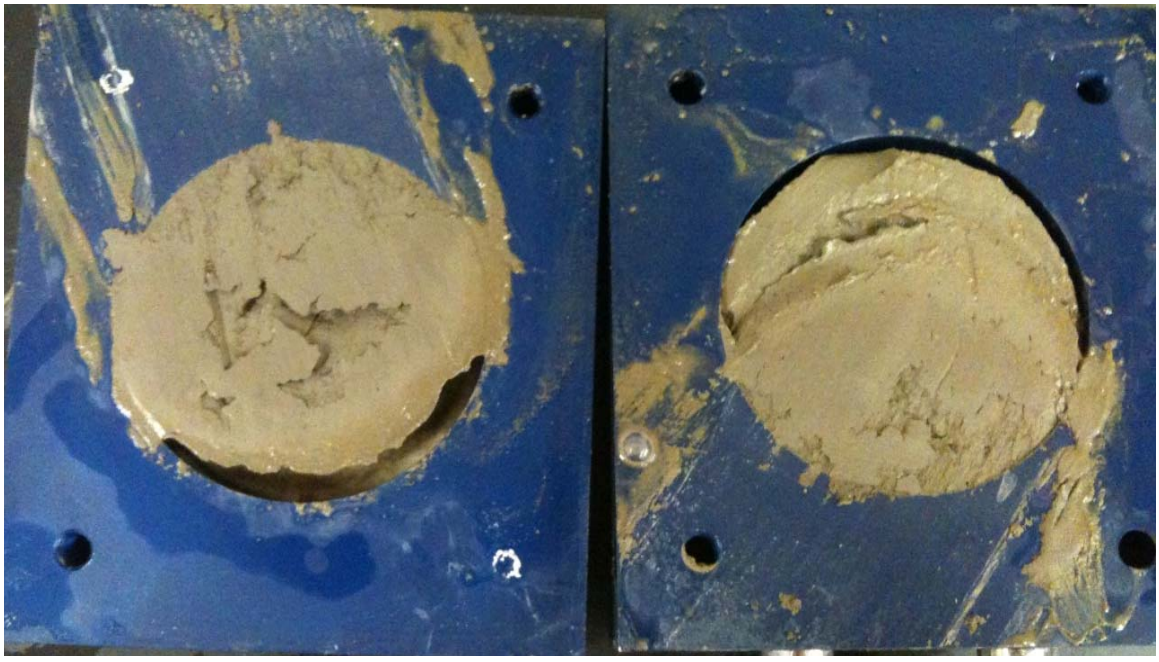

NOVA - Blenderized - 2516 psf

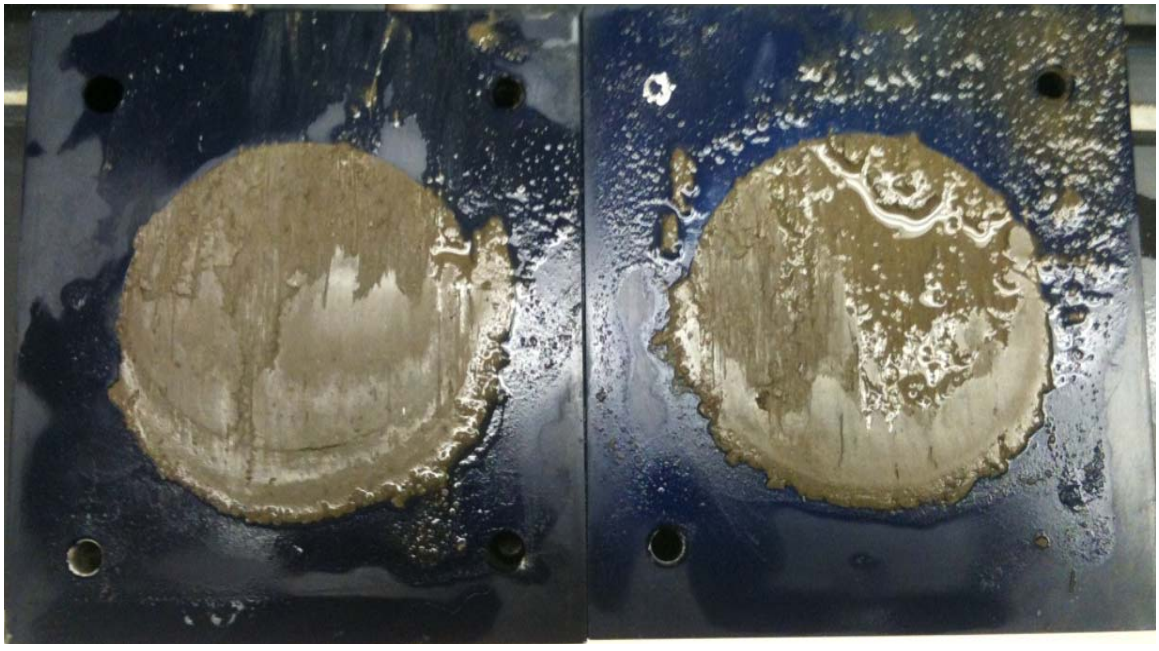

NOVA - Blenderized - 3016 psf

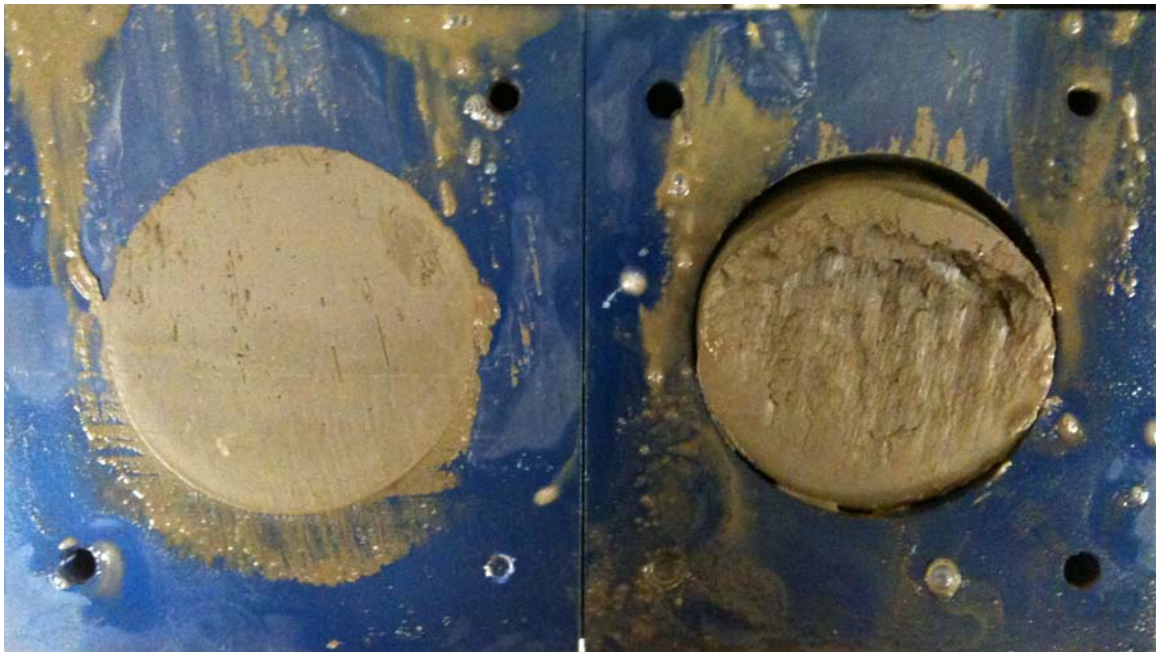

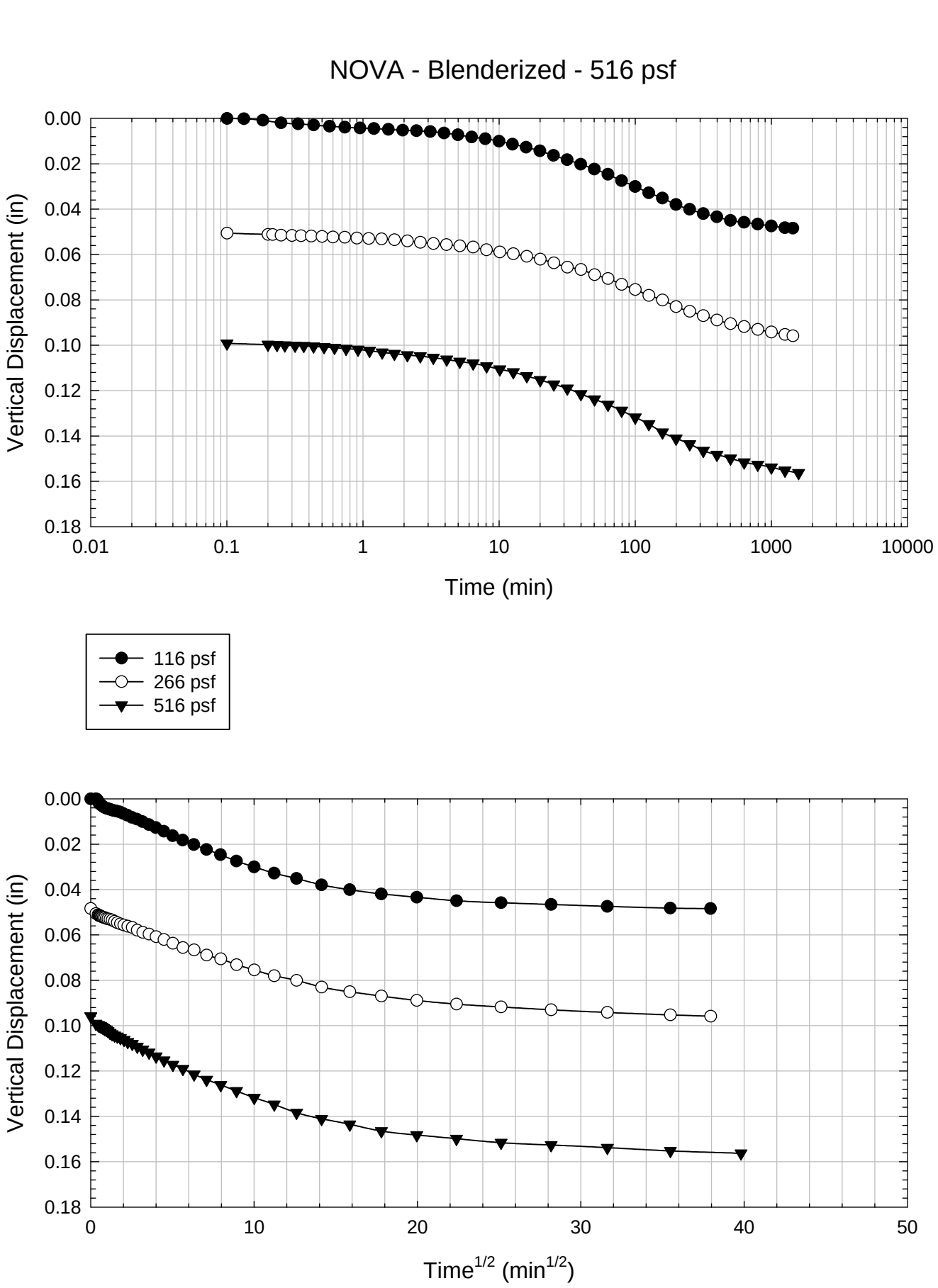
NOVA - Blenderized - 516 psf
Vertical Displacement (in)
0.00
0.02
0.04
0.06
0.08
0.10
0.12
0.14
0.16
0.18
0.01
0.1
1
10
100
1000
10000
Time (min)
116 psf
266 psf
516 psf
Vertical Displacement (in)
0
10
20
30
40
50
Time^1/2 (min^1/2)

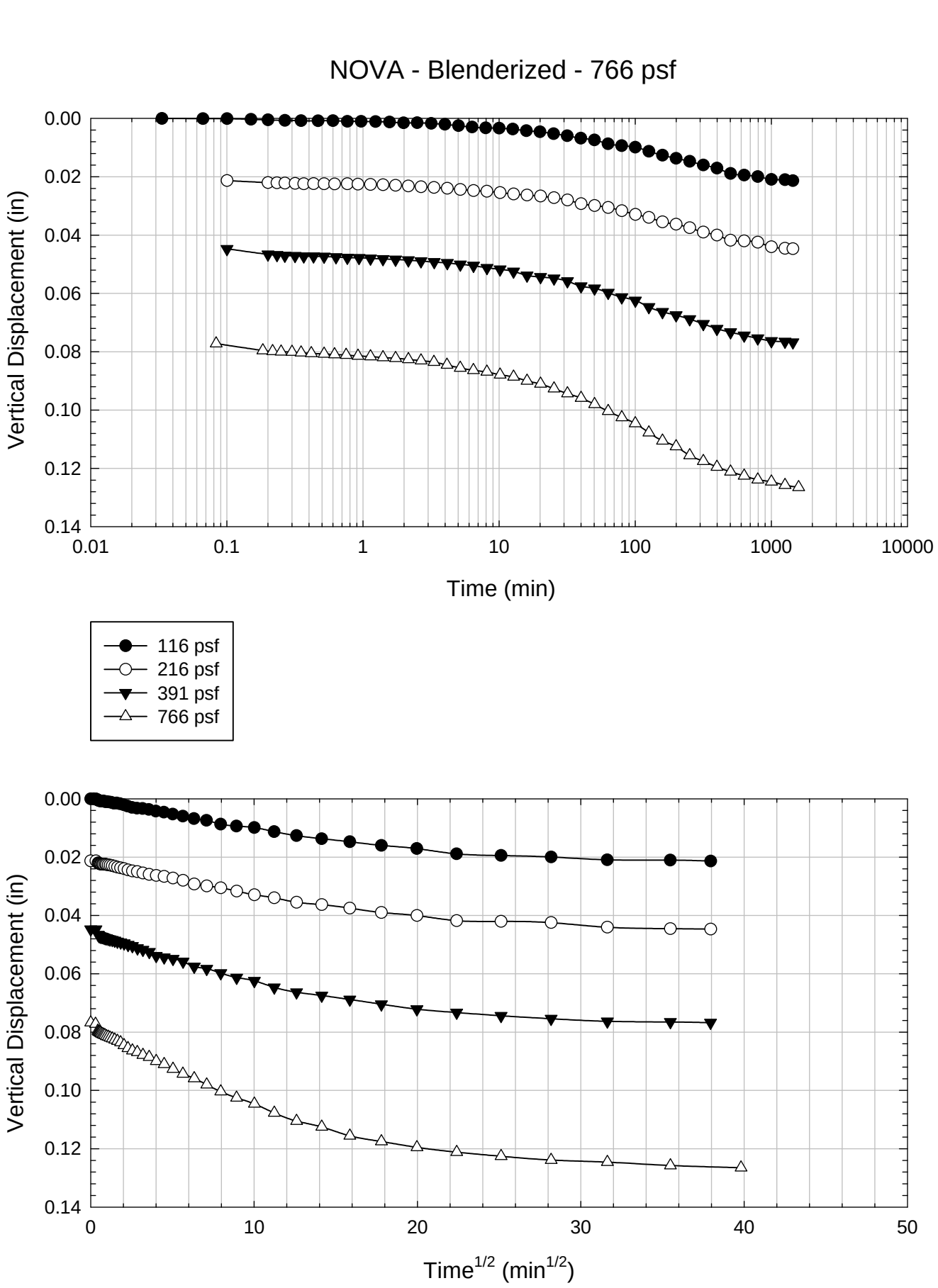
NOVA - Blenderized - 766 psf
Vertical Displacement (in)
0.00
0.02
0.04
0.06
0.08
0.10
0.12
0.14
0.01
0.1
1
10
100
1000
10000
Time (min)
116 psf
216 psf
391 psf
766 psf
Vertical Displacement (in)
0.00
0.02
0.04
0.06
0.08
0.10
0.12
0.14
0
10
20
30
40
50
Time1/2 (min1/2)

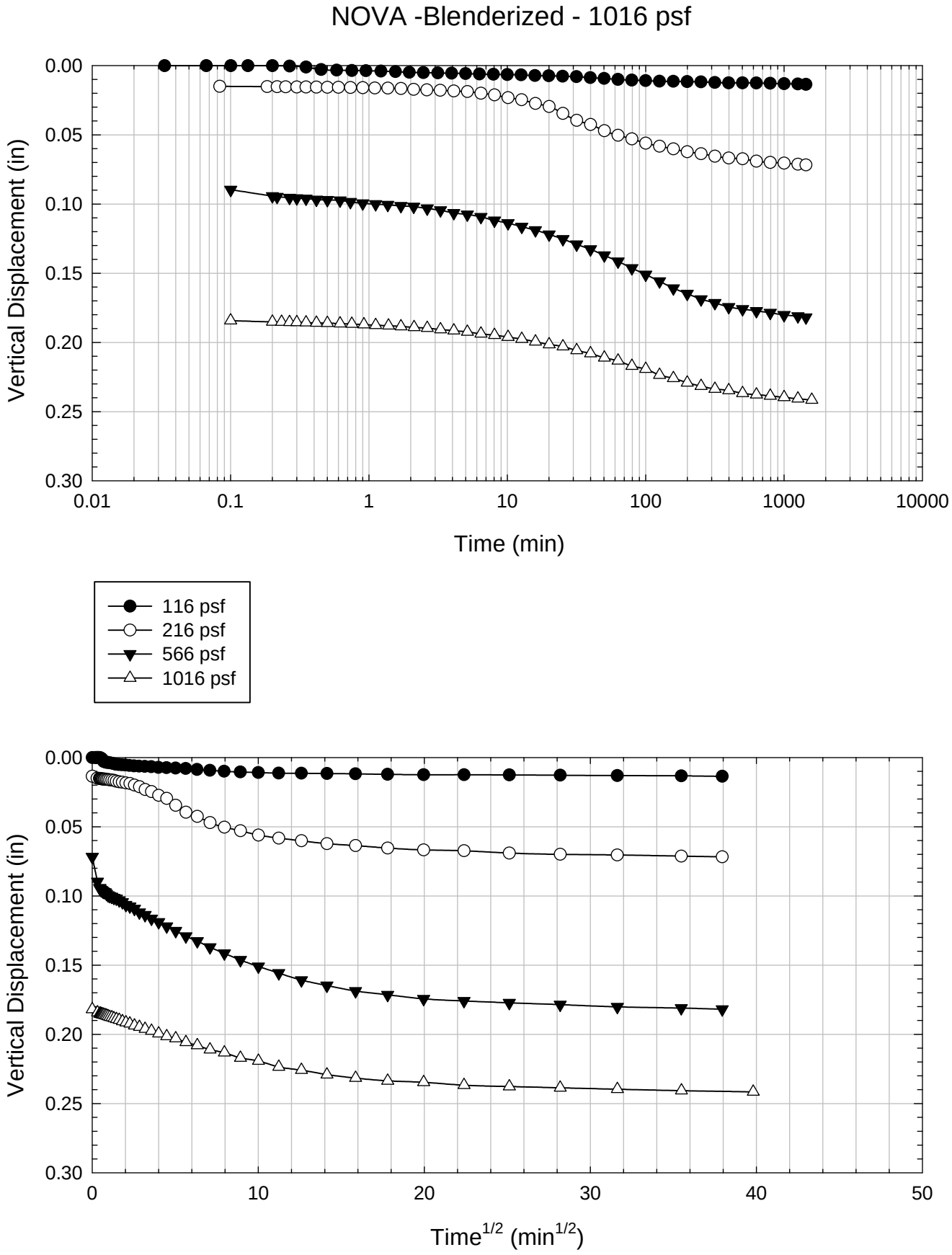
NOVA -Blenderized - 1016 psf
Vertical Displacement (in)
0.00
0.05
0.10
0.15
0.20
0.25
0.30
0.01
0.1
1
10
100
1000
10000
Time (min)
116 psf
216 psf
566 psf
1016 psf
Vertical Displacement (in)
0.00
0.05
0.10
0.15
0.20
0.25
0.30
0
10
20
30
40
50
Time^1/2 (min^1/2)

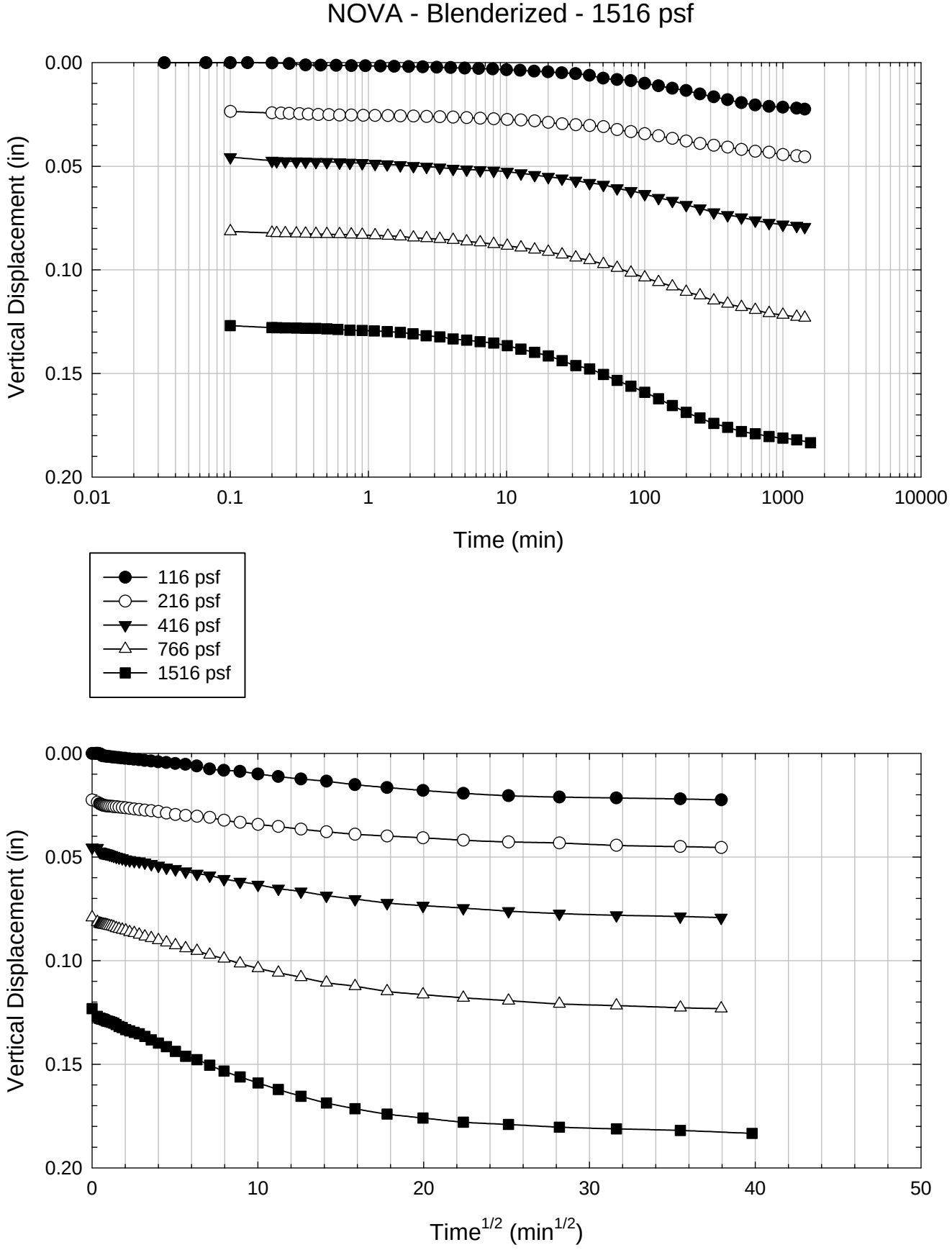
NOVA - Blenderized - 1516 psf
Vertical Displacement (in)
0.00
0.05
0.10
0.15
0.20
0.01
0.1
1
10
100
1000
10000
Time (min)
116 psf
216 psf
416 psf
766 psf
1516 psf
Vertical Displacement (in)
0.00
0.05
0.10
0.15
0.20
0
10
20
30
40
50
Time1/2 (min1/2)

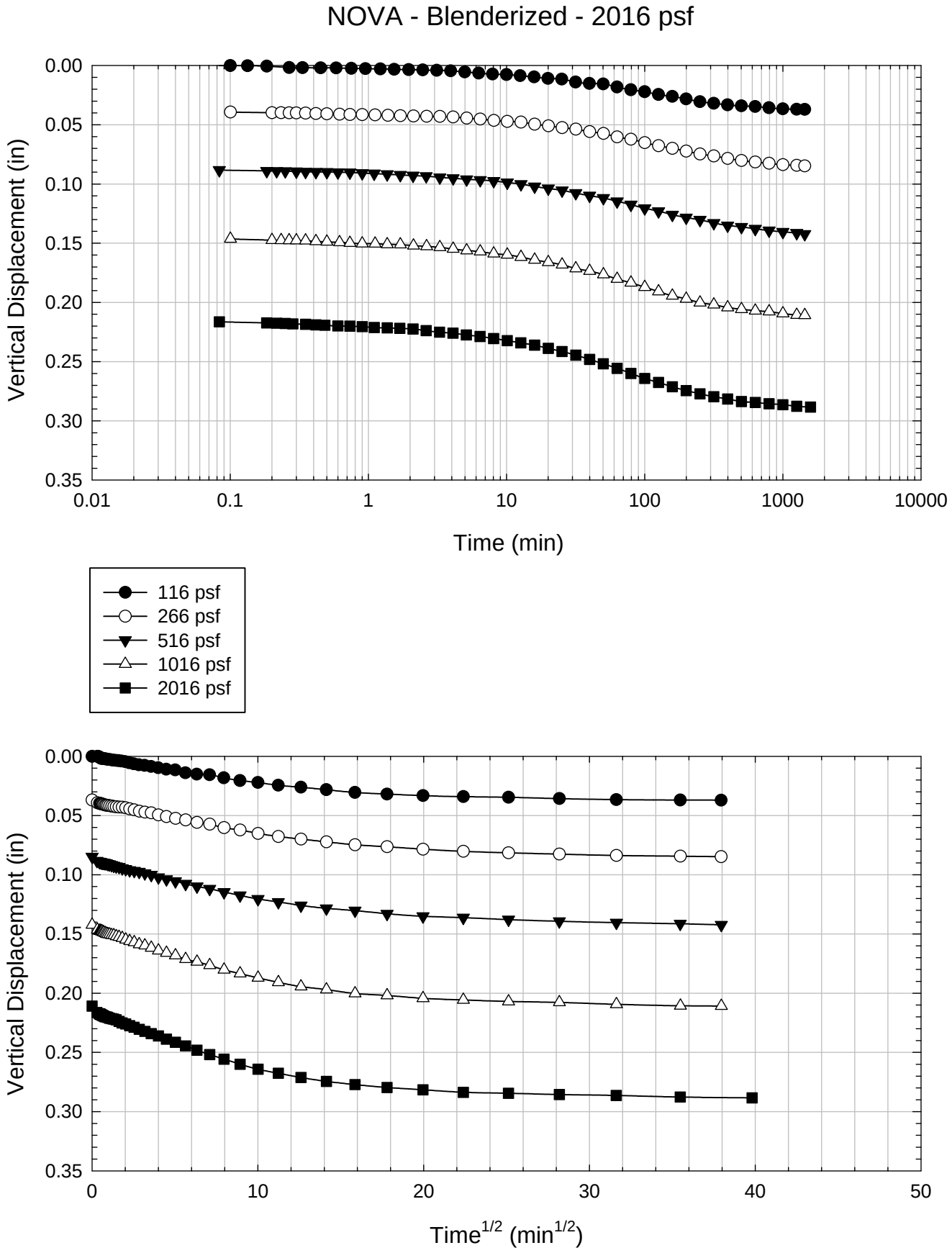
NOVA - Blenderized - 2016 psf
Vertical Displacement (in)
0.00
0.05
0.10
0.15
0.20
0.25
0.30
0.35
0.01
0.1
1
10
100
1000
10000
Time (min)
116 psf
266 psf
516 psf
1016 psf
2016 psf
Vertical Displacement (in)
0.00
0.05
0.10
0.15
0.20
0.25
0.30
0.35
0
10
20
30
40
50
Time^1/2 (min^1/2)

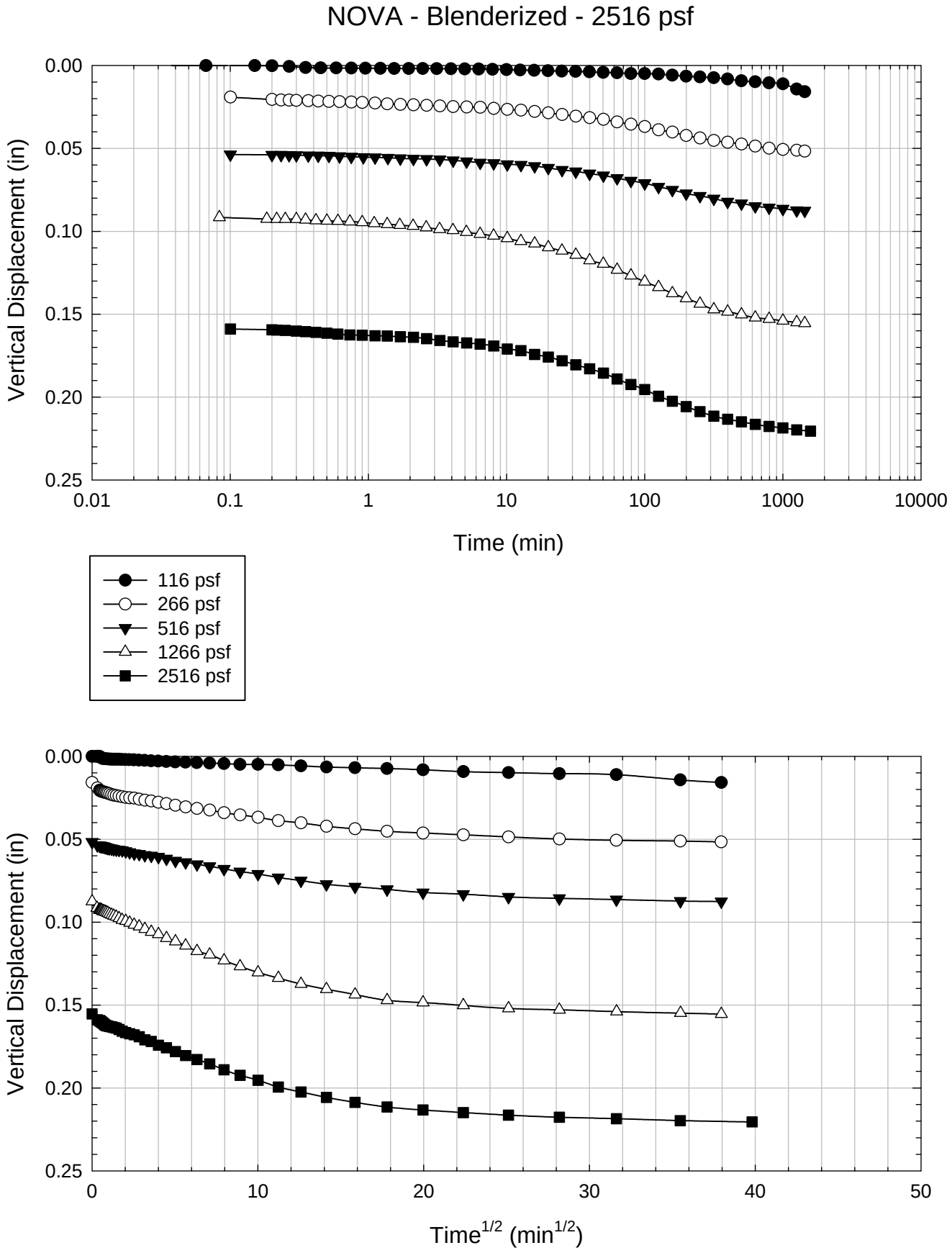
NOVA - Blenderized - 2516 psf
Vertical Displacement (in)
0.00
0.05
0.10
0.15
0.20
0.25
0.01
0.1
1
10
100
1000
10000
Time (min)
116 psf
266 psf
516 psf
1266 psf
2516 psf
Vertical Displacement (in)
0.00
0.05
0.10
0.15
0.20
0.25
0
10
20
30
40
50
Time^1/2 (min^1/2)

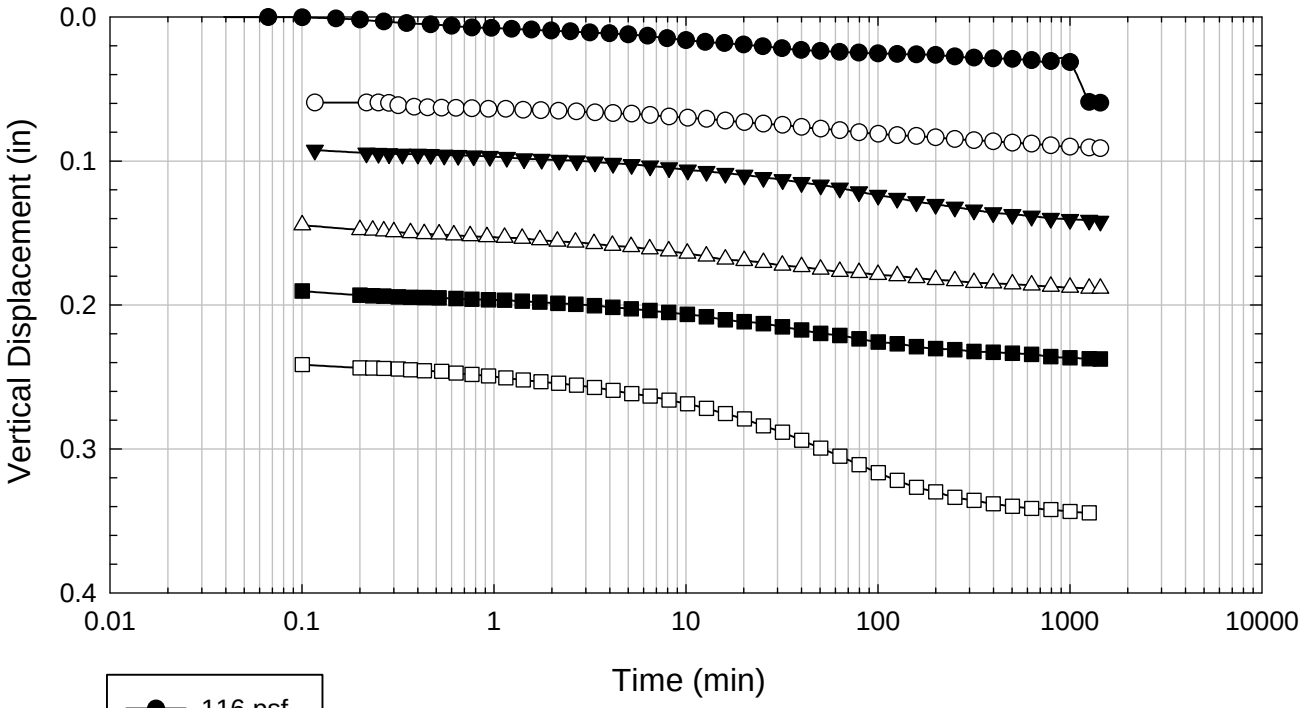
NOVA - Blenderized - 3016 psf
Vertical Displacement (in)
0.0
0.1
0.2
0.3
0.4
0.01
0.1
1
10
100
1000
10000
Time (min)

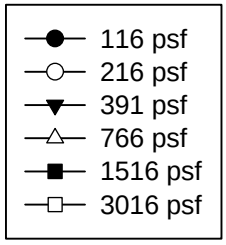
116 psf
216 psf
391 psf
766 psf
1516 psf
3016 psf

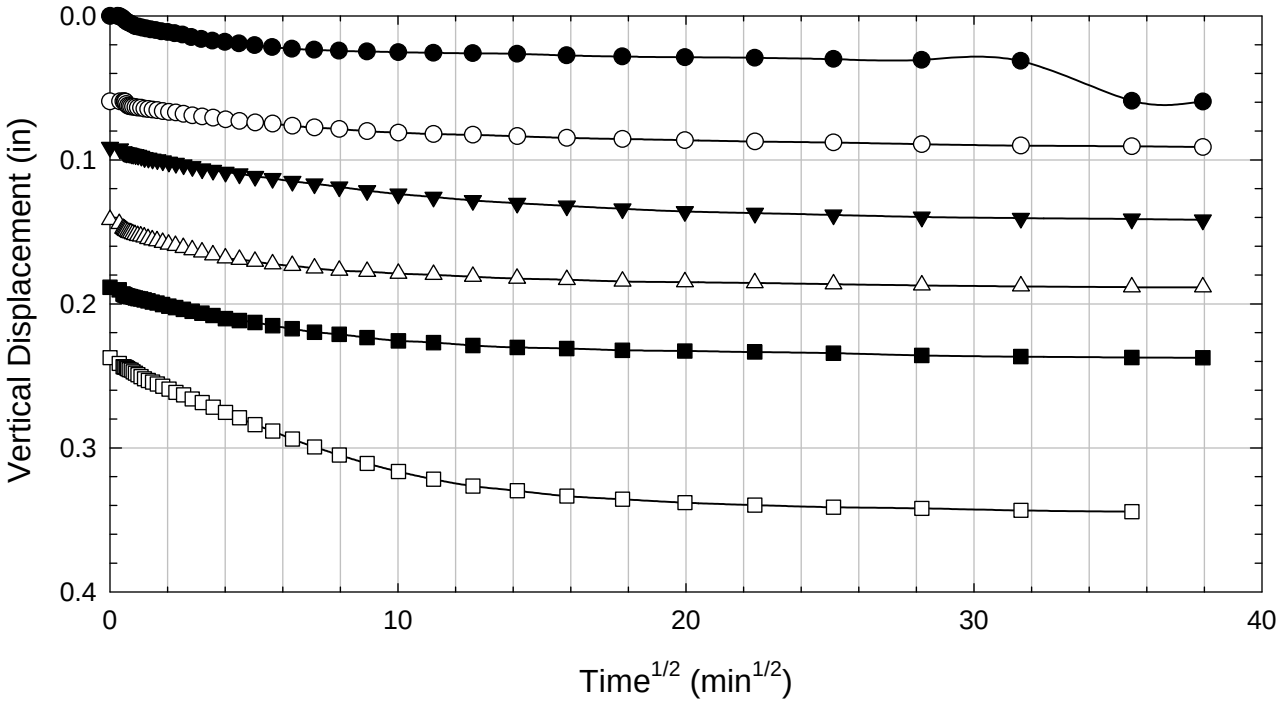
Vertical Displacement (in)
0.0
0.1
0.2
0.3
0.4
0
10
20
30
40
Time^1/2 (min^1/2)

NOVA - Blenderized

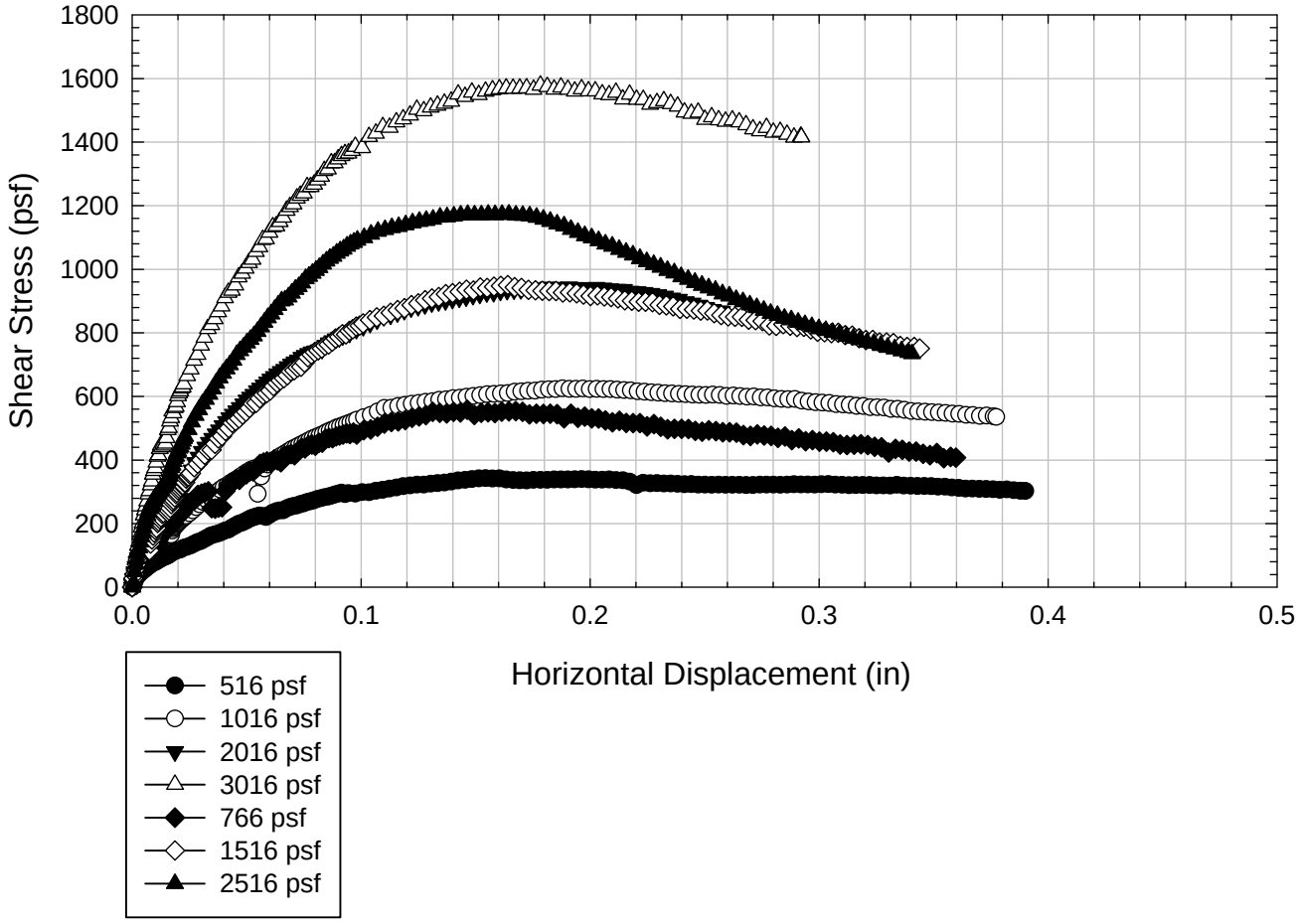

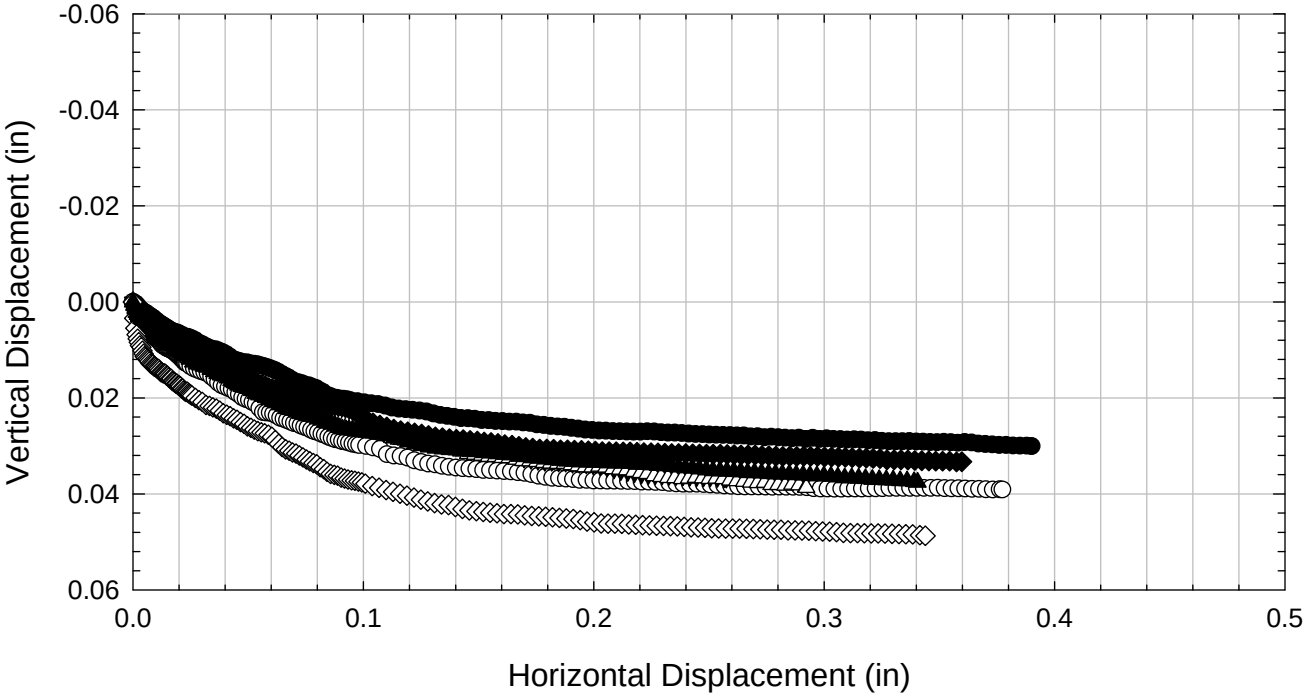

C.6.2 Non-blenderized

Virginia Polytechnic Institute and State University
Geotechnical Engineering Laboratory
Direct Shear Data Sheet

Project:	Fully Softened Shear Strength
Sample I.D./Loc.:	NOVA - Non-blenderized
Classification:	Fat Clay (CH)

Sample Preparation	Remolded at various LI	Specific Gravity	2.80

Test Number	1	2	3	4	5	6	7	8
Start Date (m/d/y)	8/21/2013	8/9/2013	12/3/2013					
End Date (m/d/y)	9/1/2013	8/16/2013	12/20/2013					
Consolidation Pressure (psf)	266	266	266					
Initial Values								
Initial Height (in)	1.30	1.38	1.42					
Initial Diameter (in)	2.50	2.50	2.50					
Initial Sample Weight (g)	166	187	184					
Water Content (%)	103.16	85.14	64.65					
Liquidity Index	2.00	1.50	1.00					
Dry Unit Weight (pcf)	48.87	56.5	61.0					
Wet Unit Weight (pcf)	99.28	104.5	100.4					
Consolidation Pressures								
Load 1 (psf)	66	116	66					
Load 2 (psf)	116	266	116					
Load 3 (psf)	266		266					
Load 4 (psf)								
Load 5 (psf)								
Load 6 (psf)								
Load 7 (psf)								
t_{50}								
Max. t_{50} for Load 1 (min)								
Max. t_{50} for Load 2 (min)								
Max. t_{50} for Load 3 (min)	55.11		130.25					
Max. t_{50} for Load 4 (min)								
Max. t_{50} for Load 5 (min)								
Max. t_{50} for Load 6 (min)								
Max. t_{50} for Load 7 (min)								
Final Values								
Water Content (%)	62.45	61.18	57.90					
Dry Unit Weight (pcf)	70.0	69.9	66.3					
Wet Unit Weight (pcf)	113.6	112.6	104.7					
Failure								
Test Performed at Shear Rate (in/min)	3.63E-05	-	1.54E-05					
Required Shear Rate (in/min)	1.07E-04	-	2.56E-05					
Displacement at Failure (in)	0.29	0.27	0.17					
Peak Shear Stress (psf)	159	146	144					
Total Change in Height at Failure (in)	0.39	0.27	0.11					
Secant Effective Friction Angle (deg)	30.8	28.8	28.5					

Comments:

NOVA - Non-blenderized - 266 psf - Liquidity Index = 2.0

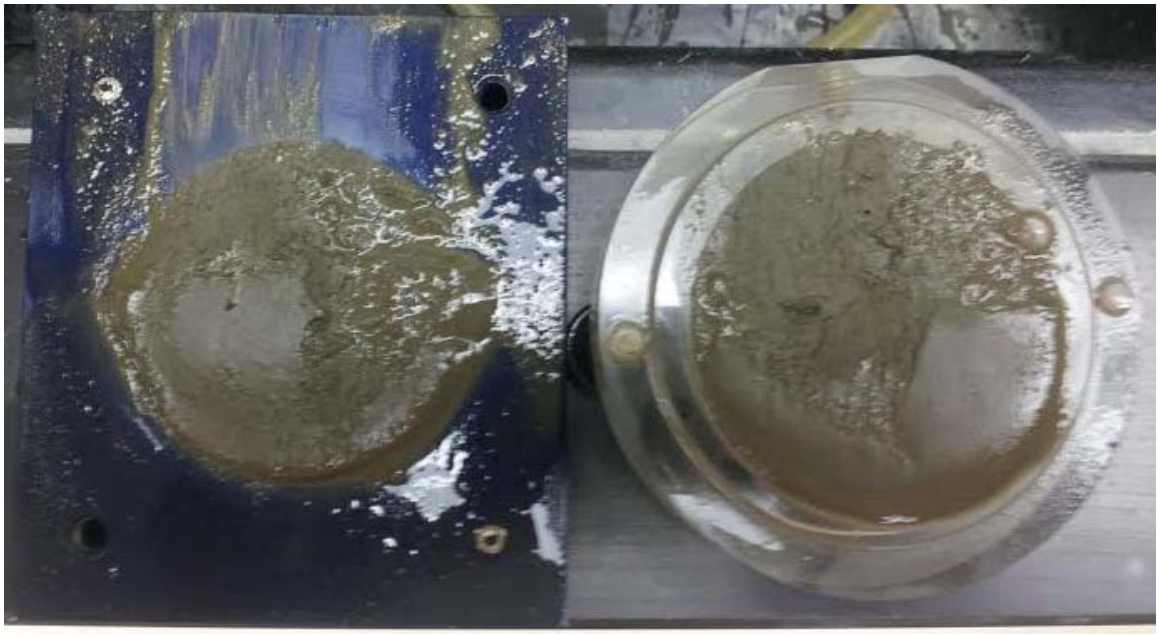

NOVA - Non-blenderized - 266 psf - Liquidity Index = 1.5

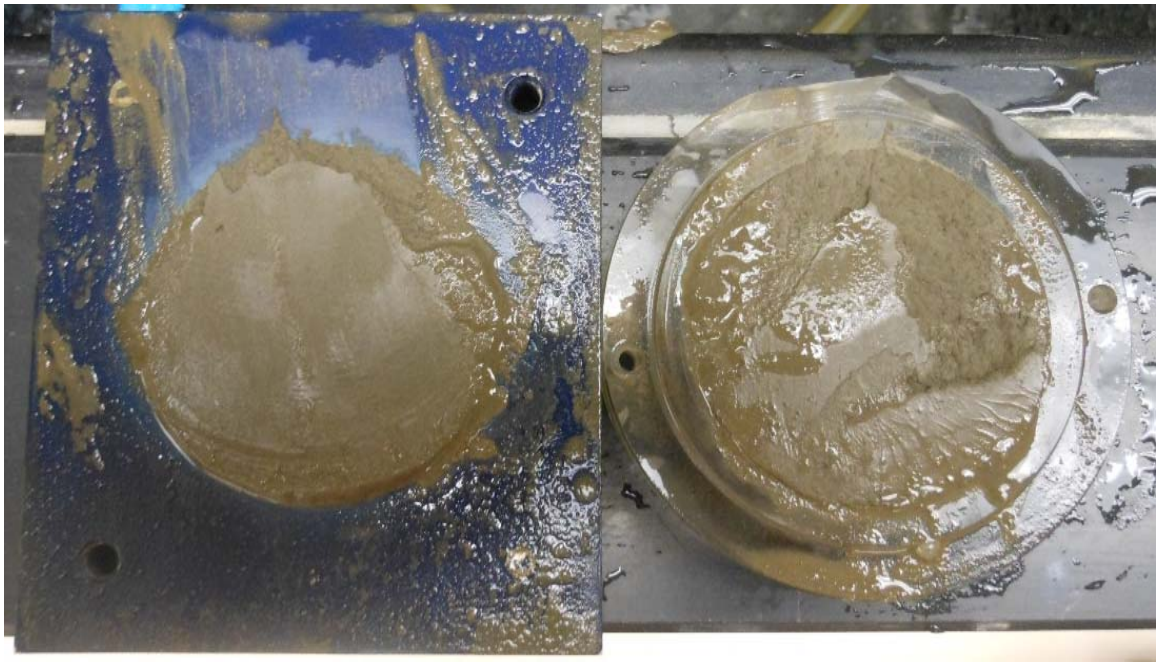

NOVA - Non-blenderized - Liquidity Index = 1.0

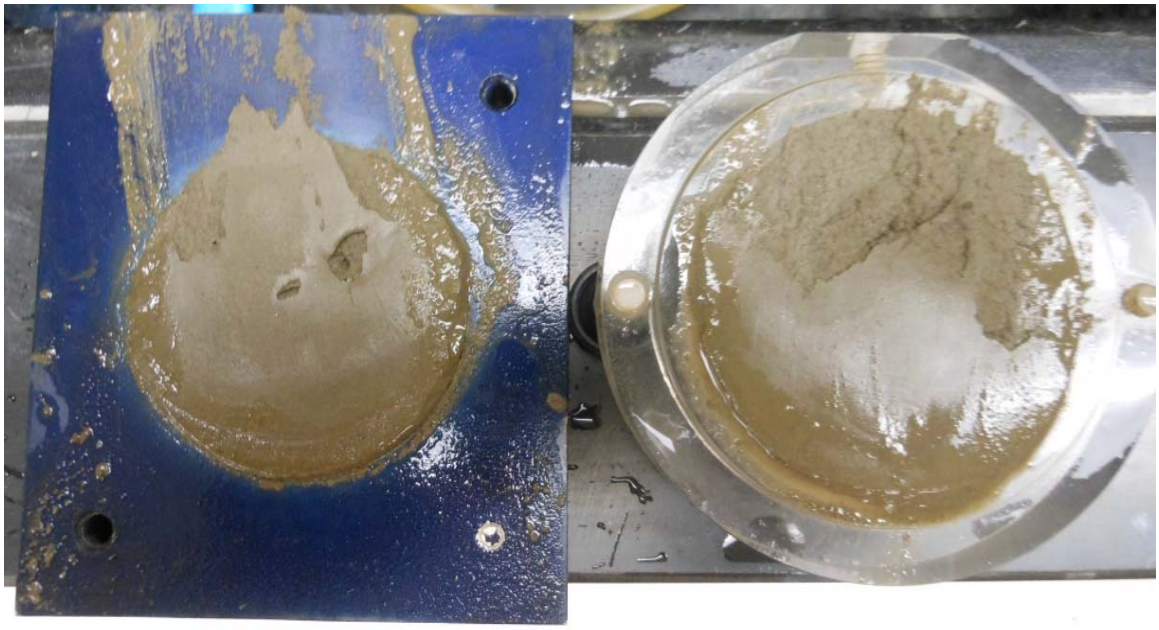

NOVA Clay - Non-blenderized - Liquidity Index = 2.0 - 266 psf

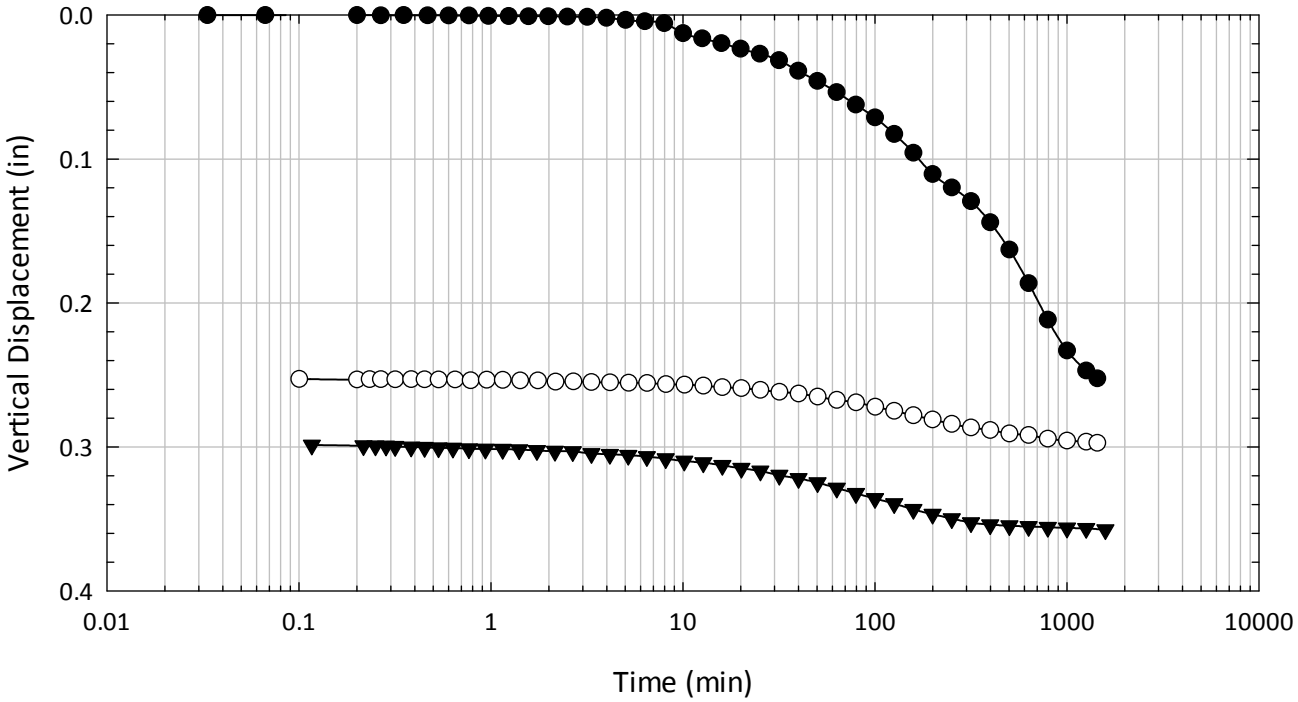

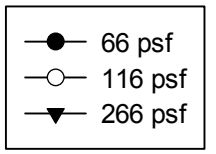

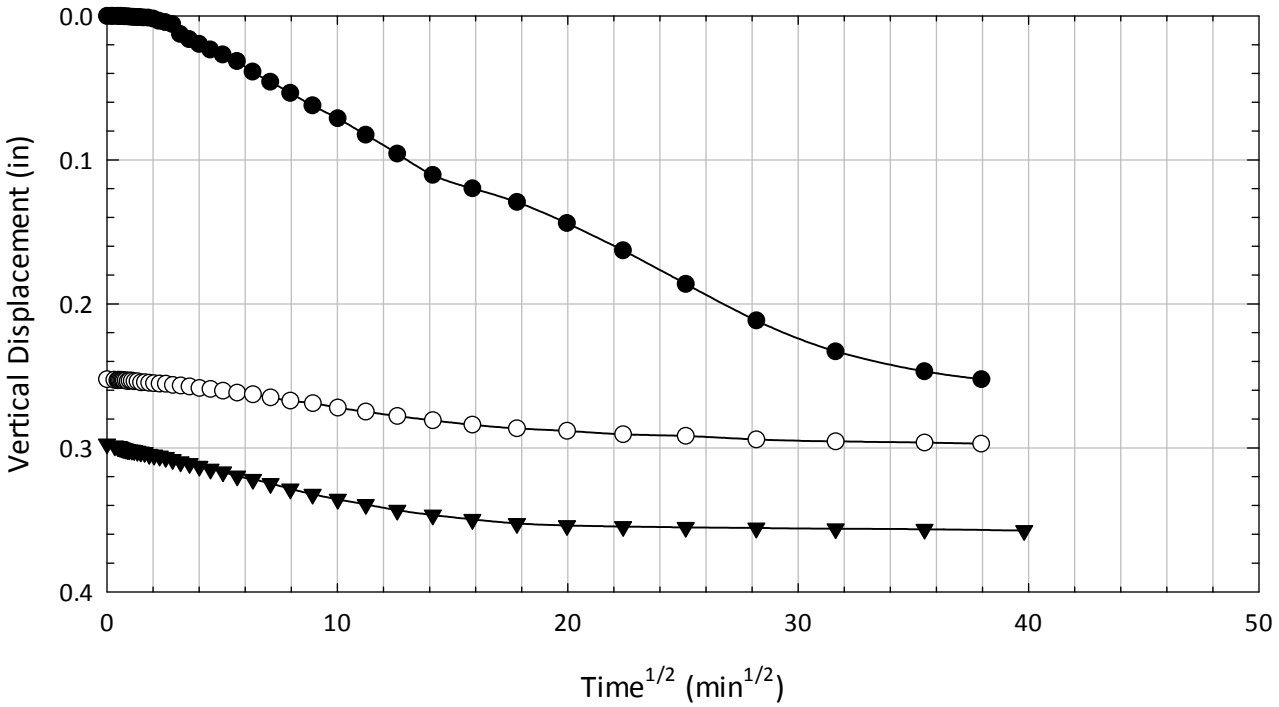

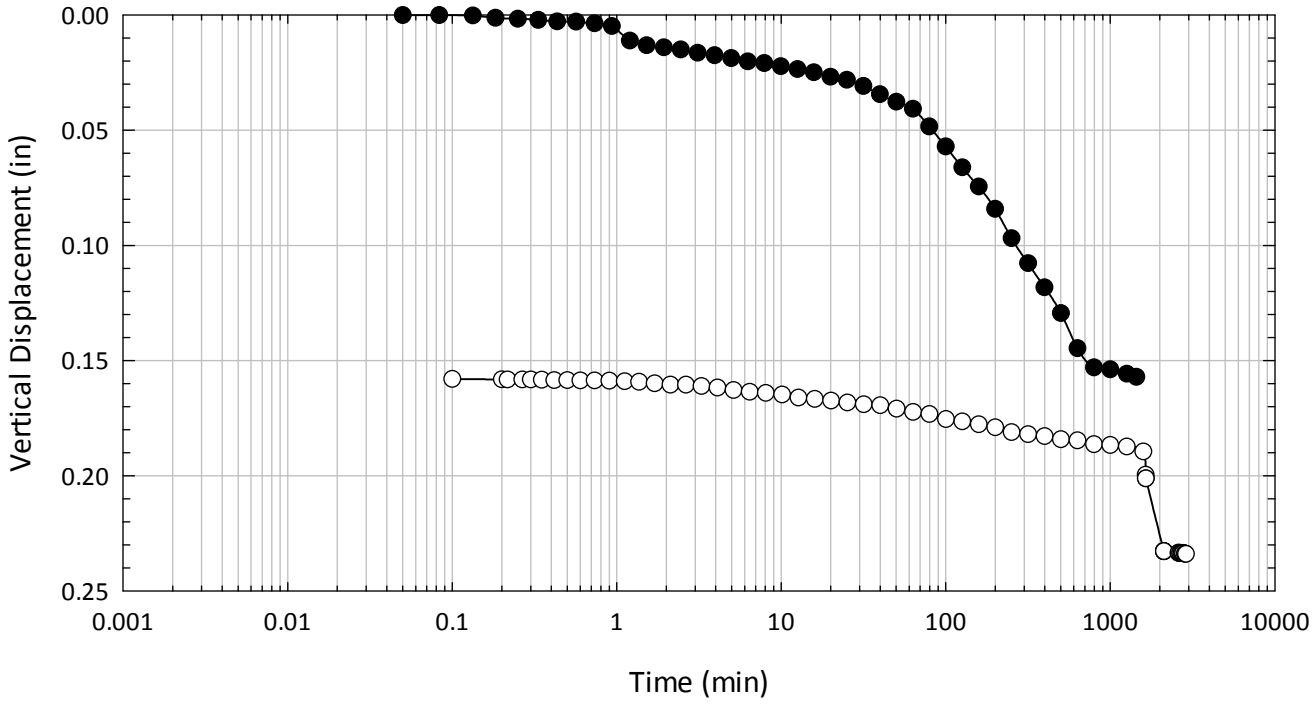
NOVA Clay - Non-blenderized - Liquidity Index = 1.5 - 266 psf
Vertical Displacement (in)
0.00
0.05
0.10
0.15
0.20
0.25
0.001
0.01
0.1
1
10
100
1000
10000
Time (min)

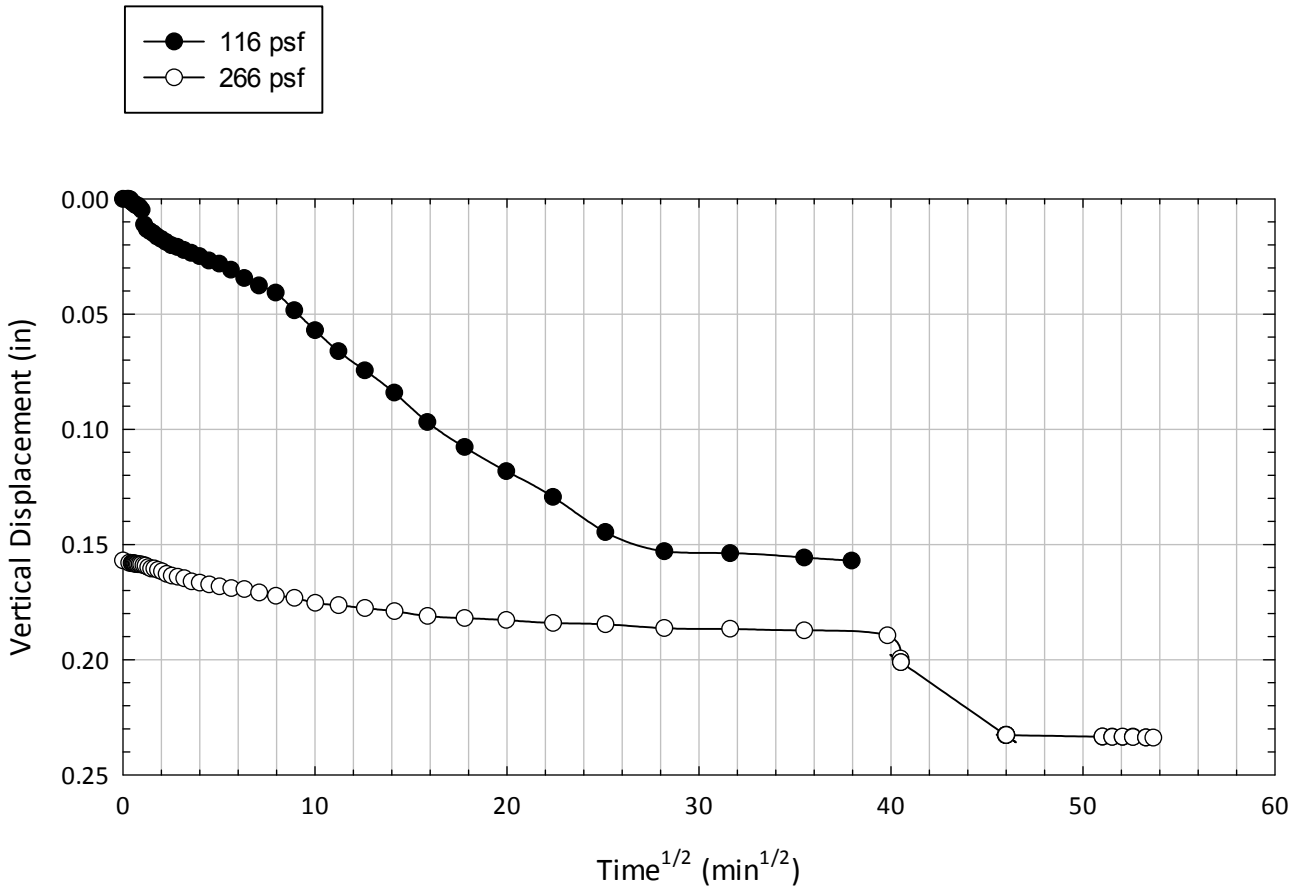
116 psf
266 psf
Vertical Displacement (in)
0.00
0.05
0.10
0.15
0.20
0.25
0
10
20
30
40
50
60
Time^1/2 (min^1/2)

NOVA Clay - Non-blenderized - Liquidity Index = 1.0 - 266 psf

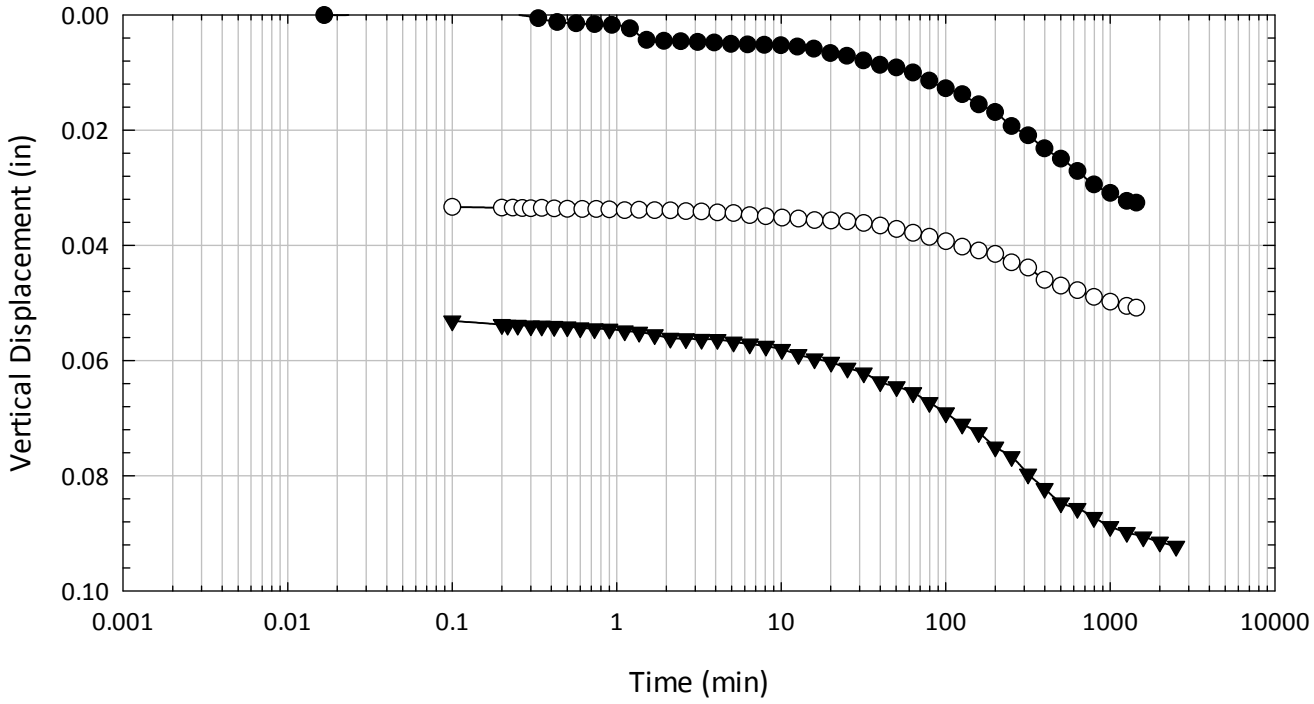

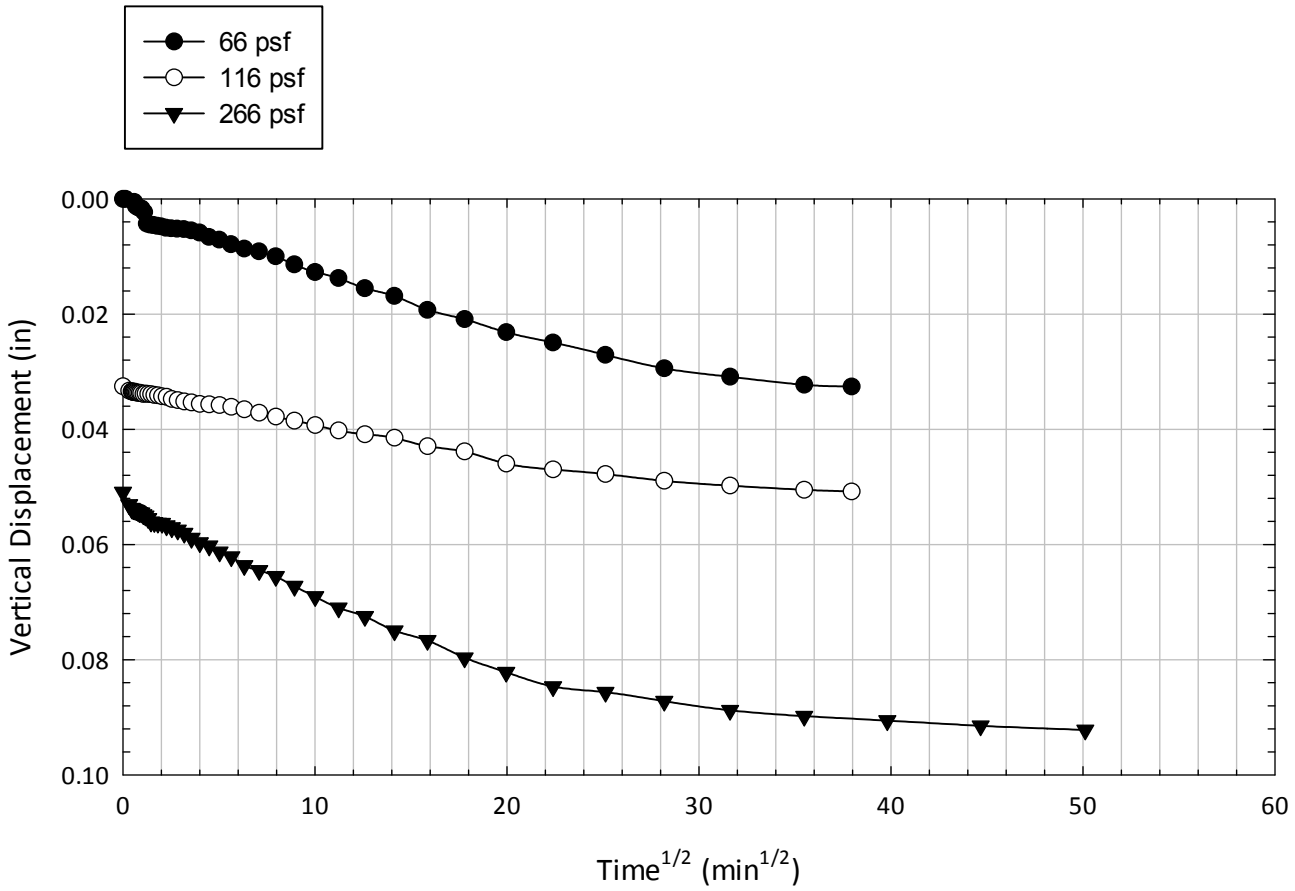

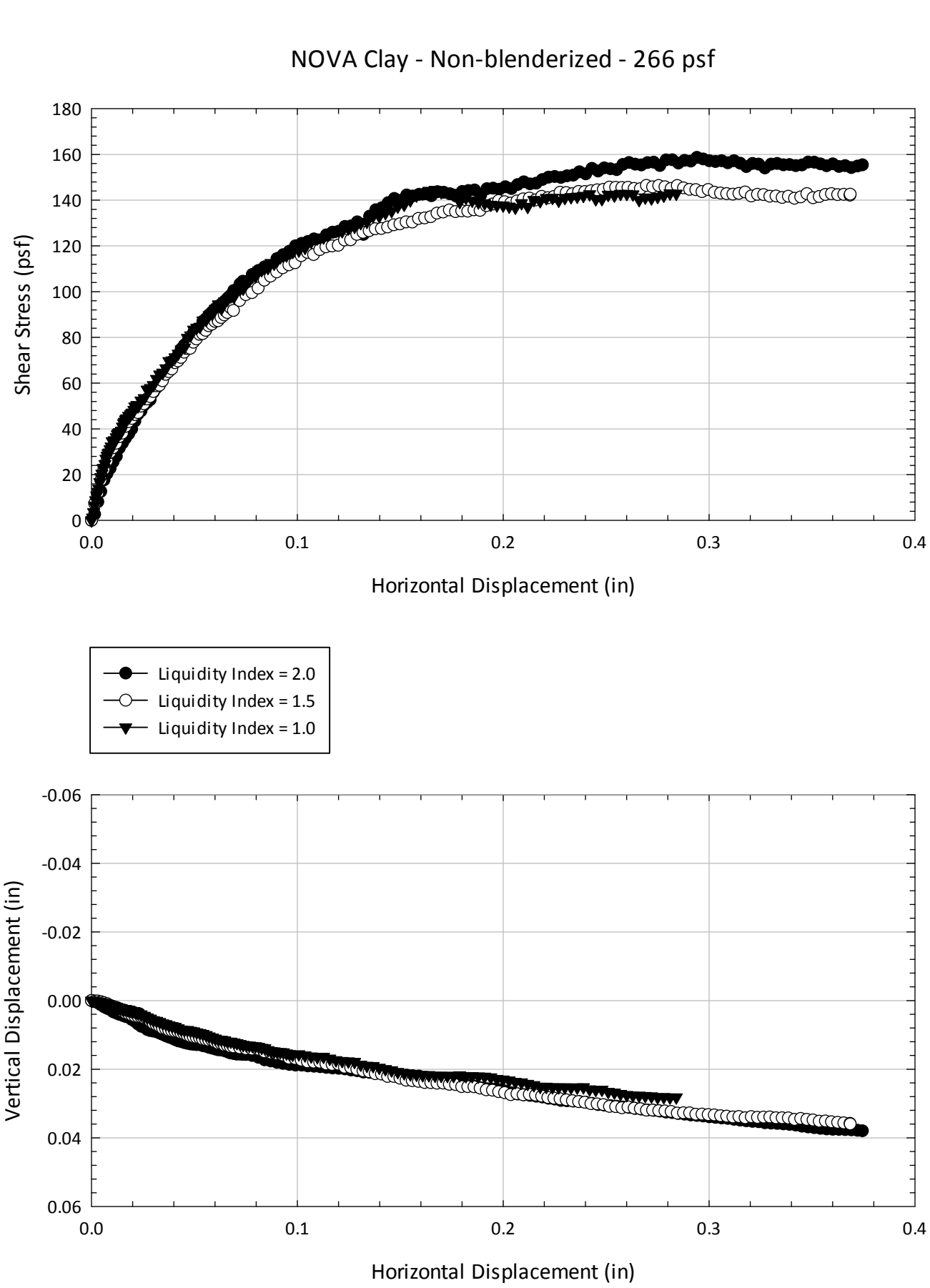
NOVA Clay - Non-blenderized - 266 psf
Shear Stress (psf)
180
160
140
120
100
80
60
40
20
0
0.0
0.1
0.2
0.3
0.4
Horizontal Displacement (in)
Liquidity Index = 2.0
Liquidity Index = 1.5
Liquidity Index = 1.0
Vertical Displacement (in)
-0.06
-0.04
-0.02
0.00
0.02
0.04
0.06
0.0
0.1
0.2
0.3
0.4
Horizontal Displacement (in)

Virginia Polytechnic Institute and State University
Geotechnical Engineering Laboratory
Direct Shear Data Sheet

Project:	Fully Softened Shear Strength
Sample I.D./Loc.:	NOVA - Non-blenderized
Classification:	Fat Clay (CH)

Sample Preparation	Remolded at LL		Specific Gravity	2.80

Test Number	1	2	3	4	5	6	7	8
Start Date (m/d/y)	11/1/2011	11/1/2011	11/7/2011	11/1/2011	11/1/2011	11/1/2011		
End Date (m/d/y)	11/7/2011	11/7/2011	11/15/2011	11/9/2011	11/9/2011	11/10/2011		
Consolidation Pressure (psf)	516	1016	2016	3016	4516	6016		
Initial Values								
Initial Height (in)	1.45	1.43	1.43	1.40	1.41	1.45		
Initial Diameter (in)	2.50	2.50	2.50	2.50	2.50	2.50		
Initial Sample Weight (g)	186	189	187	182	190	187		
Water Content (%)	68.96	69.21	67.24	69.18	70.48	70.43		
Dry Unit Weight (pcf)	58.82	60.5	60.7	59.6	61.5	58.7		
Wet Unit Weight (pcf)	99.39	102.4	101.6	100.8	104.8	100.0		
Consolidation Pressures								
Load 1 (psf)	116	116	116	116	116	116		
Load 2 (psf)	266	266	266	216	266	216		
Load 3 (psf)	516	516	516	391	516	391		
Load 4 (psf)		1016	1016	766	1141	766		
Load 5 (psf)			2016	1516	2266	1516		
Load 6 (psf)				3016	4516	3016		
Load 7 (psf)						6016		
t_{50}								
Max. t_{50} for Load 1 (min)								
Max. t_{50} for Load 2 (min)								
Max. t_{50} for Load 3 (min)	17.35							
Max. t_{50} for Load 4 (min)		17.23						
Max. t_{50} for Load 5 (min)			29.09					
Max. t_{50} for Load 6 (min)				14.01	14.00			
Max. t_{50} for Load 7 (min)						16.53		
Final Values								
Water Content (%)	57.53	54.49		47.09	44.89	41.93		
Dry Unit Weight (pcf)	66.2	71.6		78.2	88.5	84.01		
Wet Unit Weight (pcf)	104.4	110.7		115.0	128.3	119.23		
Failure								
Test Performed at Shear Rate (in/min)	1.15E-04	1.16E-04	1.43E-04	1.43E-04	1.43E-04	1.21E-04		
Required Shear Rate (in/min)	1.84E-04	2.21E-04	1.51E-04	2.86E-04	3.00E-04	2.30E-04		
Displacement at Failure (in)	0.16	0.19	0.22	0.20	0.21	0.19		
Peak Shear Stress (psf)	360	713	1143	1757	2176	3015		
Total Change in Height at Failure (in)	0.16	0.22	0.29	0.33	0.36	0.43		
Secant Effective Friction Angle (deg)	34.9	35.0	29.6	30.2	25.7	26.6		

Comments: In the test consolidated to 516 psf, power was lost during the 266 psf consolidation stress. The test was continued.
In the test consolidated to 3016 psf, power was lost during the 266 psf consolidation stress. The test was continued.

NOVA - Non-blenderized - 516 psf

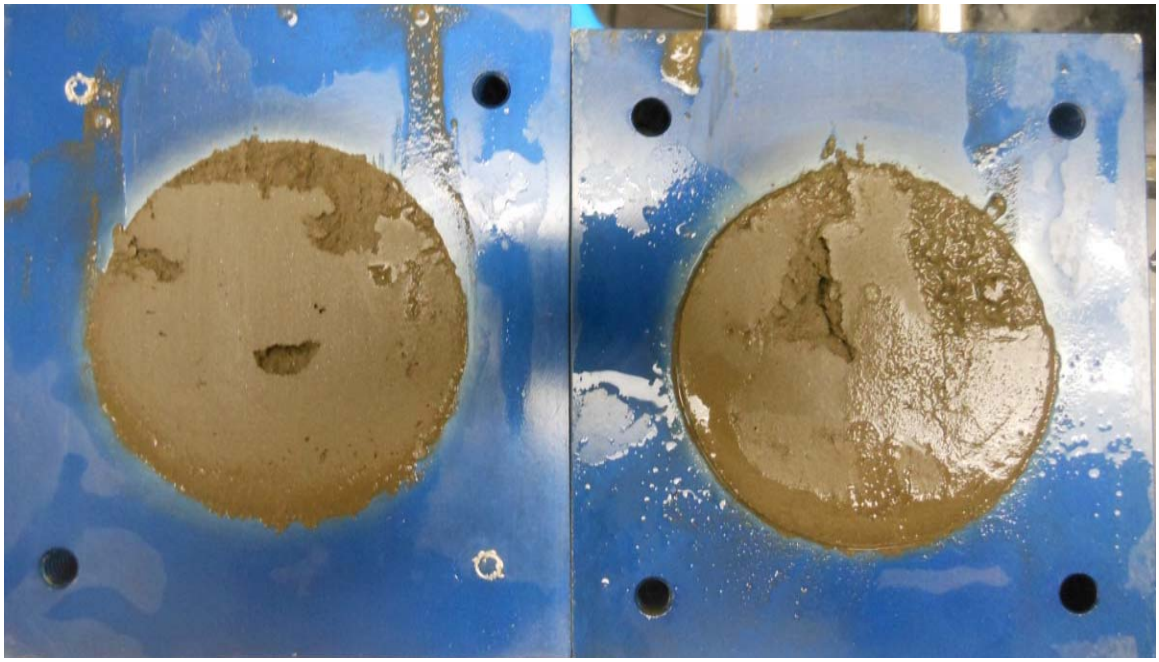

NOVA - Non-blenderized - 1016 psf

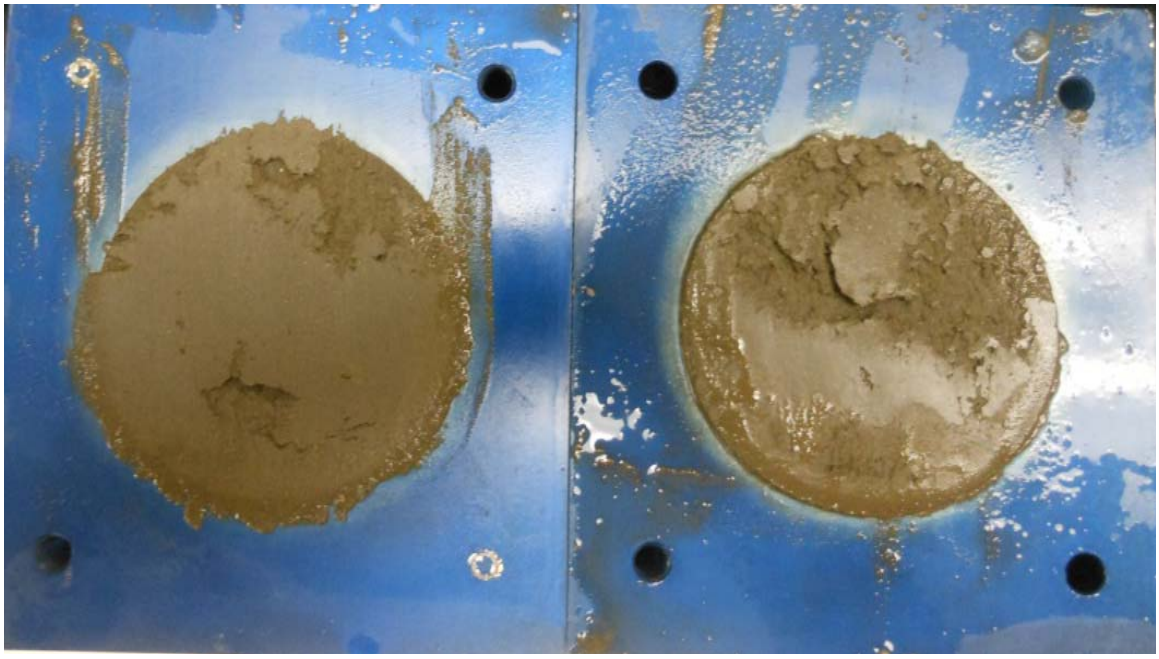

NOVA - Non-blenderized - 2016 psf

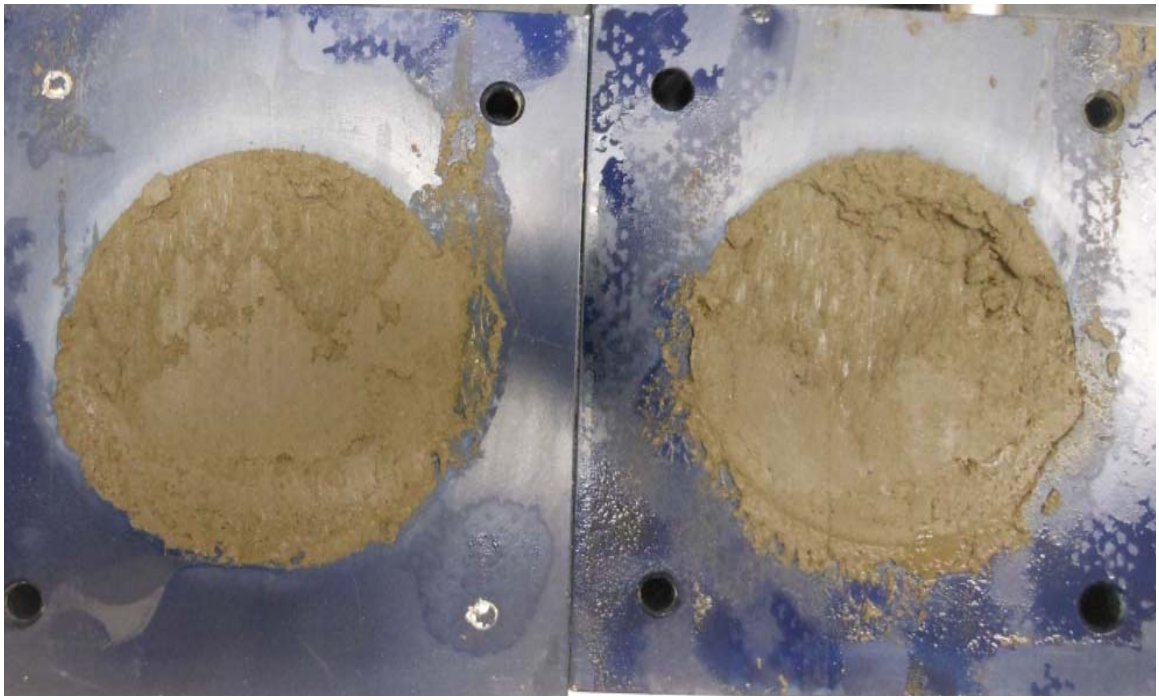

NOVA - Non-blenderized - 3016 psf

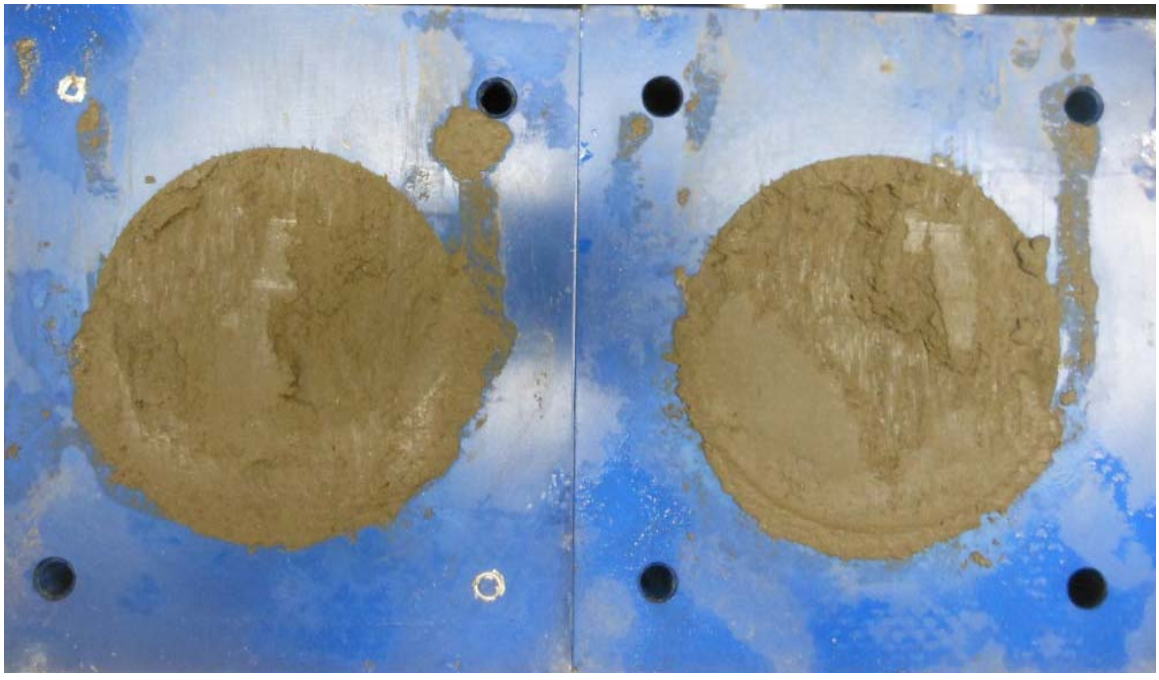

NOVA - Non-blenderized - 4516 psf

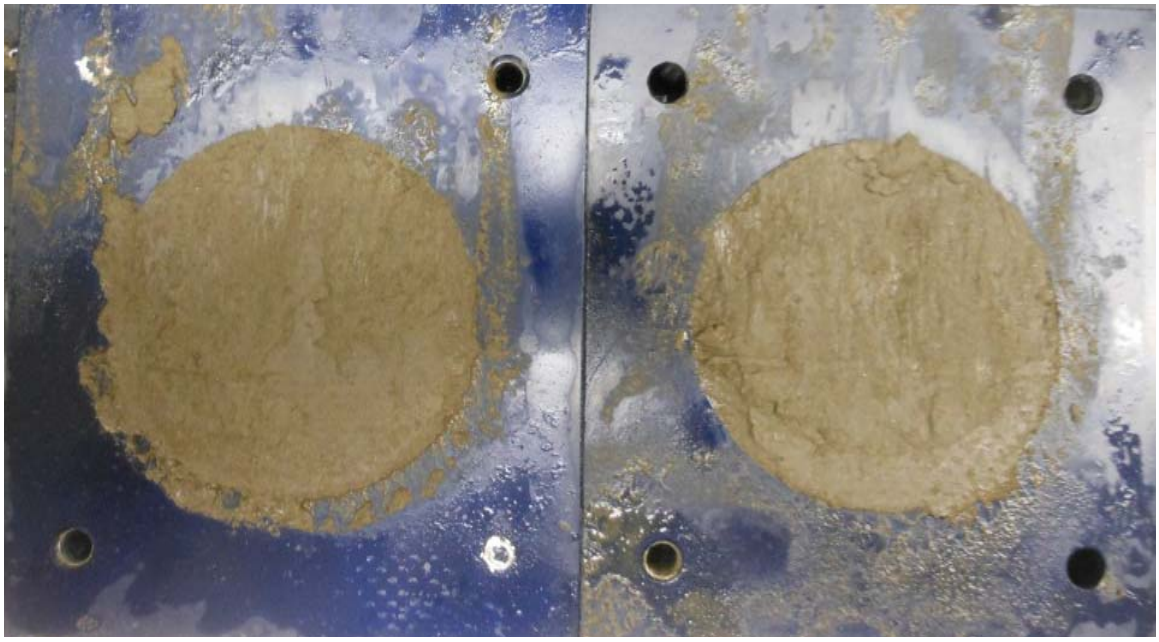

NOVA - Non-blenderized - 6016 psf

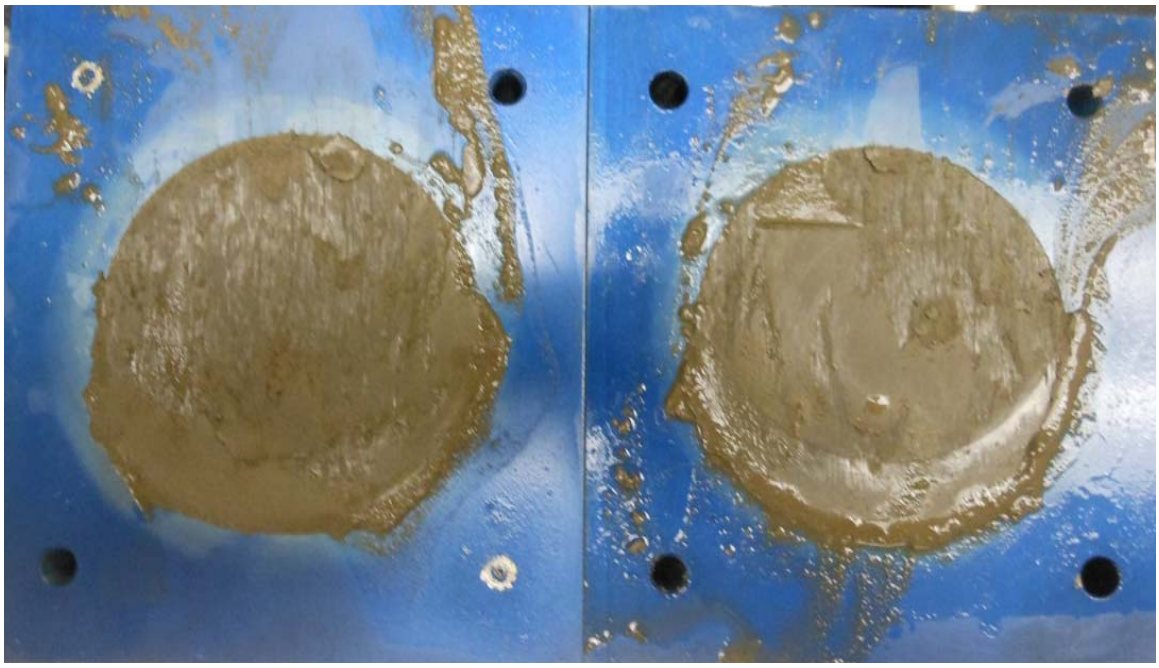

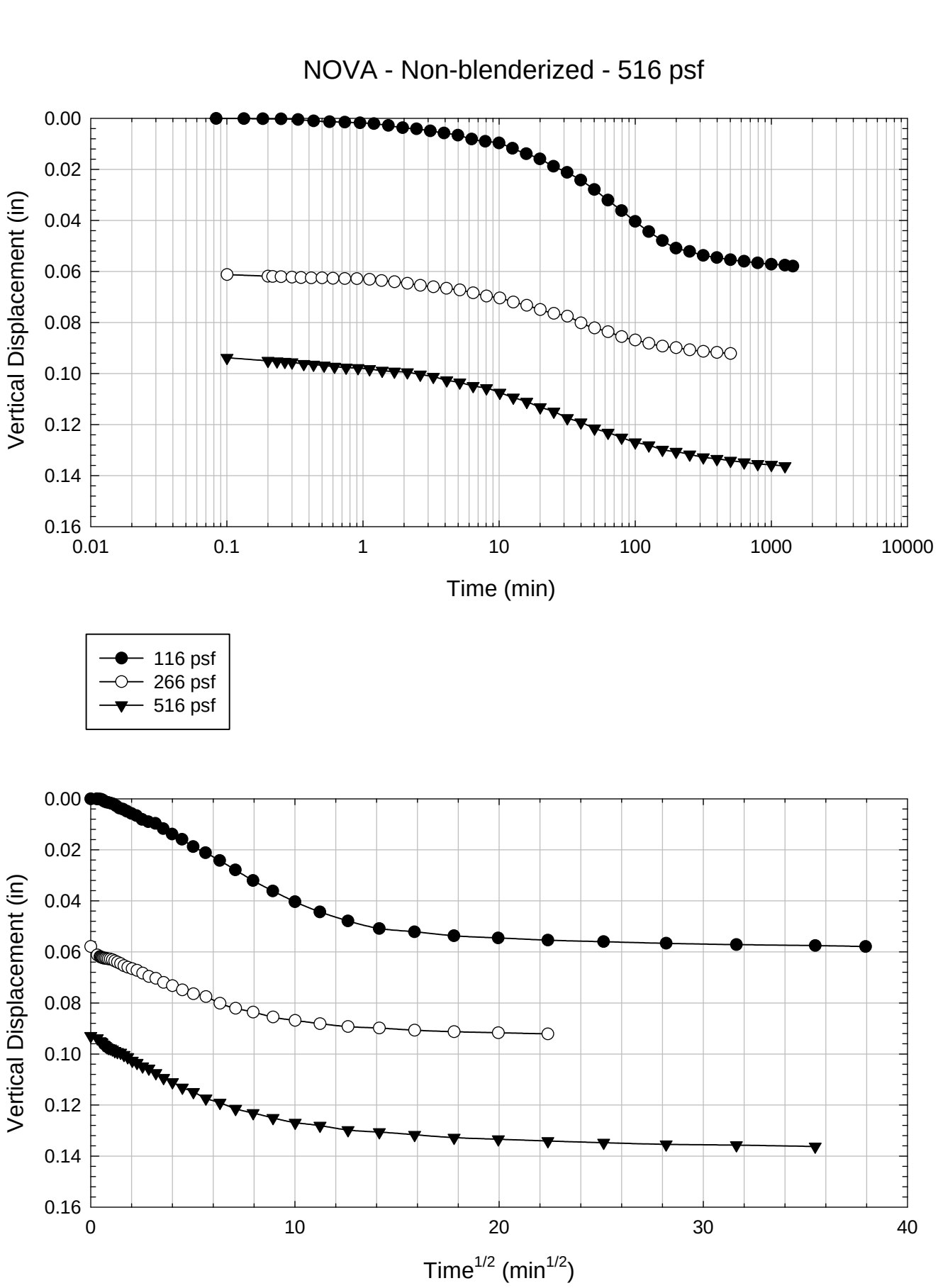
NOVA - Non-blenderized - 516 psf
Vertical Displacement (in)
0.00
0.02
0.04
0.06
0.08
0.10
0.12
0.14
0.16
0.01
0.1
1
10
100
1000
10000
Time (min)
116 psf
266 psf
516 psf
Vertical Displacement (in)
0
10
20
30
40
Time^1/2 (min^1/2)

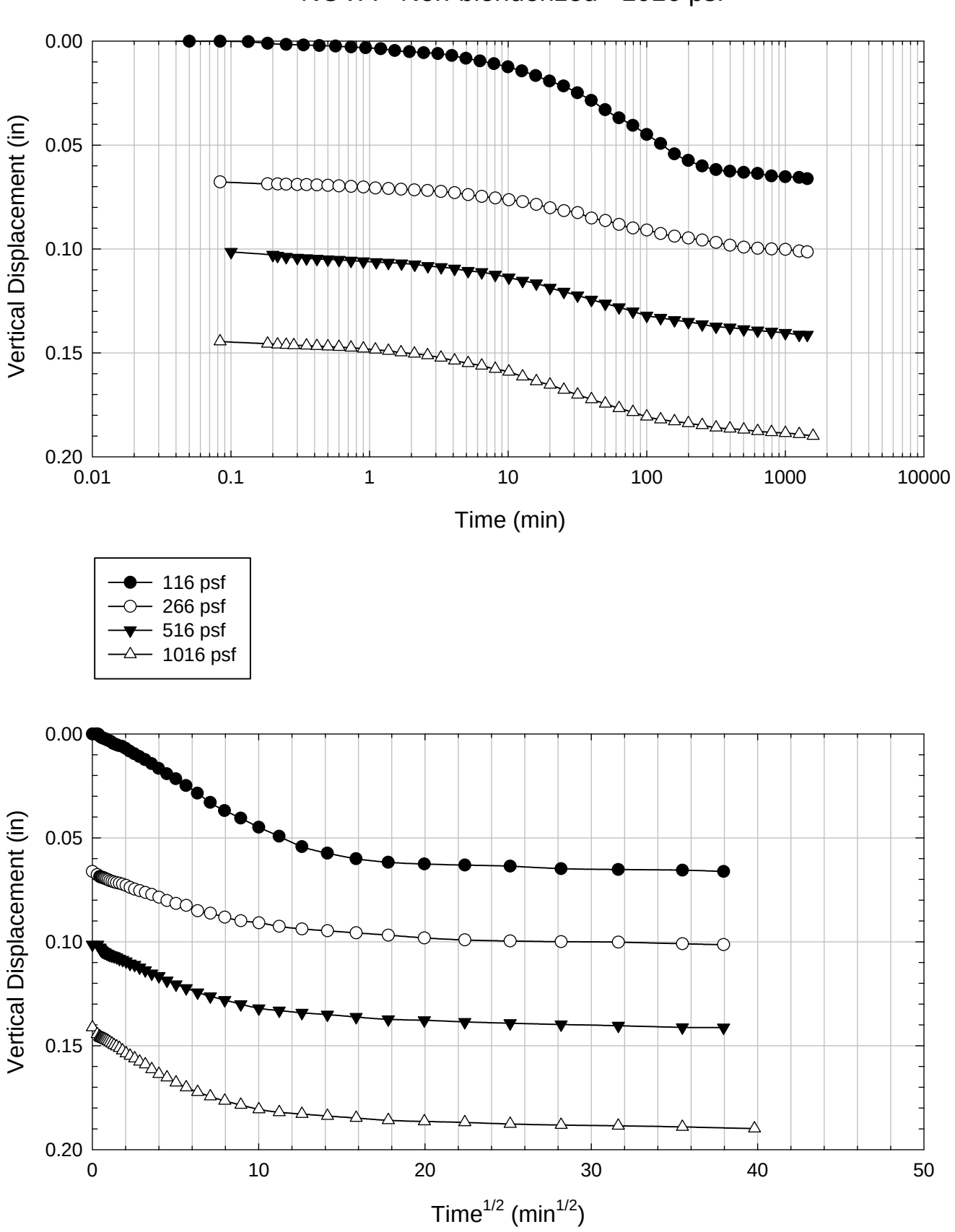
NOVA - Non-blenderized - 1016 psf
Vertical Displacement (in)
0.00
0.05
0.10
0.15
0.20
0.01
0.1
1
10
100
1000
10000
Time (min)
116 psf
266 psf
516 psf
1016 psf
Vertical Displacement (in)
0.00
0.05
0.10
0.15
0.20
0
10
20
30
40
50
Time1/2 (min1/2)

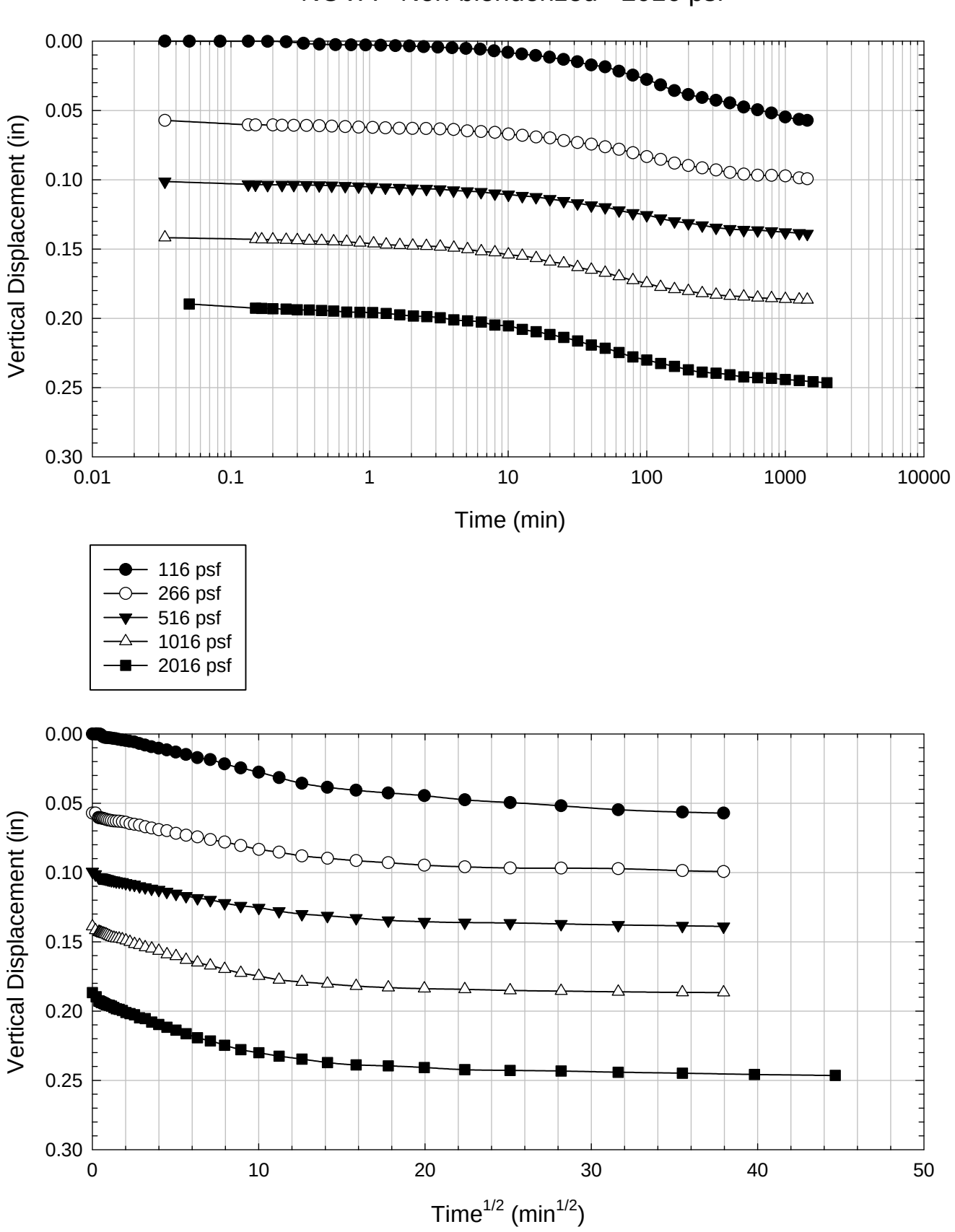
NOVA - Non-blenderized - 2016 psf
Vertical Displacement (in)
0.00
0.05
0.10
0.15
0.20
0.25
0.30
0.01
0.1
1
10
100
1000
10000
Time (min)
116 psf
266 psf
516 psf
1016 psf
2016 psf
Vertical Displacement (in)
0.00
0.05
0.10
0.15
0.20
0.25
0.30
0
10
20
30
40
50
Time1/2 (min1/2)

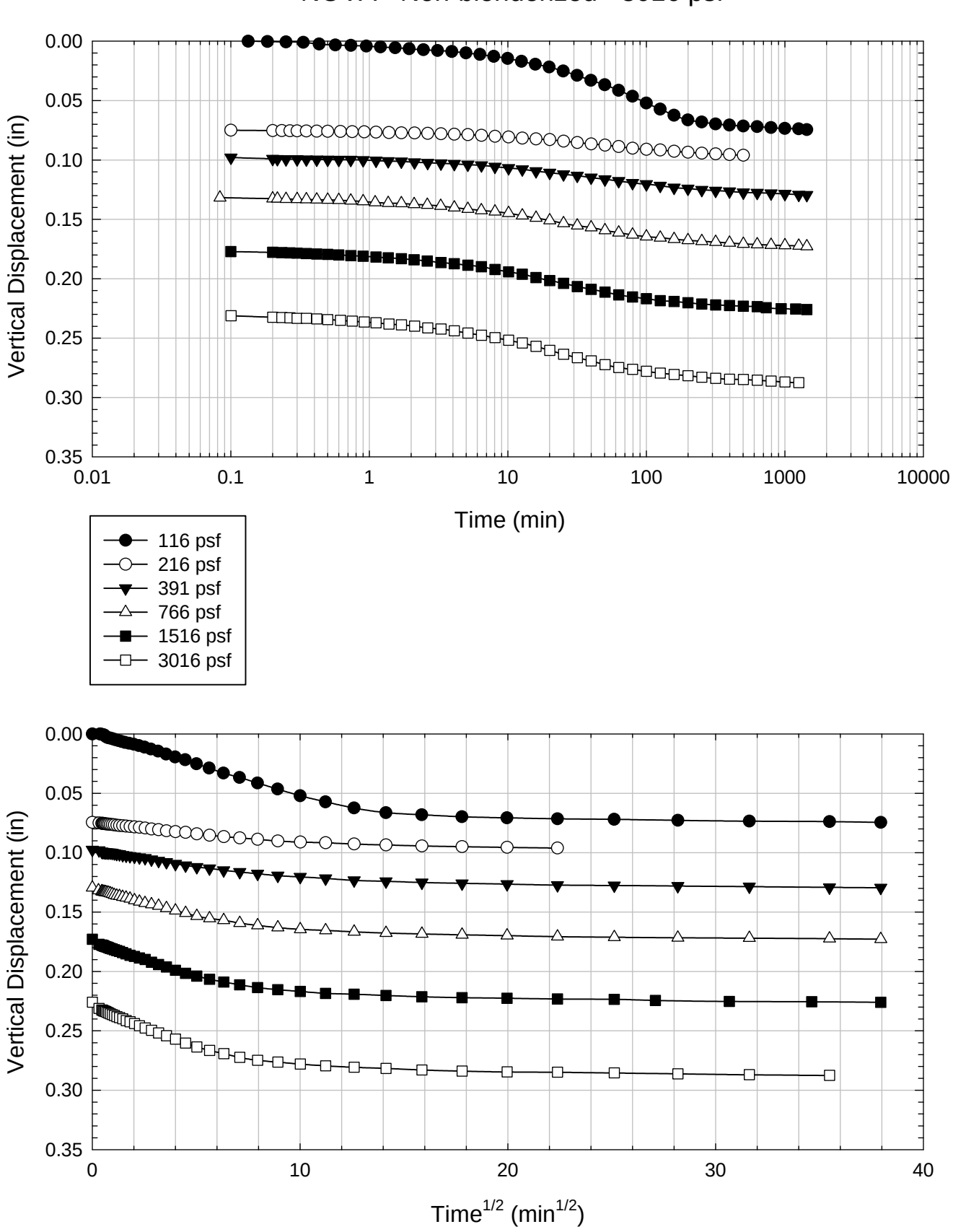
NOVA - Non-blenderized - 3016 psf
Vertical Displacement (in)
0.00
0.05
0.10
0.15
0.20
0.25
0.30
0.35
0.01
0.1
1
10
100
1000
10000
Time (min)
116 psf
216 psf
391 psf
766 psf
1516 psf
3016 psf
Vertical Displacement (in)
0.00
0.05
0.10
0.15
0.20
0.25
0.30
0.35
0
10
20
30
40
Time^1/2 (min^1/2)

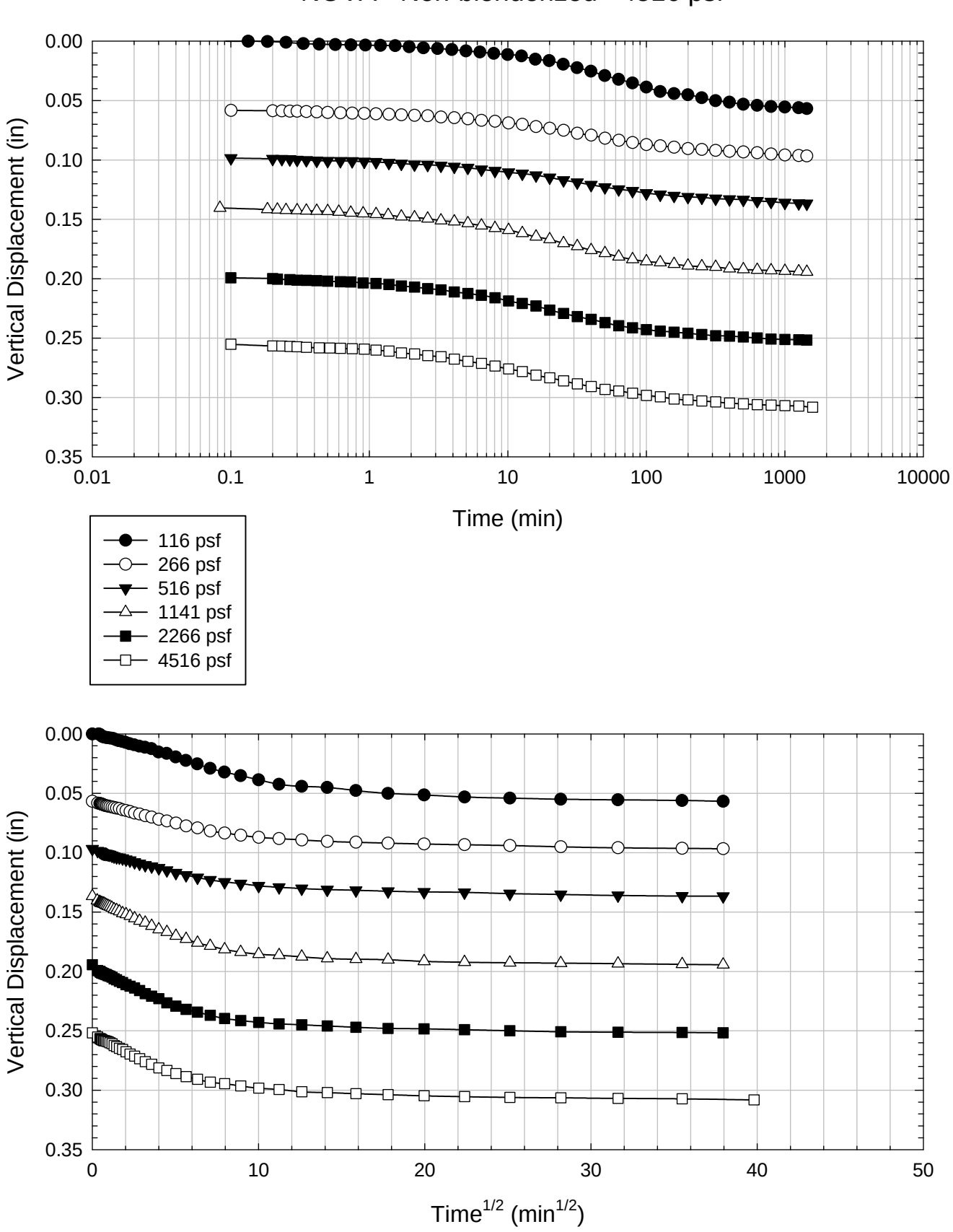
NOVA - Non-blenderized - 4516 psf
Vertical Displacement (in)
0.00
0.05
0.10
0.15
0.20
0.25
0.30
0.35
0.01
0.1
1
10
100
1000
10000
Time (min)
116 psf
266 psf
516 psf
1141 psf
2266 psf
4516 psf
Vertical Displacement (in)
0.00
0.05
0.10
0.15
0.20
0.25
0.30
0.35
0
10
20
30
40
50
Time1/2 (min1/2)

NOVA - Non-blenderized - 6016 psf

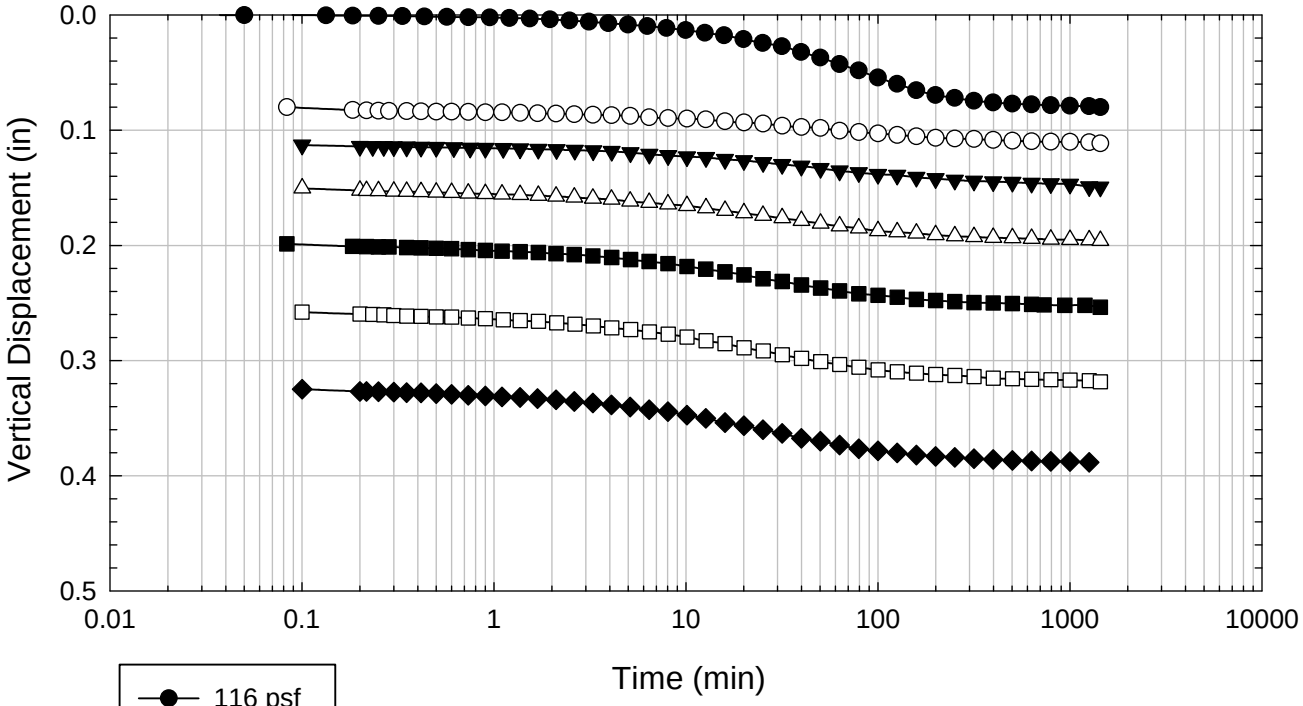

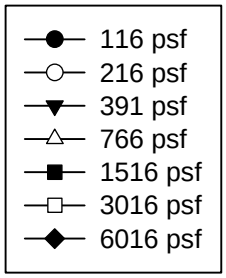

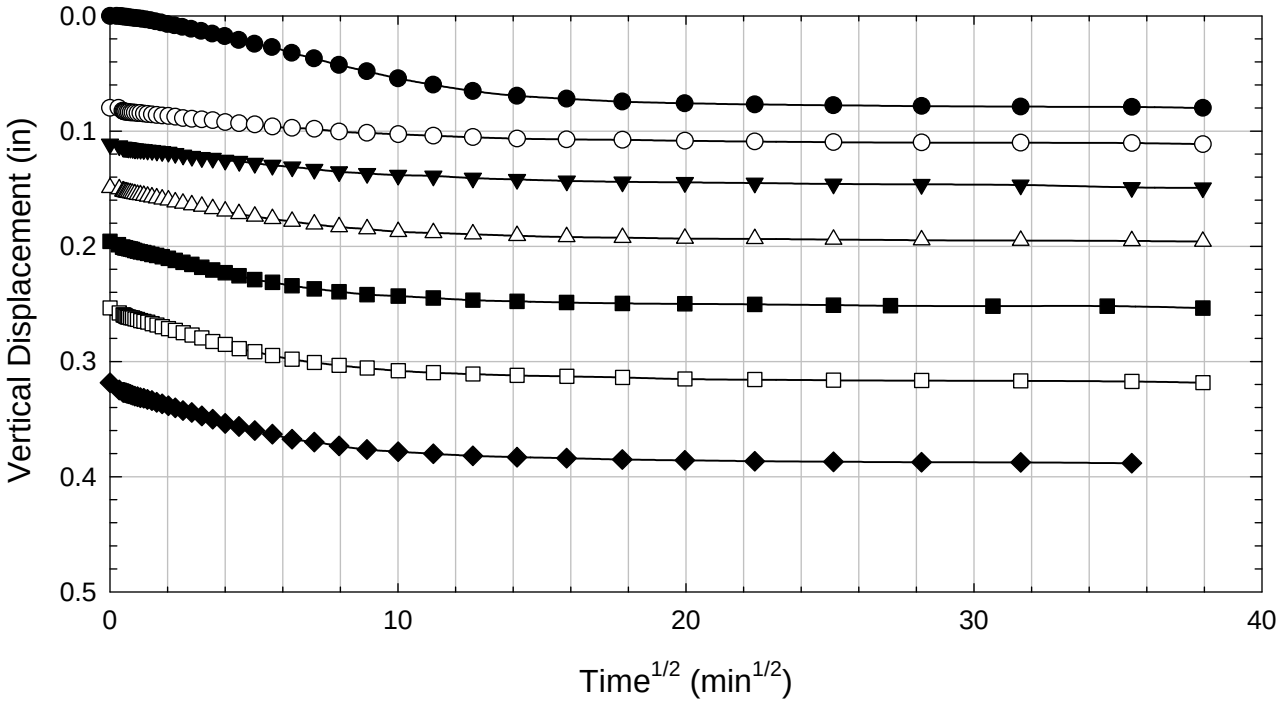

NOVA - Non-blenderized

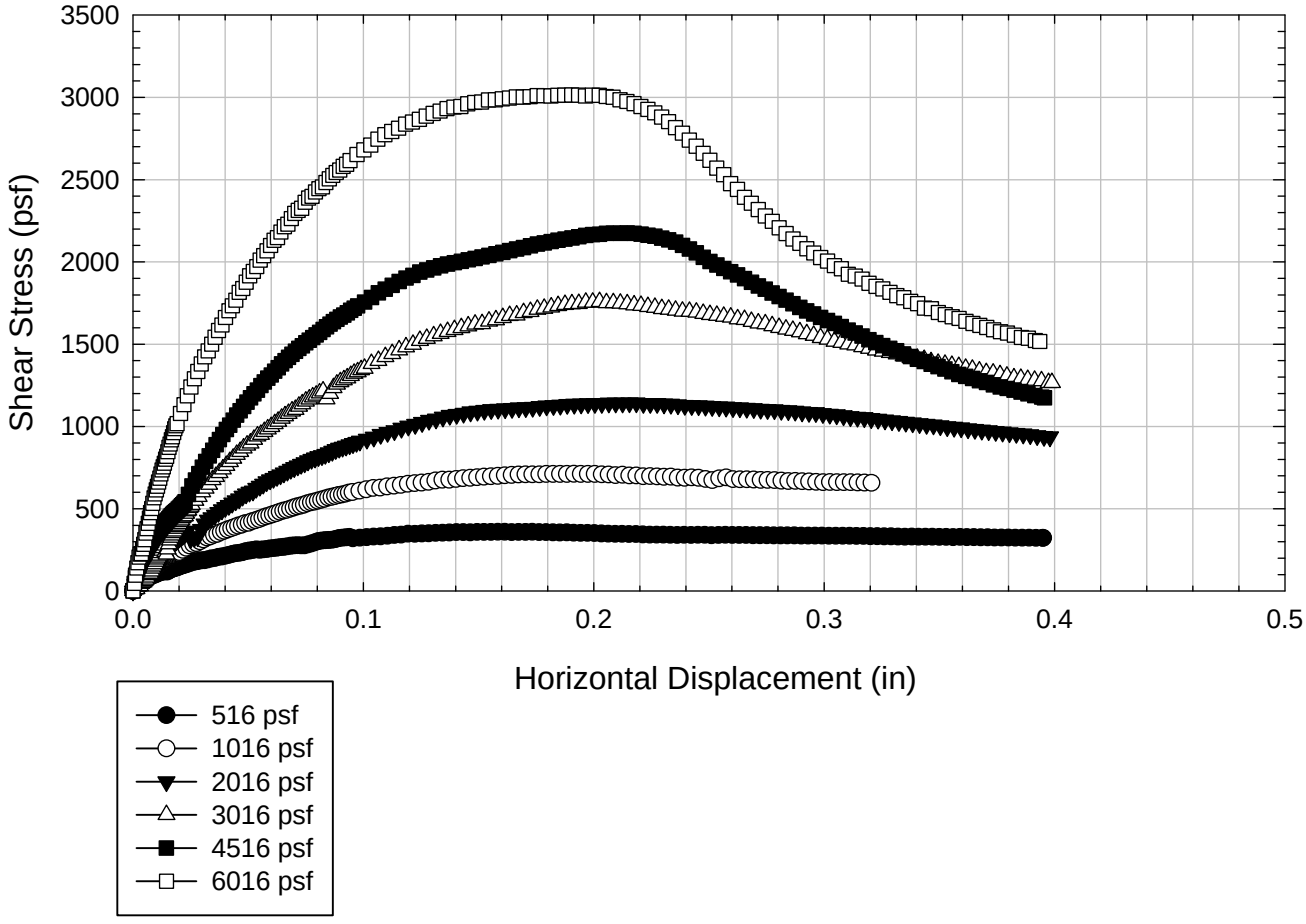

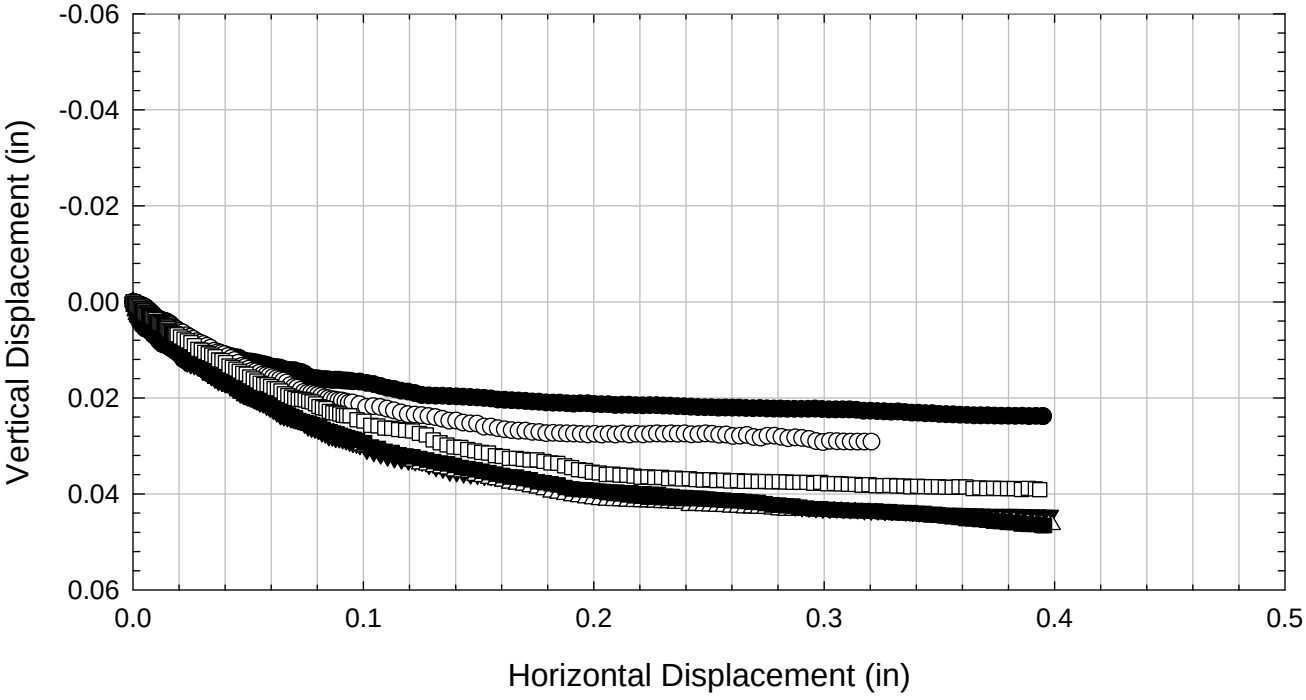

C.6.3 Liquidity Index = 1.45

Virginia Polytechnic Institute and State University
Geotechnical Engineering Laboratory
Direct Shear Data Sheet

Project:	Fully Softened Shear Strength
Sample I.D./Loc.:	NOVA - Non-blenderized - Liquidty Index = 1.45
Classification:	Fat Clay (CH)

Sample Preparation	Remolded at LI = 1.45		Specific Gravity	2.80	

Test Number	1	2	3	4	5	6	7	8
Start Date (m/d/y)	12/2/2011	12/2/2011	12/2/2011	12/2/2011	12/2/2011	2/27/2012		
End Date (m/d/y)	12/7/2011	12/8/2011	12/9/2011	12/9/2011	12/9/2011	3/9/2012		
Consolidation Pressure (psf)	516	1016	2016	3016	4516	6016		
Initial Values								
Initial Height (in)	1.42	1.41	1.42	1.38	1.40	1.40		
Initial Diameter (in)	2.50	2.50	2.50	2.50	2.50	2.50		
Initial Sample Weight (g)	182	181	180	180	184	179		
Water Content (%)	83.21	82.99	82.64	83.11	83.26	81.96		
Dry Unit Weight (pcf)	54.33	54.6	53.9	55.2	55.9	54.4		
Wet Unit Weight (pcf)	99.54	99.8	98.4	101.0	102.4	99.0		
Consolidation Pressures								
Load 1 (psf)	116	116	116	116	116	116		
Load 2 (psf)	266	266	266	216	266	216		
Load 3 (psf)	516	516	516	391	516	391		
Load 4 (psf)		1016	1016	766	1141	766		
Load 5 (psf)			2016	1516	2266	1516		
Load 6 (psf)				3016	4516	3016		
Load 7 (psf)						6016		
t_{50}								
Max. t_{50} for Load 1 (min)								
Max. t_{50} for Load 2 (min)								
Max. t_{50} for Load 3 (min)	12.17							
Max. t_{50} for Load 4 (min)		9.29						
Max. t_{50} for Load 5 (min)			7.18					
Max. t_{50} for Load 6 (min)				7.25	7.34			
Max. t_{50} for Load 7 (min)						18.12		
Final Values								
Water Content (%)	57.95	53.52	50.06	47.33	44.27	42.36		
Dry Unit Weight (pcf)	68.4	73.2	65.6	81.2	42.0	84.82		
Wet Unit Weight (pcf)	108.0	112.4	98.4	119.6	60.7	120.76		
Failure								
Test Performed at Shear Rate (in/min)	1.64E-04	1.64E-04	1.64E-04	2.76E-04	2.72E-04	1.10E-04		
Required Shear Rate (in/min)	3.62E-04	4.31E-04	6.41E-04	4.97E-04	5.72E-04	1.99E-04		
Displacement at Failure (in)	0.22	0.20	0.23	0.18	0.21	0.18		
Peak Shear Stress (psf)	358	667	1296	1701	2302	3000		
Total Change in Height at Failure (in)	0.28	0.35	0.41	0.44	0.45	0.50		
Secant Effective Friction Angle (deg)	34.7	33.3	32.7	29.4	27.0	26.5		

Comments: In the test consolidated to 6000 psf, the computer restarted during the 3000 psf consolidation stress. The test was continued.

NOVA - Non-blenderized - Liquidity Index = 1.45 - 516 psf

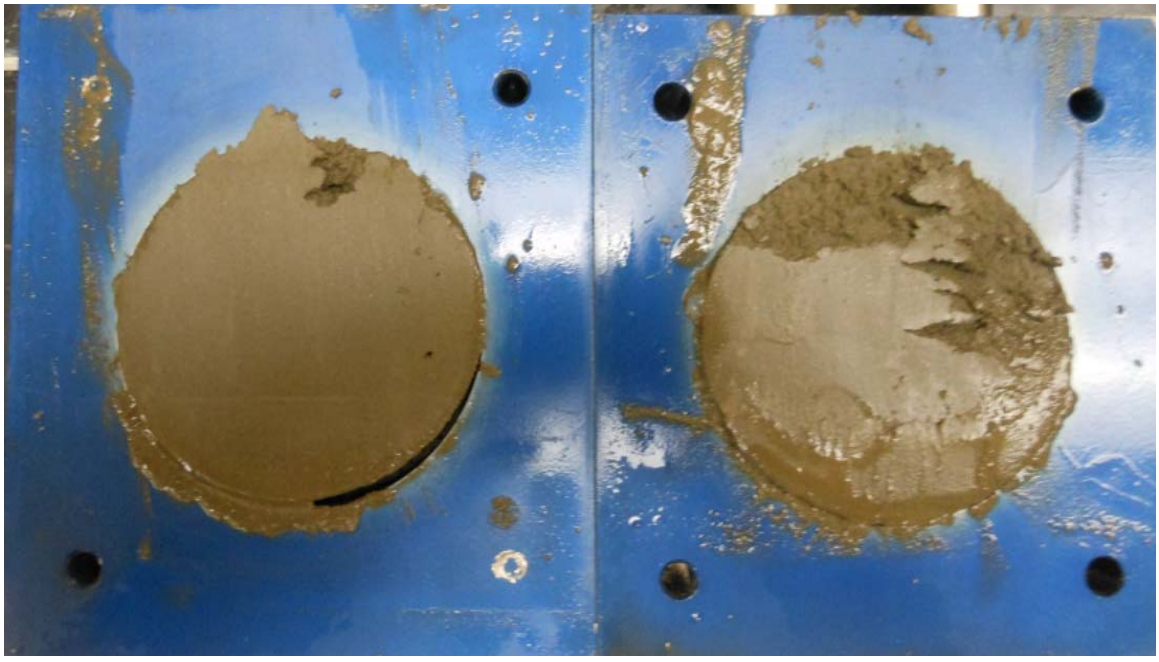

NOVA - Non-blenderized - Liquidity Index = 1.45 - 1016 psf

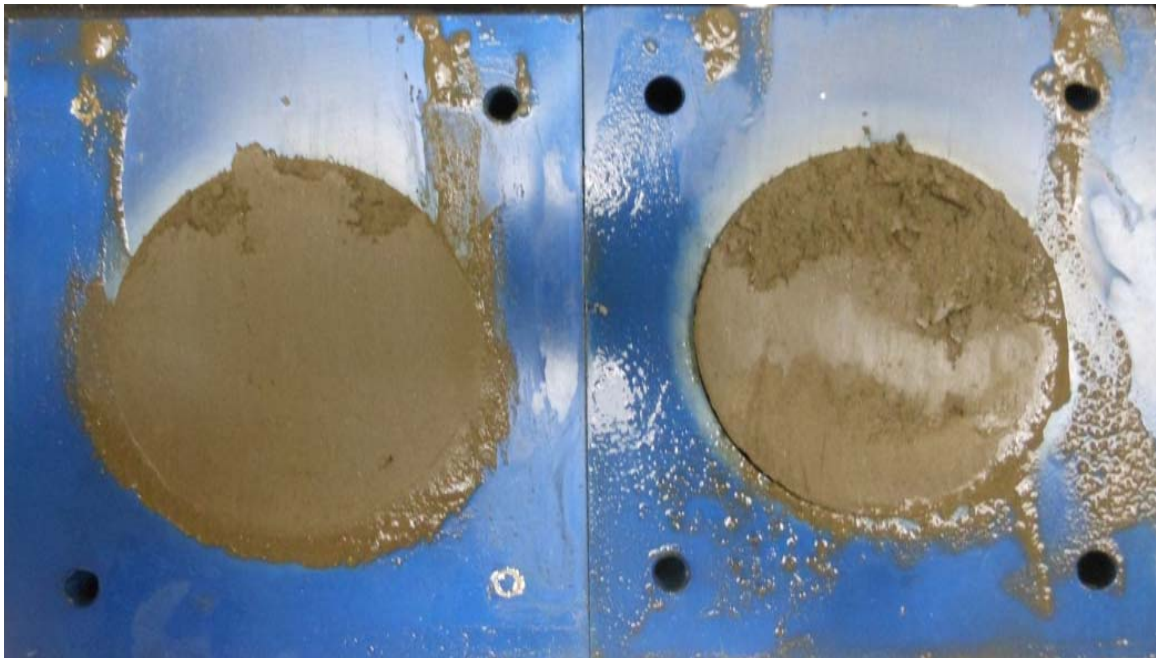

NOVA - Non-blenderized - Liquidity Index = 1.45 - 2016 psf

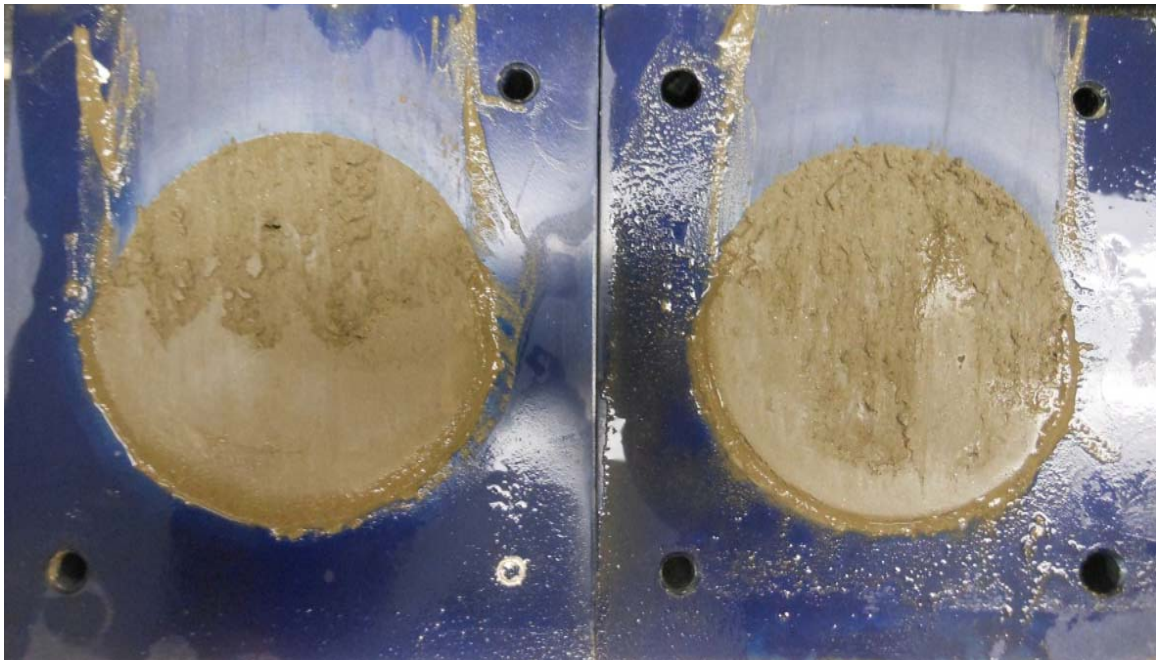

NOVA - Non-blenderized - Liquidity Index = 1.45 - 3016 psf

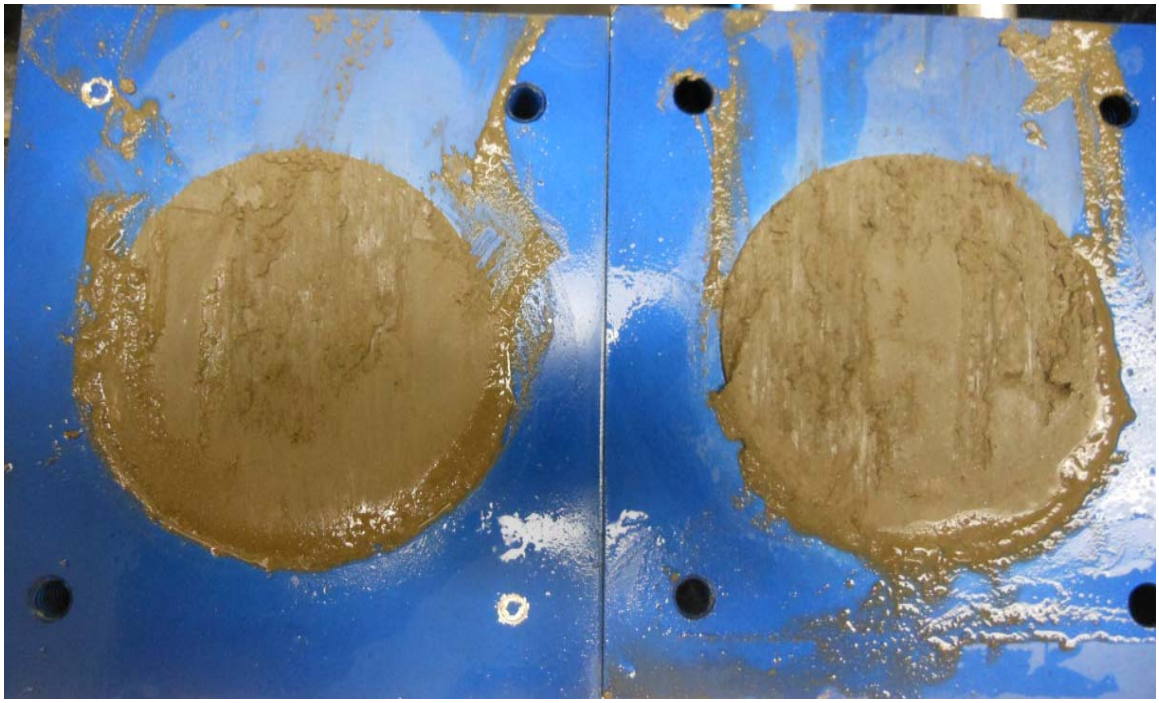

NOVA - Non-blenderized - Liquidity Index = 1.45 - 4516 psf

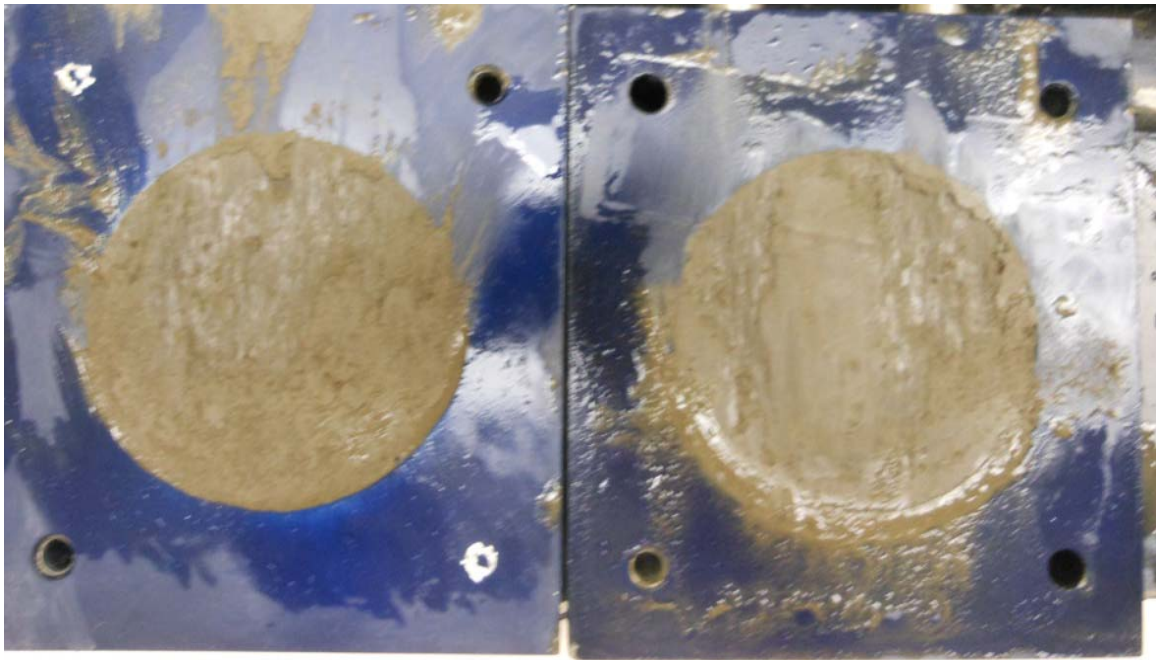

NOVA - Non-blenderized - Liquidity Index = 1.45 - 6016 psf

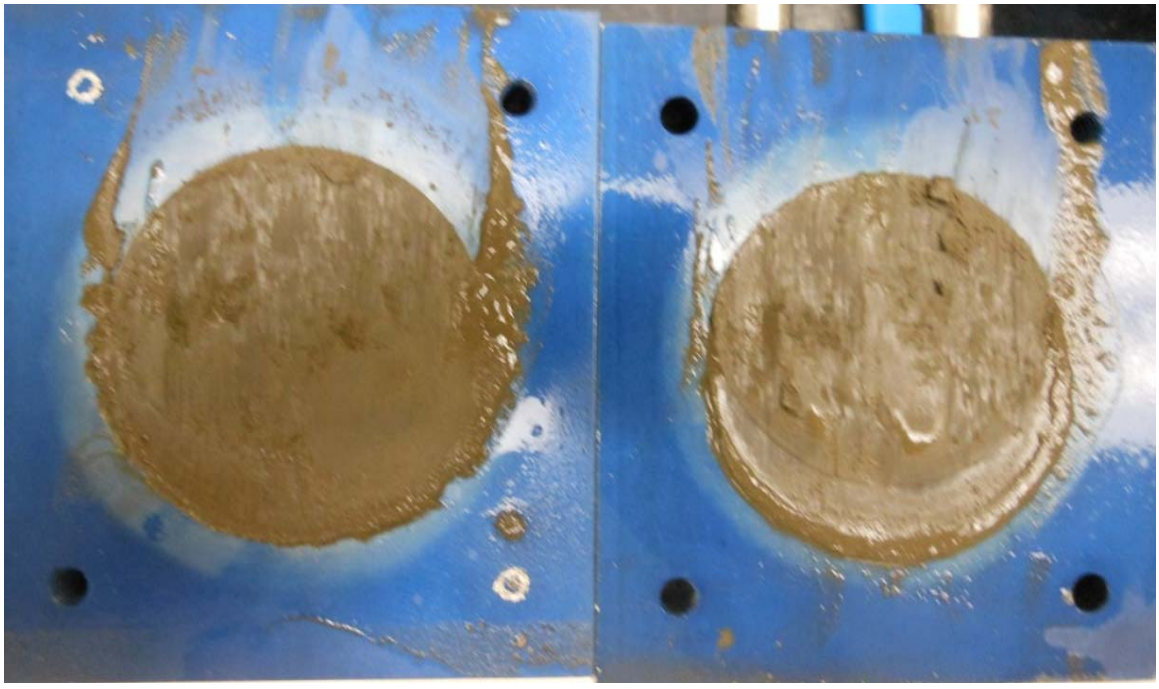

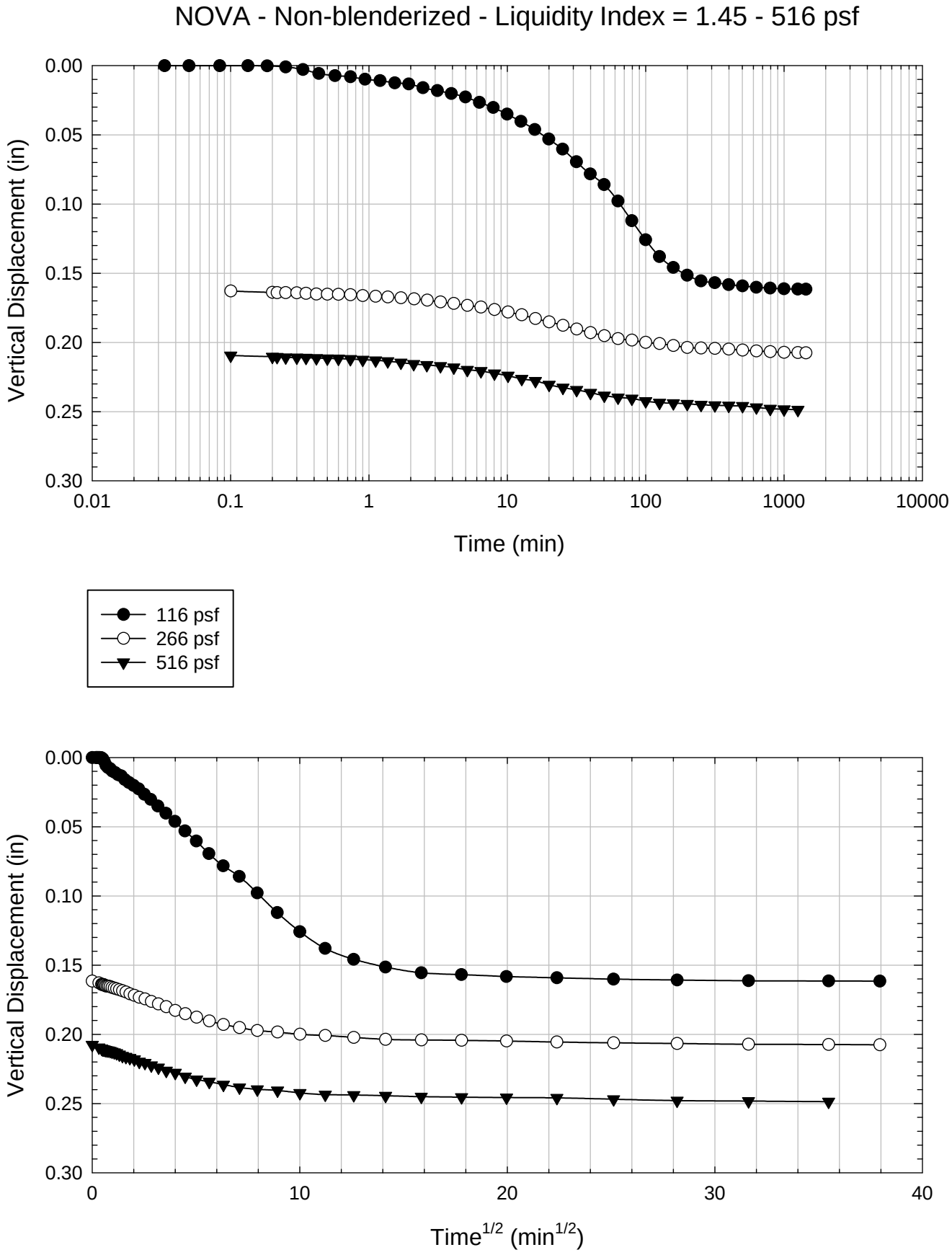
NOVA - Non-blenderized - Liquidity Index = 1.45 - 516 psf
Vertical Displacement (in)
0.00
0.05
0.10
0.15
0.20
0.25
0.30
0.01
0.1
1
10
100
1000
10000
Time (min)
116 psf
266 psf
516 psf
Vertical Displacement (in)
0.00
0.05
0.10
0.15
0.20
0.25
0.30
0
10
20
30
40
Time1/2 (min1/2)

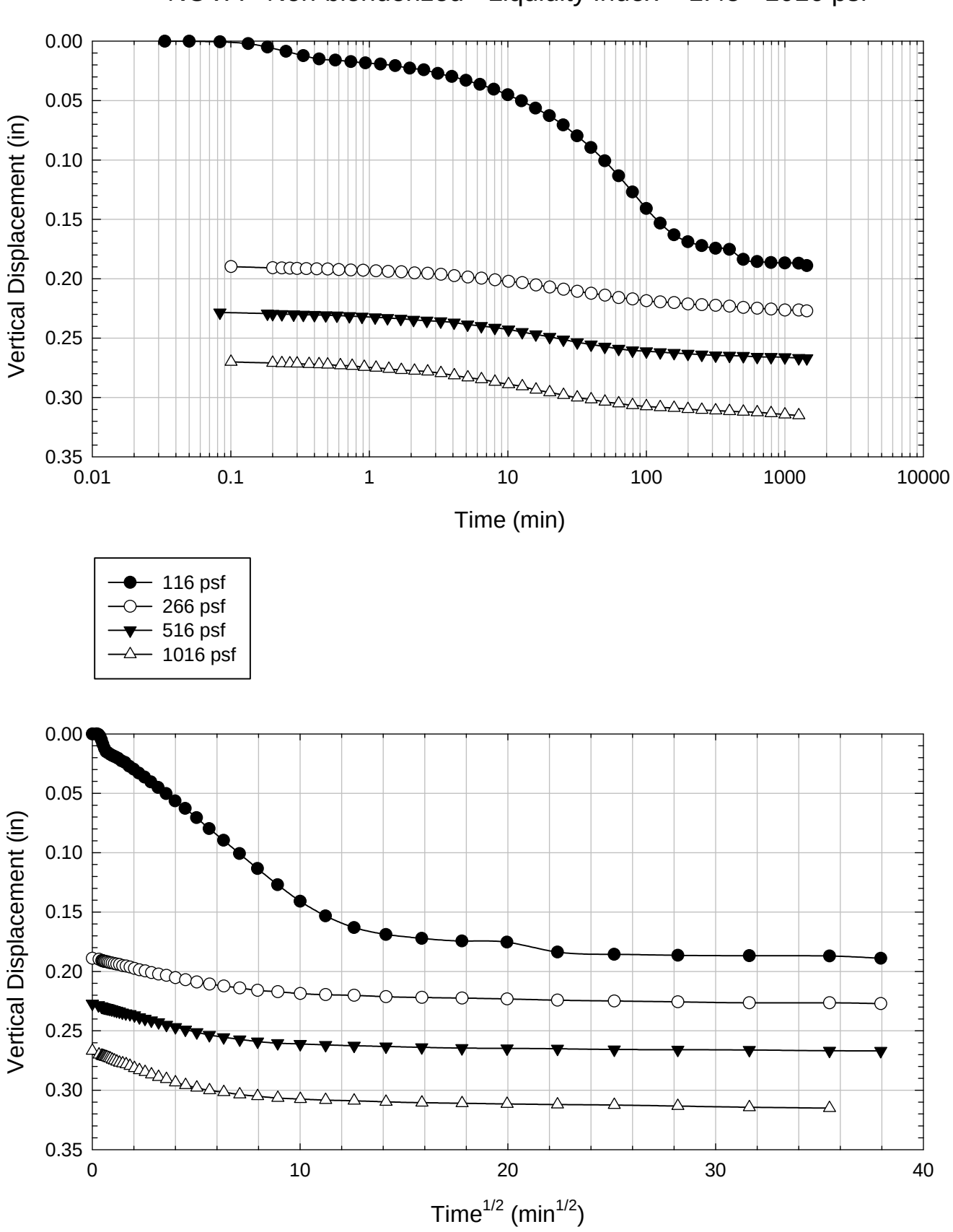
NOVA - Non-blenderized - Liquidity Index = 1.45 - 1016 psf
Vertical Displacement (in)
0.00
0.05
0.10
0.15
0.20
0.25
0.30
0.35
0.01
0.1
1
10
100
1000
10000
Time (min)
116 psf
266 psf
516 psf
1016 psf
Vertical Displacement (in)
0.00
0.05
0.10
0.15
0.20
0.25
0.30
0.35
0
10
20
30
40
Time^1/2 (min^1/2)

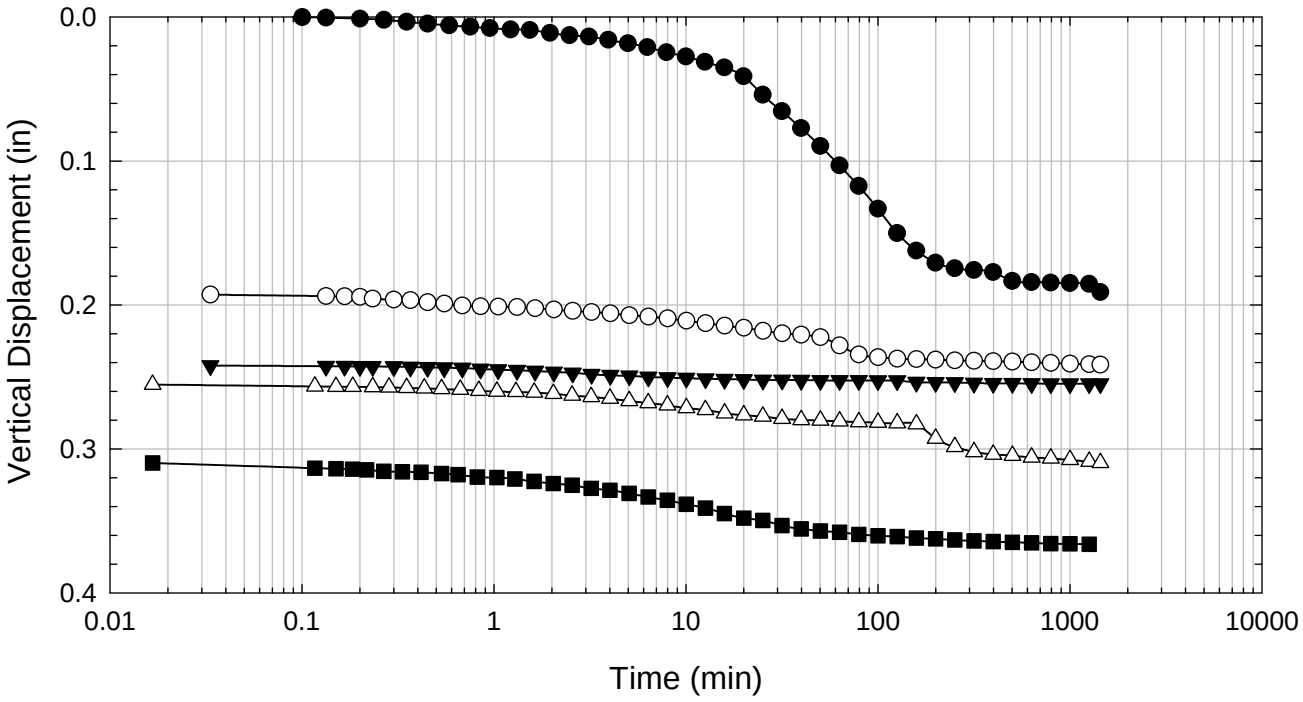
NOVA - Non-blenderized - Liquidity Index = 1.45 - 2016 psf
Vertical Displacement (in)
0.0
0.1
0.2
0.3
0.4
0.01
0.1
1
10
100
1000
10000
Time (min)

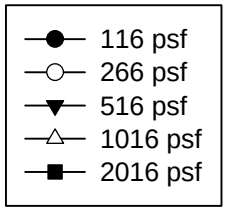
116 psf
266 psf
516 psf
1016 psf
2016 psf

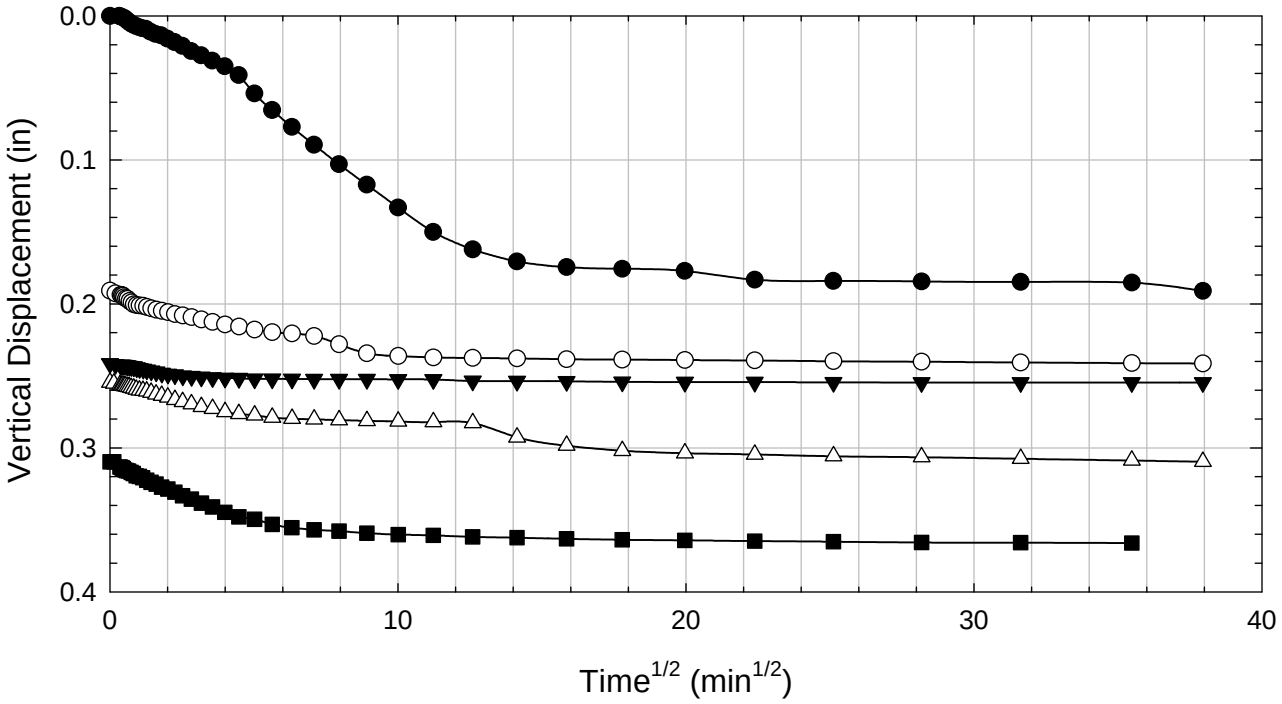
Vertical Displacement (in)
0.0
0.1
0.2
0.3
0.4
0
10
20
30
40
Time1/2 (min1/2)

NOVA - Non-blenderized - Liquidity Index = 1.45 - 3016 psf

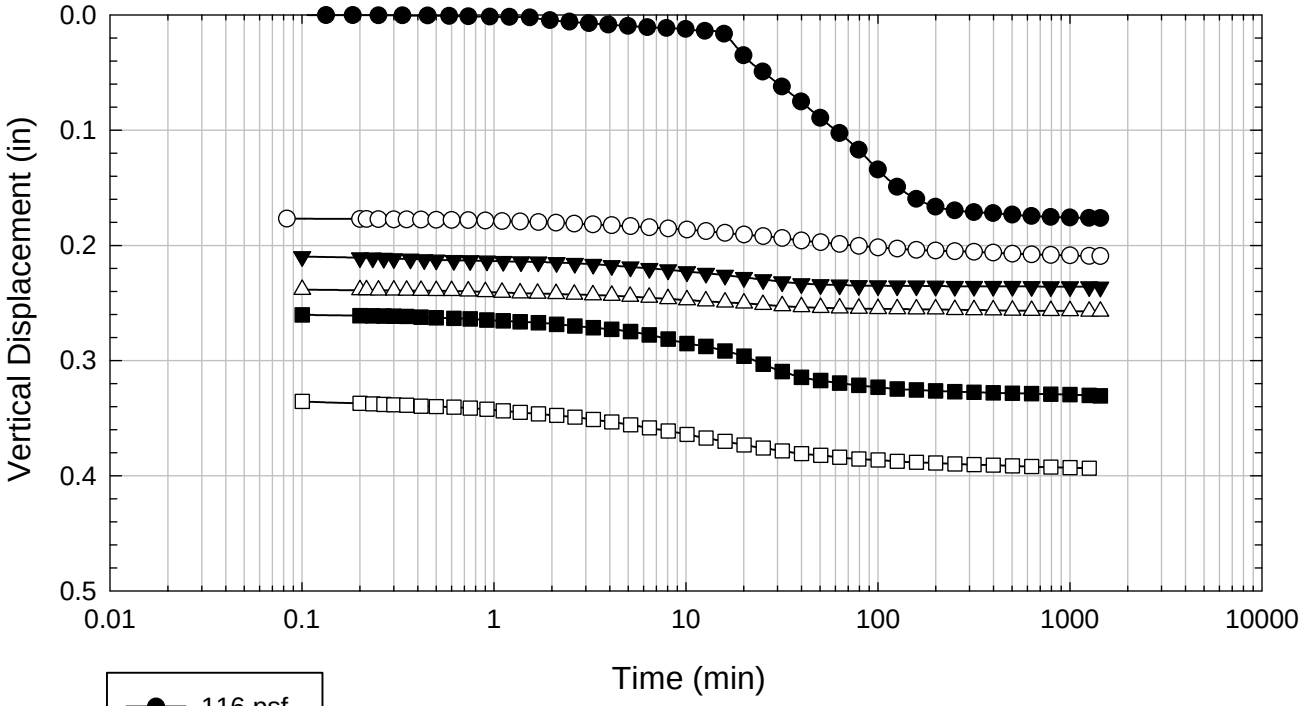

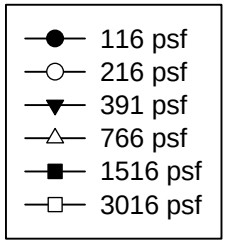

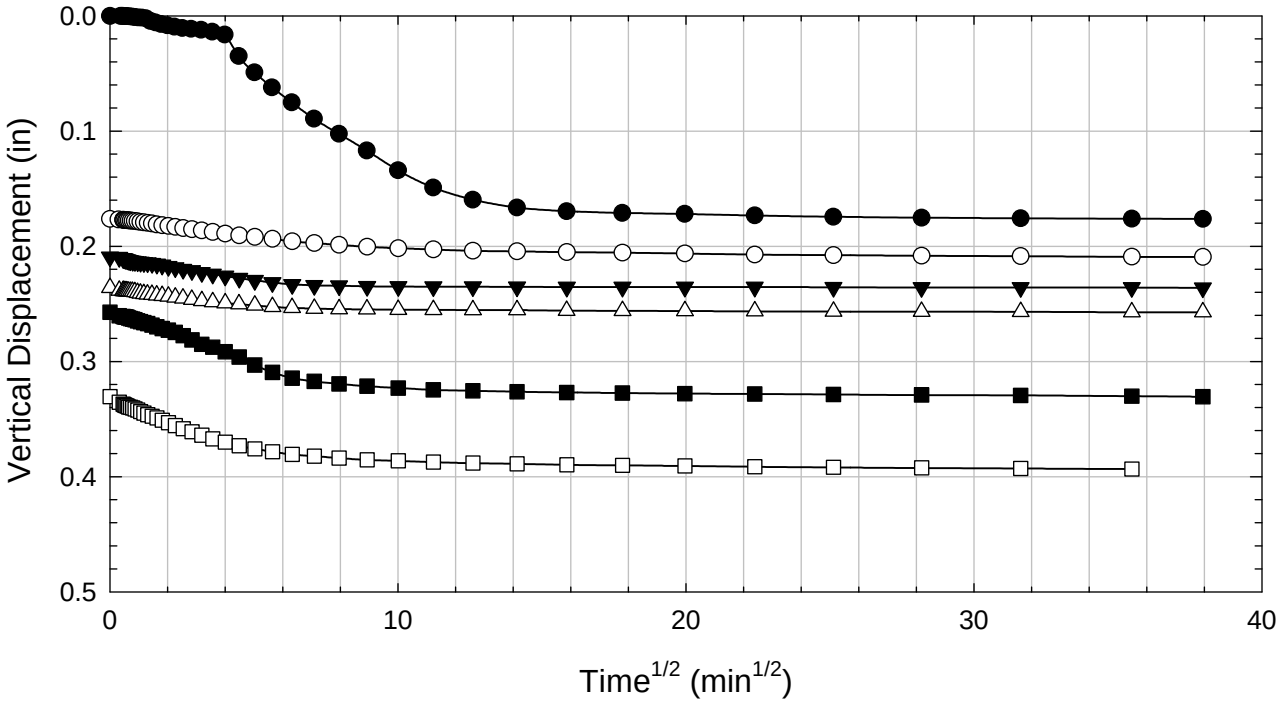

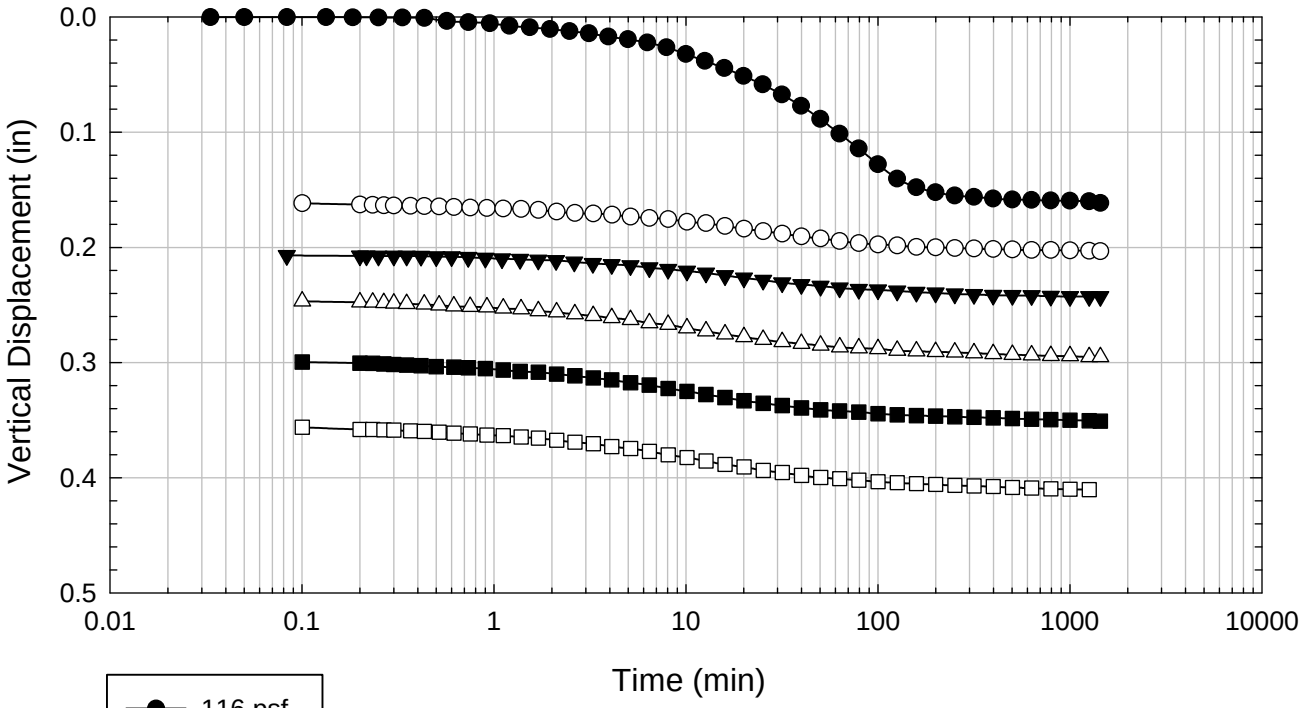
NOVA - Non-blenderized - Liquidity Index = 1.45 - 4516 psf
Vertical Displacement (in)
0.0
0.1
0.2
0.3
0.4
0.5
0.01
0.1
1
10
100
1000
10000
Time (min)

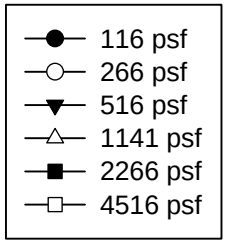
116 psf
266 psf
516 psf
1141 psf
2266 psf
4516 psf

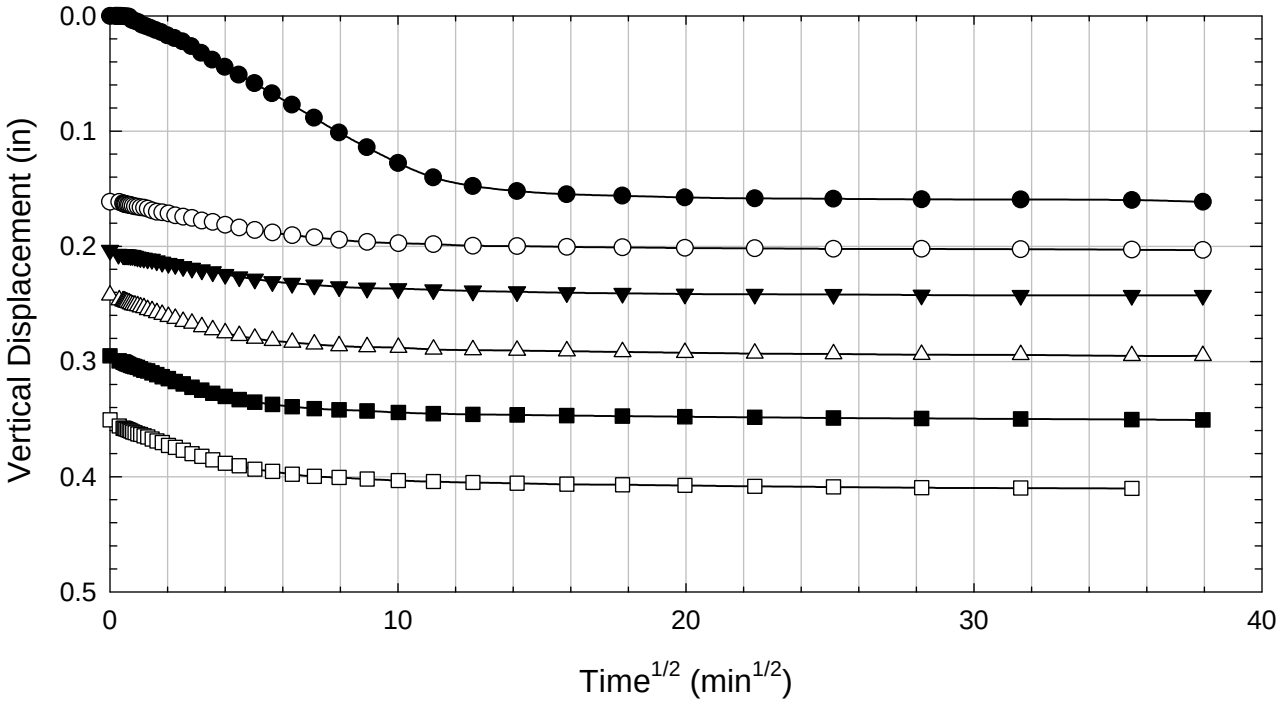
Vertical Displacement (in)
0.0
0.1
0.2
0.3
0.4
0.5
0
10
20
30
40
Time1/2 (min1/2)

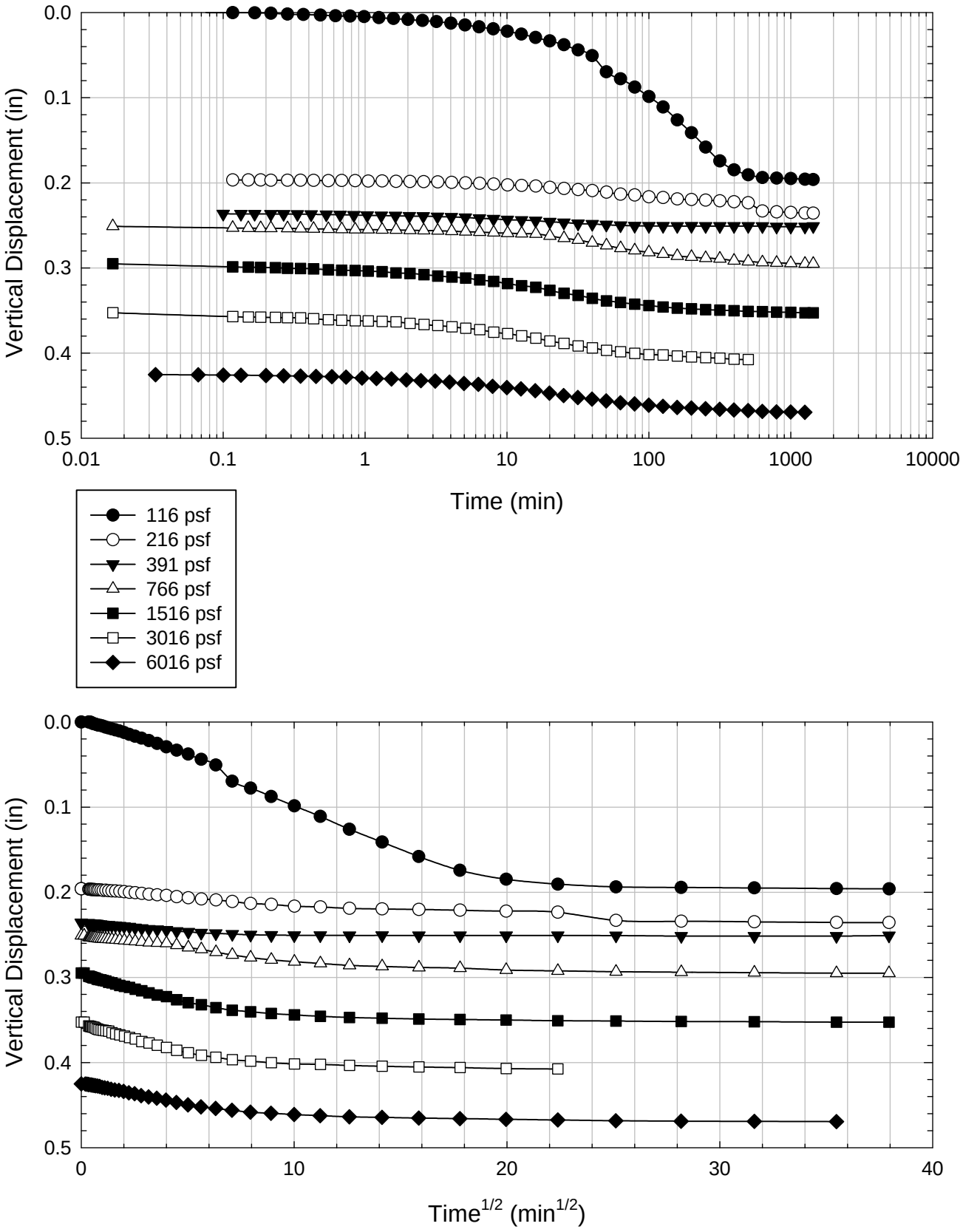
NOVA - Non-blenderized - Liquidity Index = 1.45 - 6016 psf
Vertical Displacement (in)
0.0
0.1
0.2
0.3
0.4
0.5
0.01
0.1
1
10
100
1000
10000
Time (min)
116 psf
216 psf
391 psf
766 psf
1516 psf
3016 psf
6016 psf
Vertical Displacement (in)
0.0
0.1
0.2
0.3
0.4
0.5
0
10
20
30
40
Time^1/2 (min^1/2)

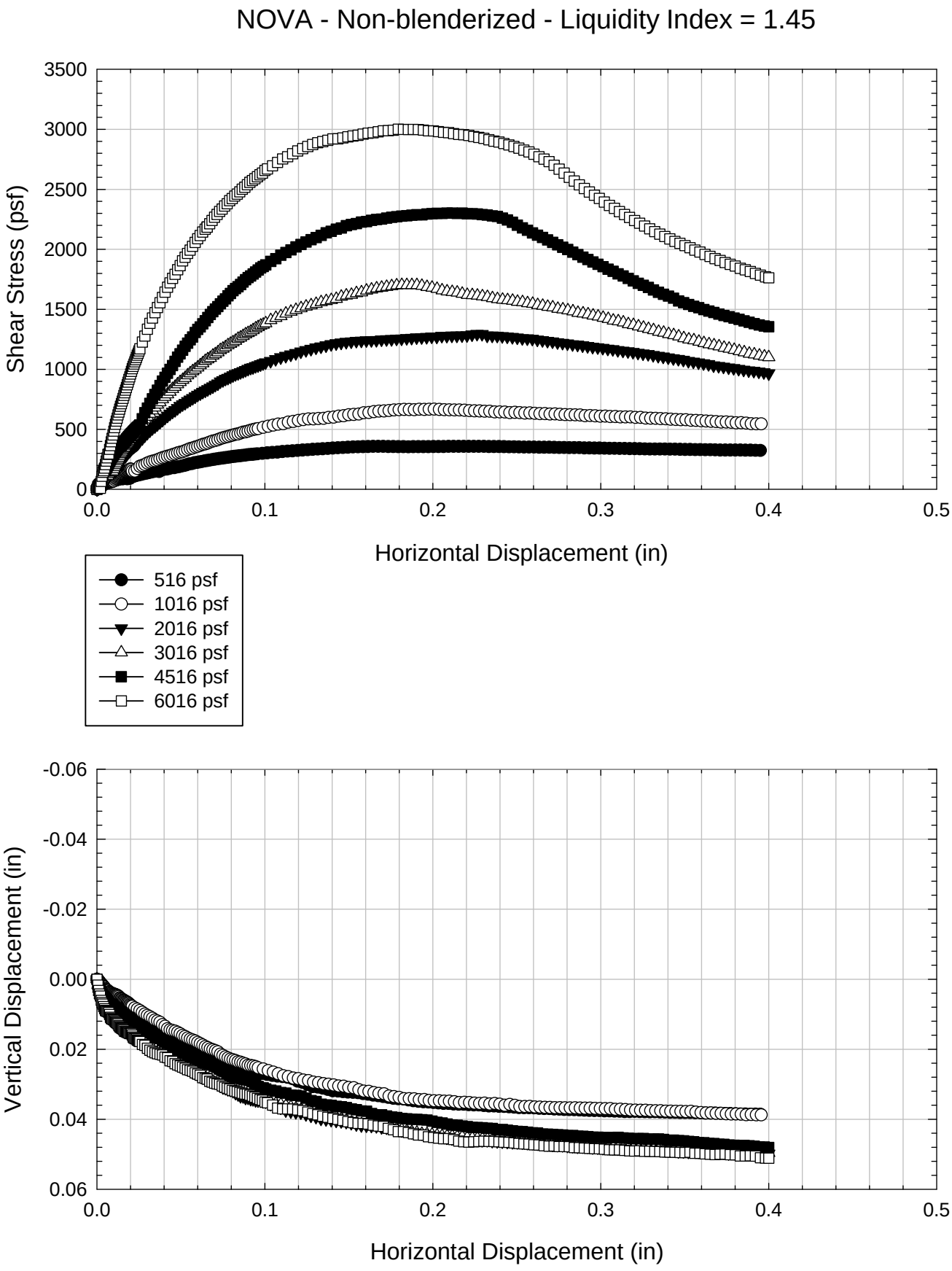
NOVA - Non-blenderized - Liquidity Index = 1.45
Shear Stress (psf)
3500
3000
2500
2000
1500
1000
500
0
0.0
0.1
0.2
0.3
0.4
0.5
Horizontal Displacement (in)
516 psf
1016 psf
2016 psf
3016 psf
4516 psf
6016 psf
Vertical Displacement (in)
-0.06
-0.04
-0.02
0.00
0.02
0.04
0.06
0.0
0.1
0.2
0.3
0.4
0.5
Horizontal Displacement (in)

C.6.4 Liquidity Index = 0.68

Virginia Polytechnic Institute and State University
Geotechnical Engineering Laboratory
Direct Shear Data Sheet

Project:	Fully Softened Shear Strength
Sample I.D./Loc.:	NOVA - Non-blenderized - Liquidty Index = 0.68
Classification:	Fat Clay (CH)

Sample Preparation	Remolded at LI = 0.68

Specific Gravity	2.80	

Test Number	1	2	3	4	5	6	7	8
Start Date (m/d/y)	12/12/2011	12/12/2011	12/12/2011	12/12/2011	12/12/2011	5/8/2012		
End Date (m/d/y)	12/20/2011	12/20/2011	12/20/2011	12/20/2011	12/20/2011	5/20/2012		
Consolidation Pressure (psf)	516	1016	2016	3016	4516	6016		
Initial Values								
Initial Height (in)	1.45	1.43	1.43	1.40	1.40	1.44		
Initial Diameter (in)	2.50	2.50	2.50	2.50	2.50	2.50		
Initial Sample Weight (g)	198	198	195	194	200	196		
Water Content (%)	53.84	53.97	54.43	53.24	53.19	53.65		
Dry Unit Weight (pcf)	68.85	69.9	68.7	70.3	72.2	68.8		
Wet Unit Weight (pcf)	105.92	107.6	106.0	107.6	110.7	105.7		
Consolidation Pressures								
Load 1 (psf)	116	116	116	116	116	116		
Load 2 (psf)	266	266	266	216	266	216		
Load 3 (psf)	516	516	516	391	516	391		
Load 4 (psf)		1016	1016	766	1141	766		
Load 5 (psf)			2016	1516	2266	1516		
Load 6 (psf)				3016	4516	3016		
Load 7 (psf)						6016		
t_{50}								
Max. t_{50} for Load 1 (min)								
Max. t_{50} for Load 2 (min)								
Max. t_{50} for Load 3 (min)	34.18							
Max. t_{50} for Load 4 (min)		30.45						
Max. t_{50} for Load 5 (min)			32.57					
Max. t_{50} for Load 6 (min)				22.43	24.36			
Max. t_{50} for Load 7 (min)						58.54		
Final Values								
Water Content (%)	51.92	49.17	45.90	43.73	41.54	39.92		
Dry Unit Weight (pcf)	71.4	75.1	76.0	80.6	85.3	85.17		
Wet Unit Weight (pcf)	108.4	112.0	110.9	115.9	120.8	119.17		
Failure								
Test Performed at Shear Rate (in/min)	5.82E-05	6.14E-05	6.14E-05	8.92E-05	8.21E-05	3.42E-05		
Required Shear Rate (in/min)	4.10E-05	7.88E-05	9.21E-05	1.52E-04	1.23E-04	5.47E-05		
Displacement at Failure (in)	0.07	0.12	0.15	0.17	0.15	0.16		
Peak Shear Stress (psf)	373	610	1128	1658	2005	2882		
Total Change in Height at Failure (in)	0.05	0.09	0.13	0.18	0.21	0.26		
Secant Effective Friction Angle (deg)	35.9	31.0	29.2	28.8	23.9	25.6		

Comments:

NOVA - Non-blenderized - Liquidity Index = 0.68 - 516 psf

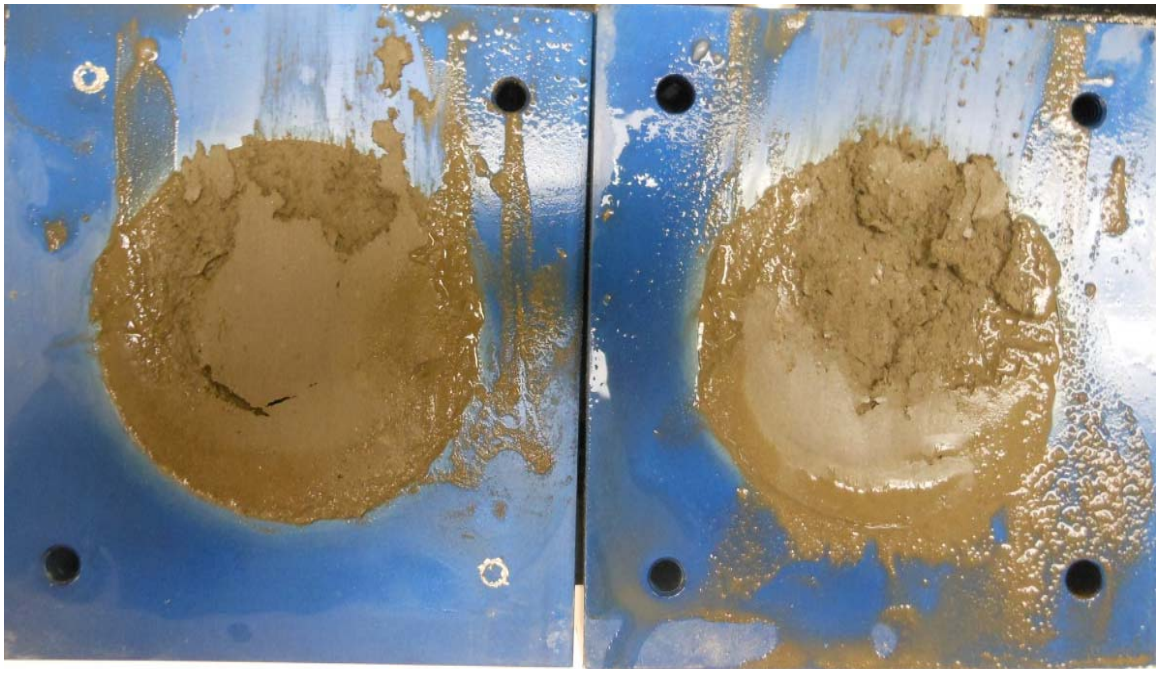

NOVA - Non-blenderized - Liquidity Index = 0.68 - 1016 psf

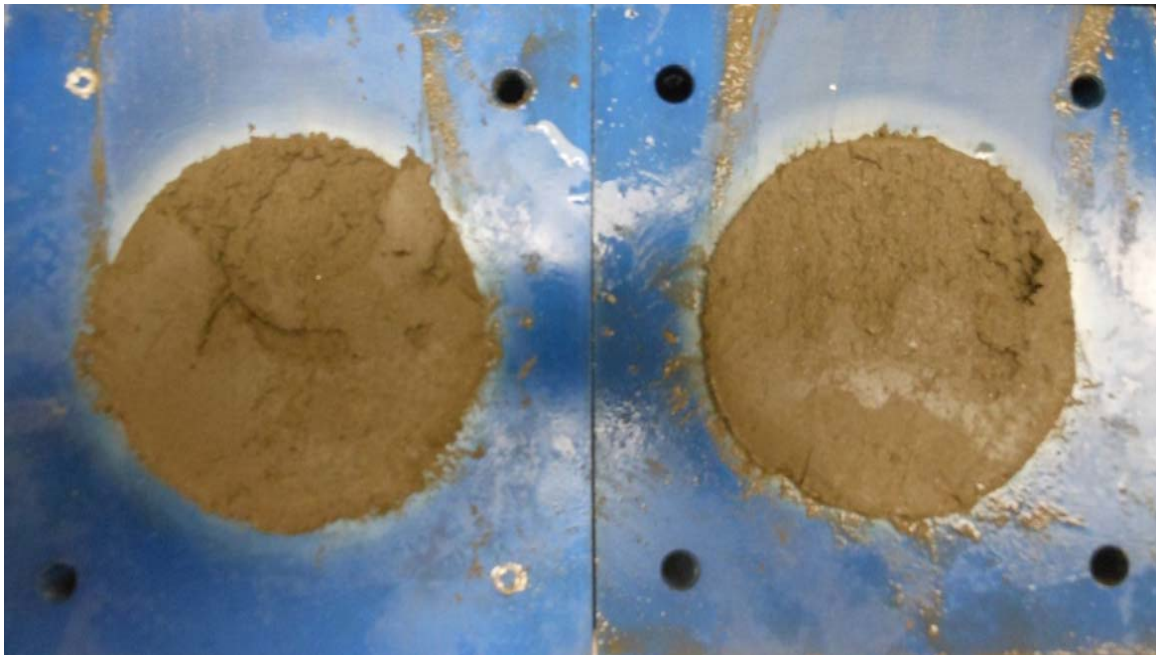

NOVA - Non-blenderized - Liquidity Index = 0.68 - 2016 psf

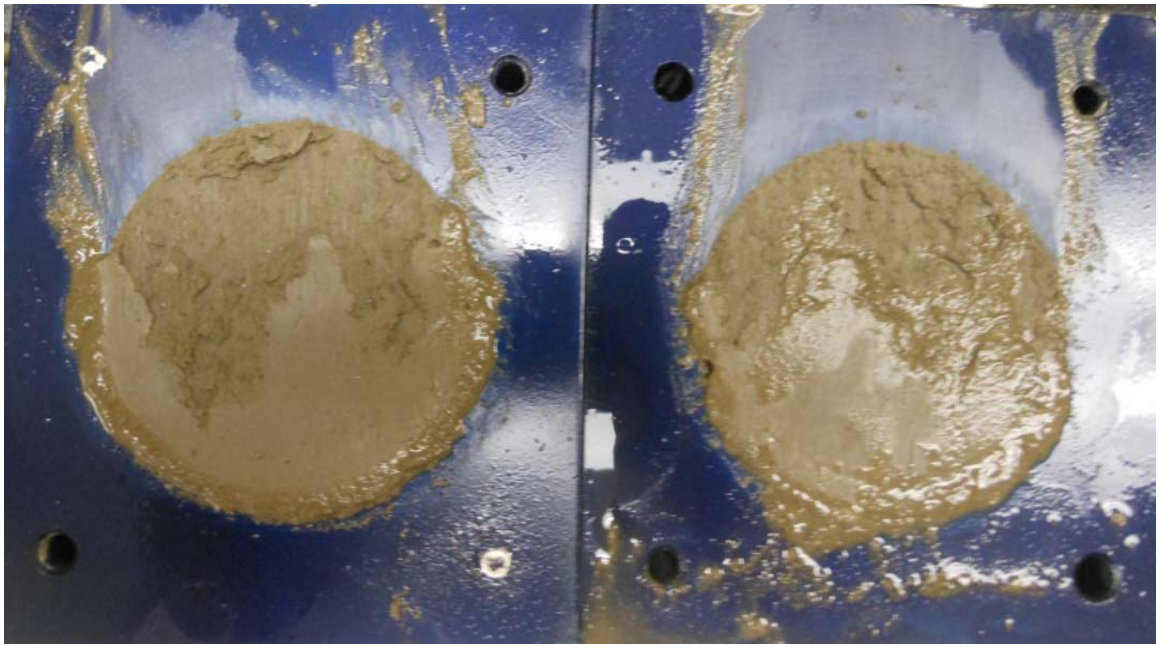

NOVA - Non-blenderized - Liquidity Index = 0.68 - 3016 psf

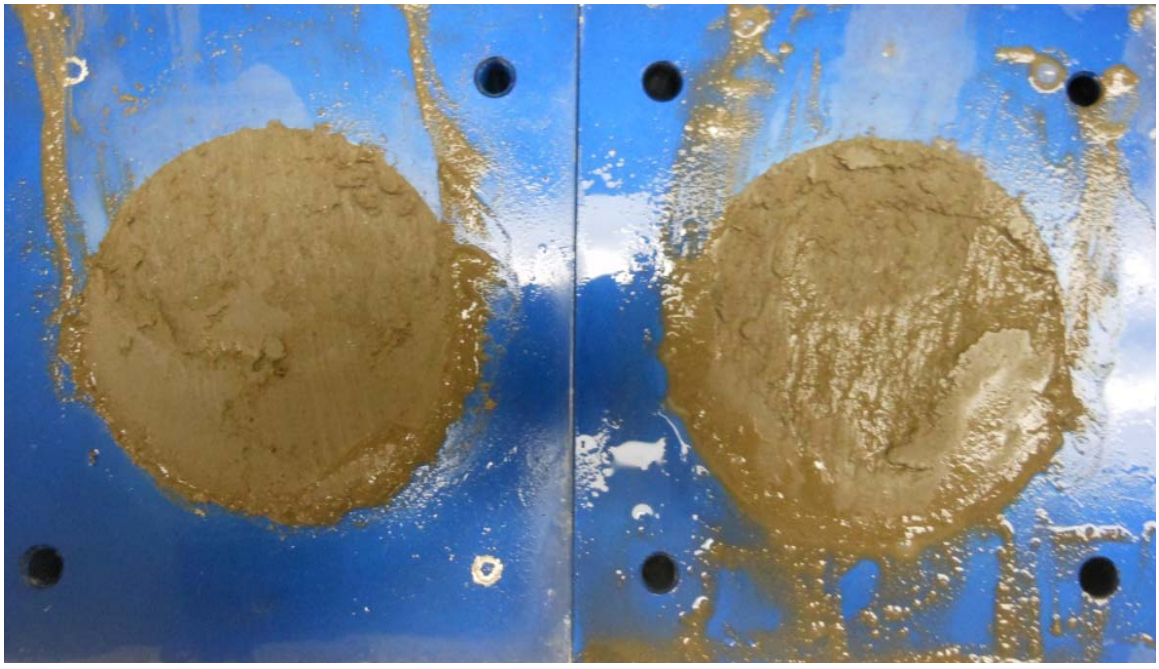

NOVA - Non-blenderized - Liquidity Index = 0.68 - 4516 psf

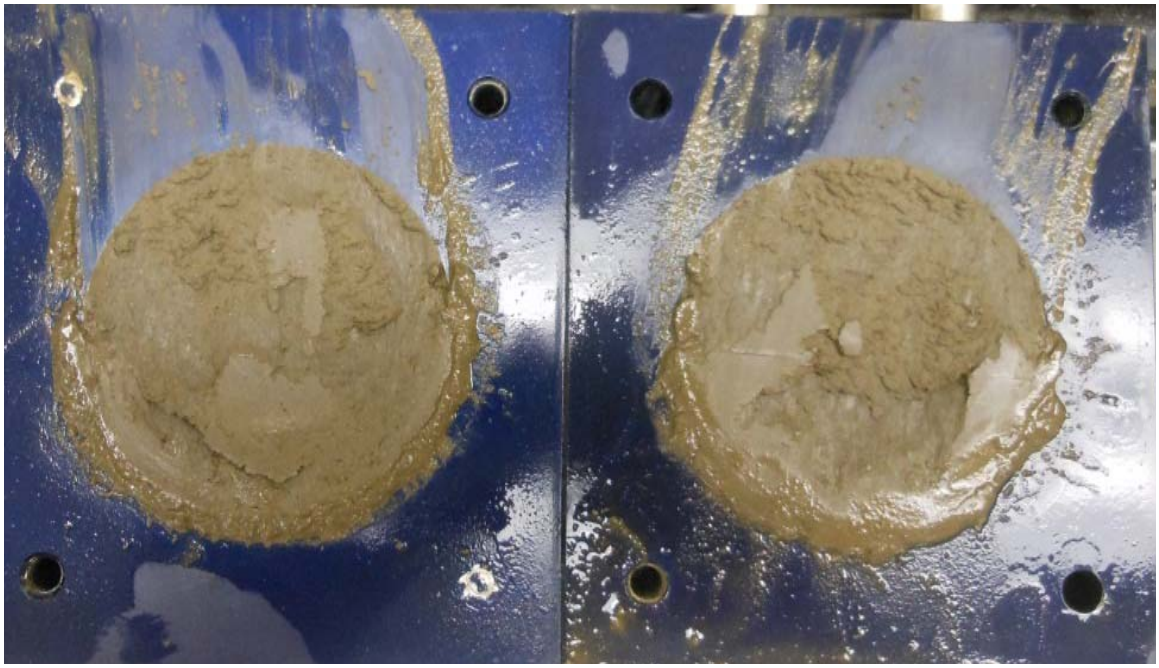

NOVA - Non-blenderized - Liquidity Index = 0.68 - 6016 psf

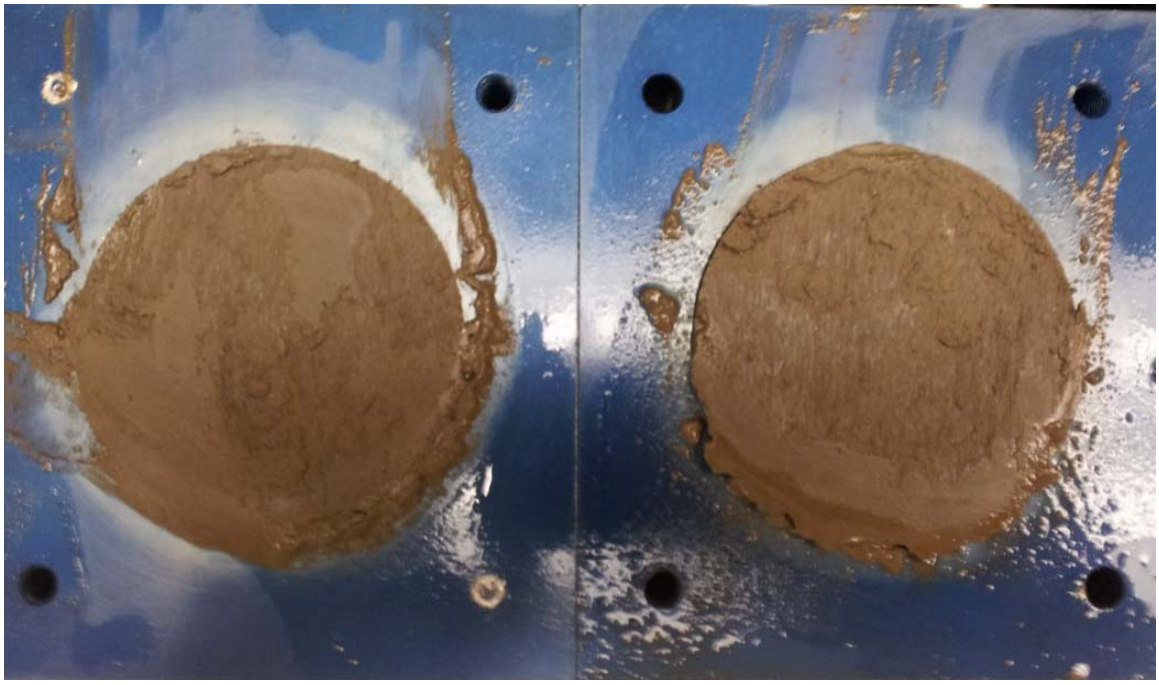

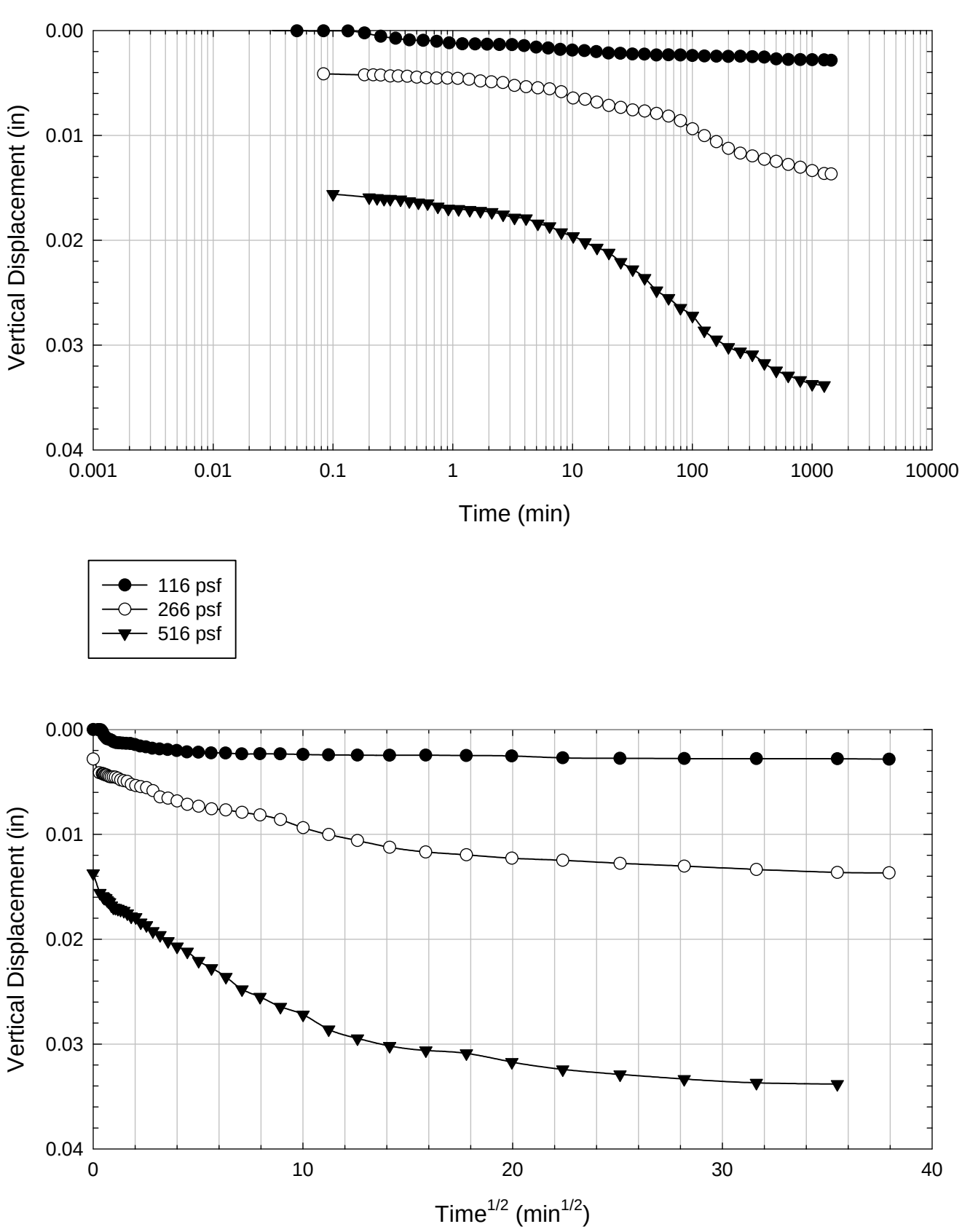
NOVA - Non-blenderized - Liquidity Index = 0.68 - 516 psf
Vertical Displacement (in)
0.00
0.01
0.02
0.03
0.04
0.001
0.01
0.1
1
10
100
1000
10000
Time (min)
116 psf
266 psf
516 psf
Vertical Displacement (in)
0.00
0.01
0.02
0.03
0.04
0
10
20
30
40
Time^1/2 (min^1/2)

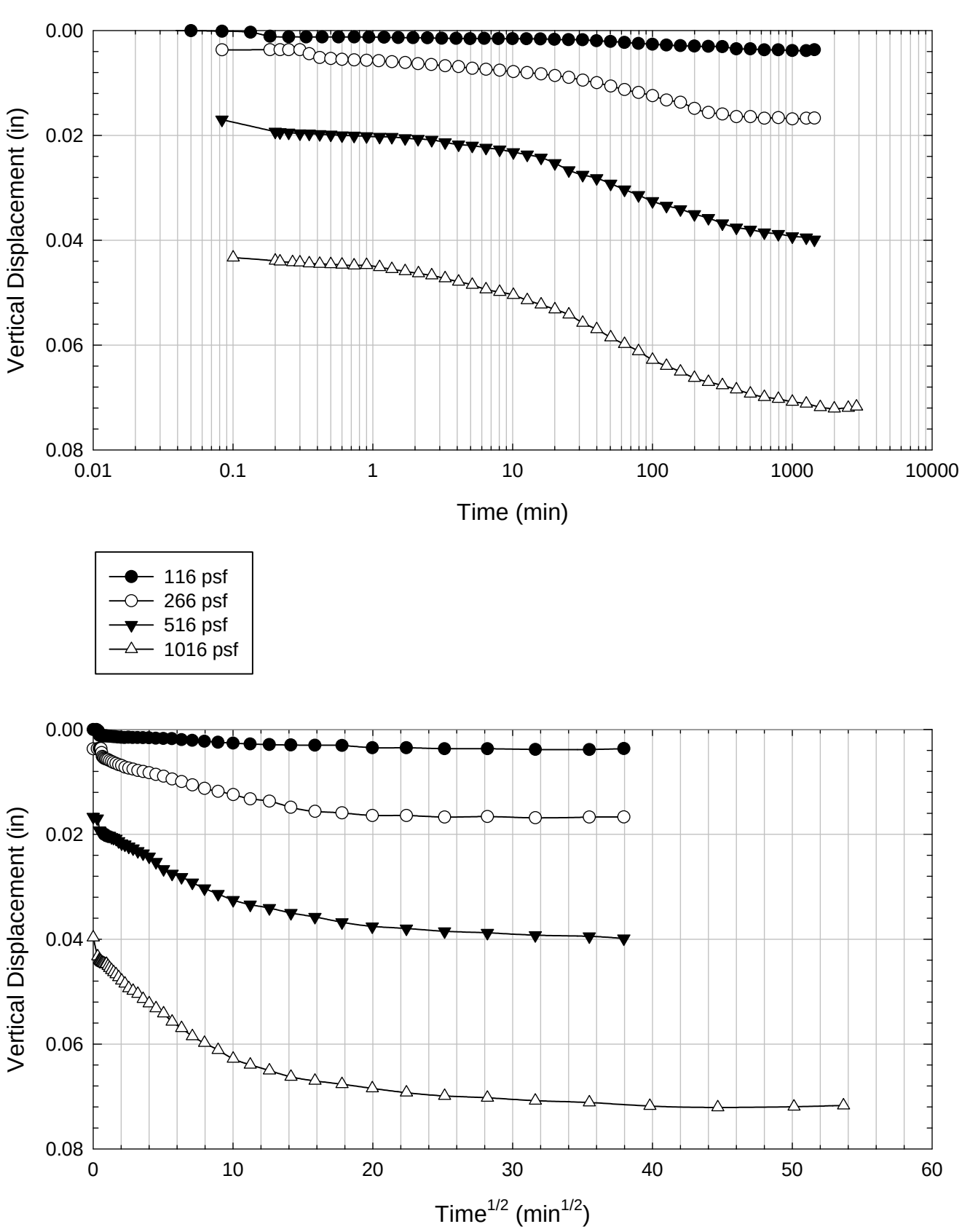
NOVA - Non-blenderized - Liquidity Index = 0.68 - 1016 psf
Vertical Displacement (in)
0.00
0.02
0.04
0.06
0.08
0.01
0.1
1
10
100
1000
10000
Time (min)
116 psf
266 psf
516 psf
1016 psf
Vertical Displacement (in)
0.00
0.02
0.04
0.06
0.08
0
10
20
30
40
50
60
Time^1/2 (min^1/2)

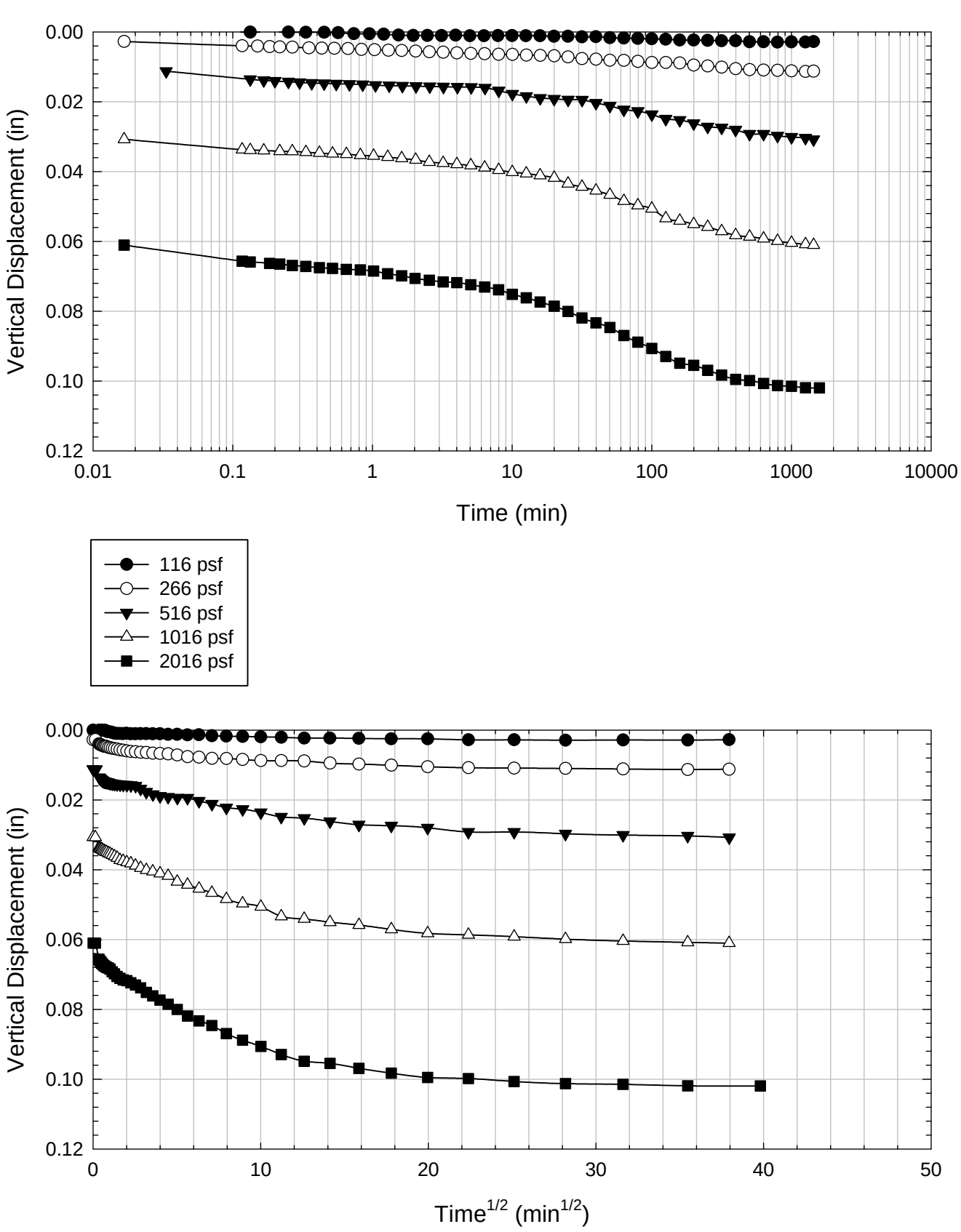
NOVA - Non-blenderized - Liquidity Index = 0.68 - 2016 psf
Vertical Displacement (in)
0.00
0.02
0.04
0.06
0.08
0.10
0.12
0.01
0.1
1
10
100
1000
10000
Time (min)
116 psf
266 psf
516 psf
1016 psf
2016 psf
Vertical Displacement (in)
0.00
0.02
0.04
0.06
0.08
0.10
0.12
0
10
20
30
40
50
Time^1/2 (min^1/2)

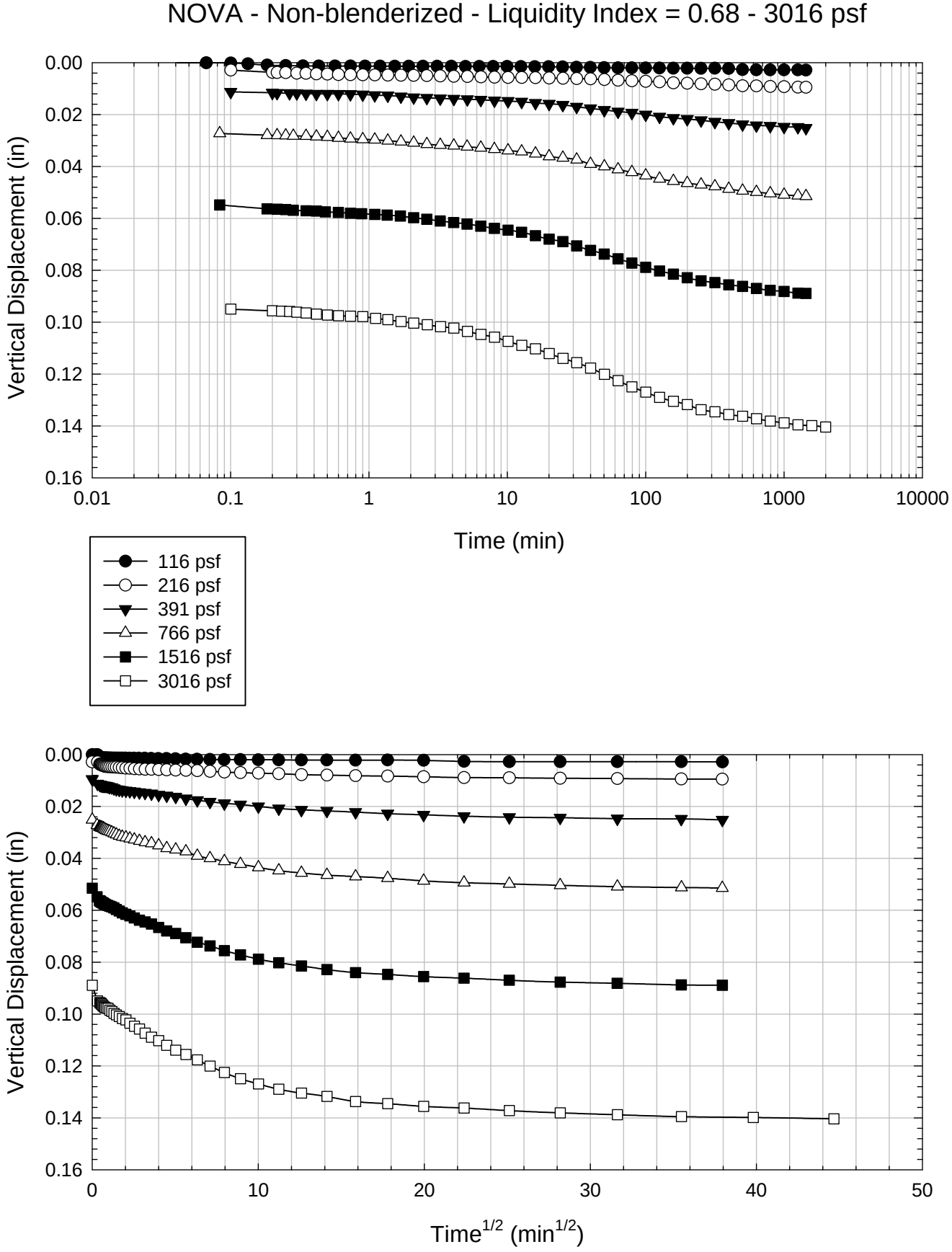
NOVA - Non-blenderized - Liquidity Index = 0.68 - 3016 psf
Vertical Displacement (in)
0.00
0.02
0.04
0.06
0.08
0.10
0.12
0.14
0.16
0.01
0.1
1
10
100
1000
10000
Time (min)
116 psf
216 psf
391 psf
766 psf
1516 psf
3016 psf
Vertical Displacement (in)
0.00
0.02
0.04
0.06
0.08
0.10
0.12
0.14
0.16
0
10
20
30
40
50
Time1/2 (min1/2)

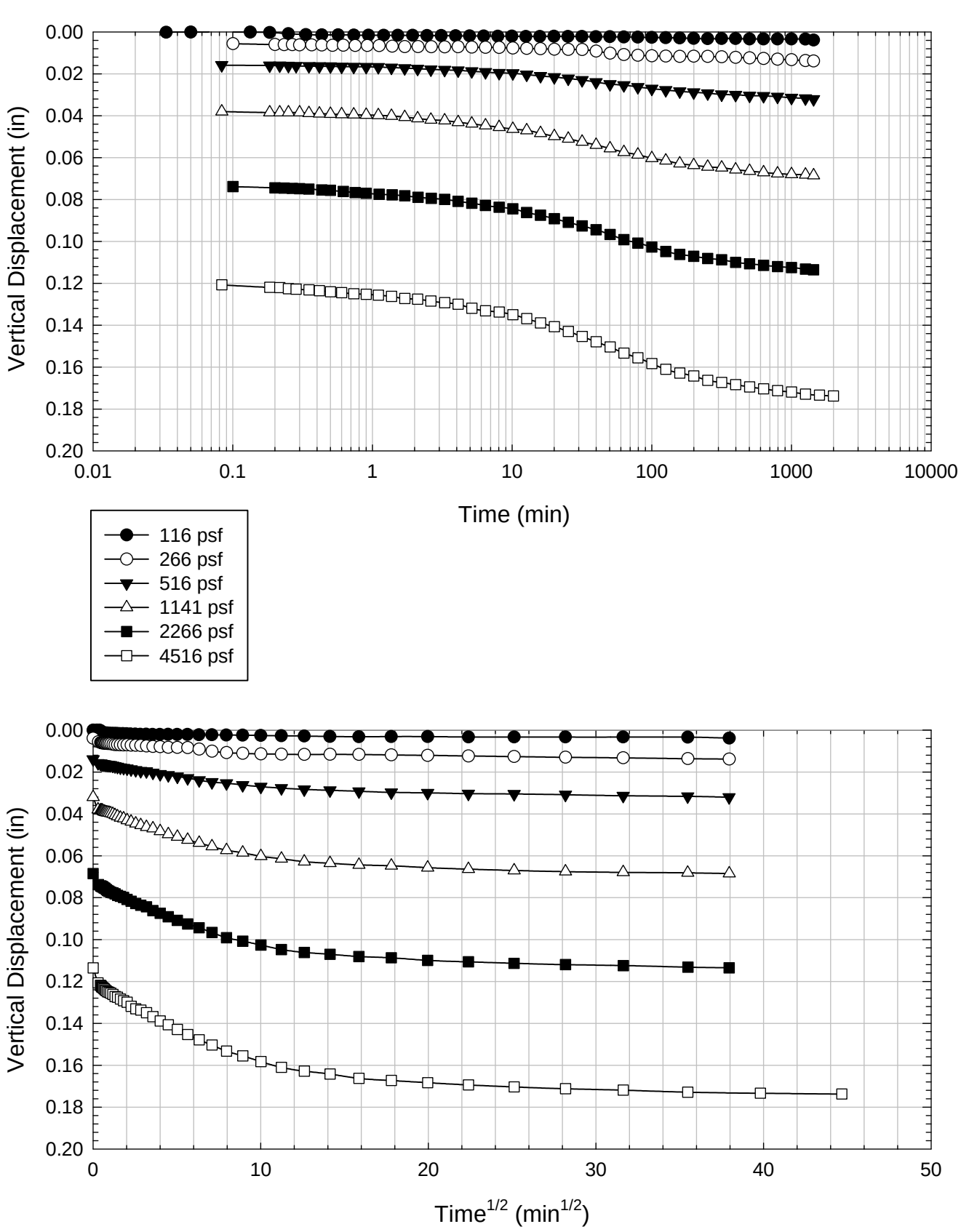
NOVA - Non-blenderized - Liquidity Index = 0.68 - 4516 psf
Vertical Displacement (in)
0.00
0.02
0.04
0.06
0.08
0.10
0.12
0.14
0.16
0.18
0.20
0.01
0.1
1
10
100
1000
10000
Time (min)
116 psf
266 psf
516 psf
1141 psf
2266 psf
4516 psf
Vertical Displacement (in)
0.00
0.02
0.04
0.06
0.08
0.10
0.12
0.14
0.16
0.18
0.20
0
10
20
30
40
50
Time1/2 (min1/2)

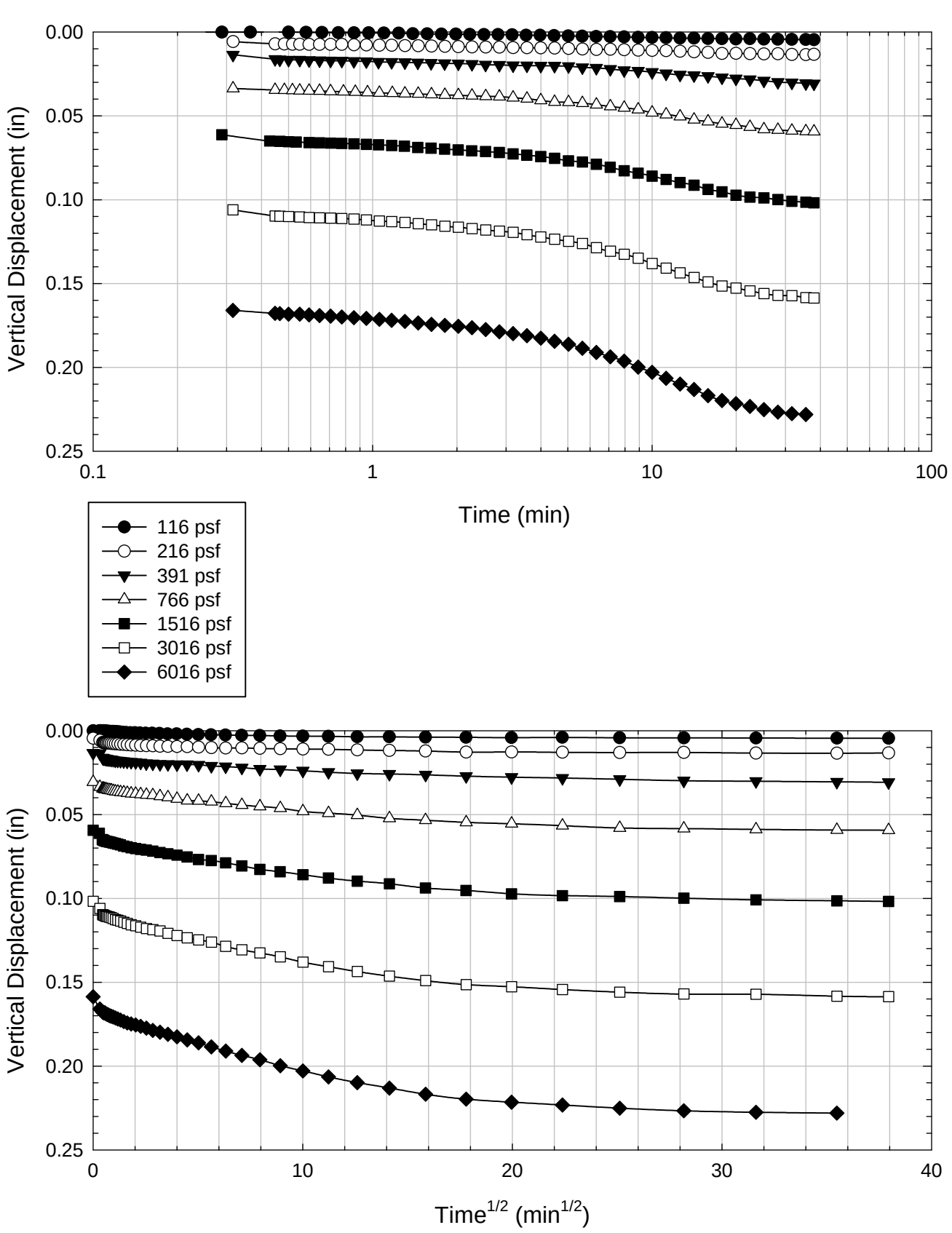
NOVA - Non-blenderized - Liquidity Index = 0.68 - 6016 psf
Vertical Displacement (in)
0.00
0.05
0.10
0.15
0.20
0.25
0.1
1
10
100
Time (min)
116 psf
216 psf
391 psf
766 psf
1516 psf
3016 psf
6016 psf
Vertical Displacement (in)
0.00
0.05
0.10
0.15
0.20
0.25
0
10
20
30
40
Time^1/2 (min^1/2)

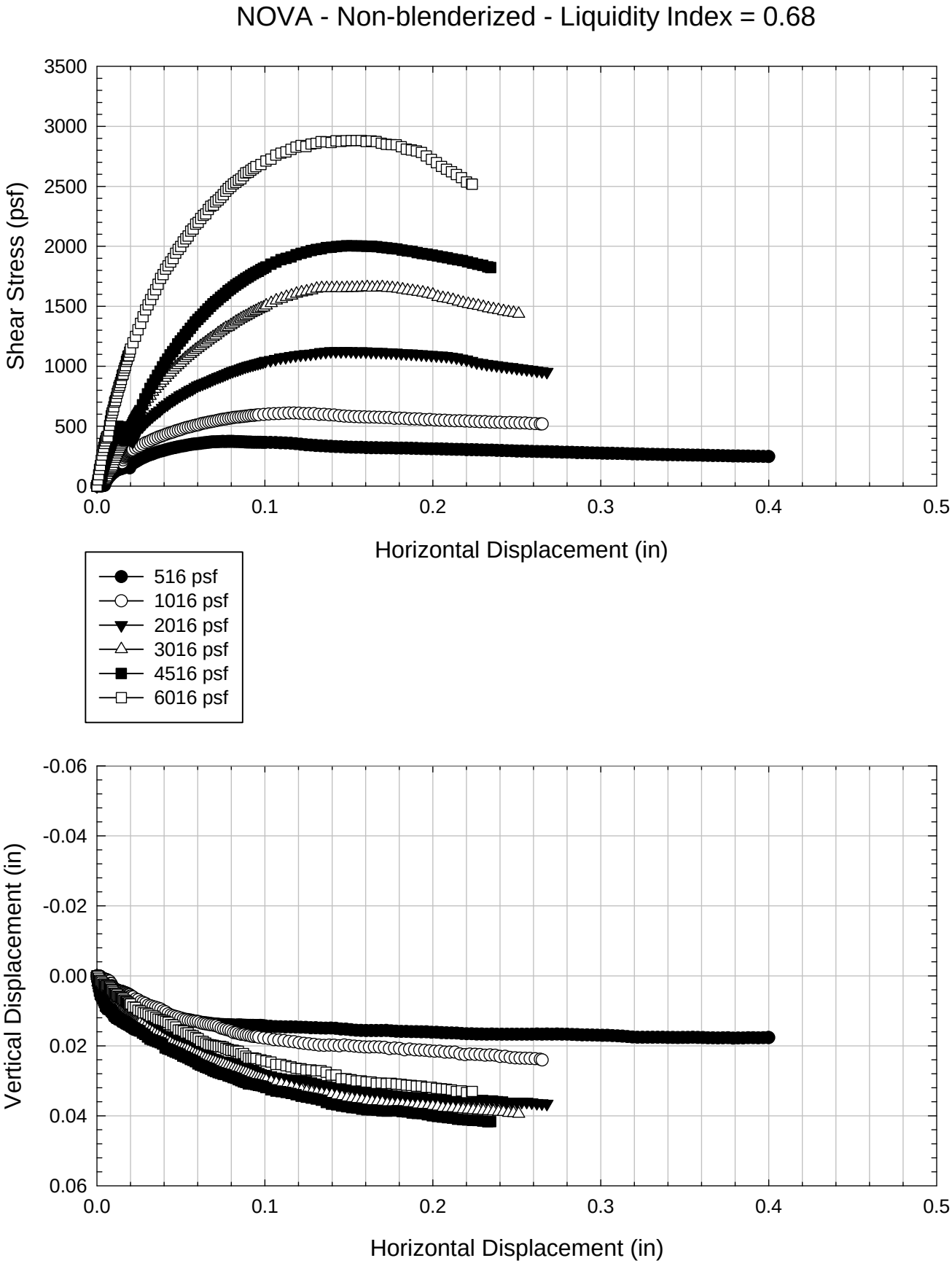
NOVA - Non-blenderized - Liquidity Index = 0.68
Shear Stress (psf)
3500
3000
2500
2000
1500
1000
500
0
0.0
0.1
0.2
0.3
0.4
0.5
Horizontal Displacement (in)
516 psf
1016 psf
2016 psf
3016 psf
4516 psf
6016 psf
Vertical Displacement (in)
-0.06
-0.04
-0.02
0.00
0.02
0.04
0.06
0.0
0.1
0.2
0.3
0.4
0.5
Horizontal Displacement (in)

C.7. Oahe

C.7.1 Blenderized

Virginia Polytechnic Institute and State University
Geotechnical Engineering Laboratory
Direct Shear Data Sheet

Project:	Fully Softened Shear Strength
Sample I.D./Loc.:	Oahe 51Y - Blenderized
Classification:	Fat Clay (CH)

Sample Preparation	Remolded at LL		Specific Gravity	2.88

Test Number	1	2	3	4	5	6	7	8
Start Date (m/d/y)	3/22/2011	3/18/2011	3/22/2011	3/18/2011	8/16/2011	8/9/2011		
End Date (m/d/y)	4/10/2011	4/12/2011	4/12/2011	4/12/2011	9/2/2011	9/2/2011		
Consolidation Pressure (psf)	516	1016	2016	3016	4516	6016		
Initial Values								
Initial Height (in) (Assumed if = 1.44)	1.44	1.44	1.44	1.44	1.41	1.43		
Initial Diameter (in)	2.50	2.50	2.50	2.50	2.50	2.50		
Initial Sample Weight (g)	153	156	162	154	165	166		
Water Content (%)	129.76	131.86	131.15	131.90	107.08	104.18		
Dry Unit Weight (pcf)	35.9	36.3	37.8	35.8	43.8	44.0		
Wet Unit Weight (pcf)	82.5	84.1	87.3	83.0	90.7	89.9		
Consolidation Pressures								
Load 1 (psf)	116	116	116	116	116	116		
Load 2 (psf)	266	216	266	216	266	216		
Load 3 (psf)	516	566	516	391	516	391		
Load 4 (psf)		1016	1016	766	1141	766		
Load 5 (psf)			2016	1516	2266	1516		
Load 6 (psf)				3016	4516	3016		
Load 7 (psf)						6016		
t_{50}								
Max. t_{50} for Load 1 (min)								
Max. t_{50} for Load 2 (min)								
Max. t_{50} for Load 3 (min)	226.17							
Max. t_{50} for Load 4 (min)		289.32						
Max. t_{50} for Load 5 (min)			282.76					
Max. t_{50} for Load 6 (min)				225.27	225.03			
Max. t_{50} for Load 7 (min)						192.49		
Final Values								
Water Content (%)	99.67	86.87	73.62	64.20	55.70	50.90		
Dry Unit Weight (pcf)	44.9	50.8	58.3	65.5	74.5	75.66		
Wet Unit Weight (pcf)	89.7	95.0	101.2	107.5	115.9	114.18		
Failure								
Test Performed at Shear Rate (in/min)	8.81E-06	6.90E-06	7.07E-06	6.90E-06	8.89E-06	1.04E-05		
Required Shear Rate (in/min)	1.06E-05	1.24E-05	8.49E-06	1.24E-05	1.51E-05	1.66E-05		
Displacement at Failure (in)	0.12	0.18	0.12	0.14	0.17	0.16		
Peak Shear Stress (psf)	263	427	646	1080	1460	1568		
Total Change in Height at Failure (in)	0.29	0.41	0.51	0.65	0.58	0.59		
Secant Effective Friction Angle (deg)	27.0	22.8	17.8	19.7	17.9	14.6		

Comments: In the test consolidated to 4515 psf, the software had to be restarted during the shearing stage due to an error.

Oahe Dam - Blenderized - 516 psf

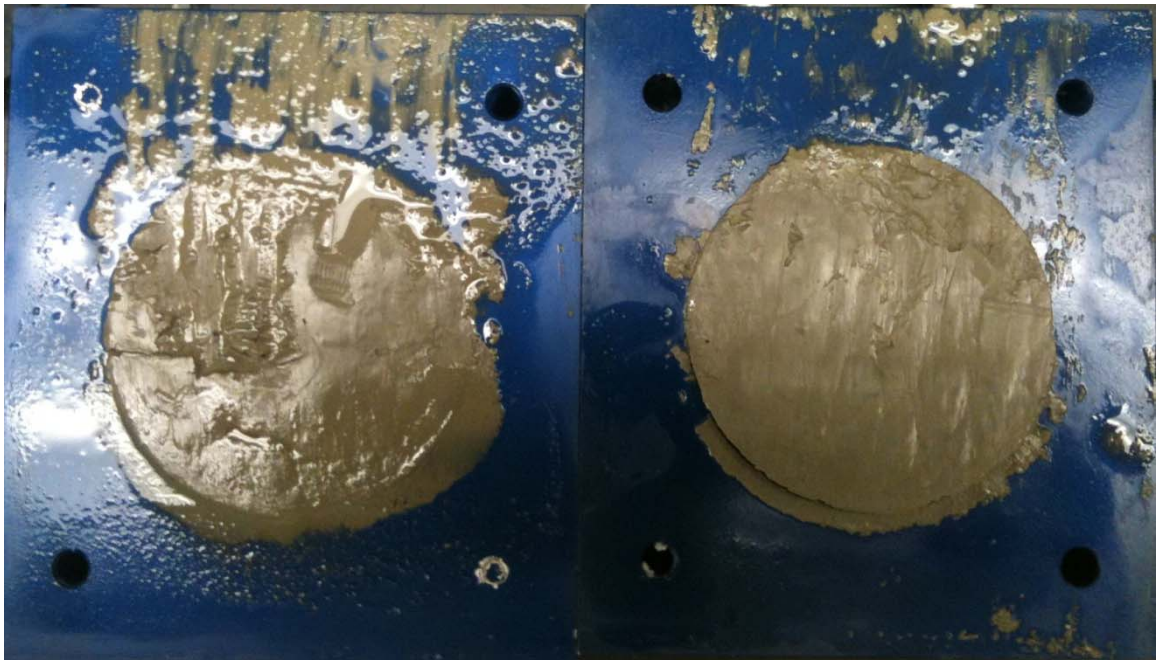

Oahe Dam - Blenderized - 1016 psf

Oahe Dam - Blenderized - 2016 psf

Oahe Dam - Blenderized - 3016 psf

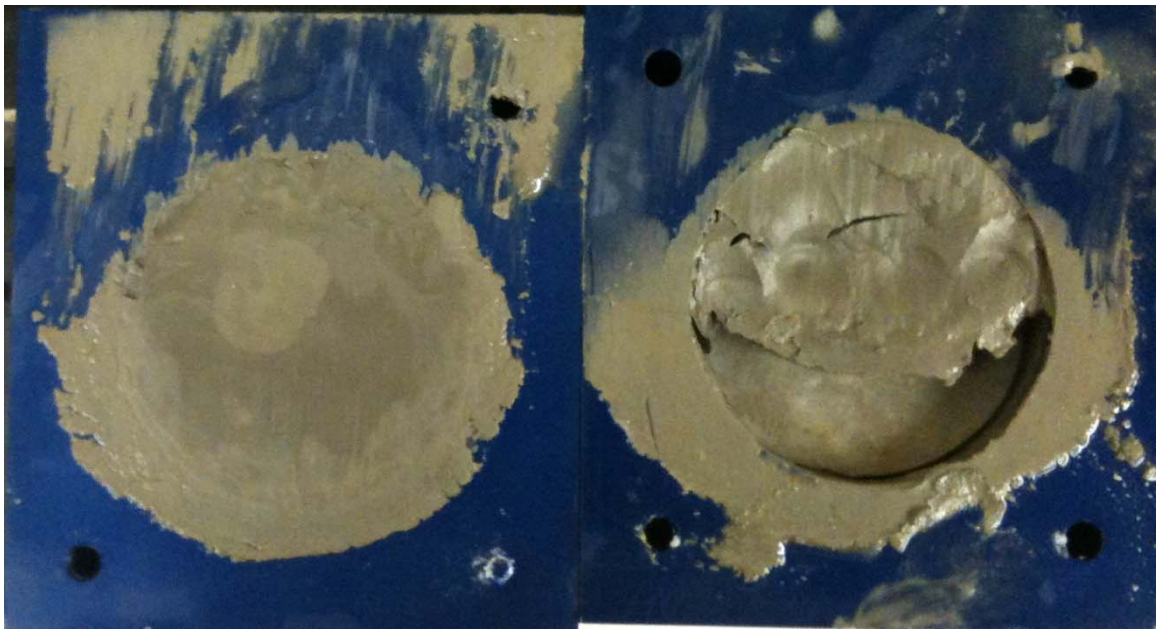

Oahe Dam - Blenderized - 4516 psf

Oahe Dam - Blenderized - 6016 psf

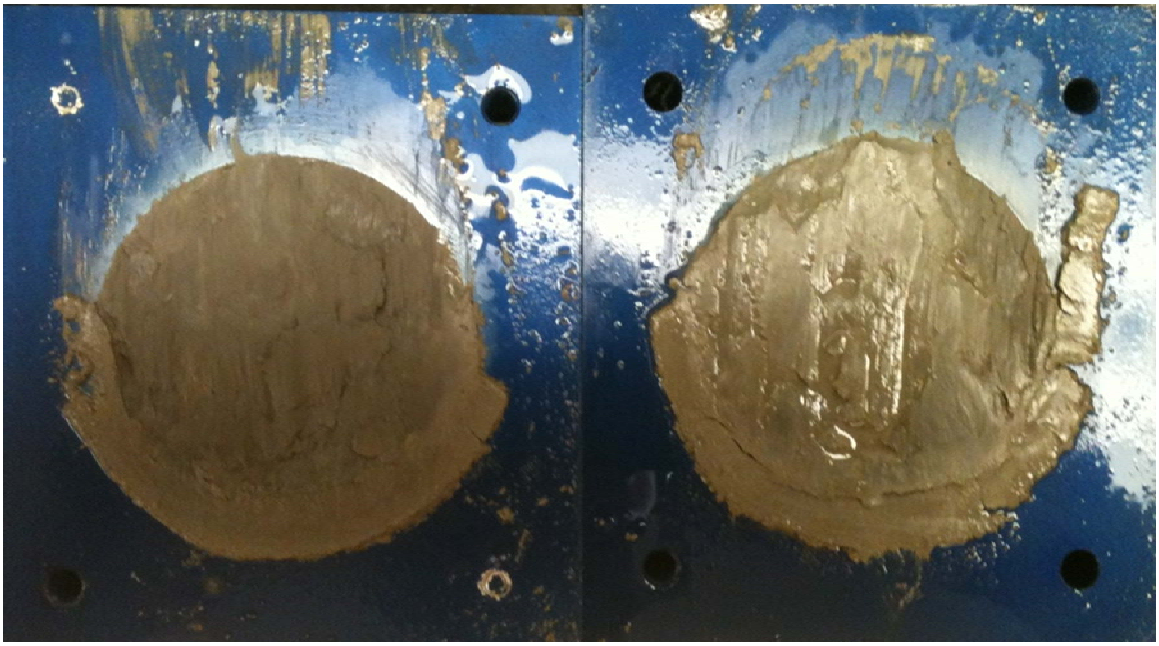

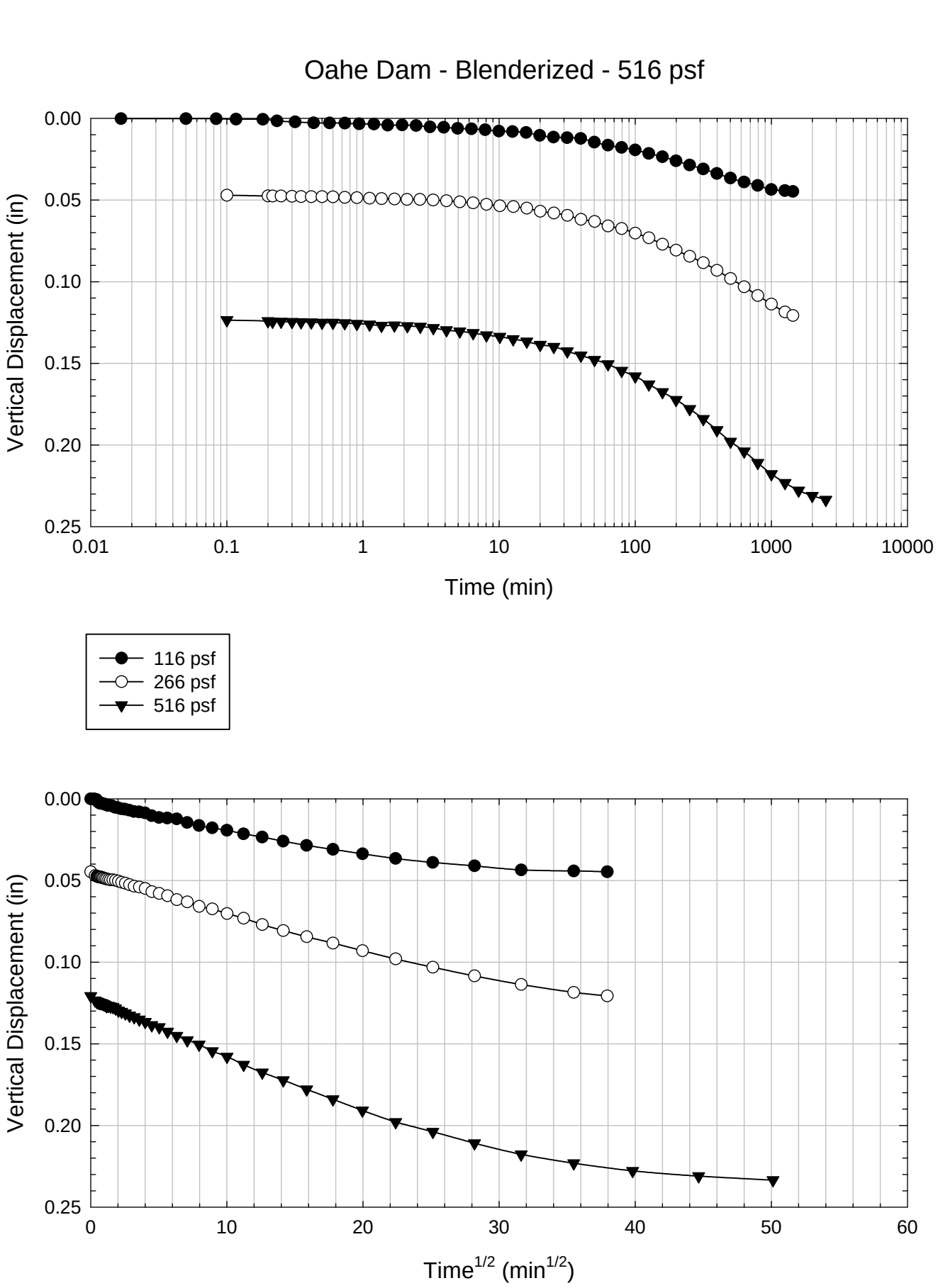
Oahe Dam - Blenderized - 516 psf
Vertical Displacement (in)
0.00
0.05
0.10
0.15
0.20
0.25
0.01
0.1
1
10
100
1000
10000
Time (min)
116 psf
266 psf
516 psf
Vertical Displacement (in)
0.00
0.05
0.10
0.15
0.20
0.25
0
10
20
30
40
50
60
Time1/2 (min1/2)

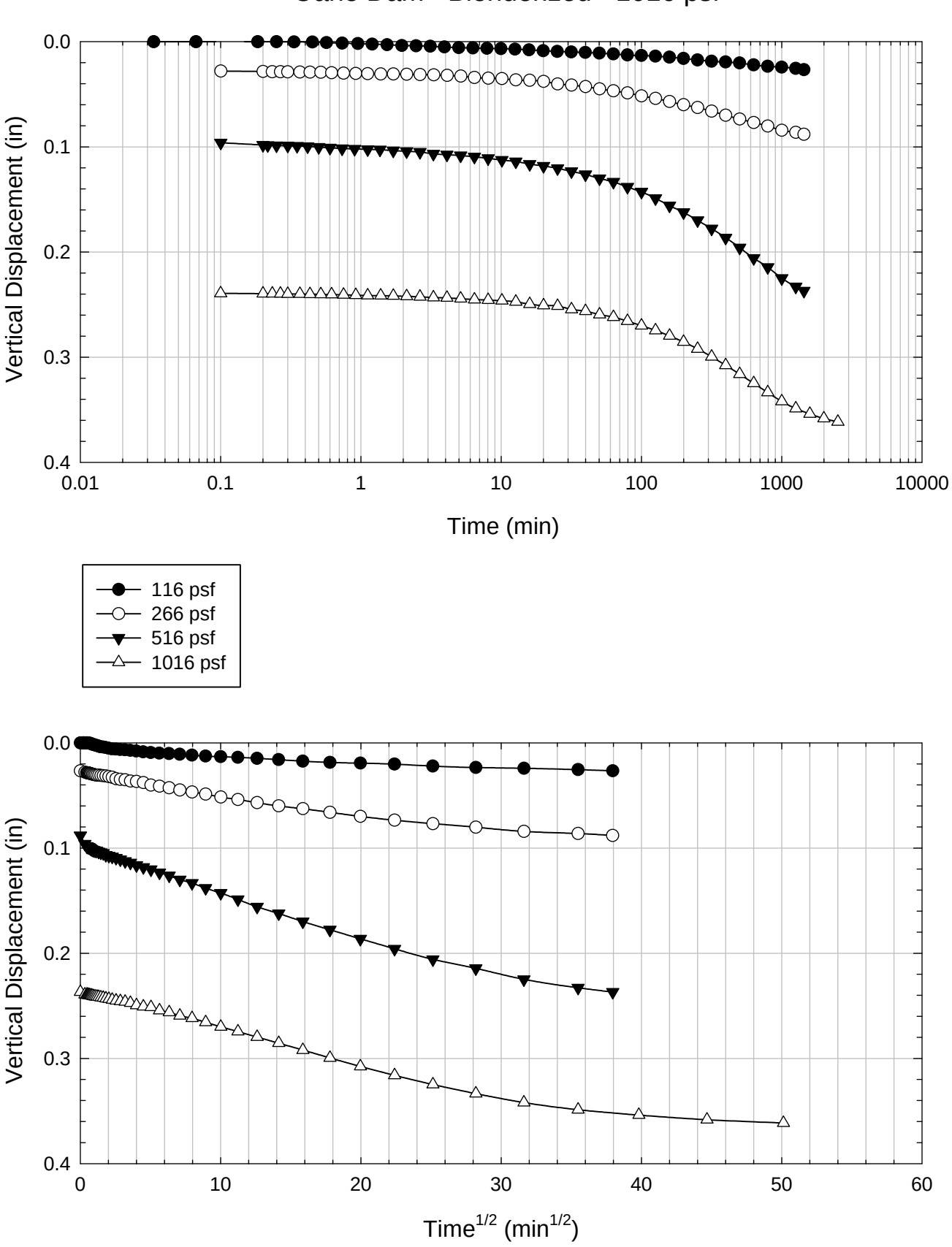
Oahe Dam - Blenderized - 1016 psf
Vertical Displacement (in)
0.0
0.1
0.2
0.3
0.4
0.01
0.1
1
10
100
1000
10000
Time (min)
116 psf
266 psf
516 psf
1016 psf
Vertical Displacement (in)
0.0
0.1
0.2
0.3
0.4
0
10
20
30
40
50
60
Time1/2 (min1/2)

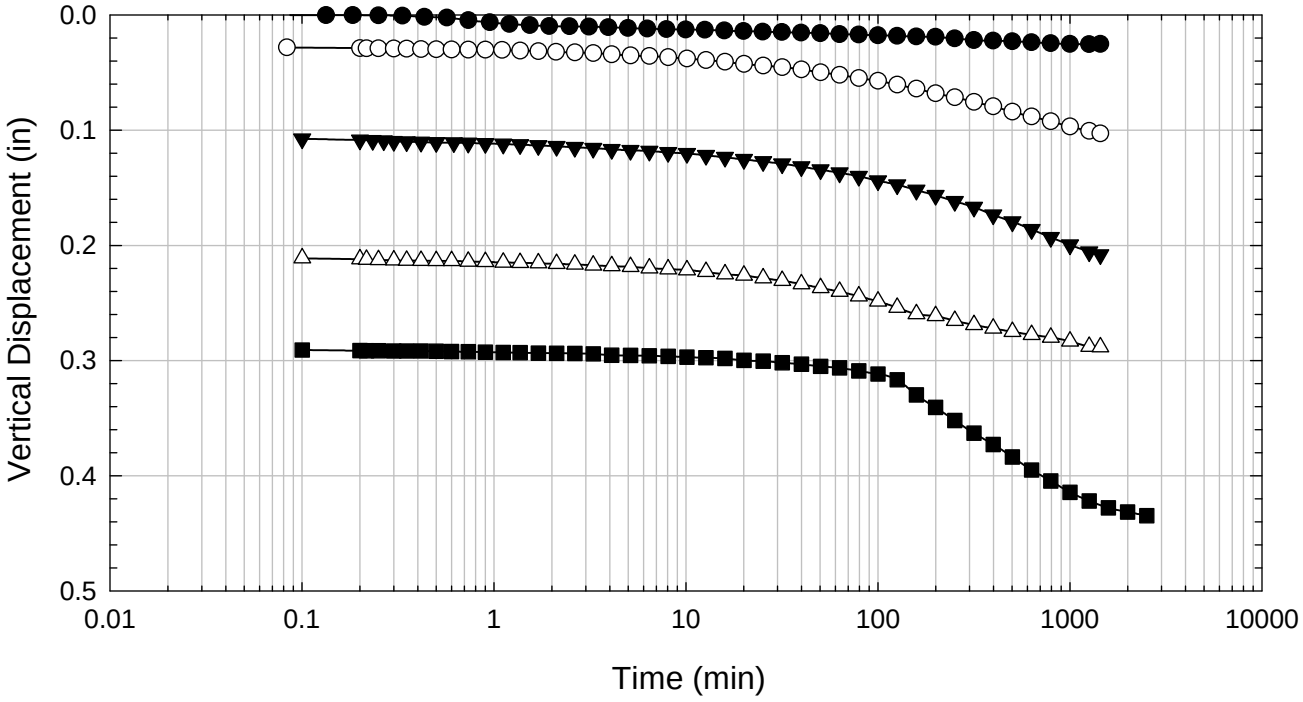
Oahe Dam - Blenderized - 2016 psf
Vertical Displacement (in)
0.0
0.1
0.2
0.3
0.4
0.5
0.01
0.1
1
10
100
1000
10000
Time (min)

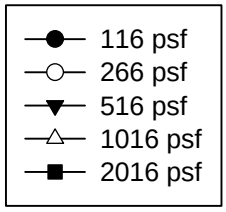
116 psf
266 psf
516 psf
1016 psf
2016 psf

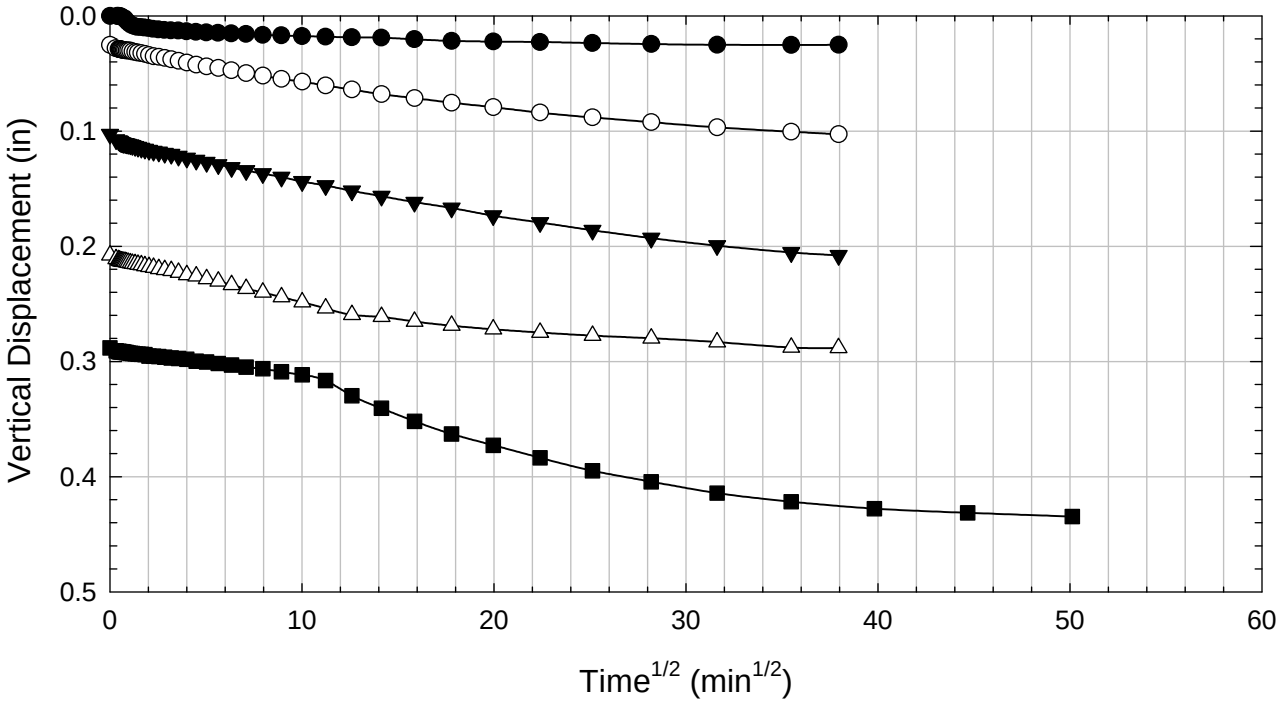
Vertical Displacement (in)
0.0
0.1
0.2
0.3
0.4
0.5
0
10
20
30
40
50
60
Time1/2 (min1/2)

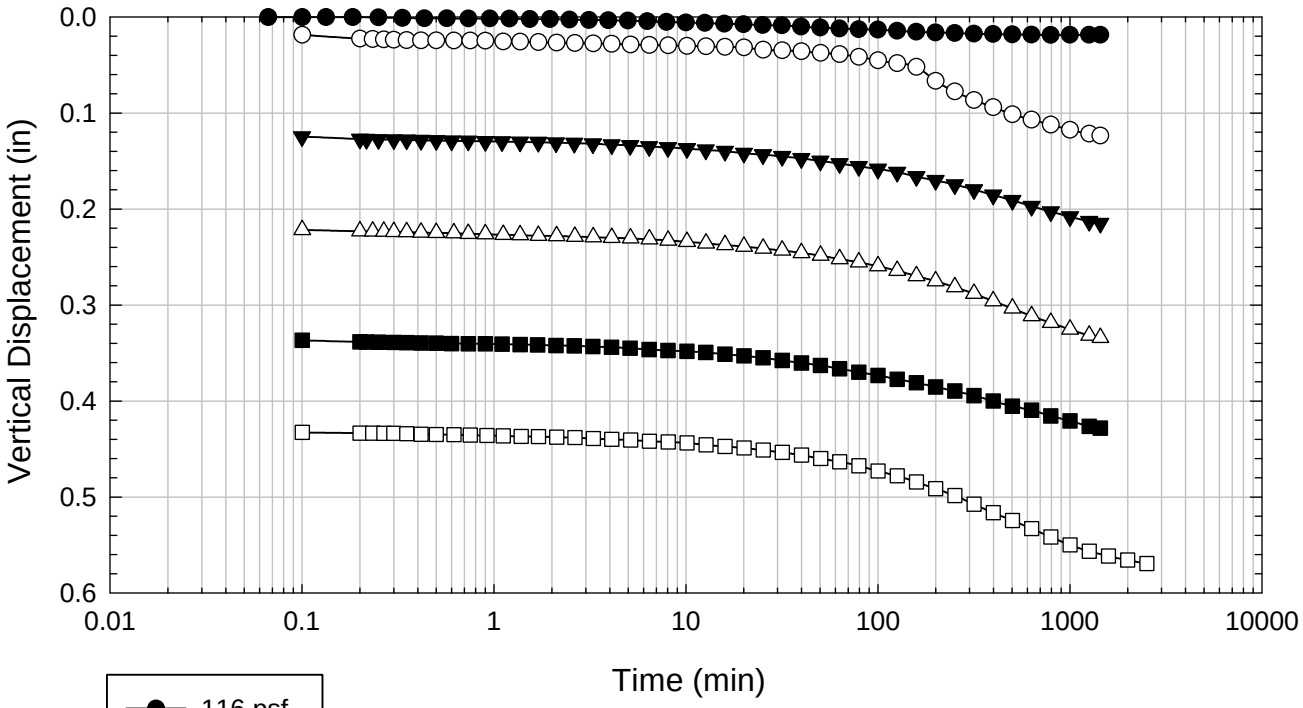
Oahe Dam - Blenderized - 3016 psf
Vertical Displacement (in)
0.0
0.1
0.2
0.3
0.4
0.5
0.6
0.01
0.1
1
10
100
1000
10000
Time (min)

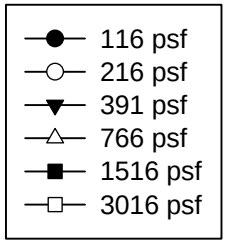
116 psf
216 psf
391 psf
766 psf
1516 psf
3016 psf

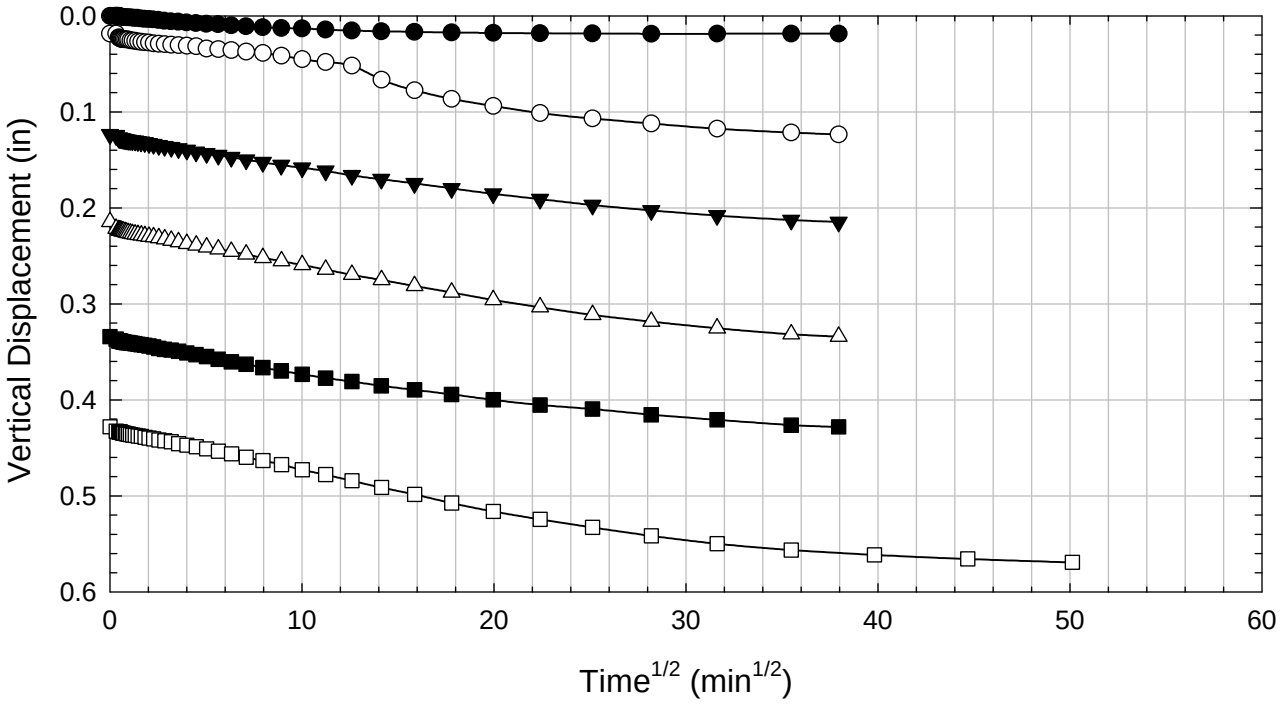
Vertical Displacement (in)
0.0
0.1
0.2
0.3
0.4
0.5
0.6
0
10
20
30
40
50
60
Time1/2 (min1/2)

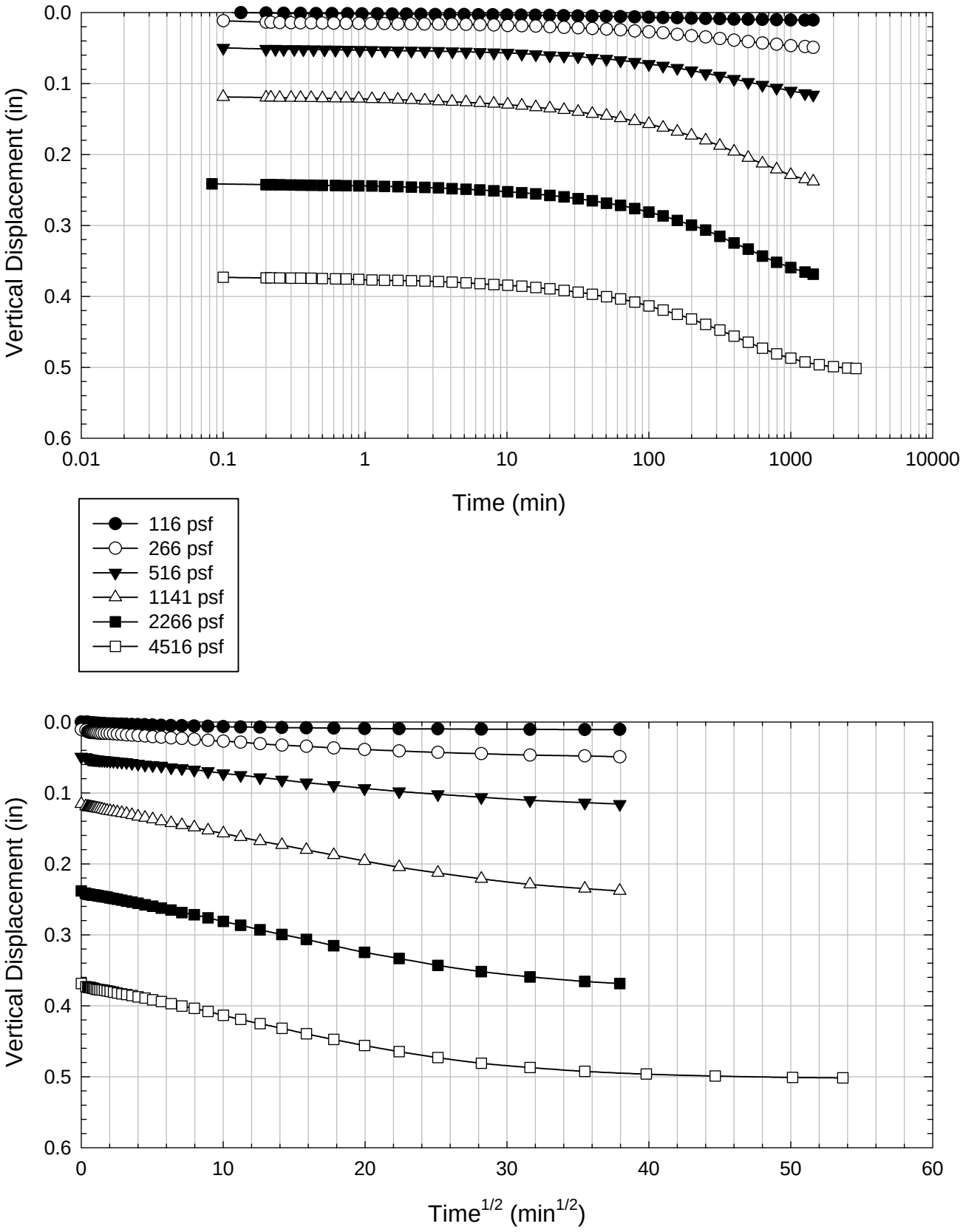
Oahe Dam - Blenderized - 4516 psf
Vertical Displacement (in)
0.0
0.1
0.2
0.3
0.4
0.5
0.6
0.01
0.1
1
10
100
1000
10000
Time (min)
116 psf
266 psf
516 psf
1141 psf
2266 psf
4516 psf
Vertical Displacement (in)
0.0
0.1
0.2
0.3
0.4
0.5
0.6
0
10
20
30
40
50
60
Time^1/2 (min^1/2)

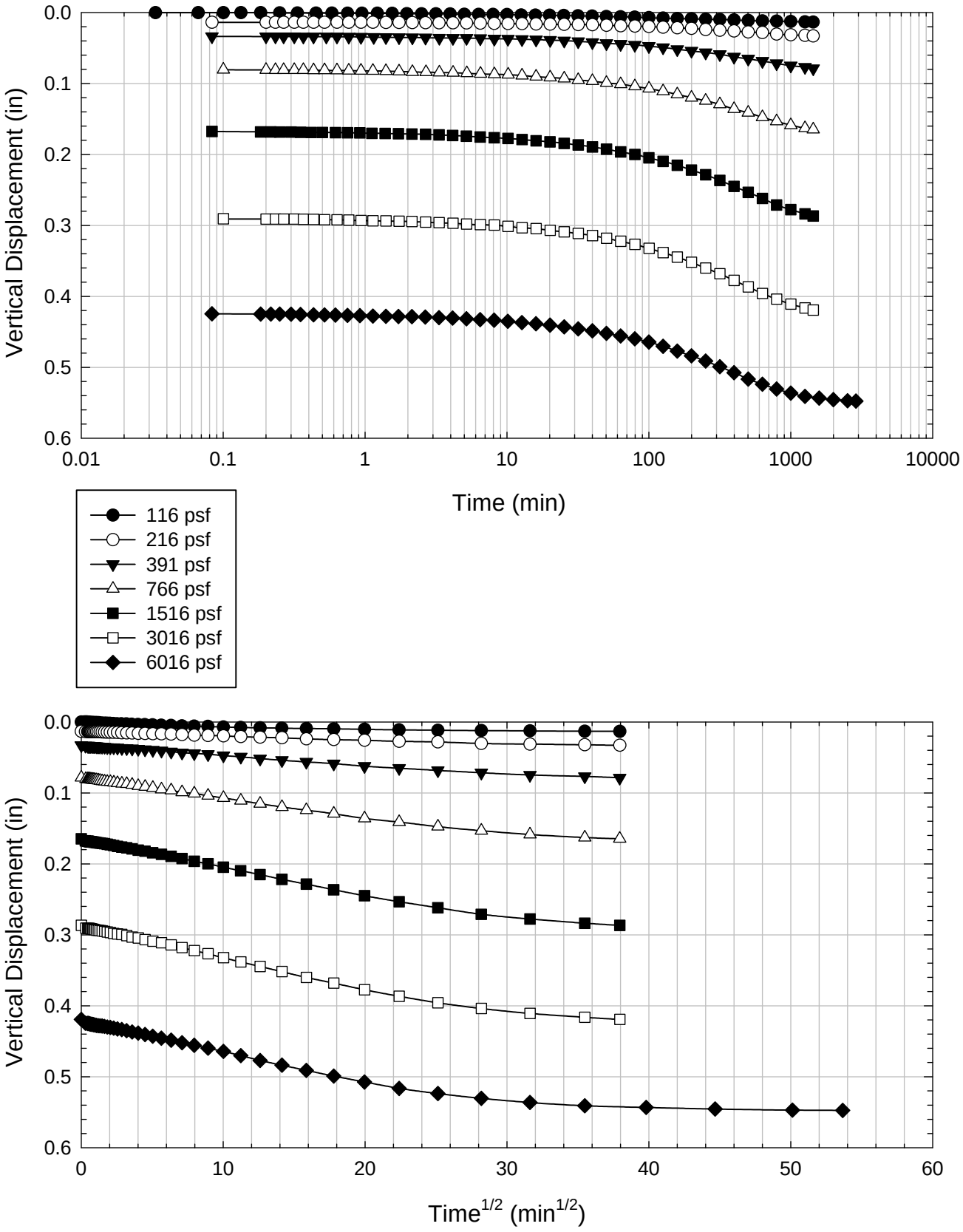
Oahe Dam - Blenderized - 6016 psf
Vertical Displacement (in)
0.0
0.1
0.2
0.3
0.4
0.5
0.6
0.01
0.1
1
10
100
1000
10000
Time (min)
116 psf
216 psf
391 psf
766 psf
1516 psf
3016 psf
6016 psf
Vertical Displacement (in)
0
10
20
30
40
50
60
Time1/2 (min1/2)

Oahe Dam - Blenderized

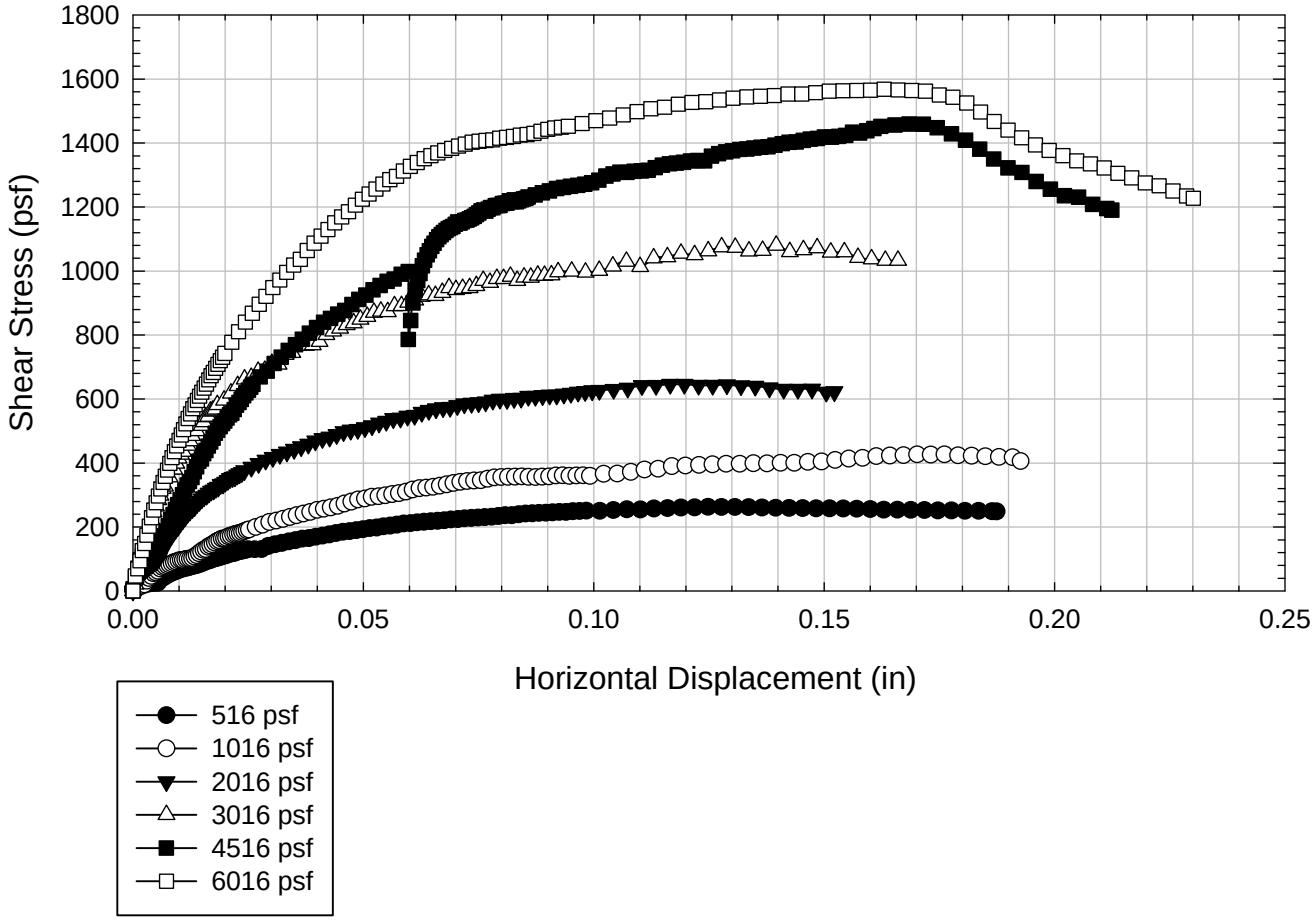

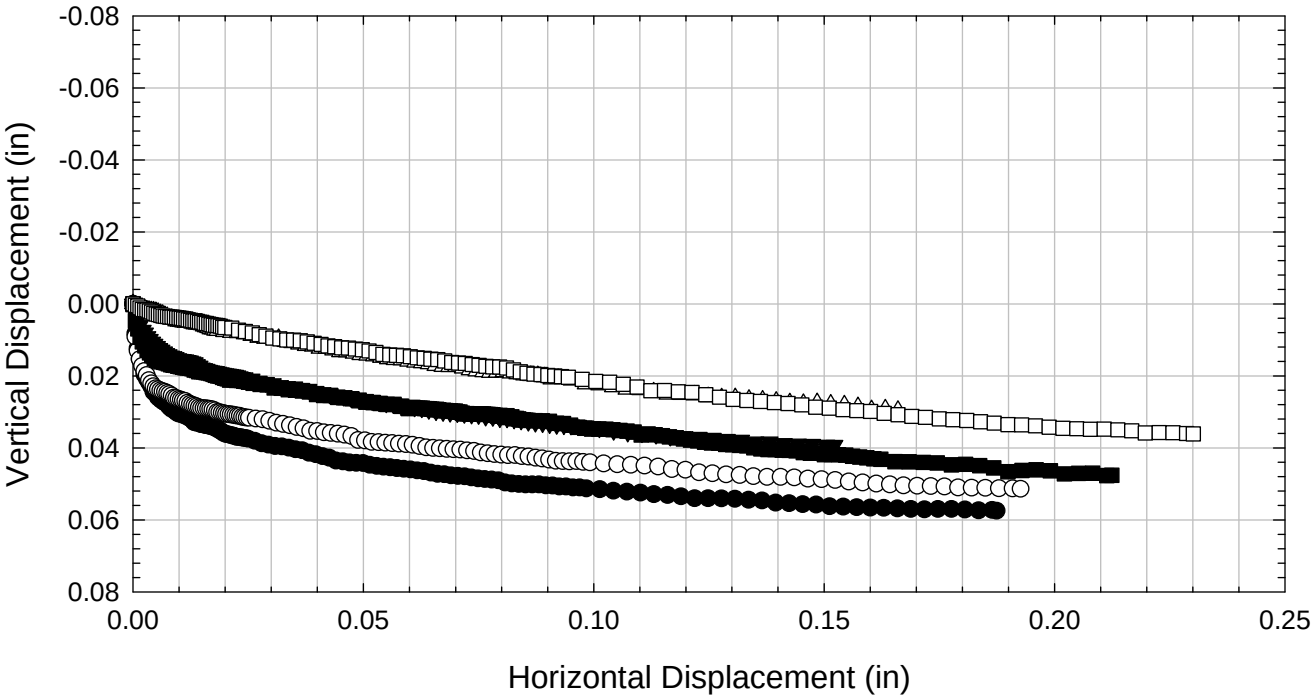

C.8. Oak Harbor

C.8.1 Non-blenderized

Virginia Polytechnic Institute and State University
Geotechnical Engineering Laboratory
Direct Shear Data Sheet

Project:	Fully Softened Shear Strength
Sample I.D./Loc.:	Oak Harbor - Non-blenderized
Classification:	Lean Clay (CL)

Sample Preparation	Remolded at LL		Specific Gravity	2.82

Test Number	1	2	3	4	5	6	7	8
Start Date (m/d/y)	9/12/2012	9/12/2012	9/12/2012	9/10/2012	4/9/2012			
End Date (m/d/y)	9/20/2012	9/20/2012	9/20/2012	9/19/2012	4/19/2012			
Consolidation Pressure (psf)	516	1016	2016	3016	6016			
Initial Values								
Initial Height (in)	1.41	1.45	1.39	1.40	1.42			
Initial Diameter (in)	2.50	2.50	2.50	2.50	2.50			
Initial Sample Weight (g)	203	210	202	205	201			
Water Content (%)	46.68	46.42	47.92	47.92	45.35			
Dry Unit Weight (pcf)	76.1	76.9	76.0	76.6	75.7			
Wet Unit Weight (pcf)	111.6	112.6	112.4	113.3	110.1			
Consolidation Pressures								
Load 1 (psf)	116	116	116	116	116			
Load 2 (psf)	266	266	266	216	216			
Load 3 (psf)	516	516	516	391	391			
Load 4 (psf)		1016	1016	766	766			
Load 5 (psf)			2016	1516	1516			
Load 6 (psf)				3016	3016			
Load 7 (psf)					6016			
t_{50}								
Max. t_{50} for Load 1 (min)								
Max. t_{50} for Load 2 (min)								
Max. t_{50} for Load 3 (min)	64.44							
Max. t_{50} for Load 4 (min)		43.27						
Max. t_{50} for Load 5 (min)			25.42					
Max. t_{50} for Load 6 (min)				22.41				
Max. t_{50} for Load 7 (min)					17.64			
Final Values								
Water Content (%)	37.19	34.17	31.22	29.94	26.25			
Dry Unit Weight (pcf)	91.1	91.7	95.6	98.8	104.2			
Wet Unit Weight (pcf)	125.0	123.0	125.5	128.4	131.5			
Failure								
Test Performed at Shear Rate (in/min)	3.10E-05	4.26E-05	7.87E-05	8.92E-05	1.13E-04			
Required Shear Rate (in/min)	3.62E-05	8.01E-05	1.33E-04	1.92E-04	2.37E-04			
Displacement at Failure (in)	0.12	0.17	0.17	0.21	0.21			
Peak Shear Stress (psf)	320	472	1169	1618	3173			
Total Change in Height at Failure (in)	0.23	0.23	0.29	0.32	0.39			
Secant Effective Friction Angle (deg)	31.8	24.9	30.1	28.2	27.8			

Comments:

Oak Harbor - Non-blenderized - 516 psf

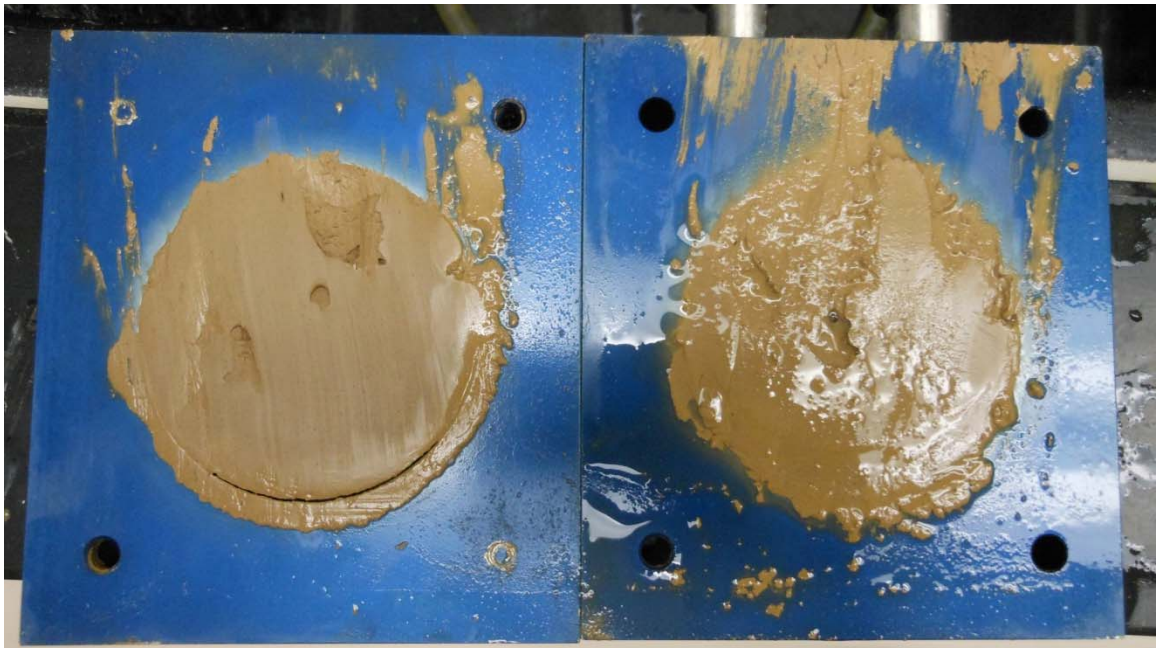

Oak Harbor - Non-blenderized - 1016 psf

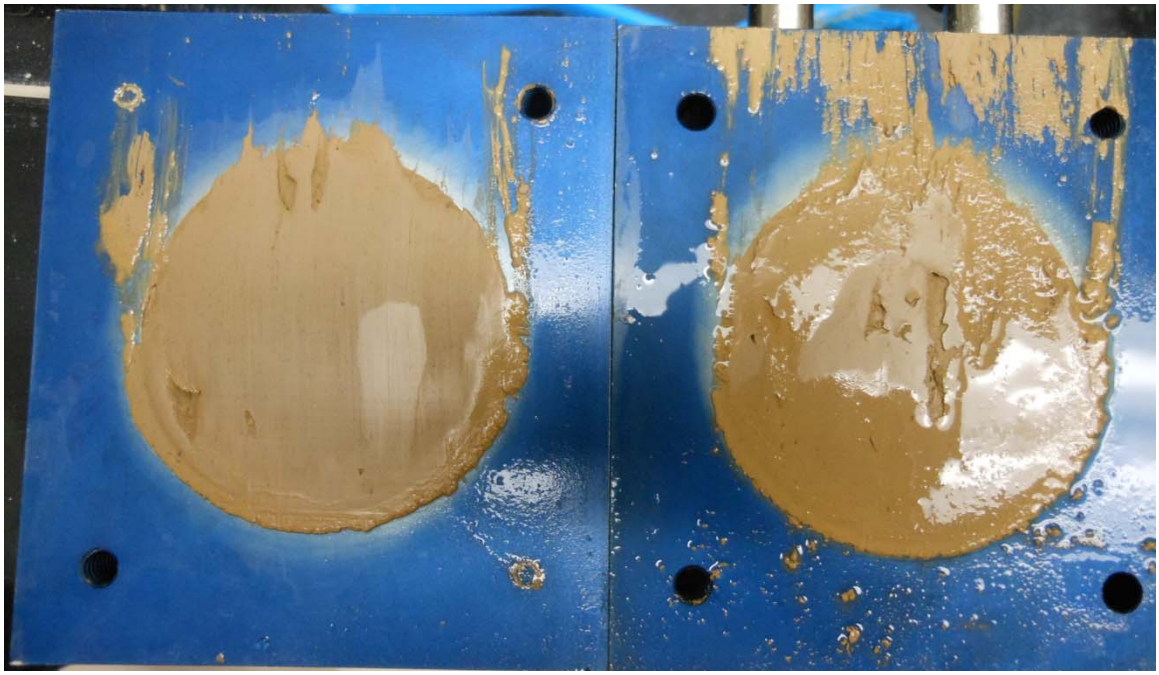

Oak Harbor - Non-blenderized - 2016 psf

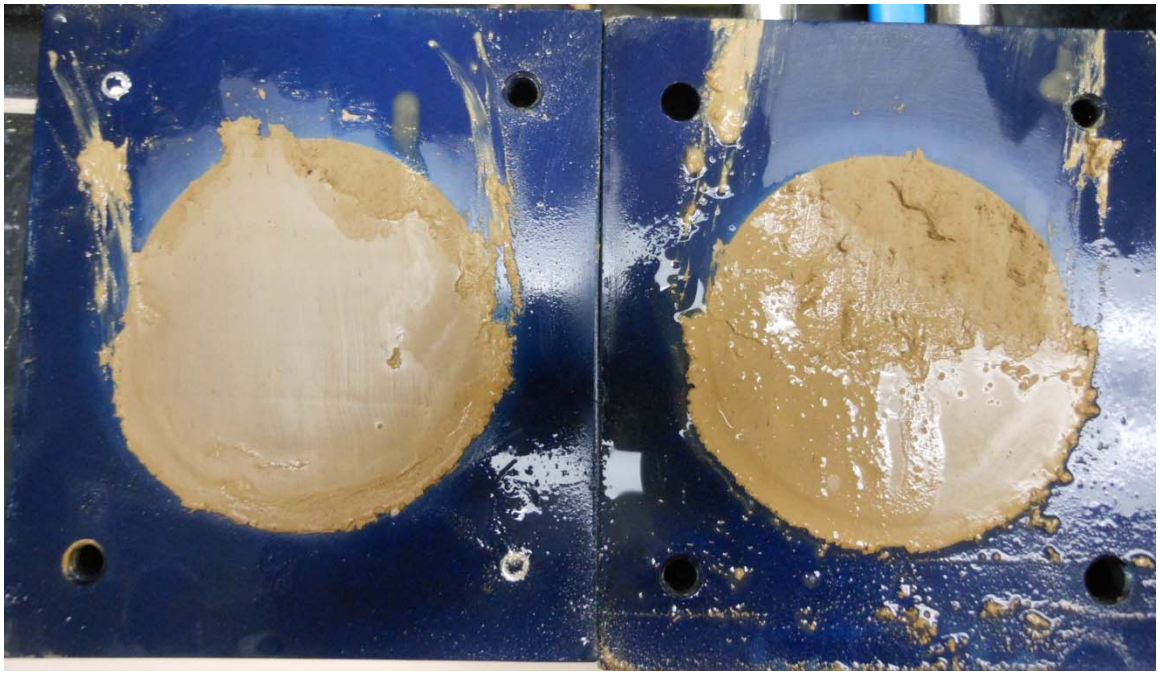

Oak Harbor - Non-blenderized - 3016 psf

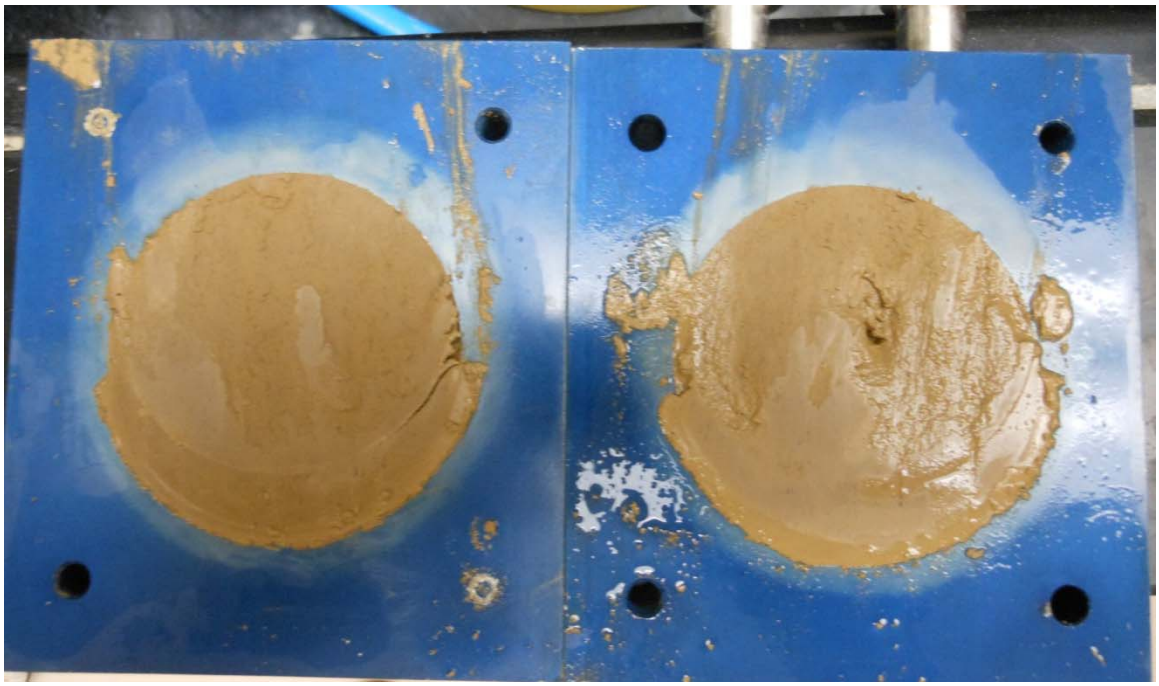

Oak Harbor - Non-blenderized - 6016 psf

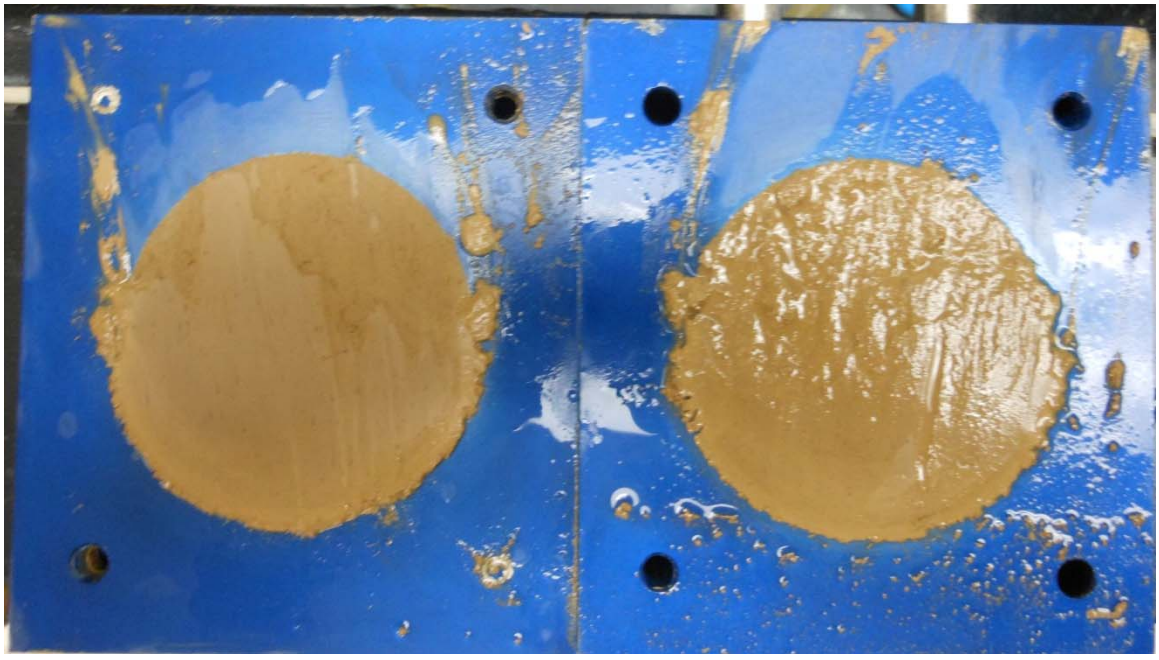

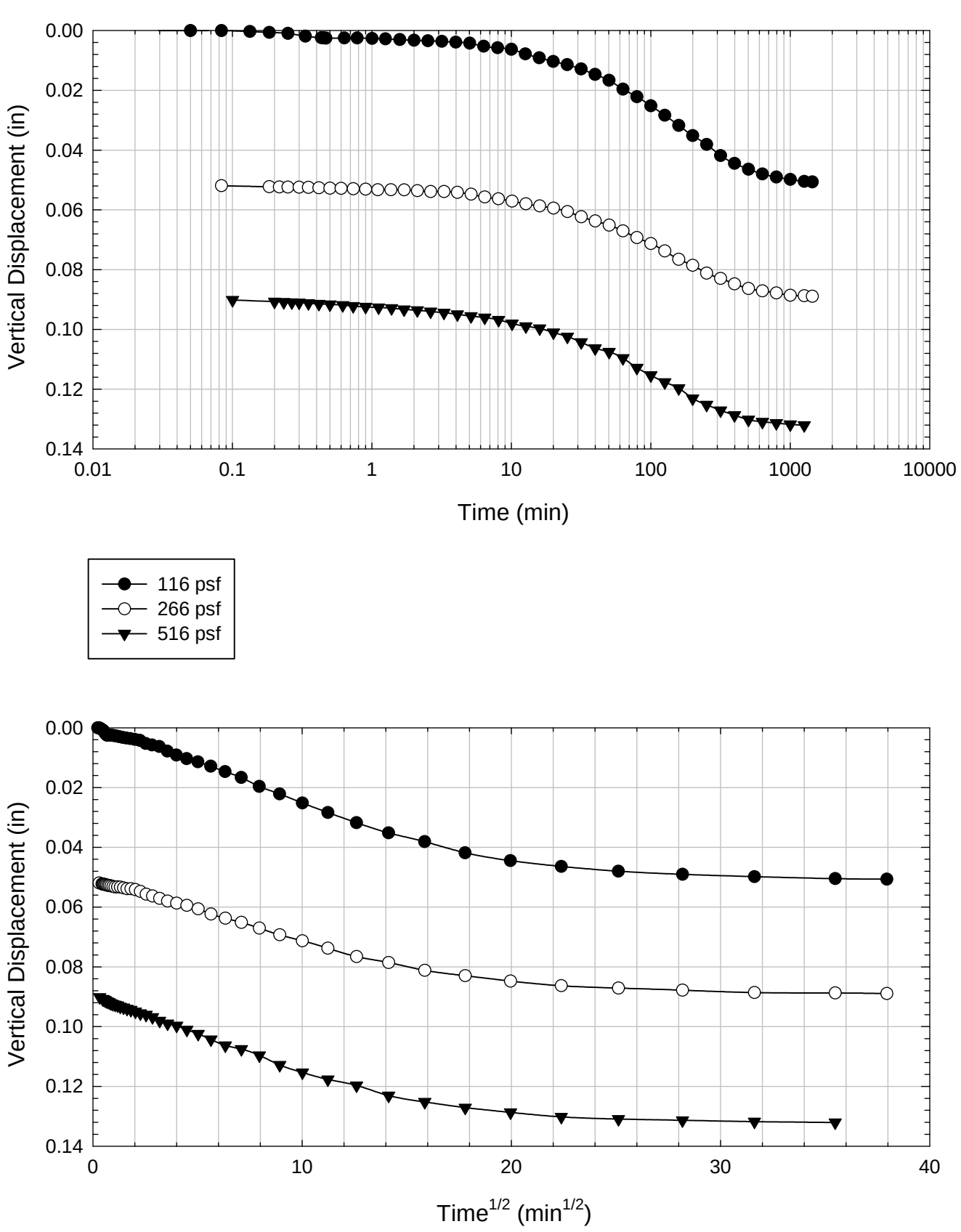
Oak Harbor - Non-blenderized - 516 psf
Vertical Displacement (in)
0.00
0.02
0.04
0.06
0.08
0.10
0.12
0.14
0.01
0.1
1
10
100
1000
10000
Time (min)
116 psf
266 psf
516 psf
Vertical Displacement (in)
0.00
0.02
0.04
0.06
0.08
0.10
0.12
0.14
0
10
20
30
40
Time^1/2 (min^1/2)

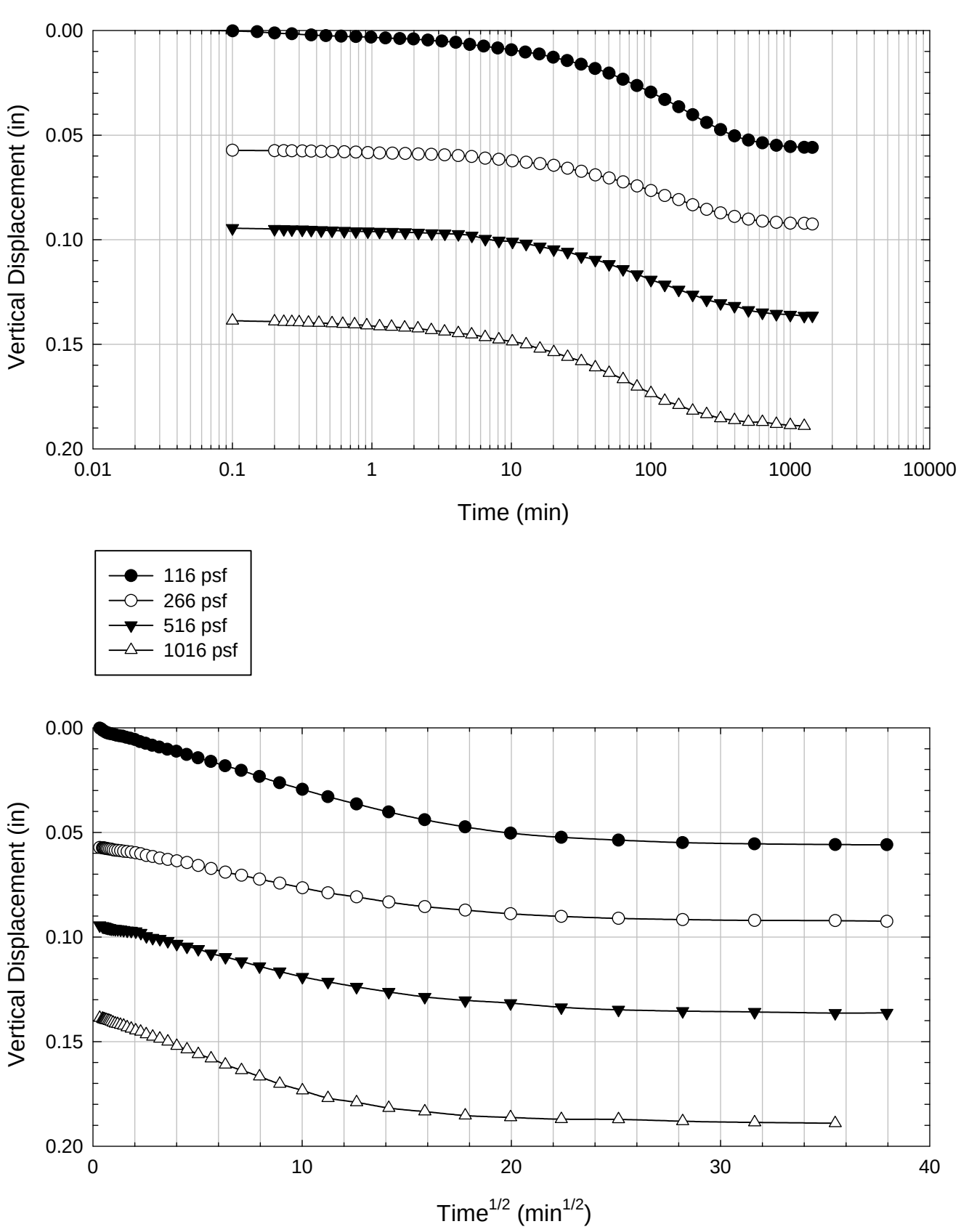
Oak Harbor - Non-blenderized - 1016 psf
Vertical Displacement (in)
0.00
0.05
0.10
0.15
0.20
0.01
0.1
1
10
100
1000
10000
Time (min)
116 psf
266 psf
516 psf
1016 psf
Vertical Displacement (in)
0.00
0.05
0.10
0.15
0.20
0
10
20
30
40
Time^1/2 (min^1/2)

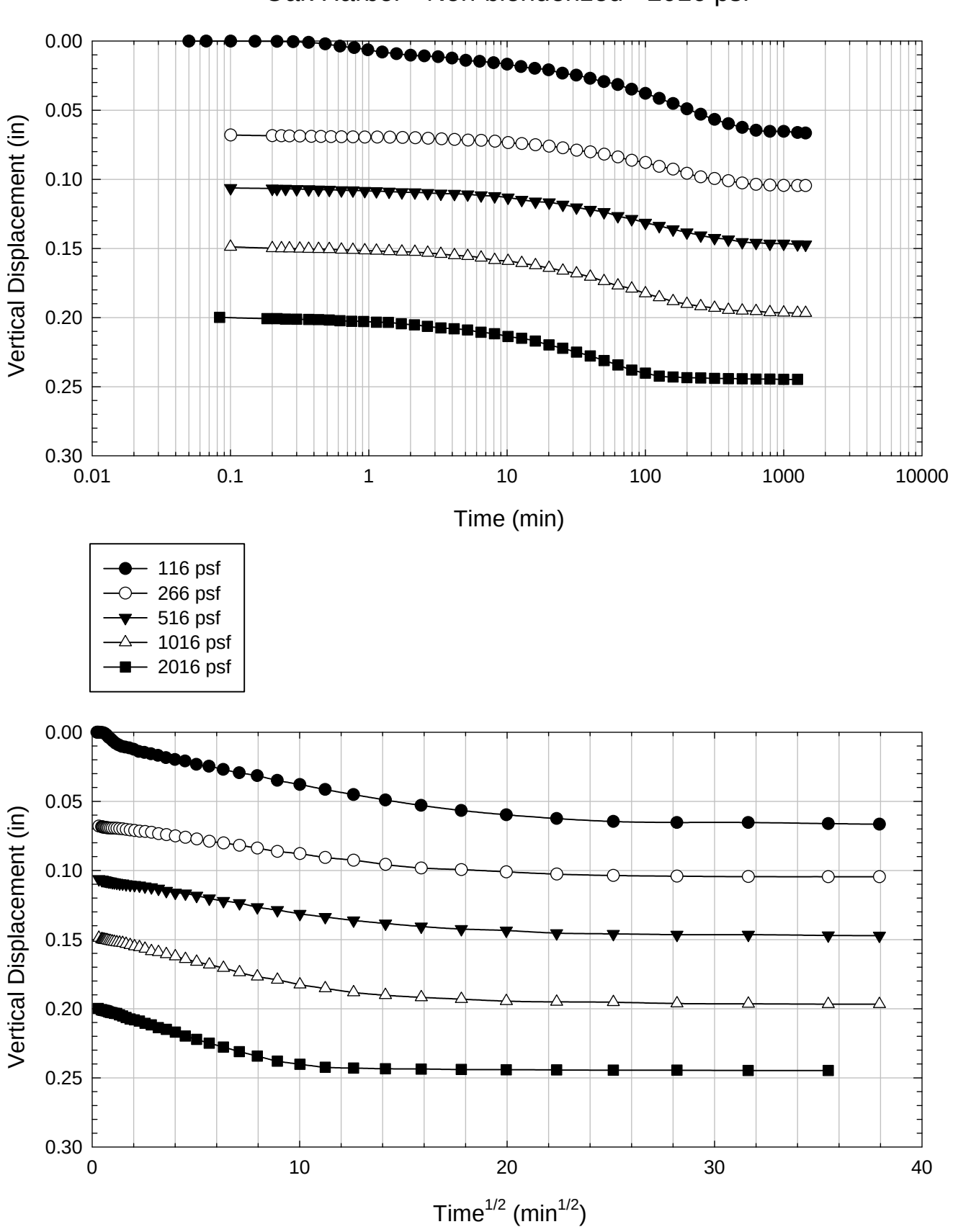
Oak Harbor - Non-blenderized - 2016 psf
Vertical Displacement (in)
0.00
0.05
0.10
0.15
0.20
0.25
0.30
0.01
0.1
1
10
100
1000
10000
Time (min)
116 psf
266 psf
516 psf
1016 psf
2016 psf
Vertical Displacement (in)
0.00
0.05
0.10
0.15
0.20
0.25
0.30
0
10
20
30
40
Time^1/2 (min^1/2)

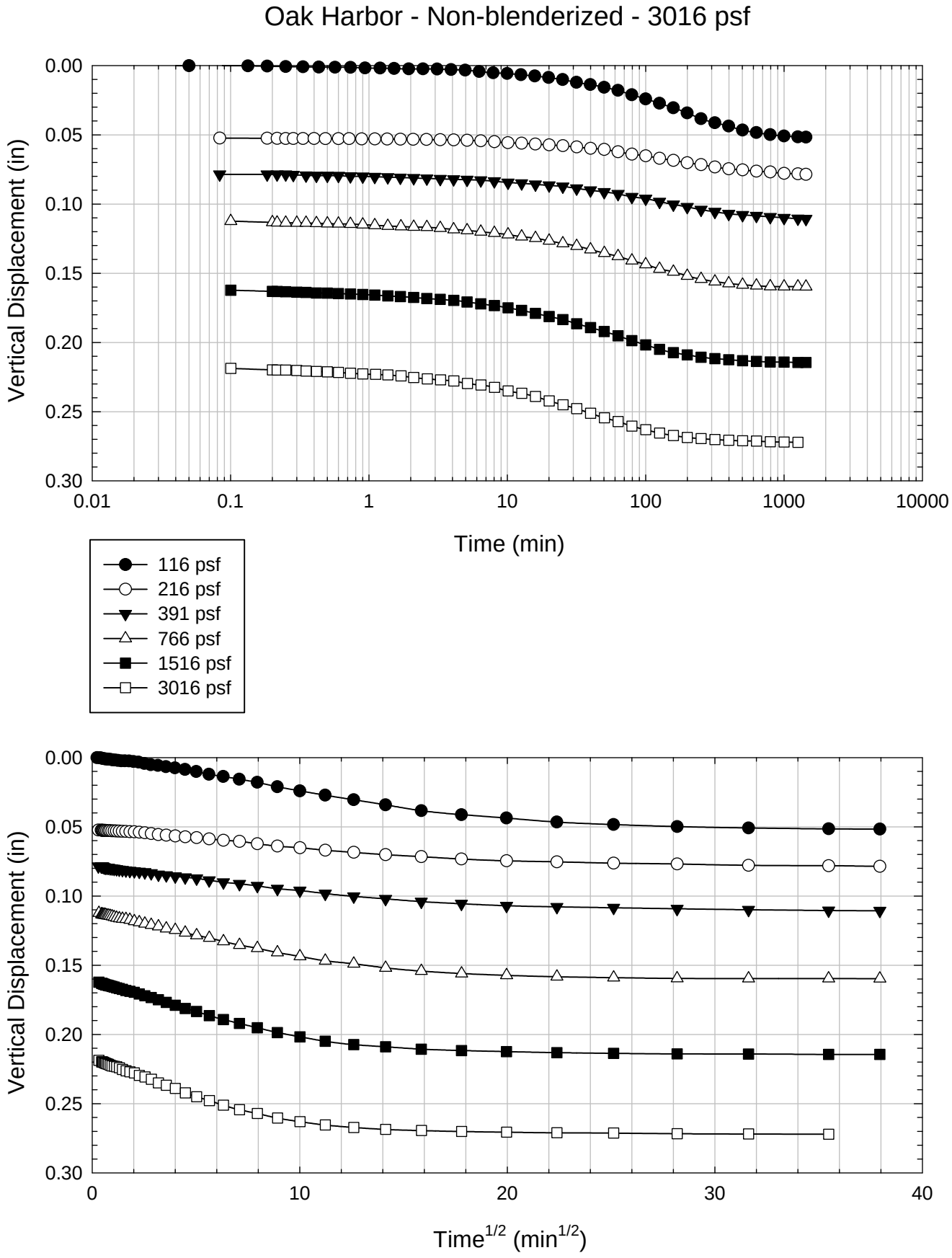
Oak Harbor - Non-blenderized - 3016 psf
Vertical Displacement (in)
0.00
0.05
0.10
0.15
0.20
0.25
0.30
0.01
0.1
1
10
100
1000
10000
Time (min)
116 psf
216 psf
391 psf
766 psf
1516 psf
3016 psf
Vertical Displacement (in)
0.00
0.05
0.10
0.15
0.20
0.25
0.30
0
10
20
30
40
Time^1/2 (min^1/2)

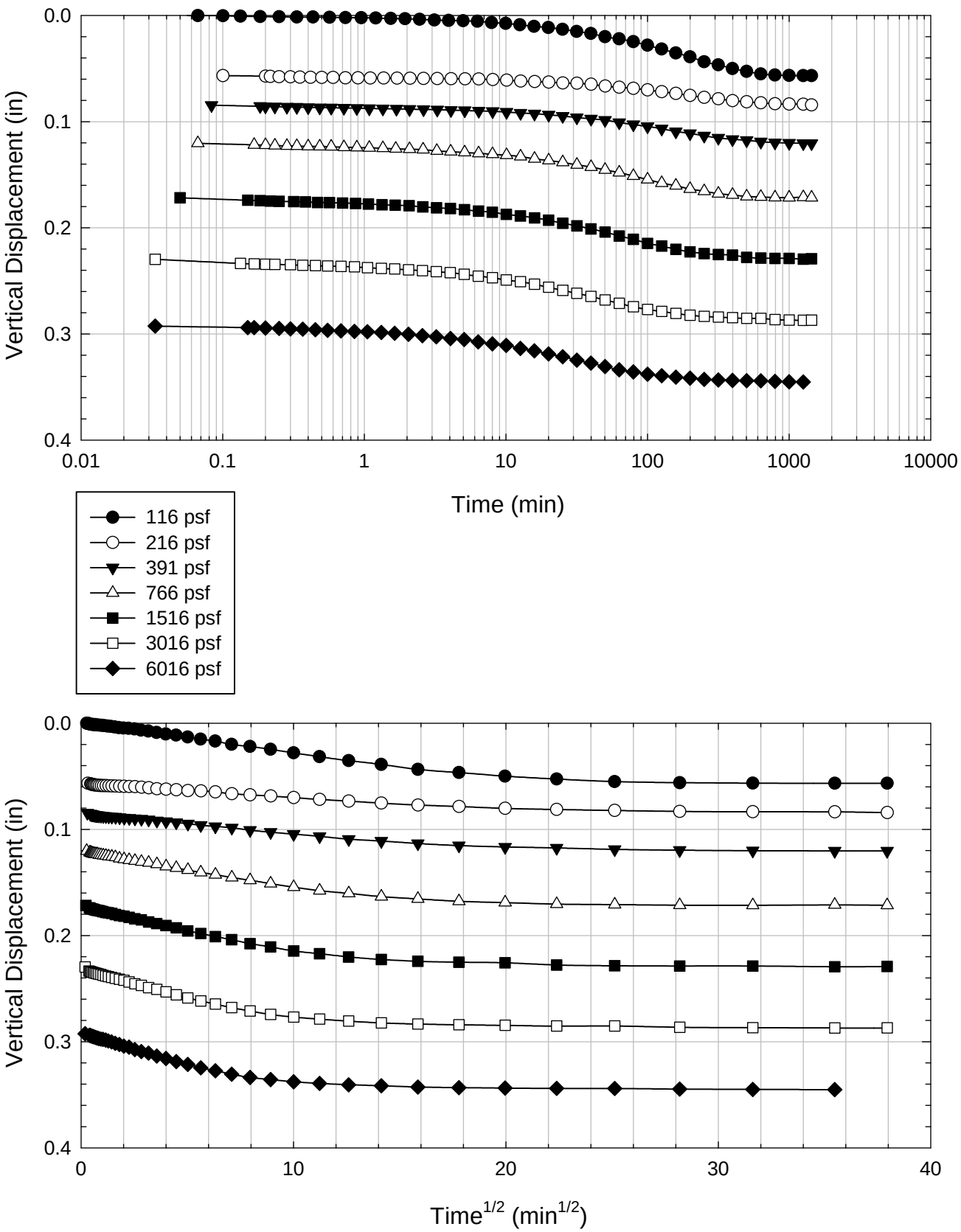
Oak Harbor - Non-blenderized - 6016 psf
Vertical Displacement (in)
0.0
0.1
0.2
0.3
0.4
0.01
0.1
1
10
100
1000
10000
Time (min)
116 psf
216 psf
391 psf
766 psf
1516 psf
3016 psf
6016 psf
Vertical Displacement (in)
0.0
0.1
0.2
0.3
0.4
0
10
20
30
40
Time^1/2 (min^1/2)

Oak Harbor - Non-blenderized

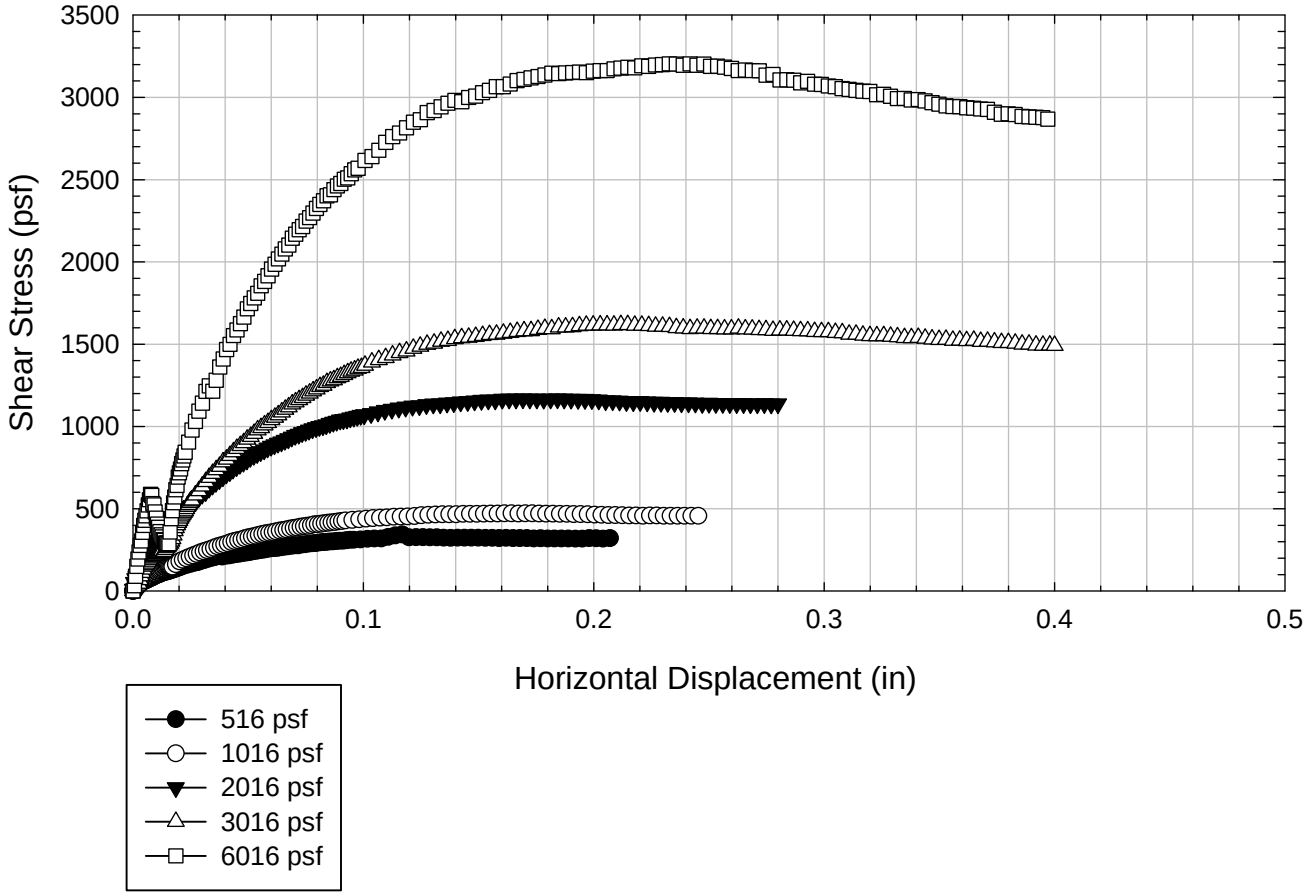

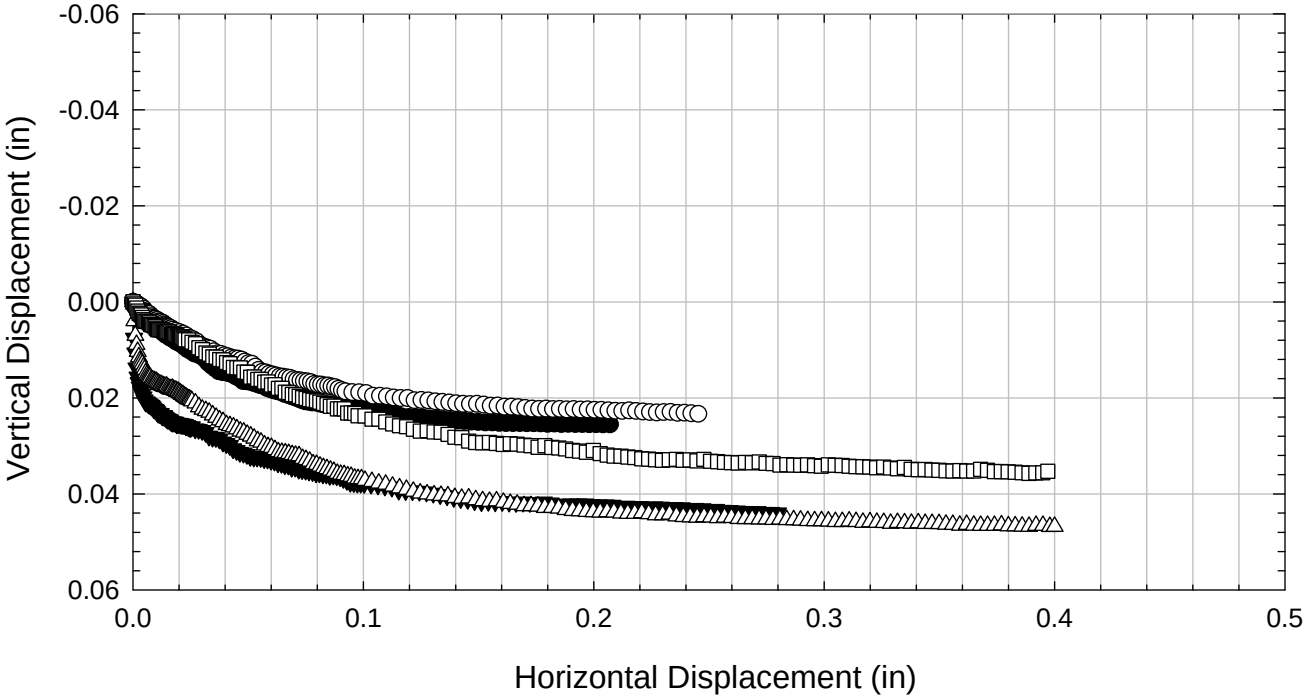

C.9. Texas 1

C.9.1 Blenderized

Virginia Polytechnic Institute and State University
Geotechnical Engineering Laboratory
Direct Shear Data Sheet

Project:	Fully Softened Shear Strength
Sample I.D./Loc.:	Texas 1 - Blenderized
Classification:	Fat Clay (CH)

Sample Preparation	Remolded at LL		Specific Gravity	2.78

Test Number	1	2	3	4	5	6	7	8
Start Date (m/d/y)	6/24/2011	6/24/2011	6/24/2011	6/24/2011				
End Date (m/d/y)	7/6/2011	7/16/2011	7/6/2011	7/6/2011				
Consolidation Pressure (psf)	516	1016	2016	3016				
Initial Values								
Initial Height (in)	1.41	1.41	1.42	1.38				
Initial Diameter (in)	2.50	2.50	2.50	2.50				
Initial Sample Weight (g)	178	181	180	176				
Water Content (%)	76.66	75.20	75.92	76.98				
Dry Unit Weight (pcf)	55.4	57.1	56.0	55.8				
Wet Unit Weight (pcf)	97.9	100.0	98.5	98.8				
Consolidation Pressures								
Load 1 (psf)	116	116	116	116				
Load 2 (psf)	266	266	266	216				
Load 3 (psf)	516	516	516	391				
Load 4 (psf)		1016	1016	766				
Load 5 (psf)			2016	1516				
Load 6 (psf)				3016				
Load 7 (psf)								
t_{50}								
Max. t_{50} for Load 1 (min)								
Max. t_{50} for Load 2 (min)								
Max. t_{50} for Load 3 (min)	98.73							
Max. t_{50} for Load 4 (min)		88.79						
Max. t_{50} for Load 5 (min)			91.66					
Max. t_{50} for Load 6 (min)				94.32				
Max. t_{50} for Load 7 (min)								
Final Values								
Water Content (%)	60.50	55.28	49.72	46.62				
Dry Unit Weight (pcf)	65.8	71.7	78.2	79.8				
Wet Unit Weight (pcf)	105.5	111.3	117.0	117.1				
Failure								
Test Performed at Shear Rate (in/min)	2.03E-05	1.00E-05	2.18E-05	2.13E-05				
Required Shear Rate (in/min)	2.84E-05	3.38E-05	1.96E-05	2.54E-05				
Displacement at Failure (in)	0.14	0.15	0.09	0.12				
Peak Shear Stress (psf)	301	570	798	1177				
Total Change in Height at Failure (in)	0.22	0.28	0.39	0.41				
Secant Effective Friction Angle (deg)	30.3	29.3	21.6	21.3				

Comments: In the test consolidated to 1016 psf, the porous stone got wedged in the last consolidation load.
In the test consolidated to 2016 psf, the porous stone was wedged until the 1000 psf consolidation load. At 1000 psf, it was freed and the sample allowed to reach end of primary consolidation.

Texas 1 - Blenderized - 516 psf

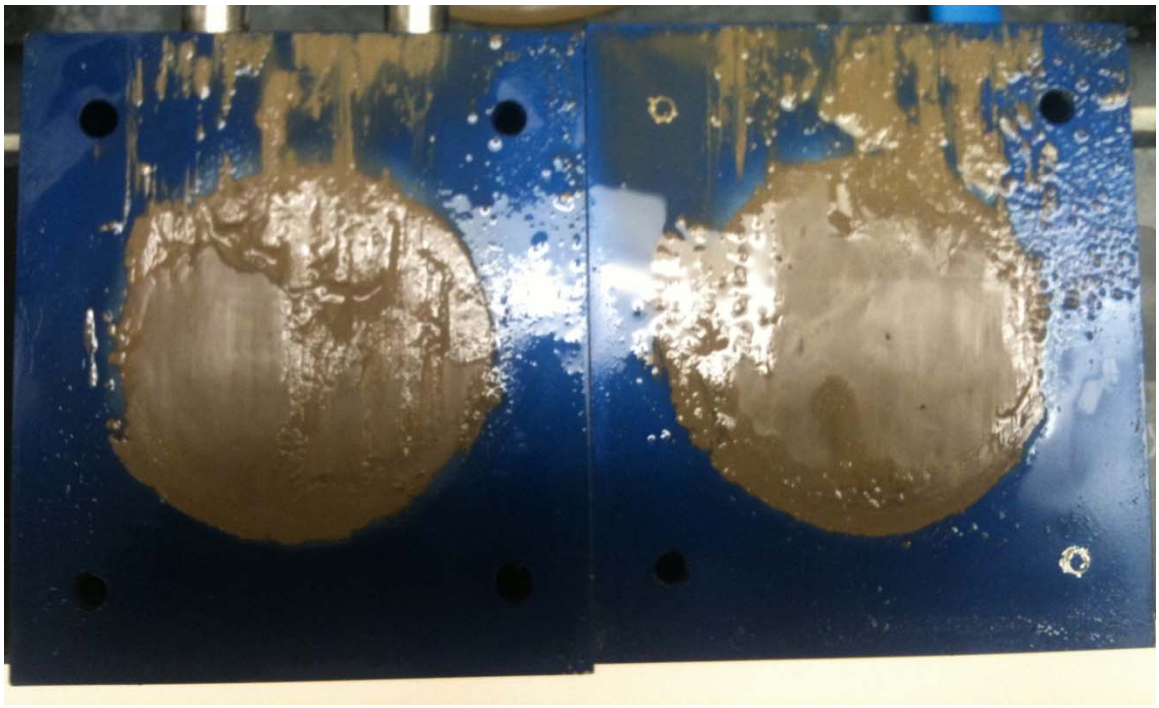

Texas 1 - Blenderized - 1016 psf

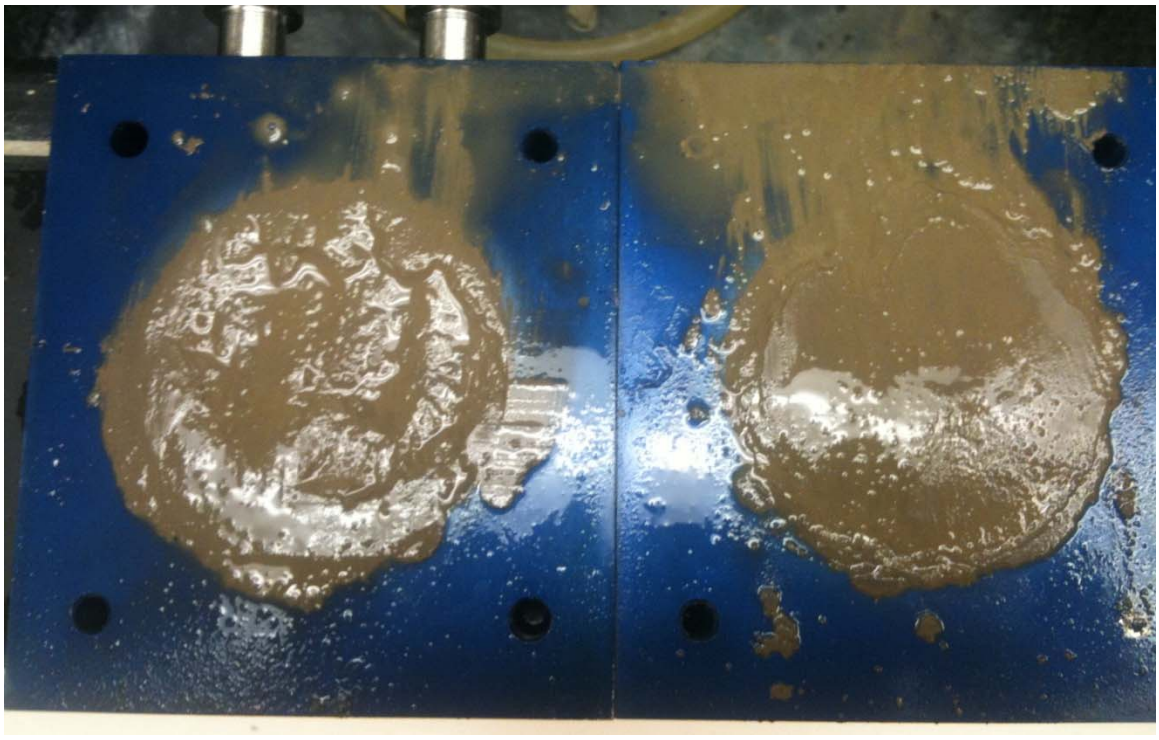

Texas 1 - Blenderized - 2016 psf

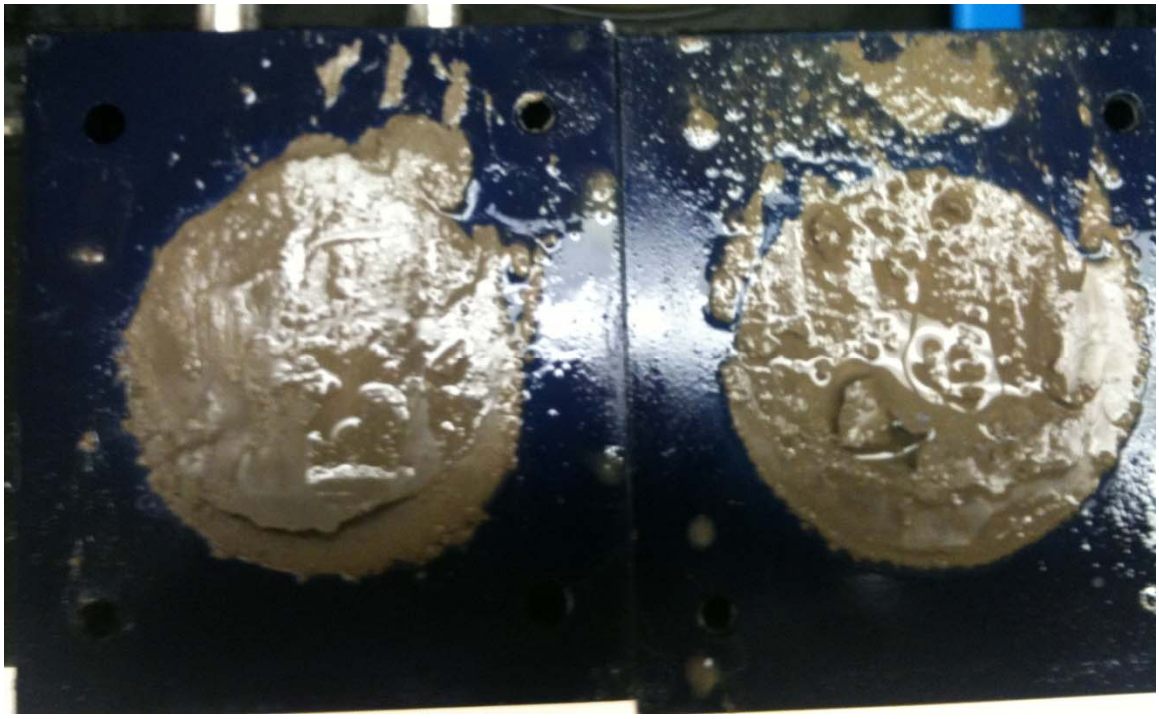

Texas 1 - Blenderized - 3016 psf

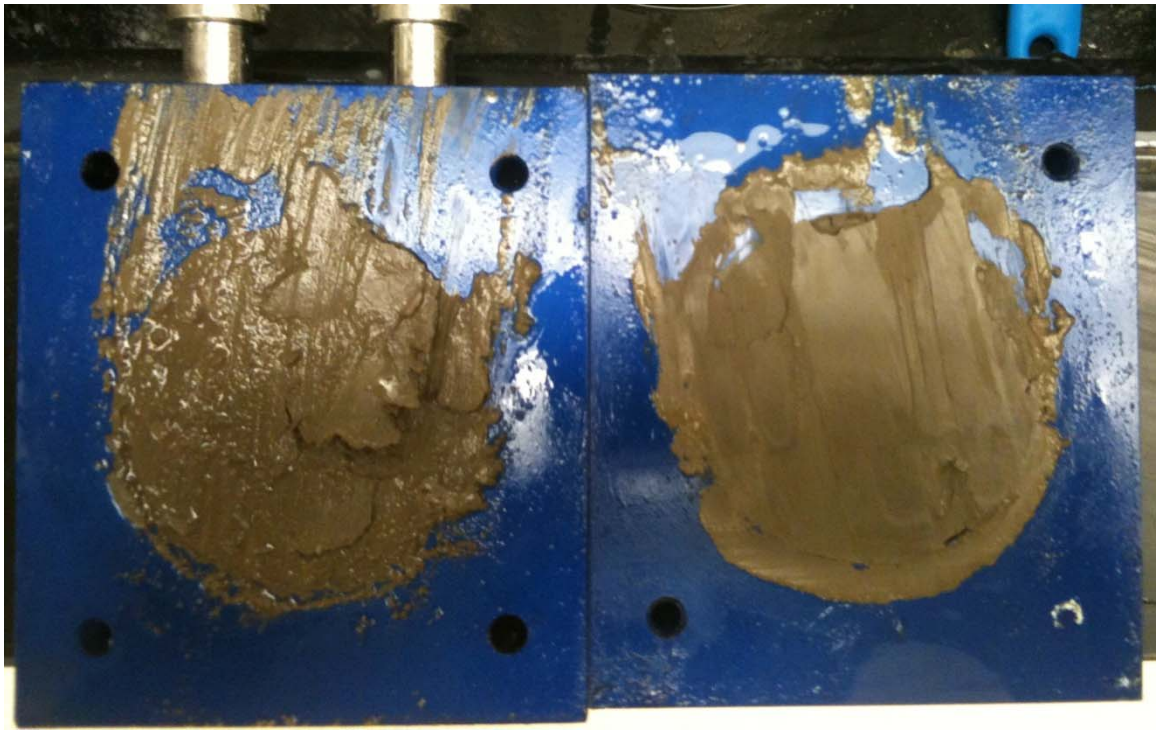

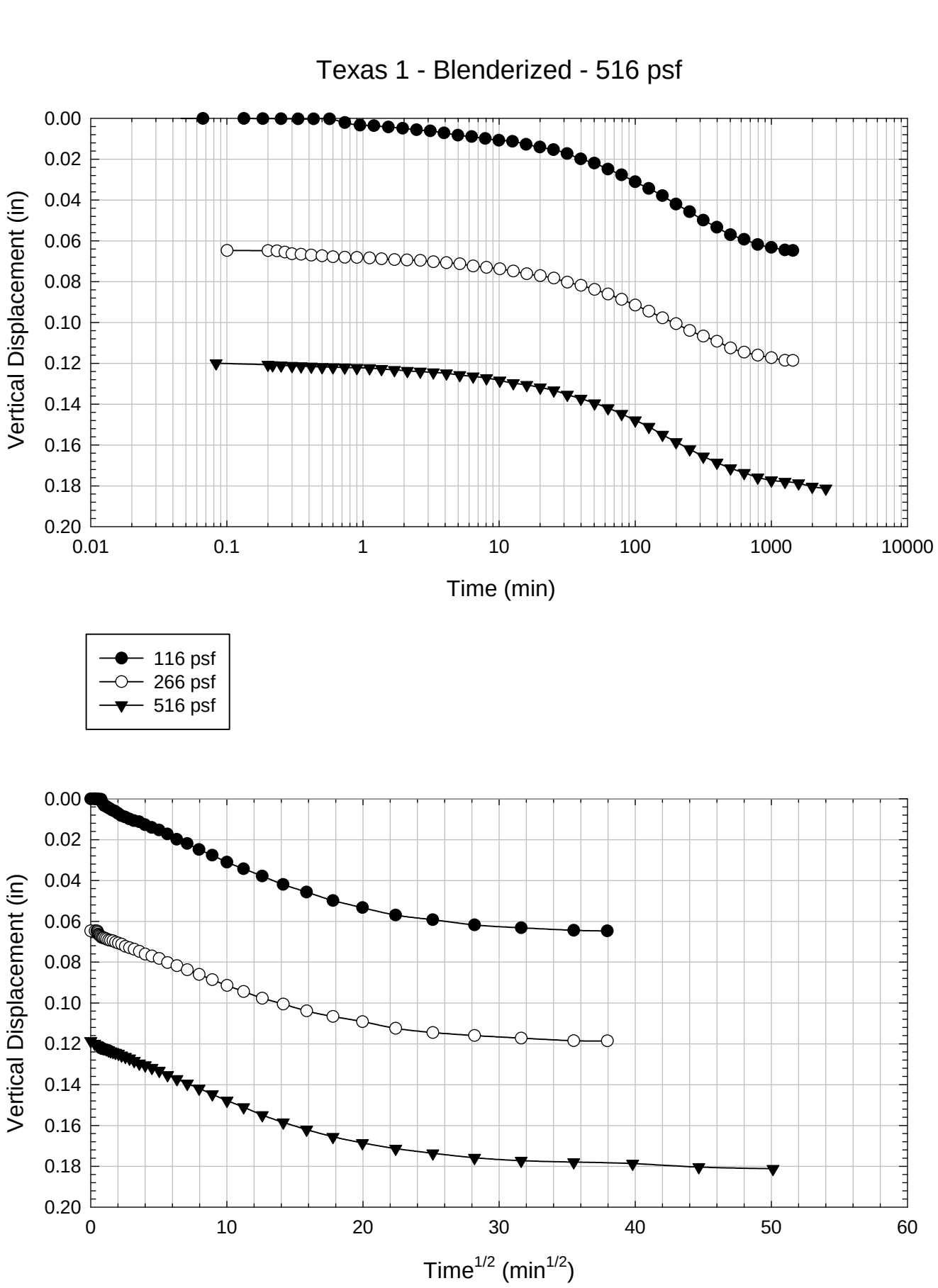
Texas 1 - Blenderized - 516 psf
Vertical Displacement (in)
0.00
0.02
0.04
0.06
0.08
0.10
0.12
0.14
0.16
0.18
0.20
0.01
0.1
1
10
100
1000
10000
Time (min)
116 psf
266 psf
516 psf
Vertical Displacement (in)
0.00
0.02
0.04
0.06
0.08
0.10
0.12
0.14
0.16
0.18
0.20
0
10
20
30
40
50
60
Time1/2 (min1/2)

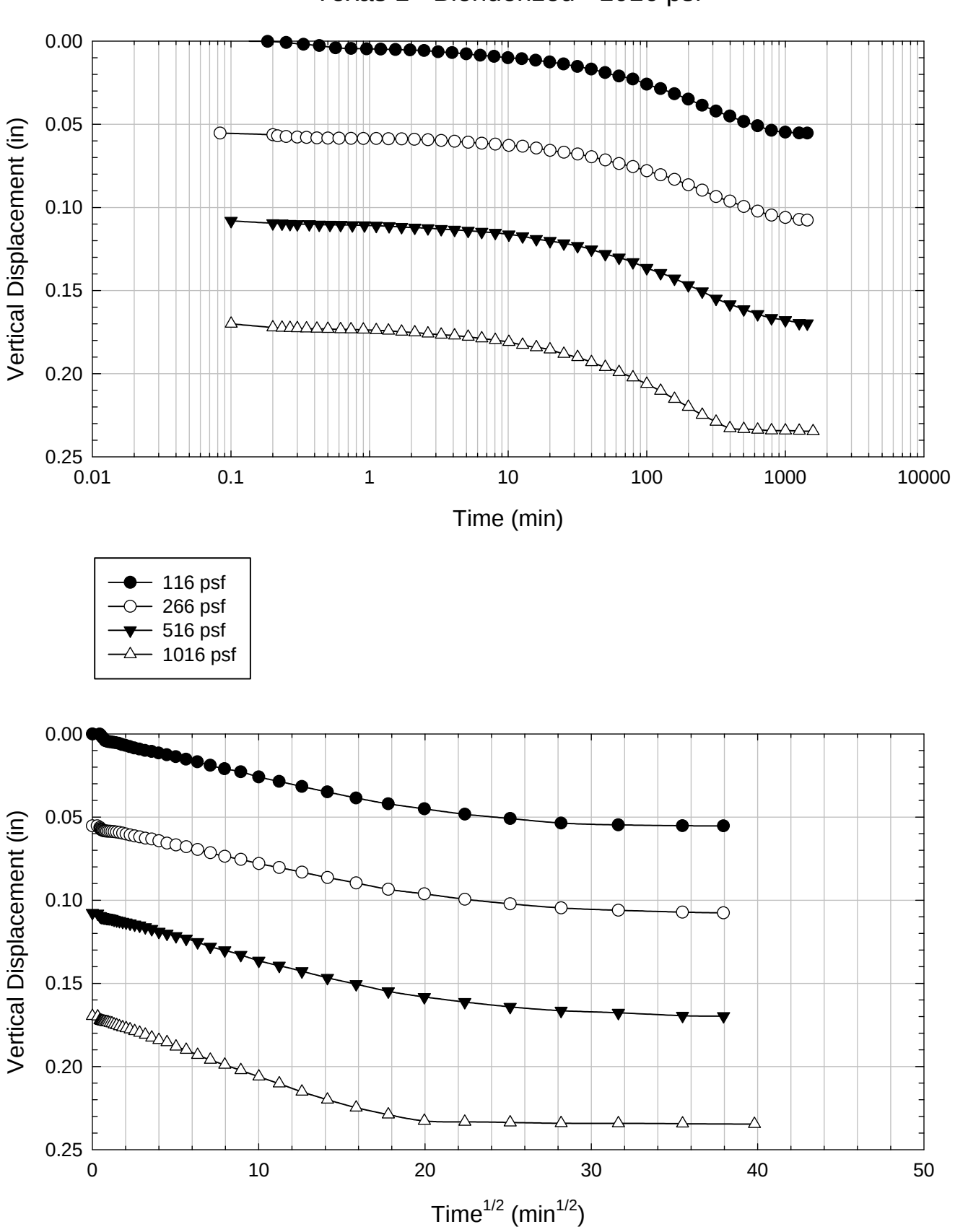
Texas 1 - Blenderized - 1016 psf
Vertical Displacement (in)
0.00
0.05
0.10
0.15
0.20
0.25
0.01
0.1
1
10
100
1000
10000
Time (min)
116 psf
266 psf
516 psf
1016 psf
Vertical Displacement (in)
0.00
0.05
0.10
0.15
0.20
0.25
0
10
20
30
40
50
Time1/2 (min1/2)

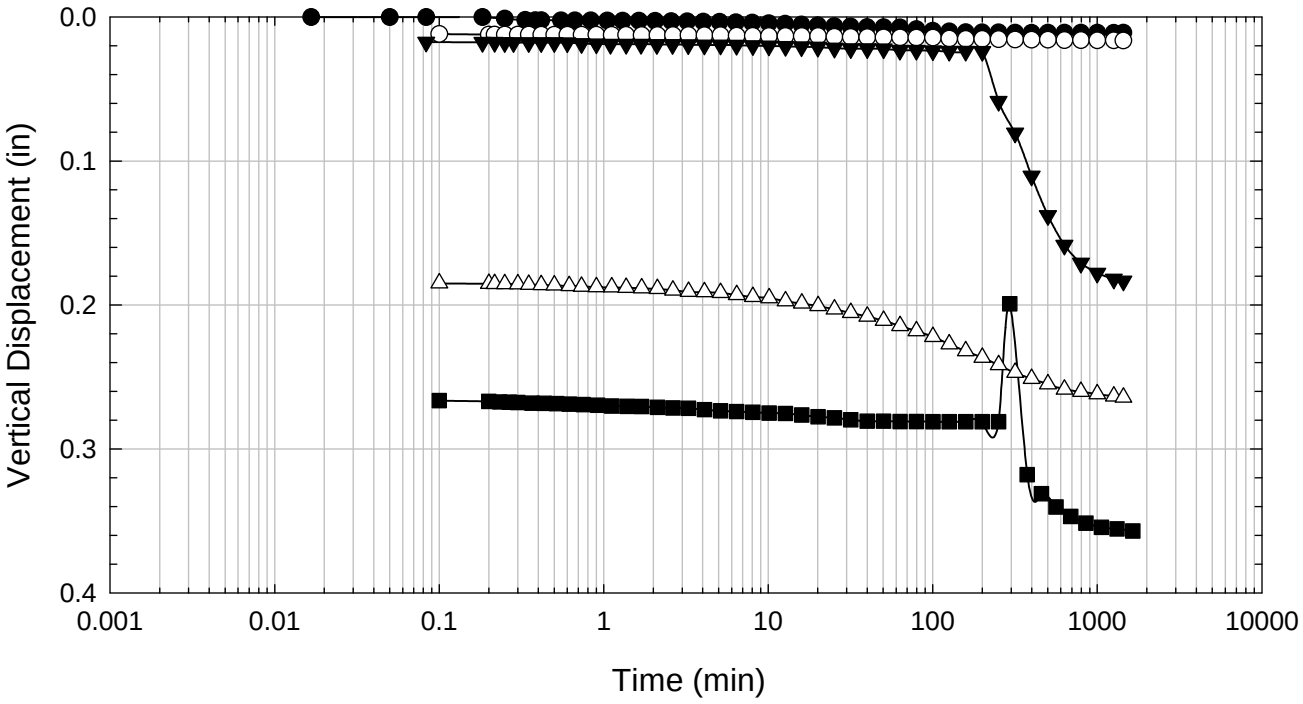
Texas 1 - Blenderized - 2016 psf
Vertical Displacement (in)
0.0
0.1
0.2
0.3
0.4
0.001
0.01
0.1
1
10
100
1000
10000
Time (min)

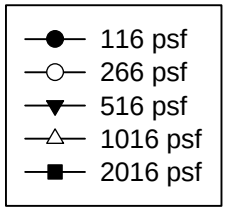
116 psf
266 psf
516 psf
1016 psf
2016 psf

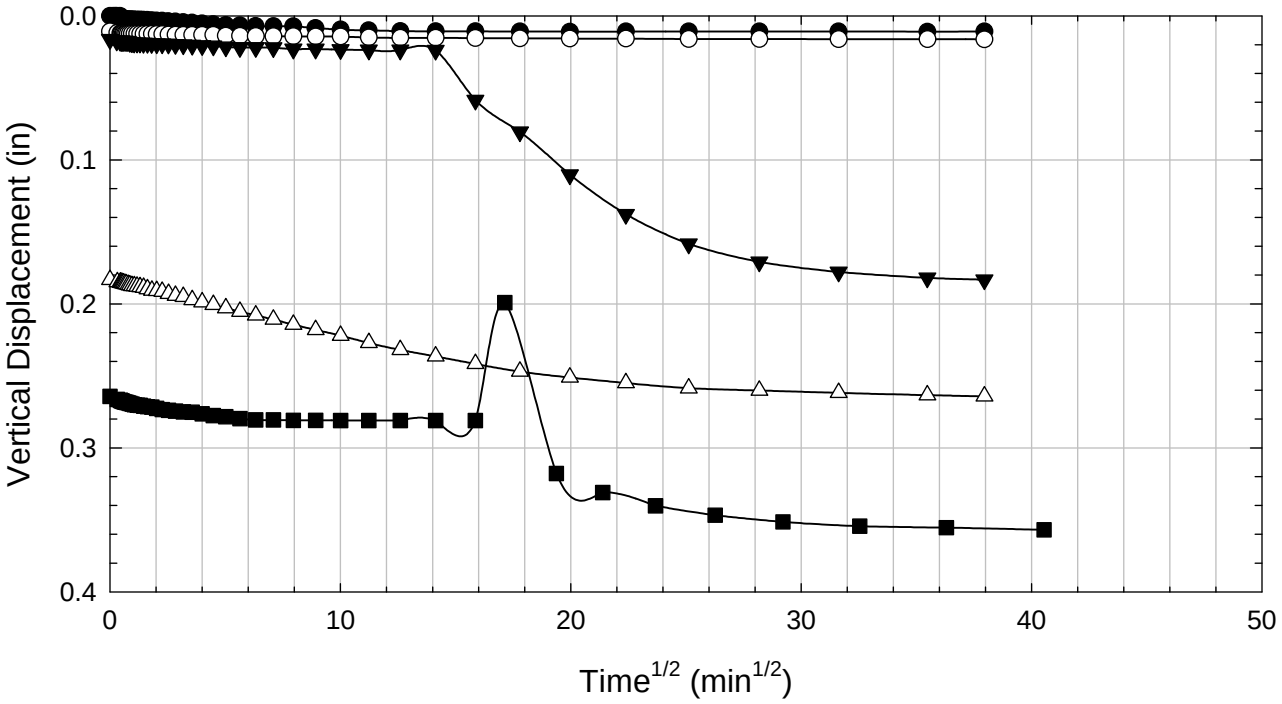
Vertical Displacement (in)
0.0
0.1
0.2
0.3
0.4
0
10
20
30
40
50
Time^1/2 (min^1/2)

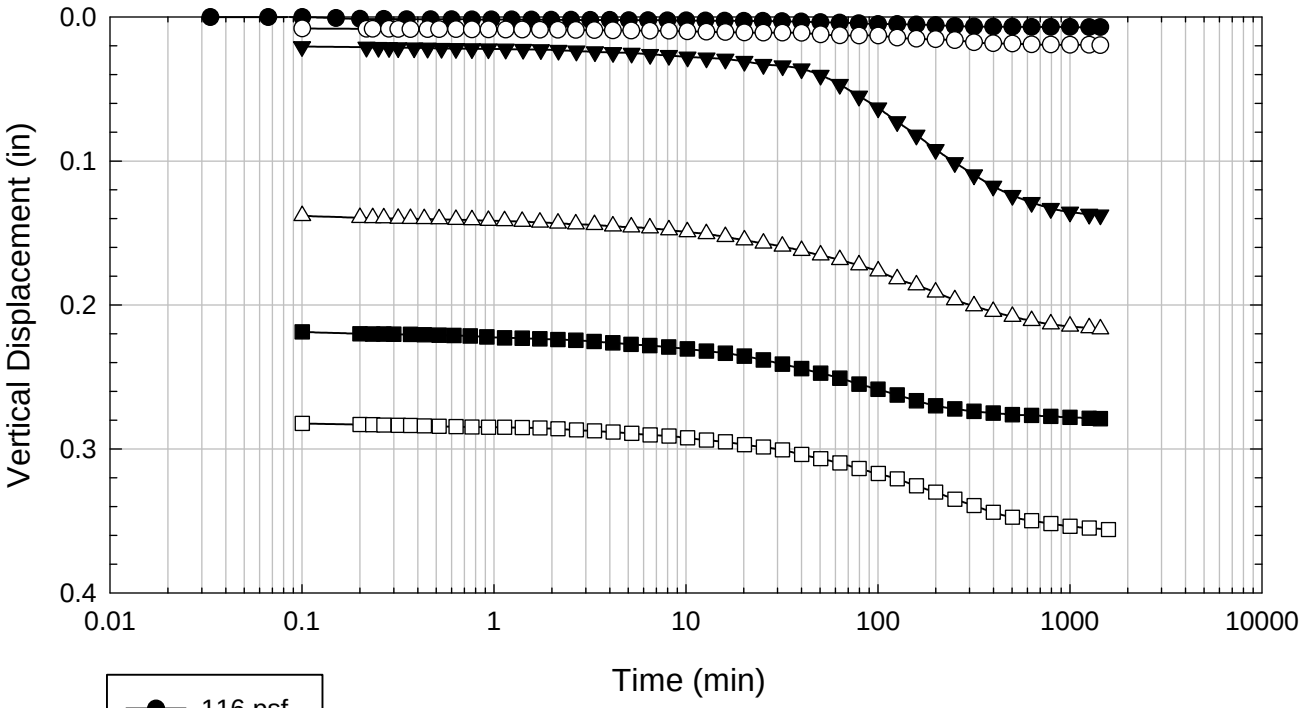
Texas 1 - Blenderized - 3016 psf
Vertical Displacement (in)
0.0
0.1
0.2
0.3
0.4
0.01
0.1
1
10
100
1000
10000
Time (min)

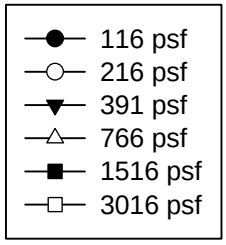
116 psf
216 psf
391 psf
766 psf
1516 psf
3016 psf

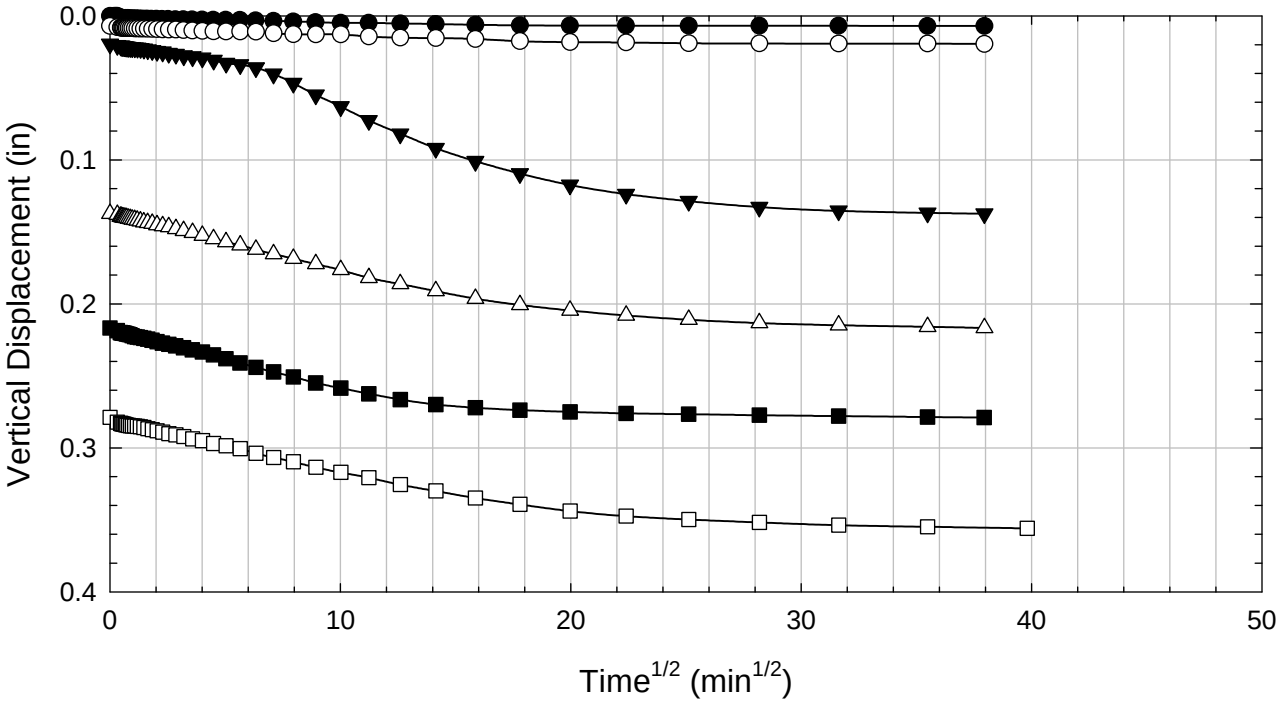
Vertical Displacement (in)
0.0
0.1
0.2
0.3
0.4
0
10
20
30
40
50
Time1/2 (min1/2)

Texas 1 - Blenderized

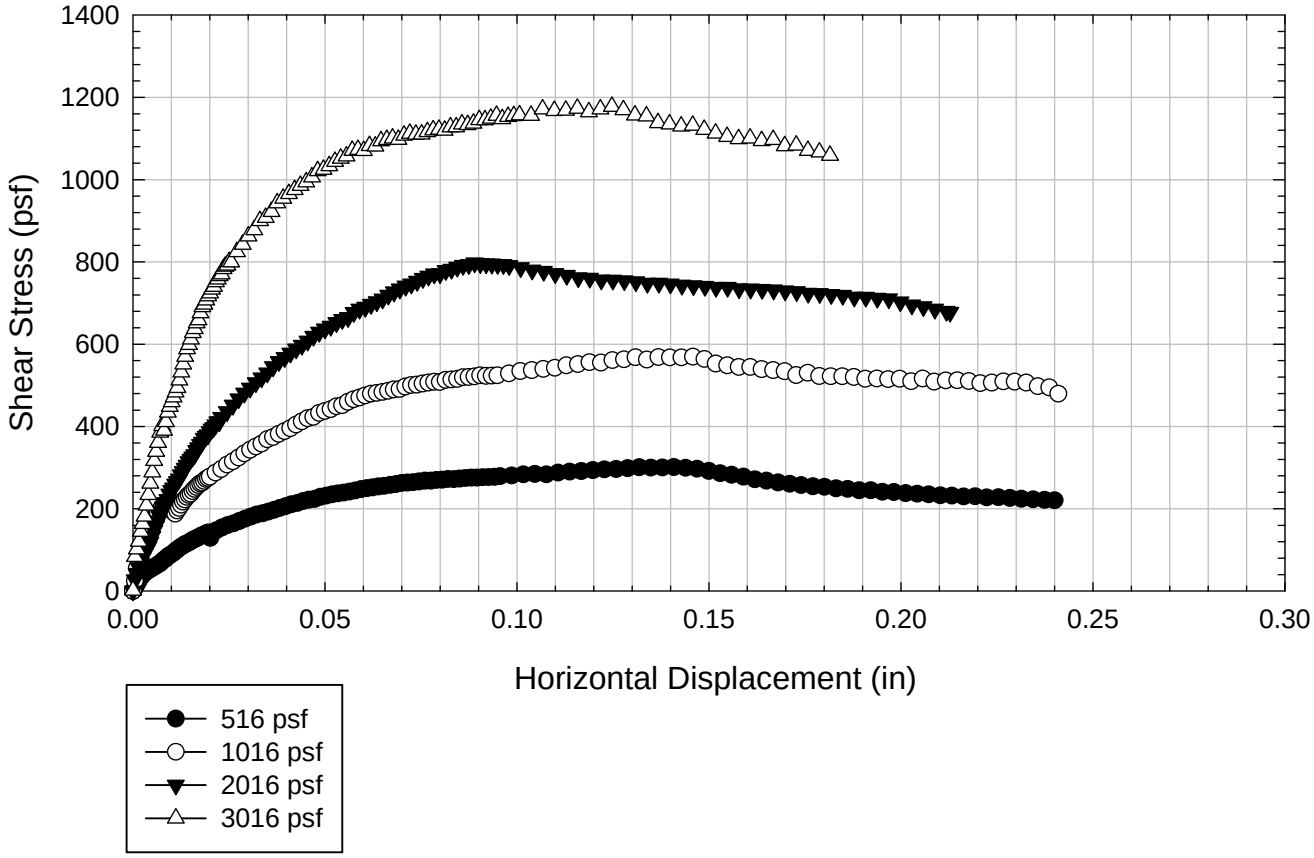

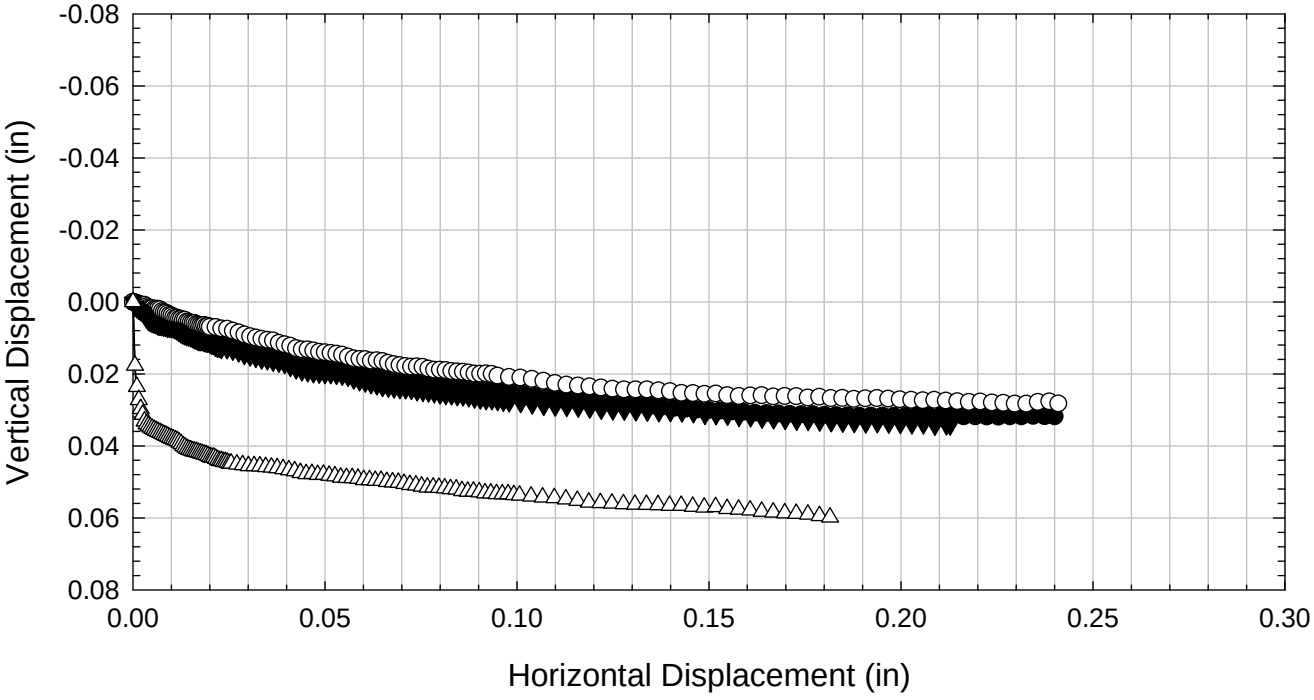

C.10. Texas 2

C.10.1 Blenderized

Virginia Polytechnic Institute and State University
Geotechnical Engineering Laboratory
Direct Shear Data Sheet

Project:	Fully Softened Shear Strength
Sample I.D./Loc.:	Texas 2 - Blenderized
Classification:	Fat Clay (CH)

Sample Preparation	Remolded at LL		Specific Gravity	2.78

Test Number	1	2	3	4	5	6	7	8
Start Date (m/d/y)	7/9/2011	7/9/2011						
End Date (m/d/y)	7/21/2011	7/21/2011						
Consolidation Pressure (psf)	516	2016						
Initial Values								
Initial Height (in)	1.43	1.40						
Initial Diameter (in)	2.50	2.50						
Initial Sample Weight (g)	183	180						
Water Content (%)	69.60	69.06						
Dry Unit Weight (pcf)	58.6	59.0						
Wet Unit Weight (pcf)	99.4	99.7						
Consolidation Pressures								
Load 1 (psf)	116	116						
Load 2 (psf)	266	266						
Load 3 (psf)	516	516						
Load 4 (psf)		1016						
Load 5 (psf)		2016						
Load 6 (psf)								
Load 7 (psf)								
t_{50}								
Max. t_{50} for Load 1 (min)								
Max. t_{50} for Load 2 (min)								
Max. t_{50} for Load 3 (min)	121.34							
Max. t_{50} for Load 4 (min)								
Max. t_{50} for Load 5 (min)		100.70						
Max. t_{50} for Load 6 (min)								
Max. t_{50} for Load 7 (min)								
Final Values								
Water Content (%)	56.75	46.38						
Dry Unit Weight (pcf)	66.7	78.5						
Wet Unit Weight (pcf)	104.6	115.0						
Failure								
Test Performed at Shear Rate (in/min)	1.65E-05	2.00E-05						
Required Shear Rate (in/min)	2.14E-05	2.58E-05						
Displacement at Failure (in)	0.13	0.13						
Peak Shear Stress (psf)	296	835						
Total Change in Height at Failure (in)	0.17	0.35						
Secant Effective Friction Angle (deg)	29.8	22.5						

Comments:

Texas 2 - Blenderized - 516 psf

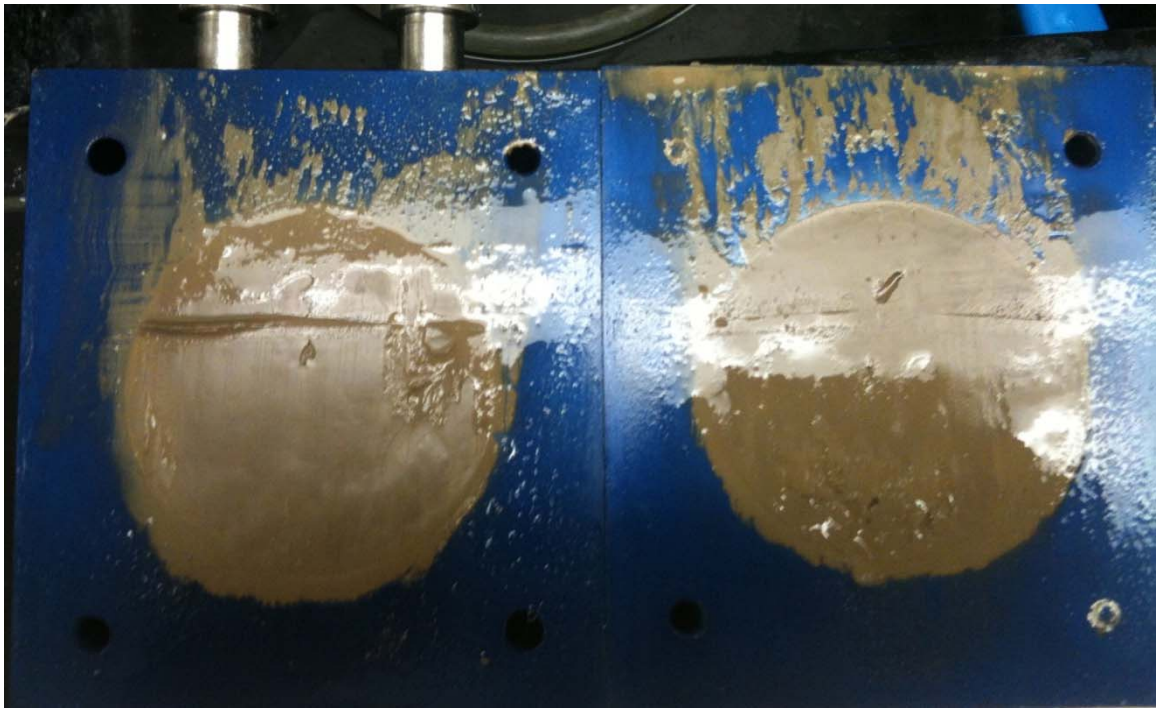

Texas 2 - Blenderized - 2016 psf

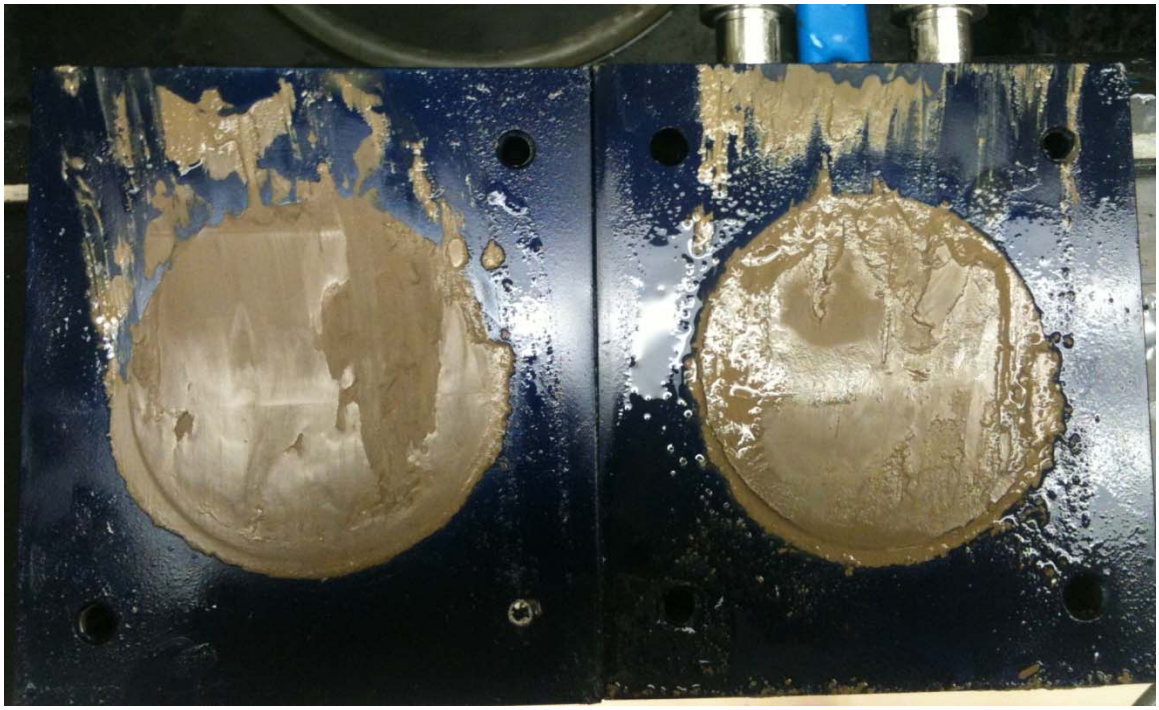

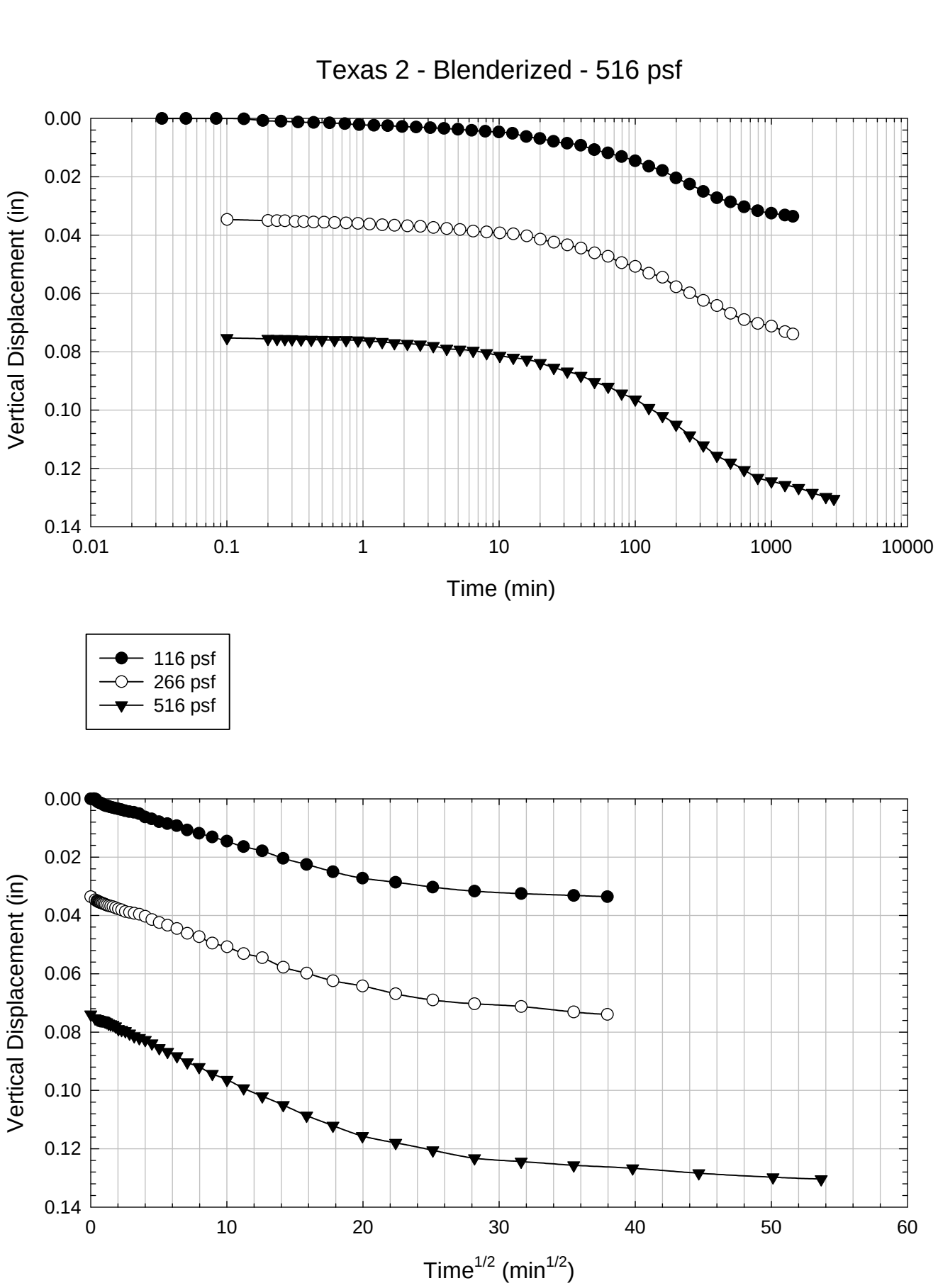
Texas 2 - Blenderized - 516 psf
Vertical Displacement (in)
0.00
0.02
0.04
0.06
0.08
0.10
0.12
0.14
0.01
0.1
1
10
100
1000
10000
Time (min)
116 psf
266 psf
516 psf
Vertical Displacement (in)
0.00
0.02
0.04
0.06
0.08
0.10
0.12
0.14
0
10
20
30
40
50
60
Time1/2 (min1/2)

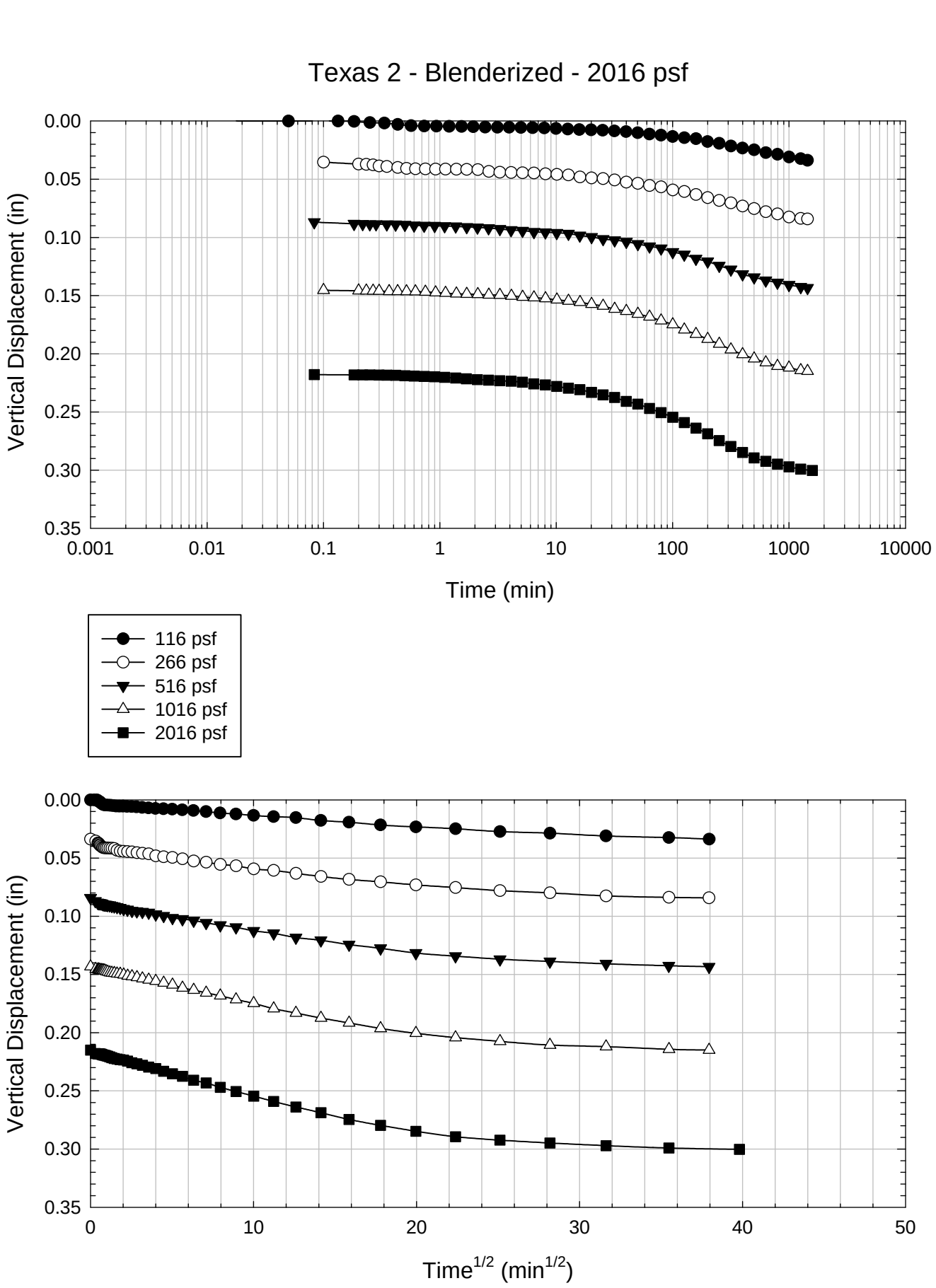
Texas 2 - Blenderized - 2016 psf
Vertical Displacement (in)
0.00
0.05
0.10
0.15
0.20
0.25
0.30
0.35
0.001
0.01
0.1
1
10
100
1000
10000
Time (min)
116 psf
266 psf
516 psf
1016 psf
2016 psf
Vertical Displacement (in)
0.00
0.05
0.10
0.15
0.20
0.25
0.30
0.35
0
10
20
30
40
50
Time1/2 (min1/2)

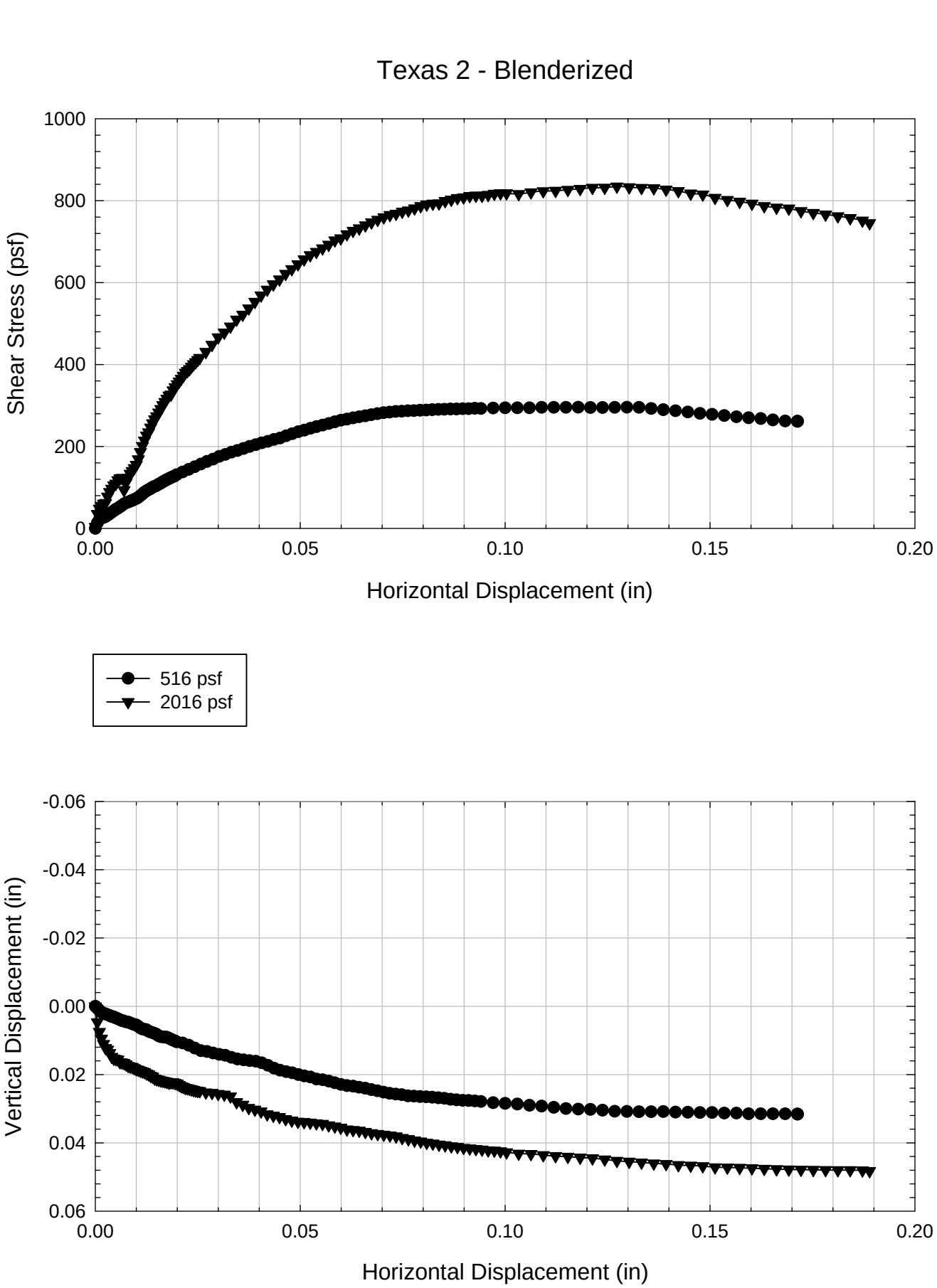
Texas 2 - Blenderized
Shear Stress (psf)
1000
800
600
400
200
0
0.00
0.05
0.10
0.15
0.20
Horizontal Displacement (in)
516 psf
2016 psf
Vertical Displacement (in)
-0.06
-0.04
-0.02
0.00
0.02
0.04
0.06
0.00
0.05
0.10
0.15
0.20
Horizontal Displacement (in)

C.11. Texas 3

C.11.1 Blenderized

Virginia Polytechnic Institute and State University
Geotechnical Engineering Laboratory
Direct Shear Data Sheet

Project:	Fully Softened Shear Strength
Sample I.D./Loc.:	Texas 3 - Blenderized
Classification:	Fat Clay (CH)

Sample Preparation	Remolded at LL		Specific Gravity	2.82

Test Number	1	2	3	4	5	6	7	8
Start Date (m/d/y)	3/11/2011	3/8/2011	3/4/2011					
End Date (m/d/y)	3/21/2011	3/18/2011	3/17/2011					
Consolidation Pressure (psf)	516	1016	2016					
Initial Values								
Initial Height (in) (Assumed)	1.44	1.44	1.44					
Initial Diameter (in)	2.50	2.50	2.50					
Initial Sample Weight (g)	161	175	189					
Water Content (%)	70.19	69.53	69.82					
Dry Unit Weight (pcf)	51.0	55.6	60.0					
Wet Unit Weight (pcf)	86.8	94.3	101.9					
Consolidation Pressures								
Load 1 (psf)	116	116	116					
Load 2 (psf)	266	216	266					
Load 3 (psf)	516	566	516					
Load 4 (psf)		1016	1016					
Load 5 (psf)			2016					
Load 6 (psf)								
Load 7 (psf)								
t_{50}								
Max. t_{50} for Load 1 (min)	13.52		77.04					
Max. t_{50} for Load 2 (min)	0.34	1.49	174.03					
Max. t_{50} for Load 3 (min)	55.74	85.16	147.53					
Max. t_{50} for Load 4 (min)		135.24	140.82					
Max. t_{50} for Load 5 (min)			37.78					
Max. t_{50} for Load 6 (min)								
Max. t_{50} for Load 7 (min)								
Final Values								
Water Content (%)	55.70	49.94	45.52					
Dry Unit Weight (pcf)	61.7	72.2	80.0					
Wet Unit Weight (pcf)	96.1	108.2	116.4					
Failure								
Test Performed at Shear Rate (in/min)	3.81E-05	4.00E-05	3.80E-05					
Required Shear Rate (in/min)	5.02E-05	2.51E-05	1.01E-04					
Displacement at Failure (in)	0.14	0.17	0.19					
Peak Shear Stress (psf)	221	539	884					
Total Change in Height at Failure (in)	0.25	0.32	0.35					
Secant Effective Friction Angle (deg)	23.2	28.0	23.7					

Comments:

Texas 3 - Blenderized - 516 psf

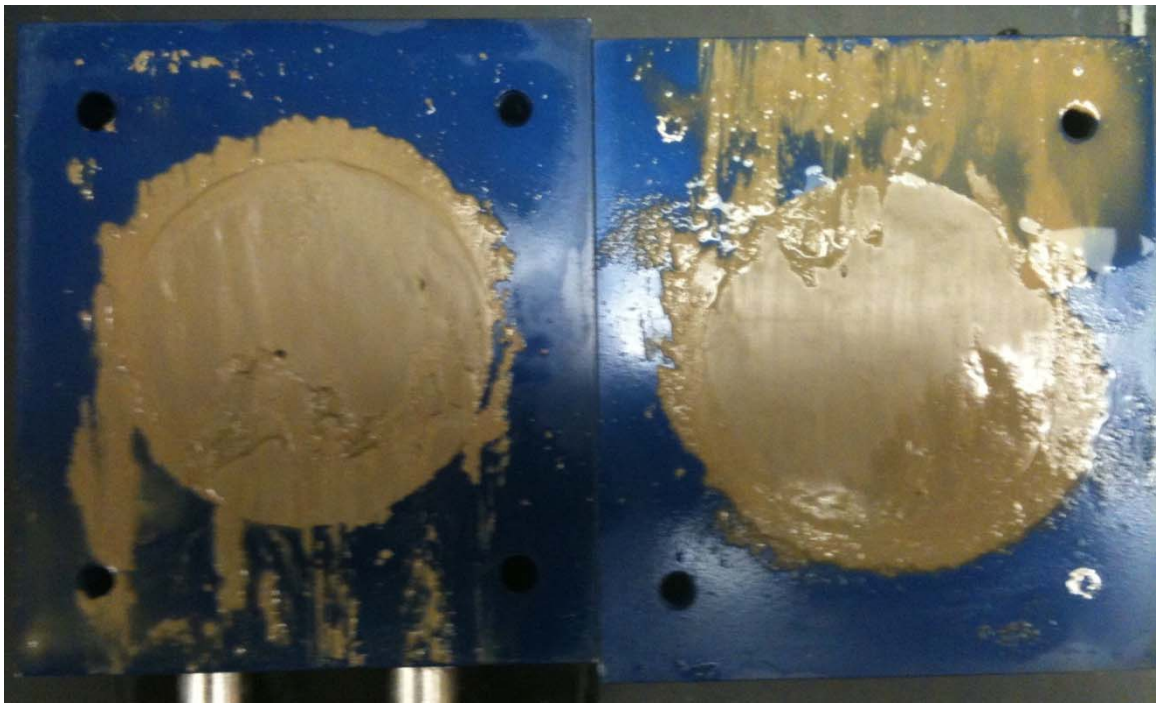

Texas 3 - Blenderized - 1016 psf

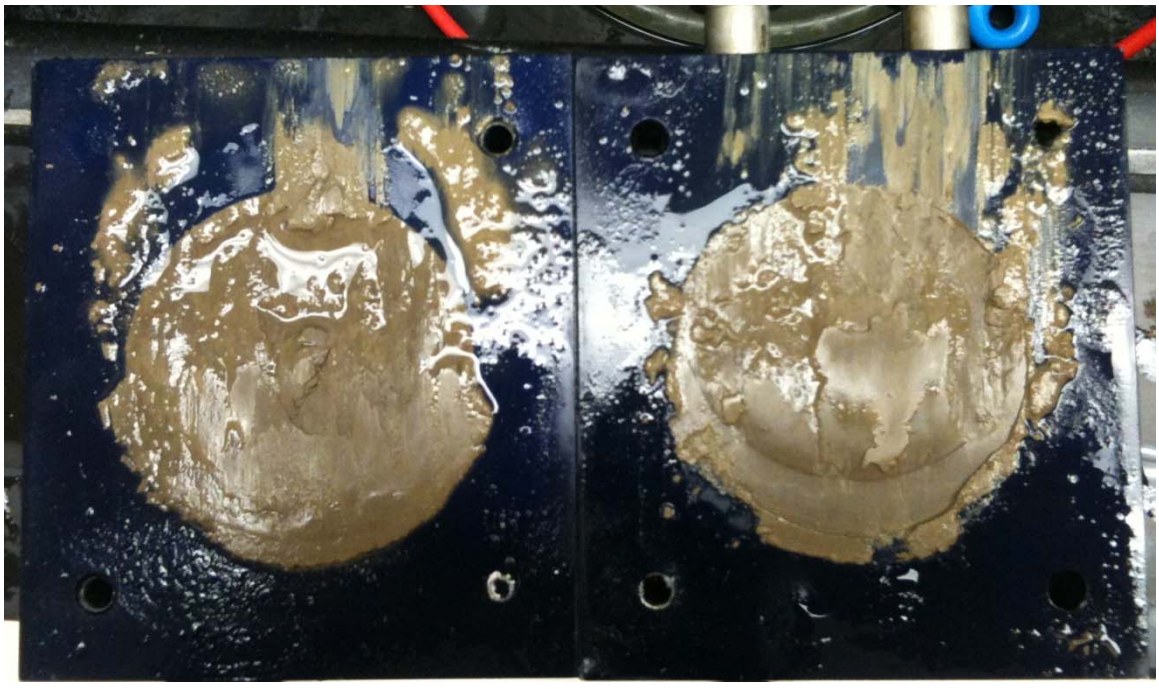

Texas 3 - Blenderized - 2016 psf

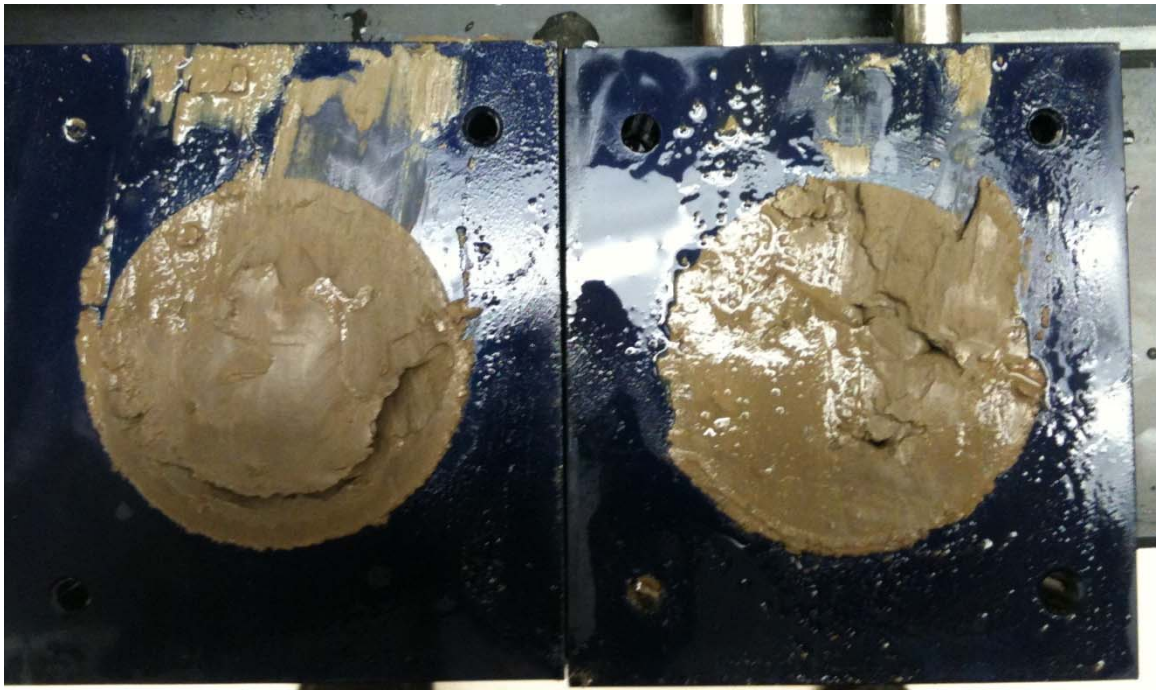

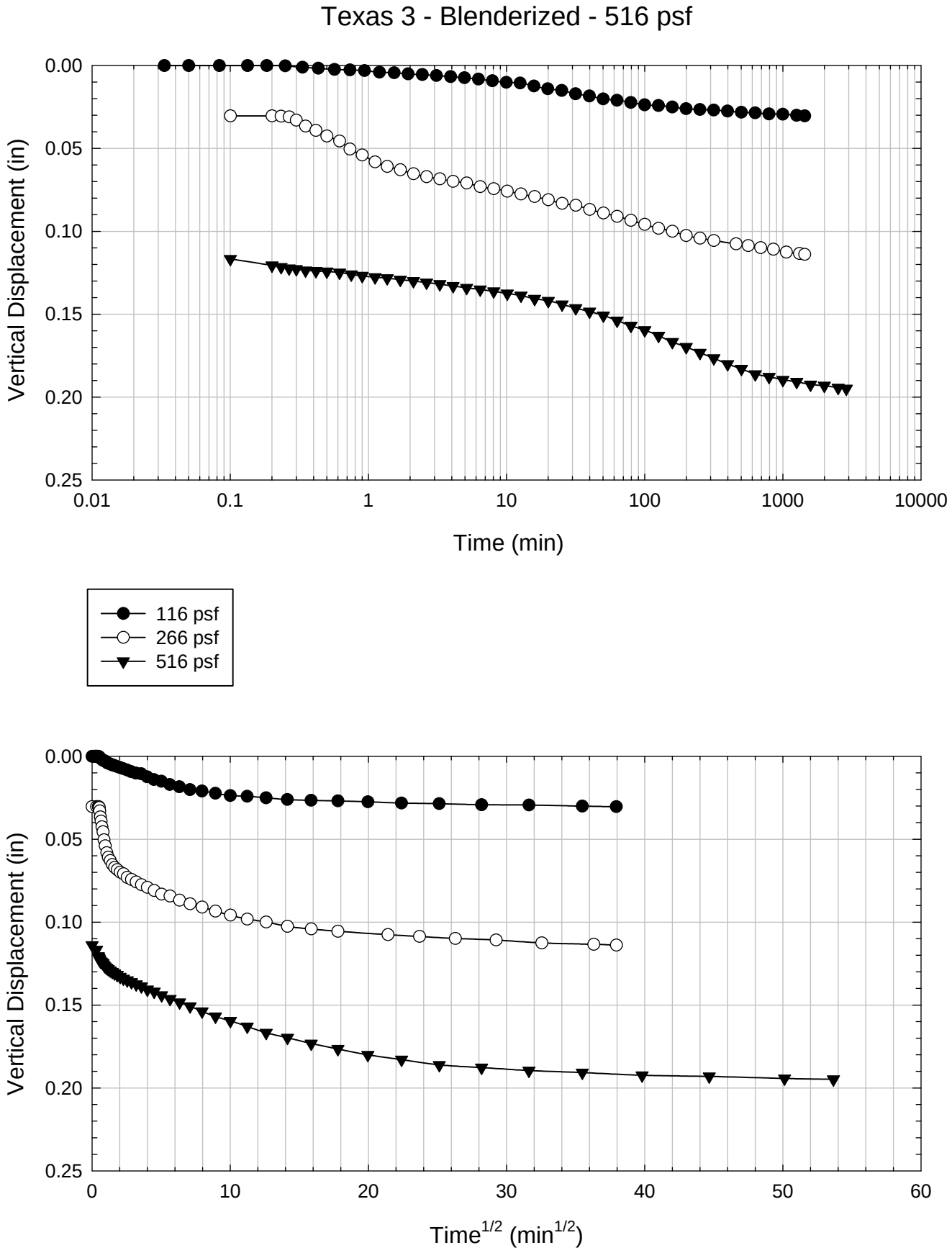
Texas 3 - Blenderized - 516 psf
Vertical Displacement (in)
0.00
0.05
0.10
0.15
0.20
0.25
0.01
0.1
1
10
100
1000
10000
Time (min)
116 psf
266 psf
516 psf
Vertical Displacement (in)
0.00
0.05
0.10
0.15
0.20
0.25
0
10
20
30
40
50
60
Time1/2 (min1/2)

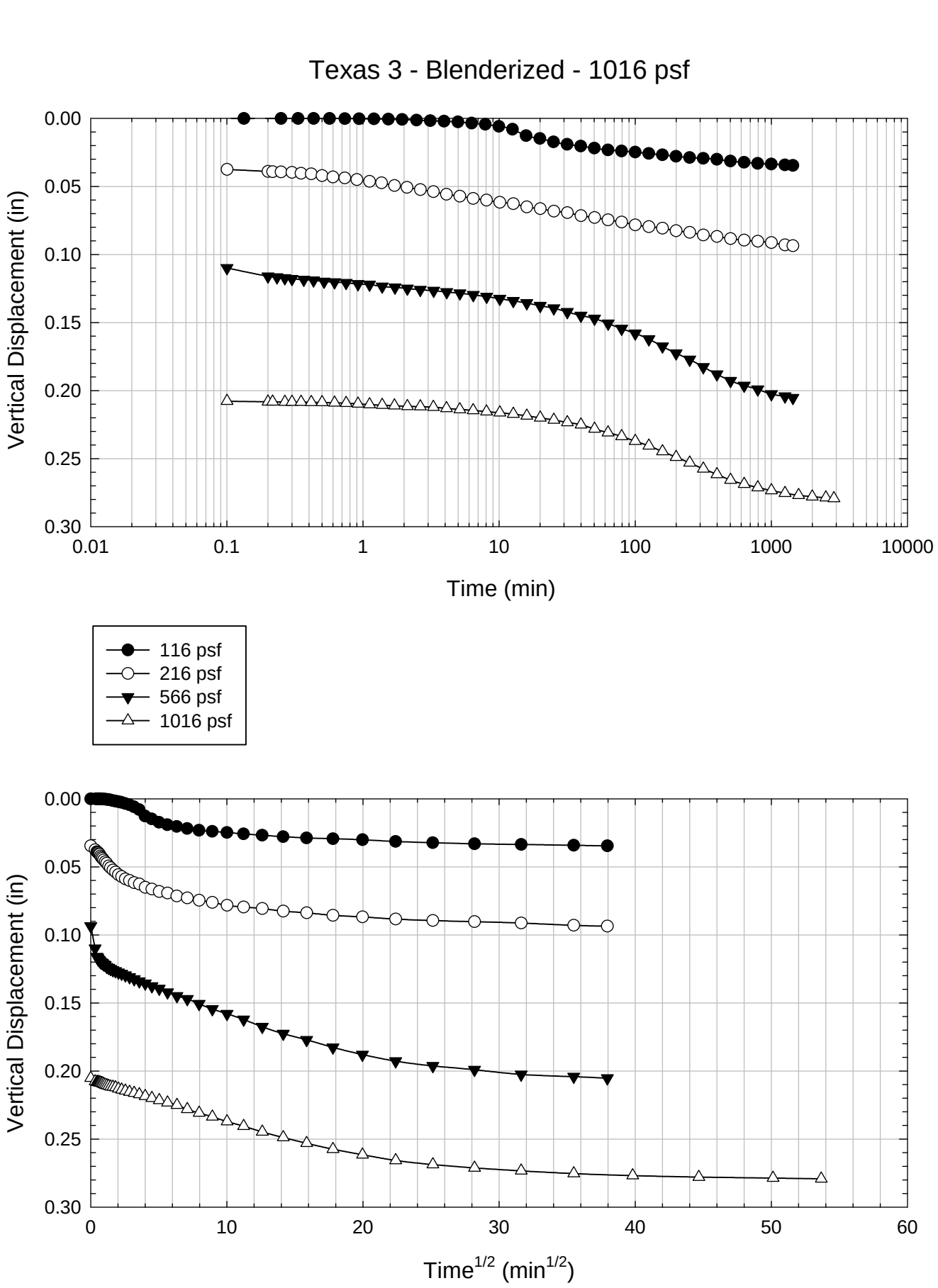
Texas 3 - Blenderized - 1016 psf
Vertical Displacement (in)
0.00
0.05
0.10
0.15
0.20
0.25
0.30
0.01
0.1
1
10
100
1000
10000
Time (min)
116 psf
216 psf
566 psf
1016 psf
Vertical Displacement (in)
0.00
0.05
0.10
0.15
0.20
0.25
0.30
0
10
20
30
40
50
60
Time1/2 (min1/2)

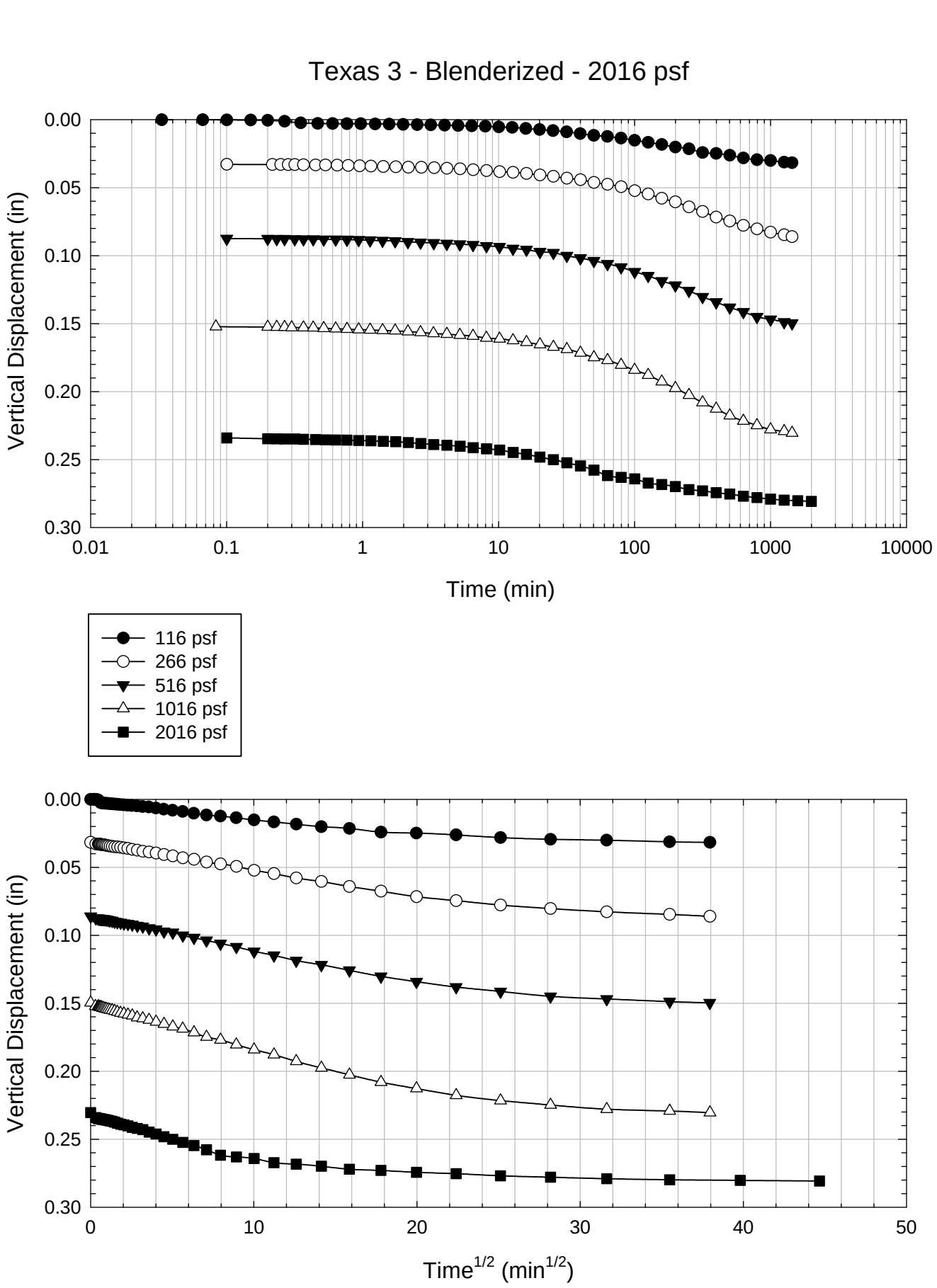
Texas 3 - Blenderized - 2016 psf
Vertical Displacement (in)
0.00
0.05
0.10
0.15
0.20
0.25
0.30
0.01
0.1
1
10
100
1000
10000
Time (min)
116 psf
266 psf
516 psf
1016 psf
2016 psf
Vertical Displacement (in)
0.00
0.05
0.10
0.15
0.20
0.25
0.30
0
10
20
30
40
50
Time1/2 (min1/2)

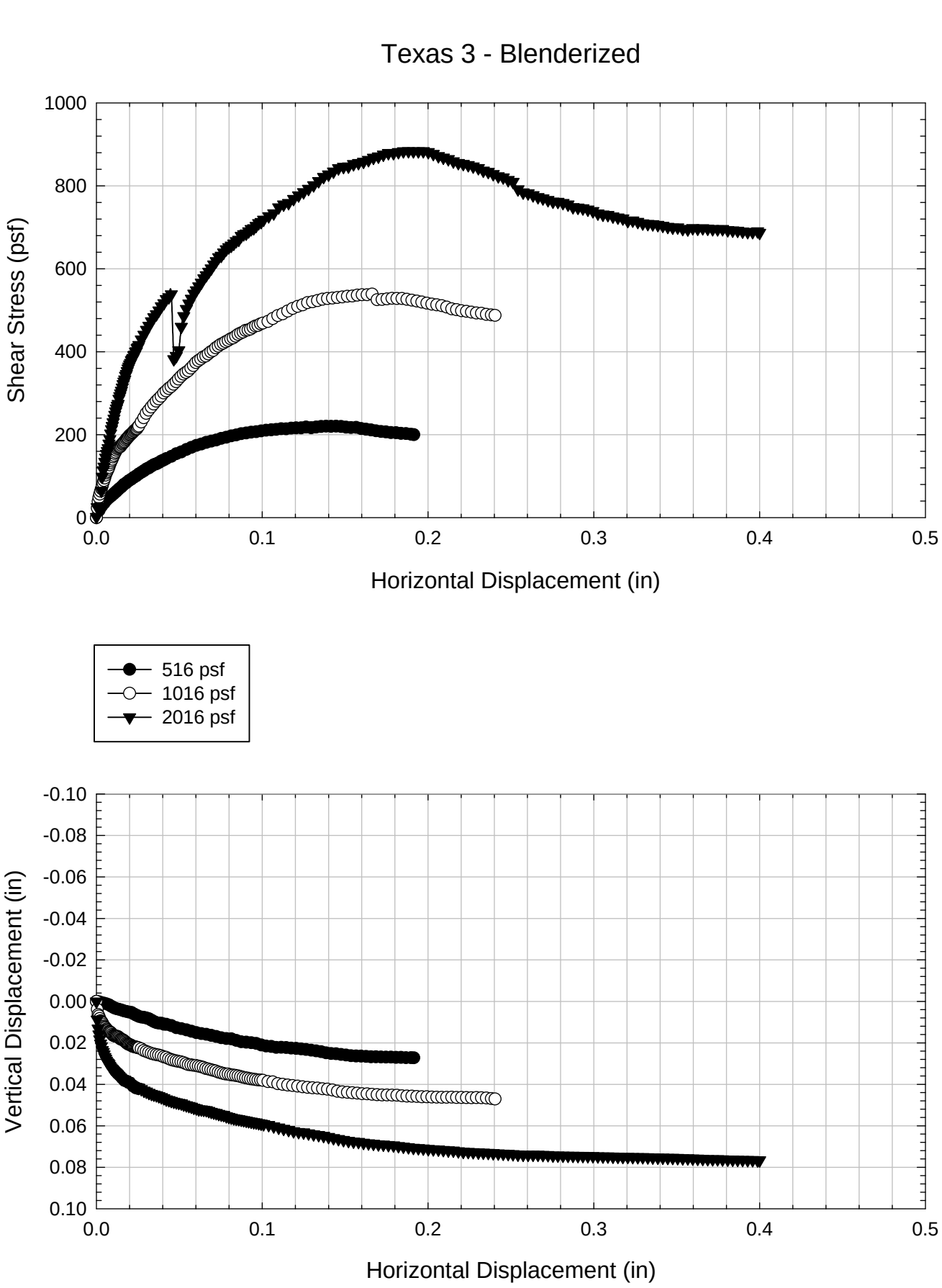
Texas 3 - Blenderized
Shear Stress (psf)
1000
800
600
400
200
0
0.0
0.1
0.2
0.3
0.4
0.5
Horizontal Displacement (in)
516 psf
1016 psf
2016 psf
Vertical Displacement (in)
-0.10
-0.08
-0.06
-0.04
-0.02
0.00
0.02
0.04
0.06
0.08
0.10
0.0
0.1
0.2
0.3
0.4
0.5
Horizontal Displacement (in)

C.12. Texas 4

C.12.1 Blenderized

Virginia Polytechnic Institute and State University
Geotechnical Engineering Laboratory
Direct Shear Data Sheet

Project:	Fully Softened Shear Strength
Sample I.D./Loc.:	Texas 4 - Blenderized
Classification:	Fat Clay (CH)

Sample Preparation	Remolded at LL		Specific Gravity	2.81

Test Number	1	2	3	4	5	6	7	8
Start Date (m/d/y)	3/18/2011	3/8/2011	3/4/2011	3/18/2011				
End Date (m/d/y)	3/28/2011	3/18/2011	3/18/2011	3/31/2011				
Consolidation Pressure (psf)	516	1016	2016	3016				
Initial Values								
Initial Height (in) (Assumed)	1.44	1.44	1.44	1.44				
Initial Diameter (in)	2.50	2.50	2.50	2.50				
Initial Sample Weight (g)	178	167	181	180				
Water Content (%)	70.91	73.28	74.61	66.96				
Dry Unit Weight (pcf)	56.1	51.9	55.9	58.1				
Wet Unit Weight (pcf)	95.9	90.0	97.6	97.0				
Consolidation Pressures								
Load 1 (psf)	116	116	116	116				
Load 2 (psf)	266	266	266	216				
Load 3 (psf)	516	516	516	416				
Load 4 (psf)		1016	1016	816				
Load 5 (psf)			2016	1616				
Load 6 (psf)				3016				
Load 7 (psf)								
t_{50}								
Max. t_{50} for Load 1 (min)		0.98						
Max. t_{50} for Load 2 (min)	62.53	10.58	150.00					
Max. t_{50} for Load 3 (min)	78.97	29.30	83.07					
Max. t_{50} for Load 4 (min)		84.48	74.41					
Max. t_{50} for Load 5 (min)			52.86	81.50				
Max. t_{50} for Load 6 (min)				85.04				
Max. t_{50} for Load 7 (min)								
Final Values								
Water Content (%)	58.56	53.68	47.36	42.85				
Dry Unit Weight (pcf)	67.9	67.4	76.6	79.7				
Wet Unit Weight (pcf)	107.7	103.6	112.9	113.8				
Failure								
Test Performed at Shear Rate (in/min)	2.50E-05	4.00E-05	3.80E-05	2.30E-05				
Required Shear Rate (in/min)	3.04E-05	4.73E-05	5.68E-05	3.29E-05				
Displacement at Failure (in)	0.12	0.20	0.15	0.14				
Peak Shear Stress (psf)	307	505	794	1149				
Total Change in Height at Failure (in)	0.25	0.33	0.38	0.38				
Secant Effective Friction Angle (deg)	30.8	26.4	21.5	20.8				

Comments:

Texas 4 - Blenderized - 516 psf

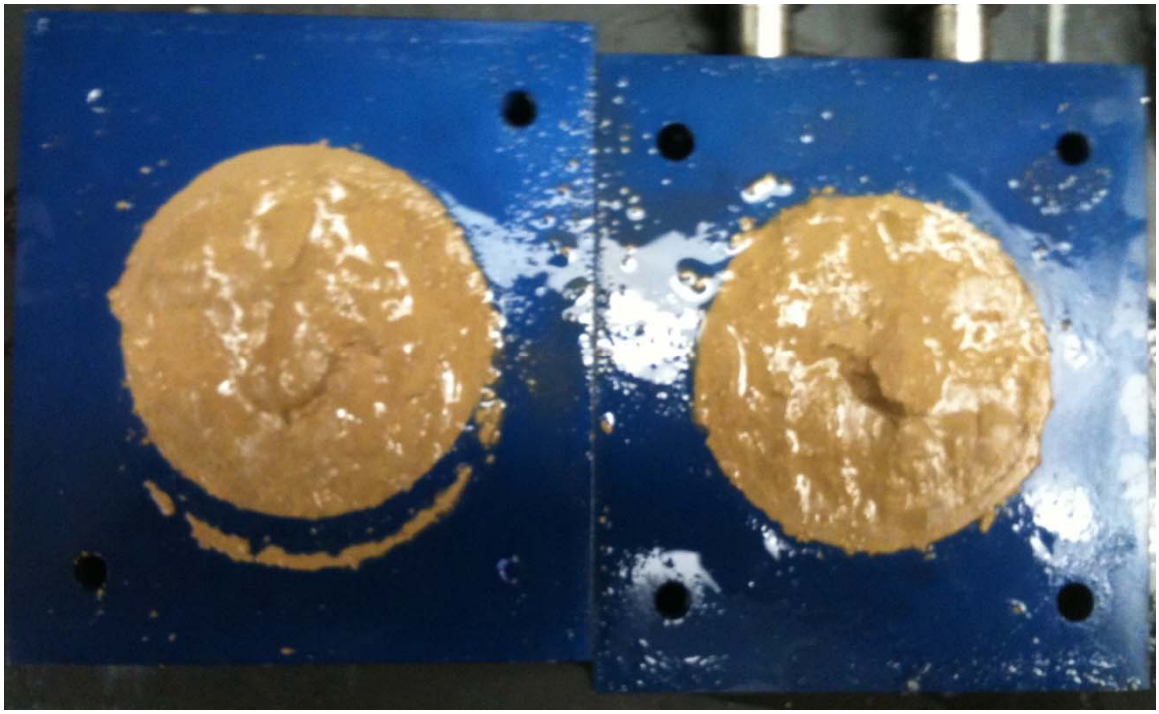

Texas 4 - Blenderized - 1016 psf

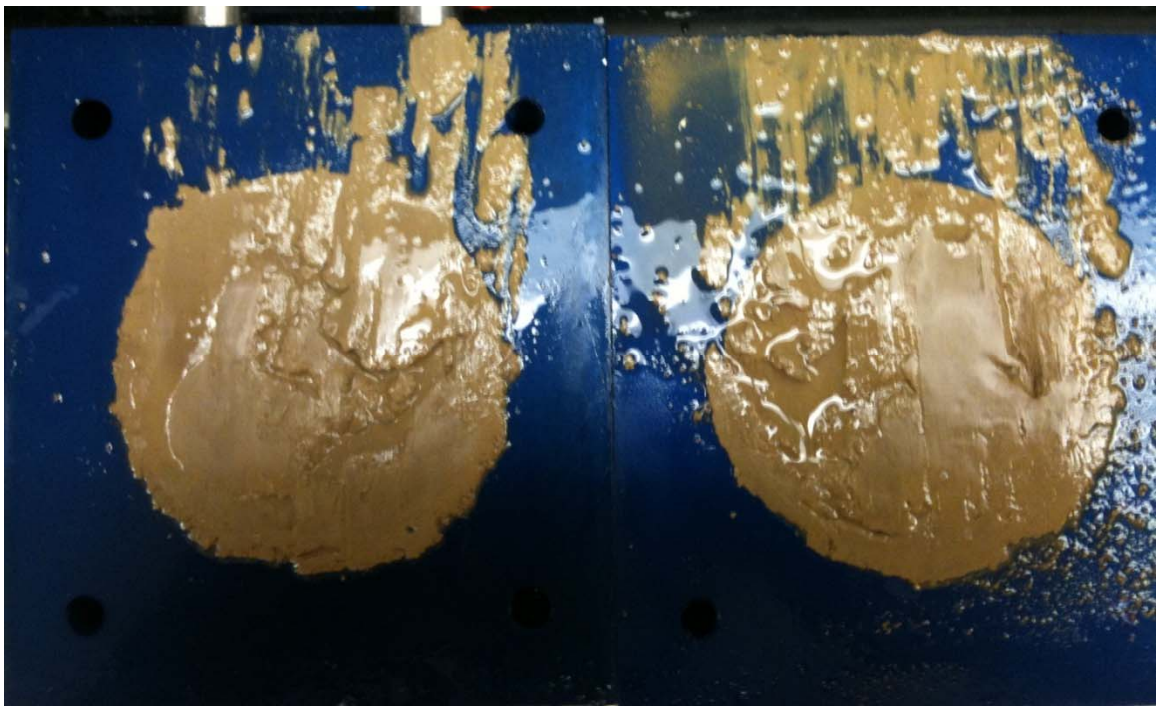

Texas 4 - Blenderized - 2016 psf

Texas 4 - Blenderized - 3016 psf

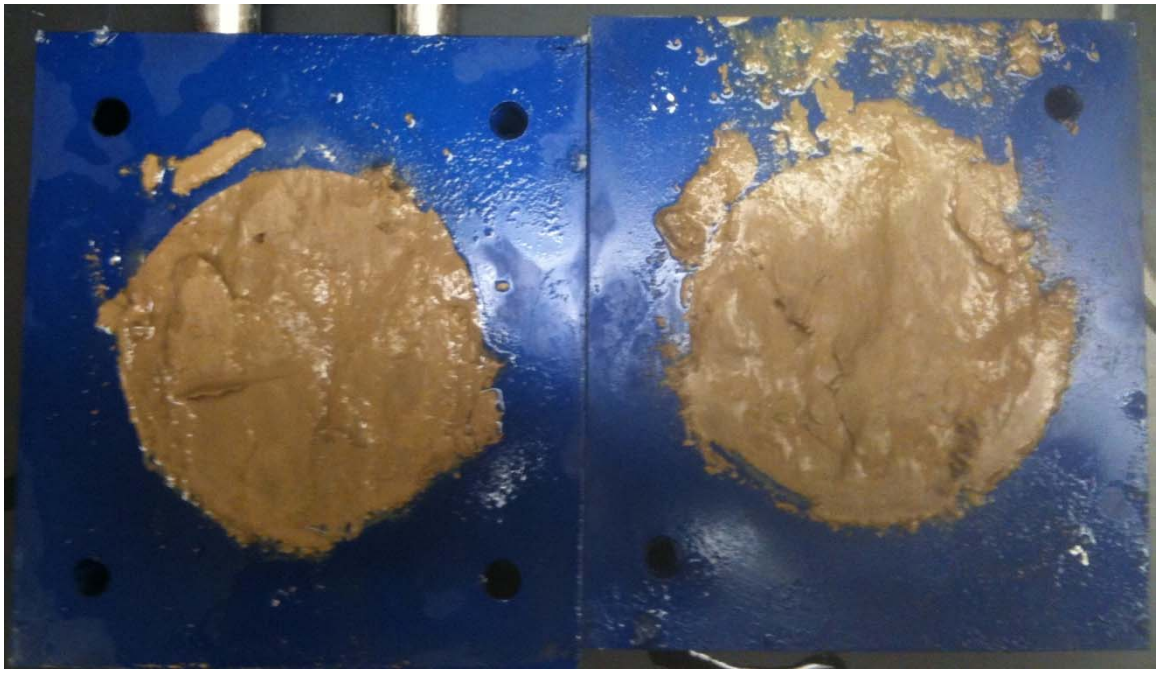

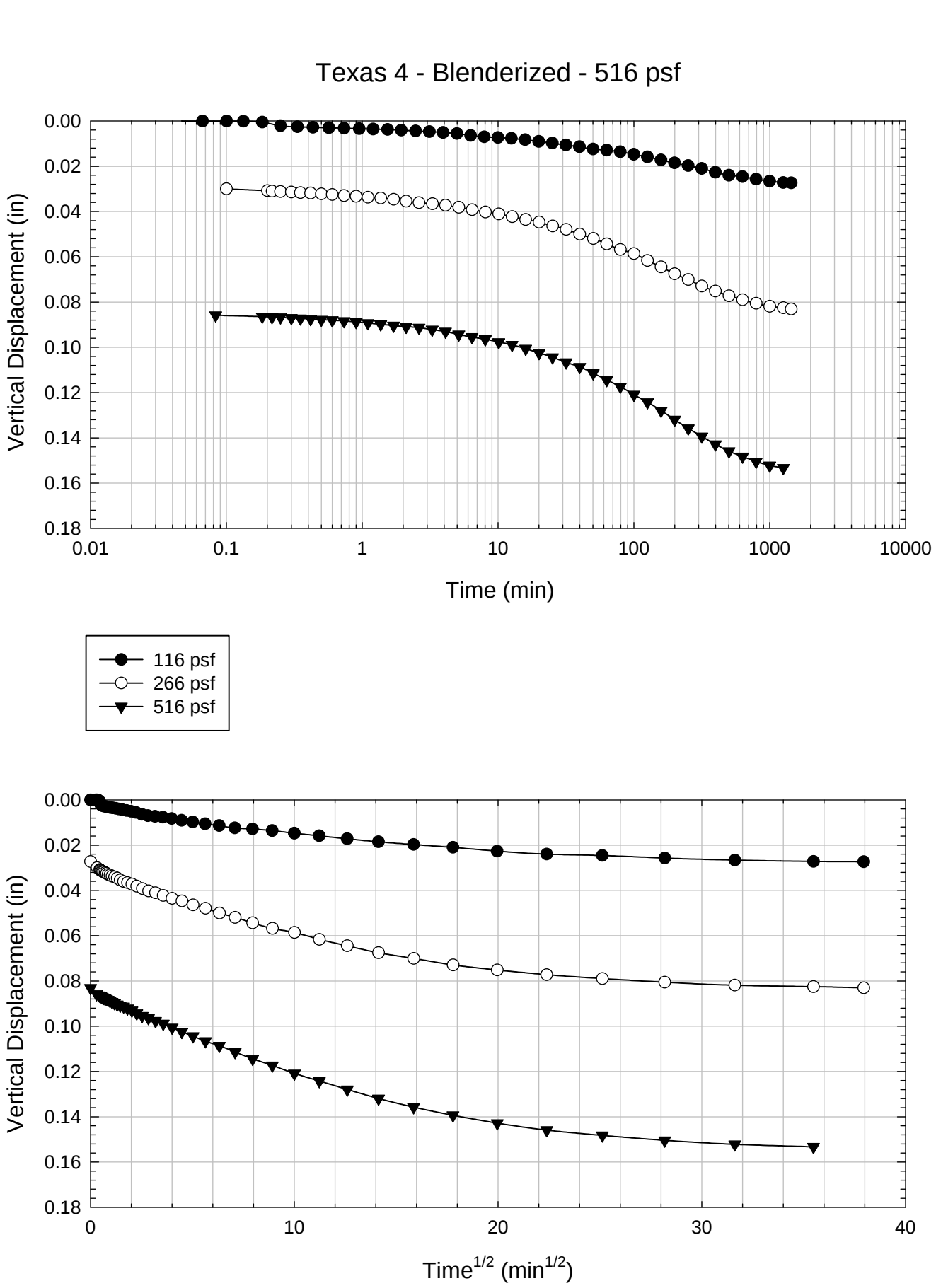
Texas 4 - Blenderized - 516 psf
Vertical Displacement (in)
0.00
0.02
0.04
0.06
0.08
0.10
0.12
0.14
0.16
0.18
0.01
0.1
1
10
100
1000
10000
Time (min)
116 psf
266 psf
516 psf
Vertical Displacement (in)
0
10
20
30
40
Time^1/2 (min^1/2)

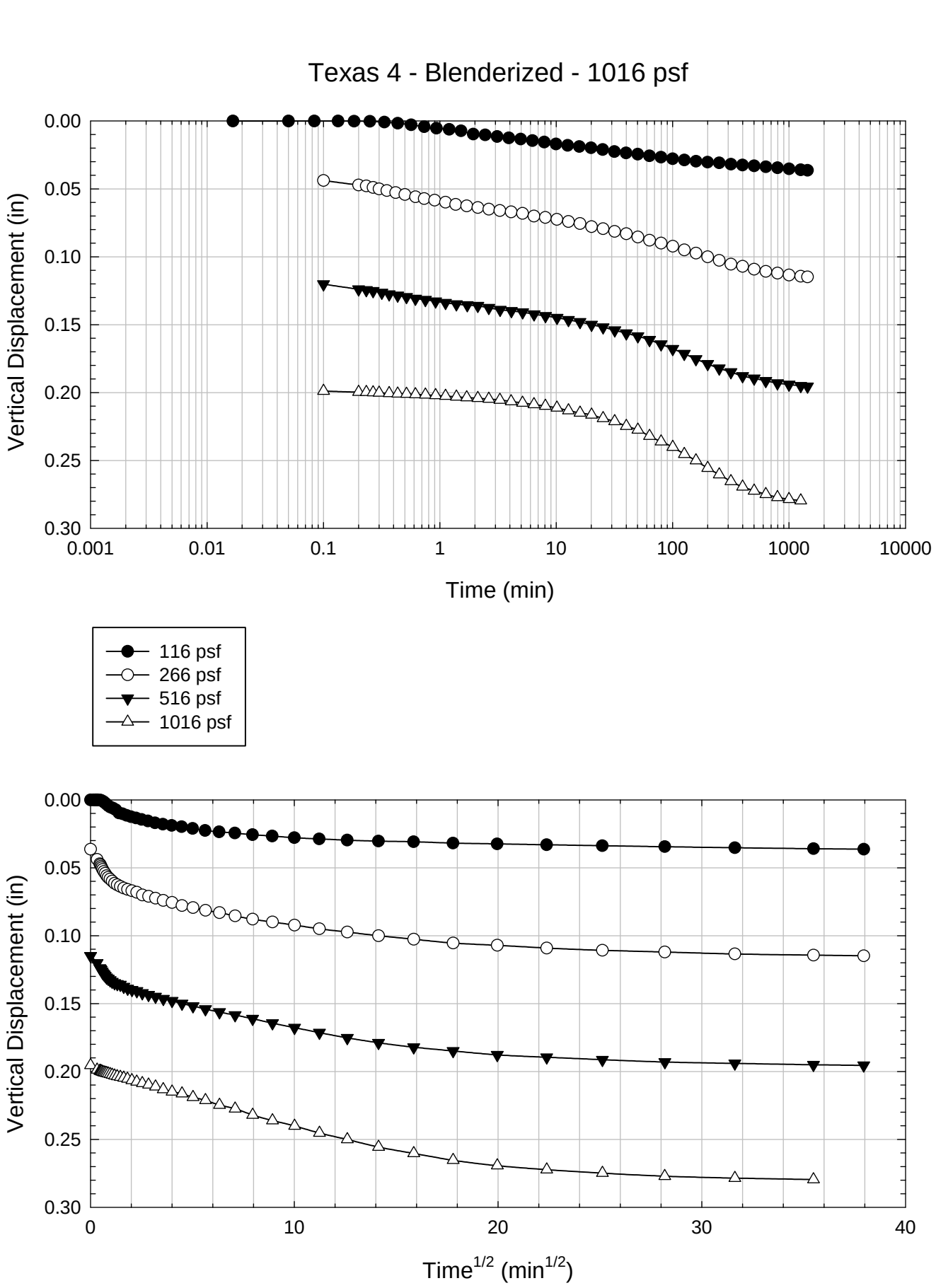
Texas 4 - Blenderized - 1016 psf
Vertical Displacement (in)
0.00
0.05
0.10
0.15
0.20
0.25
0.30
0.001
0.01
0.1
1
10
100
1000
10000
Time (min)
116 psf
266 psf
516 psf
1016 psf
Vertical Displacement (in)
0.00
0.05
0.10
0.15
0.20
0.25
0.30
0
10
20
30
40
Time^1/2 (min^1/2)

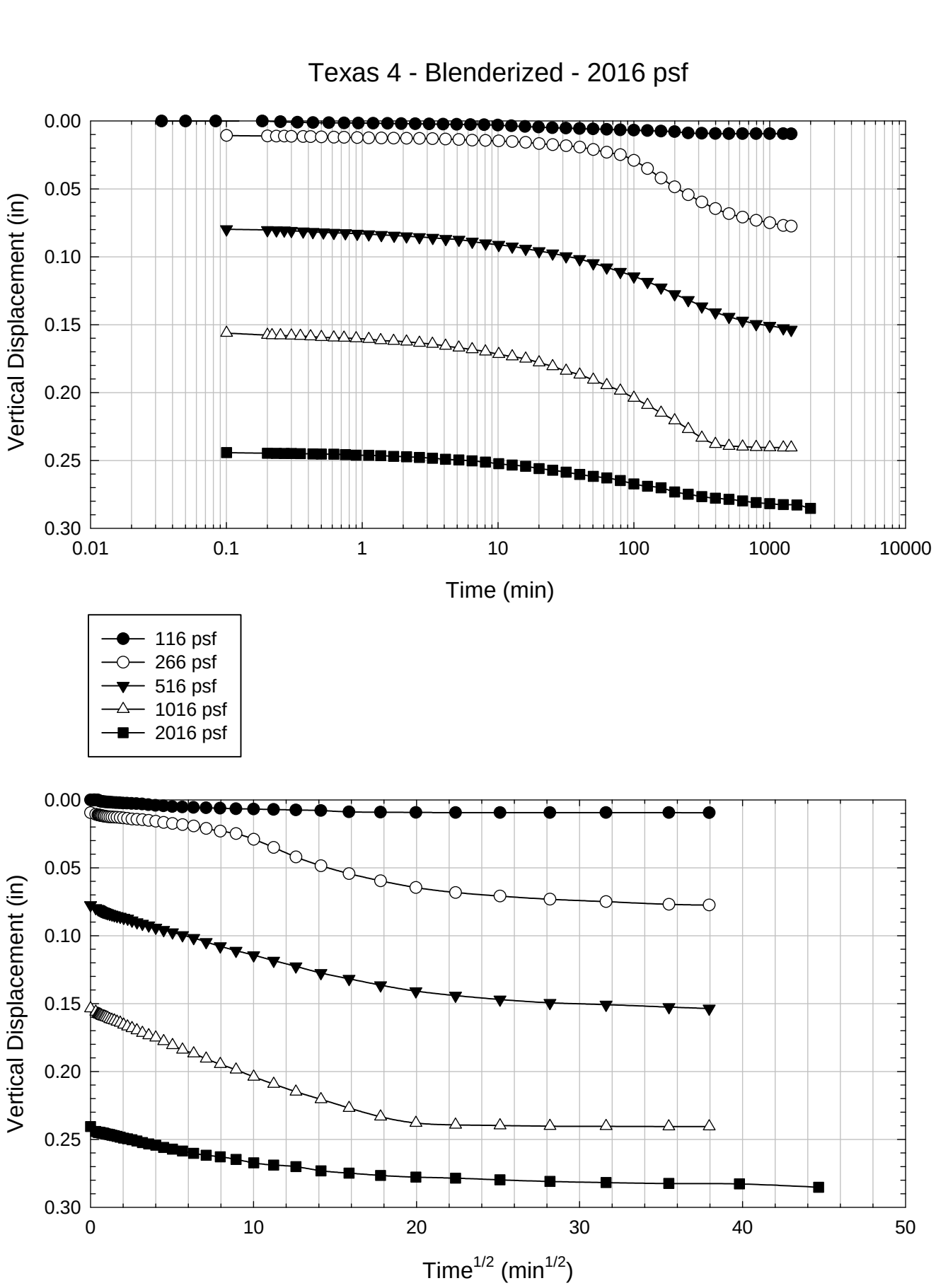
Texas 4 - Blenderized - 2016 psf
Vertical Displacement (in)
0.00
0.05
0.10
0.15
0.20
0.25
0.30
0.01
0.1
1
10
100
1000
10000
Time (min)
116 psf
266 psf
516 psf
1016 psf
2016 psf
Vertical Displacement (in)
0.00
0.05
0.10
0.15
0.20
0.25
0.30
0
10
20
30
40
50
Time1/2 (min1/2)

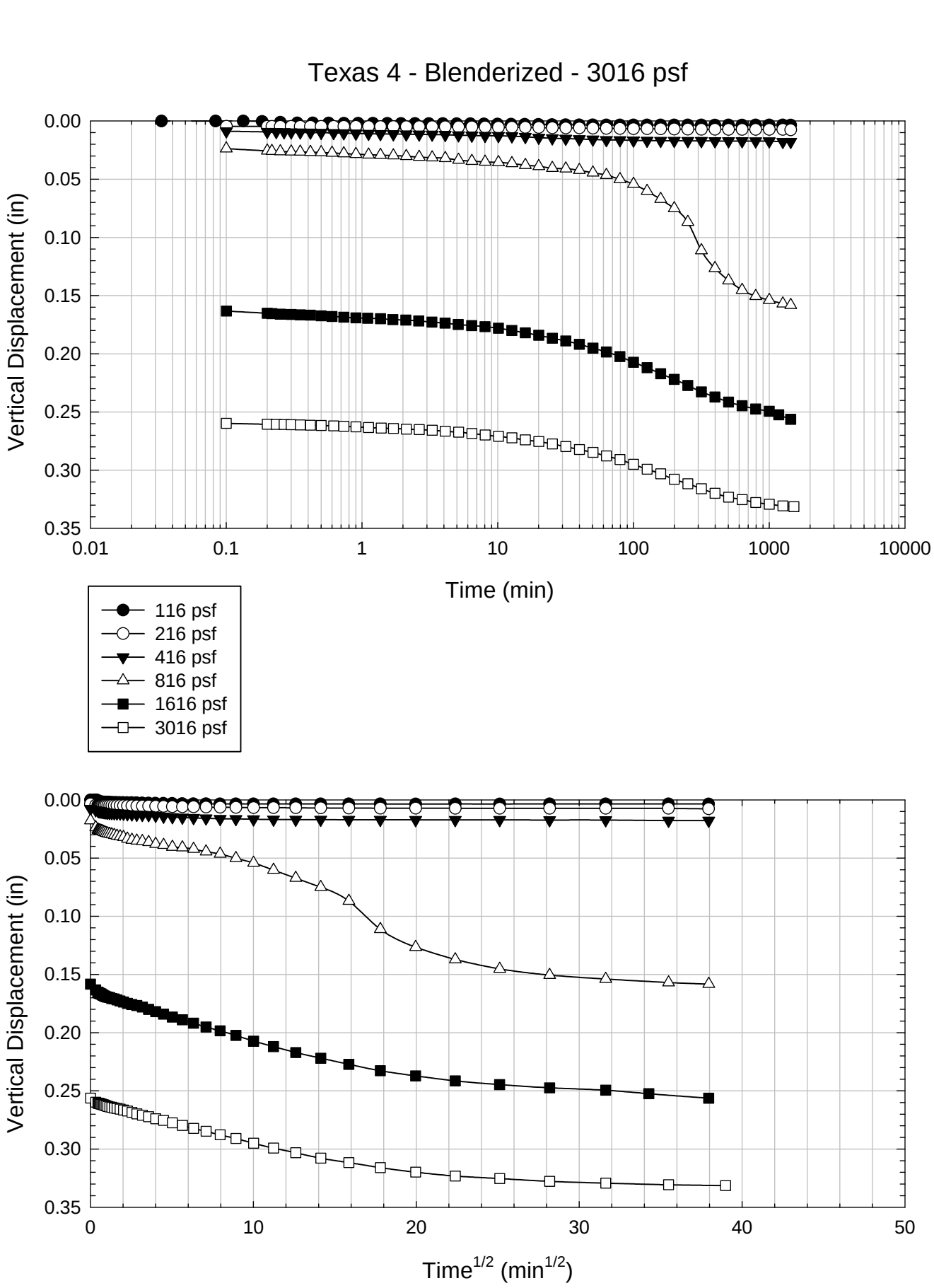
Texas 4 - Blenderized - 3016 psf
Vertical Displacement (in)
0.00
0.05
0.10
0.15
0.20
0.25
0.30
0.35
0.01
0.1
1
10
100
1000
10000
Time (min)
116 psf
216 psf
416 psf
816 psf
1616 psf
3016 psf
Vertical Displacement (in)
0.00
0.05
0.10
0.15
0.20
0.25
0.30
0.35
0
10
20
30
40
50
Time1/2 (min1/2)

Texas 4 - Blenderized

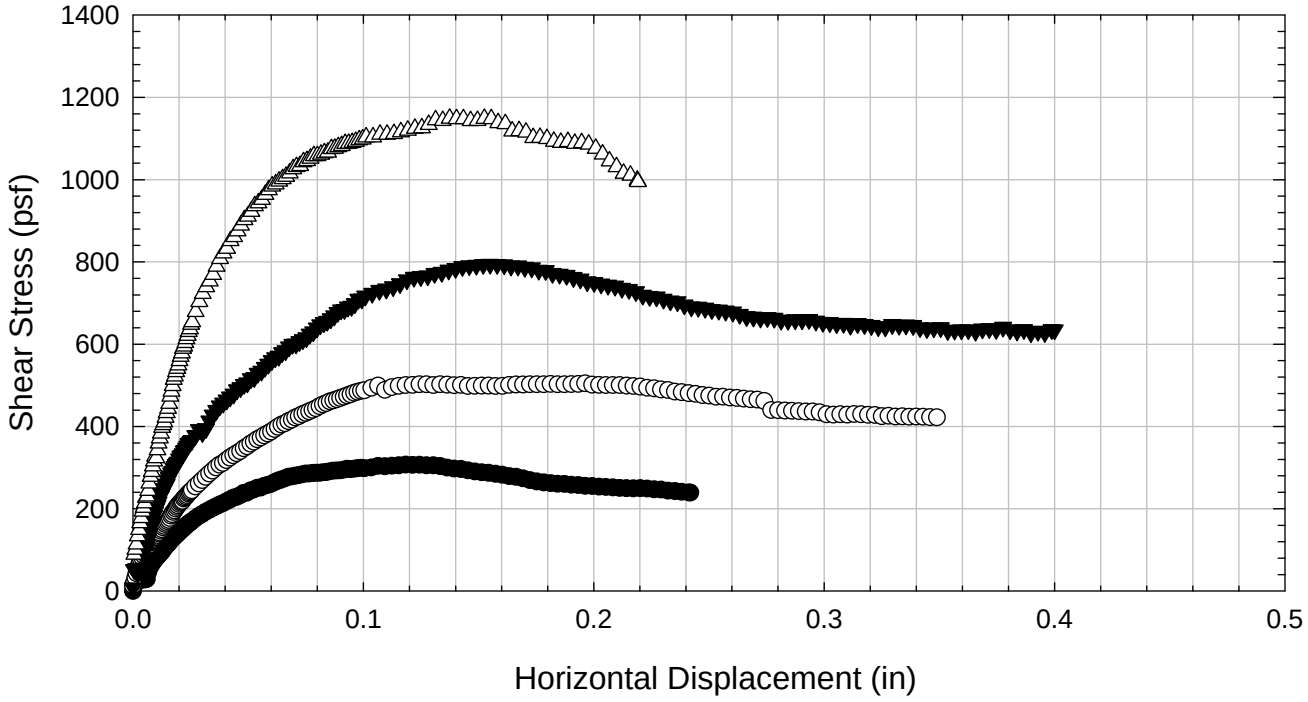

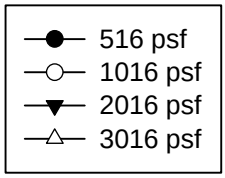

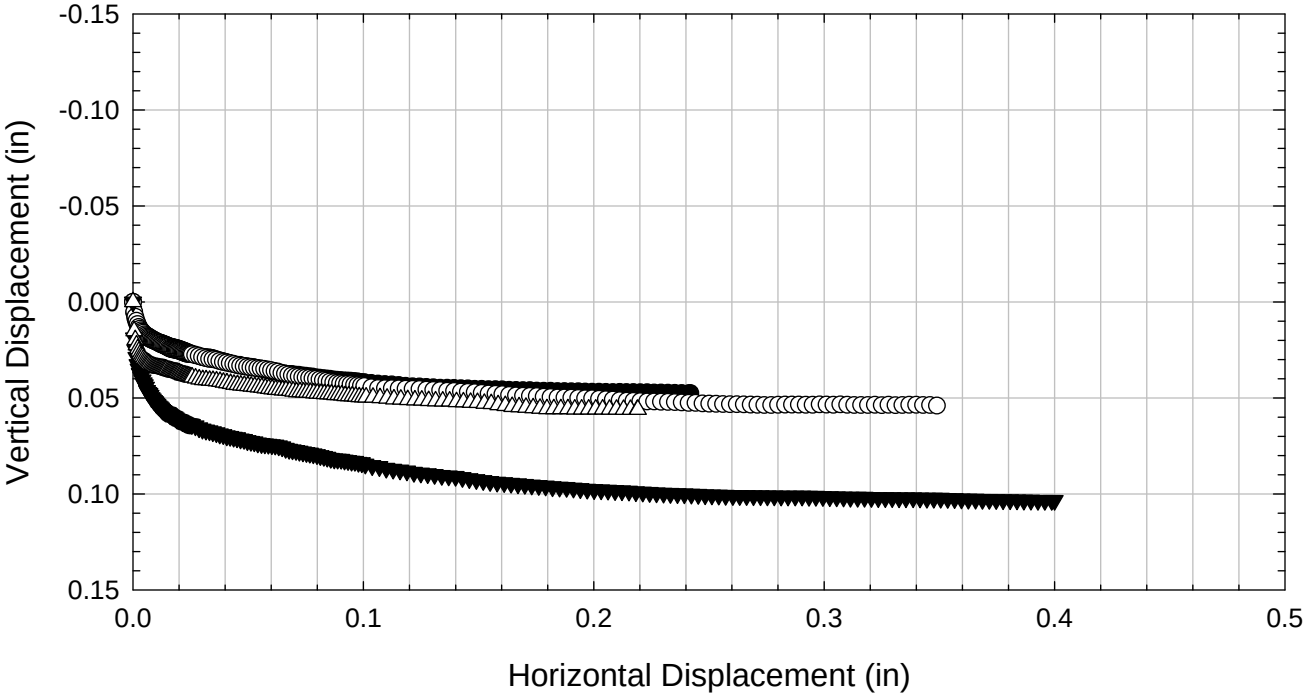

C.13. Texas 5

C.13.1 Blenderized

Virginia Polytechnic Institute and State University
Geotechnical Engineering Laboratory
Direct Shear Data Sheet

Project:	Fully Softened Shear Strength
Sample I.D./Loc.:	Texas 5 - Blenderized
Classification:	Fat Clay (CH)

Sample Preparation	Remolded at LL		Specific Gravity	2.86

Test Number	1	2	3	4	5	6	7	8
Start Date (m/d/y)	5/25/2011	5/16/2011	6/24/2011	6/24/2011	8/15/2011	8/14/2011		
End Date (m/d/y)	6/1/2011	5/24/2011	7/6/2011	7/6/2011	8/25/2011	8/25/2011		
Consolidation Pressure (psf)	516	1016	2016	3016	4516	6016		
Initial Values								
Initial Height (in)	1.43	1.42	1.38	1.41	1.40	1.45		
Initial Diameter (in)	2.50	2.50	2.50	2.50	2.50	2.50		
Initial Sample Weight (g)	177	177	181	177	175	177		
Water Content (%)	82.98	84.27	83.56	83.77	84.45	85.71		
Dry Unit Weight (pcf)	52.5	52.4	55.3	53.1	52.5	51.1		
Wet Unit Weight (pcf)	96.1	96.6	101.5	97.5	96.9	94.9		
Consolidation Pressures								
Load 1 (psf)	116	116	116	116	116	116		
Load 2 (psf)	266	266	266	216	266	216		
Load 3 (psf)	516	516	516	391	516	391		
Load 4 (psf)		1016	1016	766	1141	766		
Load 5 (psf)			2016	1516	2266	1516		
Load 6 (psf)				3016	4516	3016		
Load 7 (psf)						6016		
t_{50}								
Max. t_{50} for Load 1 (min)								
Max. t_{50} for Load 2 (min)								
Max. t_{50} for Load 3 (min)	69.67							
Max. t_{50} for Load 4 (min)		59.03						
Max. t_{50} for Load 5 (min)			74.94					
Max. t_{50} for Load 6 (min)				53.28	53.28			
Max. t_{50} for Load 7 (min)						53.04		
Final Values								
Water Content (%)	65.07	60.91	52.52	46.00	45.00	41.40		
Dry Unit Weight (pcf)	62.2	67.2	74.8	71.3	80.1	85.49		
Wet Unit Weight (pcf)	102.7	108.2	114.1	104.2	116.1	120.89		
Failure								
Test Performed at Shear Rate (in/min)	2.87E-05	3.33E-05	2.67E-05	3.73E-05	3.75E-05	3.75E-05		
Required Shear Rate (in/min)	3.44E-05	4.07E-05	3.47E-05	5.63E-05	6.38E-05	4.90E-05		
Displacement at Failure (in)	0.12	0.12	0.13	0.15	0.17	0.13		
Peak Shear Stress (psf)	287	447	687	1131	1459	2112		
Total Change in Height at Failure (in)	0.22	0.31	0.36	0.45	0.48	0.58		
Secant Effective Friction Angle (deg)	29.1	23.8	18.8	20.6	17.9	19.3		

Comments:

Texas 5 - Blenderized - 516 psf

Texas 5 - Blenderized - 1016 psf

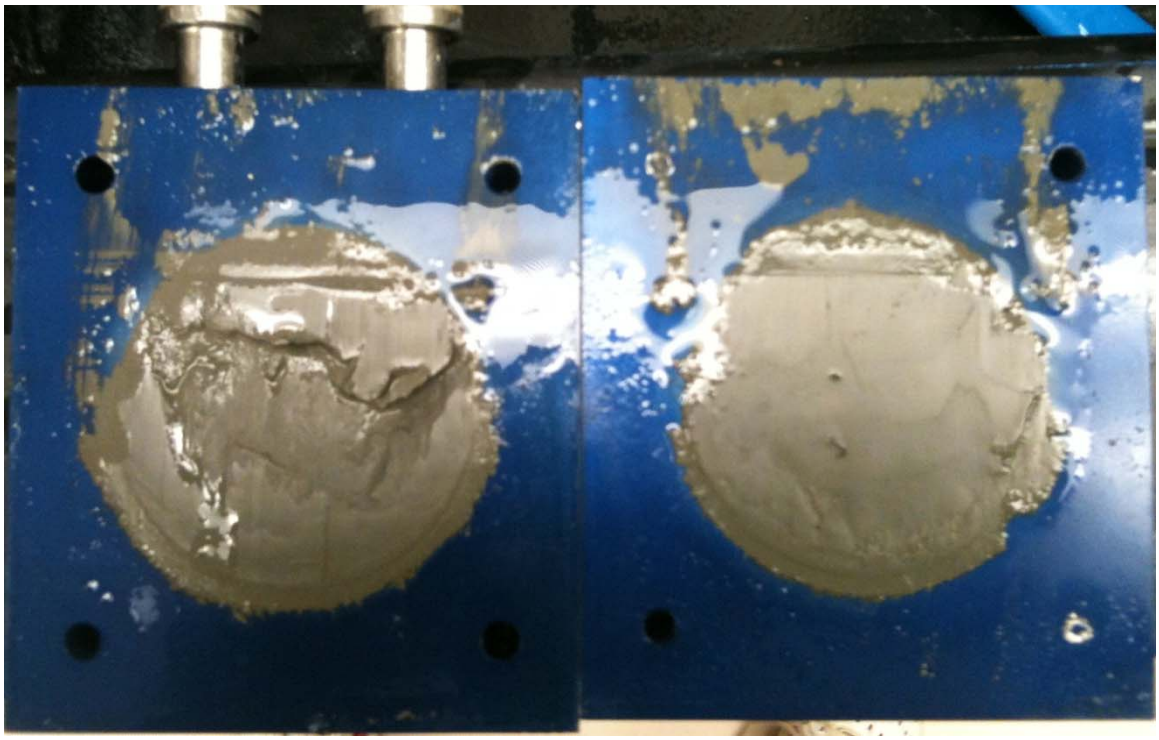

Texas 5 - Blenderized - 2016 psf

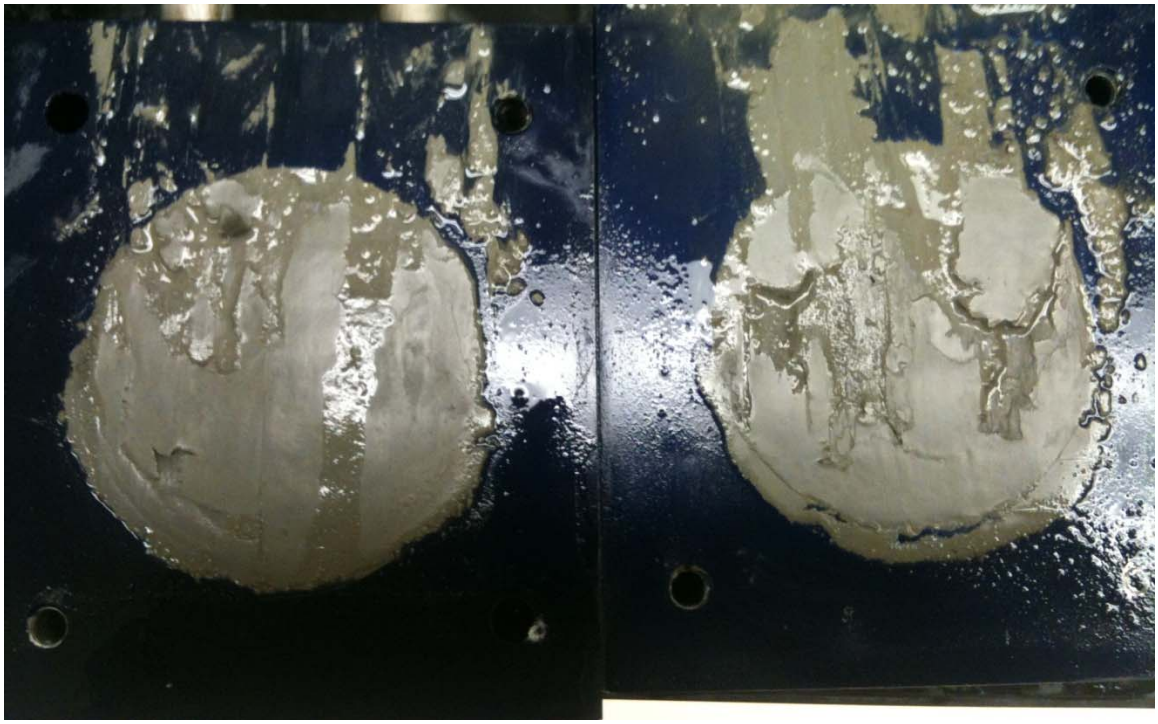

Texas 5 - Blenderized - 3016 psf

Texas 5 - Blenderized - 4516 psf

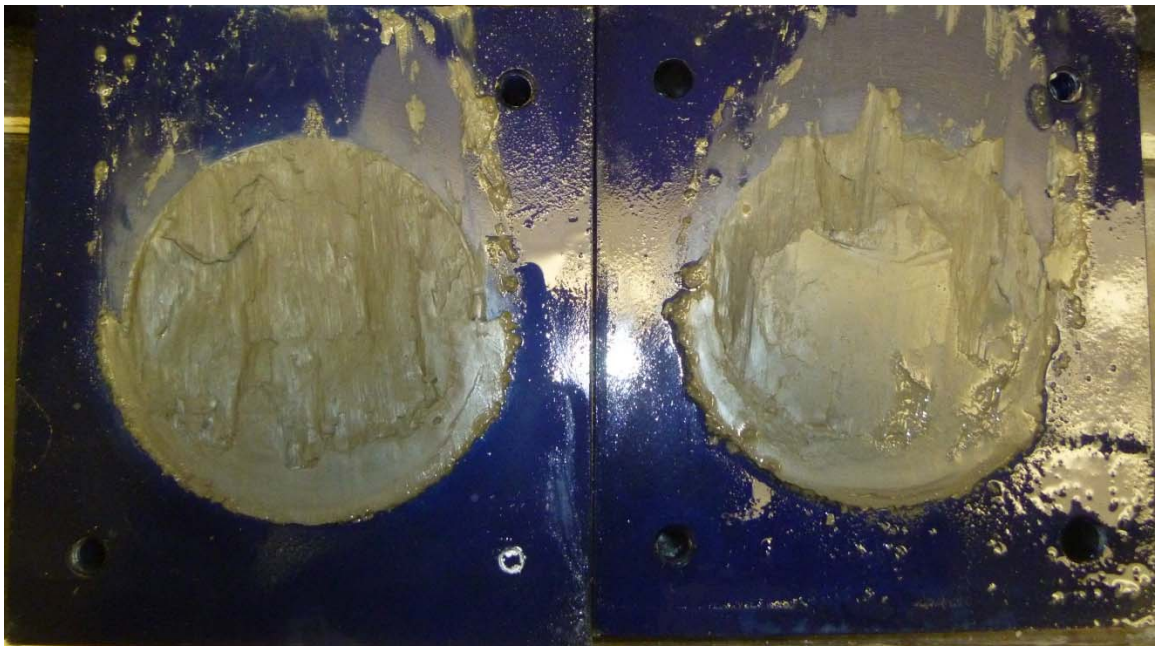

Texas 5 - Blenderized - 6016 psf

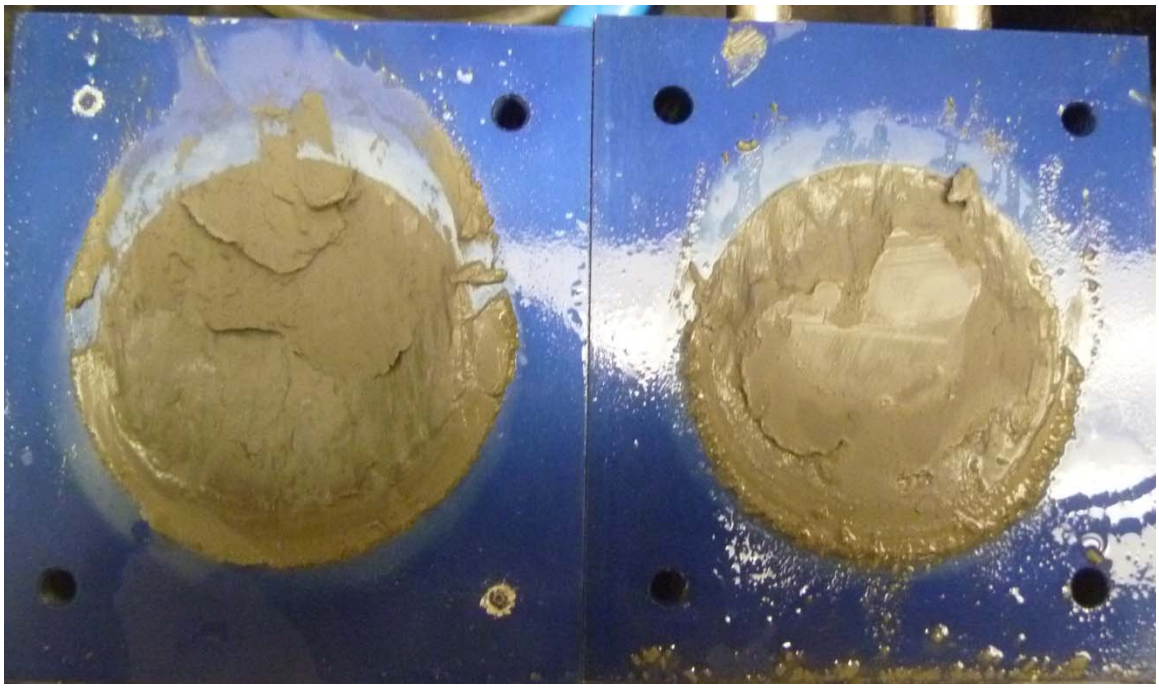

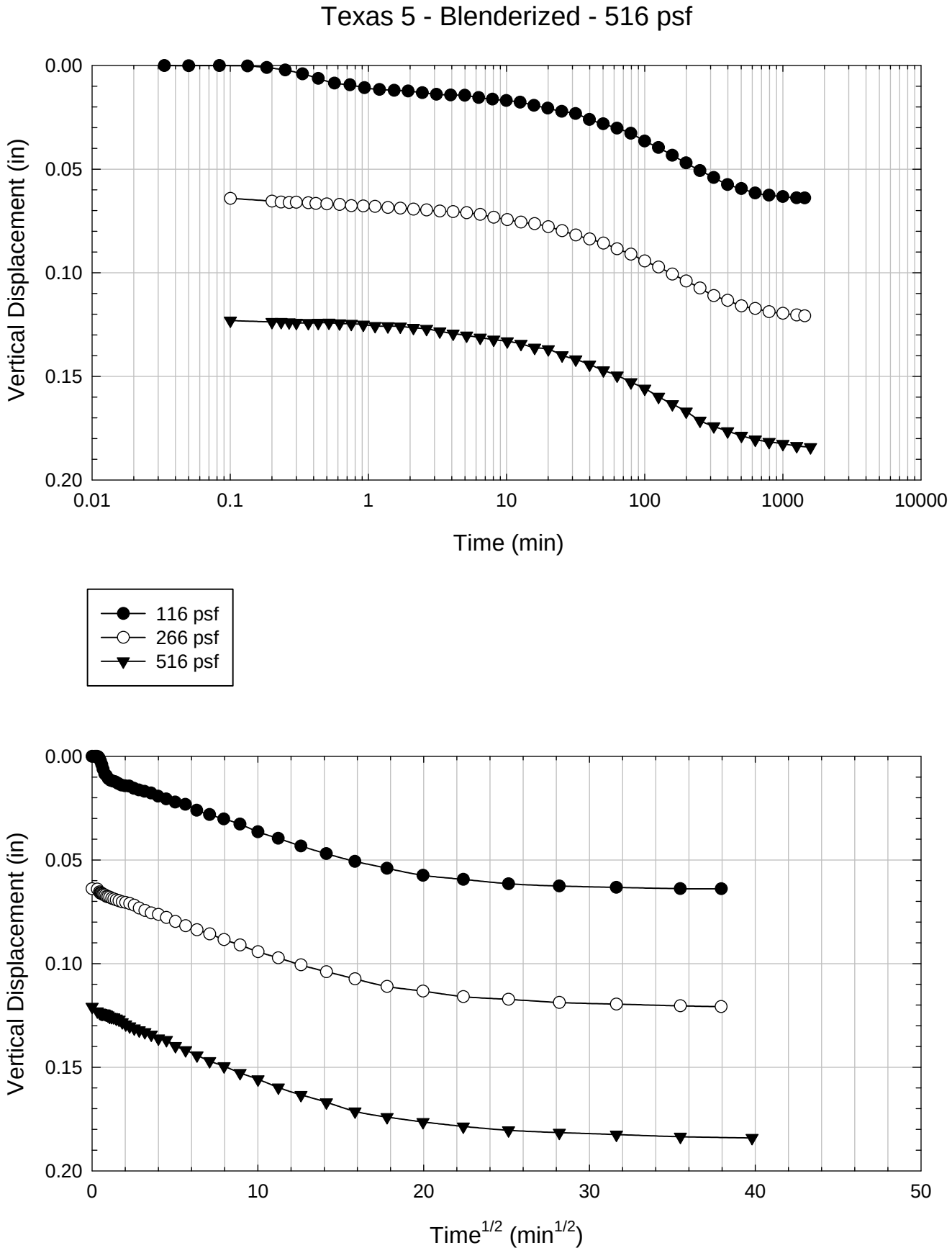
Texas 5 - Blenderized - 516 psf
Vertical Displacement (in)
0.00
0.05
0.10
0.15
0.20
0.01
0.1
1
10
100
1000
10000
Time (min)
116 psf
266 psf
516 psf
Vertical Displacement (in)
0.00
0.05
0.10
0.15
0.20
0
10
20
30
40
50
Time1/2 (min1/2)

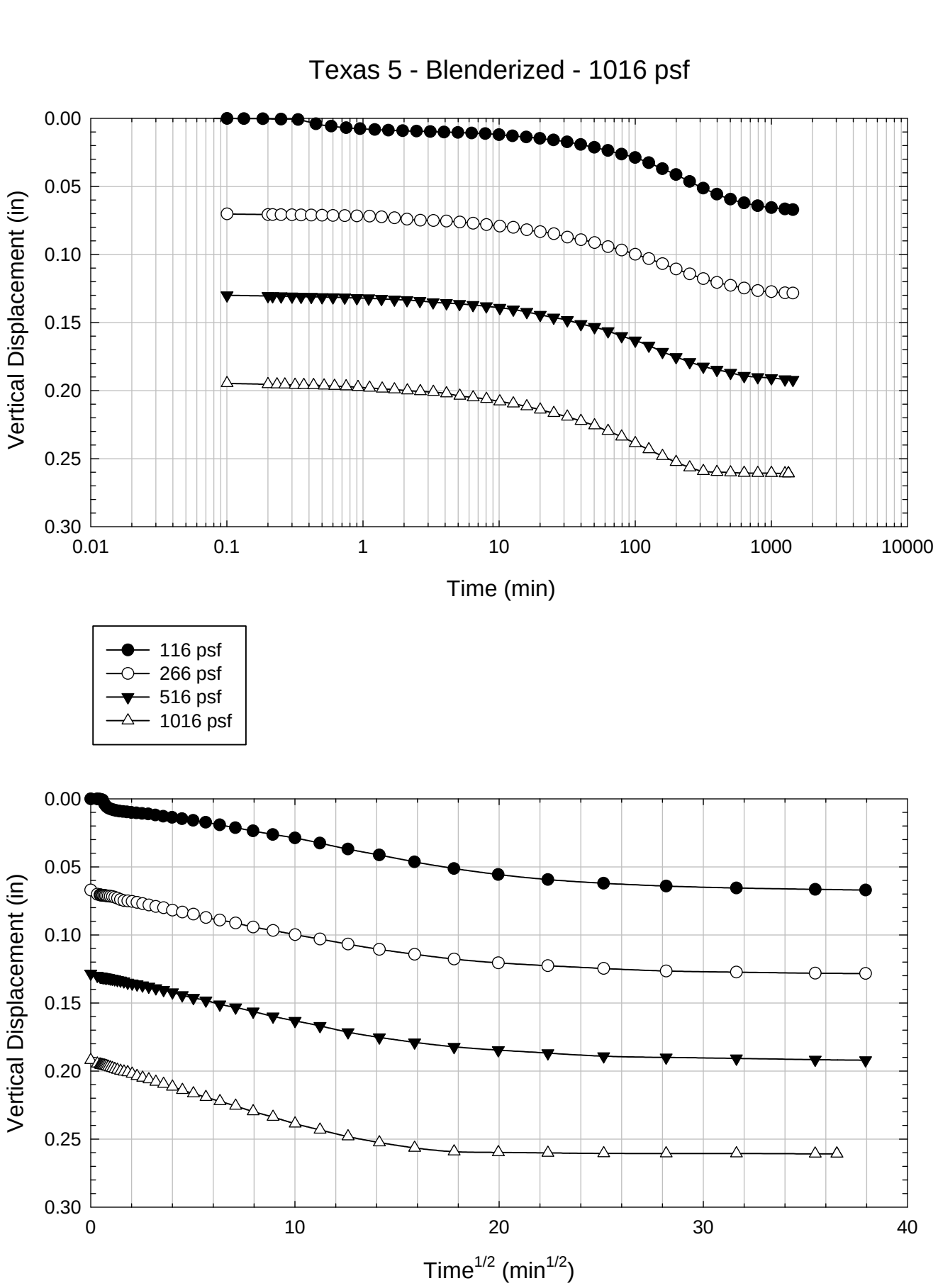
Texas 5 - Blenderized - 1016 psf
Vertical Displacement (in)
0.00
0.05
0.10
0.15
0.20
0.25
0.30
0.01
0.1
1
10
100
1000
10000
Time (min)
116 psf
266 psf
516 psf
1016 psf
Vertical Displacement (in)
0.00
0.05
0.10
0.15
0.20
0.25
0.30
0
10
20
30
40
Time^1/2 (min^1/2)

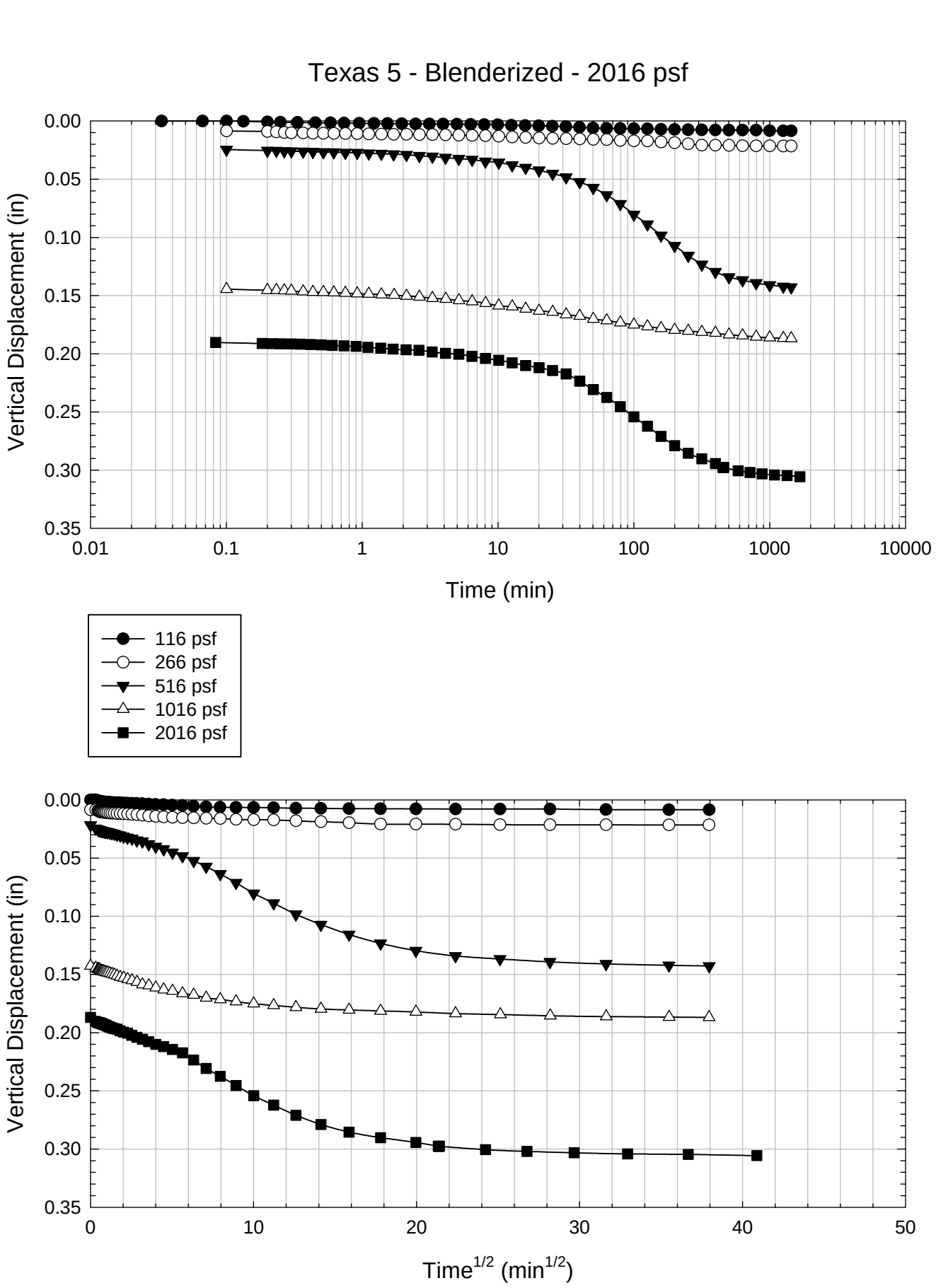
Texas 5 - Blenderized - 2016 psf
Vertical Displacement (in)
0.00
0.05
0.10
0.15
0.20
0.25
0.30
0.35
0.01
0.1
1
10
100
1000
10000
Time (min)
116 psf
266 psf
516 psf
1016 psf
2016 psf
Vertical Displacement (in)
0.00
0.05
0.10
0.15
0.20
0.25
0.30
0.35
0
10
20
30
40
50
Time1/2 (min1/2)

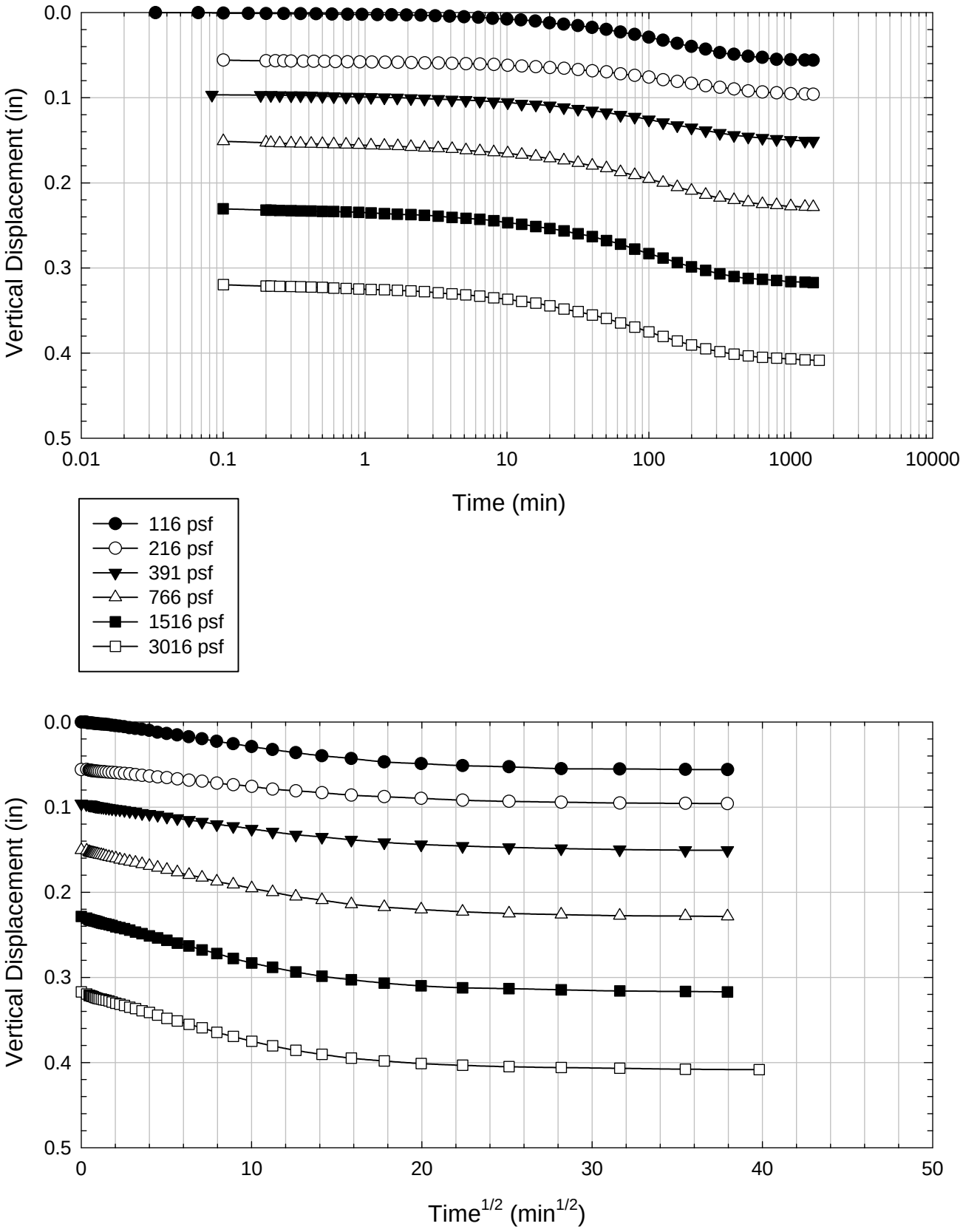
Texas 5 - Blenderized - 3016 psf
Vertical Displacement (in)
0.0
0.1
0.2
0.3
0.4
0.5
0.01
0.1
1
10
100
1000
10000
Time (min)
116 psf
216 psf
391 psf
766 psf
1516 psf
3016 psf
Vertical Displacement (in)
0.0
0.1
0.2
0.3
0.4
0.5
0
10
20
30
40
50
Time1/2 (min1/2)

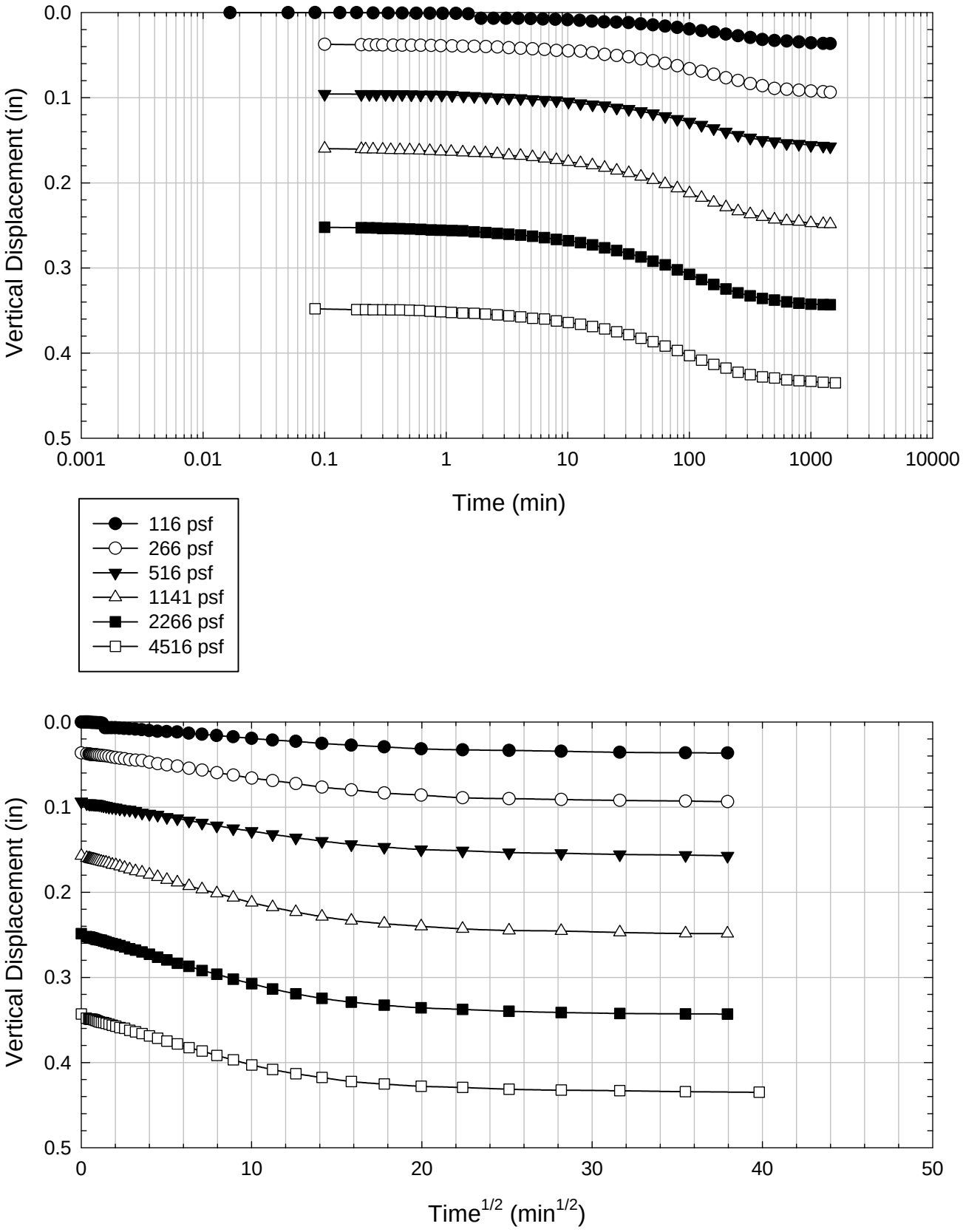
Texas 5 - Blenderized - 4516 psf
Vertical Displacement (in)
0.0
0.1
0.2
0.3
0.4
0.5
0.001
0.01
0.1
1
10
100
1000
10000
Time (min)
116 psf
266 psf
516 psf
1141 psf
2266 psf
4516 psf
Vertical Displacement (in)
0.0
0.1
0.2
0.3
0.4
0.5
0
10
20
30
40
50
Time1/2 (min1/2)

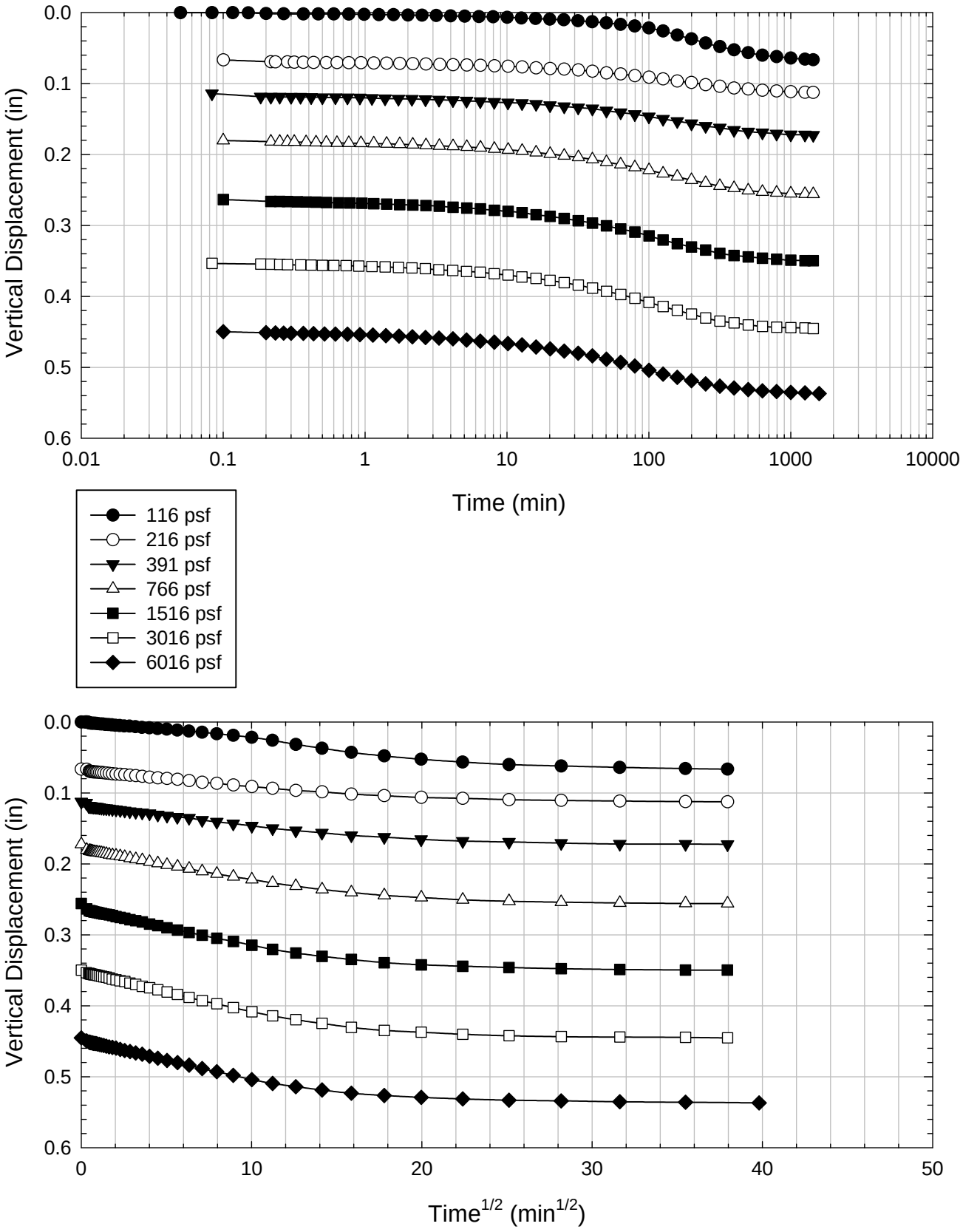
Texas 5 - Blenderized - 6016 psf
Vertical Displacement (in)
0.0
0.1
0.2
0.3
0.4
0.5
0.6
0.01
0.1
1
10
100
1000
10000
Time (min)
116 psf
216 psf
391 psf
766 psf
1516 psf
3016 psf
6016 psf
Vertical Displacement (in)
0
10
20
30
40
50
Time^1/2 (min^1/2)

Texas 5 - Blenderized

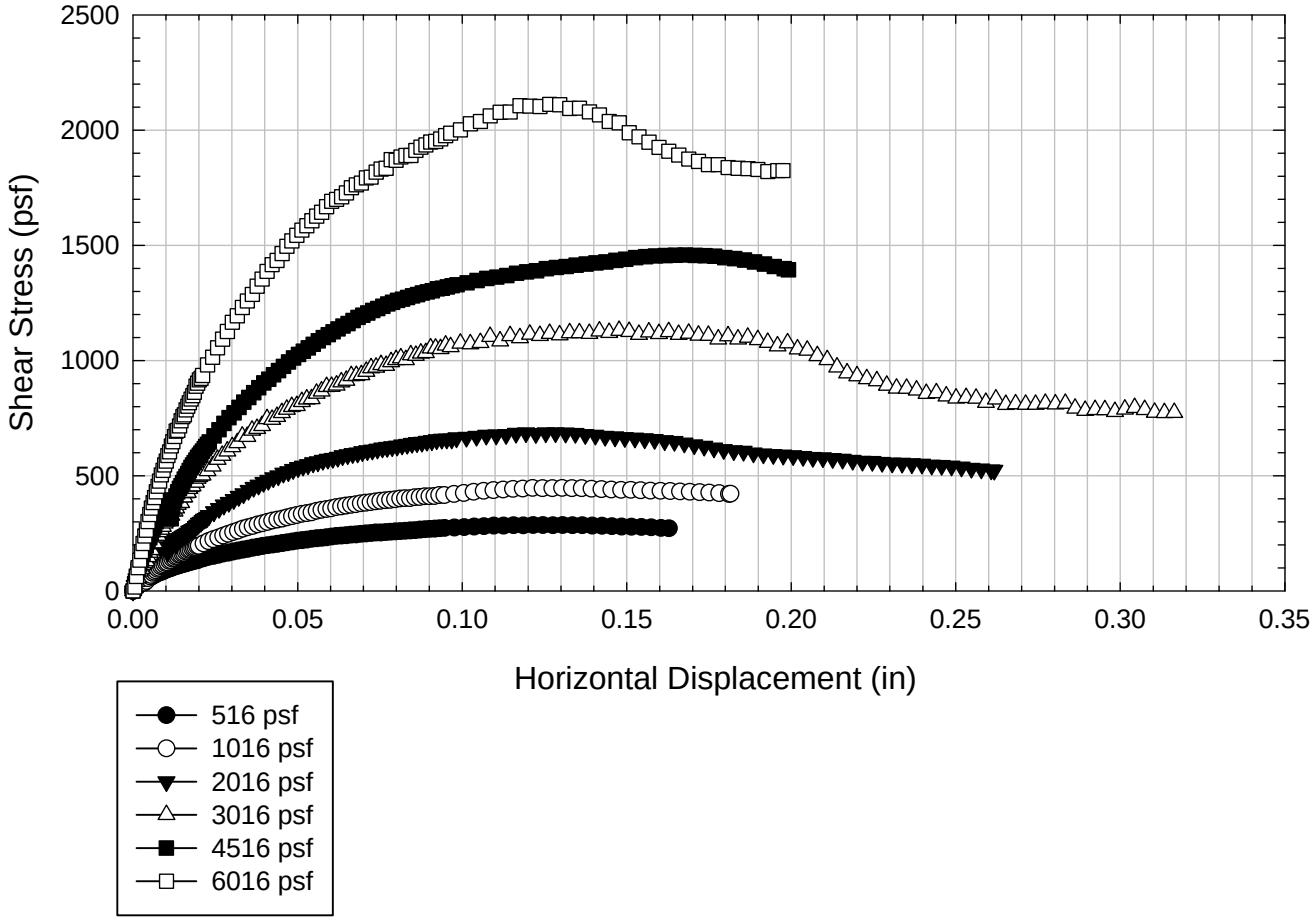

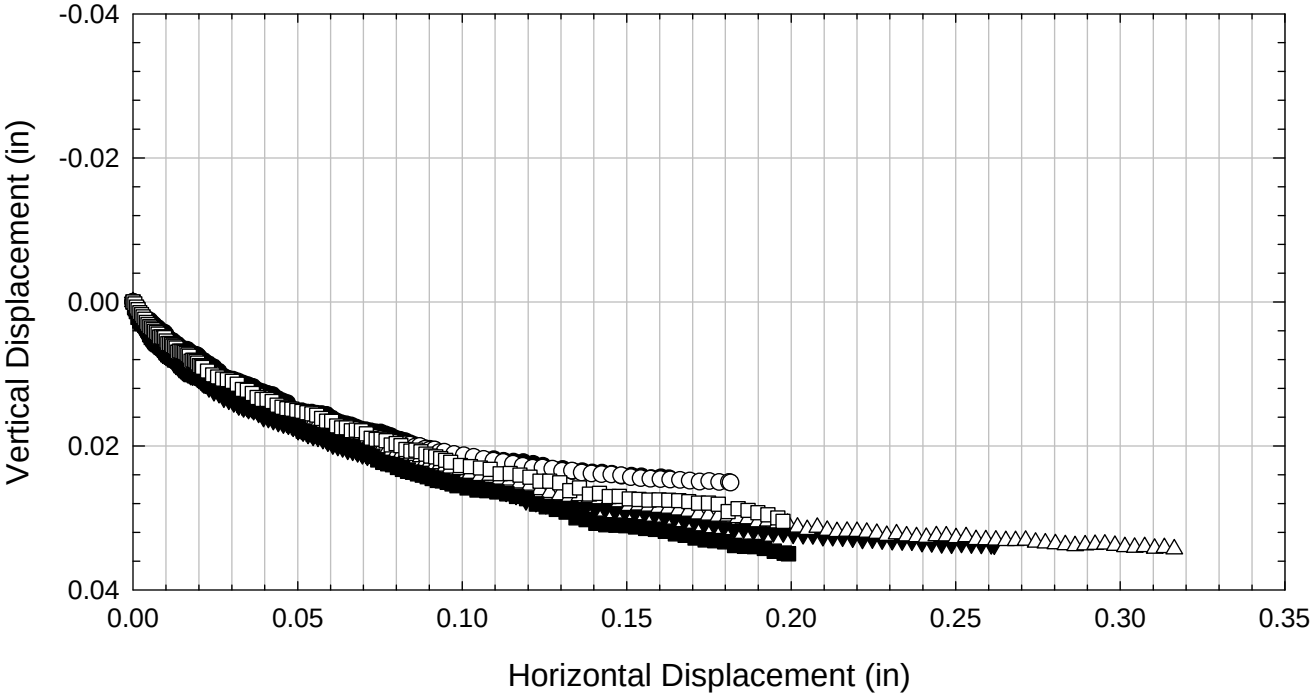

C.14. Texas 6

C.14.1 Blenderized

Virginia Polytechnic Institute and State University
Geotechnical Engineering Laboratory
Direct Shear Data Sheet

Project:	Fully Softened Shear Strength
Sample I.D./Loc.:	Texas 6 - Blenderized
Classification:	Fat Clay (CH)

Sample Preparation	Remolded at LL		Specific Gravity	2.85

Test Number	1	2	3	4	5	6	7	8
Start Date (m/d/y)	5/10/2011	5/10/2011	5/12/2011	5/10/2011	8/9/2011	8/26/2011		
End Date (m/d/y)	5/24/2011	5/24/2011	5/26/2011	5/24/2011	8/21/2011	9/10/2011		
Consolidation Pressure (psf)	516	1016	2016	3016	4516	6016		
Initial Values								
Initial Height (in)	1.44	1.41	1.41	1.41	1.38	1.47		
Initial Diameter (in)	2.50	2.50	2.50	2.50	2.50	2.50		
Initial Sample Weight (g)	181	179	176	179	183	182		
Water Content (%)	75.38	77.30	76.87	75.73	77.80	76.20		
Dry Unit Weight (pcf)	55.6	55.6	54.8	56.1	57.7	54.6		
Wet Unit Weight (pcf)	97.6	98.5	96.9	98.5	102.6	96.1		
Consolidation Pressures								
Load 1 (psf)	116	116	116	116	116	116		
Load 2 (psf)	266	216	266	216	266	216		
Load 3 (psf)	516	566	516	391	516	391		
Load 4 (psf)		1016	1016	766	1141	766		
Load 5 (psf)			2016	1516	2266	1516		
Load 6 (psf)				3016	4516	3016		
Load 7 (psf)						6016		
t_{50}								
Max. t_{50} for Load 1 (min)								
Max. t_{50} for Load 2 (min)								
Max. t_{50} for Load 3 (min)	172.89							
Max. t_{50} for Load 4 (min)		161.90						
Max. t_{50} for Load 5 (min)			33.38					
Max. t_{50} for Load 6 (min)				118.02	73.70			
Max. t_{50} for Load 7 (min)						78.82		
Final Values								
Water Content (%)	59.49	54.03	48.52	41.95	39.79	36.33		
Dry Unit Weight (pcf)	65.1	71.4	74.2	83.6	88.8	90.05		
Wet Unit Weight (pcf)	103.8	109.9	110.3	118.6	124.1	122.76		
Failure								
Test Performed at Shear Rate (in/min)	1.25E-05	1.24E-05	1.69E-05	1.69E-05	2.72E-05	2.69E-05		
Required Shear Rate (in/min)	1.62E-05	1.61E-05	1.02E-04	2.03E-05	4.07E-05	4.31E-05		
Displacement at Failure (in)	0.14	0.13	0.17	0.12	0.15	0.17		
Peak Shear Stress (psf)	274	491	968	1200	1335	2106		
Total Change in Height at Failure (in)	0.22	0.31	0.37	0.46	0.48	0.58		
Secant Effective Friction Angle (deg)	27.9	25.8	25.6	21.7	16.5	19.3		

Comments:

Texas 6 - Blenderized - 516 psf

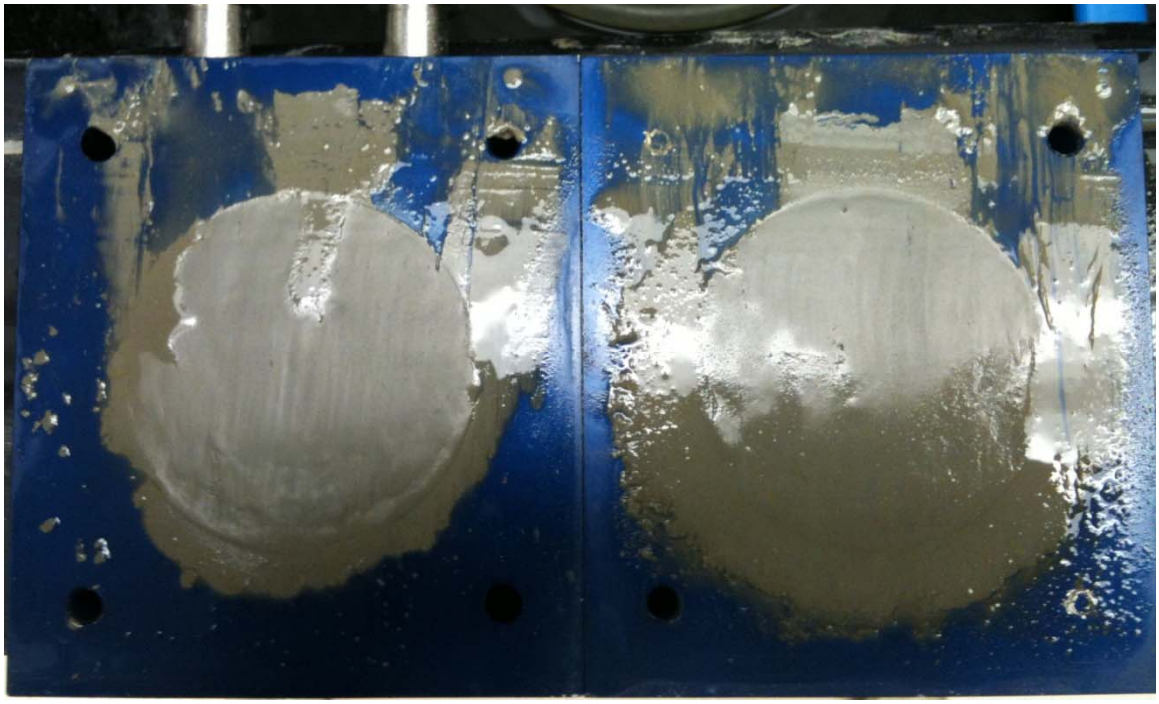

Texas 6 - Blenderized - 1016 psf

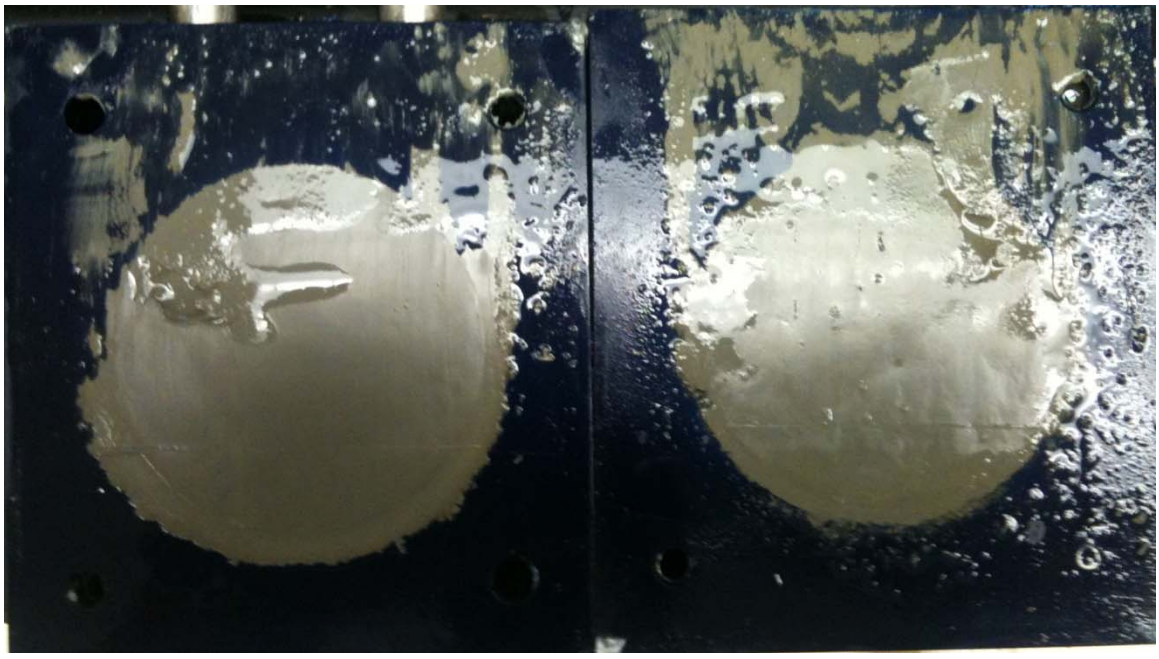

Texas 6 - Blenderized - 2016 psf

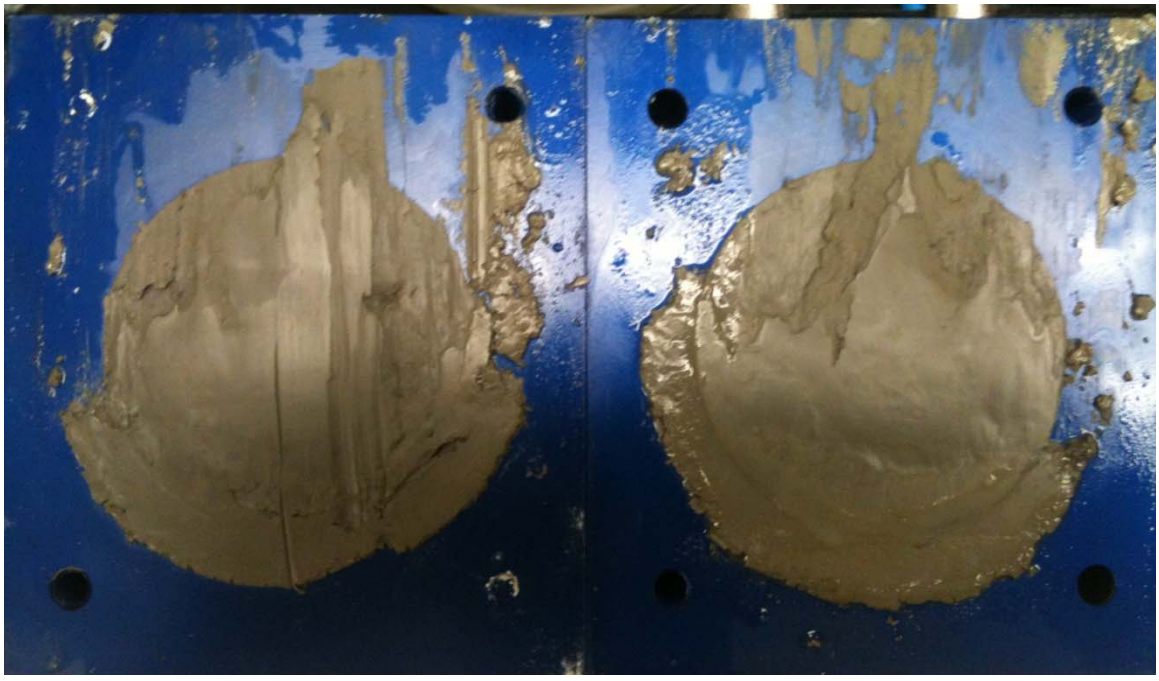

Texas 6 - Blenderized - 3016 psf

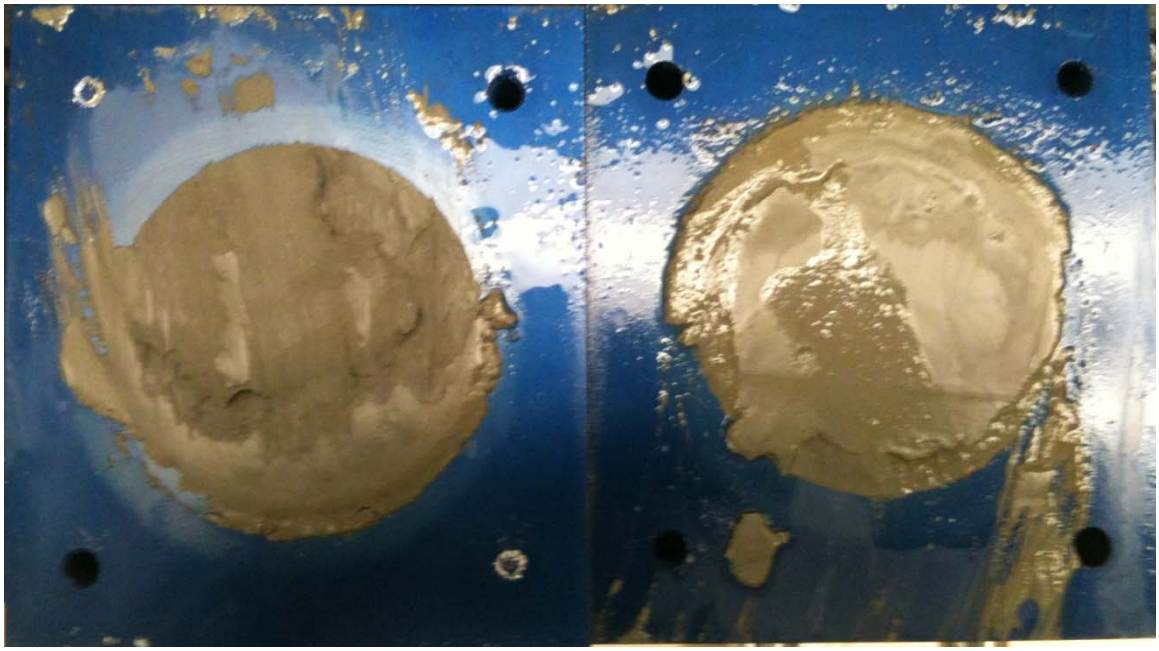

Texas 6 - Blenderized - 4516 psf

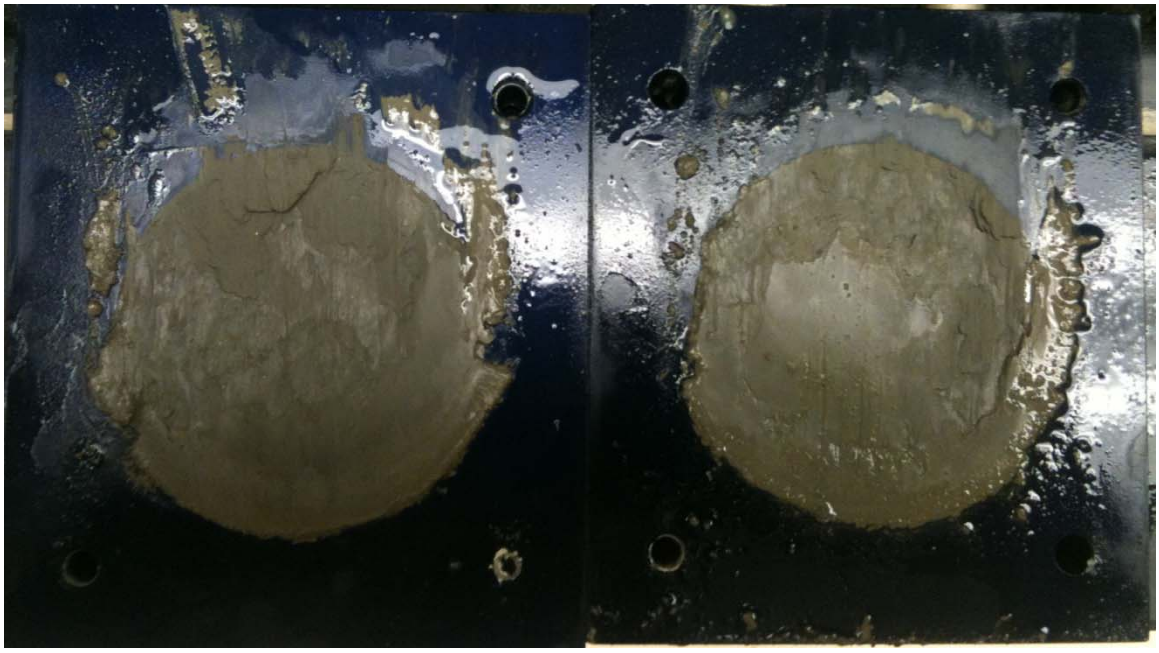

Texas 6 - Blenderized - 6016 psf

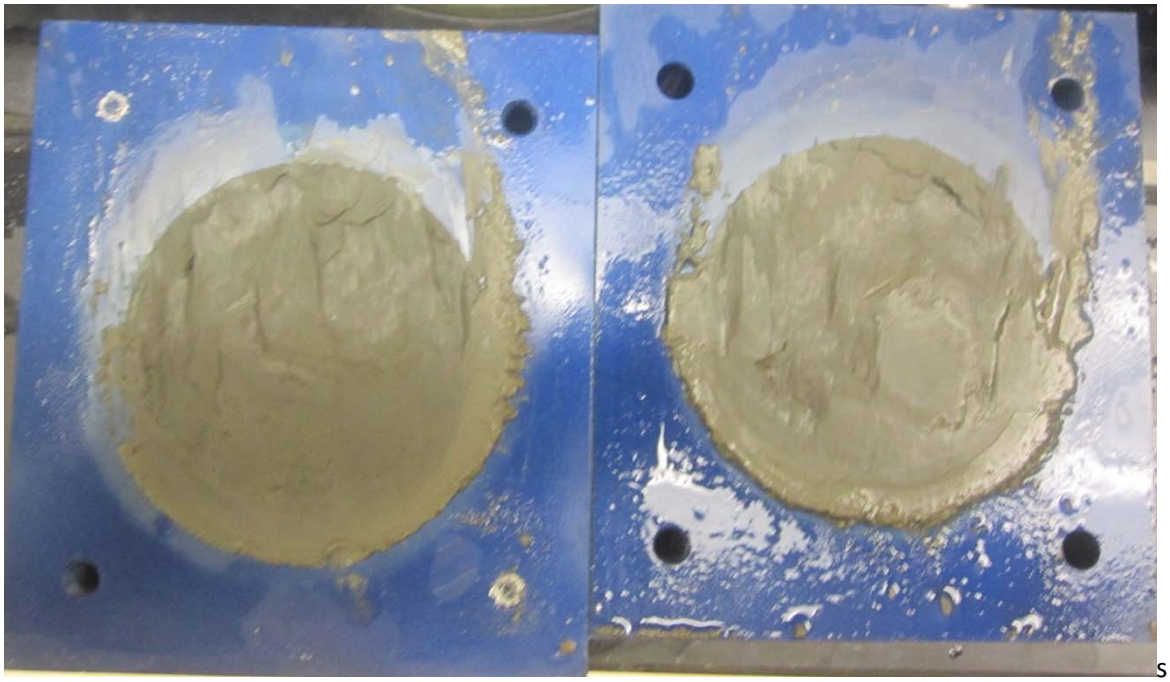

s

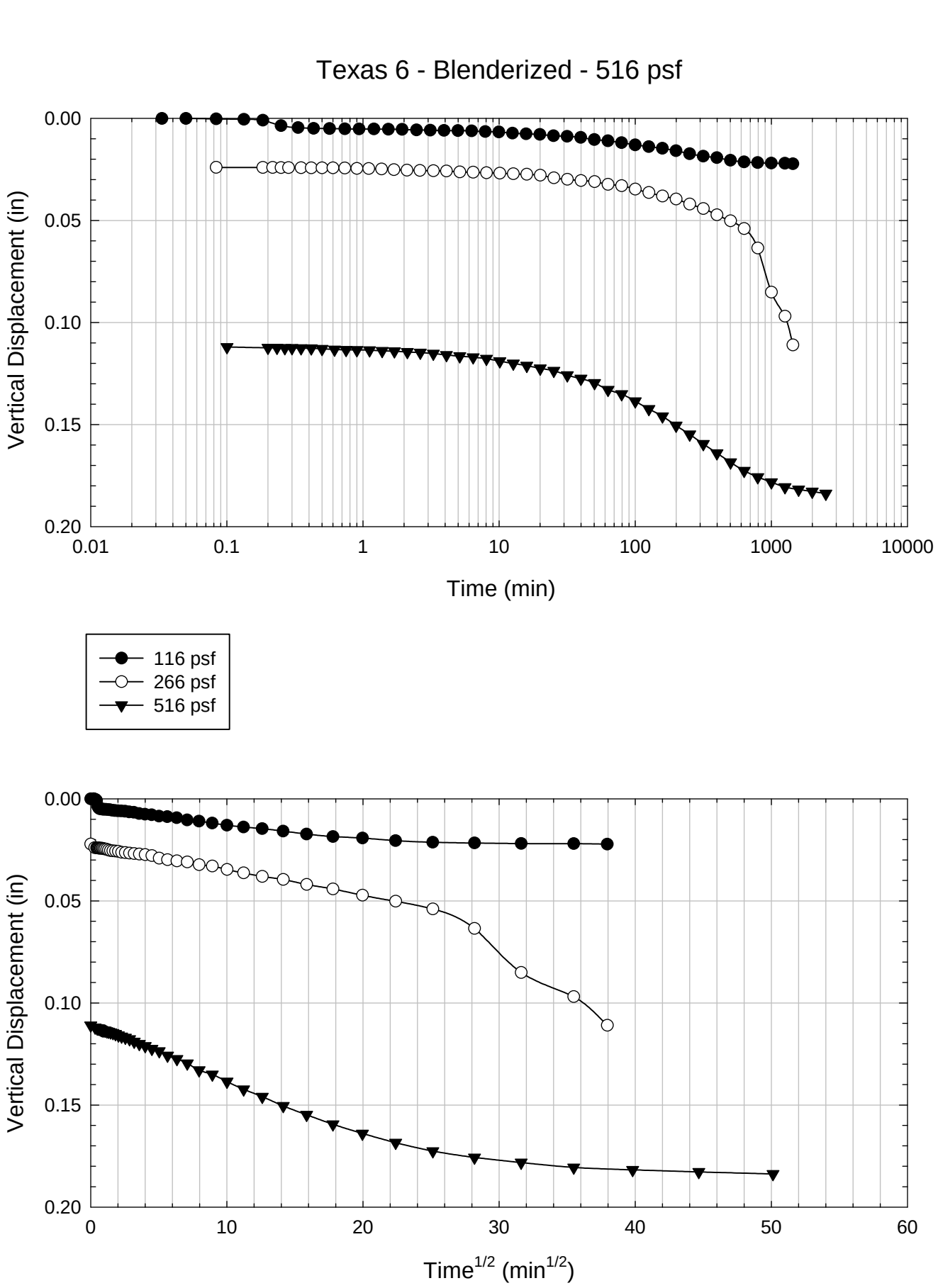
Texas 6 - Blenderized - 516 psf
Vertical Displacement (in)
0.00
0.05
0.10
0.15
0.20
0.01
0.1
1
10
100
1000
10000
Time (min)
116 psf
266 psf
516 psf
Vertical Displacement (in)
0.00
0.05
0.10
0.15
0.20
0
10
20
30
40
50
60
Time1/2 (min1/2)

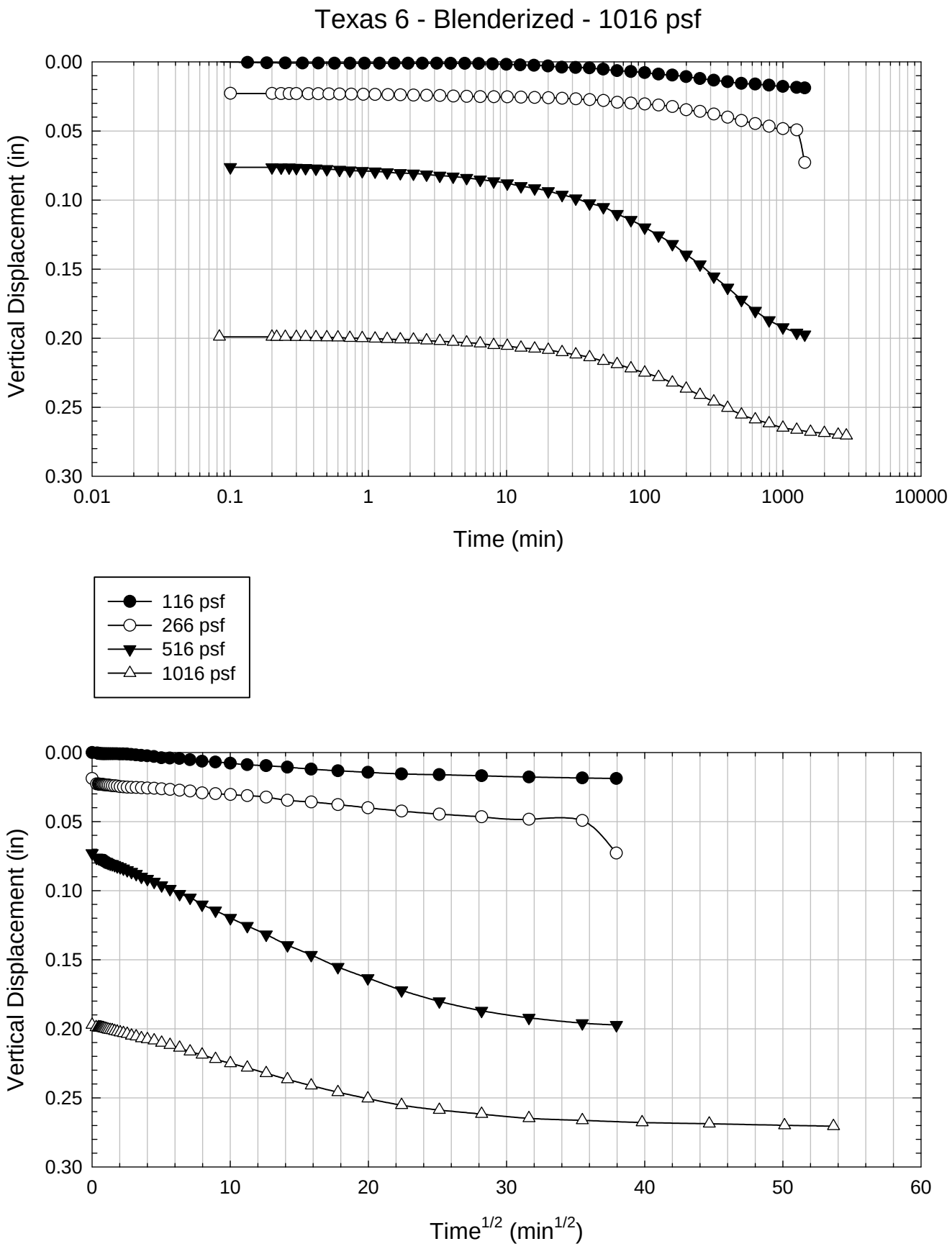
Texas 6 - Blenderized - 1016 psf
Vertical Displacement (in)
0.00
0.05
0.10
0.15
0.20
0.25
0.30
0.01
0.1
1
10
100
1000
10000
Time (min)
116 psf
266 psf
516 psf
1016 psf
Vertical Displacement (in)
0.00
0.05
0.10
0.15
0.20
0.25
0.30
0
10
20
30
40
50
60
Time^1/2 (min^1/2)

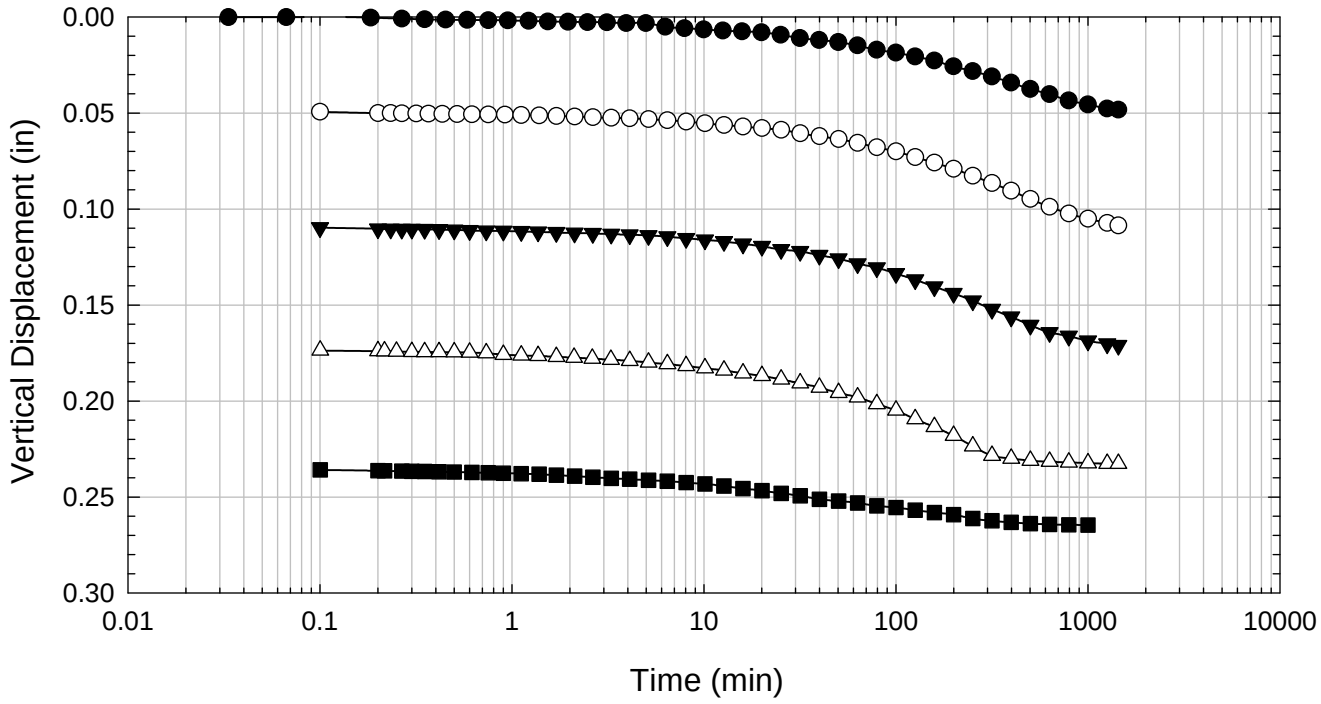
Texas 6 - Blenderized - 2016 psf
Vertical Displacement (in)
0.00
0.05
0.10
0.15
0.20
0.25
0.30
0.01
0.1
1
10
100
1000
10000
Time (min)

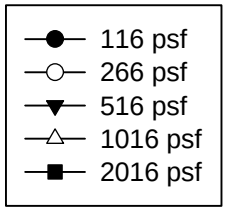
116 psf
266 psf
516 psf
1016 psf
2016 psf

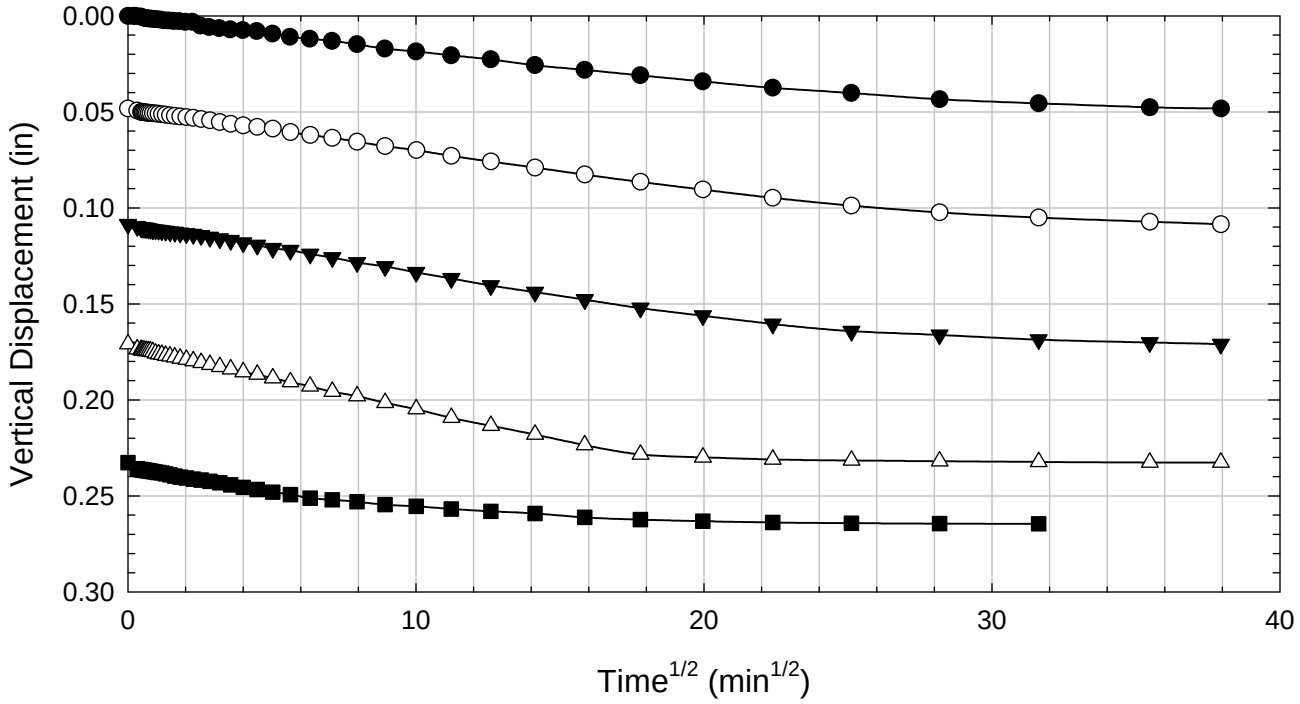
Vertical Displacement (in)
0.00
0.05
0.10
0.15
0.20
0.25
0.30
0
10
20
30
40
Time1/2 (min1/2)

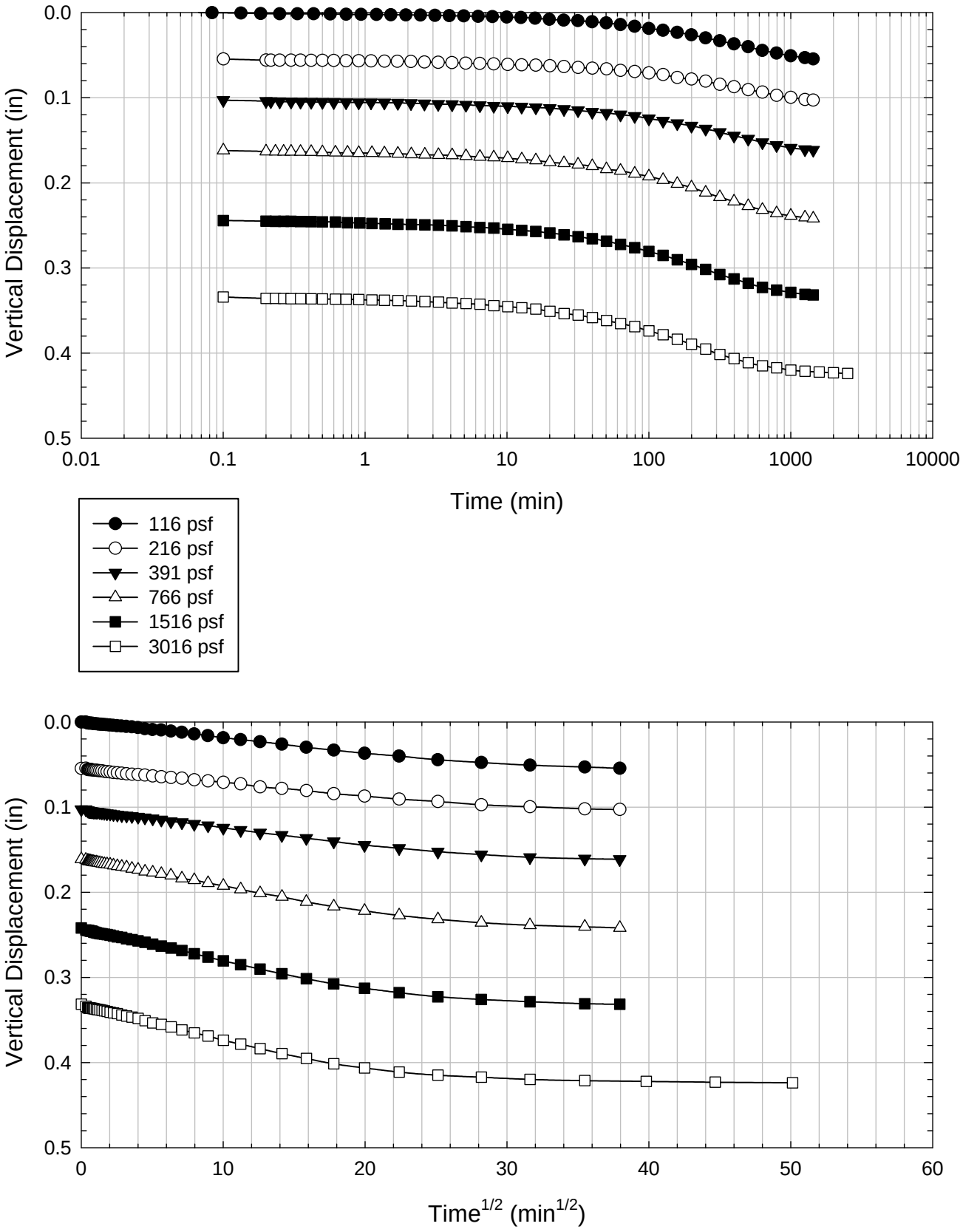
Texas 6 - Blenderized - 3016 psf
Vertical Displacement (in)
0.0
0.1
0.2
0.3
0.4
0.5
0.01
0.1
1
10
100
1000
10000
Time (min)
116 psf
216 psf
391 psf
766 psf
1516 psf
3016 psf
Vertical Displacement (in)
0.0
0.1
0.2
0.3
0.4
0.5
0
10
20
30
40
50
60
Time^1/2 (min^1/2)

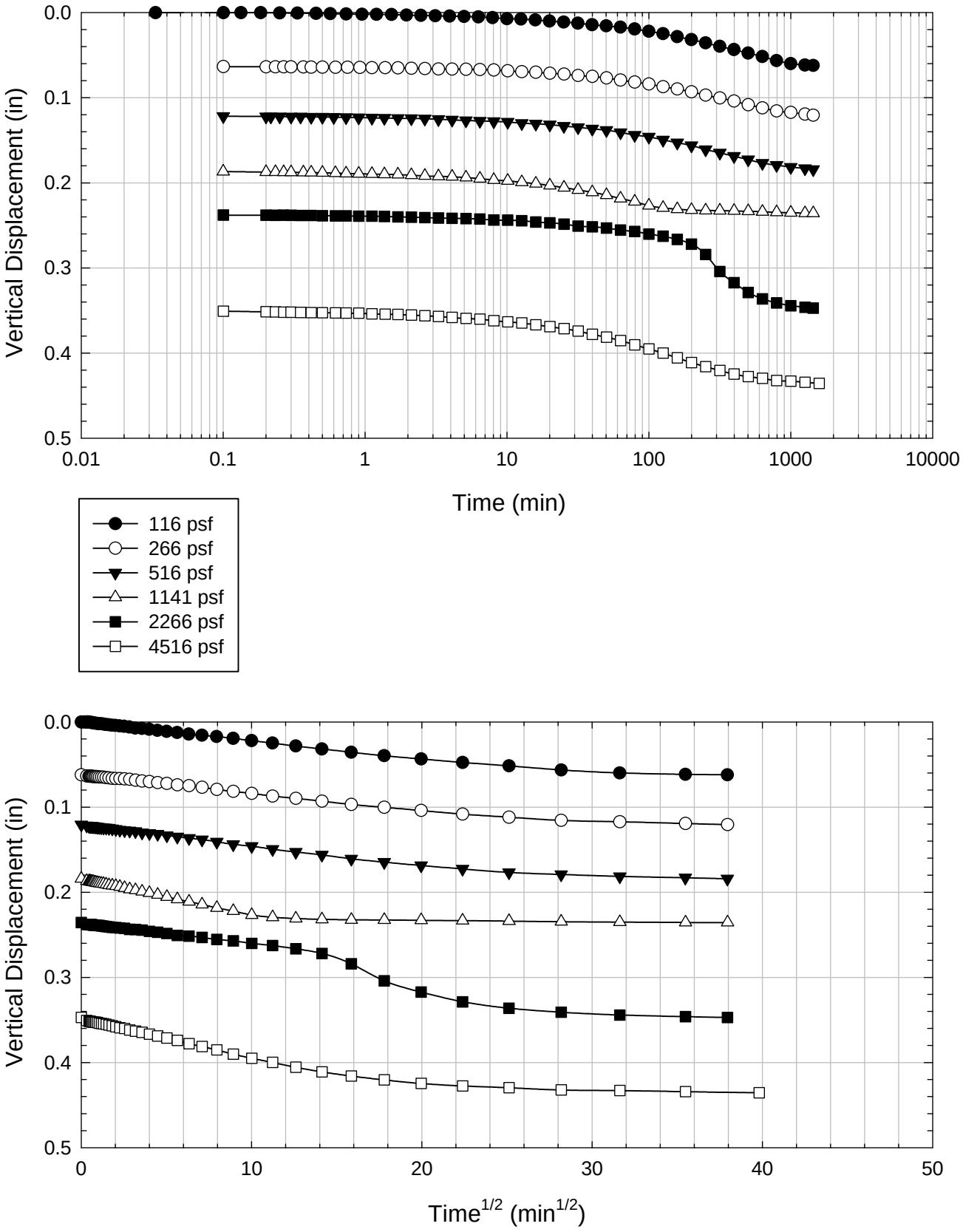
Texas 6 - Blenderized - 4516 psf
Vertical Displacement (in)
0.0
0.1
0.2
0.3
0.4
0.5
0.01
0.1
1
10
100
1000
10000
Time (min)
116 psf
266 psf
516 psf
1141 psf
2266 psf
4516 psf
Vertical Displacement (in)
0.0
0.1
0.2
0.3
0.4
0.5
0
10
20
30
40
50
Time1/2 (min1/2)

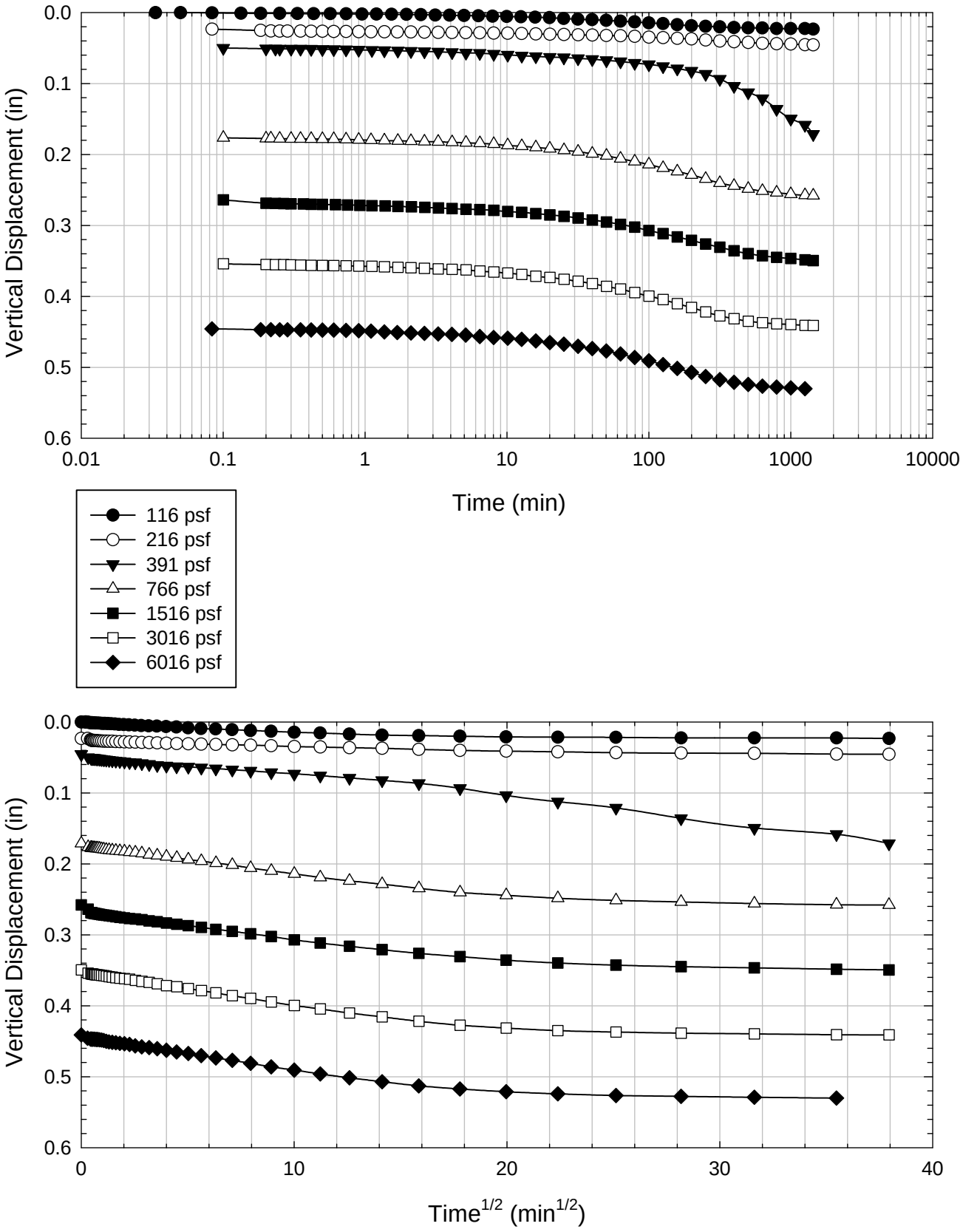
Texas 6 - Blenderized - 6016 psf
Vertical Displacement (in)
0.0
0.1
0.2
0.3
0.4
0.5
0.6
0.01
0.1
1
10
100
1000
10000
Time (min)
116 psf
216 psf
391 psf
766 psf
1516 psf
3016 psf
6016 psf
Vertical Displacement (in)
0
10
20
30
40
Time^1/2 (min^1/2)

Texas 6 - Blenderized

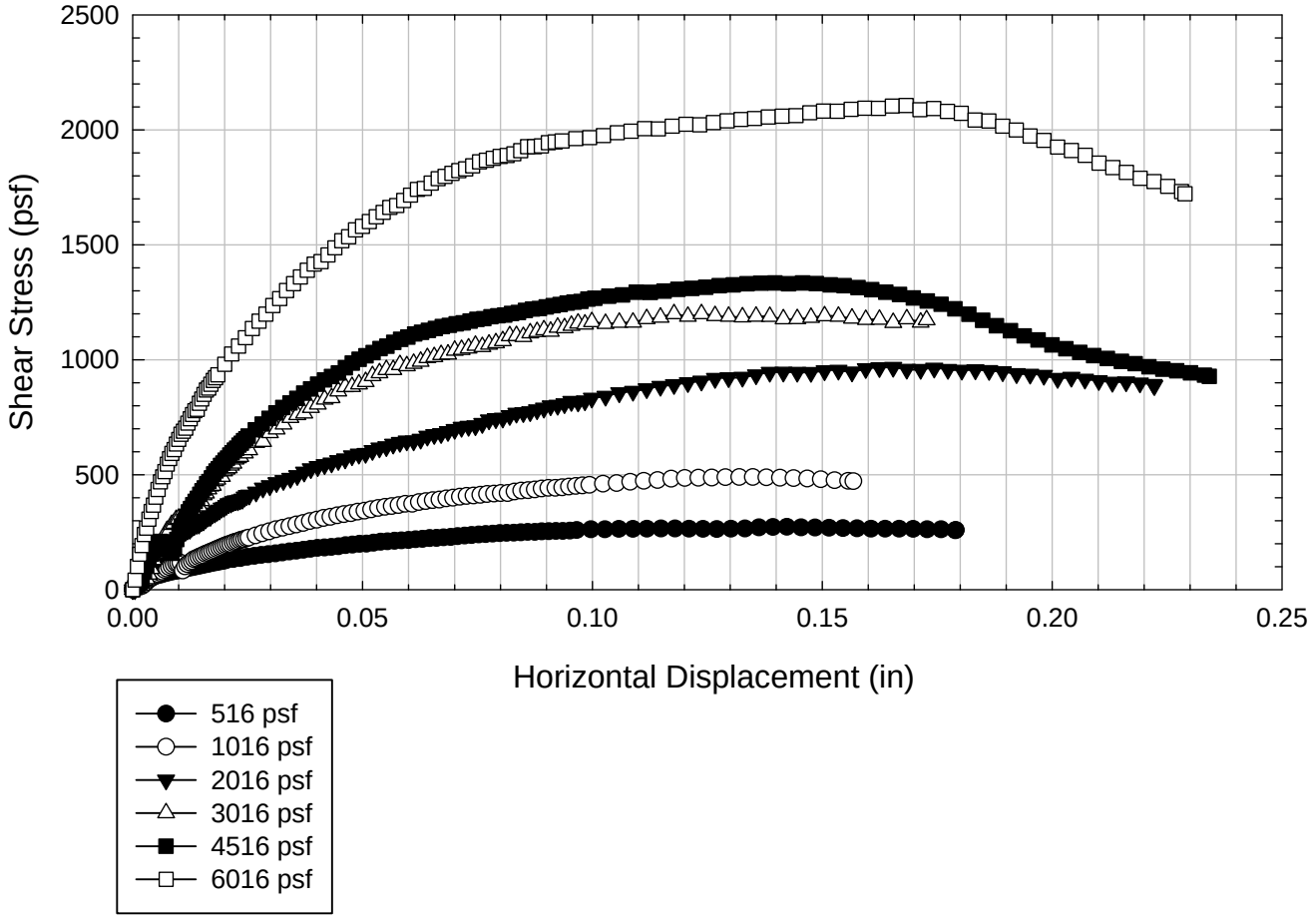

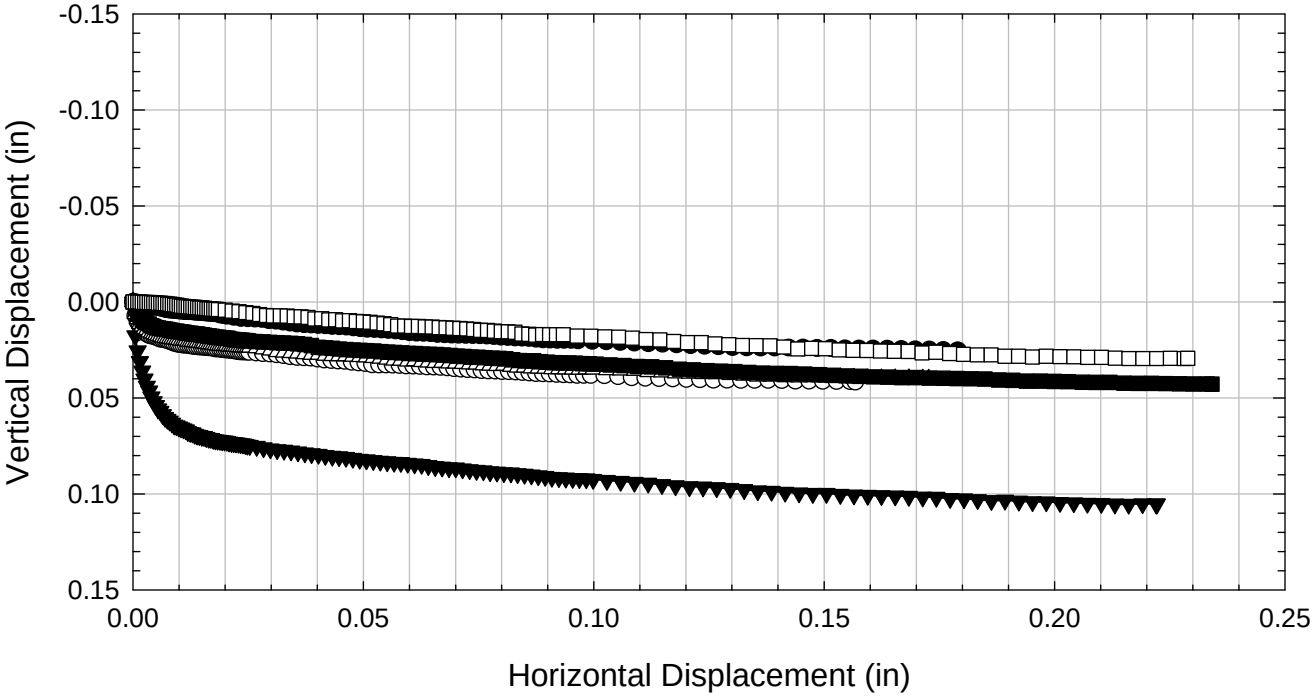

C.15. VBC

C.15.1 Blenderized

Virginia Polytechnic Institute and State University
Geotechnical Engineering Laboratory
Direct Shear Data Sheet

Project:	Fully Softened Shear Strength
Sample I.D./Loc.:	VBC - Blenderized
Classification:	Fat Clay (CH)

Sample Preparation	Remolded at LL		Specific Gravity	2.79

Test Number	1	2	3	4	5	6	7	8
Start Date (m/d/y)	10/11/2011	10/11/2011	10/15/2011	10/11/2011	10/11/2011	10/11/2011		
End Date (m/d/y)	10/31/2011	10/31/2011	10/31/2011	10/25/2011	10/25/2011	10/26/2011		
Consolidation Pressure (psf)	516	1016	2016	3016	4516	6016		
Initial Values								
Initial Height (in)	1.43	1.44	1.44	1.41	1.41	1.46		
Initial Diameter (in)	2.50	2.50	2.50	2.50	2.50	2.50		
Initial Sample Weight (g)	173	177	175	173	179	175		
Water Content (%)	92.87	93.89	93.56	93.67	91.72	93.89		
Dry Unit Weight (pcf)	48.7	49.1	48.6	49.3	51.5	48.0		
Wet Unit Weight (pcf)	94.0	95.2	94.1	95.4	98.7	93.2		
Consolidation Pressures								
Load 1 (psf)	116	116	116	116	116	116		
Load 2 (psf)	266	266	266	216	266	216		
Load 3 (psf)	516	516	516	416	516	391		
Load 4 (psf)		1016	1016	816	1141	766		
Load 5 (psf)			2016	1616	2266	1516		
Load 6 (psf)				3016	4516	3016		
Load 7 (psf)						6016		
t_{50}								
Max. t_{50} for Load 1 (min)								
Max. t_{50} for Load 2 (min)								
Max. t_{50} for Load 3 (min)	120.01							
Max. t_{50} for Load 4 (min)		165.86						
Max. t_{50} for Load 5 (min)			104.79					
Max. t_{50} for Load 6 (min)				120.61	96.39			
Max. t_{50} for Load 7 (min)						101.76		
Final Values								
Water Content (%)	69.34	58.59	53.22	50.00	44.91	42.21		
Dry Unit Weight (pcf)	60.7	65.7	75.7	76.2	82.8	83.48		
Wet Unit Weight (pcf)	102.8	104.2	116.0	114.3	120.0	118.71		
Failure								
Test Performed at Shear Rate (in/min)	1.67E-05	1.21E-05	1.91E-05	2.36E-05	2.07E-05	1.97E-05		
Required Shear Rate (in/min)	2.17E-05	2.05E-05	2.86E-05	2.49E-05	2.70E-05	2.75E-05		
Displacement at Failure (in)	0.13	0.17	0.15	0.15	0.13	0.14		
Peak Shear Stress (psf)	319	562	831	1170	1428	2120		
Total Change in Height at Failure (in)	0.28	0.40	0.51	0.49	0.53	0.62		
Secant Effective Friction Angle (deg)	31.7	28.9	22.4	21.2	17.5	19.4		

Comments: In the test consolidated at 1016 psf, the software crashed during shear and it was restarted.

VBC - Blenderized A - 516 psf

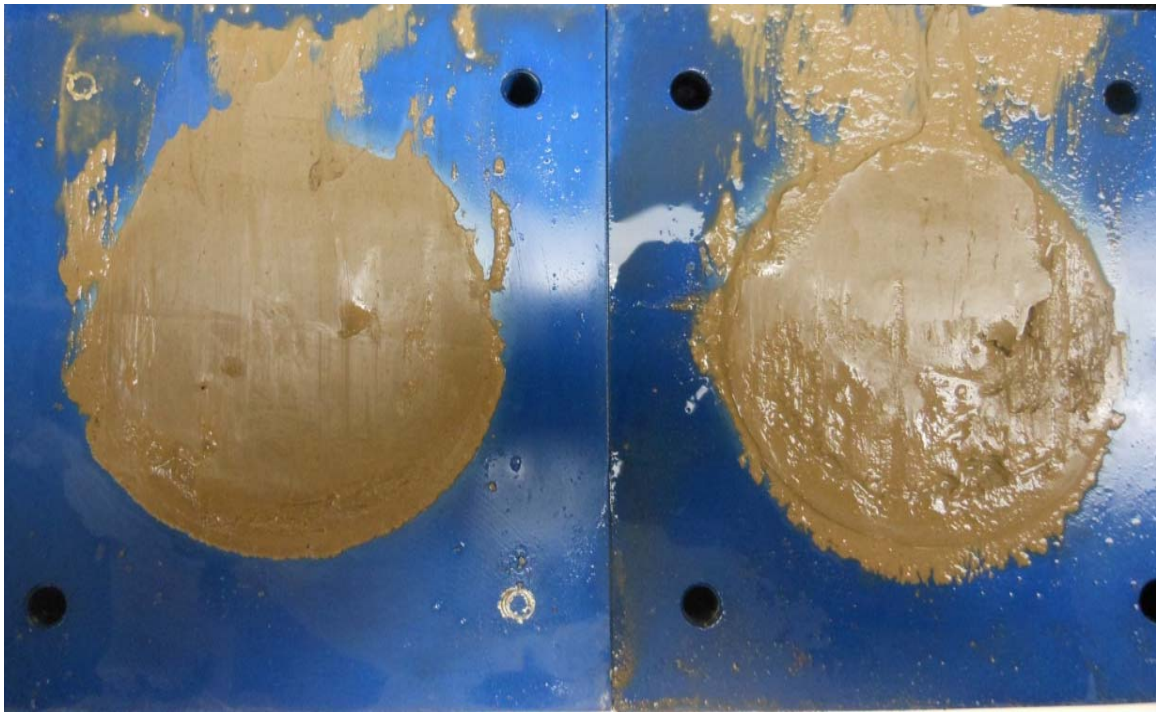

VBC - Blenderized A - 1016 psf

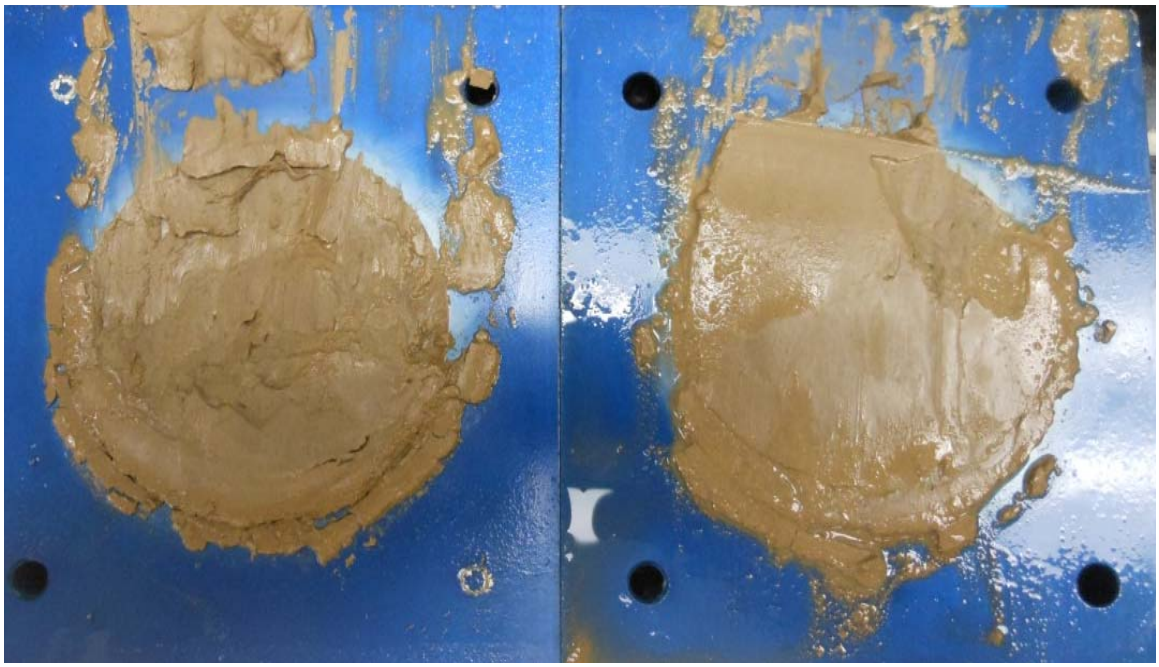

VBC - Blenderized A - 2016 psf

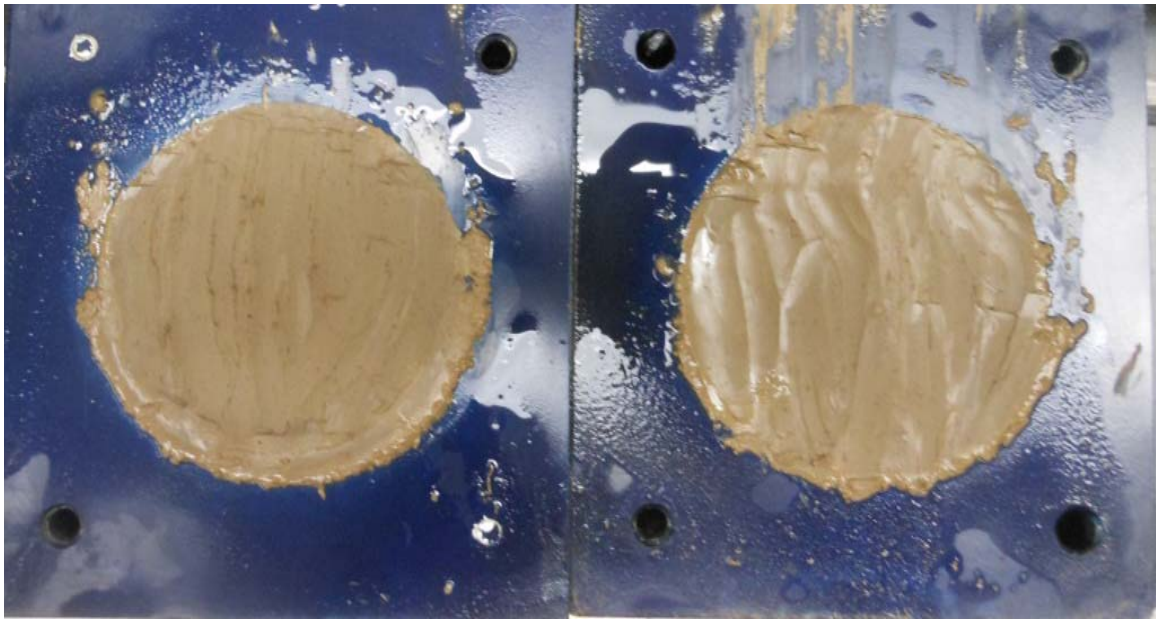

VBC - Blenderized A - 3016 psf

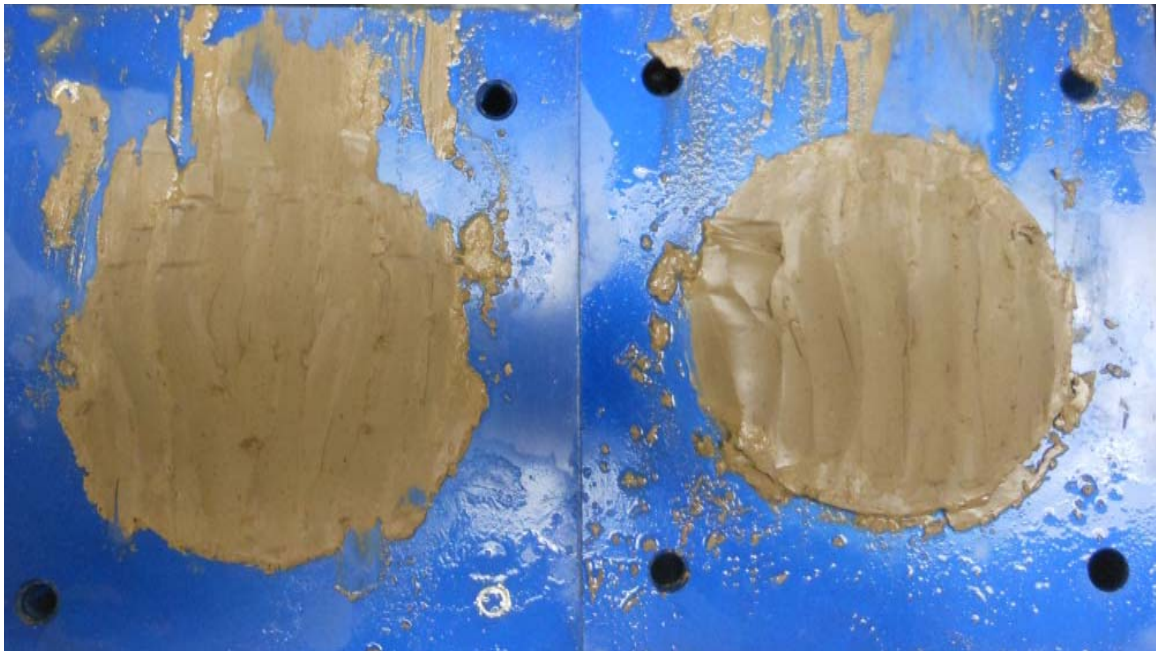

VBC - Blenderized A - 4516 psf

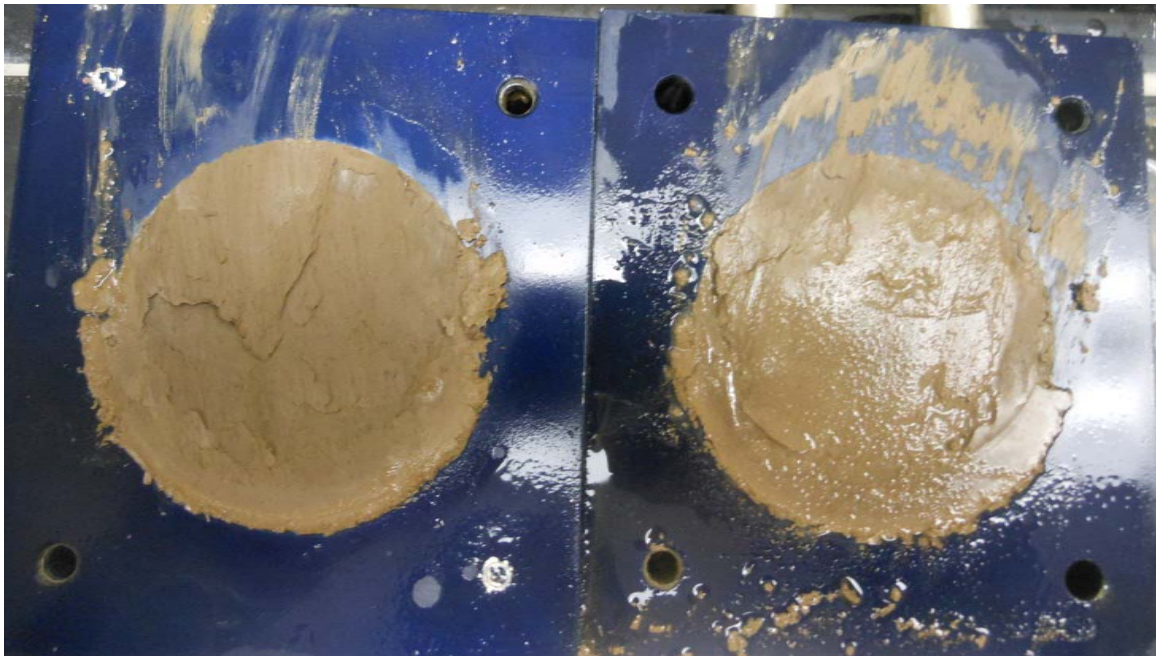

VBC - Blenderized A - 6016 psf

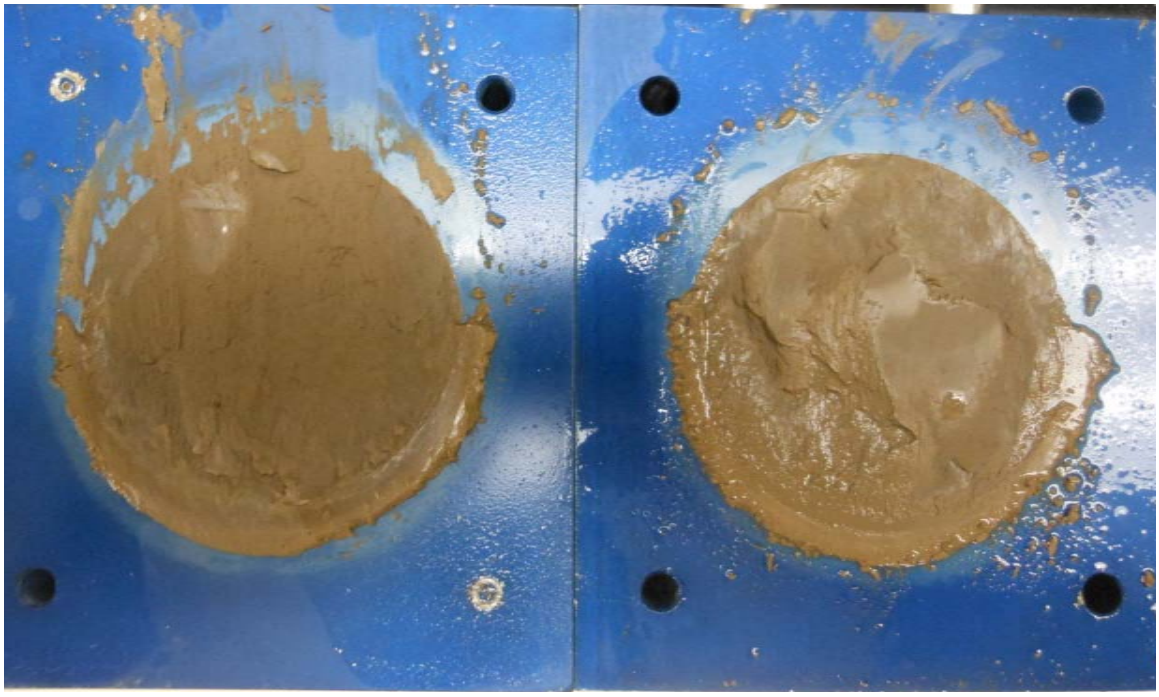

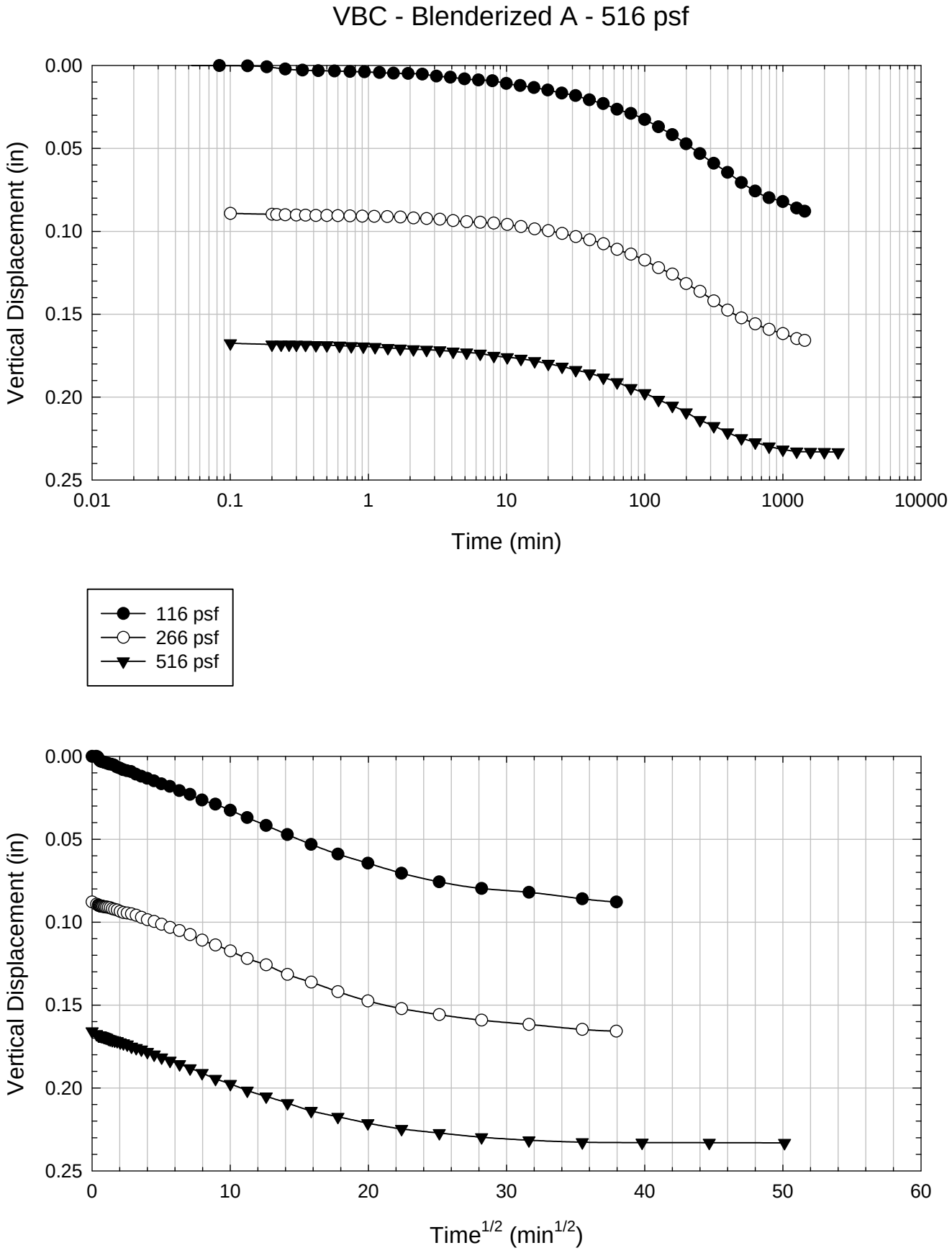
VBC - Blenderized A - 516 psf
Vertical Displacement (in)
0.00
0.05
0.10
0.15
0.20
0.25
0.01
0.1
1
10
100
1000
10000
Time (min)
116 psf
266 psf
516 psf
Vertical Displacement (in)
0.00
0.05
0.10
0.15
0.20
0.25
0
10
20
30
40
50
60
Time1/2 (min1/2)

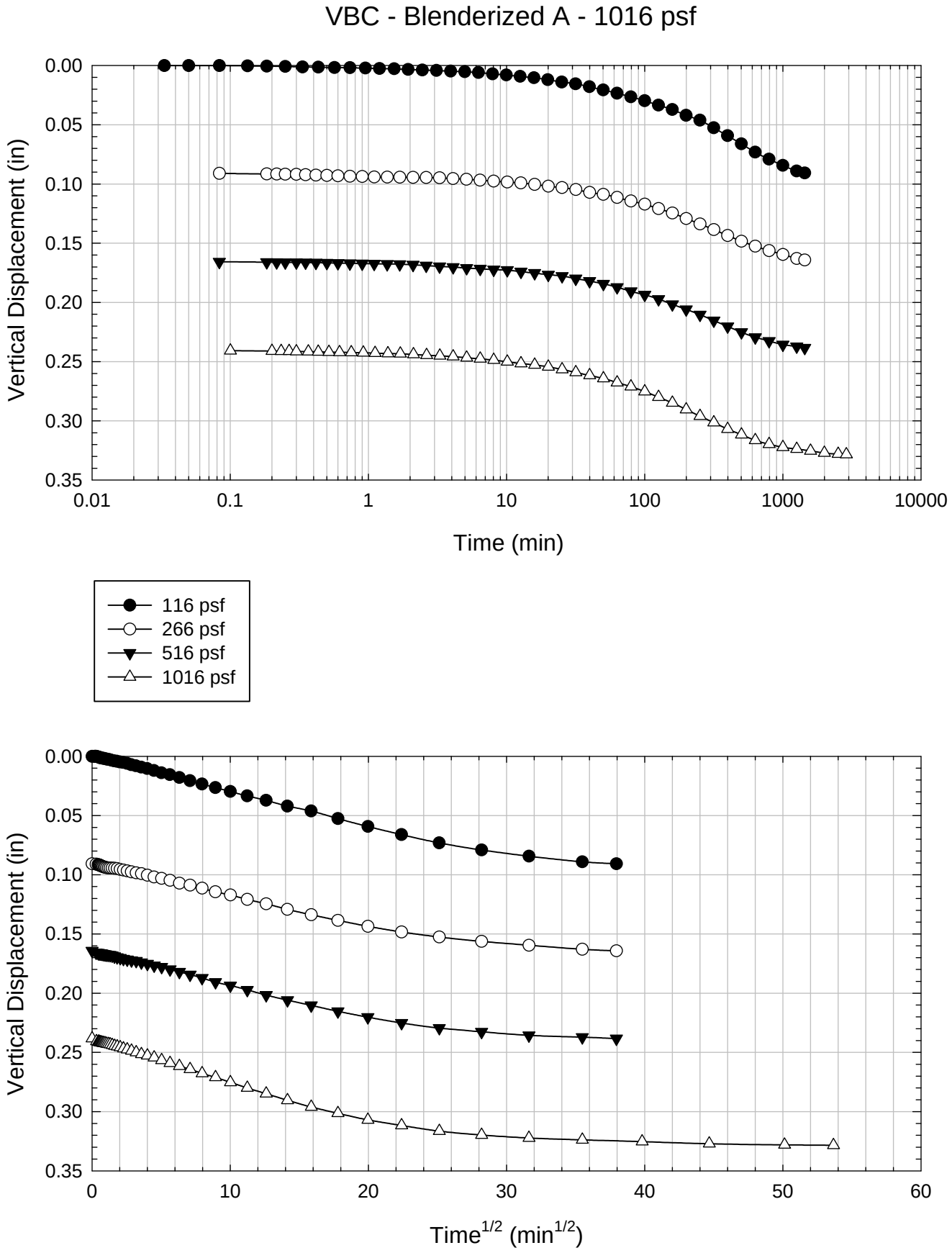
VBC - Blenderized A - 1016 psf
Vertical Displacement (in)
0.00
0.05
0.10
0.15
0.20
0.25
0.30
0.35
0.01
0.1
1
10
100
1000
10000
Time (min)
116 psf
266 psf
516 psf
1016 psf
Vertical Displacement (in)
0.00
0.05
0.10
0.15
0.20
0.25
0.30
0.35
0
10
20
30
40
50
60
Time^1/2 (min^1/2)

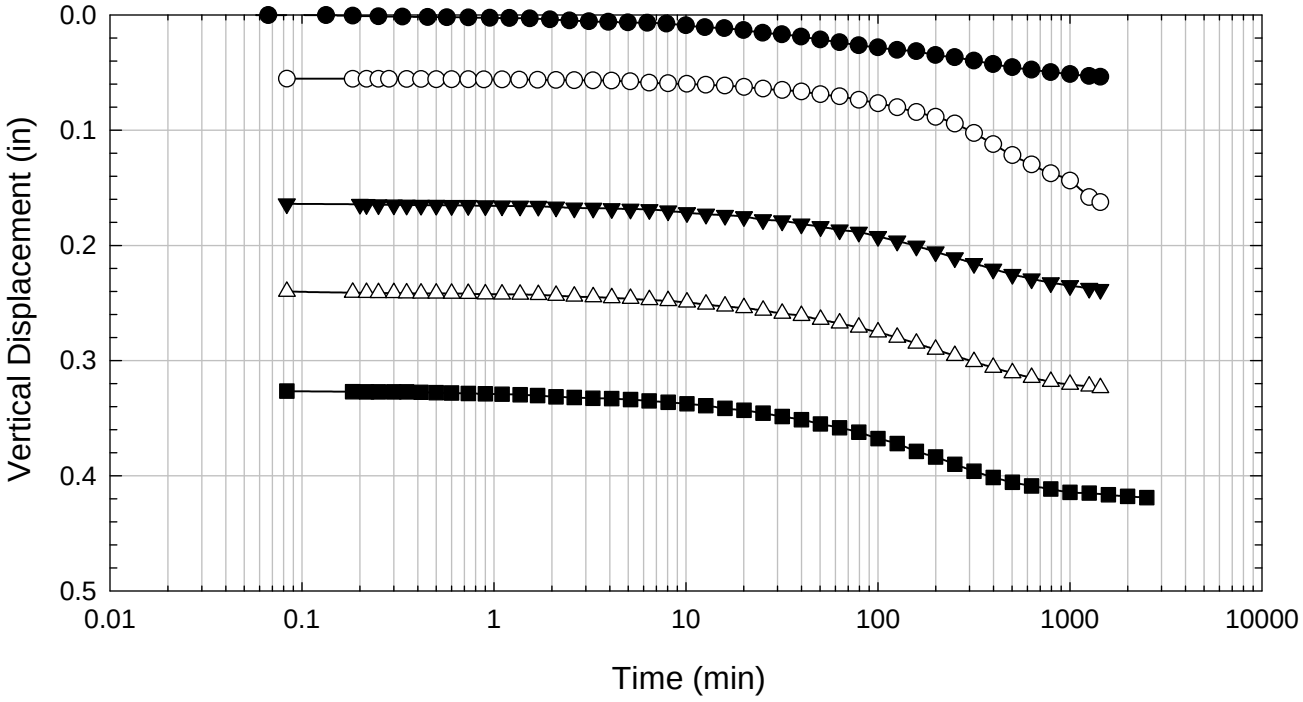
VBC - Blenderized A - 2016 psf
Vertical Displacement (in)
0.0
0.1
0.2
0.3
0.4
0.5
0.01
0.1
1
10
100
1000
10000
Time (min)

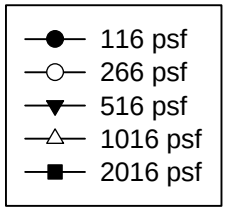
116 psf
266 psf
516 psf
1016 psf
2016 psf

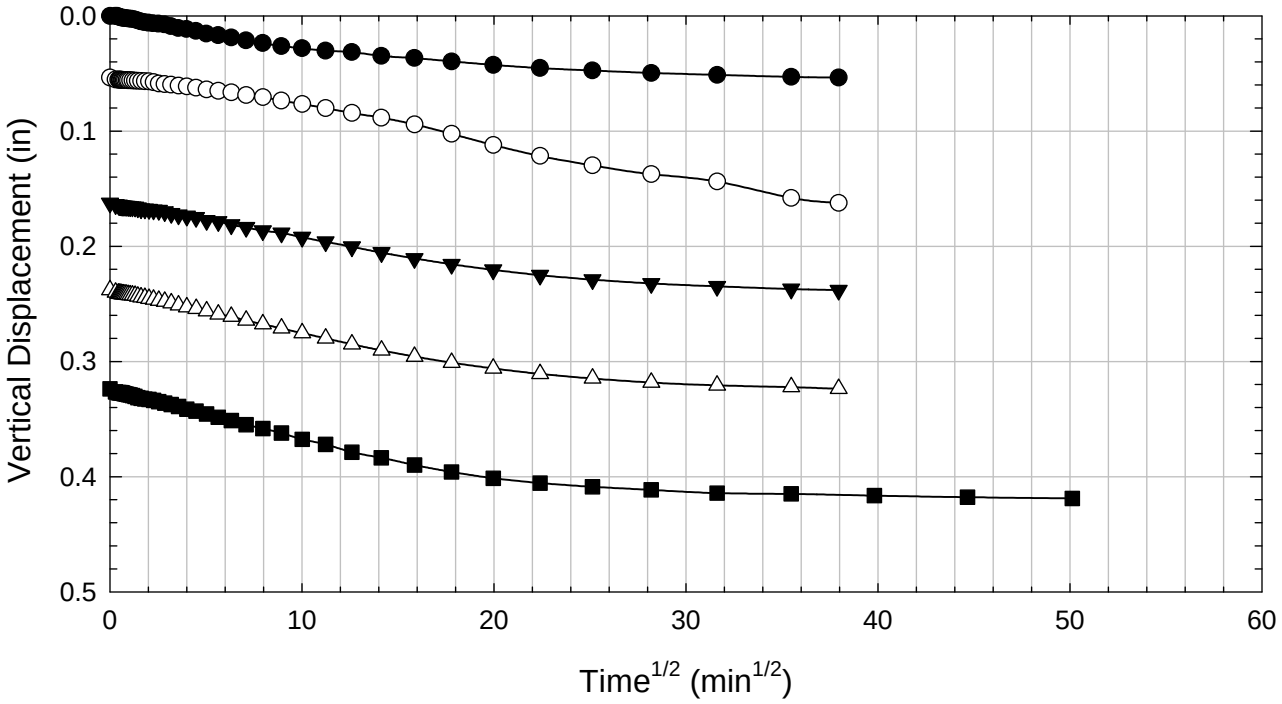
Vertical Displacement (in)
0.0
0.1
0.2
0.3
0.4
0.5
0
10
20
30
40
50
60
Time1/2 (min1/2)

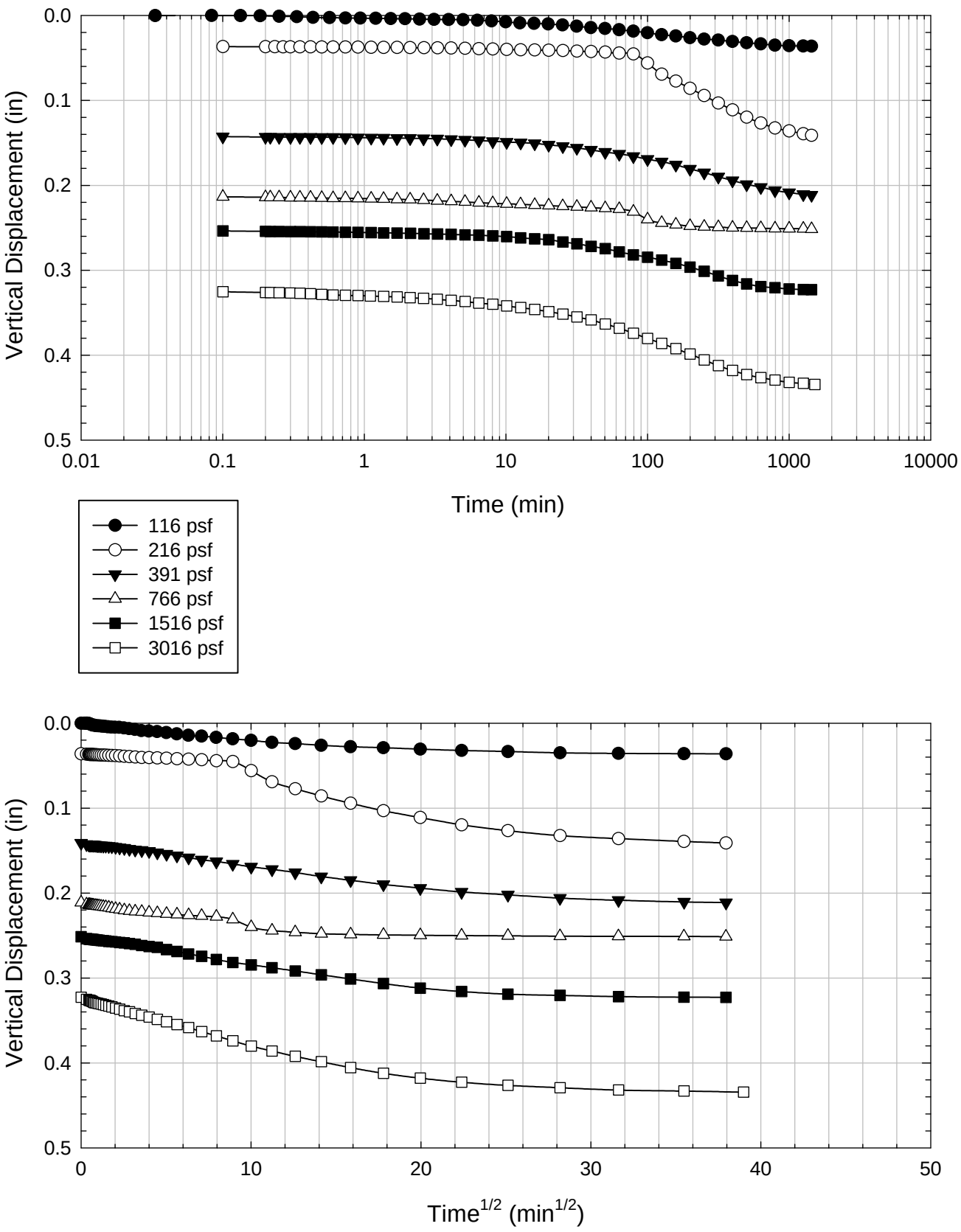
VBC - Blenderized A - 3016 psf
Vertical Displacement (in)
0.0
0.1
0.2
0.3
0.4
0.5
0.01
0.1
1
10
100
1000
10000
Time (min)
116 psf
216 psf
391 psf
766 psf
1516 psf
3016 psf
Vertical Displacement (in)
0.0
0.1
0.2
0.3
0.4
0.5
0
10
20
30
40
50
Time^1/2 (min^1/2)

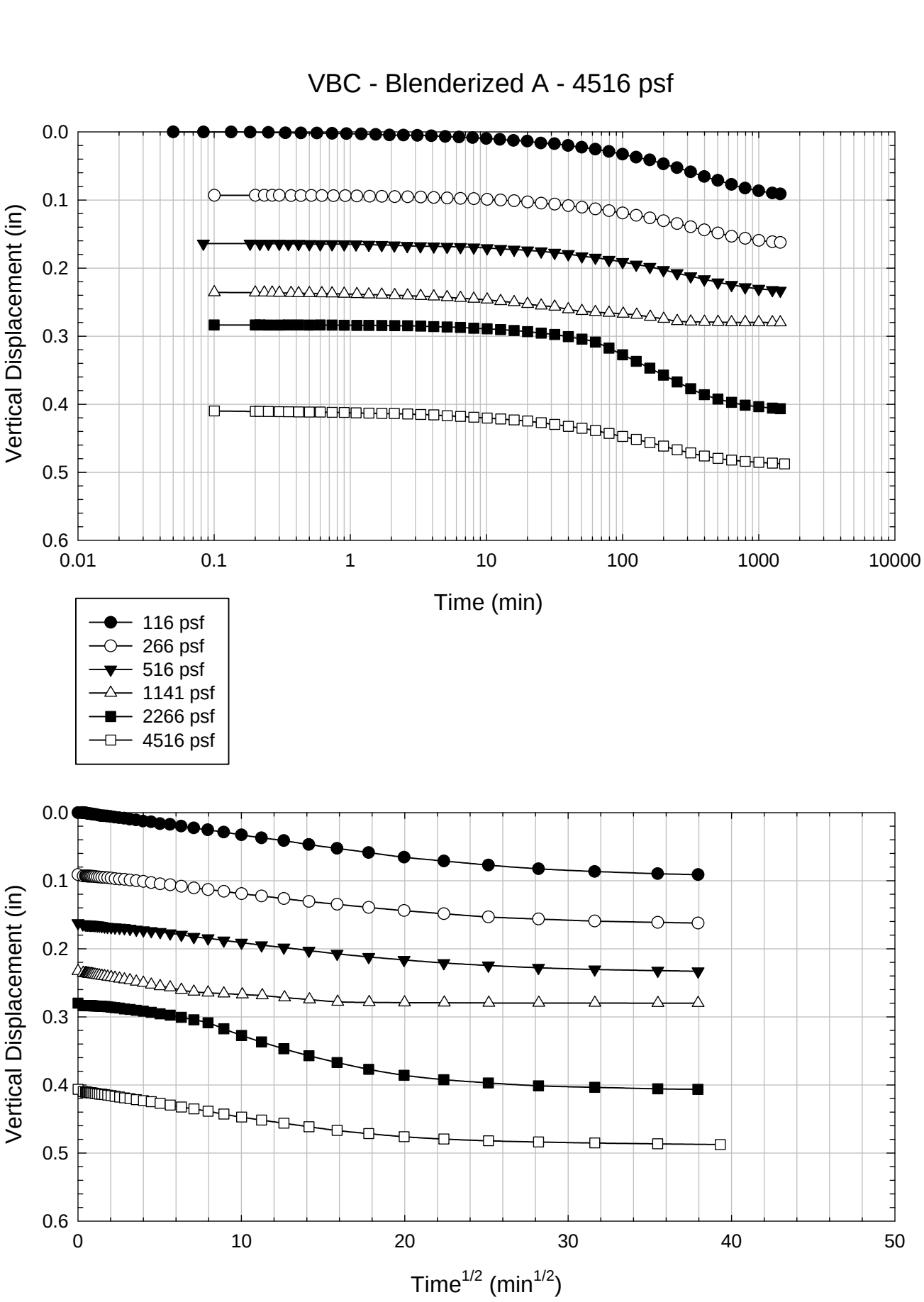
VBC - Blenderized A - 4516 psf
Vertical Displacement (in)
0.0
0.1
0.2
0.3
0.4
0.5
0.6
0.01
0.1
1
10
100
1000
10000
Time (min)
116 psf
266 psf
516 psf
1141 psf
2266 psf
4516 psf
Vertical Displacement (in)
0
10
20
30
40
50
Time^1/2 (min^1/2)

VBC - Blenderized A - 6016 psf

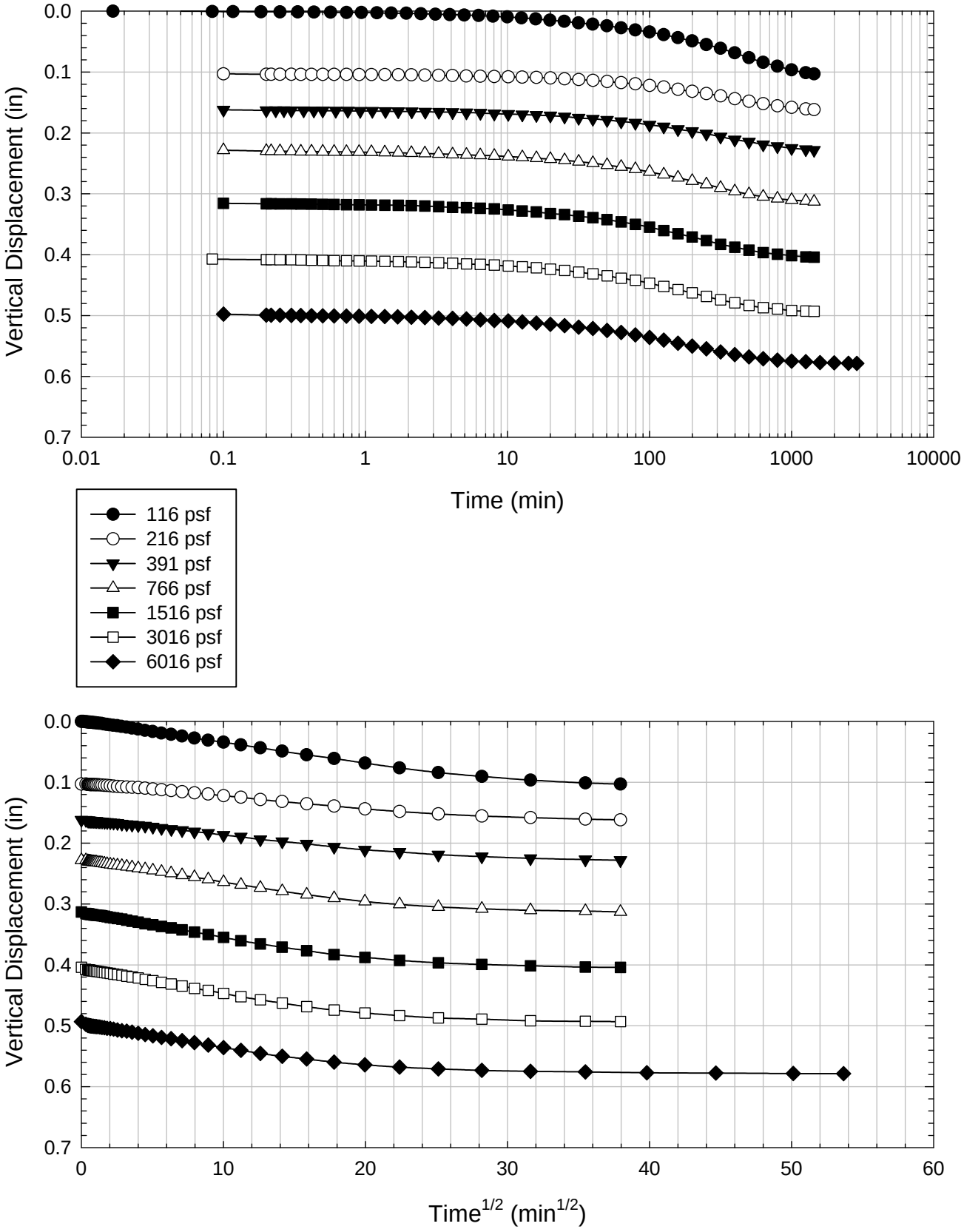

VBC - Blenderized A

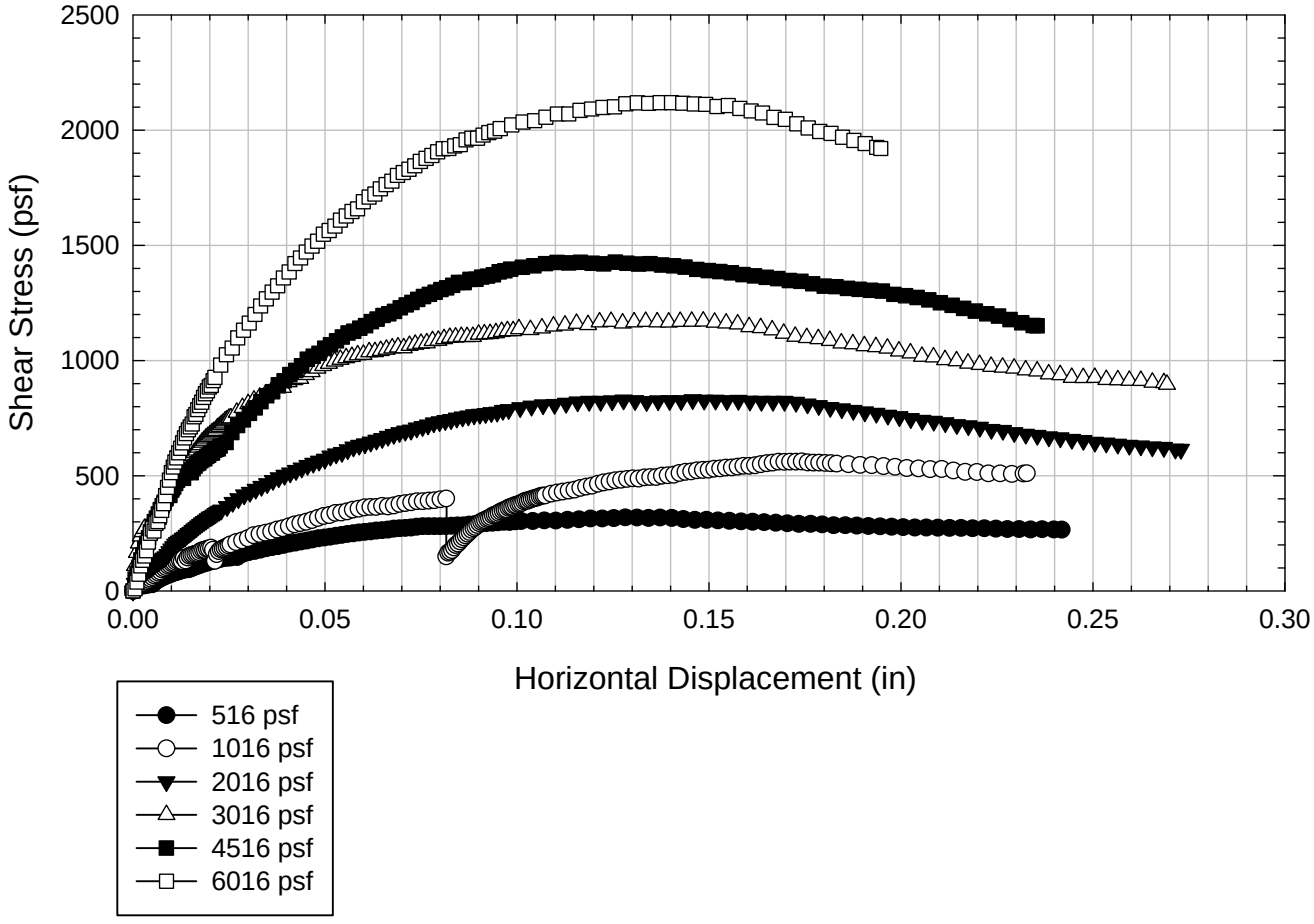

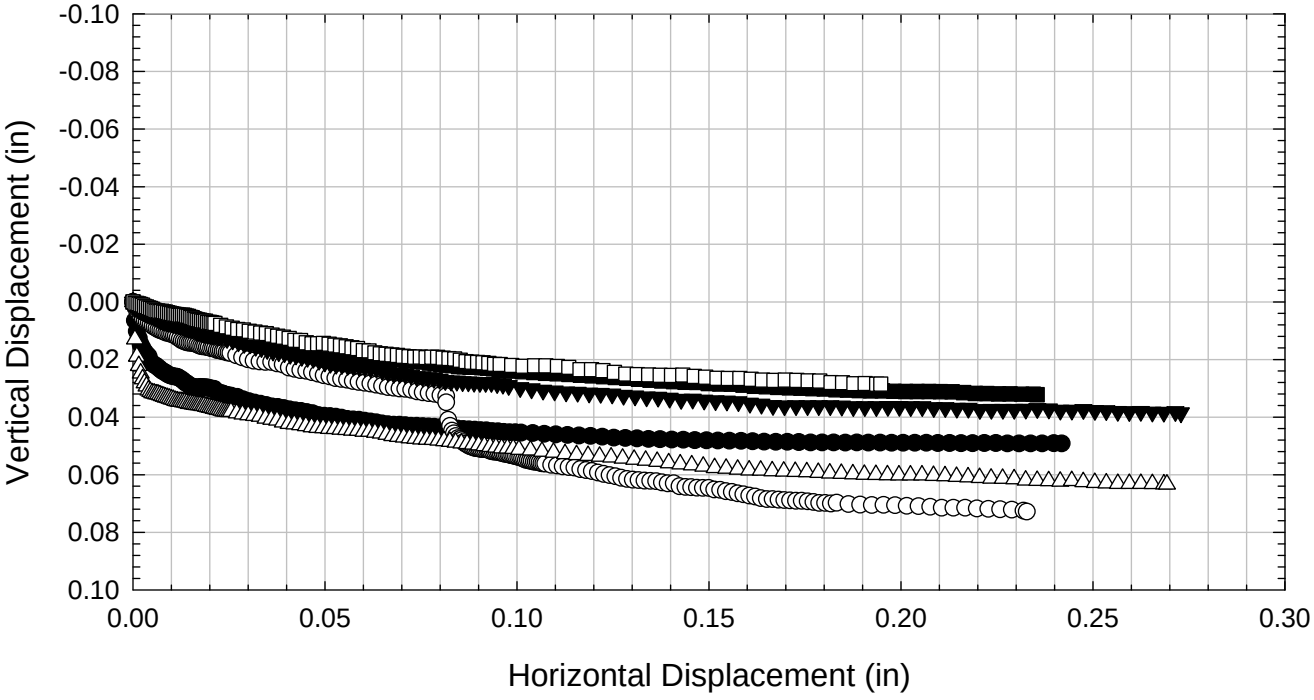

Virginia Polytechnic Institute and State University
Geotechnical Engineering Laboratory
Direct Shear Data Sheet

Project:	Fully Softened Shear Strength
Sample I.D./Loc.:	VBC - Blenderized
Classification:	Fat Clay (CH)

Sample Preparation	Remolded at LL		Specific Gravity	2.79	

Test Number	1	2	3	4	5	6	7	8	9
Start Date (m/d/y)	2/9/2011	4/8/2011	2/9/2011	4/5/2011	2/9/2011	5/10/2011	2/9/2011	8/26/2011	8/26/2011
End Date (m/d/y)	2/22/2011	4/26/2011	2/22/2011	4/26/2011	3/2/2011	5/24/2011	3/2/2011	9/10/2011	9/10/2011
Consolidation Pressure (psf)	516	766	1016	1516	2016	2516	3016	4516	6016
Initial Values									
Initial Height (in) (Assumed if = 1.44)	1.44	1.40	1.44	1.41	1.39	1.38	1.36	1.40	1.39
Initial Diameter (in)	2.50	2.50	2.50	2.50	2.50	2.50	2.50	2.50	2.50
Initial Sample Weight (g)	167	167		173	167	178	166	178	174
Water Content (%)	91.87	91.46	90.62	89.61	93.41	82.33	87.06	90.14	91.29
Dry Unit Weight (pcf)	46.9	48.4		50.2	48.3	54.8	50.6	51.95	50.7
Wet Unit Weight (pcf)	90.0	92.6		95.2	93.4	99.9	94.7	98.77	97.0
Consolidation Pressures									
Load 1 (psf)	116	116	116	116	116	116	116	116	116
Load 2 (psf)	266	216	216	216	216	266	216	266	216
Load 3 (psf)	516	391	566	416	416	532	416	516	391
Load 4 (psf)		766	1016	766	816	1266	816	1141	766
Load 5 (psf)				1516	1616	2516	1616	2266	1516
Load 6 (psf)					2016		3016	4516	3016
Load 7 (psf)									6016
t_{50}									
Max. t_{50} for Load 1 (min)	138,20		32.95		49.52		106.69		
Max. t_{50} for Load 2 (min)	161.79				80.03		123.11		
Max. t_{50} for Load 3 (min)	85.59		82.94	136.27	117.38		123.32		
Max. t_{50} for Load 4 (min)		13.90	93.17	136.80	14.32		51.93		
Max. t_{50} for Load 5 (min)					94.91	112.27			
Max. t_{50} for Load 6 (min)					185.14		199.30	92.83	
Max. t_{50} for Load 7 (min)									90.07
Final Values									
Water Content (%)	70.34	65.66	59.42	58.94	52.84	47.90	49.14	43.86	42.23
Dry Unit Weight (pcf)	57.2	63.3		67.4	74.6	77.69	86.63	83.37	77.01
Wet Unit Weight (pcf)	97.3	104.9		107.1	114.1	114.90	129.20	119.93	109.53
Failure									
Test Performed at Shear Rate (in/min)	2.30E-05	1.00E-05	2.08E-05	1.00E-05	1.31E-05	1.78E-05	1.00E-05	2.17E-05	2.27E-05
Required Shear Rate (in/min)	3.51E-05	2.16E-04	3.22E-05	2.63E-05	1.73E-05	1.96E-05	1.51E-05	2.59E-05	3.33E-05
Displacement at Failure (in)	0.15	0.15	0.15	0.18	0.16	0.11	0.15	0.12	0.15
Peak Shear Stress (psf)	301	405	624	736	835	889	1126	1551	1993
Total Change in Height at Failure (in)	0.29	0.33	0.21	0.26	0.45	0.40	0.50	0.52	0.47
Secant Effective Friction Angle (deg)	30.3	27.9	31.6	25.9	22.5	19.5	20.5	19.0	18.3

Comments:

VBC - Blenderized - 516 psf

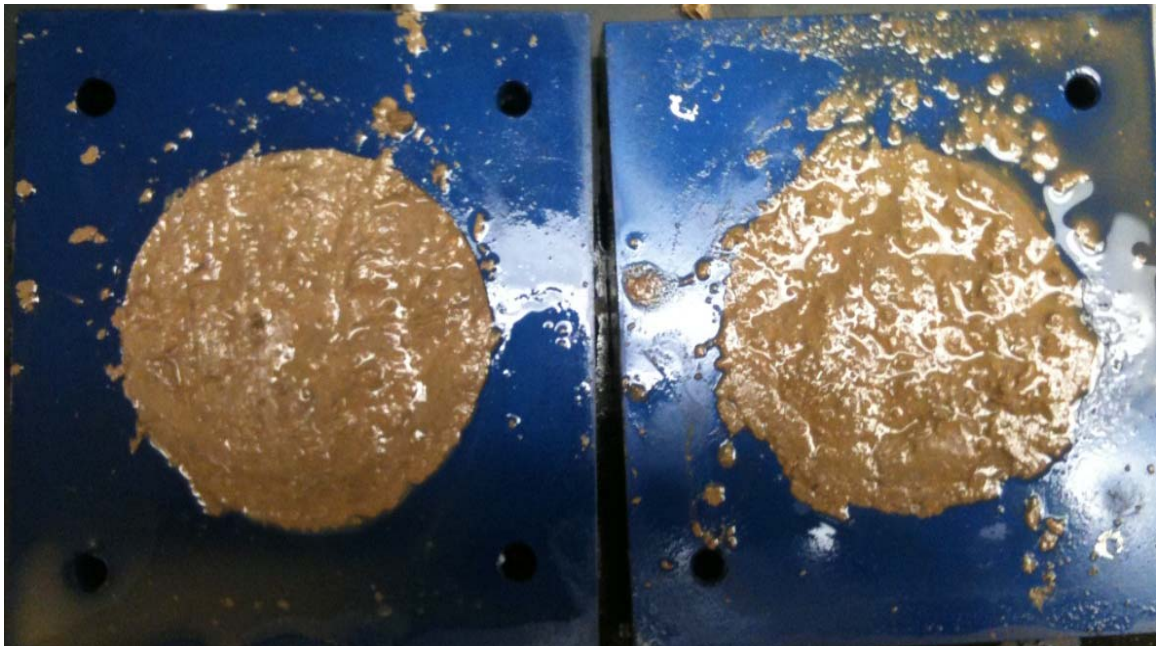

VBC - Blenderized - 766 psf

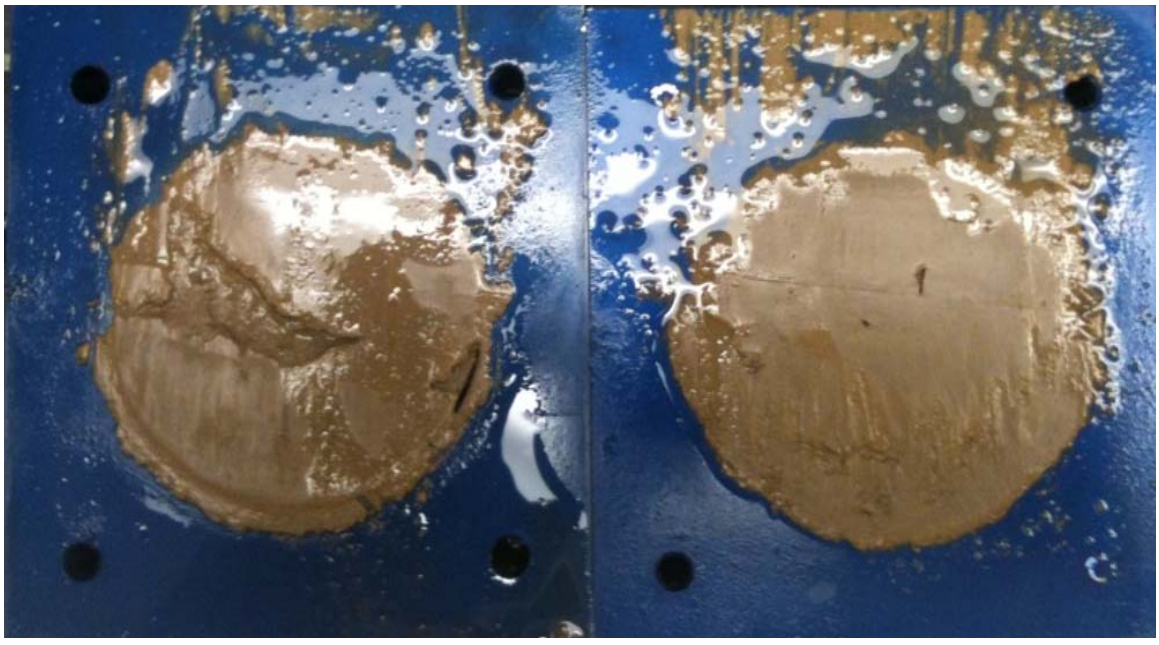

VBC - Blenderized - 1016 psf

VBC - Blenderized - 1516 psf

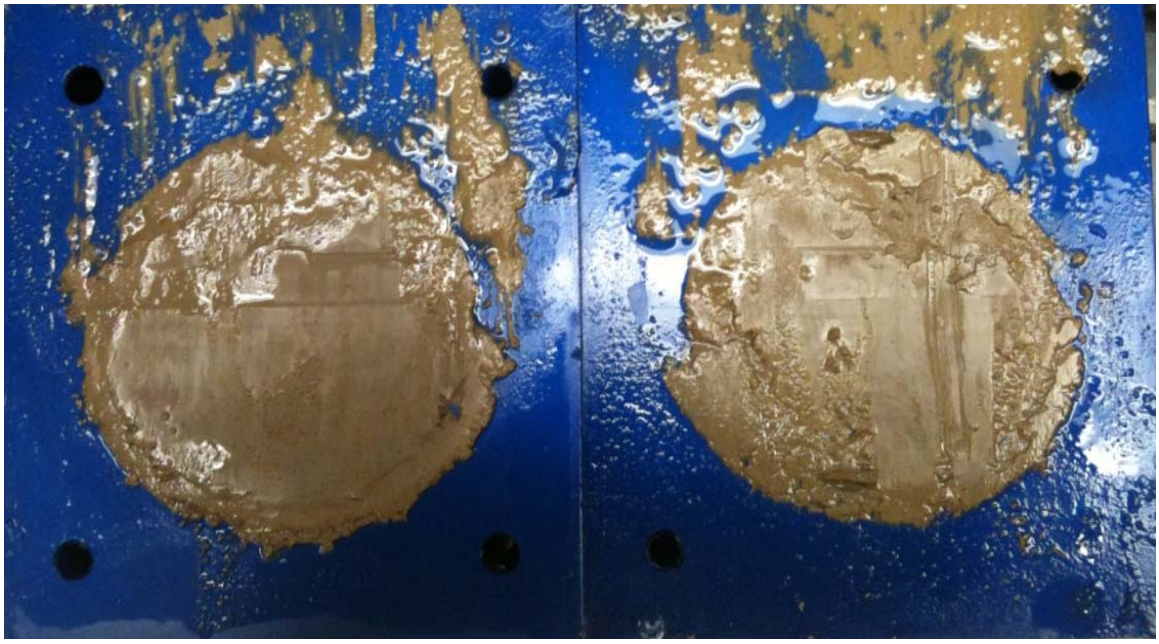

VBC - Blenderized - 2016 psf

VBC - Blenderized - 2516 psf

VBC - Blenderized - 3016 psf

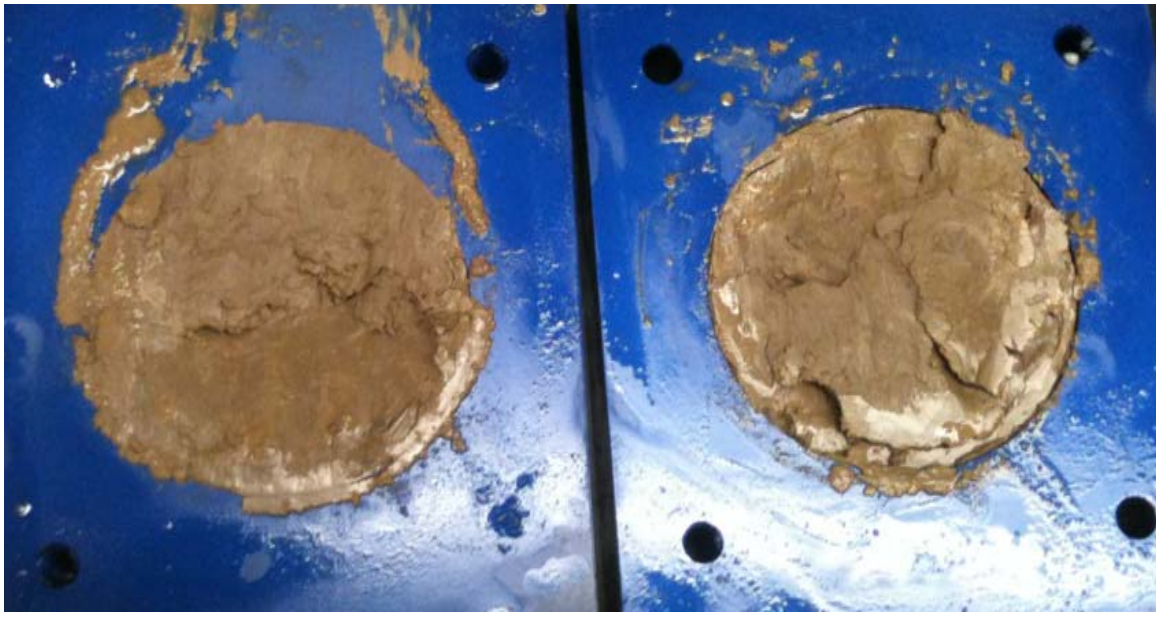

VBC - Blenderized - 4516 psf

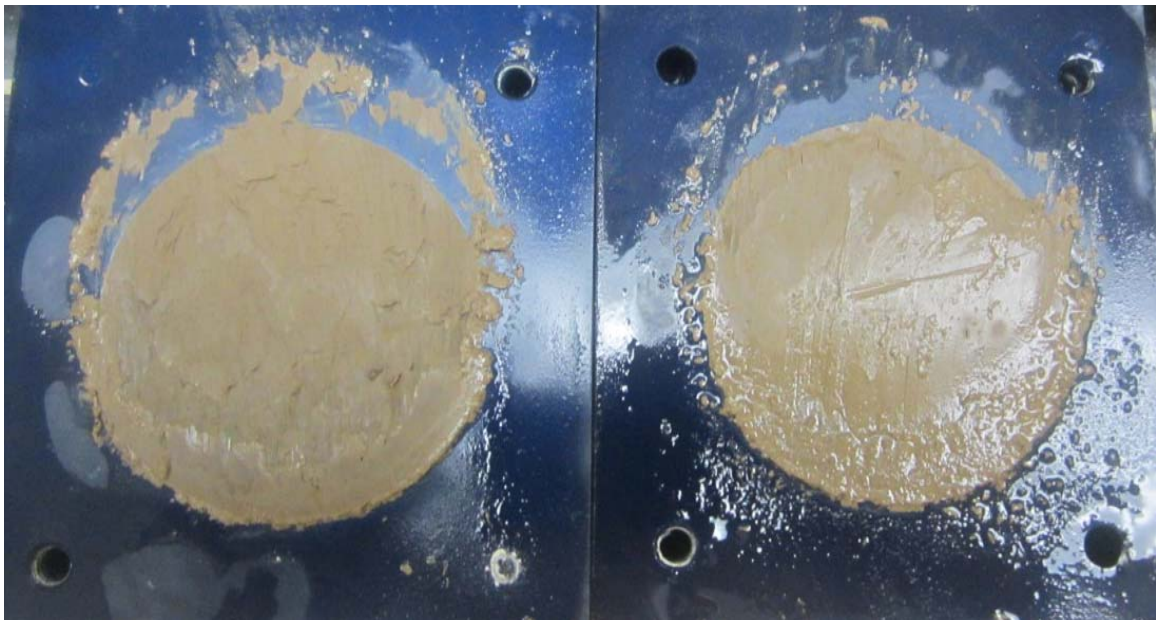

VBC - Blenderized - 6016 psf

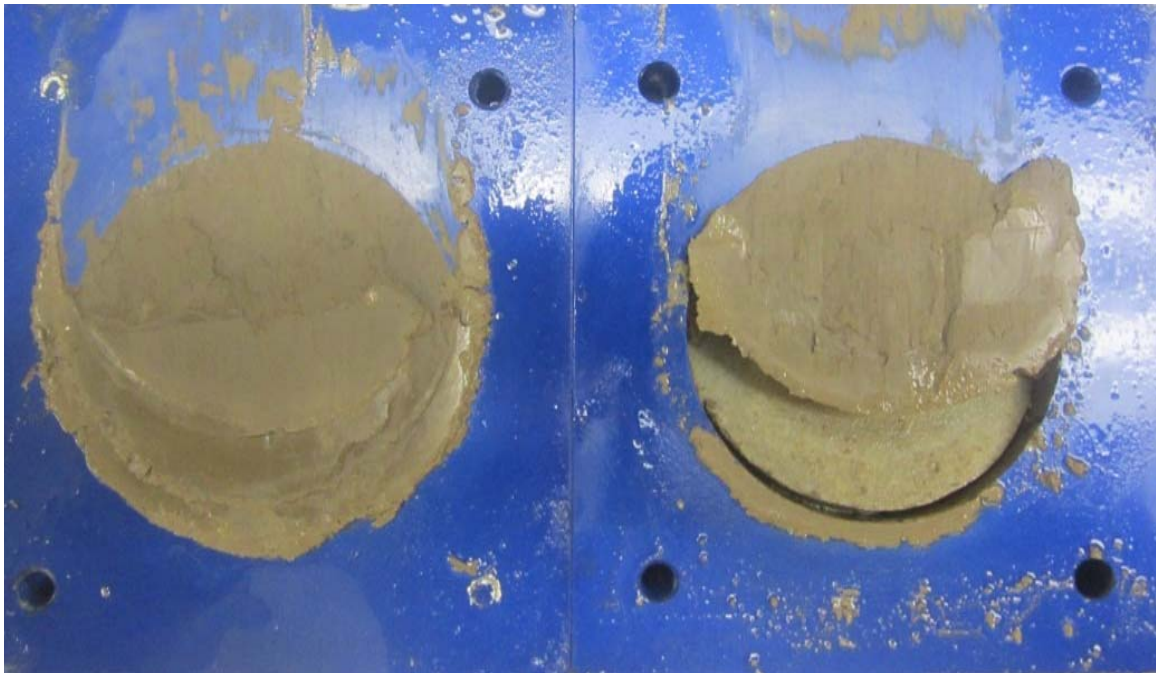

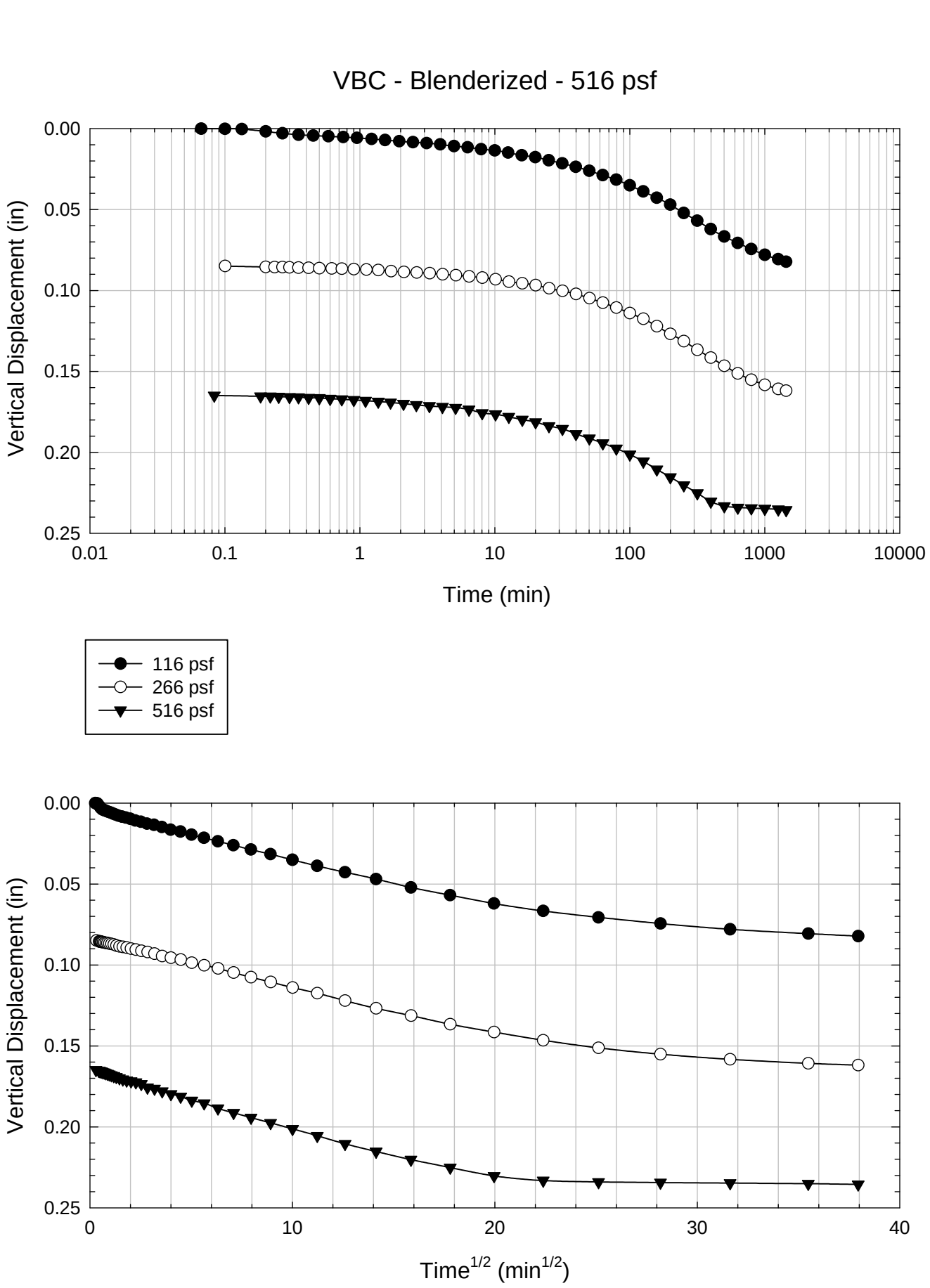
VBC - Blenderized - 516 psf
Vertical Displacement (in)
0.00
0.05
0.10
0.15
0.20
0.25
0.01
0.1
1
10
100
1000
10000
Time (min)
116 psf
266 psf
516 psf
Vertical Displacement (in)
0.00
0.05
0.10
0.15
0.20
0.25
0
10
20
30
40
Time^1/2 (min^1/2)

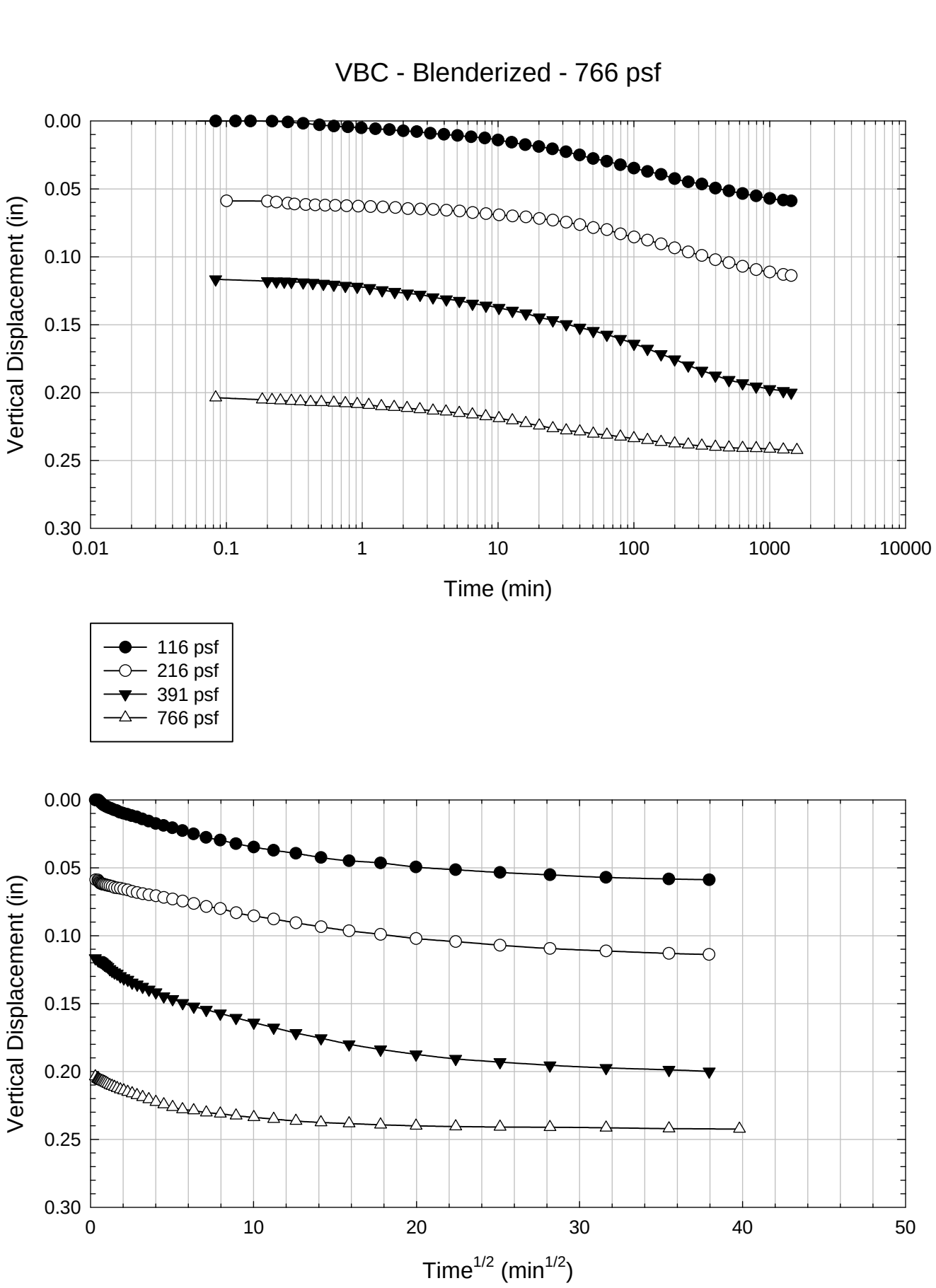
VBC - Blenderized - 766 psf
Vertical Displacement (in)
0.00
0.05
0.10
0.15
0.20
0.25
0.30
0.01
0.1
1
10
100
1000
10000
Time (min)
116 psf
216 psf
391 psf
766 psf
Vertical Displacement (in)
0.00
0.05
0.10
0.15
0.20
0.25
0.30
0
10
20
30
40
50
Time1/2 (min1/2)

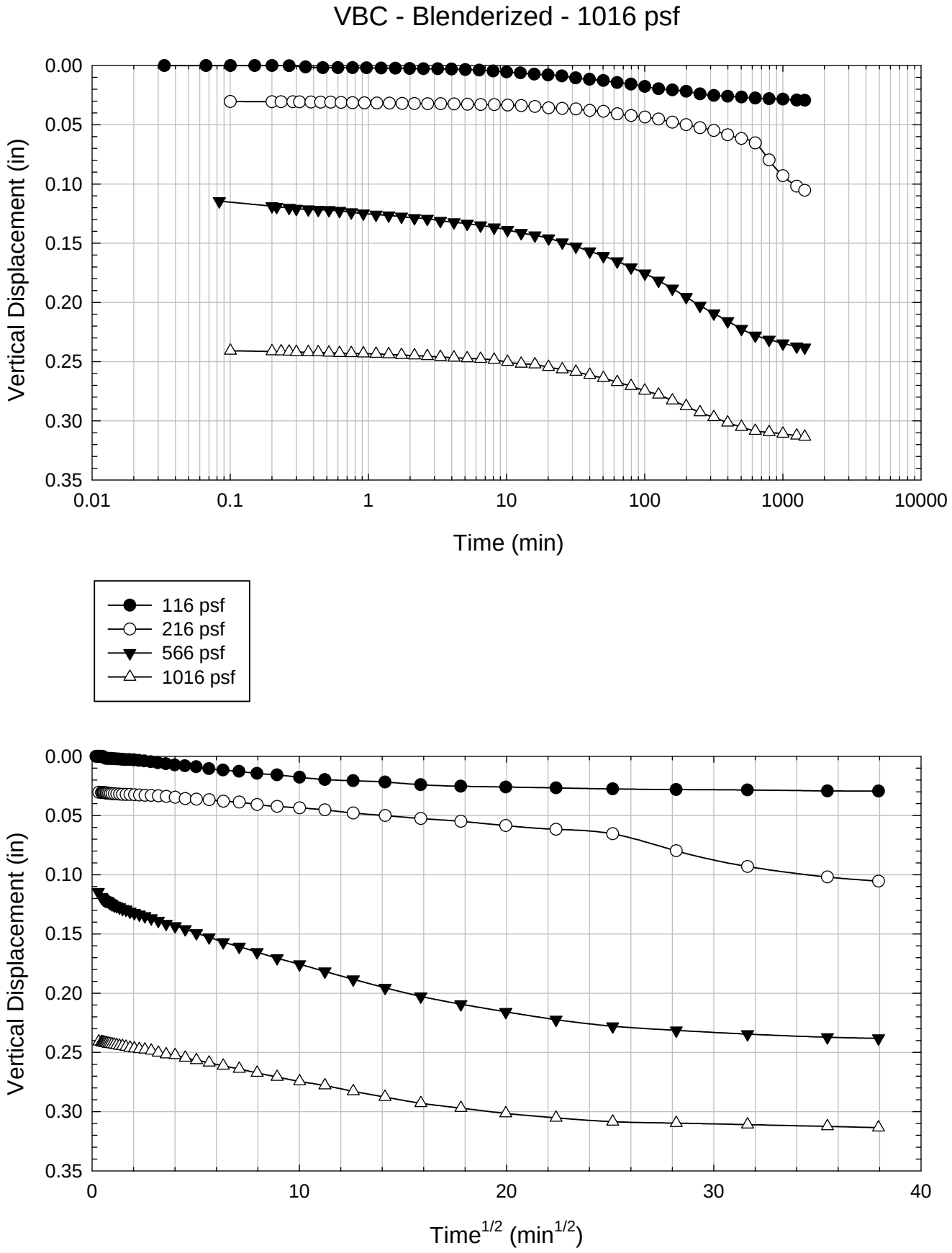
VBC - Blenderized - 1016 psf
Vertical Displacement (in)
0.00
0.05
0.10
0.15
0.20
0.25
0.30
0.35
0.01
0.1
1
10
100
1000
10000
Time (min)
116 psf
216 psf
566 psf
1016 psf
Vertical Displacement (in)
0.00
0.05
0.10
0.15
0.20
0.25
0.30
0.35
0
10
20
30
40
Time^1/2 (min^1/2)

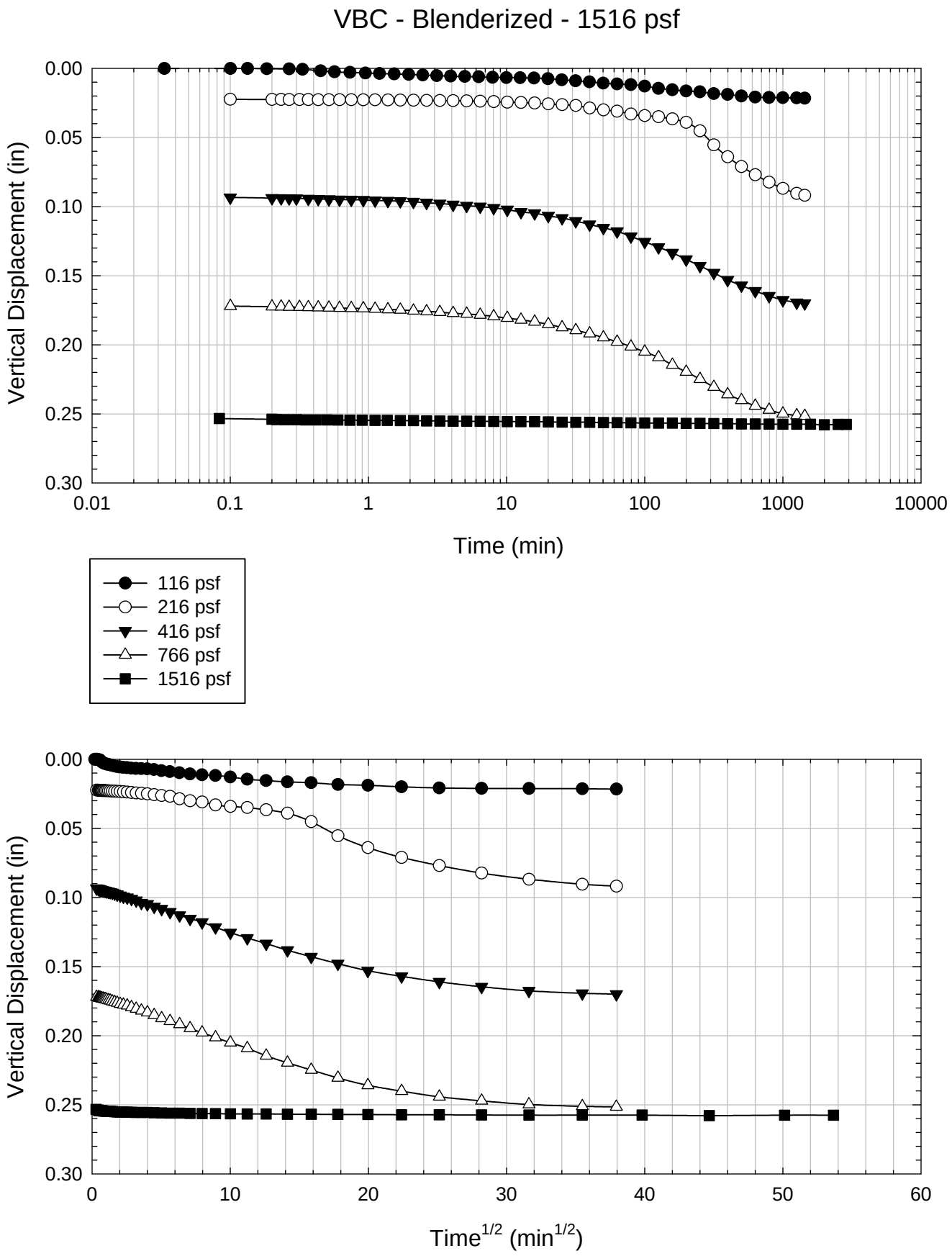
VBC - Blenderized - 1516 psf
Vertical Displacement (in)
0.00
0.05
0.10
0.15
0.20
0.25
0.30
0.01
0.1
1
10
100
1000
10000
Time (min)
116 psf
216 psf
416 psf
766 psf
1516 psf
Vertical Displacement (in)
0.00
0.05
0.10
0.15
0.20
0.25
0.30
0
10
20
30
40
50
60
Time1/2 (min1/2)

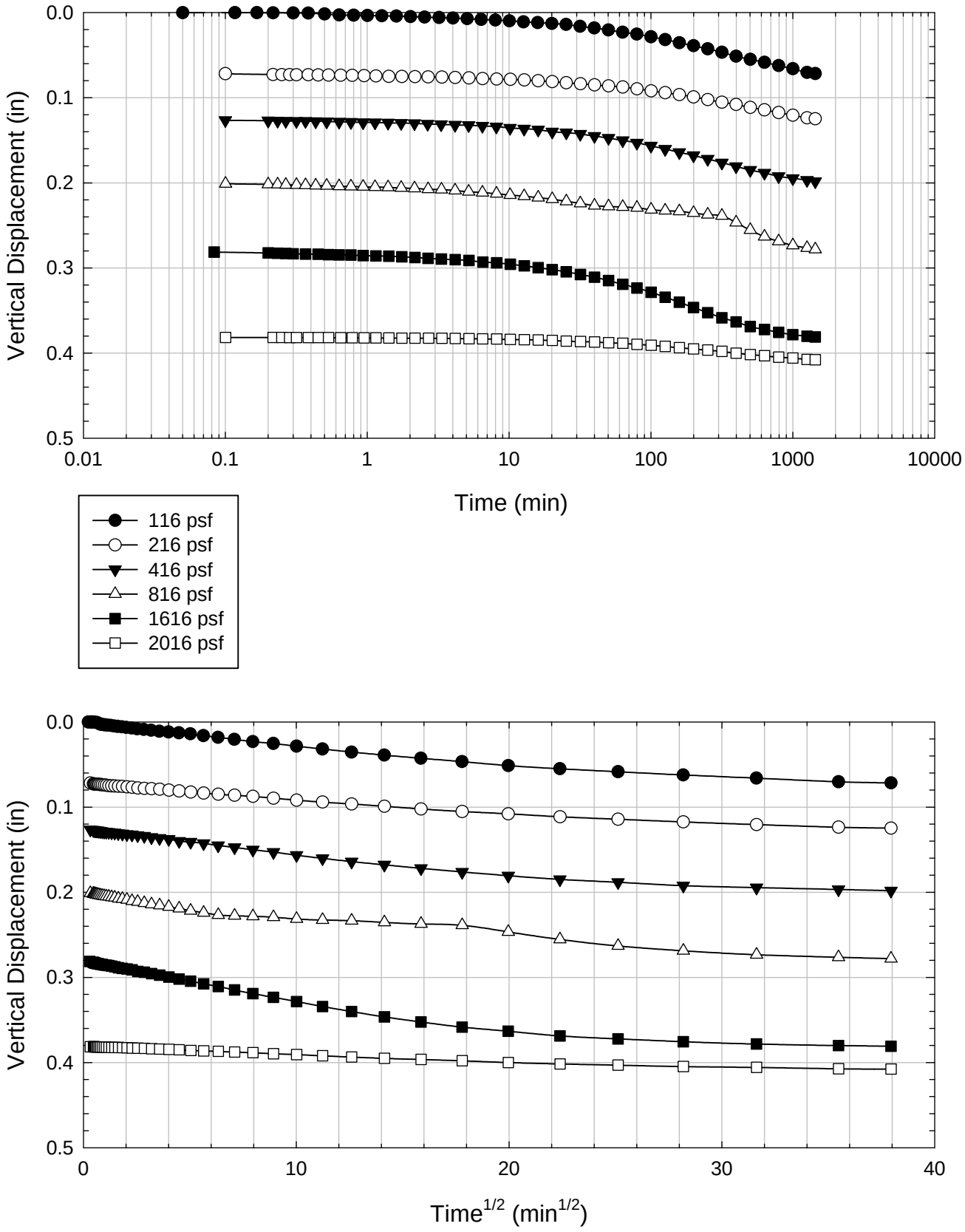
VBC - Blenderized - 2016 psf
Vertical Displacement (in)
0.0
0.1
0.2
0.3
0.4
0.5
0.01
0.1
1
10
100
1000
10000
Time (min)
116 psf
216 psf
416 psf
816 psf
1616 psf
2016 psf
Vertical Displacement (in)
0.0
0.1
0.2
0.3
0.4
0.5
0
10
20
30
40
Time^1/2 (min^1/2)

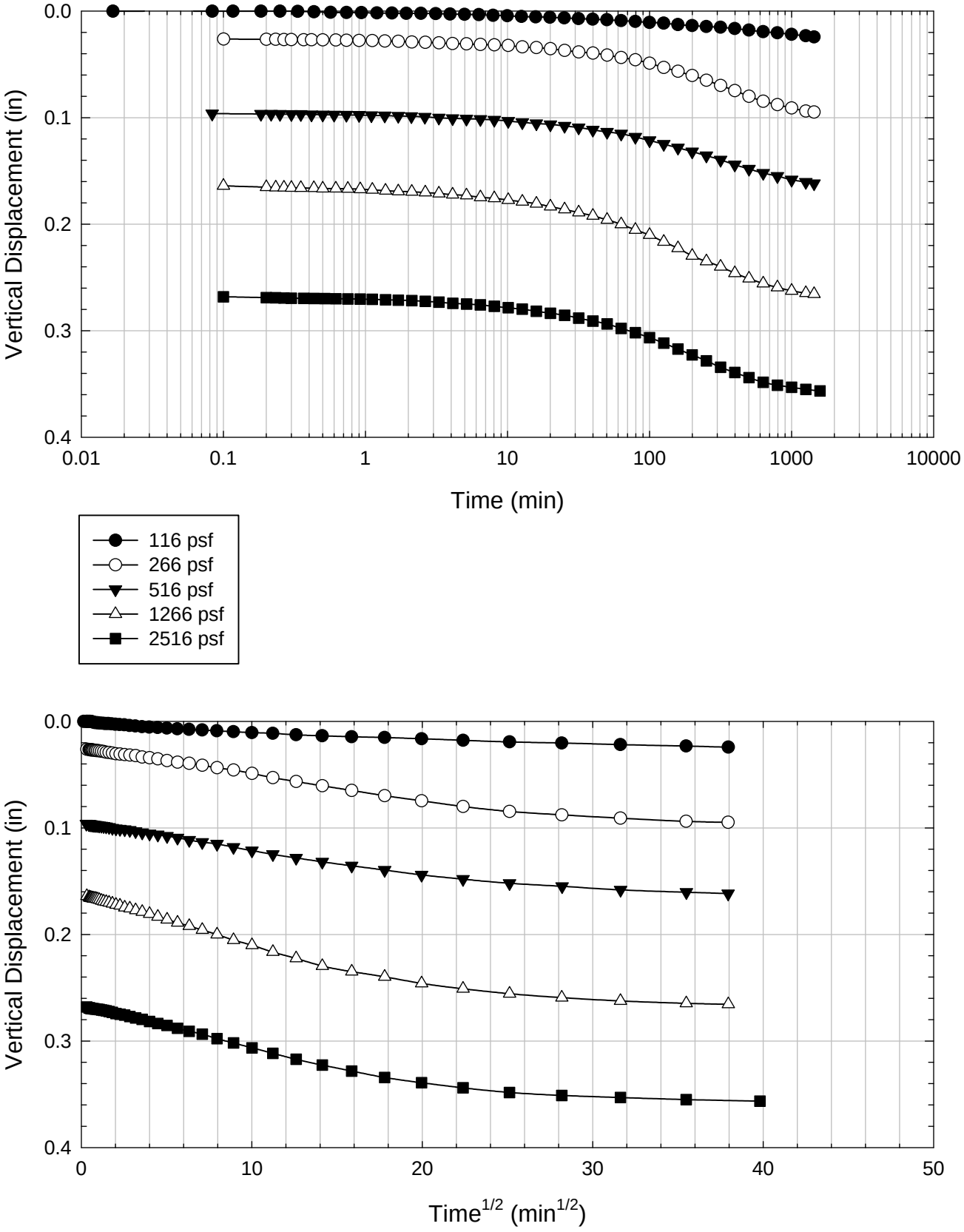
VBC - Blenderized - 2516 psf
Vertical Displacement (in)
0.0
0.1
0.2
0.3
0.4
0.01
0.1
1
10
100
1000
10000
Time (min)
116 psf
266 psf
516 psf
1266 psf
2516 psf
Vertical Displacement (in)
0.0
0.1
0.2
0.3
0.4
0
10
20
30
40
50
Time1/2 (min1/2)

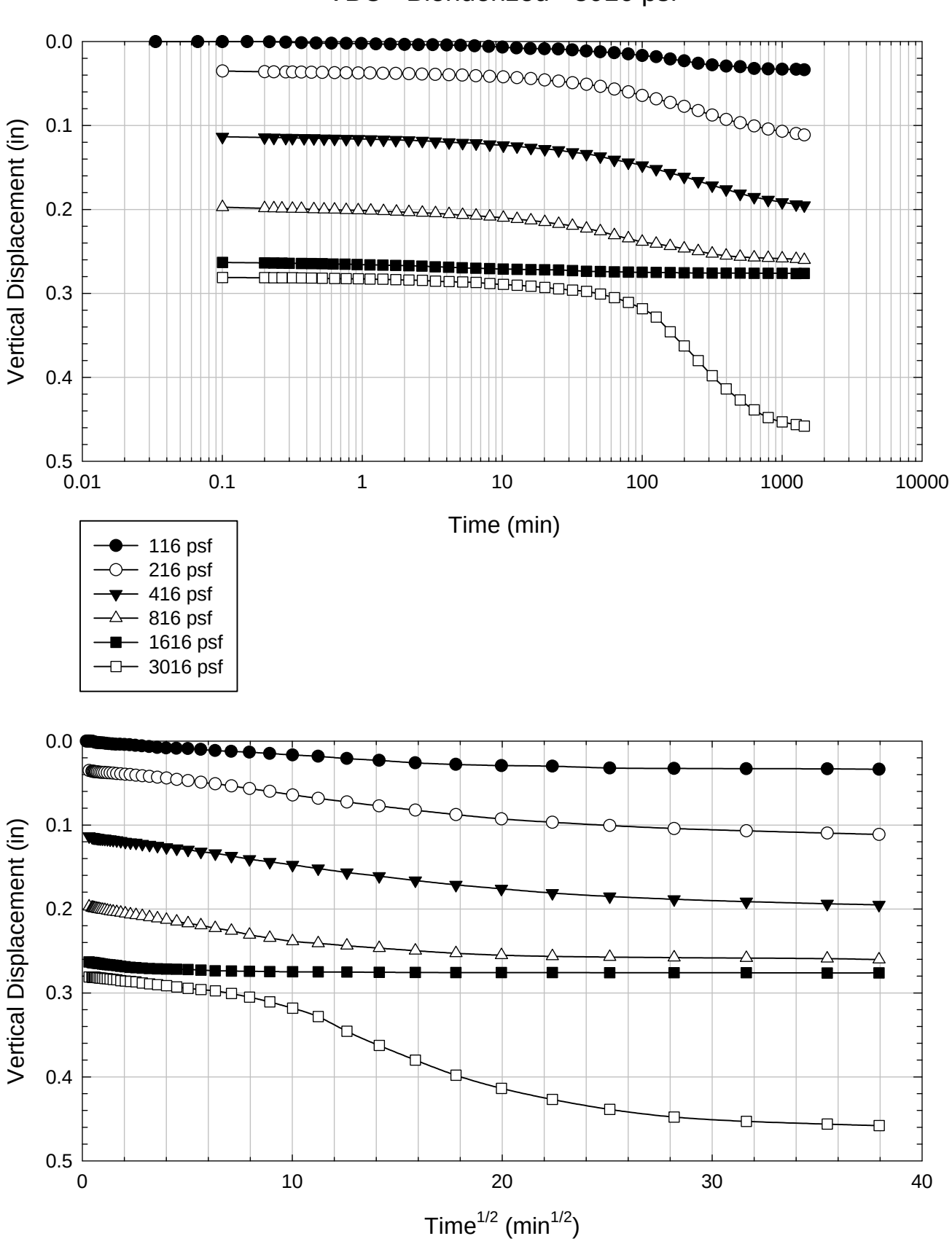
VBC - Blenderized - 3016 psf
Vertical Displacement (in)
0.0
0.1
0.2
0.3
0.4
0.5
0.01
0.1
1
10
100
1000
10000
Time (min)
116 psf
216 psf
416 psf
816 psf
1616 psf
3016 psf
Vertical Displacement (in)
0.0
0.1
0.2
0.3
0.4
0.5
0
10
20
30
40
Time^1/2 (min^1/2)

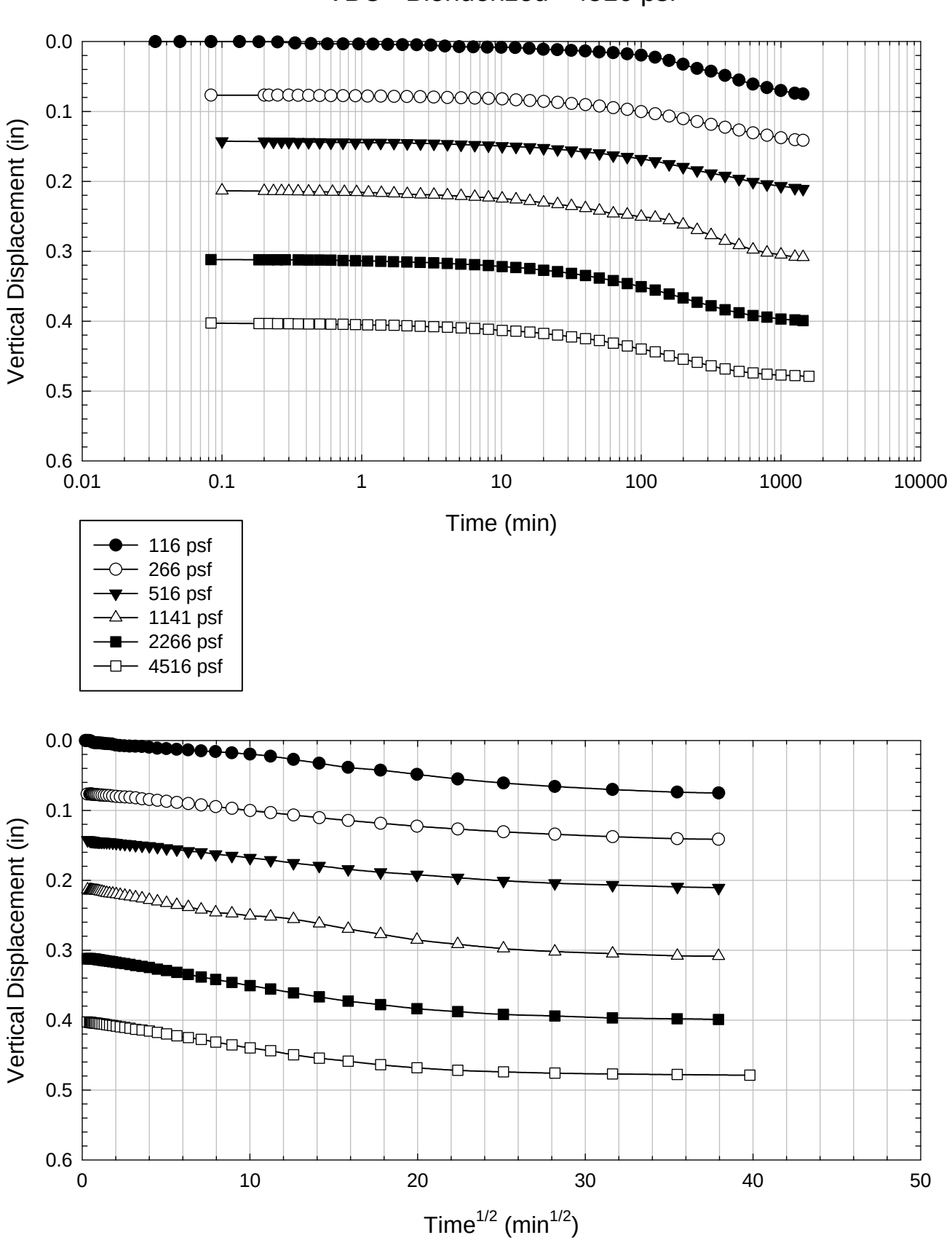
VBC - Blenderized - 4516 psf
Vertical Displacement (in)
0.0
0.1
0.2
0.3
0.4
0.5
0.6
0.01
0.1
1
10
100
1000
10000
Time (min)
116 psf
266 psf
516 psf
1141 psf
2266 psf
4516 psf
Vertical Displacement (in)
0.0
0.1
0.2
0.3
0.4
0.5
0.6
0
10
20
30
40
50
Time1/2 (min1/2)

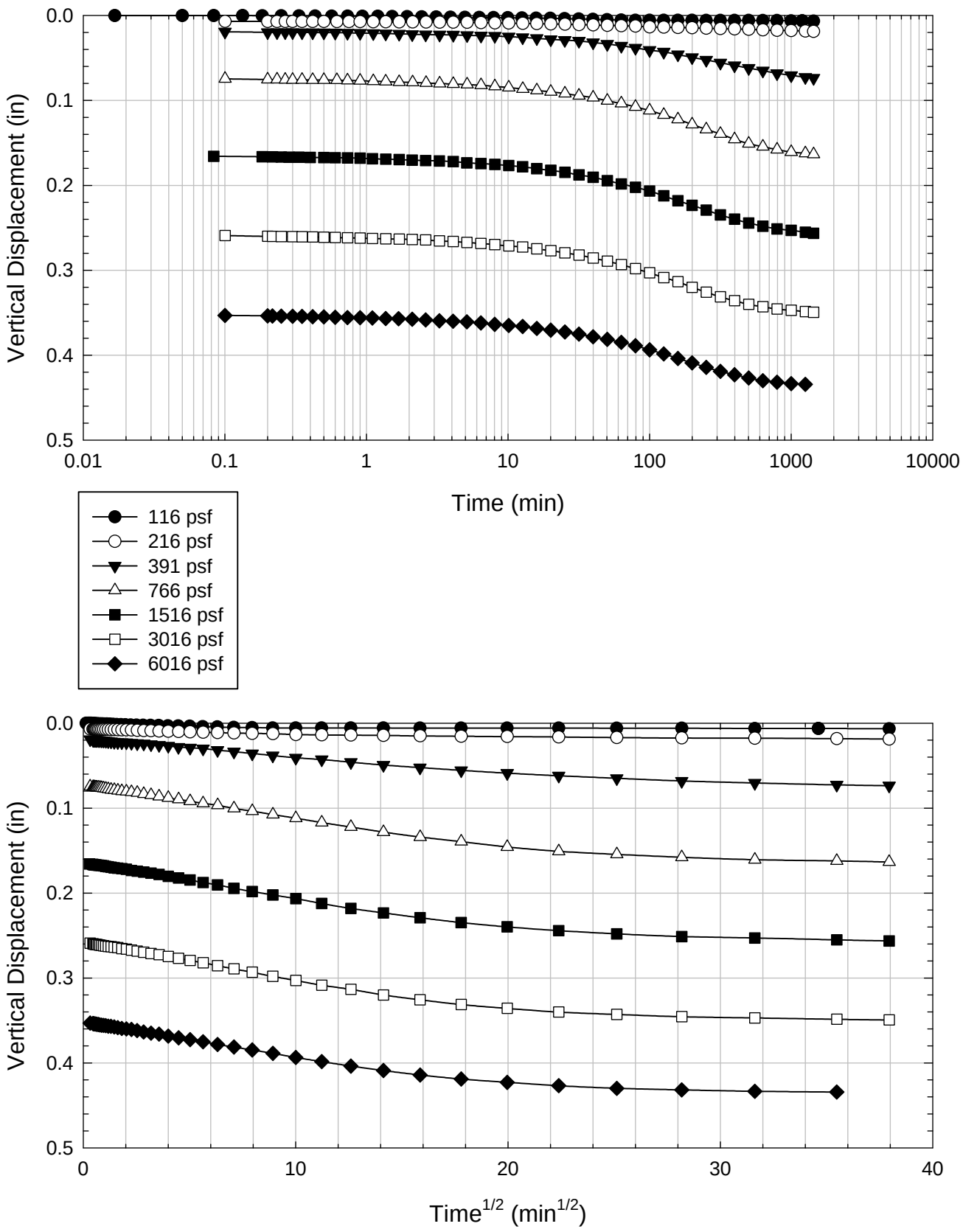
VBC - Blenderized - 6016 psf
Vertical Displacement (in)
0.0
0.1
0.2
0.3
0.4
0.5
0.01
0.1
1
10
100
1000
10000
Time (min)
116 psf
216 psf
391 psf
766 psf
1516 psf
3016 psf
6016 psf
Vertical Displacement (in)
0.0
0.1
0.2
0.3
0.4
0.5
0
10
20
30
40
Time1/2 (min1/2)

VBC - Blenderized

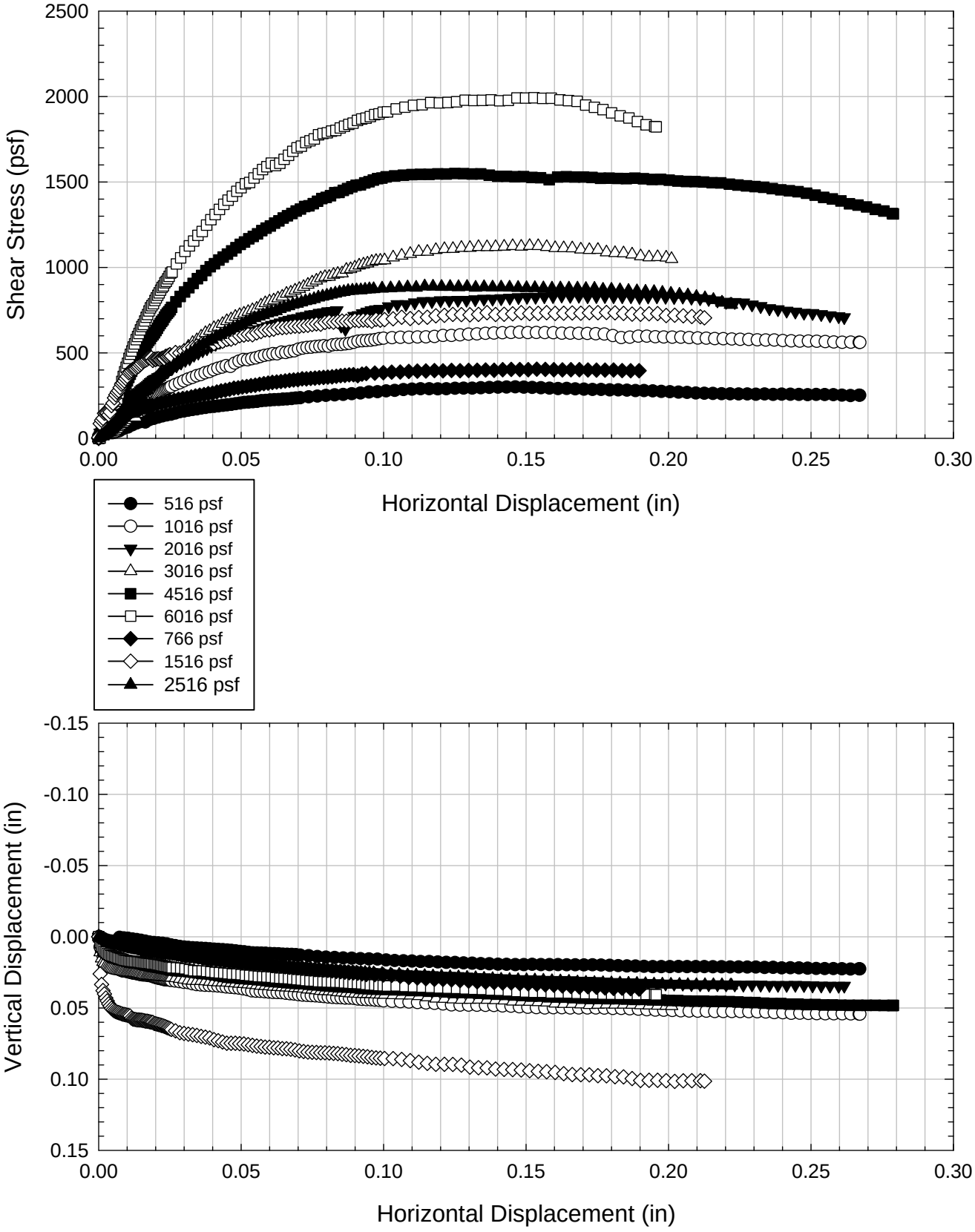

C.15.2 Non-blenderized

Virginia Polytechnic Institute and State University
Geotechnical Engineering Laboratory
Direct Shear Data Sheet

Project:	Fully Softened Shear Strength
Sample I.D./Loc.:	VBC - Non-blenderized
Classification:	Fat Clay (CH)

Sample Preparation	Remolded at LL		Specific Gravity	2.79

Test Number	1	2	3	4	5	6	7	8
Start Date (m/d/y)	11/9/2011	11/9/2011	11/15/2011	11/9/2011	19/9/11	11/14/2011		
End Date (m/d/y)	11/23/2011	11/20/2011	11/28/2011	11/20/2011	11/20/2011	11/28/2011		
Consolidation Pressure (psf)	516	1016	2016	3016	4516	6016		
Initial Values								
Initial Height (in)	1.42	1.44	1.41	1.39	1.41	1.41		
Initial Diameter (in)	2.50	2.50	2.50	2.50	2.50	2.50		
Initial Sample Weight (g)	181	179	180	178	182	180		
Water Content (%)	79.92	79.33	78.84	80.30	79.39	77.40		
Dry Unit Weight (pcf)	54.9	53.7	55.3	55.3	55.9	55.8		
Wet Unit Weight (pcf)	98.9	96.4	98.9	99.7	100.3	99.0		
Consolidation Pressures								
Load 1 (psf)	116	116	116	116	116	116		
Load 2 (psf)	266	266	266	216	266	216		
Load 3 (psf)	516	516	516	416	516	391		
Load 4 (psf)		1016	1016	816	1141	766		
Load 5 (psf)			2016	1616	2266	1516		
Load 6 (psf)				3016	4516	3016		
Load 7 (psf)						6016		
t_{50}								
Max. t_{50} for Load 1 (min)								
Max. t_{50} for Load 2 (min)								
Max. t_{50} for Load 3 (min)	109.84							
Max. t_{50} for Load 4 (min)		93.73						
Max. t_{50} for Load 5 (min)			85.22					
Max. t_{50} for Load 6 (min)				69.18	72.69			
Max. t_{50} for Load 7 (min)						79.74		
Final Values								
Water Content (%)	58.80	56.13	49.83	46.69	41.97	39.54		
Dry Unit Weight (pcf)	67.3	68.6	75.5	84.7	83.5	88.58		
Wet Unit Weight (pcf)	106.9	107.1	113.2	124.2	118.5	123.61		
Failure								
Test Performed at Shear Rate (in/min)	1.82E-05	2.13E-05	2.35E-05	2.89E-05	2.75E-05	2.51E-05		
Required Shear Rate (in/min)	2.91E-05	3.41E-05	3.75E-05	4.91E-05	4.13E-05	4.01E-05		
Displacement at Failure (in)	0.16	0.16	0.16	0.17	0.15	0.16		
Peak Shear Stress (psf)	368	509	986	1298	1575	2118		
Total Change in Height at Failure (in)	0.26	0.31	0.38	0.48	0.46	0.52		
Secant Effective Friction Angle (deg)	35.5	26.6	26.1	23.3	19.2	19.4		

Comments:

VBC - Non-blenderized - 516 psf

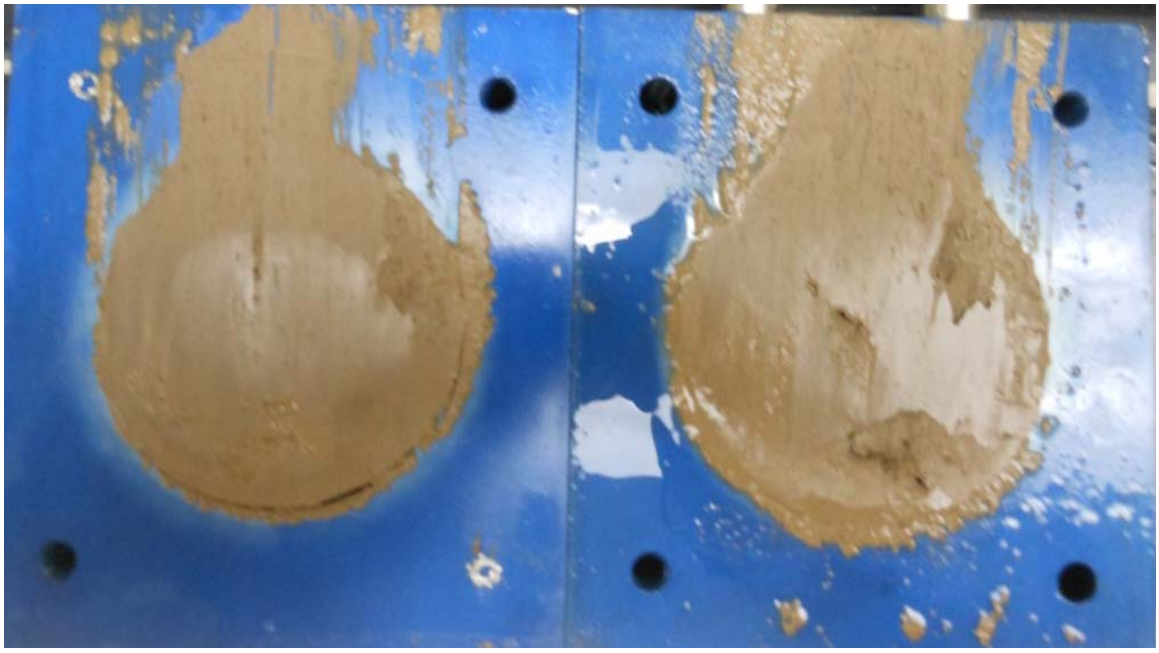

VBC - Non-blenderized - 1016 psf

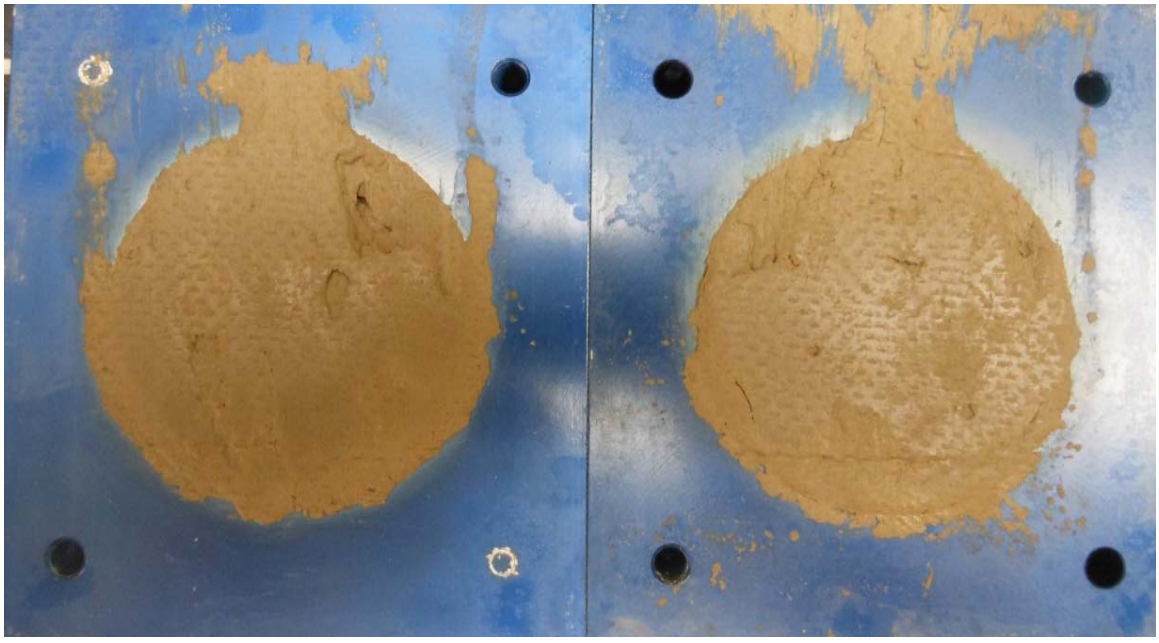

VBC - Non-blenderized - 2016 psf

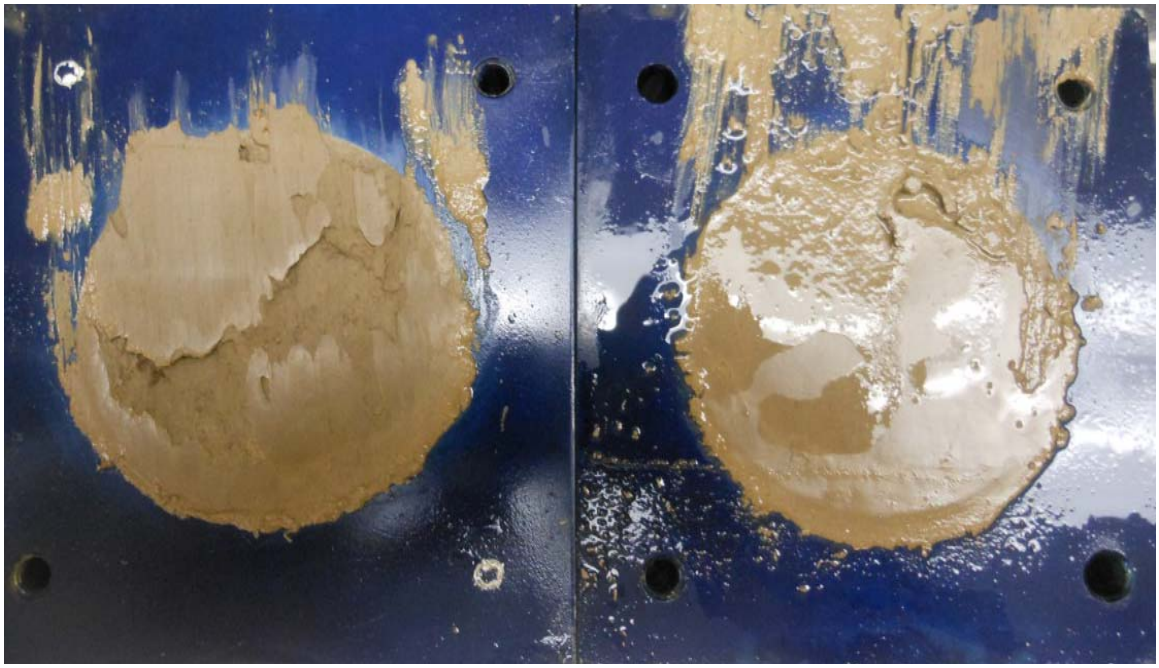

VBC - Non-blenderized - 3016 psf

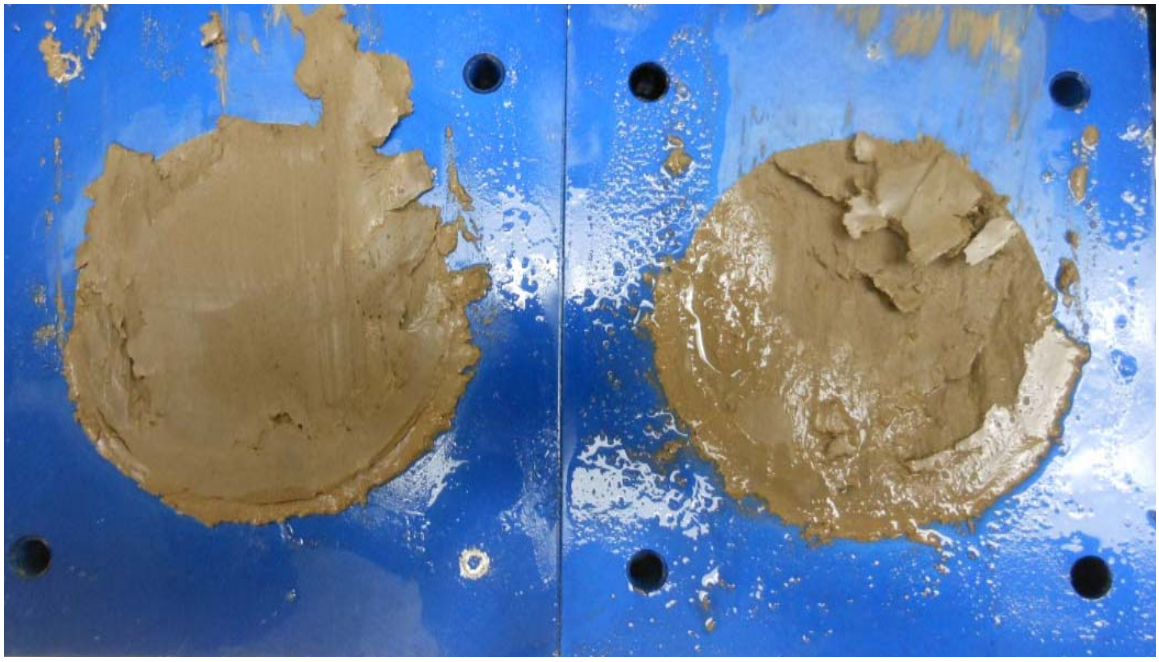

VBC - Non-blenderized - 4516 psf

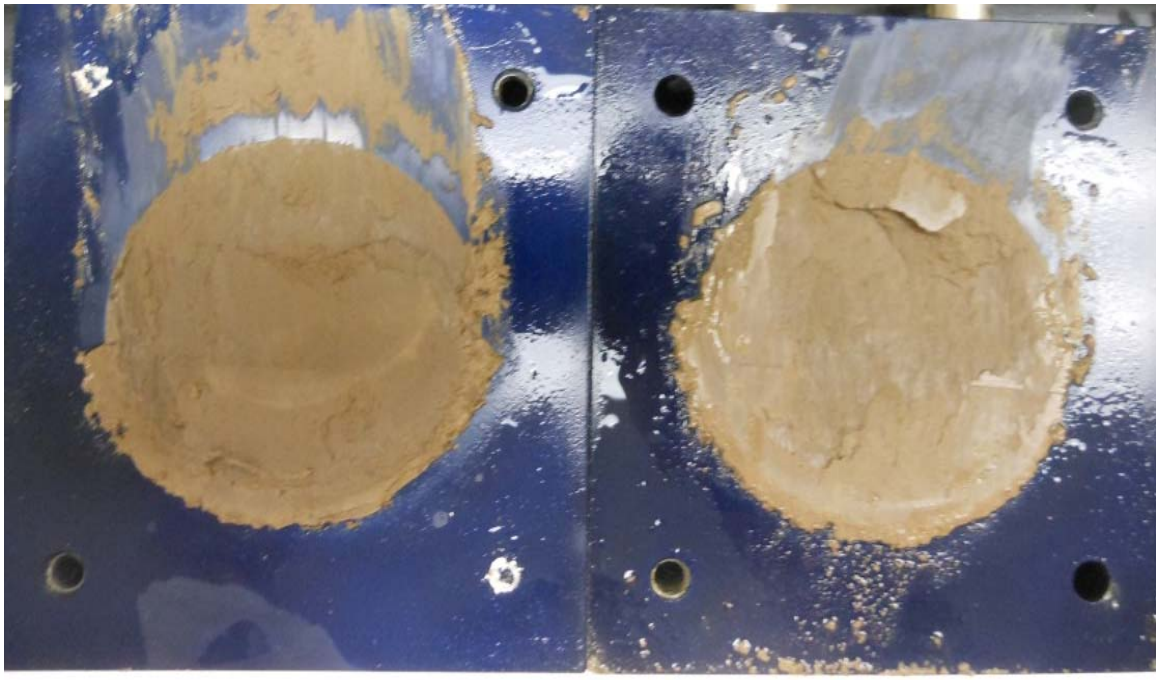

VBC - Non-blenderized - 6016 psf

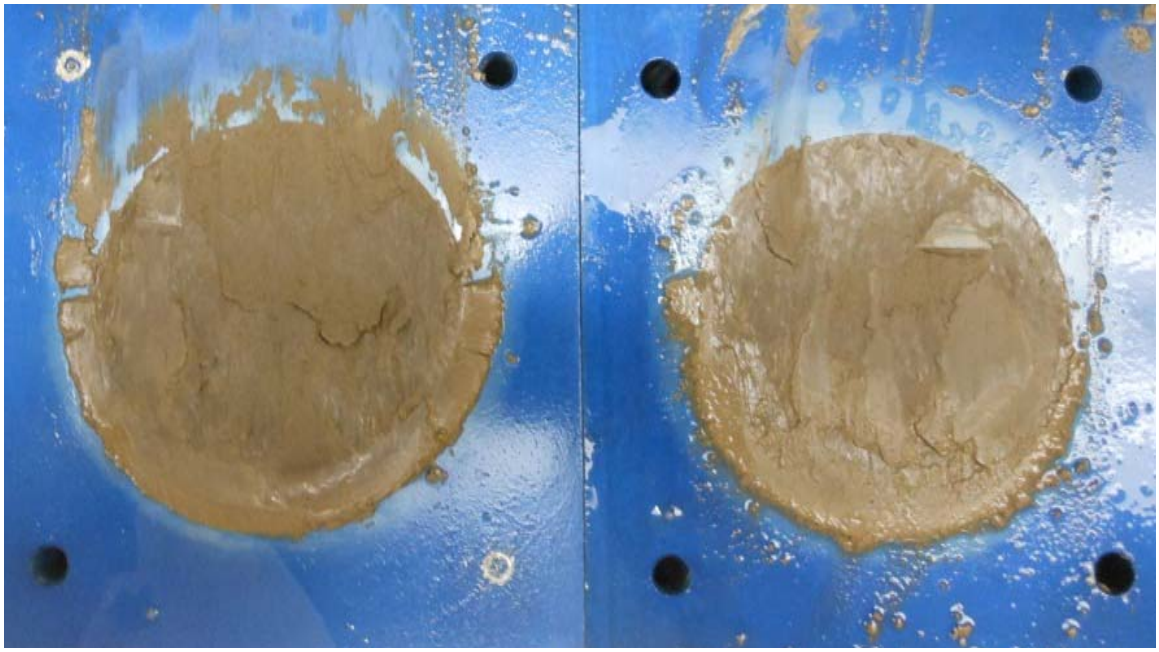

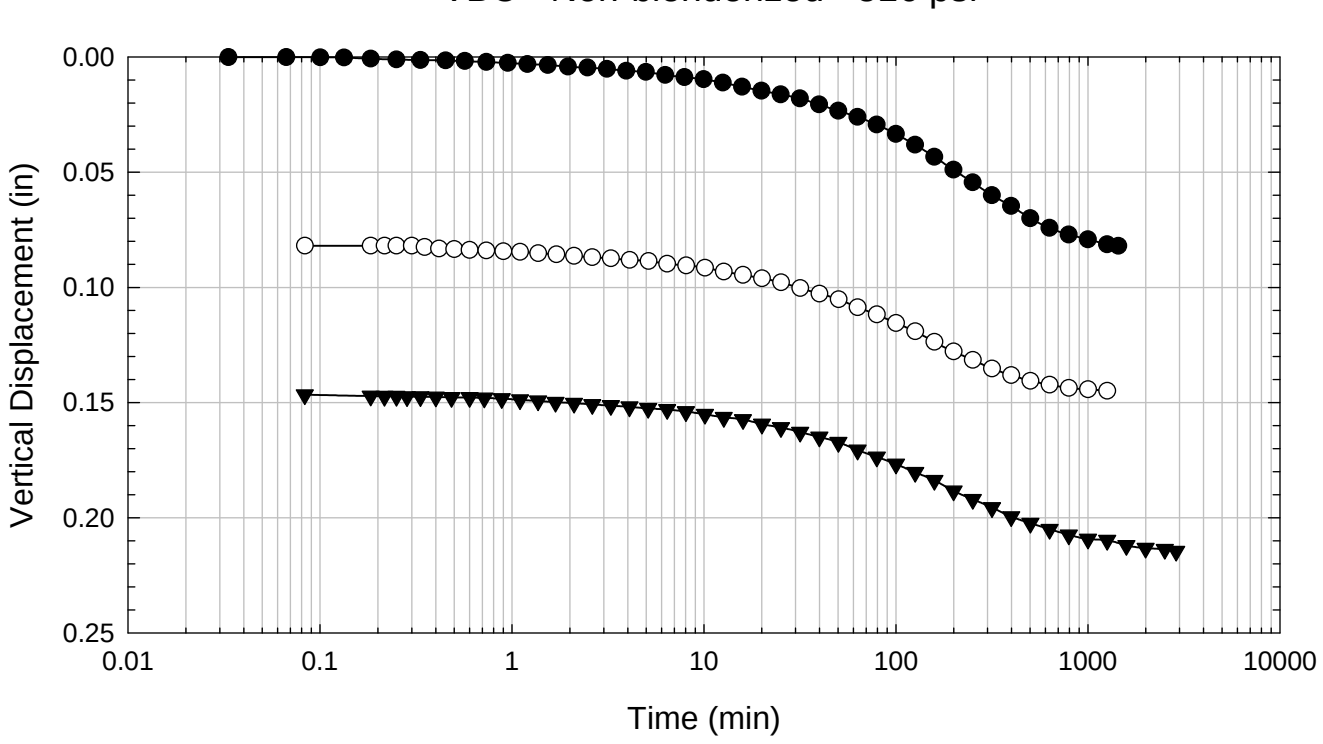
VBC - Non-blenderized - 516 psf
Vertical Displacement (in)
0.00
0.05
0.10
0.15
0.20
0.25
0.01
0.1
1
10
100
1000
10000
Time (min)

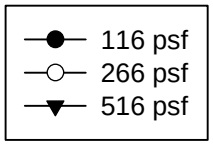
116 psf
266 psf
516 psf

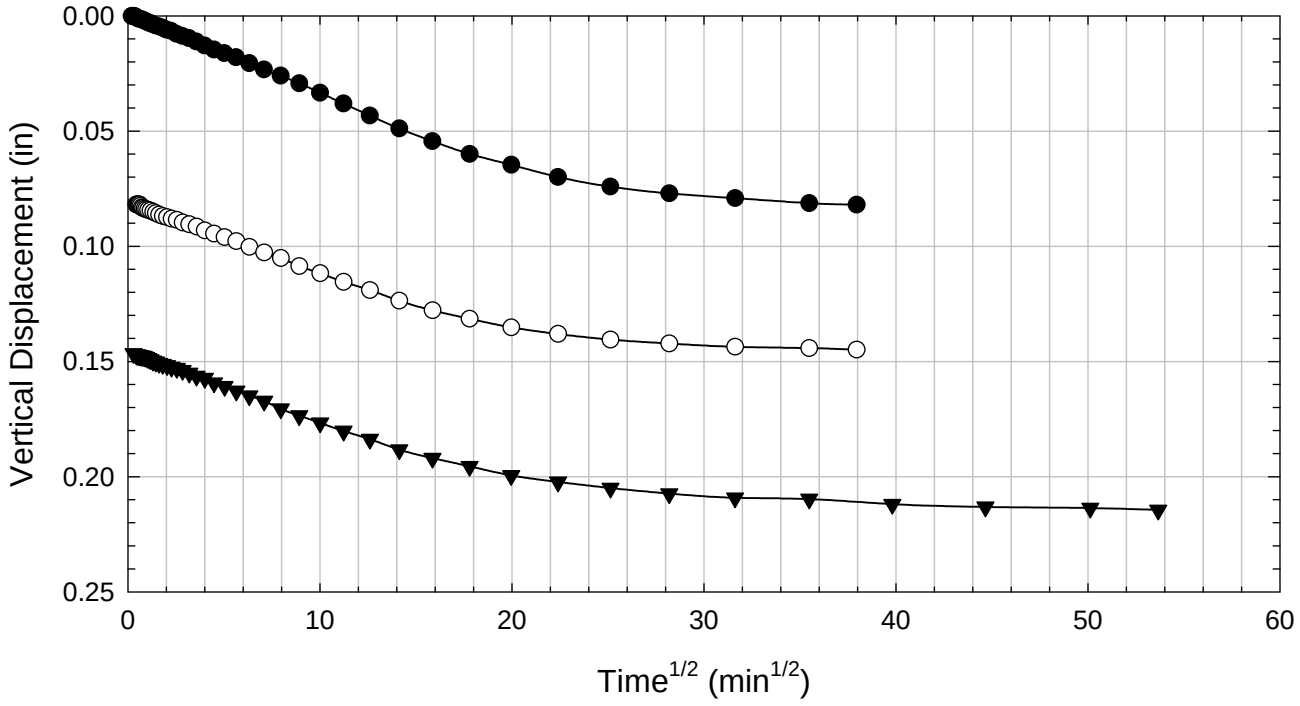
Vertical Displacement (in)
0.00
0.05
0.10
0.15
0.20
0.25
0
10
20
30
40
50
60
Time1/2 (min1/2)

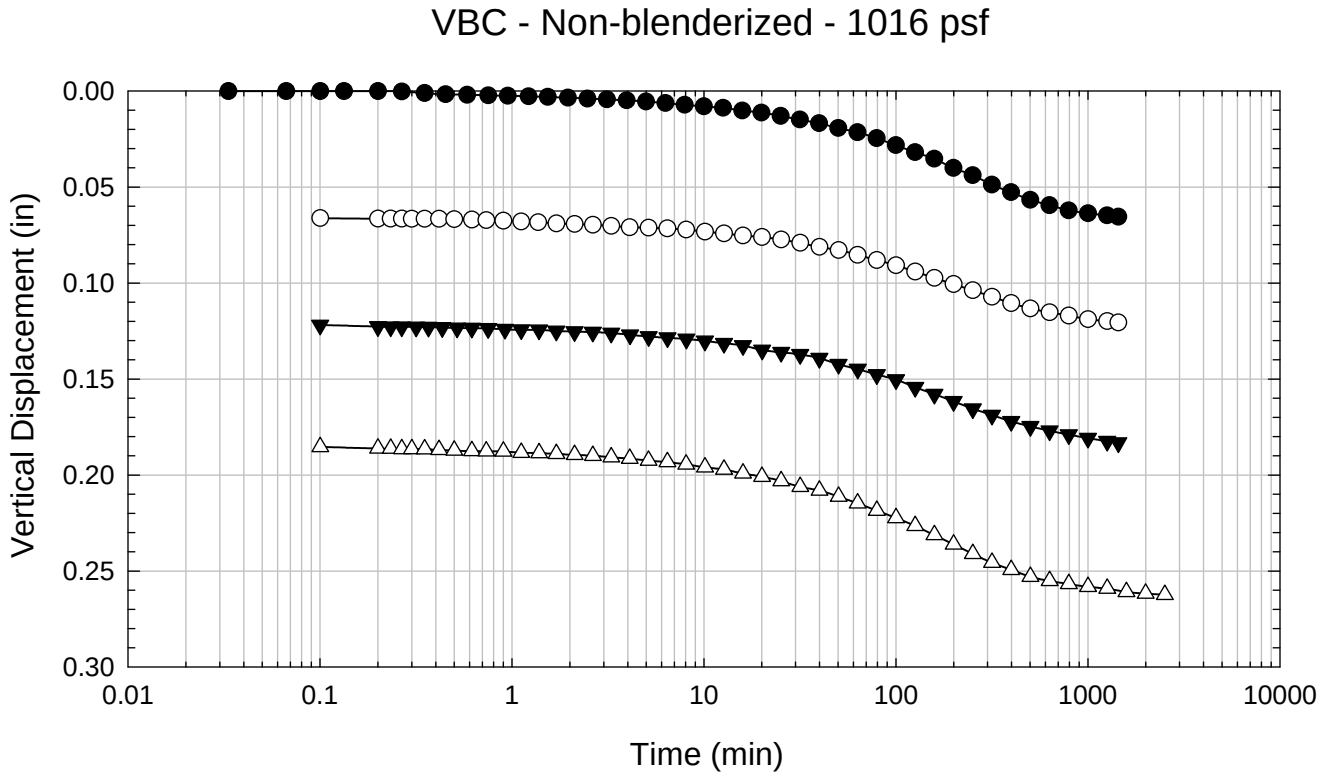
VBC - Non-blenderized - 1016 psf
Vertical Displacement (in)
0.00
0.05
0.10
0.15
0.20
0.25
0.30
0.01
0.1
1
10
100
1000
10000
Time (min)

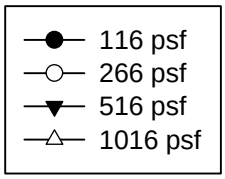
116 psf
266 psf
516 psf
1016 psf

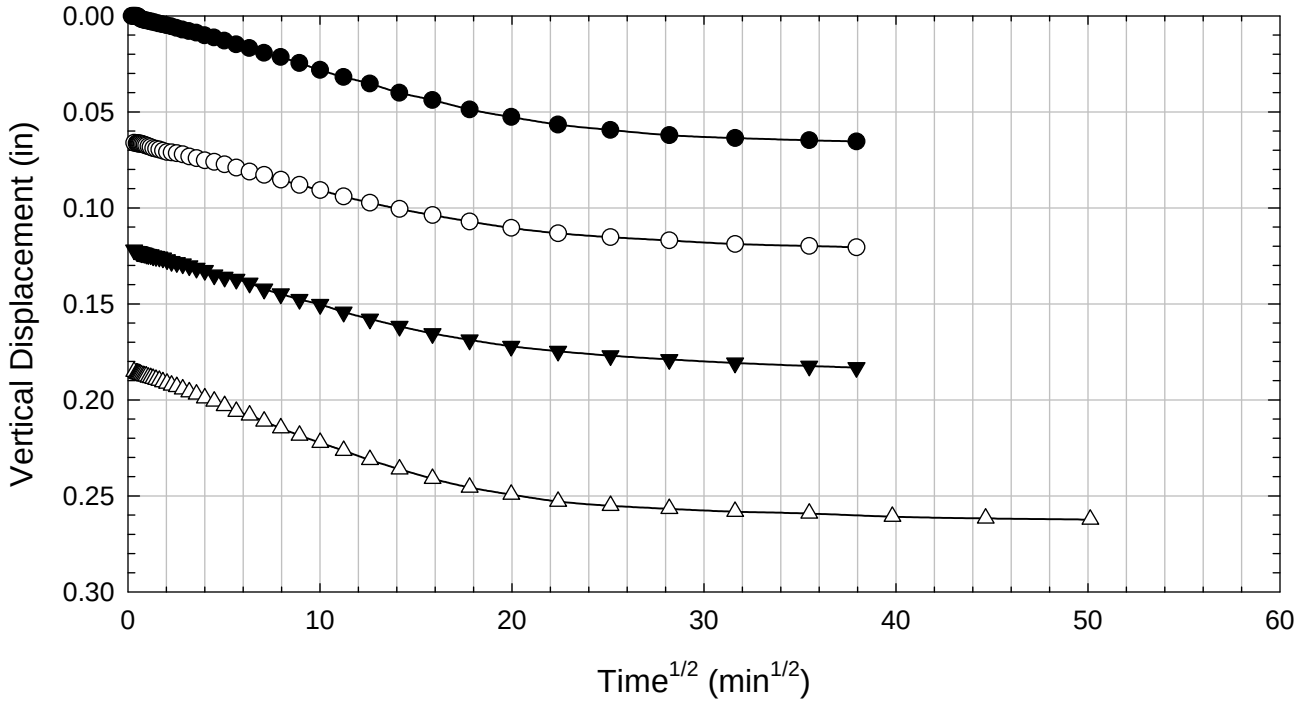
Vertical Displacement (in)
0.00
0.05
0.10
0.15
0.20
0.25
0.30
0
10
20
30
40
50
60
Time1/2 (min1/2)

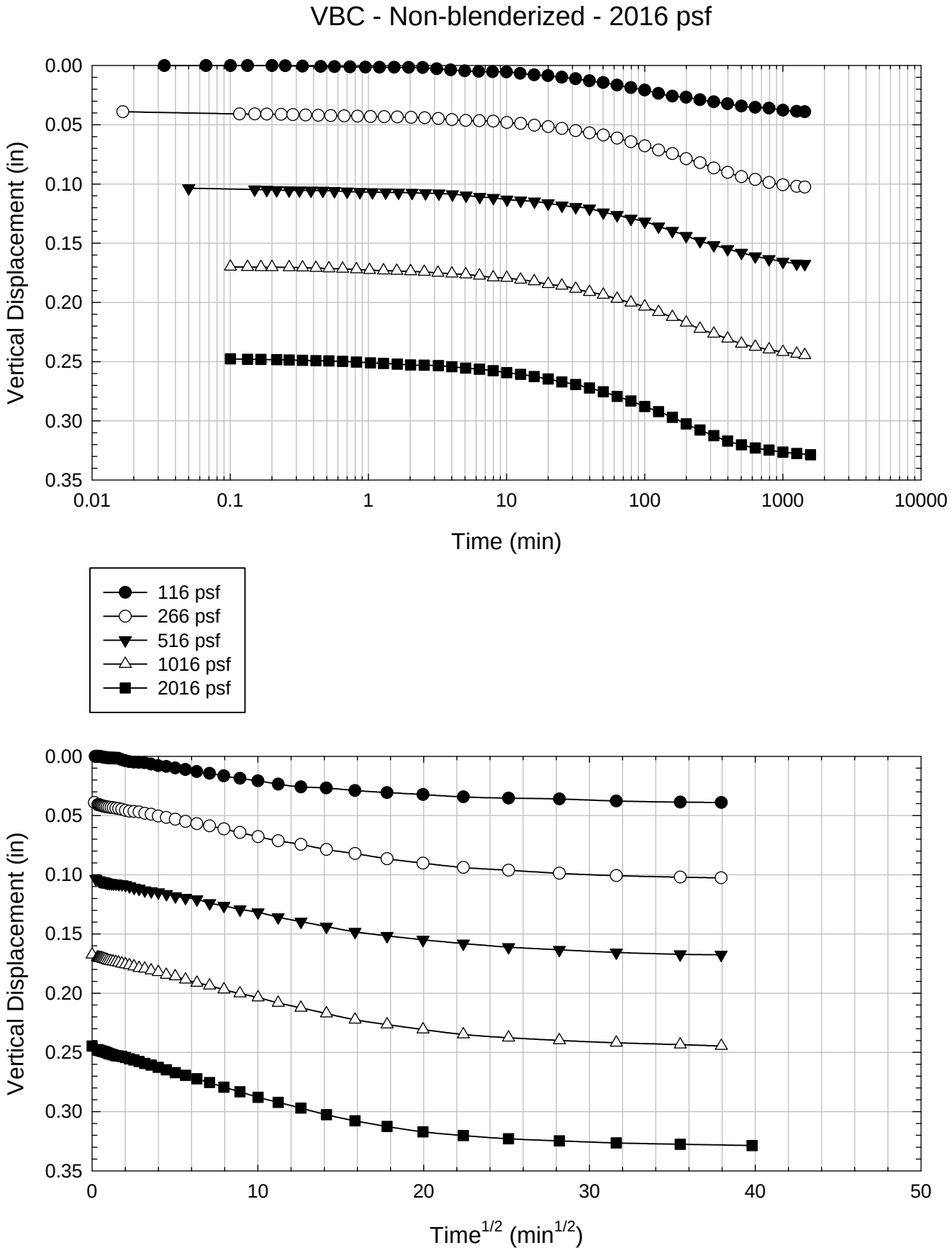
VBC - Non-blenderized - 2016 psf
Vertical Displacement (in)
0.00
0.05
0.10
0.15
0.20
0.25
0.30
0.35
0.01
0.1
1
10
100
1000
10000
Time (min)
116 psf
266 psf
516 psf
1016 psf
2016 psf
Vertical Displacement (in)
0.00
0.05
0.10
0.15
0.20
0.25
0.30
0.35
0
10
20
30
40
50
Time^1/2 (min^1/2)

VBC - Non-blenderized - 3016 psf

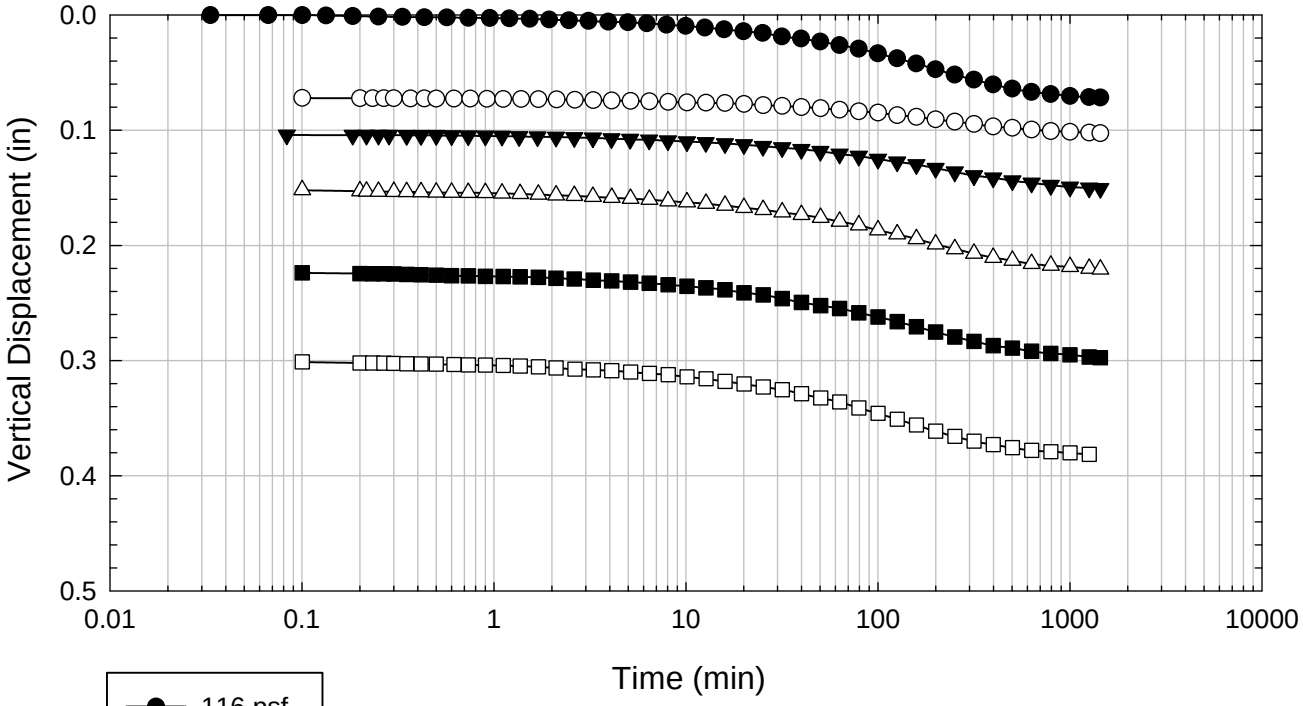

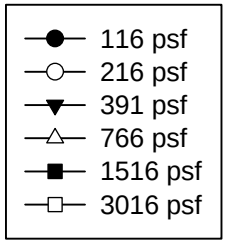

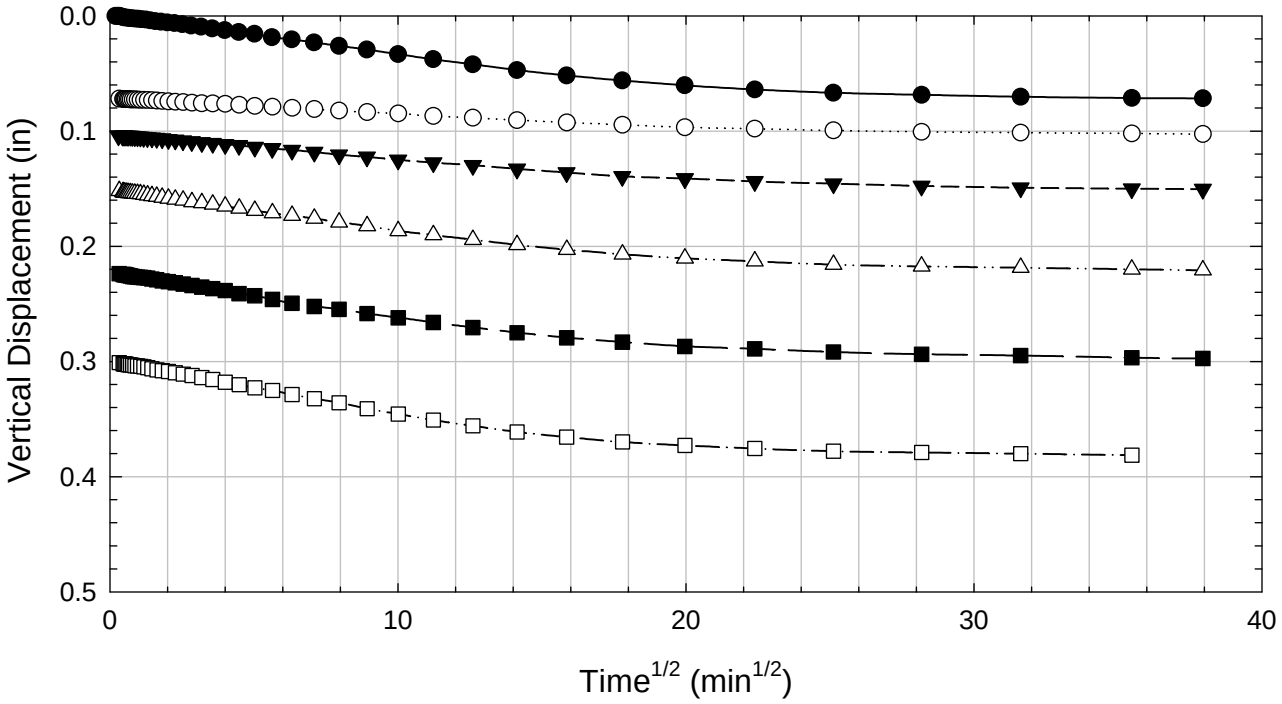

VBC - Non-blenderized - 4516 psf

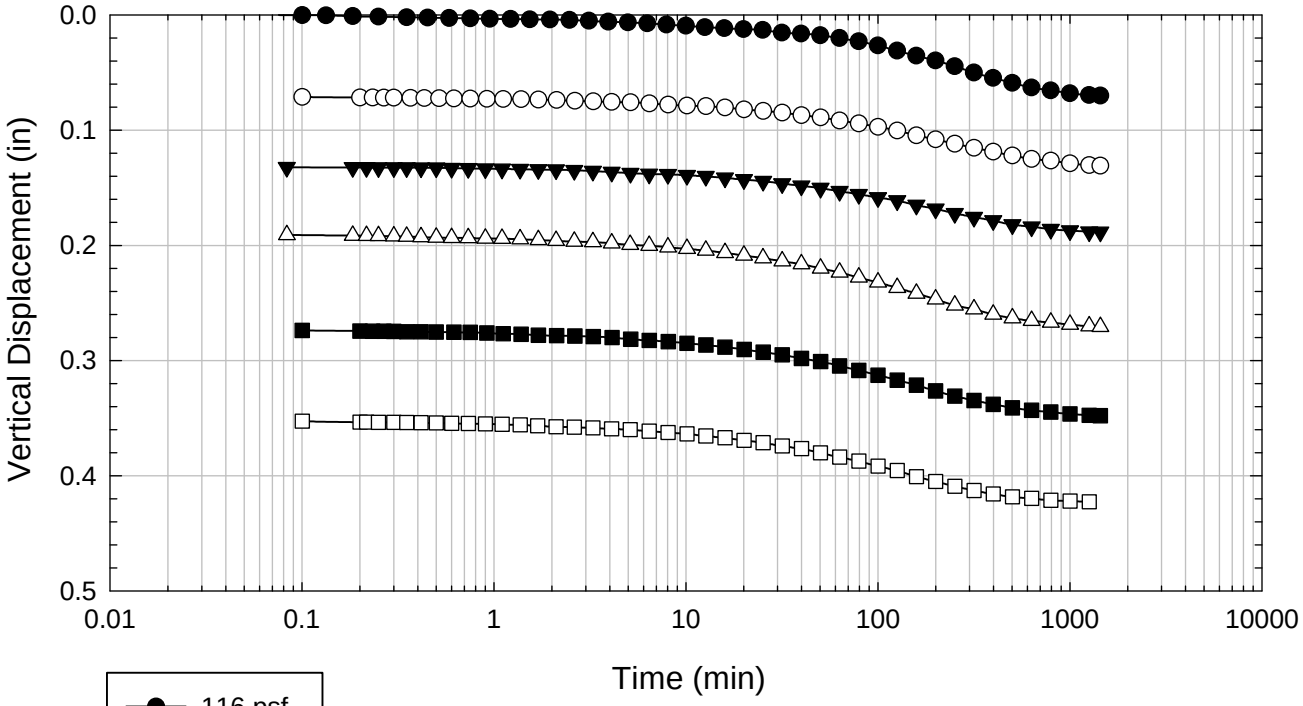

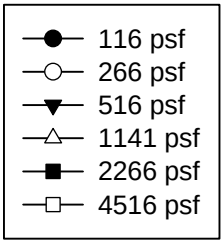

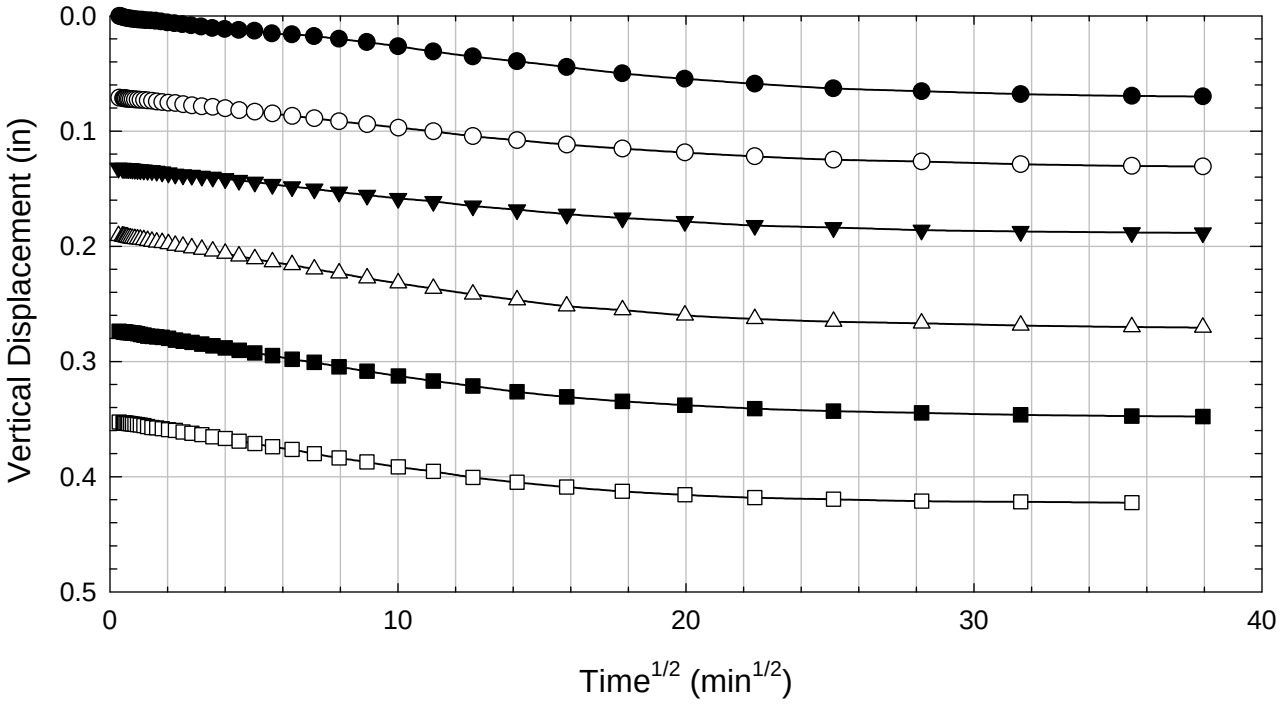

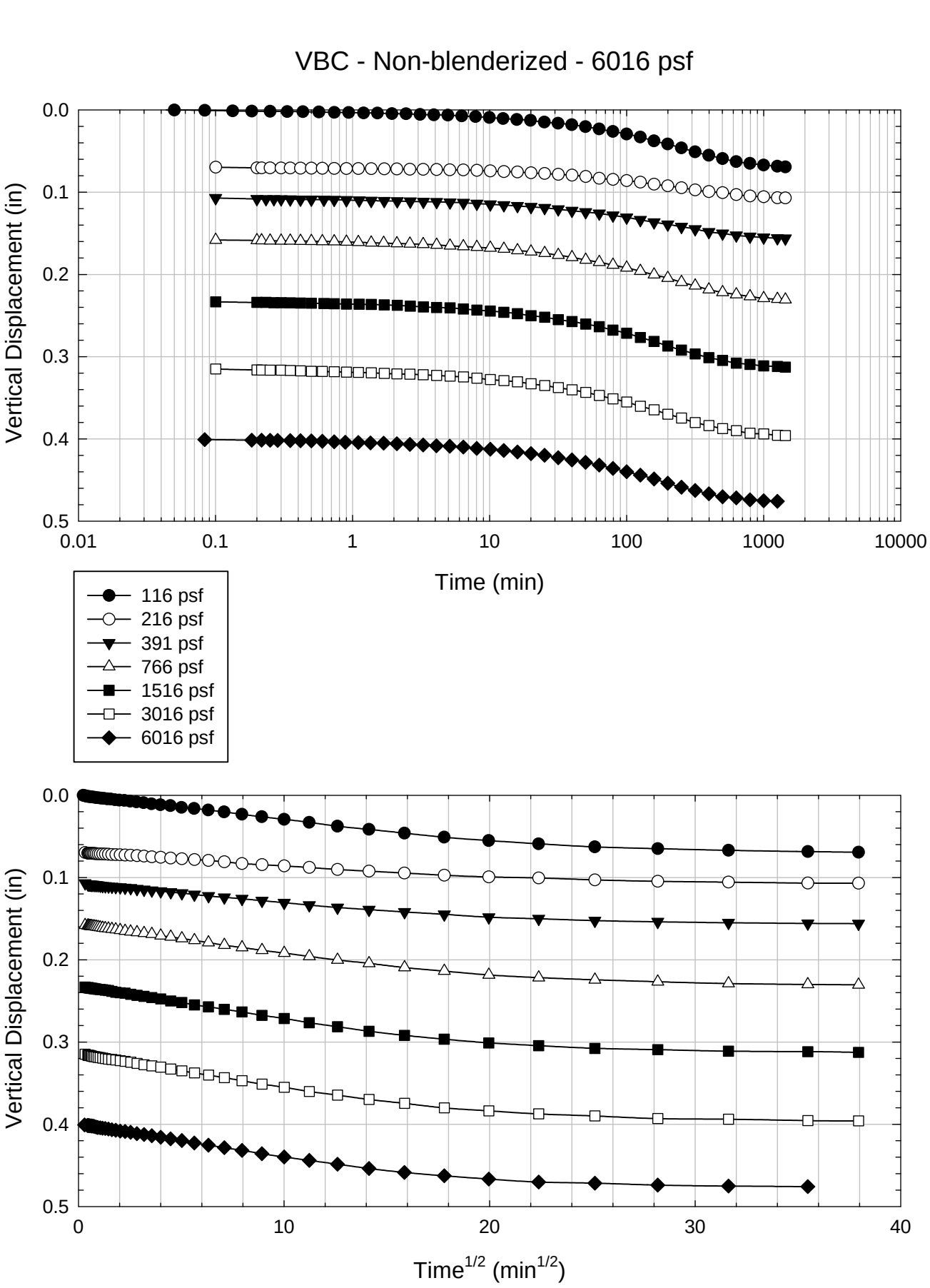
VBC - Non-blenderized - 6016 psf
Vertical Displacement (in)
0.0
0.1
0.2
0.3
0.4
0.5
0.01
0.1
1
10
100
1000
10000
Time (min)
116 psf
216 psf
391 psf
766 psf
1516 psf
3016 psf
6016 psf
Vertical Displacement (in)
0.0
0.1
0.2
0.3
0.4
0.5
0
10
20
30
40
Time^1/2 (min^1/2)

VBC - Non-blenderized

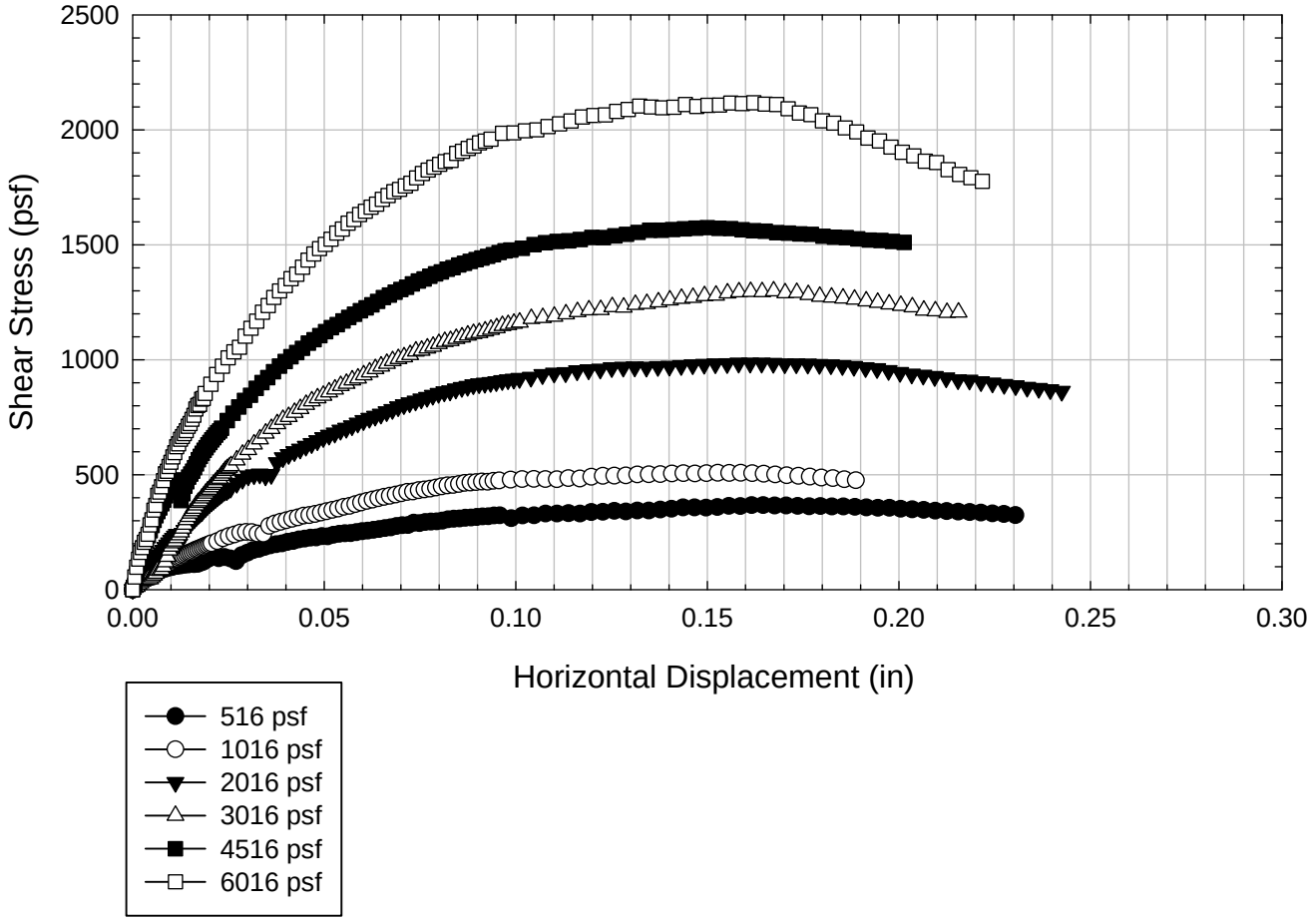

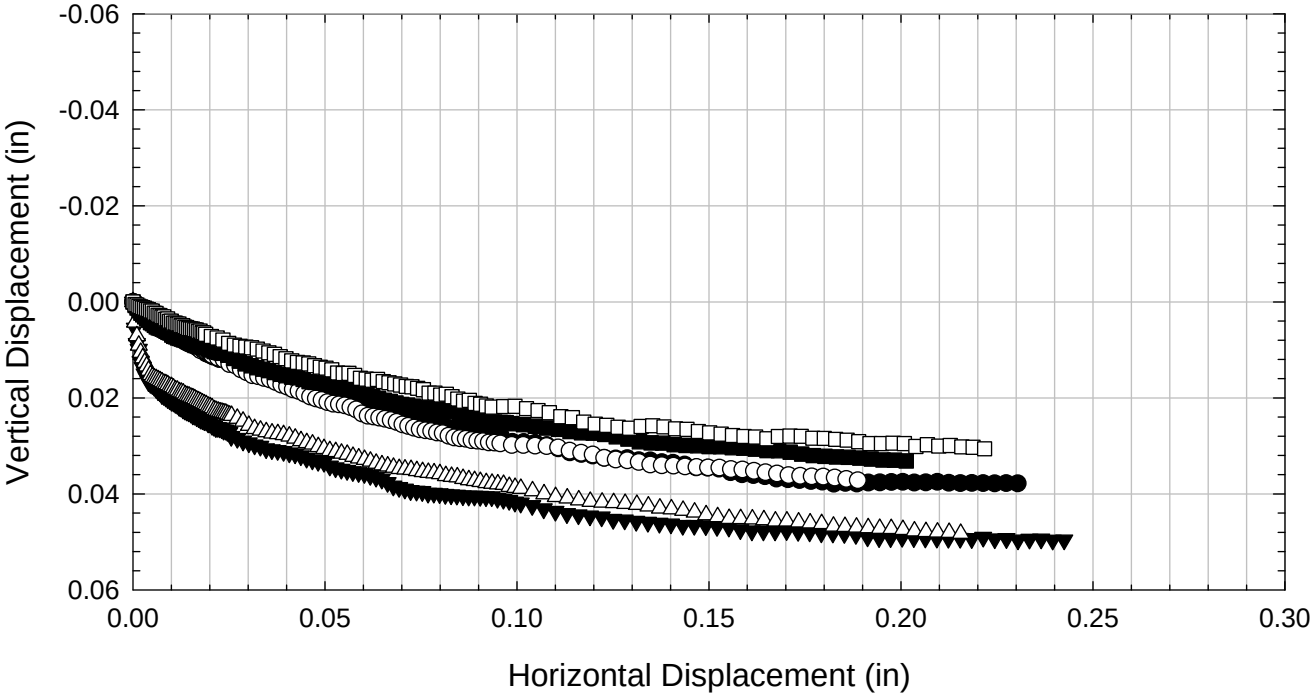

C.15.3 Liquidity Index = 1.59

Virginia Polytechnic Institute and State University
Geotechnical Engineering Laboratory
Direct Shear Data Sheet

Project:	Fully Softened Shear Strength
Sample I.D./Loc.:	VBC - Non-blenderized
Classification:	Fat Clay (CH)

Sample Preparation	Remolded at LI = 1.59		Specific Gravity	2.79

Test Number	1	2	3	4	5	6	7	8
Start Date (m/d/y)	3/13/2012	3/13/2012	3/13/2012	3/13/2012	3/13/2012	3/13/2012		
End Date (m/d/y)	3/22/2012	3/22/2012	3/22/2012	3/22/2012	3/22/2012	3/22/2012		
Consolidation Pressure (psf)	516	1016	2016	3016	4516	6016		
Initial Values								
Initial Height (in)	1.45	1.40	1.41	1.39	1.37	1.44		
Initial Diameter (in)	2.50	2.50	2.50	2.50	2.50	2.50		
Initial Sample Weight (g)	168	167	168	166	168	169		
Water Content (%)	108.27	108.99	109.99	108.54	109.64	108.01		
Dry Unit Weight (pcf)	43.3	44.2	44.1	44.4	45.3	43.9		
Wet Unit Weight (pcf)	90.1	92.4	92.7	92.6	94.9	91.2		
Consolidation Pressures								
Load 1 (psf)	116	116	116	116	116	116		
Load 2 (psf)	266	266	266	216	266	216		
Load 3 (psf)	516	516	516	391	516	391		
Load 4 (psf)		1016	1016	766	1141	766		
Load 5 (psf)			2016	1516	2266	1516		
Load 6 (psf)				3016	4516	3016		
Load 7 (psf)						6016		
t_{50}								
Max. t_{50} for Load 1 (min)								
Max. t_{50} for Load 2 (min)								
Max. t_{50} for Load 3 (min)	56.88							
Max. t_{50} for Load 4 (min)		58.35						
Max. t_{50} for Load 5 (min)			47.35					
Max. t_{50} for Load 6 (min)				42.85	52.59			
Max. t_{50} for Load 7 (min)						59.03		
Final Values								
Water Content (%)	67.18	58.93	52.75	49.97	43.28	41.02		
Dry Unit Weight (pcf)	60.9	69.1	74.1	78.0	82.6	87.34		
Wet Unit Weight (pcf)	101.8	109.7	113.2	116.9	118.4	123.16		
Failure								
Test Performed at Shear Rate (in/min)	3.52E-05	3.52E-05	4.27E-05	4.67E-05	3.80E-05	4.67E-05		
Required Shear Rate (in/min)	4.22E-05	4.46E-05	6.76E-05	7.00E-05	4.94E-05	4.74E-05		
Displacement at Failure (in)	0.12	0.13	0.16	0.15	0.13	0.14		
Peak Shear Stress (psf)	309	534	863	1253	1524	2249		
Total Change in Height at Failure (in)	0.41	0.50	0.56	0.60	0.62	0.71		
Secant Effective Friction Angle (deg)	30.9	27.7	23.2	22.6	18.7	20.5		

Comments: In the test consolidated to 516 psf, power was lost during shear but it as restarted and continued.
In the tests consolidated to 1016 and 2016 psf, power was lost during the 1016 psf consolidation stress. The tests were restarted and continued.
In the tests consolidated to 3016 and 6016 psf, power was lost during the 766 psf consolidation stress. The tests were restarted and continued.
In the test consolidated to 4516, power was lost during the 1141 psf consolidation stress. The test was restarted and continued.

VBC - Non-blenderized - Liquidity Index = 1.59 - 516 psf

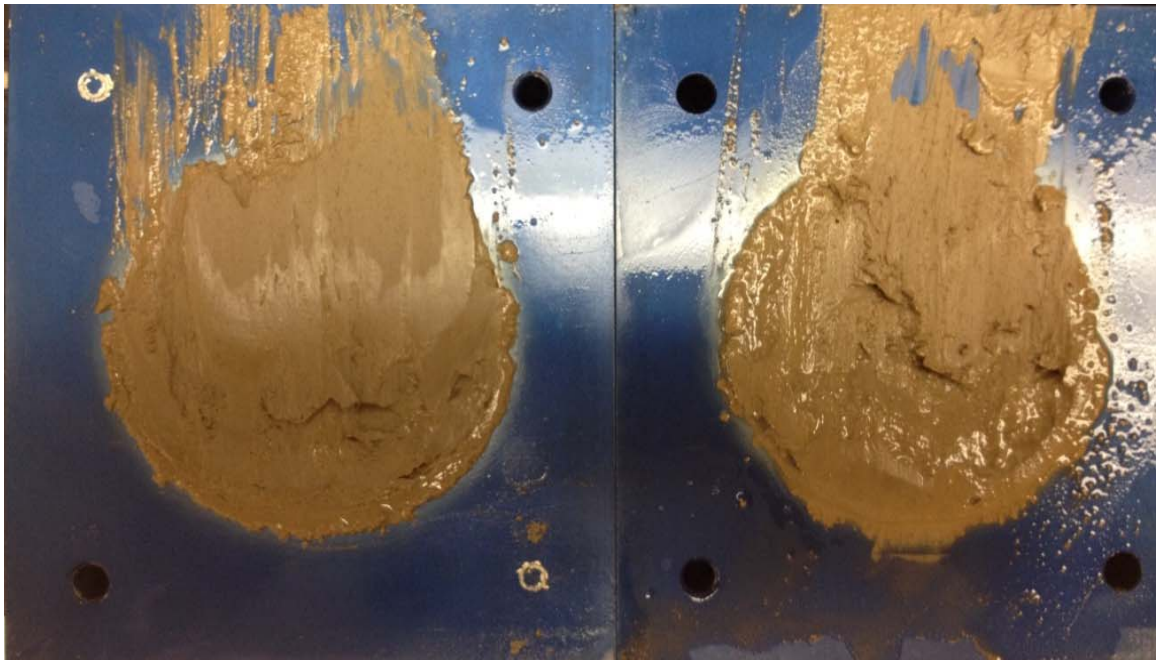

VBC - Non-blenderized - Liquidity Index = 1.59 - 1016 psf

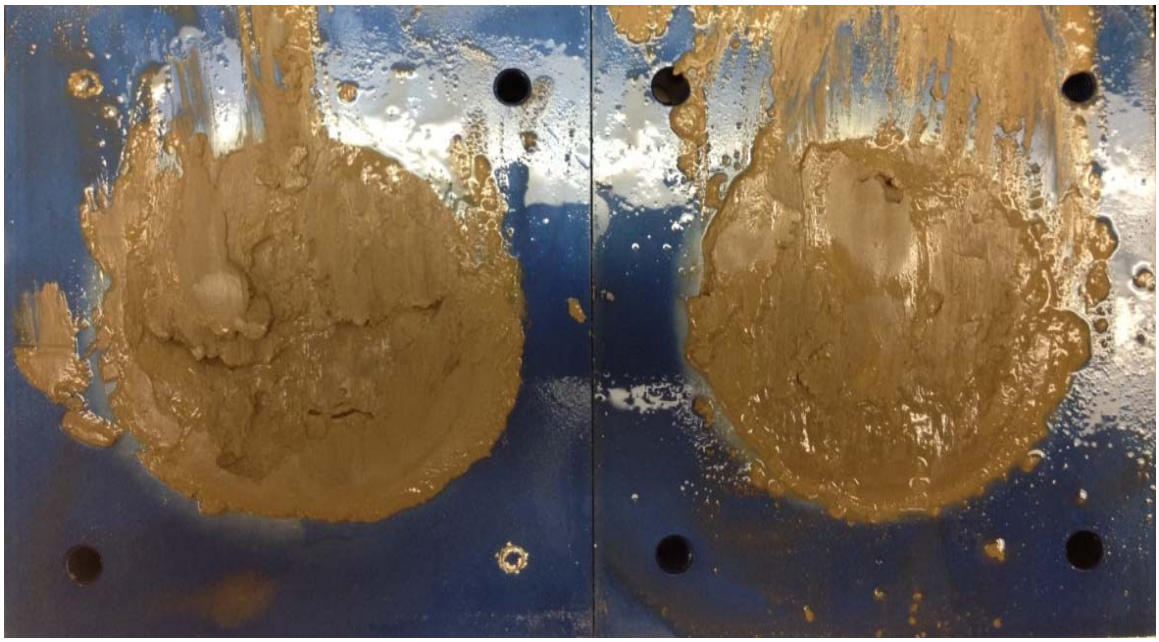

VBC - Non-blenderized - Liquidity Index = 1.59 - 2016 psf

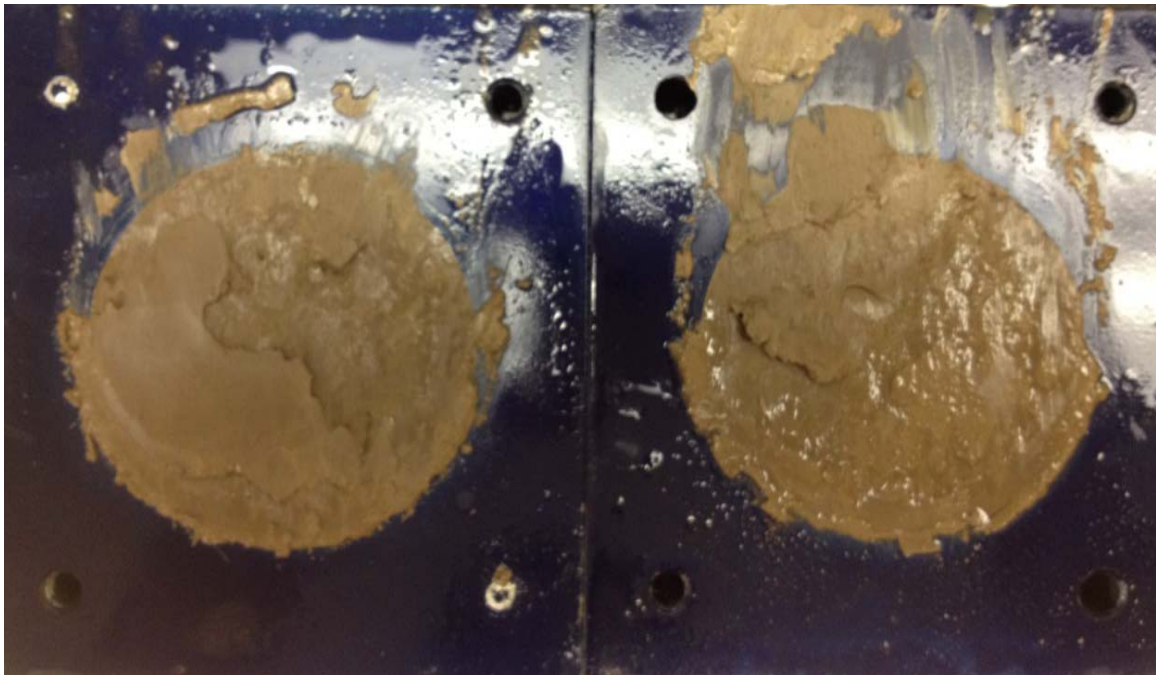

VBC - Non-blenderized - Liquidity Index = 1.59 - 3016 psf

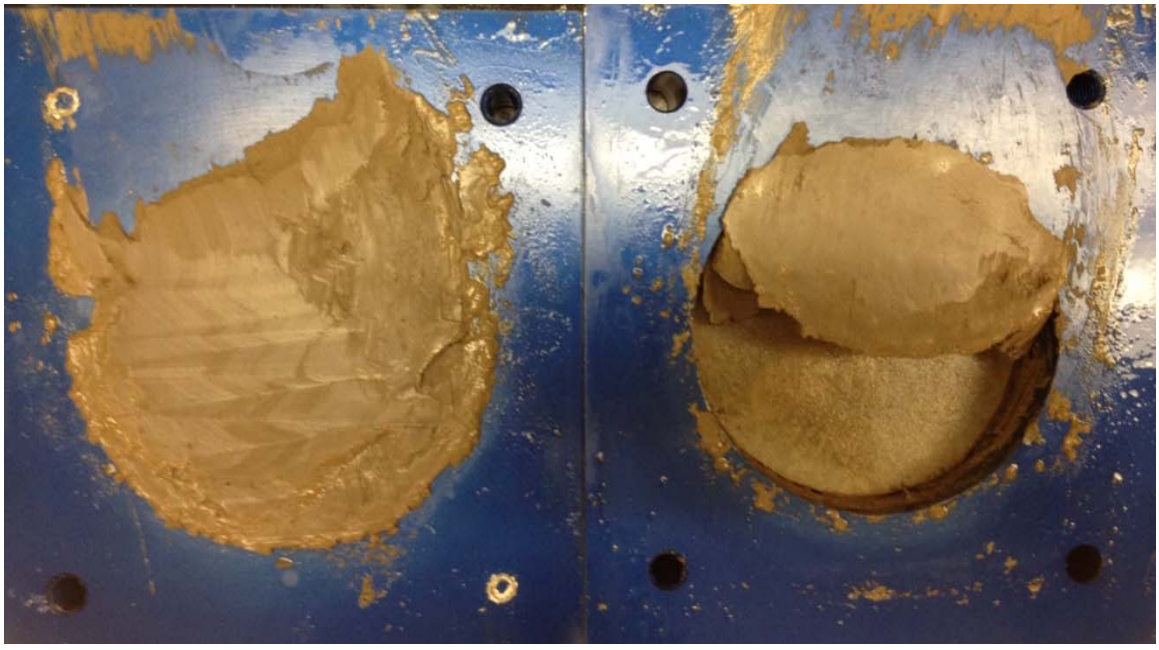

VBC - Non-blenderized - Liquidity Index = 1.59 - 4516 psf

VBC - Non-blenderized - Liquidity Index = 1.59 - 6016 psf

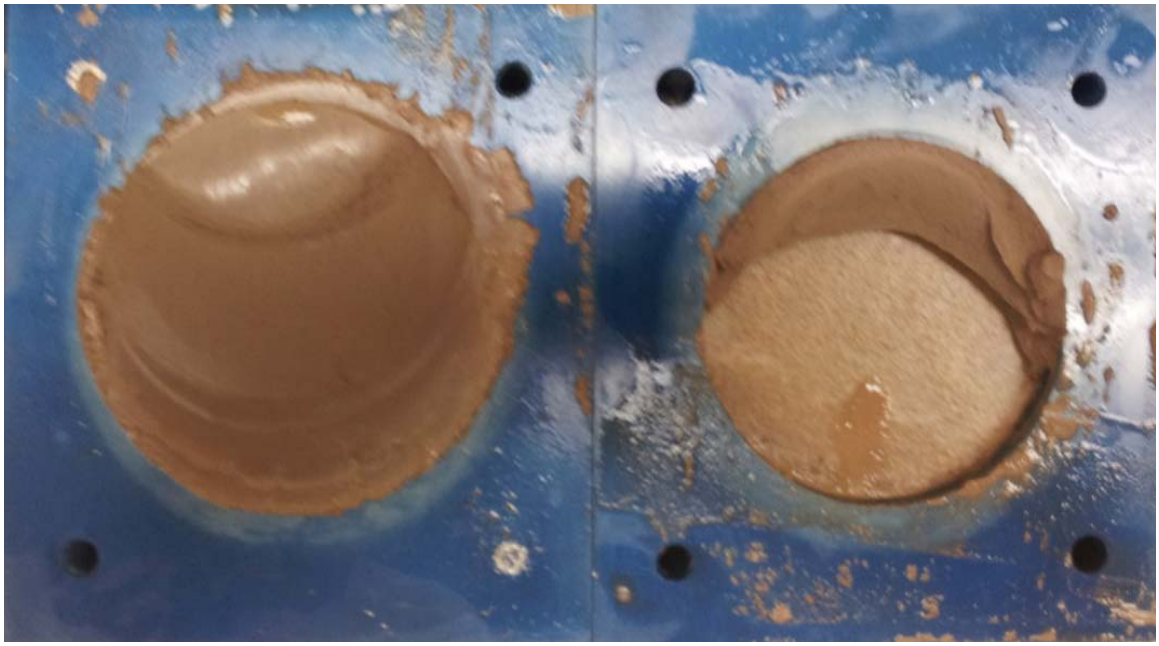

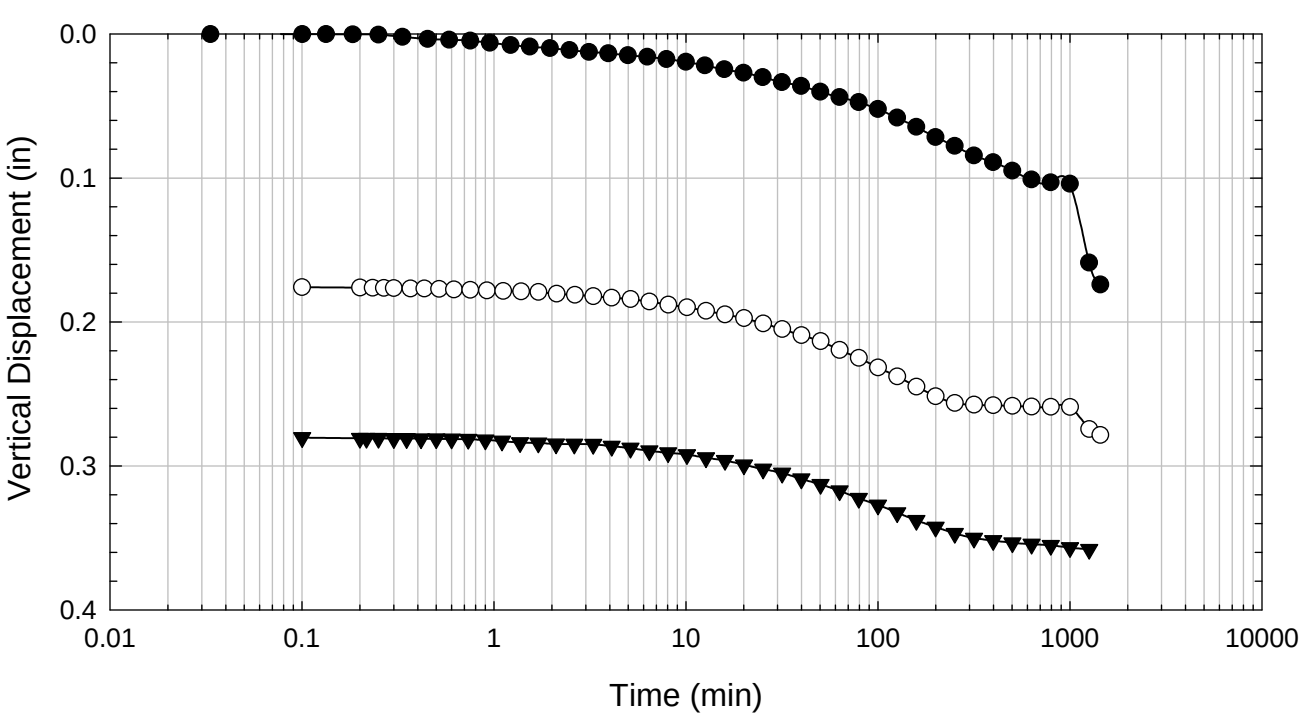
VBC - Non-blenderized - Liquidity Index = 1.59 - 516 psf
Vertical Displacement (in)
0.0
0.1
0.2
0.3
0.4
0.01
0.1
1
10
100
1000
10000
Time (min)

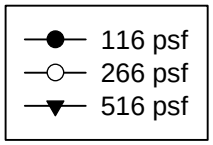
116 psf
266 psf
516 psf

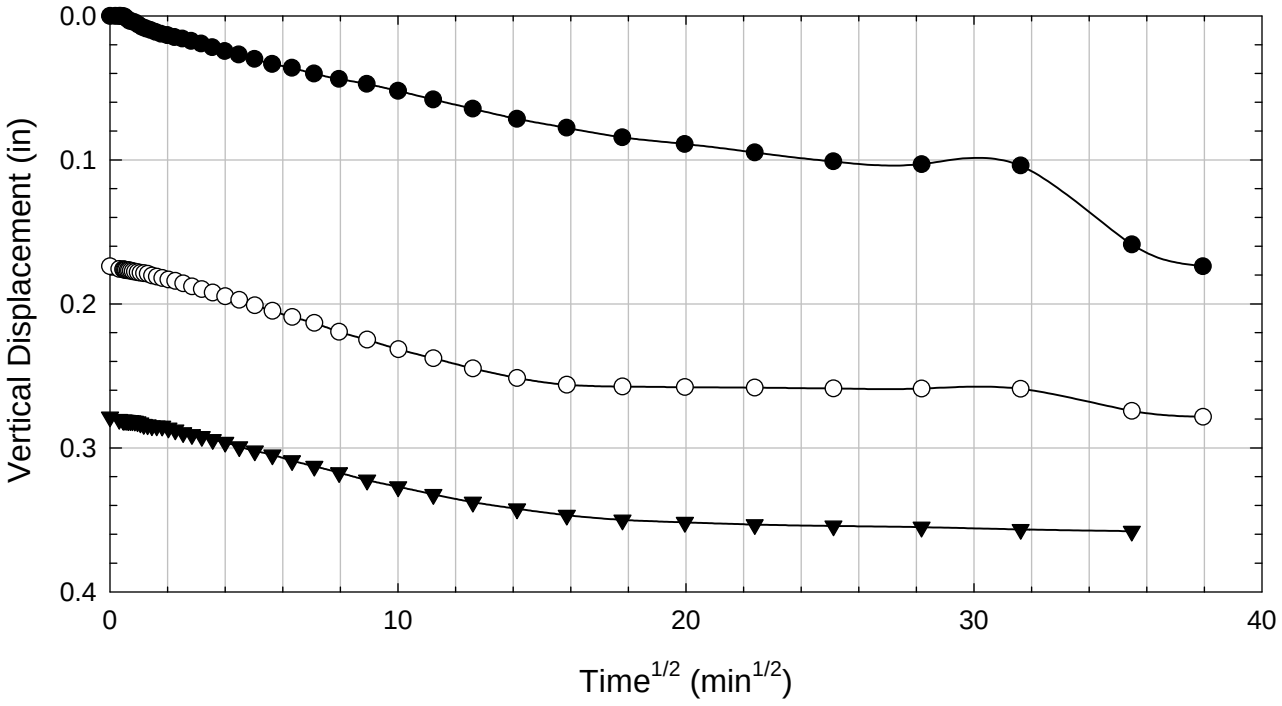
Vertical Displacement (in)
0.0
0.1
0.2
0.3
0.4
0
10
20
30
40
Time^1/2 (min^1/2)

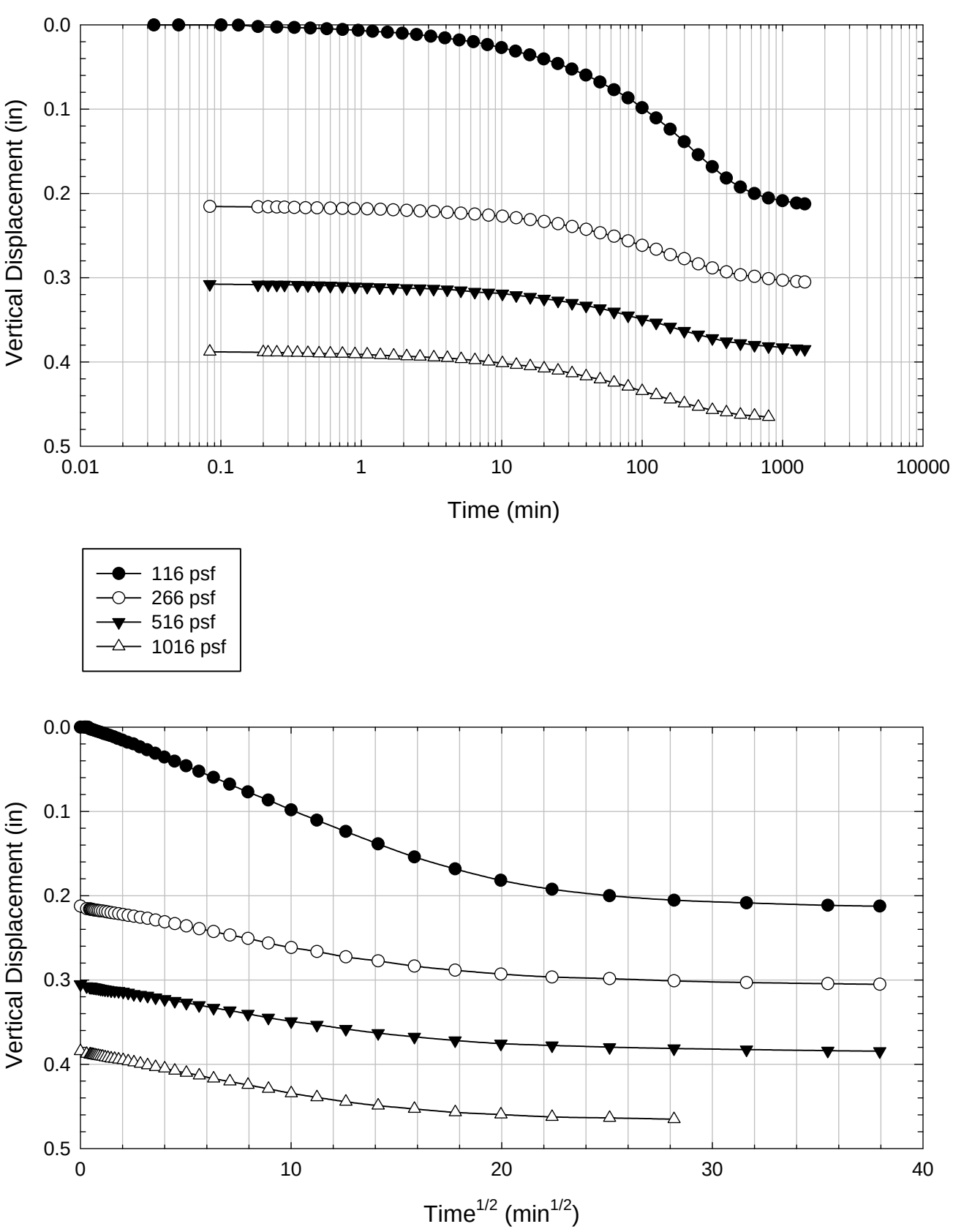
VBC - Non-blenderized - Liquidity Index = 1.59 - 1016 psf
Vertical Displacement (in)
0.0
0.1
0.2
0.3
0.4
0.5
0.01
0.1
1
10
100
1000
10000
Time (min)
116 psf
266 psf
516 psf
1016 psf
Vertical Displacement (in)
0.0
0.1
0.2
0.3
0.4
0.5
0
10
20
30
40
Time^1/2 (min^1/2)

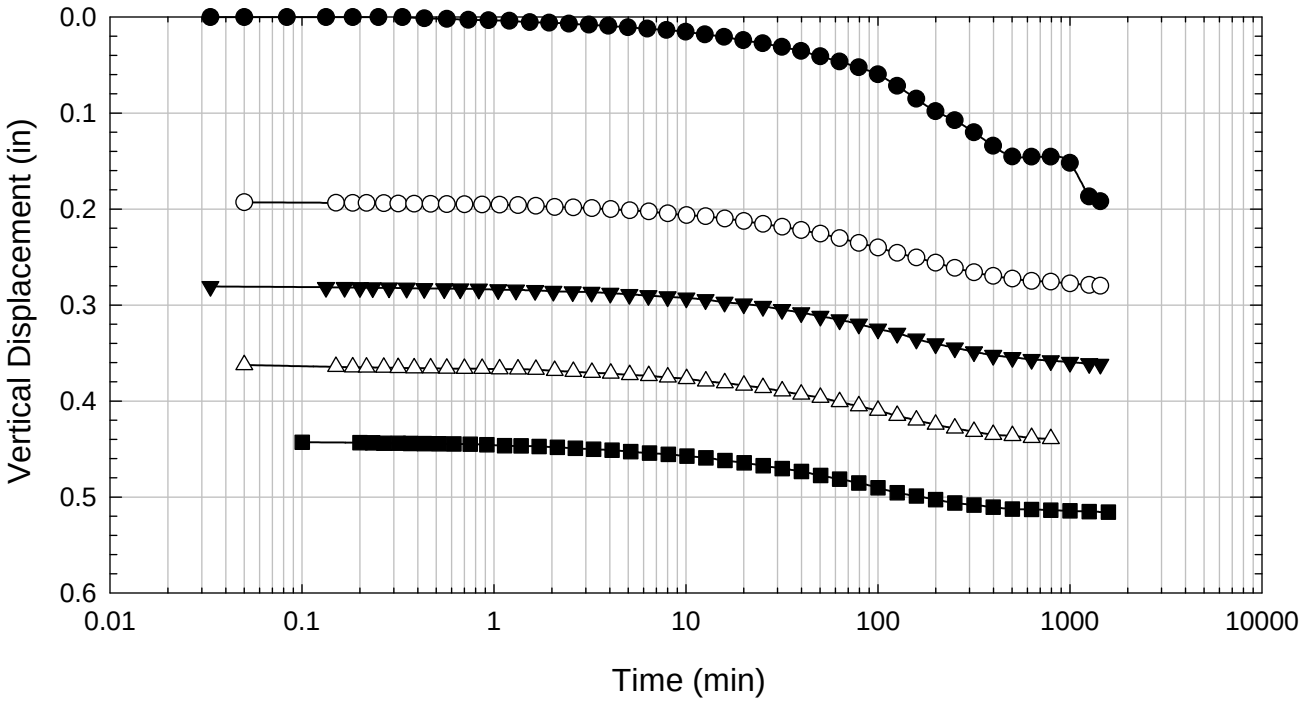
VBC - Non-blenderized - Liquidity Index = 1.59 - 2016 psf
Vertical Displacement (in)
0.0
0.1
0.2
0.3
0.4
0.5
0.6
0.01
0.1
1
10
100
1000
10000
Time (min)

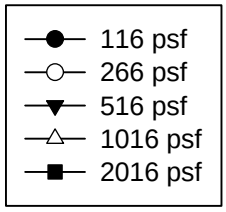
116 psf
266 psf
516 psf
1016 psf
2016 psf

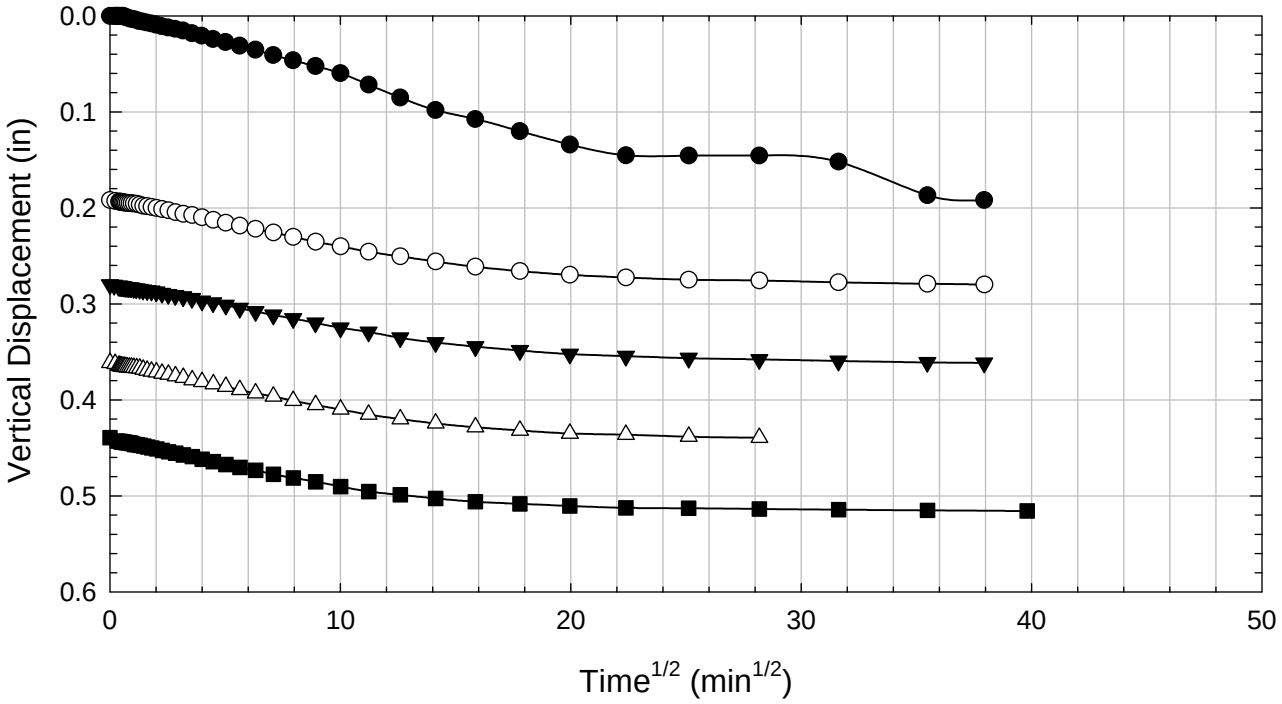
Vertical Displacement (in)
0.0
0.1
0.2
0.3
0.4
0.5
0.6
0
10
20
30
40
50
Time1/2 (min1/2)

VBC - Non-blenderized - Liquidity Index = 1.59 - 3016 psf

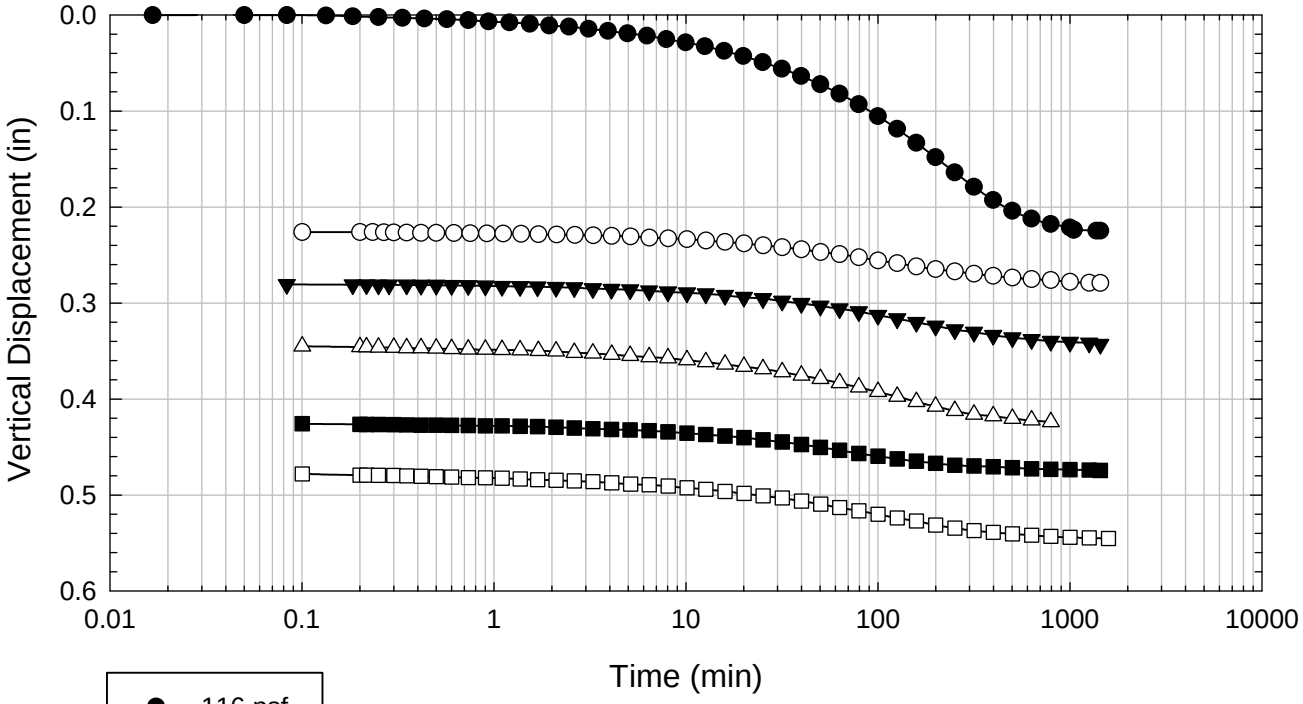

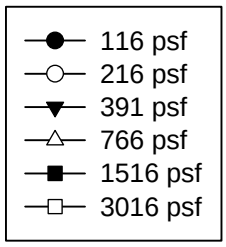

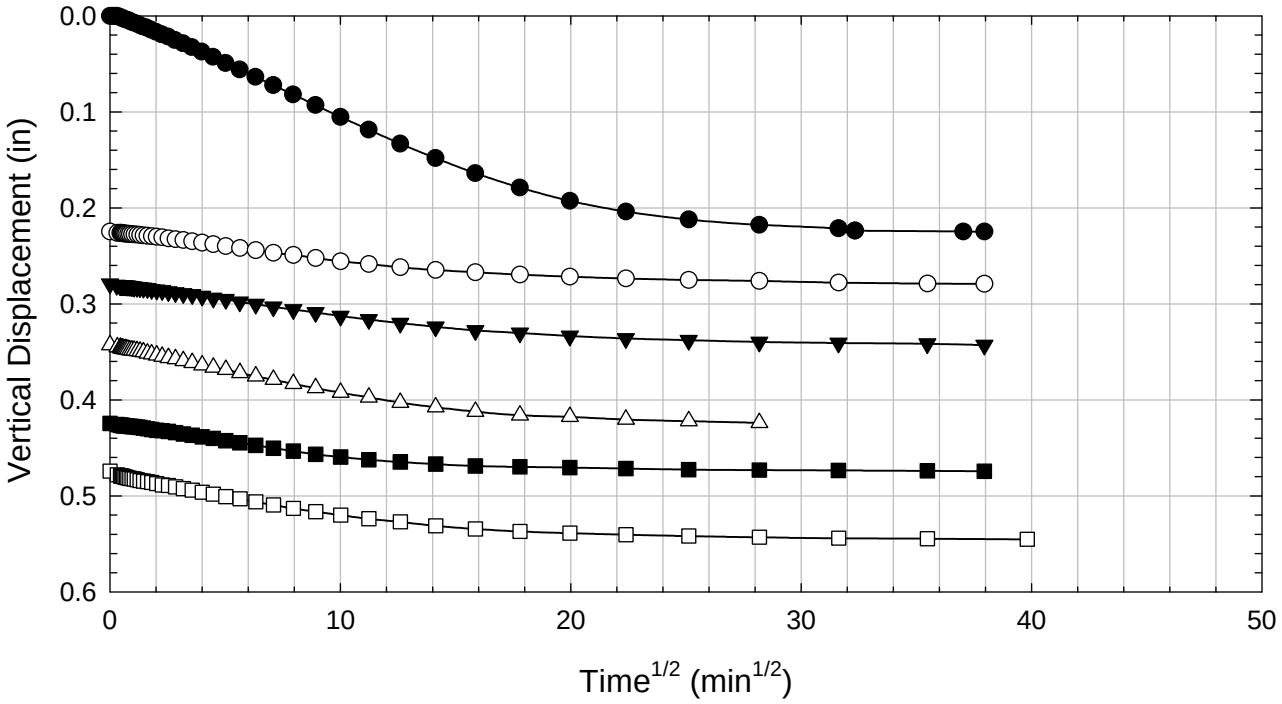

VBC - Non-blenderized - Liquidity Index = 1.59- 4516 psf

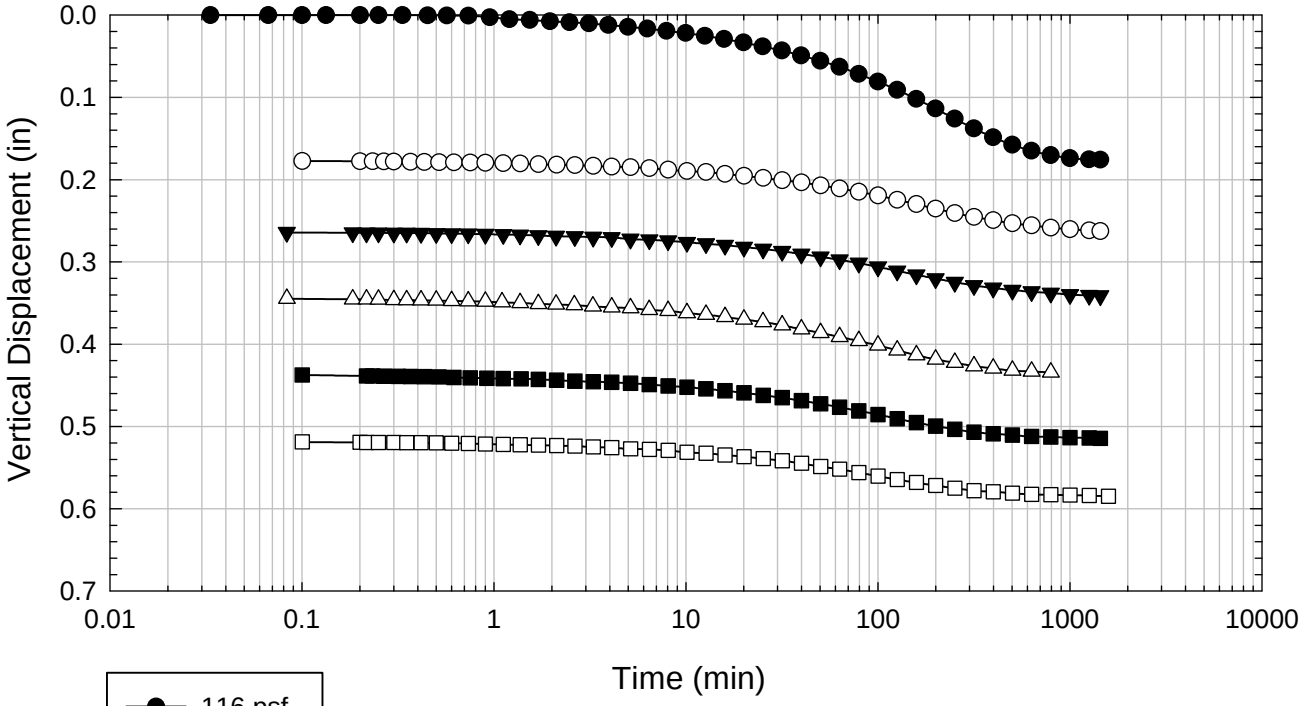

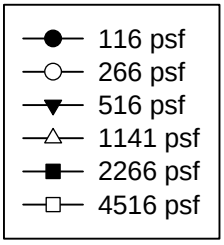

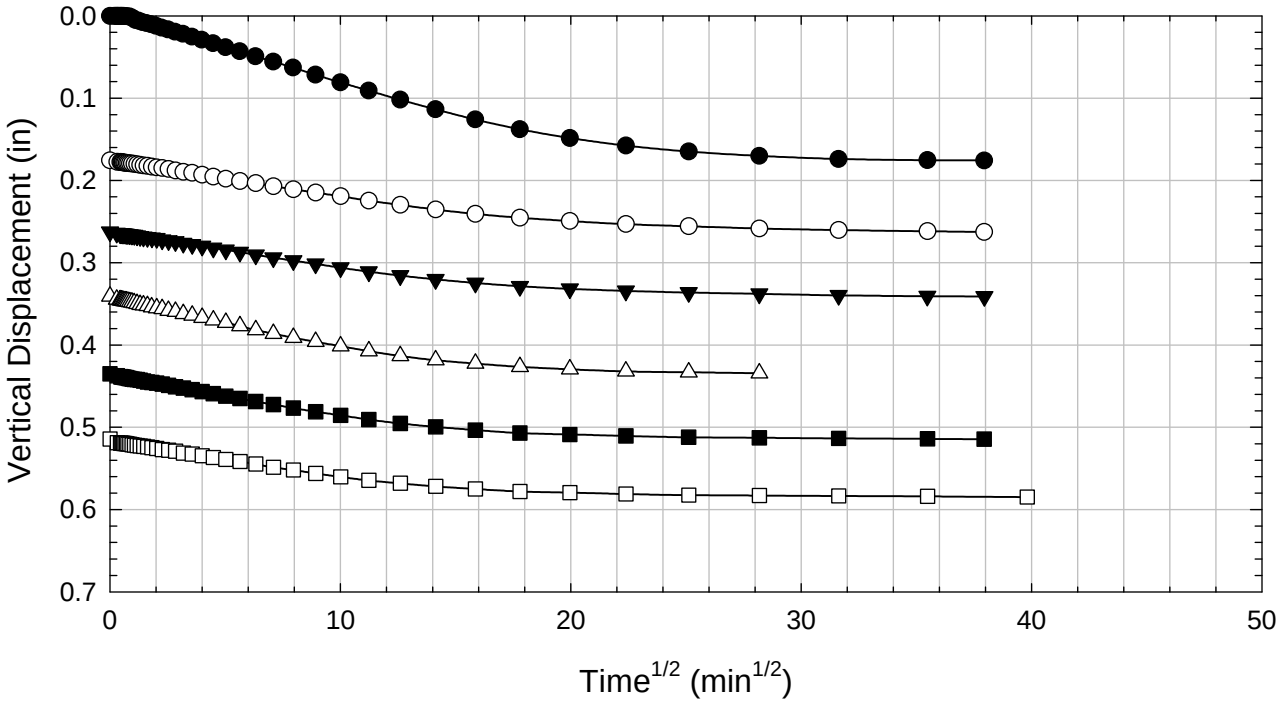

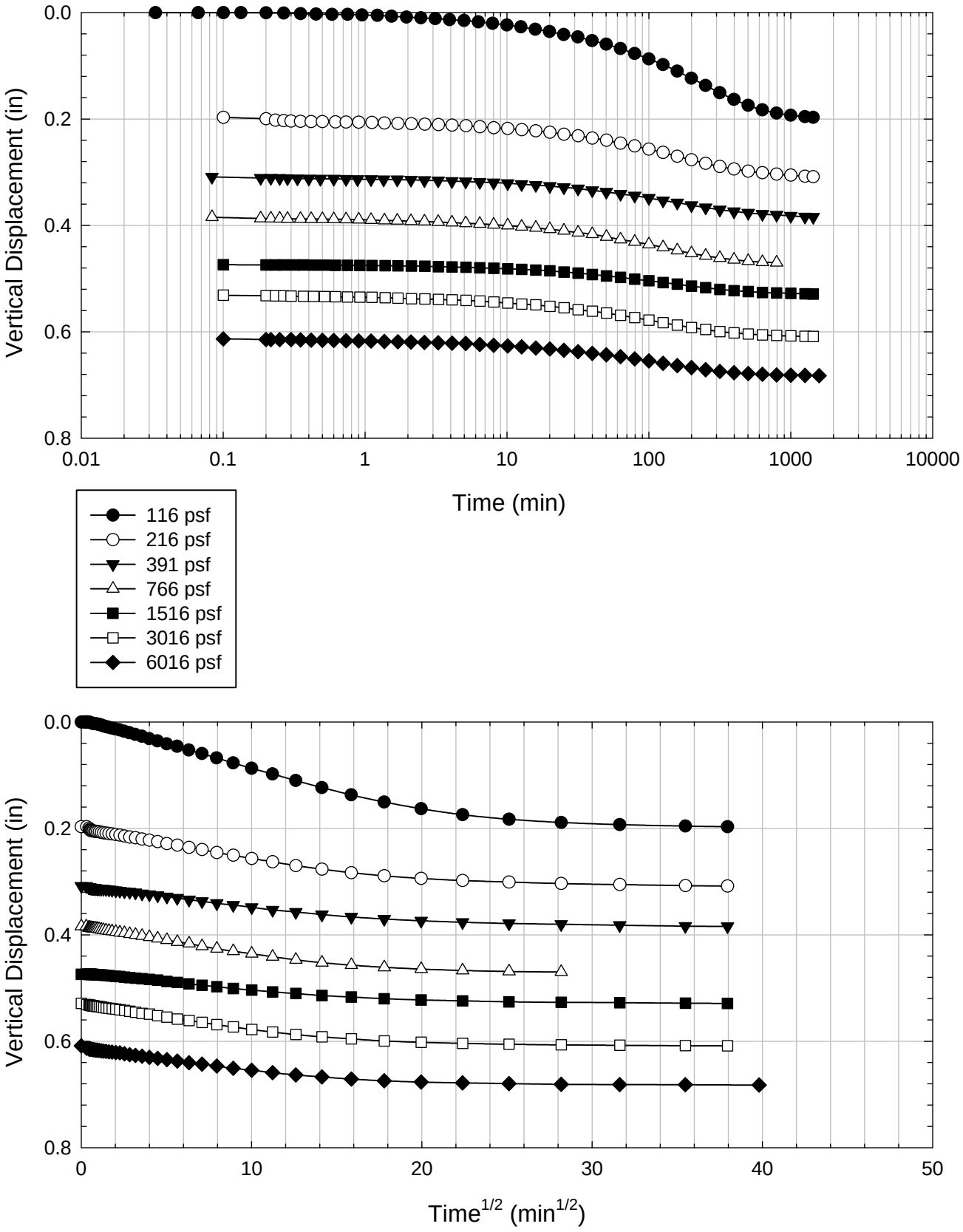
VBC - Non-blenderized - Liquidity Index = 1.59 - 6016 psf
Vertical Displacement (in)
0.0
0.2
0.4
0.6
0.8
0.01
0.1
1
10
100
1000
10000
Time (min)
116 psf
216 psf
391 psf
766 psf
1516 psf
3016 psf
6016 psf
Vertical Displacement (in)
0.0
0.2
0.4
0.6
0.8
0
10
20
30
40
50
Time^1/2 (min^1/2)

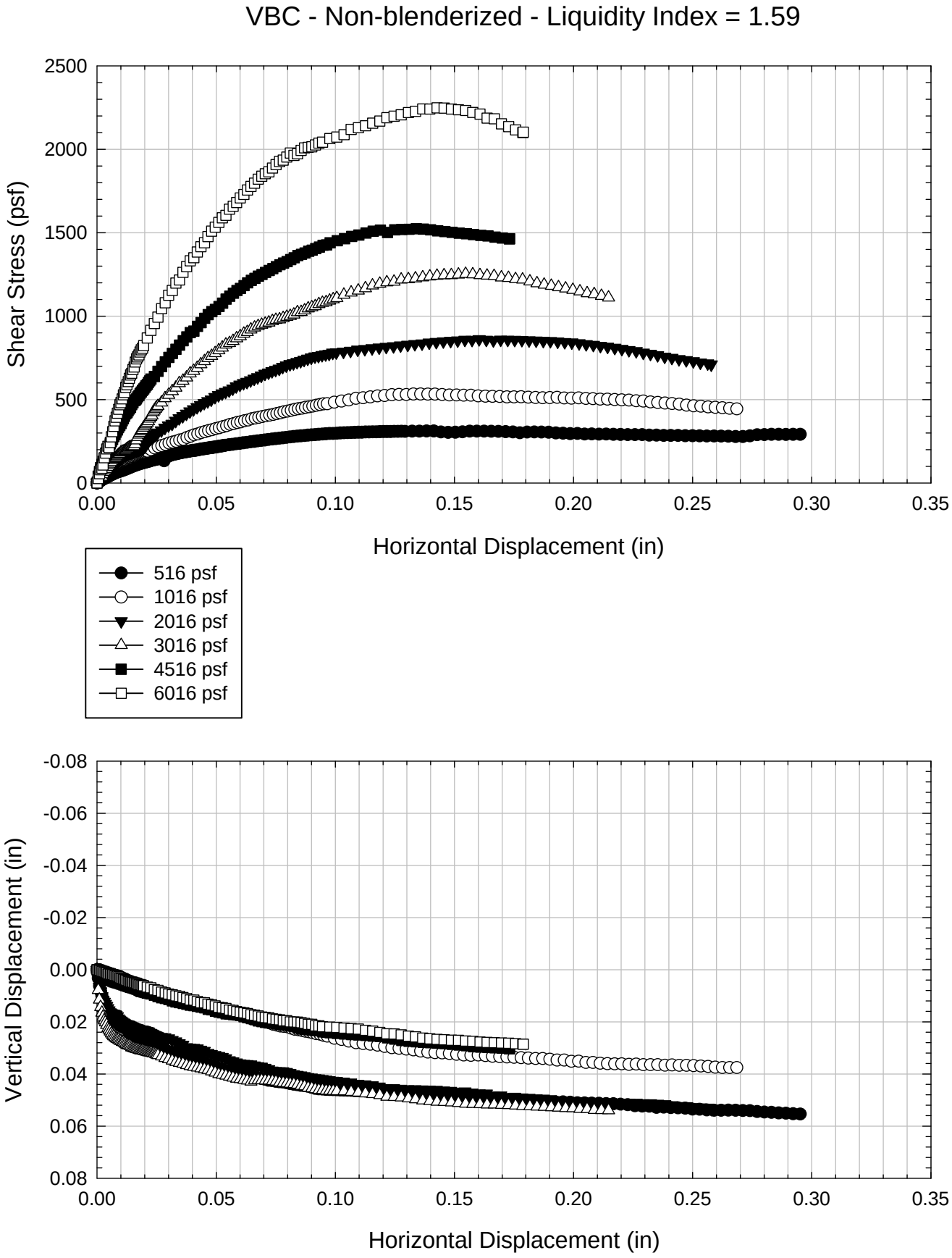
VBC - Non-blenderized - Liquidity Index = 1.59
Shear Stress (psf)
2500
2000
1500
1000
500
0
0.00
0.05
0.10
0.15
0.20
0.25
0.30
0.35
Horizontal Displacement (in)
516 psf
1016 psf
2016 psf
3016 psf
4516 psf
6016 psf
Vertical Displacement (in)
-0.08
-0.06
-0.04
-0.02
0.00
0.02
0.04
0.06
0.08
Horizontal Displacement (in)

C.15.4 Liquidity Index = 0.77

Virginia Polytechnic Institute and State University
Geotechnical Engineering Laboratory
Direct Shear Data Sheet

Project:	Fully Softened Shear Strength
Sample I.D./Loc.:	VBC - Non-blenderized
Classification:	Fat Clay (CH)

Sample Preparation	Remolded at LI = 0.77

Specific Gravity	2.79	

Test Number	1	2	3	4	5	6	7	8
Start Date (m/d/y)	2/24/2012	2/24/2012	2/24/2012	2/24/2012	6/20/1916			
End Date (m/d/y)	3/11/2012	3/11/2012	3/11/2012	3/11/2012	3/11/2012			
Consolidation Pressure (psf)	516	1016	3016	4516	6016			
Initial Values								
Initial Height (in)	1.47	1.41	1.39	1.40	1.45			
Initial Diameter (in)	2.50	2.50	2.50	2.50	2.50			
Initial Sample Weight (g)	192	189	186	190	186			
Water Content (%)	67.79	65.53	64.89	65.18	66.92			
Dry Unit Weight (pcf)	60.5	62.8	62.9	63.8	59.7			
Wet Unit Weight (pcf)	101.5	104.0	103.7	105.5	99.7			
Consolidation Pressures								
Load 1 (psf)	116	116	116	116	116			
Load 2 (psf)	266	266	216	266	216			
Load 3 (psf)	516	516	391	516	391			
Load 4 (psf)		1016	766	1141	766			
Load 5 (psf)			1516	2266	1516			
Load 6 (psf)			3016	4516	3016			
Load 7 (psf)					6016			
t_{50}								
Max. t_{50} for Load 1 (min)								
Max. t_{50} for Load 2 (min)								
Max. t_{50} for Load 3 (min)	196.32							
Max. t_{50} for Load 4 (min)		169.23						
Max. t_{50} for Load 5 (min)								
Max. t_{50} for Load 6 (min)			120.61	110.67				
Max. t_{50} for Load 7 (min)					143.02			
Final Values								
Water Content (%)	59.90	54.11	47.00	42.39	40.45			
Dry Unit Weight (pcf)	65.0	70.6	79.6	83.1	84.4			
Wet Unit Weight (pcf)	103.9	108.8	117.0	118.3	118.6			
Failure								
Test Performed at Shear Rate (in/min)	1.03E-05	1.18E-05	1.66E-05	1.81E-05	1.40E-05			
Required Shear Rate (in/min)	1.22E-05	1.54E-05	1.99E-05	2.17E-05	1.68E-05			
Displacement at Failure (in)	0.12	0.13	0.12	0.12	0.12			
Peak Shear Stress (psf)	324	525	1162	1608	2350			
Total Change in Height at Failure (in)	0.10	0.15	0.29	0.32	0.42			
Secant Effective Friction Angle (deg)	32.1	27.3	21.1	19.6	21.3			

Comments:

VBC - Non-blenderized - Liquidity Index = 0.77 - 516 psf

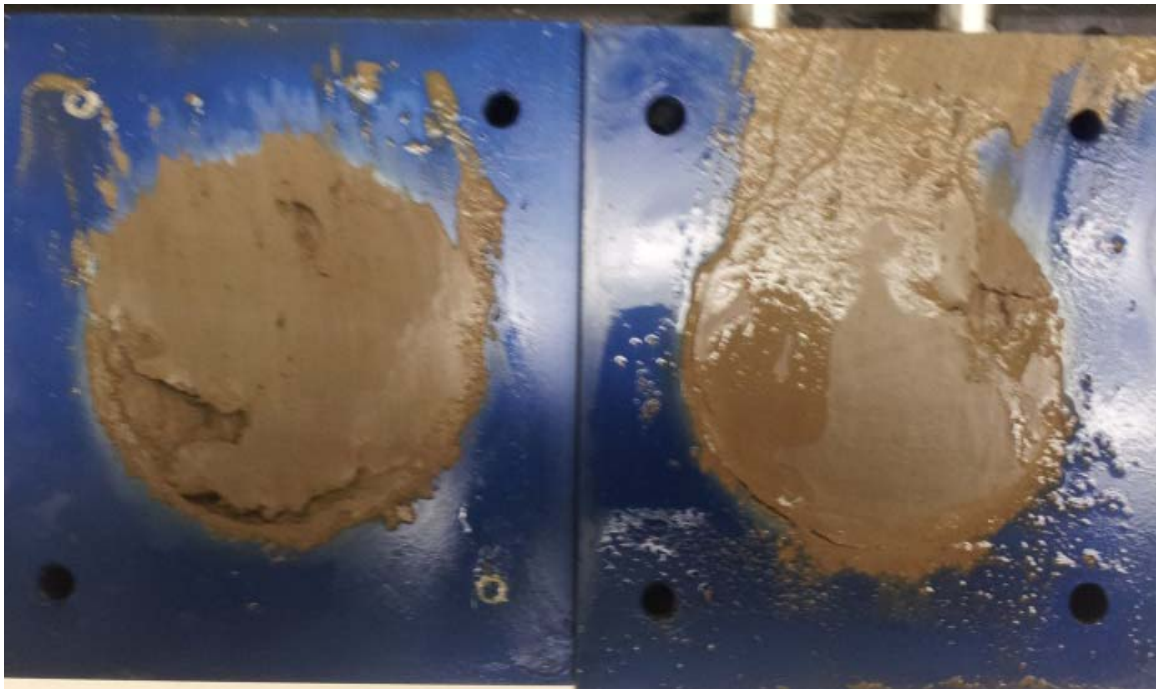

VBC - Non-blenderized - Liquidity Index = 0.77 - 1016 psf

VBC - Non-blenderized - Liquidity Index = 0.77 - 3016 psf

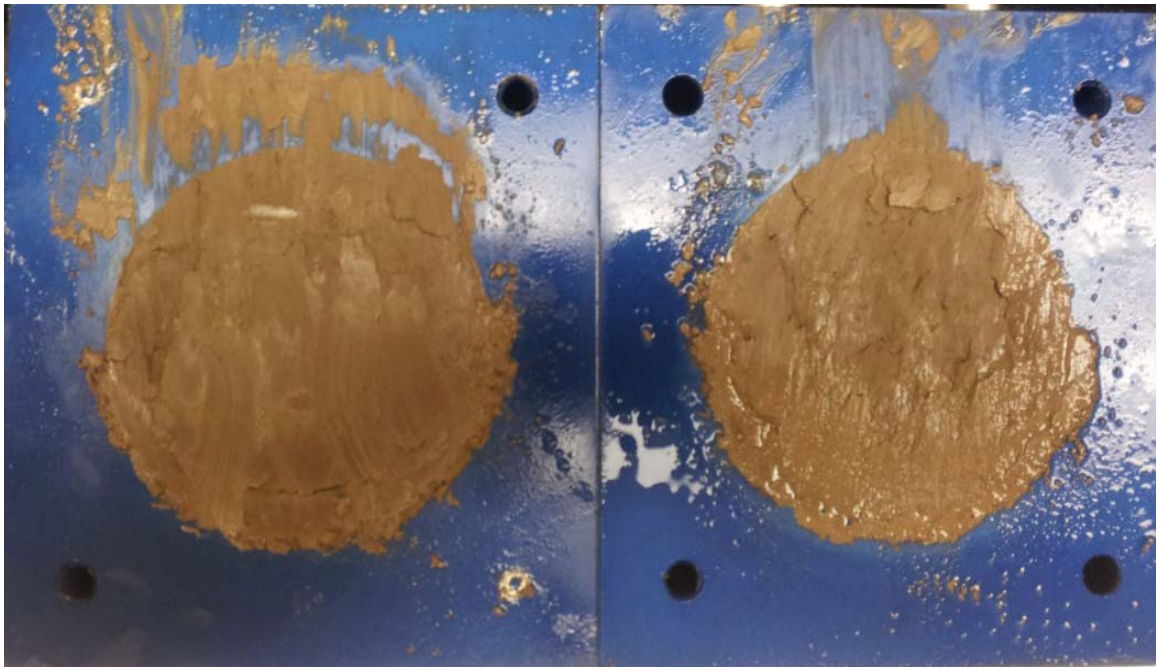

VBC - Non-blenderized - Liquidity Index = 0.77 - 4516 psf

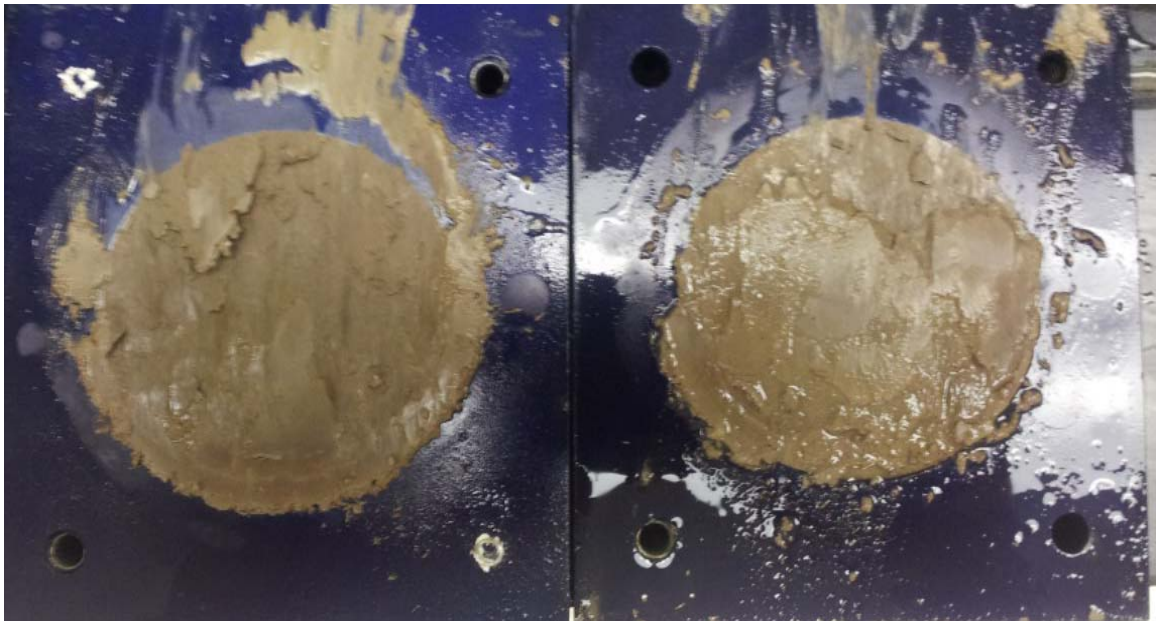

VBC - Non-blenderized - Liquidity Index = 0.77 - 6016 psf

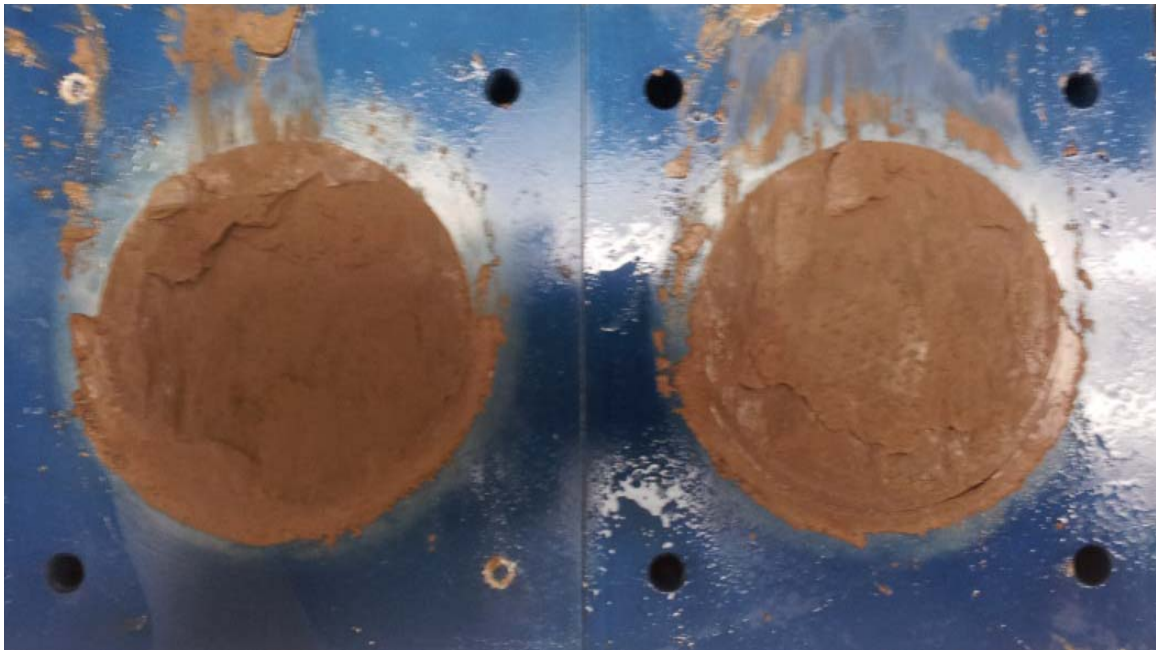

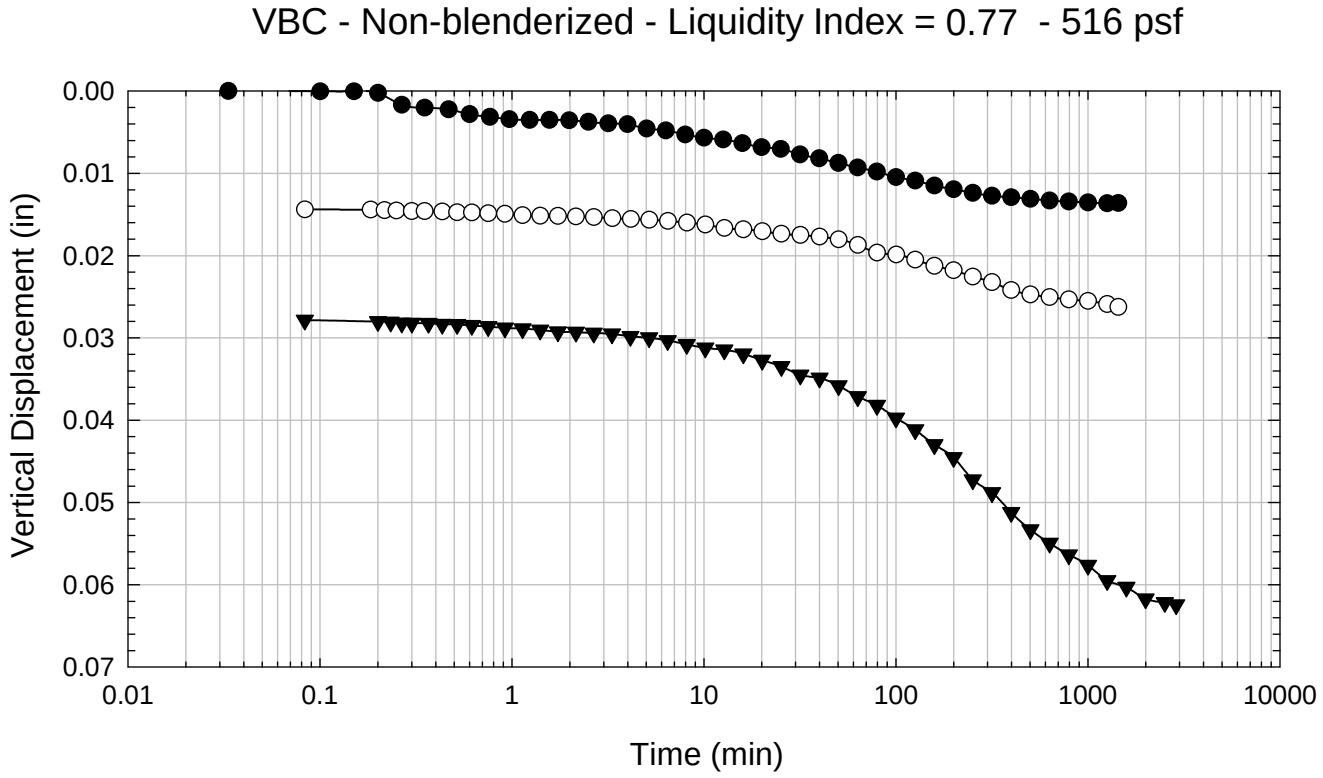
VBC - Non-blenderized - Liquidity Index = 0.77 - 516 psf
Vertical Displacement (in)
0.00
0.01
0.02
0.03
0.04
0.05
0.06
0.07
0.01
0.1
1
10
100
1000
10000
Time (min)

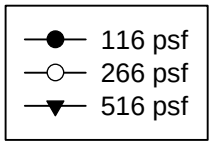
116 psf
266 psf
516 psf

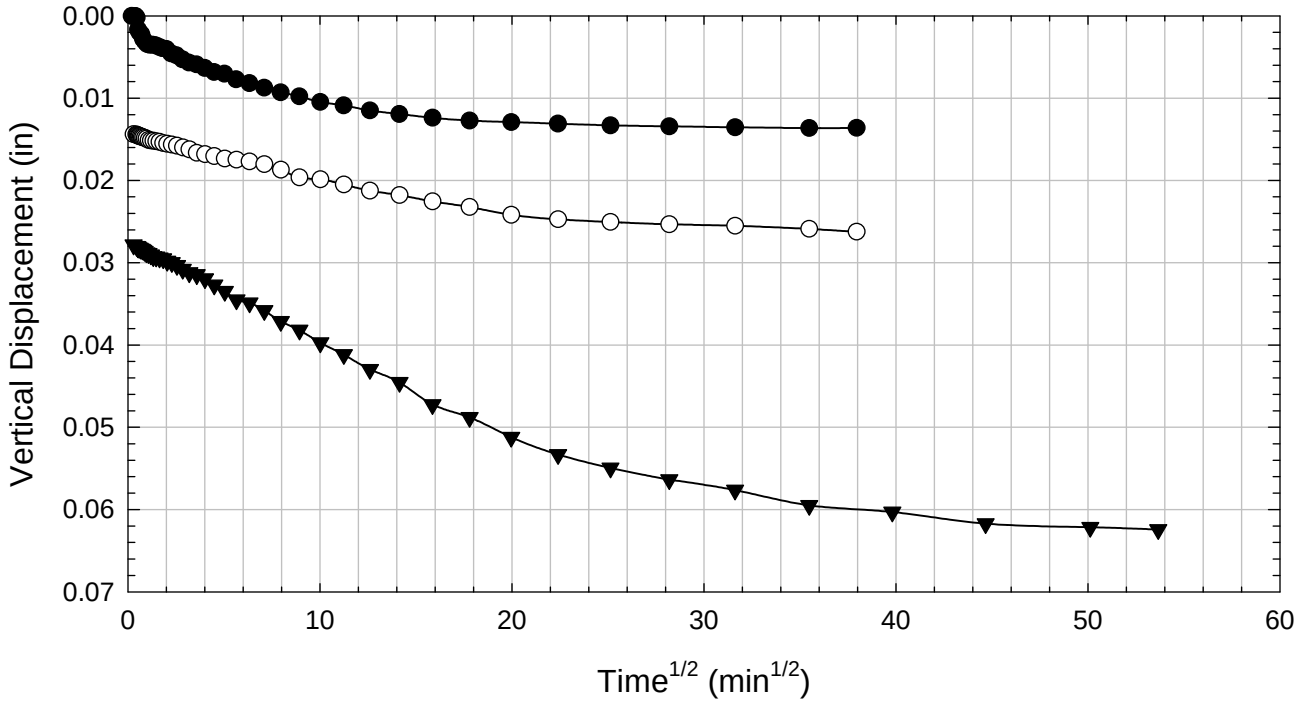
Vertical Displacement (in)
0.00
0.01
0.02
0.03
0.04
0.05
0.06
0.07
0
10
20
30
40
50
60
Time1/2 (min1/2)

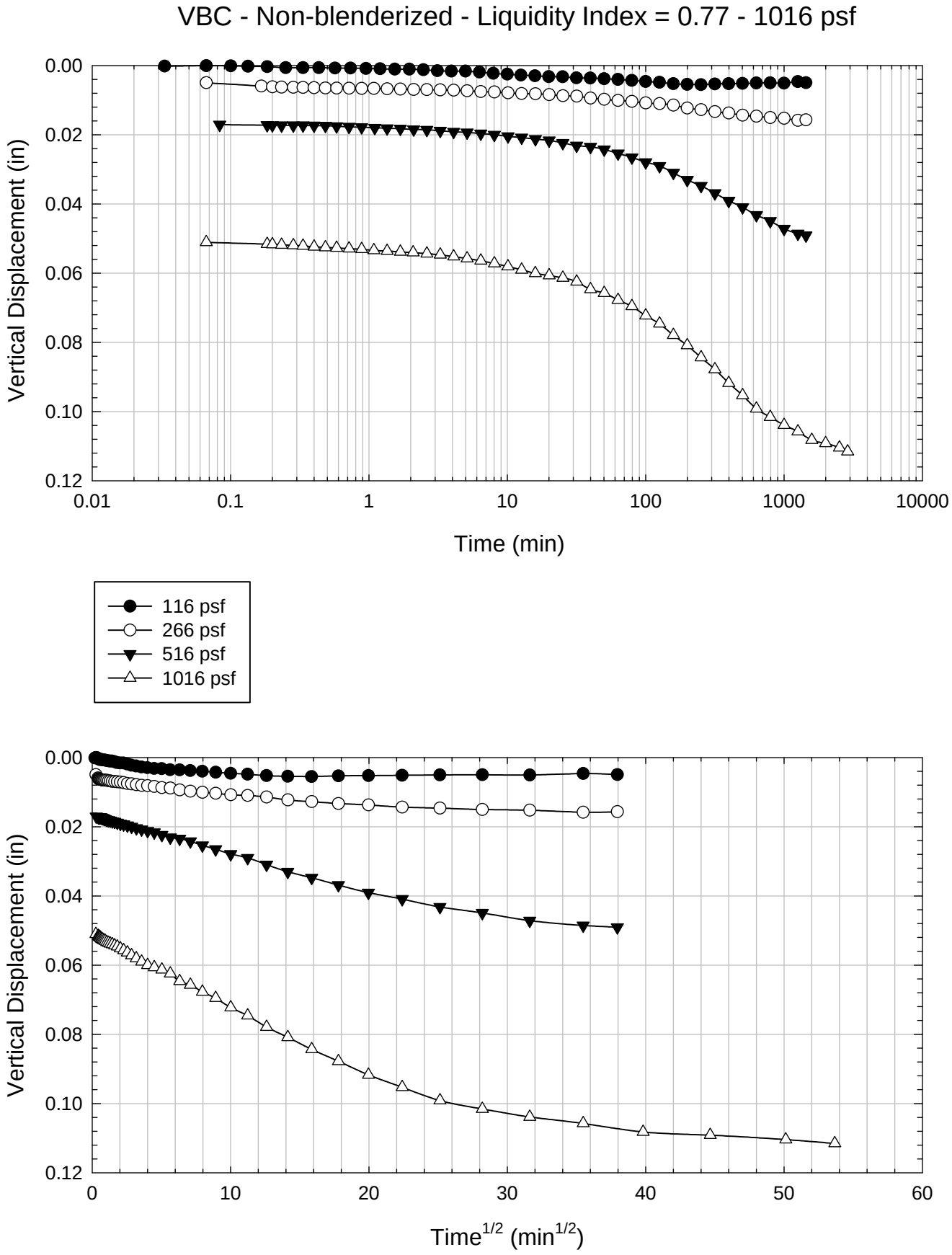
VBC - Non-blenderized - Liquidity Index = 0.77 - 1016 psf
Vertical Displacement (in)
0.00
0.02
0.04
0.06
0.08
0.10
0.12
0.01
0.1
1
10
100
1000
10000
Time (min)
116 psf
266 psf
516 psf
1016 psf
Vertical Displacement (in)
0.00
0.02
0.04
0.06
0.08
0.10
0.12
0
10
20
30
40
50
60
Time1/2 (min1/2)

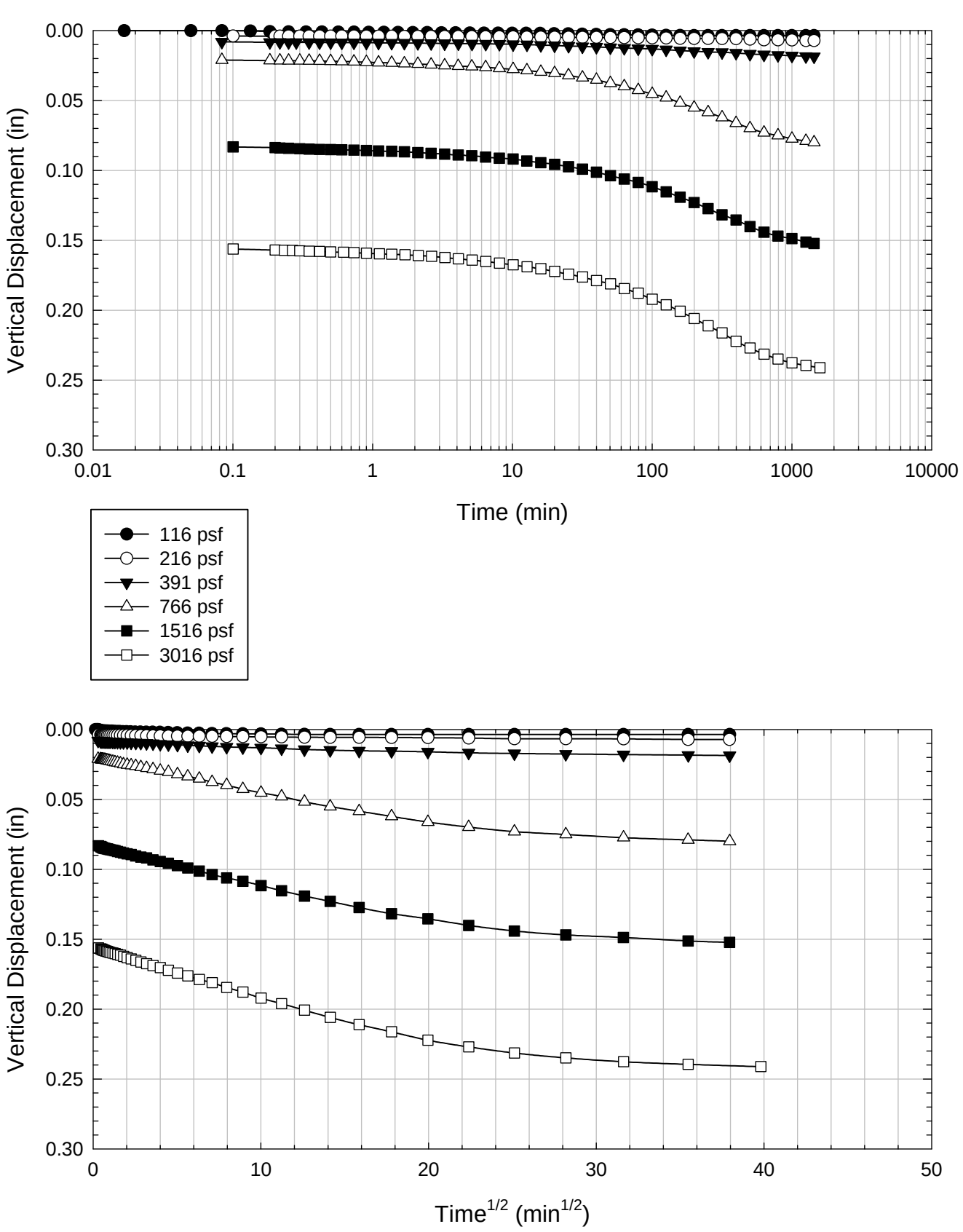
VBC - Non-blenderized - Liquidity Index = 0.77 - 3016 psf
Vertical Displacement (in)
0.00
0.05
0.10
0.15
0.20
0.25
0.30
0.01
0.1
1
10
100
1000
10000
Time (min)
116 psf
216 psf
391 psf
766 psf
1516 psf
3016 psf
Vertical Displacement (in)
0.00
0.05
0.10
0.15
0.20
0.25
0.30
0
10
20
30
40
50
Time1/2 (min1/2)

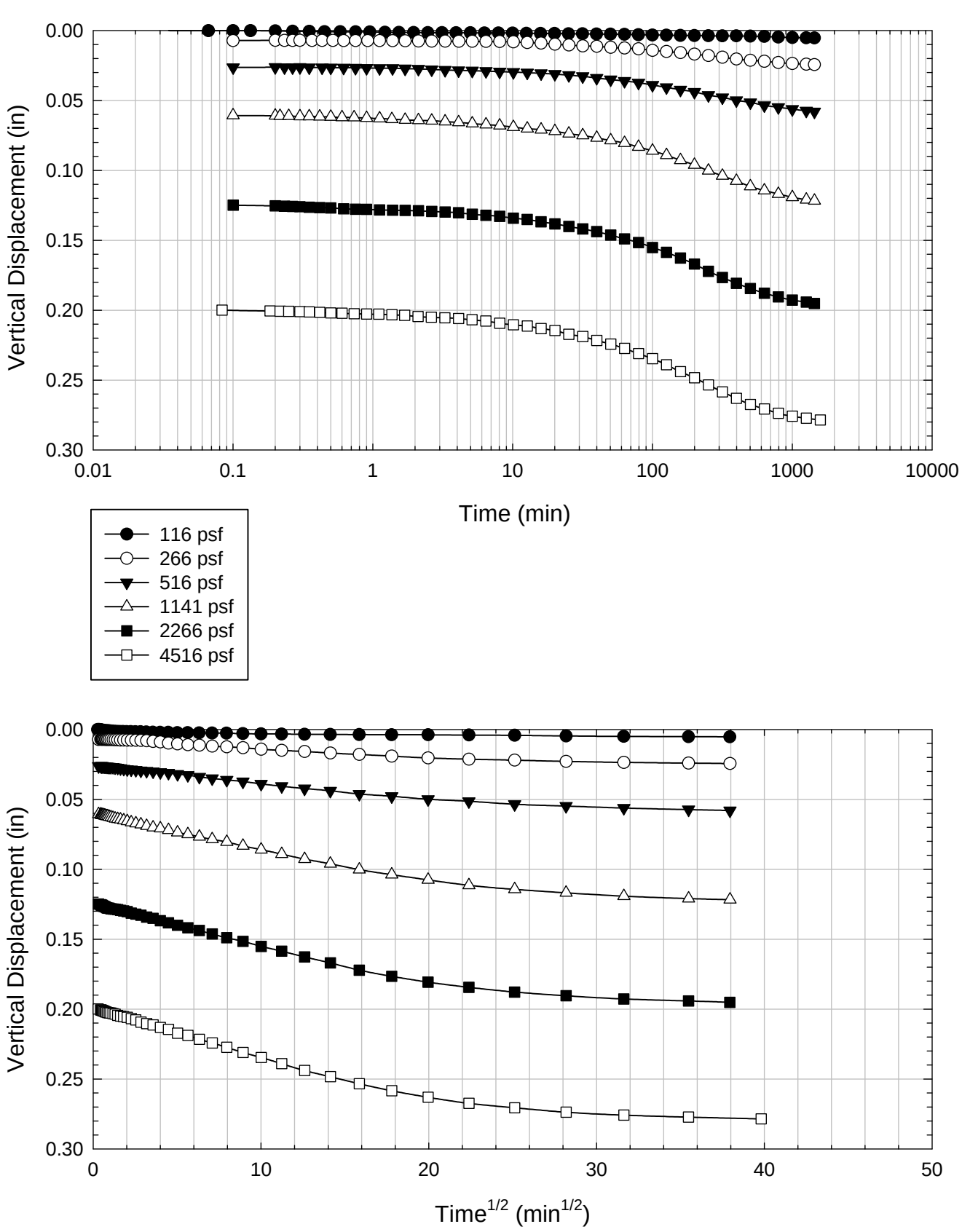
VBC - Non-blenderized - Liquidity Index = 0.77- 4516 psf
Vertical Displacement (in)
0.00
0.05
0.10
0.15
0.20
0.25
0.30
0.01
0.1
1
10
100
1000
10000
Time (min)
116 psf
266 psf
516 psf
1141 psf
2266 psf
4516 psf
Vertical Displacement (in)
0.00
0.05
0.10
0.15
0.20
0.25
0.30
0
10
20
30
40
50
Time1/2 (min1/2)

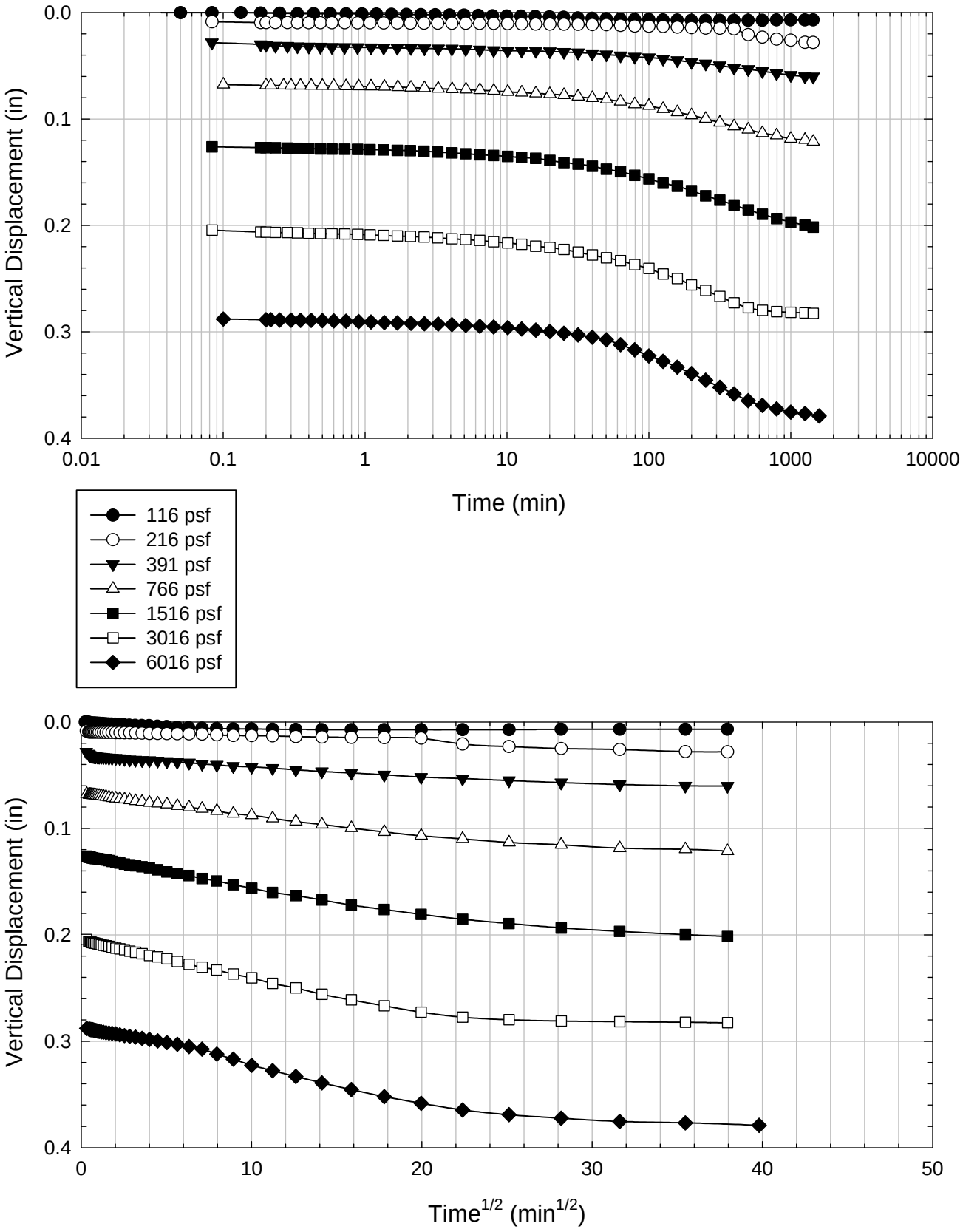
VBC - Non-blenderized - Liquidity Index = 0.77 - 6016 psf
Vertical Displacement (in)
0.0
0.1
0.2
0.3
0.4
0.01
0.1
1
10
100
1000
10000
Time (min)
116 psf
216 psf
391 psf
766 psf
1516 psf
3016 psf
6016 psf
Vertical Displacement (in)
0.0
0.1
0.2
0.3
0.4
0
10
20
30
40
50
Time^1/2 (min^1/2)

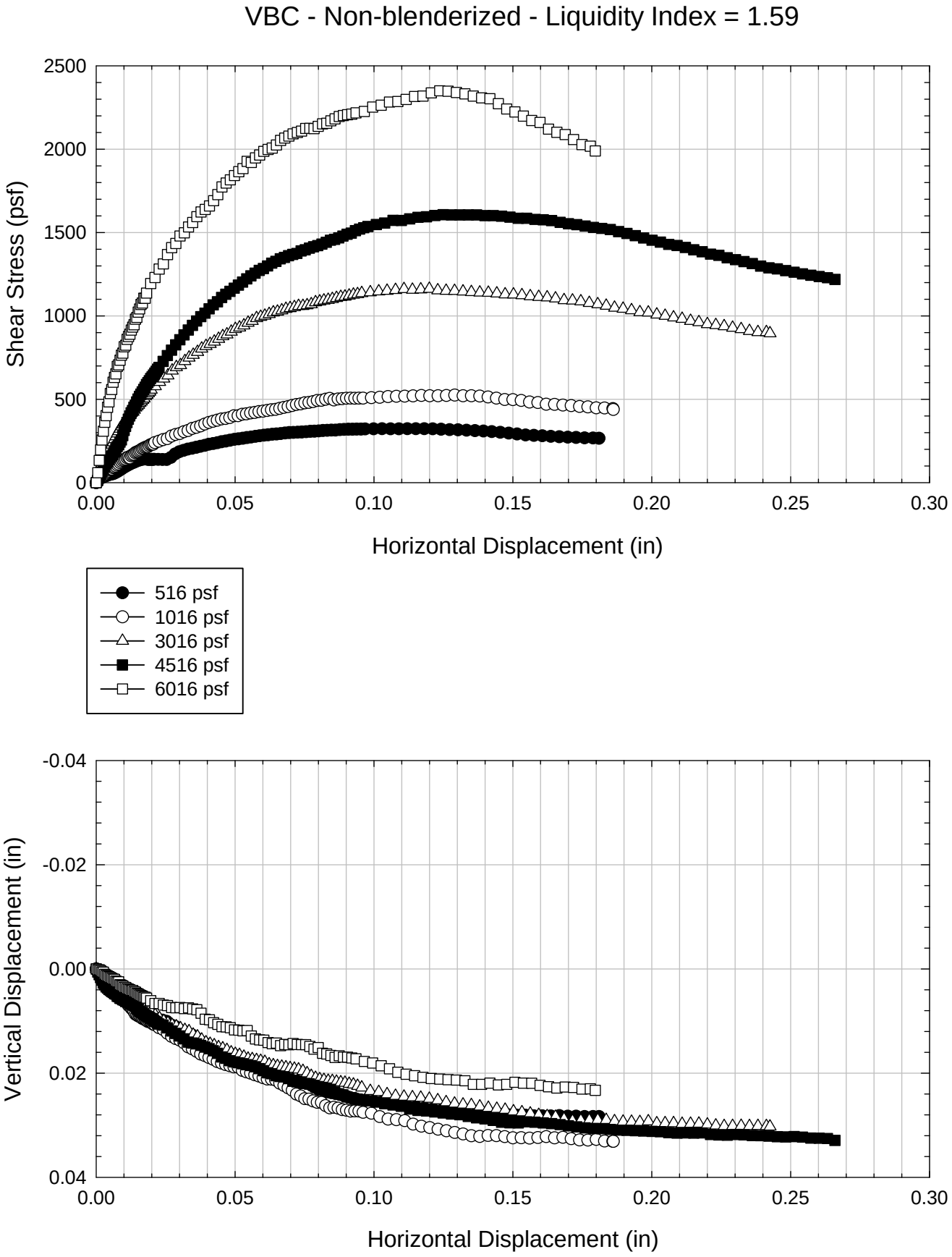
VBC - Non-blenderized - Liquidity Index = 1.59
Shear Stress (psf)
2500
2000
1500
1000
500
0
0.00
0.05
0.10
0.15
0.20
0.25
0.30
Horizontal Displacement (in)
516 psf
1016 psf
3016 psf
4516 psf
6016 psf
Vertical Displacement (in)
-0.04
-0.02
0.00
0.02
0.04
0.00
0.05
0.10
0.15
0.20
0.25
0.30
Horizontal Displacement (in)

Appendix D

Ring Shear Tests Results

Table of Contents

D.1. Alabama 1

D.1.1 Non-blenderized

Virginia Polytechnic Institute and State University
Geotechnical Engineering Laboratory
Ring Shear Data Sheet

Project:	Fully Softened Shear Strength
Sample I.D./Loc.:	Alabama 1 - Non-blenderized
Classification:	Lean Clay (CL)

Sample Preparation	Remolded at LL

Specific Gravity	2.73	
Shear Device Used	WF Bromhead Ring Shear	

Test Number	1	2	3	4	5	6	7	
Start Date (m/d/y)	1/18/2012	1/18/2013	1/19/2013					
End Date (m/d/y)	1/19/2013	1/19/2013	1/22/2013					
Consolidation Pressure (psf)	3489	7141	14473					
Initial Values								
Initial Height (in)	0.20	0.20	0.20					
Inner Radius (in)	1.38	1.38	1.38					
Outer Radius (in)	1.97	1.97	1.97					
Initial Sample Weight (g)	44.79	44.60	45.70					
Water Content (%)	41.58	40.43	40.84					
Saturation (%)	100.0	100.0	100.0					
Consolidation Pressures								
Load 1 (psf)	155	154	155					
Load 2 (psf)	254	253	254					
Load 3 (psf)	452	451	452					
Load 4 (psf)	848	847	848					
Load 5 (psf)	1641	1638	1641					
Load 6 (psf)	3489	3473	3489					
Load 7 (psf)		7141	7160					
Load 8 (psf)			14473					
t_{50}								
Max. t_{50} for Load 1 (min)								
Max. t_{50} for Load 2 (min)								
Max. t_{50} for Load 3 (min)								
Max. t_{50} for Load 4 (min)								
Max. t_{50} for Load 5 (min)								
Max. t_{50} for Load 6 (min)								
Max. t_{50} for Load 7 (min)								
Max. t_{50} for Load 8 (min)								
Final Values								
Water Content (%)	27.48	28.40	28.76					
Saturation (%)	100.0	100.0	100.0					
Failure								
Test Performed at Shear Rate (in/min)	7.00E-04	7.00E-04	7.00E-04					
Required Shear Rate (in/min)								
Displacement at Failure (in)	0.16	0.14	0.24					
Peak Shear Stress (psf)	1553	3128	6184					
Residual Shear Stress (psf)	1295	2269	4194					
Secant Peak Effective Friction Angle (deg)	24.0	23.7	23.1					
Secant Residual Effective Friction Angle (deg)	20.4	17.6	16.2					

Comments:

Alabama 1 - Non-blenderized - 3489 psf

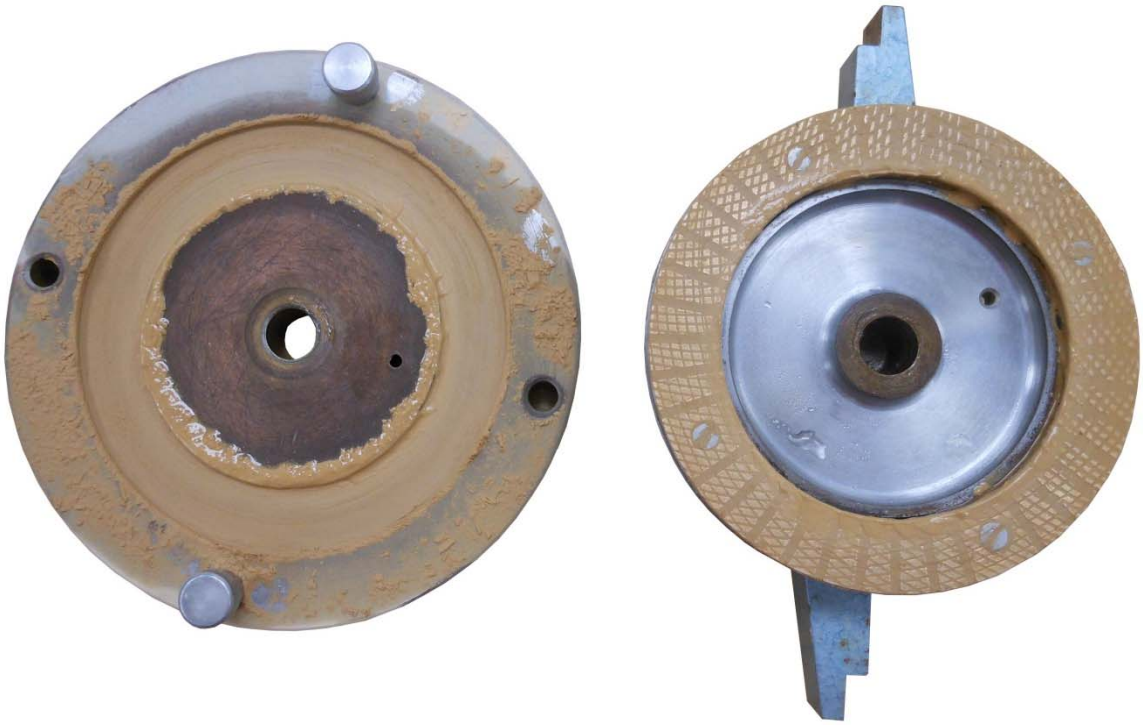

Alabama 1 - Non-blenderized - 7141 psf

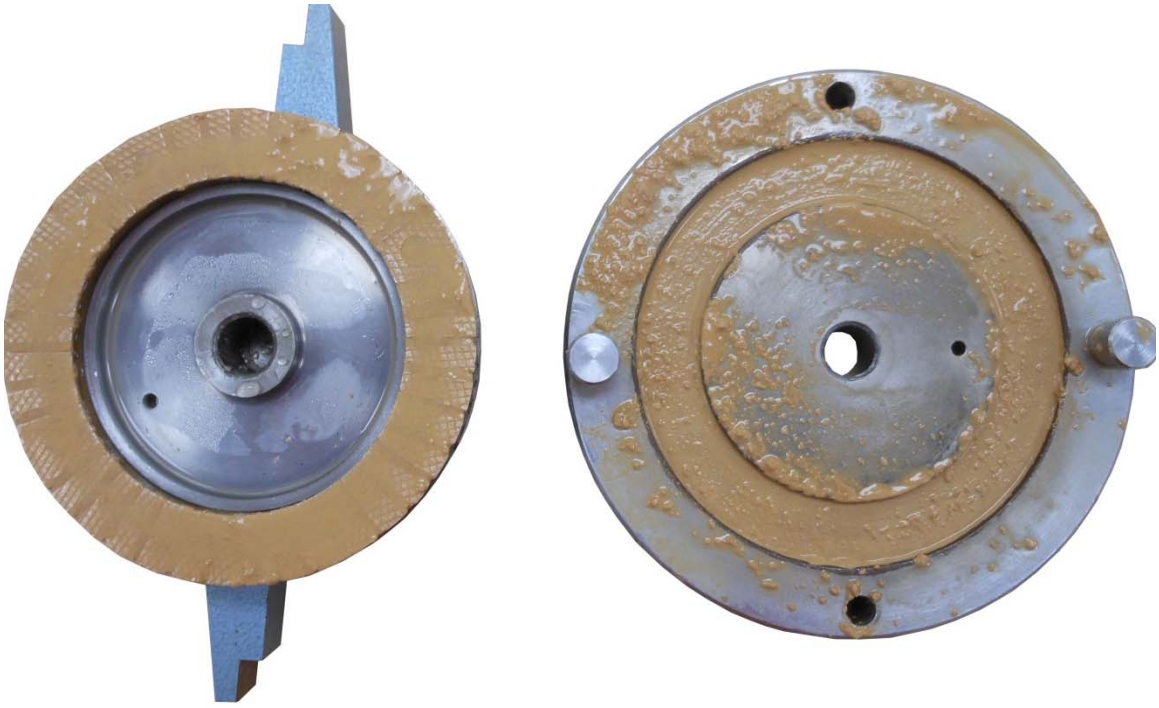

Alabama 1 - Non-blenderized - 14473 psf

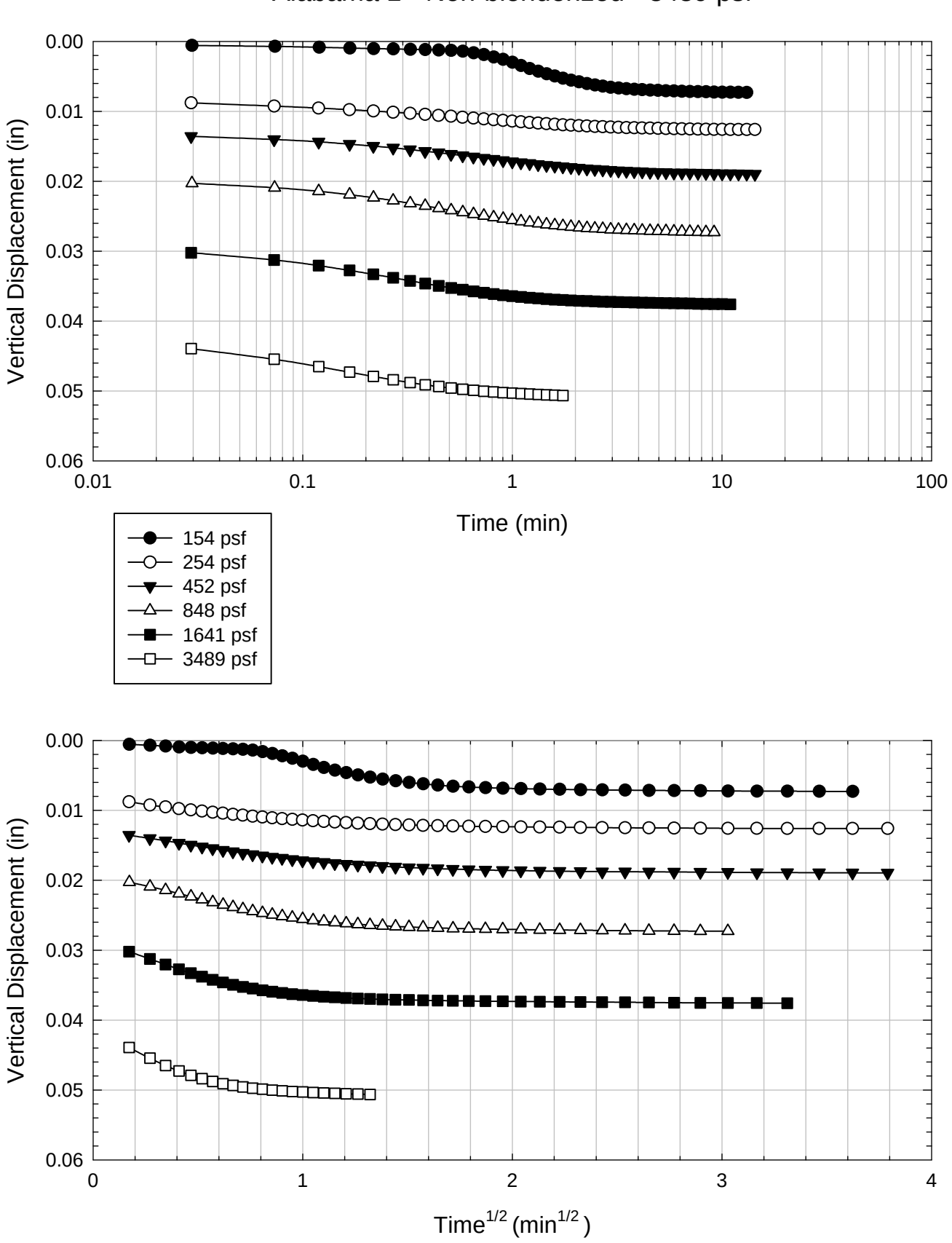
Alabama 1 - Non-blenderized - 3489 psf
Vertical Displacement (in)
0.00
0.01
0.02
0.03
0.04
0.05
0.06
0.01
0.1
1
10
100
Time (min)
154 psf
254 psf
452 psf
848 psf
1641 psf
3489 psf
Vertical Displacement (in)
0.00
0.01
0.02
0.03
0.04
0.05
0.06
0
1
2
3
4
Time^1/2 (min^1/2)

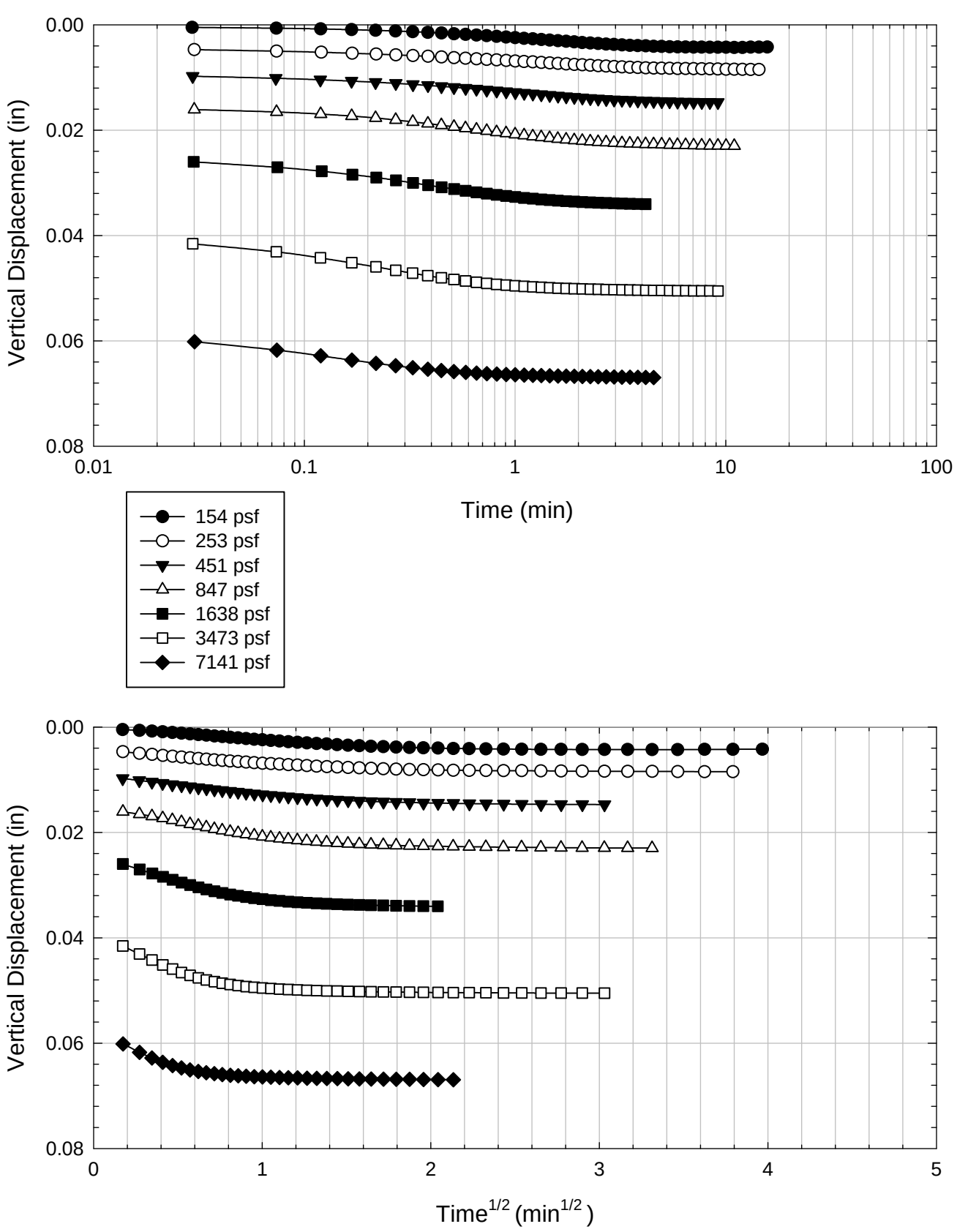
Alabama 1 - Non-blenderized - 7141 psf
Vertical Displacement (in)
0.00
0.02
0.04
0.06
0.08
0.01
0.1
1
10
100
Time (min)
154 psf
253 psf
451 psf
847 psf
1638 psf
3473 psf
7141 psf
Vertical Displacement (in)
0.00
0.02
0.04
0.06
0.08
0
1
2
3
4
5
Time^1/2 (min^1/2)

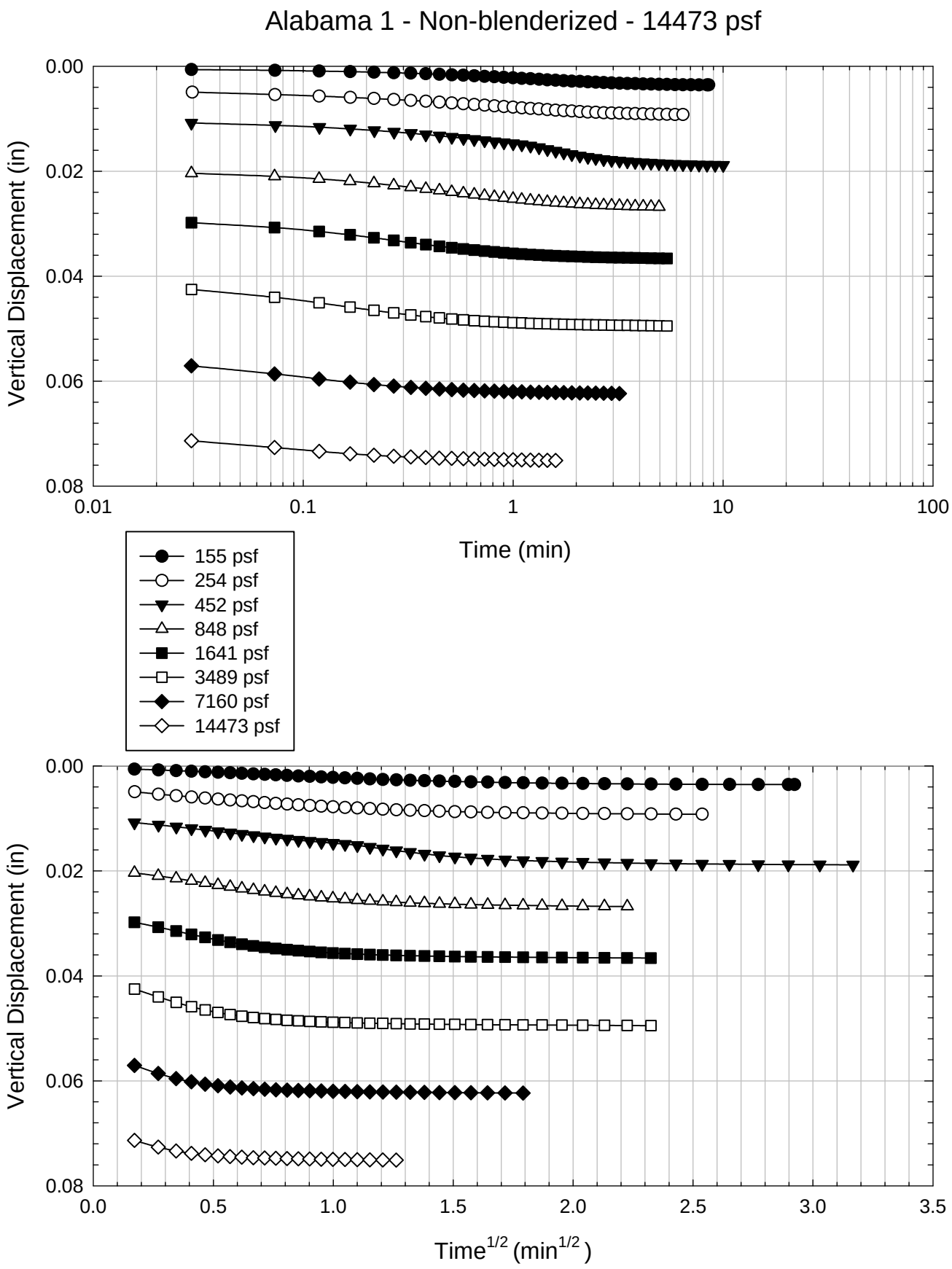
Alabama 1 - Non-blenderized - 14473 psf
Vertical Displacement (in)
0.00
0.02
0.04
0.06
0.08
0.01
0.1
1
10
100
Time (min)
155 psf
254 psf
452 psf
848 psf
1641 psf
3489 psf
7160 psf
14473 psf
Vertical Displacement (in)
0.00
0.02
0.04
0.06
0.08
0.0
0.5
1.0
1.5
2.0
2.5
3.0
3.5
Time^1/2 (min^1/2)

Alabama 1 - Non-blenderized

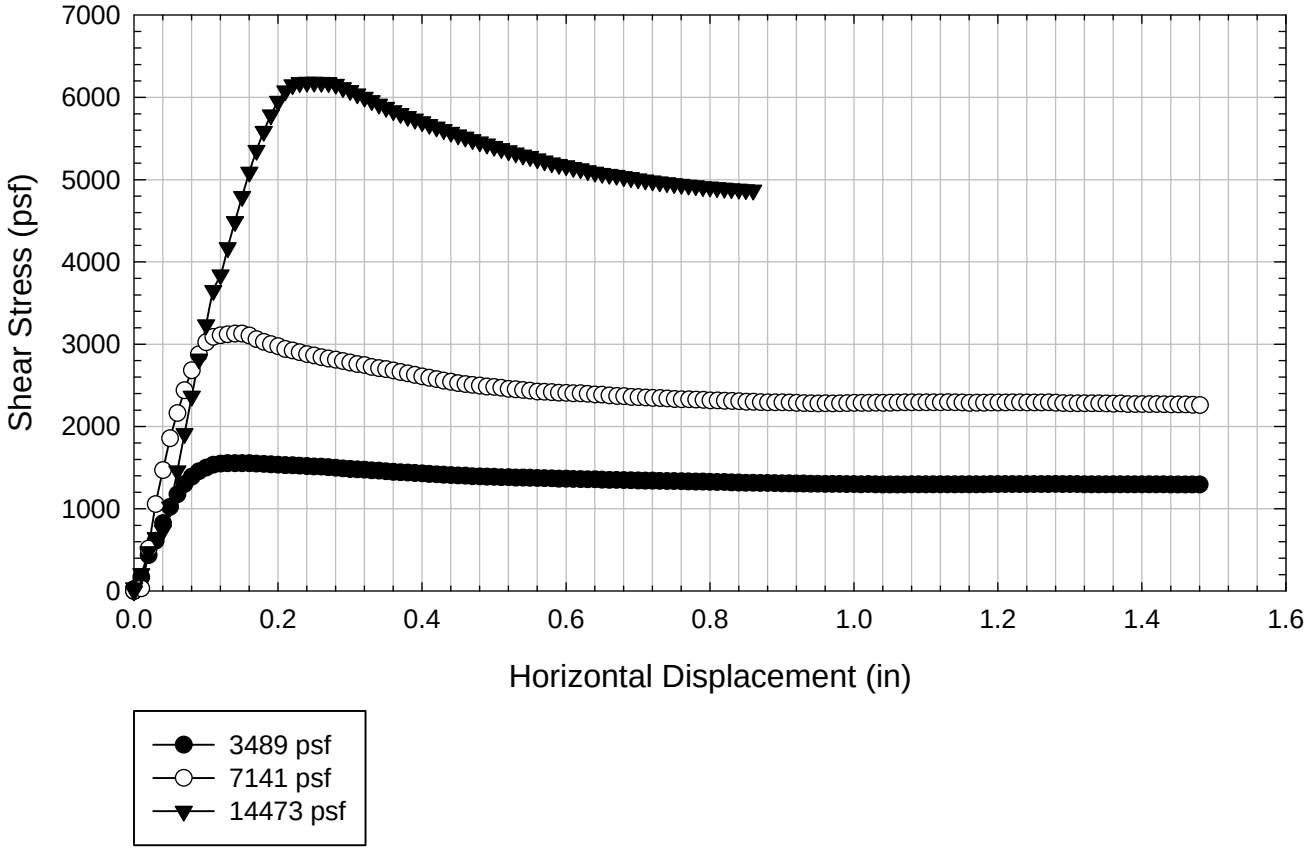

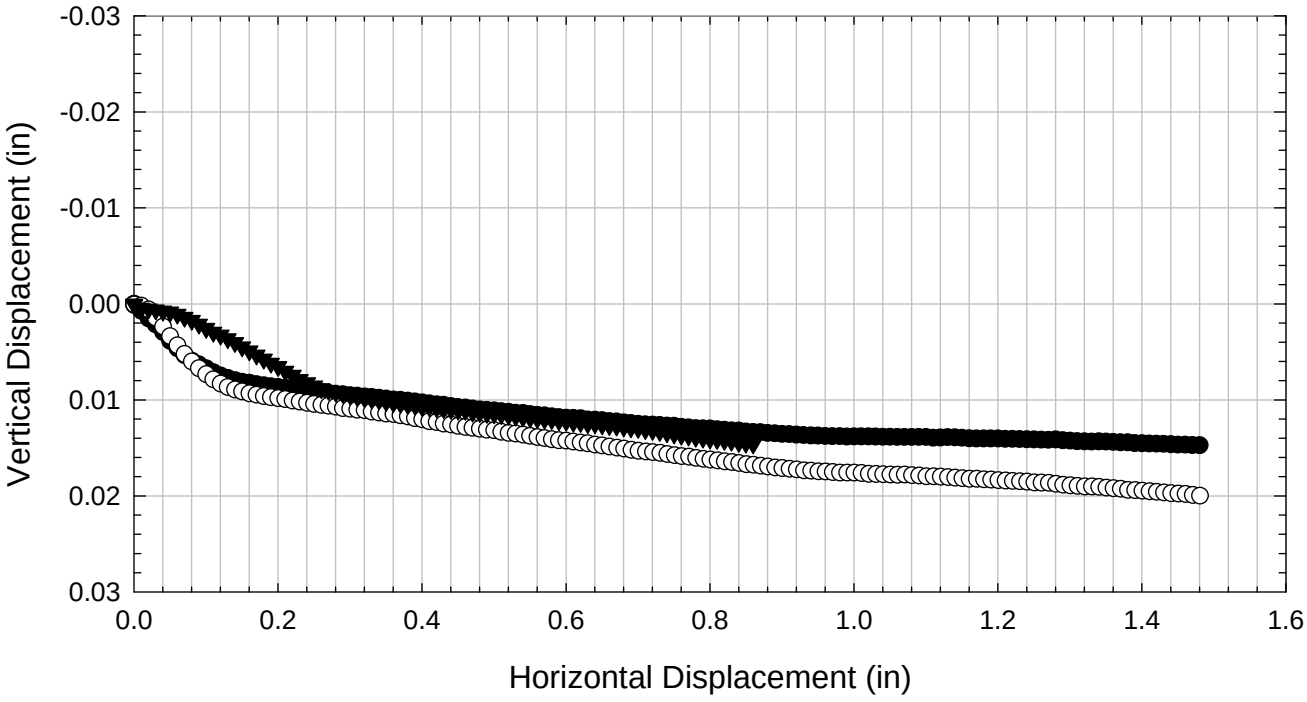

D.2. Alabama 2

D.2.1 Non-blenderized

Virginia Polytechnic Institute and State University
Geotechnical Engineering Laboratory
Ring Shear Data Sheet

Project:	Fully Softened Shear Strength
Sample I.D./Loc.:	Alabama 2 - Non-blenderized
Classification:	Sandy Fat Clay (CH)

Sample Preparation	Remolded at LL

Specific Gravity	2.72	
Shear Device Used	WF Bromhead Ring Shear	

Test Number	1	2	3	4	5	6	7	
Start Date (m/d/y)	12/5/2012	12/7/2012	12/12/2012					
End Date (m/d/y)	12/7/2012	12/9/2012	12/15/2012					
Consolidation Pressure (psf)	3473	7141	14470					
Initial Values								
Initial Height (in)	0.20	0.20	0.20					
Inner Radius (in)	1.38	1.38	1.38					
Outer Radius (in)	1.97	1.97	1.97					
Initial Sample Weight (g)	36.77	42.42	42.82					
Water Content (%)	53.15	50.19	48.98					
Saturation (%)	100.0	100.0	100.0					
Consolidation Pressures								
Load 1 (psf)	154	154	154					
Load 2 (psf)	253	253	253					
Load 3 (psf)	451	451	451					
Load 4 (psf)	847	847	847					
Load 5 (psf)	1638	1638	1638					
Load 6 (psf)	3473	3473	3473					
Load 7 (psf)		7141	7141					
Load 8 (psf)			14470					
t_{50}								
Max. t_{50} for Load 1 (min)								
Max. t_{50} for Load 2 (min)								
Max. t_{50} for Load 3 (min)								
Max. t_{50} for Load 4 (min)								
Max. t_{50} for Load 5 (min)								
Max. t_{50} for Load 6 (min)	0.93							
Max. t_{50} for Load 7 (min)		0.49						
Max. t_{50} for Load 8 (min)			0.34					
Final Values								
Water Content (%)	37.51	30.39	30.31					
Saturation (%)	100.0	100.0	100.0					
Failure								
Test Performed at Shear Rate (in/min)	7.00E-04	7.00E-04	7.00E-04					
Required Shear Rate (in/min)	4.73E-03	8.57E-03	1.59E-02					
Displacement at Failure (in)	0.22	0.21	0.27					
Peak Shear Stress (psf)	1825	3738	7512					
Residual Shear Stress (psf)	1800	3680	7459					
Secant Peak Effective Friction Angle (deg)	27.7	27.6	27.4					
Secant Residual Effective Friction Angle (deg)	27.4	27.3	27.3					

Comments:

Alabama 2 - Non-blenderized - 3473 psf

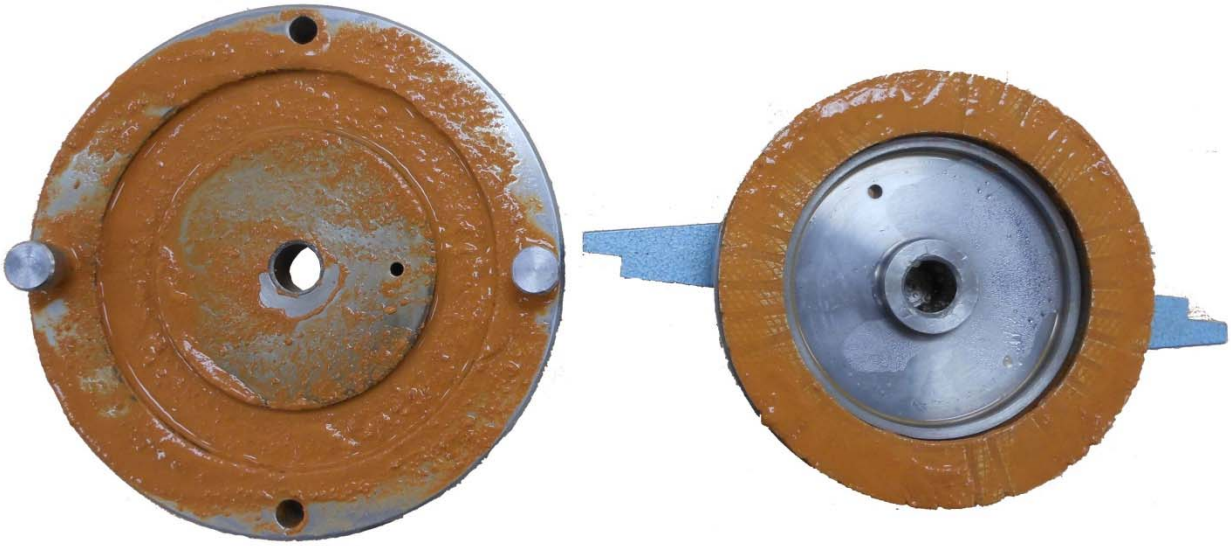

Alabama 2 - Non-blenderized - 7141 psf

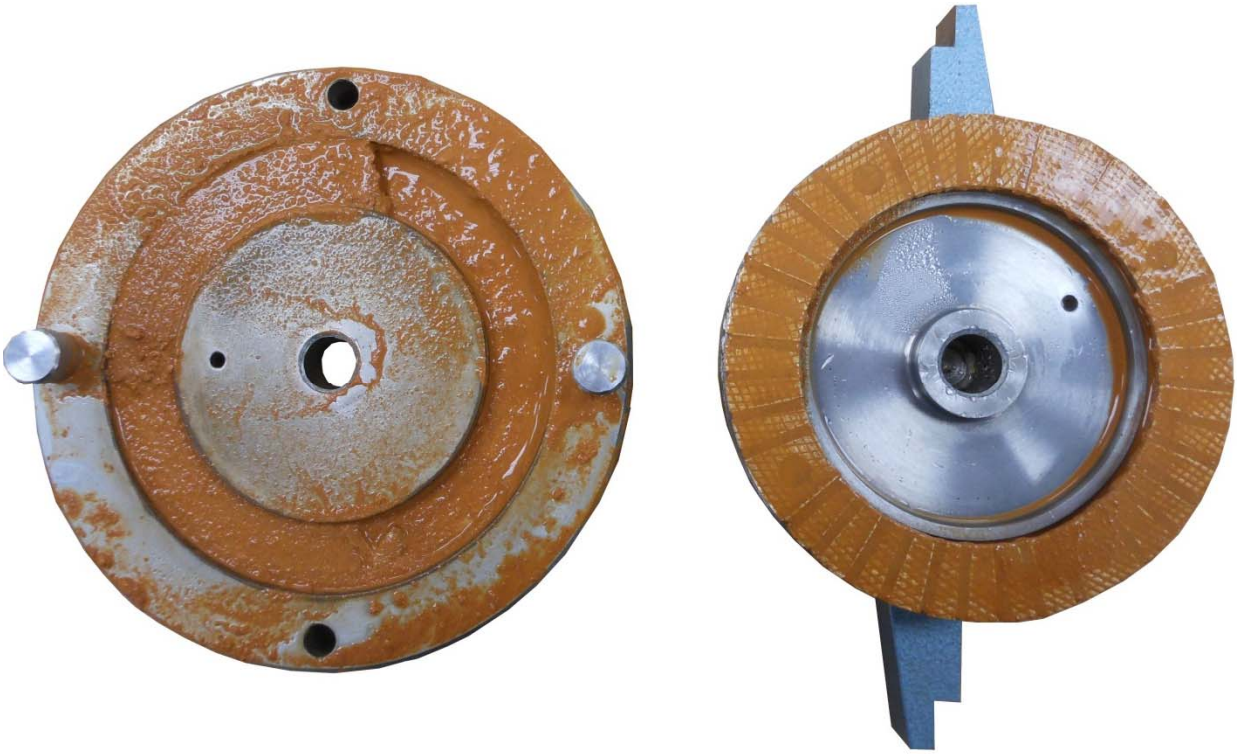

Alabama 2 - Non-blenderized - 14470 psf

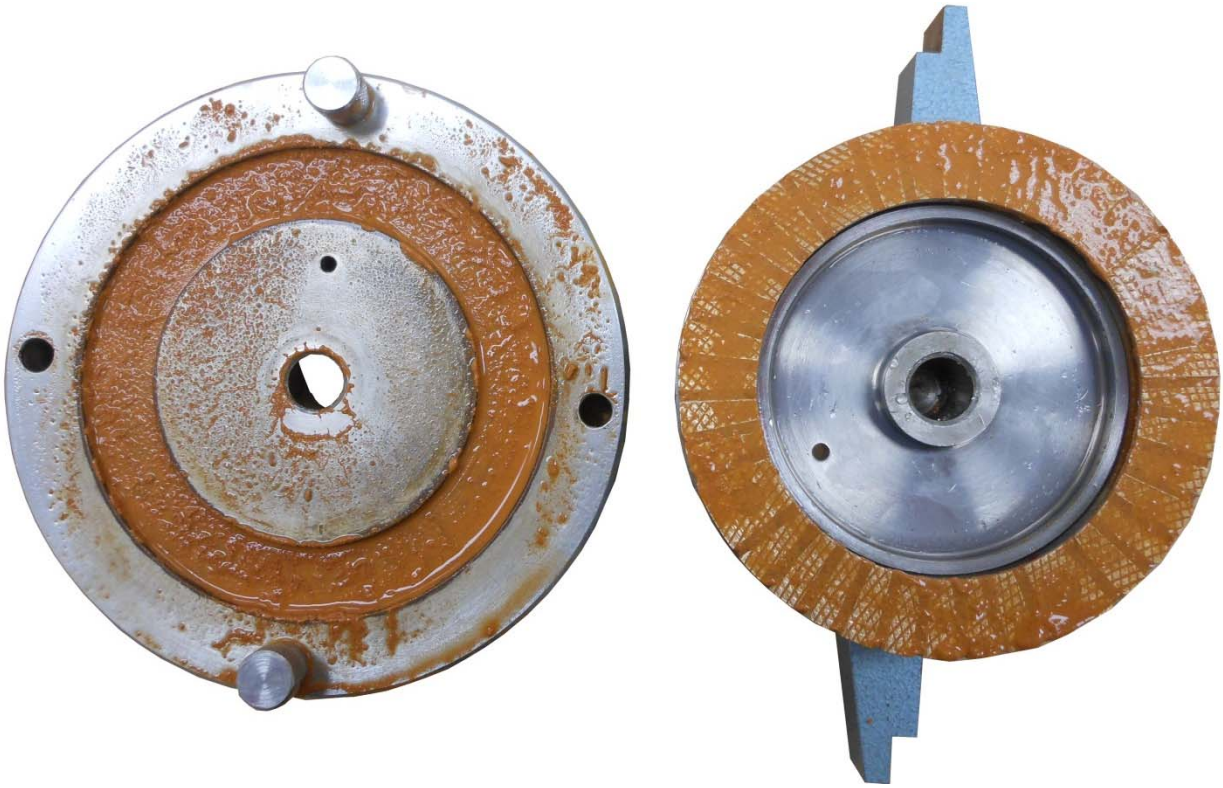

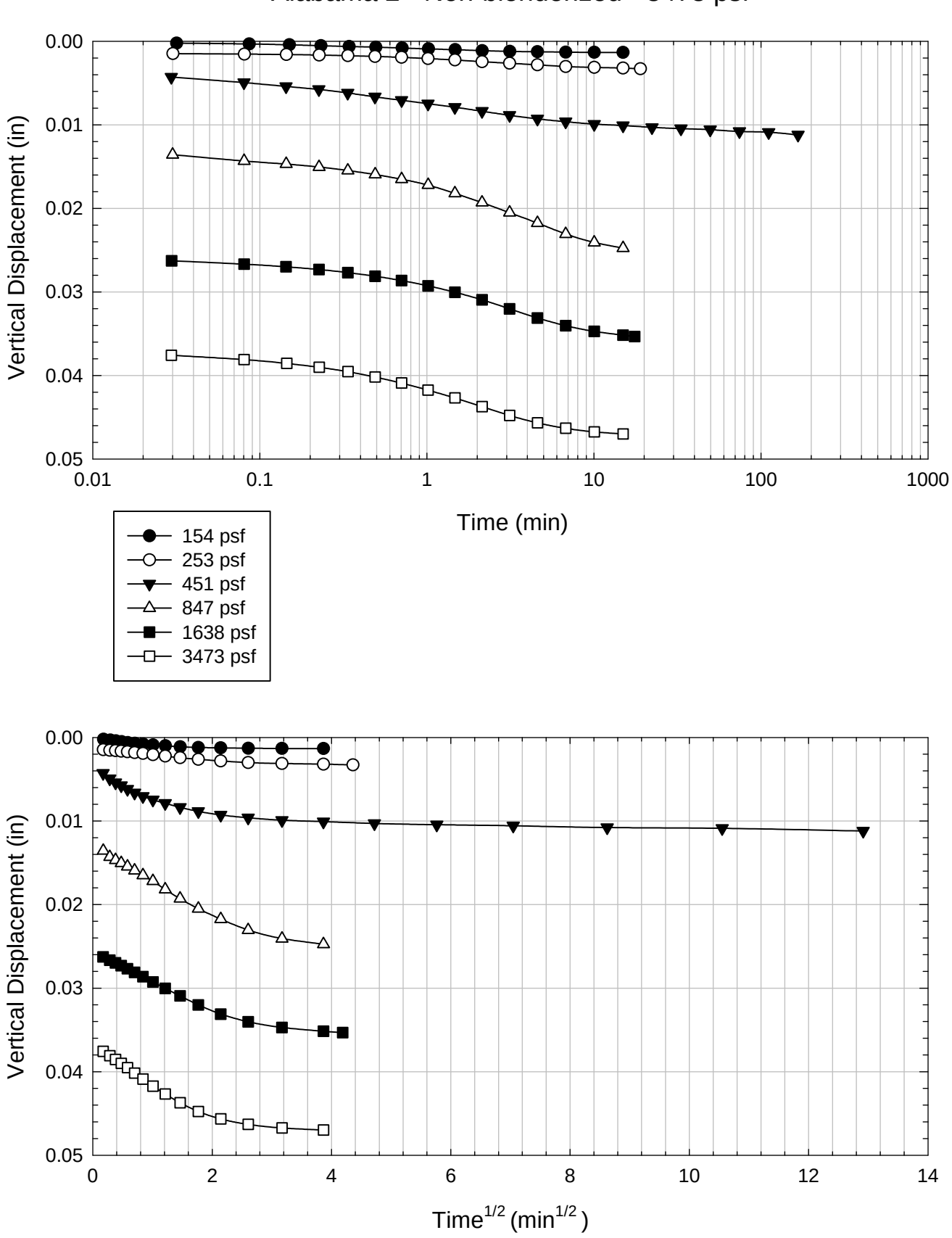
Alabama 2 - Non-blenderized - 3473 psf
Vertical Displacement (in)
0.00
0.01
0.02
0.03
0.04
0.05
0.01
0.1
1
10
100
1000
Time (min)
154 psf
253 psf
451 psf
847 psf
1638 psf
3473 psf
Vertical Displacement (in)
0.00
0.01
0.02
0.03
0.04
0.05
0
2
4
6
8
10
12
14
Time^1/2 (min^1/2)

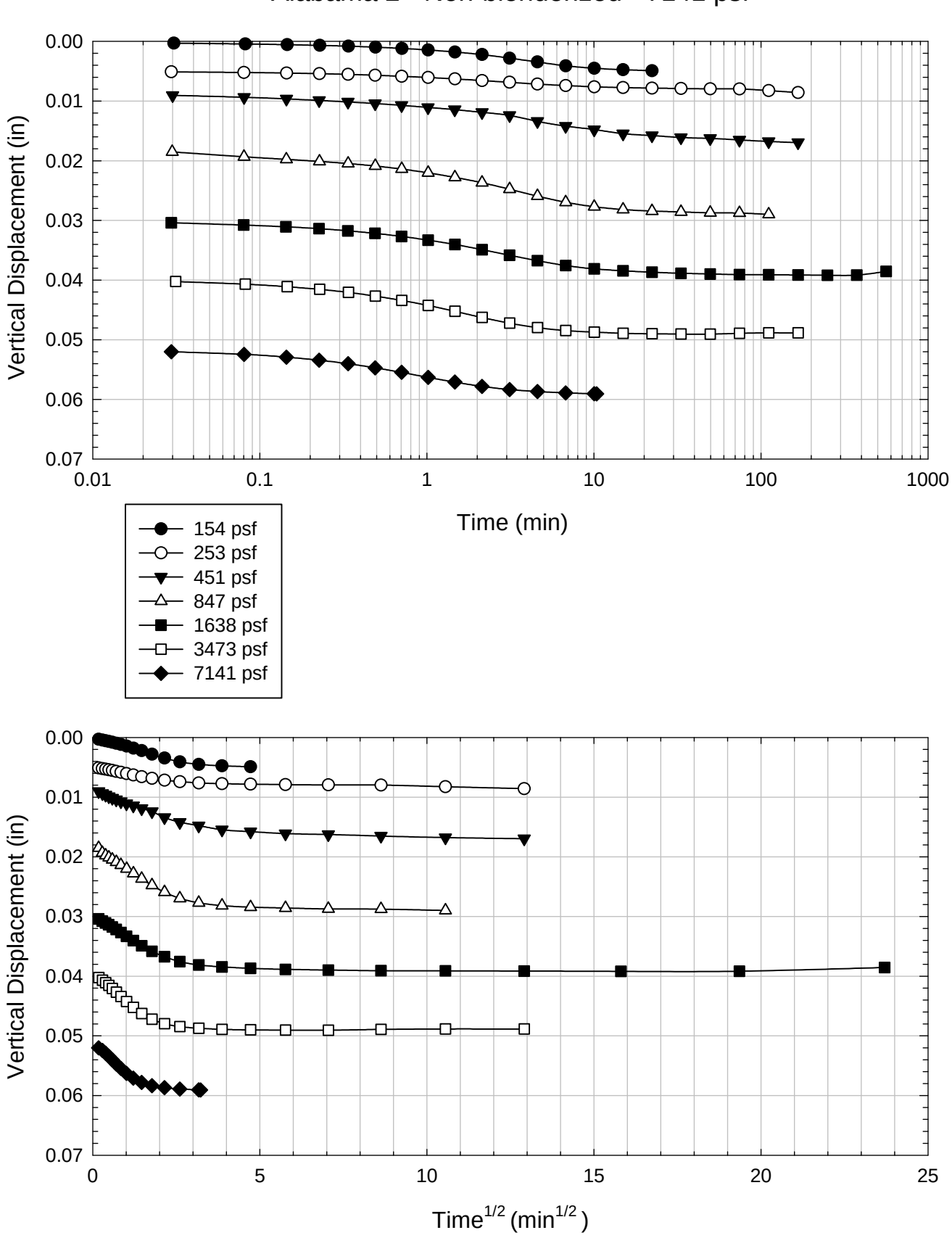
Alabama 2 - Non-blenderized - 7141 psf
Vertical Displacement (in)
0.00
0.01
0.02
0.03
0.04
0.05
0.06
0.07
0.01
0.1
1
10
100
1000
Time (min)
154 psf
253 psf
451 psf
847 psf
1638 psf
3473 psf
7141 psf
Vertical Displacement (in)
0
5
10
15
20
25
Time^1/2 (min^1/2)

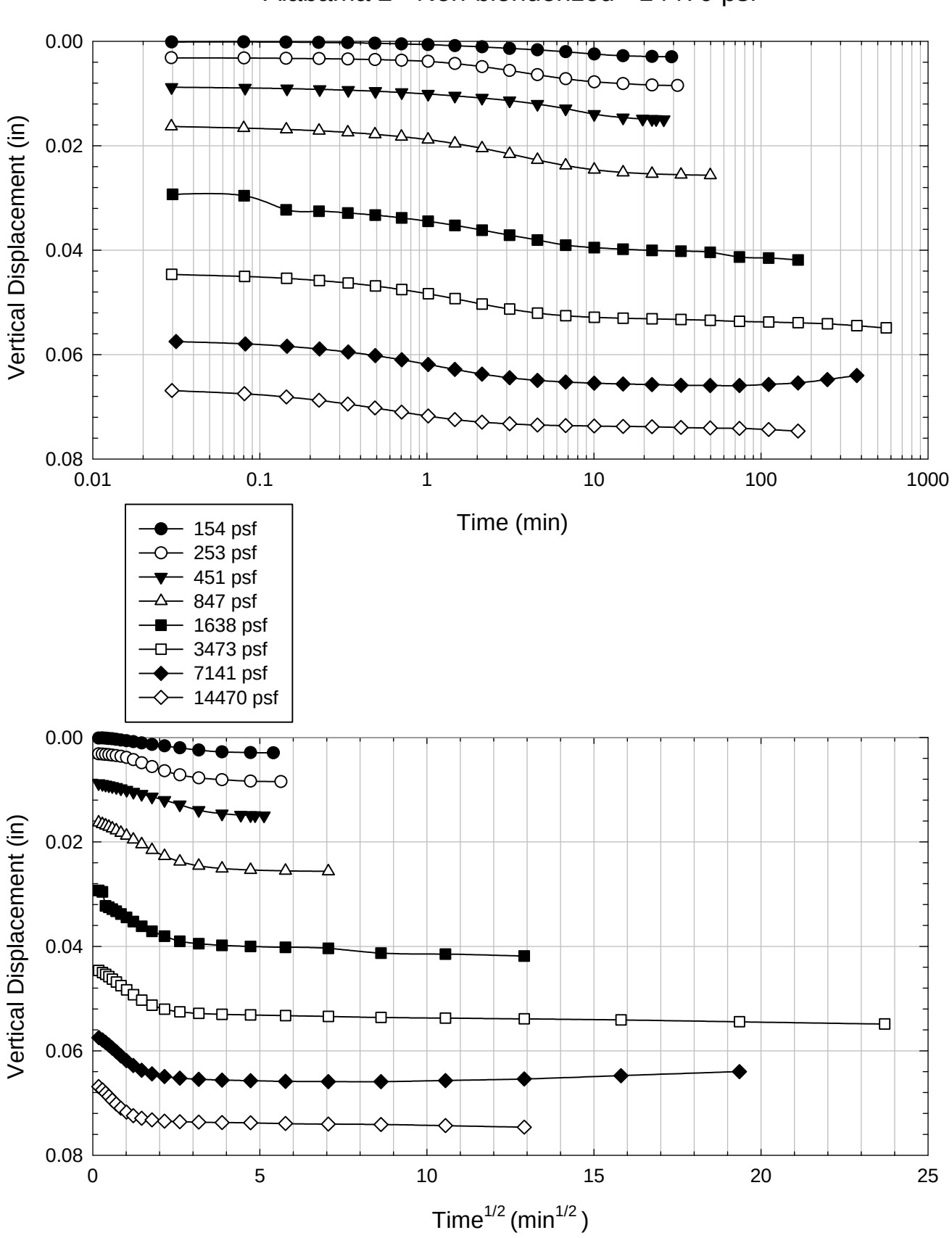
Alabama 2 - Non-blenderized - 14470 psf
Vertical Displacement (in)
0.00
0.02
0.04
0.06
0.08
0.01
0.1
1
10
100
1000
Time (min)
154 psf
253 psf
451 psf
847 psf
1638 psf
3473 psf
7141 psf
14470 psf
Vertical Displacement (in)
0.00
0.02
0.04
0.06
0.08
0
5
10
15
20
25
Time^1/2 (min^1/2)

Alabama 2 - Non-blenderized

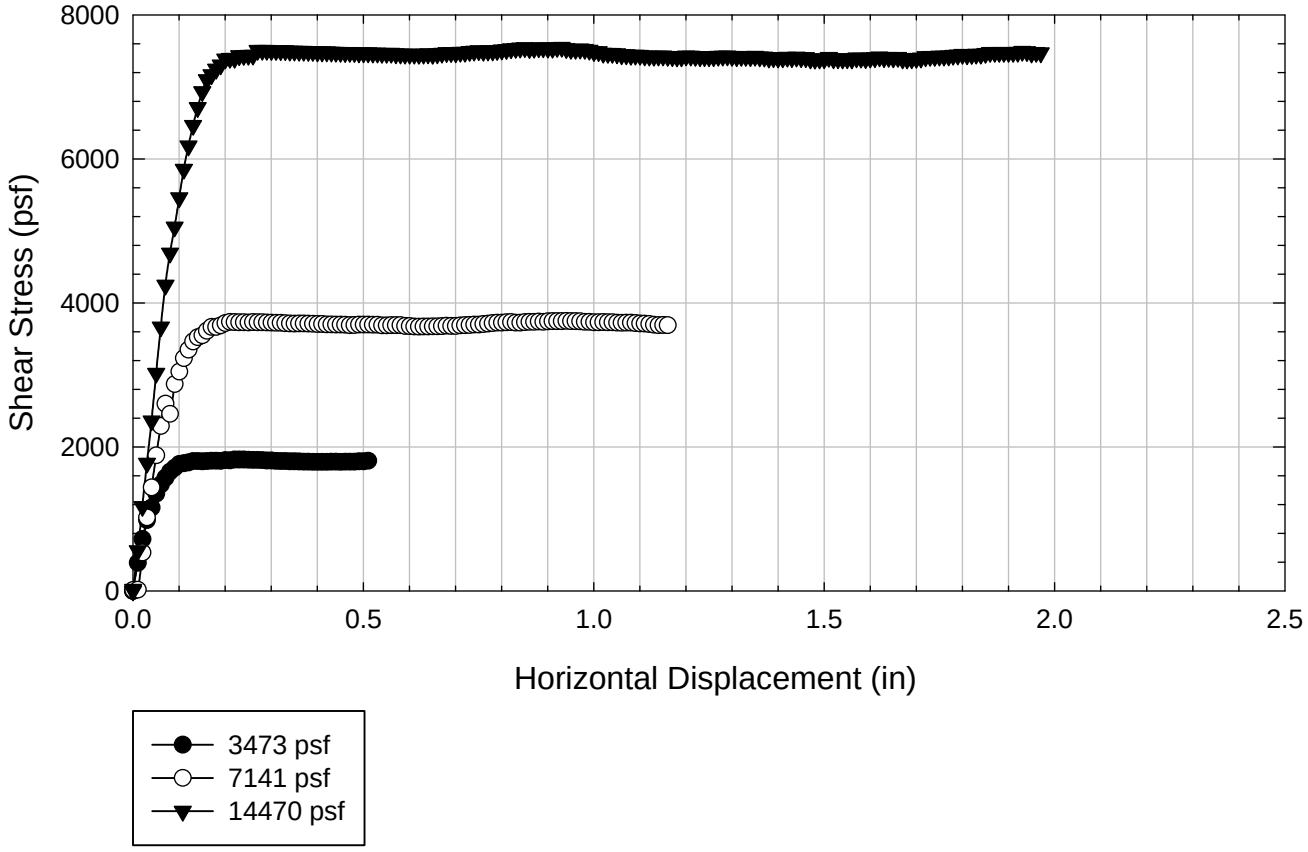

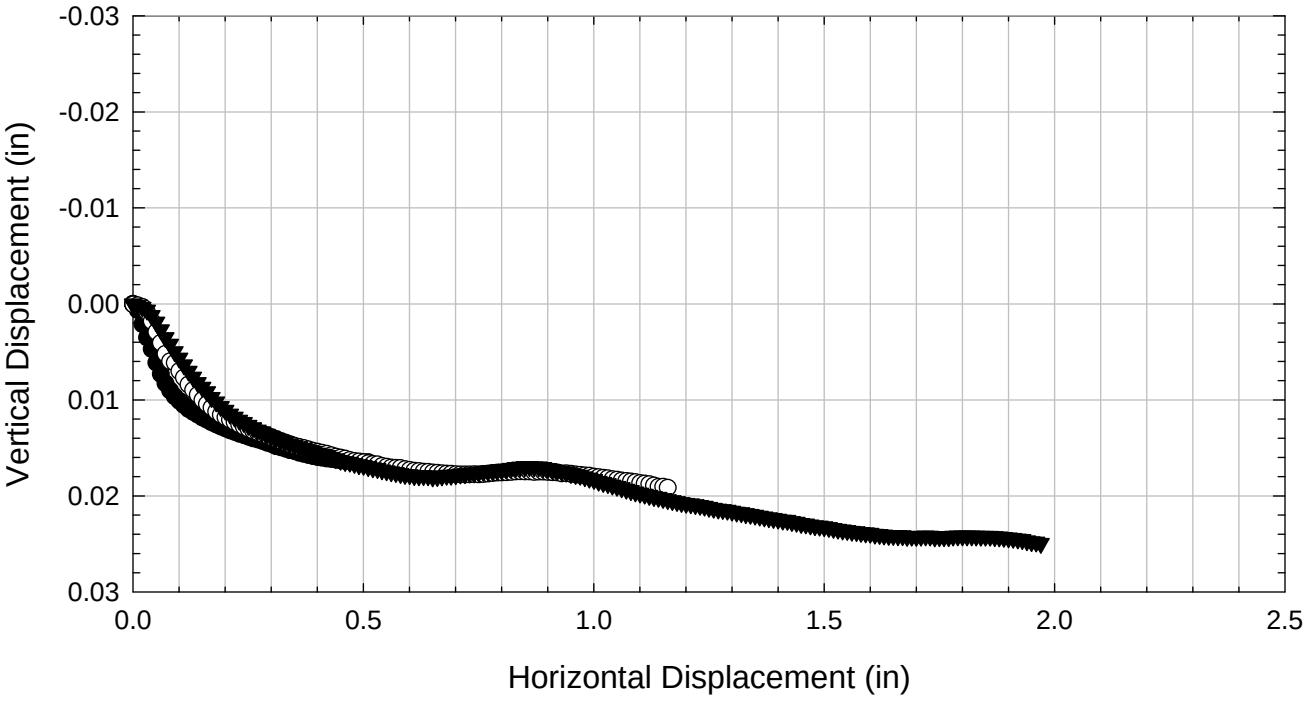

D.3. Alabama 3

D.3.1 Non-blenderized

Virginia Polytechnic Institute and State University
Geotechnical Engineering Laboratory
Ring Shear Data Sheet

Project:	Fully Softened Shear Strength
Sample I.D./Loc.:	Alabama 3 - Non-blenderized
Classification:	Low Plasticity Silt (ML)

Sample Preparation	Remolded at LL

Specific Gravity	2.79	
Shear Device Used	WF Bromhead Ring Shear	

Test Number	1	2	3	4	5	6	7	
Start Date (m/d/y)	12/16/2012	12/16/2012	12/17/2012					
End Date (m/d/y)	12/16/2012	12/17/2012	12/18/2012					
Consolidation Pressure (psf)	3473	7141	14470					
Initial Values								
Initial Height (in)	0.20	0.20	0.20					
Inner Radius (in)	1.38	1.38	1.38					
Outer Radius (in)	1.97	1.97	1.97					
Initial Sample Weight (g)	43.77	43.82	43.86					
Water Content (%)	47.26	41.04	47.01					
Saturation (%)	100.0	100.0	100.0					
Consolidation Pressures								
Load 1 (psf)	154	154	154					
Load 2 (psf)	253	253	253					
Load 3 (psf)	451	451	451					
Load 4 (psf)	847	847	847					
Load 5 (psf)	1638	1638	1638					
Load 6 (psf)	3473	3473	3473					
Load 7 (psf)		7141	7141					
Load 8 (psf)			14470					
t_{50}								
Max. t_{50} for Load 1 (min)								
Max. t_{50} for Load 2 (min)								
Max. t_{50} for Load 3 (min)								
Max. t_{50} for Load 4 (min)								
Max. t_{50} for Load 5 (min)								
Max. t_{50} for Load 6 (min)								
Max. t_{50} for Load 7 (min)								
Max. t_{50} for Load 8 (min)								
Final Values								
Water Content (%)	34.90	32.81	33.13					
Saturation (%)	100.0	100.0	100.0					
Failure								
Test Performed at Shear Rate (in/min)	7.00E-04	7.00E-04	7.00E-04					
Required Shear Rate (in/min)								
Displacement at Failure (in)	0.09	0.13	0.17					
Peak Shear Stress (psf)	1447	2866	5407					
Residual Shear Stress (psf)	993	1877	3460					
Secant Peak Effective Friction Angle (deg)	22.6	21.9	20.5					
Secant Residual Effective Friction Angle (deg)	16.0	14.7	13.4					

Comments:

Alabama 3 - Non-blenderized - 3473 psf

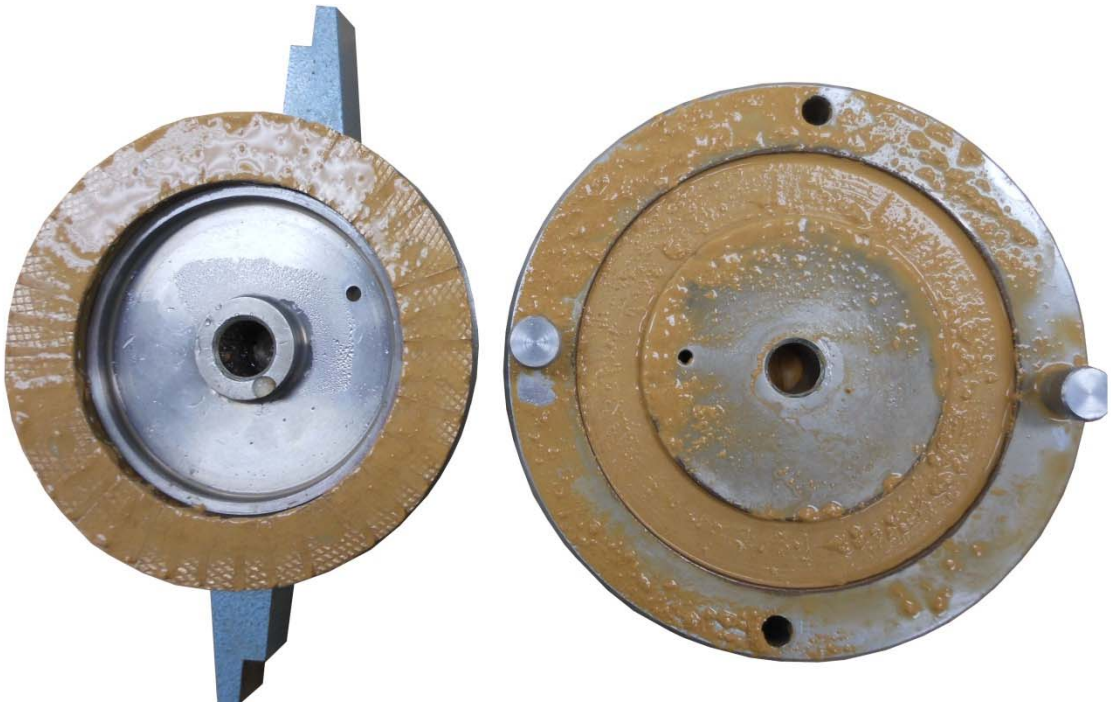

Alabama 3 - Non-blenderized - 7141 psf

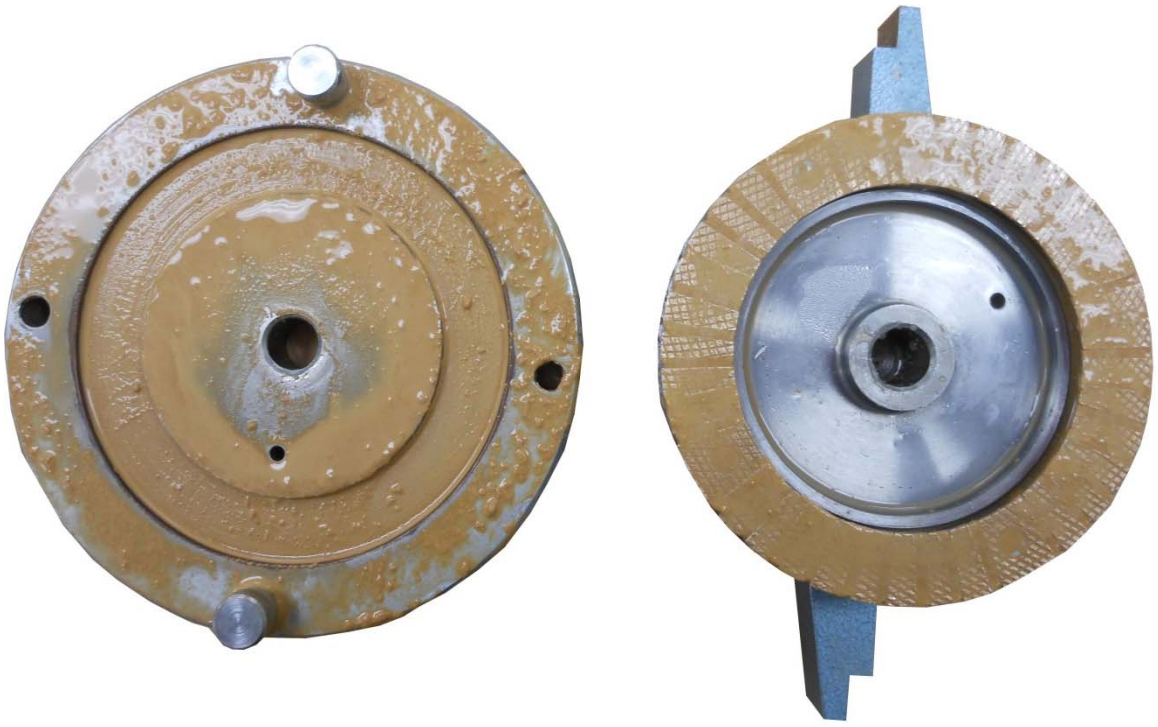

Alabama 3 - Non-blenderized - 14470 psf

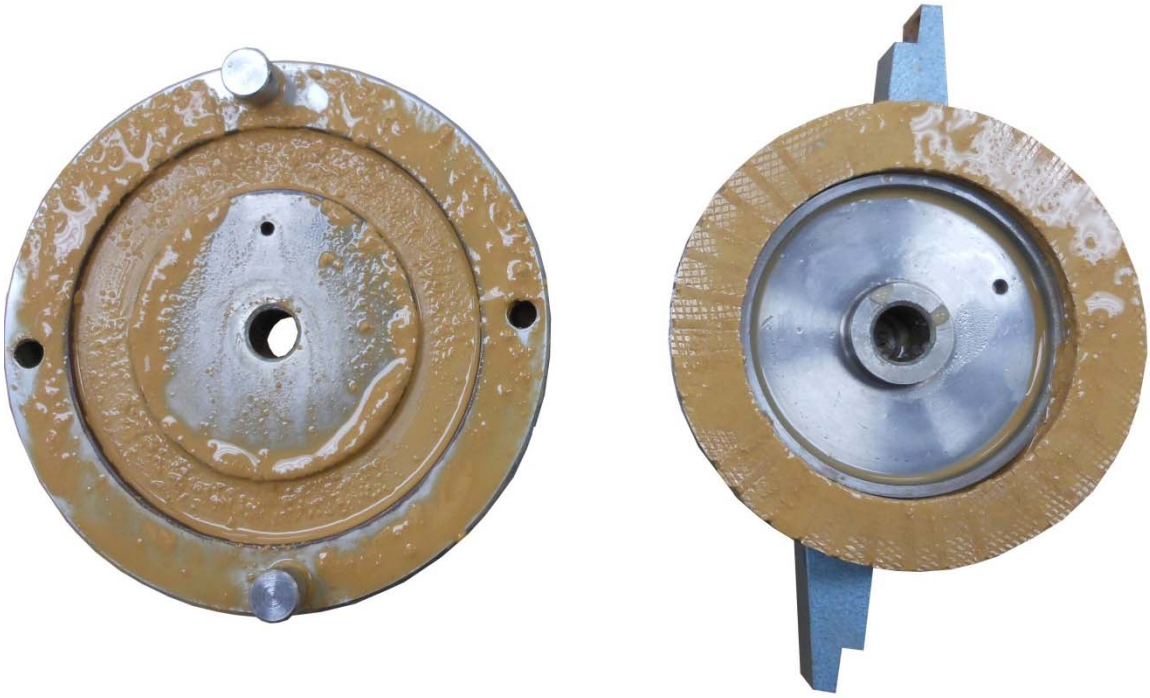

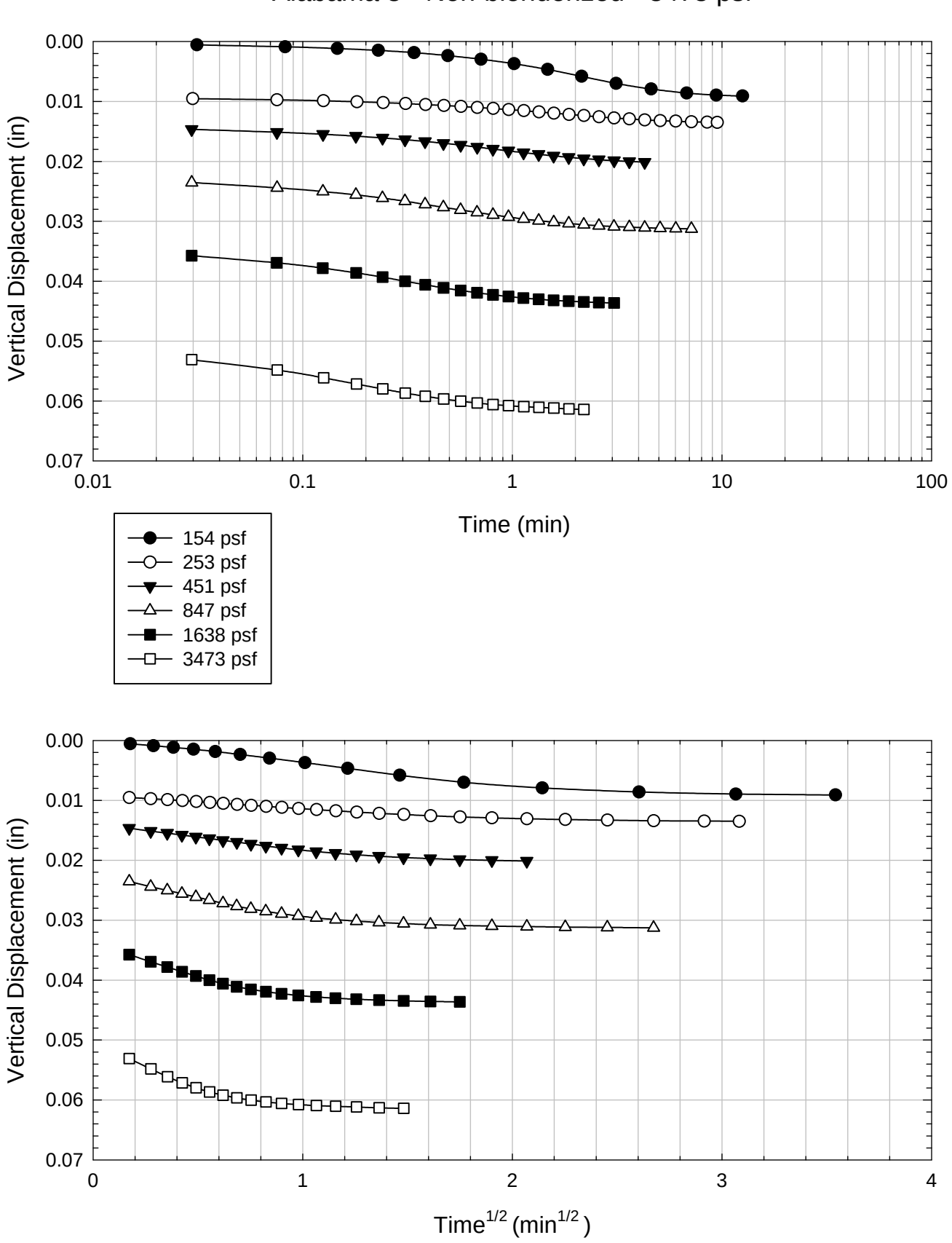
Alabama 3 - Non-blenderized - 3473 psf
Vertical Displacement (in)
0.00
0.01
0.02
0.03
0.04
0.05
0.06
0.07
0.01
0.1
1
10
100
Time (min)
154 psf
253 psf
451 psf
847 psf
1638 psf
3473 psf
Vertical Displacement (in)
0
1
2
3
4
Time^1/2 (min^1/2)

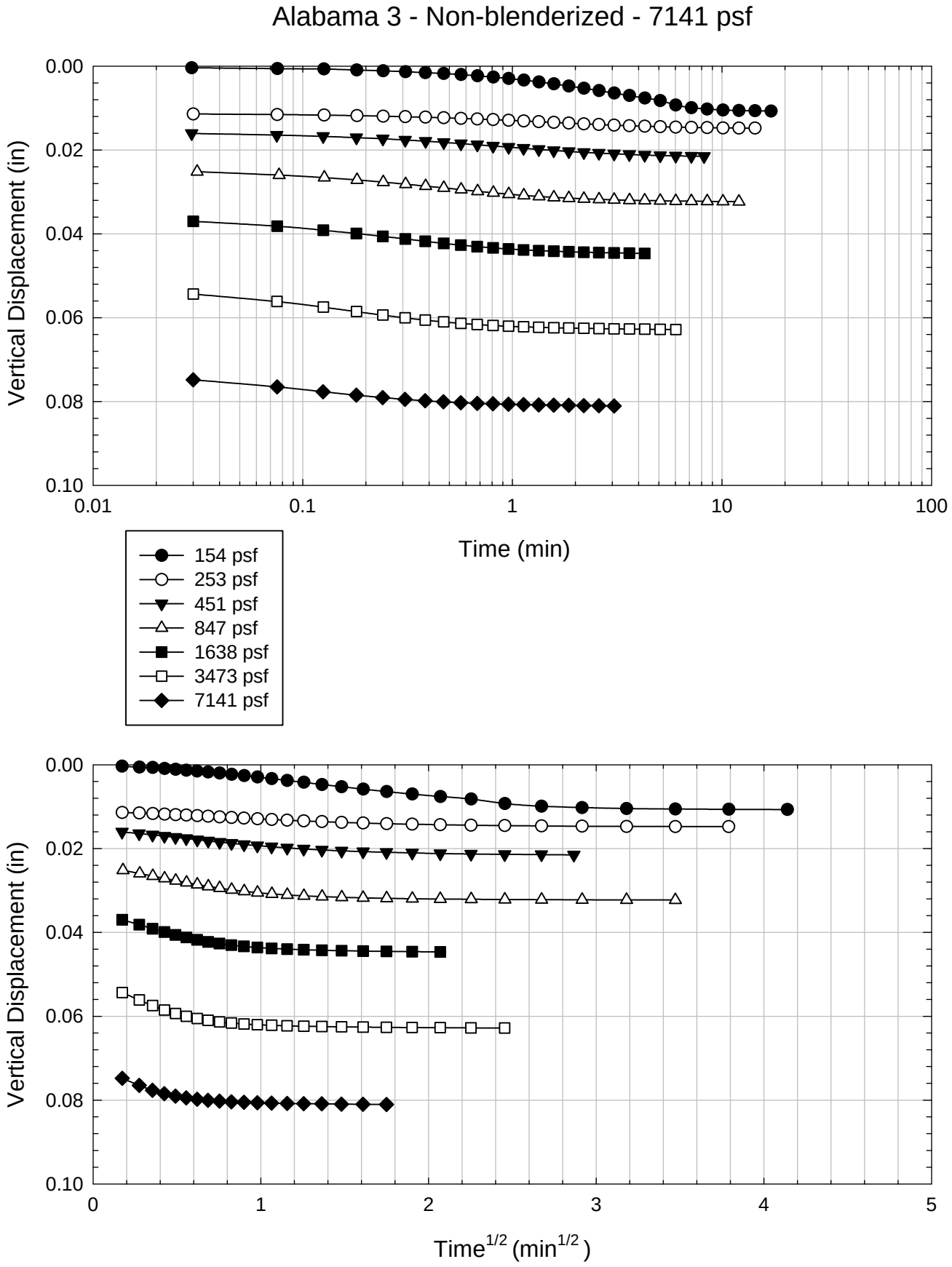
Alabama 3 - Non-blenderized - 7141 psf
Vertical Displacement (in)
0.00
0.02
0.04
0.06
0.08
0.10
0.01
0.1
1
10
100
Time (min)
154 psf
253 psf
451 psf
847 psf
1638 psf
3473 psf
7141 psf
Vertical Displacement (in)
0.00
0.02
0.04
0.06
0.08
0.10
0
1
2
3
4
5
Time^1/2 (min^1/2)

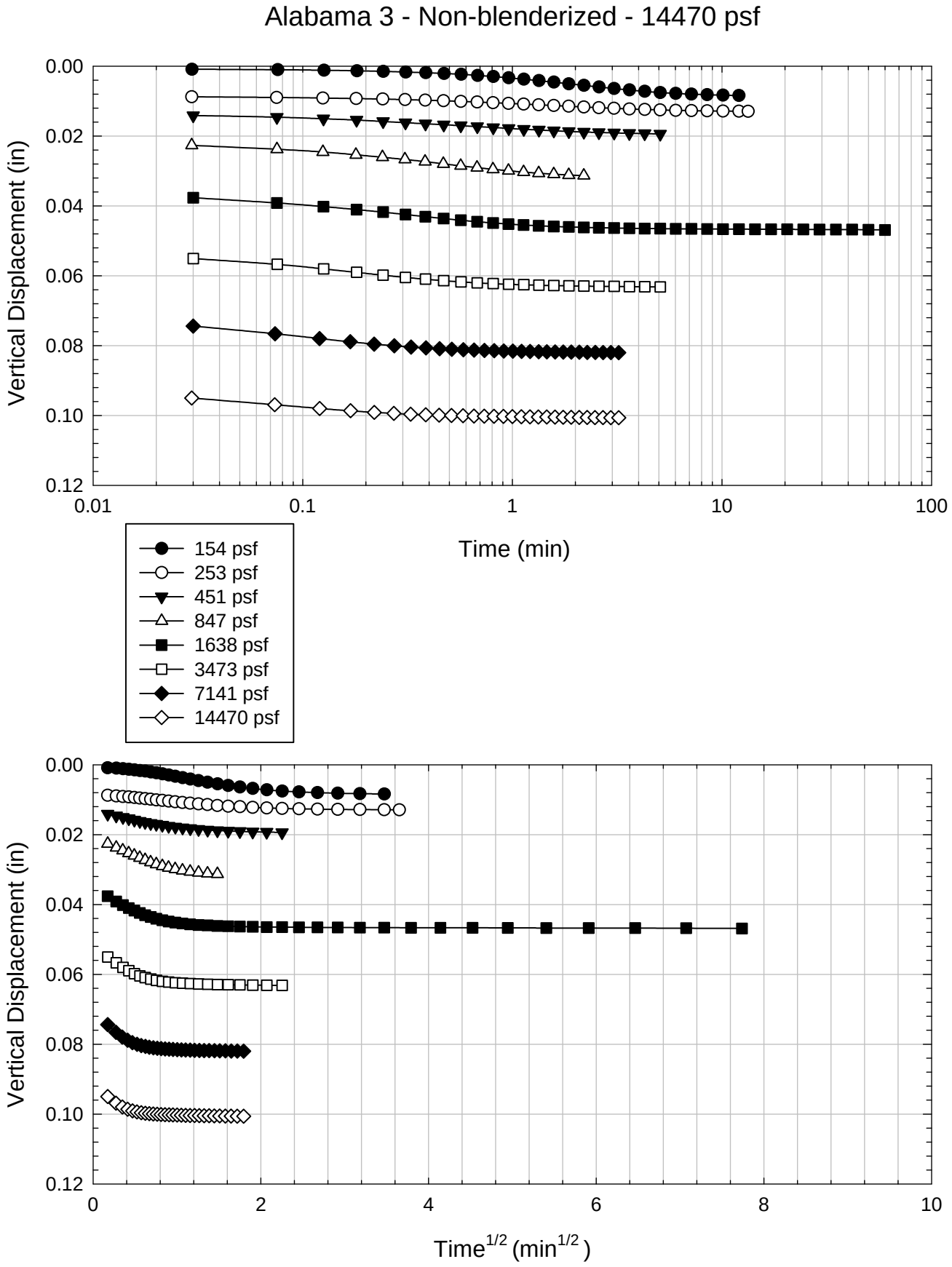
Alabama 3 - Non-blenderized - 14470 psf
Vertical Displacement (in)
0.00
0.02
0.04
0.06
0.08
0.10
0.12
0.01
0.1
1
10
100
Time (min)
154 psf
253 psf
451 psf
847 psf
1638 psf
3473 psf
7141 psf
14470 psf
Vertical Displacement (in)
0
2
4
6
8
10
Time^1/2 (min^1/2)

Alabama 3 - Non-blenderized

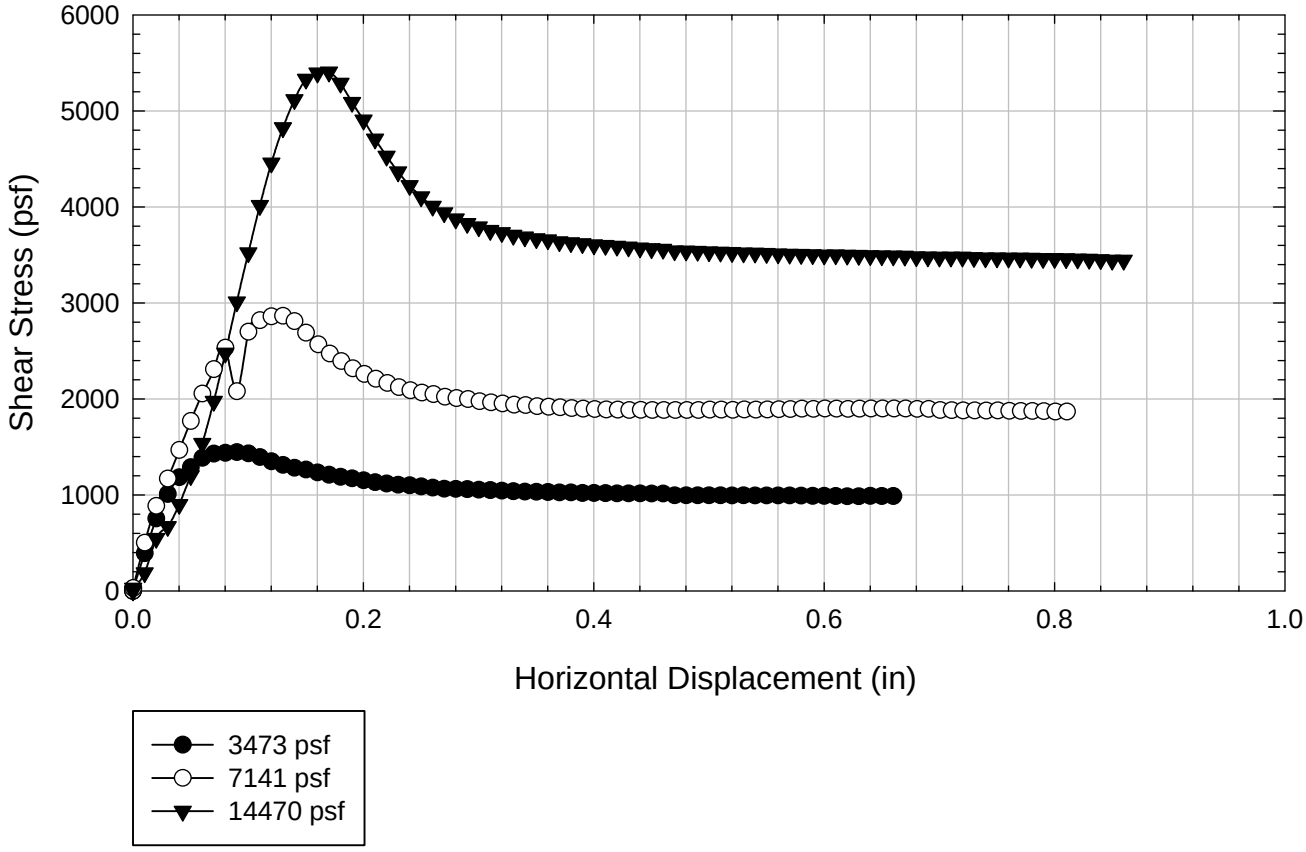

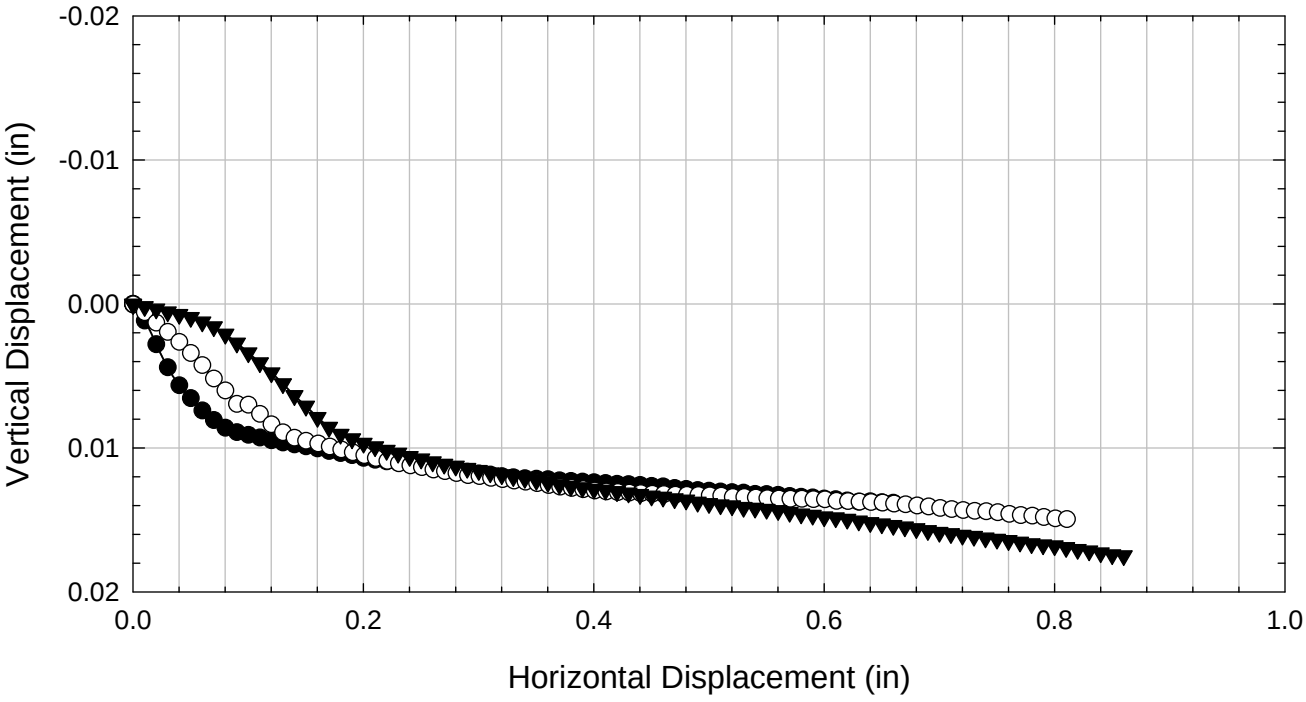

D.4. Alabama 4

D.4.1 Non-blenderized

Virginia Polytechnic Institute and State University
Geotechnical Engineering Laboratory
Ring Shear Data Sheet

Project:	Fully Softened Shear Strength
Sample I.D./Loc.:	Alabama 4 - Non-blenderized
Classification:	Lean Clay (CL)

Sample Preparation	Remolded at LL

Specific Gravity	2.71	
Shear Device Used	WF Bromhead Ring Shear	

Test Number	1	2	3	4	5	6	7	
Start Date (m/d/y)	1/14/2013	1/14/2013	1/16/2013					
End Date (m/d/y)	1/16/2013	1/16/2013	1/17/2013					
Consolidation Pressure (psf)	3473	7160	14470					
Initial Values								
Initial Height (in)	0.20	0.20	0.20					
Inner Radius (in)	1.38	1.38	1.38					
Outer Radius (in)	1.97	1.97	1.97					
Initial Sample Weight (g)	42.81	40.96	44.30					
Water Content (%)	43.79	43.07	43.10					
Saturation (%)	100.0	100.0	100.0					
Consolidation Pressures								
Load 1 (psf)	154	155	154					
Load 2 (psf)	253	254	253					
Load 3 (psf)	451	452	451					
Load 4 (psf)	847	848	847					
Load 5 (psf)	1638	1641	1638					
Load 6 (psf)	3473	3489	3473					
Load 7 (psf)		7160	7141					
Load 8 (psf)			14470					
t_{50}								
Max. t_{50} for Load 1 (min)								
Max. t_{50} for Load 2 (min)								
Max. t_{50} for Load 3 (min)								
Max. t_{50} for Load 4 (min)								
Max. t_{50} for Load 5 (min)								
Max. t_{50} for Load 6 (min)								
Max. t_{50} for Load 7 (min)								
Max. t_{50} for Load 8 (min)								
Final Values								
Water Content (%)	32.95	33.72	30.39					
Saturation (%)	100.0	100.0	100.0					
Failure								
Test Performed at Shear Rate (in/min)	7.00E-04	7.00E-04	7.00E-04					
Required Shear Rate (in/min)								
Displacement at Failure (in)	0.10	0.14	0.17					
Peak Shear Stress (psf)	1404	2805	5498					
Residual Shear Stress (psf)	857	1722	3613					
Secant Peak Effective Friction Angle (deg)	22.0	21.4	20.8					
Secant Residual Effective Friction Angle (deg)	13.9	13.5	14.0					

Comments:

Alabama 4 - Non-blenderized - 3473 psf

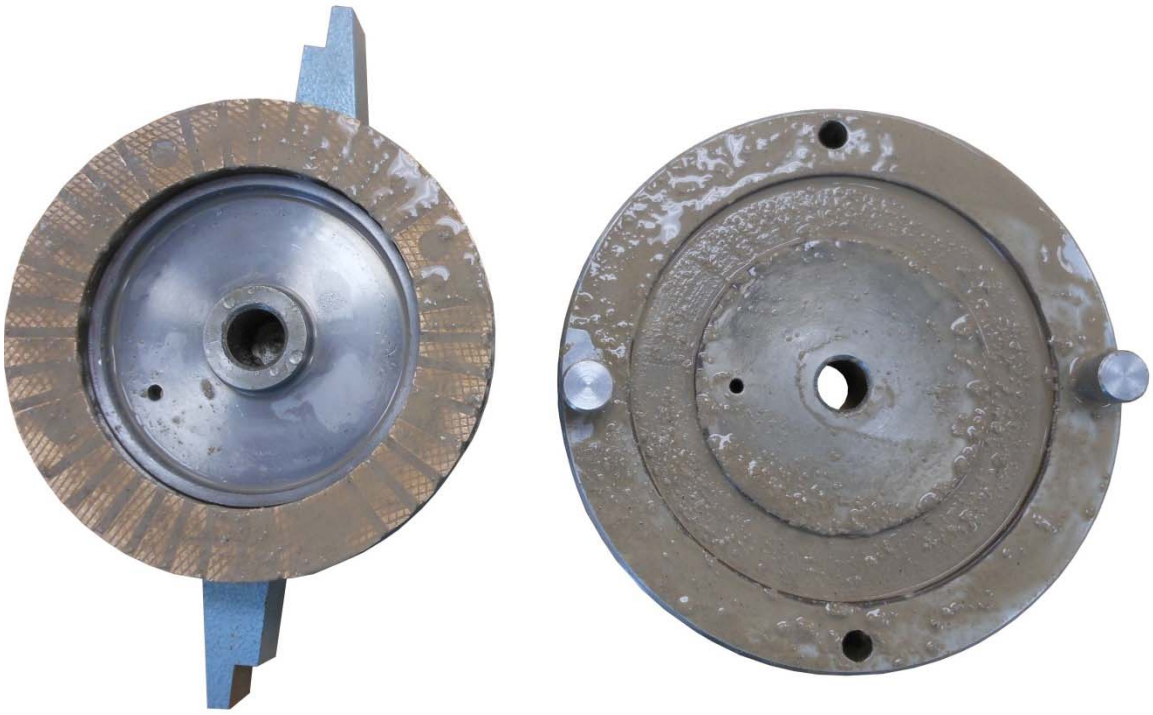

Alabama 4 - Non-blenderized - 7160 psf

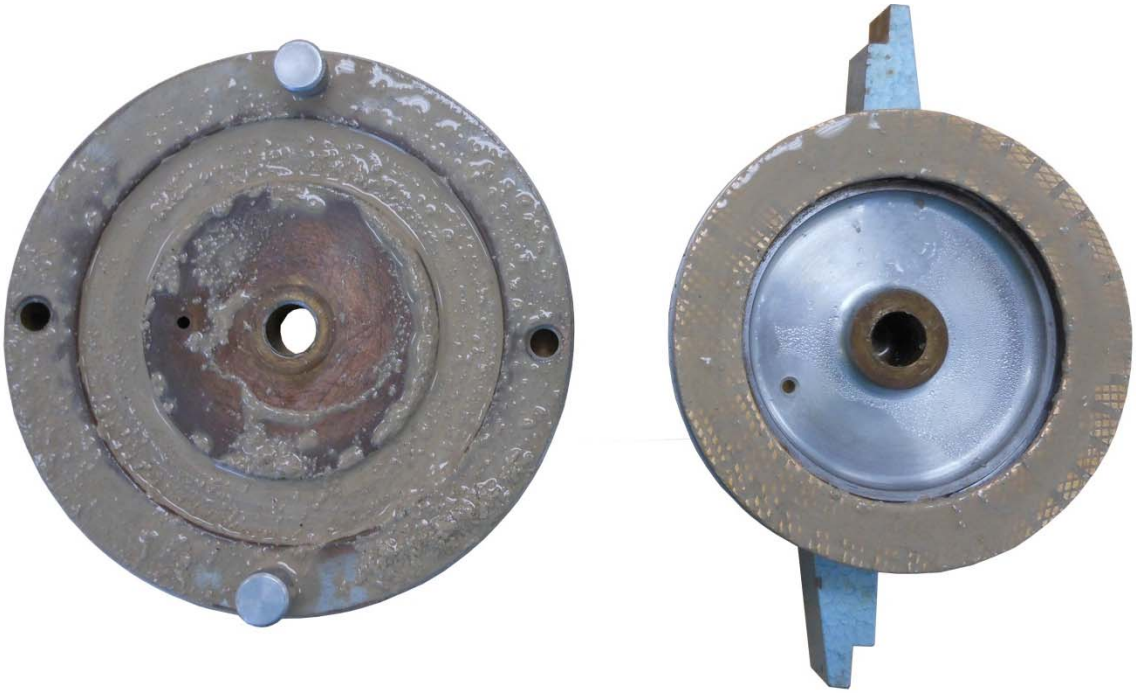

Alabama 4 - Non-blenderized - 14470 psf

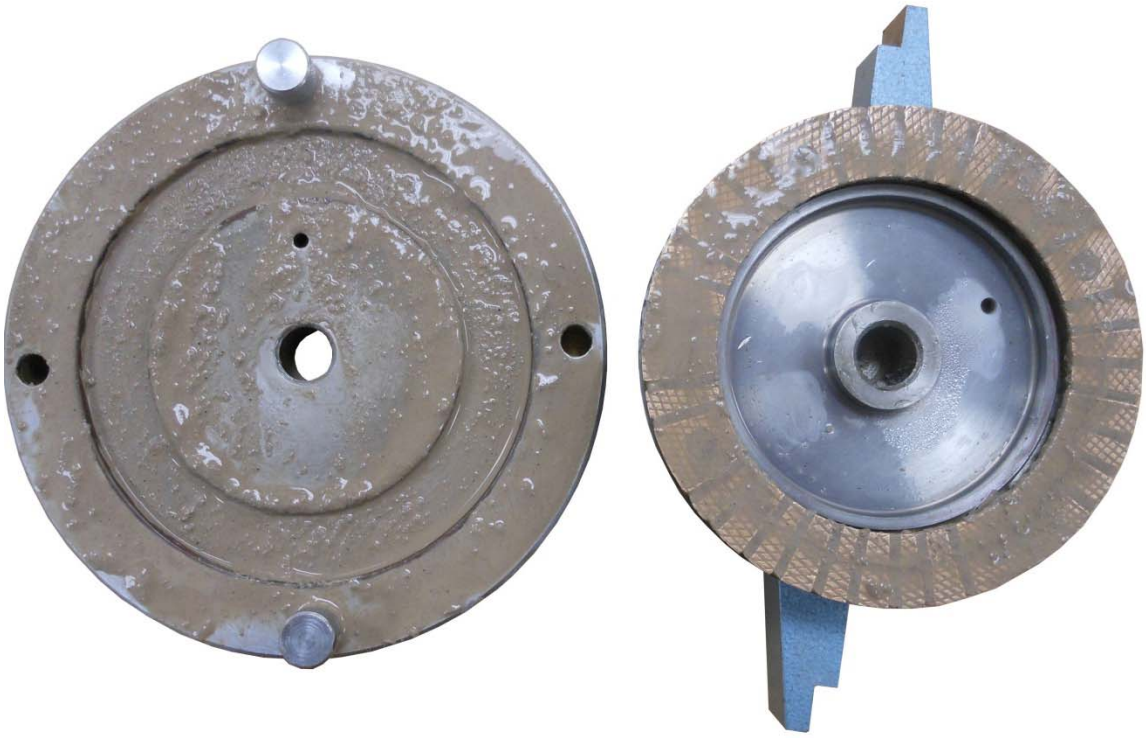

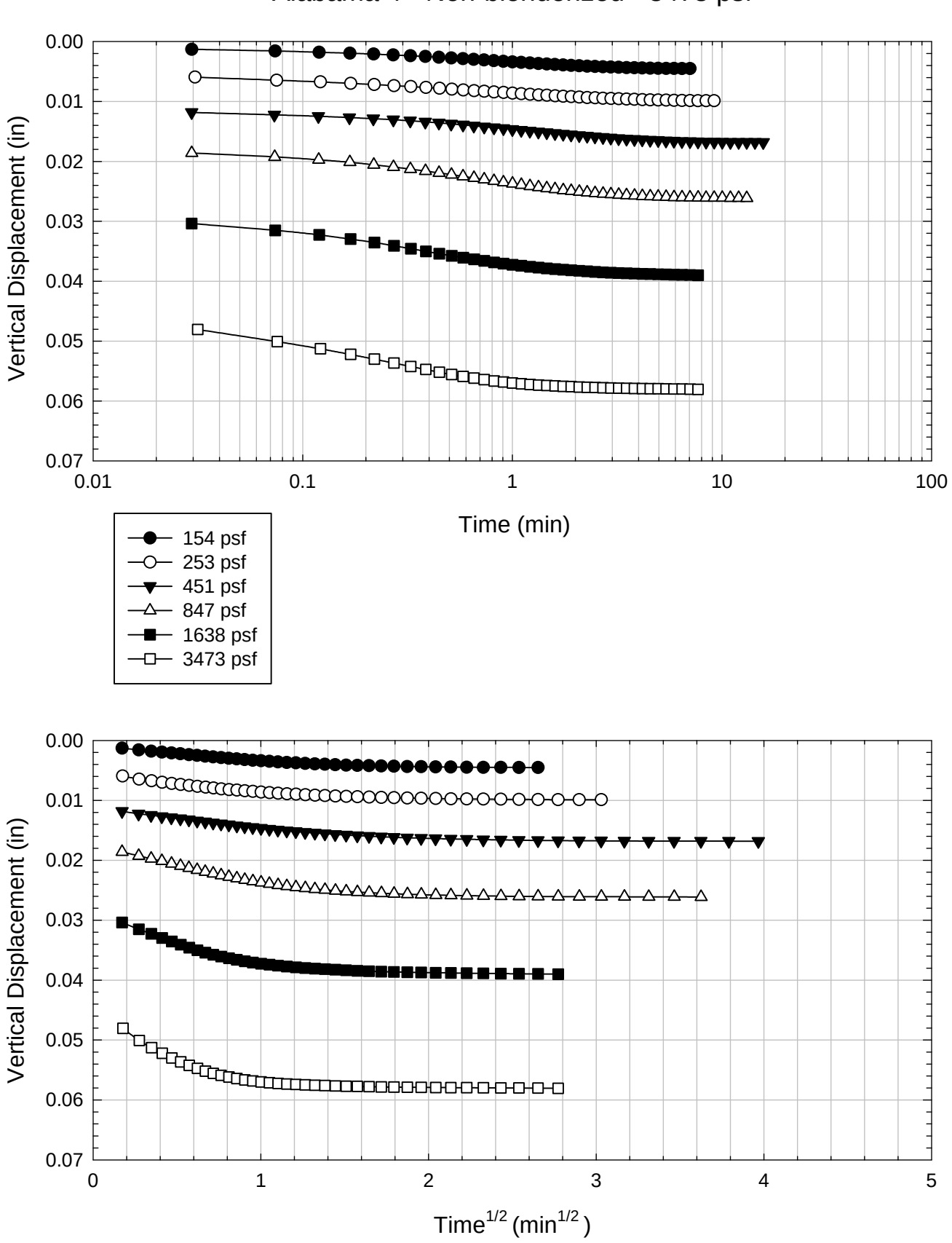
Alabama 4 - Non-blenderized - 3473 psf
Vertical Displacement (in)
0.00
0.01
0.02
0.03
0.04
0.05
0.06
0.07
0.01
0.1
1
10
100
Time (min)
154 psf
253 psf
451 psf
847 psf
1638 psf
3473 psf
Vertical Displacement (in)
0
1
2
3
4
5
Time^1/2 (min^1/2)

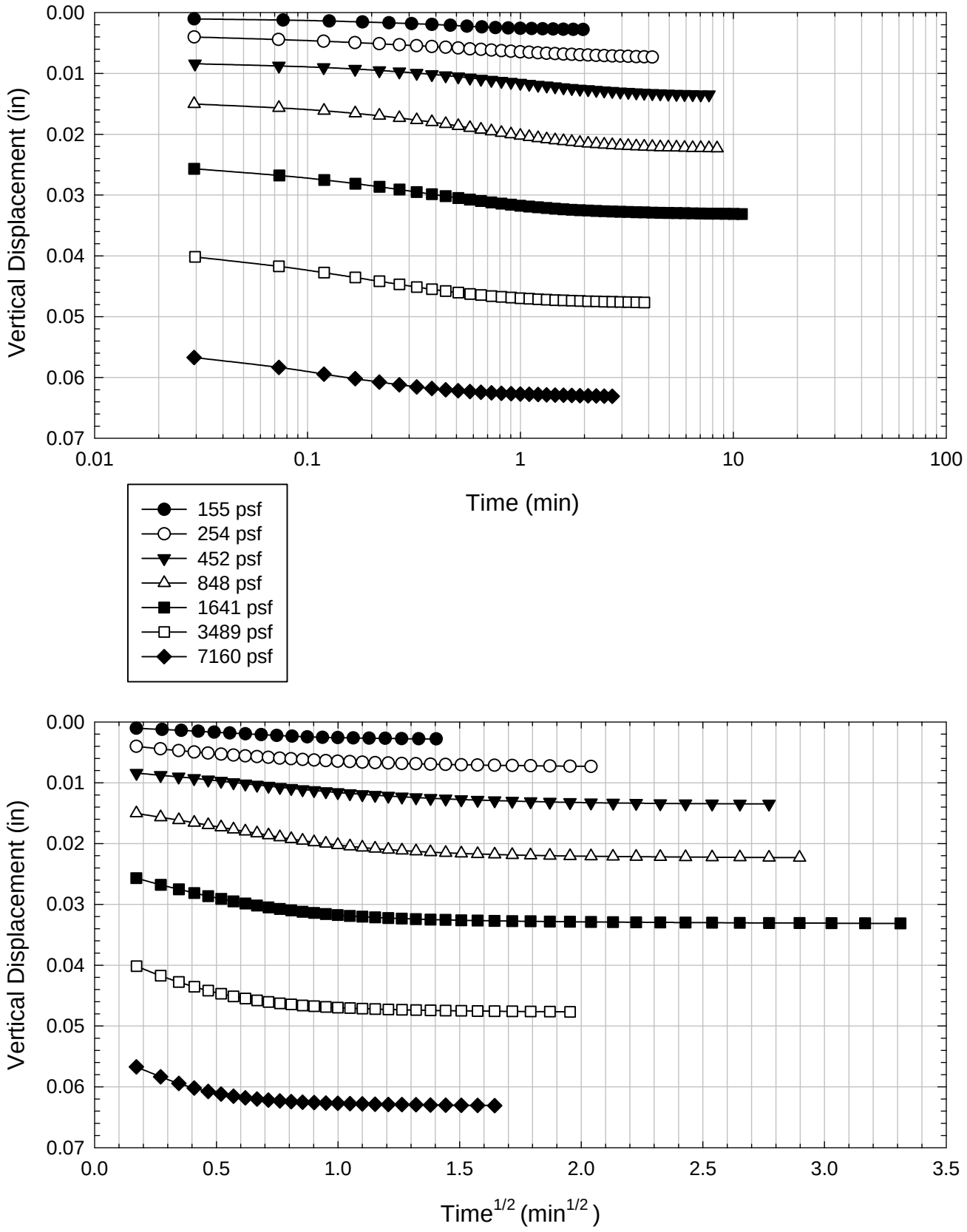
Alabama 4 - Non-blenderized - 7160 psf
Vertical Displacement (in)
0.00
0.01
0.02
0.03
0.04
0.05
0.06
0.07
0.01
0.1
1
10
100
Time (min)
155 psf
254 psf
452 psf
848 psf
1641 psf
3489 psf
7160 psf
Vertical Displacement (in)
0.0
0.5
1.0
1.5
2.0
2.5
3.0
3.5
Time^1/2 (min^1/2)

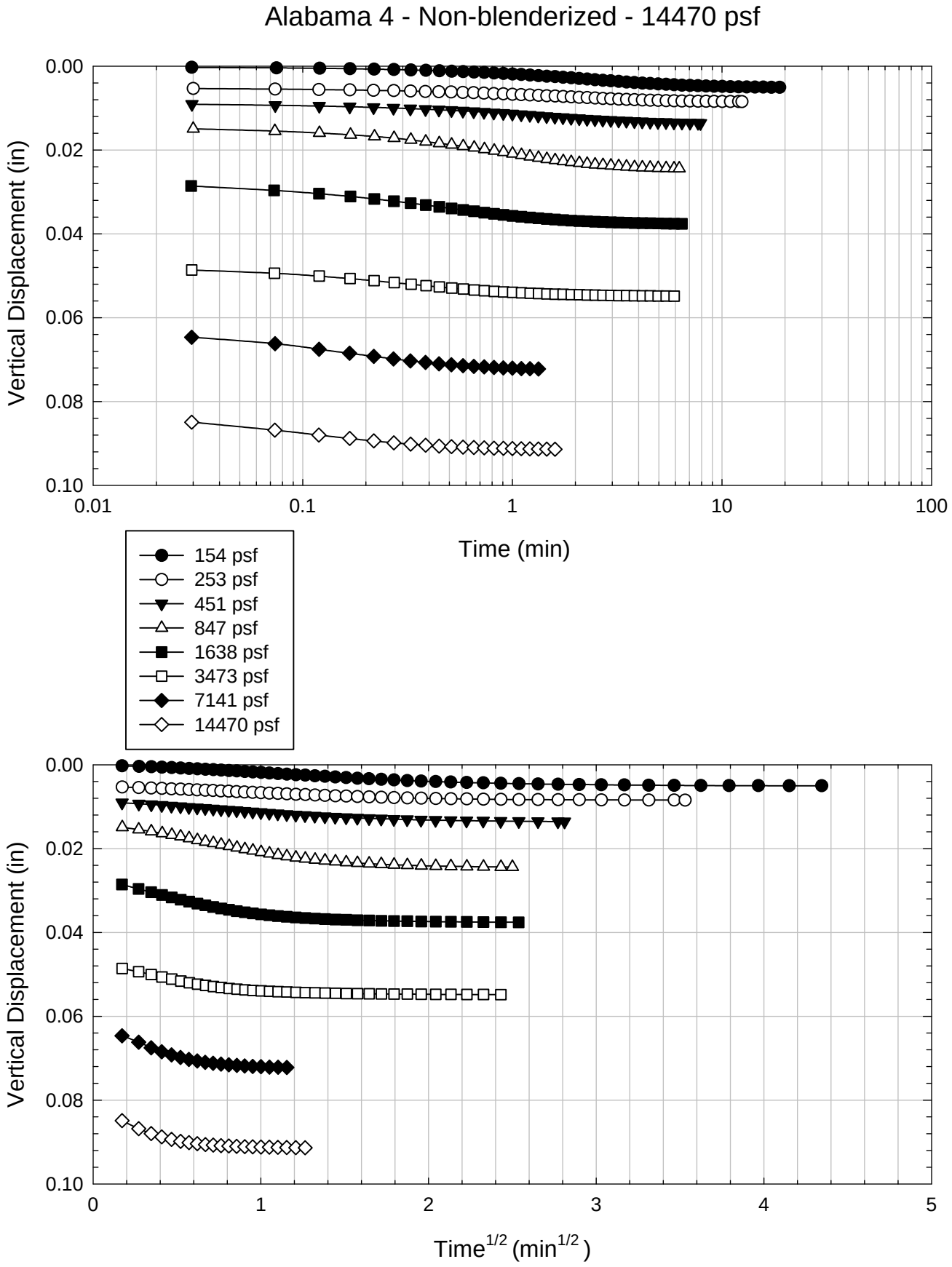
Alabama 4 - Non-blenderized - 14470 psf
Vertical Displacement (in)
0.00
0.02
0.04
0.06
0.08
0.10
0.01
0.1
1
10
100
Time (min)
154 psf
253 psf
451 psf
847 psf
1638 psf
3473 psf
7141 psf
14470 psf
Vertical Displacement (in)
0.00
0.02
0.04
0.06
0.08
0.10
0
1
2
3
4
5
Time^1/2 (min^1/2)

Alabama 4 - Non-blenderized

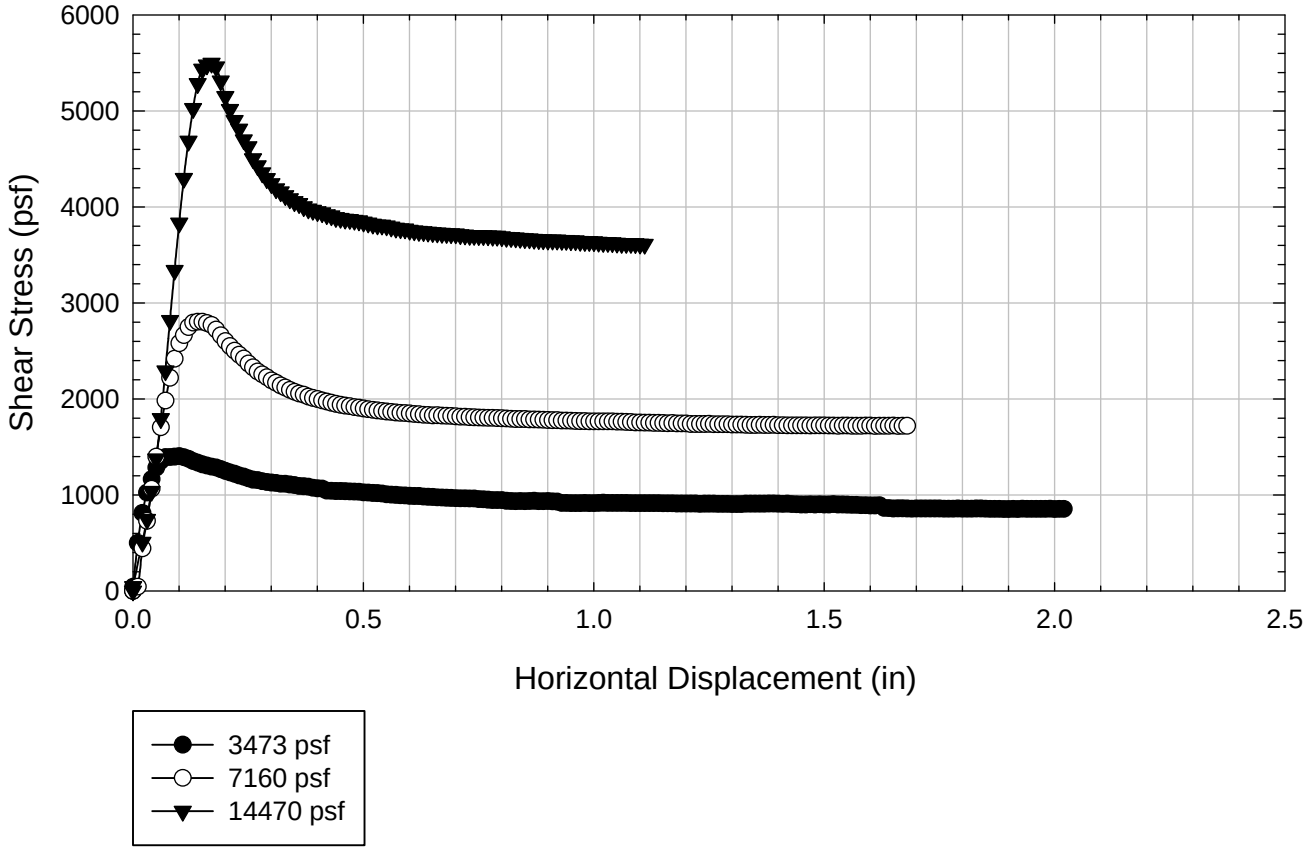

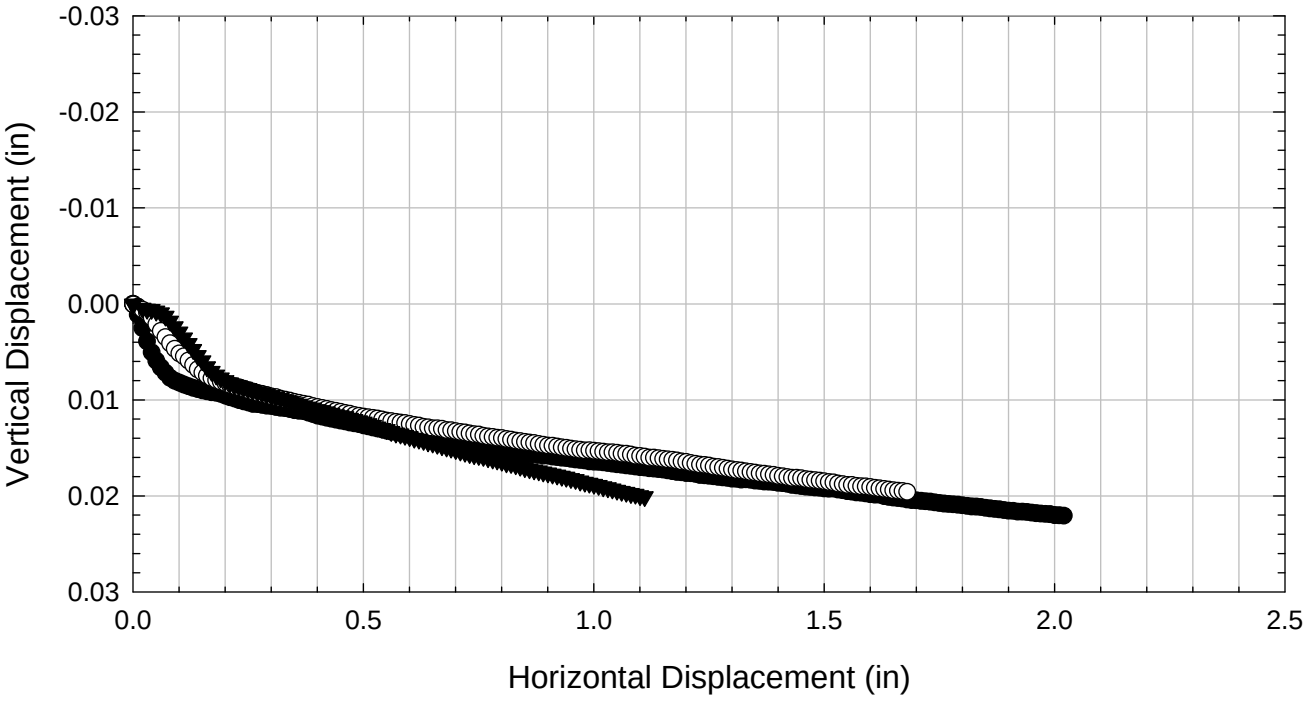

D.5. Colorado Clay

D.5.1 Blenderized

Virginia Polytechnic Institute and State University
Geotechnical Engineering Laboratory
Ring Shear Data Sheet

Project:	Fully Softened Shear Strength
Sample I.D./Loc.:	Colorado Clay - Blenderized
Classification:	Lean Clay (CL)

Sample Preparation	Remolded at LL

Specific Gravity	2.78	
Shear Device Used	WF Bromhead Ring Shear	

Test Number	1	2	3	4	5	6	7	
Start Date (m/d/y)	9/21/2011	9/19/2011	9/19/2011	9/14/2011				
End Date (m/d/y)	9/25/2011	9/21/2011	9/21/2011	9/18/2011				
Consolidation Pressure (psf)	848	1638	3213	6281				
Initial Values								
Initial Height (in)	0.20	0.20	0.20	0.20				
Inner Radius (in)	1.38	1.38	1.38	1.38				
Outer Radius (in)	1.97	1.97	1.97	1.97				
Initial Sample Weight (g)	38.63	38.28	38.22	35.49				
Water Content (%)	40.28	41.83	41.33	42.84				
Dry Unit Weight Before Shear (pcf)	83.1	95.1	107.3	78.1				
Saturation (%)	100.0	100.0	100.0	100.0				
Consolidation Pressures								
Load 1 (psf)	155	154	155	155				
Load 2 (psf)	254	253	254	254				
Load 3 (psf)	451	451	451	451				
Load 4 (psf)	848	847	848	848				
Load 5 (psf)		1638	1641	1641				
Load 6 (psf)			3213	3213				
Load 7 (psf)				6281				
t_{50}								
Max. t_{50} for Load 1 (min)								
Max. t_{50} for Load 2 (min)								
Max. t_{50} for Load 3 (min)								
Max. t_{50} for Load 4 (min)	5.51							
Max. t_{50} for Load 5 (min)		2.13						
Max. t_{50} for Load 6 (min)			0.91					
Max. t_{50} for Load 7 (min)				0.58				
Final Values								
Water Content (%)	34.96	30.71	29.91	28.90				
Saturation (%)	100.0	100.0	100.0	100.0				
Failure								
Test Performed at Shear Rate (in/min)	7.00E-04	7.00E-04	7.00E-04	7.00E-04				
Required Shear Rate (in/min)	7.99E-04	2.54E-03	5.27E-03	6.90E-03				
Displacement at Failure (in)	0.22	0.27	0.24	0.20				
Peak Shear Stress (psf)	311	774	1526	2872				
Secant Effective Friction Angle (deg)	20.2	25.3	25.4	24.6				

Comments: For the tests consolidated at 1638 and 3213 psf, the power was lost during the 451 psf consolidations stress. The tests were restarted and continued.

Colorado Clay - Blenderized - 848 psf

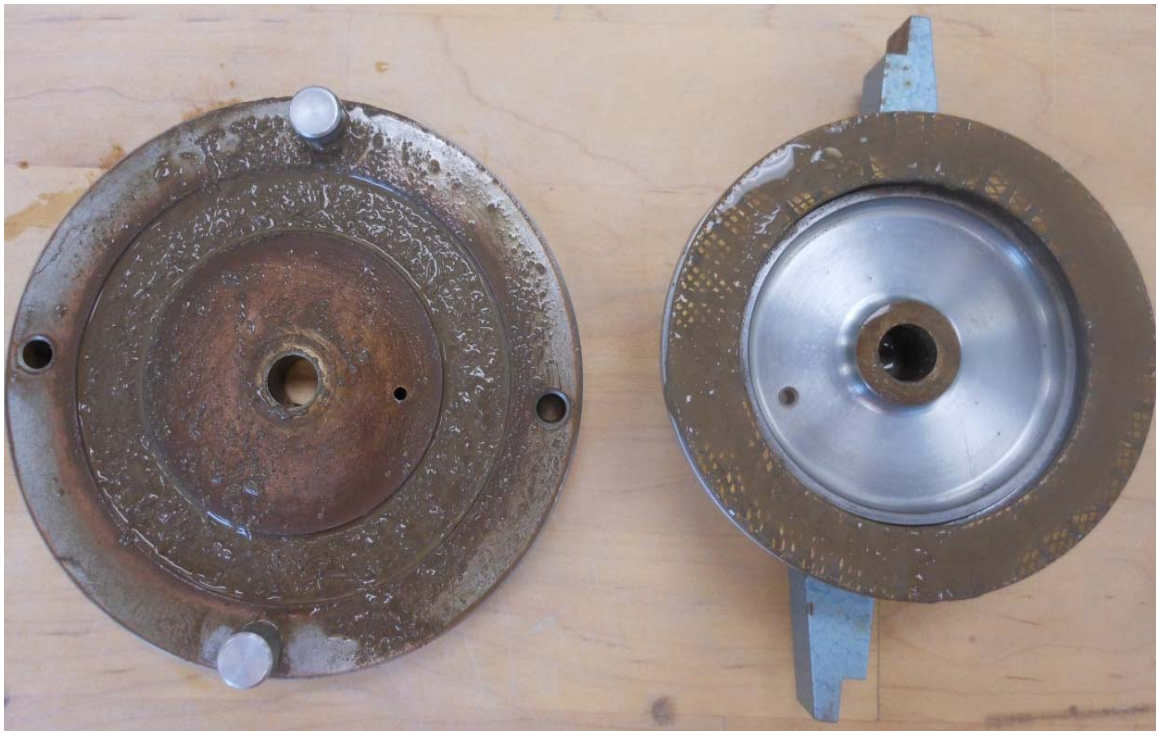

Colorado Clay - Blenderized - 1638 psf

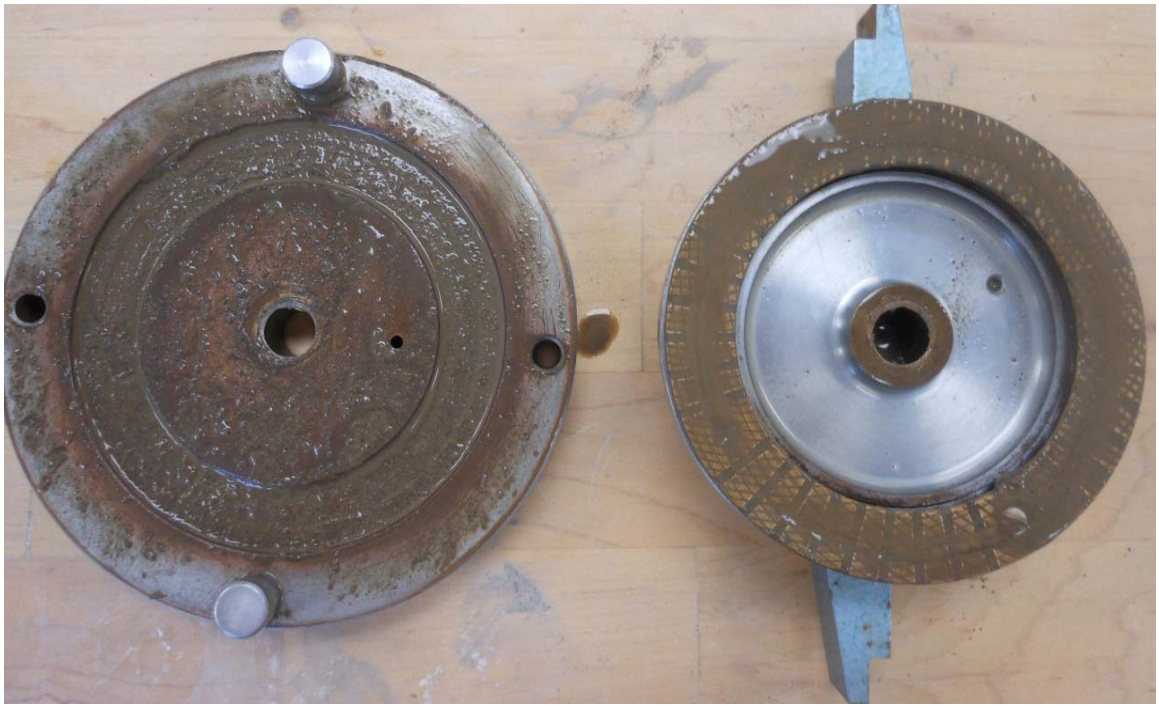

Colorado Clay - Blenderized - 3213 psf

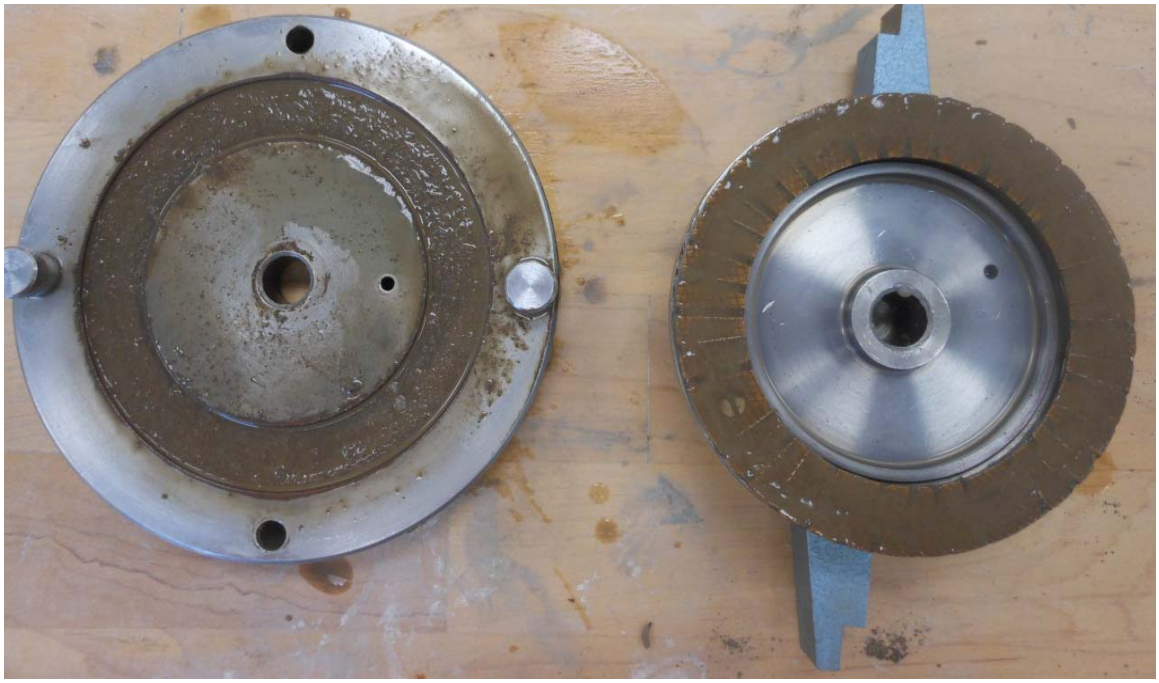

Colorado Clay - Blenderized - 6281 psf

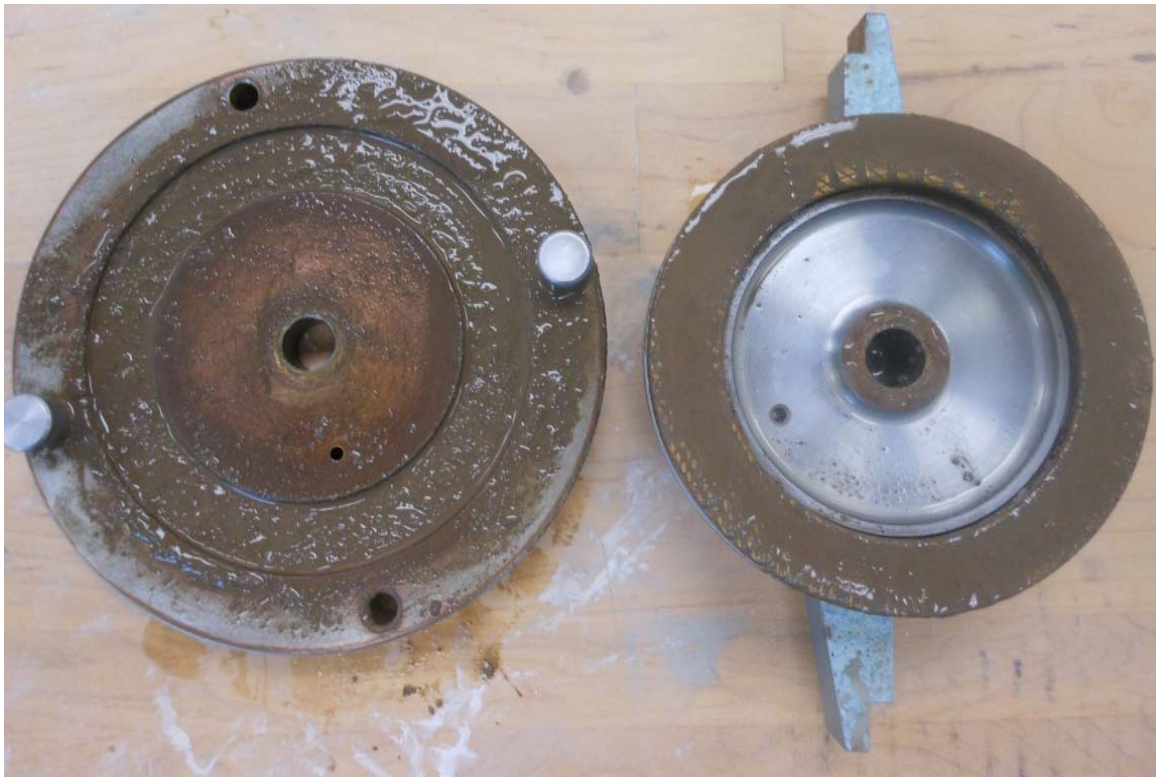

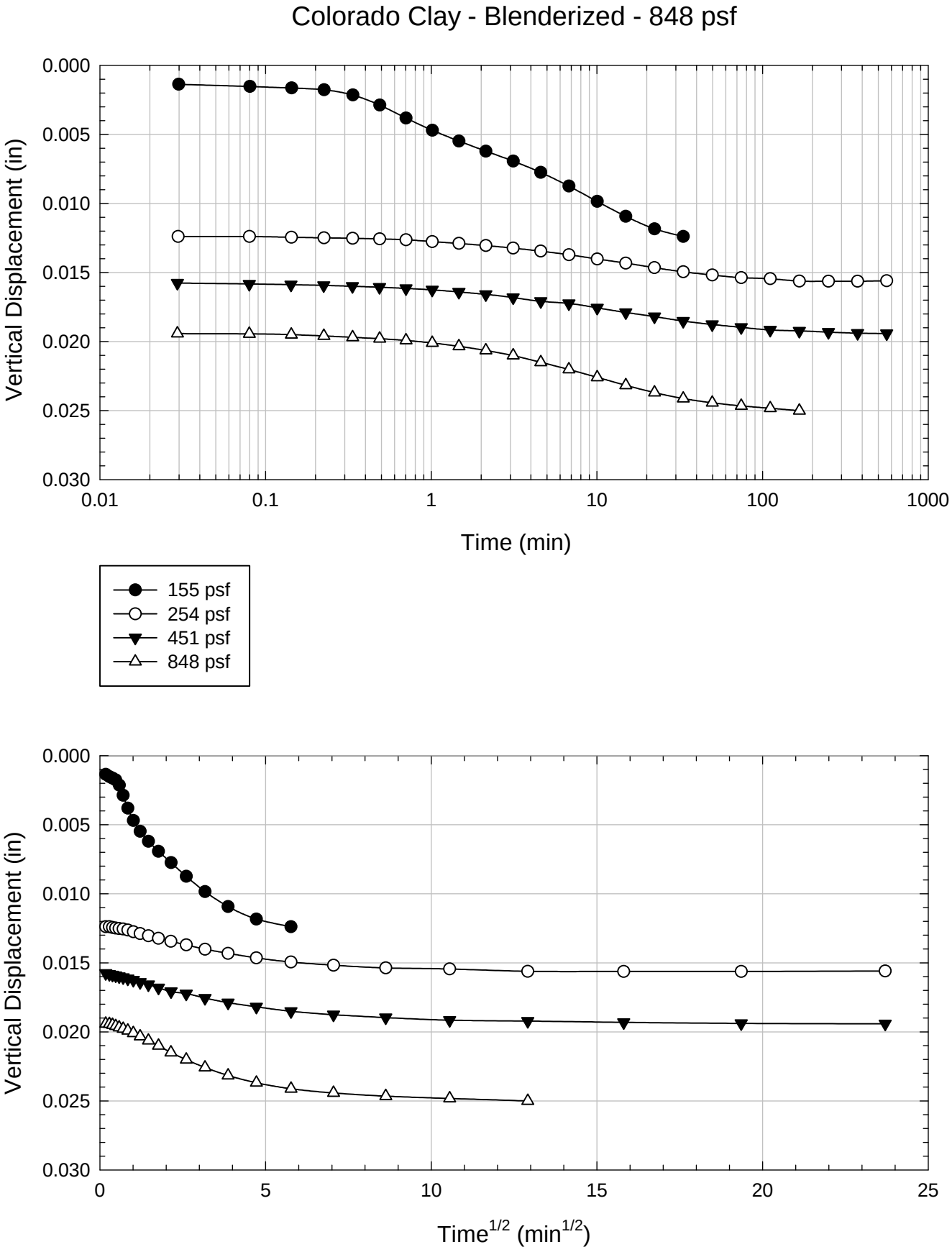
Colorado Clay - Blenderized - 848 psf
Vertical Displacement (in)
0.000
0.005
0.010
0.015
0.020
0.025
0.030
0.01
0.1
1
10
100
1000
Time (min)
155 psf
254 psf
451 psf
848 psf
Vertical Displacement (in)
0.000
0.005
0.010
0.015
0.020
0.025
0.030
0
5
10
15
20
25
Time^1/2 (min^1/2)

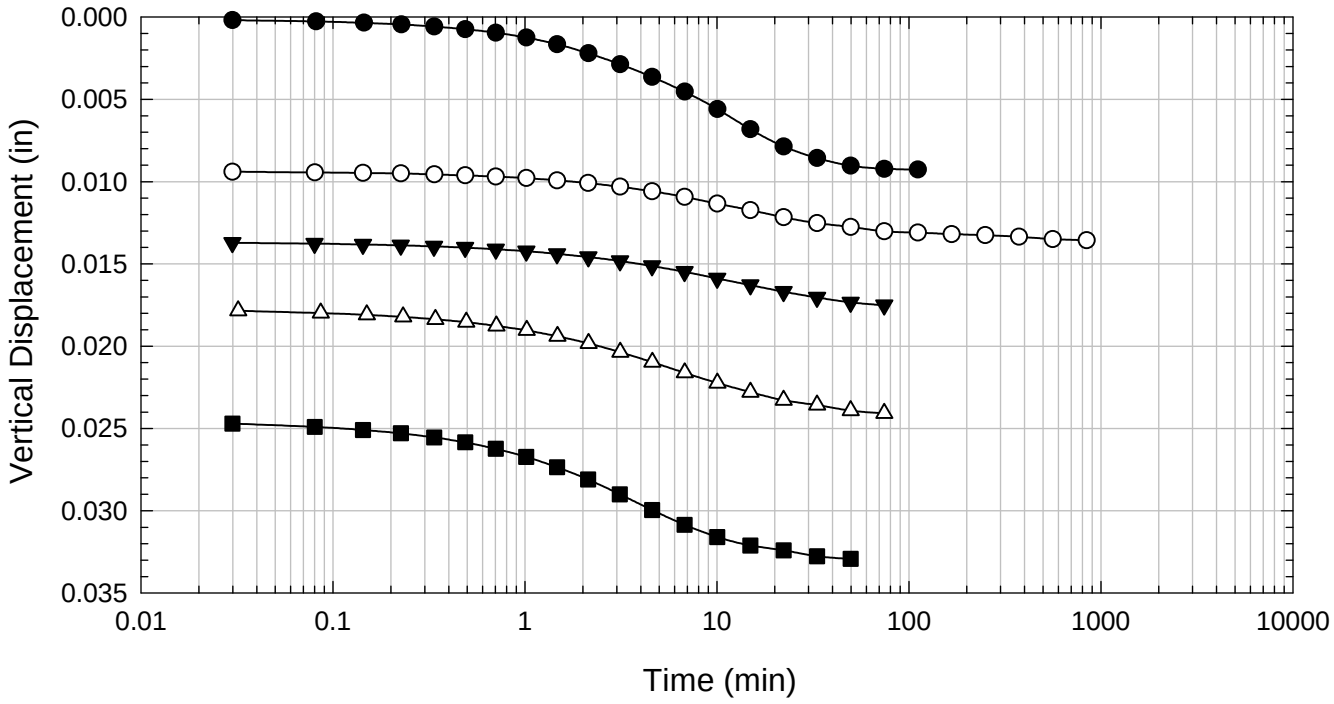
Colorado Clay - Blenderized - 1638 psf
Vertical Displacement (in)
0.000
0.005
0.010
0.015
0.020
0.025
0.030
0.035
0.01
0.1
1
10
100
1000
10000
Time (min)

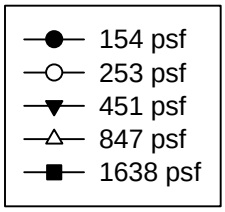
154 psf
253 psf
451 psf
847 psf
1638 psf

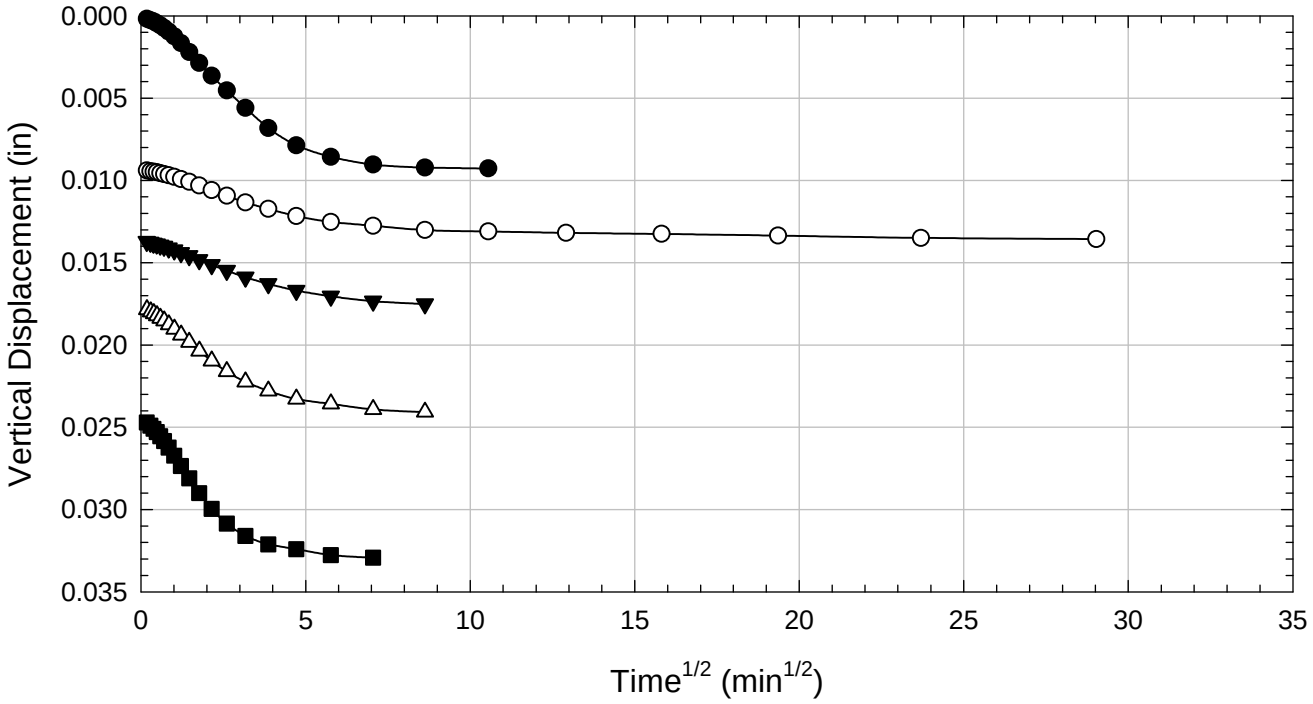
Vertical Displacement (in)
0.000
0.005
0.010
0.015
0.020
0.025
0.030
0.035
0
5
10
15
20
25
30
35
Time1/2 (min1/2)

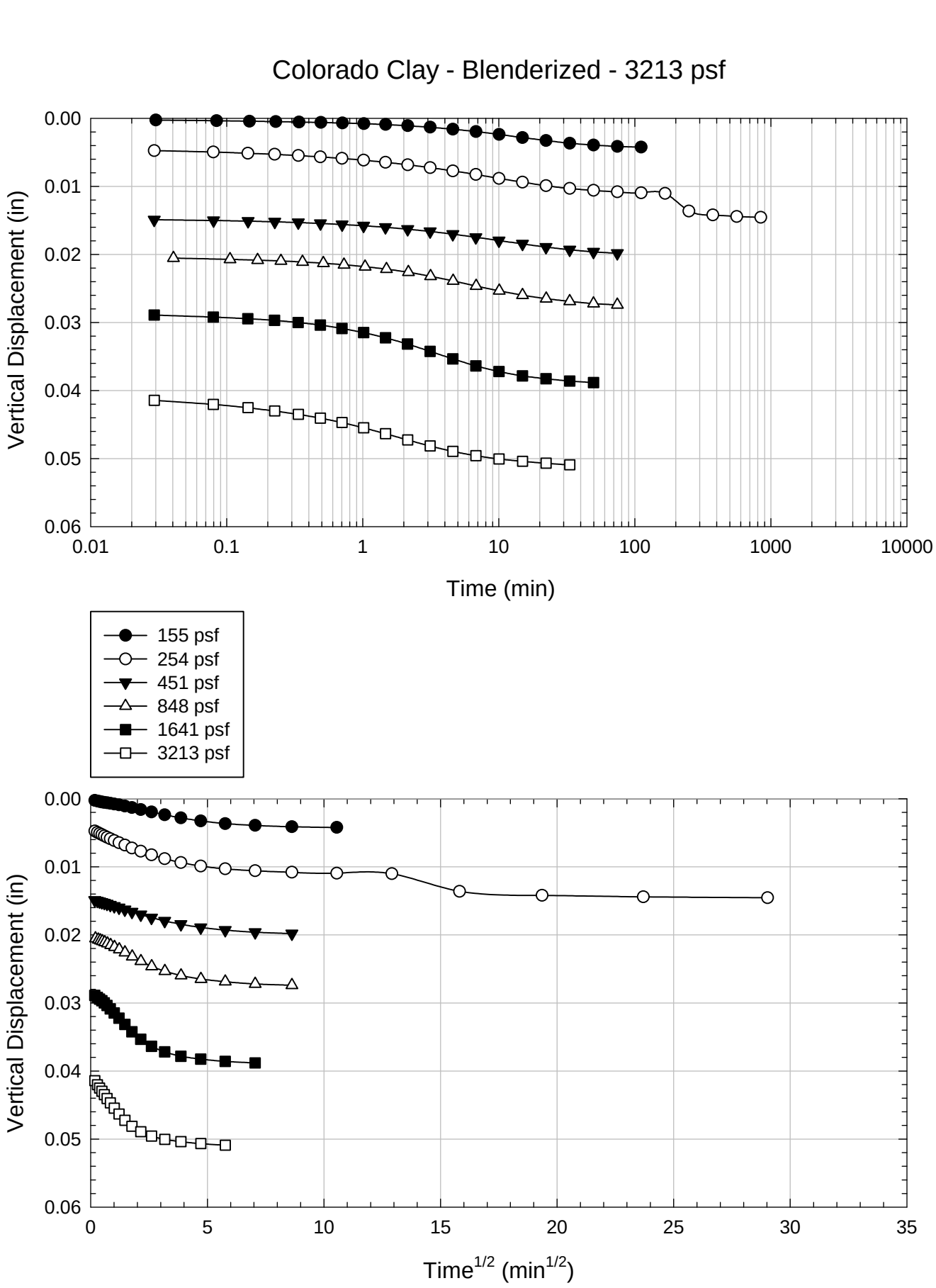
Colorado Clay - Blenderized - 3213 psf
Vertical Displacement (in)
0.00
0.01
0.02
0.03
0.04
0.05
0.06
0.01
0.1
1
10
100
1000
10000
Time (min)
155 psf
254 psf
451 psf
848 psf
1641 psf
3213 psf
Vertical Displacement (in)
0.00
0.01
0.02
0.03
0.04
0.05
0.06
0
5
10
15
20
25
30
35
Time^1/2 (min^1/2)

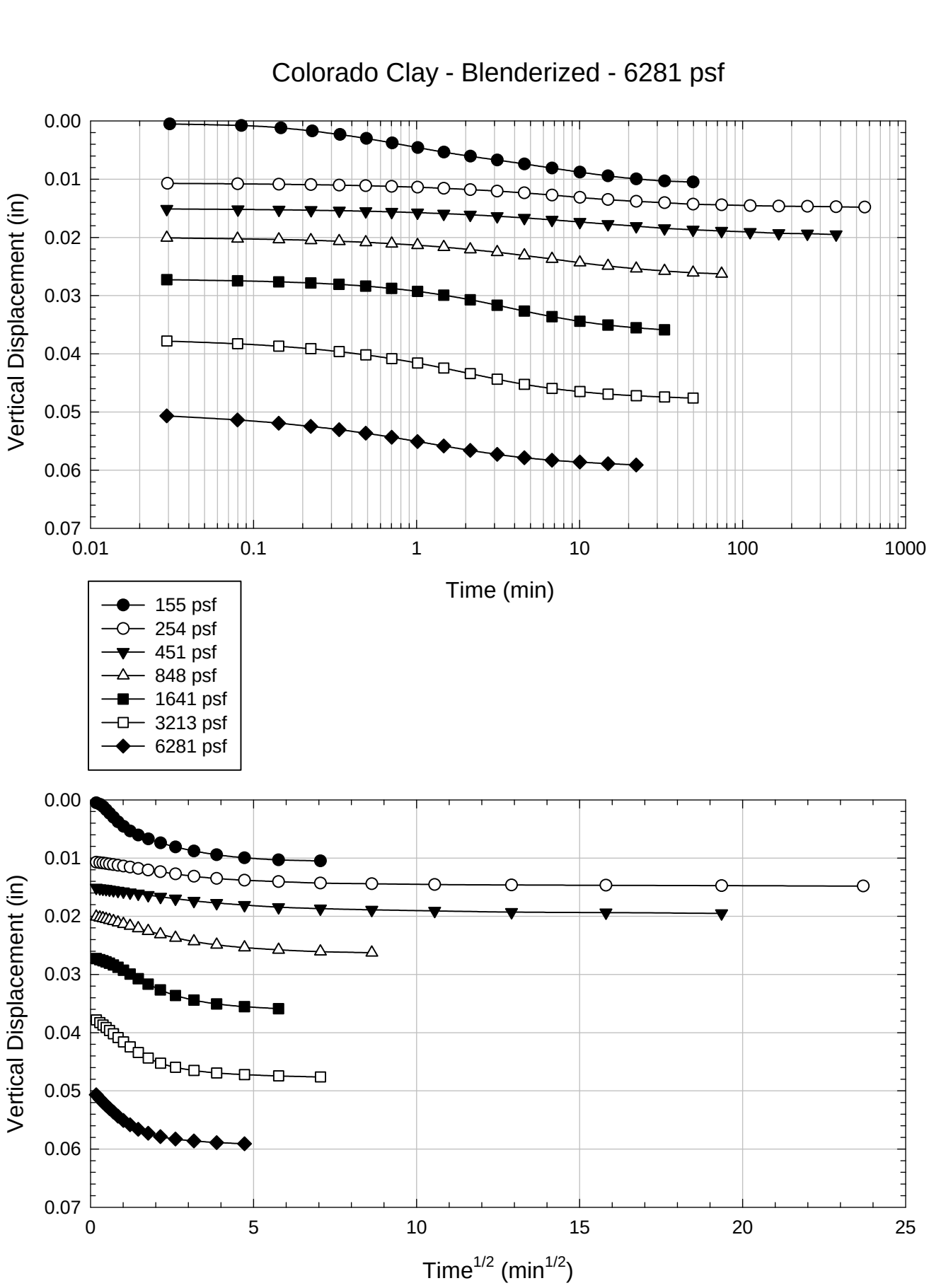
Colorado Clay - Blenderized - 6281 psf
Vertical Displacement (in)
0.00
0.01
0.02
0.03
0.04
0.05
0.06
0.07
0.01
0.1
1
10
100
1000
Time (min)
155 psf
254 psf
451 psf
848 psf
1641 psf
3213 psf
6281 psf
Vertical Displacement (in)
0
5
10
15
20
25
Time^1/2 (min^1/2)

Colorado Clay - Blenderized

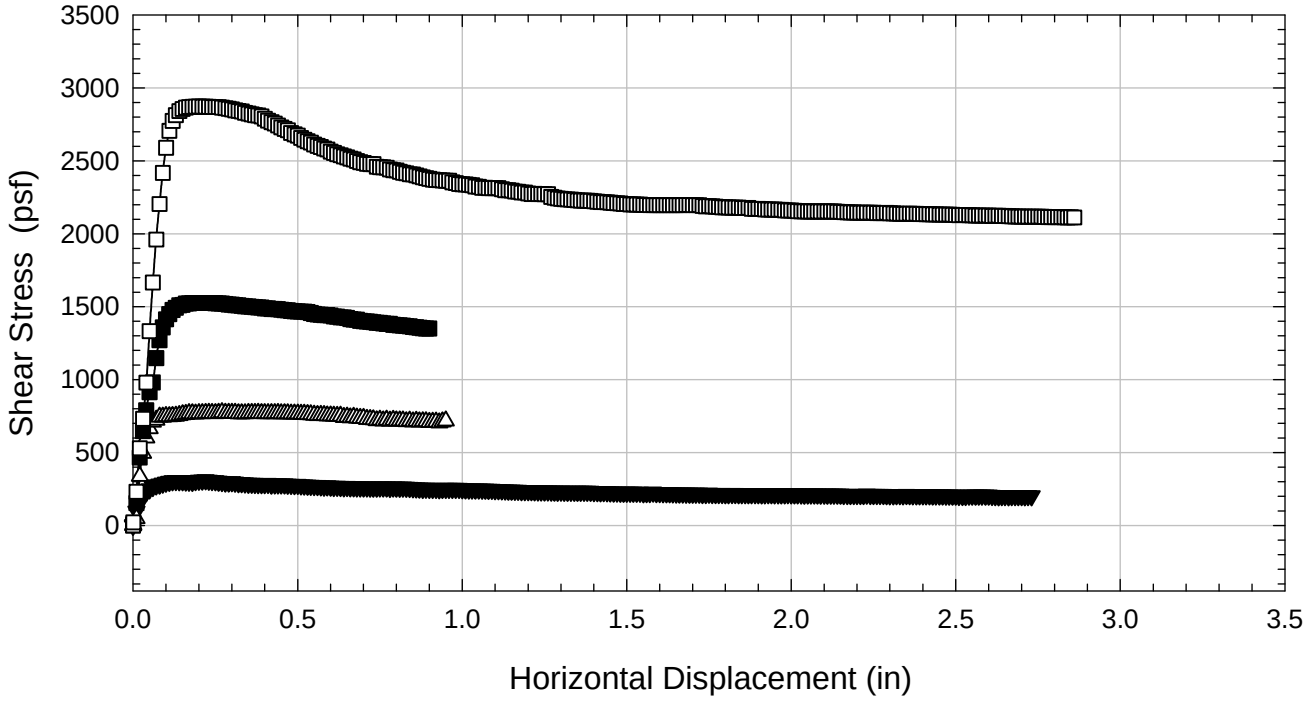

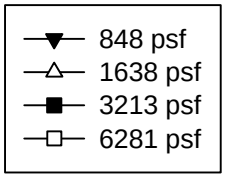

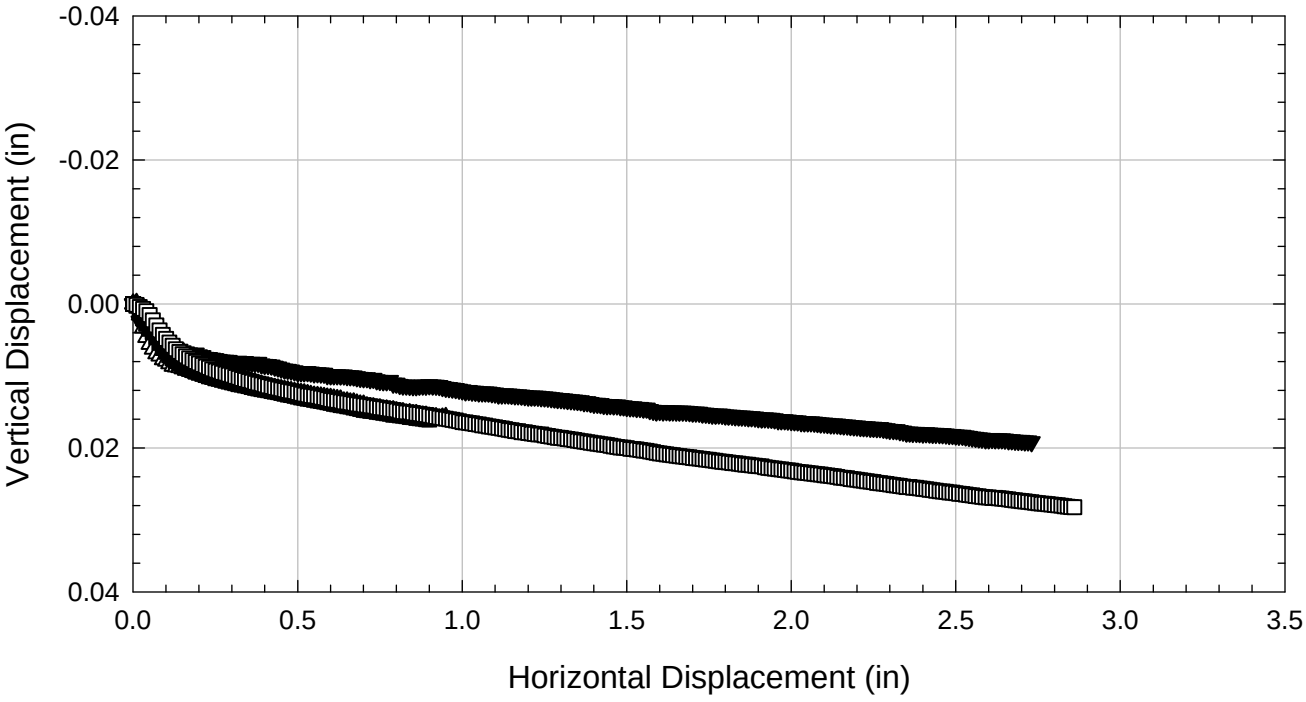

D.6. NOVA Clay

D.6.1 Blenderized

Virginia Polytechnic Institute and State University
Geotechnical Engineering Laboratory
Ring Shear Data Sheet

Project:	Fully Softened Shear Strength
Sample I.D./Loc.:	NOVA - Blenderized
Classification:	Fat Clay (CH)

Sample Preparation	Remolded at LL

Specific Gravity	2.80	
Shear Device Used	WF Bromhead Ring Shear	

Test Number	1	2	3	4	5	6	7	
Start Date (m/d/y)	4/16/2011	3/23/2011	3/27/2011	3/29/2011	4/1/2011	10/16/2011		
End Date (m/d/y)	4/18/2011	3/26/2011	3/29/2011	4/1/2011	4/6/2011	10/20/2011		
Consolidation Pressure (psf)	253	451	847	1638	3225	6281		
Initial Values								
Initial Height (in)	0.20	0.20	0.20	0.20	0.20	0.20		
Inner Radius (in)	1.38	1.38	1.38	1.38	1.38	1.38		
Outer Radius (in)	1.97	1.97	1.97	1.97	1.97	1.97		
Initial Sample Weight (g)	33.43	33.07	31.15	33.14	32.98	26.18		
Water Content (%)	71.80	72.22	70.68	70.86	71.52	80.05		
Dry Unit Weight Before Shear (pcf)	61.9	65.0	69.9	75.5	82.6	75.3		
Saturation (%)	100.0	100.0	100.0	100.0	100.0	100.0		
Consolidation Pressures								
Load 1 (psf)	154	154	154	154	154	155		
Load 2 (psf)	253	253	253	253	253	254		
Load 3 (psf)		451	451	451	451	451		
Load 4 (psf)			847	847	847	848		
Load 5 (psf)				1638	1638	1641		
Load 6 (psf)					3225	3213		
Load 7 (psf)						6281		
t_{50}								
Max. t_{50} for Load 1 (min)	5.93	9.25	3.35	7.95	8.91			
Max. t_{50} for Load 2 (min)	13.16	14.58	3.77	5.70	10.06			
Max. t_{50} for Load 3 (min)		9.88	4.96	3.35	11.88			
Max. t_{50} for Load 4 (min)			6.51	7.06	6.80			
Max. t_{50} for Load 5 (min)				6.15	6.47			
Max. t_{50} for Load 6 (min)					7.62			
Max. t_{50} for Load 7 (min)						2.84		
Final Values								
Water Content (%)	64.87	61.58	58.07	53.40	48.96	47.47		
Saturation (%)	100.0	100.0	100.0	100.0	100.0	100.0		
Failure								
Test Performed at Shear Rate (in/min)	7.00E-04	7.00E-04	7.00E-04	7.00E-04	7.00E-04	7.00E-04		
Required Shear Rate (in/min)	2.89E-04	5.87E-04	5.22E-04	3.90E-04	1.84E-04	7.75E-04		
Displacement at Failure (in)	0.19	0.29	0.17	0.12	0.07	0.11		
Peak Shear Stress (psf)	126	211	343	603	1081	1683		
Secant Effective Friction Angle (deg)	26.4	25.1	22.0	20.2	18.5	15.0		

Comments:

NOVA - Blenderized - 253 psf

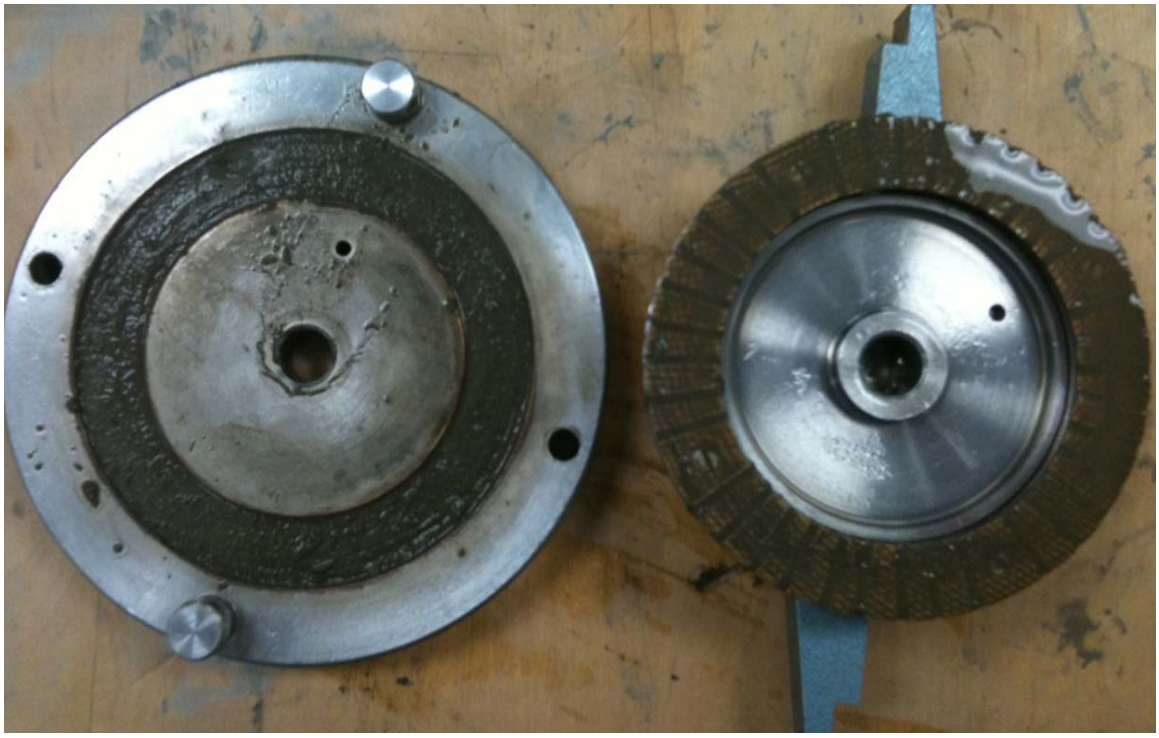

NOVA - Blenderized - 451 psf

NOVA - Blenderized - 847 psf

NOVA - Blenderized - 1638 psf

NOVA - Blenderized - 3225 psf

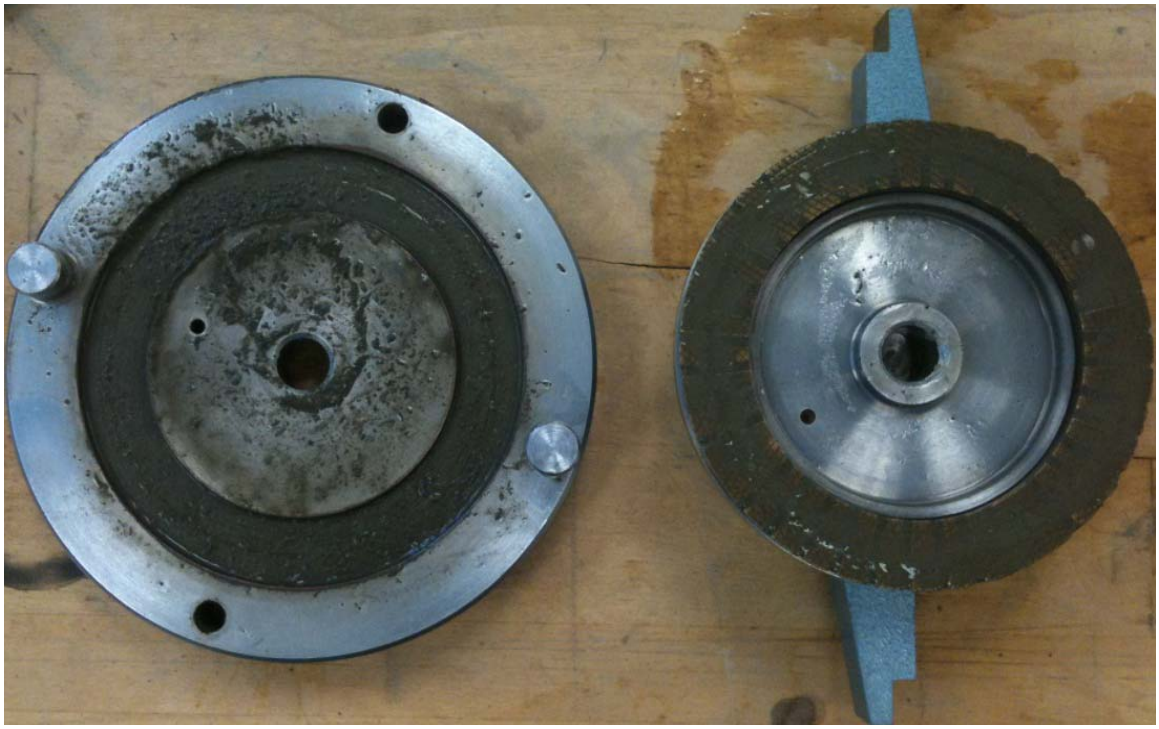

NOVA - Blenderized - 6281 psf

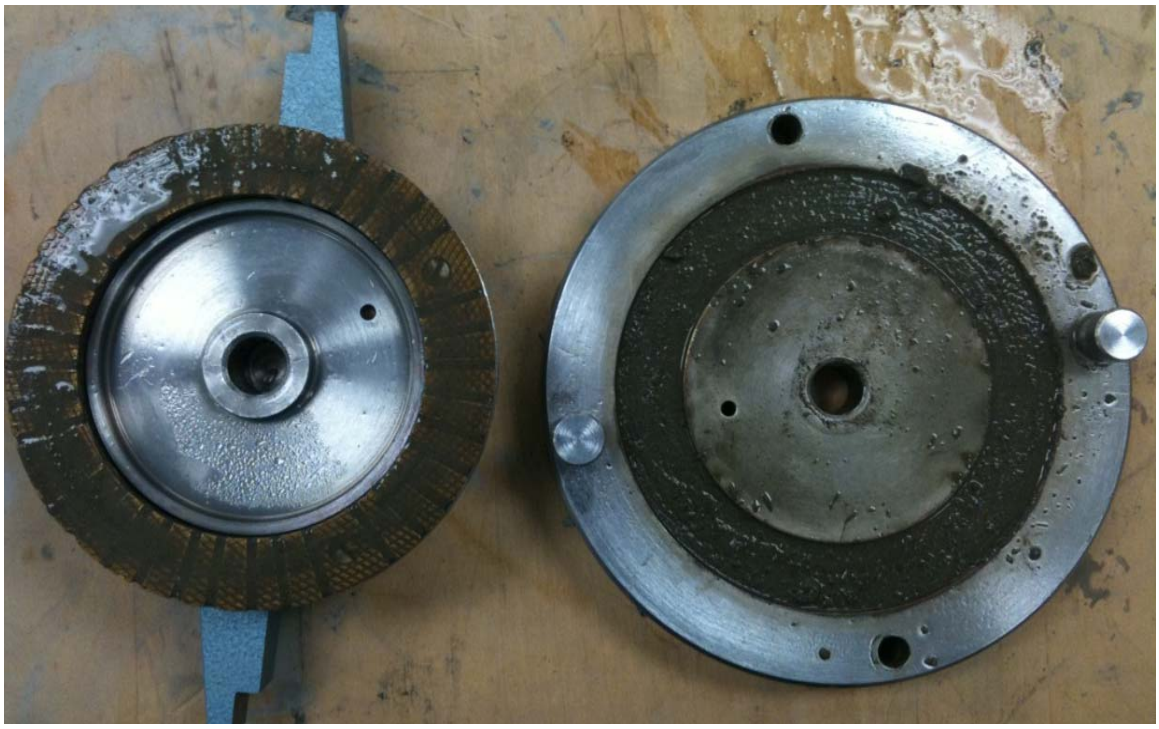

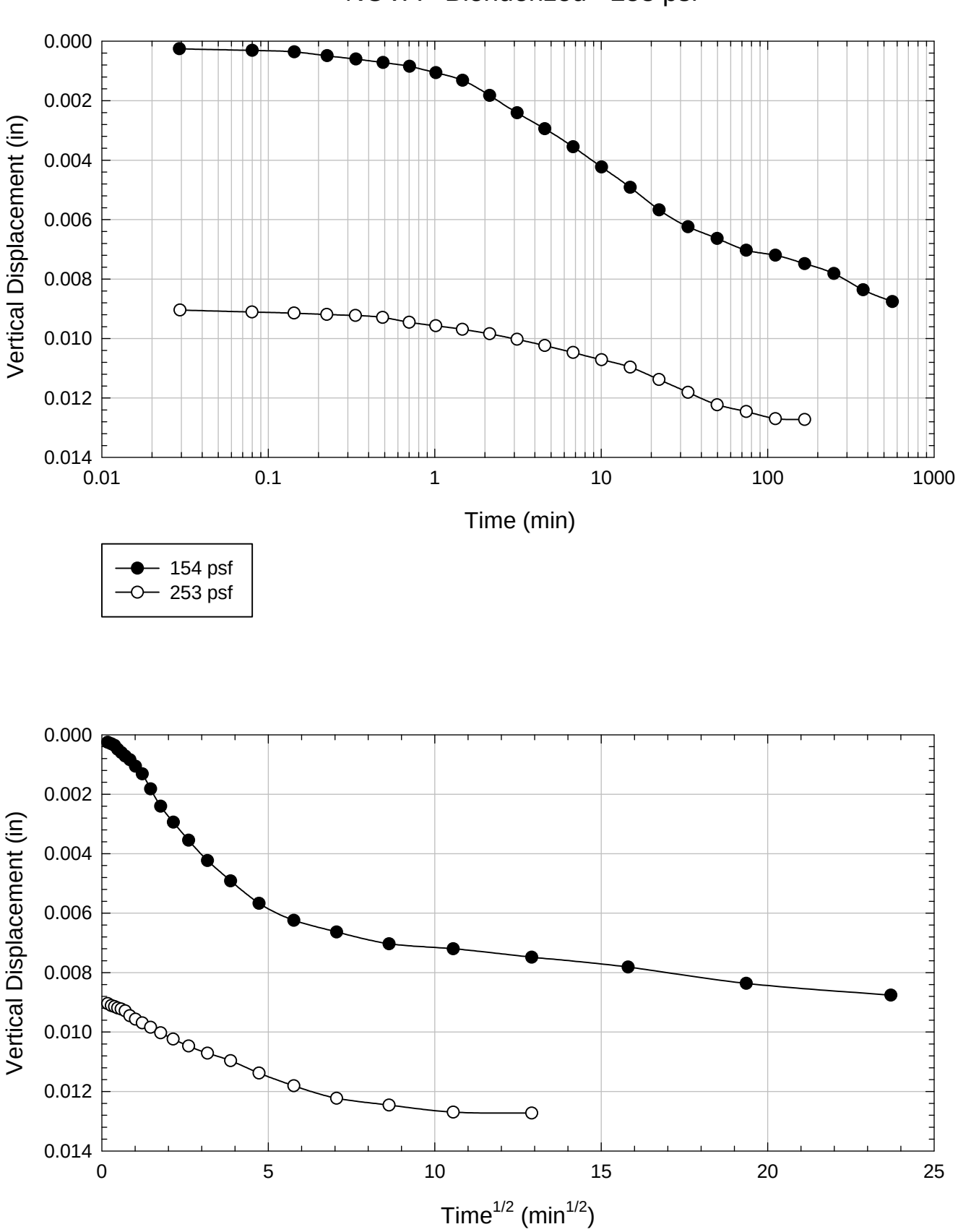
NOVA - Blenderized - 253 psf
Vertical Displacement (in)
0.000
0.002
0.004
0.006
0.008
0.010
0.012
0.014
0.01
0.1
1
10
100
1000
Time (min)
154 psf
253 psf
Vertical Displacement (in)
0.000
0.002
0.004
0.006
0.008
0.010
0.012
0.014
0
5
10
15
20
25
Time^1/2 (min^1/2)

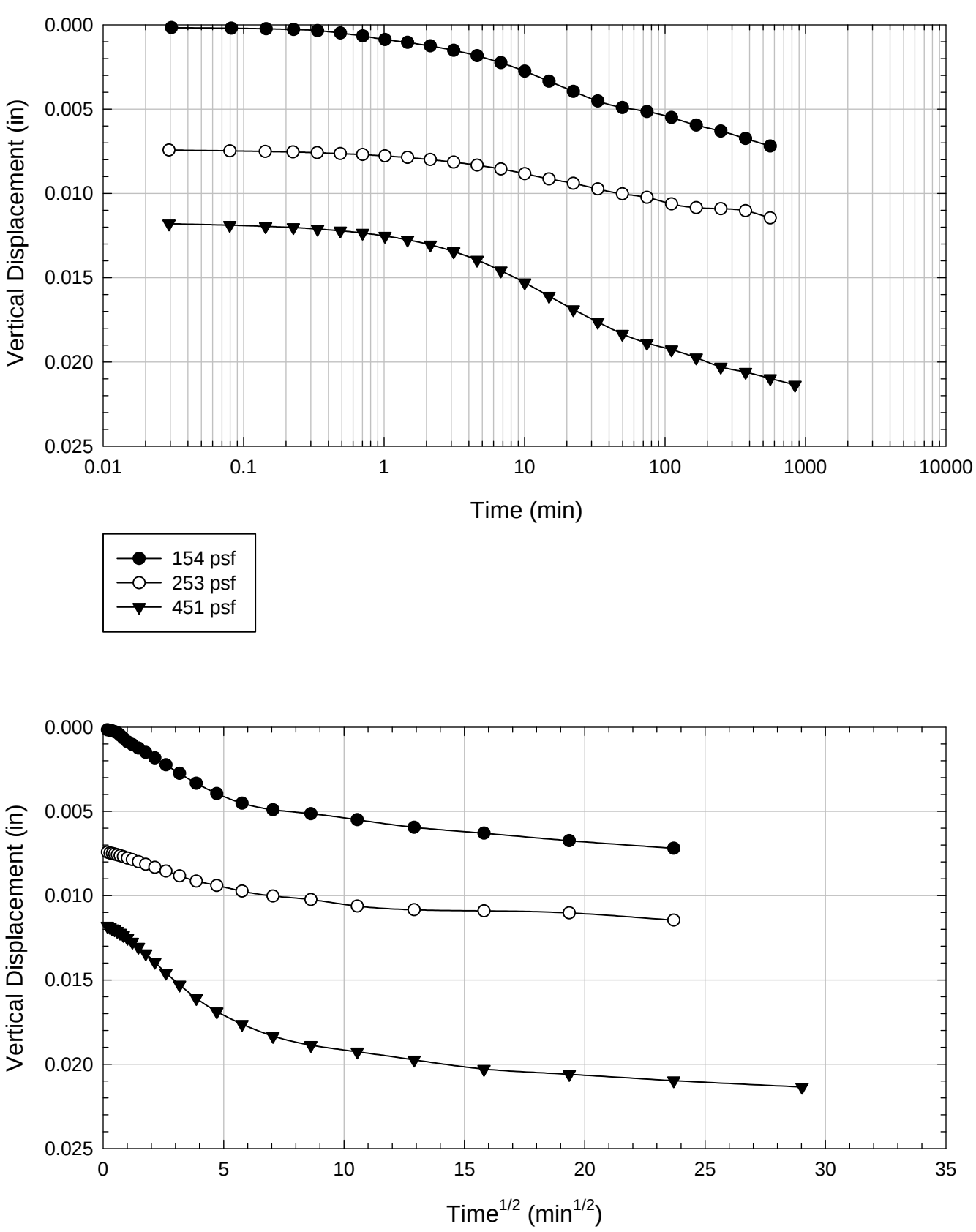
NOVA - Blenderized - 451 psf
Vertical Displacement (in)
0.000
0.005
0.010
0.015
0.020
0.025
0.01
0.1
1
10
100
1000
10000
Time (min)
154 psf
253 psf
451 psf
Vertical Displacement (in)
0.000
0.005
0.010
0.015
0.020
0.025
0
5
10
15
20
25
30
35
Time1/2 (min1/2)

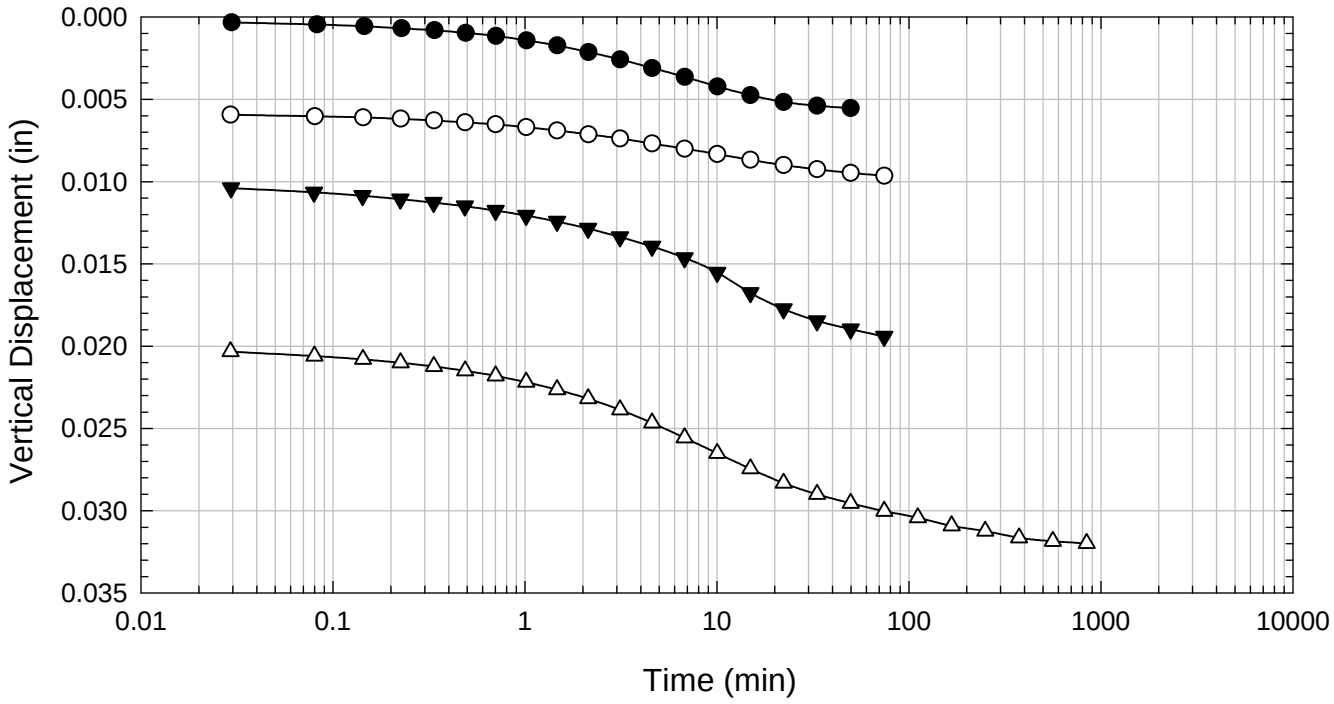
NOVA - Blenderized - 847 psf
Vertical Displacement (in)
0.000
0.005
0.010
0.015
0.020
0.025
0.030
0.035
0.01
0.1
1
10
100
1000
10000
Time (min)

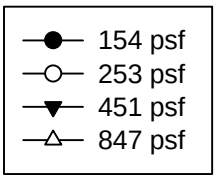
154 psf
253 psf
451 psf
847 psf

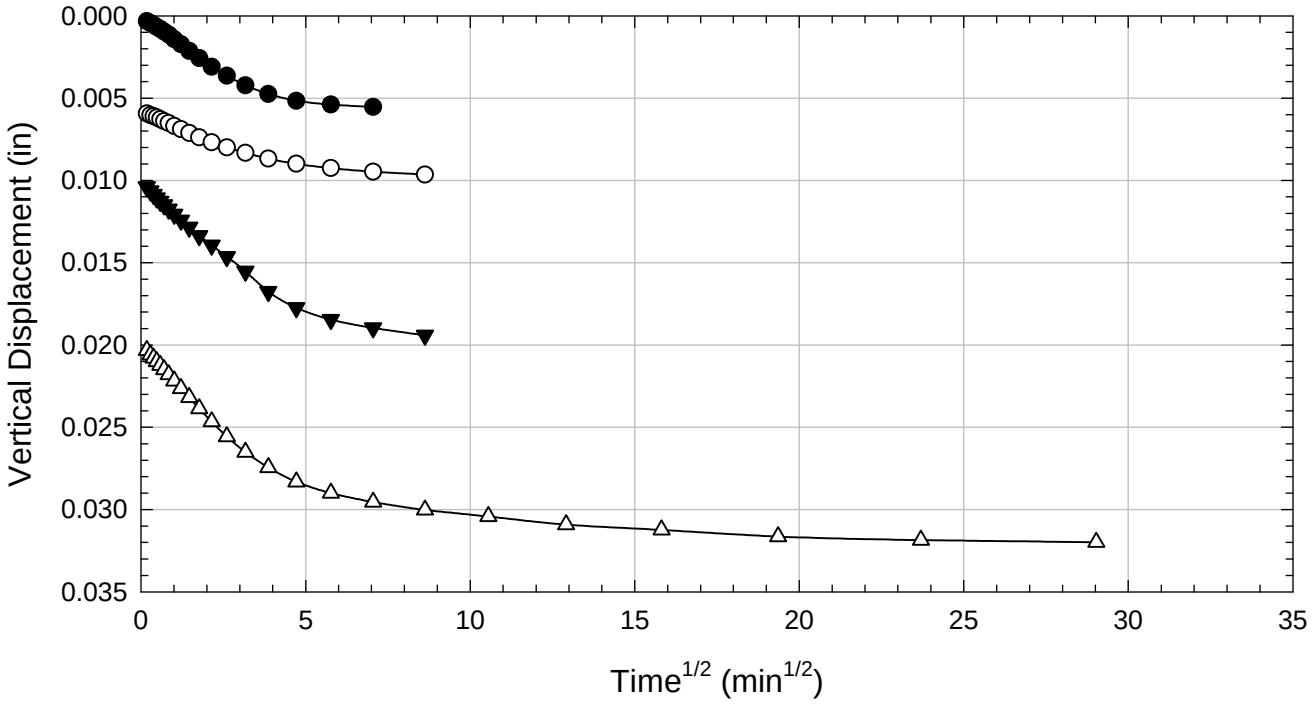
Vertical Displacement (in)
0.000
0.005
0.010
0.015
0.020
0.025
0.030
0.035
0
5
10
15
20
25
30
35
Time1/2 (min1/2)

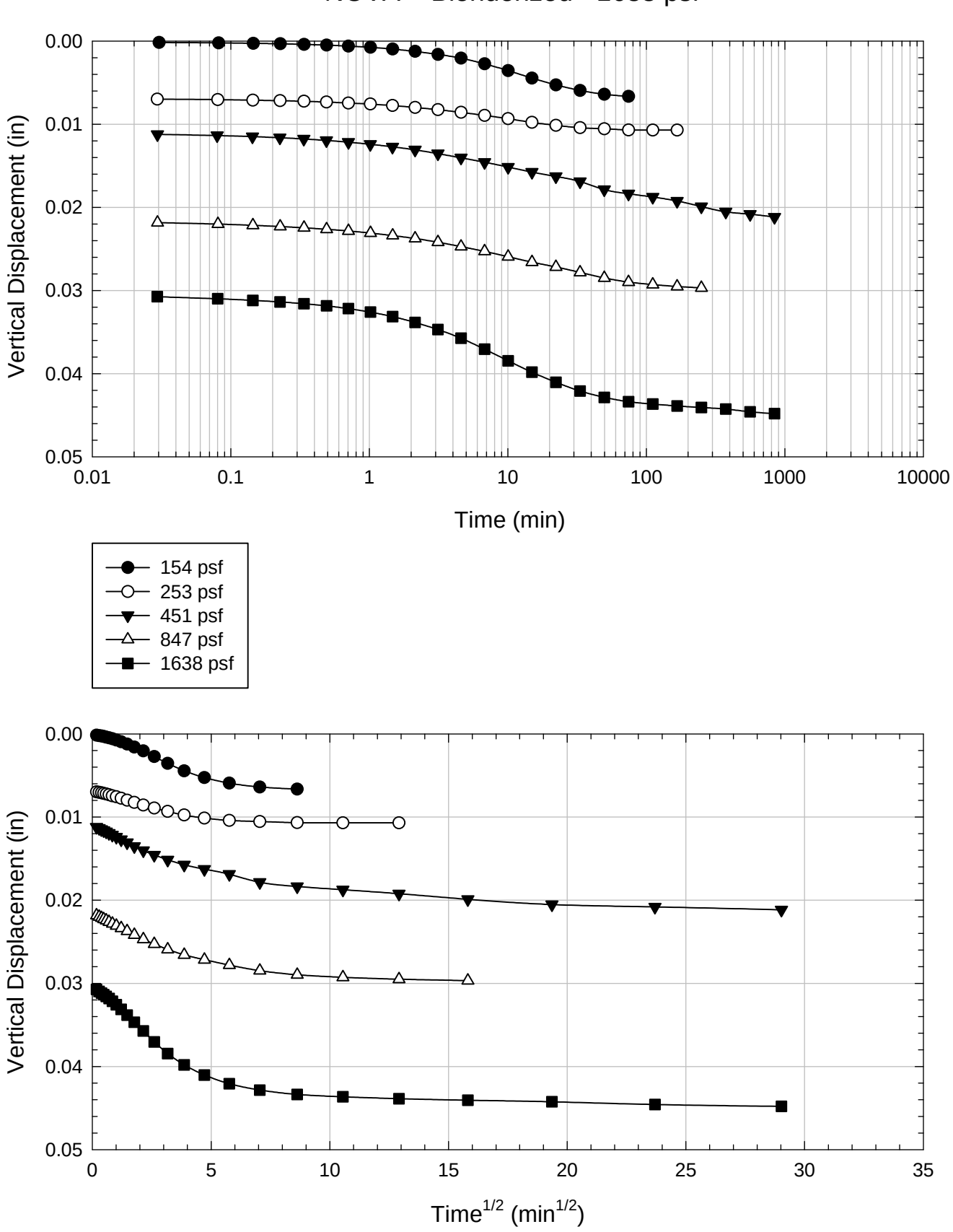
NOVA - Blenderized - 1638 psf
Vertical Displacement (in)
0.00
0.01
0.02
0.03
0.04
0.05
0.01
0.1
1
10
100
1000
10000
Time (min)
154 psf
253 psf
451 psf
847 psf
1638 psf
Vertical Displacement (in)
0.00
0.01
0.02
0.03
0.04
0.05
0
5
10
15
20
25
30
35
Time1/2 (min1/2)

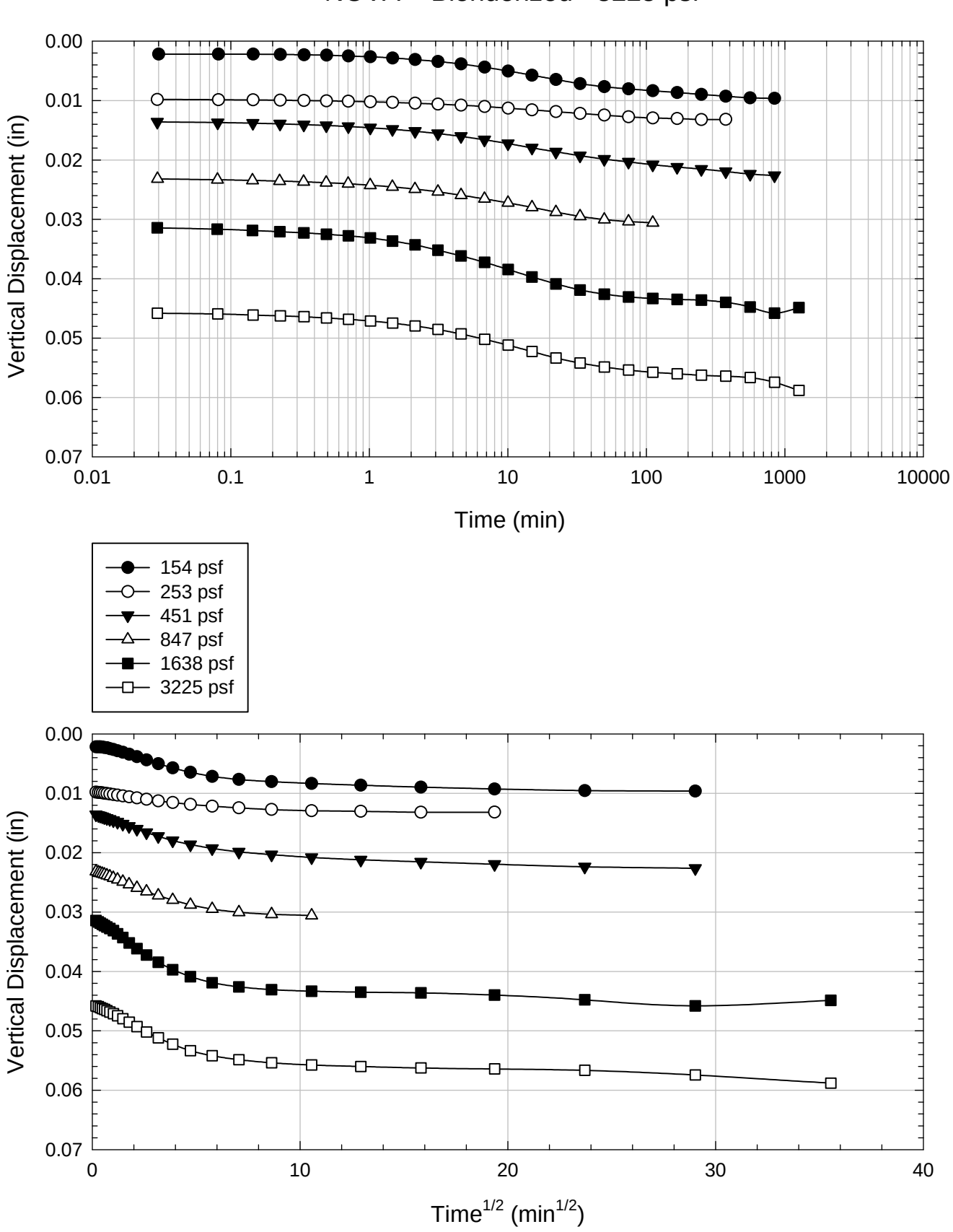
NOVA - Blenderized - 3225 psf
Vertical Displacement (in)
0.00
0.01
0.02
0.03
0.04
0.05
0.06
0.07
0.01
0.1
1
10
100
1000
10000
Time (min)
154 psf
253 psf
451 psf
847 psf
1638 psf
3225 psf
Vertical Displacement (in)
0.00
0.01
0.02
0.03
0.04
0.05
0.06
0.07
0
10
20
30
40
Time^1/2 (min^1/2)

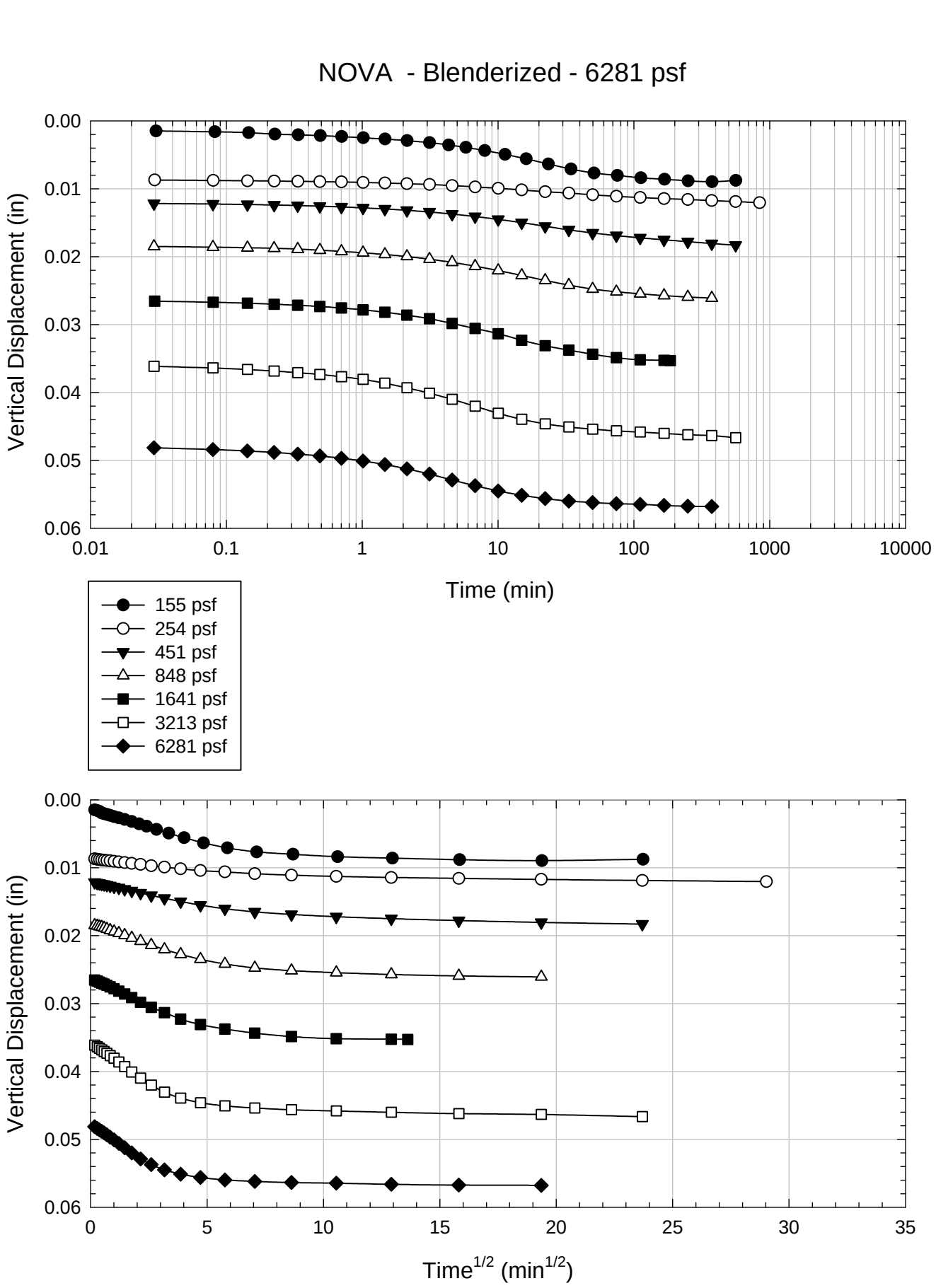
NOVA - Blenderized - 6281 psf
Vertical Displacement (in)
0.00
0.01
0.02
0.03
0.04
0.05
0.06
0.01
0.1
1
10
100
1000
10000
Time (min)
155 psf
254 psf
451 psf
848 psf
1641 psf
3213 psf
6281 psf
Vertical Displacement (in)
0
5
10
15
20
25
30
35
Time^1/2 (min^1/2)

NOVA - Blenderized

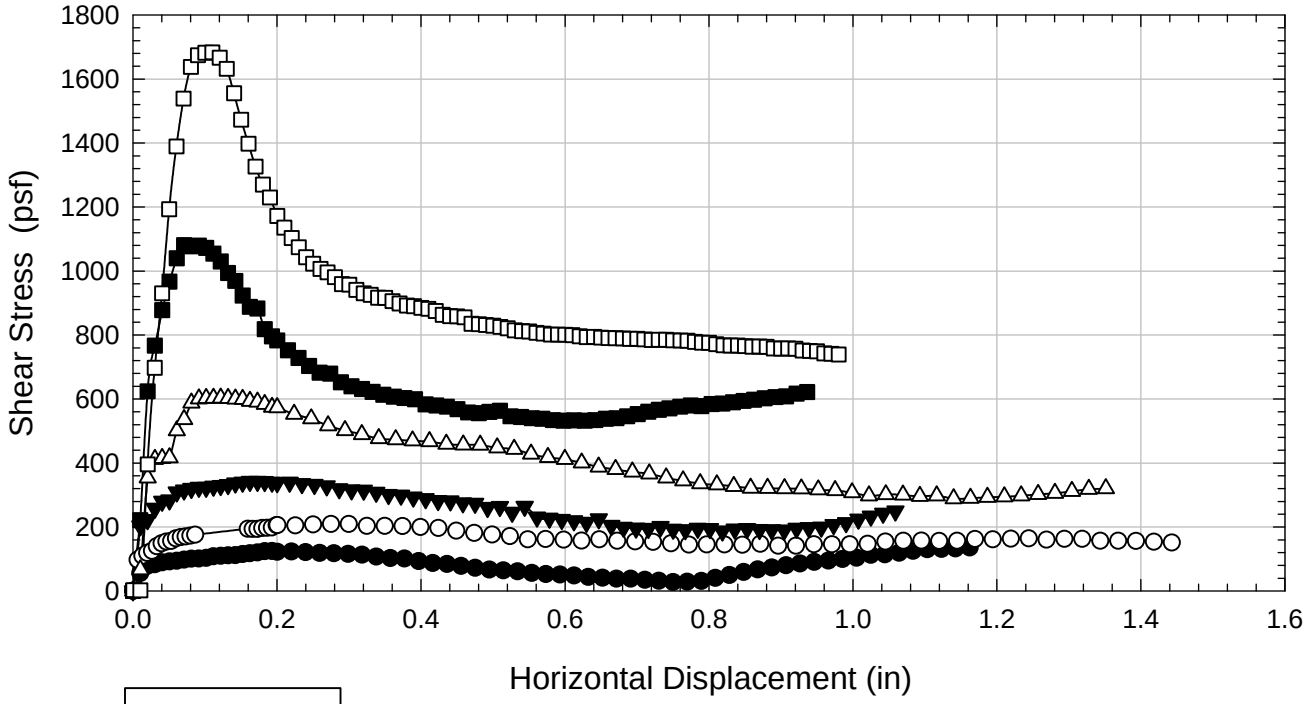

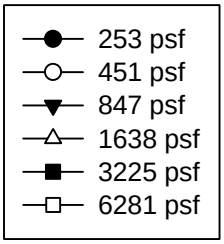

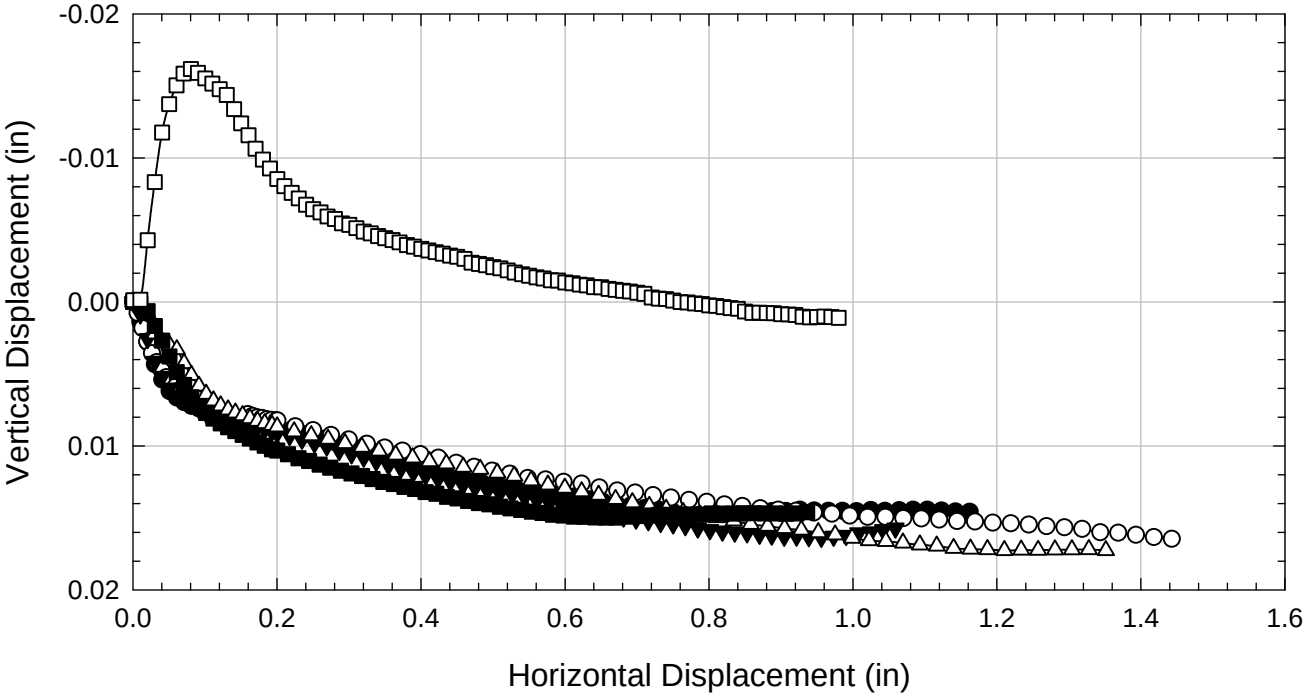

D.7. Oahe Dam

D.7.1 Blenderized

Virginia Polytechnic Institute and State University
Geotechnical Engineering Laboratory
Ring Shear Data Sheet

Project:	Fully Softened Shear Strength
Sample I.D./Loc.:	Oahe - Blenderized
Classification:	Fat Clay (CH)

Sample Preparation	Remolded at LL

Specific Gravity	2.88	
Shear Device Used	WF Bromhead Ring Shear	

Test Number	1	2	3	4	5	6	7	8
Start Date (m/d/y)	4/17/2011	5/8/2011	3/29/2011	4/9/2011	4/8/2011	8/8/2011		
End Date (m/d/y)	4/20/2011	5/10/2011	4/6/2011	4/17/2011	4/14/2011	8/13/2011		
Consolidation Pressure (psf)	254	451	848	1641	3225	6292		
Initial Values								
Initial Height (in)	0.20	0.20	0.20	0.20	0.20	0.20		
Inner Radius (in)	1.38	1.38	1.38	1.38	1.38	1.38		
Outer Radius (in)	1.97	1.97	1.97	1.97	1.97	1.97		
Initial Sample Weight (g)	29.50	29.96	29.07	29.61	29.17	28.74		
Water Content (%)	136.80	126.01	136.71	136.12	134.54	124.81		
Dry Unit Weight Before Shear (pcf)	40.1	48.1	51.1	58.8	76.3	86.6		
Saturation (%)	100.0	100.0	100.0	100.0	100.0	100.0		
Consolidation Pressures								
Load 1 (psf)	155	155	155	155	154	154		
Load 2 (psf)	254	254	254	254	253	253		
Load 3 (psf)		451	451	451	451	451		
Load 4 (psf)			848	848	847	847		
Load 5 (psf)				1641	1638	1638		
Load 6 (psf)					3225	3225		
Load 7 (psf)						6292		
t_{50}								
Max. t_{50} for Load 1 (min)								
Max. t_{50} for Load 2 (min)	39.26							
Max. t_{50} for Load 3 (min)		50.00						
Max. t_{50} for Load 4 (min)			113.86					
Max. t_{50} for Load 5 (min)				53.73				
Max. t_{50} for Load 6 (min)					28.29			
Max. t_{50} for Load 7 (min)						10.07		
Final Values								
Water Content (%)	120.24		93.45	77.39	82.63	88.07		
Saturation (%)	100.0		100.0	100.0	100.0	100.0		
Failure								
Test Performed at Shear Rate (in/min)	7.00E-04	7.00E-04	7.00E-04	7.00E-04	7.00E-04	7.00E-04		
Required Shear Rate (in/min)	1.58E-04	4.00E-05	1.41E-05	2.23E-05	4.95E-05	1.79E-04		
Displacement at Failure (in)	0.31	0.10	0.08	0.06	0.07	0.09		
Peak Shear Stress (psf)	56	92	210	454	785	1562		
Secant Effective Friction Angle (deg)	12.4	11.5	13.9	15.5	13.7	13.9		

Comments:

Oahe - Blenderized - 254 psf

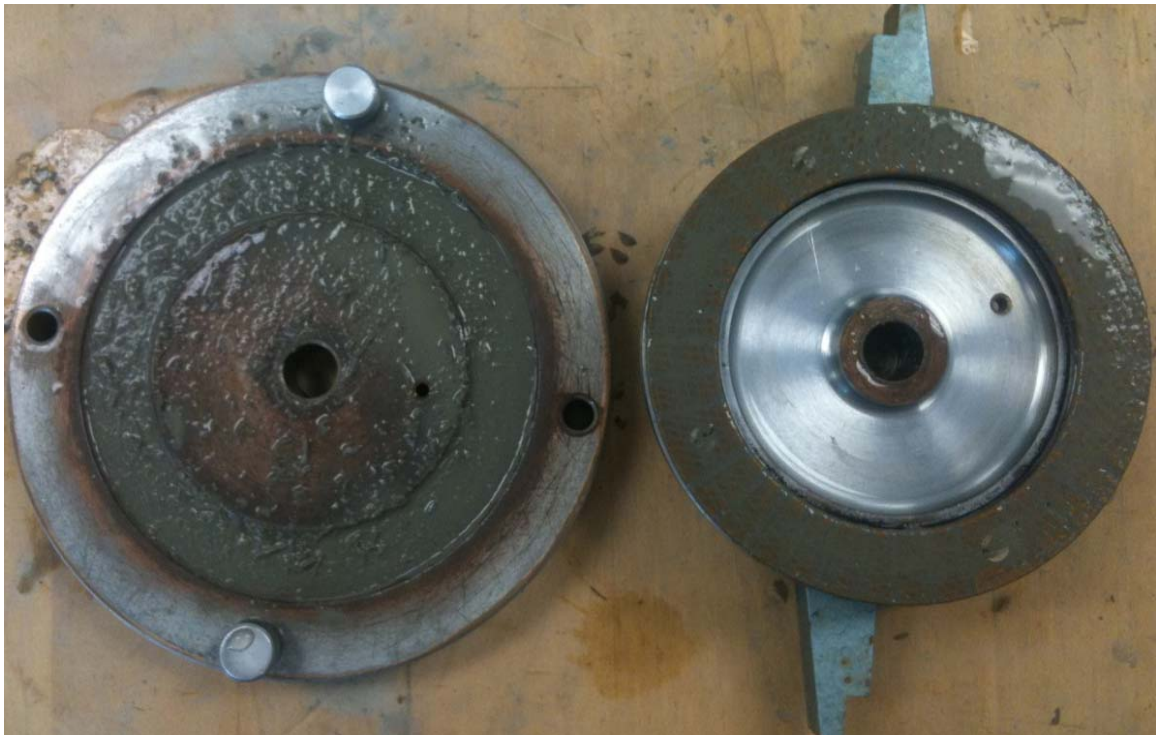

Oahe - Blenderized - 451 psf

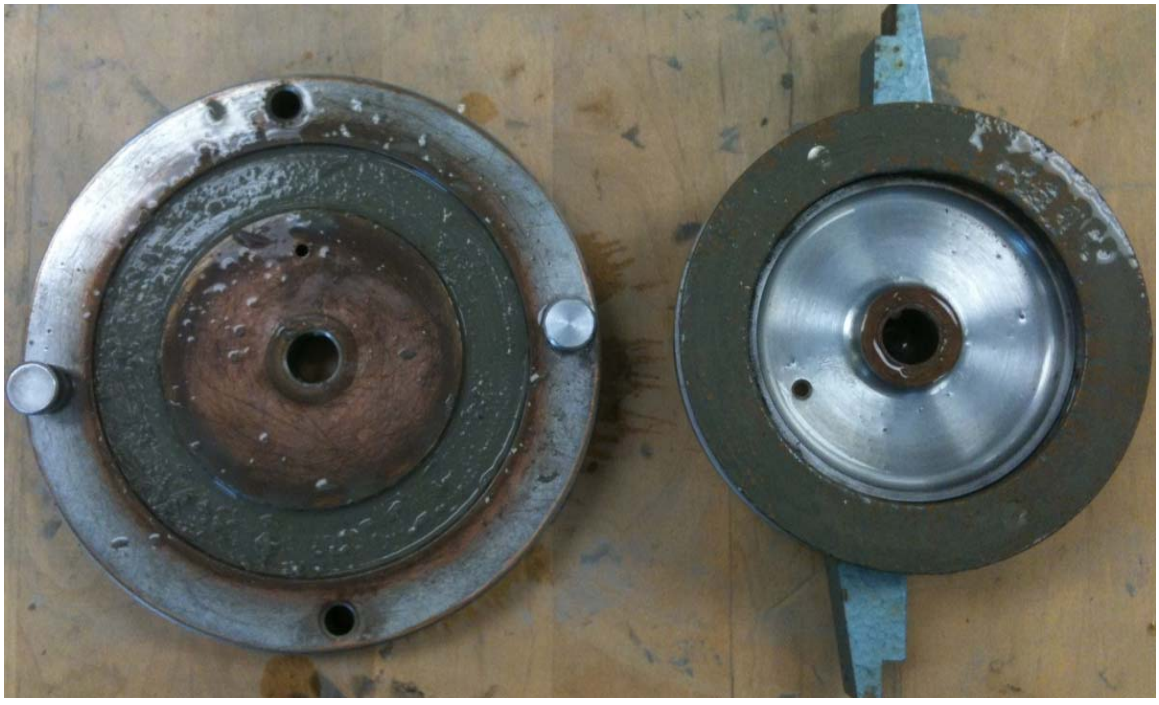

Oahe - Blenderized - 848 psf

Oahe - Blenderized - 1641 psf

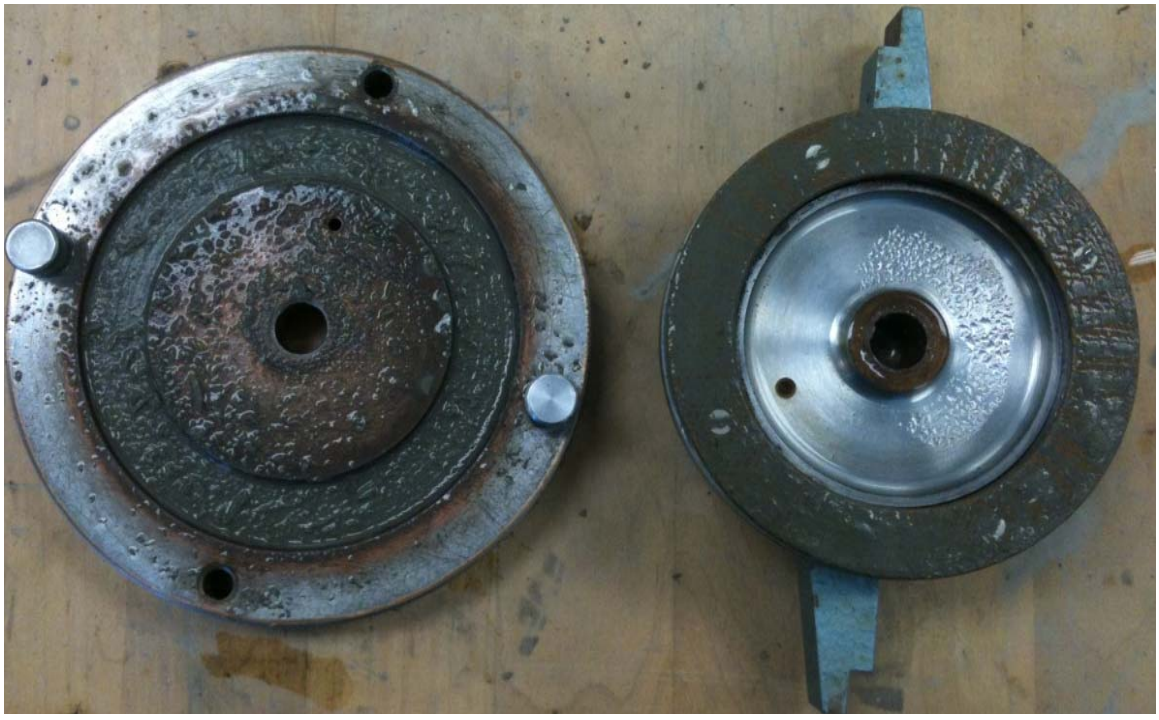

Oahe - Blenderized - 3225 psf

Oahe - Blenderized - 6292 psf

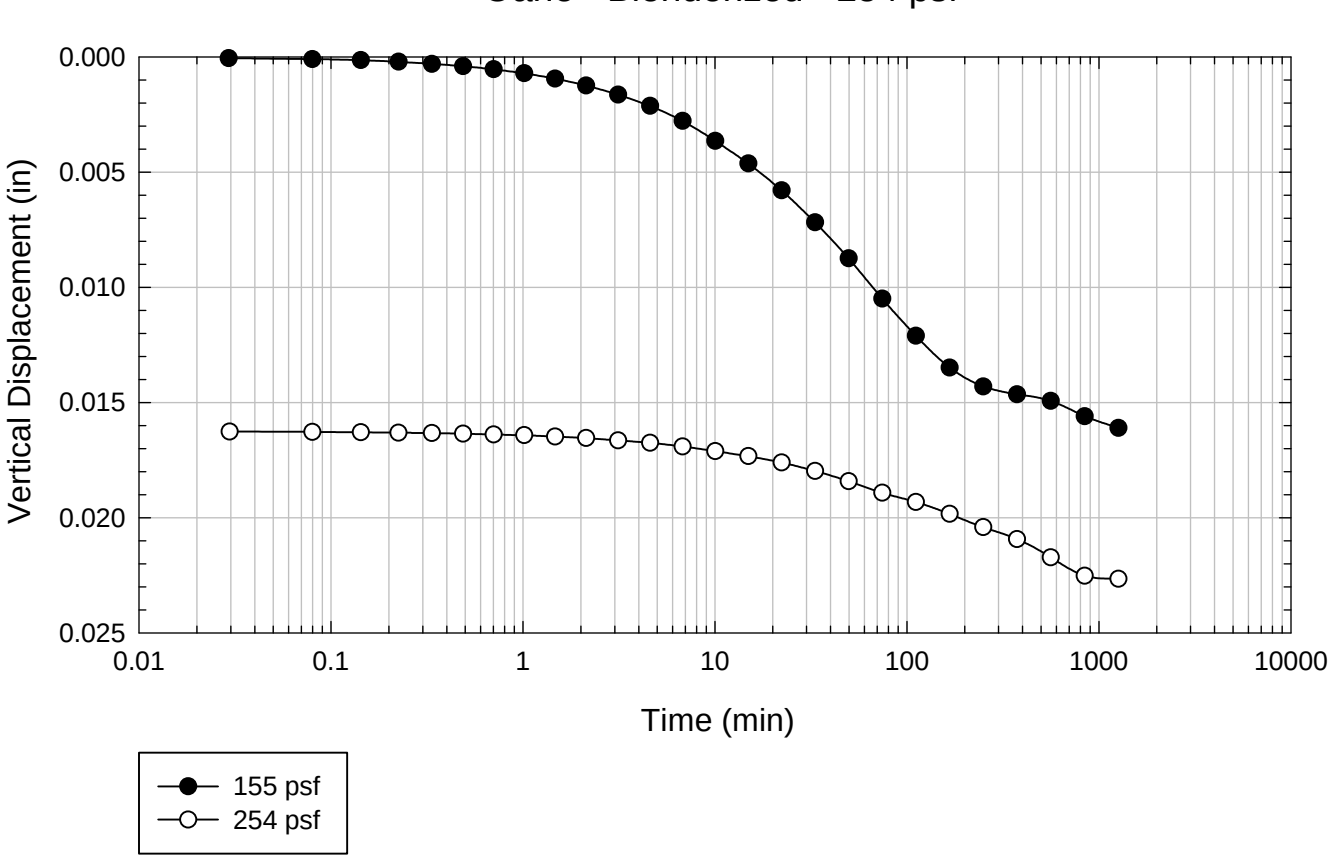
Oahe - Blenderized - 254 psf
Vertical Displacement (in)
0.000
0.005
0.010
0.015
0.020
0.025
0.01
0.1
1
10
100
1000
10000
Time (min)
155 psf
254 psf

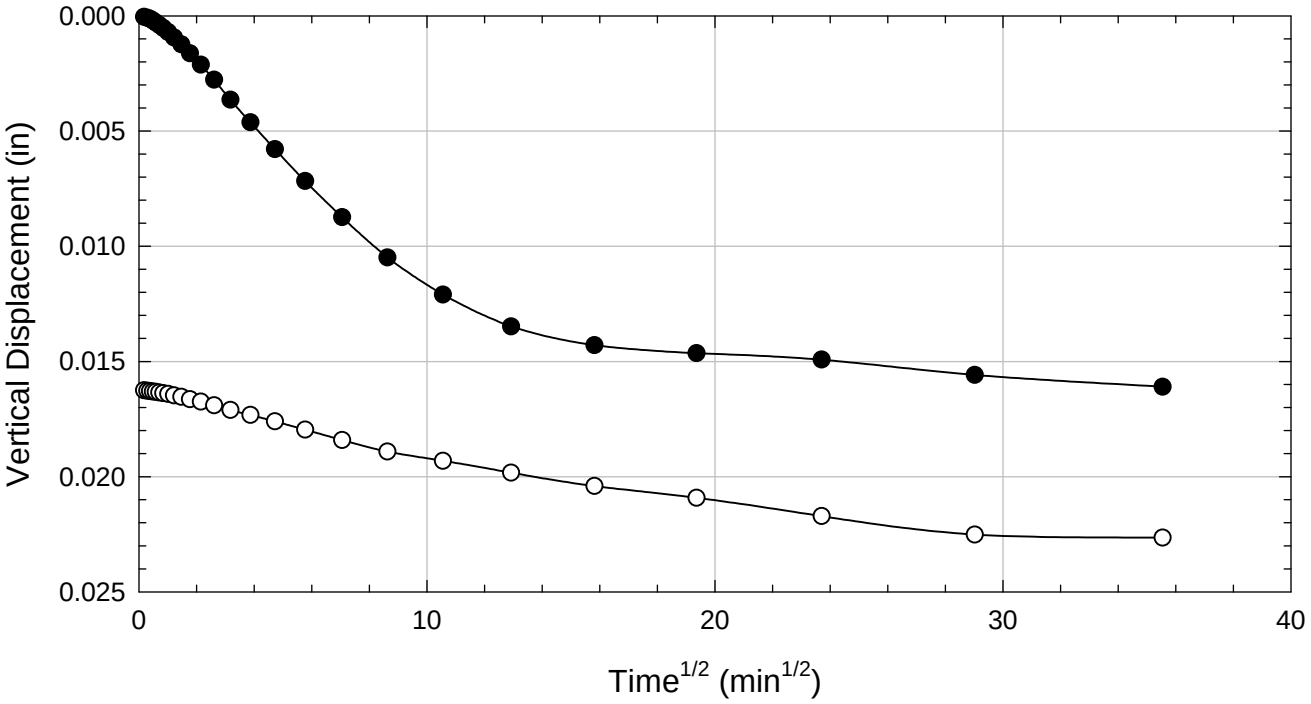
Vertical Displacement (in)
0.000
0.005
0.010
0.015
0.020
0.025
0
10
20
30
40
Time^1/2 (min^1/2)

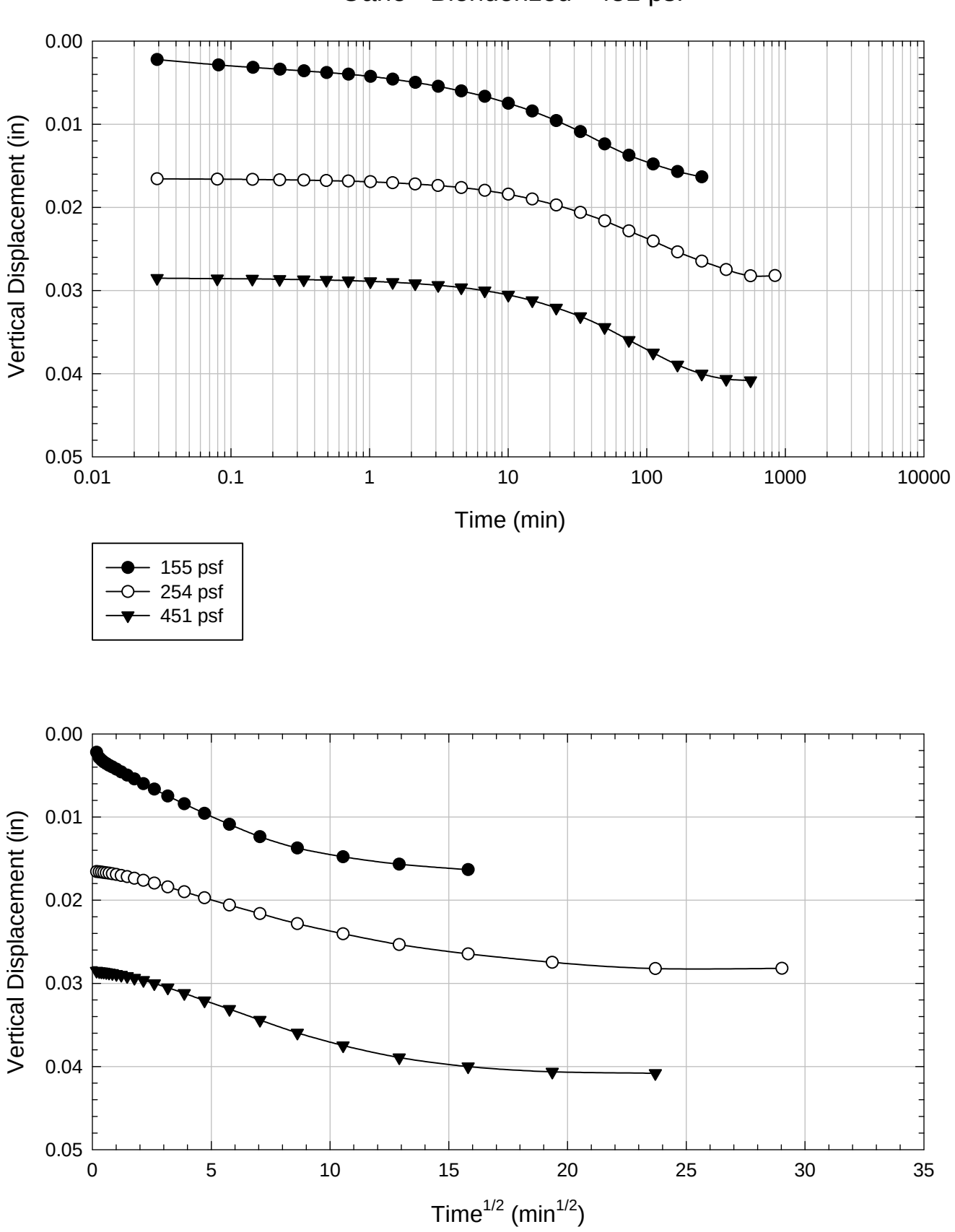
Oahe - Blenderized - 451 psf
Vertical Displacement (in)
0.00
0.01
0.02
0.03
0.04
0.05
0.01
0.1
1
10
100
1000
10000
Time (min)
155 psf
254 psf
451 psf
Vertical Displacement (in)
0.00
0.01
0.02
0.03
0.04
0.05
0
5
10
15
20
25
30
35
Time1/2 (min1/2)

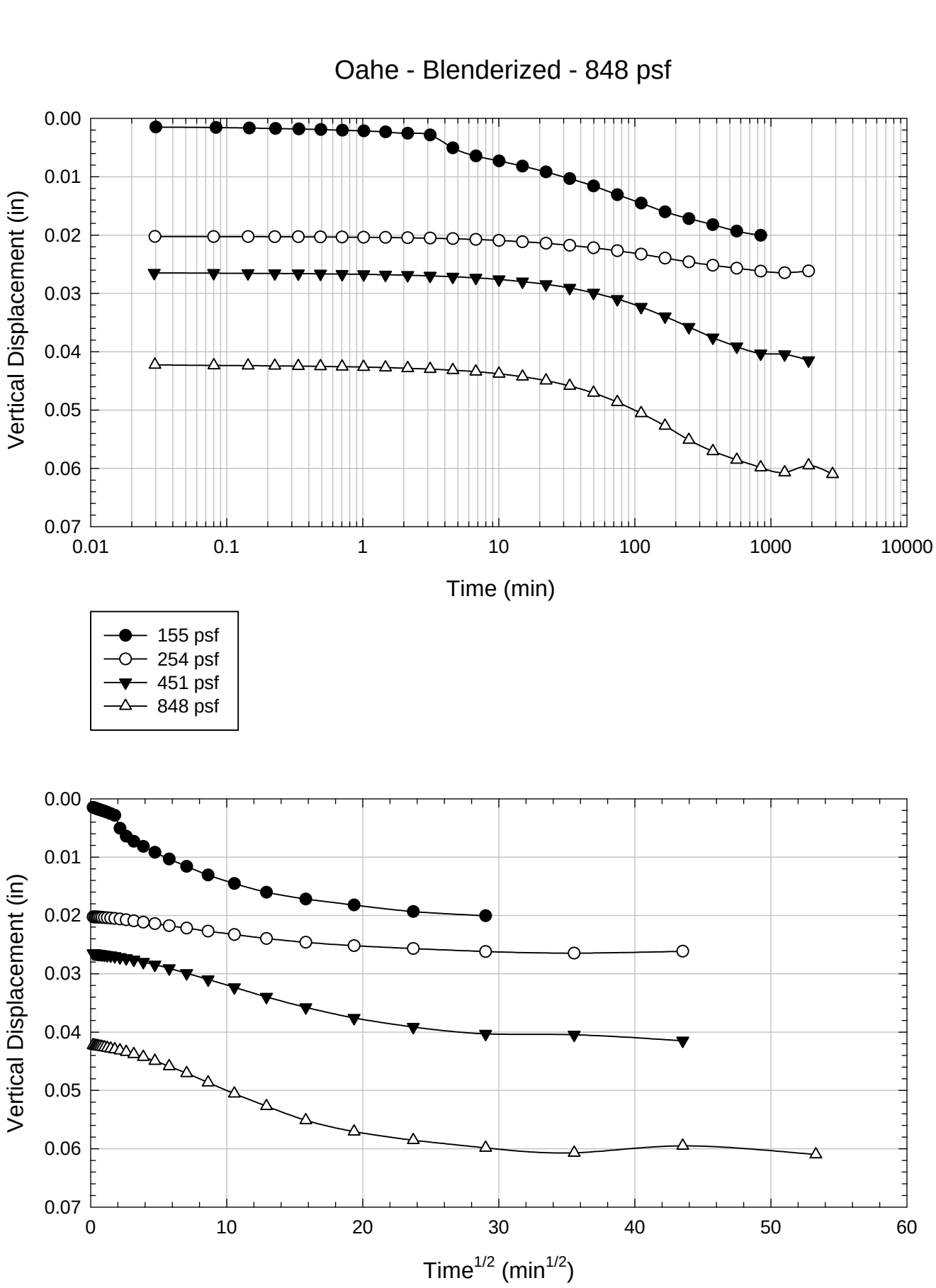
Oahe - Blenderized - 848 psf
Vertical Displacement (in)
0.00
0.01
0.02
0.03
0.04
0.05
0.06
0.07
0.01
0.1
1
10
100
1000
10000
Time (min)
155 psf
254 psf
451 psf
848 psf
Vertical Displacement (in)
0.00
0.01
0.02
0.03
0.04
0.05
0.06
0.07
0
10
20
30
40
50
60
Time1/2 (min1/2)

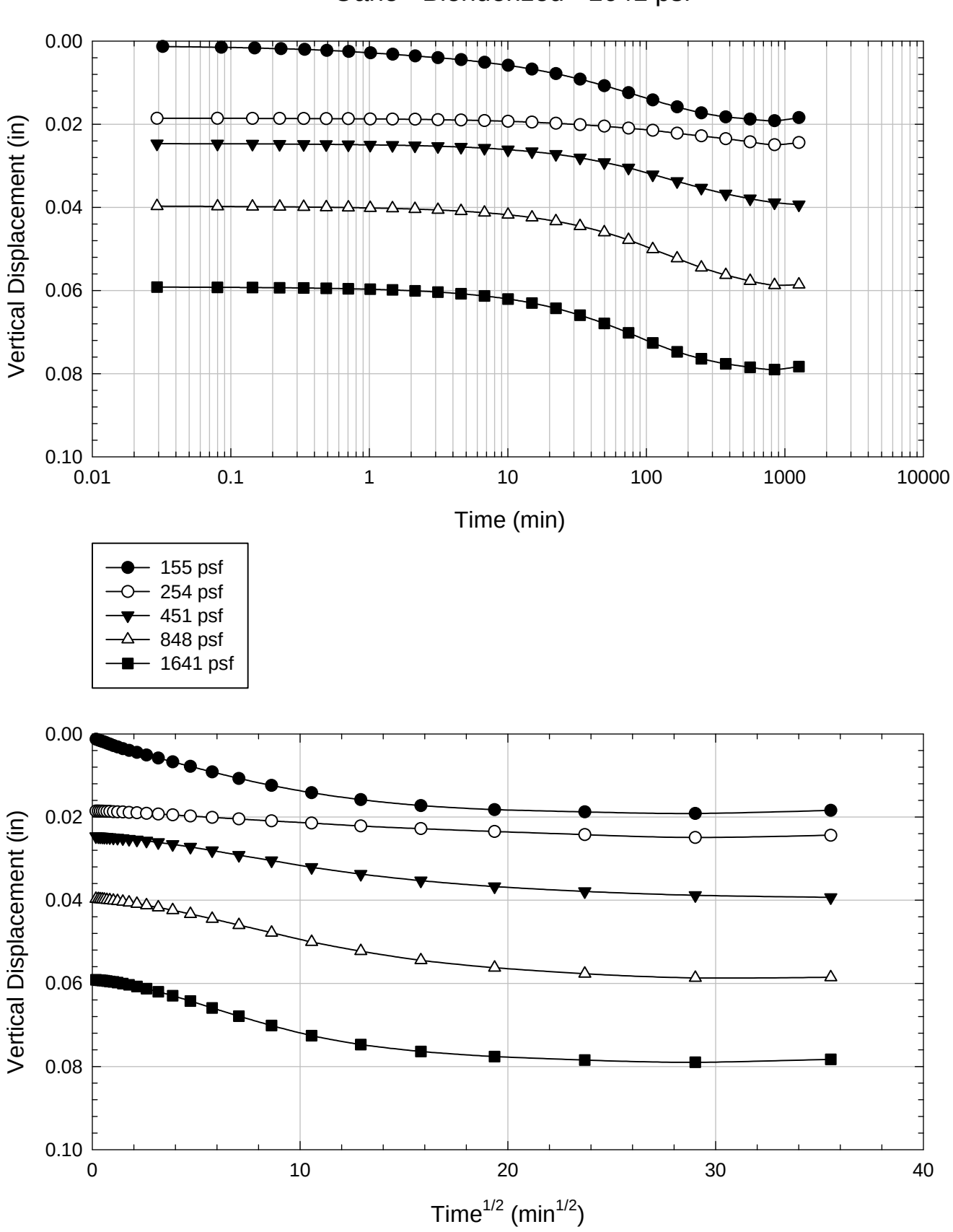
Oahe - Blenderized - 1641 psf
Vertical Displacement (in)
0.00
0.02
0.04
0.06
0.08
0.10
0.01
0.1
1
10
100
1000
10000
Time (min)
155 psf
254 psf
451 psf
848 psf
1641 psf
Vertical Displacement (in)
0.00
0.02
0.04
0.06
0.08
0.10
0
10
20
30
40
Time1/2 (min1/2)

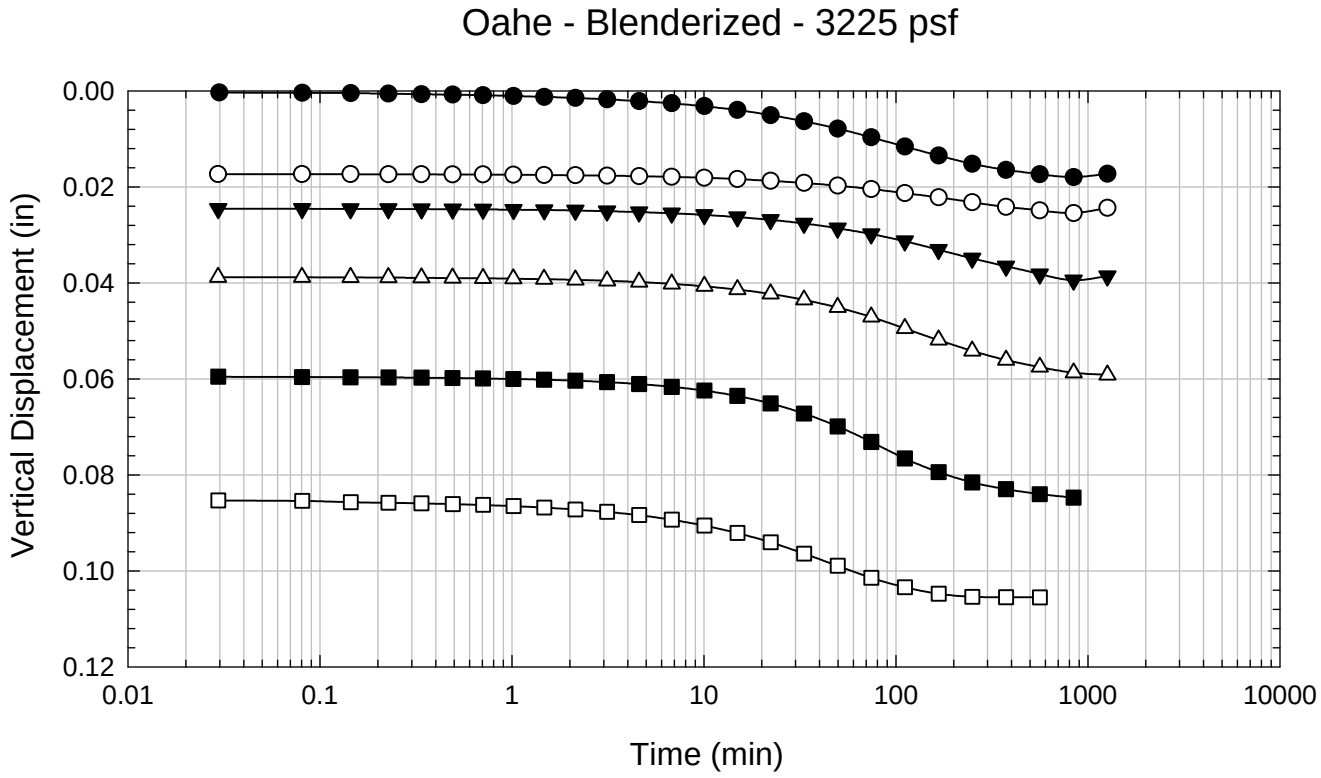
Oahe - Blenderized - 3225 psf
Vertical Displacement (in)
0.00
0.02
0.04
0.06
0.08
0.10
0.12
0.01
0.1
1
10
100
1000
10000
Time (min)

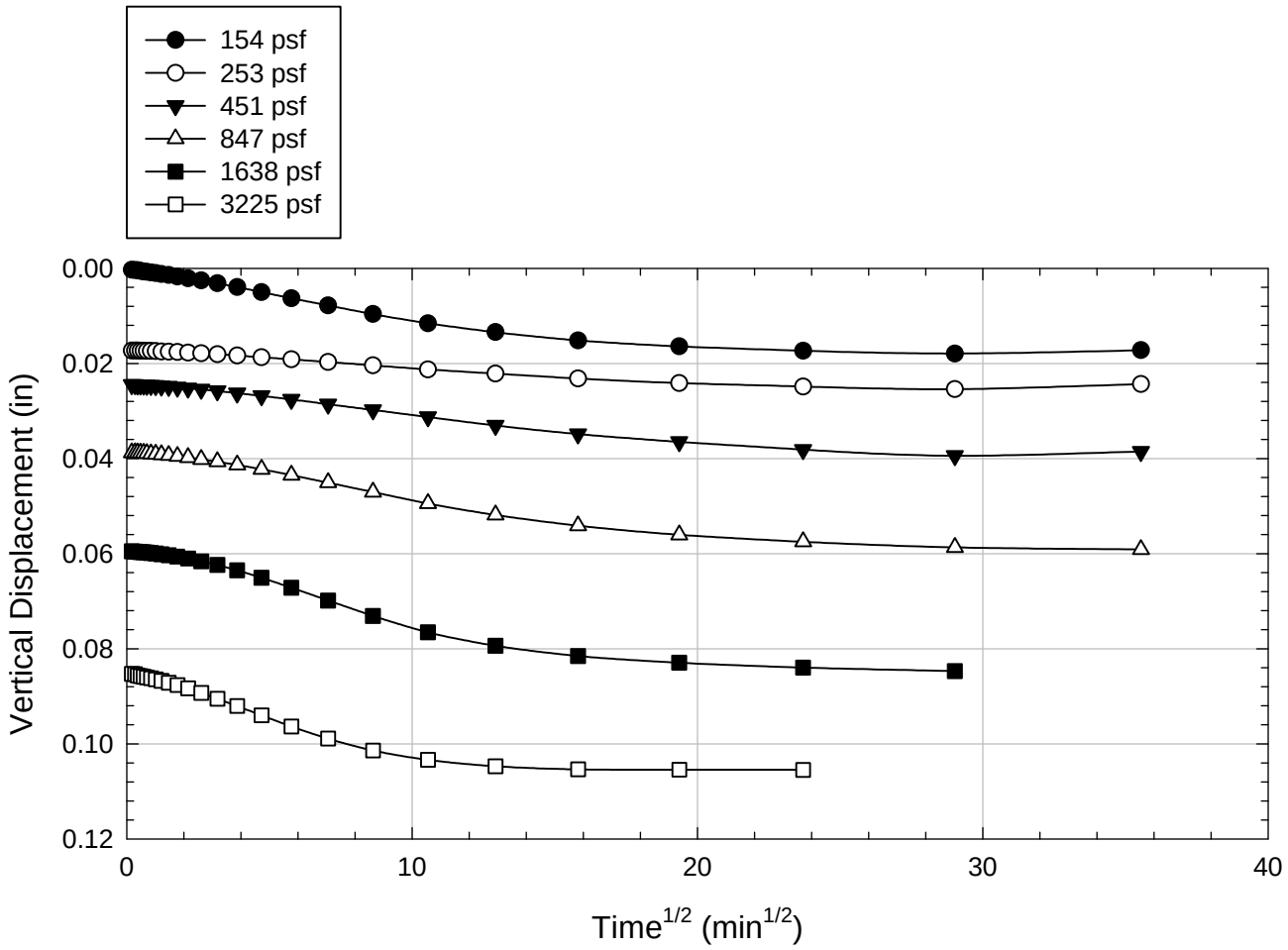
154 psf
253 psf
451 psf
847 psf
1638 psf
3225 psf
Vertical Displacement (in)
0.00
0.02
0.04
0.06
0.08
0.10
0.12
0
10
20
30
40
Time1/2 (min1/2)

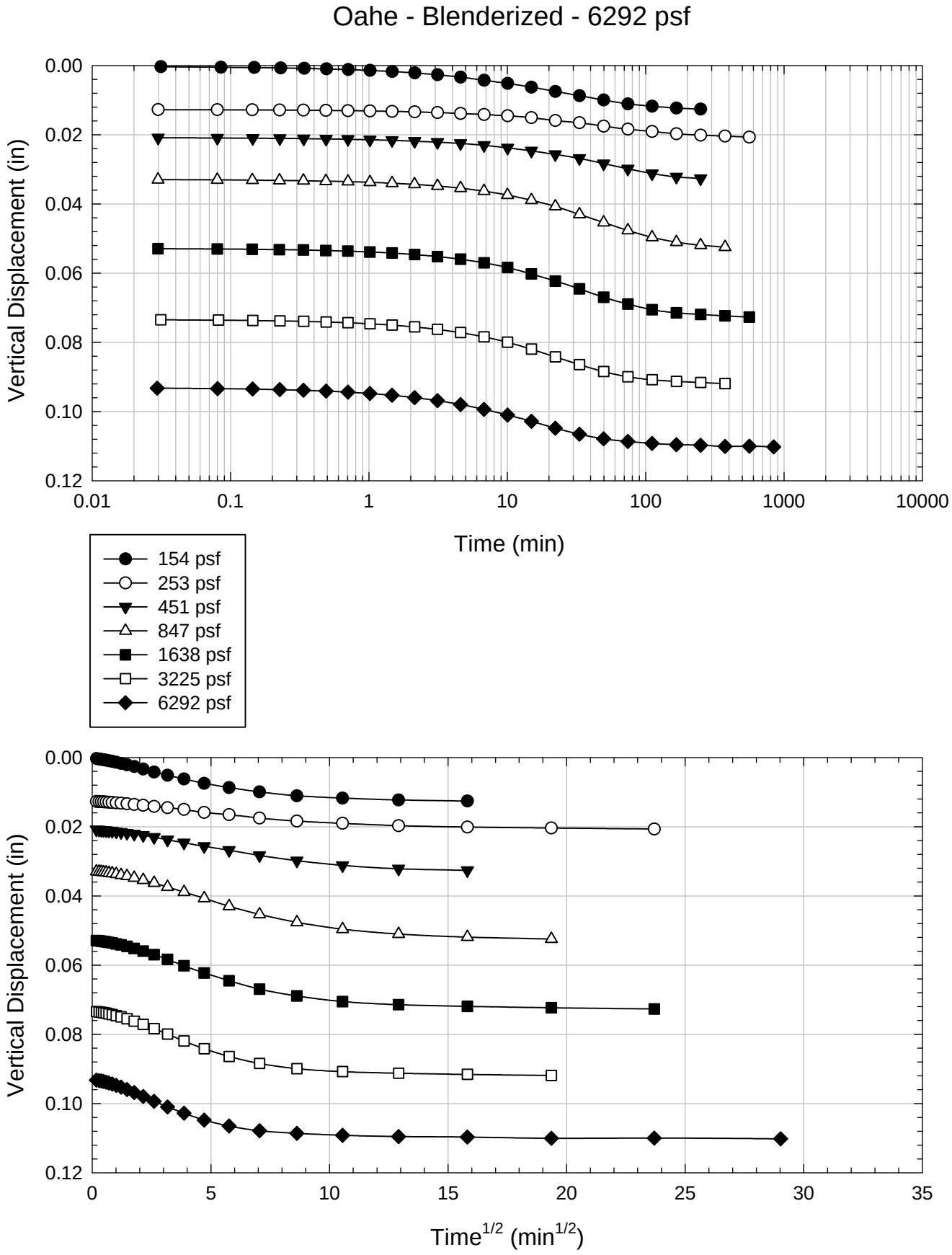
Oahe - Blenderized - 6292 psf
Vertical Displacement (in)
0.00
0.02
0.04
0.06
0.08
0.10
0.12
0.01
0.1
1
10
100
1000
10000
Time (min)
154 psf
253 psf
451 psf
847 psf
1638 psf
3225 psf
6292 psf
Vertical Displacement (in)
0
5
10
15
20
25
30
35
Time^1/2 (min^1/2)

Oahe - Blenderized

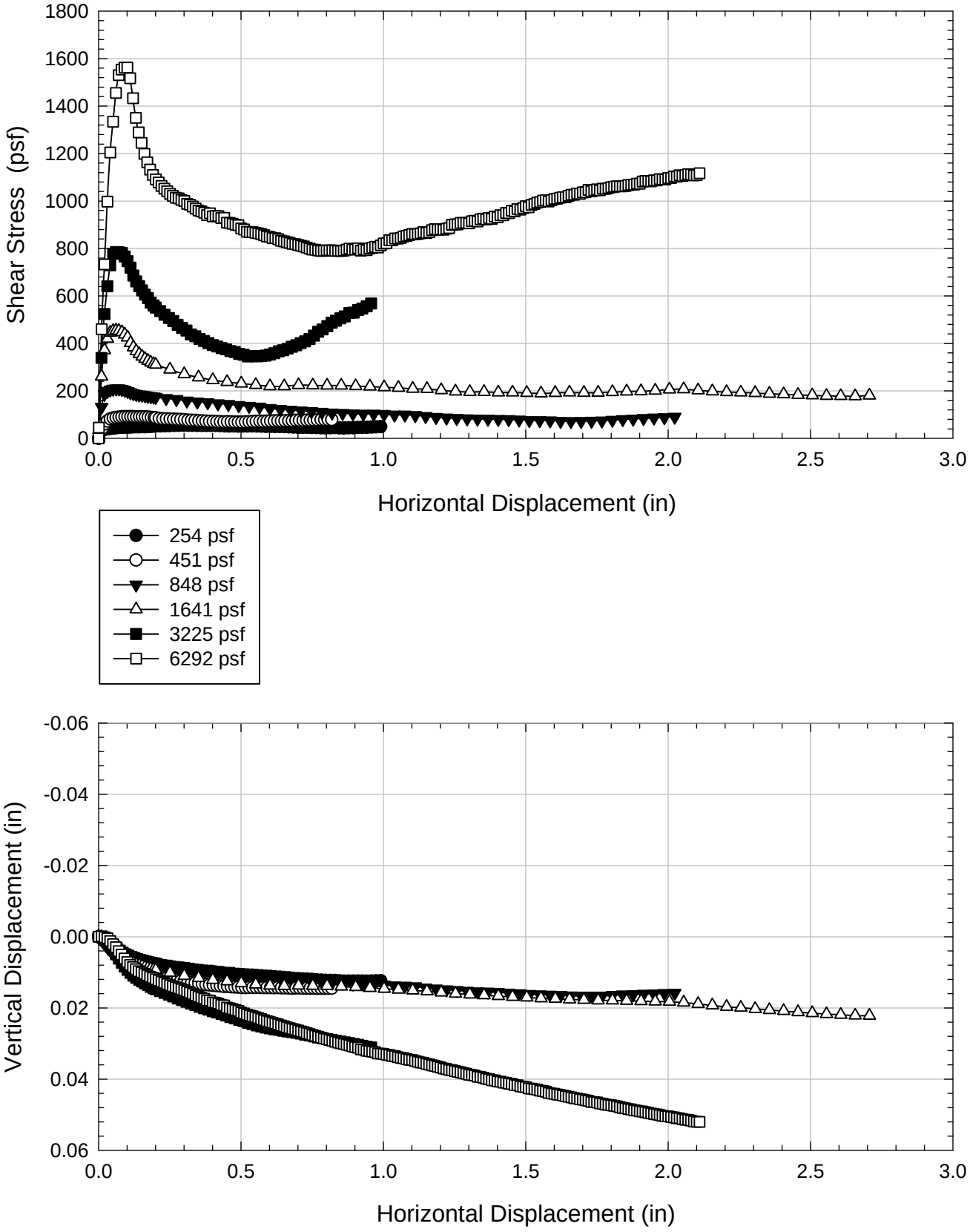

D.8. Texas 1

D.8.1 Blenderized

Virginia Polytechnic Institute and State University
Geotechnical Engineering Laboratory
Ring Shear Data Sheet

Project:	Fully Softened Shear Strength
Sample I.D./Loc.:	Texas 1 - Blenderized
Classification:	Fat Clay (CH)

Sample Preparation	Remolded at LL

Specific Gravity	2.78	
Shear Device Used	WF Bromhead Ring Shear	

Test Number	1	2	3	4	5	6	7	
Start Date (m/d/y)	5/12/2011	5/12/2011	5/16/2011	5/25/2011	5/19/2011			
End Date (m/d/y)	5/16/2011	5/16/2011	5/19/2011	5/31/2011	5/22/2011			
Consolidation Pressure (psf)	254	451	848	1641	3213			
Initial Values								
Initial Height (in)	0.20	0.20	0.20	0.20	0.20			
Inner Radius (in)	1.38	1.38	1.38	1.38	1.38			
Outer Radius (in)	1.97	1.97	1.97	1.97	1.97			
Initial Sample Weight (g)	33.00	33.48	33.51	29.51	33.59			
Water Content (%)	77.81	76.68	77.55	79.71	78.64			
Dry Unit Weight Before Shear (pcf)	54.8	55.4	55.0	53.9	54.4			
Saturation (%)	100.0	100.0	100.0	100.0	100.0			
Consolidation Pressures								
Load 1 (psf)	155	155	155	155	155			
Load 2 (psf)	254	254	254	254	254			
Load 3 (psf)		451	451	451	451			
Load 4 (psf)			848	848	848			
Load 5 (psf)				1641	1641			
Load 6 (psf)					3213			
Load 7 (psf)								
t_{50}								
Max. t_{50} for Load 1 (min)								
Max. t_{50} for Load 2 (min)	15.12							
Max. t_{50} for Load 3 (min)		16.95						
Max. t_{50} for Load 4 (min)			16.68					
Max. t_{50} for Load 5 (min)				14.30				
Max. t_{50} for Load 6 (min)					7.19			
Max. t_{50} for Load 7 (min)								
Final Values								
Water Content (%)	69.08	60.40	55.56	49.73	44.23			
Saturation (%)	100.0	100.0	100.0	100.0	100.0			
Failure								
Test Performed at Shear Rate (in/min)	7.00E-04	7.00E-04	7.00E-04	7.00E-04	7.00E-04			
Required Shear Rate (in/min)	1.06E-04	9.44E-05	1.08E-04	9.79E-05	2.23E-04			
Displacement at Failure (in)	0.08	0.08	0.09	0.07	0.08			
Peak Shear Stress (psf)	38	158	294	580	1062			
Secant Effective Friction Angle (deg)	8.6	19.3	19.1	19.5	18.3			

Comments:

Texas 1 - Blenderized - 254 psf

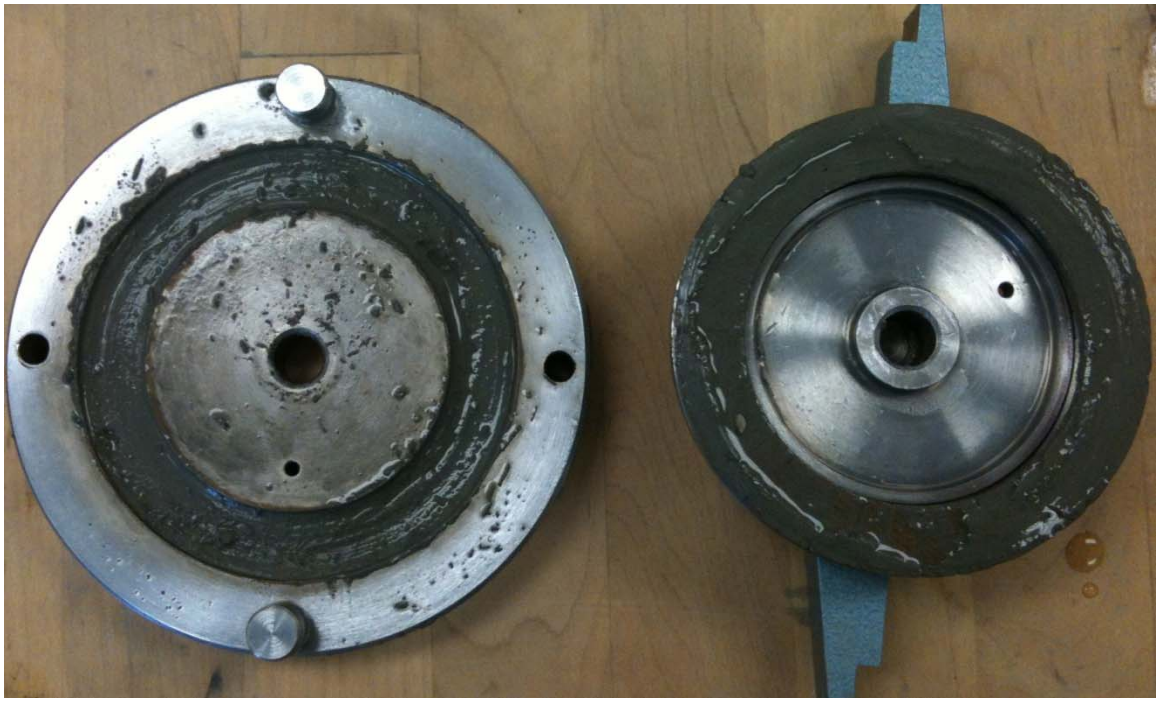

Texas 1 - Blenderized - 451 psf

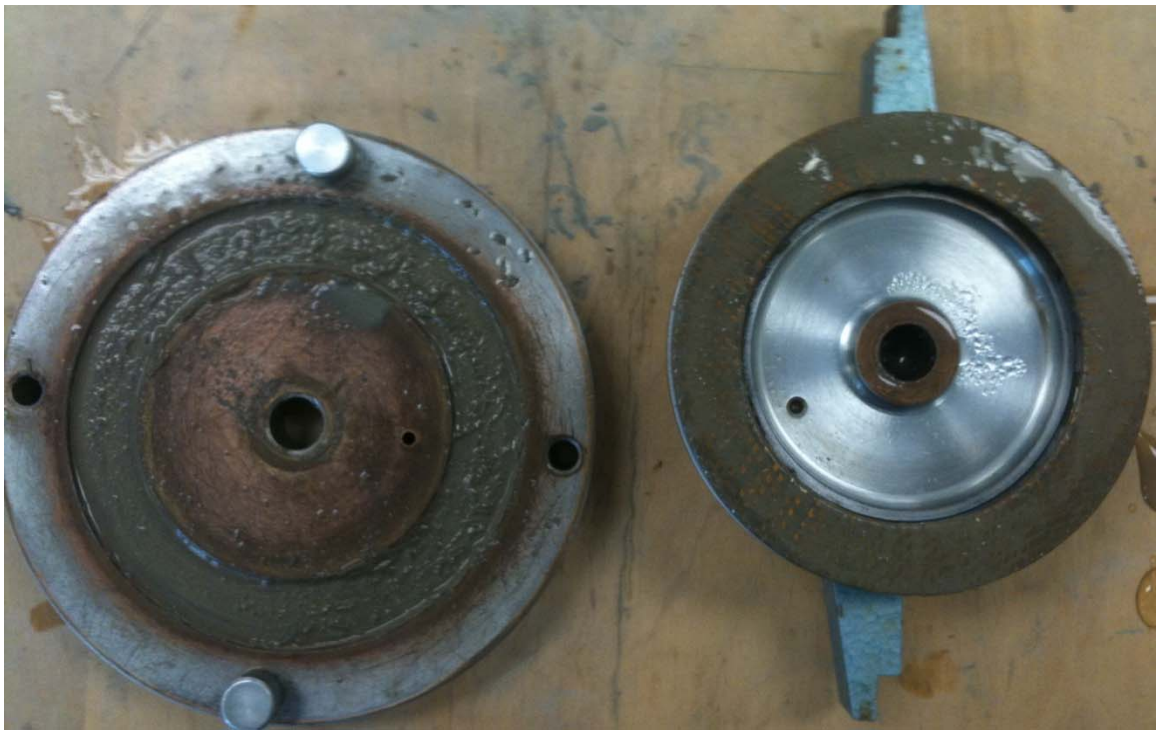

Texas 1 - Blenderized - 848 psf

Texas 1 - Blenderized - 1641 psf

Texas 1 - Blenderized - 3213 psf

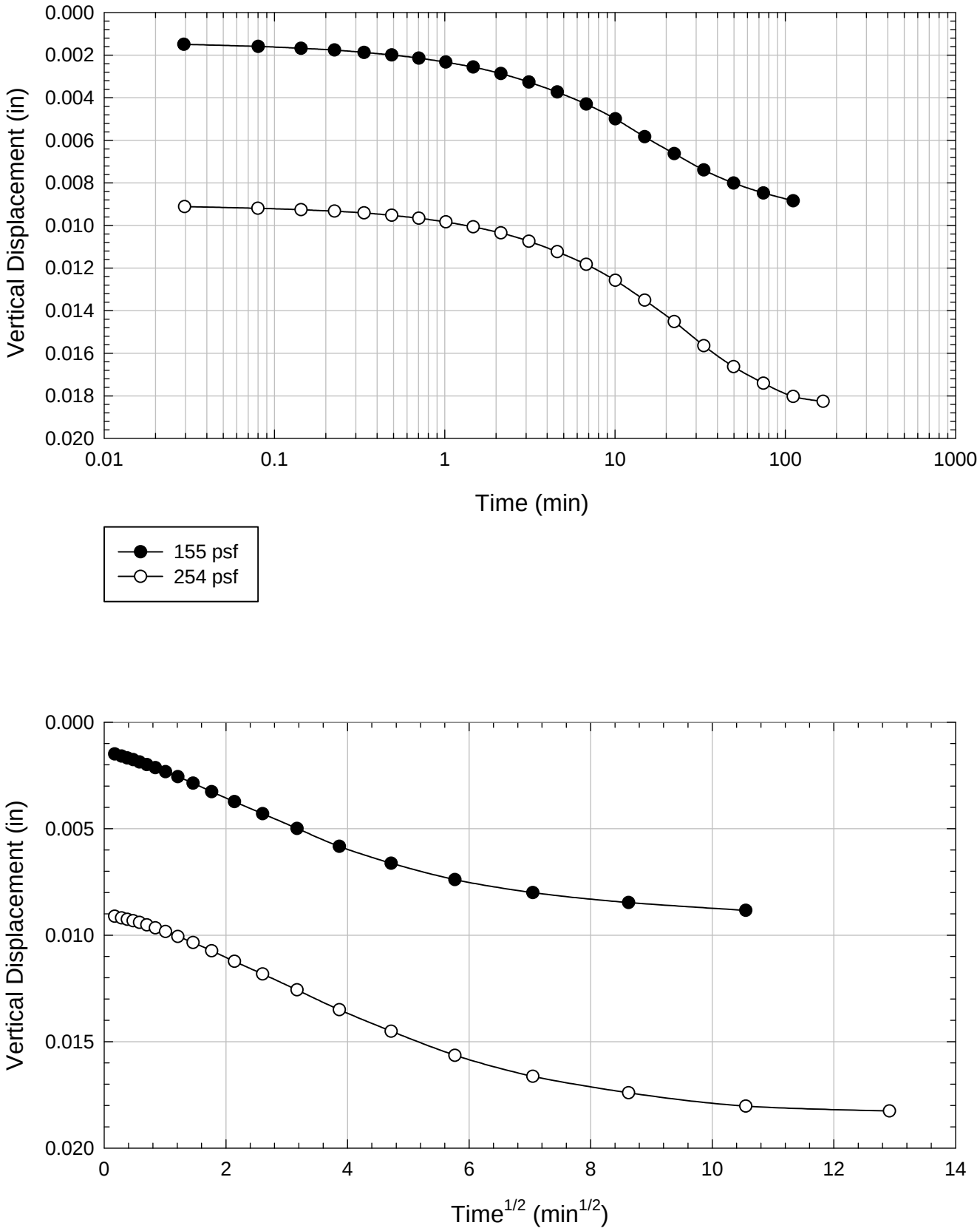
Texas 1 - Blenderized - 254 psf
Vertical Displacement (in)
0.000
0.002
0.004
0.006
0.008
0.010
0.012
0.014
0.016
0.018
0.020
0.01
0.1
1
10
100
1000
Time (min)
155 psf
254 psf
Vertical Displacement (in)
0.000
0.005
0.010
0.015
0.020
0
2
4
6
8
10
12
14
Time^1/2 (min^1/2)

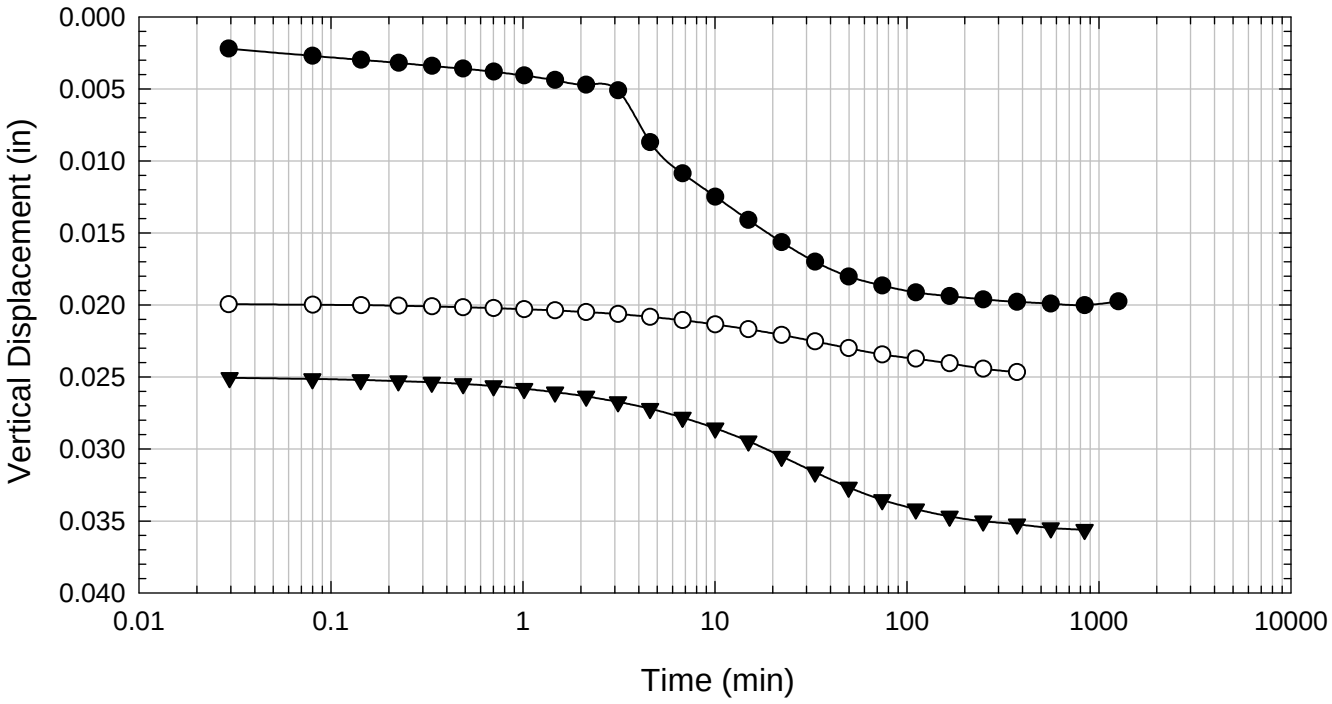
Texas 1 - Blenderized - 451 psf
Vertical Displacement (in)
0.000
0.005
0.010
0.015
0.020
0.025
0.030
0.035
0.040
0.01
0.1
1
10
100
1000
10000
Time (min)

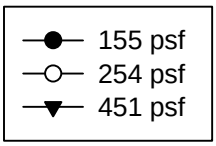
155 psf
254 psf
451 psf

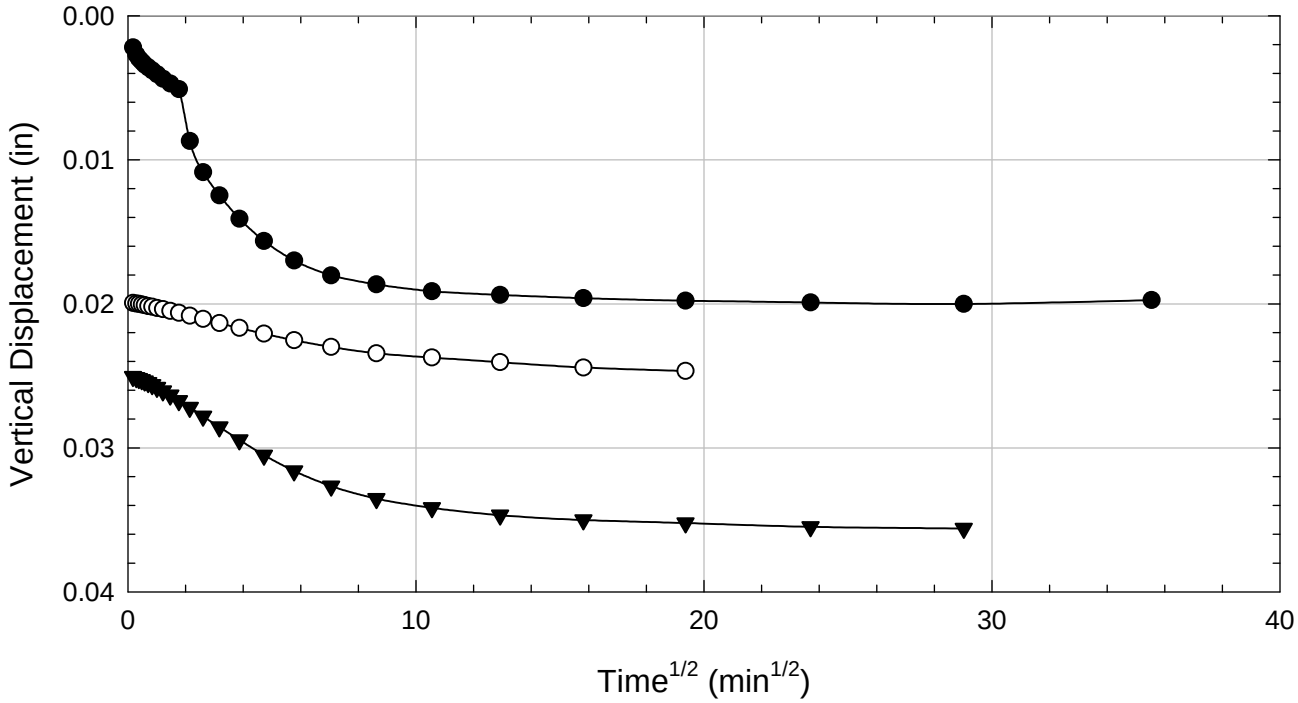
Vertical Displacement (in)
0.00
0.01
0.02
0.03
0.04
0
10
20
30
40
Time1/2 (min1/2)

Texas 1 - Blenderized - 848 psf

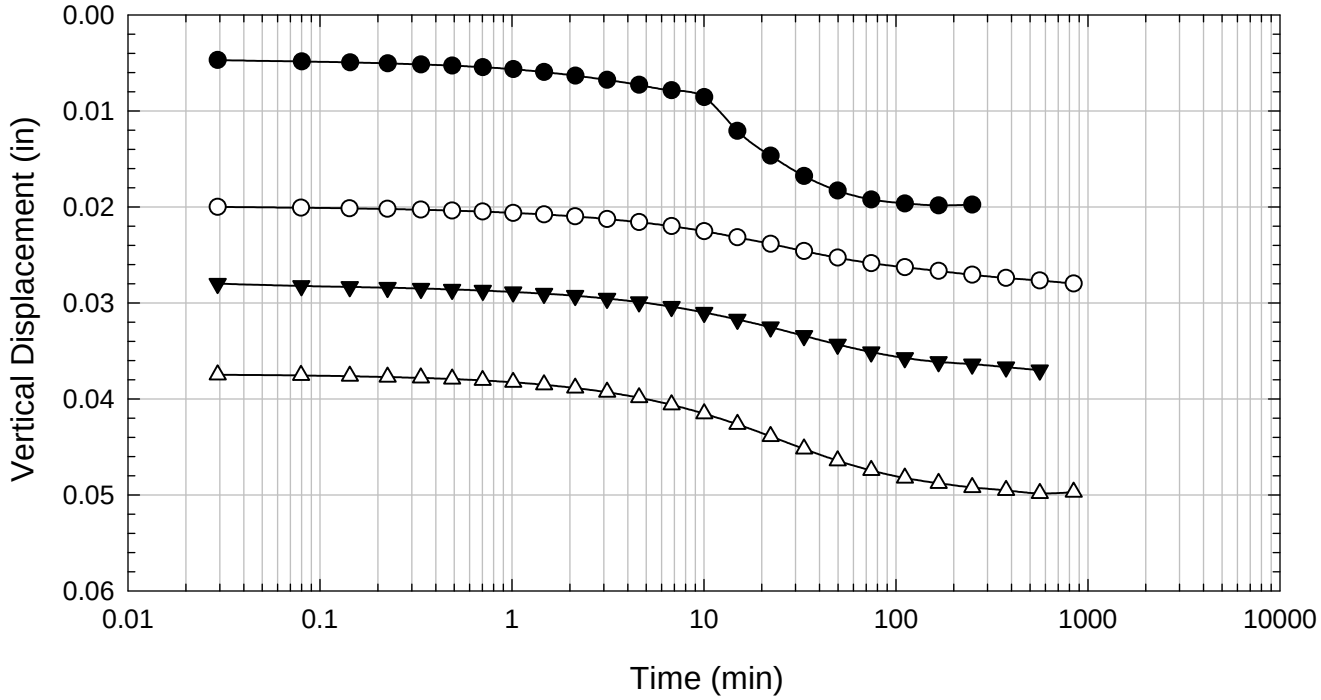

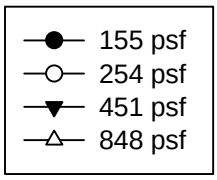

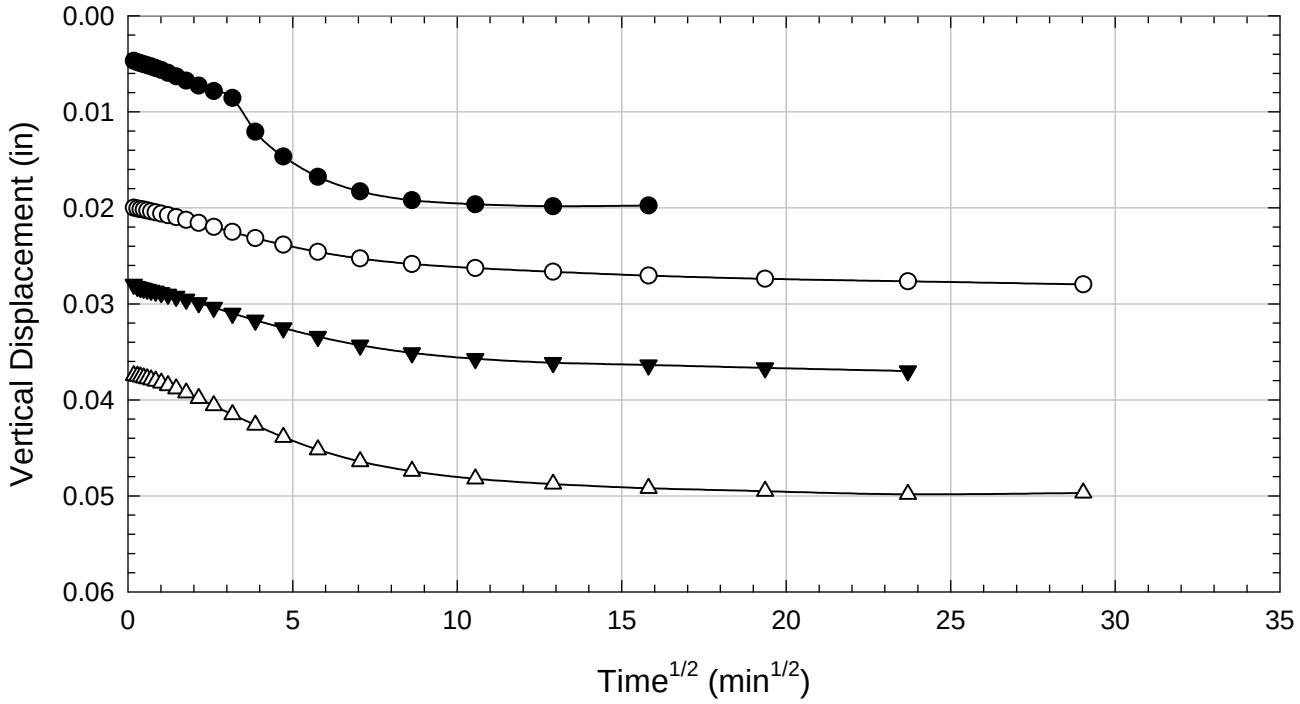

Texas 1 - Blenderized - 1641 psf

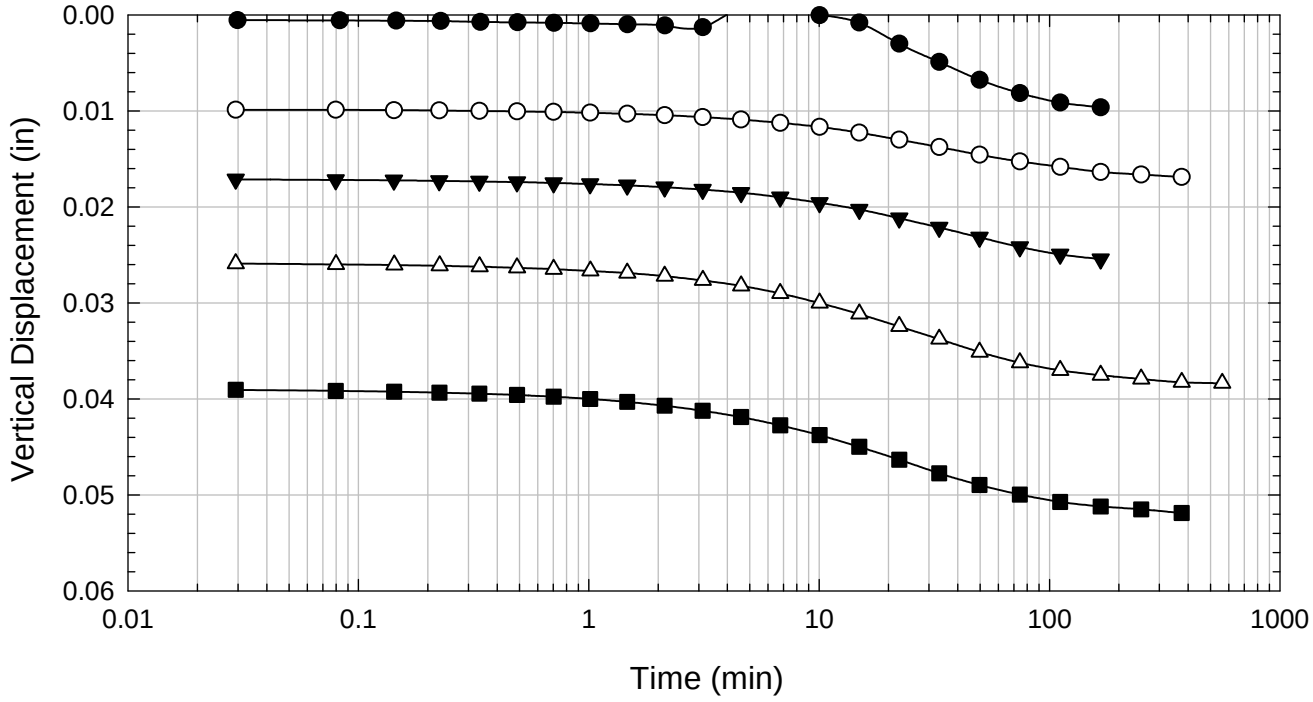

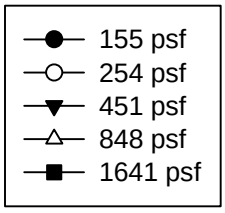

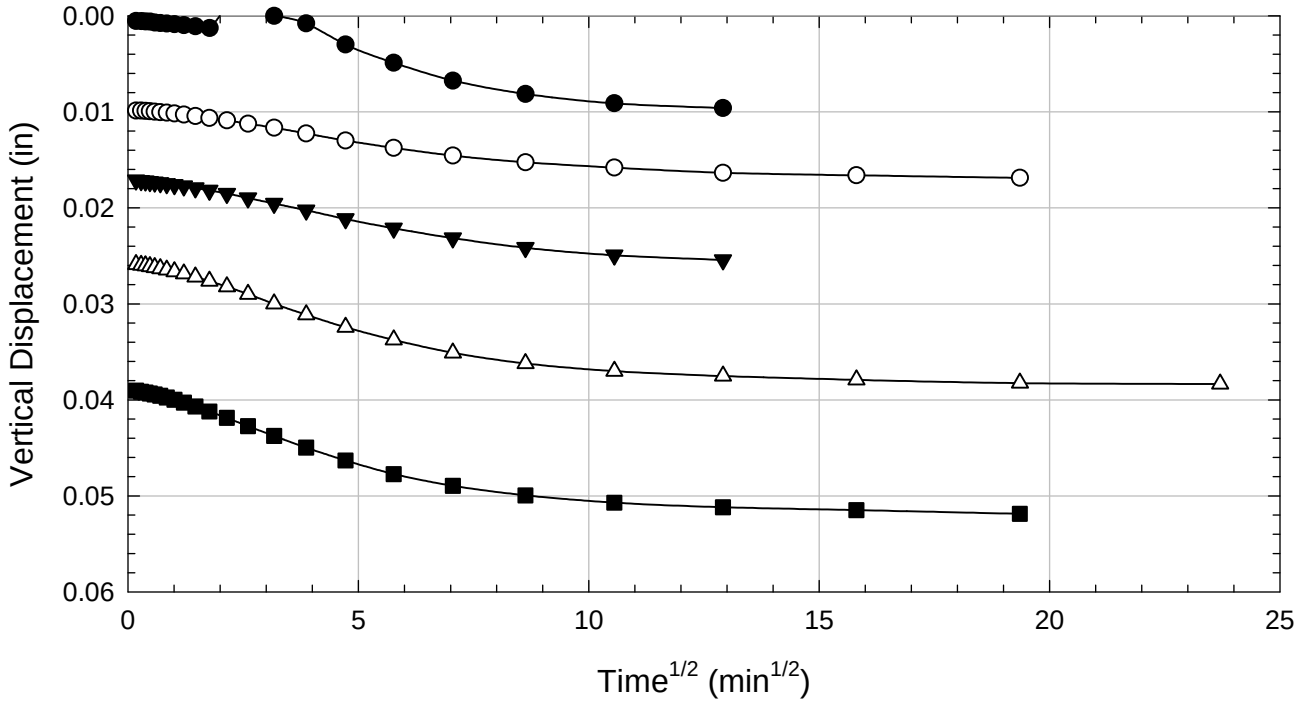

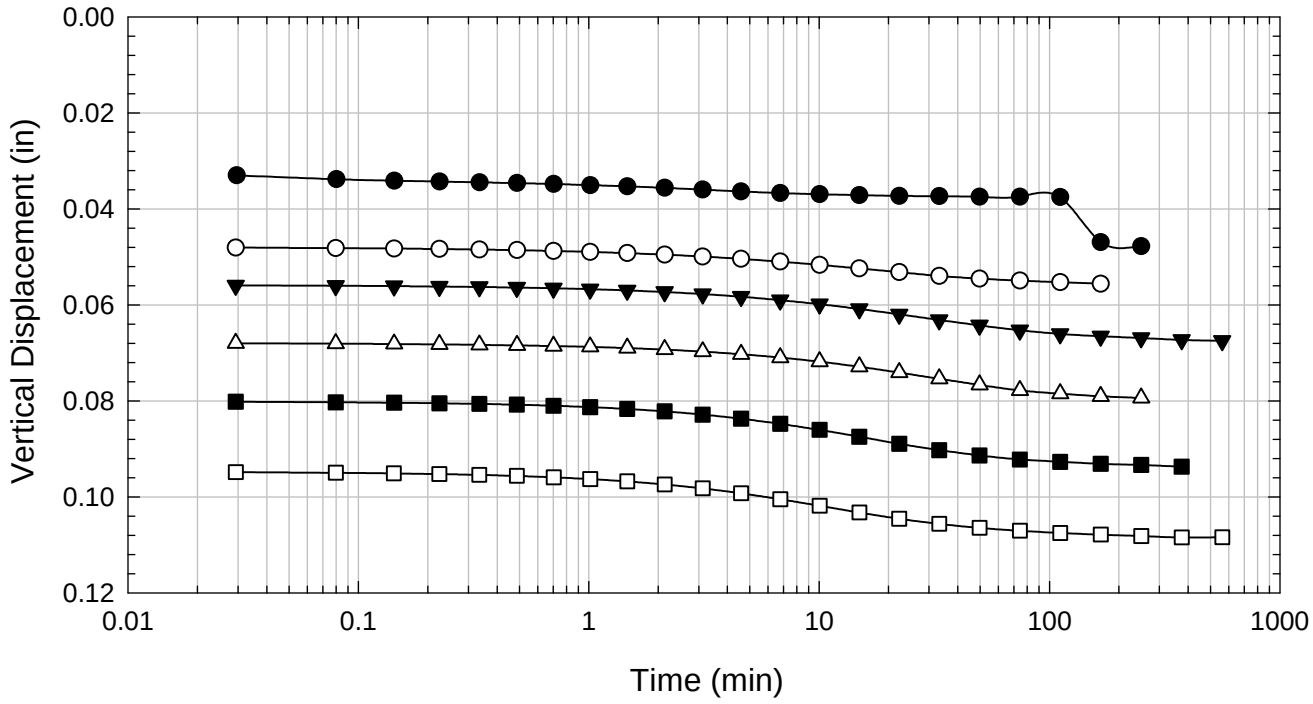
Texas 1 - Blenderized - 3213 psf
Vertical Displacement (in)
0.00
0.02
0.04
0.06
0.08
0.10
0.12
0.01
0.1
1
10
100
1000
Time (min)

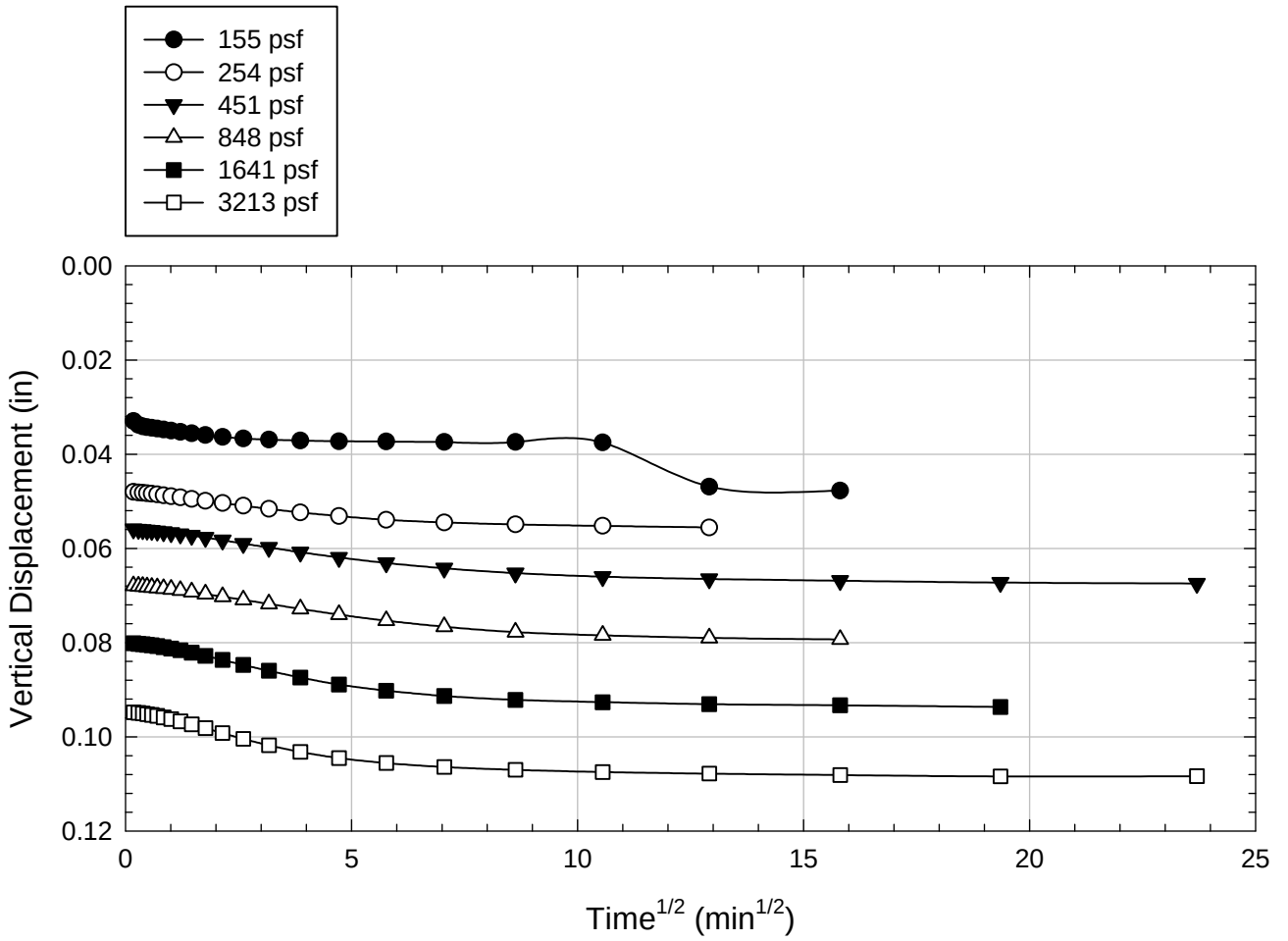
155 psf
254 psf
451 psf
848 psf
1641 psf
3213 psf
Vertical Displacement (in)
0.00
0.02
0.04
0.06
0.08
0.10
0.12
0
5
10
15
20
25
Time1/2 (min1/2)

Texas 1 - Blenderized

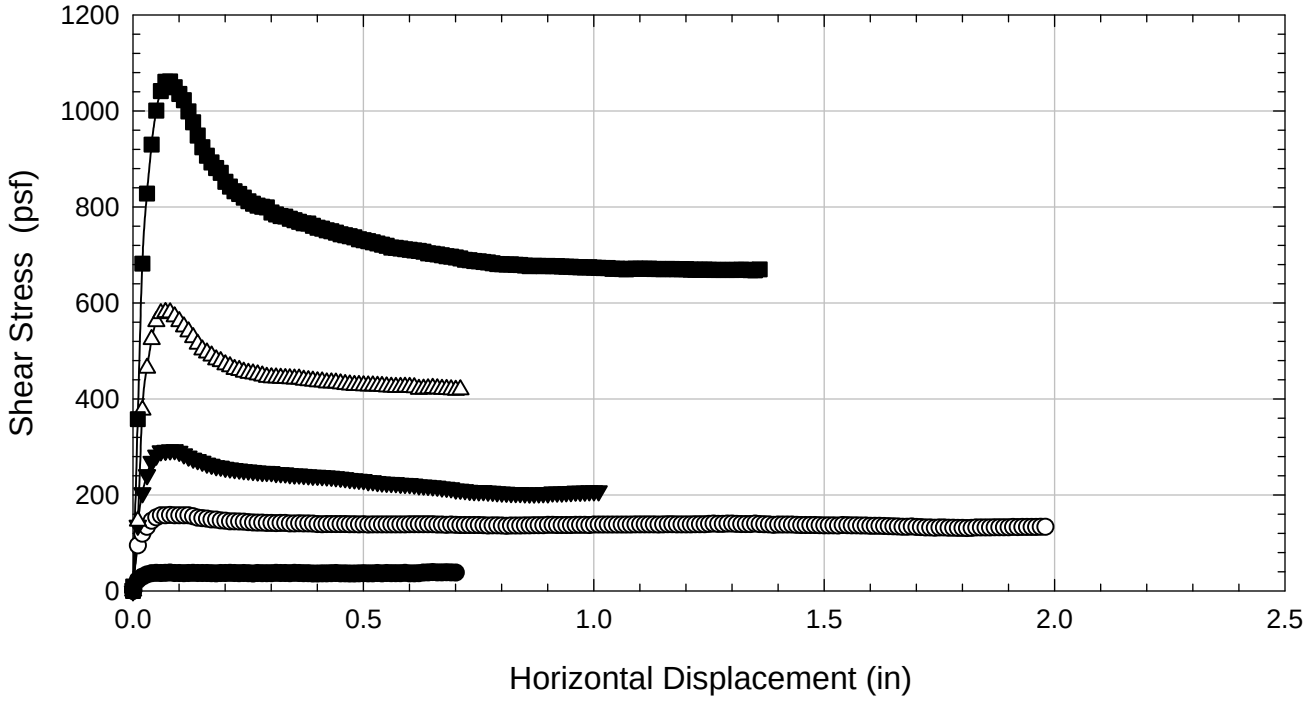

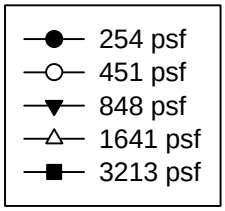

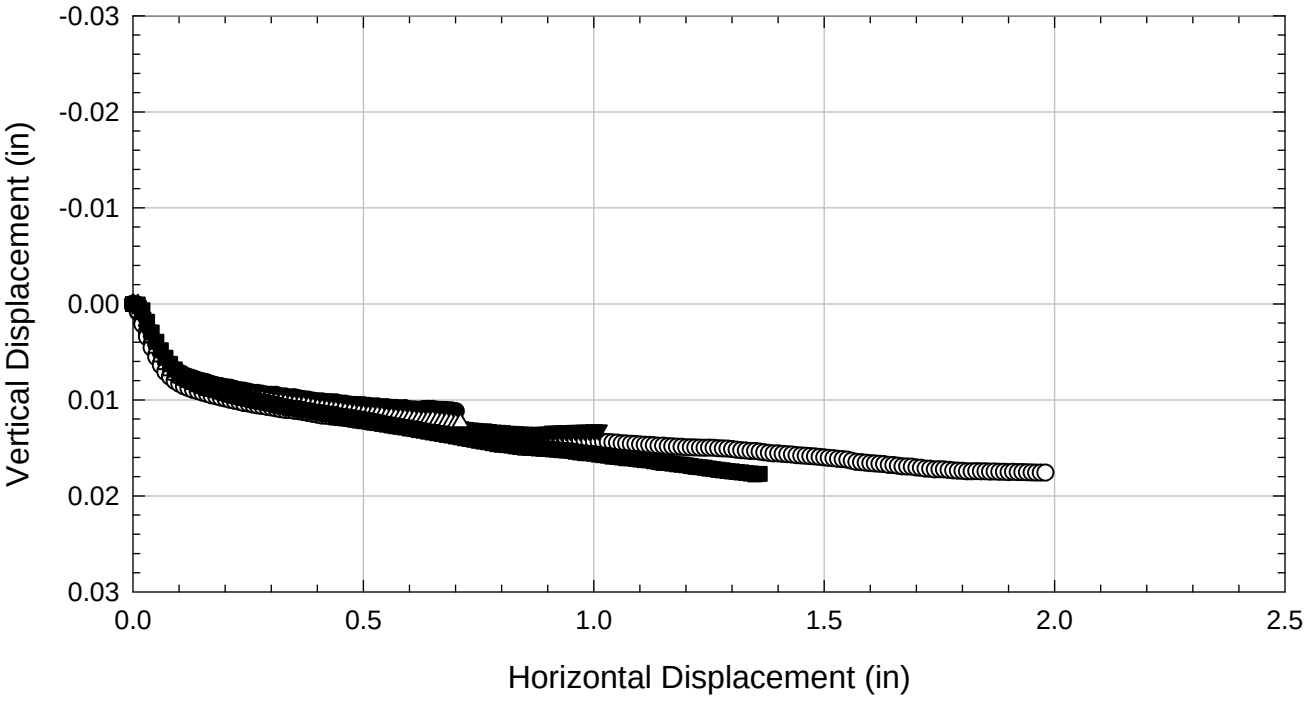

D.9. Texas 2

D.9.1 Blenderized

Virginia Polytechnic Institute and State University
Geotechnical Engineering Laboratory
Ring Shear Data Sheet

Project:	Fully Softened Shear Strength
Sample I.D./Loc.:	Texas 2 - Blenderized
Classification:	Fat Clay (CH)

Sample Preparation	Remolded at LL

Specific Gravity	2.78	
Shear Device Used	WF Bromhead Ring Shear	

Test Number	1	2	3	4	5	6	7	
Start Date (m/d/y)	5/10/2011	4/24/2011	5/2/2011	4/19/2011	4/27/2011	5/5/2011		
End Date (m/d/y)	5/12/2011	4/27/2011	5/5/2011	4/24/2011	5/2/2011	5/10/2011		
Consolidation Pressure (psf)	253	451	847	1638	1638	3225		
Initial Values								
Initial Height (in)	0.20	0.20	0.20	0.20	0.20	0.20		
Inner Radius (in)	1.38	1.38	1.38	1.38	1.38	1.38		
Outer Radius (in)	1.97	1.97	1.97	1.97	1.97	1.97		
Initial Sample Weight (g)	34.07	33.79	33.95	32.86	34.18	34.07		
Water Content (%)	66.62	67.70	68.81	70.70	69.34	67.66		
Dry Unit Weight Before Shear (pcf)	66.8	69.2	75.1	77.3	80.1	92.3		
Saturation (%)	100.0	100.0	100.0	100.0	100.0	100.0		
Consolidation Pressures								
Load 1 (psf)	154	154	154	154	154	154		
Load 2 (psf)	253	253	253	253	253	253		
Load 3 (psf)		451	451	451	451	451		
Load 4 (psf)			847	847	847	847		
Load 5 (psf)				1638	1638	1638		
Load 6 (psf)						3225		
Load 7 (psf)								
t_{50}								
Max. t_{50} for Load 1 (min)								
Max. t_{50} for Load 2 (min)	15.65							
Max. t_{50} for Load 3 (min)		20.26						
Max. t_{50} for Load 4 (min)			23.28					
Max. t_{50} for Load 5 (min)				19.88	21.97			
Max. t_{50} for Load 6 (min)						11.15		
Max. t_{50} for Load 7 (min)								
Final Values								
Water Content (%)	66.31	57.18	51.28	47.19	47.98	43.44		
Saturation (%)	100.0	100.0	100.0	100.0	100.0	100.00		
Failure								
Test Performed at Shear Rate (in/min)	7.00E-04	7.00E-04	7.00E-04	7.00E-04	7.00E-04	7.00E-04		
Required Shear Rate (in/min)	1.28E-04	1.78E-04	6.01E-05	1.51E-04	1.00E-04	2.33E-04		
Displacement at Failure (in)	0.10	0.18	0.07	0.15	0.11	0.13		
Peak Shear Stress (psf)	69	147	288	577	513	1067		
Secant Effective Friction Angle (deg)	15.2	18.0	18.8	19.4	17.4	18.3		

Comments: During second test consolidated to 1638 psf power was lost during the 154 psf consolidation stress. The test was restarted and continued.

Texas 2 - Blenderized - 253 psf

Texas 2 - Blenderized - 451 psf

Texas 2 - Blenderized - 847 psf

Texas 2 - Blenderized - 1638 psf

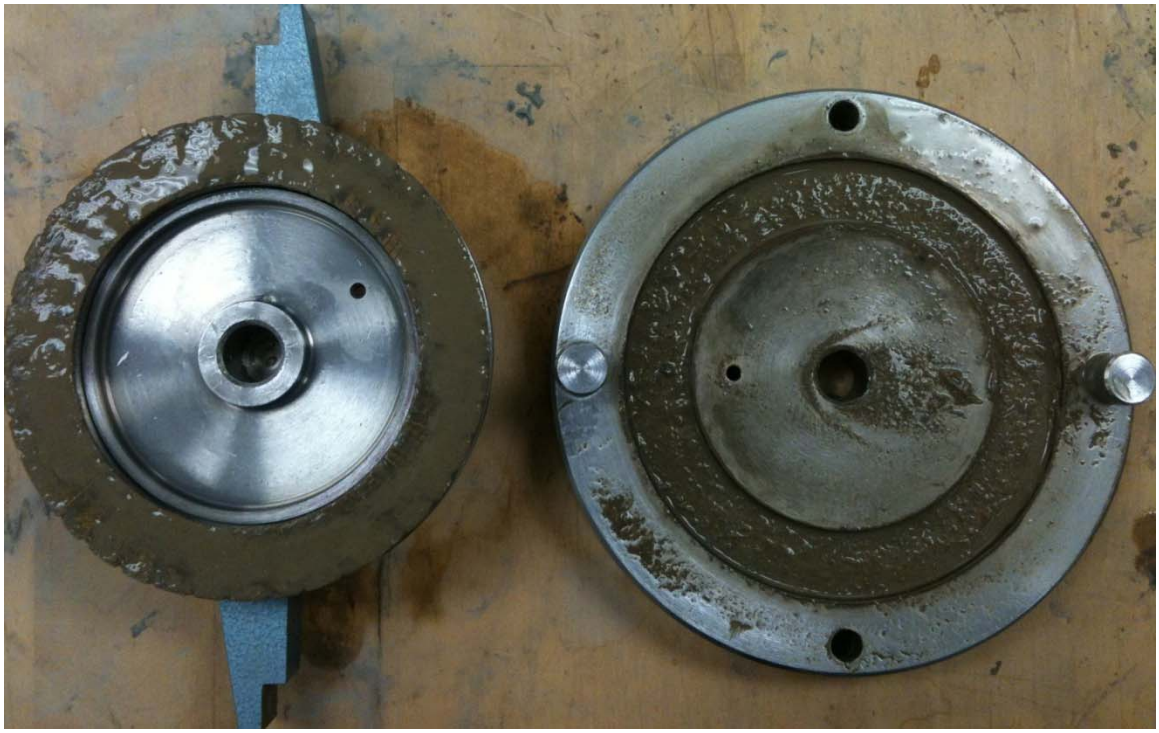

Texas 2 - Blenderized - 1638 A psf

Texas 2 - Blenderized - 3225 psf

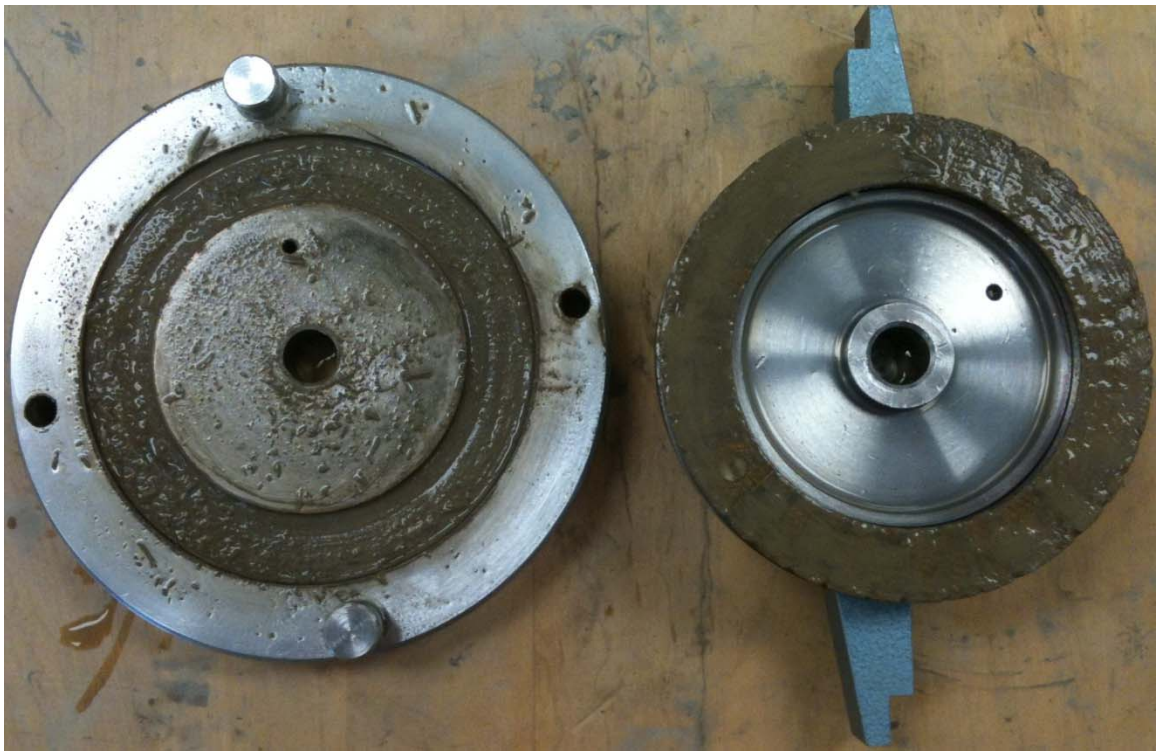

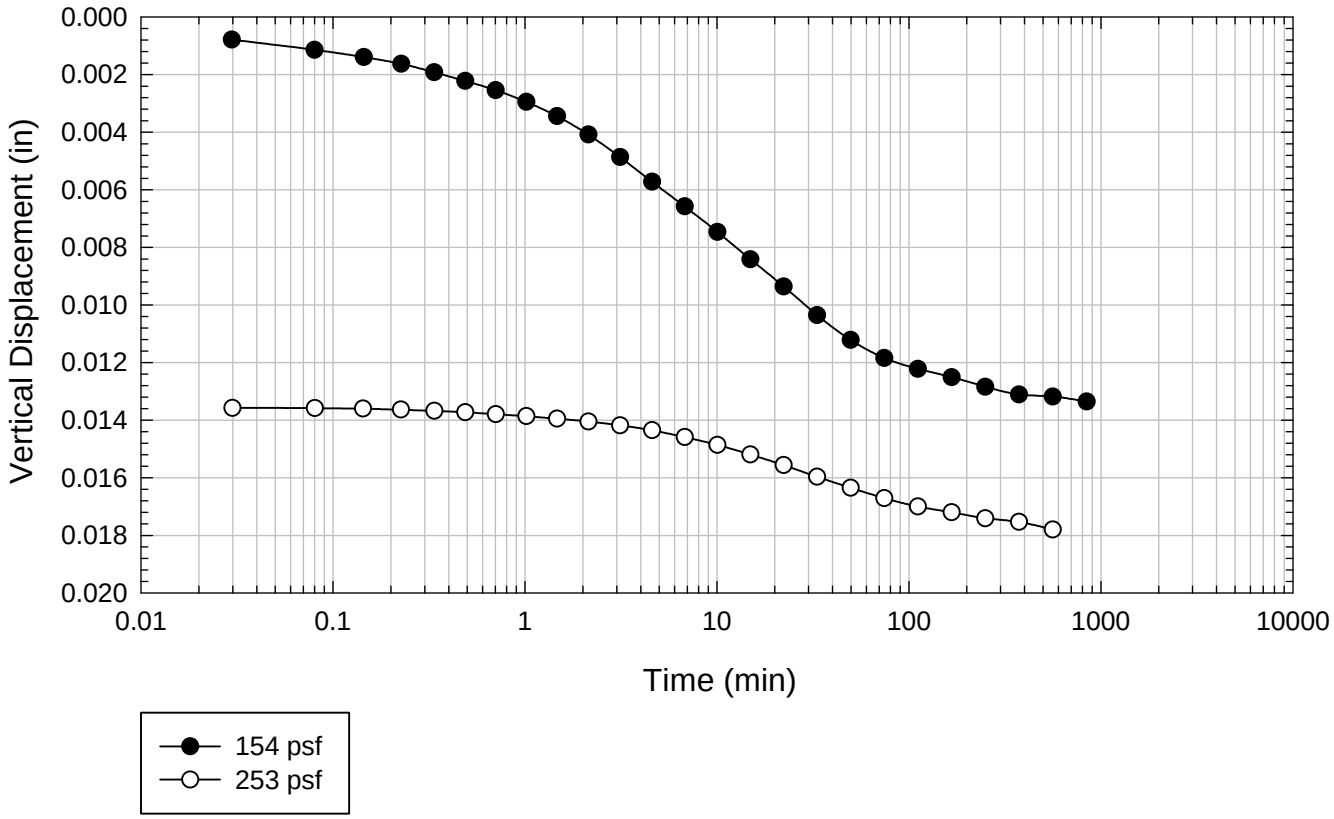
Texas 2 - Blenderized - 253 psf
Vertical Displacement (in)
0.000
0.002
0.004
0.006
0.008
0.010
0.012
0.014
0.016
0.018
0.020
0.01
0.1
1
10
100
1000
10000
Time (min)
154 psf
253 psf

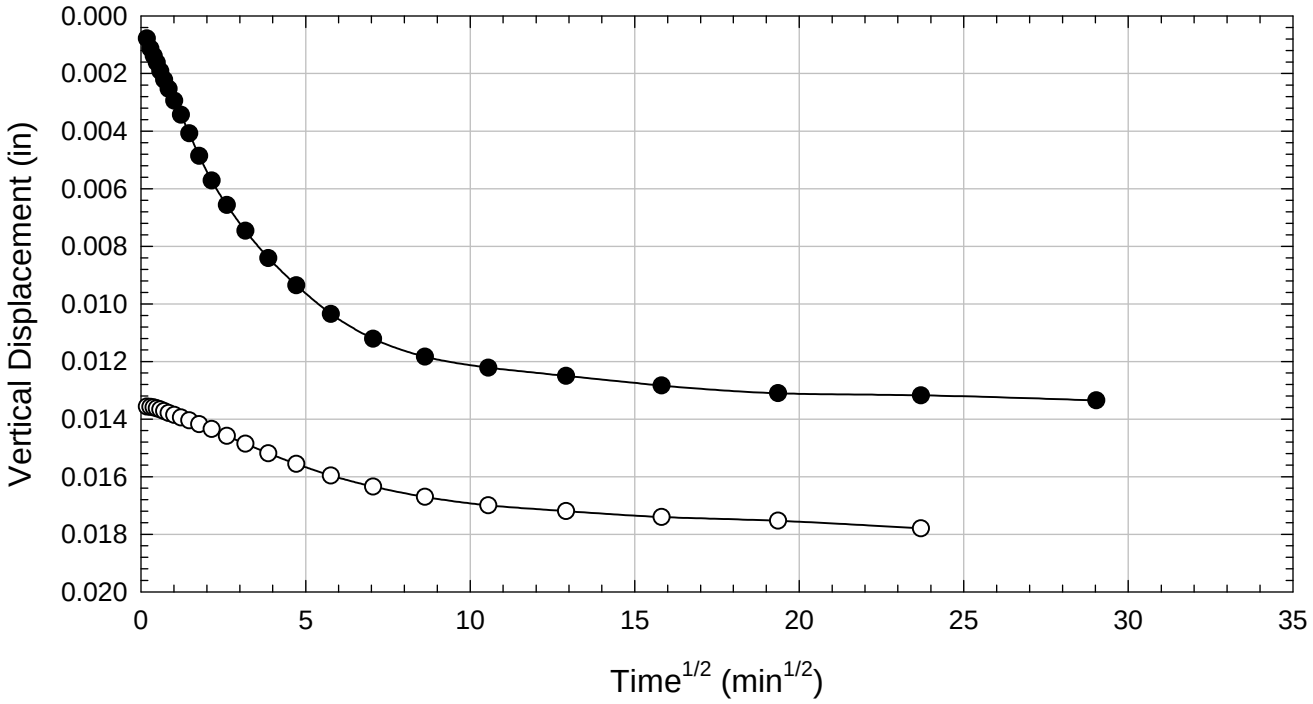
Vertical Displacement (in)
0.000
0.002
0.004
0.006
0.008
0.010
0.012
0.014
0.016
0.018
0.020
0
5
10
15
20
25
30
35
Time1/2 (min1/2)

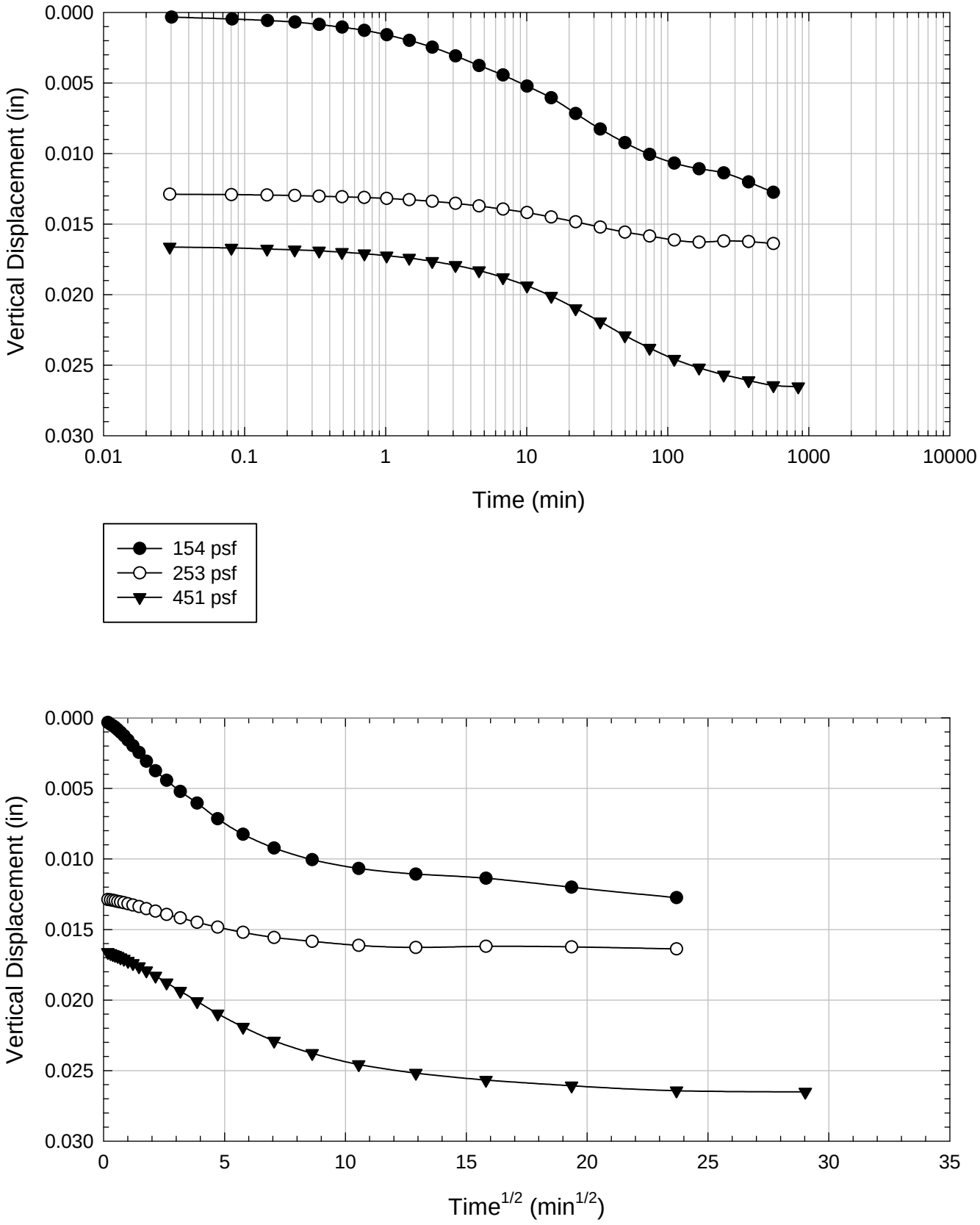
Texas 2 - Blenderized - 451 psf
Vertical Displacement (in)
0.000
0.005
0.010
0.015
0.020
0.025
0.030
0.01
0.1
1
10
100
1000
10000
Time (min)
154 psf
253 psf
451 psf
Vertical Displacement (in)
0.000
0.005
0.010
0.015
0.020
0.025
0.030
0
5
10
15
20
25
30
35
Time^1/2 (min^1/2)

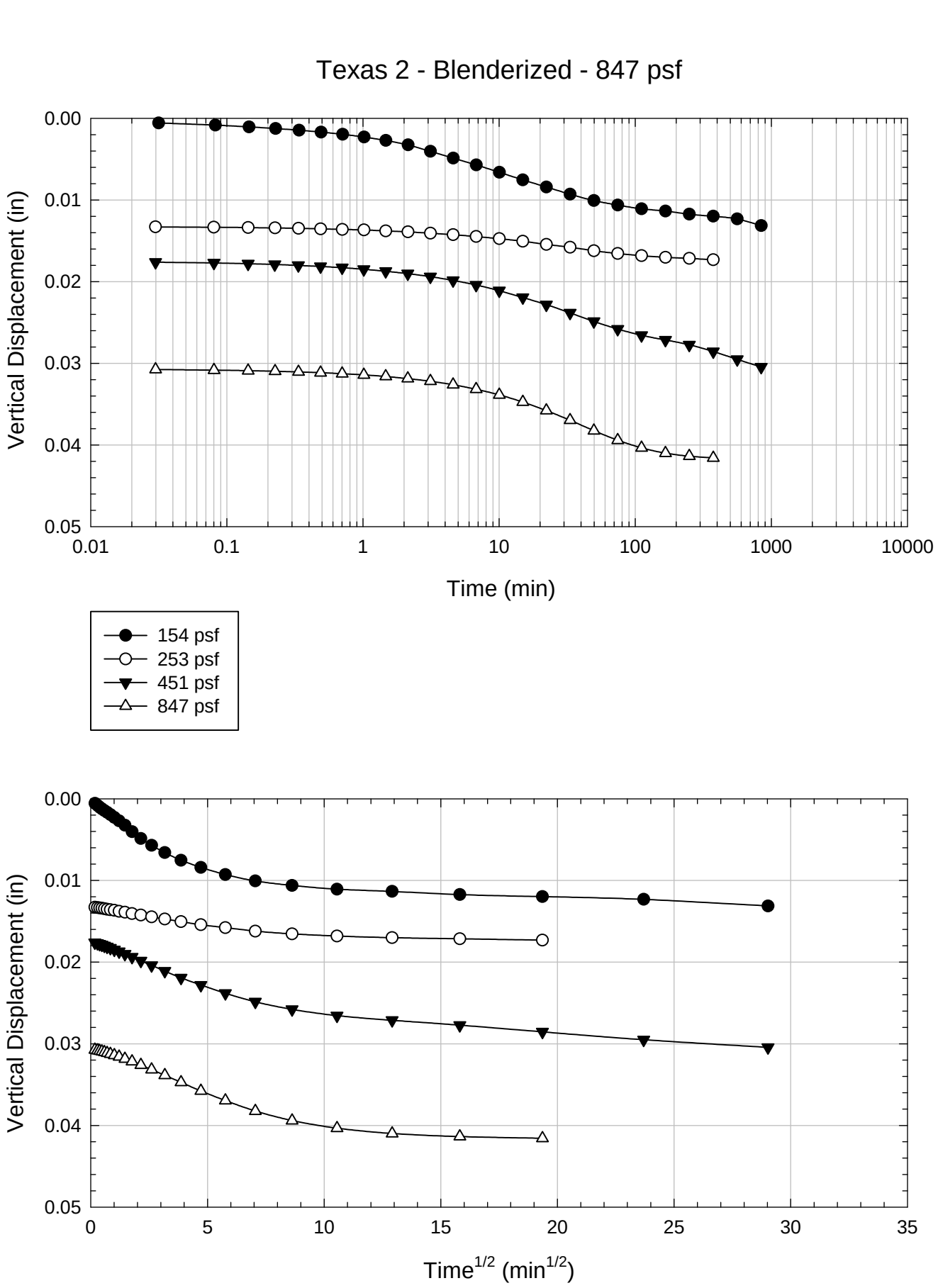
Texas 2 - Blenderized - 847 psf
Vertical Displacement (in)
0.00
0.01
0.02
0.03
0.04
0.05
0.01
0.1
1
10
100
1000
10000
Time (min)
154 psf
253 psf
451 psf
847 psf
Vertical Displacement (in)
0.00
0.01
0.02
0.03
0.04
0.05
0
5
10
15
20
25
30
35
Time1/2 (min1/2)

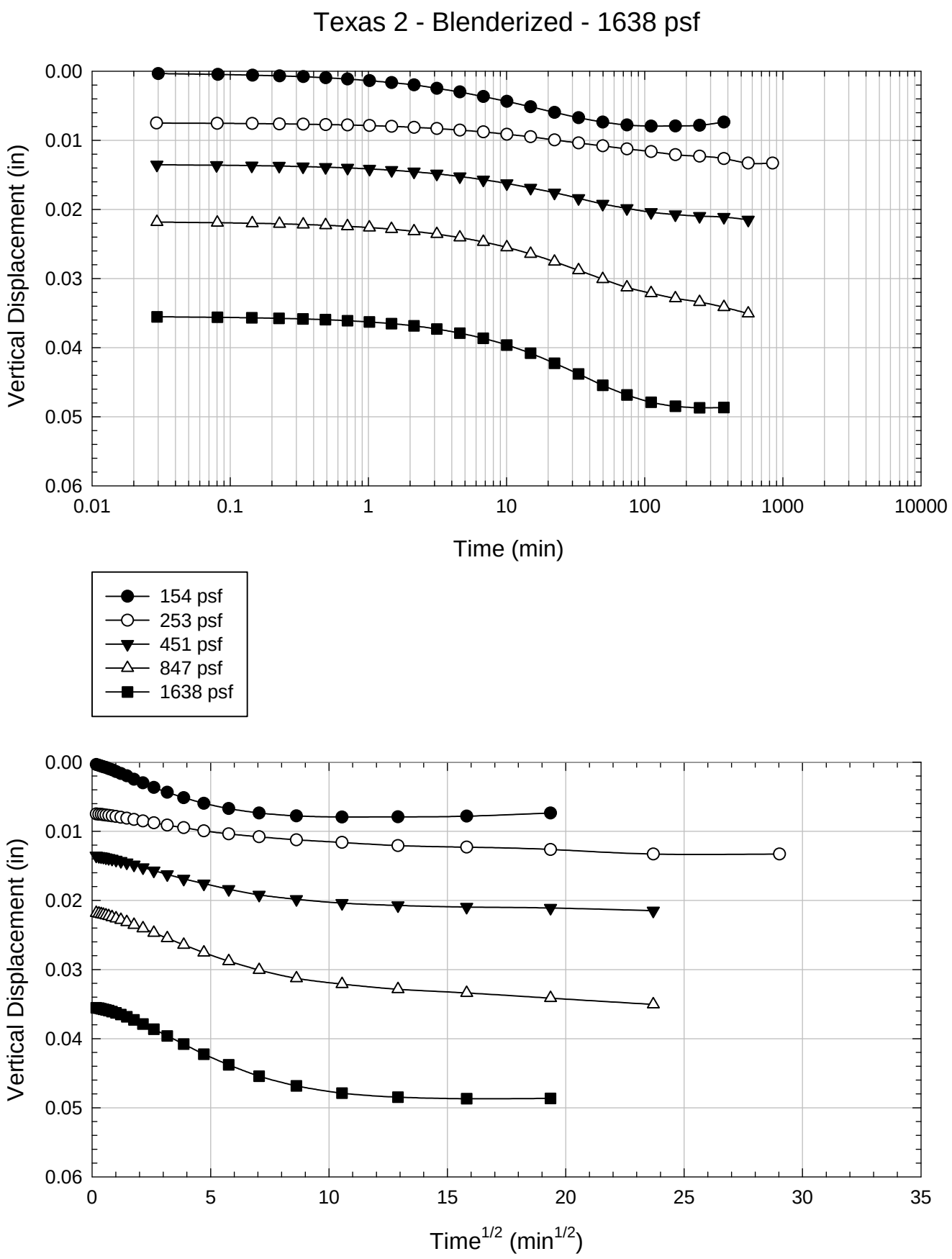
Texas 2 - Blenderized - 1638 psf
Vertical Displacement (in)
0.00
0.01
0.02
0.03
0.04
0.05
0.06
0.01
0.1
1
10
100
1000
10000
Time (min)
154 psf
253 psf
451 psf
847 psf
1638 psf
Vertical Displacement (in)
0.00
0.01
0.02
0.03
0.04
0.05
0.06
0
5
10
15
20
25
30
35
Time1/2 (min1/2)

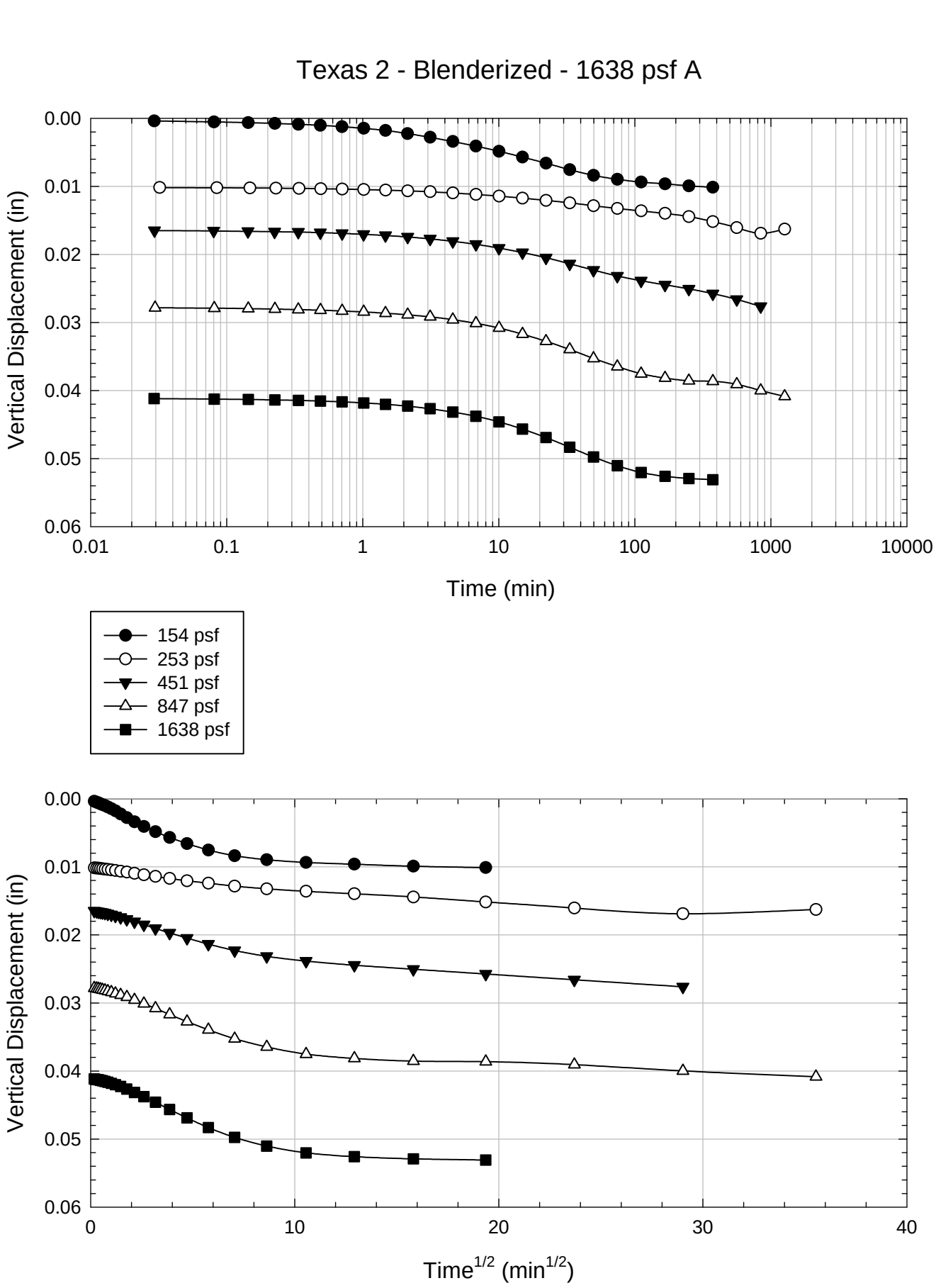
Texas 2 - Blenderized - 1638 psf A
Vertical Displacement (in)
0.00
0.01
0.02
0.03
0.04
0.05
0.06
0.01
0.1
1
10
100
1000
10000
Time (min)
154 psf
253 psf
451 psf
847 psf
1638 psf
Vertical Displacement (in)
0.00
0.01
0.02
0.03
0.04
0.05
0.06
0
10
20
30
40
Time1/2 (min1/2)

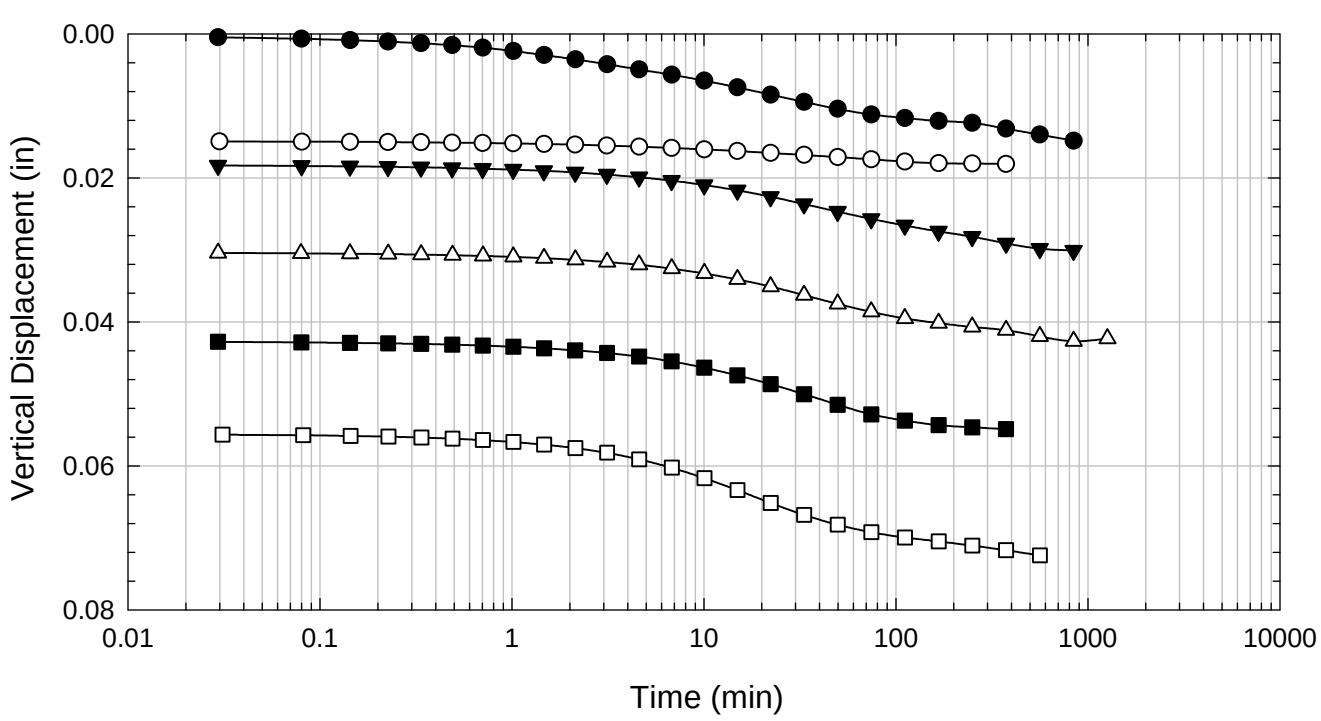
Texas 2 - Blenderized - 3225 psf
Vertical Displacement (in)
0.00
0.02
0.04
0.06
0.08
0.01
0.1
1
10
100
1000
10000
Time (min)

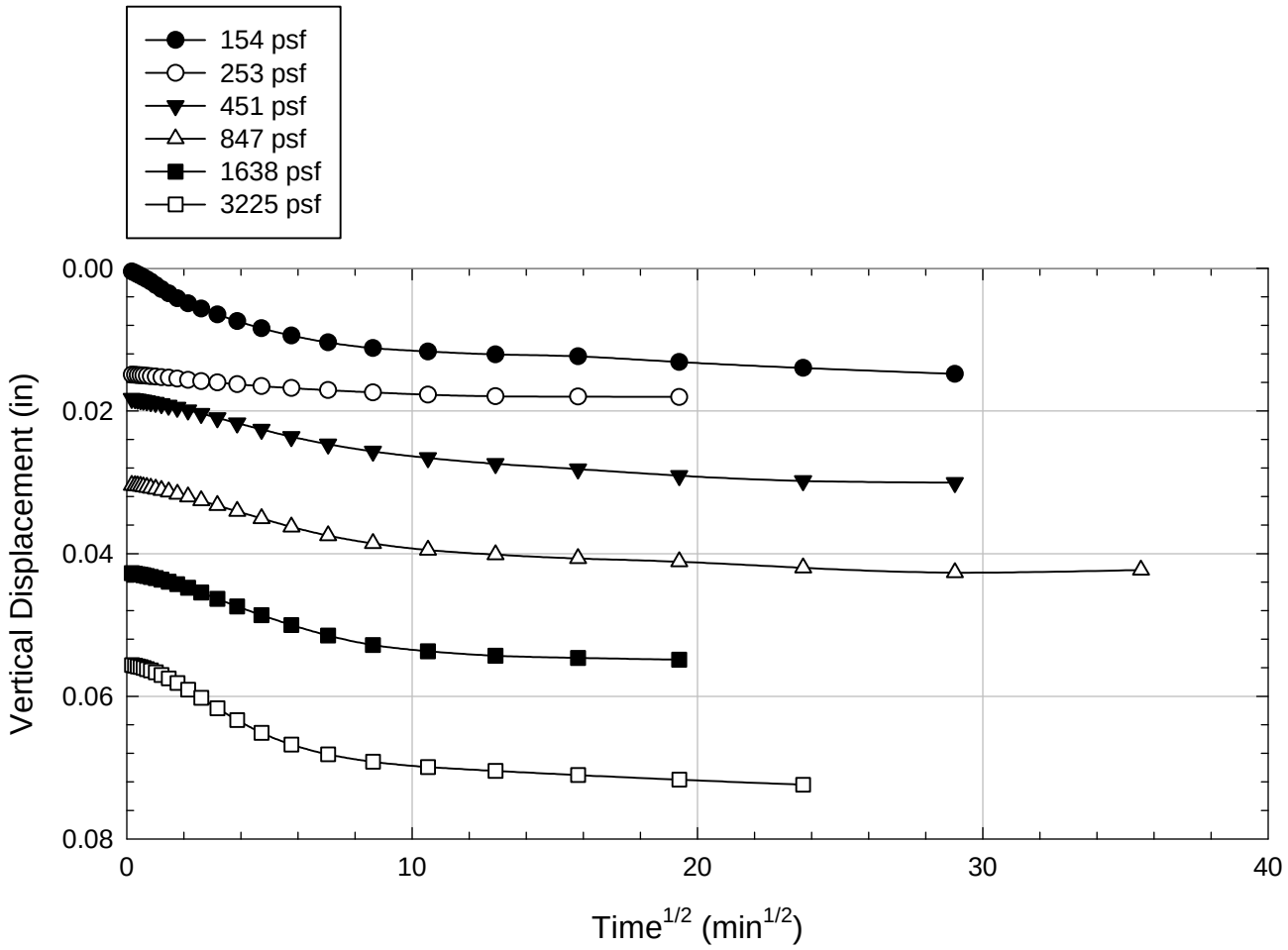
154 psf
253 psf
451 psf
847 psf
1638 psf
3225 psf
Vertical Displacement (in)
0.00
0.02
0.04
0.06
0.08
0
10
20
30
40
Time1/2 (min1/2)

Texas 2 - Blenderized

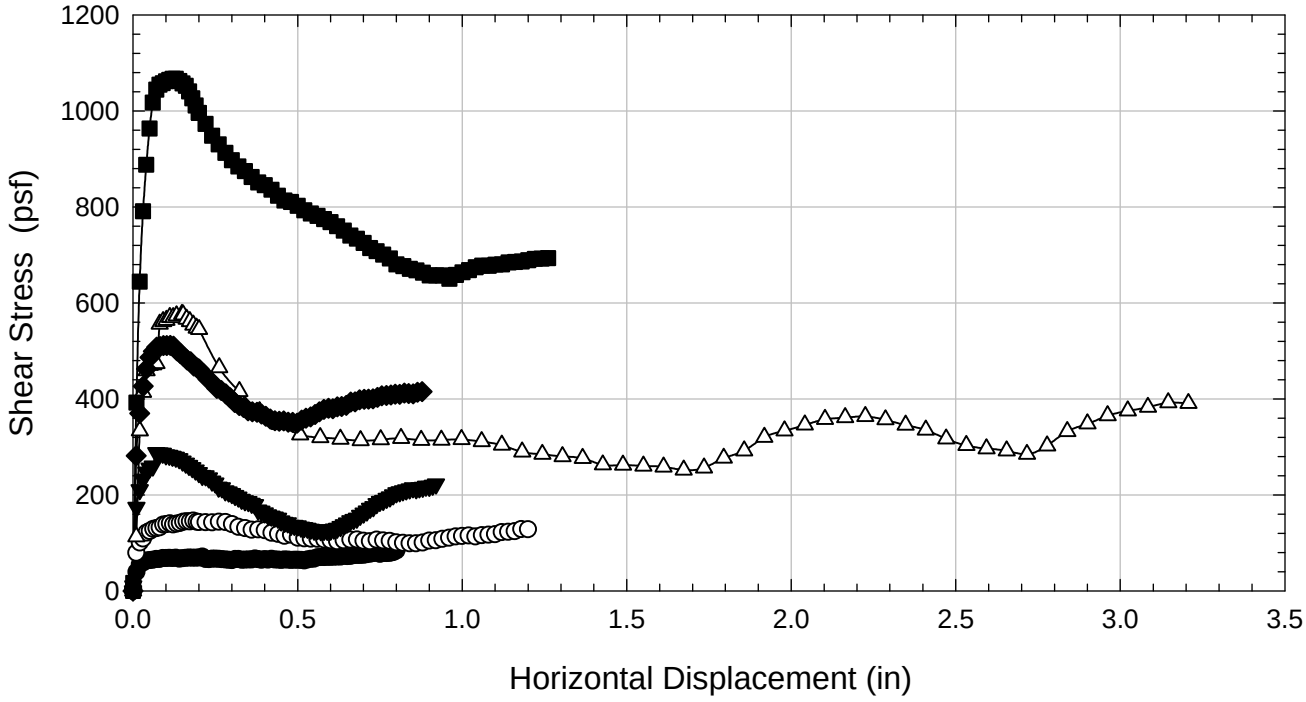

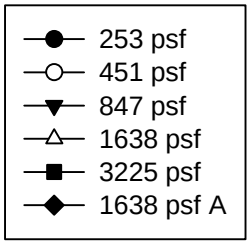

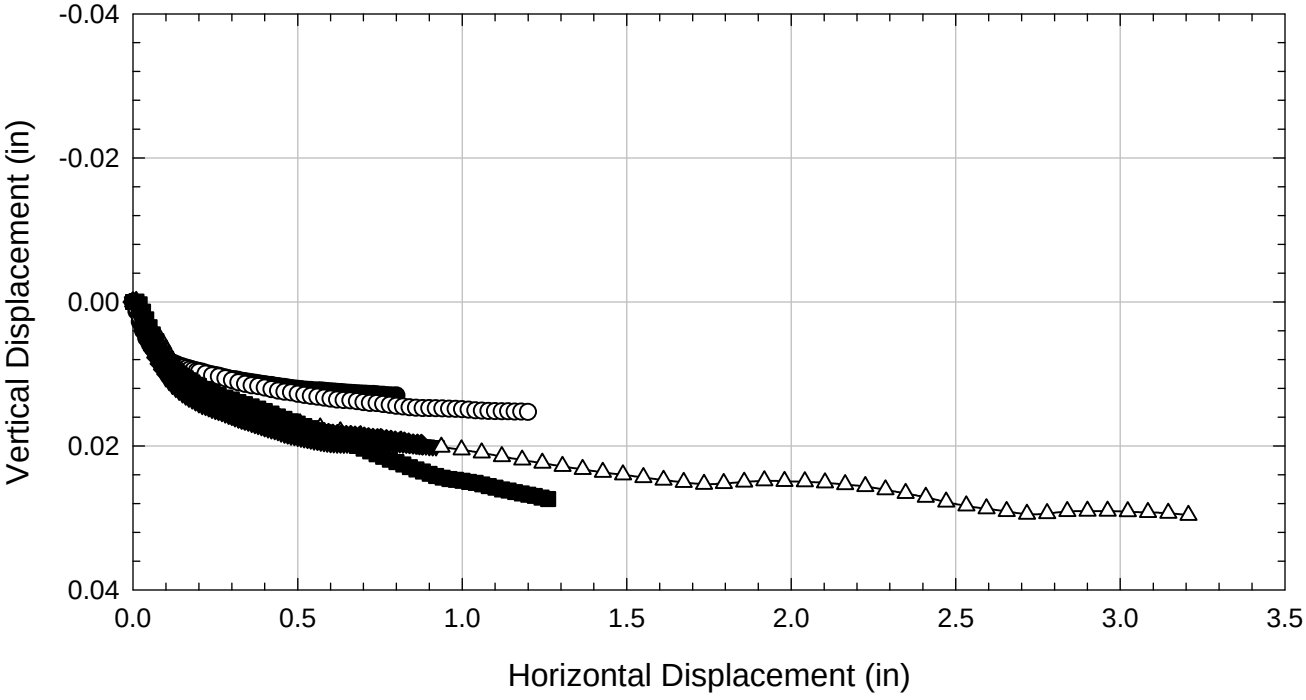

D.10. Texas 3

D.10.1 Blenderized

Virginia Polytechnic Institute and State University
Geotechnical Engineering Laboratory
Ring Shear Data Sheet

Project:	Fully Softened Shear Strength
Sample I.D./Loc.:	Texas 3 - Blenderized
Classification:	Fat Clay (CH)

Sample Preparation	Remolded at LL

Specific Gravity	2.82	
Shear Device Used	WF Bromhead Ring Shear	

Test Number	1	2	3	4	5	6	7	
Start Date (m/d/y)	3/3/2011	1/31/2011	2/4/2011	2/13/2011	2/19/2011			
End Date (m/d/y)	3/5/2011	2/4/2011	2/9/2011	2/19/2011	2/24/2011			
Consolidation Pressure (psf)	253	451	847	1638	3225			
Initial Values								
Initial Height (in)	0.20	0.20	0.20	0.20	0.20			
Inner Radius (in)	1.38	1.38	1.38	1.38	1.38			
Outer Radius (in)	1.97	1.97	1.97	1.97	1.97			
Initial Sample Weight (g)	34.16	31.50	29.89	34.19	33.81			
Water Content (%)	70.63	69.37	70.10	70.38	70.94			
Dry Unit Weight Before Shear (pcf)	63.3	68.7	74.8	82.6	100.3			
Saturation (%)	100.0	100.0	100.0	100.0	100.0			
Consolidation Pressures								
Load 1 (psf)	154	154	154	154	154			
Load 2 (psf)	253	253	253	253	253			
Load 3 (psf)		451	451	451	451			
Load 4 (psf)			847	847	847			
Load 5 (psf)				1638	1638			
Load 6 (psf)					3225			
Load 7 (psf)								
t_{50}								
Max. t_{50} for Load 1 (min)	29.07	9.26	35.35	51.04	8.67			
Max. t_{50} for Load 2 (min)	35.87	39.17	27.50	60.67	25.32			
Max. t_{50} for Load 3 (min)		19.00	36.09	60.00	45.24			
Max. t_{50} for Load 4 (min)			28.53	50.41	38.49			
Max. t_{50} for Load 5 (min)				49.27	26.37			
Max. t_{50} for Load 6 (min)					18.92			
Max. t_{50} for Load 7 (min)								
Final Values								
Water Content (%)	63.36	55.82	54.74	48.43	48.02			
Saturation (%)	100.0	100.0	100.0	100.0	100.0			
Failure								
Test Performed at Shear Rate (in/min)	7.00E-04	7.00E-04	7.00E-04	7.00E-04	7.00E-04			
Required Shear Rate (in/min)	5.58E-05	6.32E-05	7.01E-05	3.65E-05	1.06E-04			
Displacement at Failure (in)	0.10	0.06	0.10	0.09	0.14			
Peak Shear Stress (psf)	70	130	265	493	890			
Secant Effective Friction Angle (deg)	15.5	16.1	17.4	16.7	15.4			

Comments:

Texas 3 - Blenderized - 253 psf

Texas 3 - Blenderized - 451 psf

Texas 3 - Blenderized - 847 psf

Texas 3 - Blenderized - 3225 psf

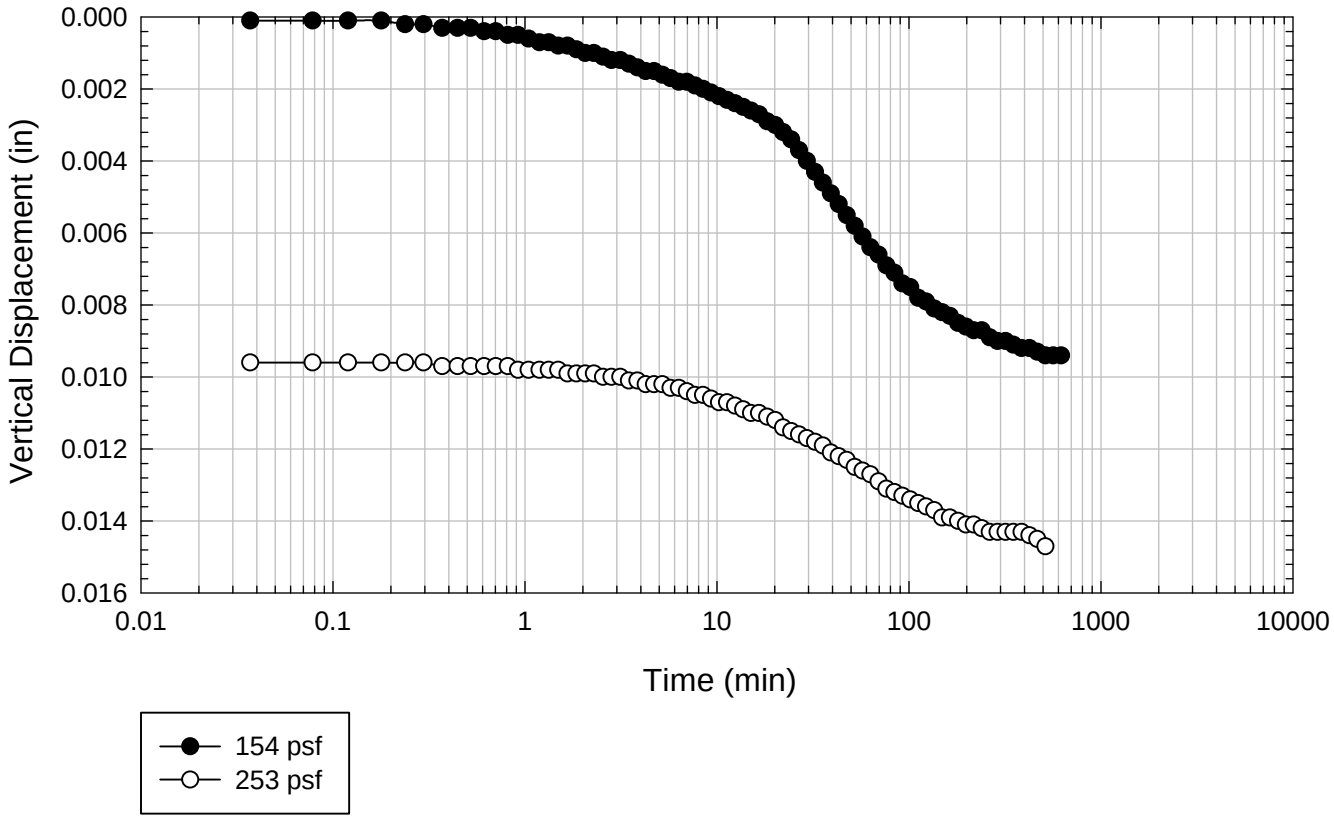
Texas 3 - Blenderized - 253 psf
Vertical Displacement (in)
0.000
0.002
0.004
0.006
0.008
0.010
0.012
0.014
0.016
0.01
0.1
1
10
100
1000
10000
Time (min)
154 psf
253 psf

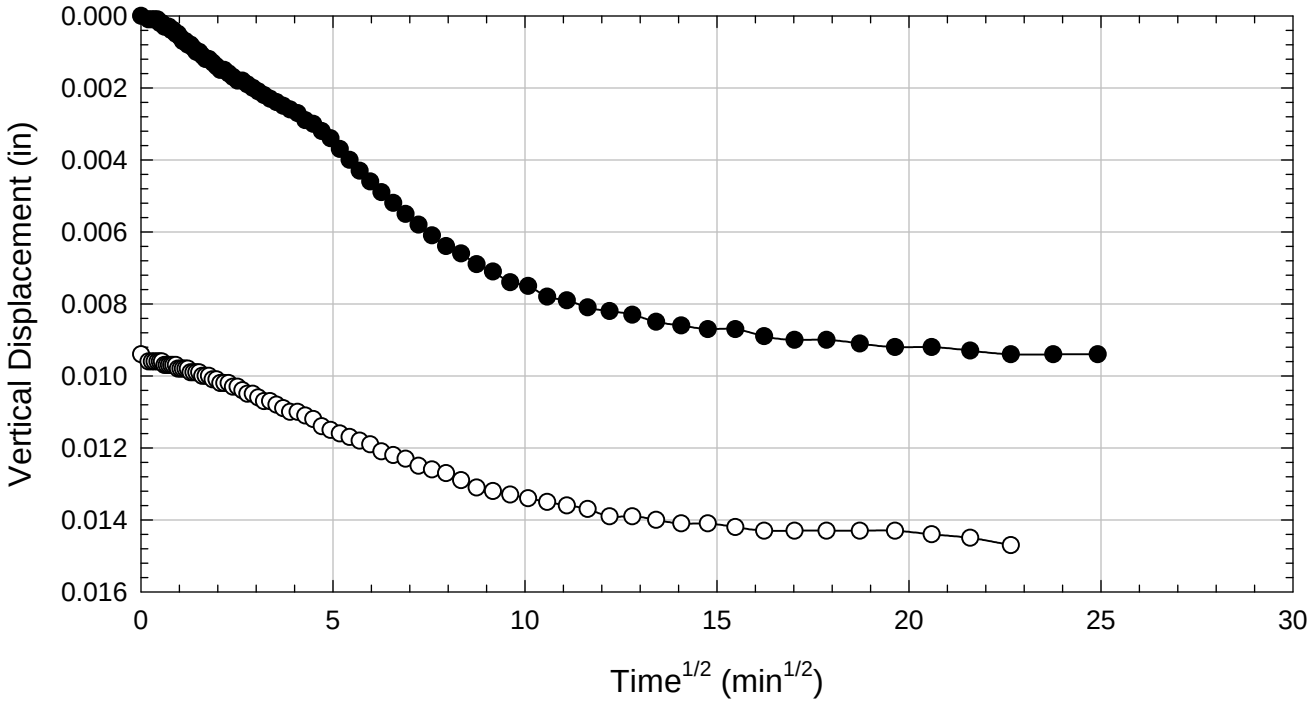
Vertical Displacement (in)
0.000
0.002
0.004
0.006
0.008
0.010
0.012
0.014
0.016
0
5
10
15
20
25
30
Time1/2 (min1/2)

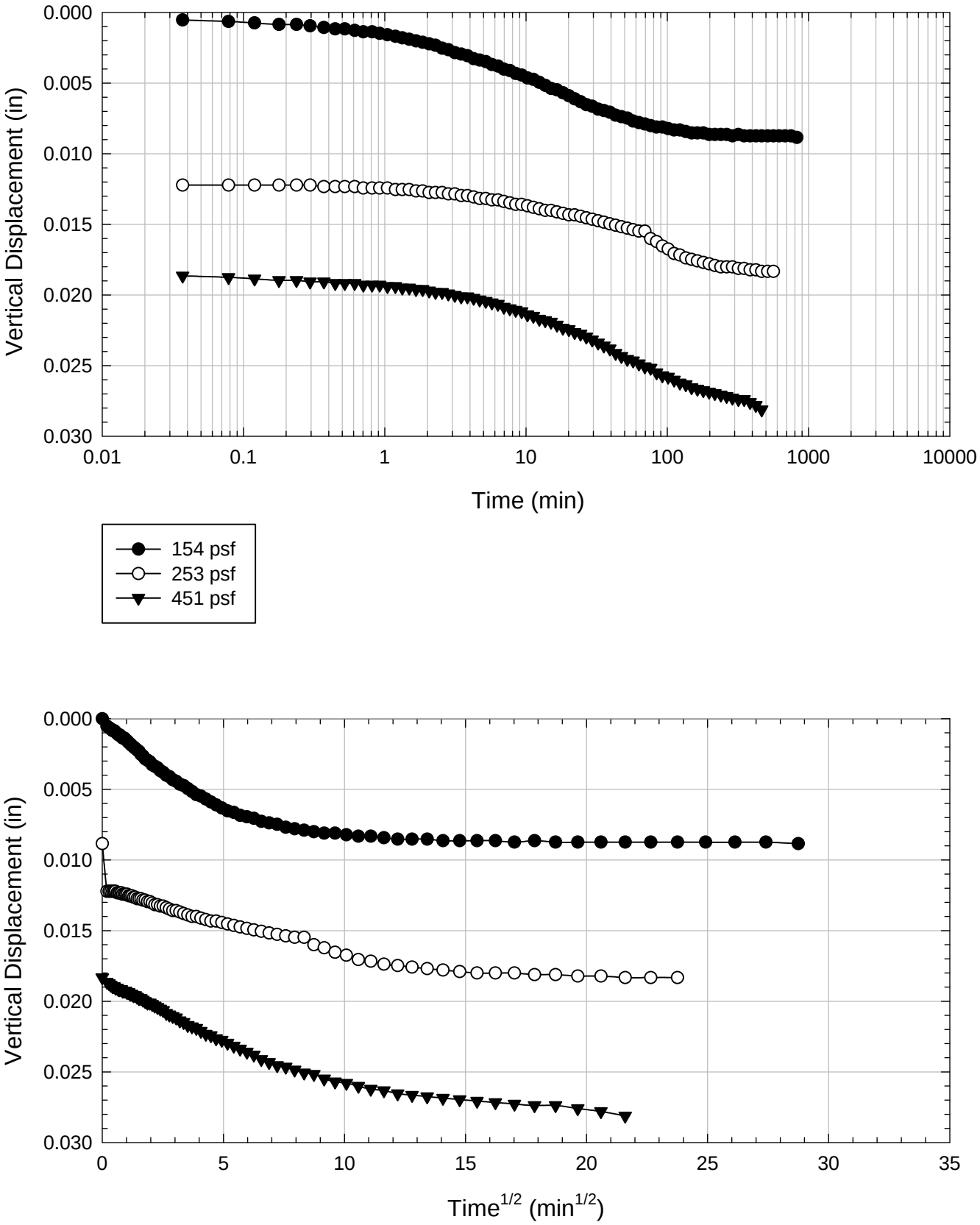
Texas 3 - Blenderized - 451 psf
Vertical Displacement (in)
0.000
0.005
0.010
0.015
0.020
0.025
0.030
0.01
0.1
1
10
100
1000
10000
Time (min)
154 psf
253 psf
451 psf
Vertical Displacement (in)
0.000
0.005
0.010
0.015
0.020
0.025
0.030
0
5
10
15
20
25
30
35
Time^1/2 (min^1/2)

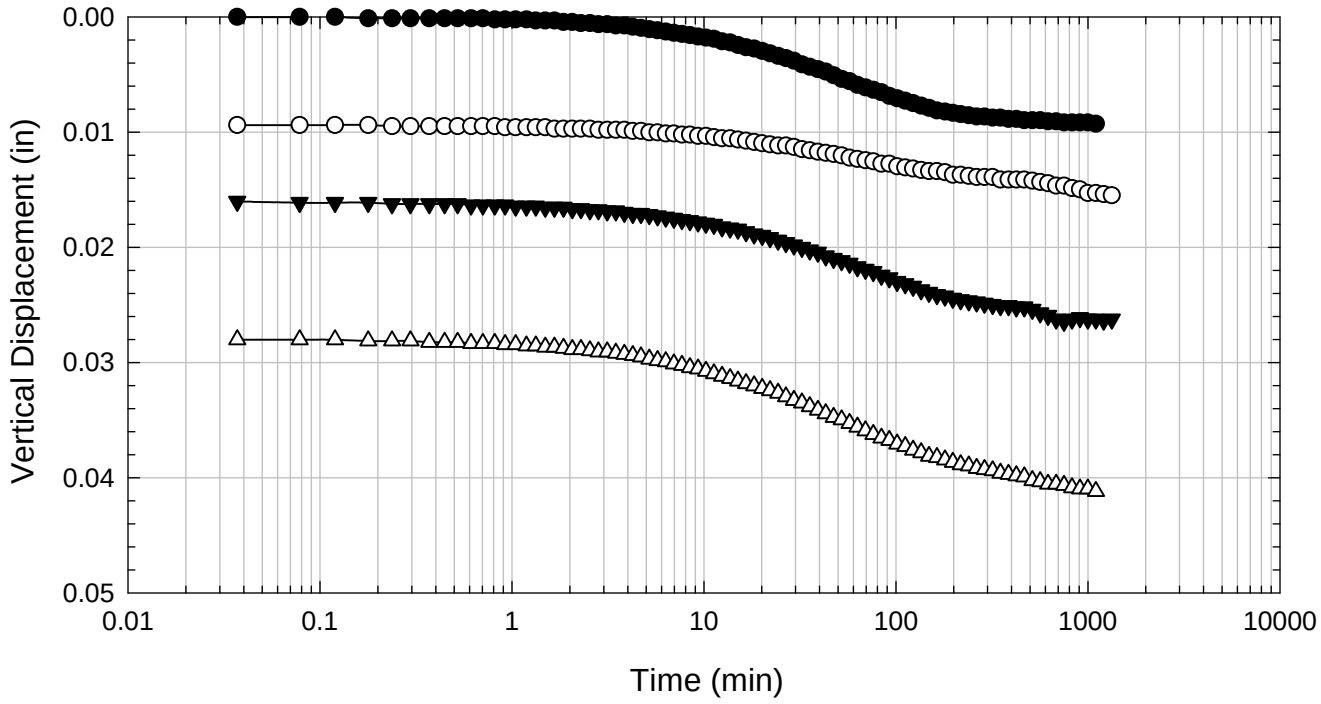
Texas 3 - Blenderized - 847 psf
Vertical Displacement (in)
0.00
0.01
0.02
0.03
0.04
0.05
0.01
0.1
1
10
100
1000
10000
Time (min)

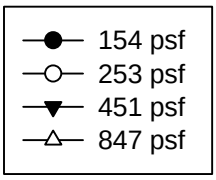
154 psf
253 psf
451 psf
847 psf

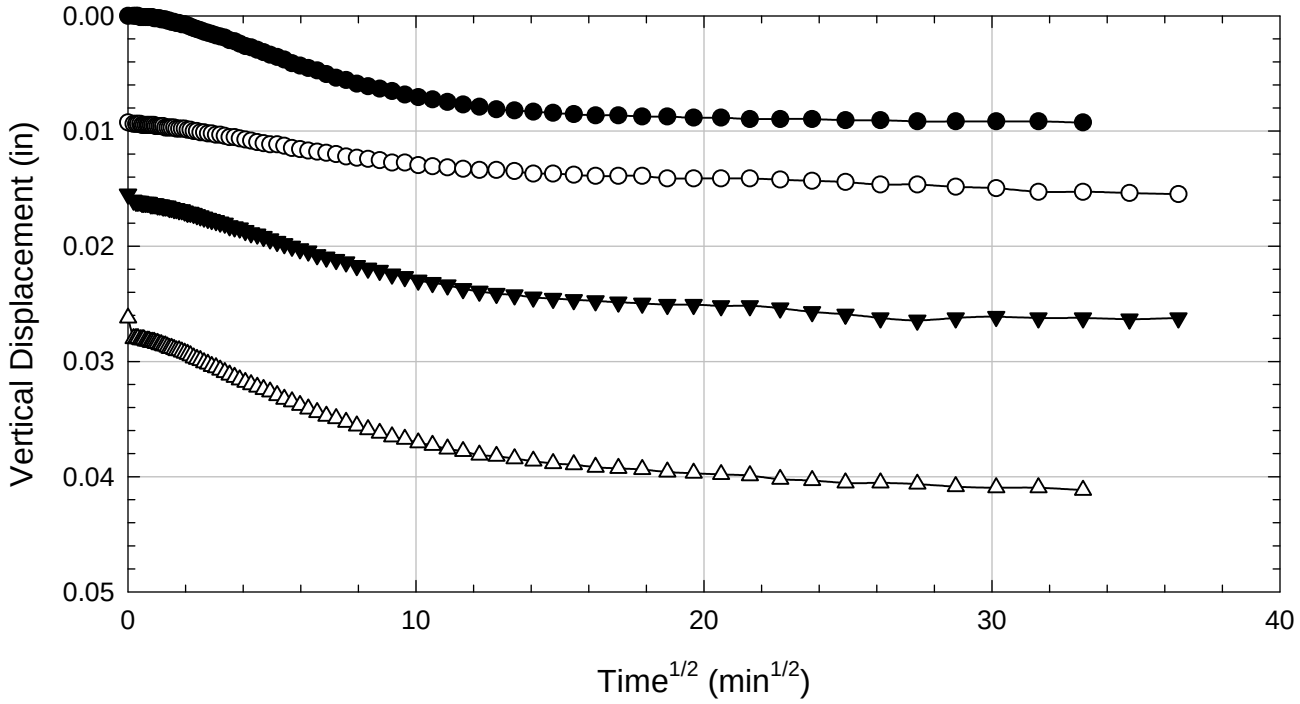
Vertical Displacement (in)
0.00
0.01
0.02
0.03
0.04
0.05
0
10
20
30
40
Time1/2 (min1/2)

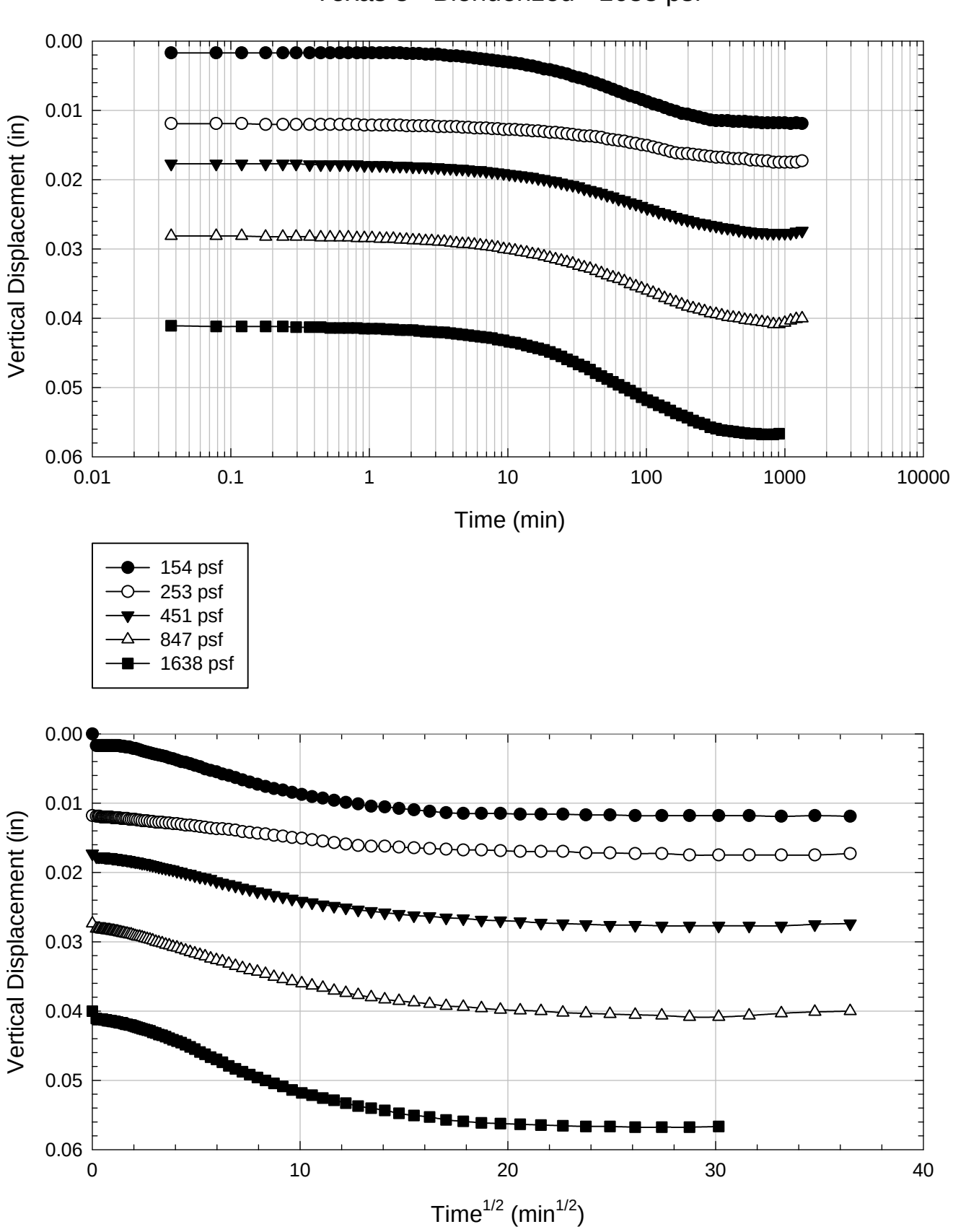
Texas 3 - Blenderized - 1638 psf
Vertical Displacement (in)
0.00
0.01
0.02
0.03
0.04
0.05
0.06
0.01
0.1
1
10
100
1000
10000
Time (min)
154 psf
253 psf
451 psf
847 psf
1638 psf
Vertical Displacement (in)
0.00
0.01
0.02
0.03
0.04
0.05
0.06
0
10
20
30
40
Time^1/2 (min^1/2)

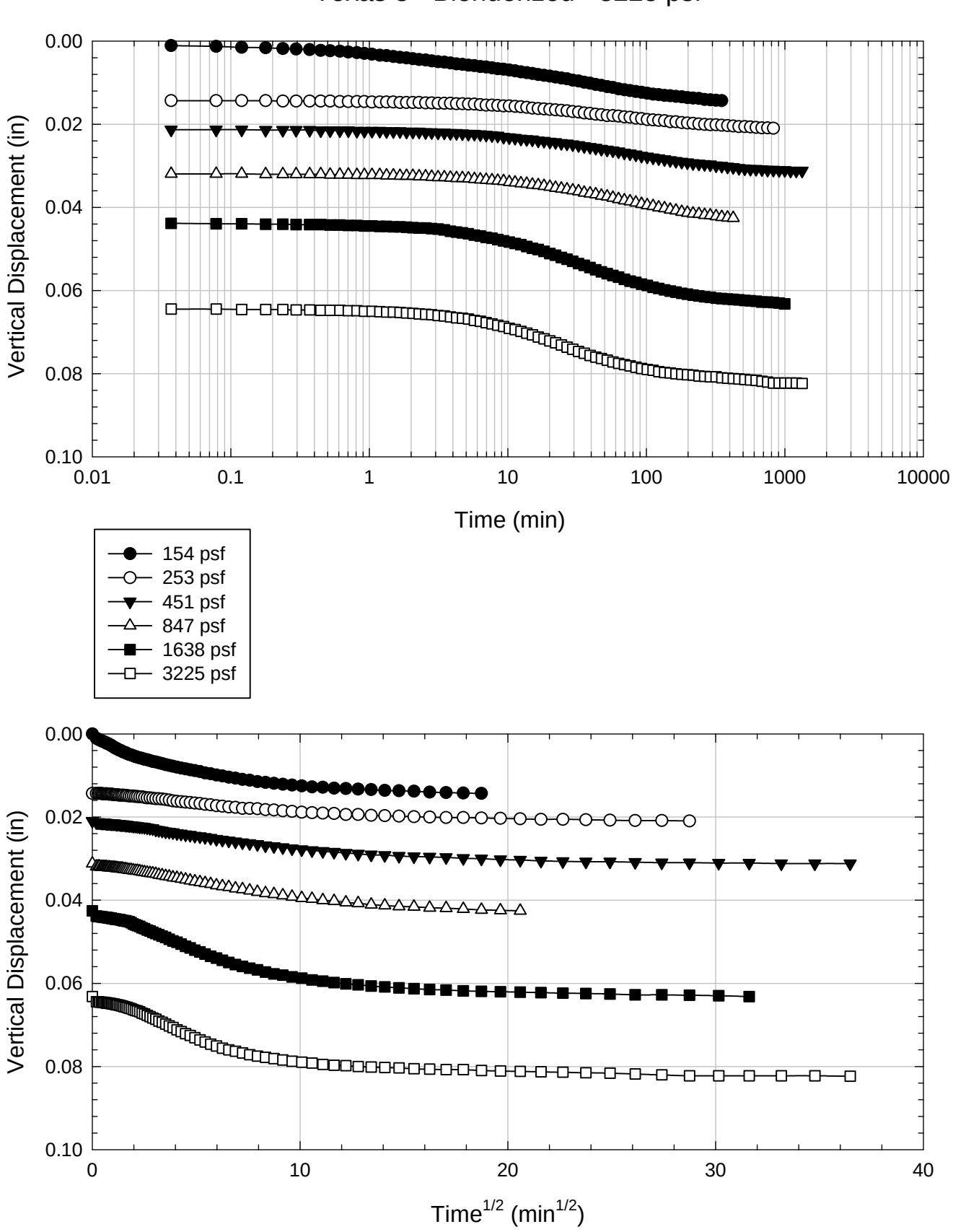
Texas 3 - Blenderized - 3225 psf
Vertical Displacement (in)
0.00
0.02
0.04
0.06
0.08
0.10
0.01
0.1
1
10
100
1000
10000
Time (min)
154 psf
253 psf
451 psf
847 psf
1638 psf
3225 psf
Vertical Displacement (in)
0.00
0.02
0.04
0.06
0.08
0.10
0
10
20
30
40
Time^1/2 (min^1/2)

Texas 3 - Blenderized

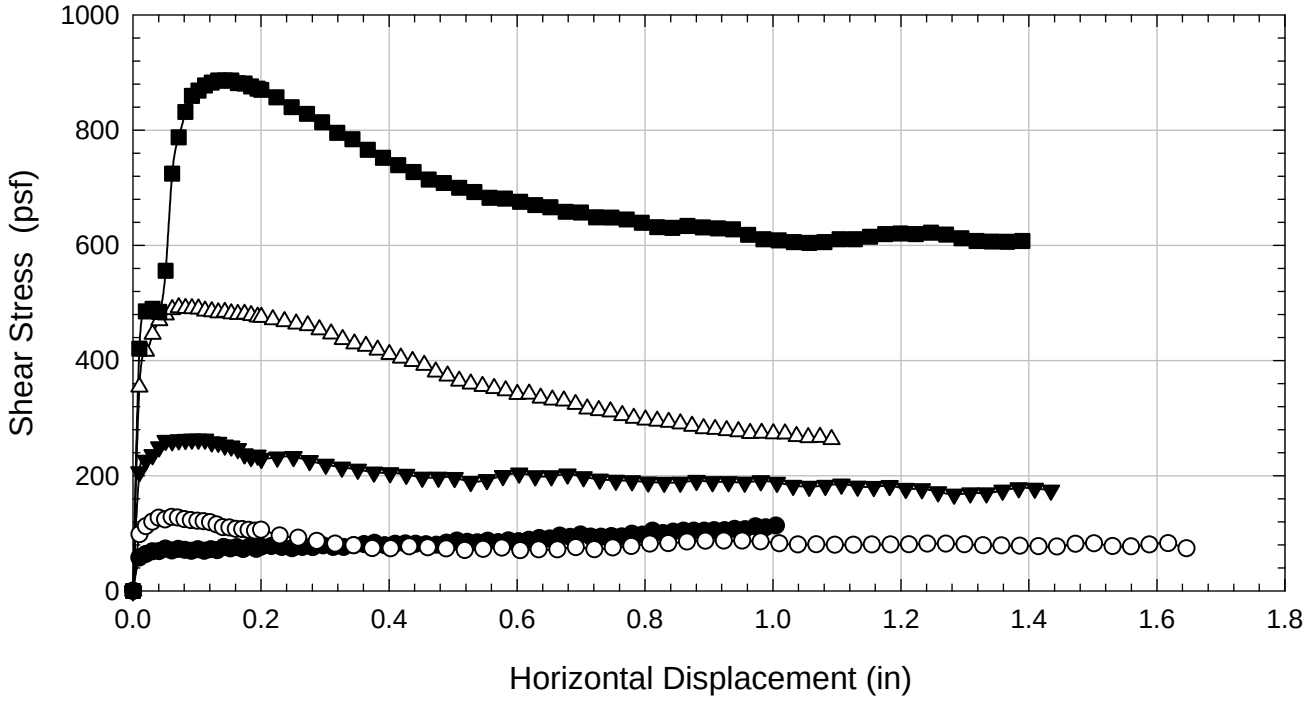

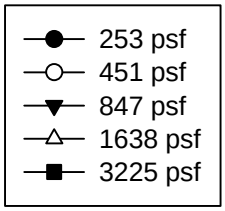

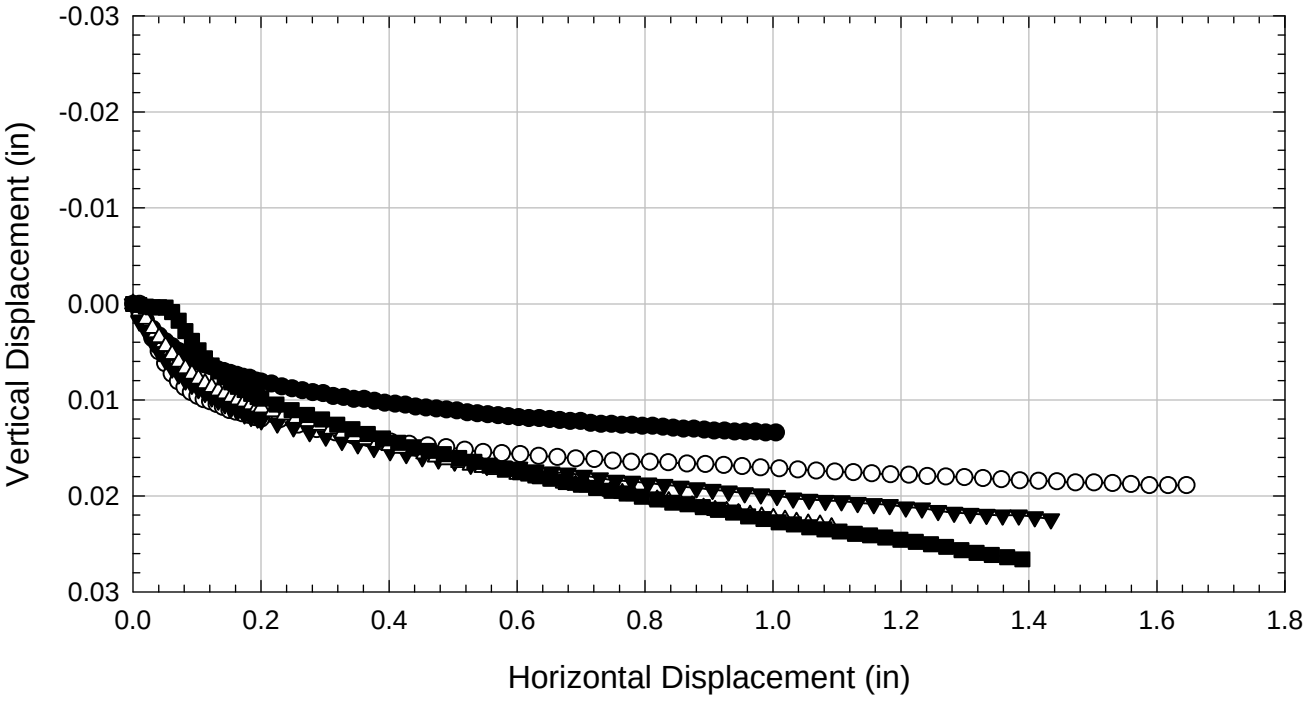

D.11. Texas 4

D.11.1 Blenderized

Virginia Polytechnic Institute and State University
Geotechnical Engineering Laboratory
Ring Shear Data Sheet

Project:	Fully Softened Shear Strength
Sample I.D./Loc.:	Texas 4 - Blenderized
Classification:	Fat Clay (CH)

Sample Preparation	Remolded at LL

Specific Gravity	2.81	
Shear Device Used	WF Bromhead Ring Shear	

Test Number	1	2	3	4	5	6	7	
Start Date (m/d/y)	3/3/2011	1/31/2011	2/4/2011	2/13/2011	2/19/2011			
End Date (m/d/y)	3/5/2011	2/4/2011	2/9/2011	2/19/2011	2/24/2011			
Consolidation Pressure (psf)	254	451	848	1641	3213			
Initial Values								
Initial Height (in)	0.20	0.20	0.20	0.20	0.20			
Inner Radius (in)	1.38	1.38	1.38	1.38	1.38			
Outer Radius (in)	1.97	1.97	1.97	1.97	1.97			
Initial Sample Weight (g)	34.30	33.70	39.80	33.52	33.57			
Water Content (%)	73.75	75.27	75.19	75.99	75.85			
Dry Unit Weight Before Shear (pcf)	63.0	61.5	71.8	79.4	92.5			
Saturation (%)	100.0	100.0	100.0	100.0	100.0			
Consolidation Pressures								
Load 1 (psf)	155	155	155	155	155			
Load 2 (psf)	254	254	254	254	254			
Load 3 (psf)		451	451	451	451			
Load 4 (psf)			848	848	848			
Load 5 (psf)				1641	1641			
Load 6 (psf)					3213			
Load 7 (psf)								
t_{50}								
Max. t_{50} for Load 1 (min)	15.76	15.94	17.52	24.31	11.24			
Max. t_{50} for Load 2 (min)	32.79		37.00	56.17	26.92			
Max. t_{50} for Load 3 (min)		20.35	51.30	50.48	36.02			
Max. t_{50} for Load 4 (min)			29.46	35.73	25.83			
Max. t_{50} for Load 5 (min)				26.63	17.76			
Max. t_{50} for Load 6 (min)					12.46			
Max. t_{50} for Load 7 (min)								
Final Values								
Water Content (%)	66.17	61.88	58.30	54.60	49.75			
Saturation (%)	100.0	100.0	100.0	100.0	100.0			
Failure								
Test Performed at Shear Rate (in/min)	7.00E-04	7.00E-04	7.00E-04	7.00E-04	7.00E-04			
Required Shear Rate (in/min)	6.10E-05	5.90E-05	6.11E-05	5.26E-05	6.76E-05			
Displacement at Failure (in)	0.10	0.06	0.09	0.07	0.06			
Peak Shear Stress (psf)	41	119	246	413	791			
Secant Effective Friction Angle (deg)	9.2	14.8	16.2	14.1	13.8			

Comments:

Texas 4 - Blenderized - 254 psf

Texas 4 - Blenderized - 848 psf

Texas 4 - Blenderized - 1641 psf

Texas 4 - Blenderized - 3213 psf

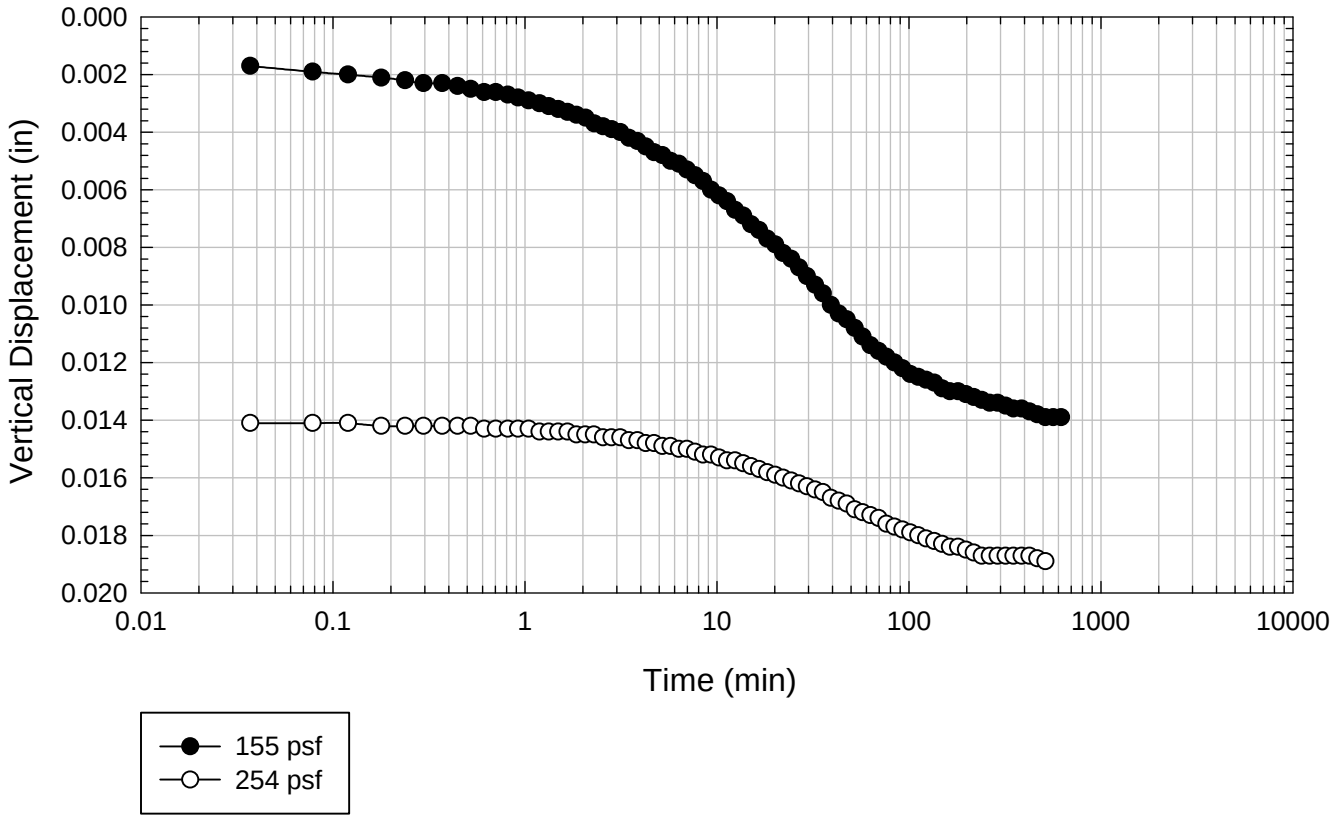
Texas 4 - Blenderized - 254 psf
Vertical Displacement (in)
0.000
0.002
0.004
0.006
0.008
0.010
0.012
0.014
0.016
0.018
0.020
0.01
0.1
1
10
100
1000
10000
Time (min)
155 psf
254 psf

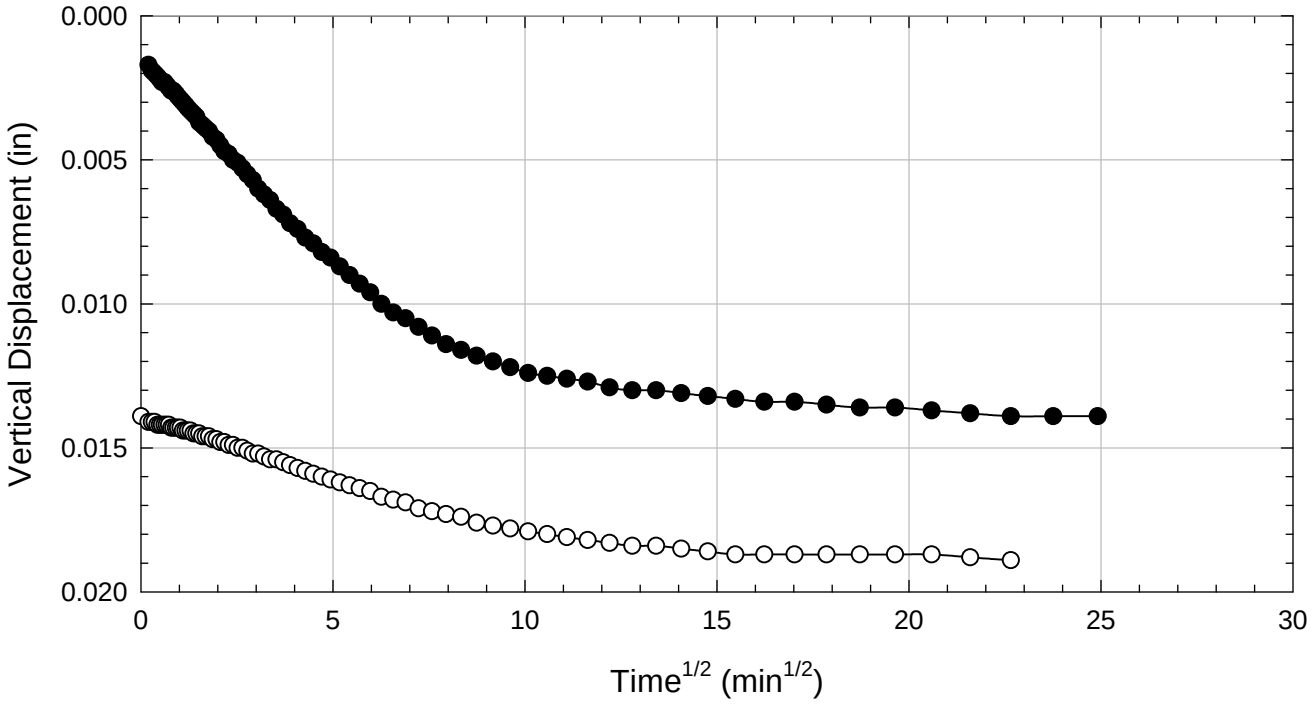
Vertical Displacement (in)
0.000
0.005
0.010
0.015
0.020
0
5
10
15
20
25
30
Time^1/2 (min^1/2)

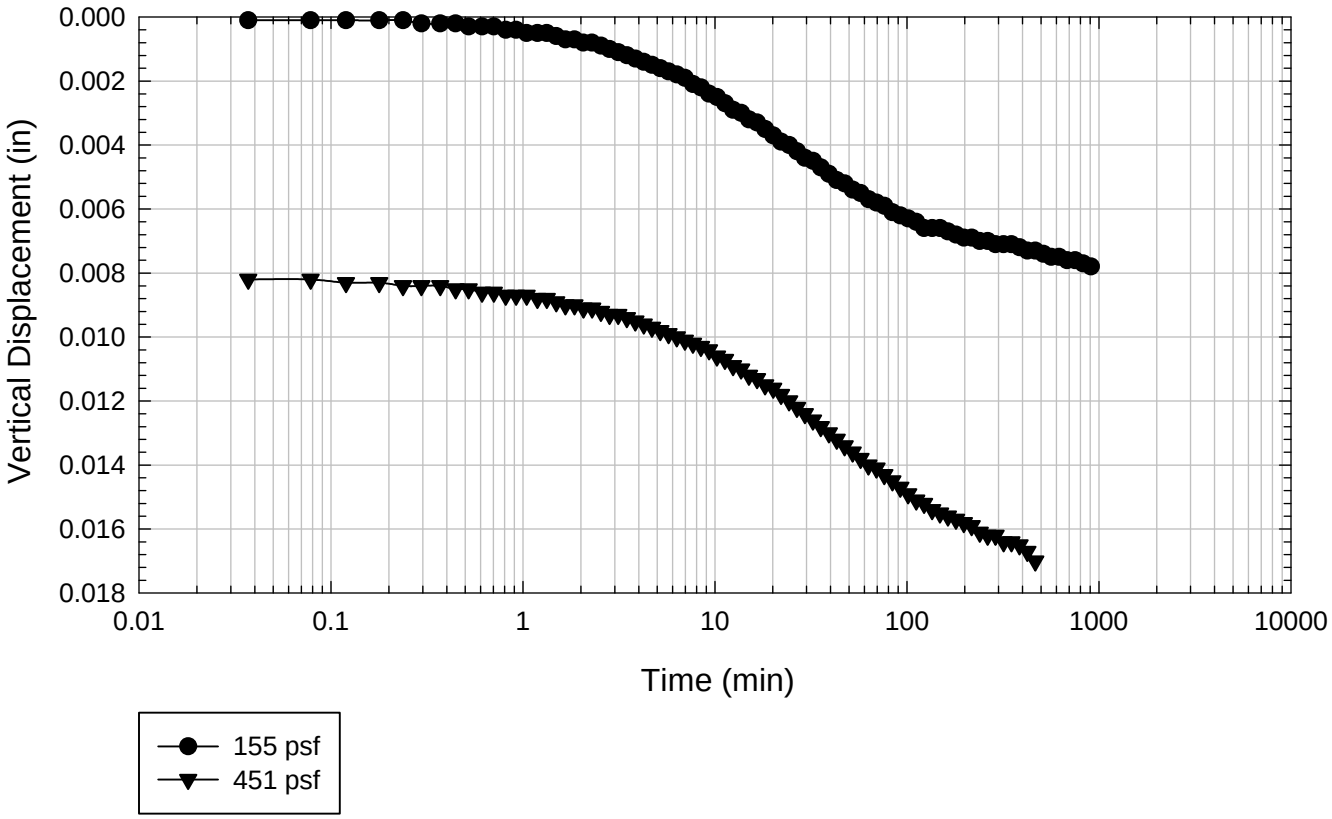
Texas 4 - Blenderized - 451 psf
Vertical Displacement (in)
0.000
0.002
0.004
0.006
0.008
0.010
0.012
0.014
0.016
0.018
0.01
0.1
1
10
100
1000
10000
Time (min)
155 psf
451 psf

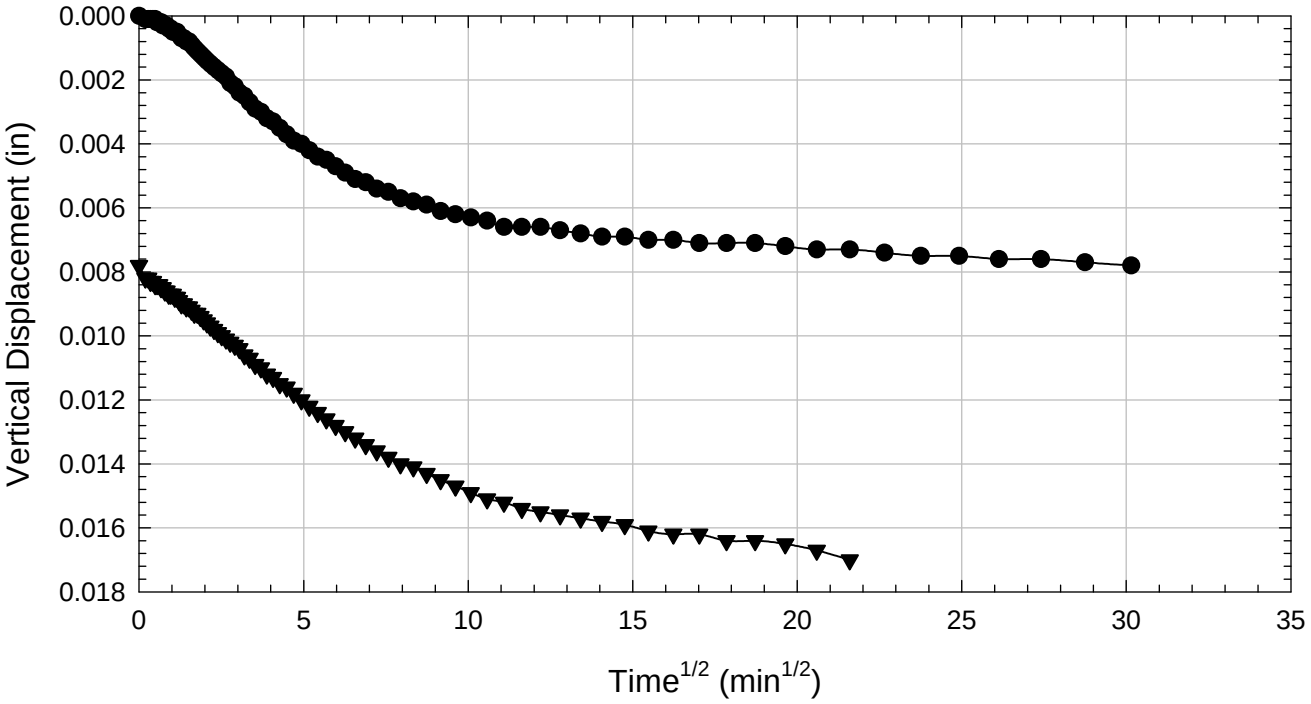
Vertical Displacement (in)
0.000
0.002
0.004
0.006
0.008
0.010
0.012
0.014
0.016
0.018
0
5
10
15
20
25
30
35
Time1/2 (min1/2)

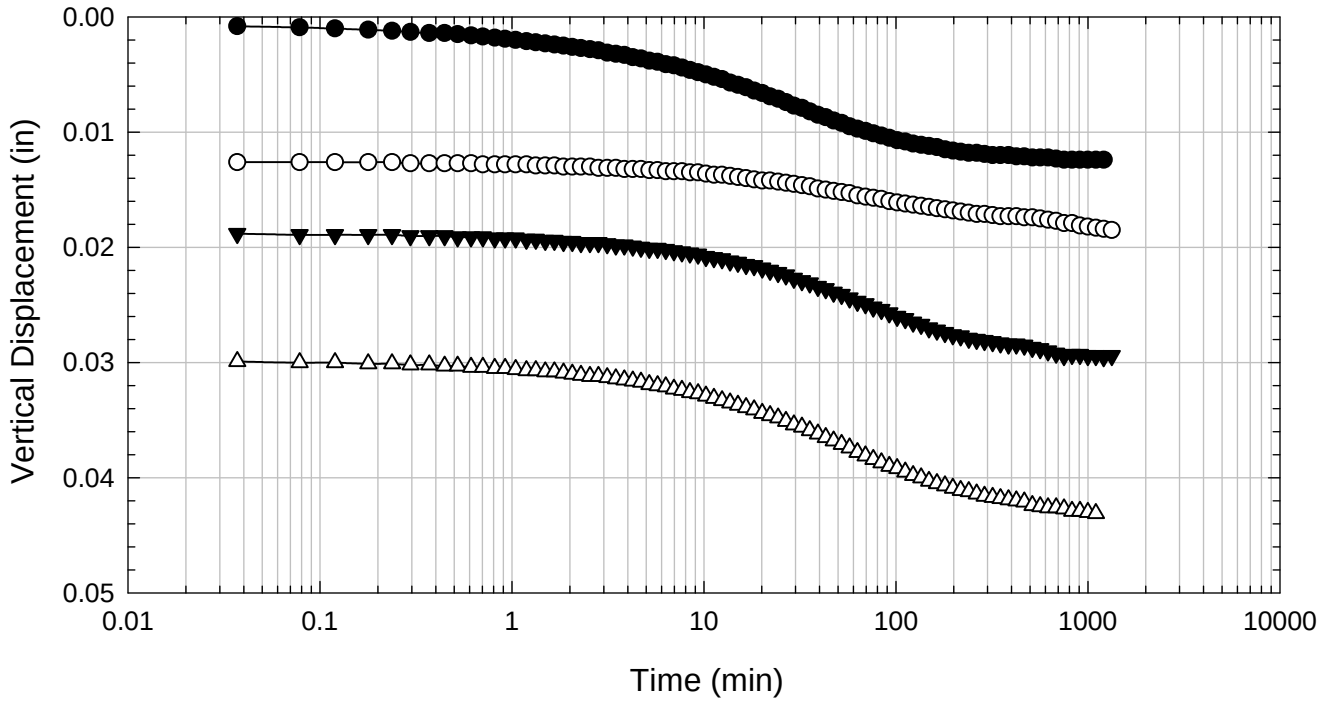
Texas 4 - Blenderized - 848 psf
Vertical Displacement (in)
0.00
0.01
0.02
0.03
0.04
0.05
0.01
0.1
1
10
100
1000
10000
Time (min)

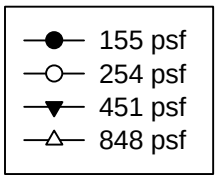
155 psf
254 psf
451 psf
848 psf

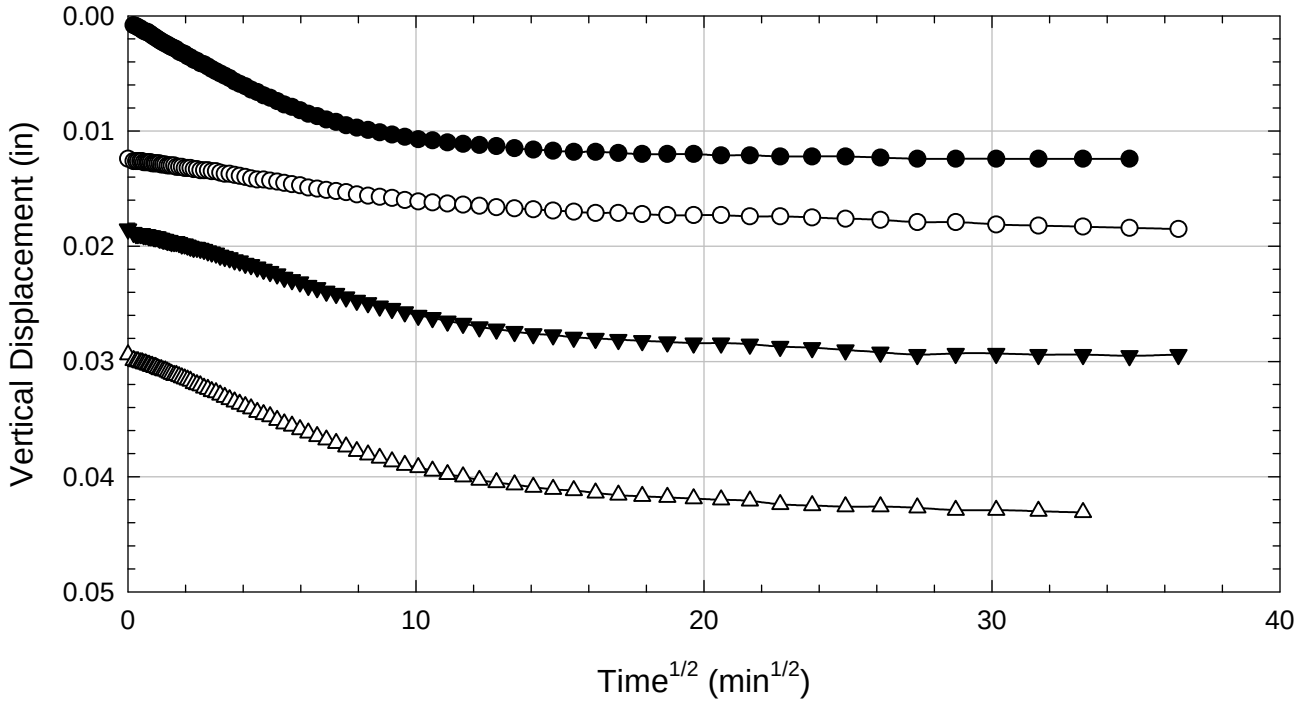
Vertical Displacement (in)
0.00
0.01
0.02
0.03
0.04
0.05
0
10
20
30
40
Time^1/2 (min^1/2)

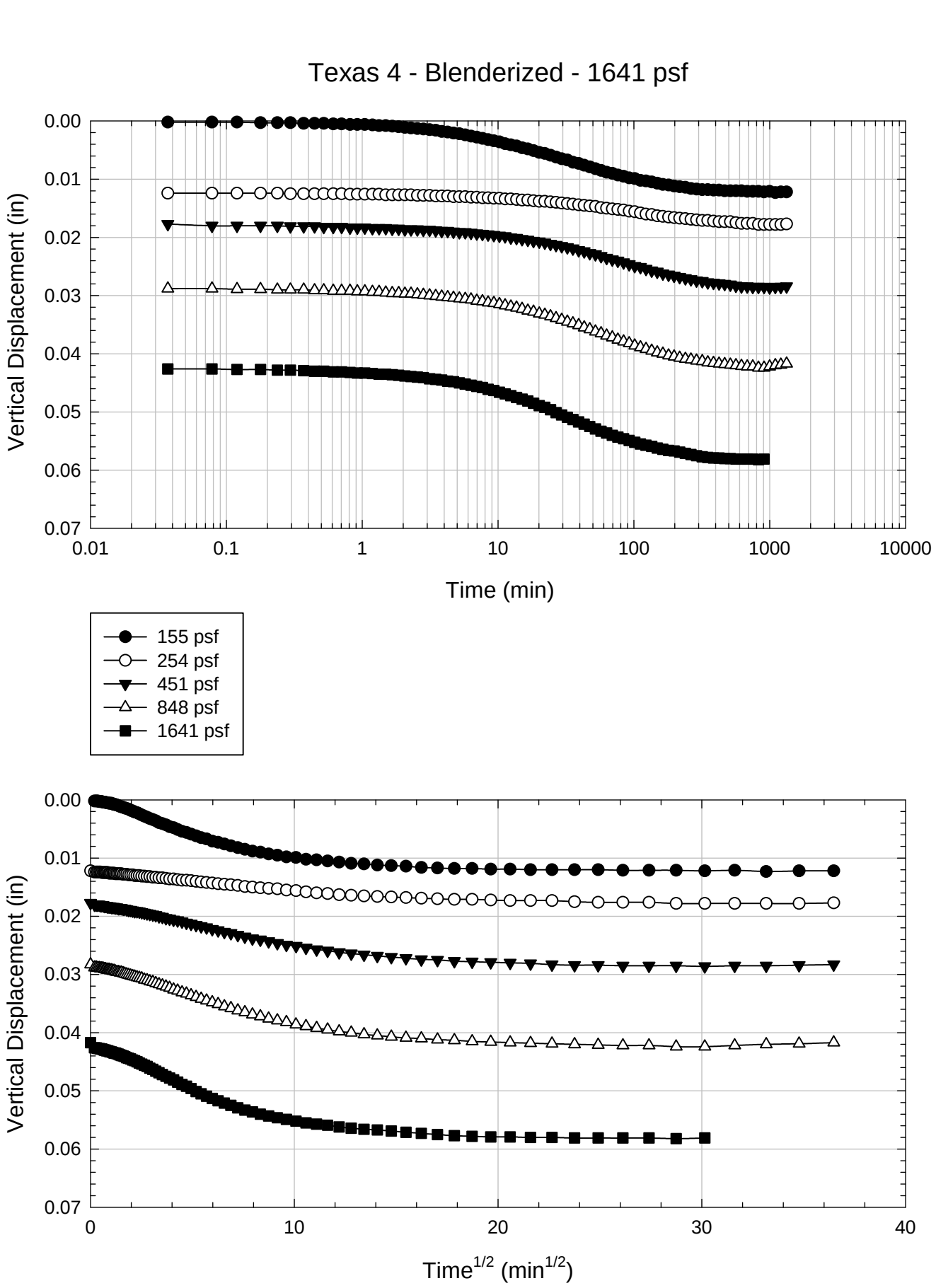
Texas 4 - Blenderized - 1641 psf
Vertical Displacement (in)
0.00
0.01
0.02
0.03
0.04
0.05
0.06
0.07
0.01
0.1
1
10
100
1000
10000
Time (min)
155 psf
254 psf
451 psf
848 psf
1641 psf
Vertical Displacement (in)
0.00
0.01
0.02
0.03
0.04
0.05
0.06
0.07
0
10
20
30
40
Time^1/2 (min^1/2)

Texas 4 - Blenderized - 3213 psf

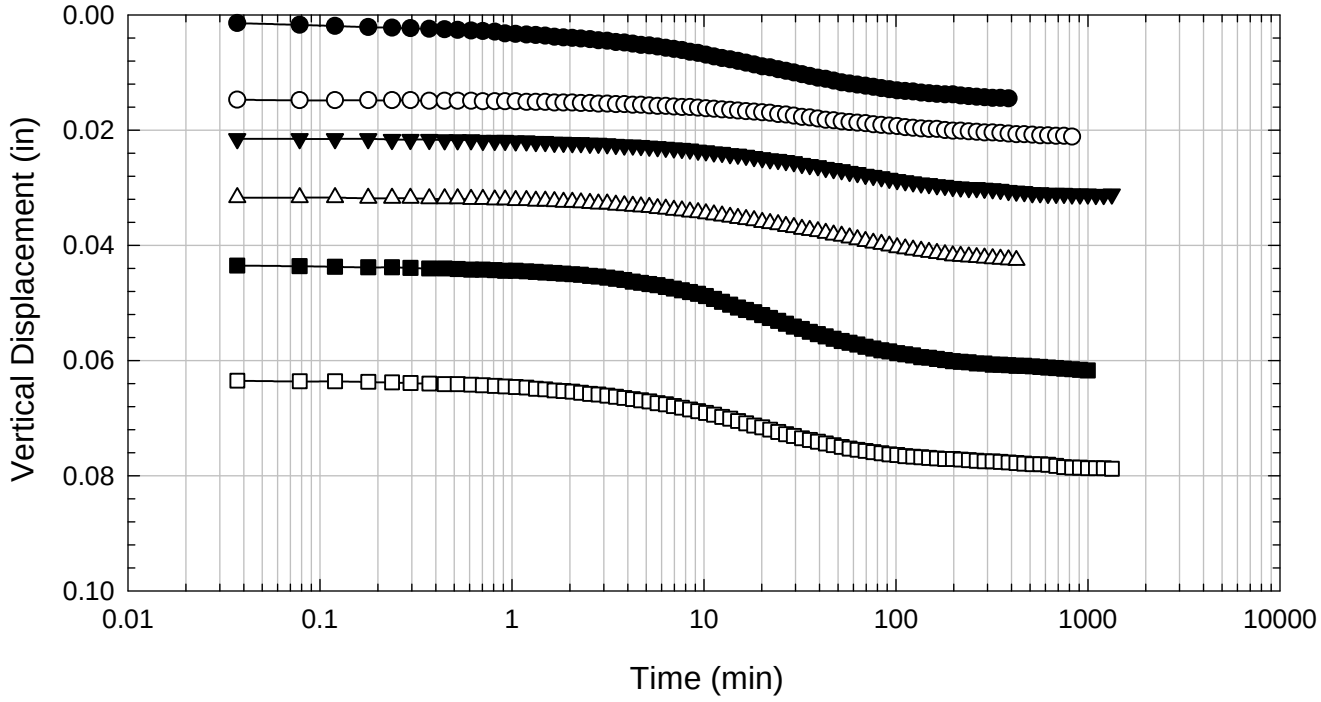

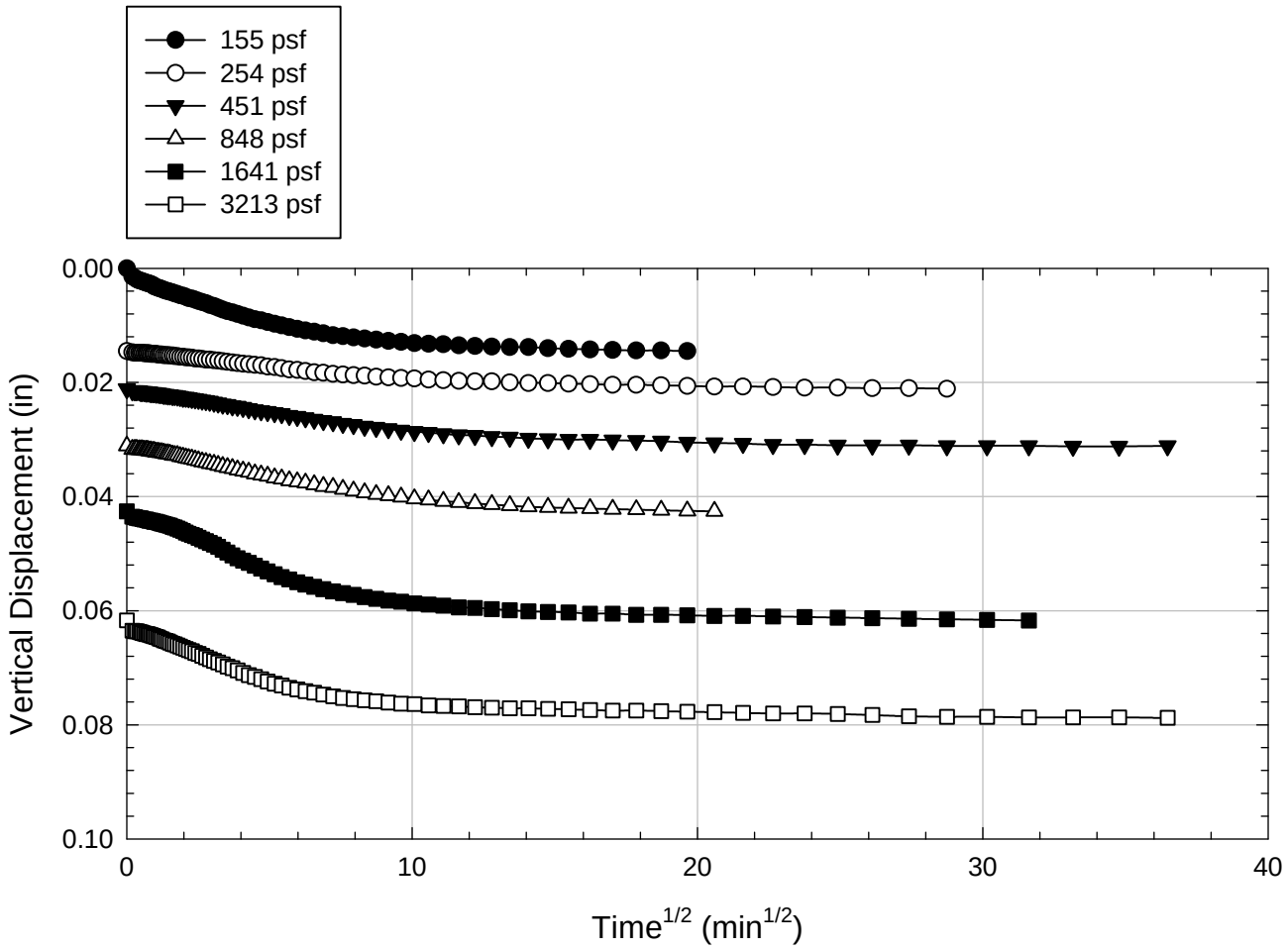

Texas 4 - Blenderized

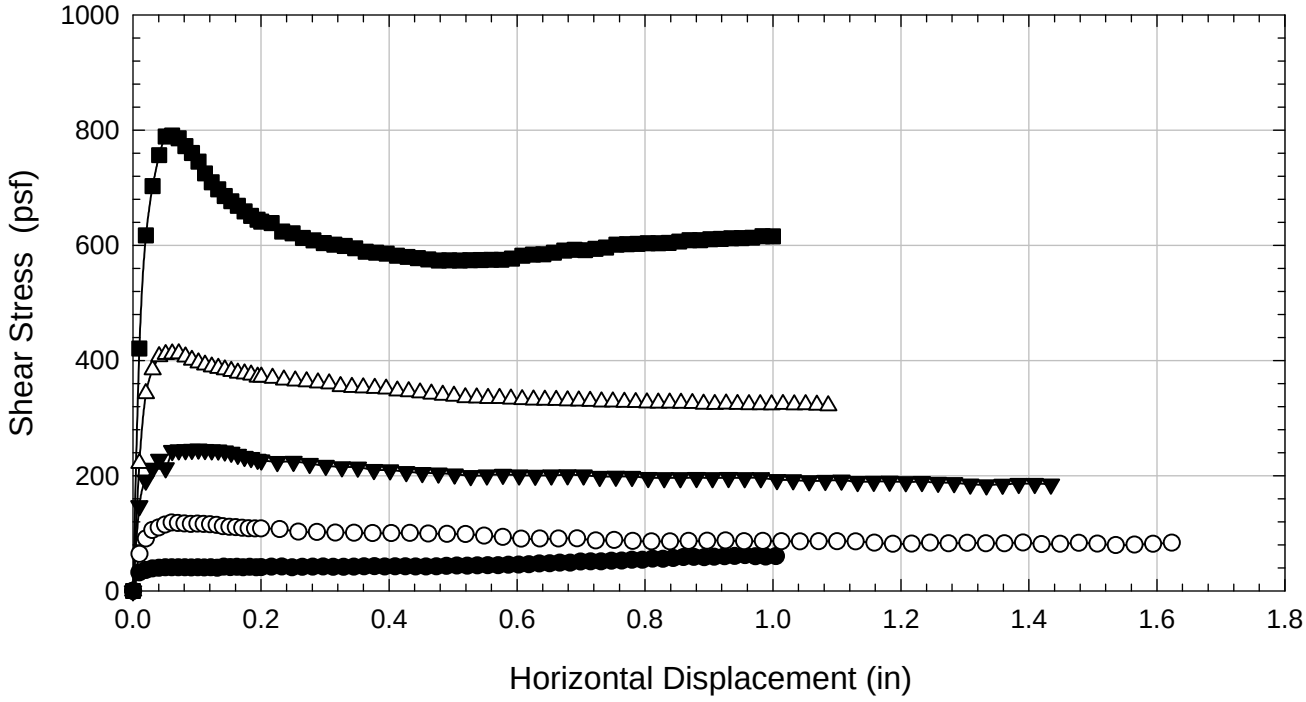

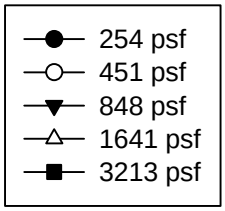

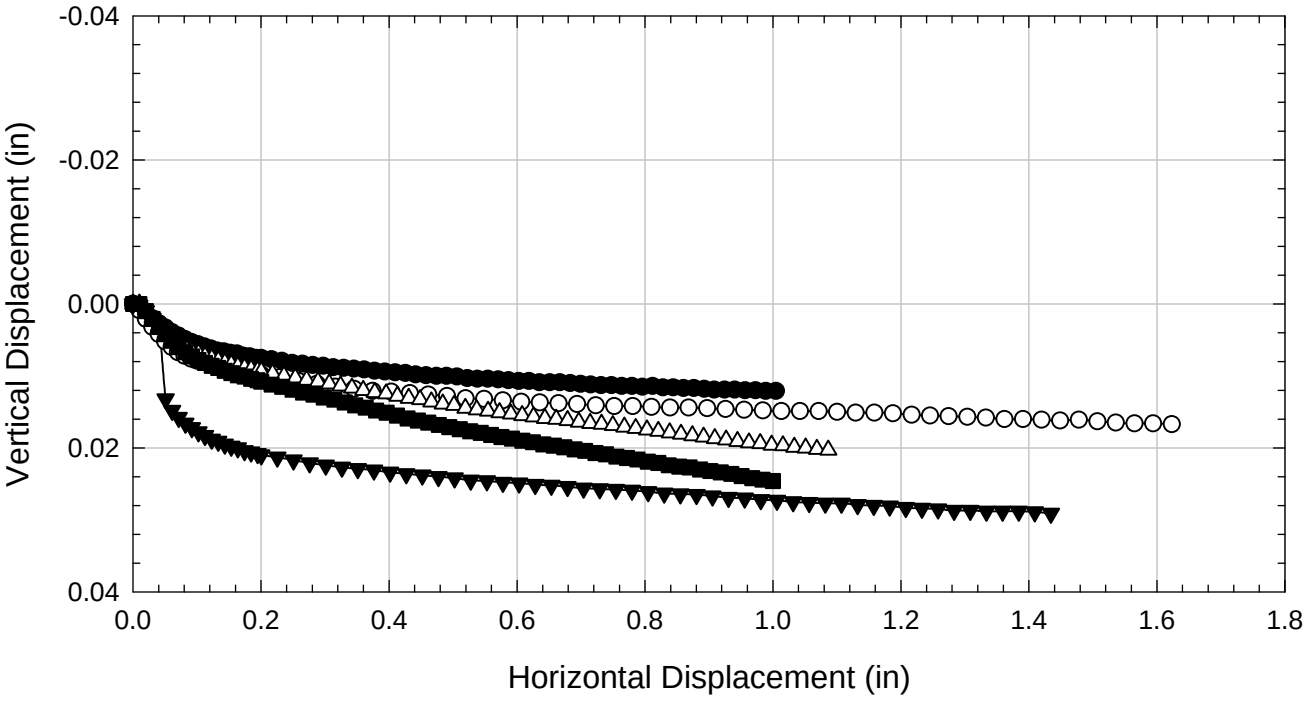

D.12. Texas 5

D.12.1 Blenderized

Virginia Polytechnic Institute and State University
Geotechnical Engineering Laboratory
Ring Shear Data Sheet

Project:	Fully Softened Shear Strength
Sample I.D./Loc.:	Texas 5 - Blenderized
Classification:	Fat Clay (CH)

Sample Preparation	Remolded at LL

Specific Gravity	2.86	
Shear Device Used	WF Bromhead Ring Shear	

Test Number	1	2	3	4	5	6	7	
Start Date (m/d/y)	5/31/2011	5/12/2011	5/16/2011	5/25/2011	5/19/2011	8/19/2011		
End Date (m/d/y)	6/1/2011	5/16/2011	5/19/2011	5/31/2011	5/22/2011	8/24/2011		
Consolidation Pressure (psf)	253	451	847	1638	3225	6281		
Initial Values								
Initial Height (in)	0.20	0.20	0.20	0.20	0.20	0.20		
Inner Radius (in)	1.38	1.38	1.38	1.38	1.38	1.38		
Outer Radius (in)	1.97	1.97	1.97	1.97	1.97	1.97		
Initial Sample Weight (g)	31.87	32.67	32.84	27.89	32.69	26.94		
Water Content (%)	86.83	87.00	87.96	87.13	86.92	79.28		
Dry Unit Weight Before Shear (pcf)	58.8	61.6	65.6	76.1	85.5	96.1		
Saturation (%)	100.0	100.0	100.0	100.0	100.0	100.0		
Consolidation Pressures								
Load 1 (psf)	154	154	154	154	154	155		
Load 2 (psf)	253	253	253	253	253	254		
Load 3 (psf)		451	451	451	451	451		
Load 4 (psf)			847	847	847	848		
Load 5 (psf)				1638	1638	1641		
Load 6 (psf)					3225	3213		
Load 7 (psf)						6281		
t_{50}								
Max. t_{50} for Load 1 (min)								
Max. t_{50} for Load 2 (min)	11.07							
Max. t_{50} for Load 3 (min)		18.03						
Max. t_{50} for Load 4 (min)			13.71					
Max. t_{50} for Load 5 (min)				7.84				
Max. t_{50} for Load 6 (min)					4.53			
Max. t_{50} for Load 7 (min)						2.69		
Final Values								
Water Content (%)	77.17	67.60	61.15	57.43	54.95	57.37		
Saturation (%)	100.0	100.0	100.0	100.0	100.0	100.0		
Failure								
Test Performed at Shear Rate (in/min)	7.00E-04	7.00E-04	7.00E-04	7.00E-04	7.00E-04	7.00E-04		
Required Shear Rate (in/min)	9.03E-05	2.22E-04	1.60E-04	3.06E-04	5.74E-04	8.18E-04		
Displacement at Failure (in)	0.05	0.20	0.11	0.12	0.13	0.11		
Peak Shear Stress (psf)	63	181	312	568	1008	1929		
Secant Effective Friction Angle (deg)	13.9	21.8	20.2	19.1	17.4	17.1		

Comments:

Texas 5 - Blenderized - 253 psf

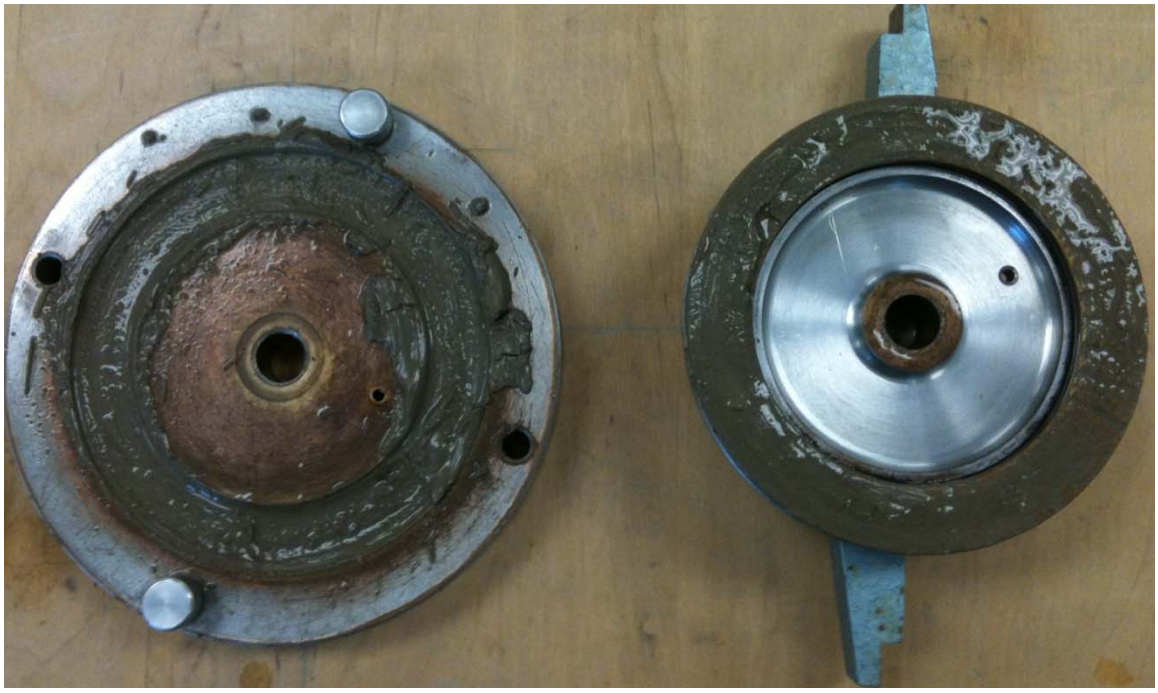

Texas 5 - Blenderized - 451 psf

Texas 5 - Blenderized - 847 psf

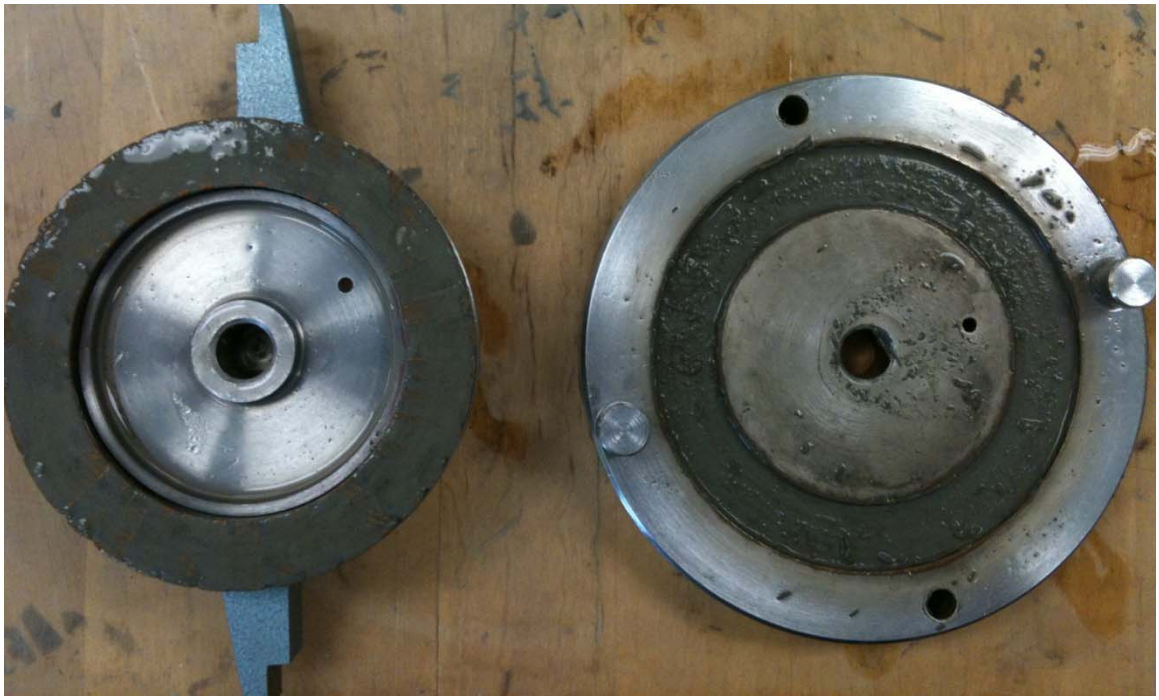

Texas 5 - Blenderized - 1638 psf

Texas 5 - Blenderized - 3225 psf

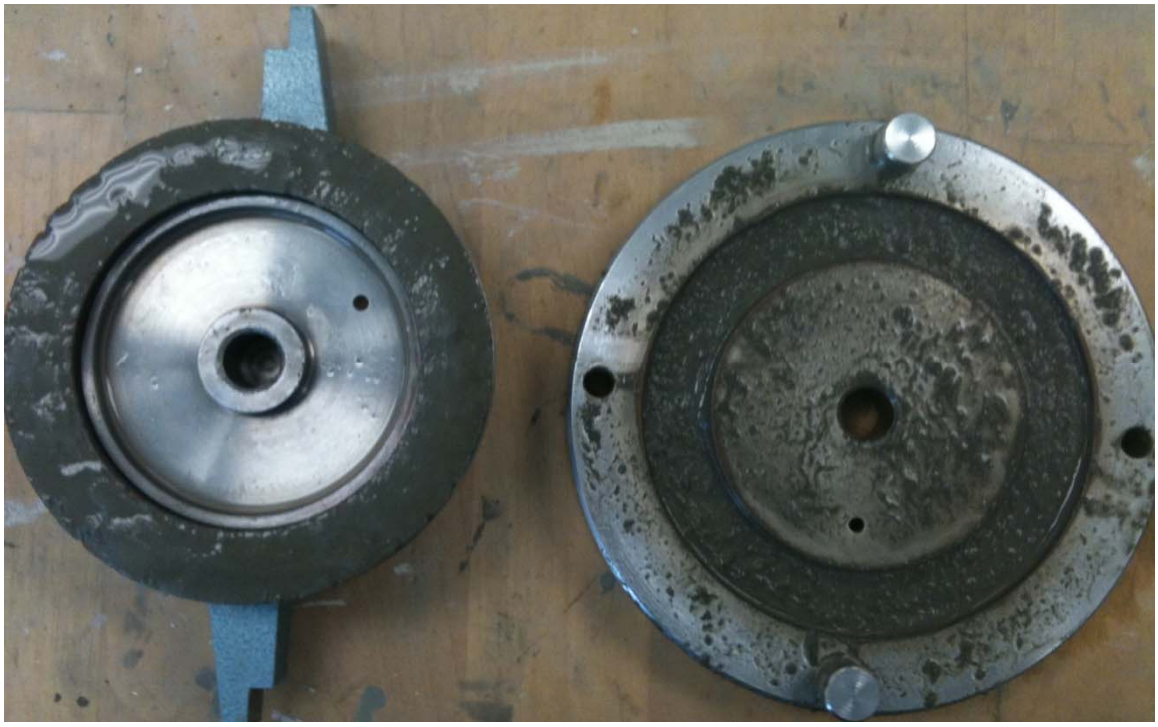

Texas 5 - Blenderized - 6281 psf

Texas 5 - Blenderized - 253 psf

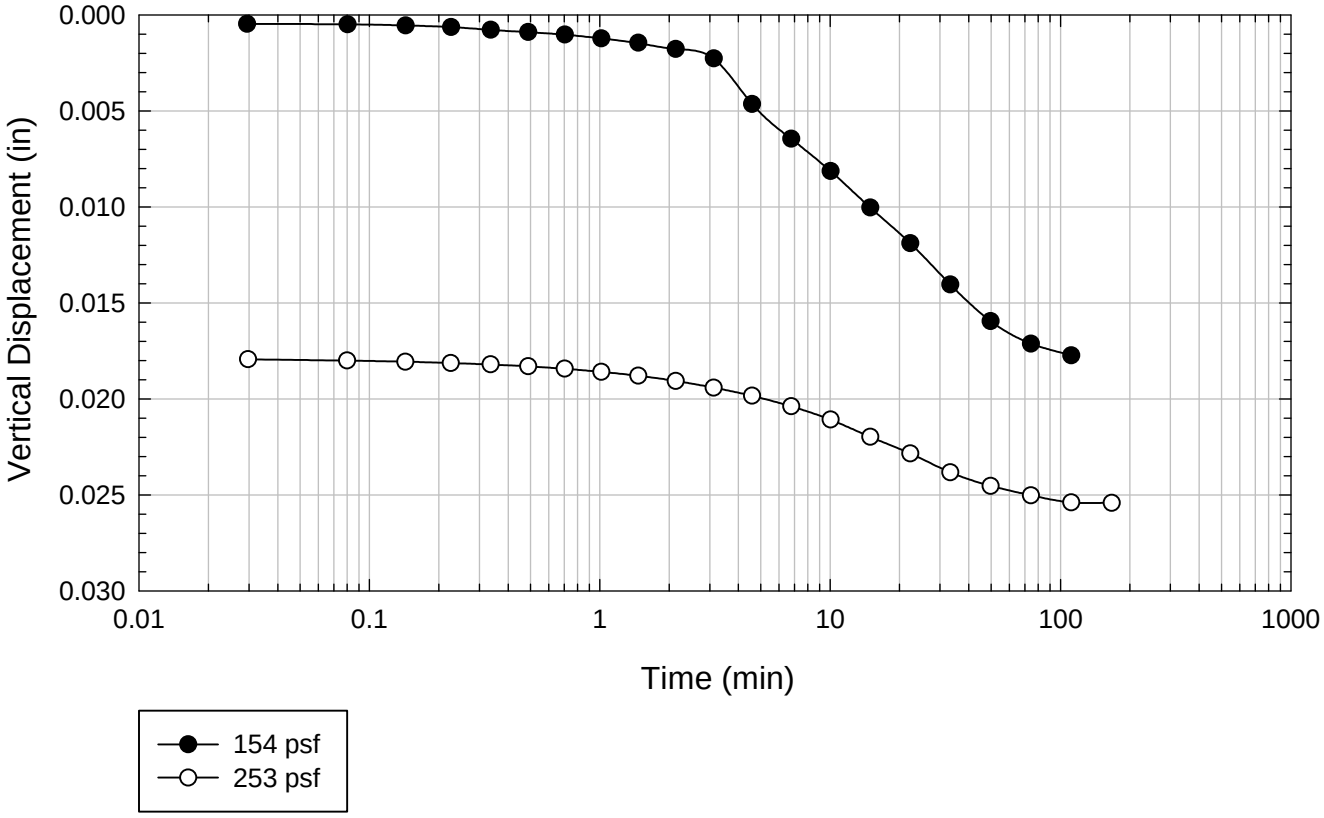

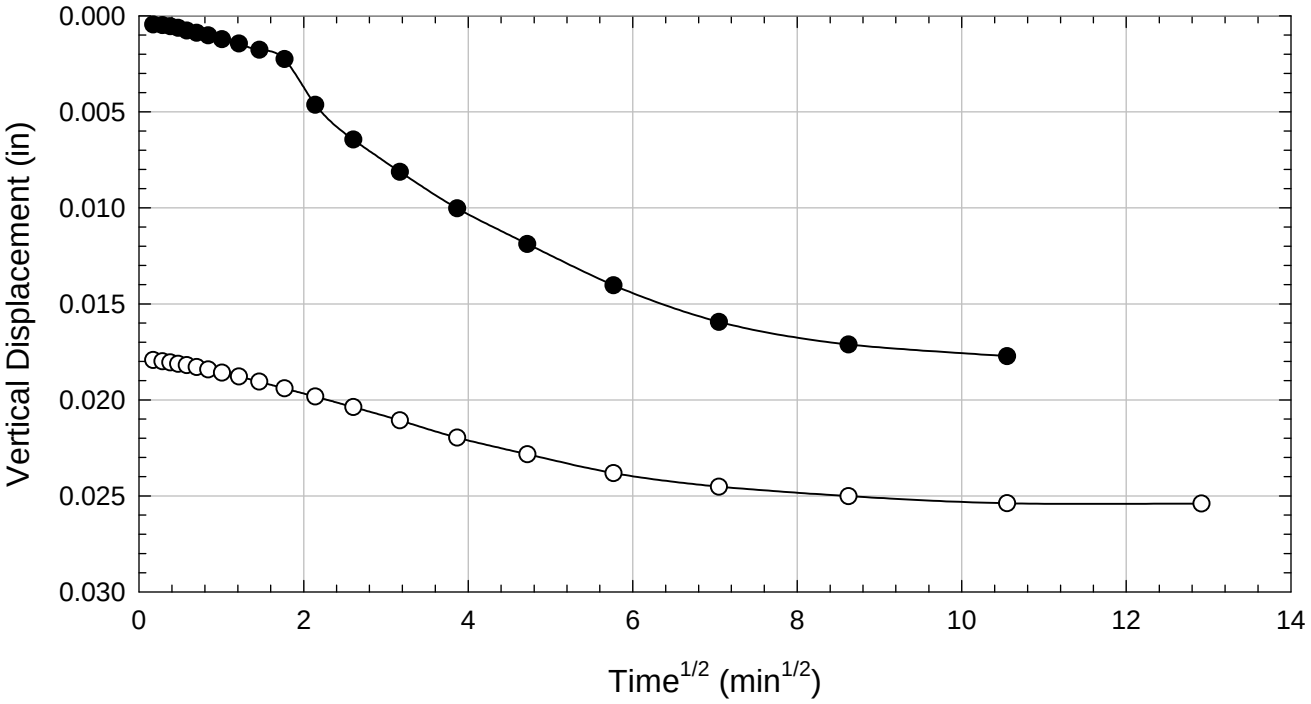

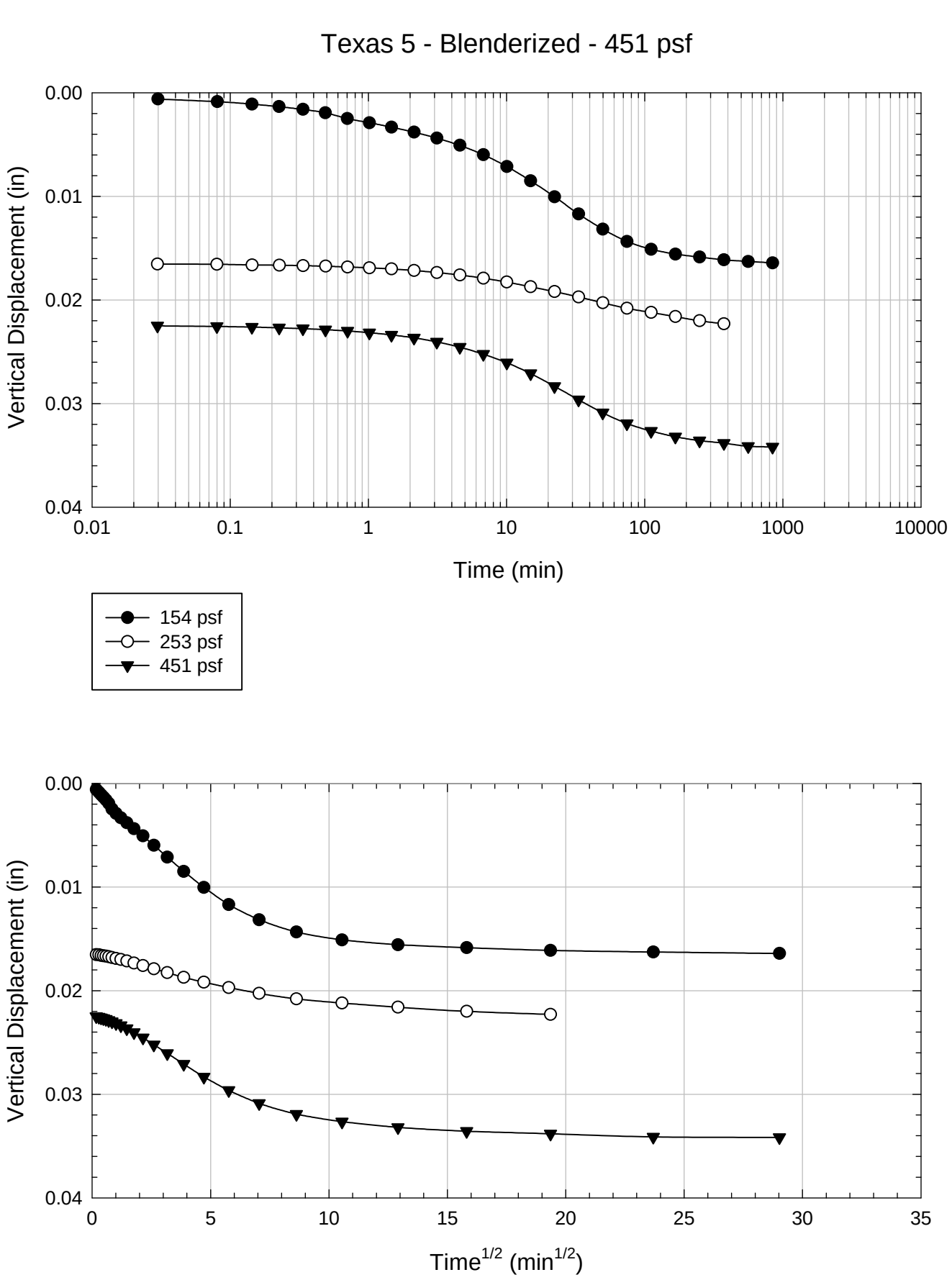
Texas 5 - Blenderized - 451 psf
Vertical Displacement (in)
0.00
0.01
0.02
0.03
0.04
0.01
0.1
1
10
100
1000
10000
Time (min)
154 psf
253 psf
451 psf
Vertical Displacement (in)
0.00
0.01
0.02
0.03
0.04
0
5
10
15
20
25
30
35
Time^1/2 (min^1/2)

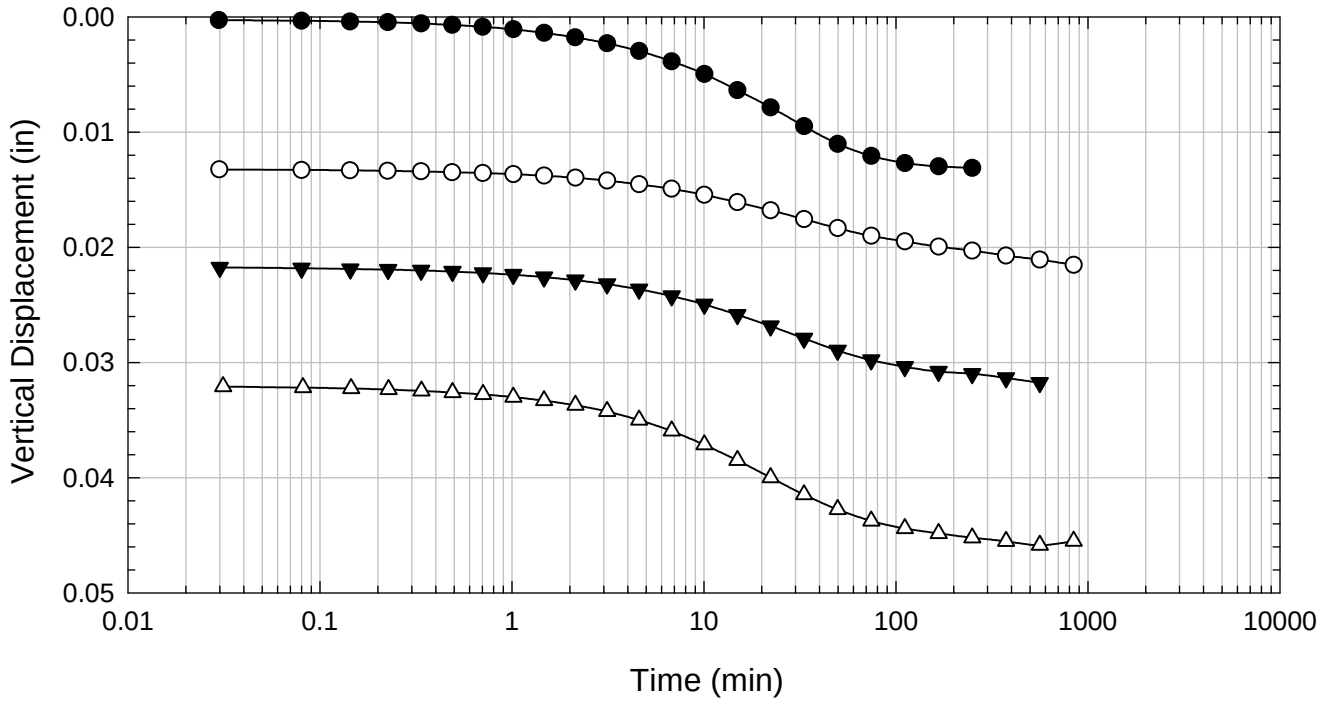
Texas 5 - Blenderized - 847 psf
Vertical Displacement (in)
0.00
0.01
0.02
0.03
0.04
0.05
0.01
0.1
1
10
100
1000
10000
Time (min)

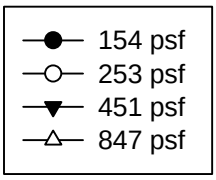
154 psf
253 psf
451 psf
847 psf

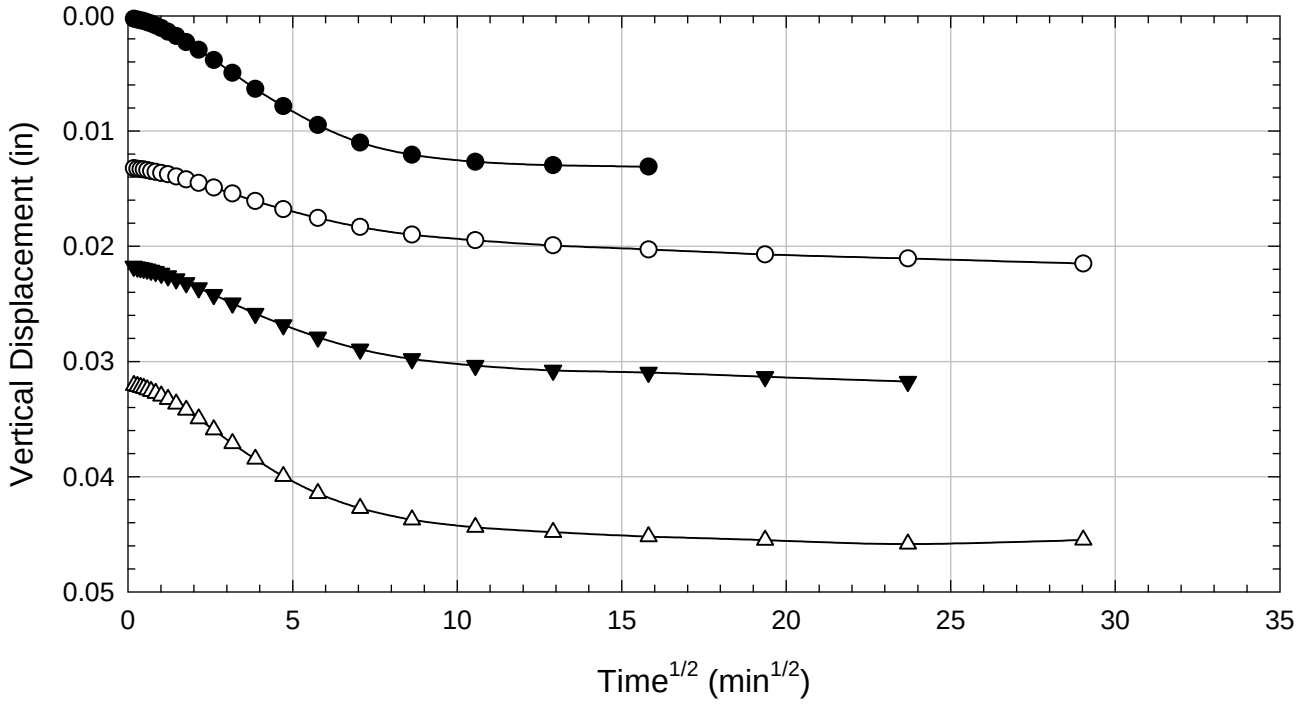
Vertical Displacement (in)
0.00
0.01
0.02
0.03
0.04
0.05
0
5
10
15
20
25
30
35
Time^1/2 (min^1/2)

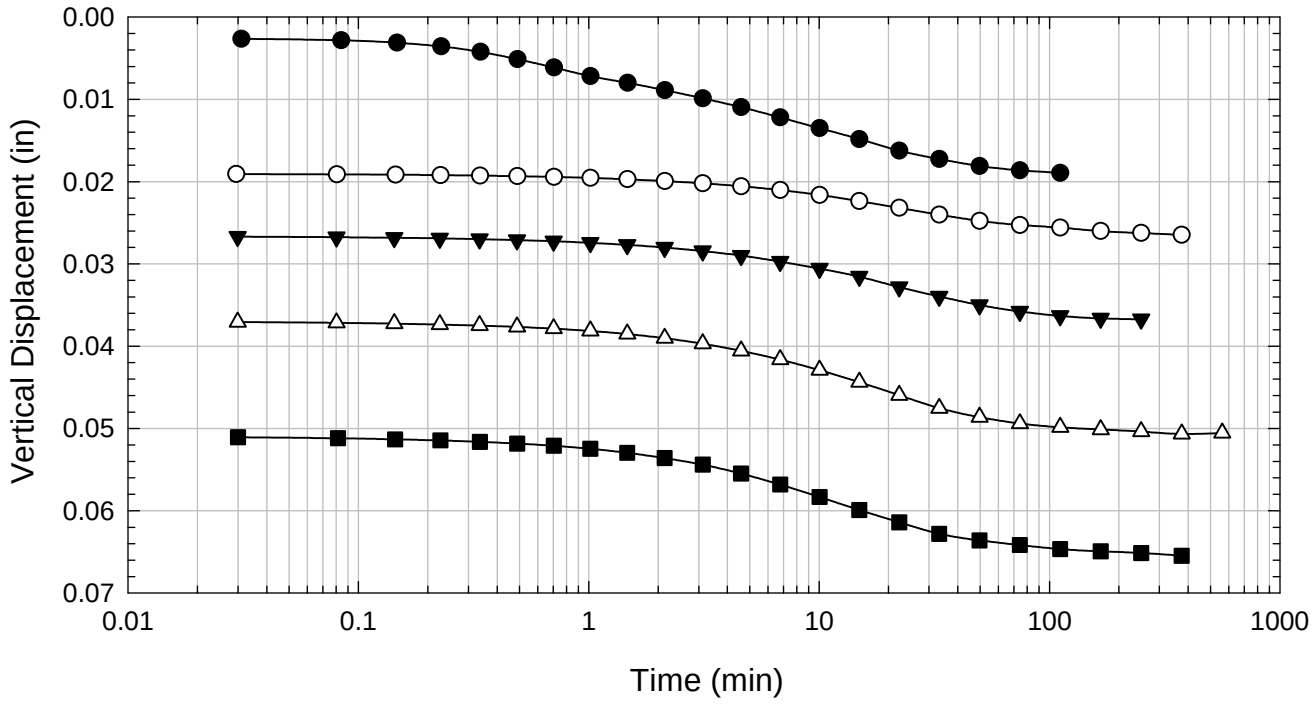
Texas 5 - Blenderized - 1638 psf
Vertical Displacement (in)
0.00
0.01
0.02
0.03
0.04
0.05
0.06
0.07
0.01
0.1
1
10
100
1000
Time (min)

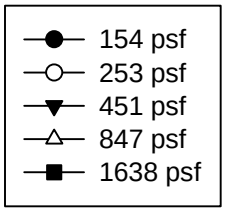
154 psf
253 psf
451 psf
847 psf
1638 psf

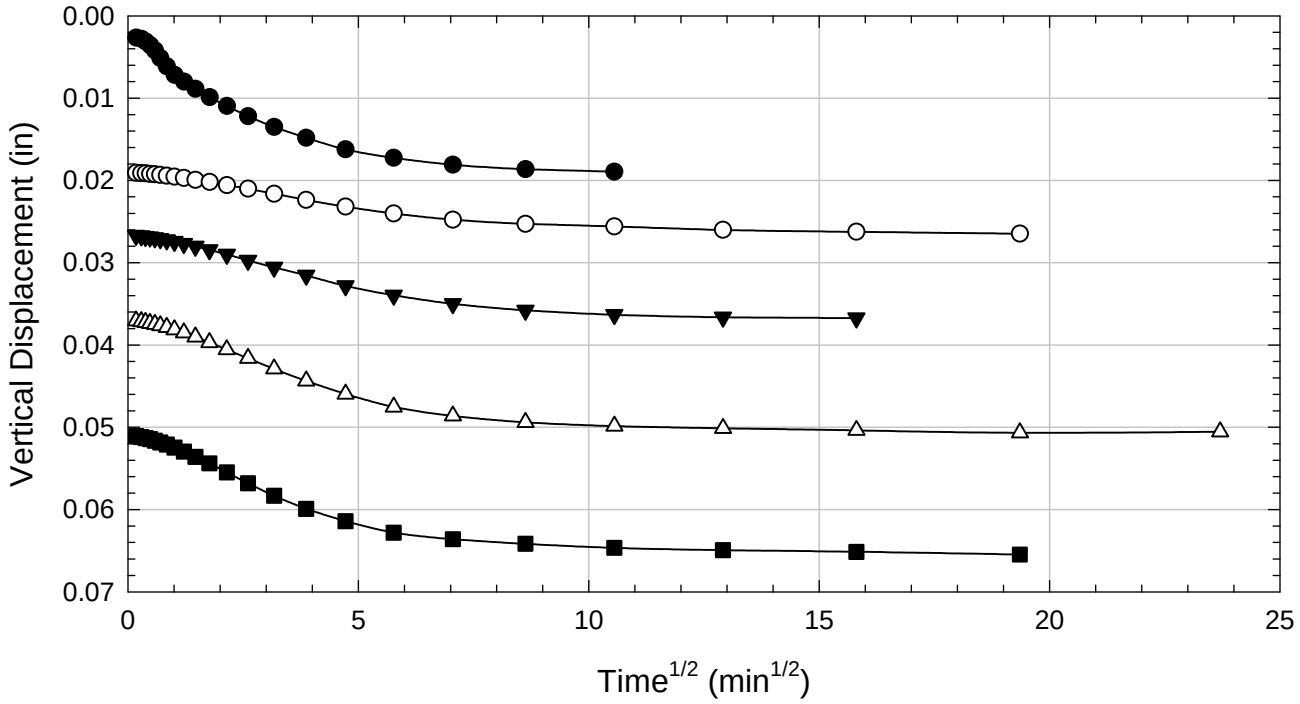
Vertical Displacement (in)
0.00
0.01
0.02
0.03
0.04
0.05
0.06
0.07
0
5
10
15
20
25
Time1/2 (min1/2)

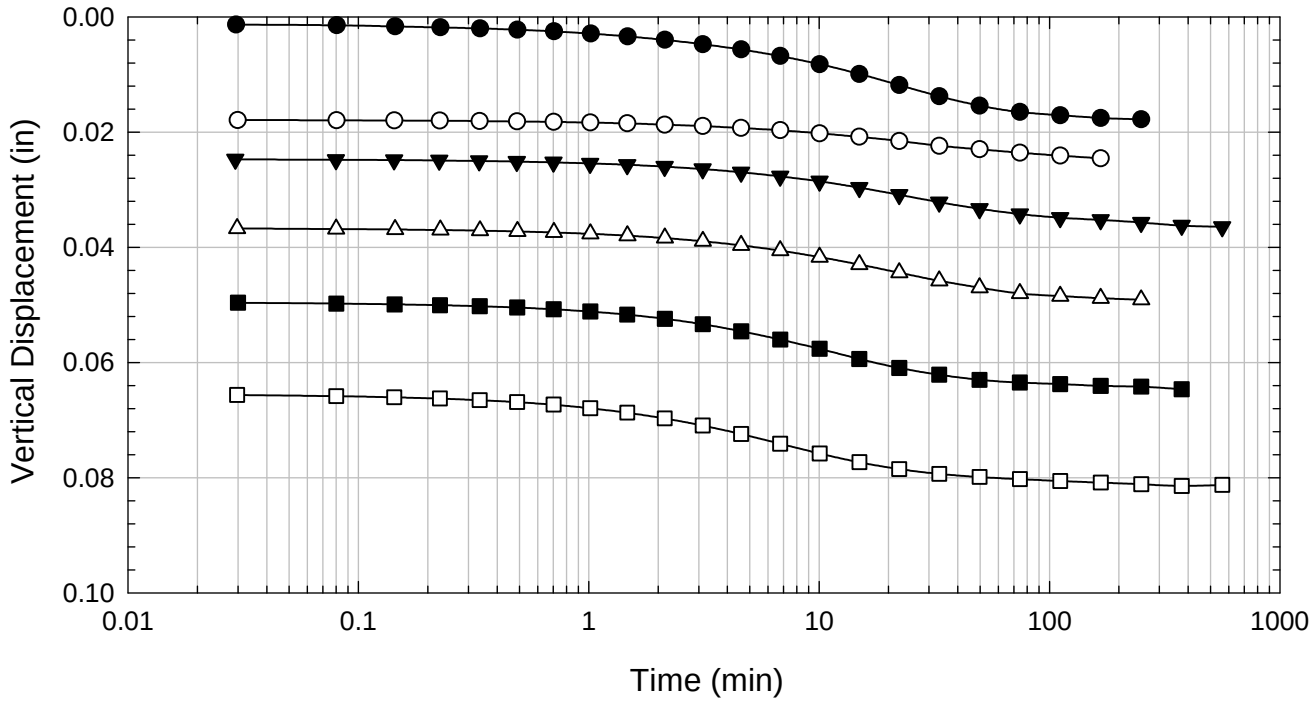
Texas 5 - Blenderized - 3225 psf
Vertical Displacement (in)
0.00
0.02
0.04
0.06
0.08
0.10
0.01
0.1
1
10
100
1000
Time (min)

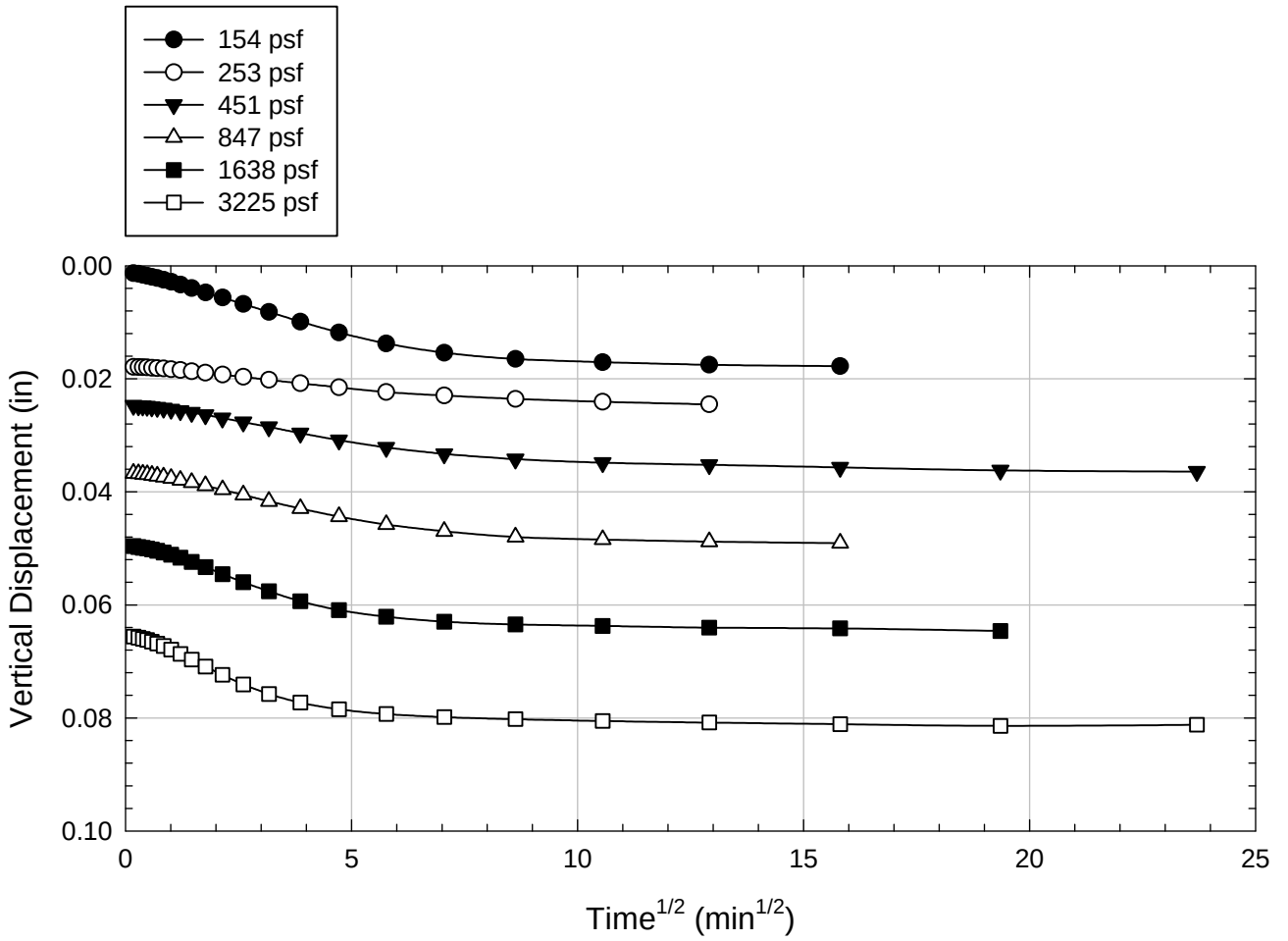
154 psf
253 psf
451 psf
847 psf
1638 psf
3225 psf
Vertical Displacement (in)
0.00
0.02
0.04
0.06
0.08
0.10
0
5
10
15
20
25
Time1/2 (min1/2)

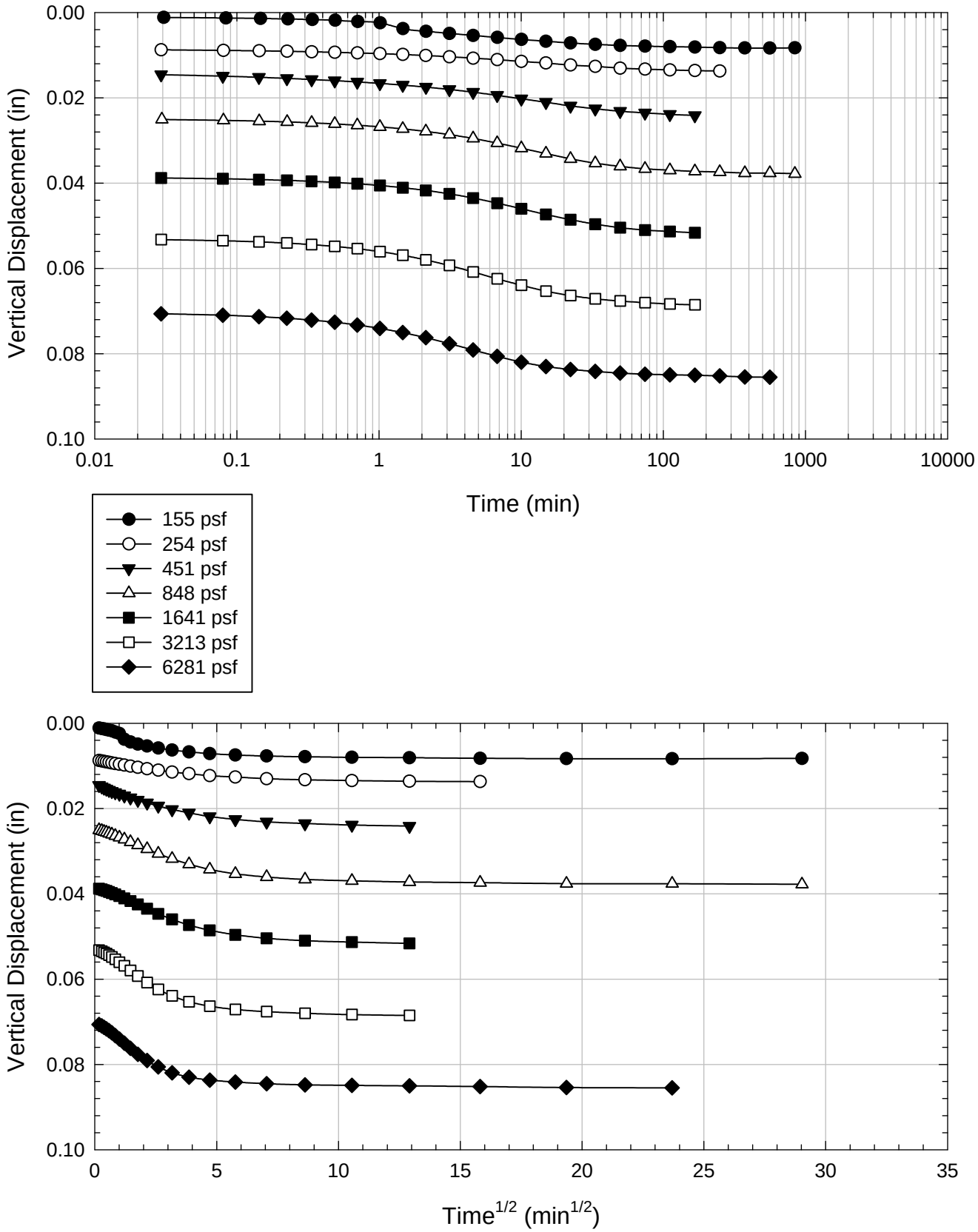
Texas 5 - Blenderized - 6281 psf
Vertical Displacement (in)
0.00
0.02
0.04
0.06
0.08
0.10
0.01
0.1
1
10
100
1000
10000
Time (min)
155 psf
254 psf
451 psf
848 psf
1641 psf
3213 psf
6281 psf
Vertical Displacement (in)
0.00
0.02
0.04
0.06
0.08
0.10
0
5
10
15
20
25
30
35
Time1/2 (min1/2)

Texas 5 - Blenderized

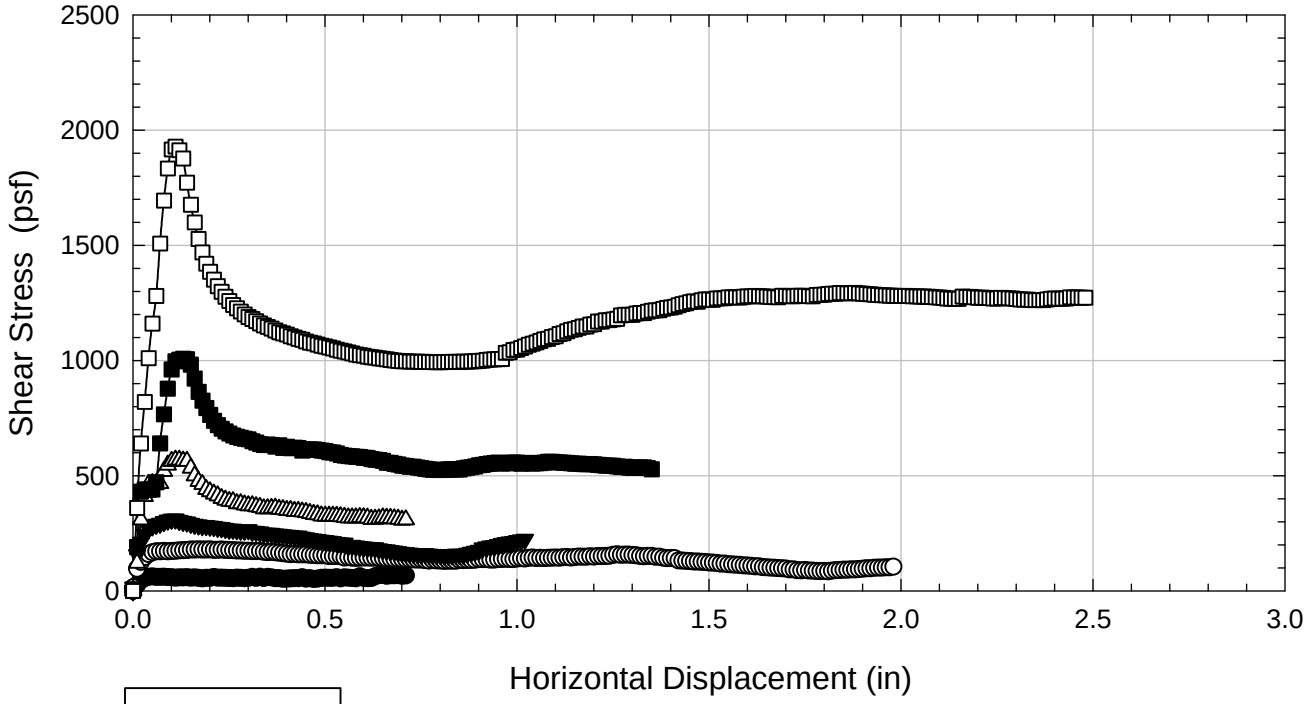

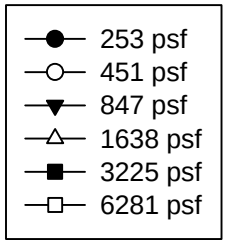

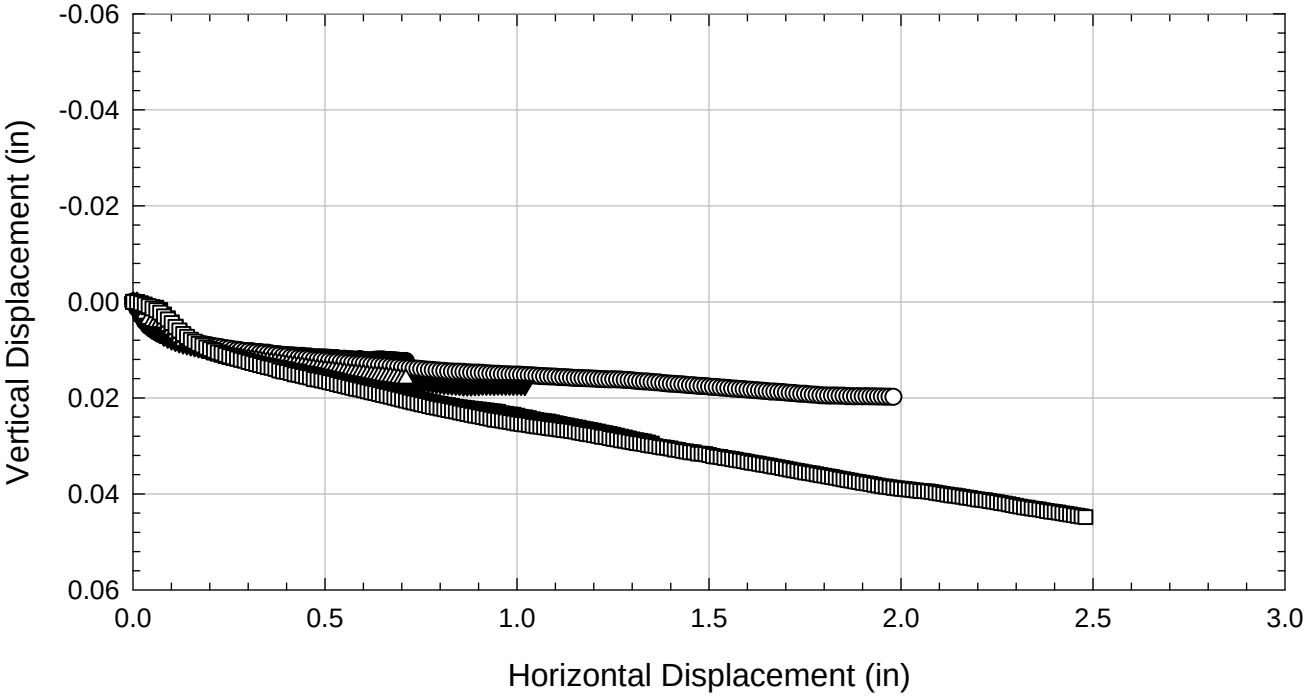

D.13. Texas 6

D.13.1 Blenderized

Virginia Polytechnic Institute and State University
Geotechnical Engineering Laboratory
Ring Shear Data Sheet

Project:	Fully Softened Shear Strength
Sample I.D./Loc.:	Texas 6 - Blenderized
Classification:	Fat Clay (CH)

Sample Preparation	Remolded at LL

Specific Gravity	2.85	
Shear Device Used	WF Bromhead Ring Shear	

Test Number	1	2	3	4	5	6	7	
Start Date (m/d/y)	5/10/2011	4/20/2011	4/24/2011	5/3/2011	4/28/2011	8/8/2011		
End Date (m/d/y)	5/12/2011	4/24/2011	4/28/2011	5/8/2011	5/3/2011	8/13/2011		
Consolidation Pressure (psf)	254	451	848	1641	3213	6281		
Initial Values								
Initial Height (in)	0.20	0.20	0.20	0.20	0.20	0.20		
Inner Radius (in)	1.38	1.38	1.38	1.38	1.38	1.38		
Outer Radius (in)	1.97	1.97	1.97	1.97	1.97	1.97		
Initial Sample Weight (g)	33.27	33.17	33.09	33.10	33.42	33.45		
Water Content (%)	80.04	79.24	79.74	82.26	79.89	68.50		
Dry Unit Weight Before Shear (pcf)	54.2	54.6	54.3	53.2	54.3	60.2		
Saturation (%)	100.0	100.0	100.0	100.0	100.0	100.0		
Consolidation Pressures								
Load 1 (psf)	155	155	155	155	155	155		
Load 2 (psf)	254	254	254	254	254	254		
Load 3 (psf)		451	451	451	451	451		
Load 4 (psf)			848	848	848	848		
Load 5 (psf)				1641	1641	1641		
Load 6 (psf)					3213	3213		
Load 7 (psf)						6281		
t_{50}								
Max. t_{50} for Load 1 (min)								
Max. t_{50} for Load 2 (min)	22.59							
Max. t_{50} for Load 3 (min)		32.88						
Max. t_{50} for Load 4 (min)			19.29					
Max. t_{50} for Load 5 (min)				11.64				
Max. t_{50} for Load 6 (min)					6.58			
Max. t_{50} for Load 7 (min)						3.79		
Final Values								
Water Content (%)	76.48	66.40	59.45	55.00	55.20	57.86		
Saturation (%)	100.0	100.0	100.0	100.0	100.0	100.0		
Failure								
Test Performed at Shear Rate (in/min)	7.00E-04	7.00E-04	7.00E-04	7.00E-04	7.00E-04	7.00E-04		
Required Shear Rate (in/min)	8.85E-05	9.12E-05	1.04E-04	1.72E-04	2.43E-04	5.28E-04		
Displacement at Failure (in)	0.10	0.15	0.10	0.10	0.08	0.10		
Peak Shear Stress (psf)	84	106	255	536	858	1791		
Secant Effective Friction Angle (deg)	18.3	13.2	16.7	18.1	15.0	15.9		

Comments:

Texas 6 - Blenderized - 254 psf

Texas 6 - Blenderized - 451 psf

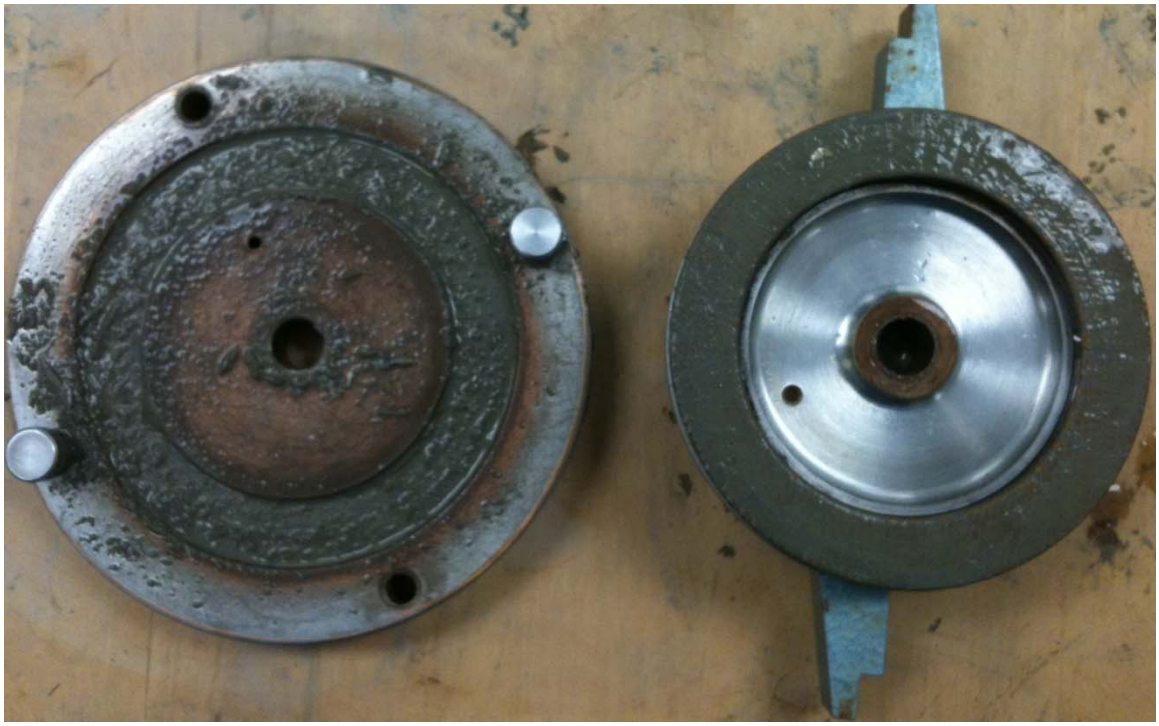

Texas 6 - Blenderized - 848 psf

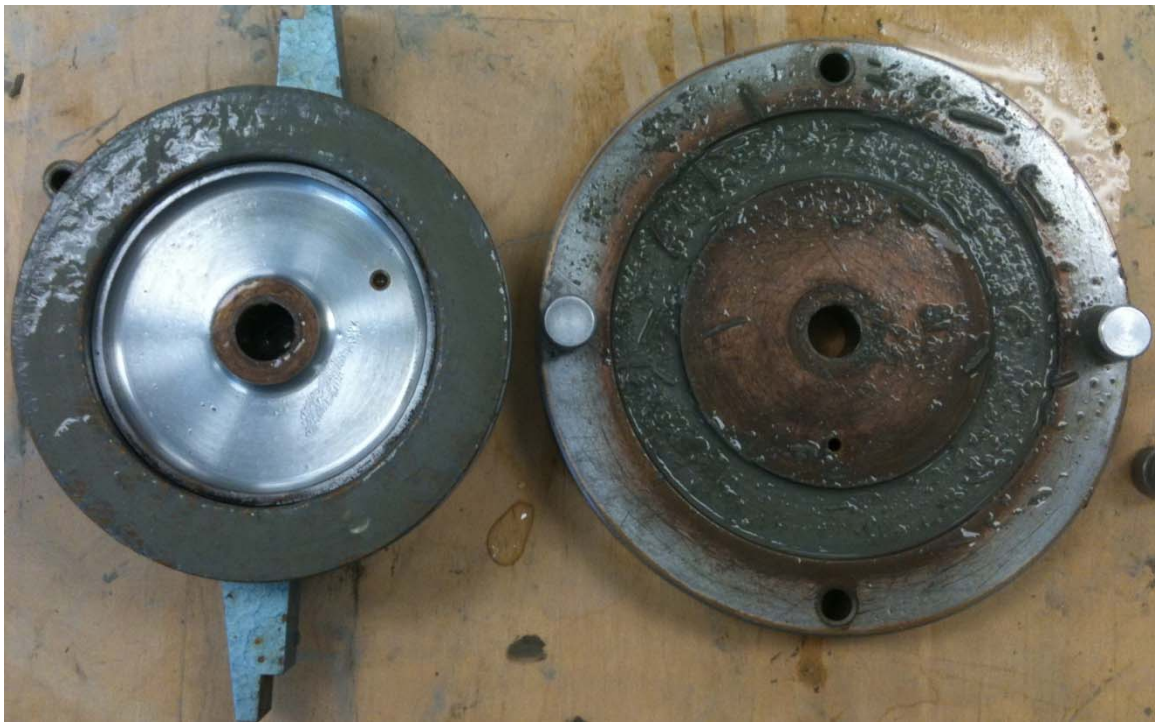

Texas 6 - Blenderized - 1641 psf

Texas 6 - Blenderized - 3213 psf

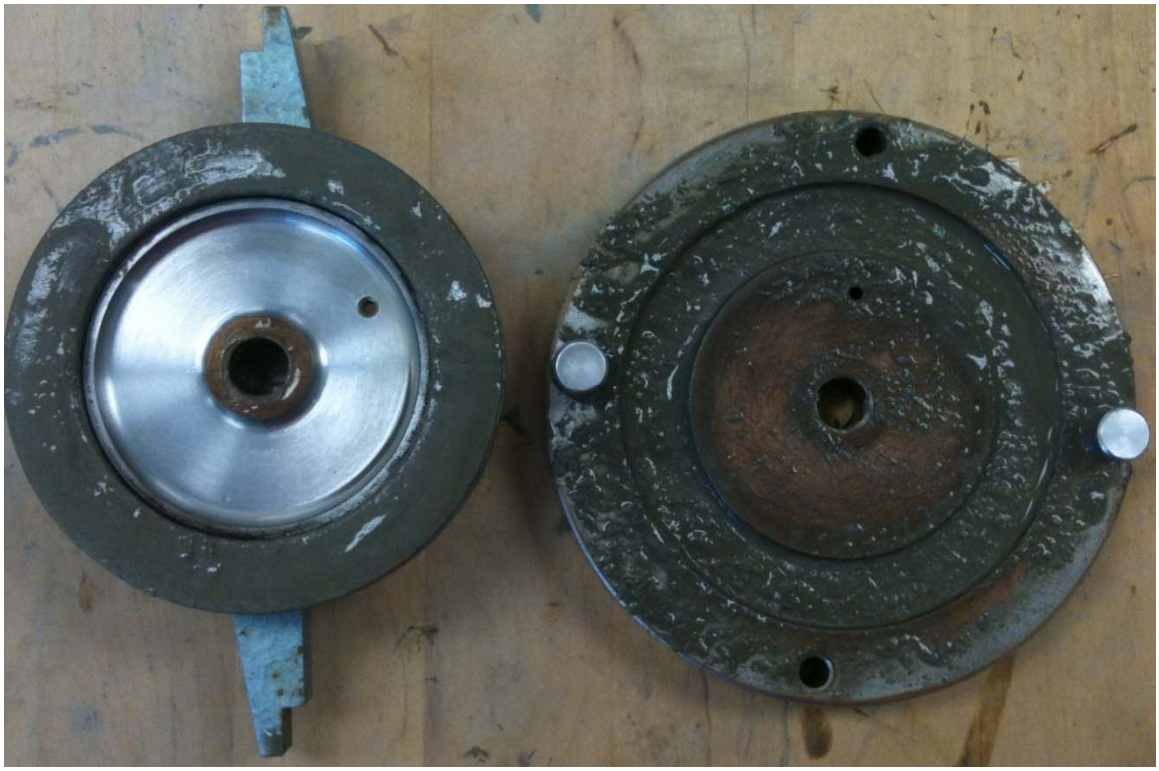

Texas 6 - Blenderized - 6281 psf

Texas 6 - Blenderized - 254 psf

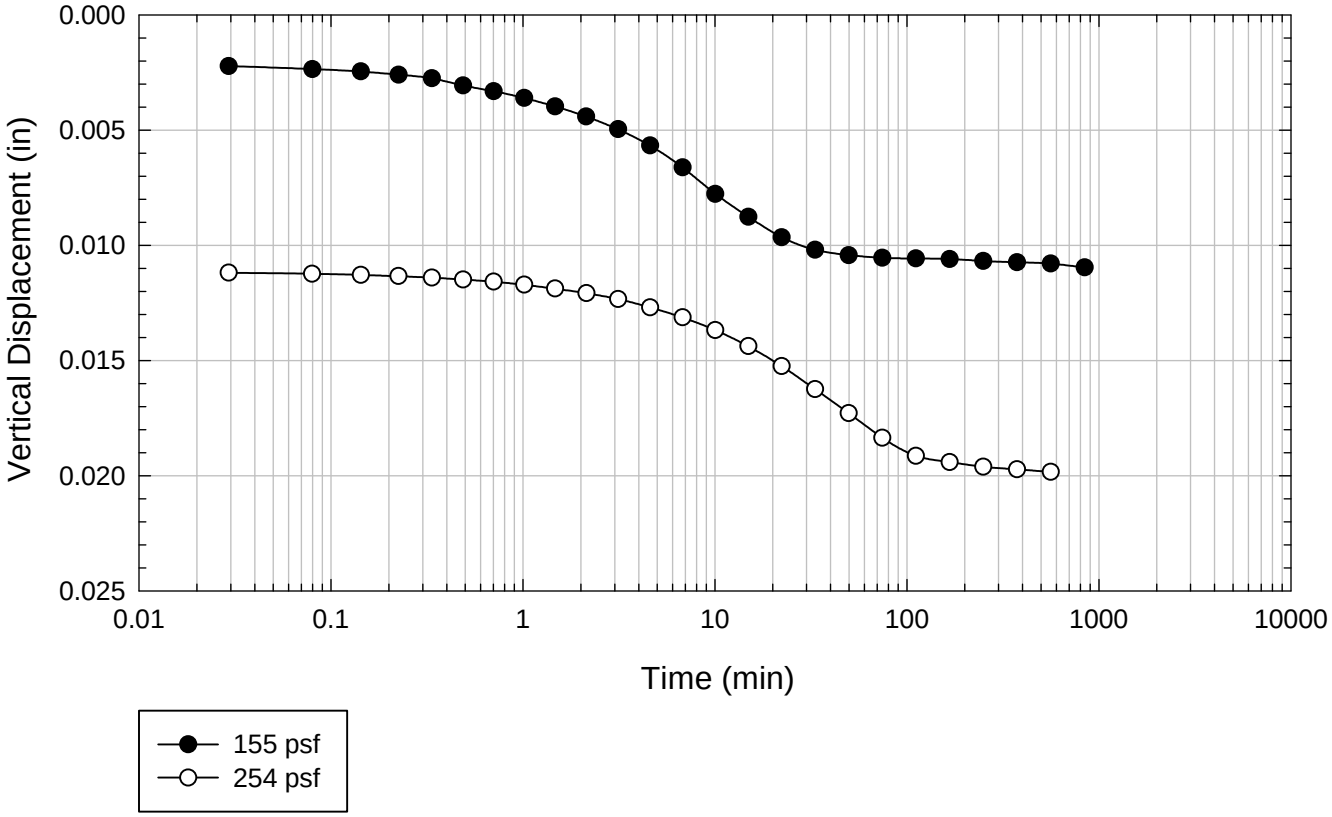

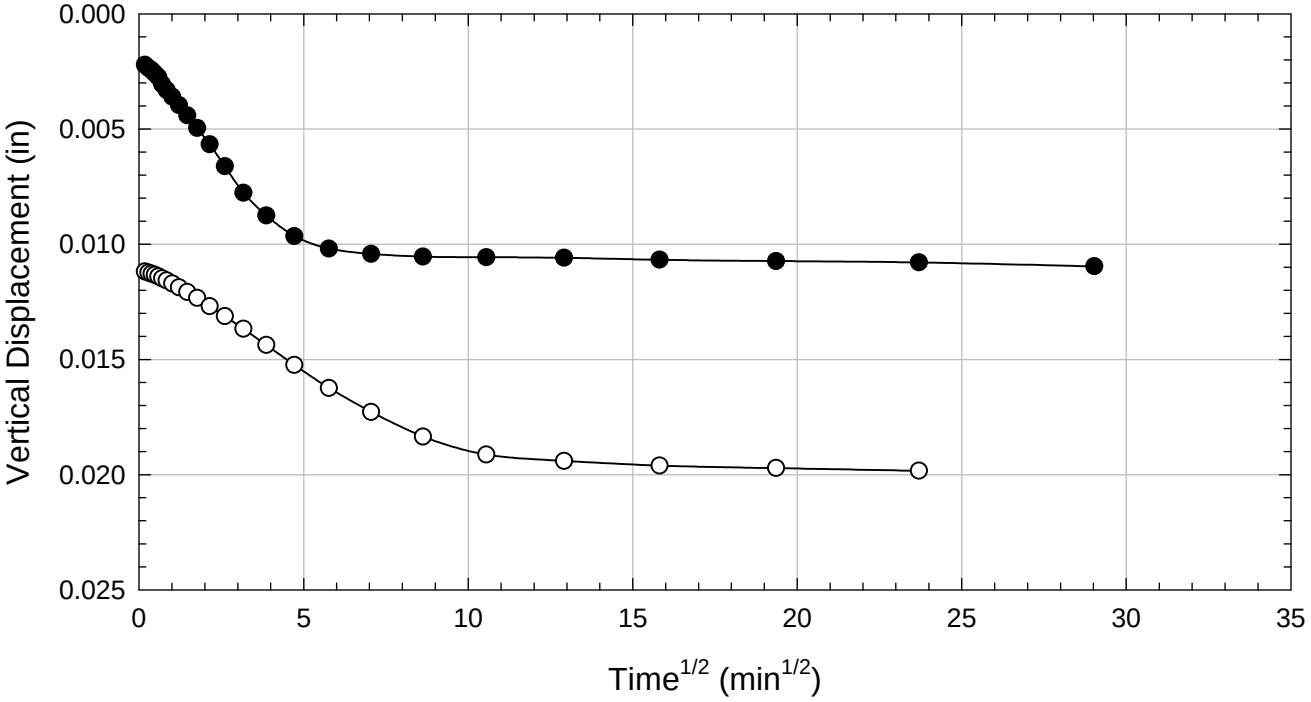

Texas 6 - Blenderized - 451 psf

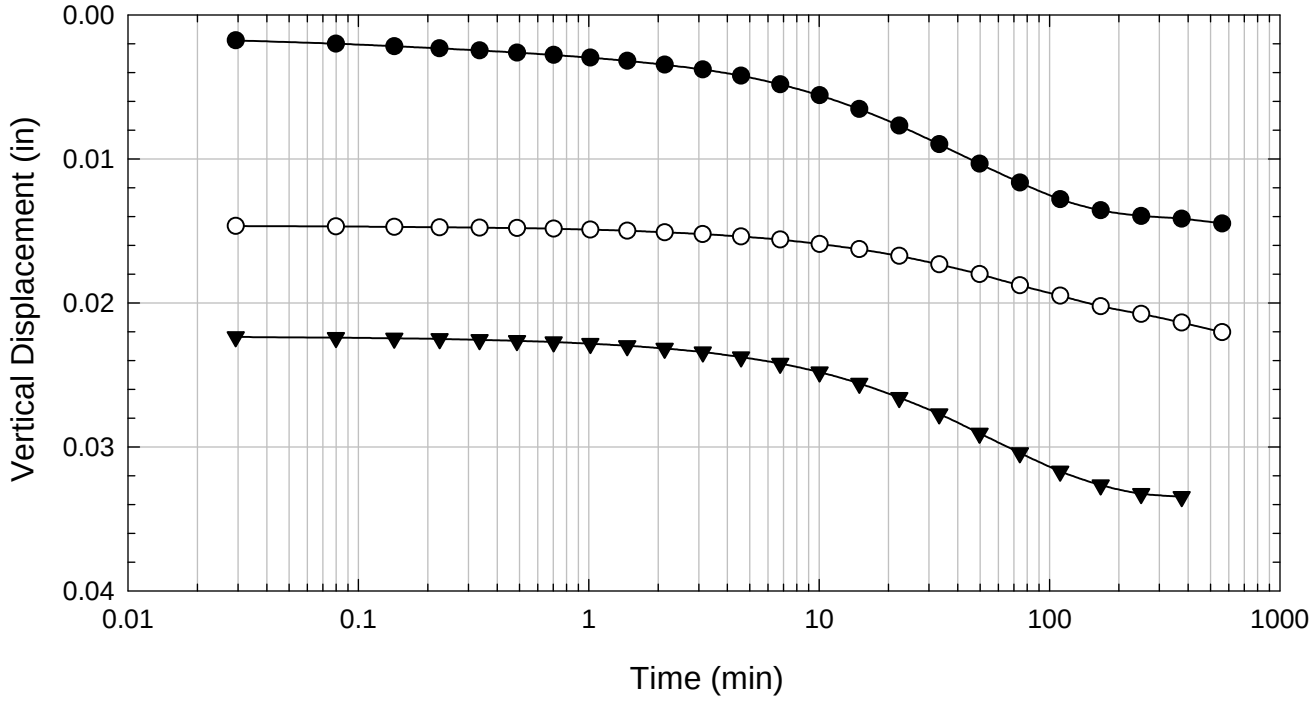

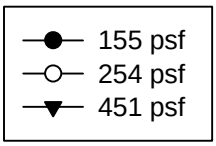

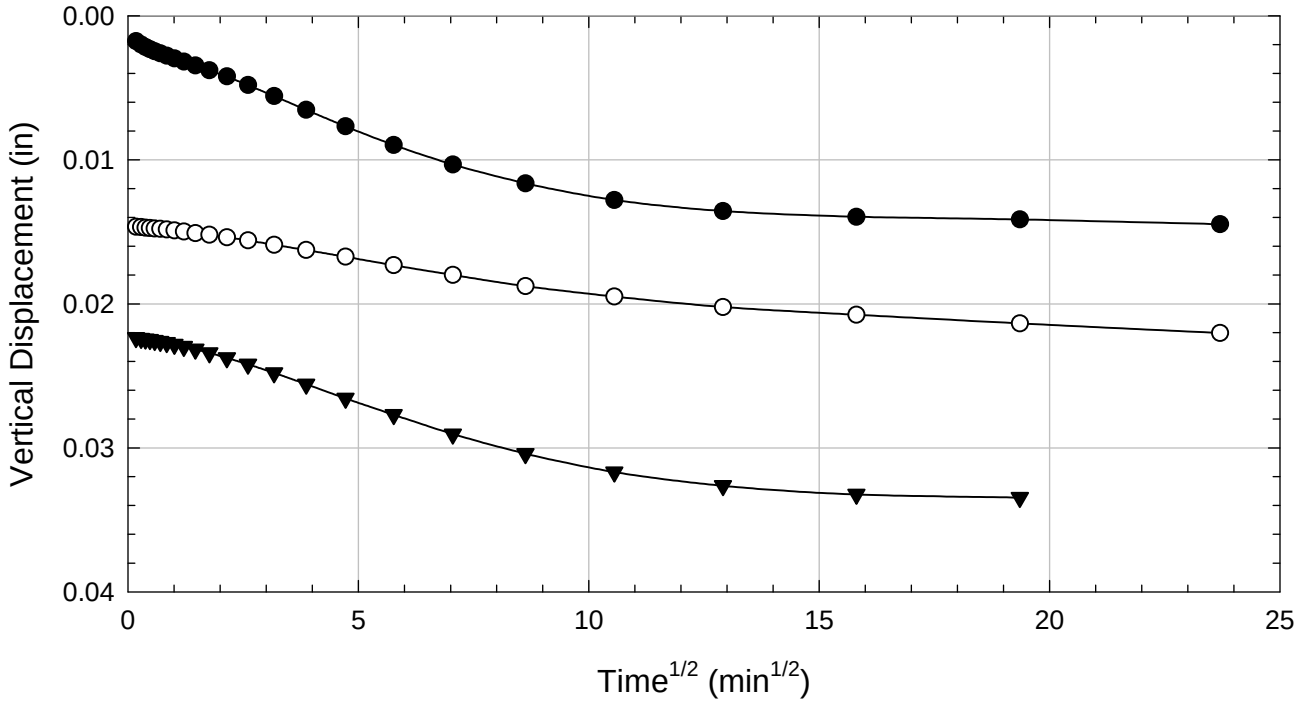

Texas 6 - Blenderized - 848 psf

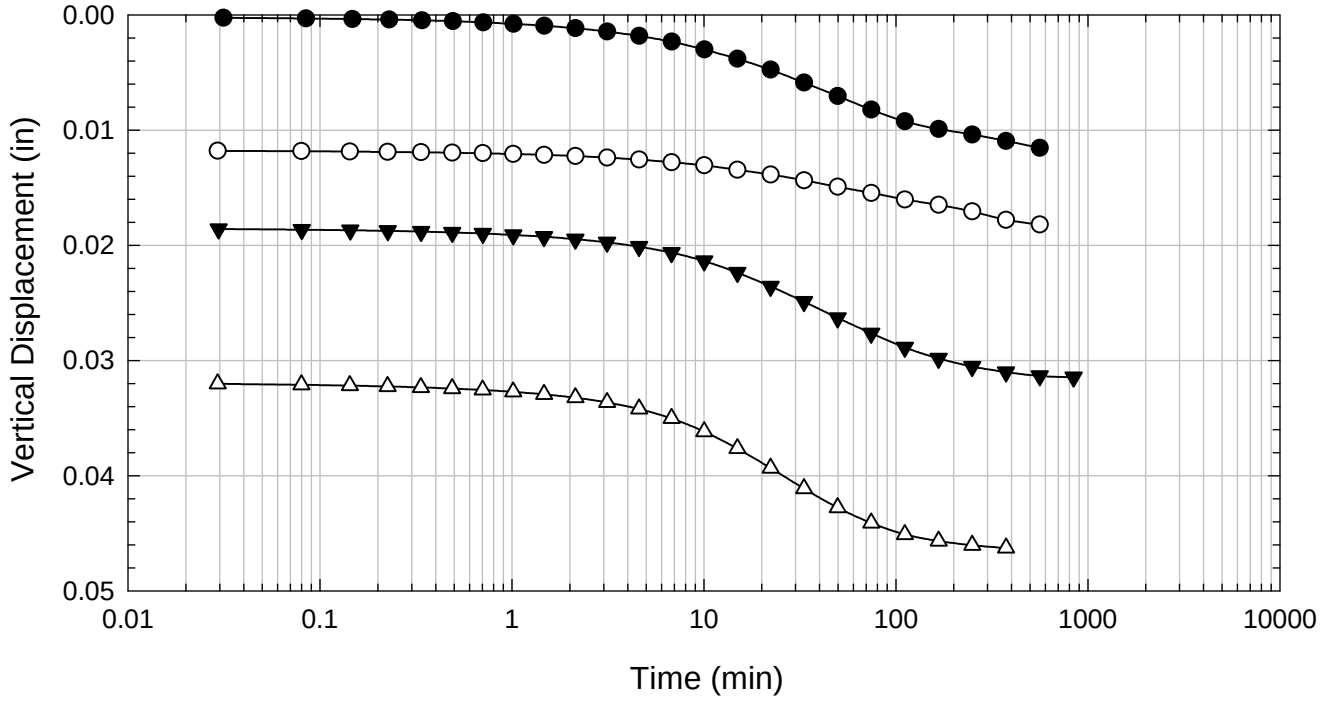

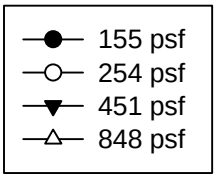

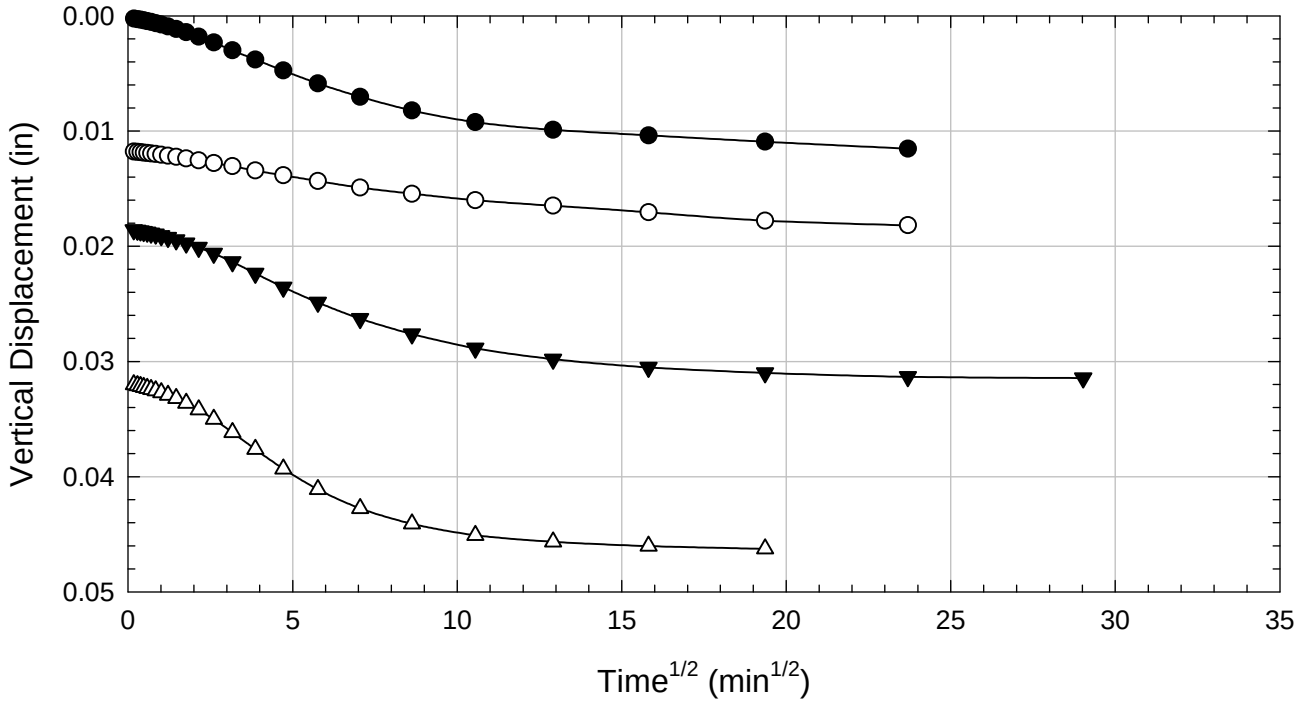

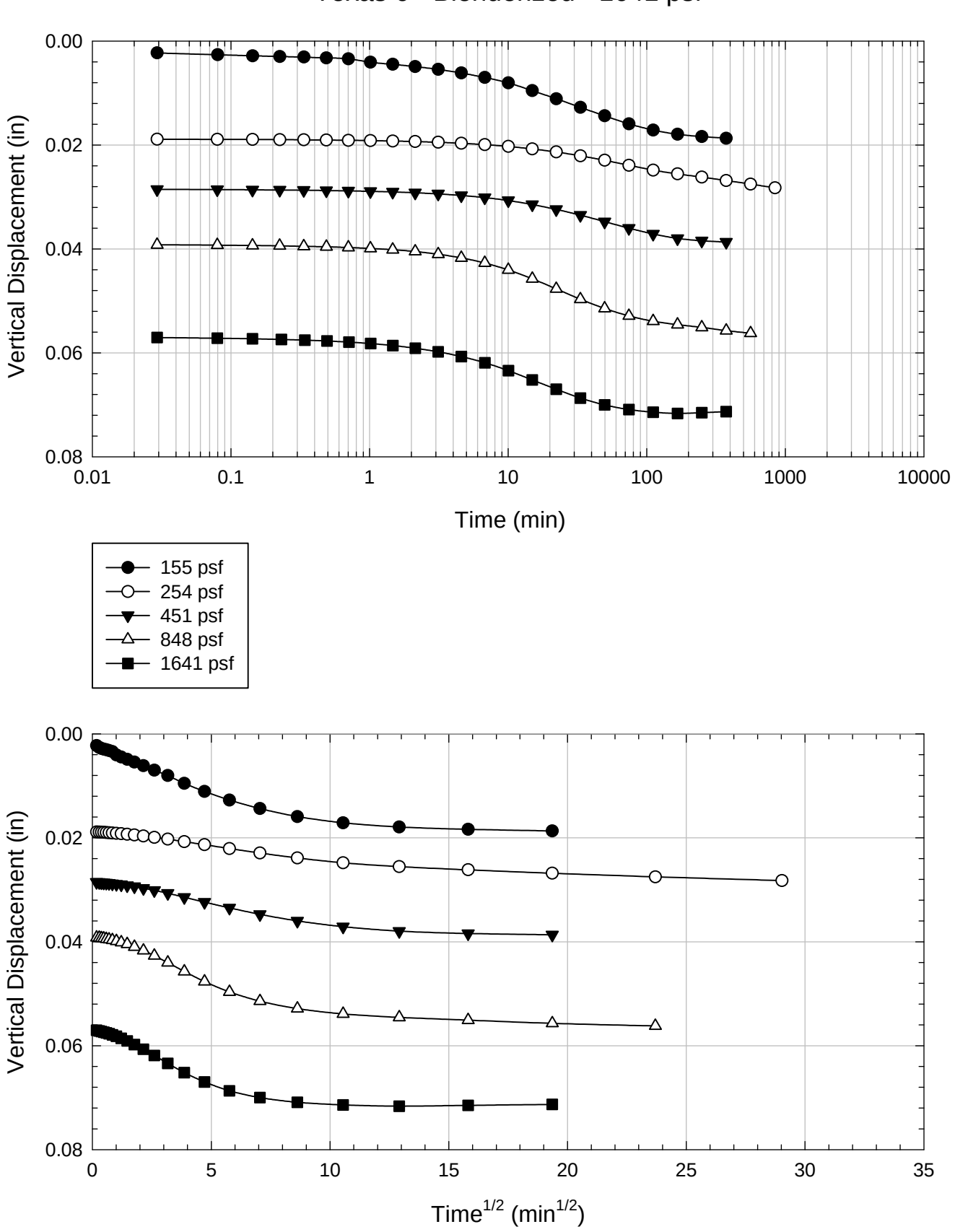
Texas 6 - Blenderized - 1641 psf
Vertical Displacement (in)
0.00
0.02
0.04
0.06
0.08
0.01
0.1
1
10
100
1000
10000
Time (min)
155 psf
254 psf
451 psf
848 psf
1641 psf
Vertical Displacement (in)
0.00
0.02
0.04
0.06
0.08
0
5
10
15
20
25
30
35
Time1/2 (min1/2)

Texas 6 - Blenderized - 3213 psf

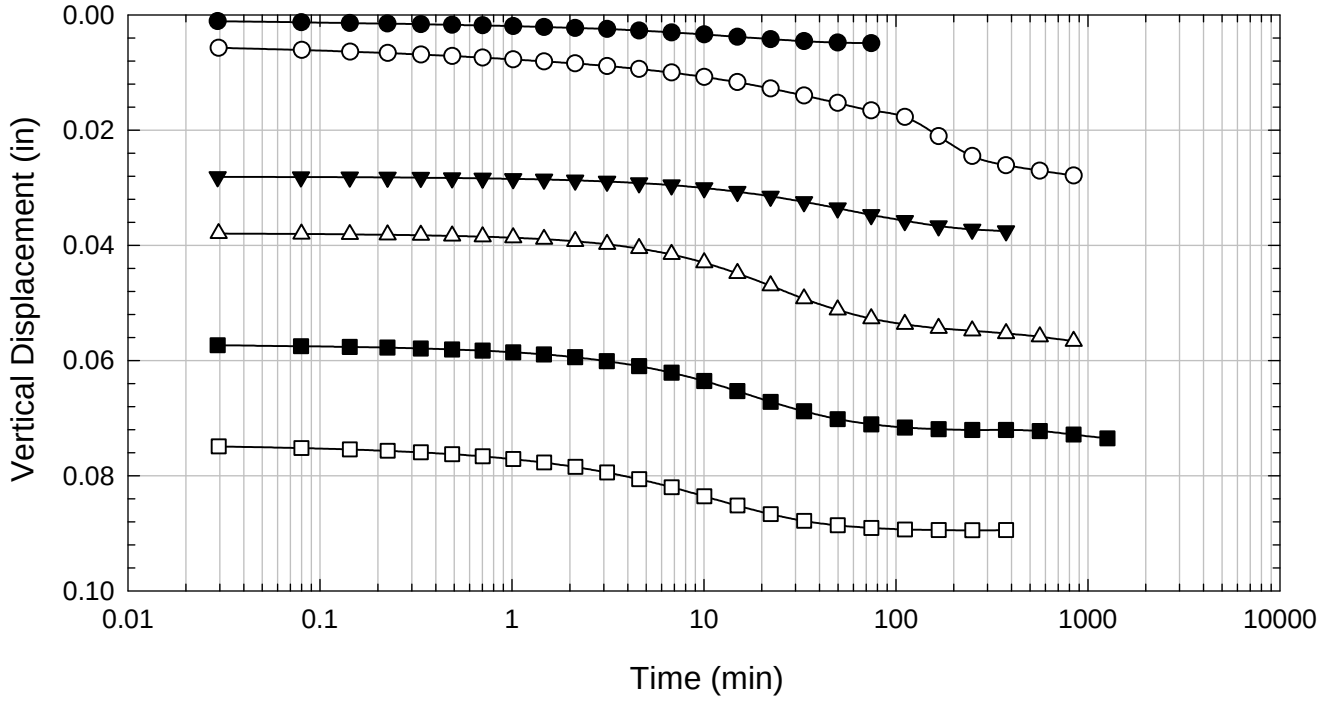

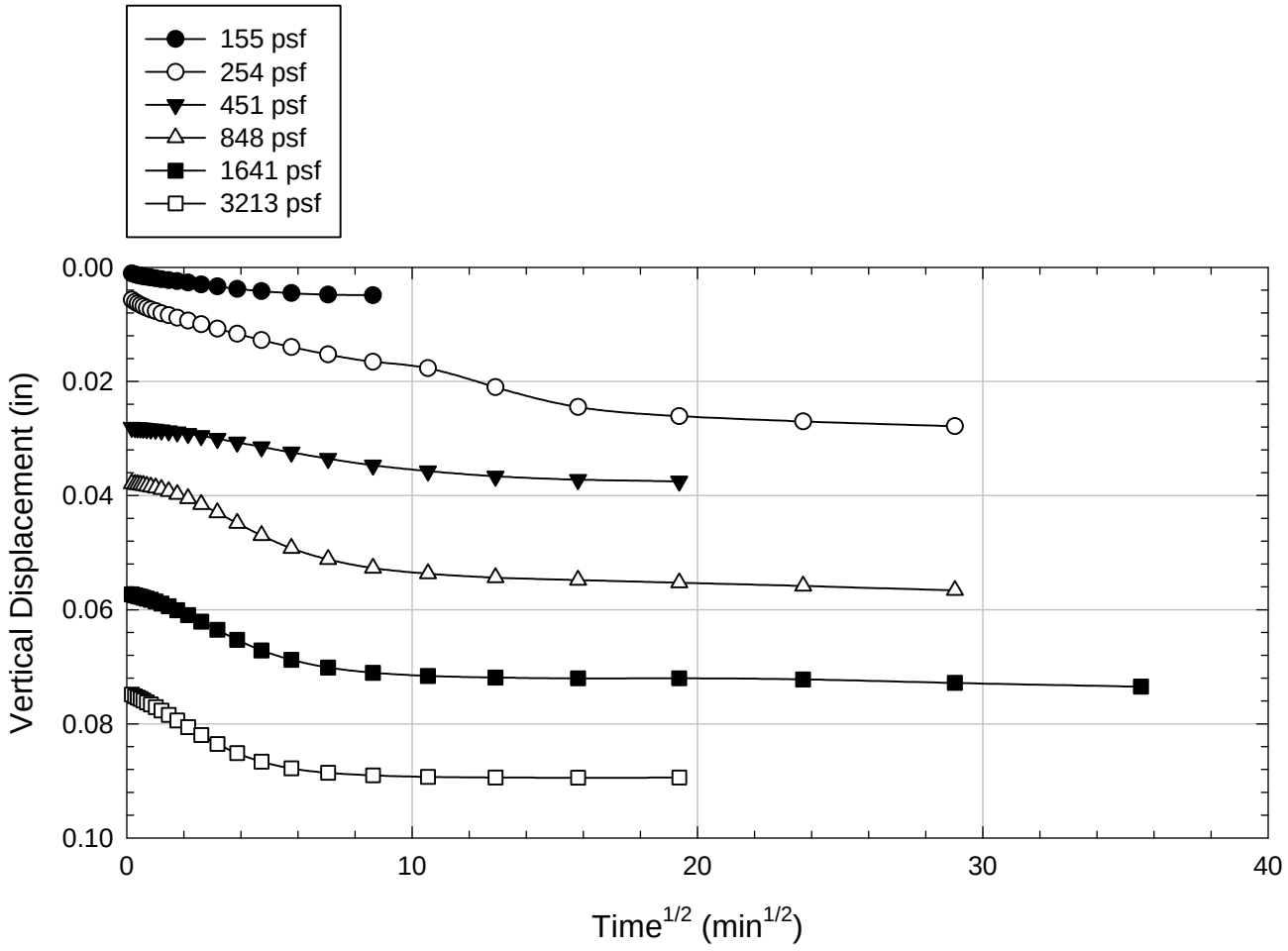

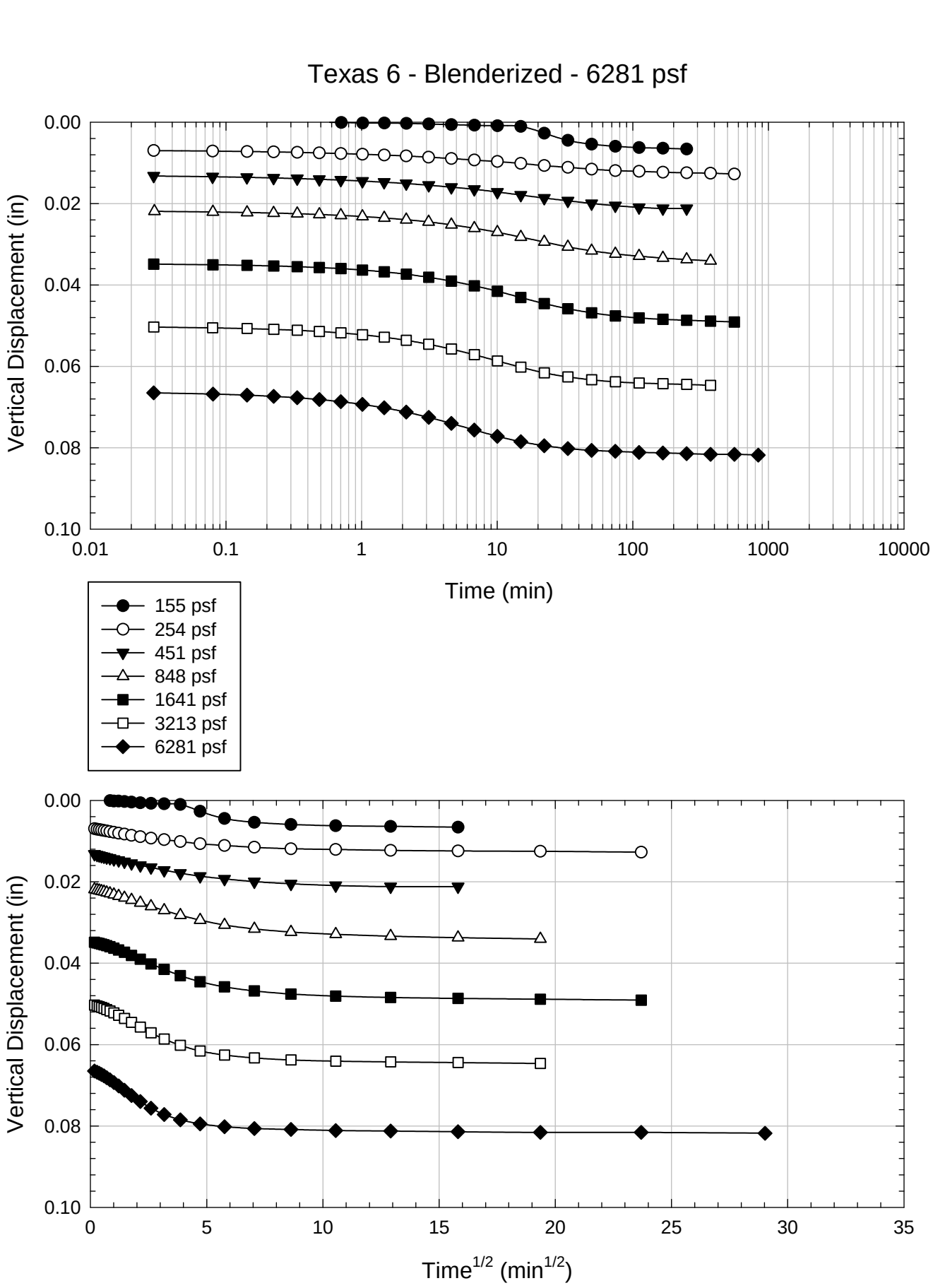
Texas 6 - Blenderized - 6281 psf
Vertical Displacement (in)
0.00
0.02
0.04
0.06
0.08
0.10
0.01
0.1
1
10
100
1000
10000
Time (min)
155 psf
254 psf
451 psf
848 psf
1641 psf
3213 psf
6281 psf
Vertical Displacement (in)
0.00
0.02
0.04
0.06
0.08
0.10
0
5
10
15
20
25
30
35
Time1/2 (min1/2)

Texas 6 - Blenderized

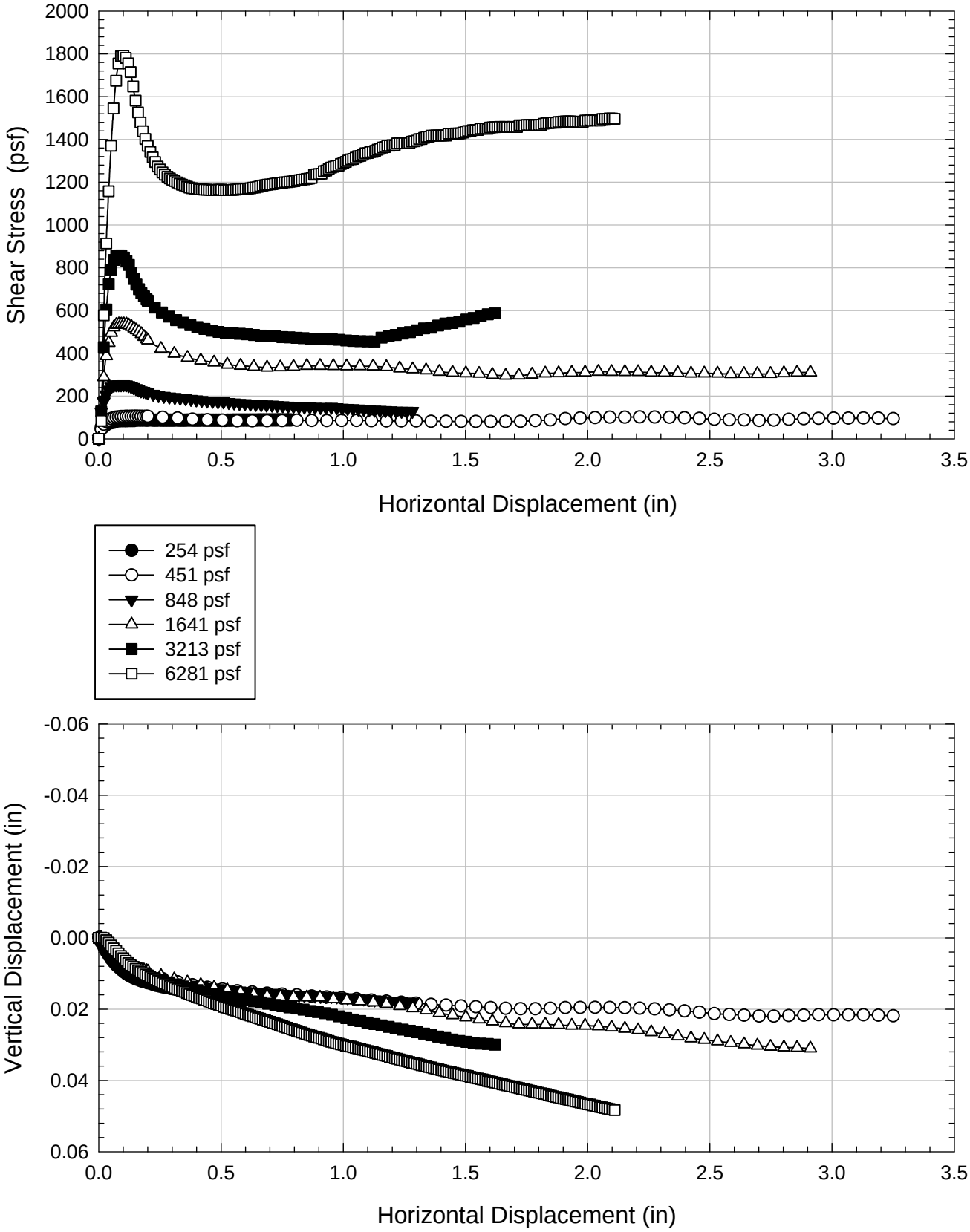

D.14. VBC

D.14.1 Blenderized

Virginia Polytechnic Institute and State University
Geotechnical Engineering Laboratory
Ring Shear Data Sheet

Project:	Fully Softened Shear Strength
Sample I.D./Loc.:	VBC - Blenderized
Classification:	Fat Clay (CH)

Sample Preparation	Remolded at LL

Specific Gravity	2.79	
Shear Device Used	WF Bromhead Ring Shear	

Test Number	1	2	3	4	5	6	7	8
Start Date (m/d/y)	3/21/2011	3/10/2011	24/2/11	3/10/2011	3/18/2011	8/19/2011		
End Date (m/d/y)	3/23/2011		3/3/2011	3/19/2011	3/23/2011	8/24/2011		
Consolidation Pressure (psf)	253	451	847	1638	3213	6292		
Initial Values								
Initial Height (in)	0.20	0.20	0.20	0.20	0.20	0.20		
Inner Radius (in)	1.38	1.38	1.38	1.38	1.38	1.38		
Outer Radius (in)	1.97	1.97	1.97	1.97	1.97	1.97		
Initial Sample Weight (g)	25.19	30.65	31.57	30.93	25.28	25.92		
Water Content (%)	91.82	91.65	92.72	91.34	94.17	88.84		
Dry Unit Weight Before Shear (pcf)	55.2	59.6	67.5	71.8	79.4	50.0		
Saturation (%)	100.0	100.0	100.0	100.0	100.0	100.0		
Consolidation Pressures								
Load 1 (psf)	154	155	154	154	155	154		
Load 2 (psf)	253	254	253	253	254	253		
Load 3 (psf)		451	451	451	451	451		
Load 4 (psf)			847	847	848	847		
Load 5 (psf)				1638	1641	1638		
Load 6 (psf)					3213	3225		
Load 7 (psf)						6292		
t_{50}								
Max. t_{50} for Load 1 (min)	17.11	23.91		44.87	21.79			
Max. t_{50} for Load 2 (min)	24.12	47.41	132.81	86.42	45.92			
Max. t_{50} for Load 3 (min)		27.17	76.61	49.40	40.73			
Max. t_{50} for Load 4 (min)			61.04	102.36	61.89			
Max. t_{50} for Load 5 (min)				60.72	17.37			
Max. t_{50} for Load 6 (min)					14.30			
Max. t_{50} for Load 7 (min)						6.19		
Final Values								
Water Content (%)	74.82	72.21	62.39	55.41	56.19	50.81		
Saturation (%)	100.0	100.0	100.0	100.0	100.0	100.0		
Failure								
Test Performed at Shear Rate (in/min)	7.00E-04	7.00E-04	7.00E-04	7.00E-04	7.00E-04	7.00E-04		
Required Shear Rate (in/min)	8.29E-05	1.18E-04	5.24E-05	3.95E-05	1.26E-04	5.49E-04		
Displacement at Failure (in)	0.10	0.16	0.16	0.12	0.09	0.17		
Peak Shear Stress (psf)	86	154	351	534	986	1954		
Secant Effective Friction Angle (deg)	18.8	18.8	22.5	18.1	17.1	17.2		

Comments:

VBC - Blenderized - 253 psf

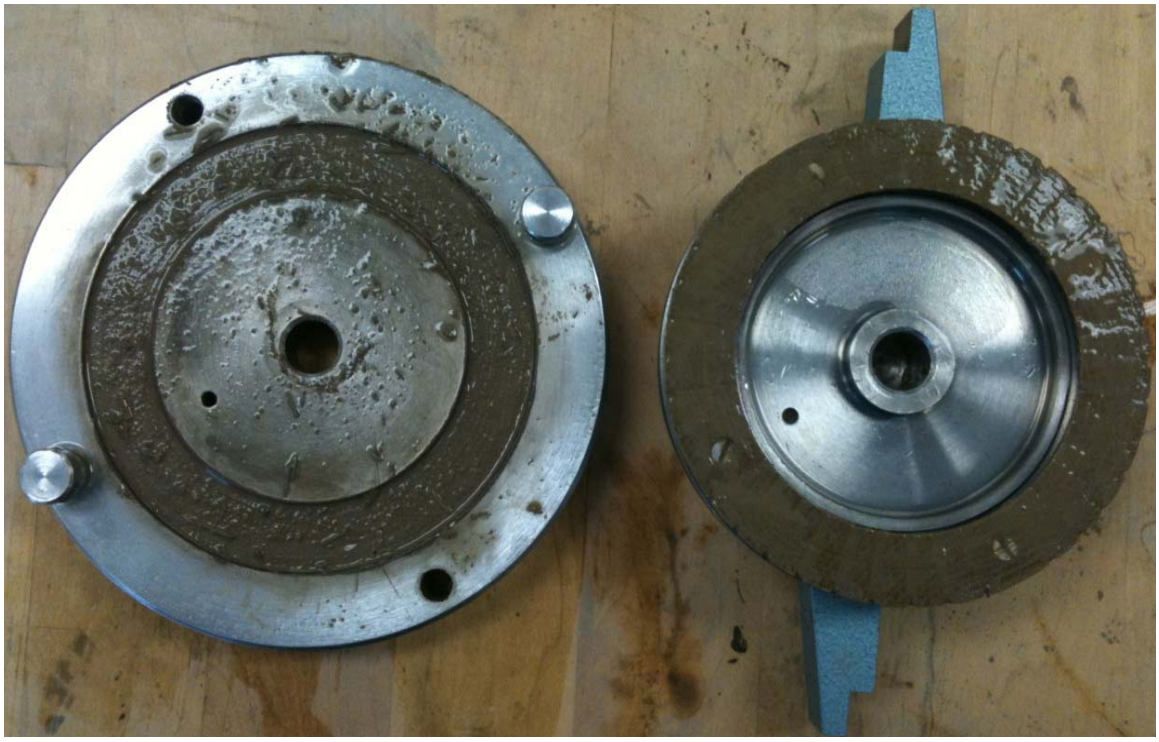

VBC - Blenderized - 451 psf

VBC - Blenderized - 847 psf

VBC - Blenderized - 1638 psf

VBC - Blenderized - 3213 psf

VBC - Blenderized - 6292 psf

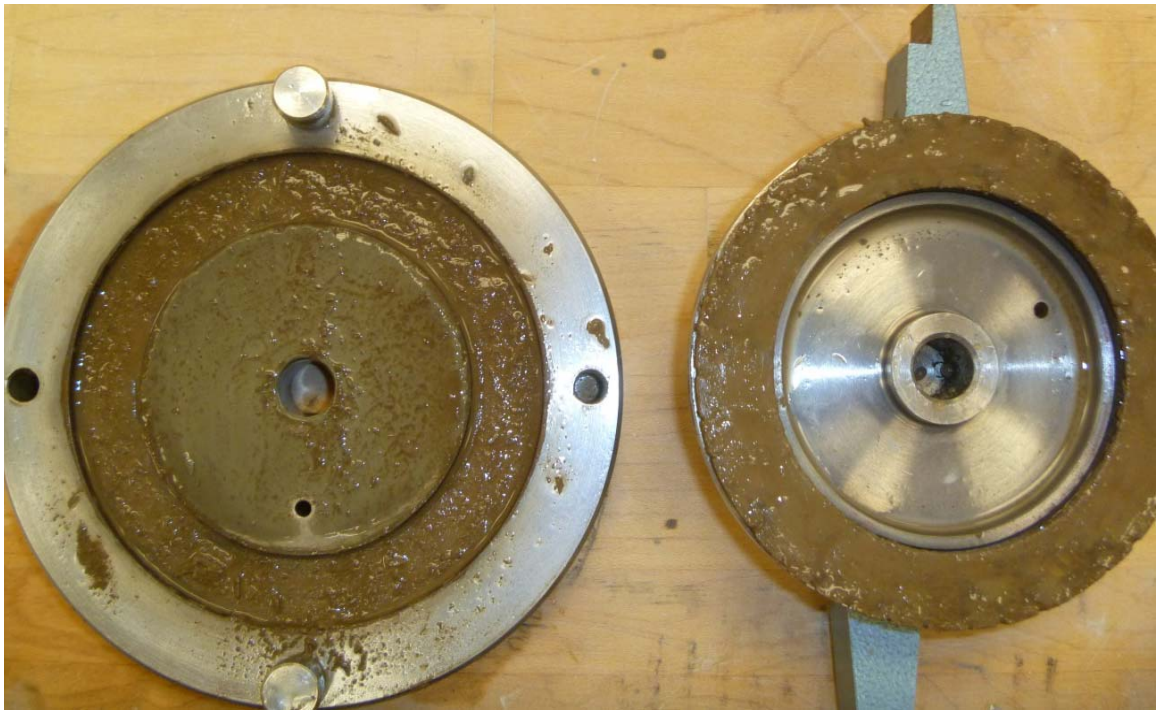

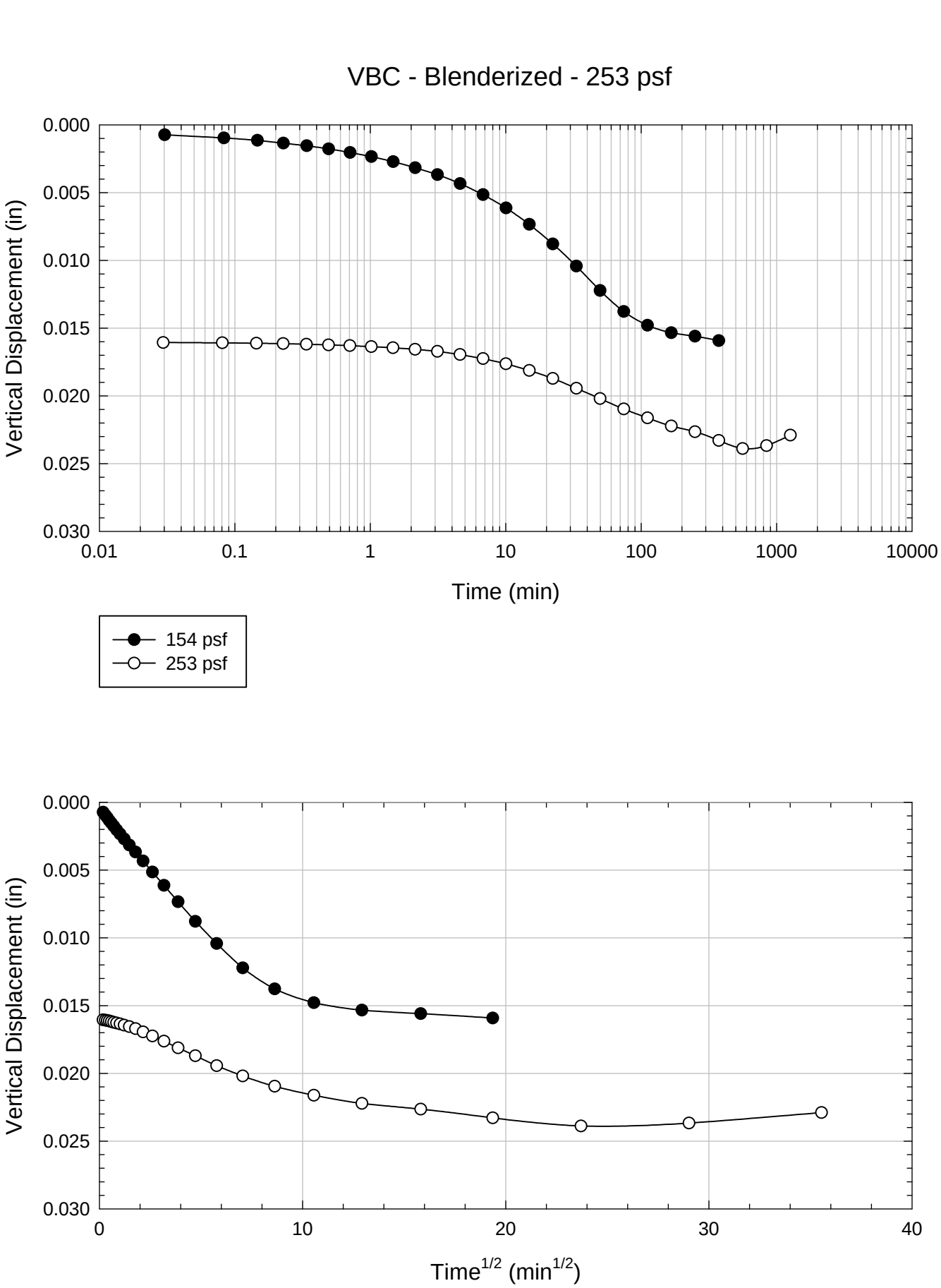
VBC - Blenderized - 253 psf
Vertical Displacement (in)
0.000
0.005
0.010
0.015
0.020
0.025
0.030
0.01
0.1
1
10
100
1000
10000
Time (min)
154 psf
253 psf
Vertical Displacement (in)
0.000
0.005
0.010
0.015
0.020
0.025
0.030
0
10
20
30
40
Time^1/2 (min^1/2)

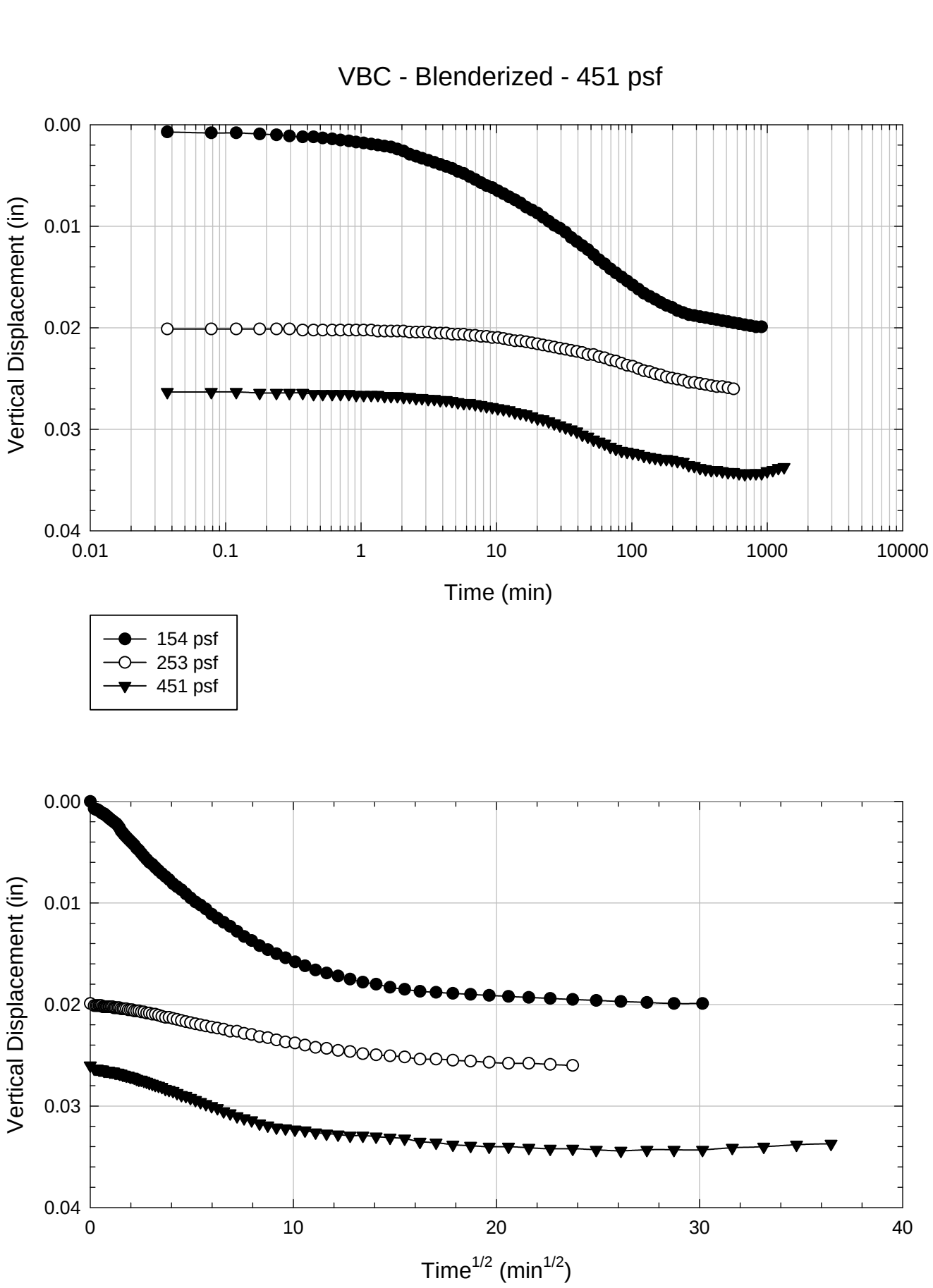
VBC - Blenderized - 451 psf
Vertical Displacement (in)
0.00
0.01
0.02
0.03
0.04
0.01
0.1
1
10
100
1000
10000
Time (min)
154 psf
253 psf
451 psf
Vertical Displacement (in)
0.00
0.01
0.02
0.03
0.04
0
10
20
30
40
Time^1/2 (min^1/2)

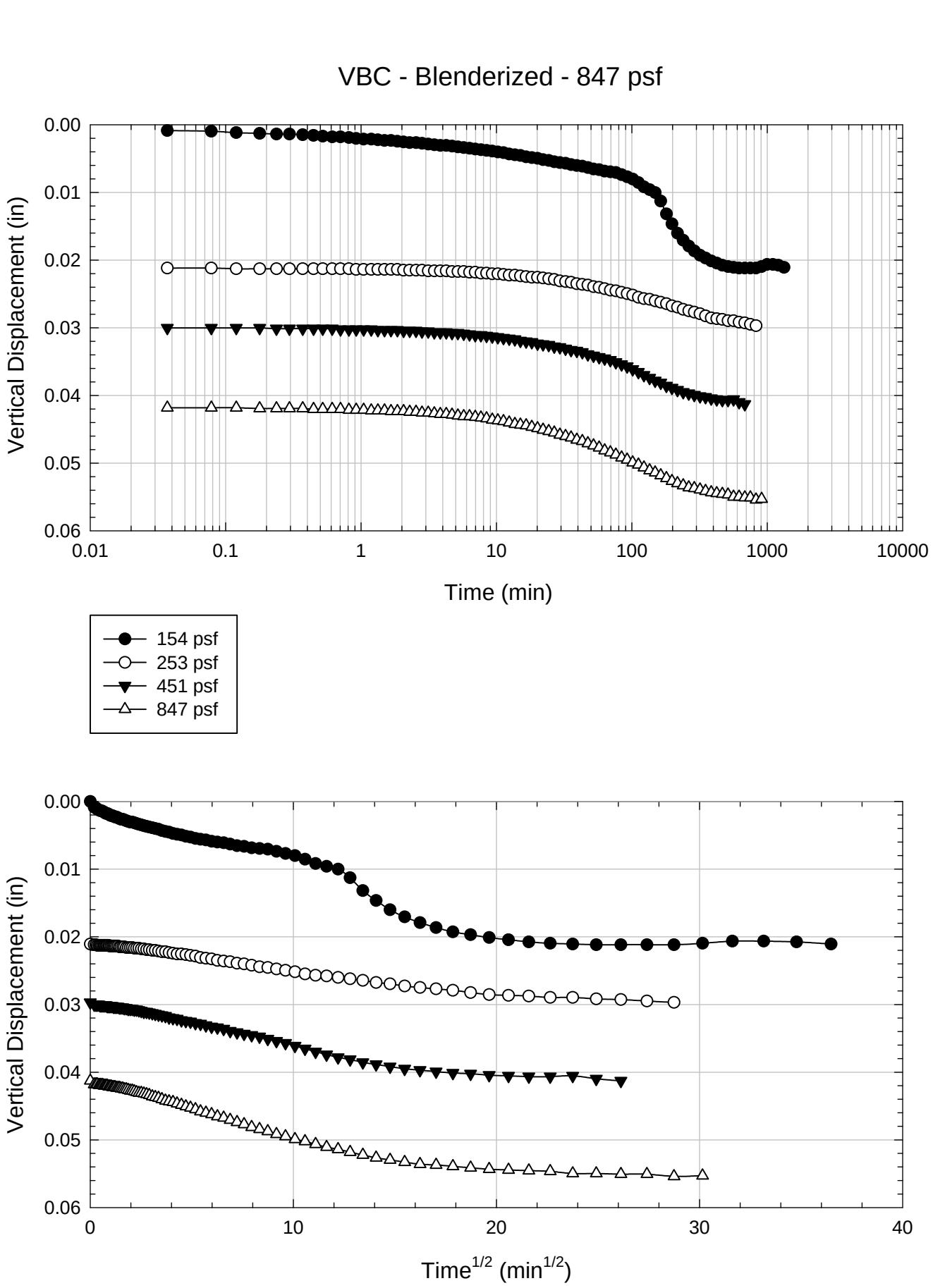
VBC - Blenderized - 847 psf
Vertical Displacement (in)
0.00
0.01
0.02
0.03
0.04
0.05
0.06
0.01
0.1
1
10
100
1000
10000
Time (min)
154 psf
253 psf
451 psf
847 psf
Vertical Displacement (in)
0.00
0.01
0.02
0.03
0.04
0.05
0.06
0
10
20
30
40
Time1/2 (min1/2)

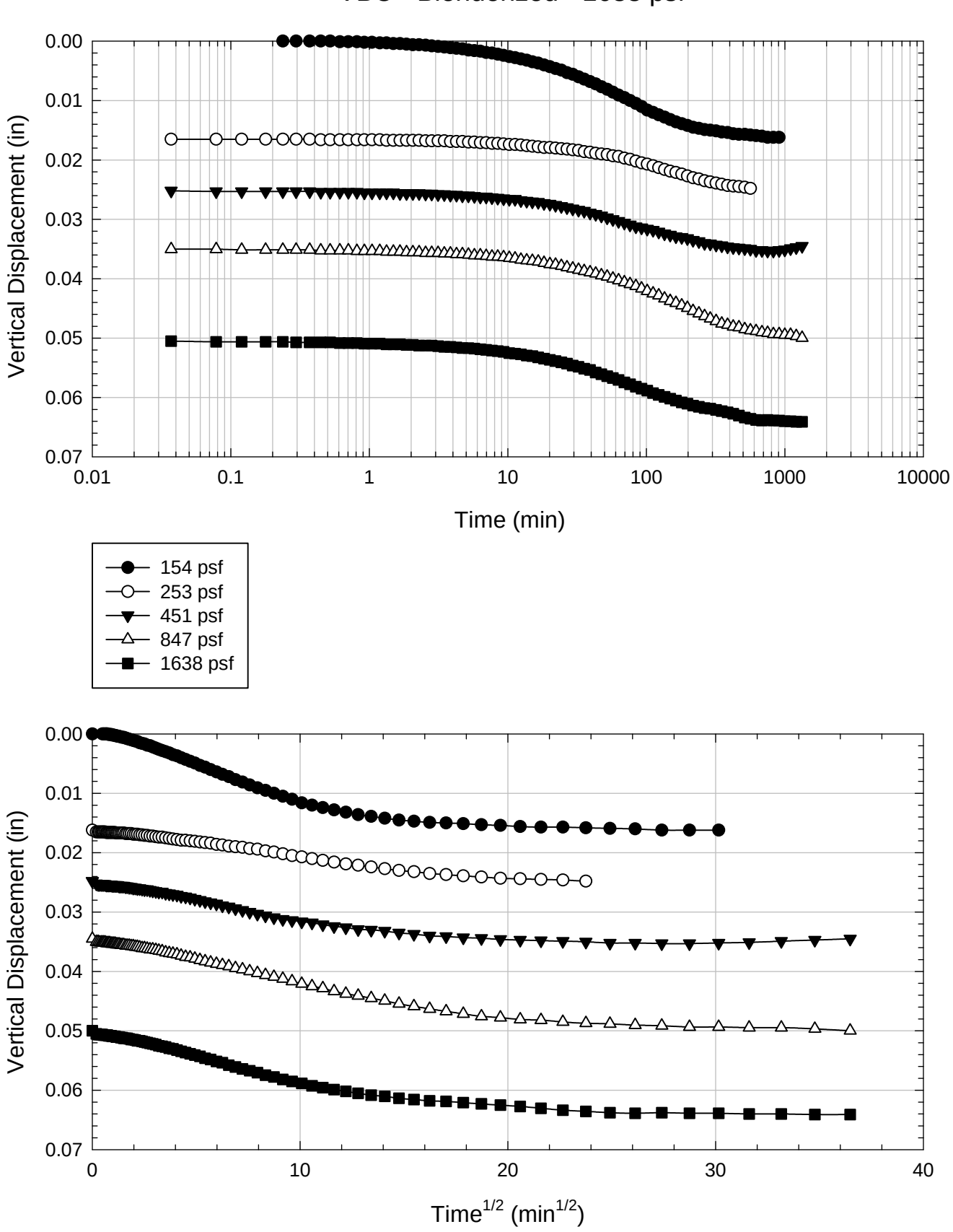
VBC - Blenderized - 1638 psf
Vertical Displacement (in)
0.00
0.01
0.02
0.03
0.04
0.05
0.06
0.07
0.01
0.1
1
10
100
1000
10000
Time (min)
154 psf
253 psf
451 psf
847 psf
1638 psf
Vertical Displacement (in)
0.00
0.01
0.02
0.03
0.04
0.05
0.06
0.07
0
10
20
30
40
Time^1/2 (min^1/2)

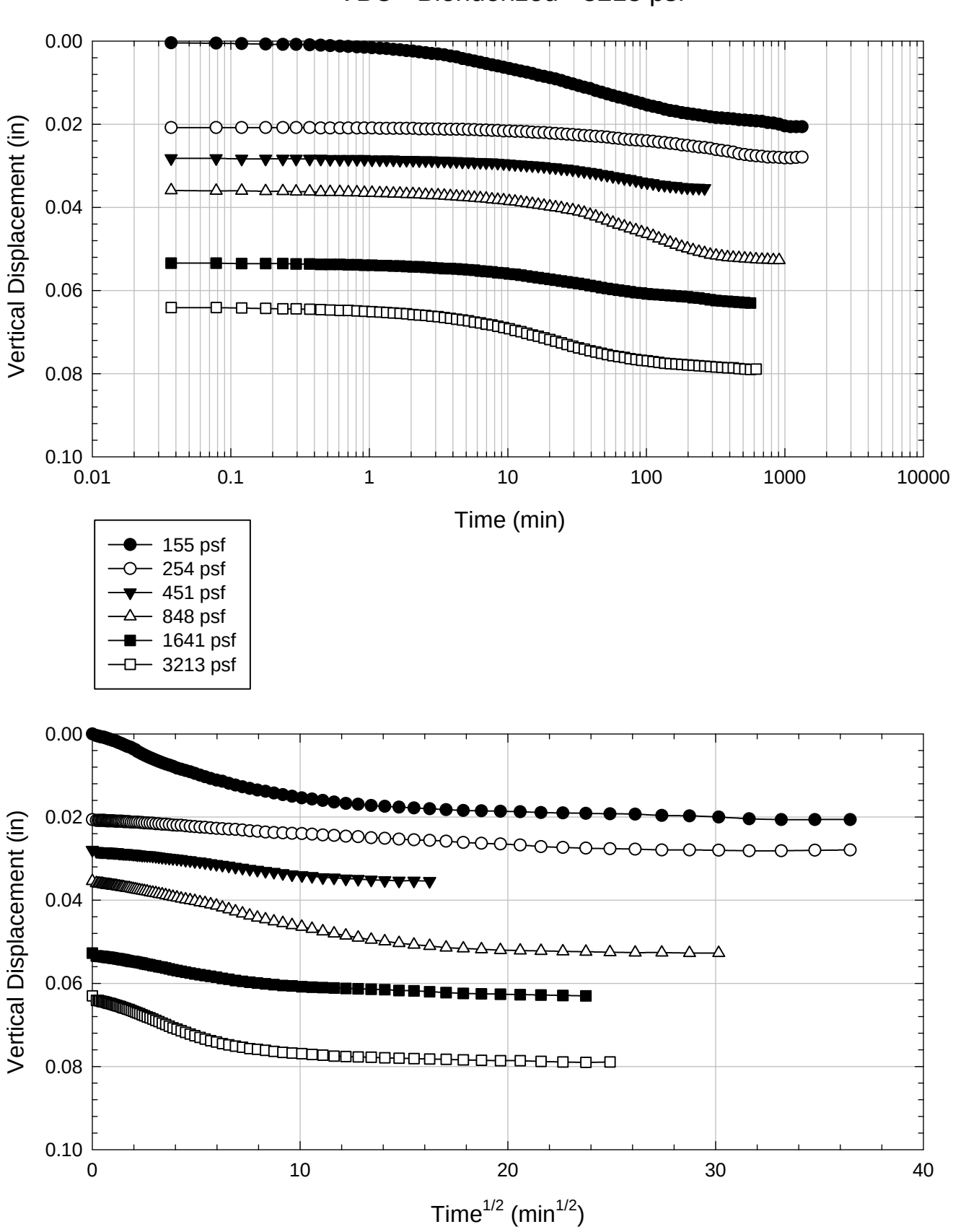
VBC - Blenderized - 3213 psf
Vertical Displacement (in)
0.00
0.02
0.04
0.06
0.08
0.10
0.01
0.1
1
10
100
1000
10000
Time (min)
155 psf
254 psf
451 psf
848 psf
1641 psf
3213 psf
Vertical Displacement (in)
0.00
0.02
0.04
0.06
0.08
0.10
0
10
20
30
40
Time1/2 (min1/2)

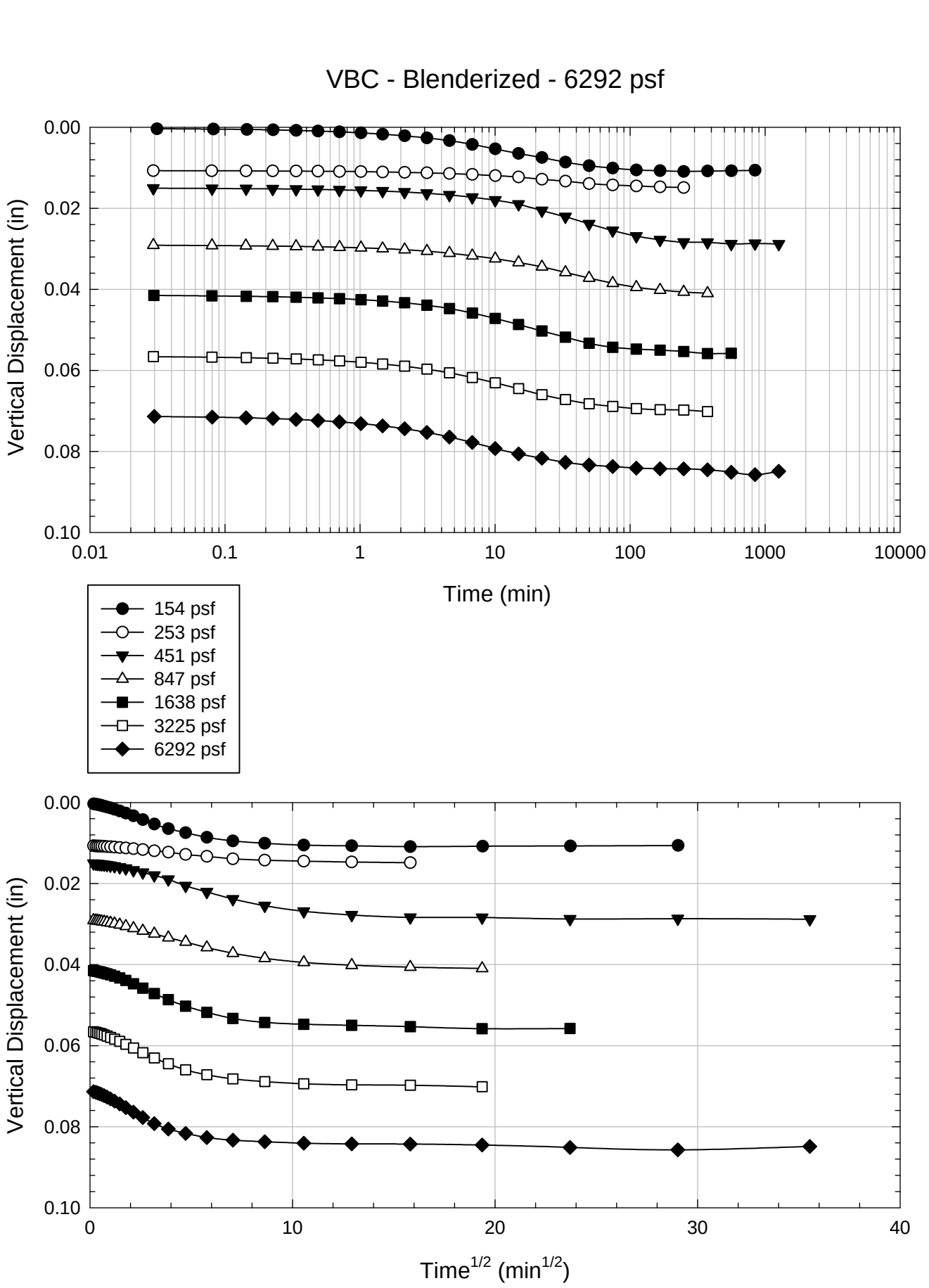
VBC - Blenderized - 6292 psf
Vertical Displacement (in)
0.00
0.02
0.04
0.06
0.08
0.10
0.01
0.1
1
10
100
1000
10000
Time (min)
154 psf
253 psf
451 psf
847 psf
1638 psf
3225 psf
6292 psf
Vertical Displacement (in)
0.00
0.02
0.04
0.06
0.08
0.10
0
10
20
30
40
Time^1/2 (min^1/2)

VBC - Blenderized

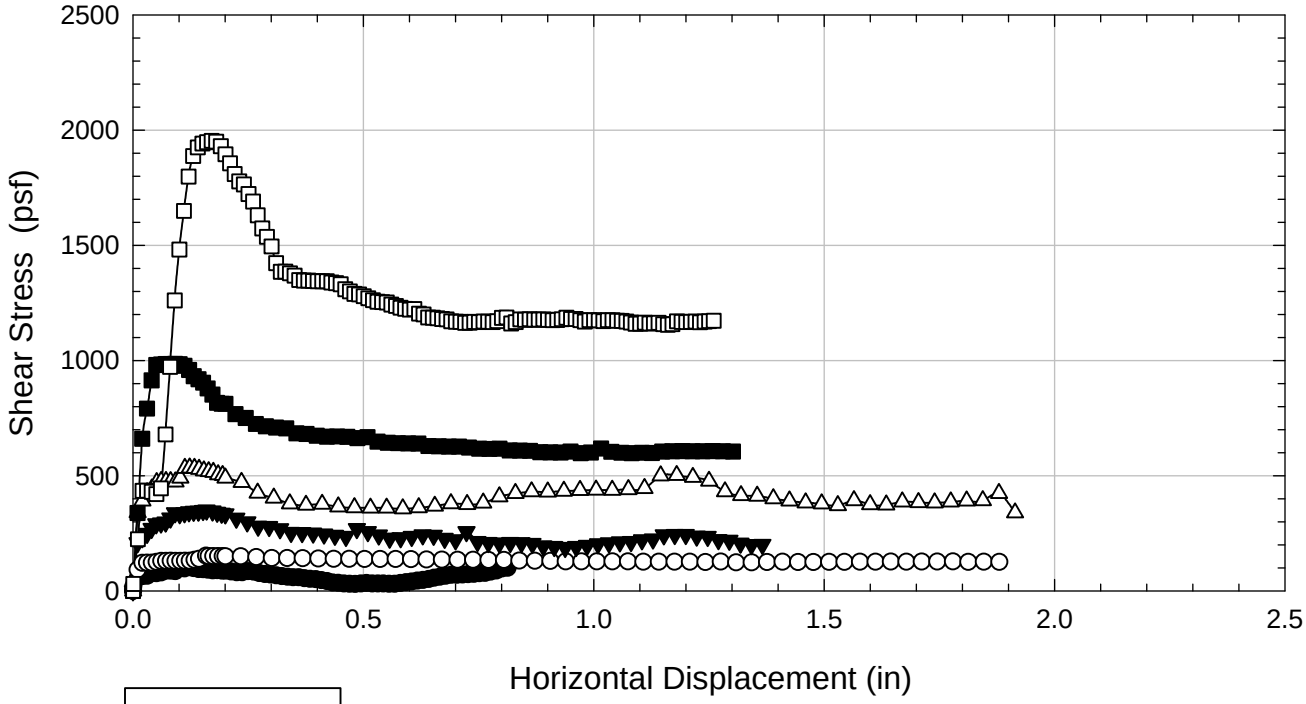

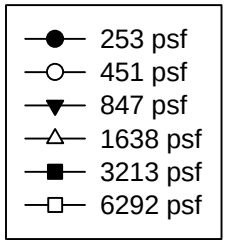

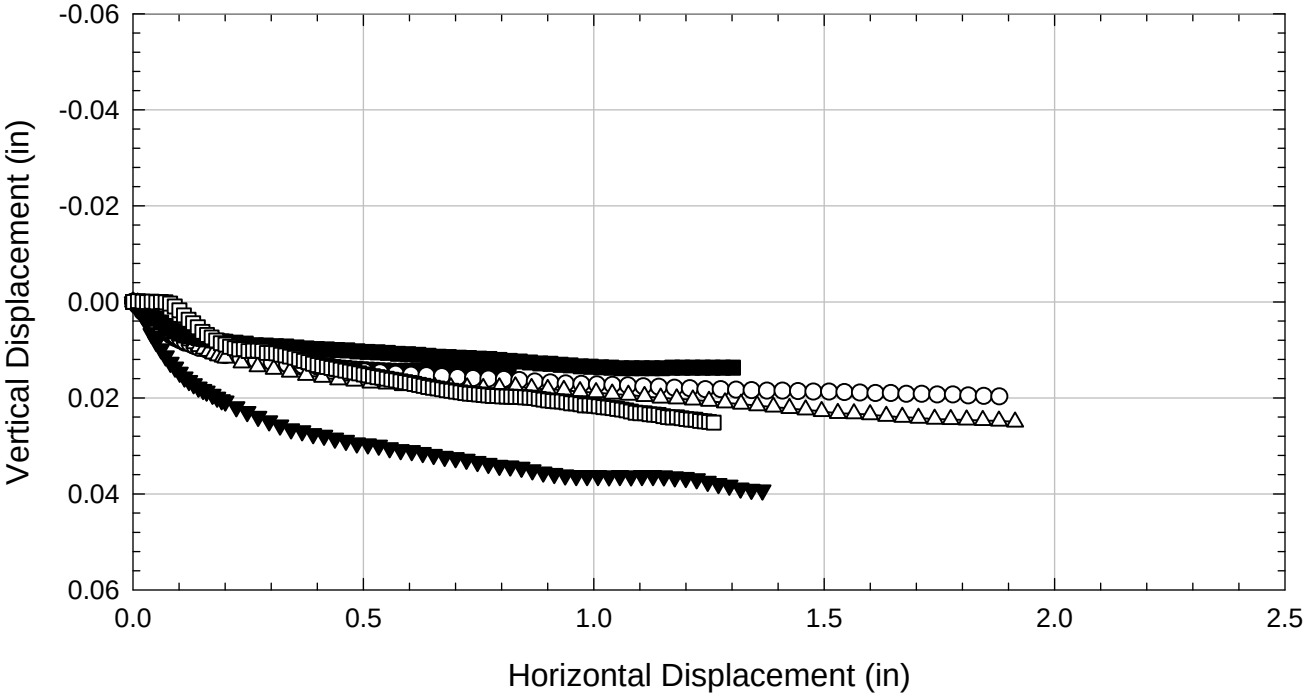

Appendix E

Consolidated Undrained Triaxial Tests Results

Table of Contents

E.1. Alabama 1

E.1.1 Non-blenderized

Virginia Polytechnic Institute and State University
Geotechnical Engineering Laboratory
Triaxial Data Sheet

Project:	Fully Softened Shear Strength
Sample I.D./Loc.:	Alabama 1- Non-blenderized - Consolidated Undrained
Classification:	Lean Clay (CL)

Sample Preparation	Remolded at LL
Specimen Saturation Method	Wet

Specific Gravity	2.73	
Method for Dimensions After Consol.	Case and Chilver (1959)	

Test Number	1	2	3	4	5	6	7	
Start Date (m/d/y)	2/17/2013	2/17/2013	2/17/2013	2/18/2013	2/17/2013			
End Date (m/d/y)	2/19/2013	2/19/2013	2/19/2013	2/20/2013	2/19/2013			
Backpressure (psf)	7200	7200	7200	7200	7200			
Consolidation Pressure (psf)	1008	3024	5472	8064	10080			
B value	1.00	0.99	0.95	0.98	0.98			
Initial Values								
Initial Height (in.)	3.054	3.016	3.093	3.033	3.074			
Initial Diameter (in.)	1.372	1.374	1.375	1.386	1.369			
Initial Sample Weight (g.)	141.73	139.57	144.33	145.55	141.30			
Water Content (%)	31.52	29.86	31.21	31.17	31.46			
Dry Unit Weight (pcf)	90.9	91.6	91.2	92.4	90.5			
Wet Unit Weight (pcf)	119.6	118.9	119.7	121.2	119.0			
Saturation (%)	98.5	94.7	98.3	100.0	97.3			
Void Ratio	0.87	0.86	0.87	0.84	0.88			
After Consolidation								
t_{100} Using Casagrande Method (min)	103.94	56.91	56.90	56.86	55.13			
Volumetric Strain (%)	2.06	6.01	9.12	10.76	11.86			
Height After Consolidation (in.)	3.033	2.956	2.999	2.924	2.952			
Area After Consolidation (in.)	1.458	1.423	1.395	1.401	1.356			
Final Values								
Water Content (%)	29.74	27.75	25.76	24.66	23.79			
Dry Unit Weight (pcf)	92.0	95.1	99.0	100.4	101.4			
Wet Unit Weight (pcf)	119.4	121.5	124.5	125.1	125.5			
Saturation (%)	95.3	95.7	97.5	96.6	95.5			
Void Ratio	0.85	0.79	0.72	0.70	0.68			
Failure								
Failure Criteria	Max PSR	Max PSR	Max PSR	Max PSR	Max PSR			
Deviator Stress at failure (psf)	1317.69	2552.62	4277.64	6373.63	7449.43			
Principal Stress Ratio at failure	2.56	2.68	2.77	2.73	2.85			
Minor Principal Effective Stress at fail. (psf)	877.5	1540.2	2432.0	3699.7	4046.0			
Major Principal Effective Stress at fail. (psf)	2242.2	4120.7	6736.8	10114.1	11532.3			
Corrections Applied	Membrane	Membrane	Membrane	Membrane	Membrane			
Axial Strain at failure (%)	15.09	8.54	8.21	12.69	11.15			
Test performed at strain rate (%/hr)	1.00	1.00	1.00	1.00	1.00			

Comments:

Alabama 1 - Non-blenderized - 1,008 psf

Alabama 1 - Non-blenderized - 3,024 psf

Alabama 1 - Non-blenderized - 5,472 psf

Alabama 1 - Non-blenderized - 8,064 psf

Alabama 1 - Non-blenderized - 10,080 psf

Alabama 1 - Non-blenderized

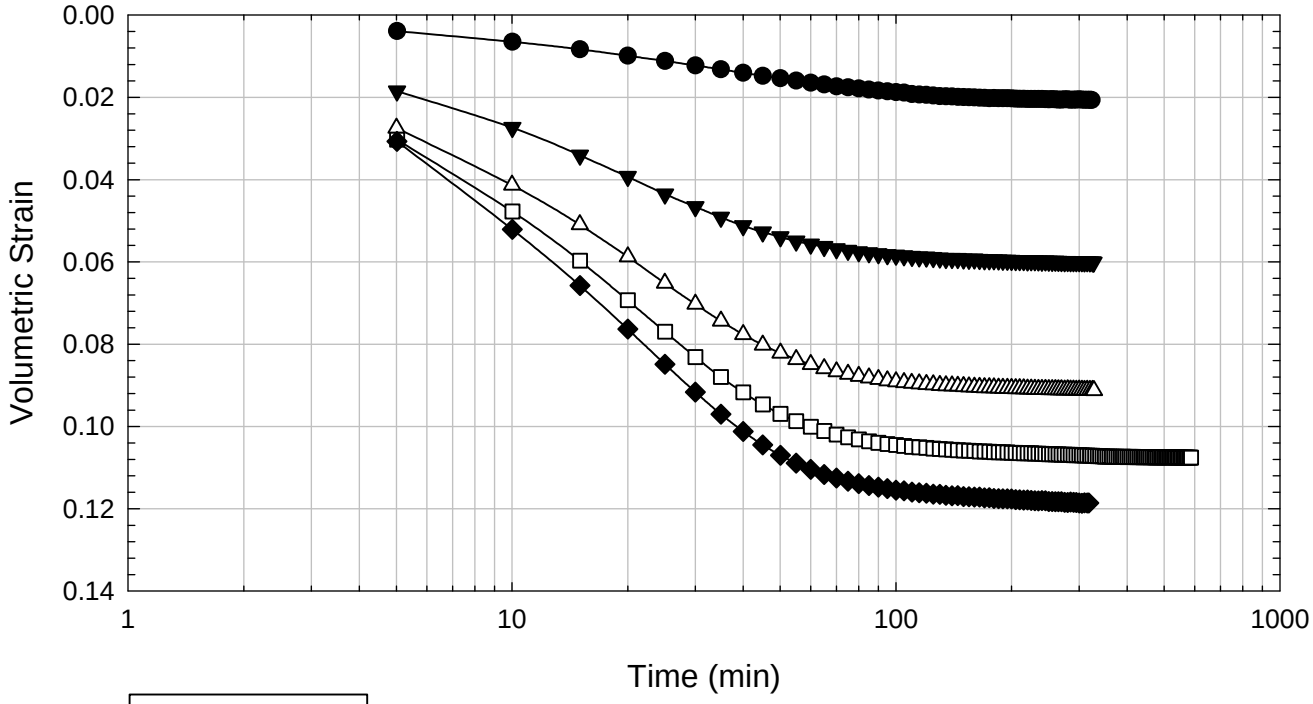

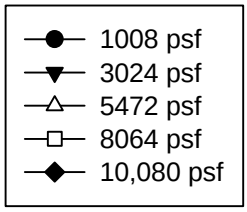

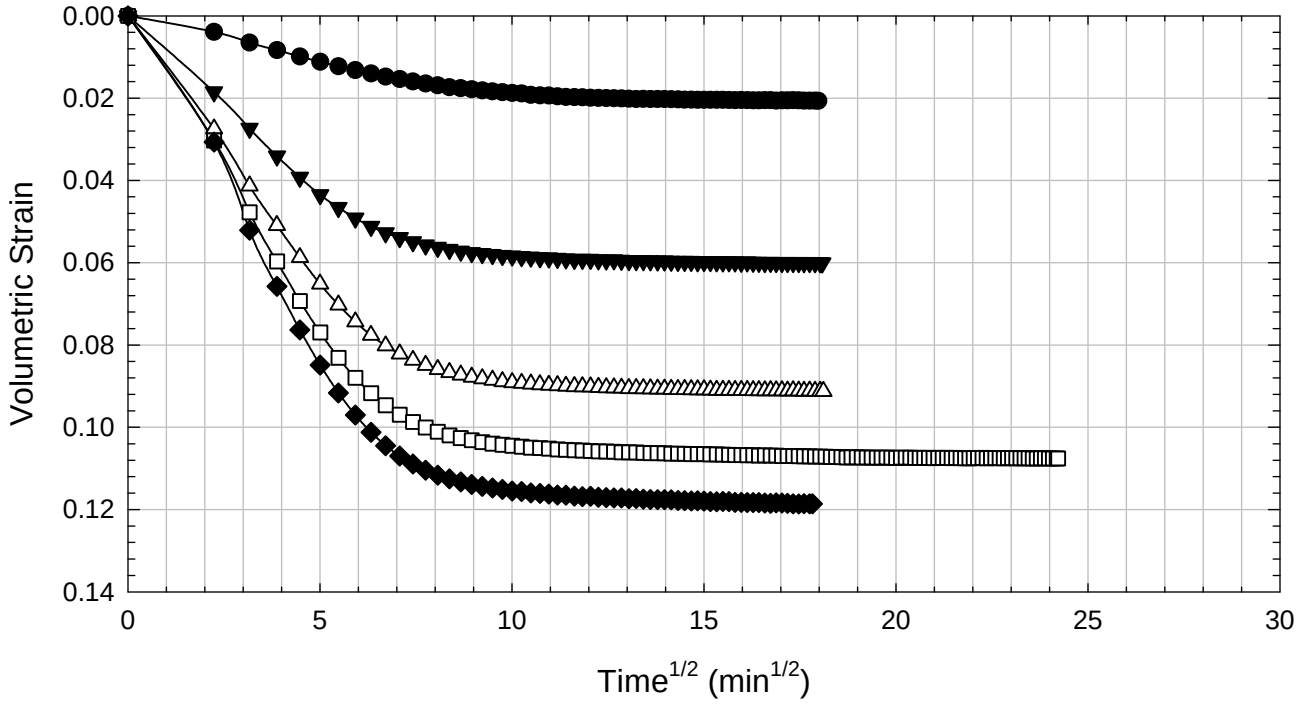

Alabama 1 - Non-blenderized

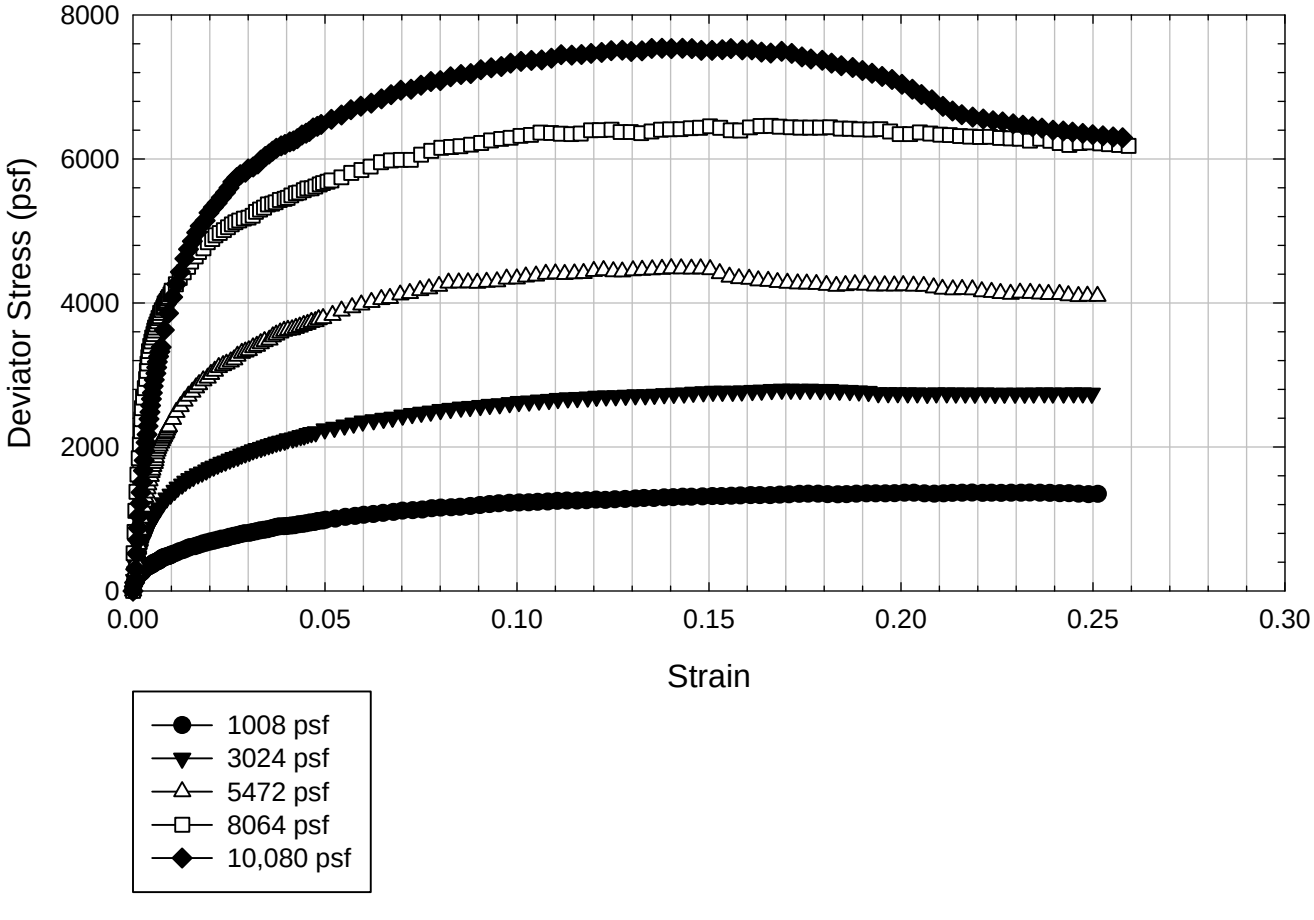

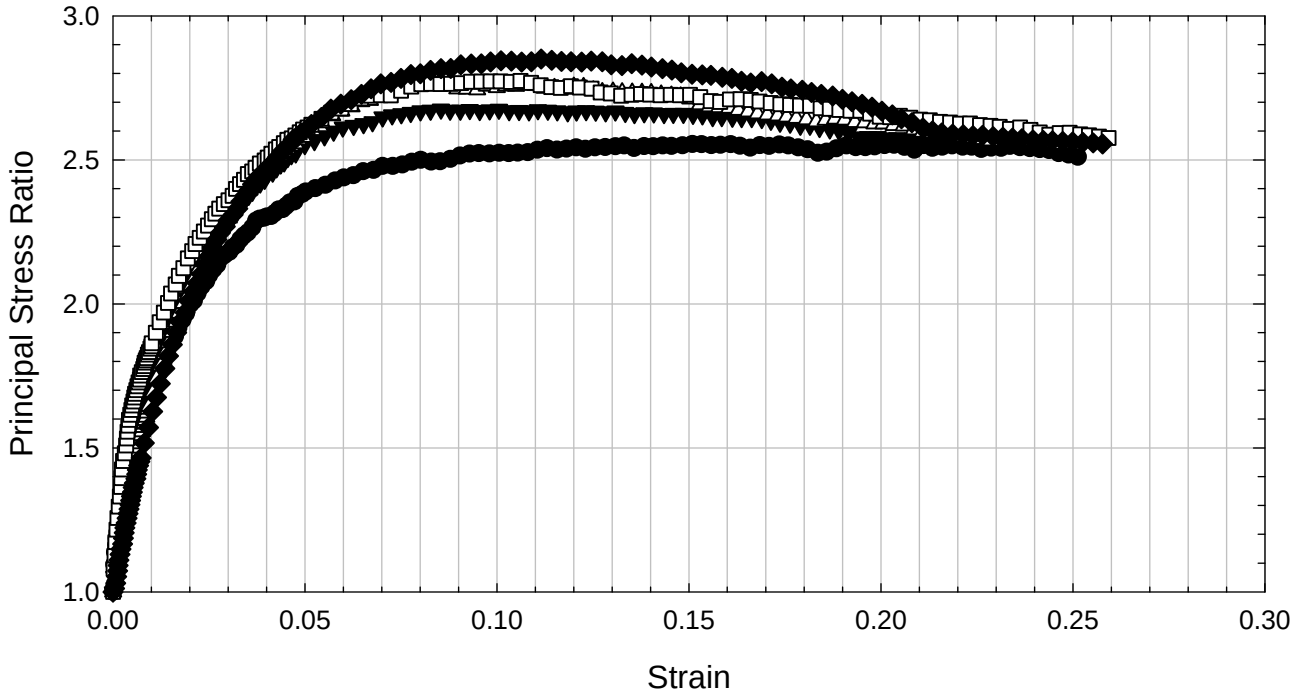

Alabama 1 - Non-blenderized

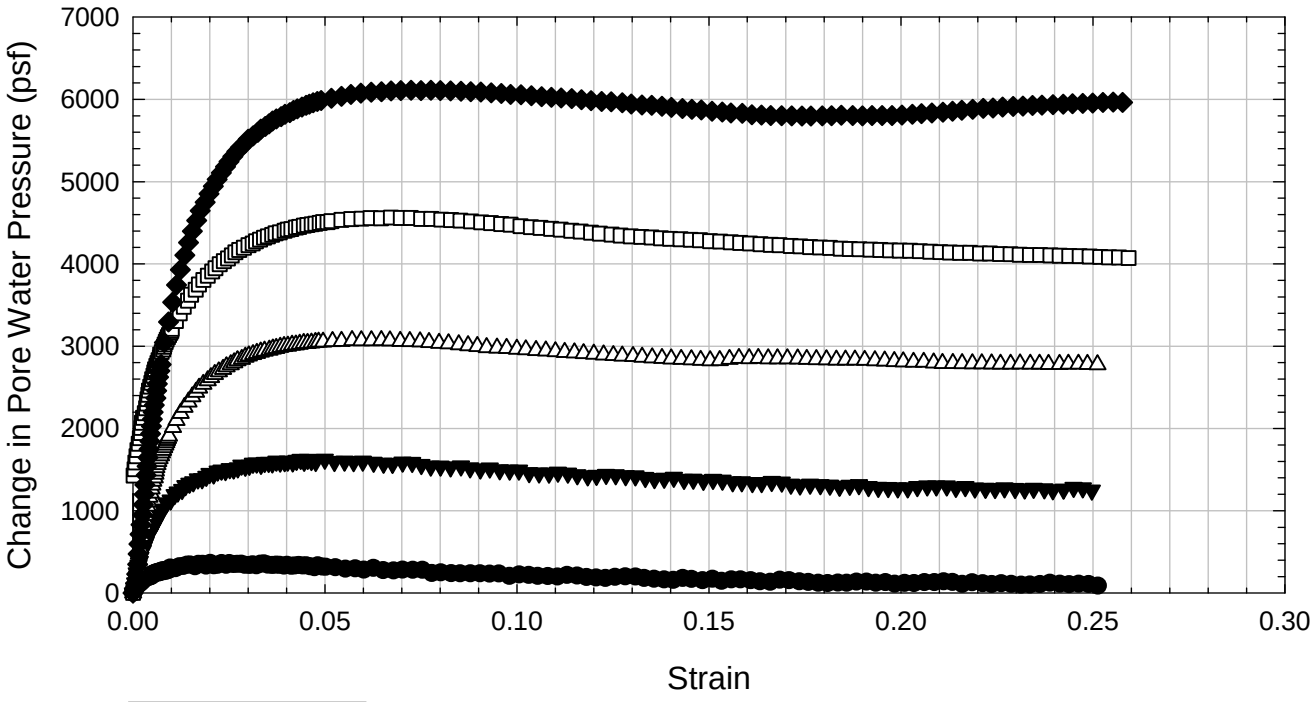

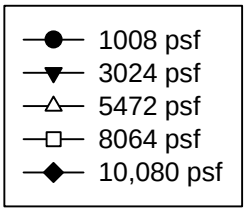

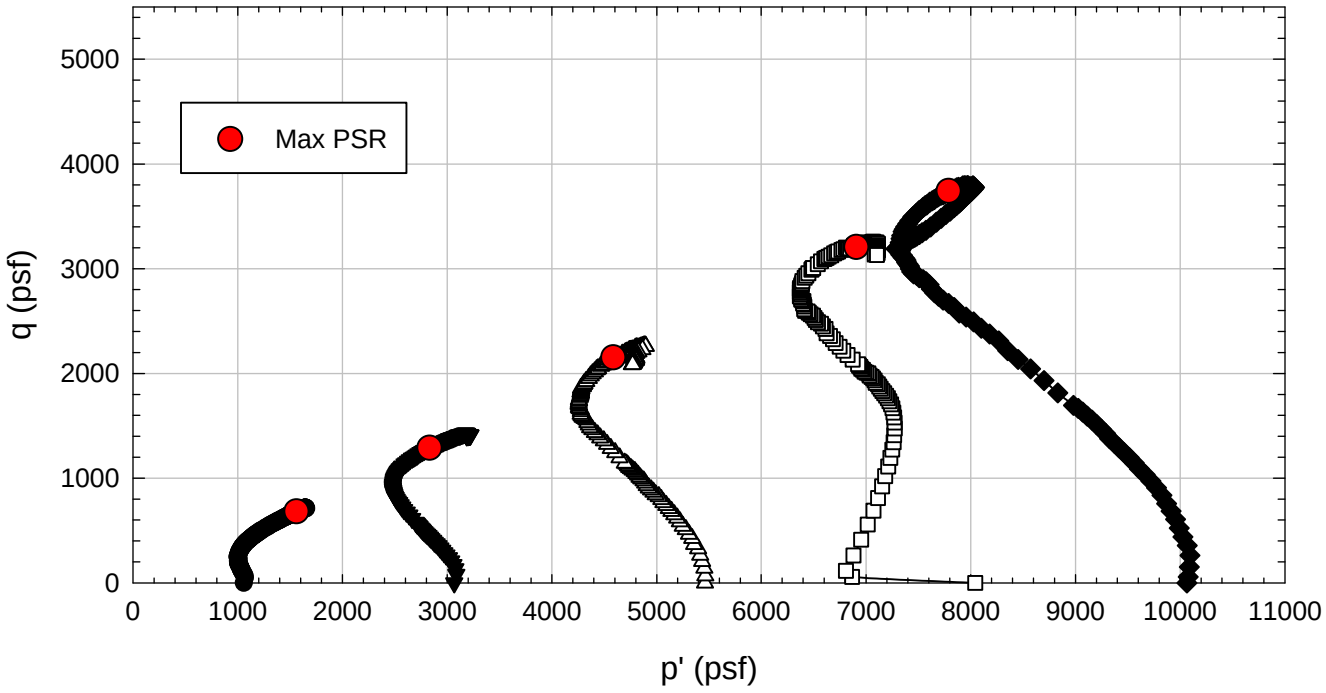

Alabama 1 - Non-blenderized

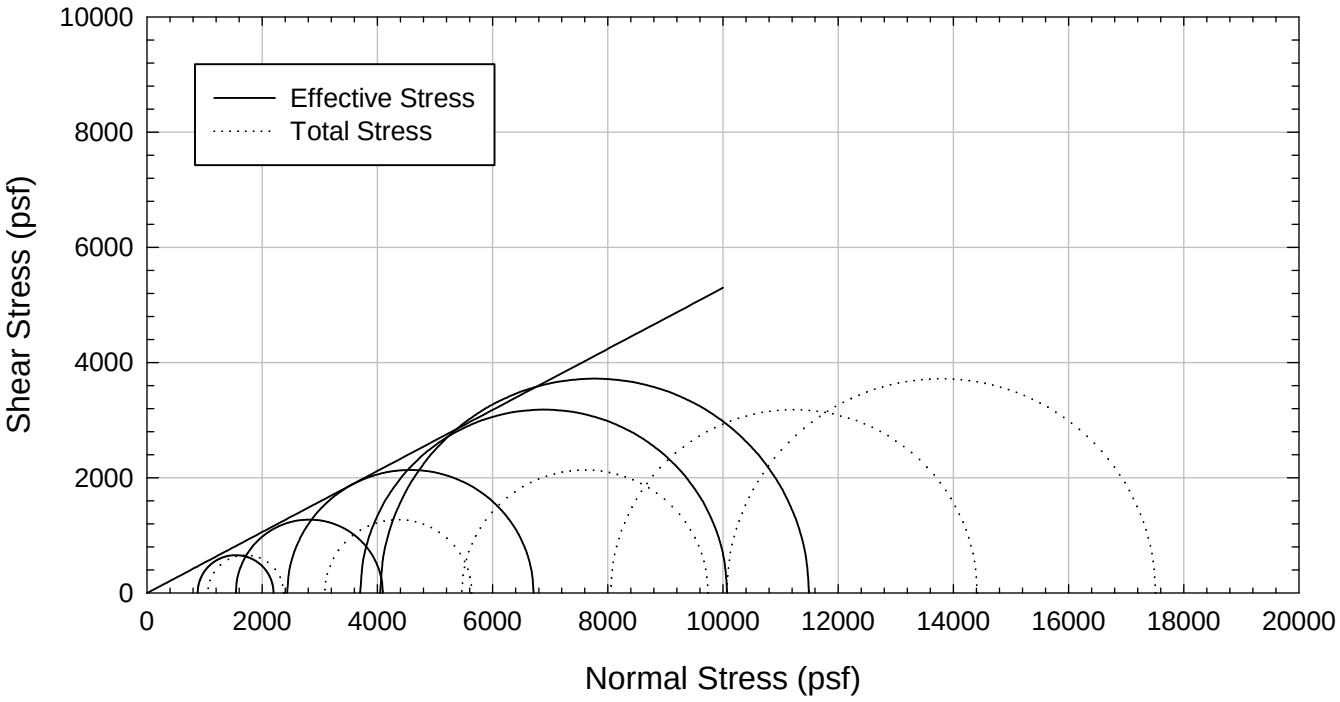

E.2. Colorado Clay

E.2.1 Non-blenderized

Virginia Polytechnic Institute and State University
Geotechnical Engineering Laboratory
Triaxial Data Sheet

Project:	Fully Softened Shear Strength
Sample I.D./Loc.:	Colorado Clay - Non-blenderized - Consolidated Undrained
Classification:	Lean Clay (CL)

Sample Preparation	Remolded at LL
Specimen Saturation Method	Wet

Specific Gravity	2.78	Assumed
Method for Dimensions After Consol.	Case and Chilver (1959)	

Test Number	1	2	3	4	5	6	7	
Start Date (m/d/y)	4/21/2012	4/21/2012	4/21/2012	4/21/2012	4/21/2012			
End Date (m/d/y)	4/29/2012	4/29/2012	4/28/2012	4/28/2012	4/28/2012			
Backpressure (psf)	7200	7200	7200	7200	7200			
Consolidation Pressure (psf)	1008	2016	3024	8064	10080			
B value	0.96	1.00	0.96	1.00	0.99			
Initial Values								
Initial Height (in.)	3.038	2.991	2.991	3.011	2.980			
Initial Diameter (in.)	1.386	1.371	1.363	1.363	1.361			
Initial Sample Weight (g.)	138.76	135.47	135.55	135.53	134.47			
Water Content (%)	32.66	33.15	33.54	33.61	34.32			
Dry Unit Weight (pcf)	86.9	87.8	88.6	88.0	88.0			
Wet Unit Weight (pcf)	115.3	116.9	118.3	117.5	118.2			
Saturation (%)	91.2	94.4	97.3	96.1	98.2			
Void Ratio	1.00	0.98	0.96	0.97	0.97			
After Consolidation								
t_{100} Using Casagrande Method (min)	807.95	814.51	676.50	574.81	548.86			
Volumetric Strain (%)	3.16	6.98	8.76	14.61	15.67			
Height After Consolidation (in.)	3.006	2.921	2.904	2.864	2.824			
Area After Consolidation (in.)	1.477	1.408	1.374	1.317	1.303			
Final Values								
Water Content (%)	31.88	29.71	28.04	24.69	24.02			
Dry Unit Weight (pcf)	87.8	92.6	95.6	101.1	102.7			
Wet Unit Weight (pcf)	115.9	120.1	122.4	126.1	127.3			
Saturation (%)	90.9	94.5	95.7	95.9	96.8			
Void Ratio	0.97	0.87	0.81	0.72	0.69			
Failure								
Failure Criteria	Max PSR	Max PSR	Max PSR	Max PSR	Max PSR			
Deviator Stress at failure (psf)	897.25	1755.27	2575.51	5915.90	7452.95			
Principal Stress Ratio at failure	3.26	3.25	3.54	2.76	2.94			
Minor Principal Effective Stress at fail. (psf)	407.9	796.7	1024.4	3384.3	3865.9			
Major Principal Effective Stress at fail. (psf)	1330.3	2587.9	3629.5	9335.2	11352.7			
Corrections Applied	Membrane	Membrane	Membrane	Membrane	Membrane			
Axial Strain at failure (%)	7.80	11.08	8.92	10.40	9.97			
Test performed at strain rate (%/hr)	0.58	0.58	0.70	0.82	0.86			

Comments:

Colorado - Non-blenderized - 1008 psf

Colorado - Non-blenderized - 3024 psf

Colorado - Non-blenderized - 8064 psf

Colorado - Non-blenderized - 10,080 psf

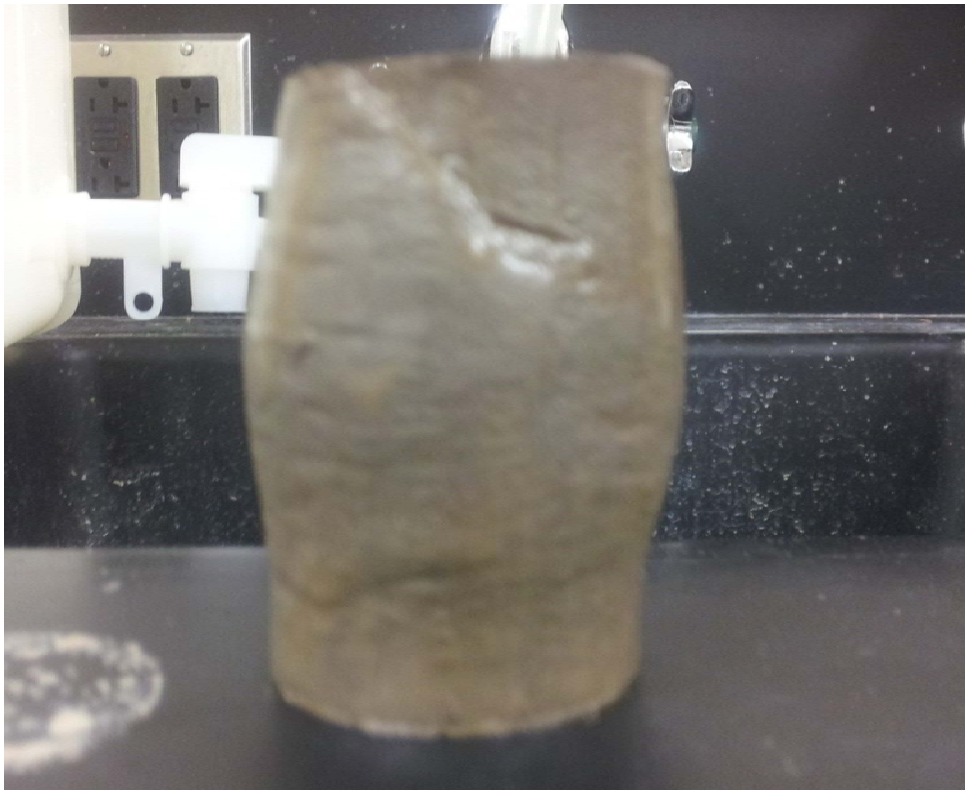

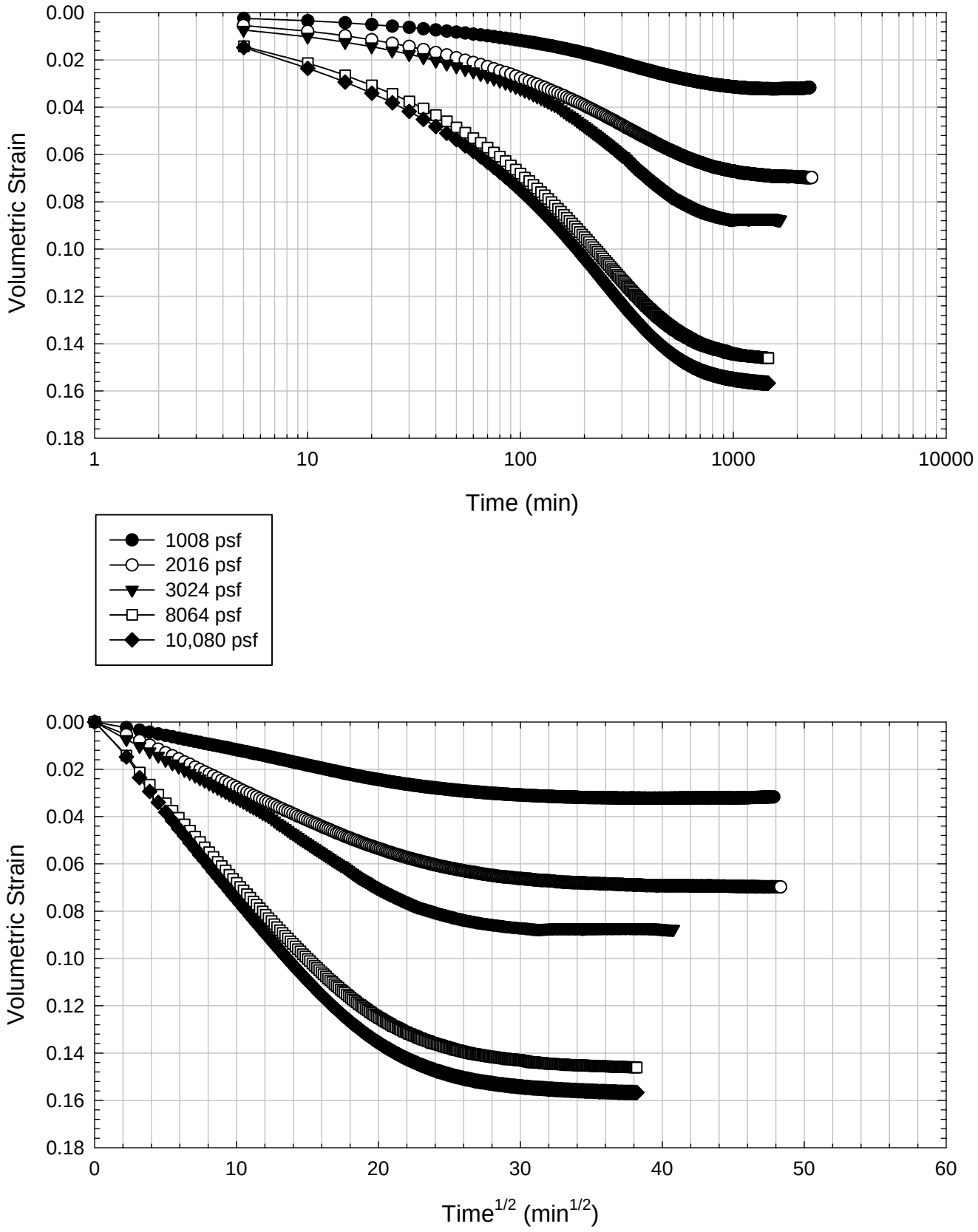
Colorado Clay - Non-blenderized
Volumetric Strain
0.00
0.02
0.04
0.06
0.08
0.10
0.12
0.14
0.16
0.18
1
10
100
1000
10000
Time (min)
1008 psf
2016 psf
3024 psf
8064 psf
10,080 psf
Volumetric Strain
0.00
0.02
0.04
0.06
0.08
0.10
0.12
0.14
0.16
0.18
0
10
20
30
40
50
60
Time^1/2 (min^1/2)

Colorado Clay - Non-blenderized

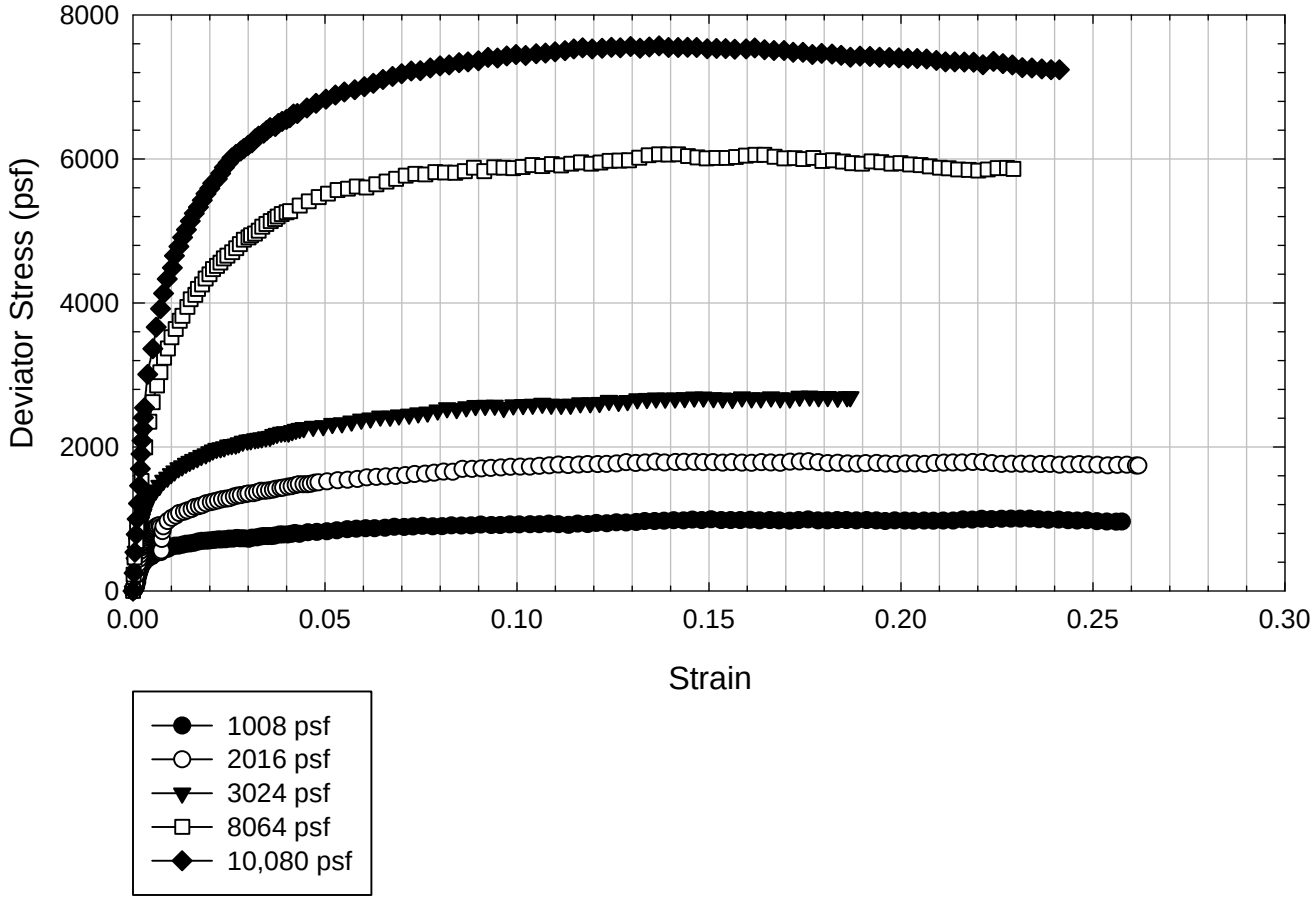

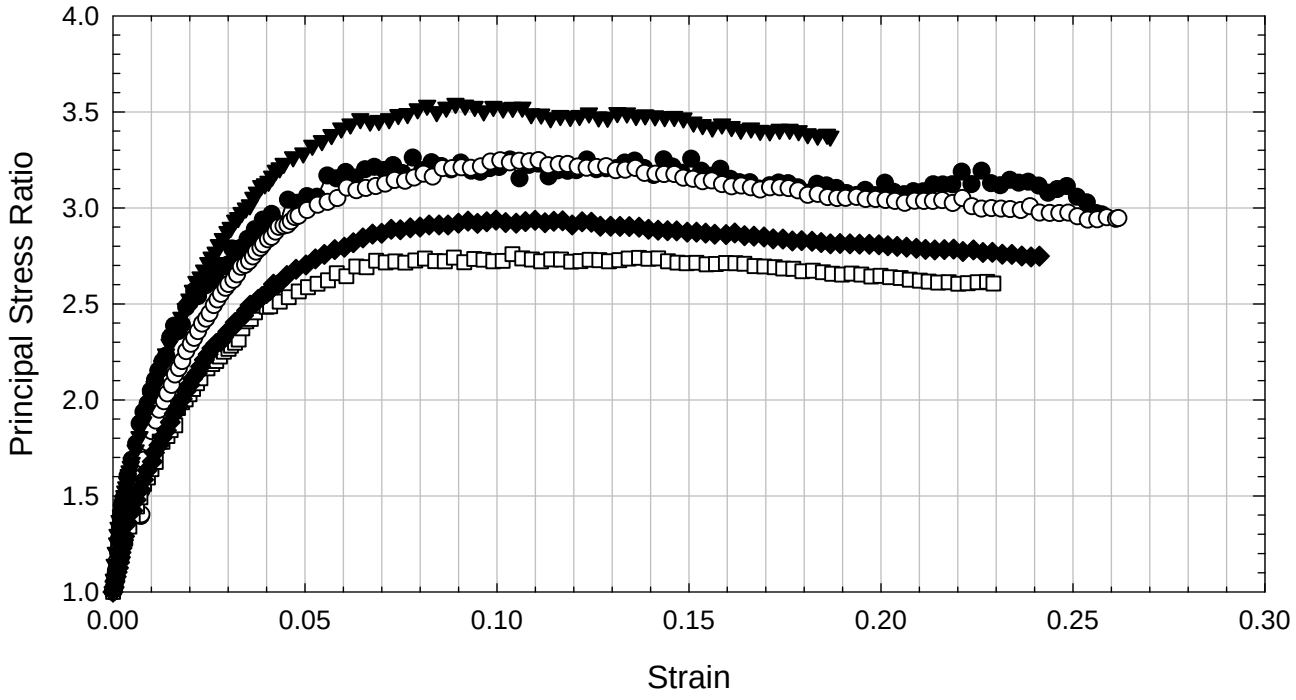

Colorado Clay - Non-blenderized

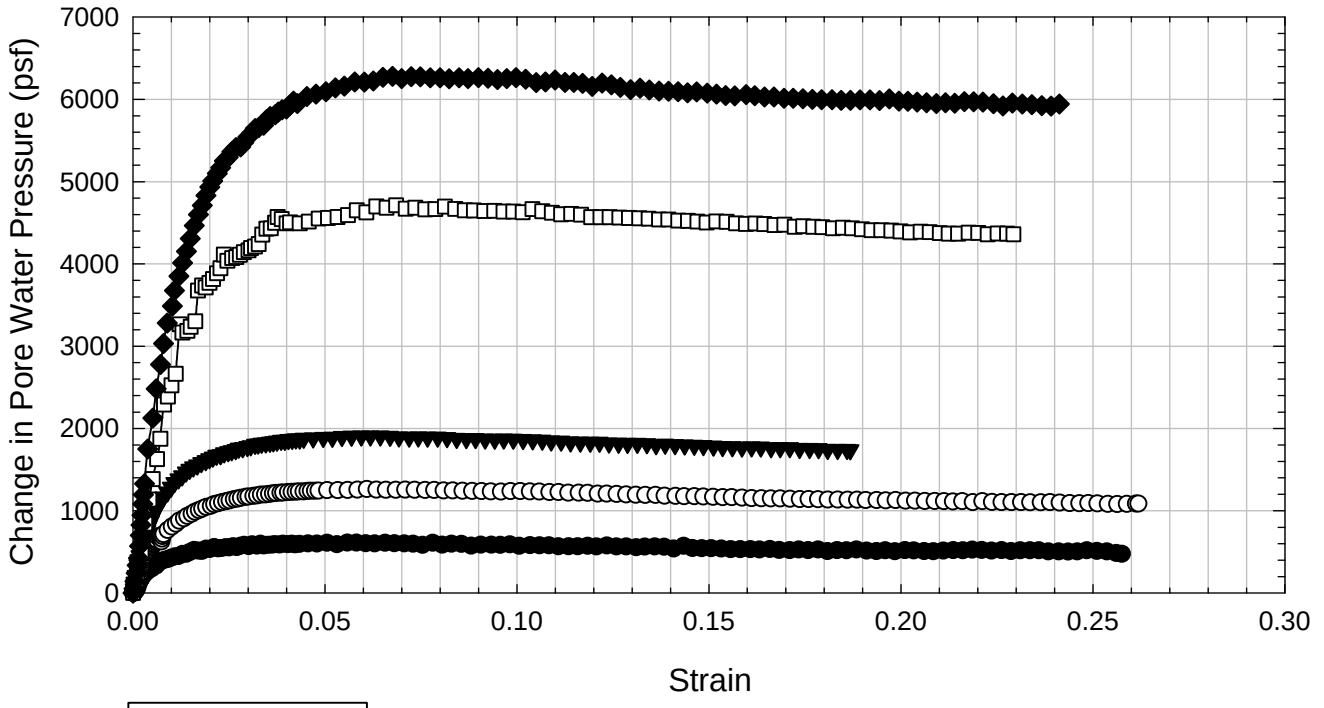

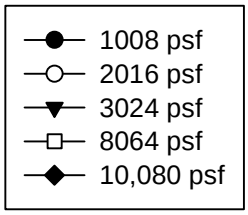

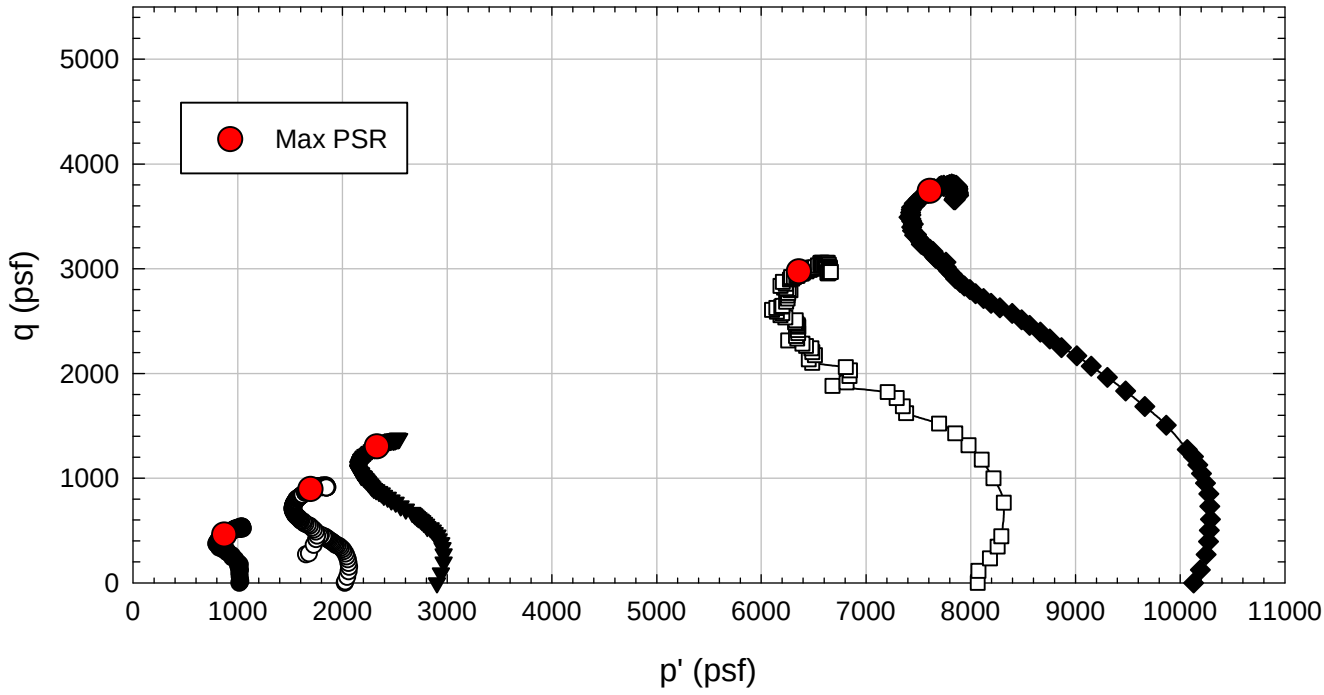

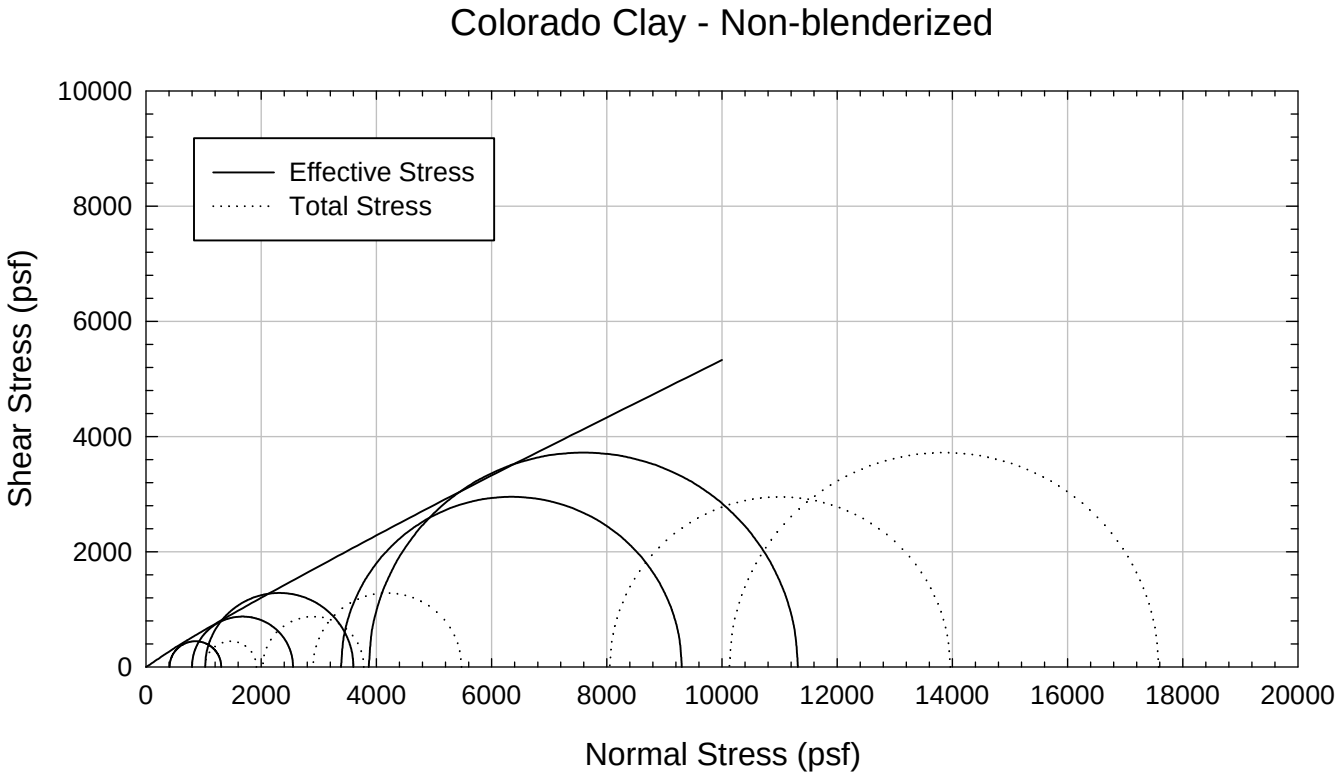
Colorado Clay - Non-blenderized
Effective Stress
Total Stress
Shear Stress (psf)
Normal Stress (psf)
0
2000
4000
6000
8000
10000
12000
14000
16000
18000
20000

E.3. NOVA Clay

E.3.1 Non-blenderized

Virginia Polytechnic Institute and State University
Geotechnical Engineering Laboratory
Triaxial Data Sheet

Project:	Fully Softened Shear Strength
Sample I.D./Loc.:	NOVA - Non-blenderized - Consolidated Undrained
Classification:	Fat Clay (CH)

Sample Preparation	Remolded at LL
Specimen Saturation Method	Wet

Specific Gravity	2.80	Assumed
Method for Dimensions After Consol.	Case and Chilver (1959)	

Test Number	1	2	3	4	5	6	7	
Start Date (m/d/y)	2/23/2012	2/23/2012	2/23/2012	2/23/2012	2/23/2012	3/1/2012	3/7/2012	
End Date (m/d/y)	2/29/2012	3/1/2012	3/1/2012	3/1/2012	3/1/2012	3/9/2012	3/15/2012	
Backpressure (psf)	7200	7200	7200	7200	7200	7200	7200	
Consolidation Pressure (psf)	1008	2016	3024	4464	6048	8064	10080	
B value	0.98	0.98	0.96	0.97	0.97	0.99	0.98	
Initial Values								
Initial Height (in.)	3.018	3.087	2.979	3.100	3.01	3.05	2.99	
Initial Diameter (in.)	1.379	1.313	1.374	1.385	1.38	1.38	1.39	
Initial Sample Weight (g.)	122.77	122.49	121.36	126.35	121.10	125.12	125.50	
Water Content (%)	56.32	55.49	56.93	56.29	56.80	53.17	51.20	
Dry Unit Weight (pcf)	66.4	71.8	66.7	65.9	65.8	68.5	69.5	
Wet Unit Weight (pcf)	103.8	111.6	104.7	103.1	103.1	104.9	105.1	
Saturation (%)	96.6	100.0	98.4	95.5	96.0	95.9	94.7	
Void Ratio	1.63	1.55	1.62	1.65	1.66	1.55	1.51	
After Consolidation								
t_{100} Using Casagrande Method (min)	382.16	694.10	554.76	972.40	951.88	934.25	812.65	
Volumetric Strain (%)	2.92	8.43	9.84	12.11	14.37	15.79	16.91	
Height After Consolidation (in.)	2.988	3.000	2.881	2.975	2.868	2.891	2.822	
Area After Consolidation (in.)	1.464	1.278	1.385	1.385	1.343	1.332	1.350	
Final Values								
Water Content (%)	53.67	50.58	48.00	45.77	44.13	42.97	40.34	
Dry Unit Weight (pcf)	68.0	72.3	73.9	74.5	76.41	79.31	82.05	
Wet Unit Weight (pcf)	104.5	108.9	109.4	108.6	110.13	113.38	115.14	
Saturation (%)	95.7	100.0	98.5	95.3	96.04	100.00	100.00	
Void Ratio	1.57	1.42	1.36	1.34	1.29	1.20	1.13	
Failure								
Failure Criteria	Max PSR	Max PSR	Max PSR	Max PSR	Max PSR	Max PSR	Max PSR	
Deviator Stress at failure (psf)	936.27	1792.01	2450.34	3224.93	4103.55	5187.98	6767.33	
Principal Stress Ratio at failure	3.23	3.07	2.90	2.61	2.46	2.35	2.40	
Minor Principal Effective Stress at fail. (psf)	432.6	881.4	1306.6	2025.9	2837.5	3875.9	4863.1	
Major Principal Effective Stress at fail. (psf)	1399.3	2705.5	3792.4	5285.1	6971.5	9094.5	11666.2	
Corrections Applied	Membrane	Membrane	Membrane	Membrane	Membrane	Membrane	Membrane	
Axial Strain at failure (%)	9.49	9.31	10.84	10.45	9.04	9.07	10.76	
Test performed at strain rate (%/hr)	1.00	0.50	0.50	0.50	0.50	0.50	0.50	

Comments:

NOVA - Non-blenderized - 1008 psf

NOVA - Non-blenderized - 2016 psf

NOVA - Non-blenderized - 3024 psf

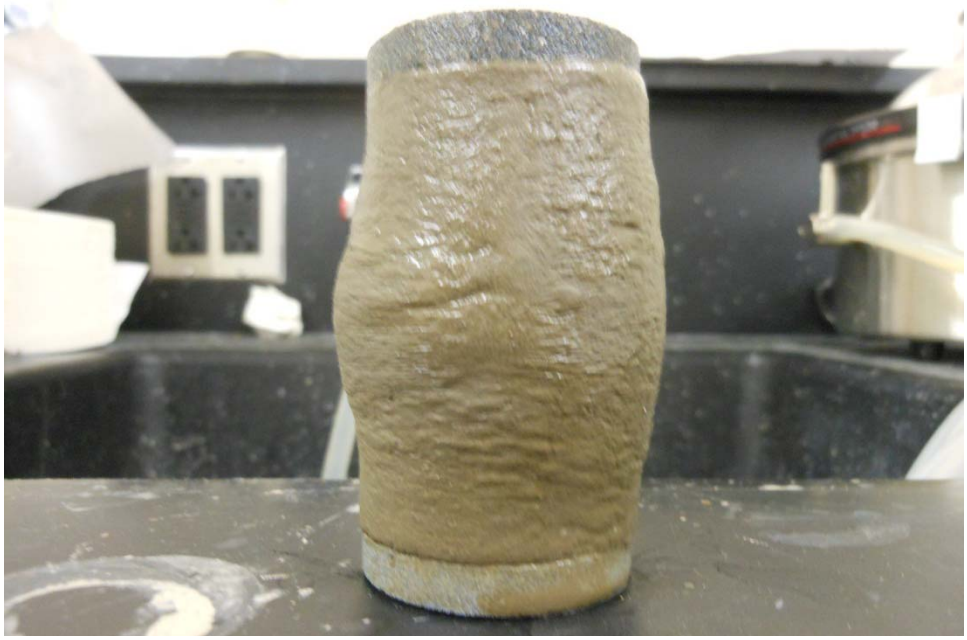

NOVA - Non-blenderized - 4464 psf

NOVA - Non-blenderized - 6048 psf

NOVA - Non-blenderized - 8064 psf

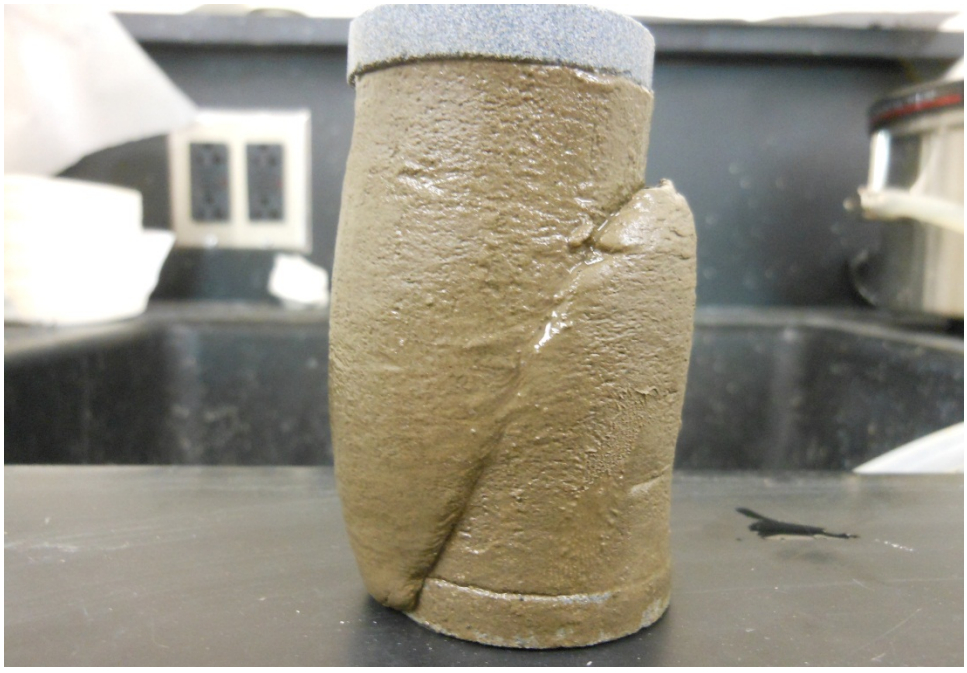

NOVA - Non-blenderized – 10,080 psf

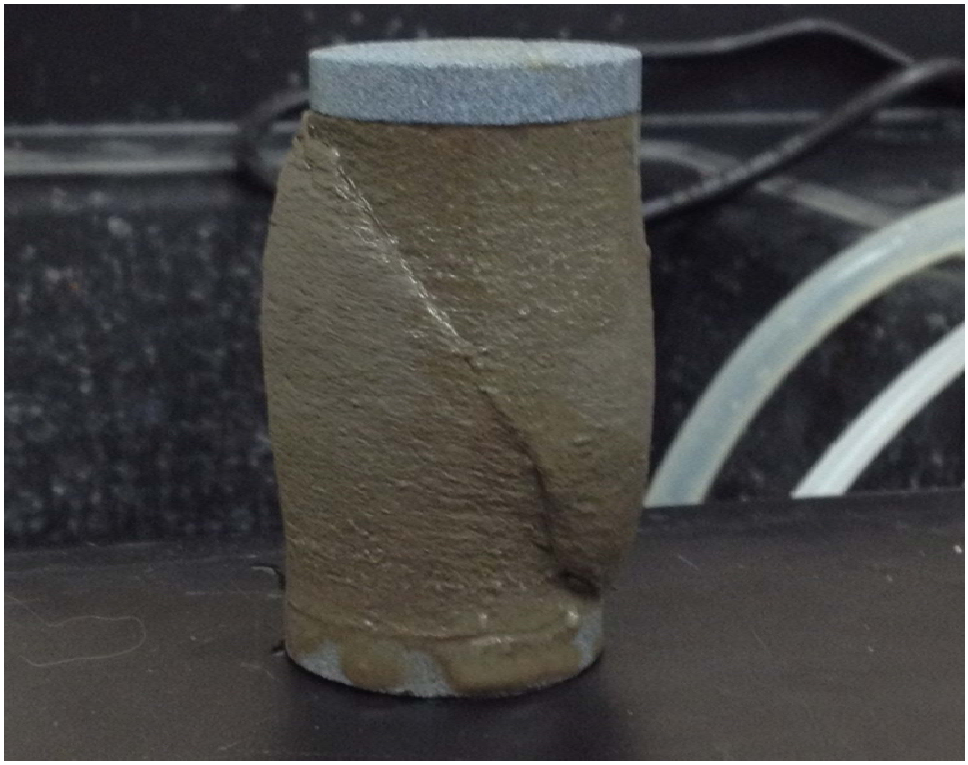

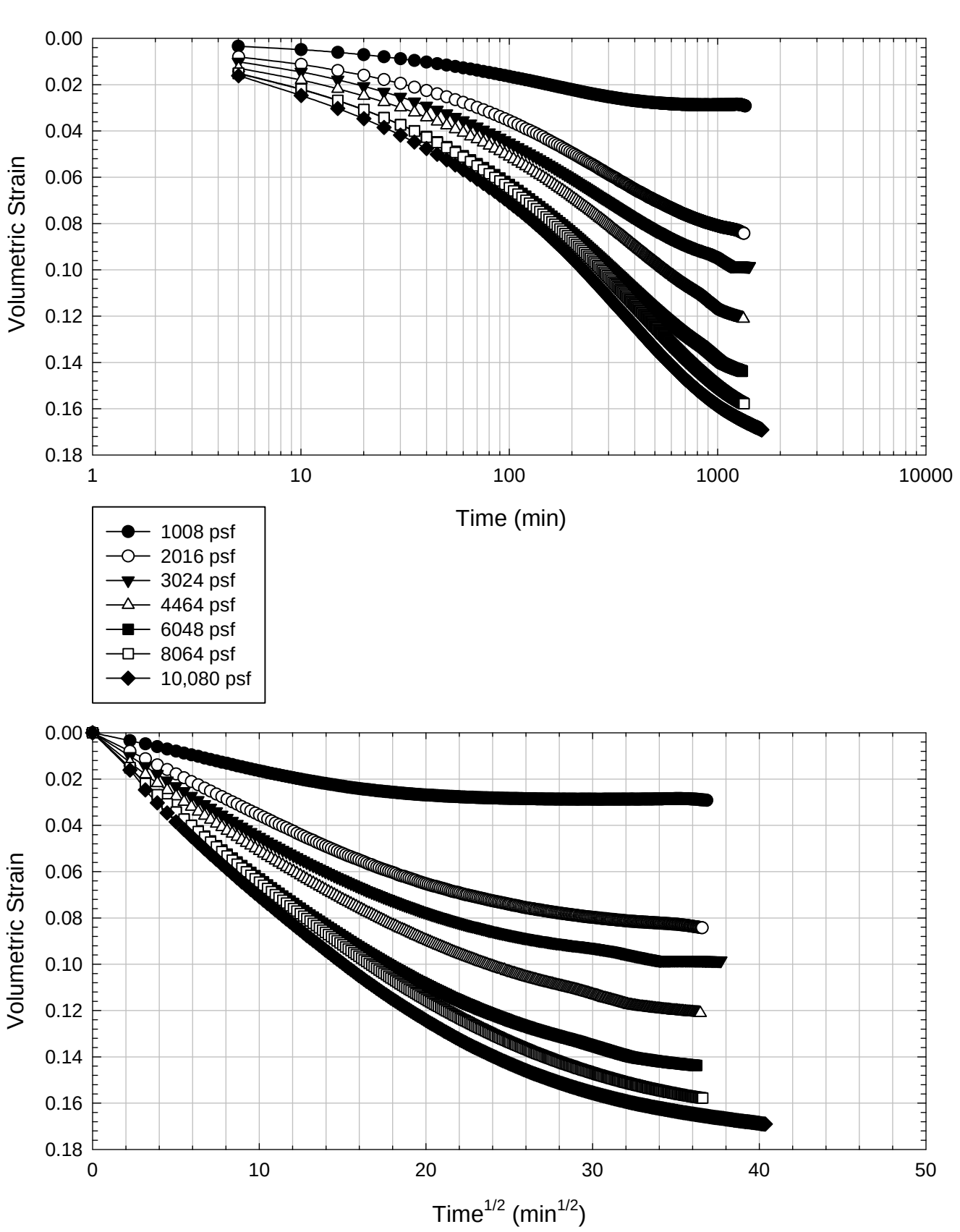
NOVA - Non-blenderized
Volumetric Strain
0.00
0.02
0.04
0.06
0.08
0.10
0.12
0.14
0.16
0.18
1
10
100
1000
10000
Time (min)
1008 psf
2016 psf
3024 psf
4464 psf
6048 psf
8064 psf
10,080 psf
Volumetric Strain
0.00
0.02
0.04
0.06
0.08
0.10
0.12
0.14
0.16
0.18
0
10
20
30
40
50
Time^1/2 (min^1/2)

NOVA - Non-blenderized

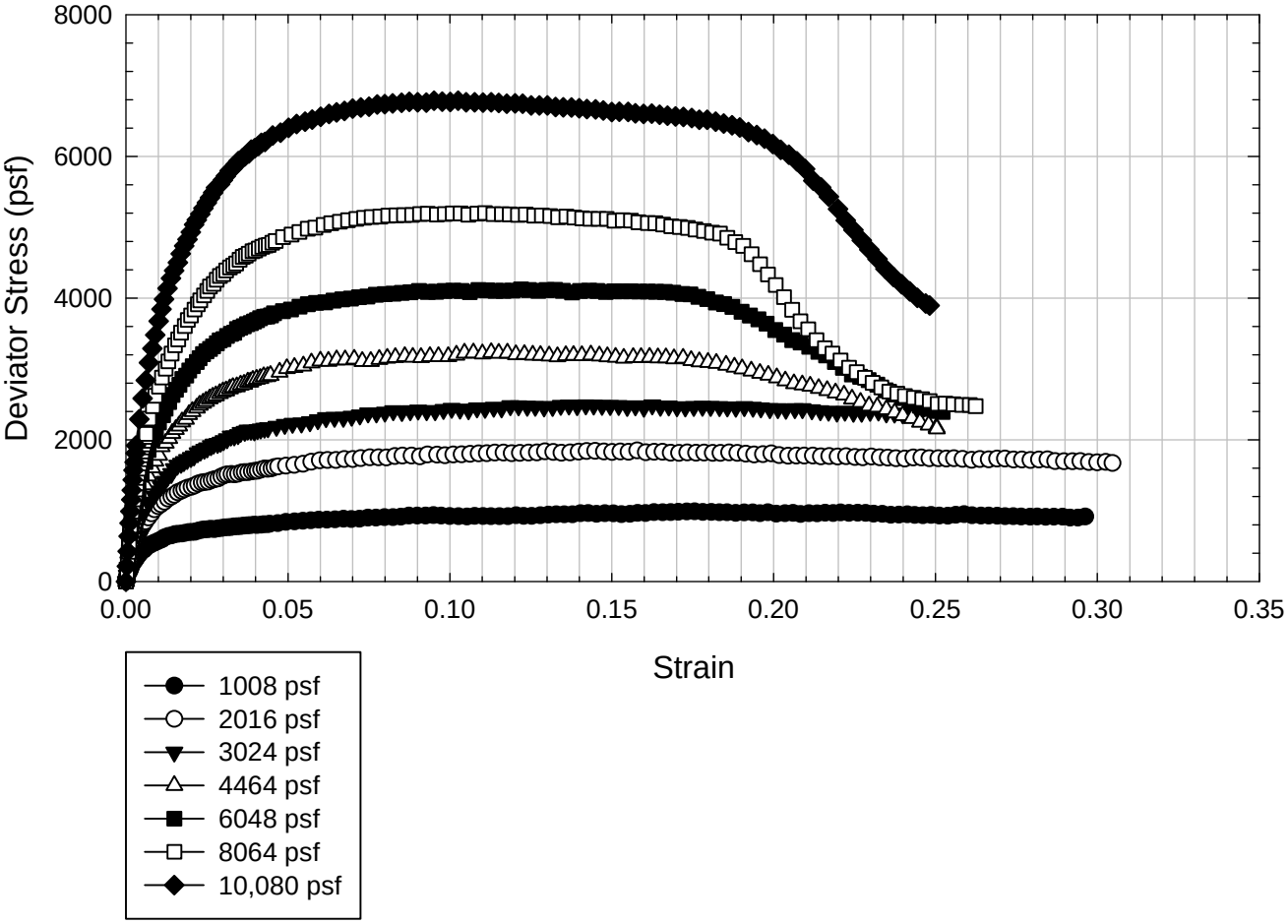

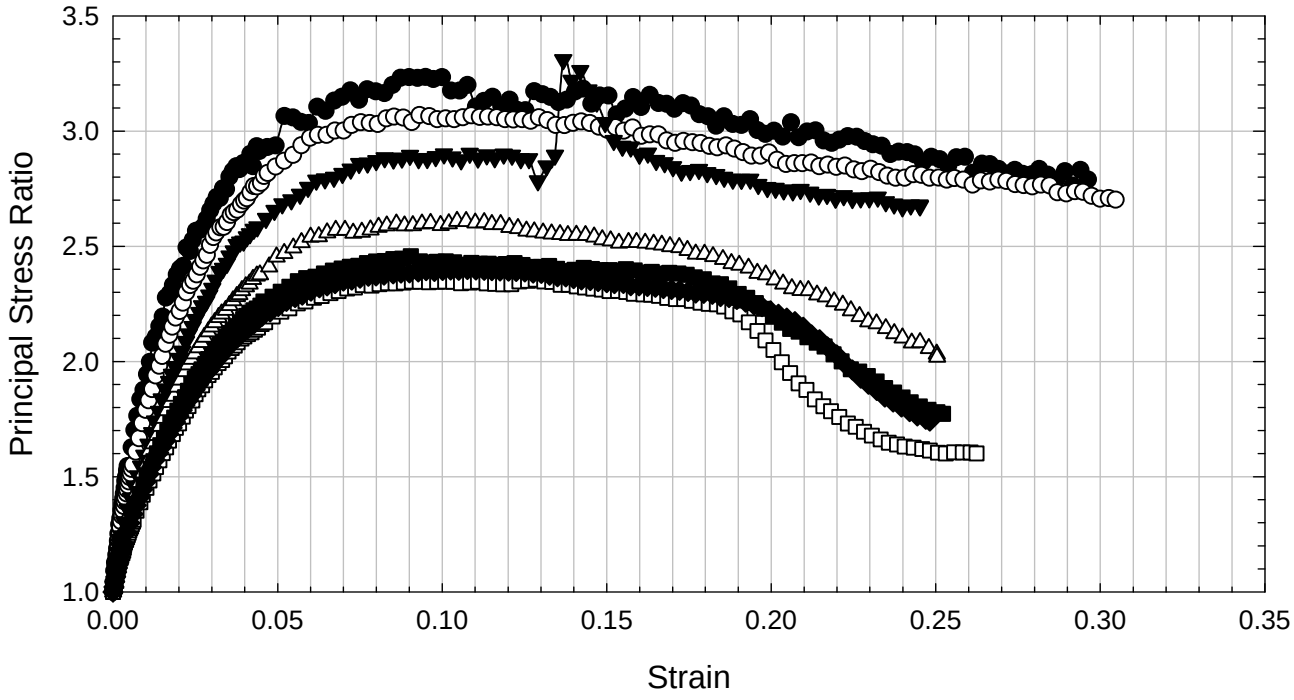

NOVA - Non-blenderized

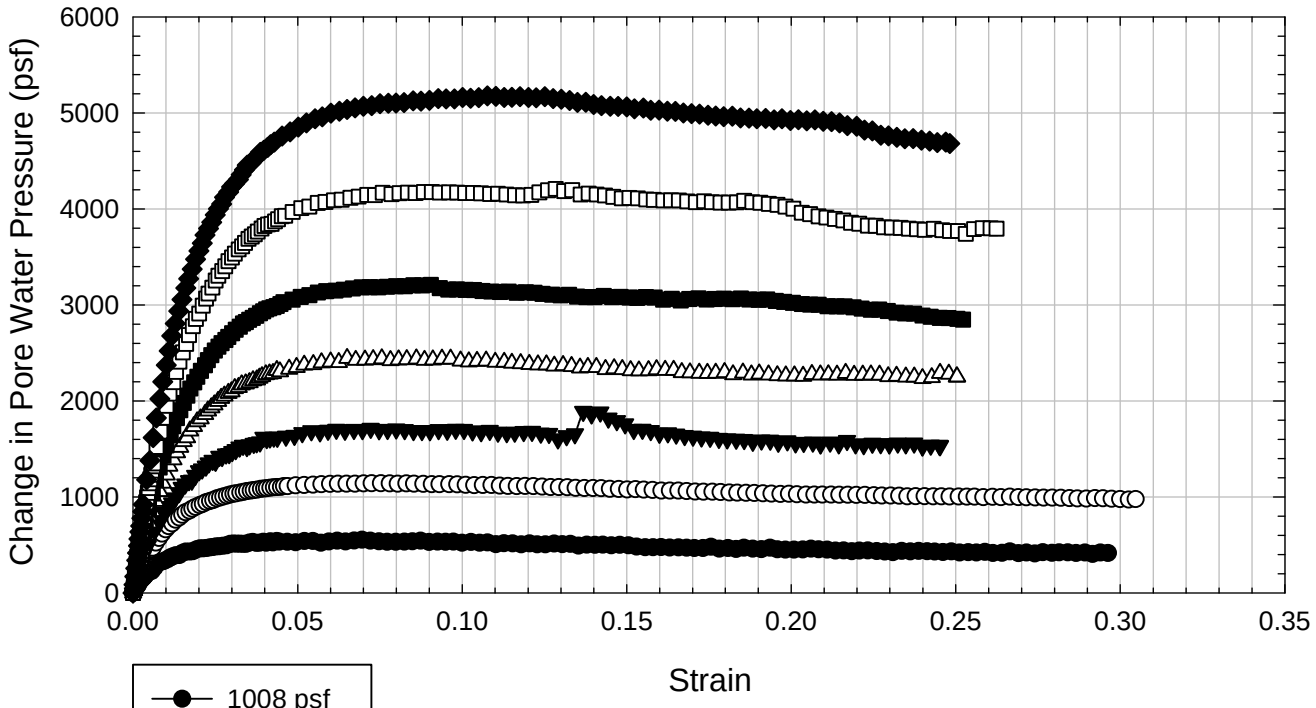

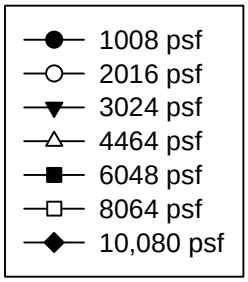

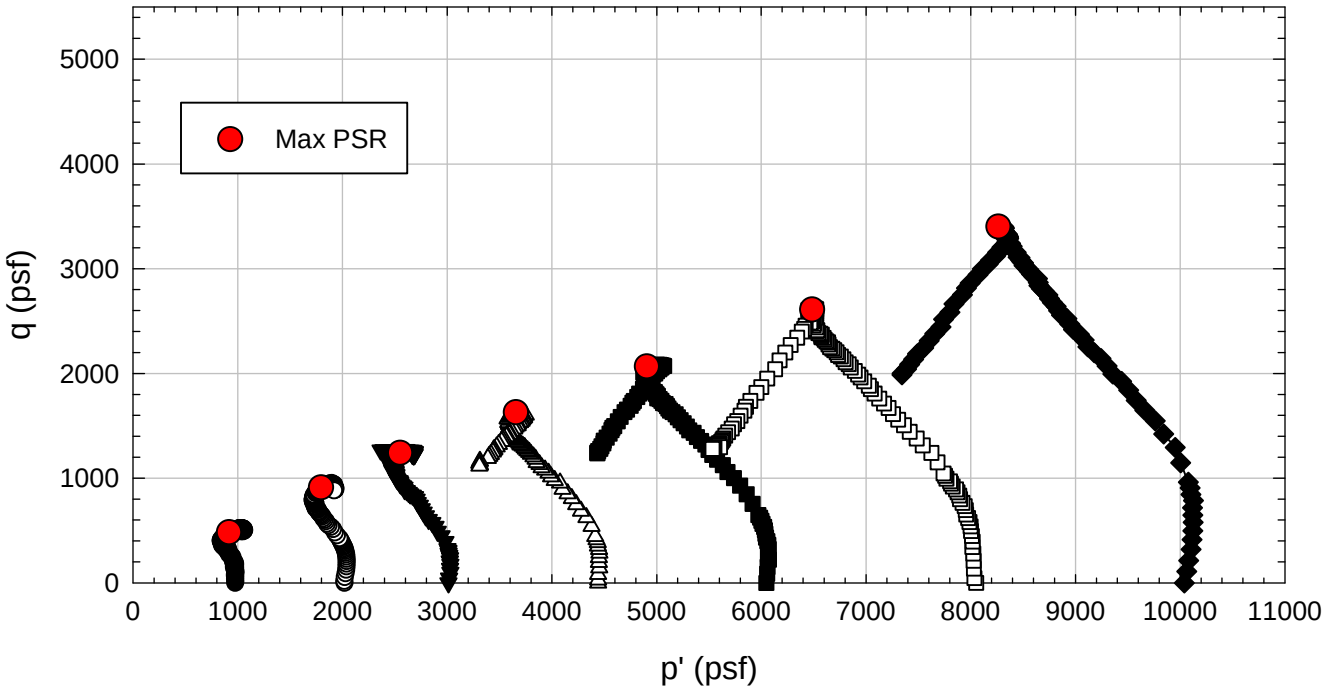

NOVA - Non-blenderized

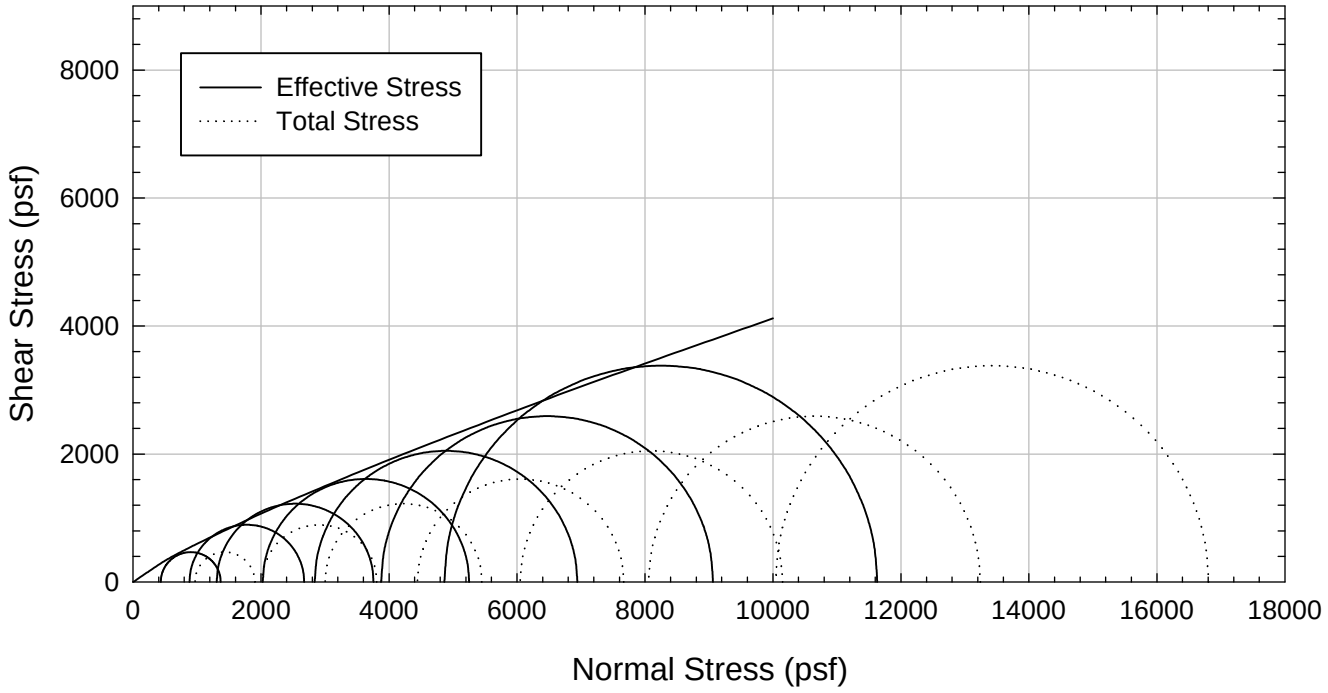

E.3.2 Packed

Virginia Polytechnic Institute and State University
Geotechnical Engineering Laboratory
Triaxial Data Sheet

Project:	Fully Softened Shear Strength
Sample I.D./Loc.:	NOVA - Non-blenderized - Packed - Consolidated Undrained
Classification:	Fat Clay (CH)

Sample Preparation	Packed
Specimen Saturation Method	Wet

Specific Gravity	2.80	Assumed
Method for Dimensions After Consol.	Case and Chilver (1959)	

Test Number	1	2	3	4	5	6	7	8
Start Date (m/d/y)	6/14/2013	8/9/2013						
End Date (m/d/y)	7/3/2013	8/18/2013						
Backpressure (psf)	7200	7200						
Consolidation Pressure (psf)	432	432						
B value	0.98	0.99						
Initial Values								
Initial Height (in.)	2.825	2.816						
Initial Diameter (in.)	1.320	1.310						
Initial Sample Weight (g.)	104.57	102.04						
Water Content (%)	53.66	58.18						
Dry Unit Weight (pcf)	67.1	64.7						
Wet Unit Weight (pcf)	103.0	102.4						
Saturation (%)	93.6	95.9						
Void Ratio	1.61	1.70						
After Consolidation								
t_{100} Using Casagrande Method (min)	1700	1500.00						
Volumetric Strain (%)	2.83	2.83						
Height After Consolidation (in.)	2.798	2.789						
Area After Consolidation (in.)	1.343	1.322						
Final Values								
Water Content (%)	53.24	55.58						
Dry Unit Weight (pcf)	69.2	66.4						
Wet Unit Weight (pcf)	106.1	103.3						
Saturation (%)	97.8	95.4						
Void Ratio	1.52	1.63						
Failure								
Failure Criteria	Max PSR	Max PSR						
Deviator Stress at failure (psf)	615.33	540.20						
Principal Stress Ratio at failure	4.53	3.87						
Minor Principal Effective Stress at fail. (psf)	178.0	197.6						
Major Principal Effective Stress at fail. (psf)	807.1	764.2						
Corrections Applied	Membrane	Membrane						
Axial Strain at failure (%)	4.00	7.74						
Test performed at strain rate (%/hr)	0.25	0.25						

Comments:

NOVA - Non-blenderized - Packed Liquidity Index = 0.53 - 432 psf

NOVA - Non-blenderized - Packed Liquidity Index = 0.80 - 432 psf

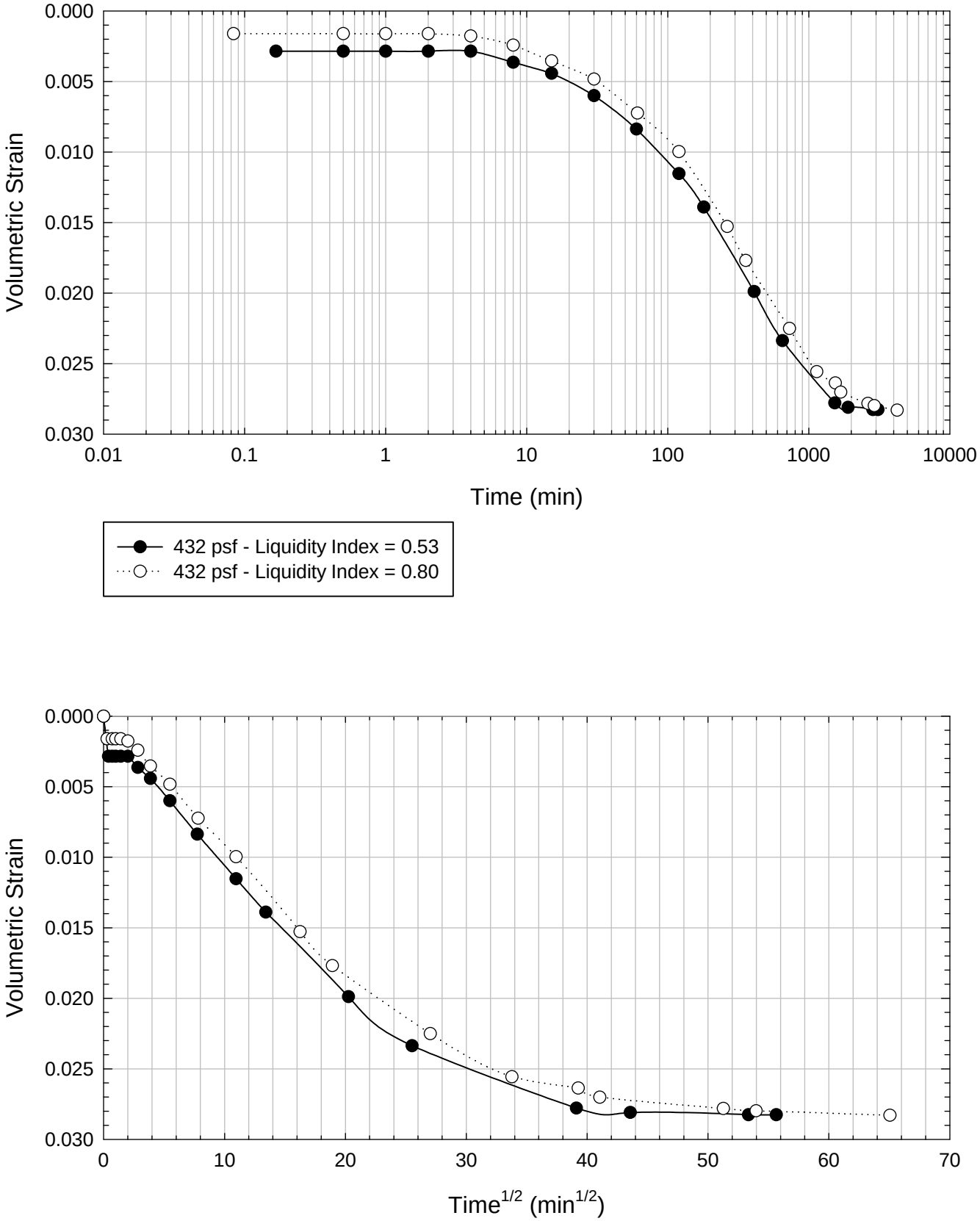
NOVA - Non-blenderized - Packed
Volumetric Strain
0.000
0.005
0.010
0.015
0.020
0.025
0.030
0.01
0.1
1
10
100
1000
10000
Time (min)
432 psf - Liquidity Index = 0.53
432 psf - Liquidity Index = 0.80
Volumetric Strain
0.000
0.005
0.010
0.015
0.020
0.025
0.030
0
10
20
30
40
50
60
70
Time^1/2 (min^1/2)

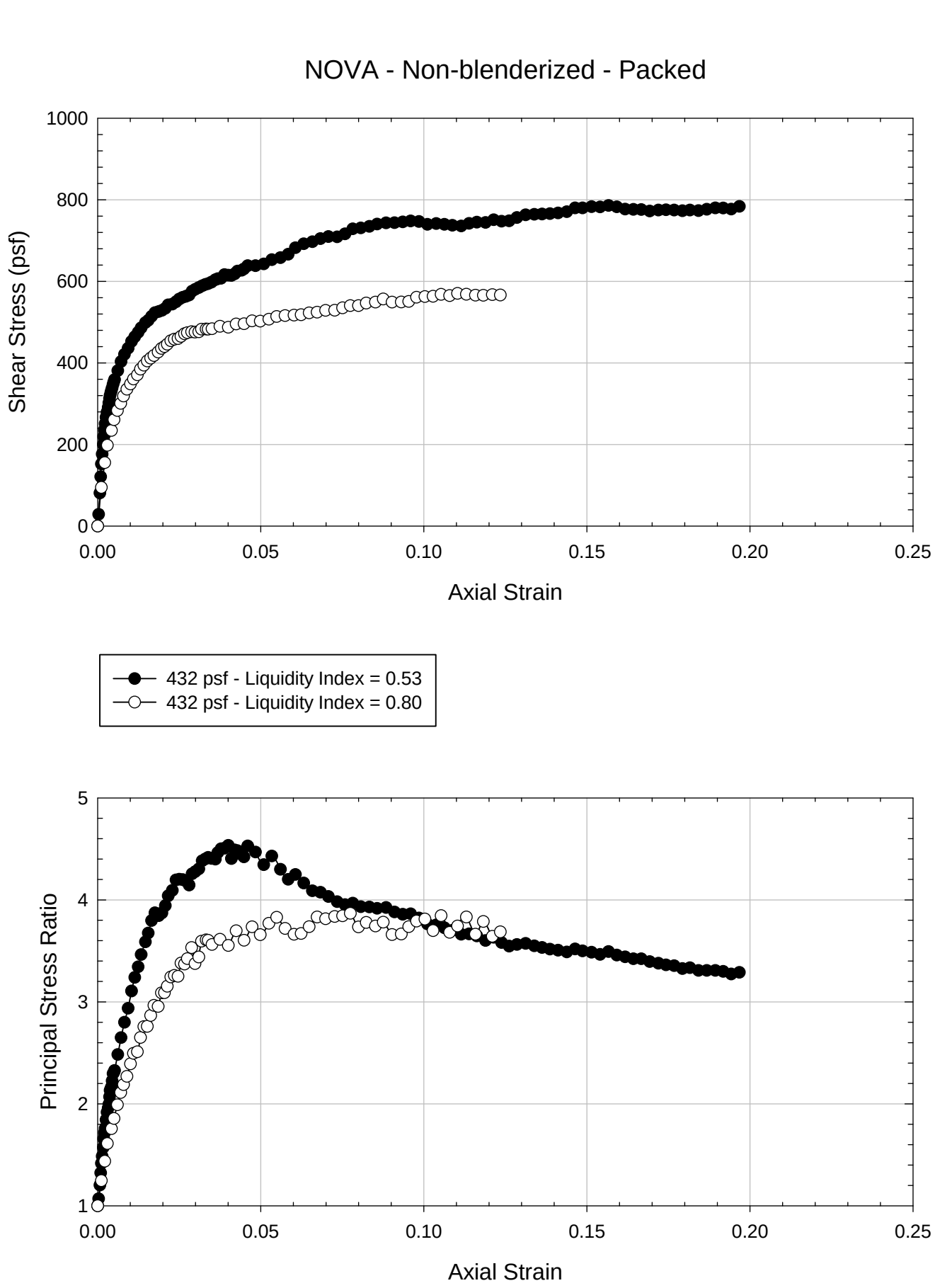
NOVA - Non-blenderized - Packed
Shear Stress (psf)
1000
800
600
400
200
0
0.00
0.05
0.10
0.15
0.20
0.25
Axial Strain
432 psf - Liquidity Index = 0.53
432 psf - Liquidity Index = 0.80
Principal Stress Ratio
5
4
3
2
1
0.00
0.05
0.10
0.15
0.20
0.25
Axial Strain

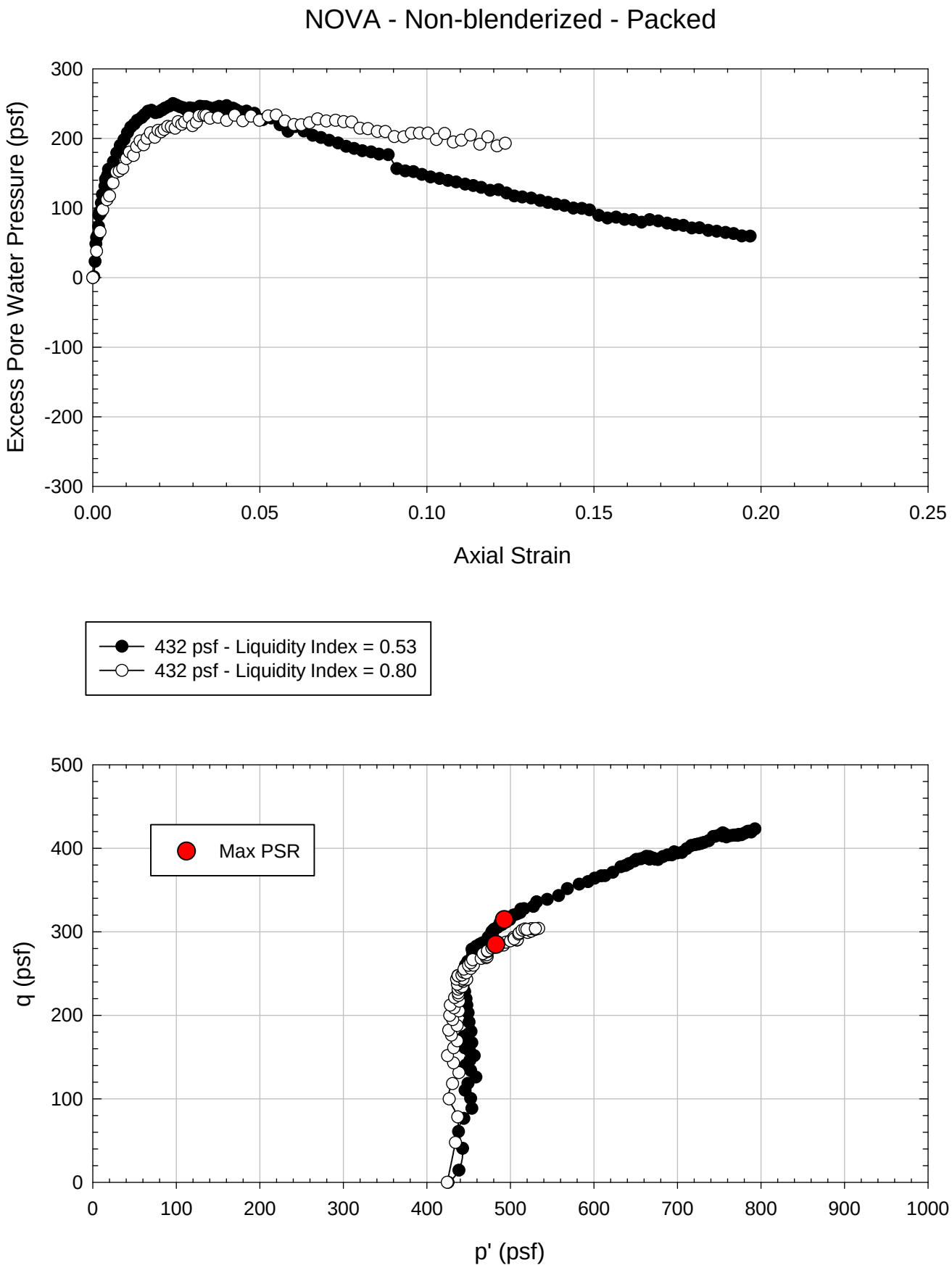
NOVA - Non-blenderized - Packed
Excess Pore Water Pressure (psf)
300
200
100
0
-100
-200
-300
0.00
0.05
0.10
0.15
0.20
0.25
Axial Strain
432 psf - Liquidity Index = 0.53
432 psf - Liquidity Index = 0.80
Max PSR
q (psf)
500
400
300
200
100
0
0
100
200
300
400
500
600
700
800
900
1000
p' (psf)

Virginia Polytechnic Institute and State University
Geotechnical Engineering Laboratory
Triaxial Data Sheet

Project:	Fully Softened Shear Strength
Sample I.D./Loc.:	NOVA - Non-blenderized - Consolidated Undrained - Packed
Classification:	Fat Clay (CH)

Sample Preparation	Packed
Specimen Saturation Method	Wet

Specific Gravity	2.80	Assumed
Method for Dimensions After Consol.	Case and Chilver (1959)	

Test Number	1	2	3	4	5	6	7	8
Start Date (m/d/y)	12/7/2012	12/9/2012	12/8/2012					
End Date (m/d/y)	12/12/2012	12/13/2012	12/13/2012					
Backpressure (psf)	7200	7200	7200					
Consolidation Pressure (psf)	2016	3024	4464					
B value	0.97	0.98	0.98					
Initial Values								
Initial Height (in.)	2.850	2.811	2.834					
Initial Diameter (in.)	1.307	1.305	1.307					
Initial Sample Weight (g.)	105.39	105.73	105.45					
Water Content (%)	53.37	51.84	51.99					
Dry Unit Weight (pcf)	68.5	70.6	69.5					
Wet Unit Weight (pcf)	105.0	107.1	105.6					
Saturation (%)	96.3	98.3	96.2					
Void Ratio	1.55	1.48	1.51					
After Consolidation								
t_{100} Using Casagrande Method (min)	733.26	1118.45	1494.23					
Volumetric Strain (%)	4.81	7.95	10.15					
Height After Consolidation (in.)	2.804	2.737	2.738					
Area After Consolidation (in.)	1.299	1.267	1.251					
Final Values								
Water Content (%)	48.70	45.66	43.26					
Dry Unit Weight (pcf)	71.0	76.2	77.3					
Wet Unit Weight (pcf)	105.6	110.9	110.7					
Saturation (%)	93.4	98.8	96.1					
Void Ratio	1.46	1.29	1.26					
Failure								
Failure Criteria	Max PSR	Max PSR	Max PSR					
Deviator Stress at failure (psf)	1764.85	2531.33	3432.52					
Principal Stress Ratio at failure	2.95	2.73	2.73					
Minor Principal Effective Stress at fail. (psf)	916.2	1477.7	2009.1					
Major Principal Effective Stress at fail. (psf)	2704.5	4038.0	5474.9					
Corrections Applied	Membrane	Membrane	Membrane					
Axial Strain at failure (%)	6.78	8.34	9.59					
Test performed at strain rate (%/hr)	0.50	0.30	0.30					

Comments:

NOVA - Non-blenderized - Packed - 2016 psf

NOVA - Non-blenderized - Packed - 3024 psf

NOVA - Non-blenderized - Packed - 4464 psf

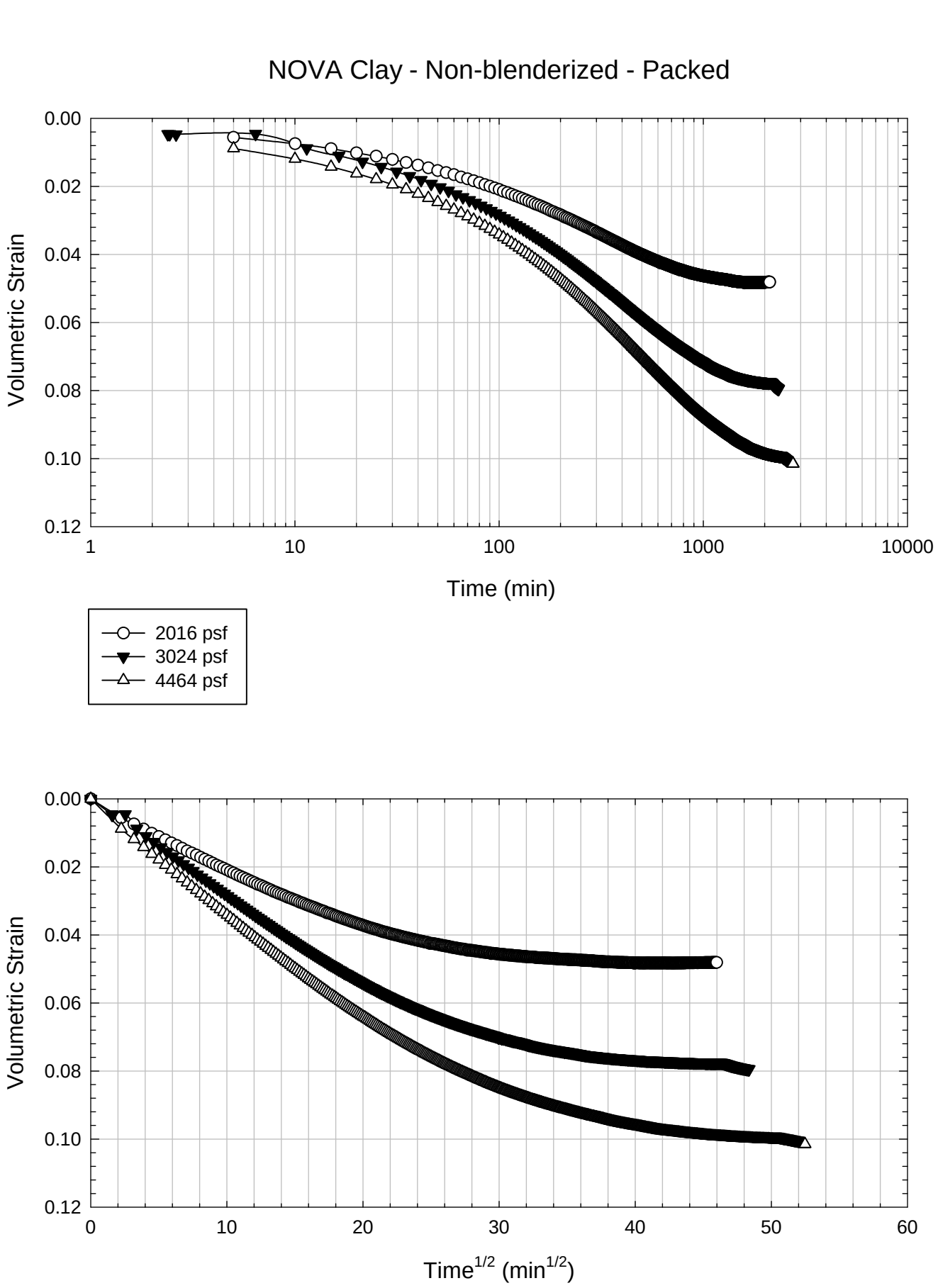
NOVA Clay - Non-blenderized - Packed
Volumetric Strain
0.00
0.02
0.04
0.06
0.08
0.10
0.12
1
10
100
1000
10000
Time (min)
2016 psf
3024 psf
4464 psf
Volumetric Strain
0.00
0.02
0.04
0.06
0.08
0.10
0.12
0
10
20
30
40
50
60
Time^1/2 (min^1/2)

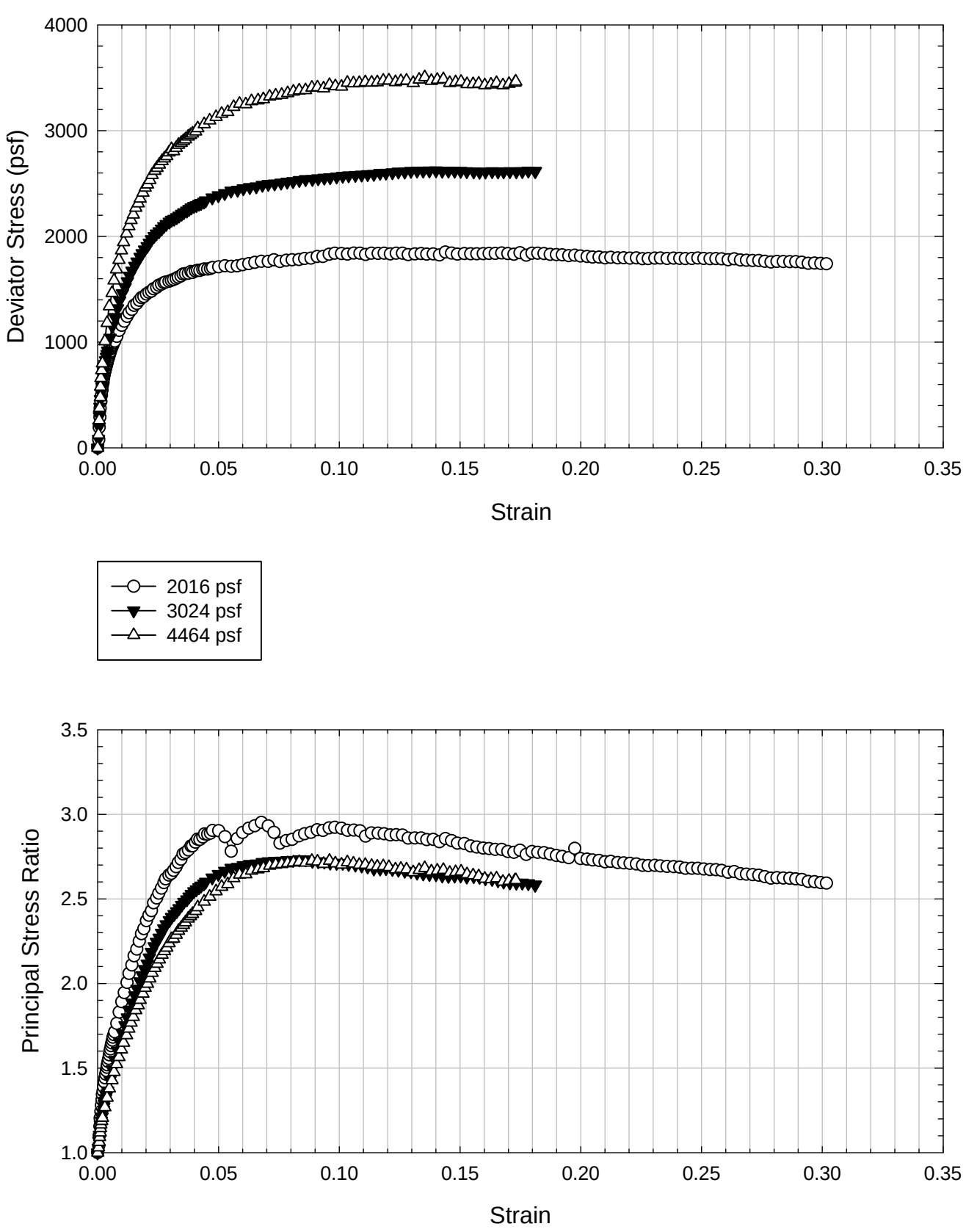
NOVA Clay - Non-blenderized - Packed
Deviator Stress (psf)
4000
3000
2000
1000
0
0.00
0.05
0.10
0.15
0.20
0.25
0.30
0.35
Strain
2016 psf
3024 psf
4464 psf
Principal Stress Ratio
3.5
3.0
2.5
2.0
1.5
1.0
0.00
0.05
0.10
0.15
0.20
0.25
0.30
0.35
Strain

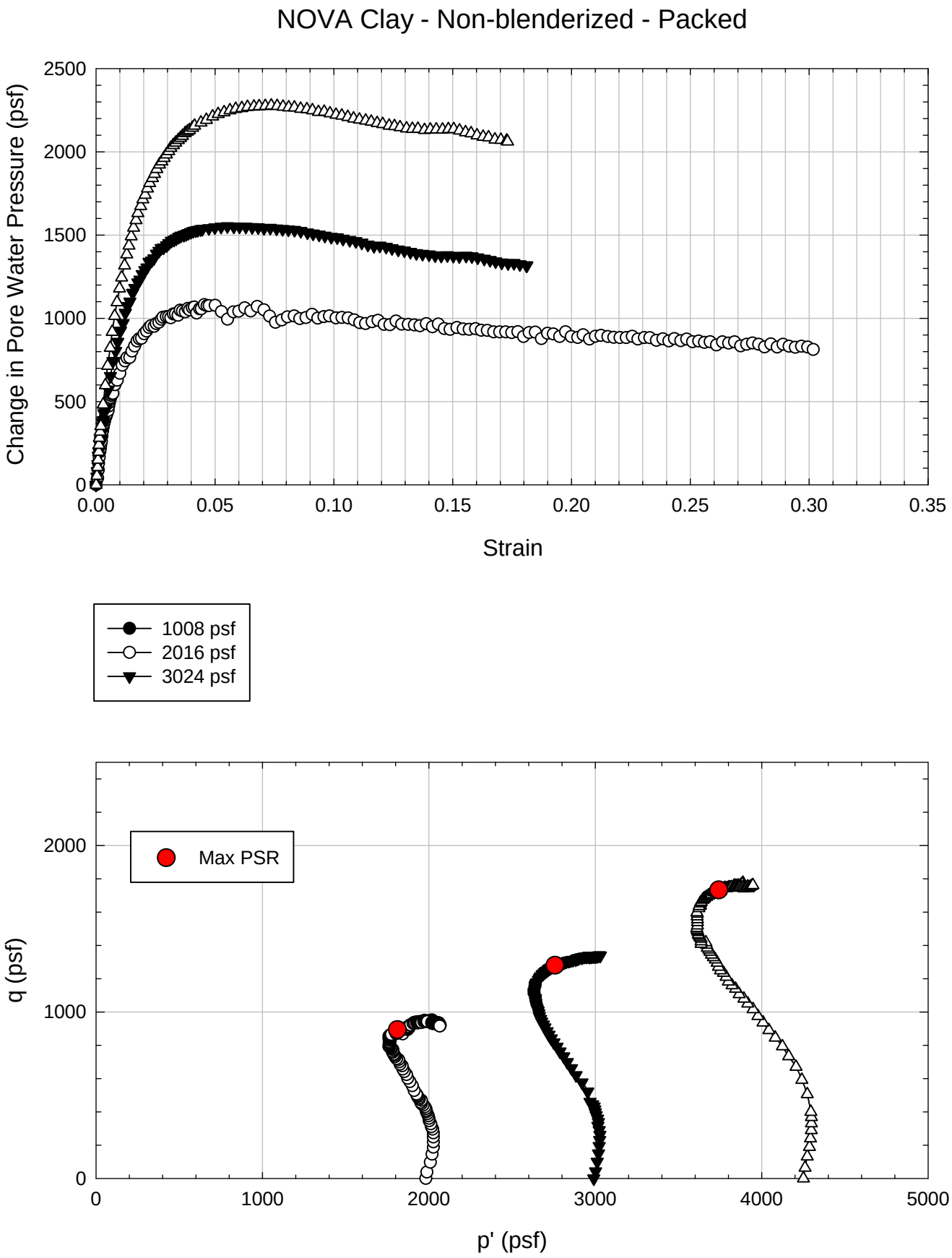
NOVA Clay - Non-blenderized - Packed
Change in Pore Water Pressure (psf)
2500
2000
1500
1000
500
0
0.00
0.05
0.10
0.15
0.20
0.25
0.30
0.35
Strain
1008 psf
2016 psf
3024 psf
Max PSR
q (psf)
2000
1000
0
0
1000
2000
3000
4000
5000
p' (psf)

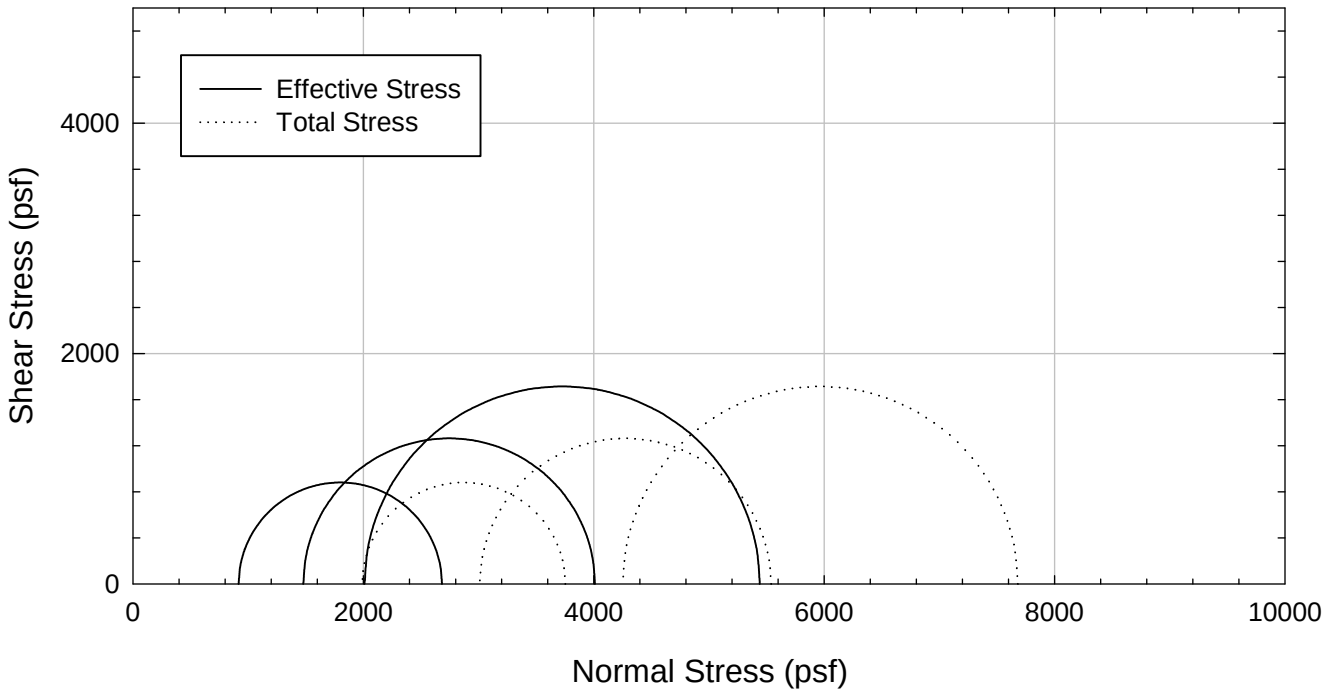
NOVA Clay - Non-blenderized - Packed
Effective Stress
Total Stress
Shear Stress (psf)
Normal Stress (psf)
0
2000
4000
6000
8000
10000

E.4. Oak Harbor

E.4.1 Non-blenderized

Virginia Polytechnic Institute and State University
Geotechnical Engineering Laboratory
Triaxial Data Sheet

Project:	Fully Softened Shear Strength
Sample I.D./Loc.:	Oak Harbor - Non-blenderized - Consolidated Undrained
Classification:	Lean Clay (CL)

Sample Preparation	Remolded at LL
Specimen Saturation Method	Wet

Specific Gravity	2.82	
Method for Dimensions After Consol.	Case and Chilver (1959)	

Test Number	1	2	3	4	5	6	7	
Start Date (m/d/y)	2/24/2013	2/24/2013	2/24/2013	2/24/2013	2/24/2013			
End Date (m/d/y)	2/28/2013	2/28/2013	2/28/2013	2/28/2013	2/27/2013			
Backpressure (psf)	7200	7200	7200	7200	7200			
Consolidation Pressure (psf)	1008	2016	5472	8064	10080			
B value	1.00	0.97	0.95	0.98	0.99			
Initial Values								
Initial Height (in.)	3.011	2.979	3.015	2.981	3.026			
Initial Diameter (in.)	1.359	1.368	1.372	1.360	1.371			
Initial Sample Weight (g.)	131.65	130.67	133.80	130.17	133.28			
Water Content (%)	36.51	36.54	36.84	36.10	35.98			
Dry Unit Weight (pcf)	84.1	83.3	83.6	84.1	83.6			
Wet Unit Weight (pcf)	114.8	113.7	114.4	114.5	113.7			
Saturation (%)	94.3	92.6	94.0	93.3	91.8			
Void Ratio	1.09	1.11	1.11	1.09	1.11			
After Consolidation								
t_{100} Using Casagrande Method (min)	878.23	724.11	664.40	614.90	580.73			
Volumetric Strain (%)	3.69	7.51	13.31	13.73	15.75			
Height After Consolidation (in.)	2.974	2.904	2.881	2.845	2.867			
Area After Consolidation (in.)	1.415	1.396	1.347	1.320	1.321			
Final Values								
Water Content (%)	34.51	31.70	27.72	25.95	25.12			
Dry Unit Weight (pcf)	86.1	88.4	94.8	95.6	97.2			
Wet Unit Weight (pcf)	115.8	116.4	121.1	120.4	121.6			
Saturation (%)	93.2	90.1	91.3	87.0	87.3			
Void Ratio	1.04	0.99	0.86	0.84	0.81			
Failure								
Failure Criteria	Max PSR	Max PSR	Max PSR	Max PSR	Max PSR			
Deviator Stress at failure (psf)	750.78	1426.79	3398.88	4954.31	6241.89			
Principal Stress Ratio at failure	2.60	2.15	2.46	2.50	2.52			
Minor Principal Effective Stress at fail. (psf)	491.8	1270.5	2355.5	3320.7	4125.7			
Major Principal Effective Stress at fail. (psf)	1276.7	2735.1	5800.9	8311.7	10400.4			
Corrections Applied	Membrane	Membrane	Membrane	Membrane	Membrane			
Axial Strain at failure (%)	10.52	11.63	14.28	10.93	9.72			
Test performed at strain rate (%/hr)	0.50	0.50	0.50	0.50	0.50			

Comments: The computer crashed during the shearing stage of the sample consolidated to 10,080 psf. The test was included because it stopped close to the maximum principal stress ratio.

Oak Harbor - Non-blenderized - 1008 psf

Oak Harbor - Non-blenderized – 2016 psf

Oak Harbor - Non-blenderized - 5472 psf

Oak Harbor - Non-blenderized - 8064 psf

Oak Harbor - Non-blenderized - 10,080 psf

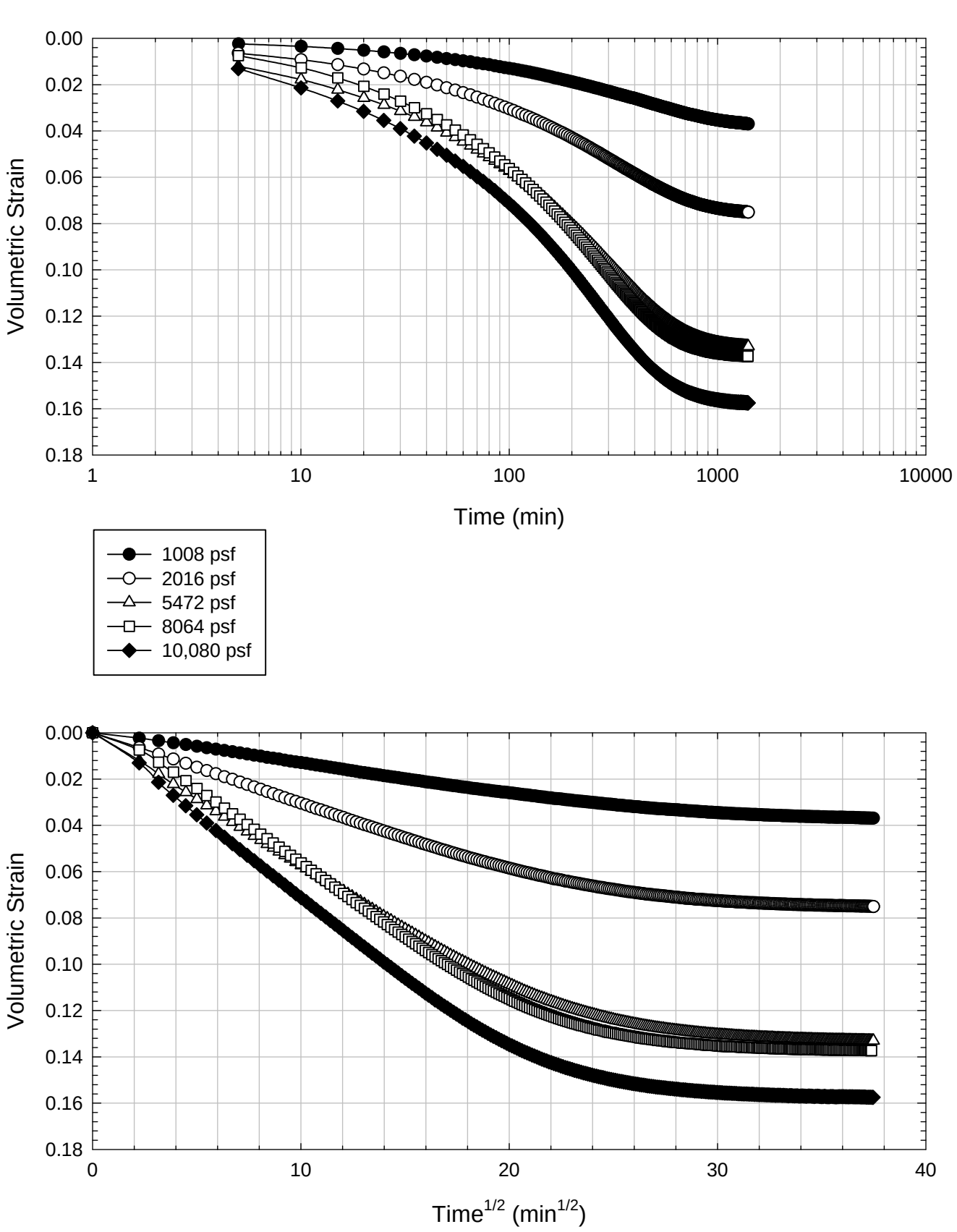
Oak Harbor - Non-blenderized
Volumetric Strain
0.00
0.02
0.04
0.06
0.08
0.10
0.12
0.14
0.16
0.18
1
10
100
1000
10000
Time (min)
1008 psf
2016 psf
5472 psf
8064 psf
10,080 psf
Volumetric Strain
0.00
0.02
0.04
0.06
0.08
0.10
0.12
0.14
0.16
0.18
0
10
20
30
40
Time^1/2 (min^1/2)

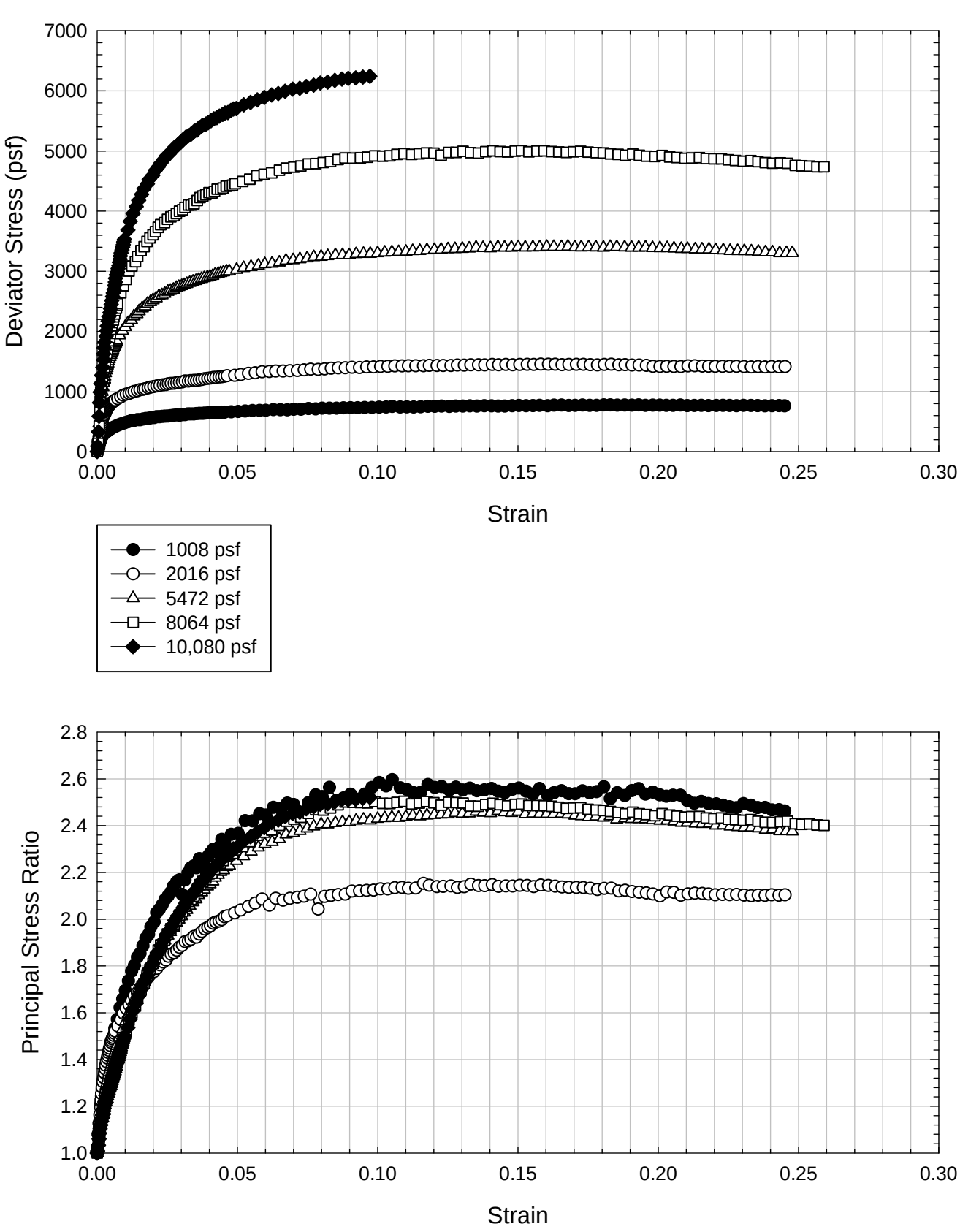
Oak Harbor - Non-blenderized
Deviator Stress (psf)
7000
6000
5000
4000
3000
2000
1000
0
0.00
0.05
0.10
0.15
0.20
0.25
0.30
Strain
1008 psf
2016 psf
5472 psf
8064 psf
10,080 psf
Principal Stress Ratio
2.8
2.6
2.4
2.2
2.0
1.8
1.6
1.4
1.2
1.0
0.00
0.05
0.10
0.15
0.20
0.25
0.30
Strain

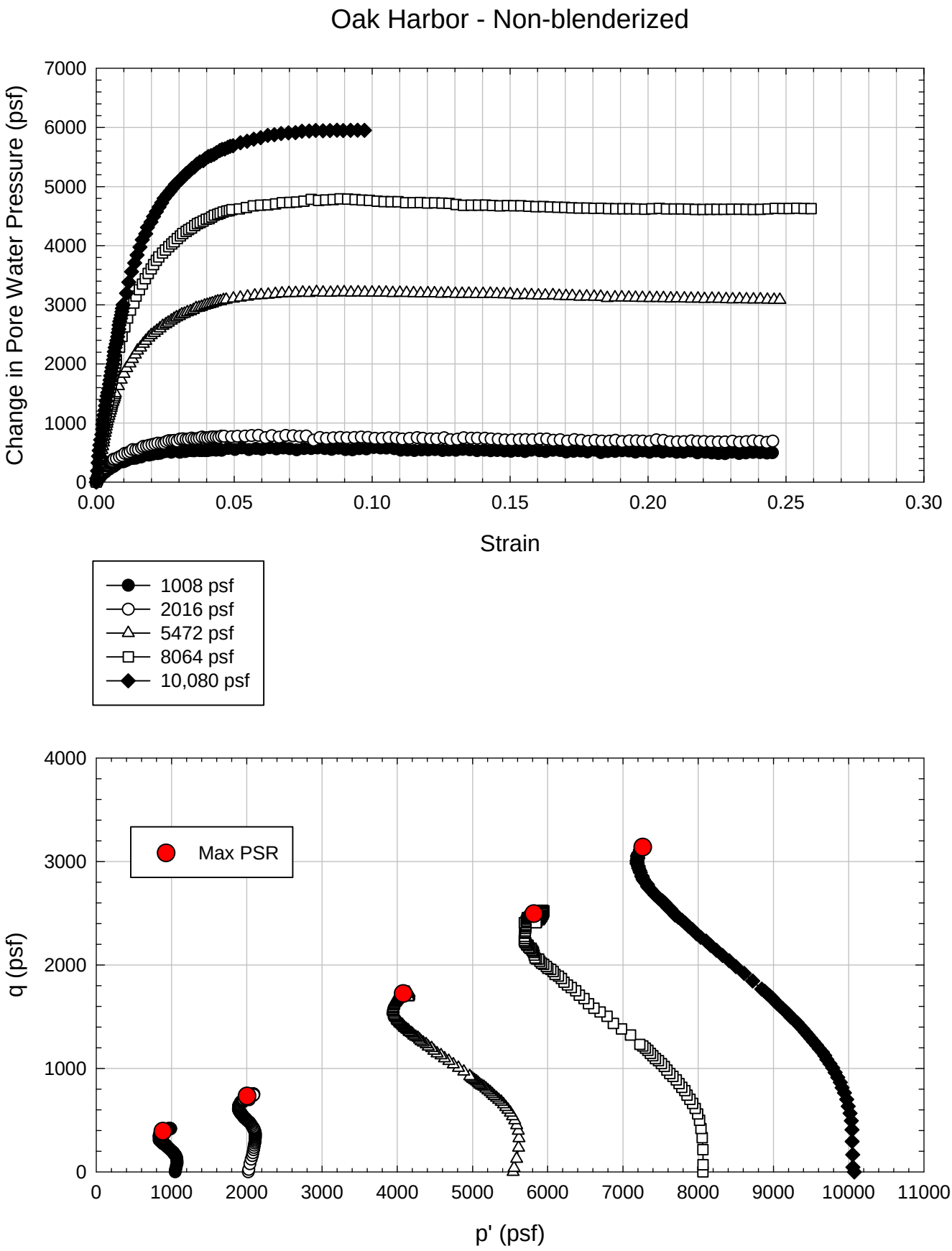
Oak Harbor - Non-blenderized
Change in Pore Water Pressure (psf)
7000
6000
5000
4000
3000
2000
1000
0
0.00
0.05
0.10
0.15
0.20
0.25
0.30
Strain
1008 psf
2016 psf
5472 psf
8064 psf
10,080 psf
q (psf)
4000
3000
2000
1000
0
Max PSR
0
1000
2000
3000
4000
5000
6000
7000
8000
9000
10000
11000
p' (psf)

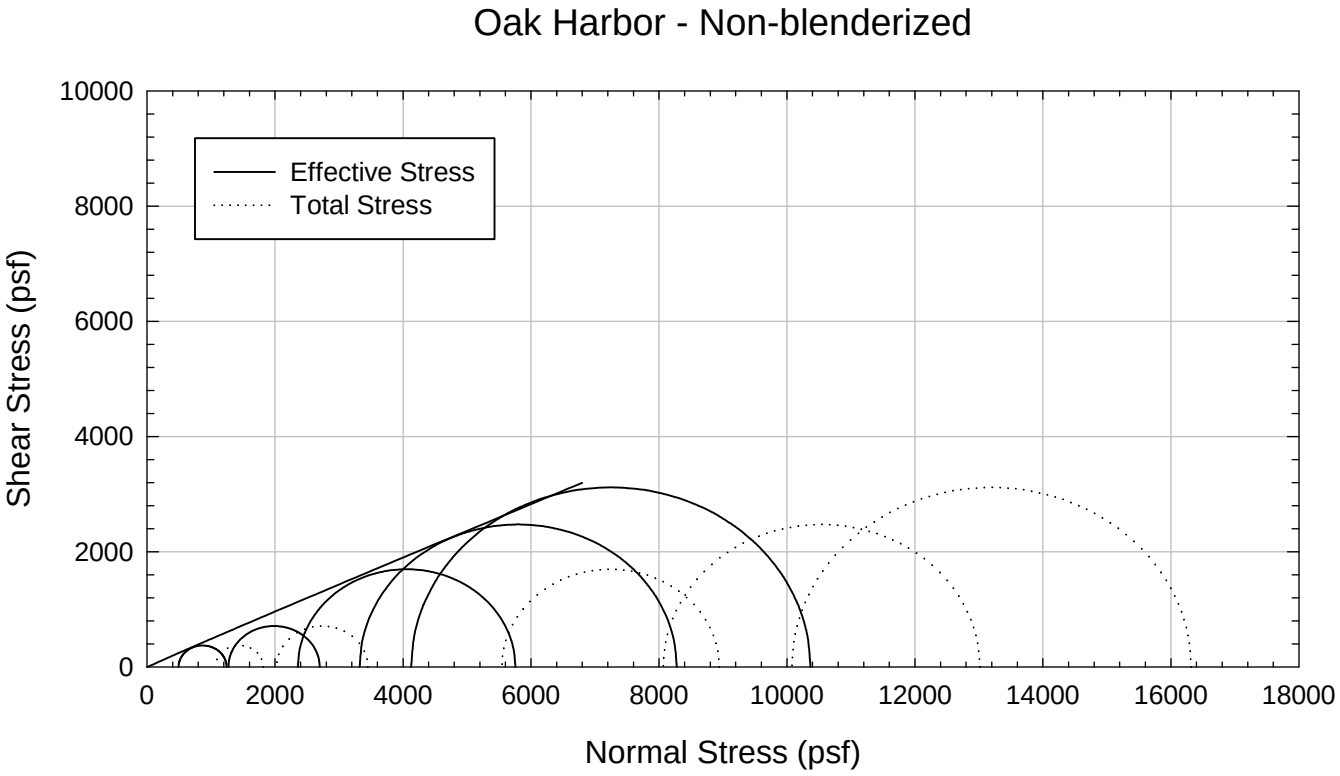
Oak Harbor - Non-blenderized
Effective Stress
Total Stress
Shear Stress (psf)
Normal Stress (psf)
0
2000
4000
6000
8000
10000
12000
14000
16000
18000

E.4.2 Packed

Virginia Polytechnic Institute and State University
Geotechnical Engineering Laboratory
Triaxial Data Sheet

Project:	Fully Softened Shear Strength
Sample I.D./Loc.:	Oak Harbor - Non-blenderized - Packed - Consolidated Undrained
Classification:	Lean Clay (CL)

Sample Preparation	Packed
Specimen Saturation Method	Wet

Specific Gravity	2.82	
Method for Dimensions After Consol.	Case and Chilver (1959)	

Test Number	1	2	3	4	5	6	7	8
Start Date (m/d/y)	5/22/2013	5/31/2013						
End Date (m/d/y)	5/30/2013	6/12/2013						
Backpressure (psf)	7200	7200						
Consolidation Pressure (psf)	144	432						
B value	1.00	0.97						
Initial Values								
Initial Height (in.)	2.849	2.778						
Initial Diameter (in.)	1.311	1.307						
Initial Sample Weight (g.)	113.35	114.81						
Water Content (%)	36.61	35.82						
Dry Unit Weight (pcf)	82.2	86.4						
Wet Unit Weight (pcf)	112.3	117.4						
Saturation (%)	90.5	97.4						
Void Ratio	1.14	1.04						
After Consolidation								
t_{100} Using Casagrande Method (min)	1300.00	2200.00						
Volumetric Strain (%)	0.49	3.13						
Height After Consolidation (in.)	2.844	2.749						
Area After Consolidation (in.)	1.345	1.314						
Final Values								
Water Content (%)	36.23	33.97						
Dry Unit Weight (pcf)	83.0	89.4						
Wet Unit Weight (pcf)	113.0	119.7						
Saturation (%)	91.2	98.9						
Void Ratio	1.12	0.97						
Failure								
Failure Criteria	Max PSR	Max PSR						
Deviator Stress at failure (psf)	276.12	589.34						
Principal Stress Ratio at failure	4.76	3.90						
Minor Principal Effective Stress at fail. (psf)	74.9	209.0						
Major Principal Effective Stress at fail. (psf)	356.2	814.7						
Corrections Applied	Membrane	Membrane						
Axial Strain at failure (%)	1.50	4.78						
Test performed at strain rate (%/hr)	0.50	0.25						

Comments:

Oak Harbor - Non-blenderized - Packed - 144 psf

Oak Harbor - Non-blenderized - Packed - 432 psf

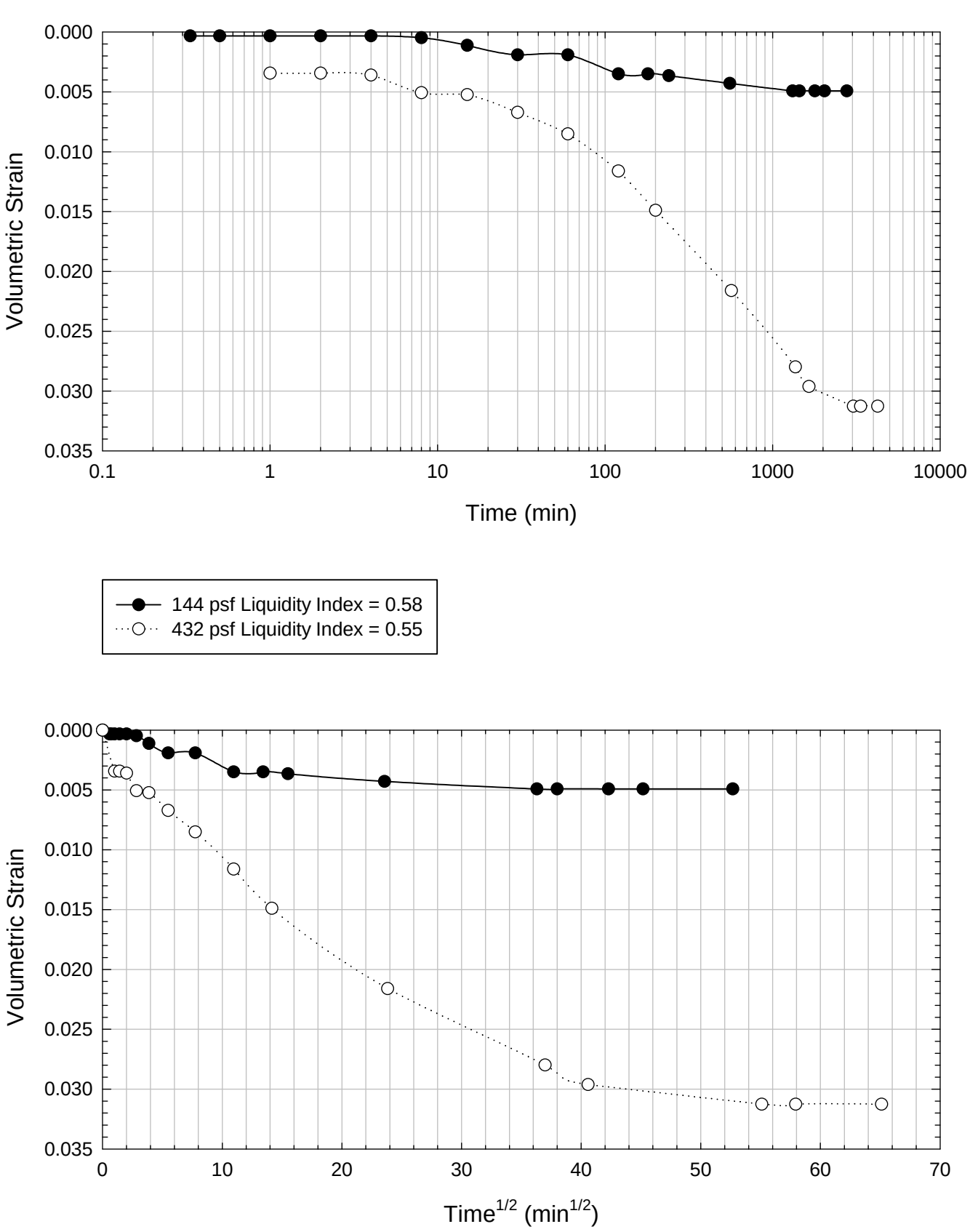
Oak Harbor - Non-blenderized - Packed
Volumetric Strain
0.000
0.005
0.010
0.015
0.020
0.025
0.030
0.035
0.1
1
10
100
1000
10000
Time (min)
144 psf Liquidity Index = 0.58
432 psf Liquidity Index = 0.55
Volumetric Strain
0.000
0.005
0.010
0.015
0.020
0.025
0.030
0.035
0
10
20
30
40
50
60
70
Time^1/2 (min^1/2)

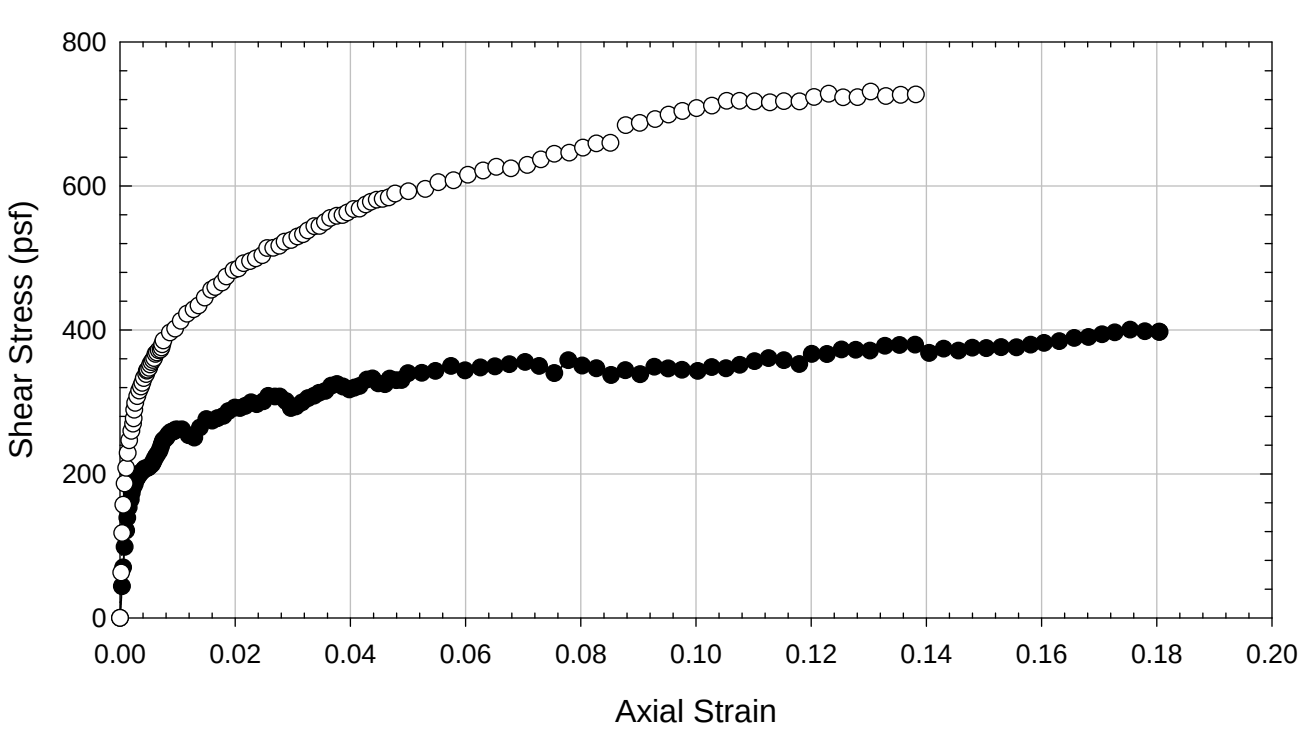
Oak Harbor - Non-blenderized - Packed
Shear Stress (psf)
800
600
400
200
0
0.00
0.02
0.04
0.06
0.08
0.10
0.12
0.14
0.16
0.18
0.20
Axial Strain

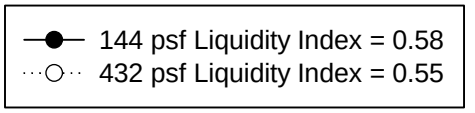
144 psf Liquidity Index = 0.58
432 psf Liquidity Index = 0.55

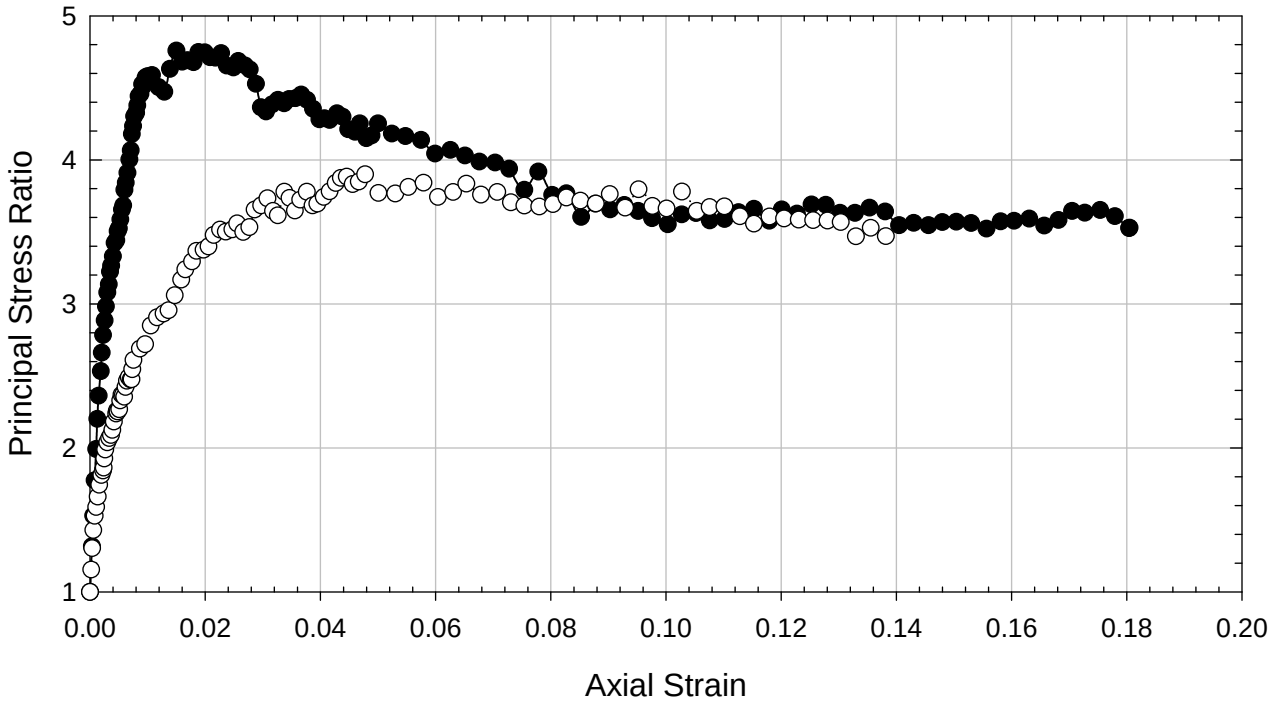
Principal Stress Ratio
5
4
3
2
1
0.00
0.02
0.04
0.06
0.08
0.10
0.12
0.14
0.16
0.18
0.20
Axial Strain

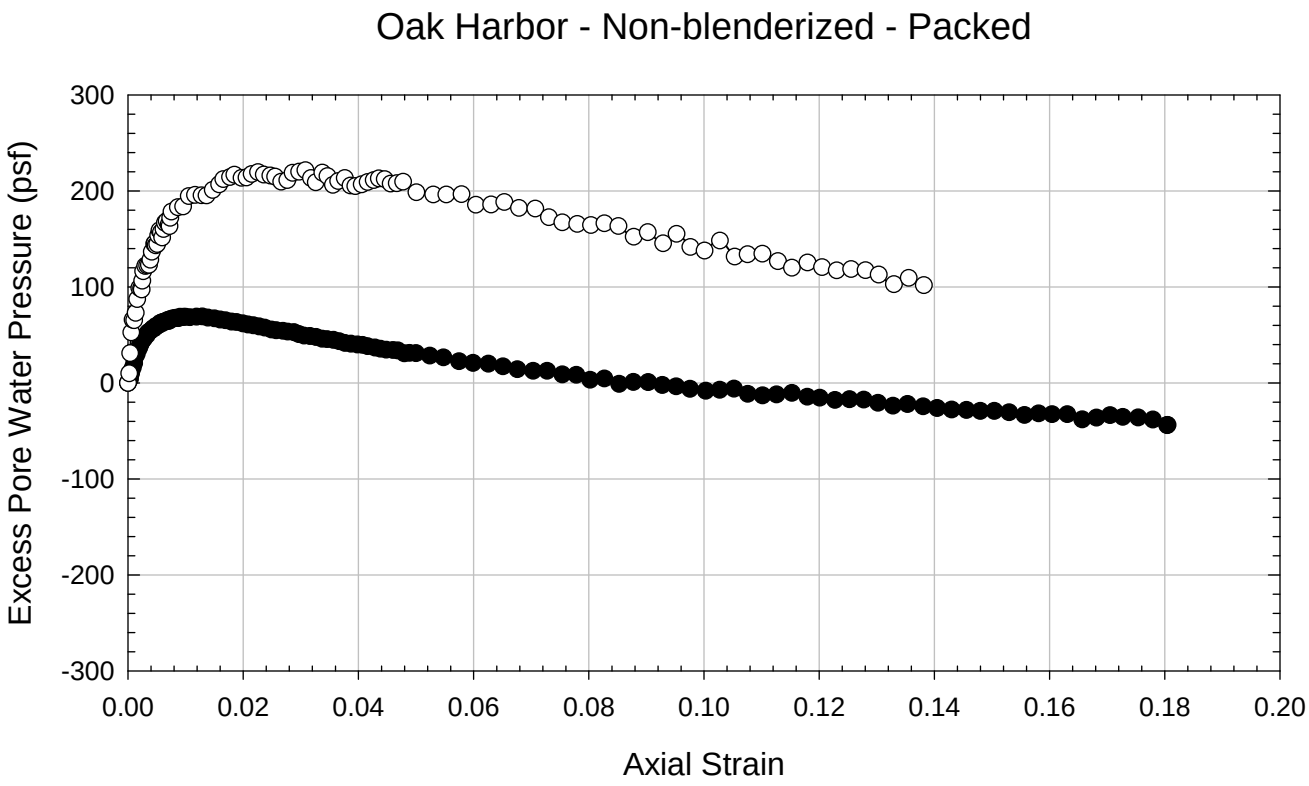
Oak Harbor - Non-blenderized - Packed
Excess Pore Water Pressure (psf)
300
200
100
0
-100
-200
-300
0.00
0.02
0.04
0.06
0.08
0.10
0.12
0.14
0.16
0.18
0.20
Axial Strain
144 psf, Liquidity Index = 0.58
432 psf, Liquidity Index = 0.55

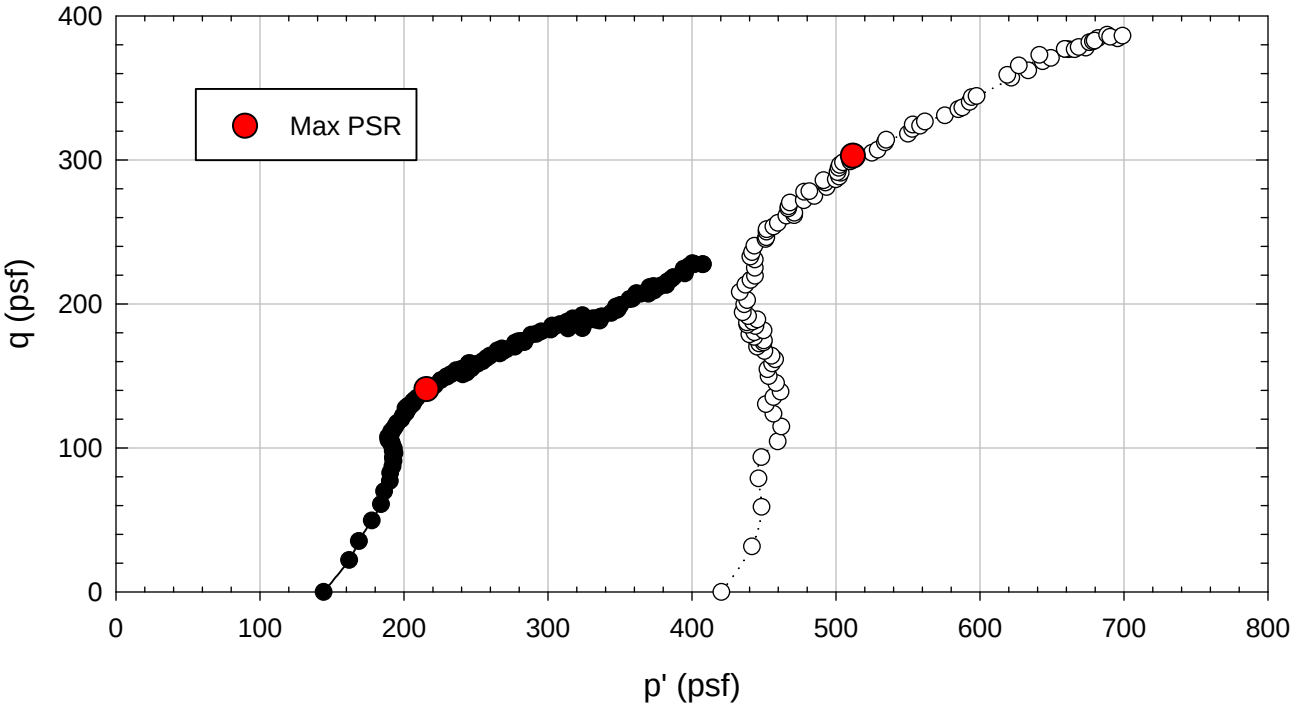
Max PSR
q (psf)
400
300
200
100
0
0
100
200
300
400
500
600
700
800
p' (psf)

E.5. VBC

E.5.1 Non-blenderized

Virginia Polytechnic Institute and State University
Geotechnical Engineering Laboratory
Triaxial Data Sheet

Project:	Fully Softened Shear Strength
Sample I.D./Loc.:	VBC - Non-blenderized - Consolidated Undrained
Classification:	Fat Clay (CH)

Sample Preparation	Remolded at LL
Specimen Saturation Method	Wet

Specific Gravity	2.79	
Method for Dimensions After Consol.	Case and Chilver (1959)	

Test Number	1	2	3	4	5	6	7	
Start Date (m/d/y)	5/14/2012	5/14/2012	5/14/2012	6/4/2012	5/14/2012	5/14/2012		
End Date (m/d/y)	5/25/2012	5/25/2012	5/25/2012	6/14/2012	5/25/2012	5/25/2012		
Backpressure (psf)	7200	7200	7200	7200	7200	7200		
Consolidation Pressure (psf)	1008	2016	3024	5472	8064	10080		
B value	0.97	0.99	0.98	0.98	0.96	1.00		
Initial Values								
Initial Height (in.)	2.951	2.980	3.078	3.008	3.074	3.000		
Initial Diameter (in.)	1.372	1.374	1.371	1.374	1.373	1.353		
Initial Sample Weight (g.)	116.94	118.12	122.40	121.30	122.72	118.99		
Water Content (%)	63.45	61.23	62.95	61.87	62.15	64.64		
Dry Unit Weight (pcf)	62.5	63.2	63.0	64.0	63.3	63.8		
Wet Unit Weight (pcf)	102.1	101.9	102.6	103.6	102.7	105.1		
Saturation (%)	99.1	97.3	99.5	100.0	99.2	100.0		
Void Ratio	1.79	1.76	1.76	1.72	1.75	1.73		
After Consolidation								
t_{100} Using Casagrande Method (min)	3246.95	3277.75	3832.12	3667.55	3778.01	3553.90		
Volumetric Strain (%)	5.79	11.64	15.83	19.54	24.86	25.72		
Height After Consolidation (in.)	2.894	2.864	2.916	2.812	2.819	2.743		
Area After Consolidation (in.)	1.421	1.368	1.320	1.290	1.235	1.191		
Final Values								
Water Content (%)	54.30	58.76	48.39	44.48	41.21	39.33		
Dry Unit Weight (pcf)	67.6	66.0	73.3	77.7	81.0	83.0		
Wet Unit Weight (pcf)	104.3	104.7	108.8	112.2	114.4	115.7		
Saturation (%)	96.1	100.0	98.2	100.0	100.0	100.0		
Void Ratio	1.58	1.64	1.38	1.24	1.15	1.10		
Failure								
Failure Criteria	Max PSR	Max PSR	Max PSR	Max PSR	Max PSR	Max PSR		
Deviator Stress at failure (psf)	839.72	1449.38	1968.46	3013.61	4476.76	4891.79		
Principal Stress Ratio at failure	3.12	2.65	2.68	2.06	2.11	1.98		
Minor Principal Effective Stress at fail. (psf)	408.6	898.3	1195.1	2888.3	4058.3	5052.6		
Major Principal Effective Stress at fail. (psf)	1275.7	2380.6	3198.4	5936.5	8575.9	9988.0		
Corrections Applied	Membrane	Membrane	Membrane	Membrane	Membrane	Membrane		
Axial Strain at failure (%)	8.34	9.92	10.36	10.14	11.83	12.45		
Test performed at strain rate (%/hr)	0.14	0.14	0.12	0.12	0.12	0.12		

Comments:

VBC - Non-blenderized - 1008 psf

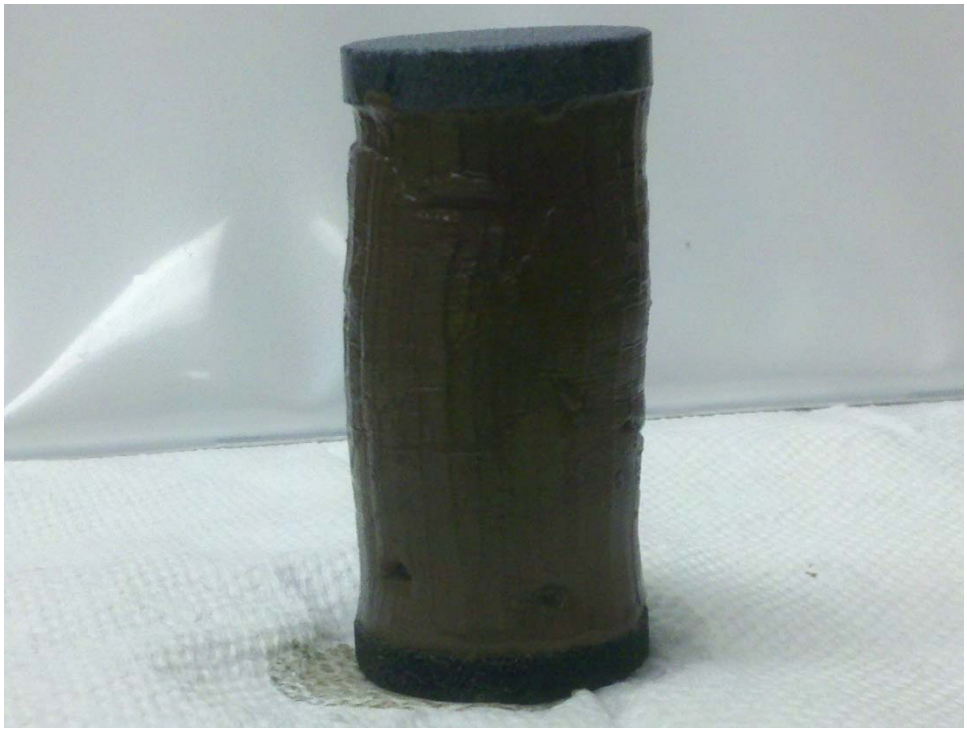

VBC - Non-blenderized - 2016 psf

VBC - Non-blenderized - 5472 psf

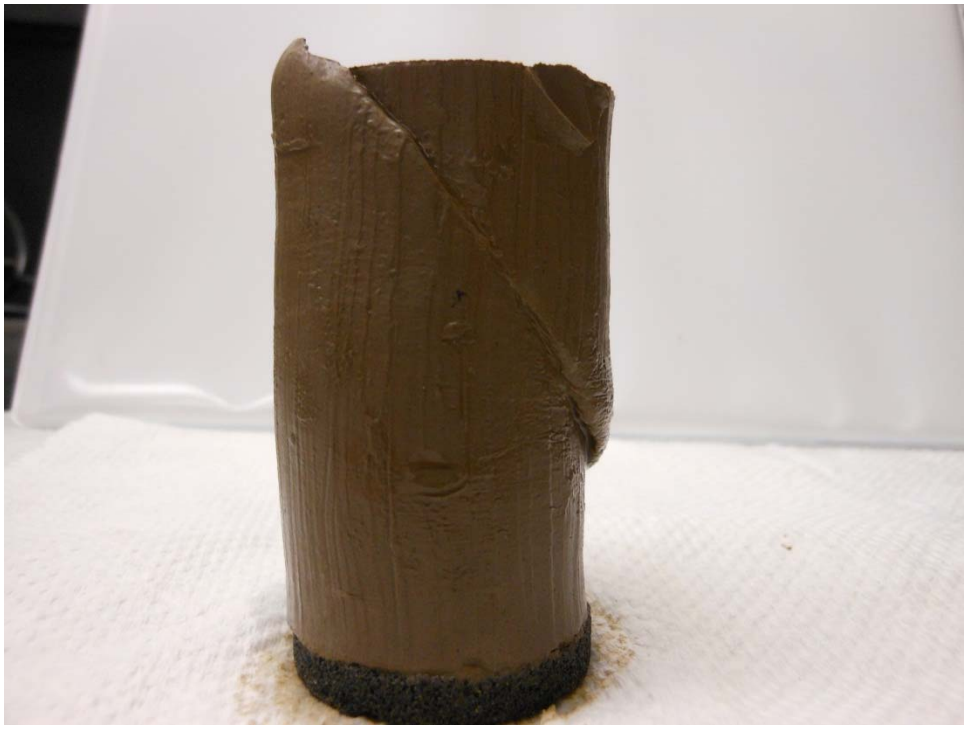

VBC - Non-blenderized - 8064 psf

VBC - Non-blenderized - 10,080 psf

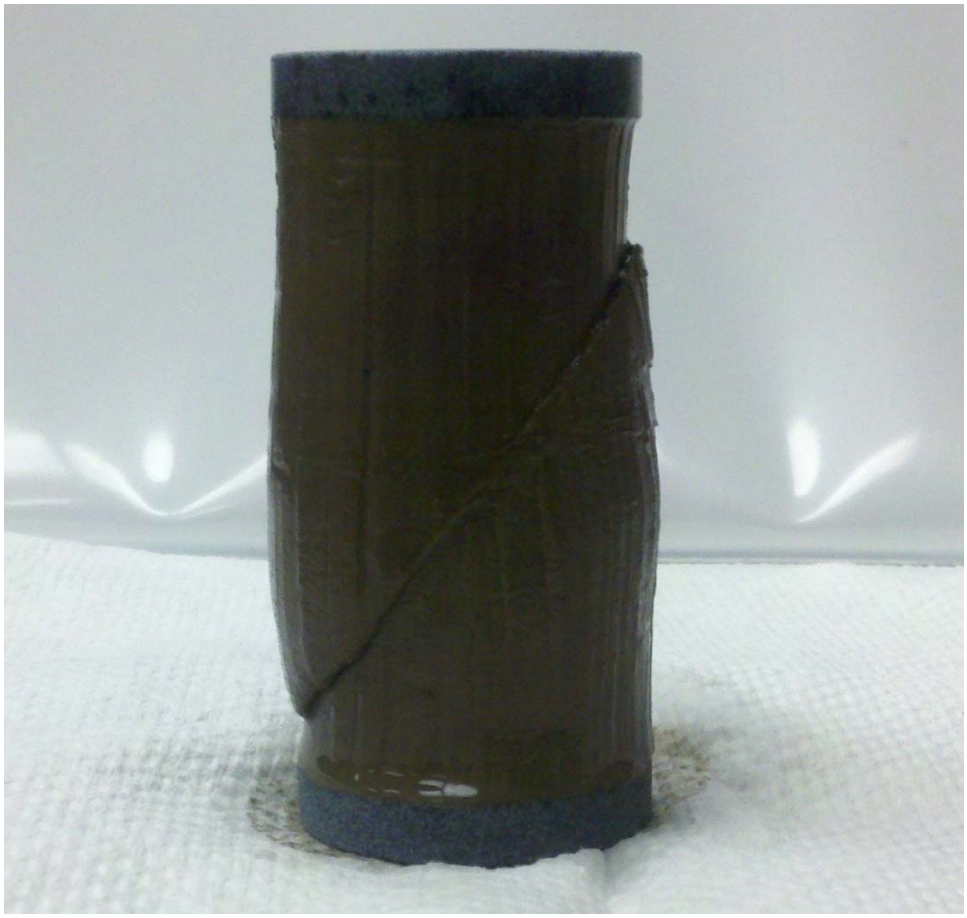

VBC - Non-blenderized

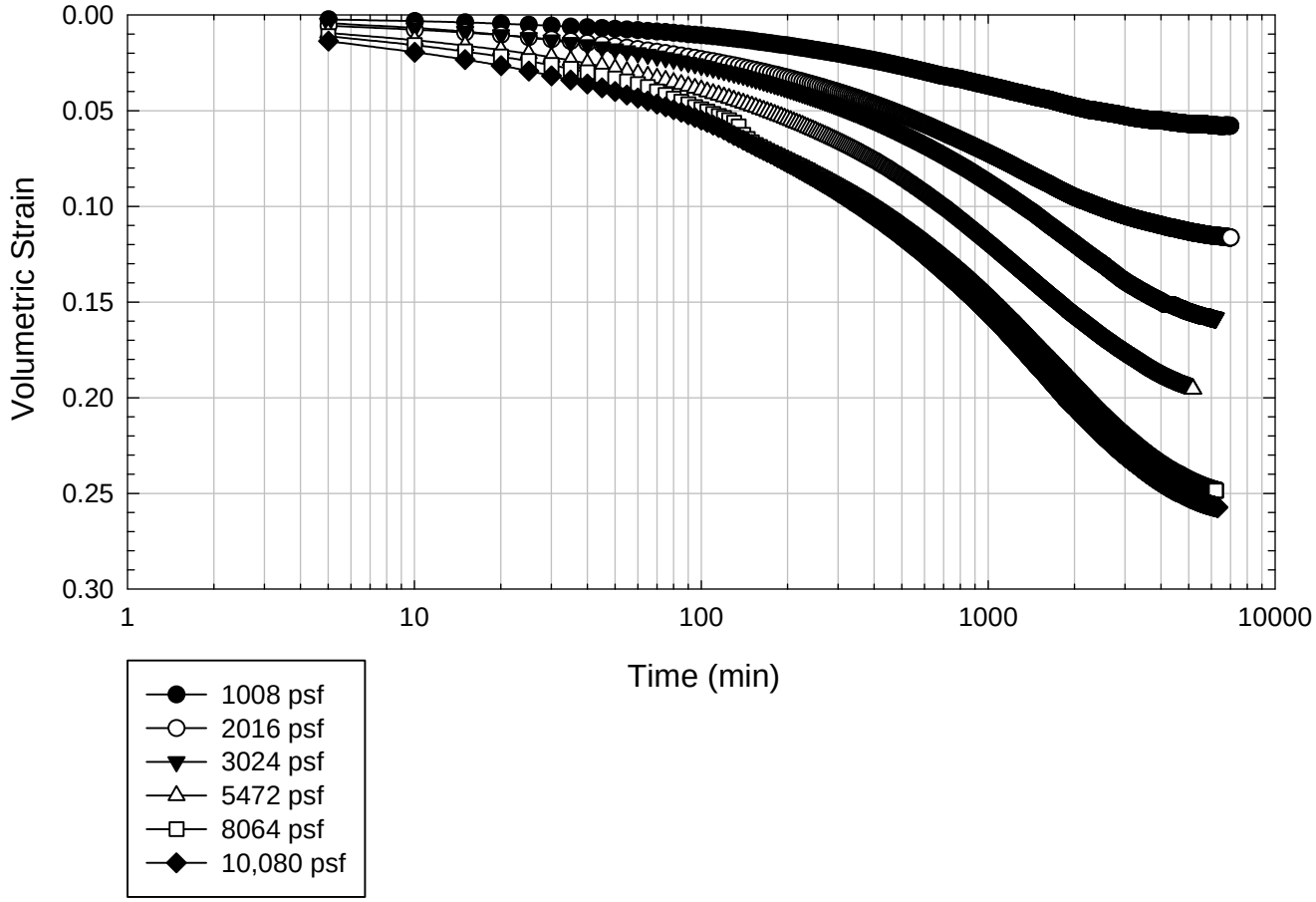

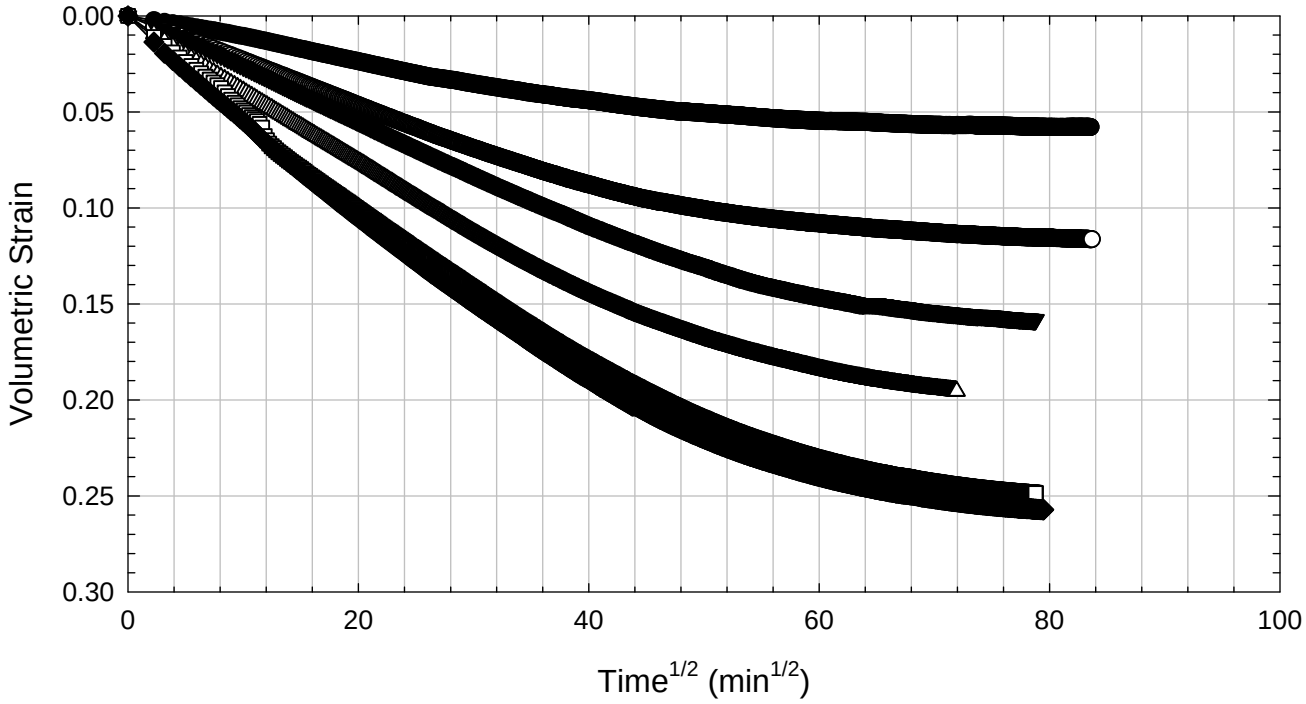

VBC - Non-blenderized

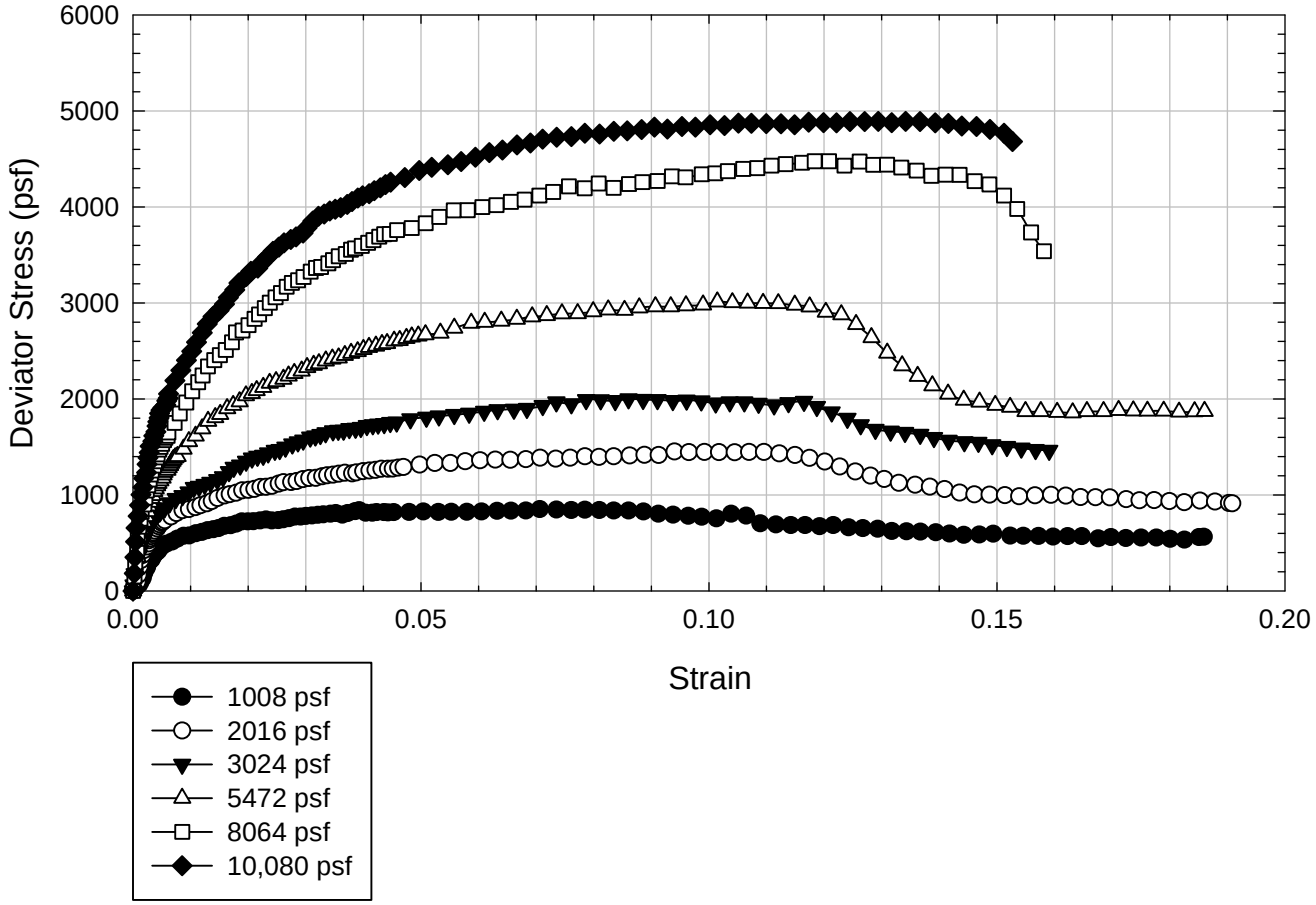

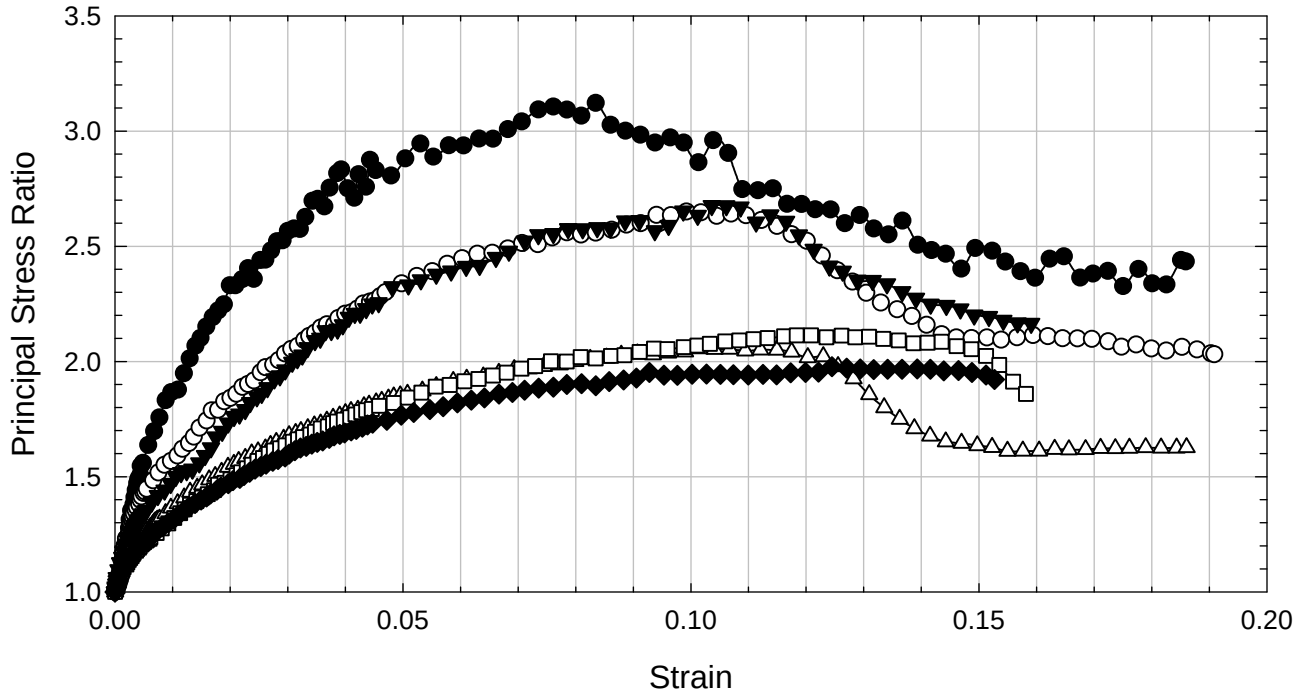

VBC - Non-blenderized

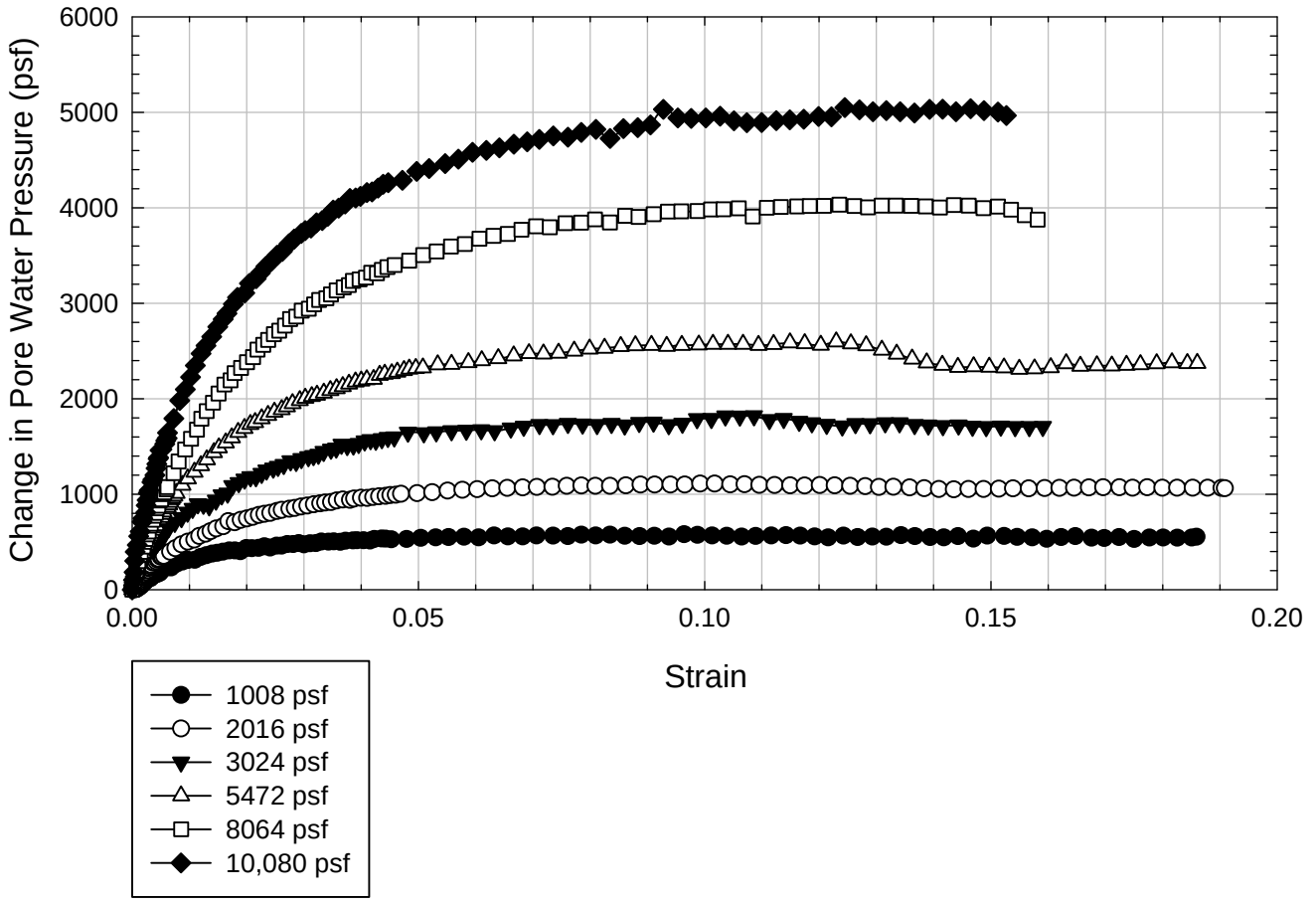

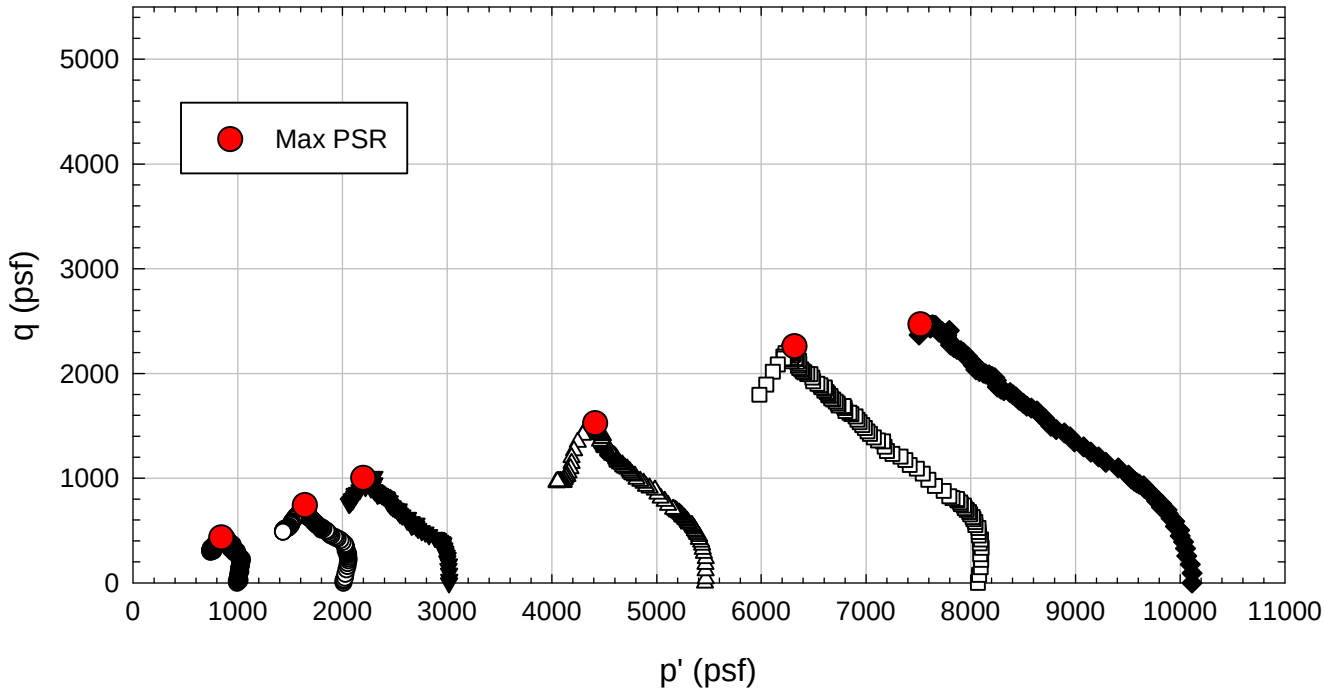

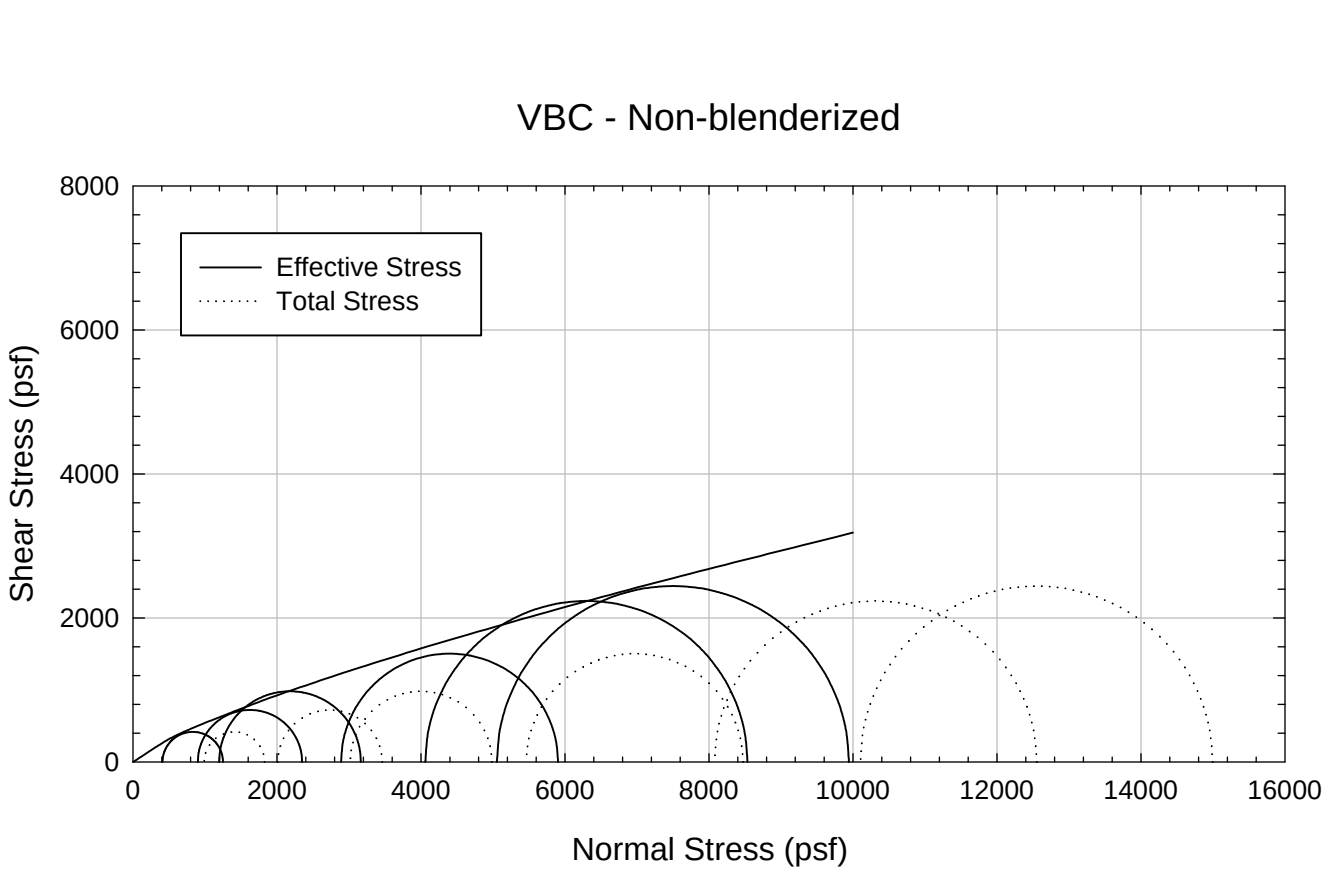
VBC - Non-blenderized
Effective Stress
Total Stress
Shear Stress (psf)
Normal Stress (psf)
0
2000
4000
6000
8000
10000
12000
14000
16000

Appendix F

Direct Shear Fully Softened Shear Strength Measurement Performed by ERDC

Soil	USCS		Specific Gravity	Non-blenderized				Blenderized			Direct Shear		
	Symbol	Group Name		LL	PL	PI	Clay-sized Fraction	LL	PL	PI	σ'_n (psf)	τ_f (psf)	ϕ'_{sec} (deg)
Texas 1	CH	Fat Clay	2.78	68	24	44	63	76	25	51	250	185	36.5
											500	285	29.7
											1000	550	28.8
											1500	710	25.3
											2000	810	22.0
											4000	1560	21.3
Texas 2	CH	Fat Clay	2.78	66	23	43	58	74	21	53	500	320	32.6
											1000	465	24.9
											1500	750	26.6
											2000	870	23.5
											4000	1635	22.2
Texas 3	CH	Fat Clay	2.82	65	21	44	54.5	71	22	49	500	240	25.6
											1000	520	27.5
											1500	685	24.5
											2000	765	20.9
											4000	1430	19.7
Texas 4	CH	Fat Clay	2.81	66	24	42	66.5	76	23	53	500	335	33.8
											1000	480	25.6
											1500	610	22.1
											2000	760	20.8
											4000	1045	14.6
Texas 7	CH	Fat Clay	2.76	56	16	40	46	65	21	44	600	430	35.6
											700	445	32.4
											1000	540	28.4
											1500	645	23.3
											3000	1390	24.9
											4000	1430	19.7
Texas 8	CH	Fat Clay	2.77	70	25	45	60	75	24	51	500	410	39.4
											1000	545	28.6
											1500	750	26.6
											2000	880	23.7
											4000	1490	20.4
Texas 9	CH	Fat Clay	2.83	83	26	57	63	81	24	57	500	315	32.2
											1000	468	25.1
											1500	625	22.6
											2000	795	21.7
											4000	1230	17.1
Texas 10	CH	Fat Clay	2.82	80	27	53	70	84	25	59	250	166	33.6
											500	280	29.2
											1000	490	26.1
											1500	660	23.7
											2000	770	21.1
											4000	1560	21.3
Texas 11	CH	Fat Clay	2.82	88	27	61	66	85	22	63	500	310	31.8
											1000	400	21.8
											1500	555	20.3
											2000	770	21.1
											4000	1270	17.6
Texas 12	CL	Lean Clay	2.73	35	14	21	29	39	14	25	600	460	37.5
											700	485	34.7
											1000	700	35.0
											1500	930	31.8
											3000	1680	29.2
Texas 13	CH	Fat Clay	2.84	79	24	55	65	76	22	54	250	180	35.8
											1000	470	25.2
											1500	695	24.9
											2000	765	20.9
											4000	1360	18.8
Texas 14	CH	Fat Clay	2.84	75	23	52	65	77	23	54	500	230	24.7
											1000	530	27.9
											1500	620	22.5
											2000	880	23.7
											4000	1120	15.6
Texas 15	CH	Fat Clay	2.80	52	17	35	42	53	16	37	600	390	33.0
											700	540	37.6
											1000	580	30.1
											1500	820	28.7
											3000	1425	25.4

Texas 16	CH	Fat Clay	2.80	69	23	46	64	75	24	51	250	178	35.5
											500	275	28.8
											1000	540	28.4
											1500	740	26.3
											2000	850	23.0
											4000	1560	21.3
Texas 17	CH	Fat Clay	2.80	76	26	50	66	82	26	56	500	250	26.6
											1000	540	28.4
											1500	645	23.3
											2000	870	23.5
											4000	1410	19.4
Texas 18	CH	Fat Clay	2.79	72	25	47	60	77	27	50	500	330	33.4
											1000	610	31.4
											1500	830	29.0
											2000	1020	27.0
											4000	1685	22.8
Texas 19	CH	Fat Clay	2.79	69	25	44	64	80	26	54	500	310	31.8
											1000	550	28.8
											1500	685	24.5
											2000	965	25.8
											4000	1510	20.7
Texas 20	CL	Lean Clay	2.72	31	13	18	25	34	13	21	250	205	39.4
											500	290	30.1
											750	510	34.2
											4000	2250	29.4
Texas 21	CH	Fat Clay	2.82	71	21	50	58	77	23	54	600	350	30.3
											700	340	25.9
											1000	520	27.5
											1500	725	25.8
											3000	1210	22.0
Texas 22	CL	Lean Clay	2.73	45	17	28	37	46	16	30	500	460	42.6
											1000	745	36.7
											1500	850	29.5
											2000	1085	28.5
											4000	1950	26.0
Texas 23	CH	Fat Clay	2.76	52	16	36	43	52	16	36	250	180	35.8
											500	370	36.5
											1000	580	30.1
											1500	760	26.9
											2000	970	25.9
											4000	1690	22.9
Texas 24	CL	Lean Clay	2.72	33	14	19	23	33	15	18	500	500	45.0
											1000	710	35.4
											1500	1010	34.0
											2000	1230	31.6
											4000	2450	31.5
Texas 25	CH	Fat Clay	2.79	73	22	51	59	73	22	51	500	285	29.7
											1000	475	25.4
											1500	660	23.7
											2000	905	24.3
											4000	1400	19.3
Texas 26	CH	Fat Clay	2.82	72	29	43	67	91	27	64	500	295	30.5
											1000	545	28.6
											1500	645	23.3
											2000	695	19.2
											4000	1200	16.7
Texas 27	CH	Fat Clay	2.82	73	24	49	70	86	28	58	500	320	32.6
											1000	470	25.2
											1500	615	22.3
											2000	770	21.1
											4000	1400	19.3
Texas 28	CH	Fat Clay	2.83	85	30	55	70	93	29	64	500	240	25.6
											1000	538	28.3
											1500	520	19.1
											2000	835	22.7
											4000	1115	15.6
Texas 29	CH	Fat Clay	2.87	77	26	51	61	75	23	52	500	280	29.2
											1000	545	28.6
											1500	695	24.9
											2000	855	23.1
											4000	1575	21.5

Texas 30	CH	Fat Clay	2.81	N/A	N/A	N/A	63	93	33	60	500	299	30.9
											1000	508	26.9
											2000	780	21.3
											6000	1930	17.8
											12000	3055	14.3
Texas 31	CH	Fat Clay	2.83	N/A	N/A	N/A	64	84	27	57	500	262	27.7
											1000	425	23.0
											1500	574	20.9
											2000	900	24.2
											4000	1300	18.0
											6000	1745	16.2
											12000	3326	15.5
Texas 32	CH	Fat Clay	2.77	N/A	N/A	N/A	57	83	26	57	500	290	30.1
											1000	517	27.3
											2000	835	22.7
											6000	1984	18.3
											12000	3605	16.7
Texas 33	CH	Fat Clay	2.73	N/A	N/A	N/A	56	79	25	54	500	303	31.2
											1000	453	24.4
											2000	818	22.2
											6000	1878	17.4
											12000	3553	16.5
Texas 34	CH	Fat Clay	2.71	N/A	N/A	N/A	42	57	18	39	500	182	20.0
											1000	569	29.6
											2000	957	25.6
											6000	2522	22.8
											12000	4203	19.3
Texas 35	CH	Fat Clay	2.84	N/A	N/A	N/A	47	64	20	44	500	207	22.5
											1000	546	28.6
											2000	849	23.0
											6000	2102	19.3
											12000	3974	18.3

Texas 1 - Blenderized

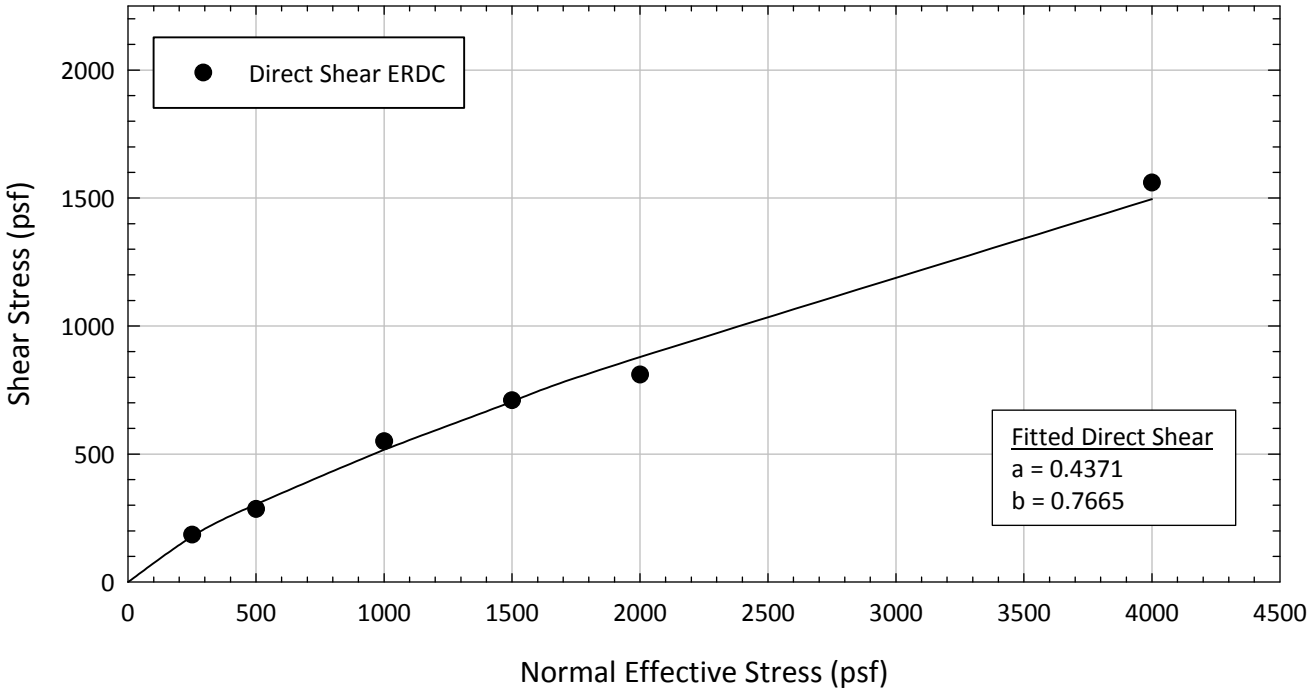

Texas 2 - Blenderized

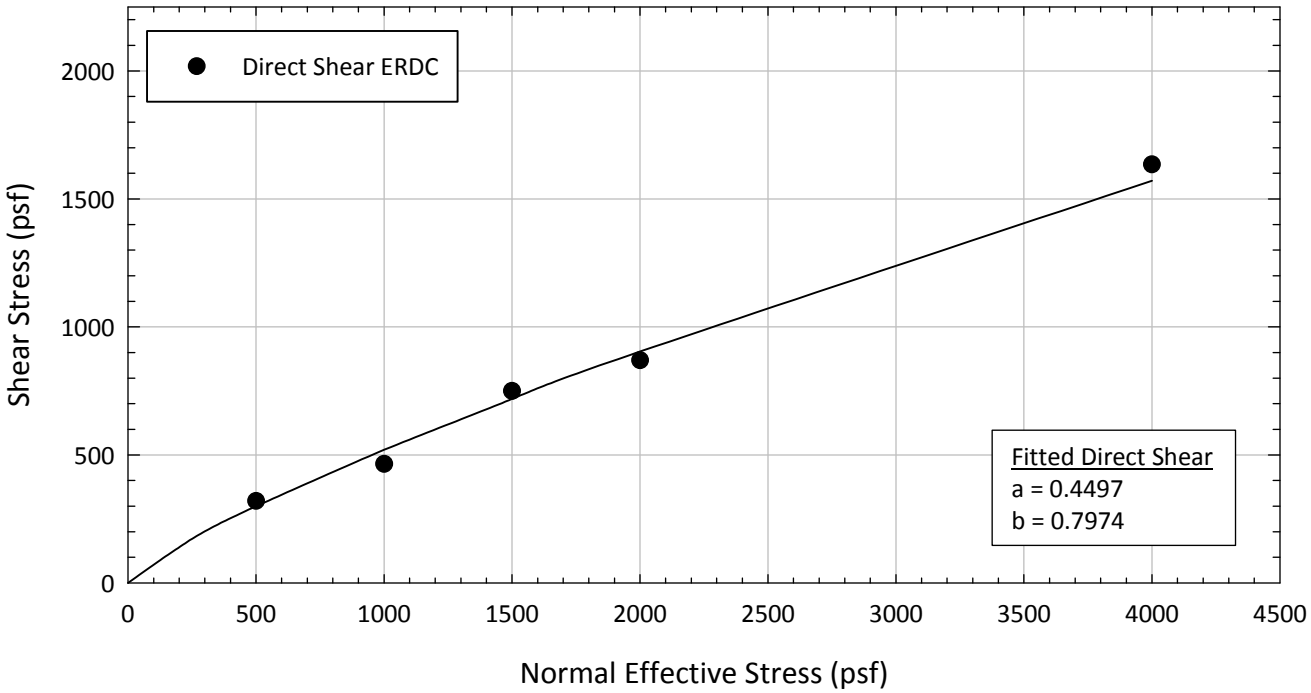

Texas 3 - Blenderized

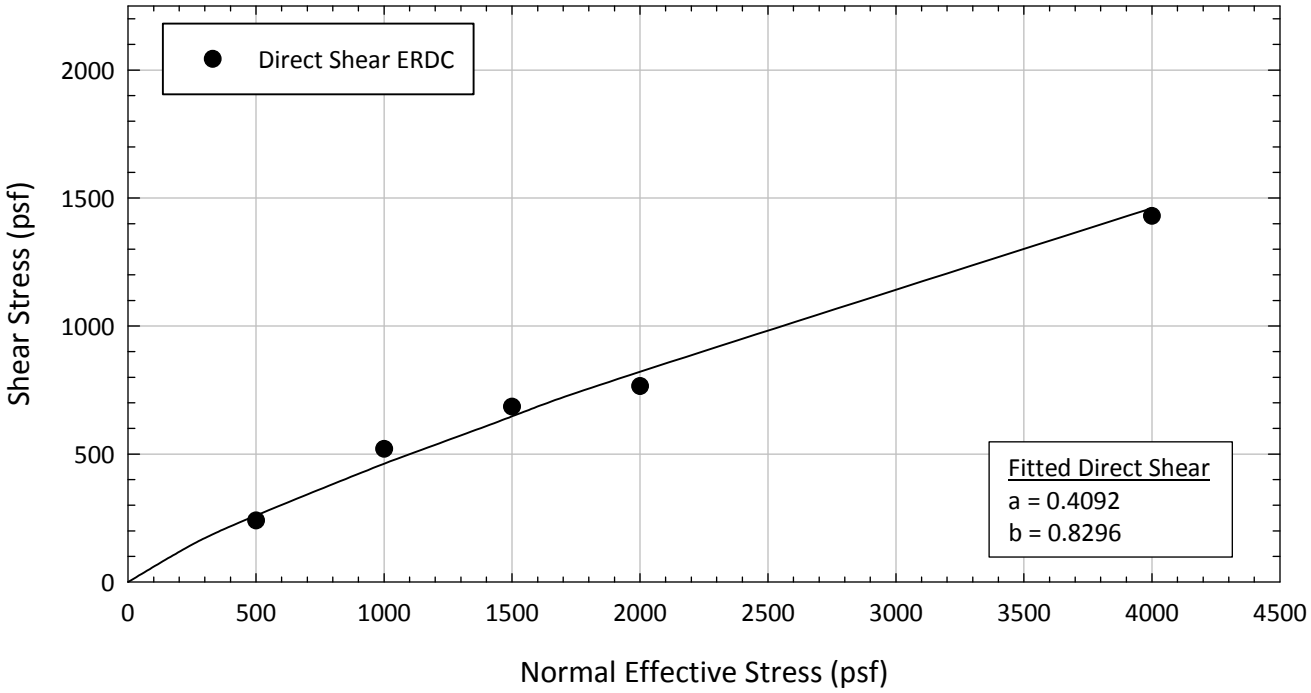

Texas 4 - Blenderized

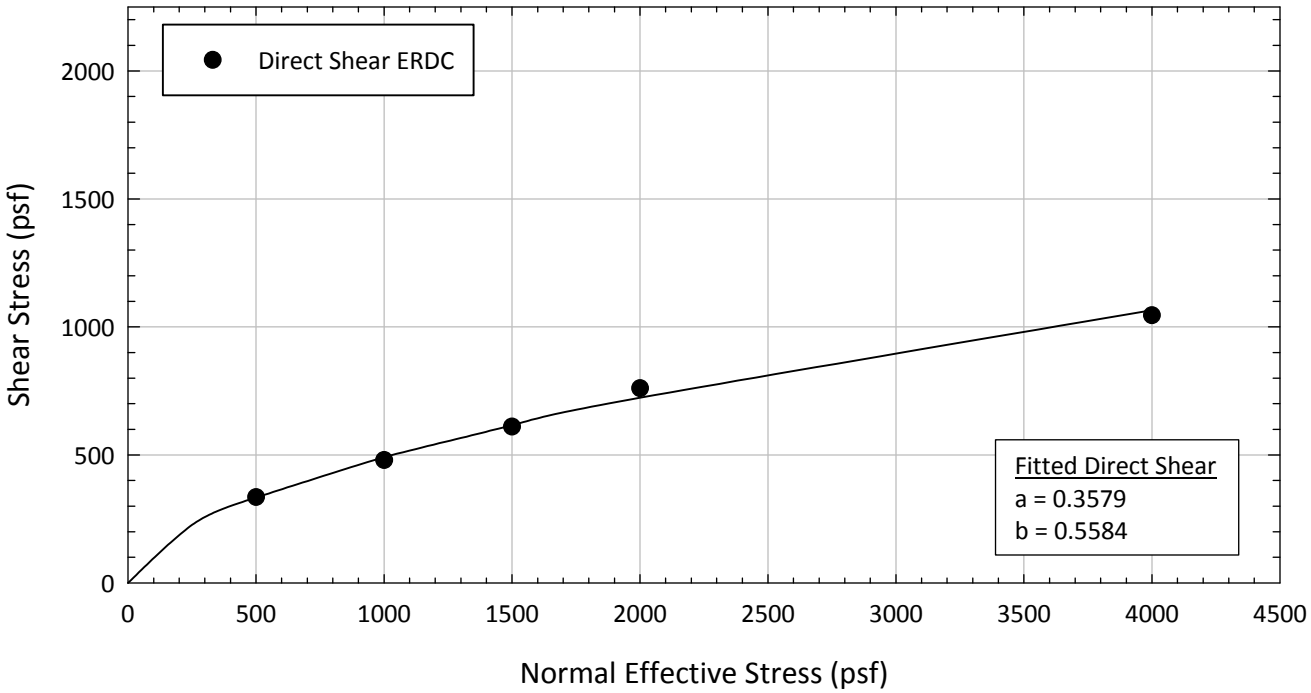

Texas 7 - Blenderized

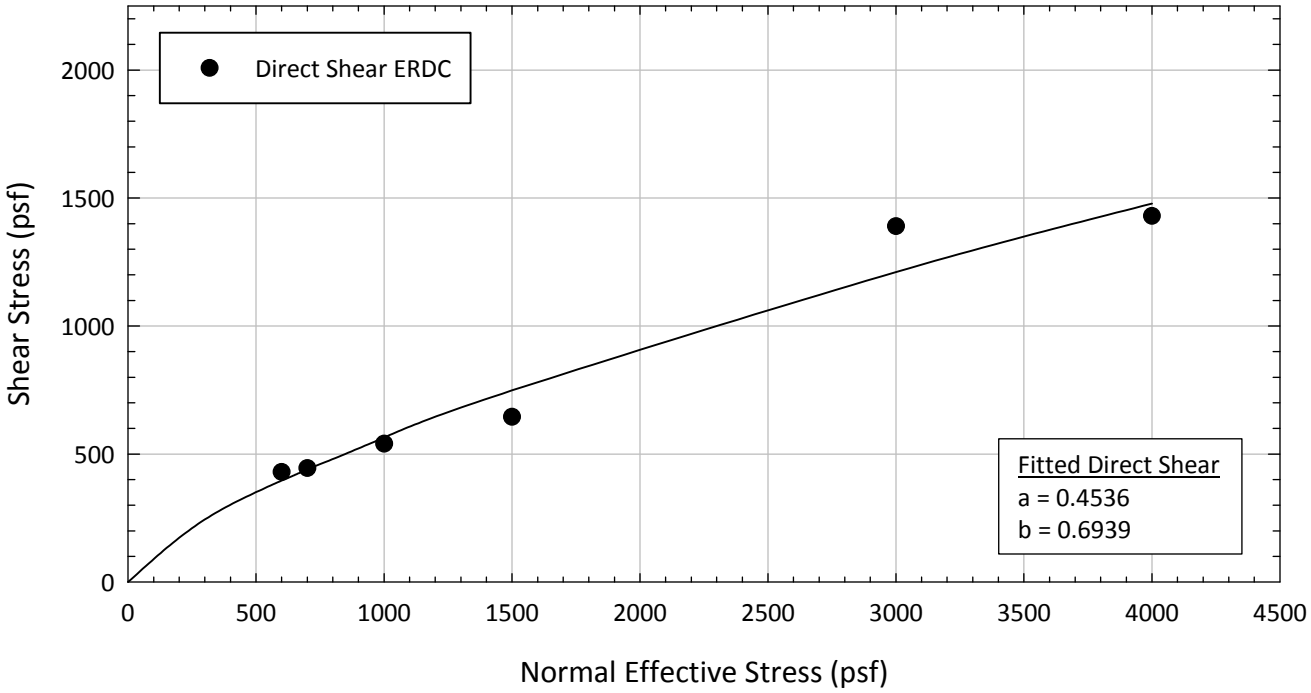

Texas 8 - Blenderized

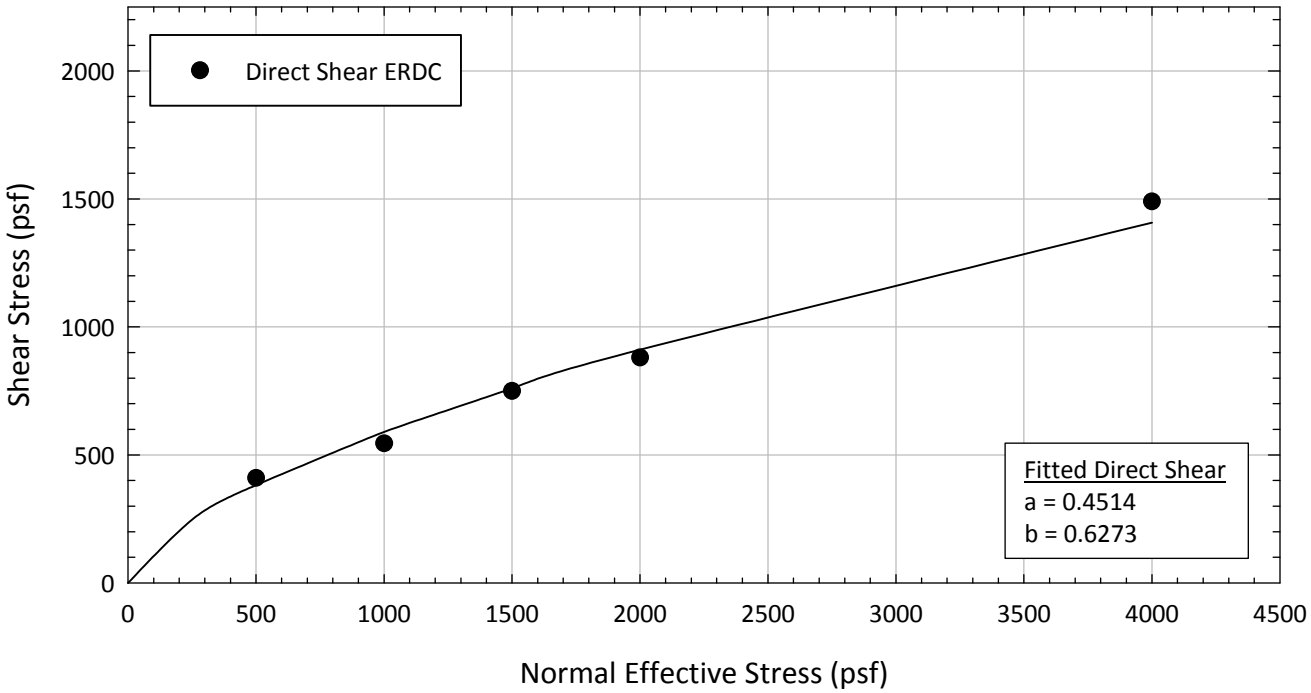

Texas 9 - Blenderized

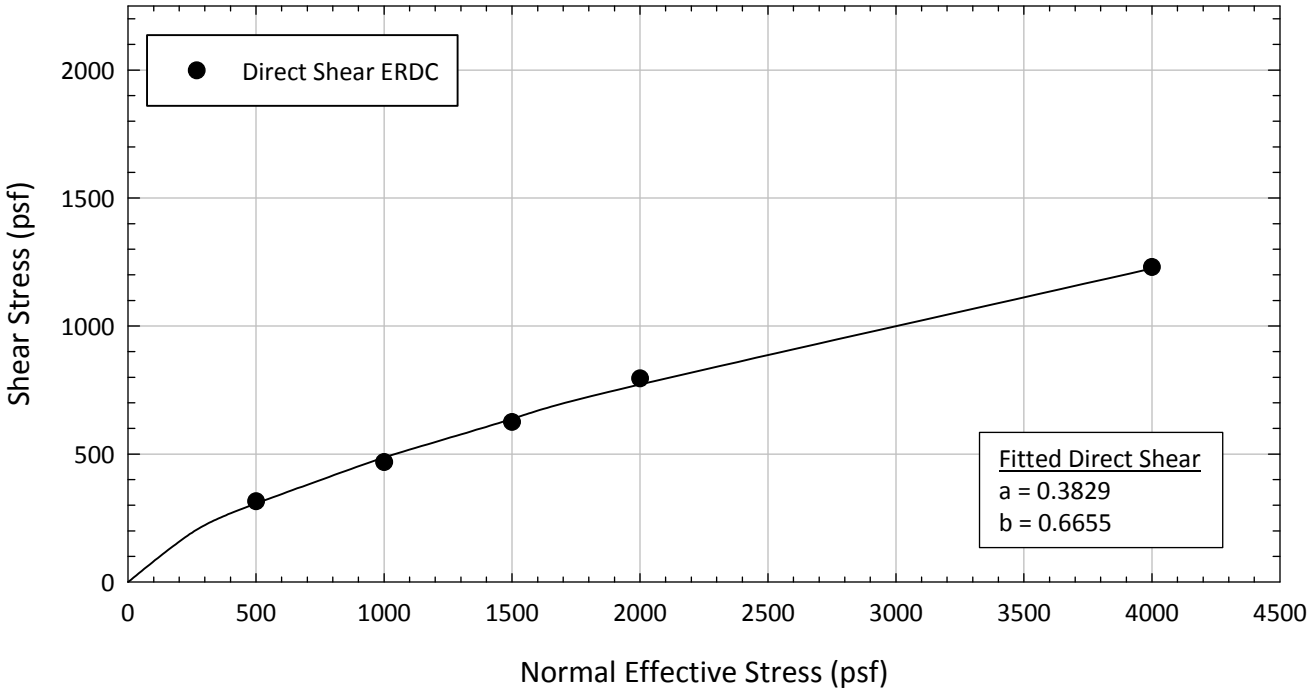

Texas 10 - Blenderized

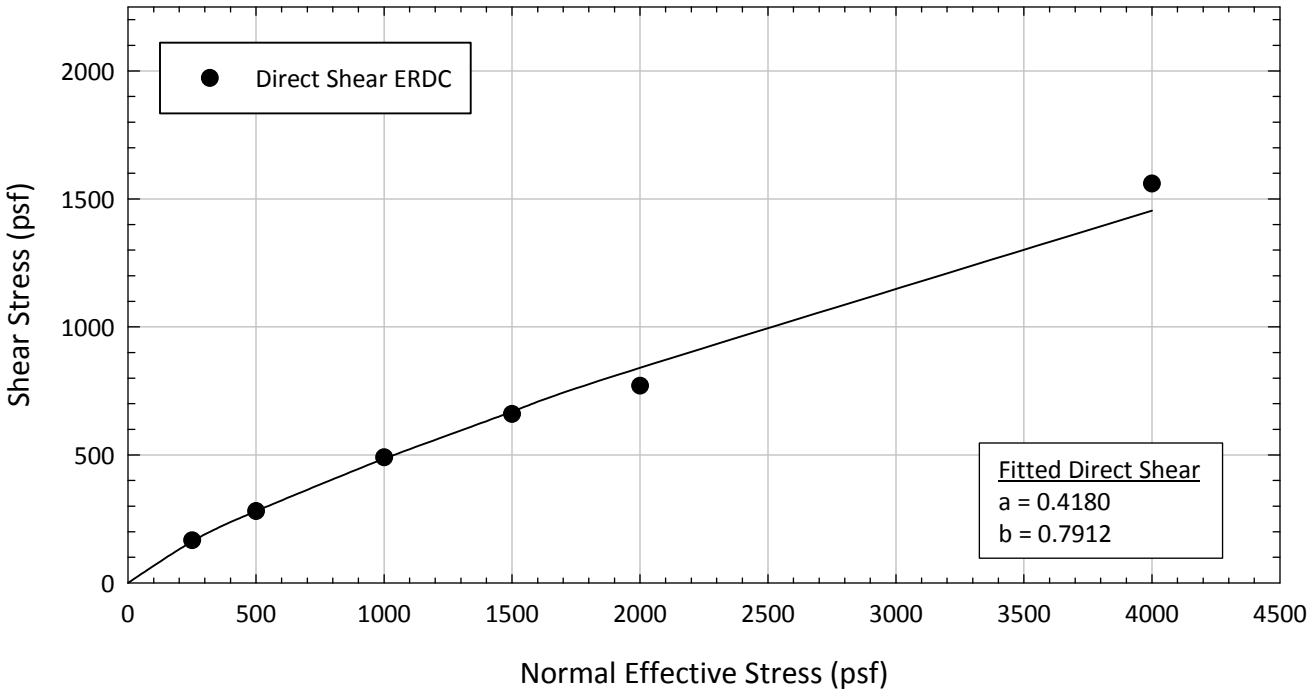

Texas 11 - Blenderized

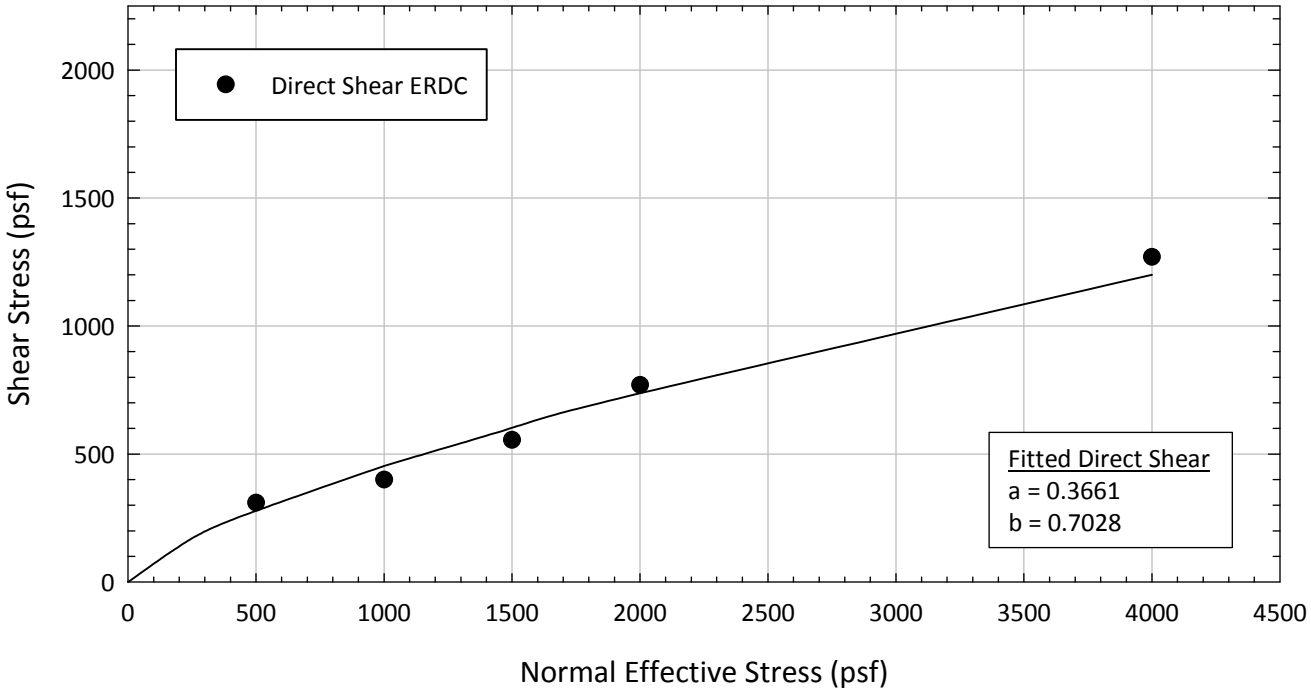

Texas 12 - Blenderized

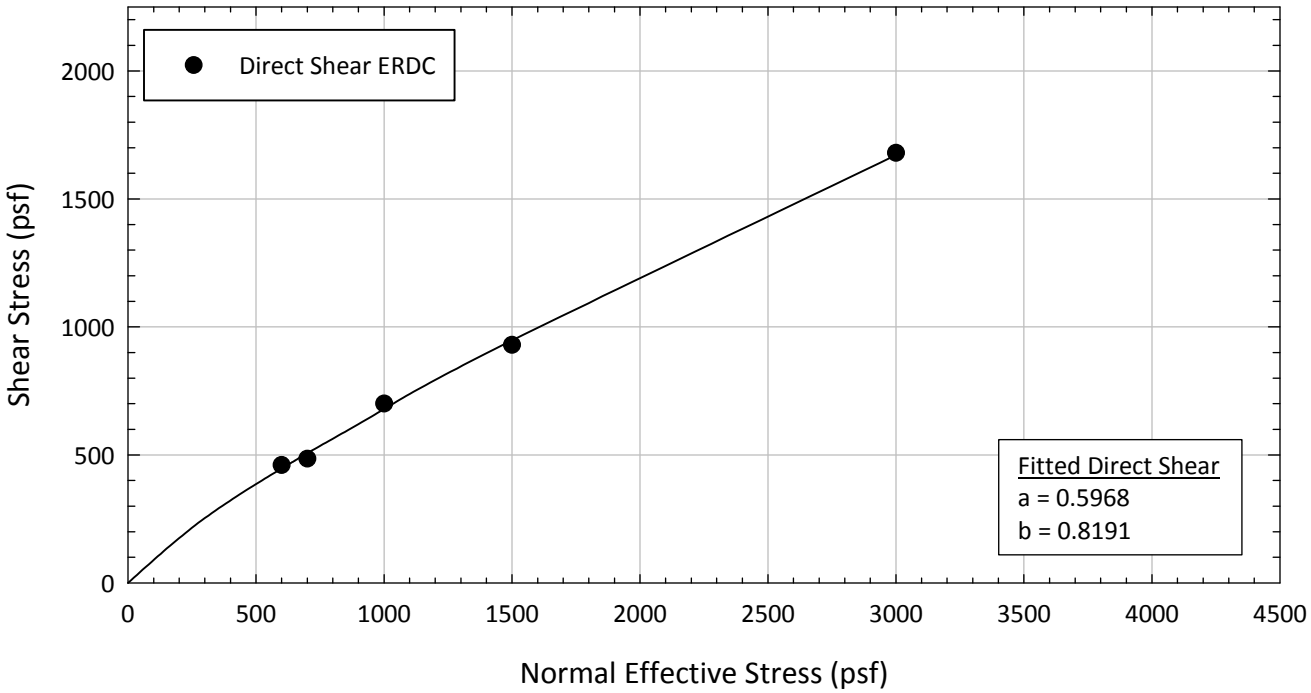

Texas 13 - Blenderized

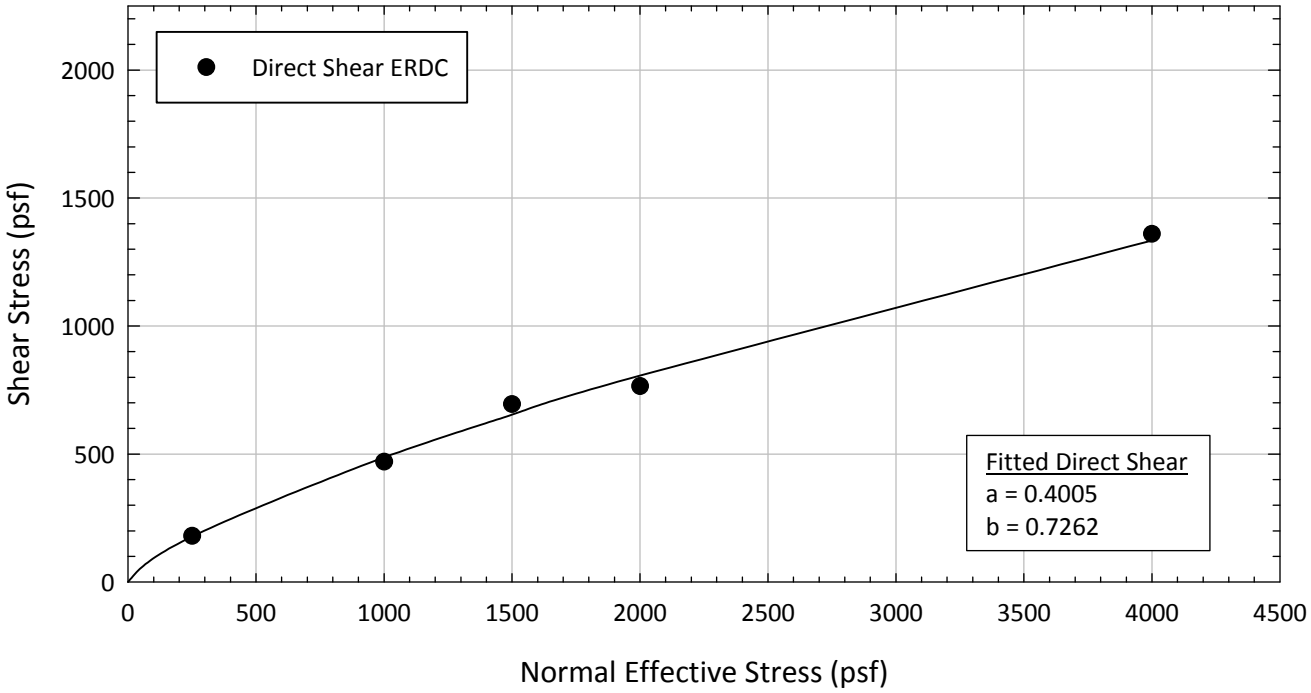

Texas 14 - Blenderized

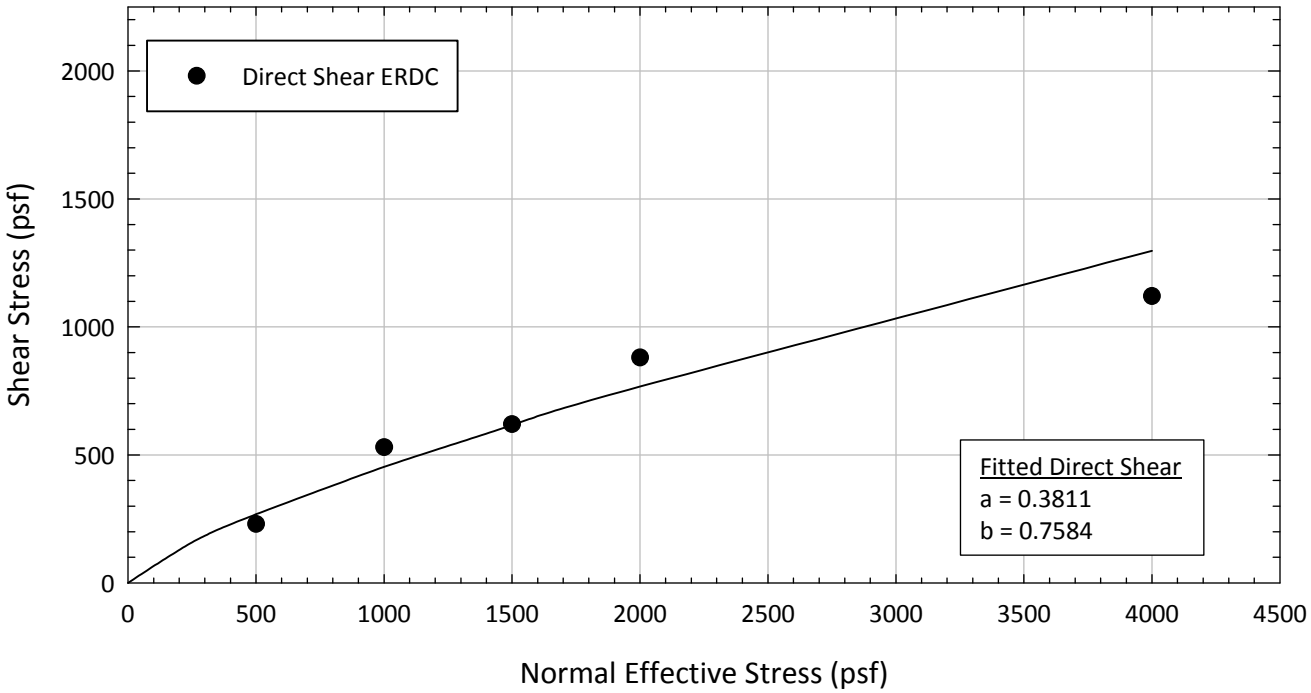

Texas 15 - Blenderized

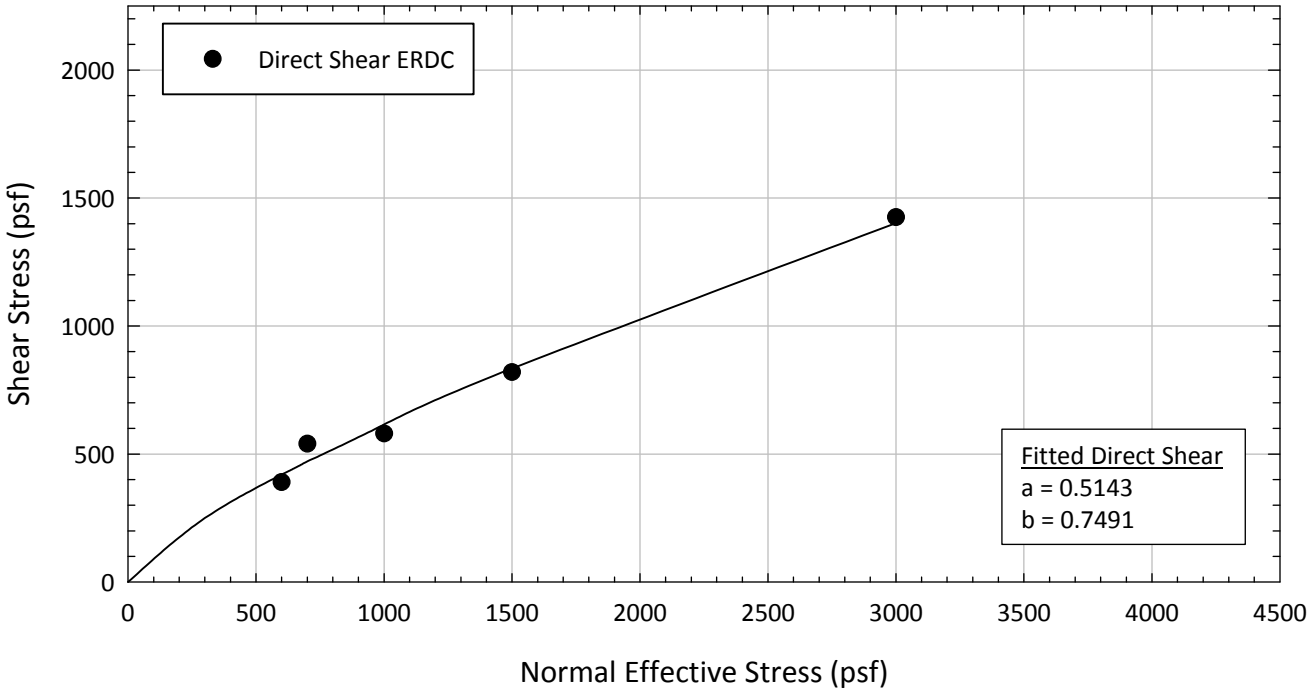

Texas 16 - Blenderized

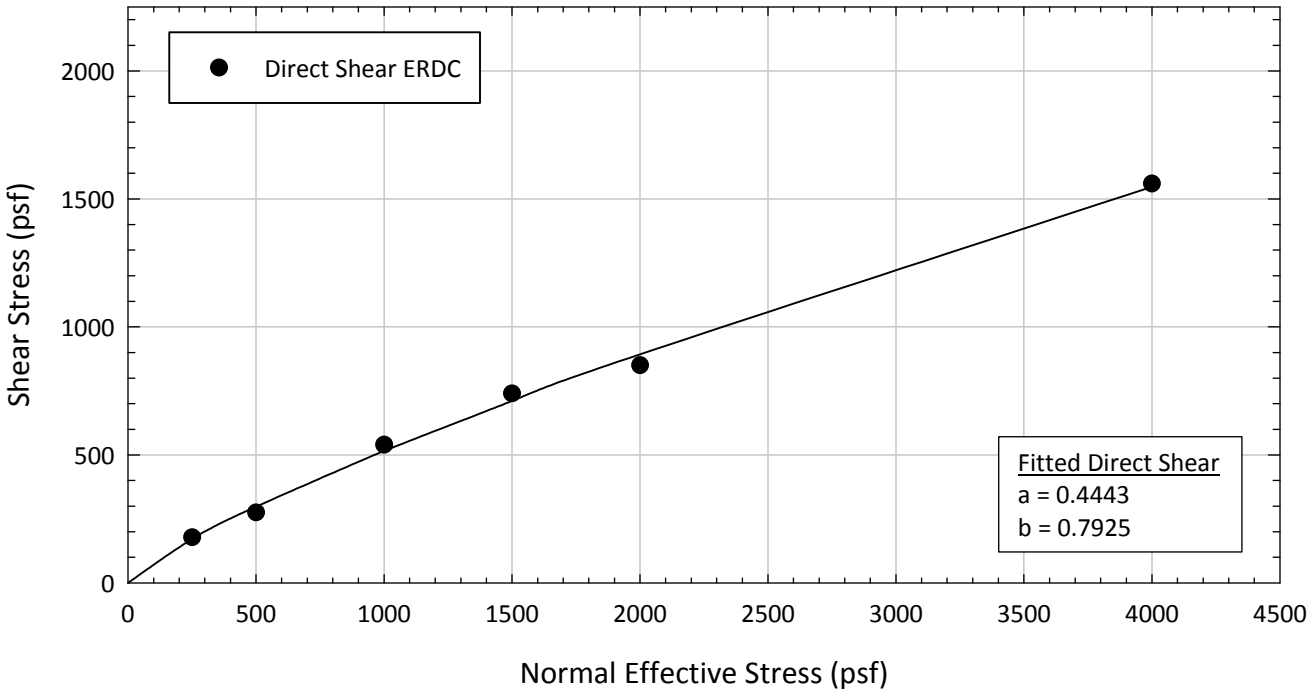

Texas 17 - Blenderized

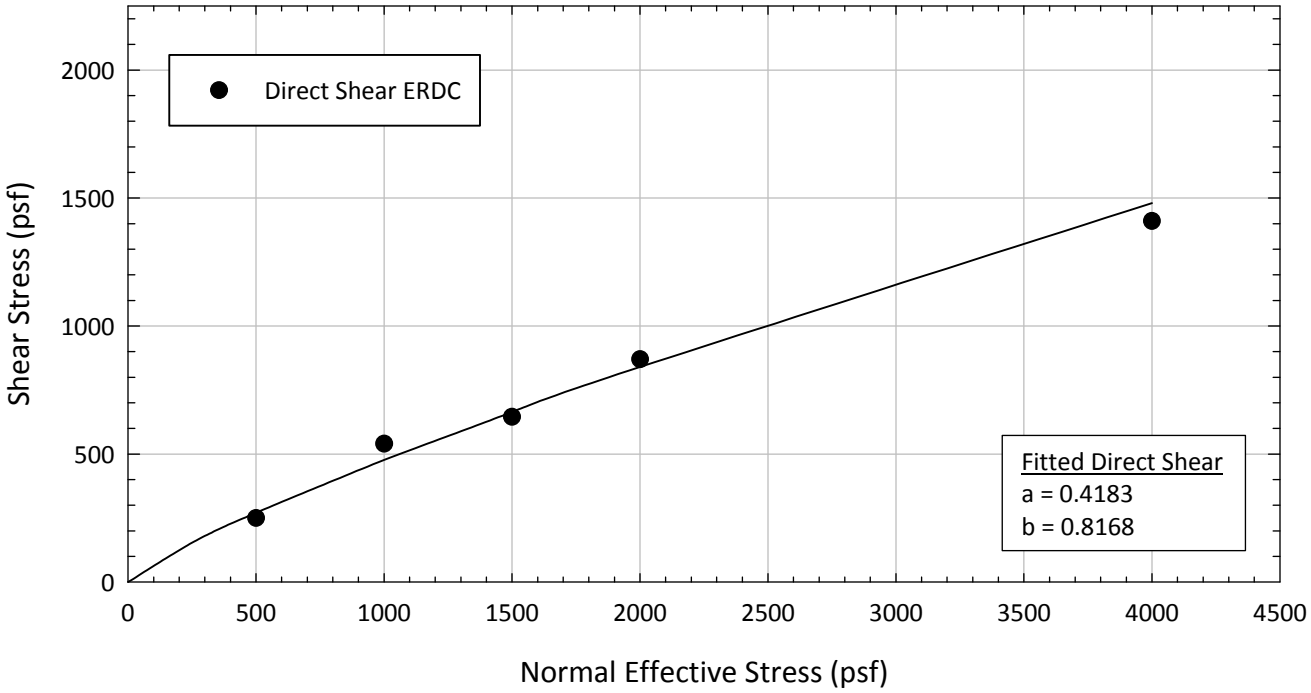

Texas 18 - Blenderized

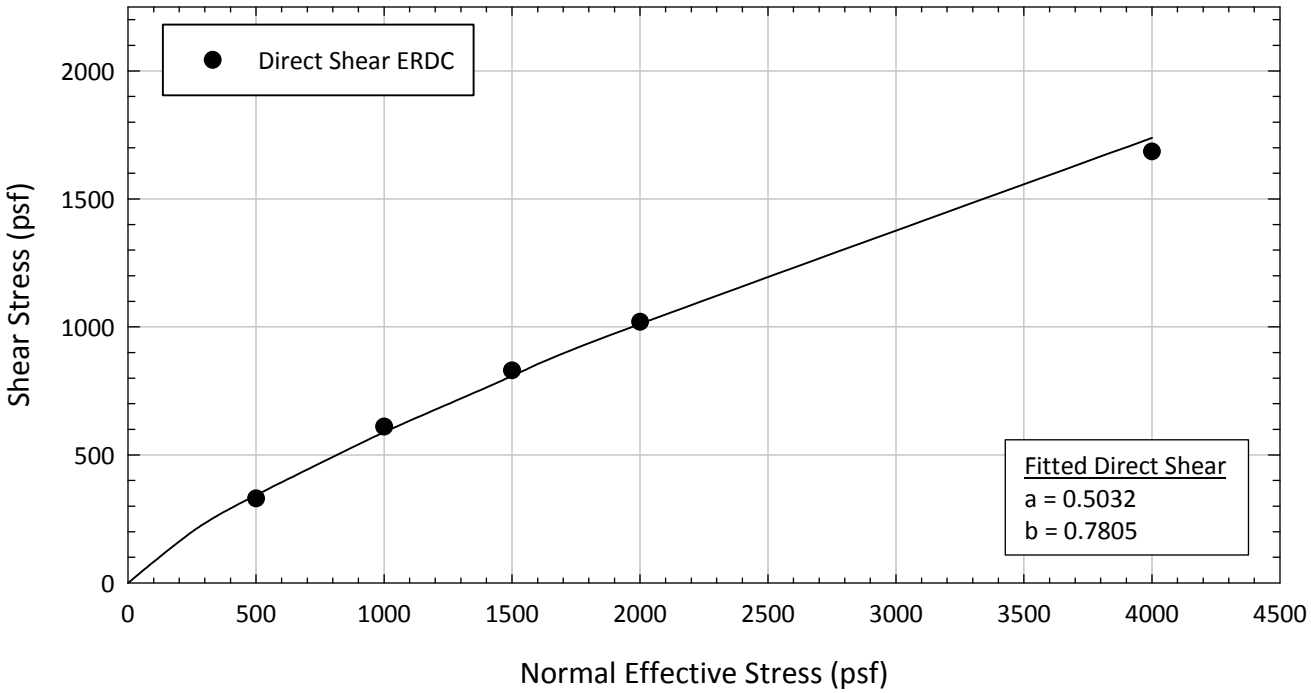

Texas 19 - Blenderized

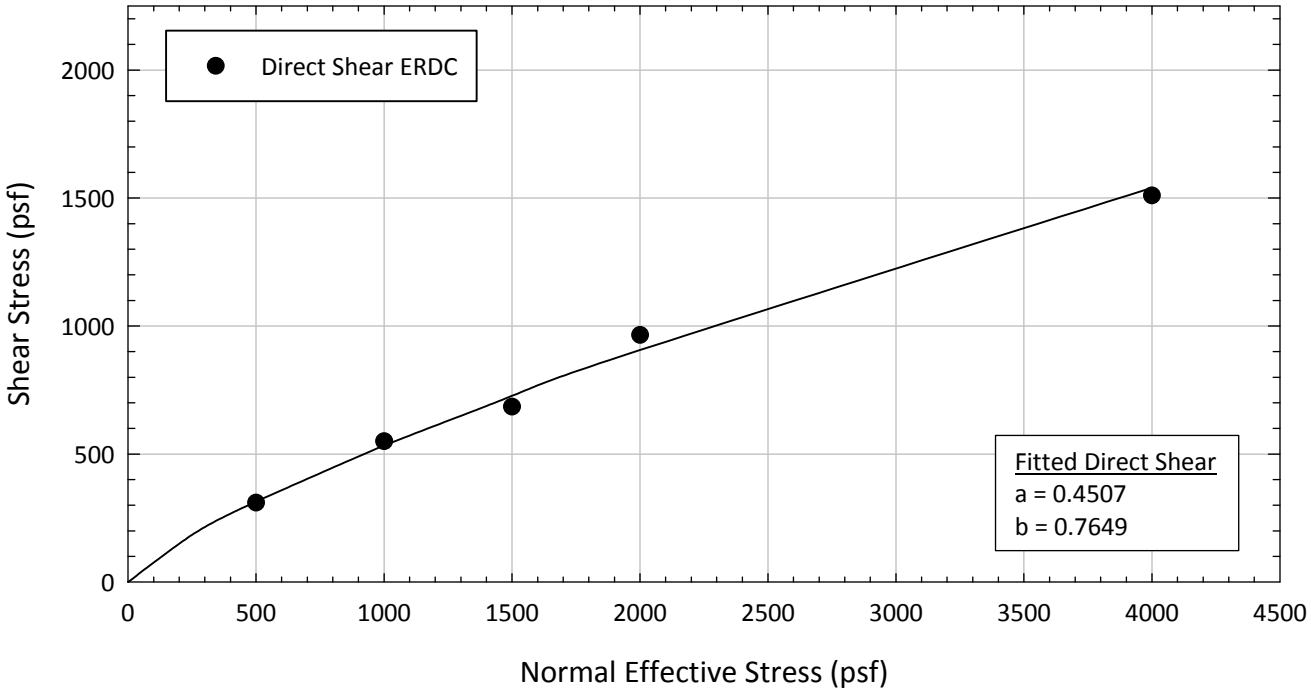

Texas 20 - Blenderized

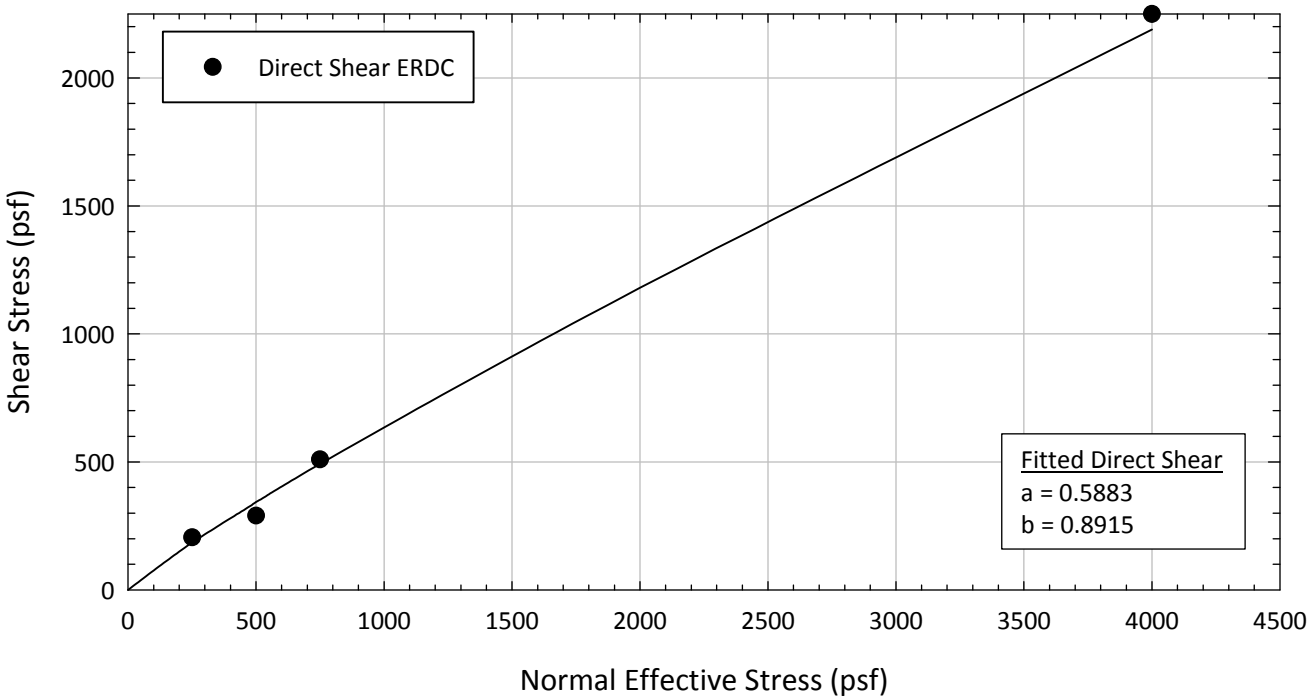

Texas 21 - Blenderized

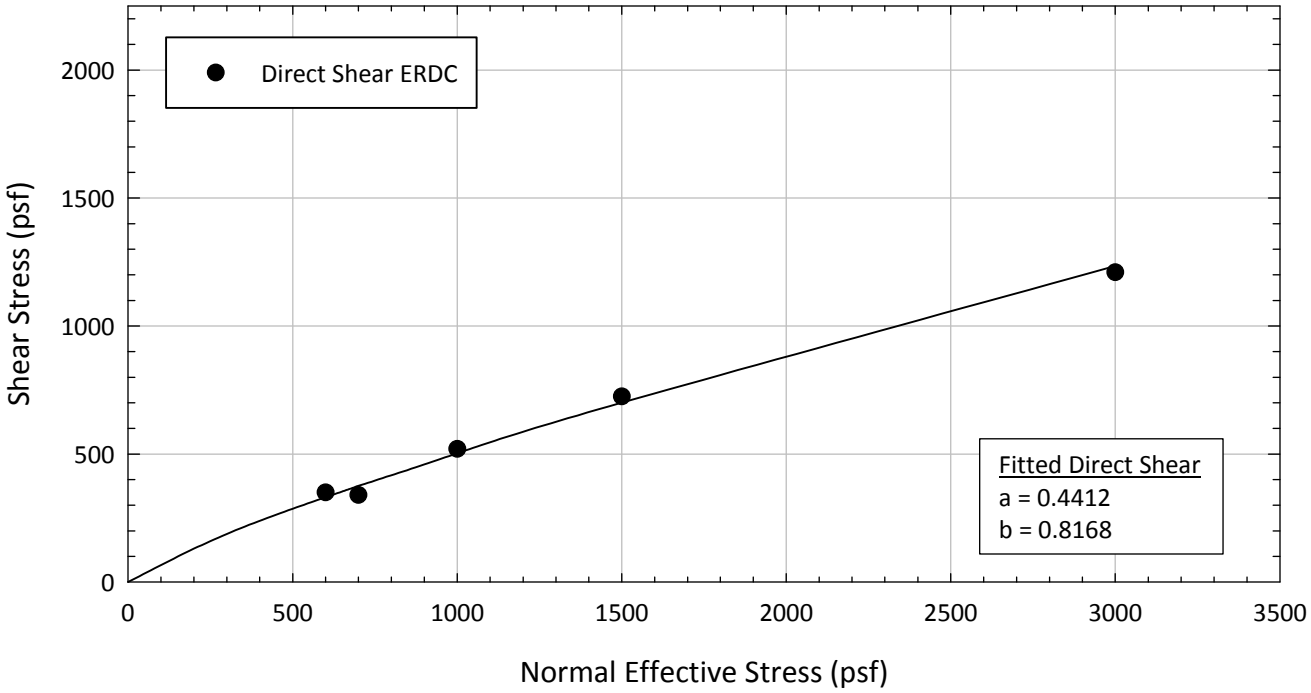

Texas 22 - Blenderized

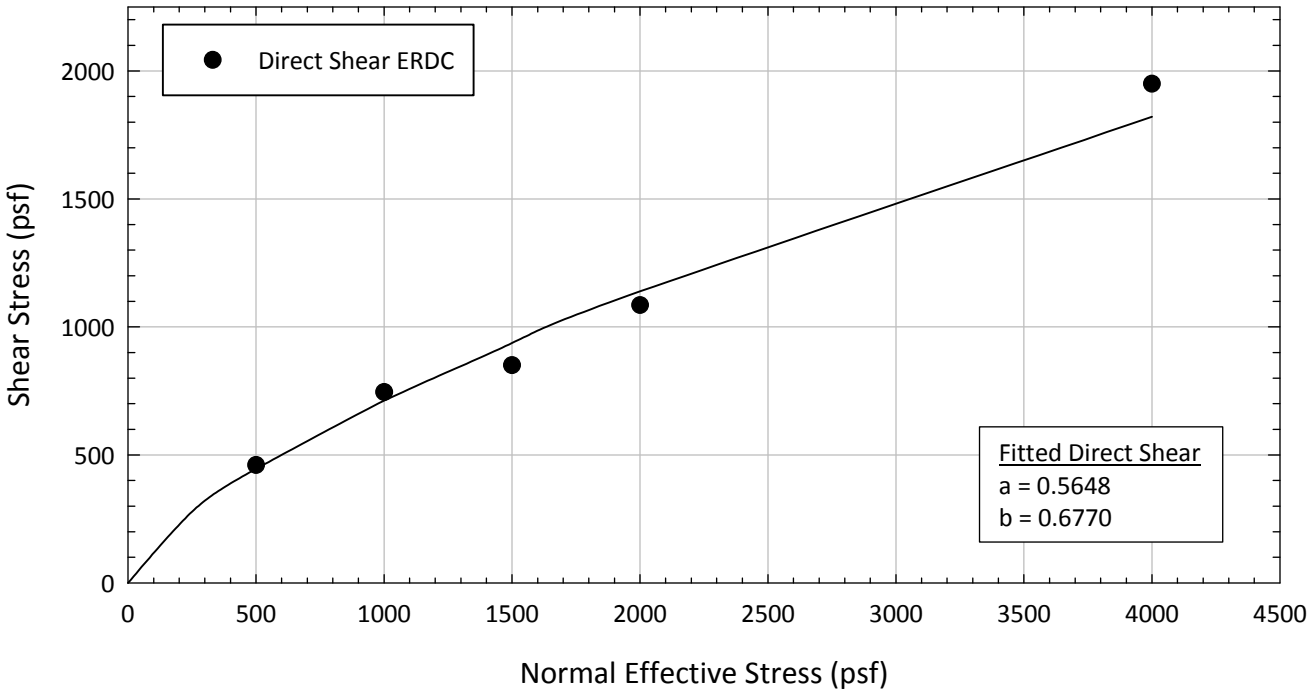

Texas 23 - Blenderized

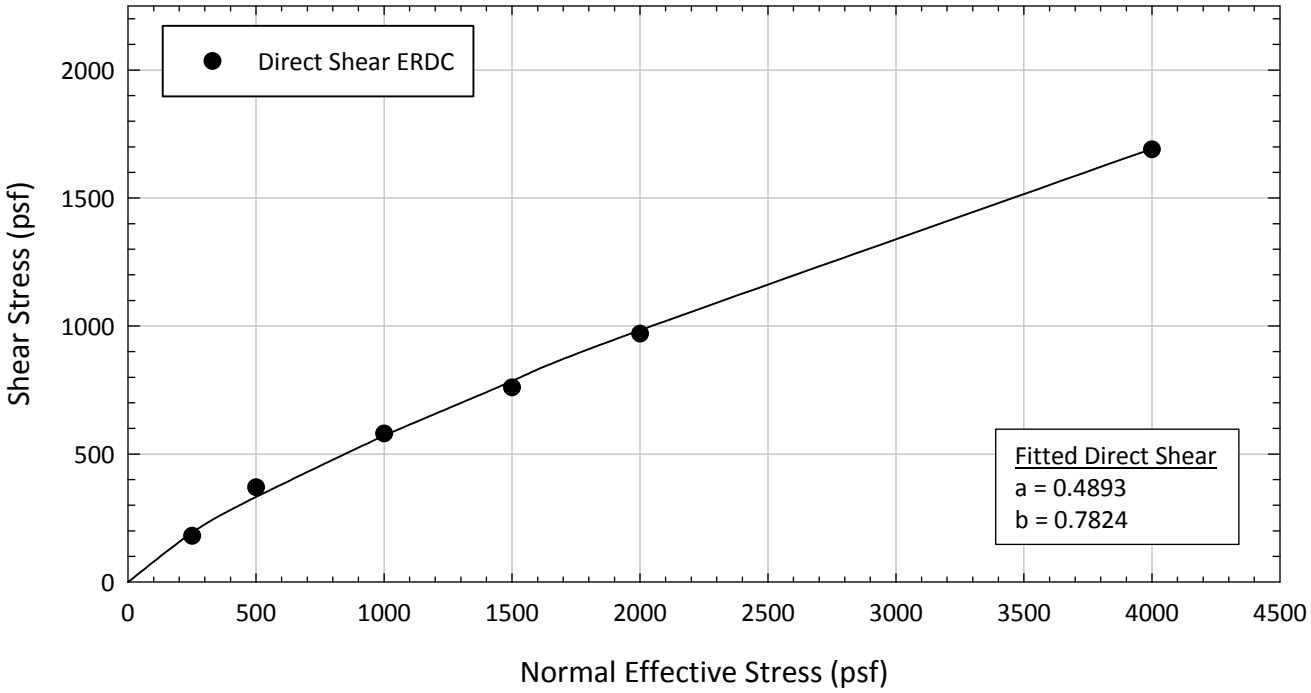

Texas 24 - Blenderized

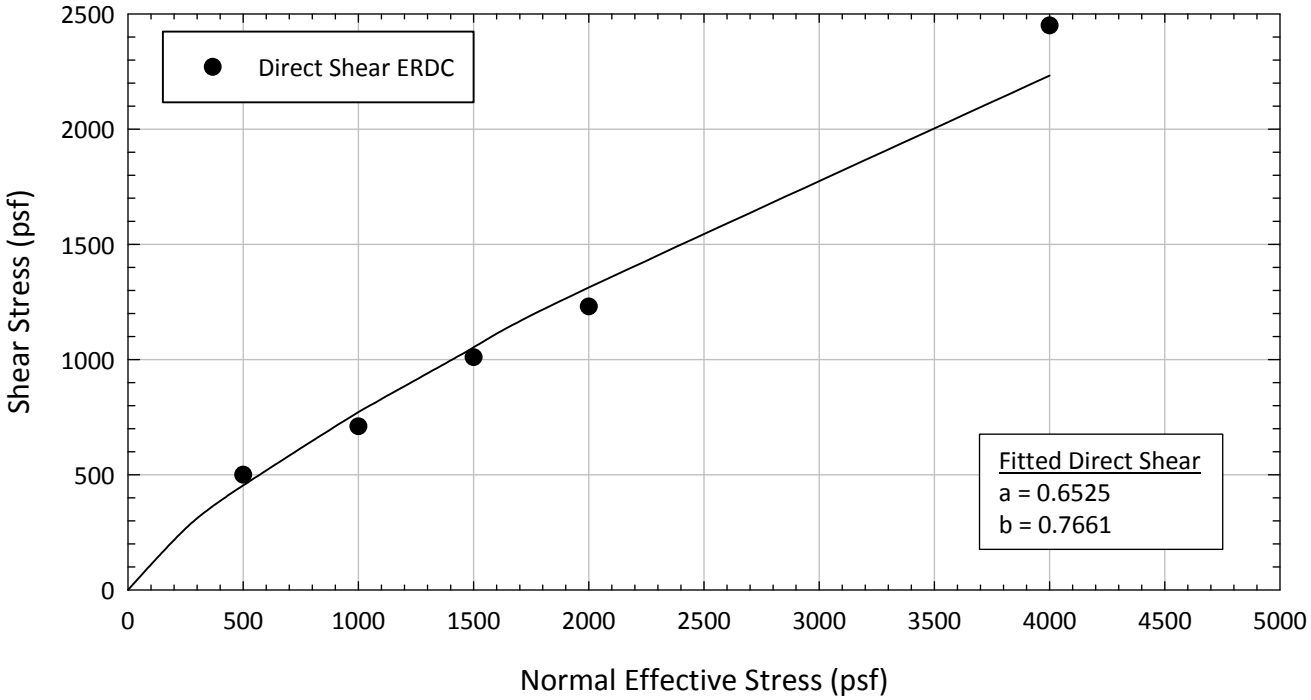

Texas 25 - Blenderized

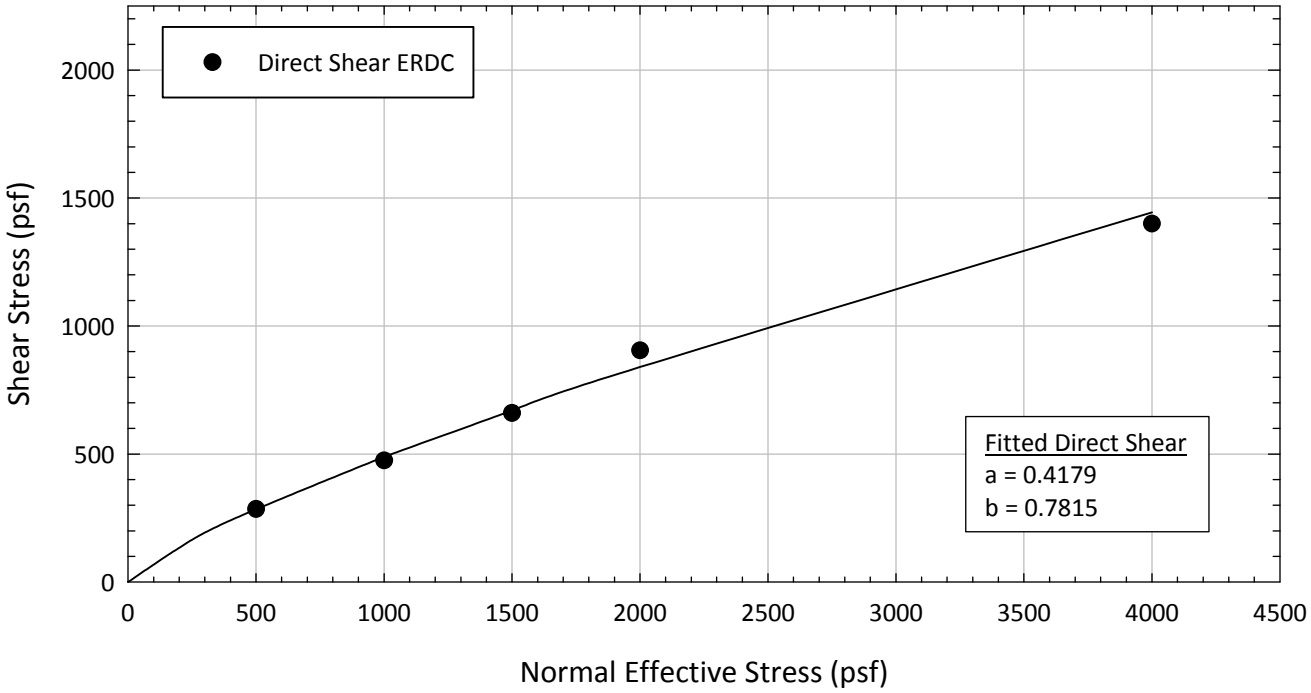

Texas 26 - Blenderized

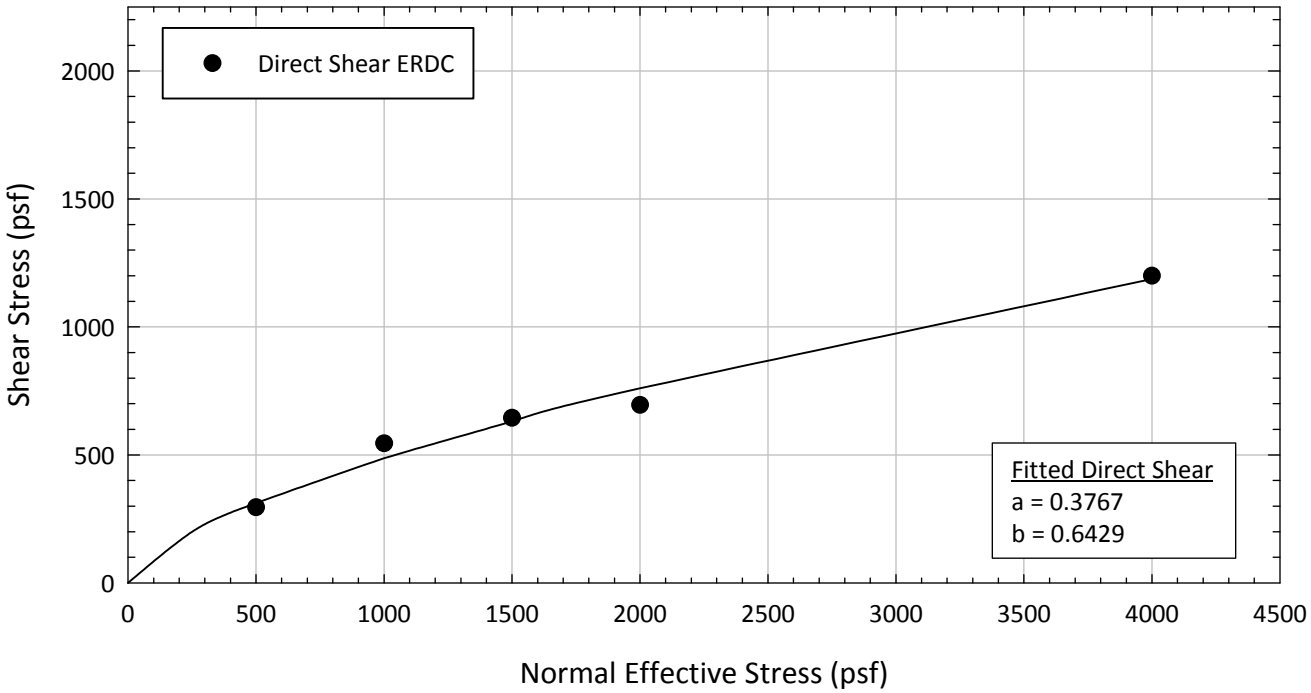

Texas 27 - Blenderized

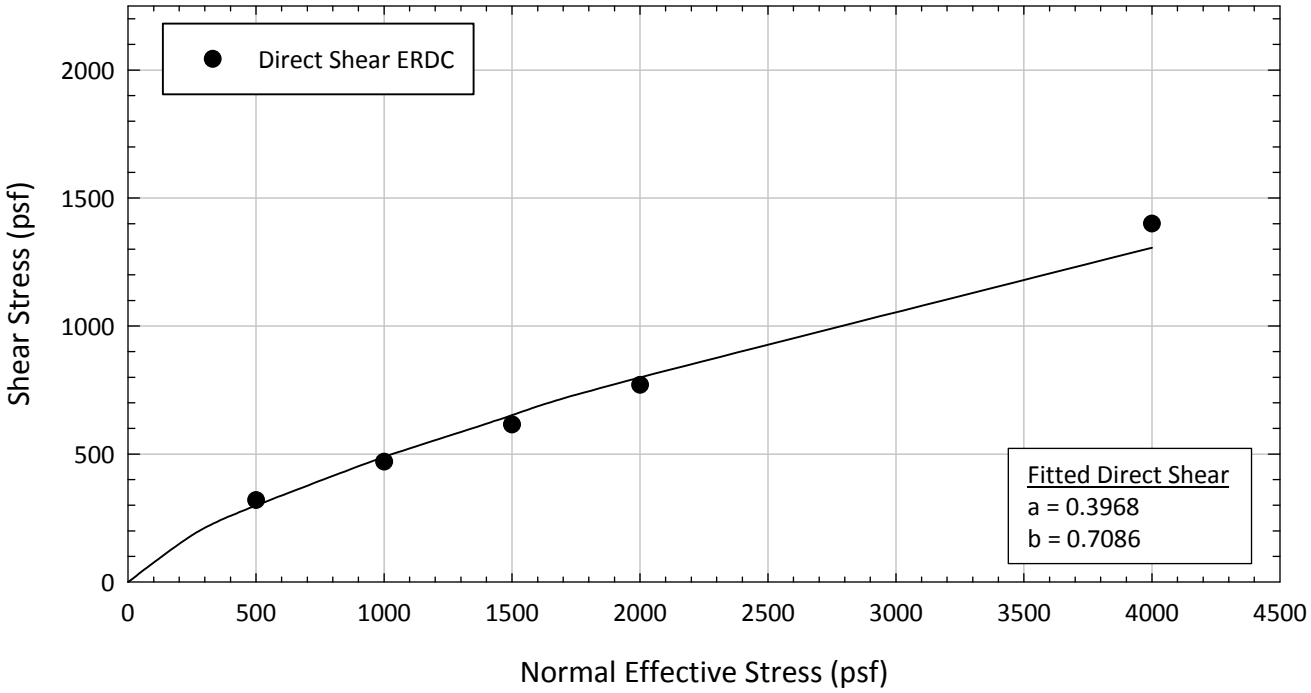

Texas 28 - Blenderized

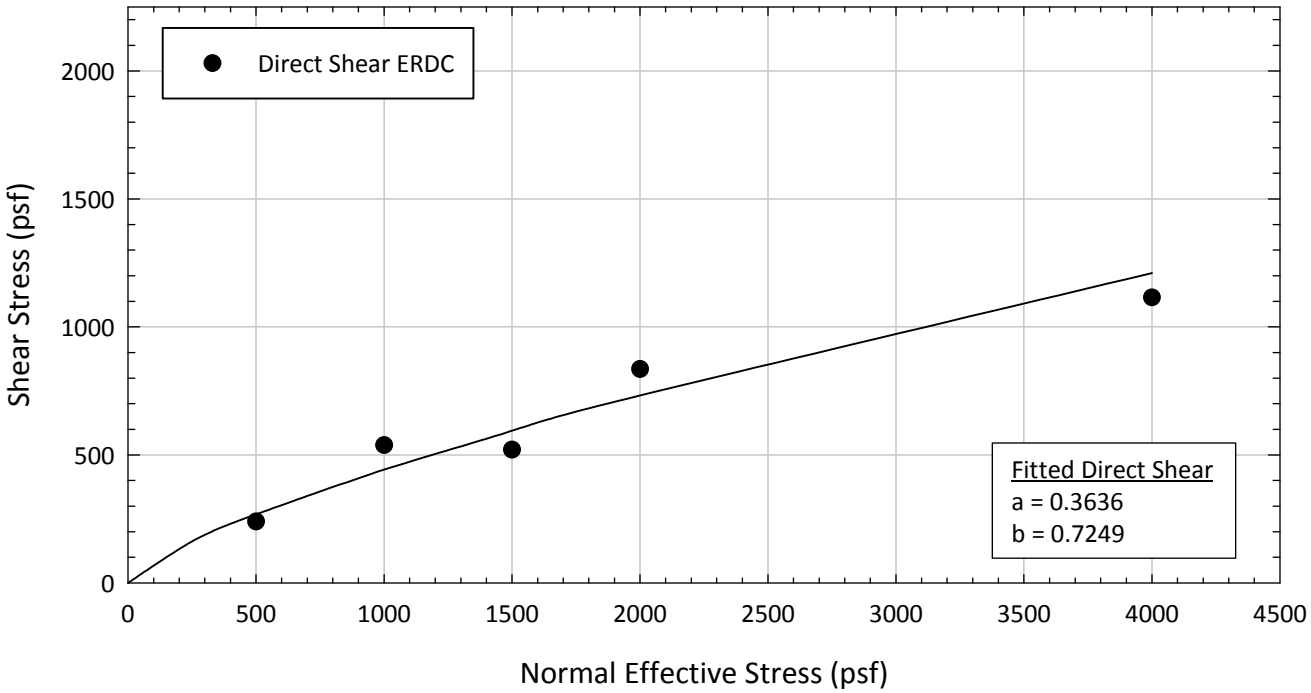

Texas 29 - Blenderized

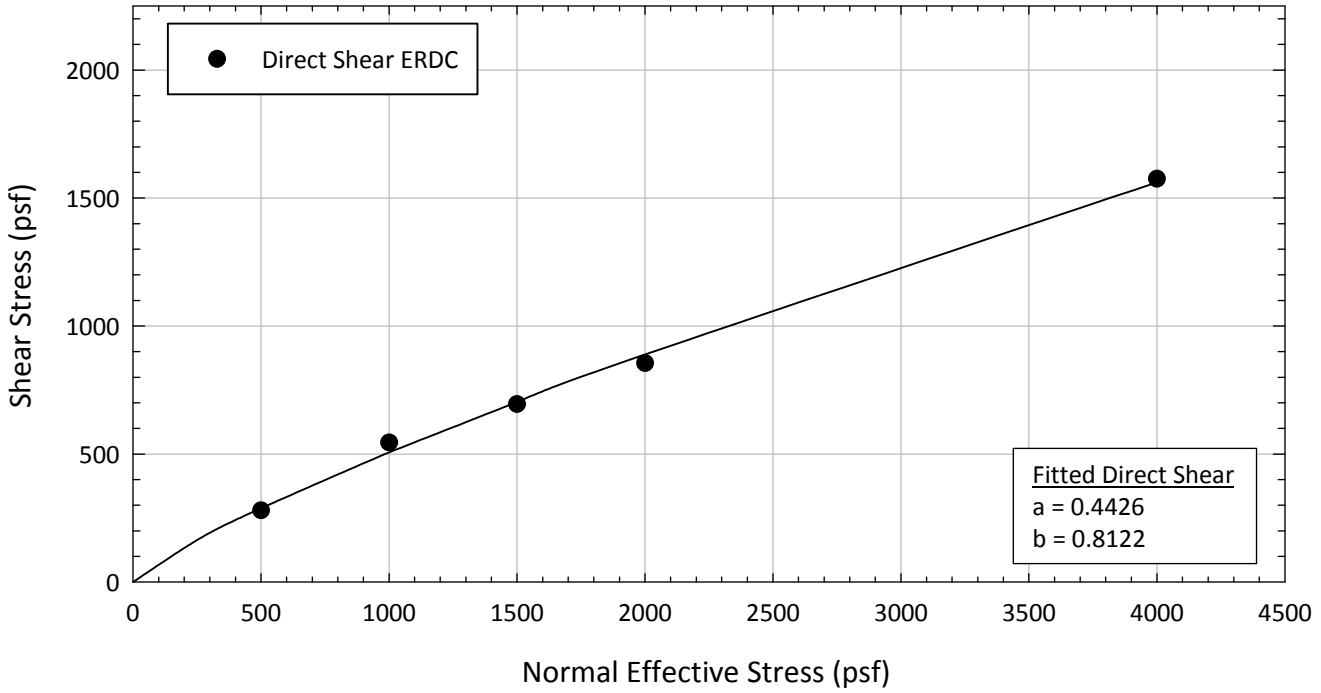

Texas 30 - Blenderized

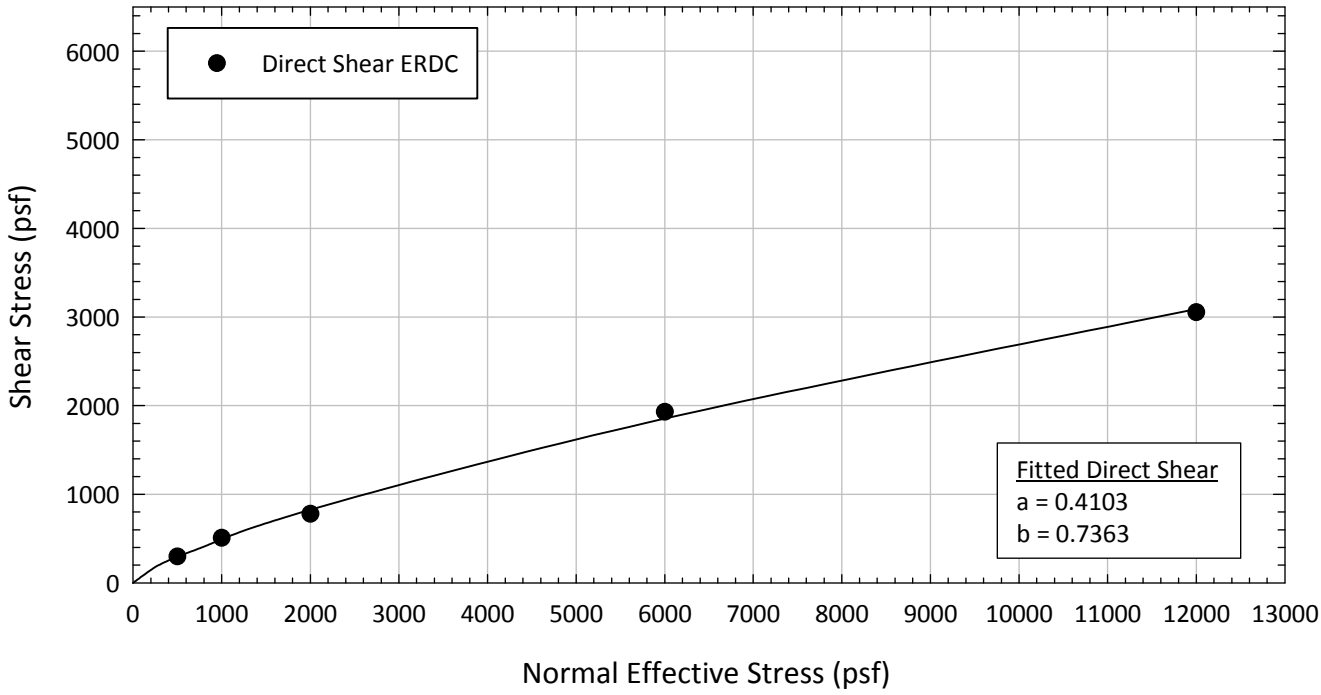

Texas 31 - Blenderized

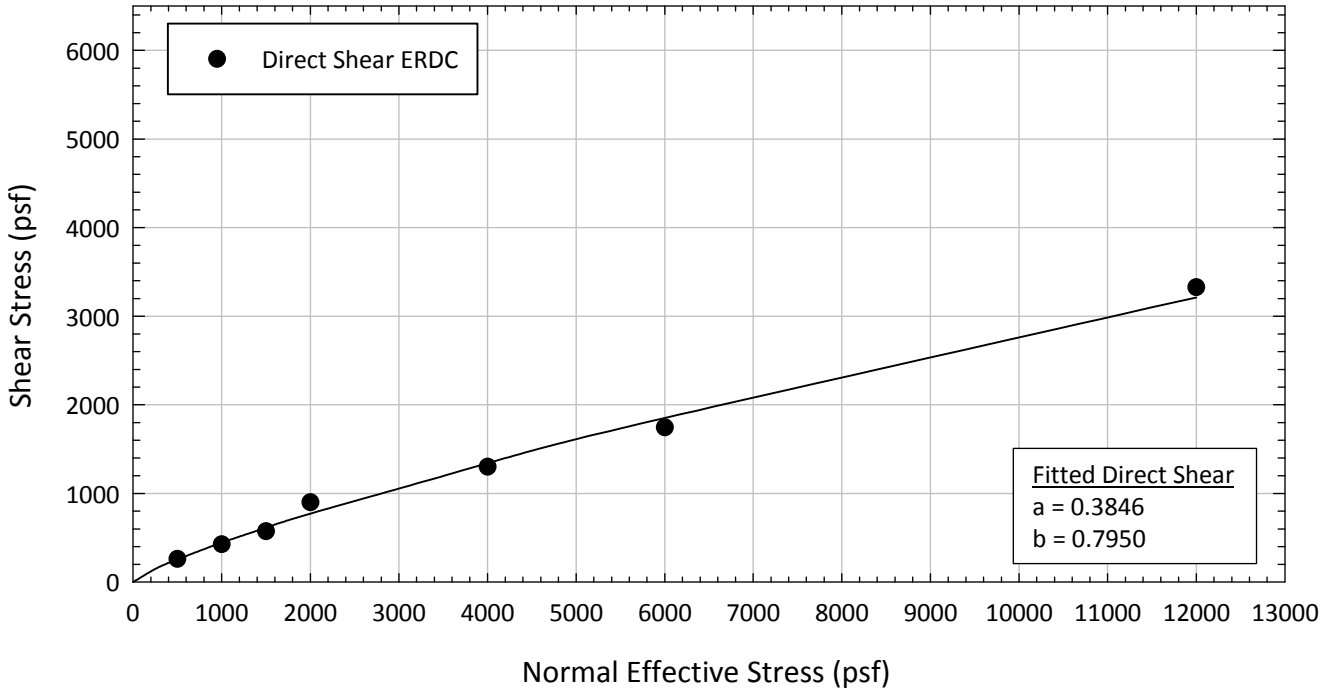

Texas 32 - Blenderized

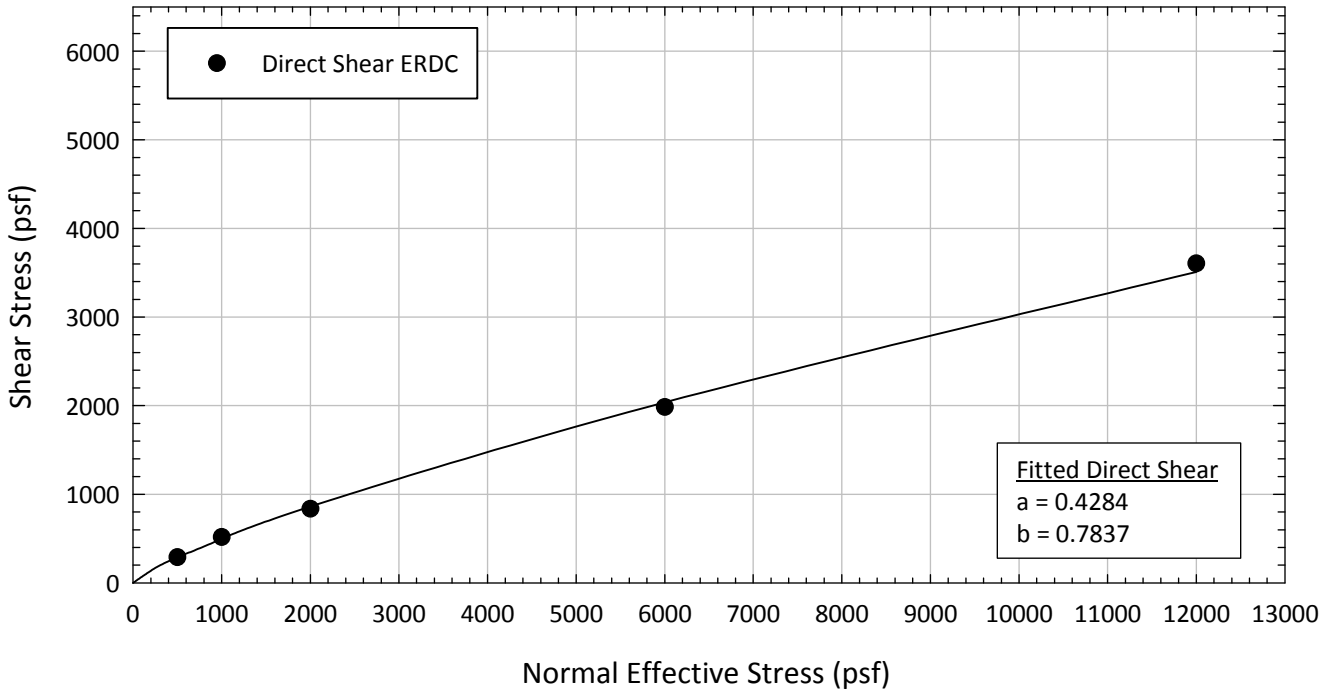

Texas 33 - Blenderized

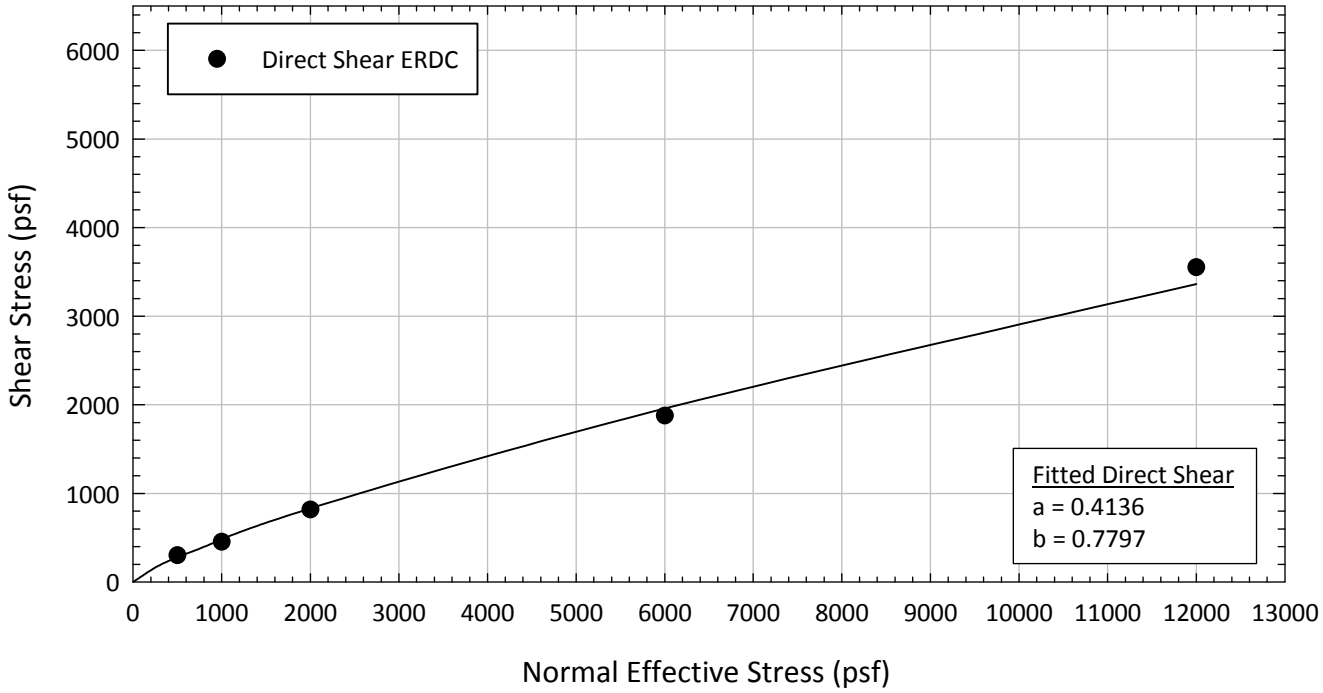

Texas 34 - Blenderized

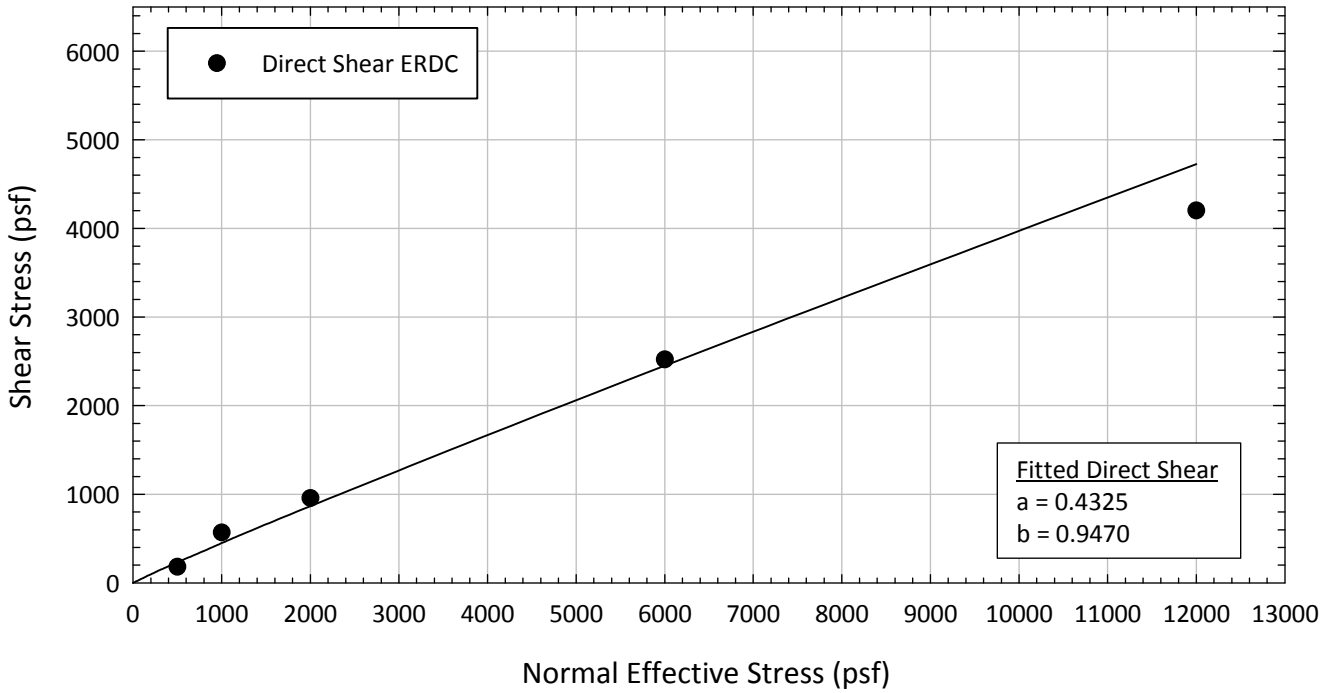

Texas 35 - Blenderized

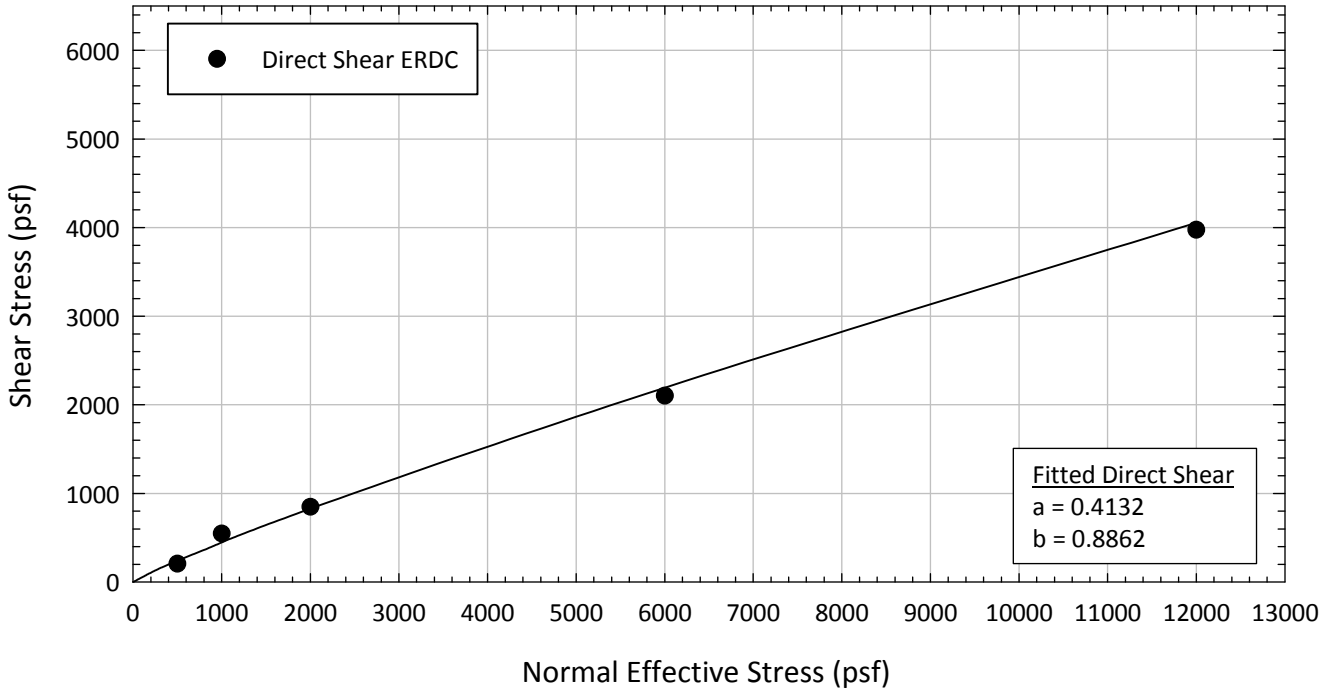

Appendix G

Triaxial Tests Allowed to Swell

Table of Contents

G.1. Oak Harbor

G.1.1 ICU Triaxials

Virginia Polytechnic Institute and State University
Geotechnical Engineering Laboratory
Triaxial Data Sheet

Project:	Fully Softened Shear Strength
Sample I.D./Loc.:	Oak Harbor - Compacted - Allowed to Swell - Consolidated Undrained
Classification:	Lean Clay (CL)

Sample Preparation	Compacted
Specimen Saturation Method	Wet

Specific Gravity	2.82	
Method for Dimensions After Consol.	Case and Chilver (1959)	

Test Number	1	2	3	4	5	6	7	8
Start Date (m/d/y)	7/16/2012	7/16/2012	7/10/2012	7/10/2012	7/10/2012	7/10/2012		
End Date (m/d/y)	7/23/2012	7/23/2012	7/14/2012	7/14/2012	7/14/2012	7/14/2012		
Backpressure (psf)	14400	14400	12946	12946	12946	9360		
Consolidation Pressure (psf)	541	720	1008	2016	4608	7920		
B value	1.00	0.99	0.98	1.00	0.97	0.98		
Initial Values								
Initial Height (in.)	2.788	2.789	2.797	2.784	2.799	2.73		
Initial Diameter (in.)	1.312	1.312	1.310	1.310	1.309	1.31		
Initial Sample Weight (g.)	127.39	128.22	128.03	128.33	129.41	126.51		
Water Content (%)	20.18	20.45	19.70	20.11	20.10	20.20		
Dry Unit Weight (pcf)	106.9	107.7	107.8	108.5	109.0	108.9		
Wet Unit Weight (pcf)	128.4	129.7	129.0	130.4	130.9	130.9		
Saturation (%)	88.9	90.2	88.9	91.1	92.2	92.2		
Void Ratio	0.65	0.64	0.63	0.62	0.62	0.62		
After Swelling and Consolidation								
t_{100} Using Casagrande Method (min)	150.00	600.00	110.00	325.00	400.00	350.00		
Volumetric Strain (%)	-4.32	-6.12	-4.30	-2.00	-0.50	0.73		
Height After Consolidation (in.)	2.793	2.799	2.800	2.784	2.805	2.736		
Area After Consolidation (in.)	1.409	1.430	1.405	1.374	1.349	1.337		
Final Values								
Water Content (%)	25.50	26.08	24.94	23.23	22.09	21.47		
Dry Unit Weight (pcf)	102.4	101.5	103.4	106.4	108.5	109.69		
Wet Unit Weight (pcf)	128.6	127.9	129.2	131.1	132.5	133.2		
Saturation (%)	100.0	100.0	100.0	100.0	100.0	100.0		
Void Ratio	0.72	0.74	0.70	0.66	0.62	0.61		
Failure								
Failure Criteria	Max PSR	Max PSR	Max PSR	Max PSR	Max PSR	Max PSR		
Deviator Stress at failure (psf)	1110.41	1164.51	1961.17	3233.99	5970.67	9061.81		
Principal Stress Ratio at failure	5.56	4.37	3.74	2.90	2.75	2.62		
Minor Principal Effective Stress at fail. (psf)	243.2	345.6	716.2	1704.8	3419.8	5609.5		
Major Principal Effective Stress at fail. (psf)	1353.7	1510.1	2677.4	4939.0	9390.5	14671.3		
Corrections Applied	Membrane	Membrane	Membrane	Membrane	Membrane	Membrane		
Axial Strain at failure (%)	0.69	1.20	2.61	4.48	5.88	7.60		
Test performed at strain rate (%/hr)	0.35	0.25	0.25	0.25	0.25	0.25		

Comments: All test specimens were allowed to swell during/after consolidation. The piston was in contact with the top platen during swelling. For this reason, a small vertical stress was already being applied to the sample at the beginning of shearing.
Volumetric strain is positive for compression and negative for swelling.

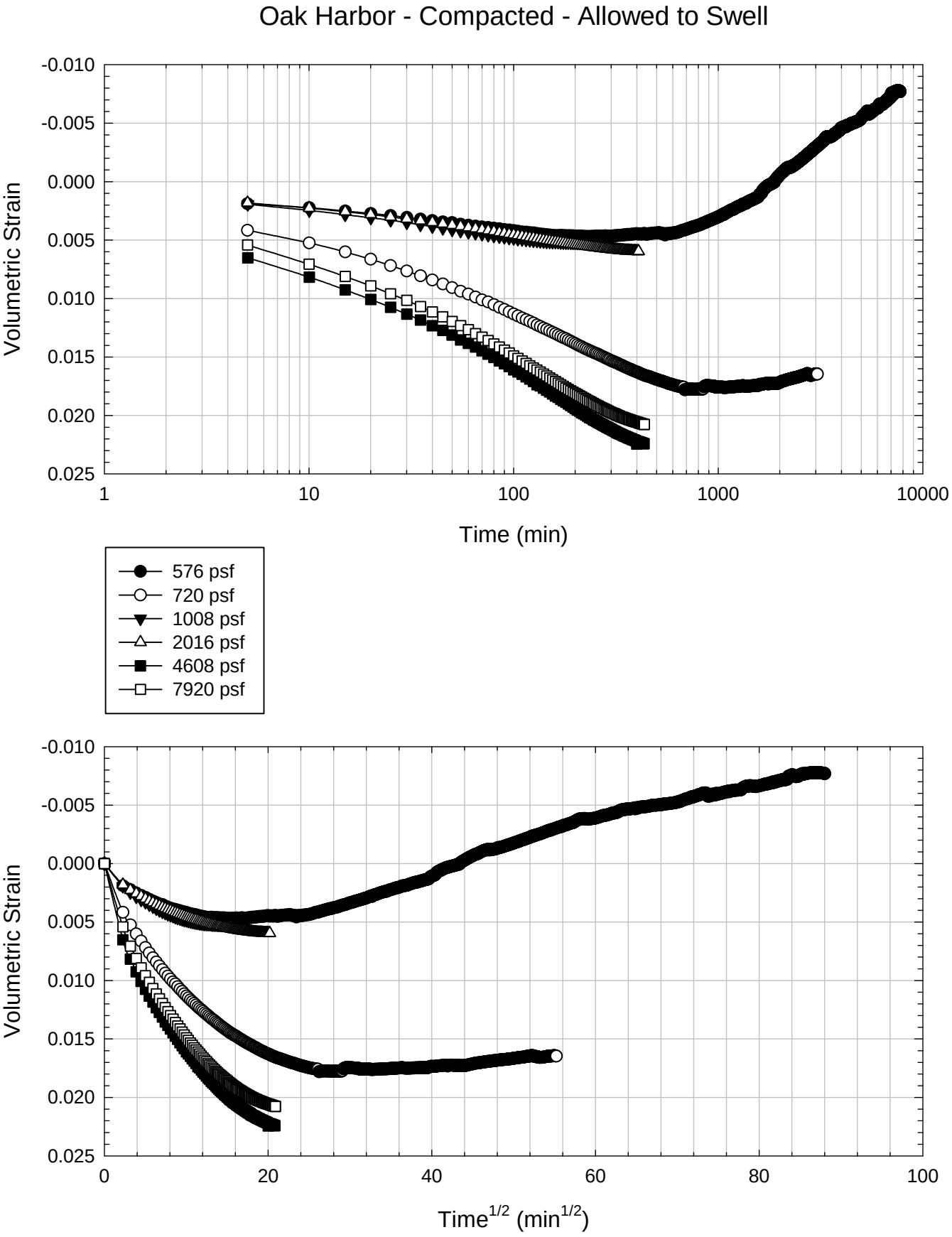
Oak Harbor - Compacted - Allowed to Swell
Volumetric Strain
-0.010
-0.005
0.000
0.005
0.010
0.015
0.020
0.025
1
10
100
1000
10000
Time (min)
576 psf
720 psf
1008 psf
2016 psf
4608 psf
7920 psf
Volumetric Strain
-0.010
-0.005
0.000
0.005
0.010
0.015
0.020
0.025
0
20
40
60
80
100
Time^1/2 (min^1/2)

Oak Harbor - Compacted - Allowed to Swell

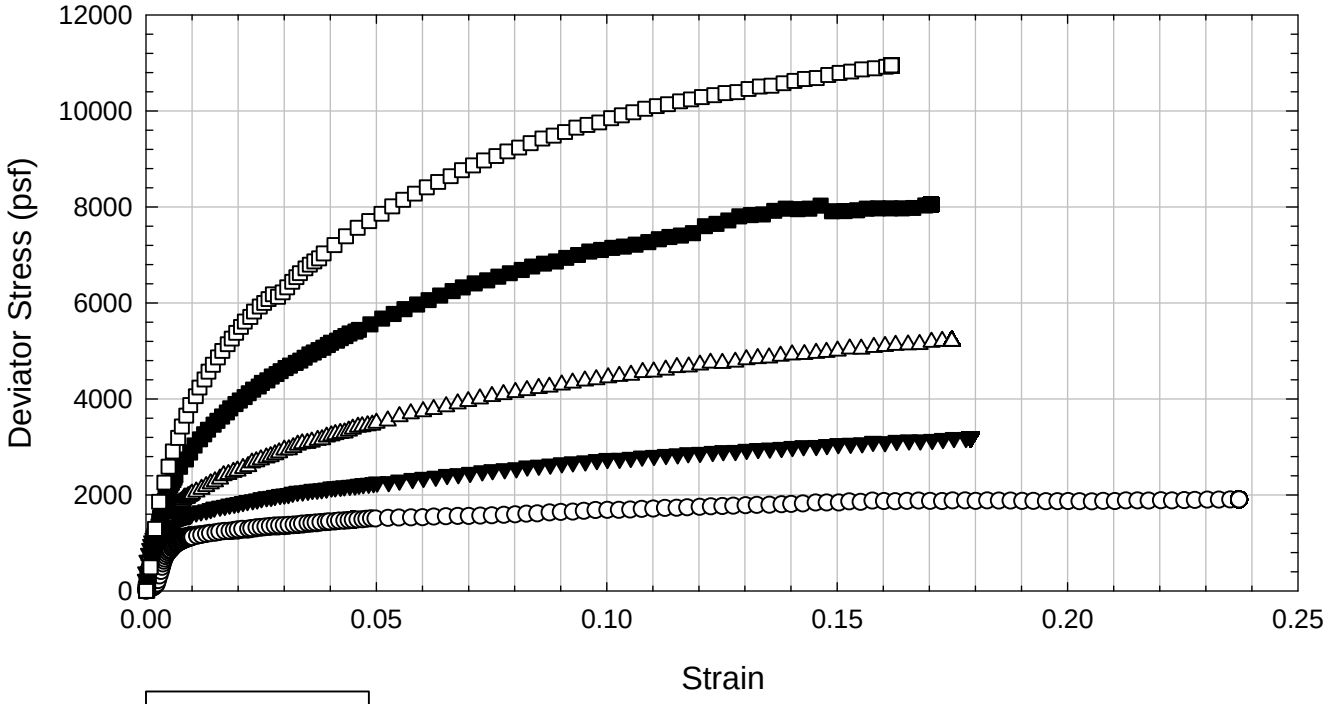

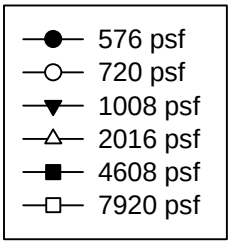

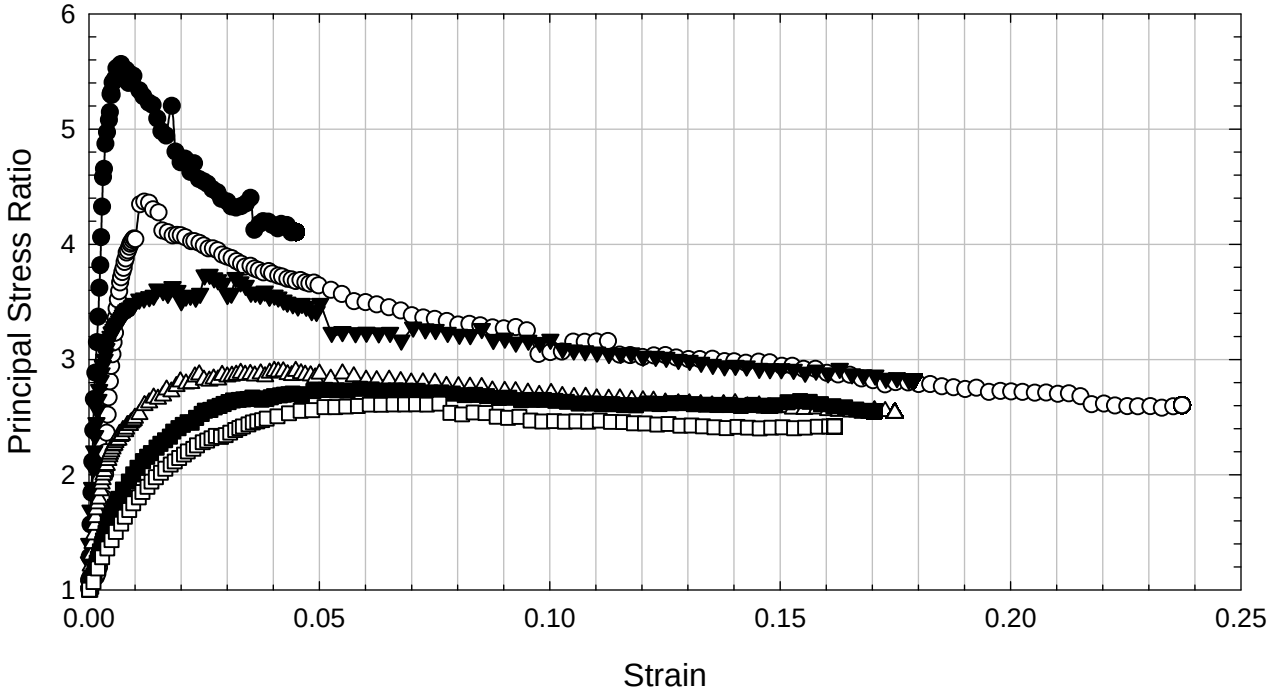

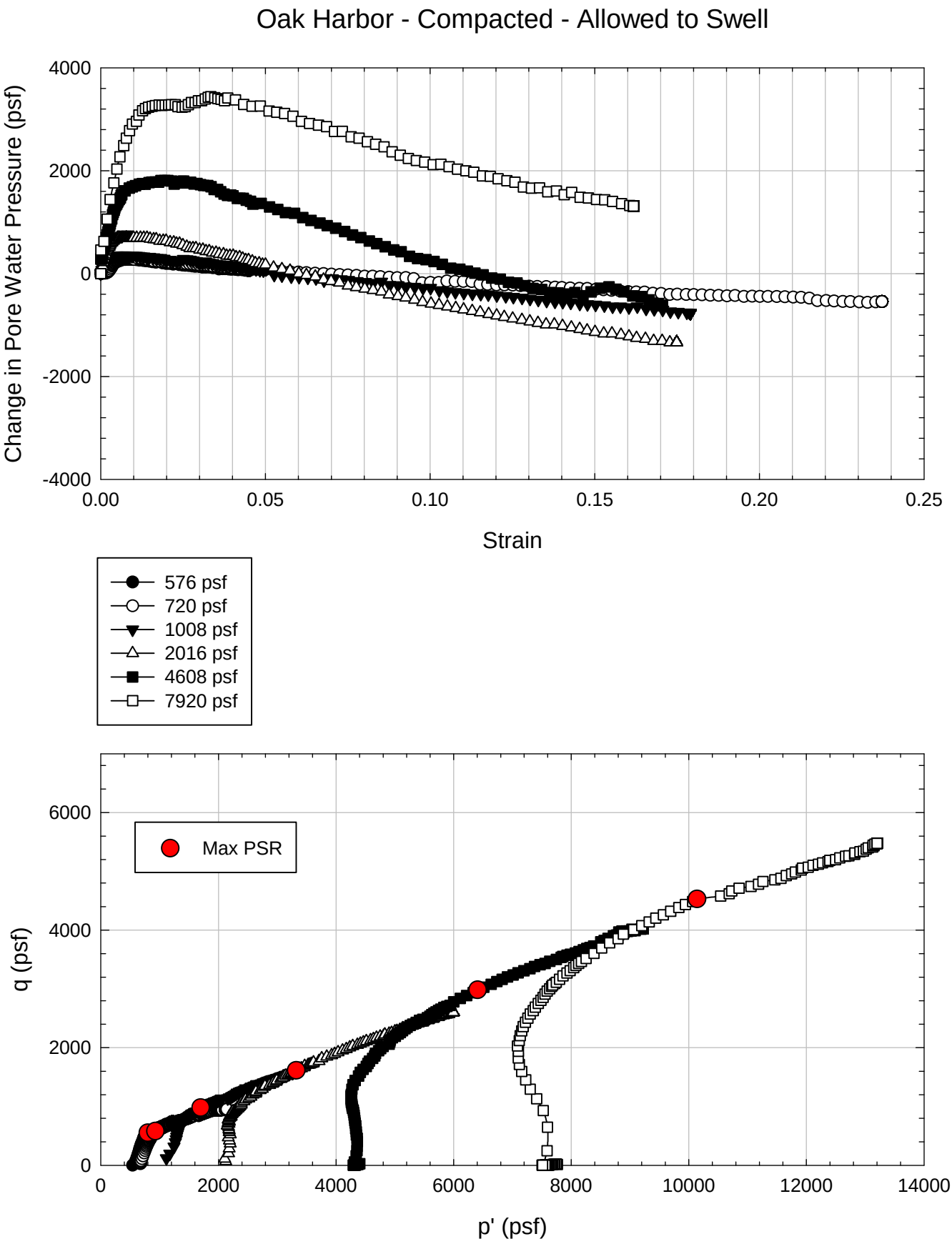
Oak Harbor - Compacted - Allowed to Swell
Change in Pore Water Pressure (psf)
4000
2000
0
-2000
-4000
0.00
0.05
0.10
0.15
0.20
0.25
Strain
576 psf
720 psf
1008 psf
2016 psf
4608 psf
7920 psf
Max PSR
q (psf)
6000
4000
2000
0
0
2000
4000
6000
8000
10000
12000
14000
p' (psf)

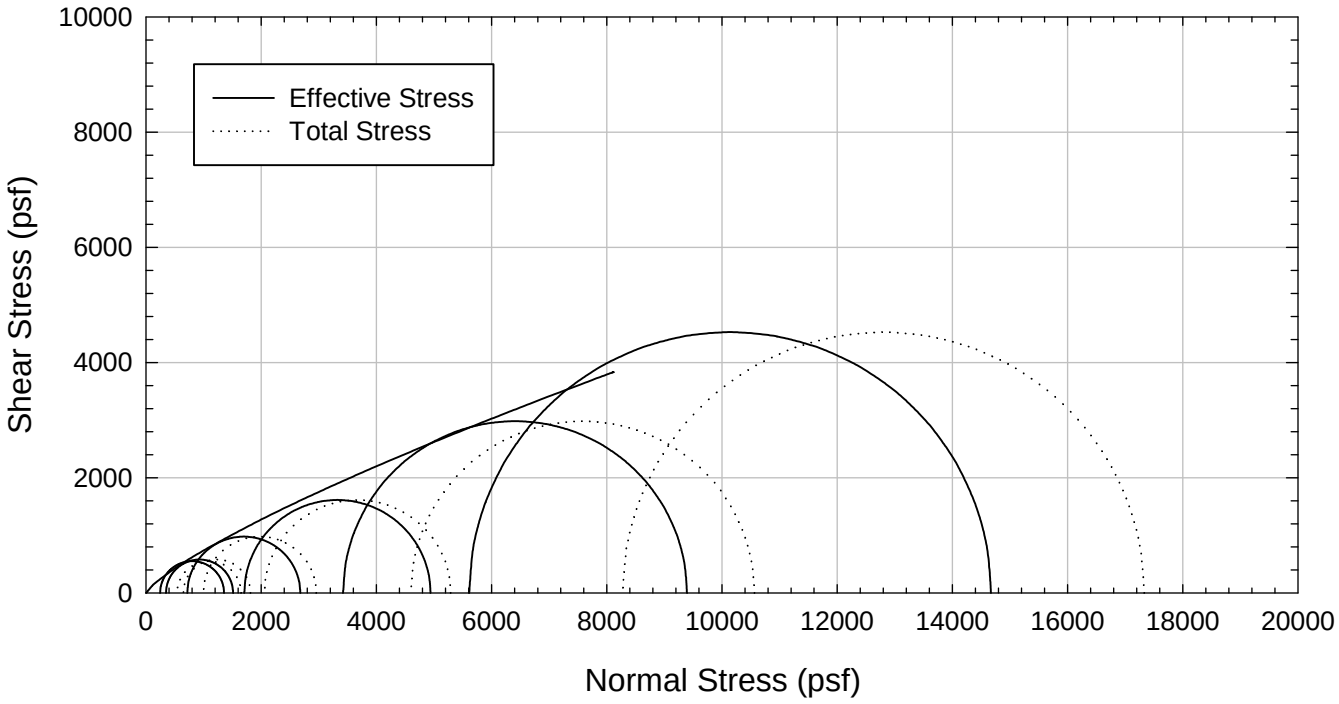
Oak Harbor - Compacted - Allowed to Swell
Effective Stress
Total Stress
Shear Stress (psf)
Normal Stress (psf)
0
2000
4000
6000
8000
10000
12000
14000
16000
18000
20000

Virginia Polytechnic Institute and State University
Geotechnical Engineering Laboratory
Triaxial Data Sheet

Project:	Fully Softened Shear Strength
Sample I.D./Loc.:	Oak Harbor - Compacted - Allowed to Swell - Consolidated Undrained
Classification:	Lean Clay (CL)

Sample Preparation	Compacted
Specimen Saturation Method	Wet

Specific Gravity	2.82	
Method for Dimensions After Consol.	Method B	

Test Number	1	2	3	4	5	6	7	8
Start Date (m/d/y)	11/5/2012	11/5/2012	10/29/2012	10/29/2012	10/16/2012	10/17/2012		
End Date (m/d/y)	11/14/2012	11/12/2012	11/5/2012	11/4/2012	10/26/2012	10/26/2012		
Backpressure (psf)	8480	9598	11762	12951	9105	8319		
Consolidation Pressure (psf)	864	1008	3024	3312	5040	5040		
B value	0.95	0.92	0.99	0.97	0.96	0.97		
Initial Values								
Initial Height (in.)	2.798	2.798	2.796	2.793	2.799	2.792		
Initial Diameter (in.)	1.315	1.314	1.313	1.312	1.314	1.314		
Initial Sample Weight (g.)	124.60	125.30	125.85	125.58	127.33	127.34		
Water Content (%)	18.20	18.50	19.00	19.00	19.50	19.40		
Dry Unit Weight (pcf)	105.8	106.2	106.4	106.5	106.9	107.3		
Wet Unit Weight (pcf)	125.1	125.8	126.6	126.7	127.7	128.1		
Saturation (%)	77.1	79.2	81.7	82.0	85.1	85.5		
Void Ratio	0.67	0.66	0.66	0.65	0.65	0.64		
After Swelling and Consolidation								
t_{100} Using Casagrande Method (min)	---	100	500	350	500	480		
Volumetric Strain (%)	-4.89	-5.95	-2.01	-1.38	0.31	-0.86		
Height After Consolidation (in.)	2.752	2.742	2.777	2.780	2.802	2.784		
Area After Consolidation (in.)	1.447	1.466	1.391	1.377	1.351	1.372		
Final Values								
Water Content (%)	26.50	26.90	24.40	24.00	22.80	23.20		
Dry Unit Weight (pcf)	100.8	100.2	104.3	105.0	107.2	106.4		
Wet Unit Weight (pcf)	127.5	127.2	129.7	130.2	131.6	131.1		
Saturation (%)	100.0	100.0	100.0	100.0	100.0	100.0		
Void Ratio	0.75	0.76	0.69	0.68	0.64	0.66		
Failure								
Failure Criteria	Max PSR	Max PSR	Max PSR	Max PSR	Max PSR	Max PSR		
Deviator Stress at failure (psf)	1164	1358	3590	3775	6540	5711		
Principal Stress Ratio at failure	2.78	3.26	2.78	2.79	2.63	2.68		
Minor Principal Effective Stress at fail. (psf)	674	608	2027	2127	4020	3409		
Major Principal Effective Stress at fail. (psf)	1873	1982	5642	5926	10589	9143		
Corrections Applied	Membrane	Membrane	Membrane	Membrane	Membrane	Membrane		
Axial Strain at failure (%)	10.8	4.8	7.4	7.0	8.6	7.1		
Test performed at strain rate (%/hr)	0.43	0.36	0.36	0.43	0.36	0.43		

Comments: Volumetric strain is positive for compression and negative for swelling.

Oak Harbor - Compacted - Allowed to Swell

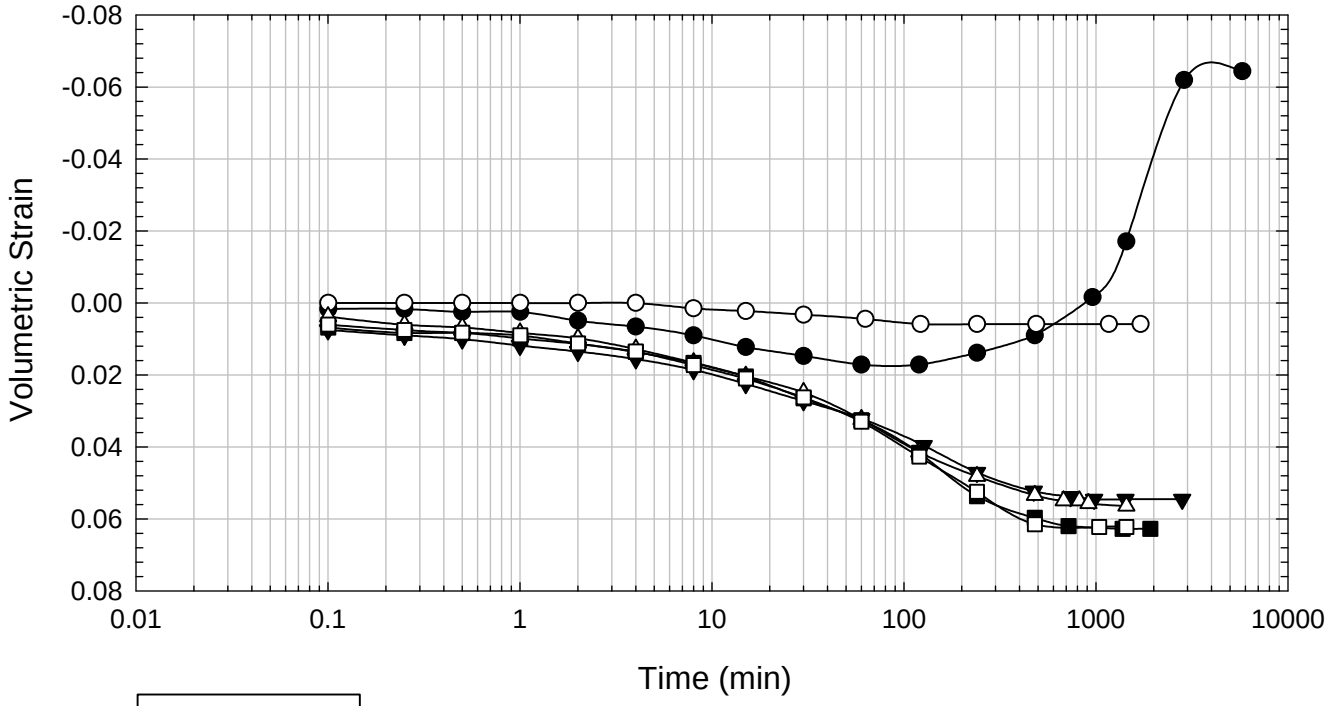

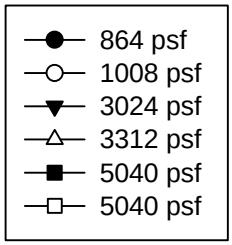

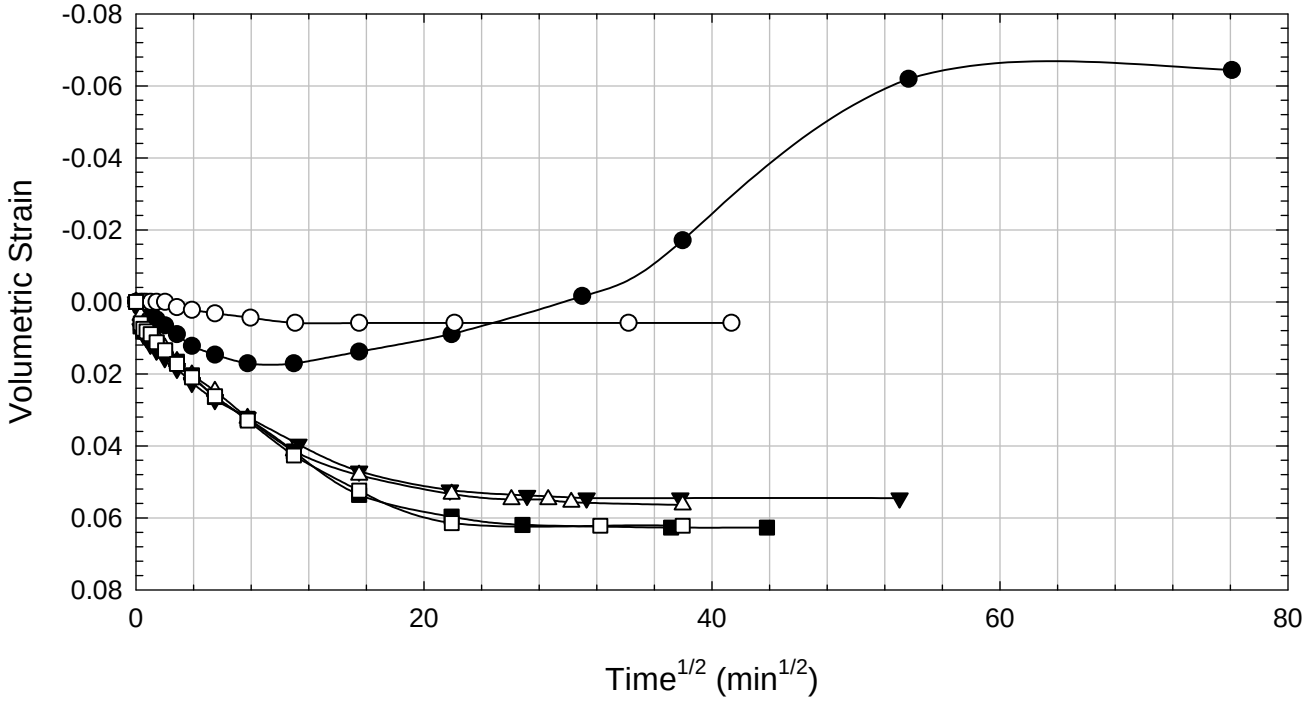

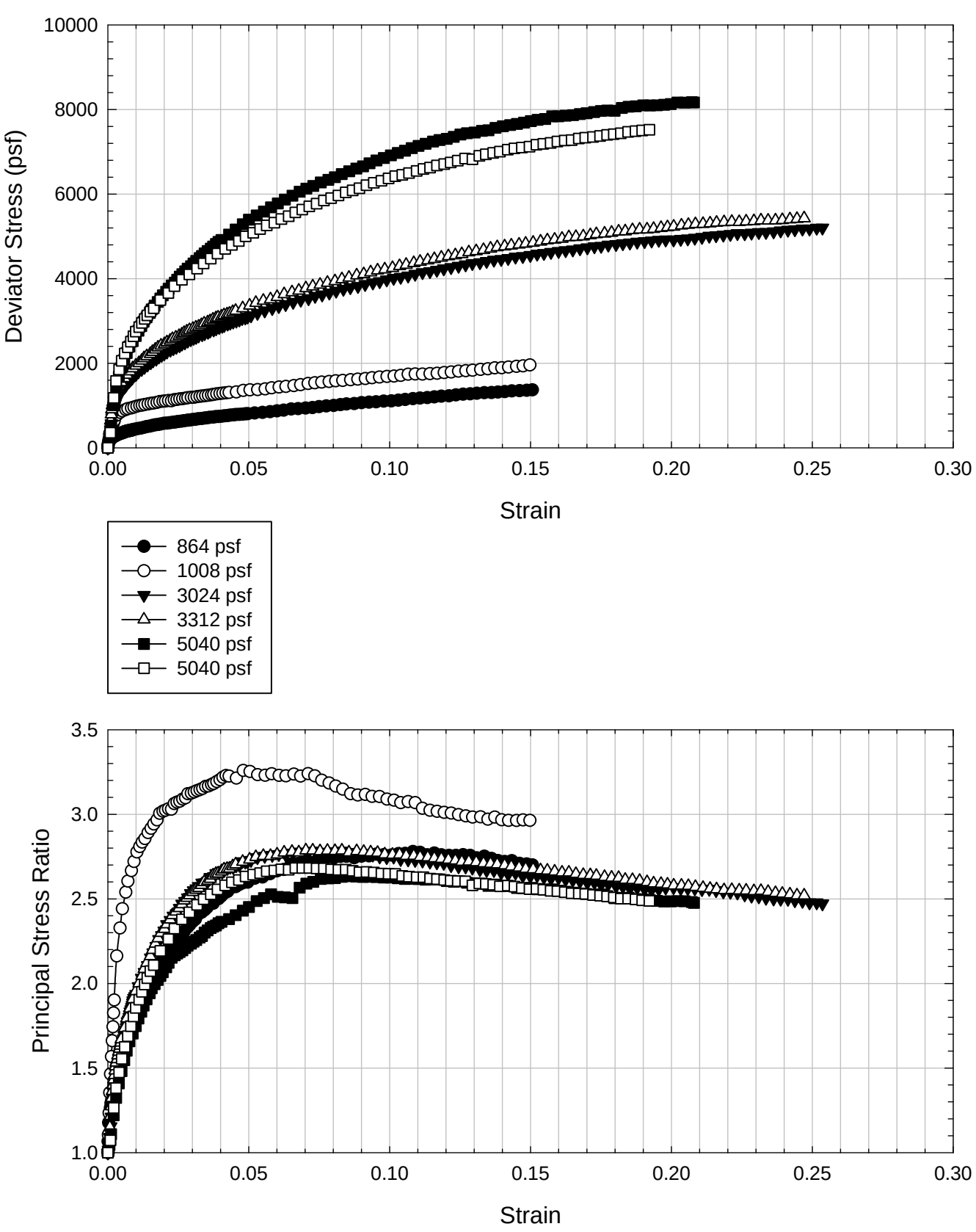
Oak Harbor - Compacted - Allowed to Swell
Deviator Stress (psf)
10000
8000
6000
4000
2000
0
0.00
0.05
0.10
0.15
0.20
0.25
0.30
Strain
864 psf
1008 psf
3024 psf
3312 psf
5040 psf
5040 psf
Principal Stress Ratio
3.5
3.0
2.5
2.0
1.5
1.0
0.00
0.05
0.10
0.15
0.20
0.25
0.30
Strain

Oak Harbor - Compacted - Allowed to Swell

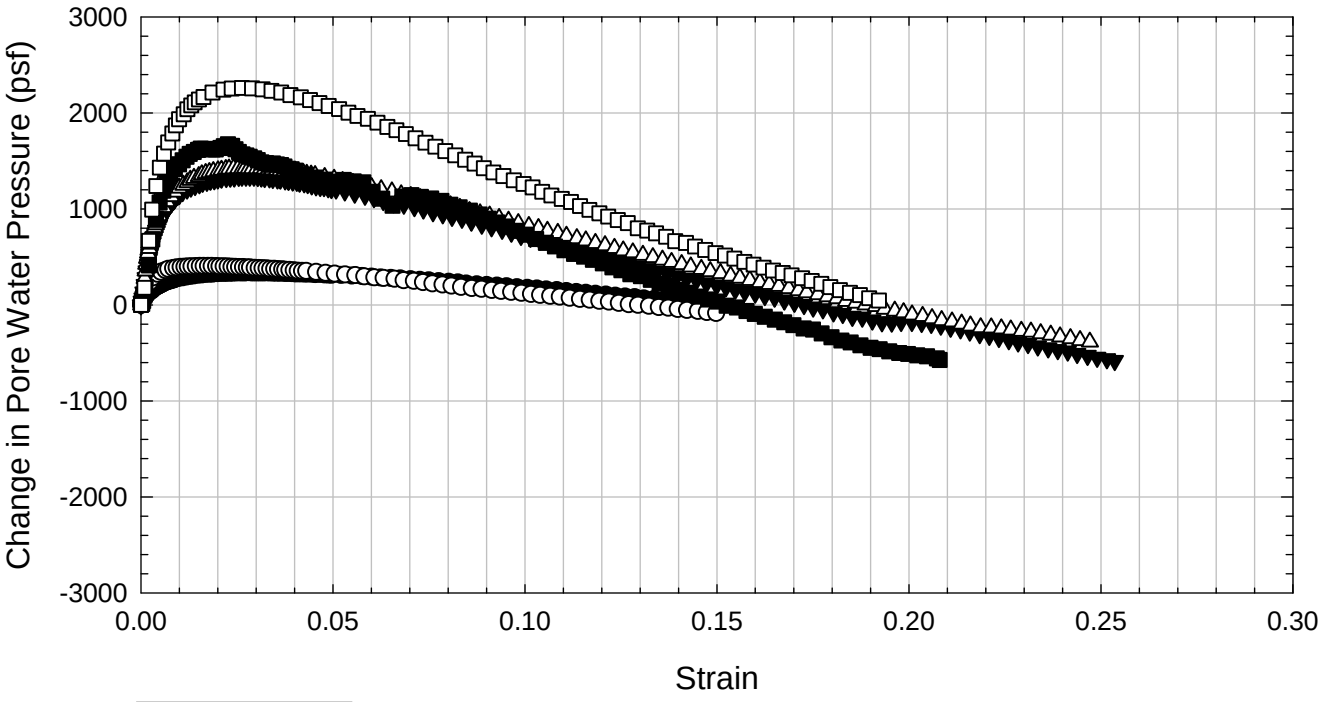

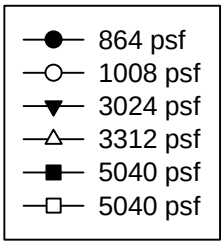

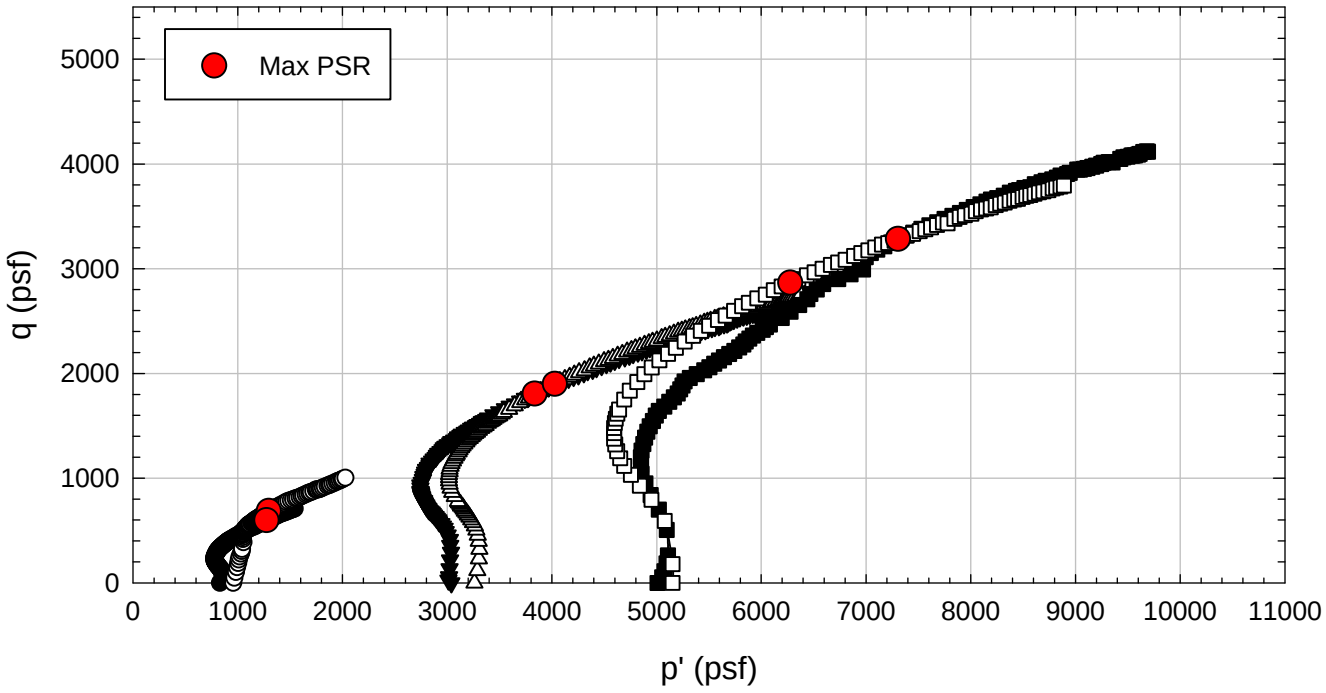

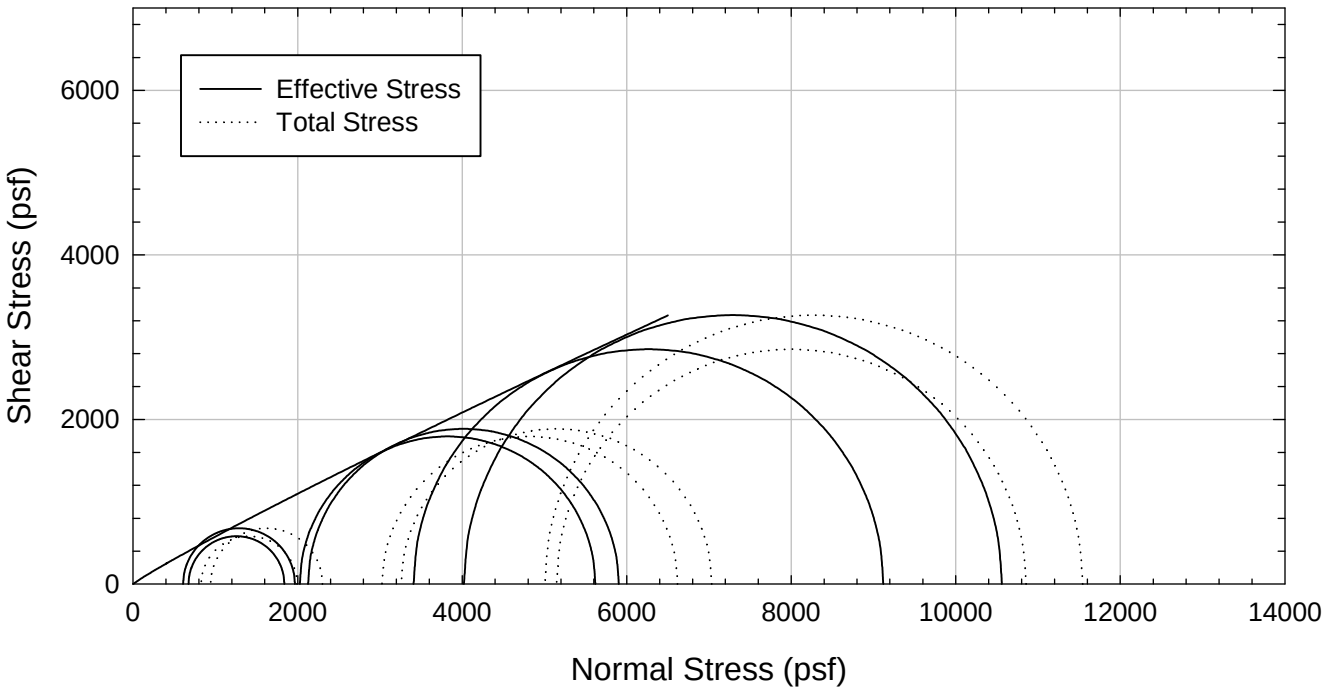
Oak Harbor - Compacted - Allowed to Swell
Effective Stress
Total Stress
Shear Stress (psf)
Normal Stress (psf)
0
2000
4000
6000
8000
10000
12000
14000

Virginia Polytechnic Institute and State University
Geotechnical Engineering Laboratory
Triaxial Data Sheet

Project:	Fully Softened Shear Strength
Sample I.D./Loc.:	Oak Harbor - Compacted - Allowed to Swell - Consolidated Undrained
Classification:	Lean Clay (CL)

Sample Preparation	Compacted
Specimen Saturation Method	Wet

Specific Gravity	2.82	
Method for Dimensions After Consol.	Method B	

Test Number	1	2	3	4	5	6	7	8
Start Date (m/d/y)	11/5/2012	1/5/2012	10/29/2012	10/29/2012	10/17/2012	10/22/2012		
End Date (m/d/y)	11/11/2012	11/11/2012	11/5/2012	11/4/2012	10/27/2012	10/29/2012		
Backpressure (psf)	13673	11894	12211	11622	9068	9468		
Consolidation Pressure (psf)	1008	2016	3024	4032	5040	7200		
B value	1.00	1.00	0.97	0.99	0.98	0.98		
Initial Values								
Initial Height (in.)	2.795	2.794	2.792	2.795	2.790	2.792		
Initial Diameter (in.)	1.315	1.316	1.313	1.312	1.312	1.313		
Initial Sample Weight (g.)	125.49	125.22	125.40	126.39	127.46	127.13		
Water Content (%)	18.60	18.80	18.90	19.30	19.60	19.80		
Dry Unit Weight (pcf)	106.1	105.7	106.2	106.8	107.7	107.0		
Wet Unit Weight (pcf)	125.8	125.6	126.3	127.4	128.8	128.2		
Saturation (%)	79.7	79.5	81.2	83.9	87.0	86.5		
Void Ratio	0.66	0.67	0.66	0.65	0.63	0.65		
After Swelling and Consolidation								
t_{100} Using Casagrande Method (min)	180	400	550	500	550	650		
Volumetric Strain (%)	-5.05	-3.37	-1.88	-1.21	-0.39	1.75		
Height After Consolidation (in.)	2.748	2.763	2.774	2.784	2.786	2.808		
Area After Consolidation (in.)	1.452	1.422	1.389	1.374	1.358	1.322		
Final Values								
Water Content (%)	26.40	25.60	24.40	23.70	22.80	21.90		
Dry Unit Weight (pcf)	101.0	102.3	104.3	105.5	107.3	108.9		
Wet Unit Weight (pcf)	127.7	128.5	129.7	130.5	131.8	132.7		
Saturation (%)	100.0	100.0	100.0	100.0	100.0	100.0		
Void Ratio	0.74	0.72	0.69	0.67	0.64	0.62		
Failure								
Failure Criteria	Max PSR	Max PSR	Max PSR	Max PSR	Max PSR	Max PSR		
Deviator Stress at failure (psf)	1334	2397	3668	4390	5531	9003		
Principal Stress Ratio at failure	3.46	3.04	2.79	2.71	2.66	2.68		
Minor Principal Effective Stress at fail. (psf)	549	1185	2065	2575	3340	5359		
Major Principal Effective Stress at fail. (psf)	1902	3609	5762	6990	8892	14380		
Corrections Applied	Membrane	Membrane	Membrane	Membrane	Membrane	Membrane		
Axial Strain at failure (%)	5.9	8.0	8.6	7.4	6.5	5.1		
Test performed at strain rate (%/hr)	0.36	0.49	0.36	0.49	0.36	0.49		

Comments: Volumetric strain is positive for compression and negative for swelling.

Oak Harbor - Compacted - Allowed to Swell

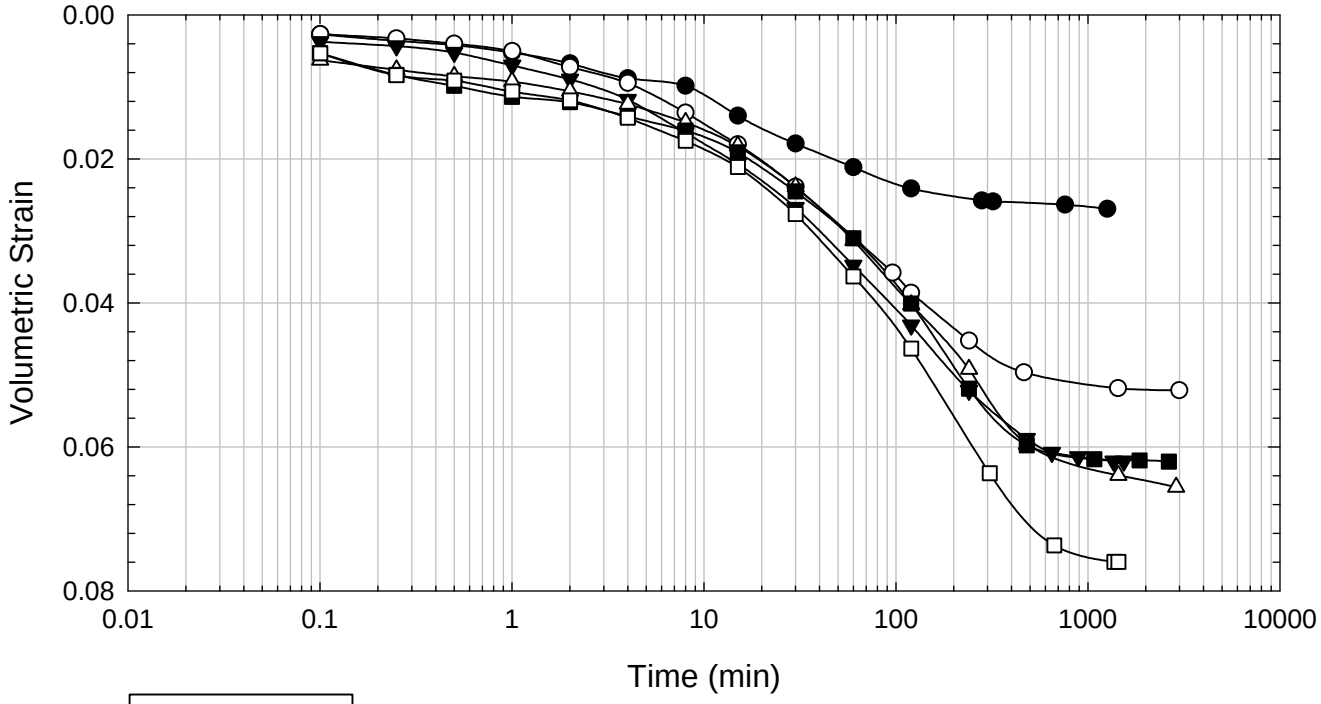

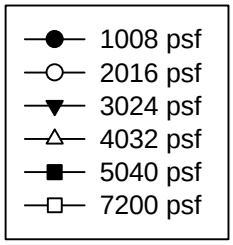

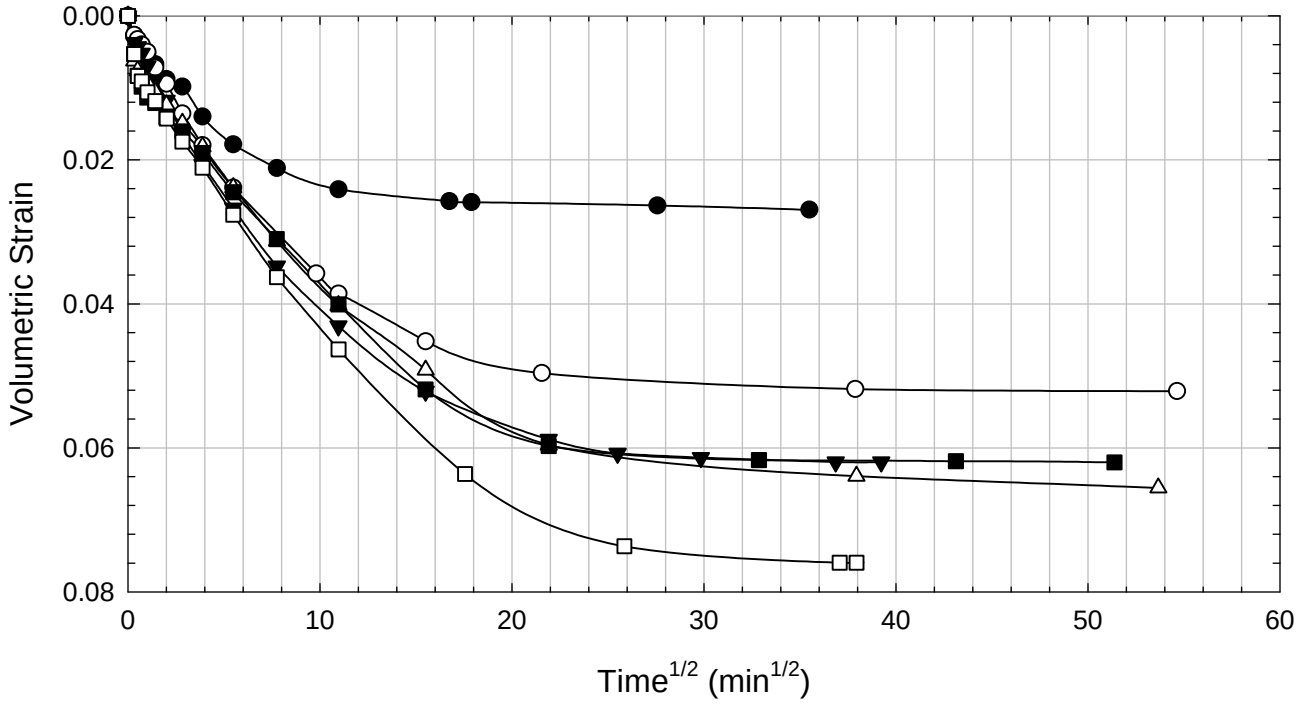

Oak Harbor - Compacted - Allowed to Swell

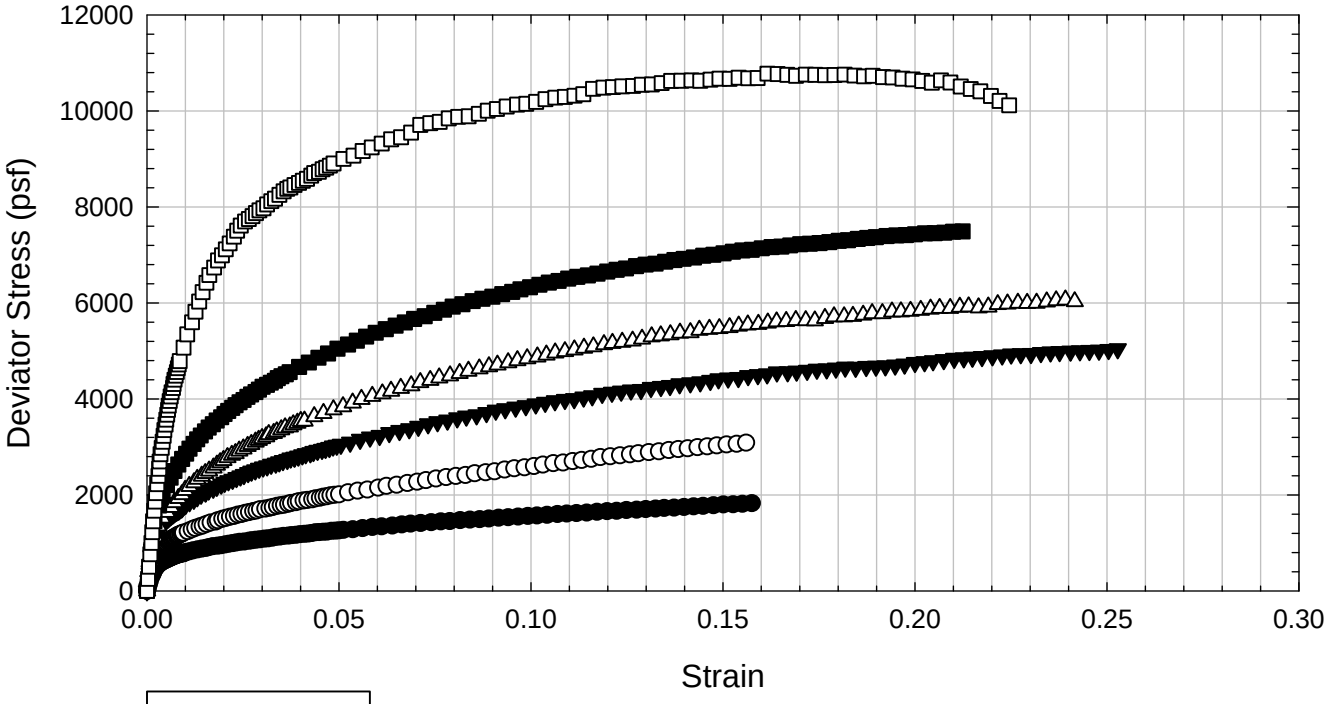

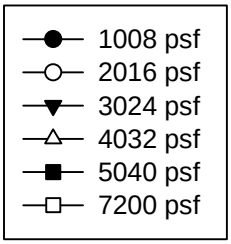

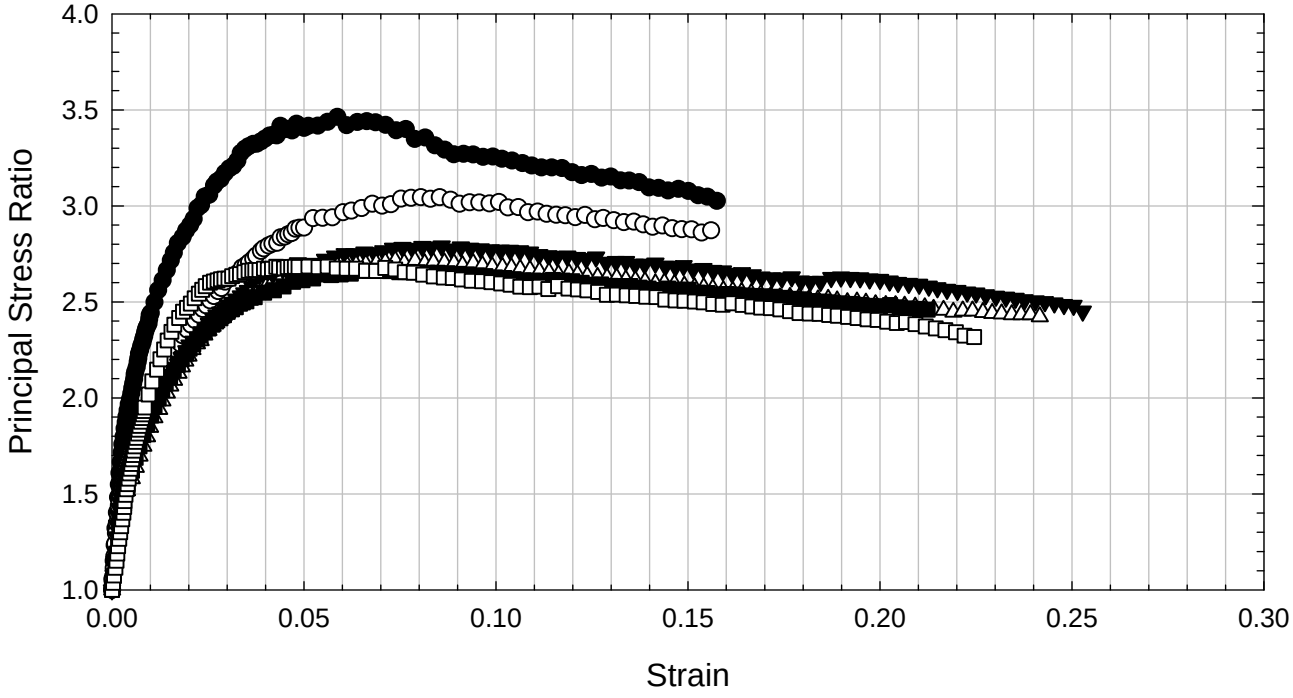

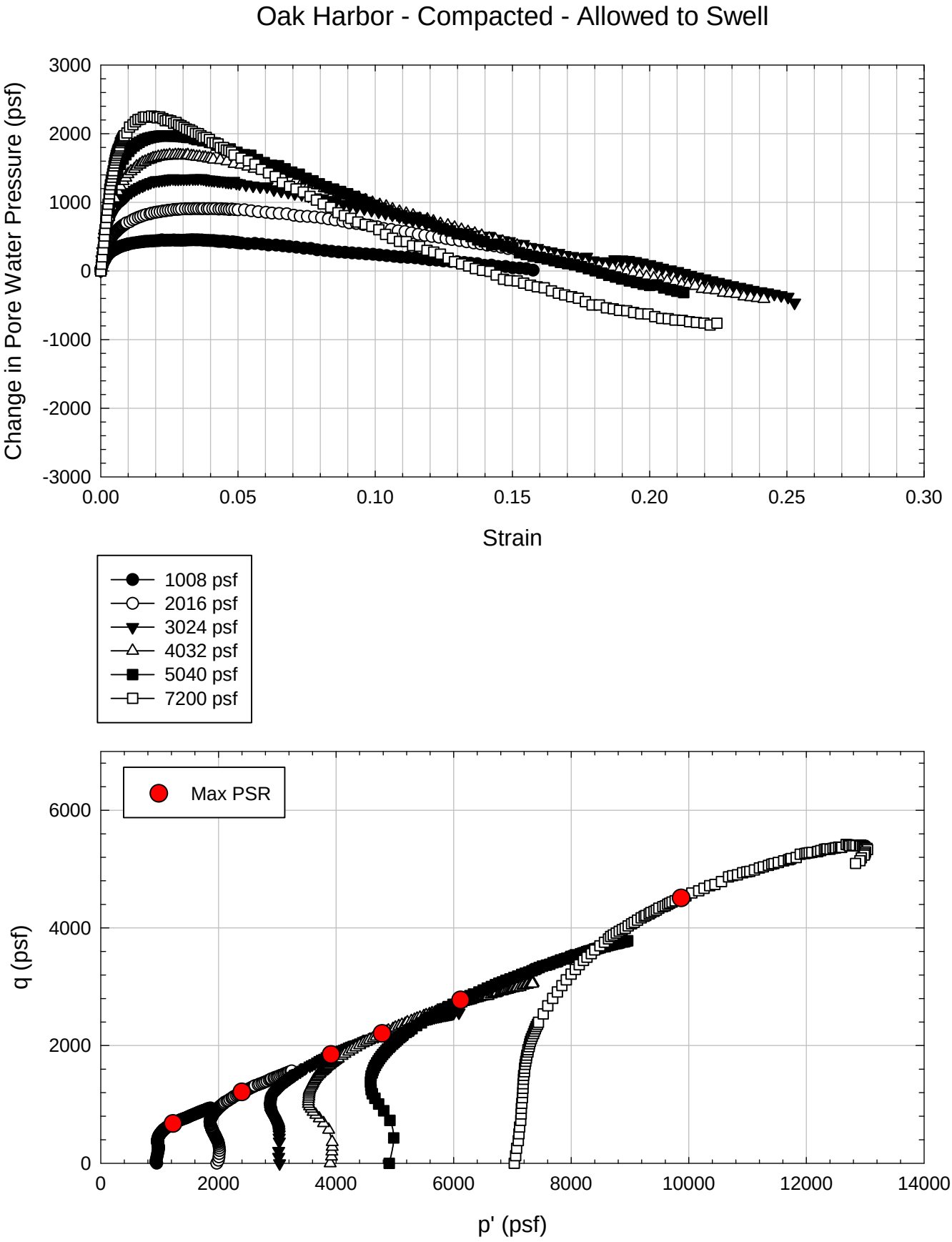
Oak Harbor - Compacted - Allowed to Swell
Change in Pore Water Pressure (psf)
3000
2000
1000
0
-1000
-2000
-3000
0.00
0.05
0.10
0.15
0.20
0.25
0.30
Strain
1008 psf
2016 psf
3024 psf
4032 psf
5040 psf
7200 psf
Max PSR
q (psf)
6000
4000
2000
0
0
2000
4000
6000
8000
10000
12000
14000
p' (psf)

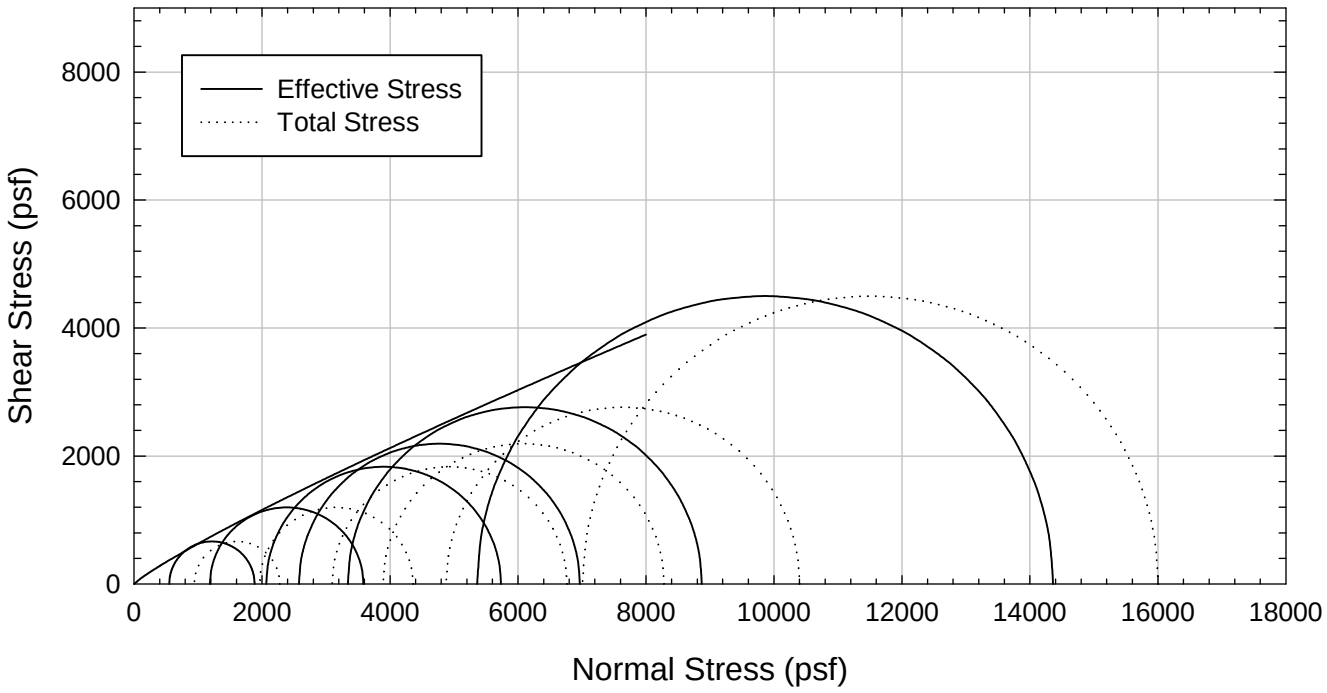
Oak Harbor - Compacted - Allowed to Swell
Effective Stress
Total Stress
Shear Stress (psf)
Normal Stress (psf)
0
2000
4000
6000
8000
10000
12000
14000
16000
18000

Virginia Polytechnic Institute and State University
Geotechnical Engineering Laboratory
Triaxial Data Sheet

Project:	Fully Softened Shear Strength
Sample I.D./Loc.:	Oak Harbor - Compacted - Allowed to Swell - Consolidated Undrained
Classification:	Lean Clay (CL)

Sample Preparation	Compacted
Specimen Saturation Method	Wet

Specific Gravity	2.82	
Method for Dimensions After Consol.	Method B	

Test Number	1	2	3	4	5	6	7	8
Start Date (m/d/y)	11/5/2012	11/4/2012	10/22/2012	10/29/2012	10/29/2012	10/22/2012		
End Date (m/d/y)	11/11/2012	11/11/2012	10/28/2012	11/4/2012	11/5/2012	10/28/2012		
Backpressure (psf)	12552	9232	10570	15237	8669	8748		
Consolidation Pressure (psf)	1872	2016	3600	4032	7200	7488		
B value	1.00	0.98	0.97	0.99	1.00	0.97		
Initial Values								
Initial Height (in.)	2.79	2.795	2.792	2.792	2.793	2.785		
Initial Diameter (in.)	1.31	1.315	1.311	1.311	1.312	1.313		
Initial Sample Weight (g.)	126.45	124.58	125.88	125.88	126.08	126.21		
Water Content (%)	19.40	18.30	19.40	19.40	19.40	19.70		
Dry Unit Weight (pcf)	106.5	105.8	106.7	106.7	106.5	106.6		
Wet Unit Weight (pcf)	127.2	125.2	127.4	127.4	127.2	127.6		
Saturation (%)	83.6	77.5	83.9	83.9	83.8	85.0		
Void Ratio	0.65	0.66	0.65	0.65	0.65	0.65		
After Swelling and Consolidation								
t_{100} Using Casagrande Method (min)	200	250	500	700	600	470		
Volumetric Strain (%)	-4.58	-3.39	-1.38	-0.59	1.76	1.47		
Height After Consolidation (in.)	2.750	2.763	2.780	2.786	2.809	2.799		
Area After Consolidation (in.)	1.441	1.420	1.377	1.360	1.320	1.328		
Final Values								
Water Content (%)	25.90	25.60	24.00	23.40	22.10	22.30		
Dry Unit Weight (pcf)	101.80	102.3	105.0	106.00	108.4	108.10		
Wet Unit Weight (pcf)	128.2	128.5	130.2	130.8	132.4	132.2		
Saturation (%)	100.0	100.0	100.0	100.0	100.0	100.0		
Void Ratio	0.73	0.72	0.68	0.66	0.63	0.63		
Failure								
Failure Criteria	Max PSR	Max PSR	Max PSR	Max PSR	Max PSR	Max PSR		
Deviator Stress at failure (psf)	2443	2389	4826	4876	7583	7969		
Principal Stress Ratio at failure	2.86	2.94	2.73	2.78	2.63	2.59		
Minor Principal Effective Stress at fail. (psf)	1328	1246	2807	2759	4673	5020		
Major Principal Effective Stress at fail. (psf)	3798	3663	7655	7660	12285	13018		
Corrections Applied	Membrane	Membrane	Membrane	Membrane	Membrane	Membrane		
Axial Strain at failure (%)	8.5	8.5	6.5	7.5	8.5	8.6		
Test performed at strain rate (%/hr)	0.50	0.39	0.39	0.50	0.39	0.50		

Comments: Volumetric strain is positive for compression and negative for swelling

Oak Harbor - Compacted - Allowed to Swell

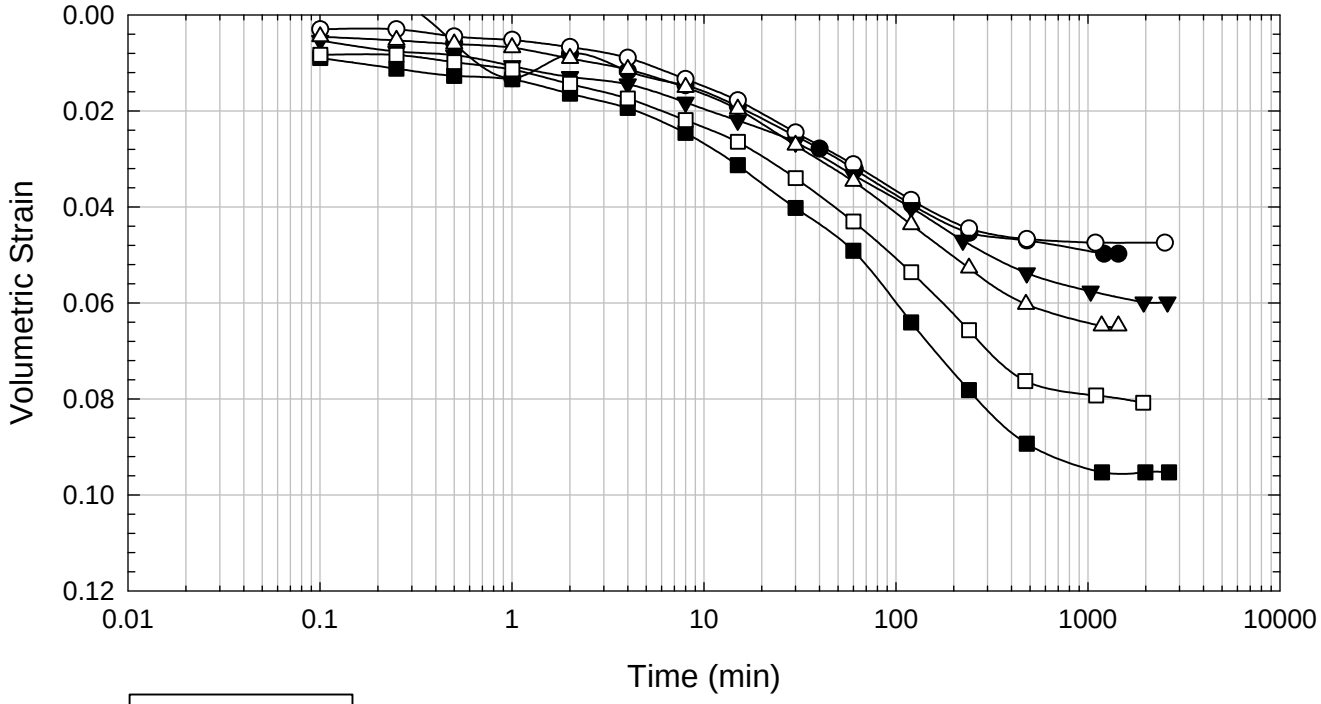

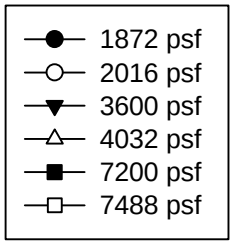

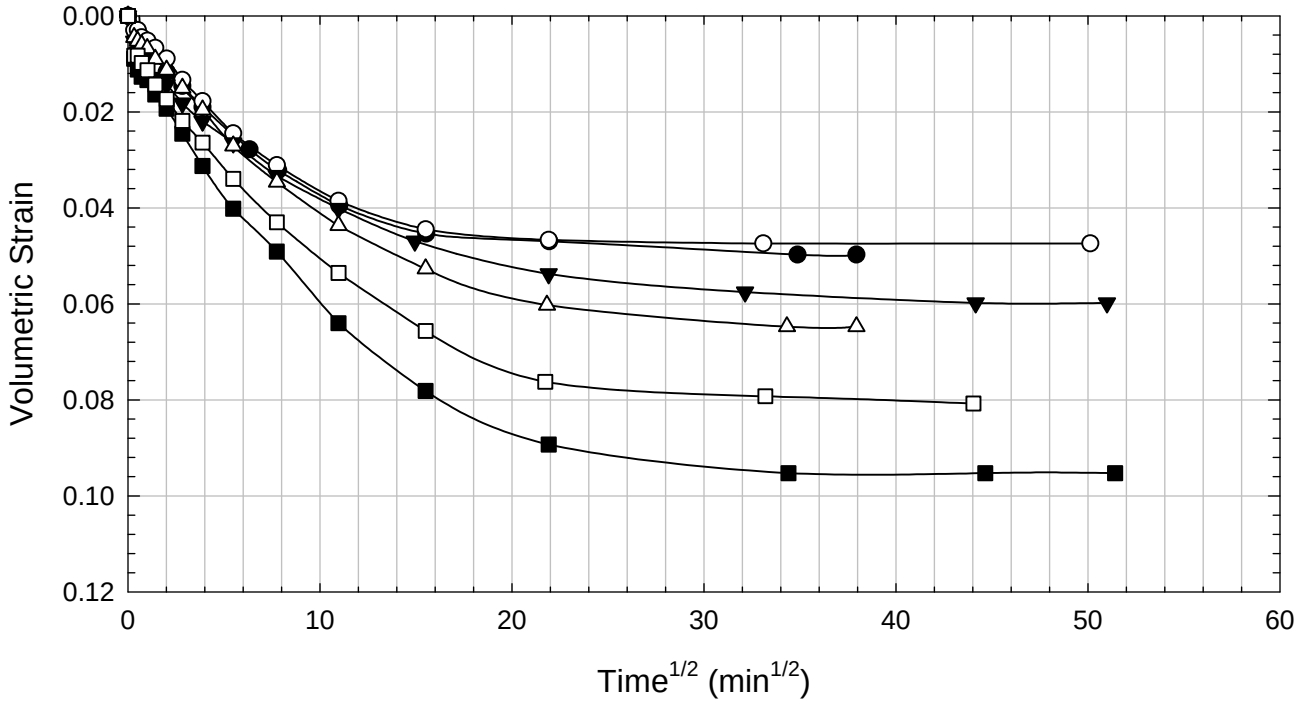

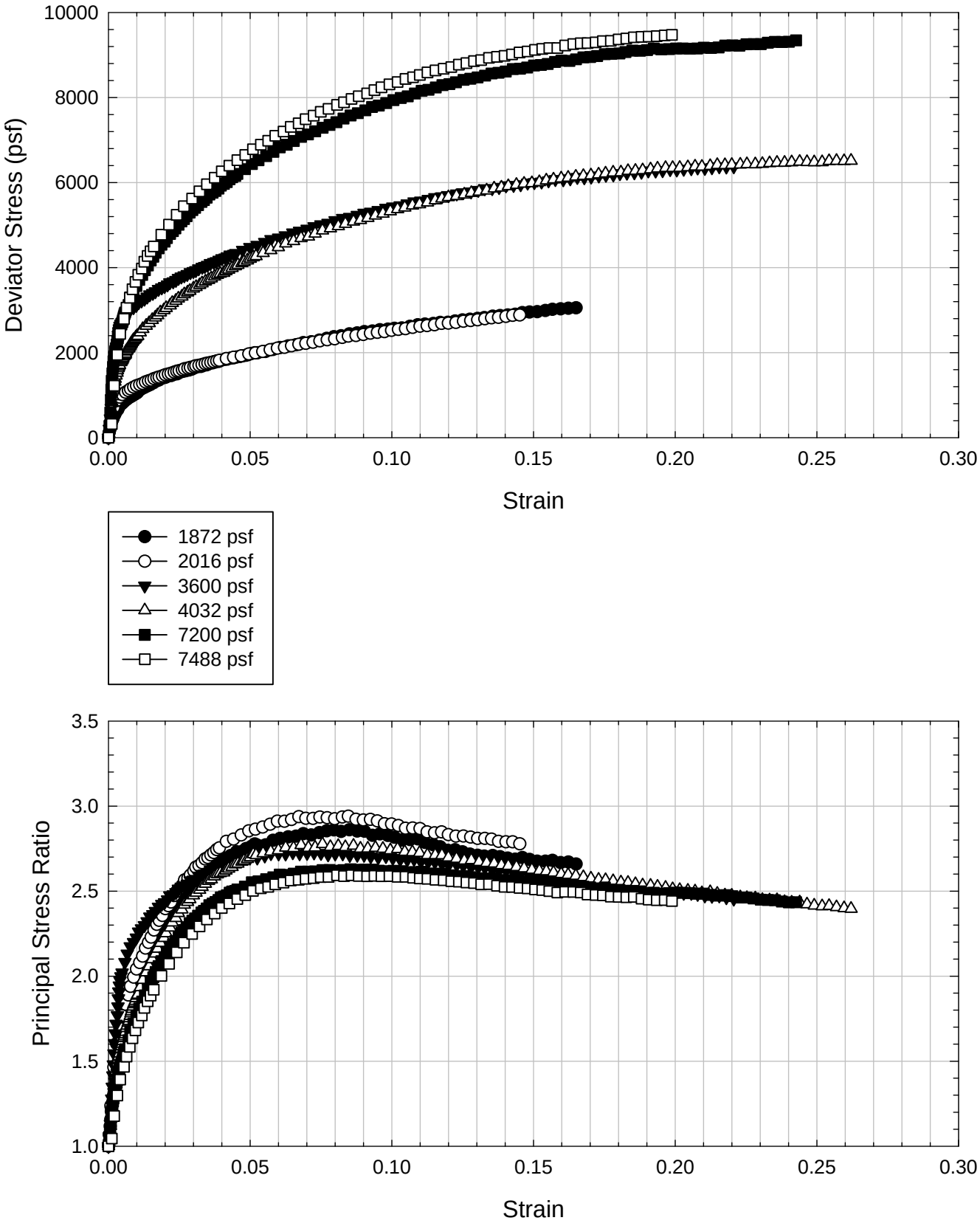
Oak Harbor - Compacted - Allowed to Swell
Deviator Stress (psf)
10000
8000
6000
4000
2000
0
0.00
0.05
0.10
0.15
0.20
0.25
0.30
Strain
1872 psf
2016 psf
3600 psf
4032 psf
7200 psf
7488 psf
Principal Stress Ratio
3.5
3.0
2.5
2.0
1.5
1.0
0.00
0.05
0.10
0.15
0.20
0.25
0.30
Strain

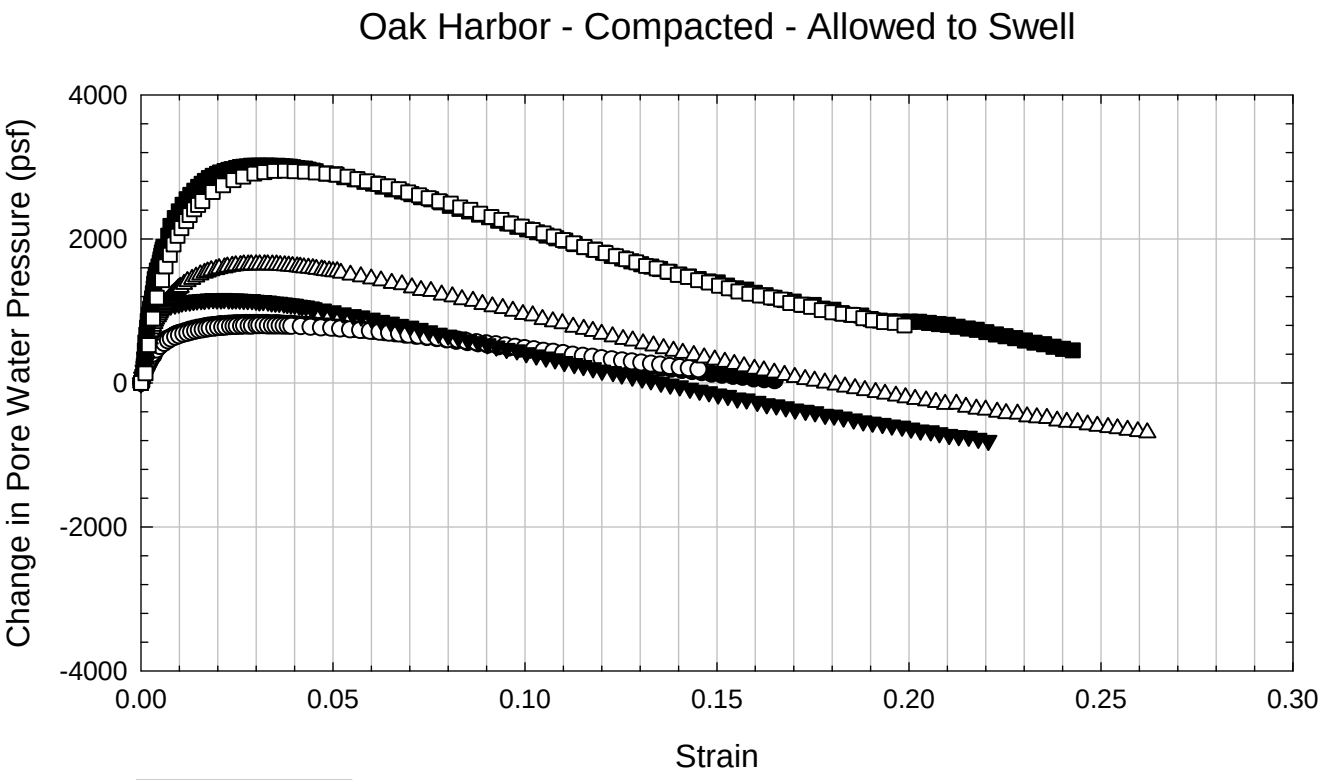
Oak Harbor - Compacted - Allowed to Swell
Change in Pore Water Pressure (psf)
4000
2000
0
-2000
-4000
0.00
0.05
0.10
0.15
0.20
0.25
0.30
Strain

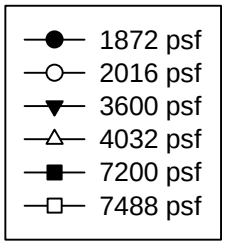
1872 psf
2016 psf
3600 psf
4032 psf
7200 psf
7488 psf

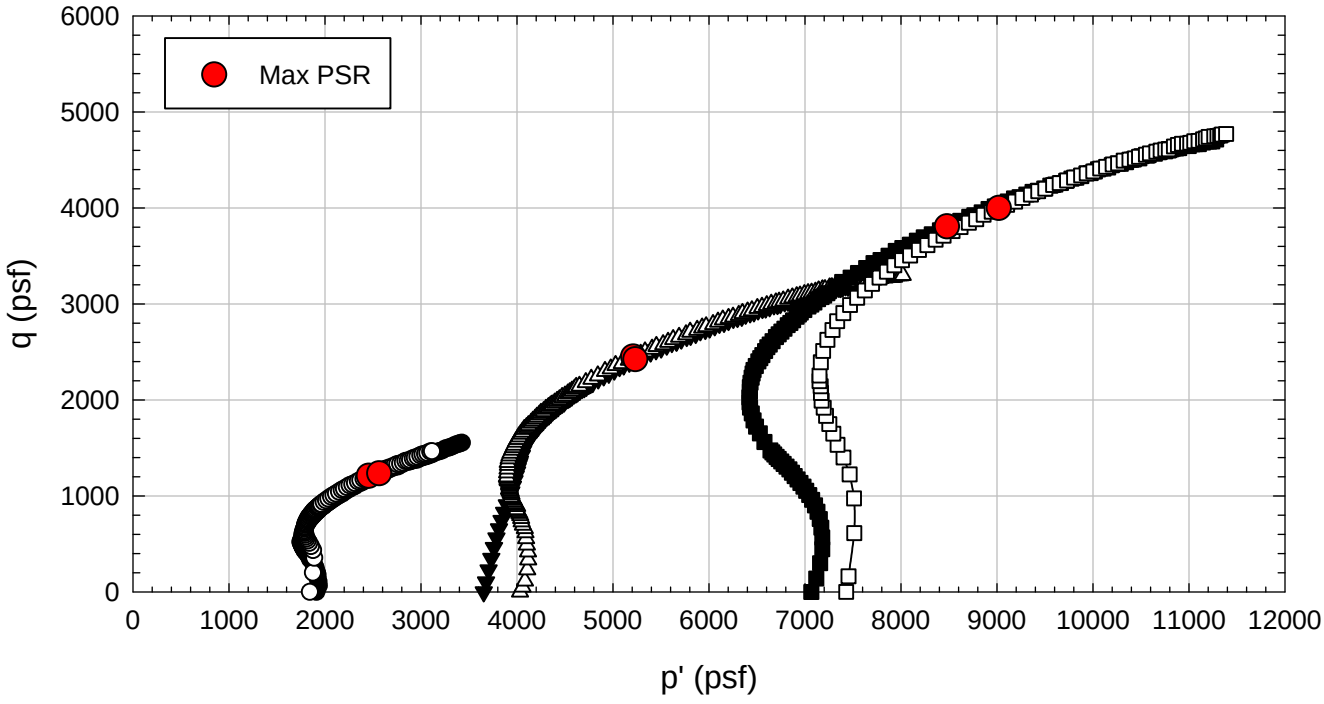
Max PSR
q (psf)
6000
5000
4000
3000
2000
1000
0
0
1000
2000
3000
4000
5000
6000
7000
8000
9000
10000
11000
12000
p' (psf)

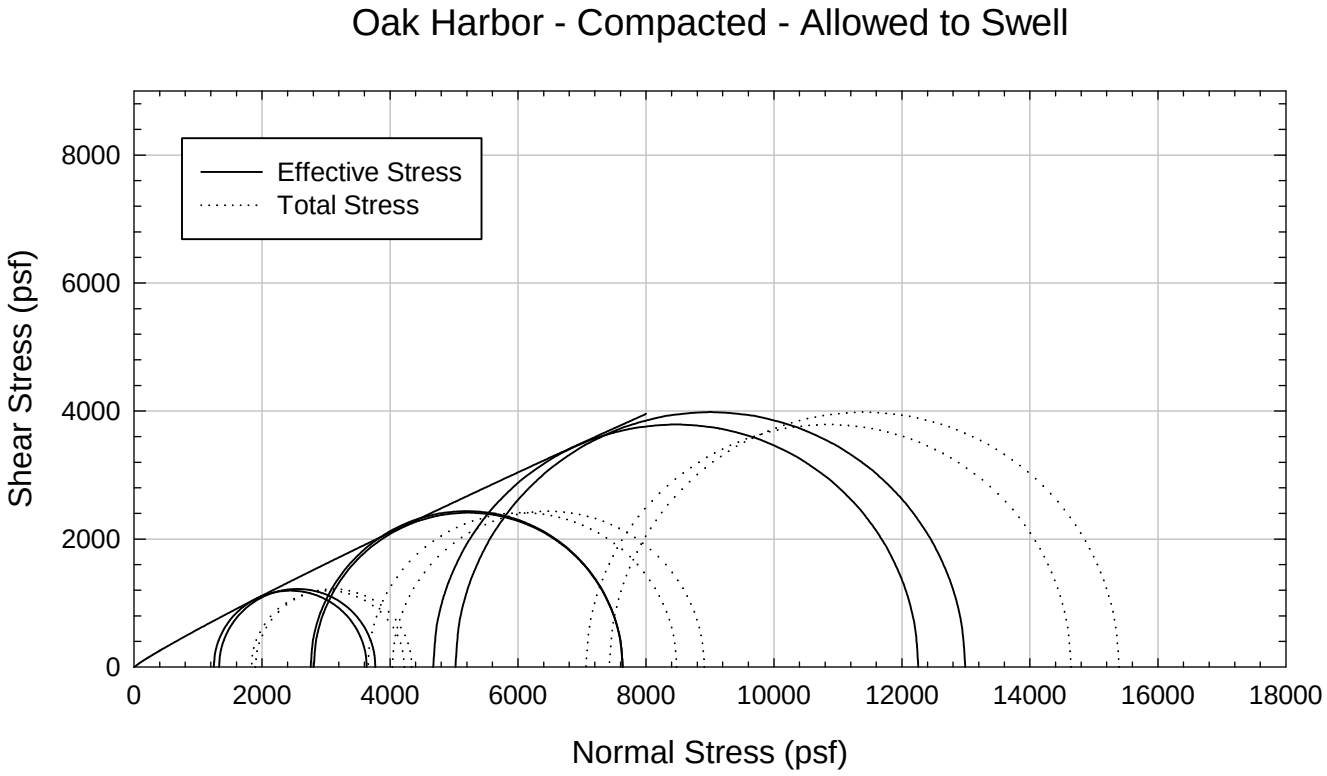
Oak Harbor - Compacted - Allowed to Swell
Effective Stress
Total Stress
Shear Stress (psf)
Normal Stress (psf)
0
2000
4000
6000
8000
10000
12000
14000
16000
18000

G.1.2 ACU Triaxials

Virginia Polytechnic Institute and State University
Geotechnical Engineering Laboratory
Triaxial Data Sheet

Project:	Fully Softened Shear Strength
Sample I.D./Loc.:	Oak Harbor - Compacted - Allowed to Swell - Anisotropically Consolidated Undrained
Classification:	Lean Clay (CL)

Sample Preparation	Compacted
Specimen Saturation Method	Wet

Specific Gravity	2.82	
Method for Dimensions After Consol.	Method B	

Test Number	1	2	3	4				
Start Date (m/d/y)	8/29/2012	8/20/2012	8/29/2012	8/29/2012				
End Date (m/d/y)	9/6/2012	8/27/2012	9/6/2012	9/6/2012				
Backpressure (psf)	12902	12960	12931	12931				
Major Effective Consolidation Pressure (psf)	950	2036	4005	8333				
Consolidation stress ratio ($\sigma'_{1c}/\sigma'_{3c}$)	1.34	1.95	2.06	1.91				
B value	1.00	1.00	0.99	0.99				
Initial Values								
Initial Height (in.)	2.782	2.783	2.782	2.783				
Initial Diameter (in.)	1.316	1.313	1.316	1.315				
Initial Sample Weight (g.)	129.27	122.17	128.01	128.24				
Water Content (%)	19.5	18.0	19.9	16.4				
Dry Unit Weight (pcf)	109.0	104.6	107.4	111.1				
Wet Unit Weight (pcf)	130.3	123.4	128.8	129.3				
Saturation (%)	89.1	74.3	88.9	79.1				
Void Ratio	0.62	0.68	0.63	0.59				
After Swelling and Consolidation								
t_{100} Using Casagrande Method (min)	---	250	---	---				
Volumetric Strain (Initial to Final) (%)	-4.72	-4.27	-2.06	-0.65				
Height After Consolidation (in.)	2.827	2.755	2.625	2.533				
Area After Consolidation (in.)	1.401	1.427	1.472	1.501				
Final Values								
Water Content (%)	24.50	26.77	23.59	21.12				
Dry Unit Weight (pcf)	104.1	100.4	105.3	110.4				
Wet Unit Weight (pcf)	129.6	127.3	130.1	133.7				
Saturation (%)	100.0	100.0	100.0	100.0				
Void Ratio	0.69	0.76	0.66	0.60				
Failure								
Failure Criteria	Max PSR	Max PSR	Max PSR	Max PSR				
Deviator Stress at failure (psf)	1472	1600	3121	7092				
Principal Stress Ratio at failure	3.59	2.96	2.87	2.69				
Minor Principal Effective Stress at fail. (psf)	567	817	1665	4196				
Major Principal Effective Stress at fail. (psf)	2040	2417	4786	11288				
Corrections Applied	Membrane	Membrane	Membrane	Membrane				
Axial Strain at failure (%)	3.3	8.6	3.5	8.5				
Test performed at strain rate (%/hr)	0.25	0.25	0.25	0.25				

Comments: Volumetric strain is positve for compression and negative for swelling.

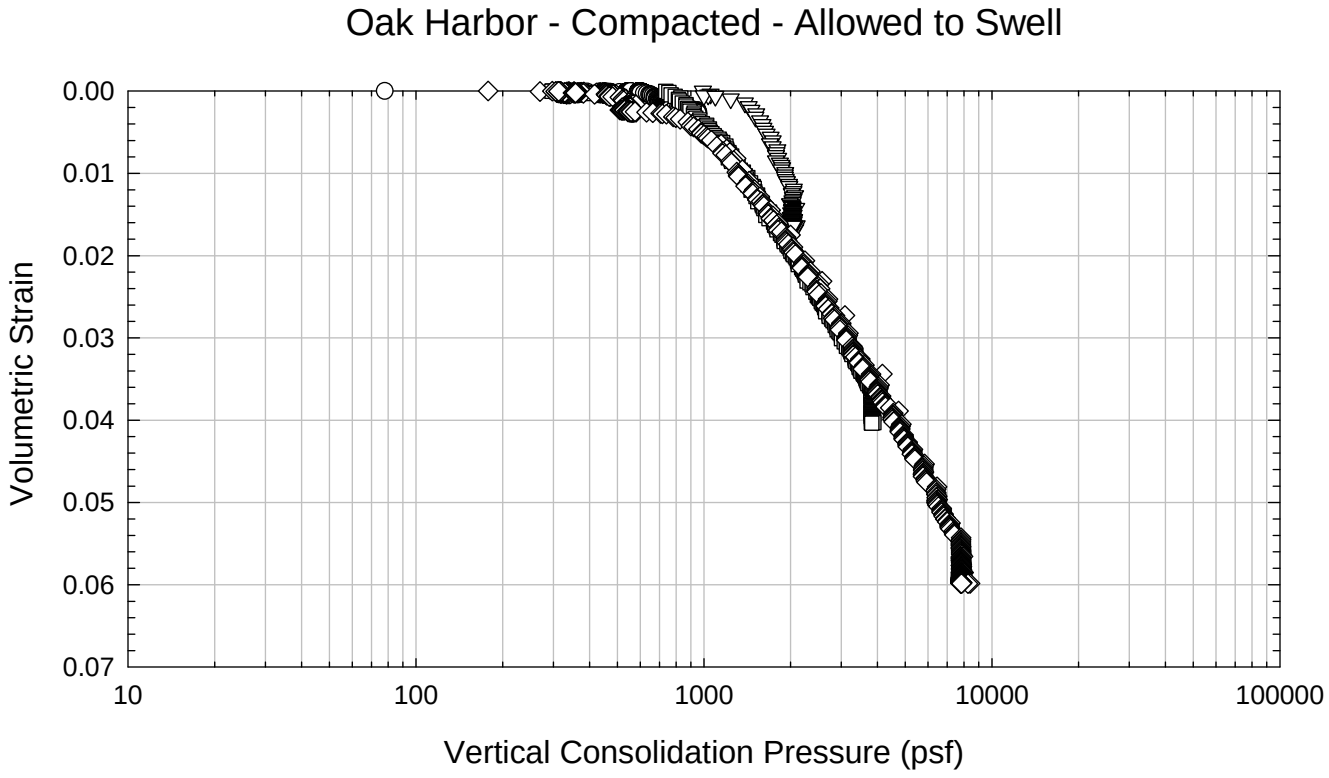
Oak Harbor - Compacted - Allowed to Swell
Volumetric Strain
0.00
0.01
0.02
0.03
0.04
0.05
0.06
0.07
10
100
1000
10000
100000
Vertical Consolidation Pressure (psf)

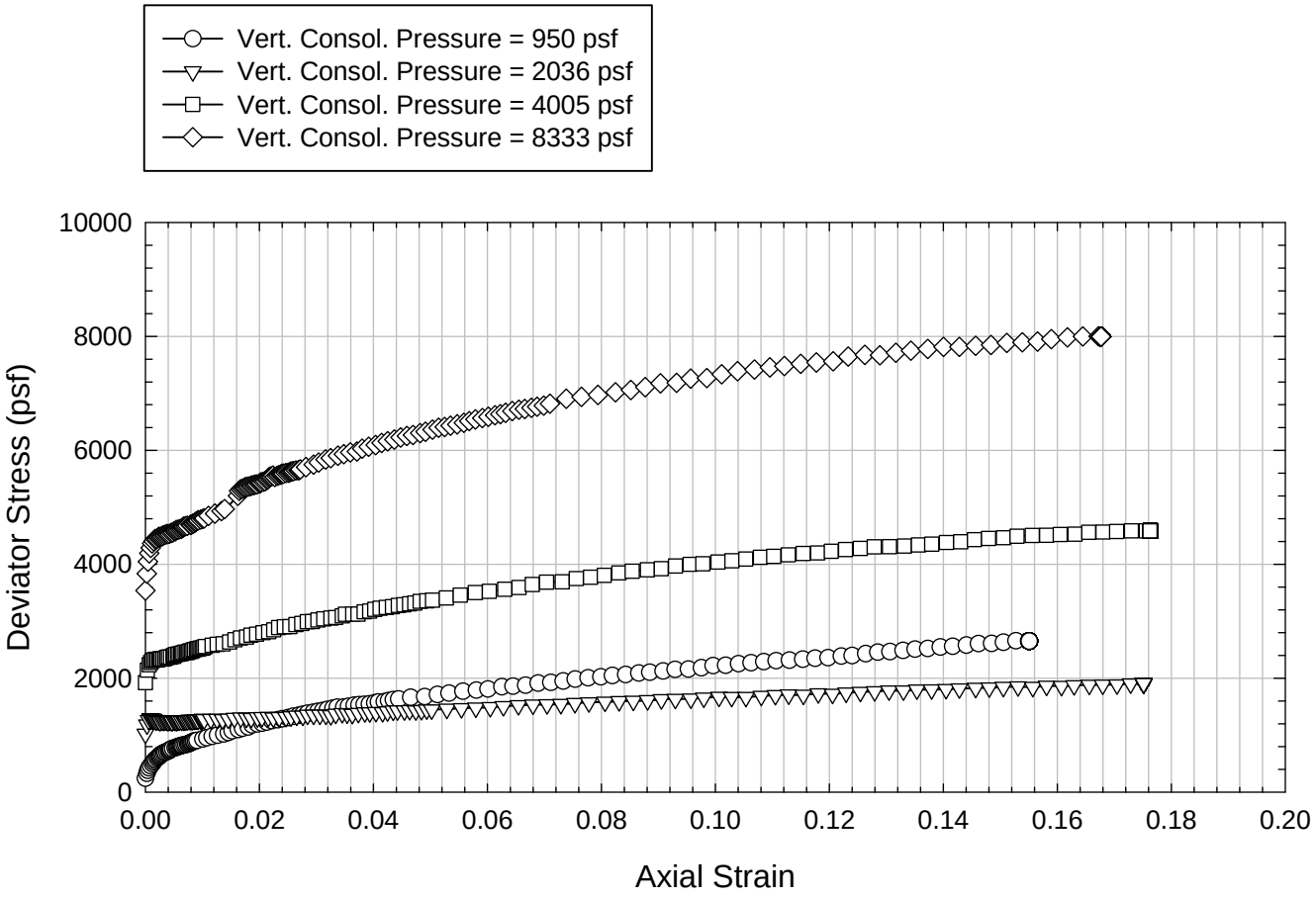
Vert. Consol. Pressure = 950 psf
Vert. Consol. Pressure = 2036 psf
Vert. Consol. Pressure = 4005 psf
Vert. Consol. Pressure = 8333 psf
Deviator Stress (psf)
10000
8000
6000
4000
2000
0
0.00
0.02
0.04
0.06
0.08
0.10
0.12
0.14
0.16
0.18
0.20
Axial Strain

Oak Harbor - Compacted - Allowed to Swell

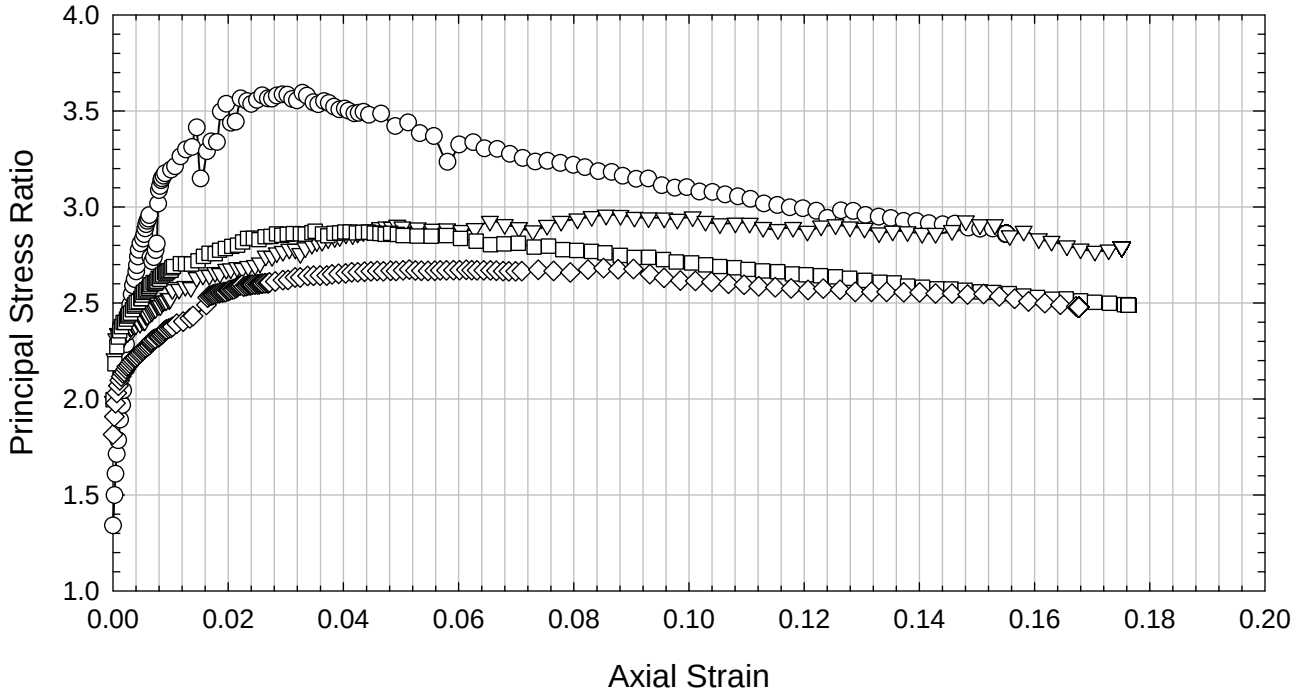

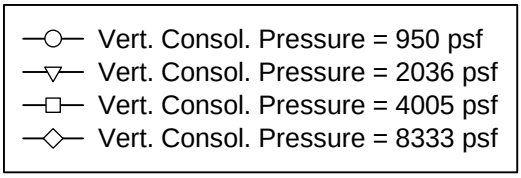

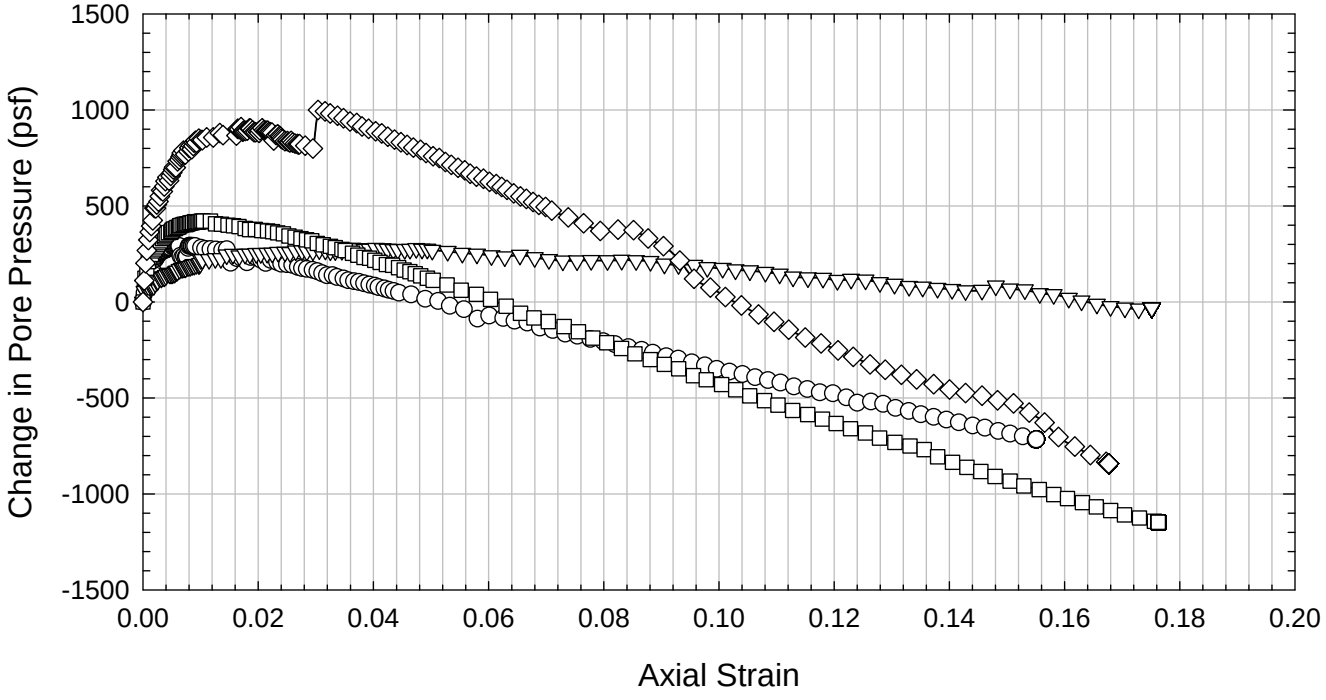

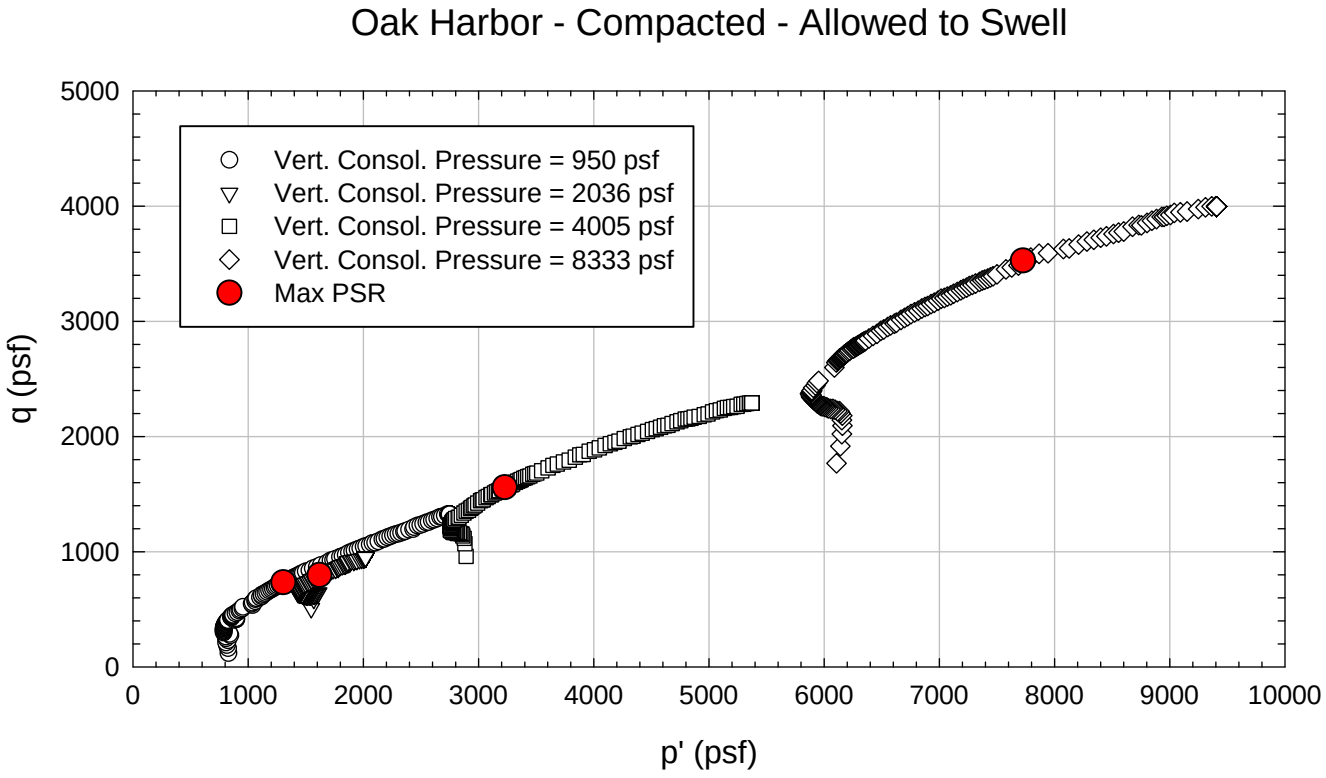
Oak Harbor - Compacted - Allowed to Swell
Vert. Consol. Pressure = 950 psf
Vert. Consol. Pressure = 2036 psf
Vert. Consol. Pressure = 4005 psf
Vert. Consol. Pressure = 8333 psf
Max PSR
q (psf)
p' (psf)
0
1000
2000
3000
4000
5000
6000
7000
8000
9000
10000

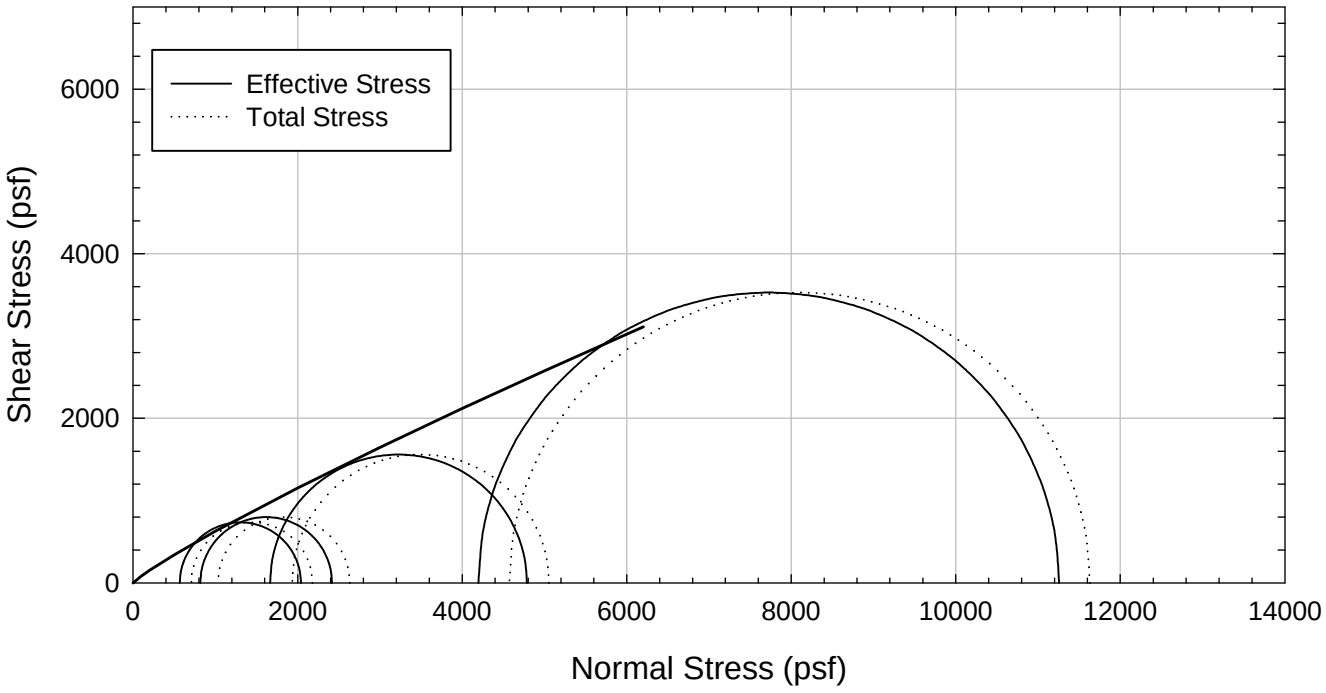
Effective Stress
Total Stress
Shear Stress (psf)
Normal Stress (psf)
0
2000
4000
6000
8000
10000
12000
14000

Virginia Polytechnic Institute and State University
Geotechnical Engineering Laboratory
Triaxial Data Sheet

Project:	Fully Softened Shear Strength
Sample I.D./Loc.:	Oak Harbor - Compacted - Allowed to Swell - Anisotropically Consolidated Undrained
Classification:	Lean Clay (CL)

Sample Preparation	Compacted
Specimen Saturation Method	Wet

Specific Gravity	2.82	
Method for Dimensions After Consol.	Method B	

Test Number	1	2	3	4	5	6	7	8
Start Date (m/d/y)	11/14/2012	11/12/2012	10/17/2012	11/12/2012	11/7/2012	10/31/2012		
End Date (m/d/y)	11/19/2012	11/17/2012	10/26/2012	11/16/2012	11/14/2012	11/8/2012		
Backpressure (psf)	12960	12960	10080	11520	12082	10080		
Major Effective Consolidation Pressure (psf)	876	1008	2267	2801	4036	7517		
Consolidation stress ratio ($\sigma'_{1c}/\sigma'_{3c}$)	1.93	2.05	2.09	1.77	1.79	2.03		
B value	0.97	0.95	0.95	0.95	> 0.90	0.97		
Initial Values								
Initial Height (in.)	2.796	2.801	2.80	2.795	2.792	2.791		
Initial Diameter (in.)	1.311	1.312	1.31	1.313	1.315	1.314		
Initial Sample Weight (g.)	128.85	129.45	126.89	128.62	125.67	125.36		
Water Content (%)	19.6	19.9	19.50	19.8	18.5	19.10		
Dry Unit Weight (pcf)	108.7	108.6	107.2	108.0	106.5	105.9		
Wet Unit Weight (pcf)	130.0	130.2	128.1	129.4	126.2	126.1		
Saturation (%)	89.2	90.2	86.5	88.8	80.0	81.3		
Void Ratio	0.62	0.62	0.63	0.63	0.65	0.66		
After Swelling and Consolidation								
t_{100} Using Casagrande Method (min)	---	---	---	---	---	---		
Volumetric Strain (Initial to Final) (%)	-5.69	-4.85	-4.69	-2.70	-2.65	0.32		
Height After Consolidation (in.)	2.650	2.851	2.793	2.751	2.525	2.636		
Area After Consolidation (in.)	1.506	1.393	1.415	1.413	1.542	1.432		
Final Values								
Water Content (%)	25.30	24.80	25.30	23.90	24.70	23.30		
Dry Unit Weight (pcf)	102.8	103.6	102.40	105.1	103.8	106.2		
Wet Unit Weight (pcf)	128.8	129.3	128.3	130.2	129.4	130.9		
Saturation (%)	100.0	100.0	100.0	100.0	100.0	100.0		
Void Ratio	0.71	0.70	0.71	0.68	0.70	0.66		
Failure								
Failure Criteria	Max PSR	Max PSR	Max PSR	Max PSR	Max PSR	Max PSR		
Deviator Stress at failure (psf)	1152	1189	2015	2872	3226	5274		
Principal Stress Ratio at failure	5.01	4.89	3.43	3.12	2.75	2.46		
Minor Principal Effective Stress at fail. (psf)	287	306	830	1352	1838	3618		
Major Principal Effective Stress at fail. (psf)	1439	1495	2845	4224	5064	8892		
Corrections Applied	Membrane	Membrane	Membrane	Membrane	Membrane	Membrane		
Axial Strain at failure (%)	2.0	1.4	1.9	2.7	6.7	6.8		
Test performed at strain rate (%/hr)	0.25	0.25	0.25	0.25	0.25	0.25		

Comments: Volumetric strain is positive for compression and negative for swelling.

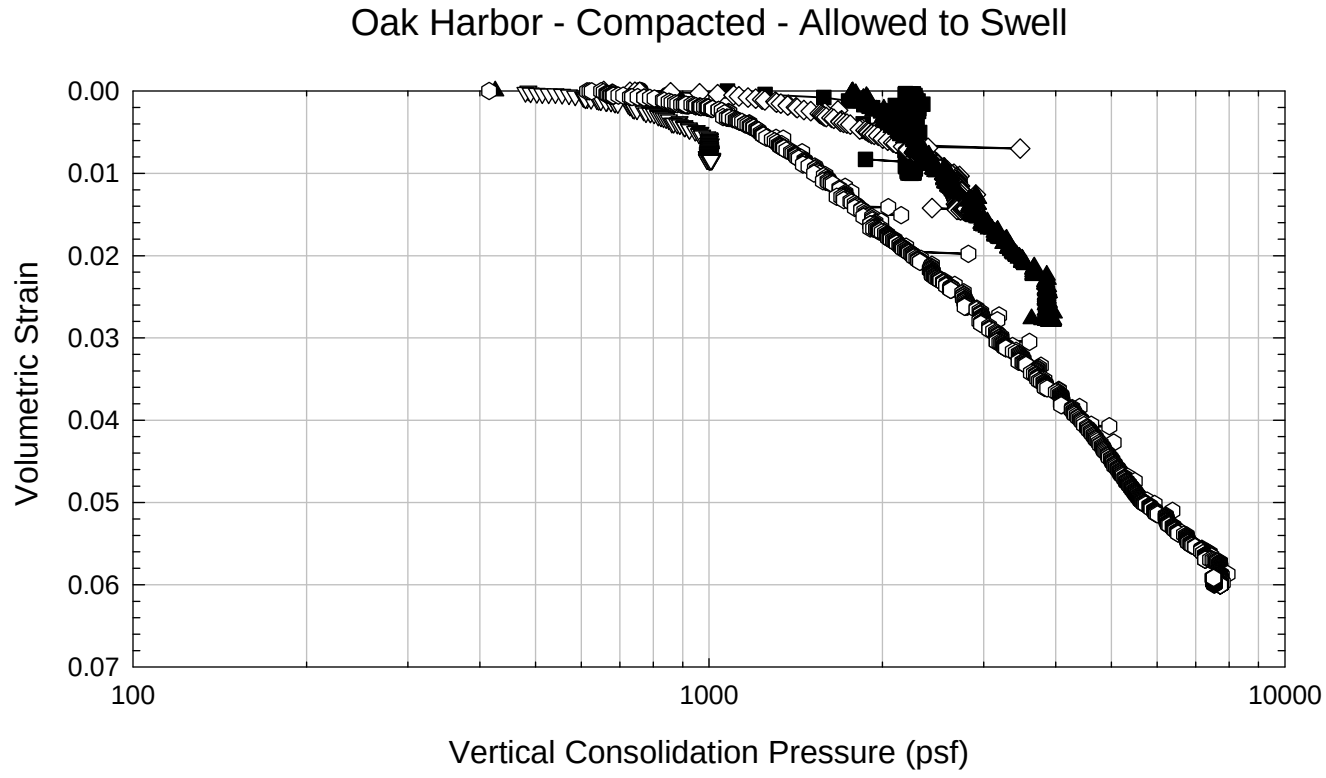
Oak Harbor - Compacted - Allowed to Swell
Volumetric Strain
0.00
0.01
0.02
0.03
0.04
0.05
0.06
0.07
100
1000
10000
Vertical Consolidation Pressure (psf)

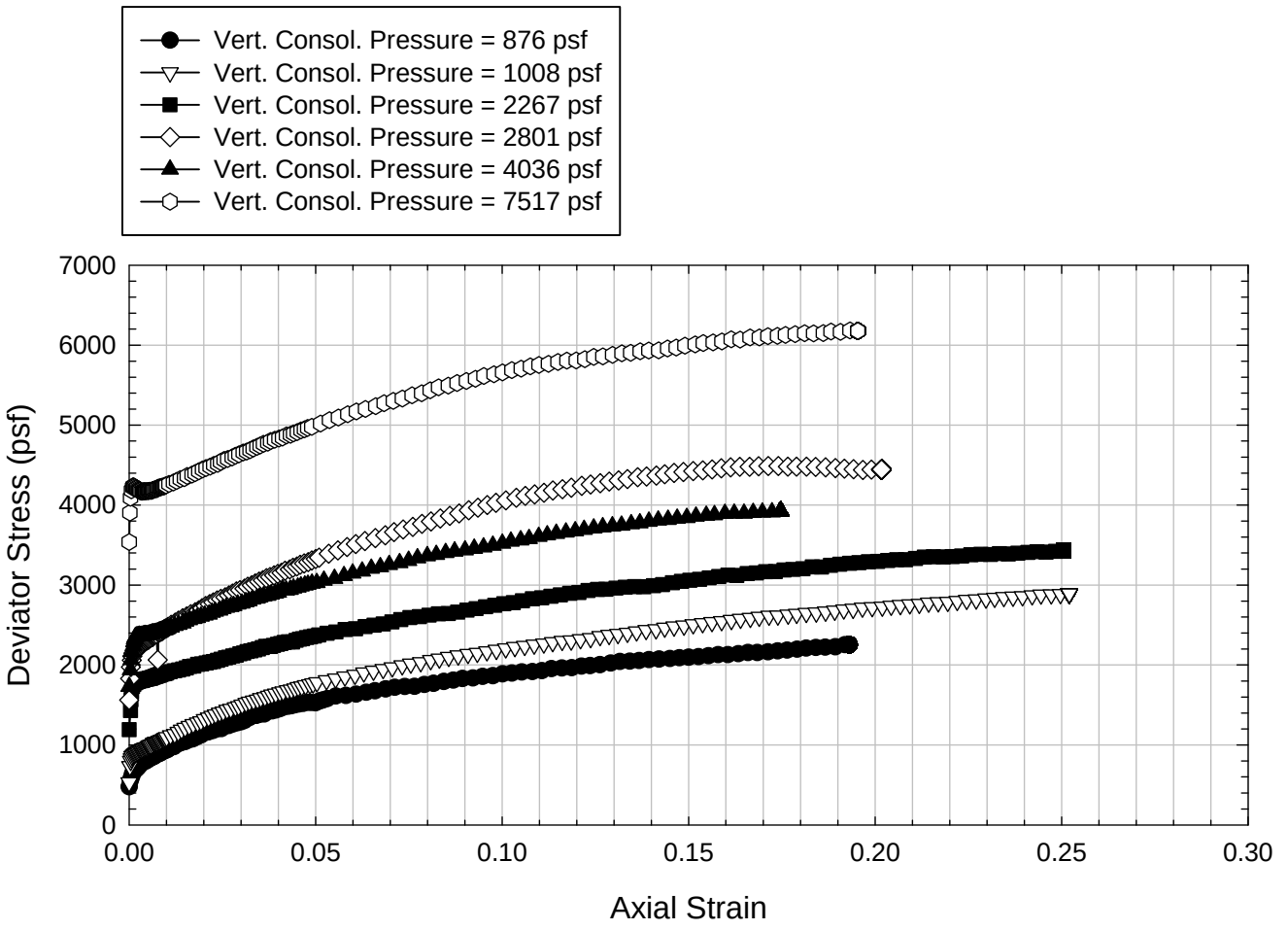
Vert. Consol. Pressure = 876 psf
Vert. Consol. Pressure = 1008 psf
Vert. Consol. Pressure = 2267 psf
Vert. Consol. Pressure = 2801 psf
Vert. Consol. Pressure = 4036 psf
Vert. Consol. Pressure = 7517 psf
Deviator Stress (psf)
7000
6000
5000
4000
3000
2000
1000
0
0.00
0.05
0.10
0.15
0.20
0.25
0.30
Axial Strain

Oak Harbor - Compacted - Allowed to Swell

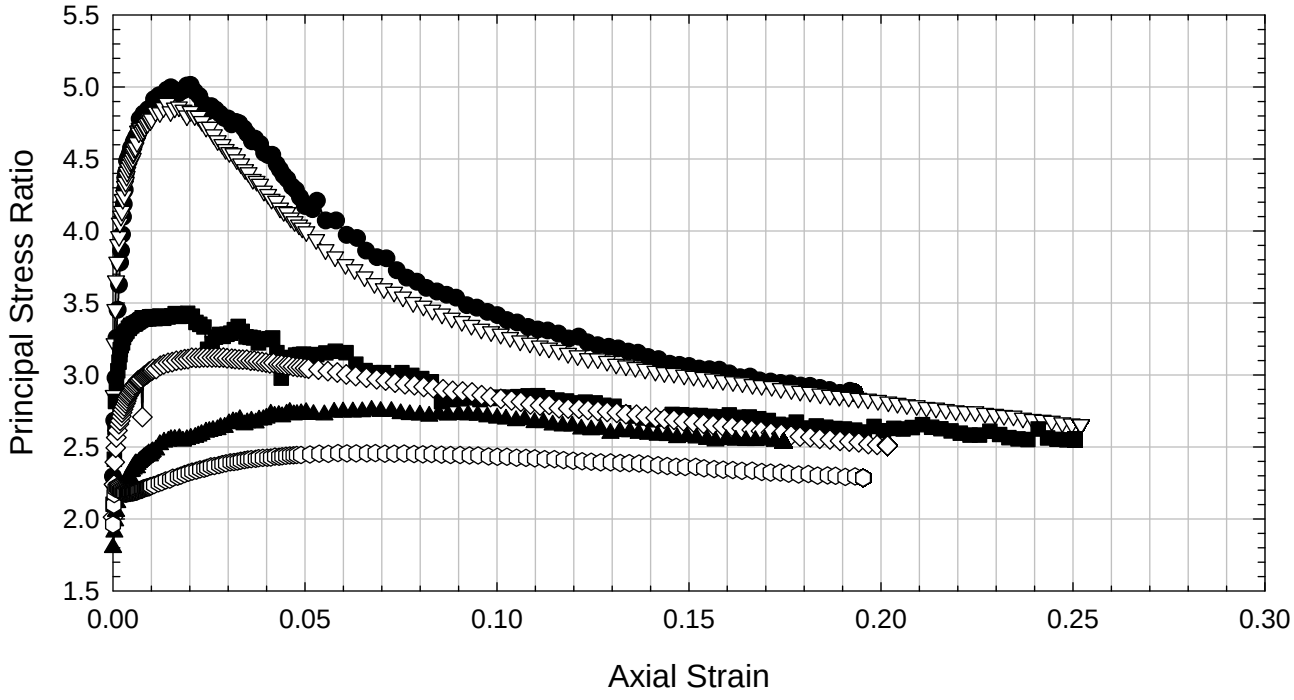

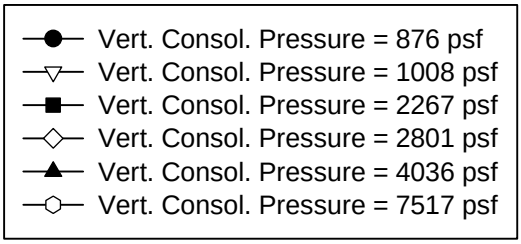

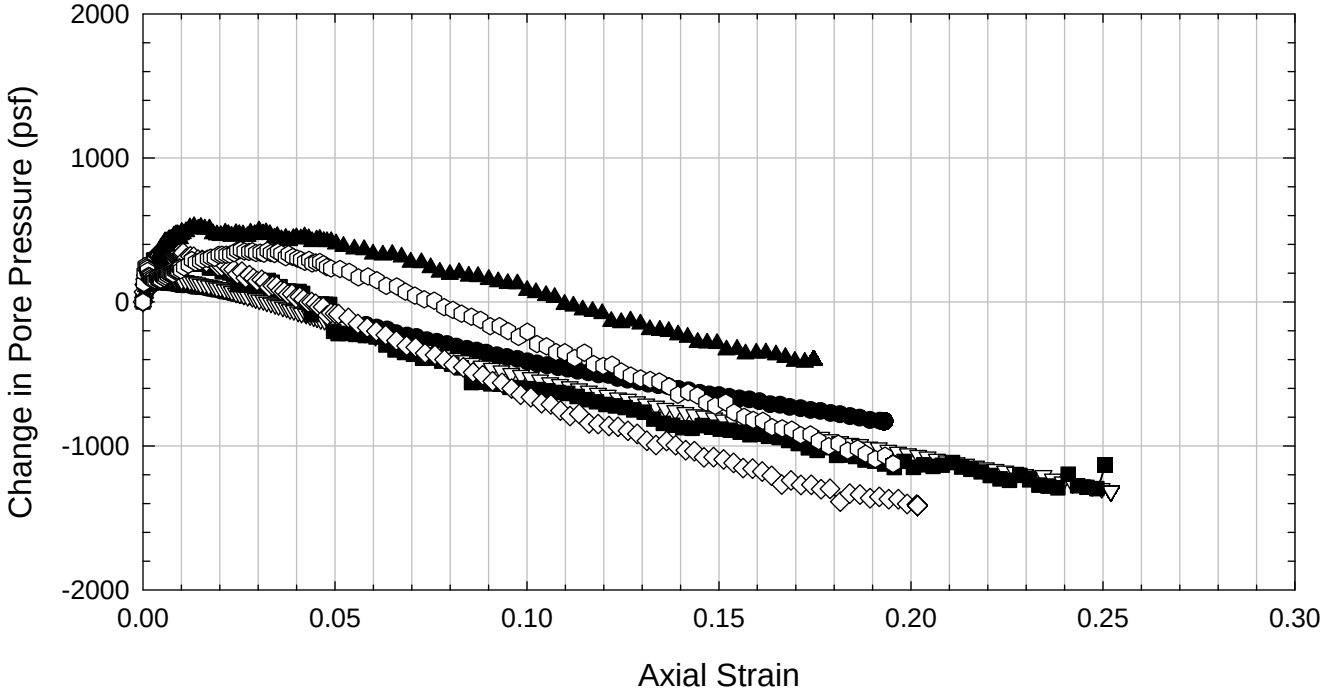

Oak Harbor - Compacted - Allowed to Swell

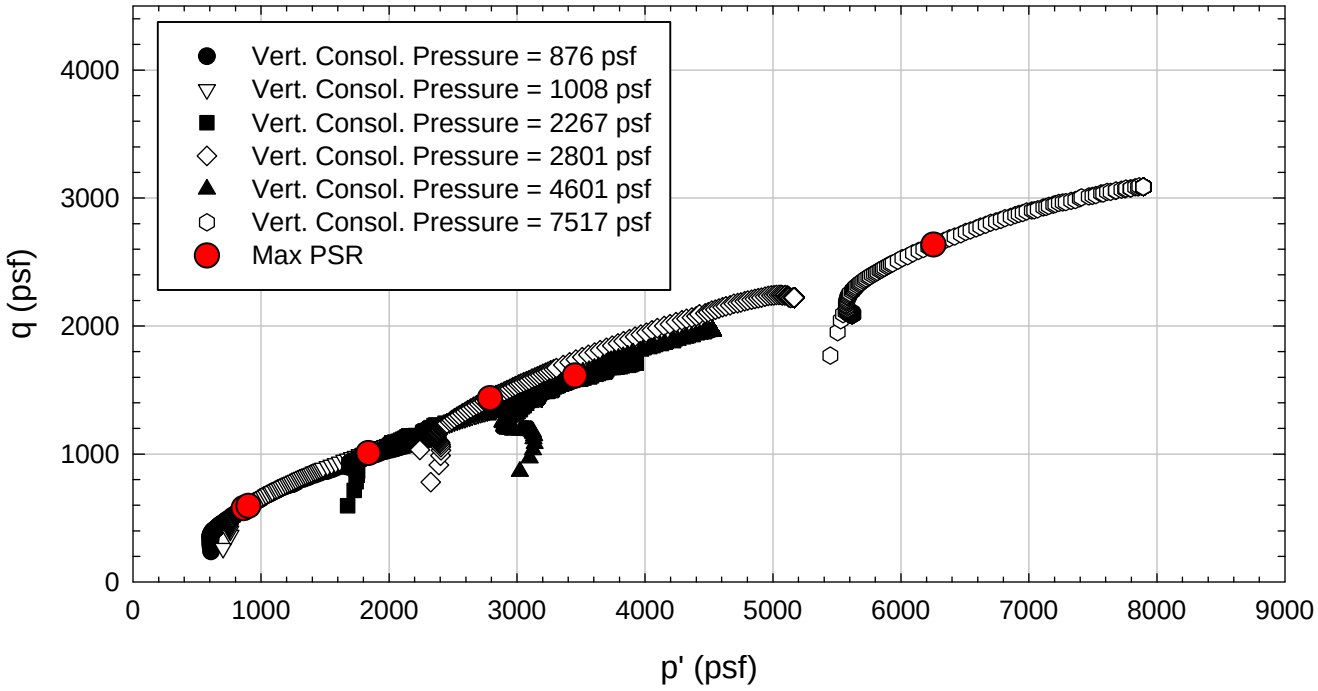

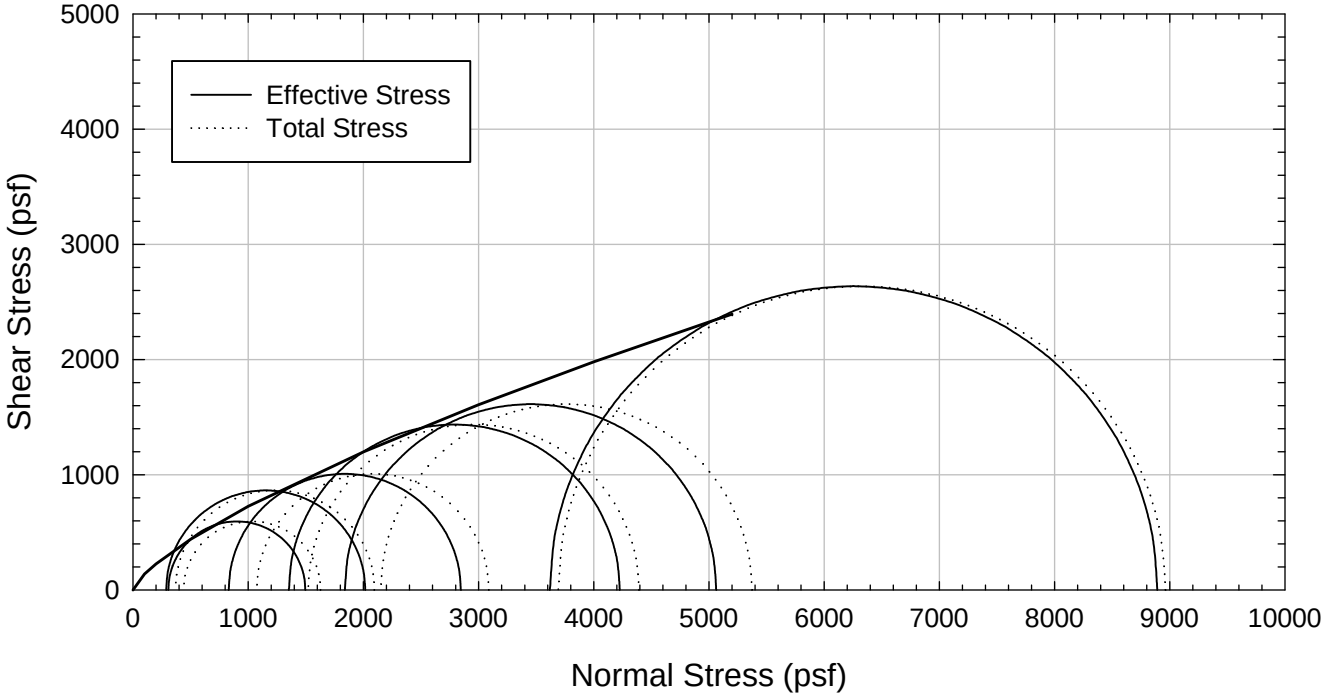

G.2. VBC

G.2.1 ICU Triaxials

Virginia Polytechnic Institute and State University
Geotechnical Engineering Laboratory
Triaxial Data Sheet

Project:	Fully Softened Shear Strength
Sample I.D./Loc.:	VBC - Compacted - Allowed to Swell - Consolidated Undrained
Classification:	Fat Clay (CH)

Sample Preparation	Compacted
Specimen Saturation Method	Wet

Specific Gravity	2.79	
Method for Dimensions After Consol.	Method B	

Test Number	1	2	3	4	5	6	7	8
Start Date (m/d/y)	6/21/2013	6/21/2013	6/21/2013	7/18/2013	7/18/2013			
End Date (m/d/y)	7/16/2013	7/17/2013	7/18/2013	8/22/2013	8/22/2013			
Backpressure (psf)	11520	11520	11520	11520	13680			
Consolidation Pressure (psf)	1008	2016	3024	3600	3600			
B value	-	-	-	-	-			
Initial Values								
Initial Height (in.)	2.791	2.782	2.774	2.773	2.776			
Initial Diameter (in.)	1.315	1.312	1.314	1.315	1.315			
Initial Sample Weight (g.)	118.64	118.31	118.16	117.87	118.14			
Water Content (%)	28.61	28.94	27.98	27.05	28.04			
Dry Unit Weight (pcf)	92.7	92.9	93.5	93.8	93.2			
Wet Unit Weight (pcf)	119.2	119.8	119.7	119.2	119.4			
Saturation (%)	90.9	92.5	90.6	88.3	90.2			
Void Ratio	0.88	0.87	0.86	0.86	0.87			
After Swelling and Consolidation								
t_{100} Using Casagrande Method (min)	3000.00	3000.00	3000.00	6000.00	-			
Volumetric Strain (%)	-7.90	-5.94	-2.83	-1.86	0.27			
Height After Consolidation (in.)	2.758	2.765	2.757	2.794	2.779			
Area After Consolidation (in.)	1.483	1.441	1.403	1.373	1.353			
Final Values								
Water Content (%)	37.02	35.99	33.07	33.51	31.64			
Dry Unit Weight (pcf)	85.6	86.9	90.6	90.0	92.5			
Wet Unit Weight (pcf)	117.3	118.1	120.5	120.1	121.7			
Saturation (%)	100.0	100.0	100.0	100.0	100.0			
Void Ratio	1.03	1.00	0.92	0.93	0.88			
Failure								
Failure Criteria	Max PSR	Max PSR	Max PSR	Max PSR	Max PSR			
Deviator Stress at failure (psf)	1897.81	2266.88	4124.27	4144.37	4816.82			
Principal Stress Ratio at failure	8.48	3.53	3.80	3.78	2.82			
Minor Principal Effective Stress at fail. (psf)	254.9	900.3	1477.0	1496.7	2648.4			
Major Principal Effective Stress at fail. (psf)	2161.5	3175.0	5615.5	5652.7	7476.7			
Corrections Applied	Membrane	Membrane	Membrane	Membrane	Membrane			
Axial Strain at failure (%)	2.65	2.33	4.22	3.41	3.33			
Test performed at strain rate (%/hr)	0.12	0.12	0.12	0.12	0.12			

Comments: All test specimens were allowed to swell during/after consolidation. The piston was in contact with the top platen during swelling. For this reason, a small vertical stress was already being applied to the sample at the beginning of shearing.
Volumetric strain is positive for compression and negative for swelling.
Sample 5 was not allowed to swell. It was tested at the swelling pressure.

VBC - Compacted - Allowed to Swell - 1008 psf

VBC - Compacted - Allowed to Swell - 2016 psf

VBC - Compacted - Allowed to Swell - 3024 psf

VBC - Compacted - Allowed to Swell - 3600 psf

VBC - Compacted - Not Allowed to Swell - 3600 psf

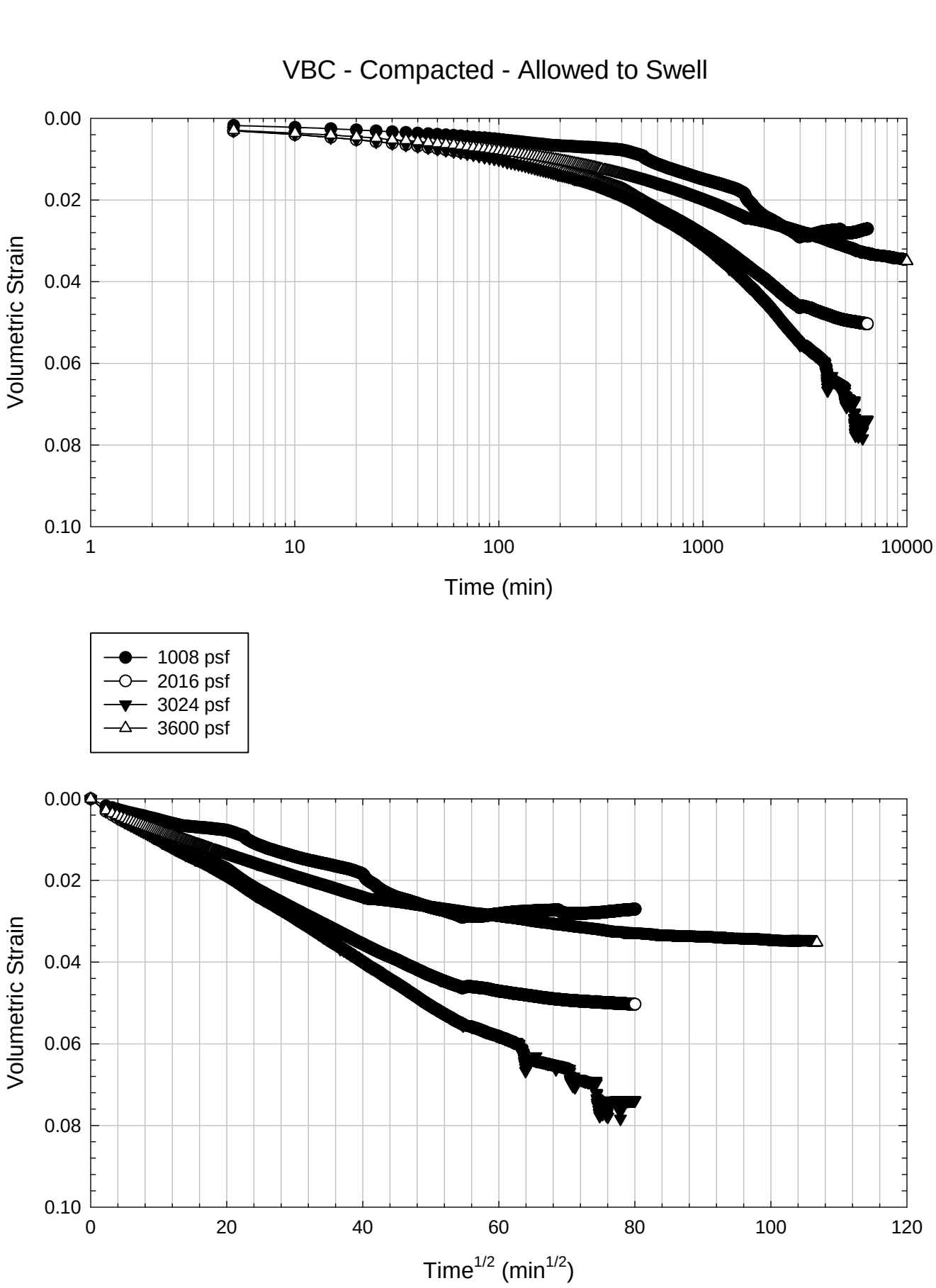
VBC - Compacted - Allowed to Swell
Volumetric Strain
0.00
0.02
0.04
0.06
0.08
0.10
1
10
100
1000
10000
Time (min)
1008 psf
2016 psf
3024 psf
3600 psf
Volumetric Strain
0.00
0.02
0.04
0.06
0.08
0.10
0
20
40
60
80
100
120
Time^1/2 (min^1/2)

VBC - Compacted - Allowed to Swell

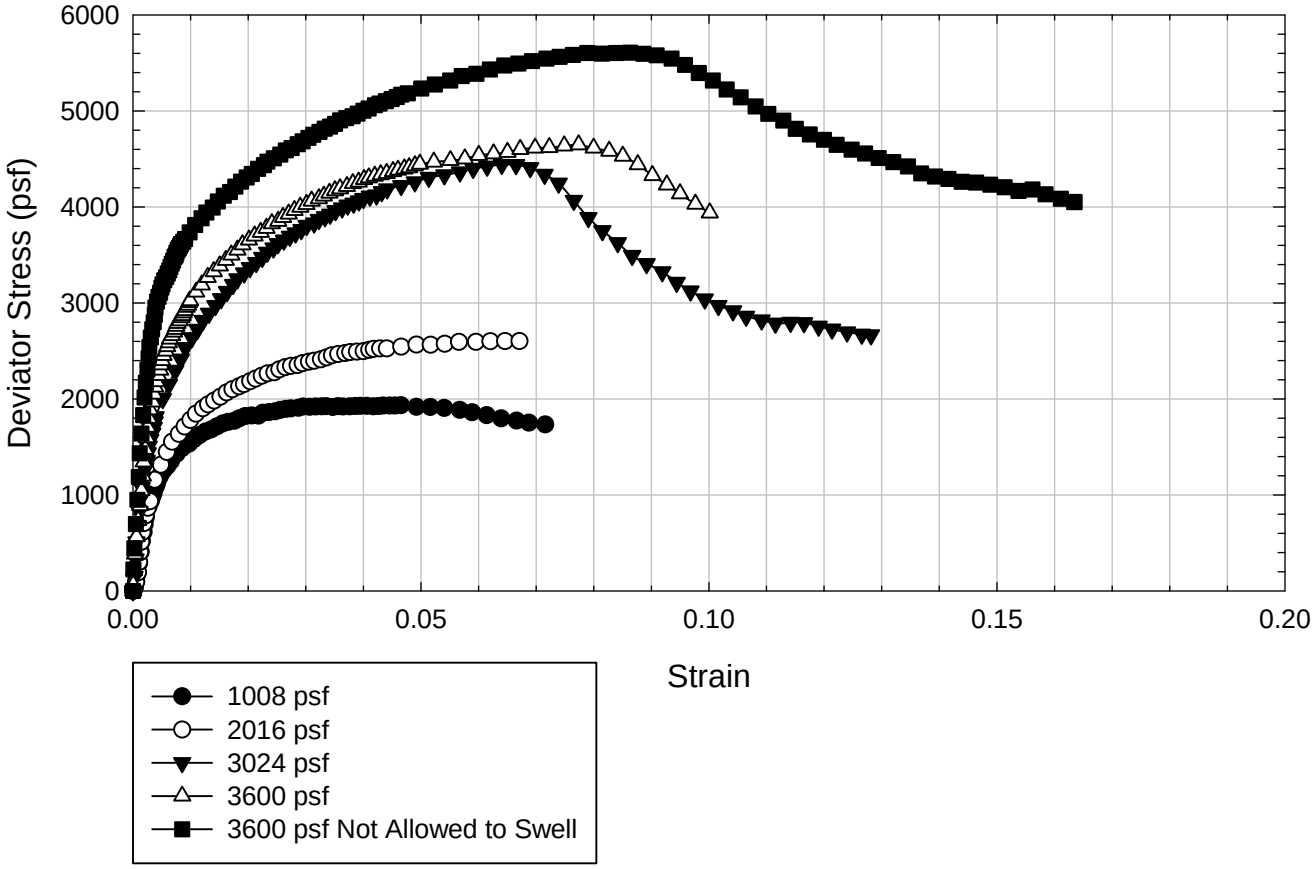

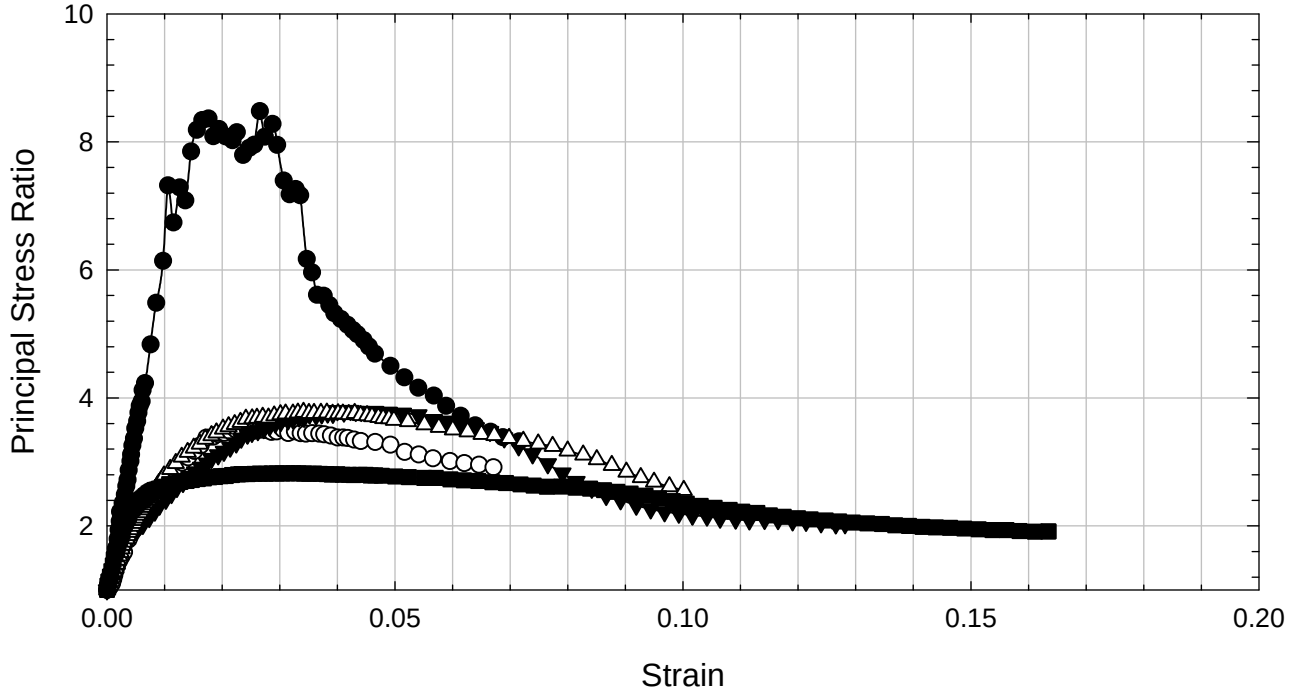

VBC - Compacted - Allowed to Swell

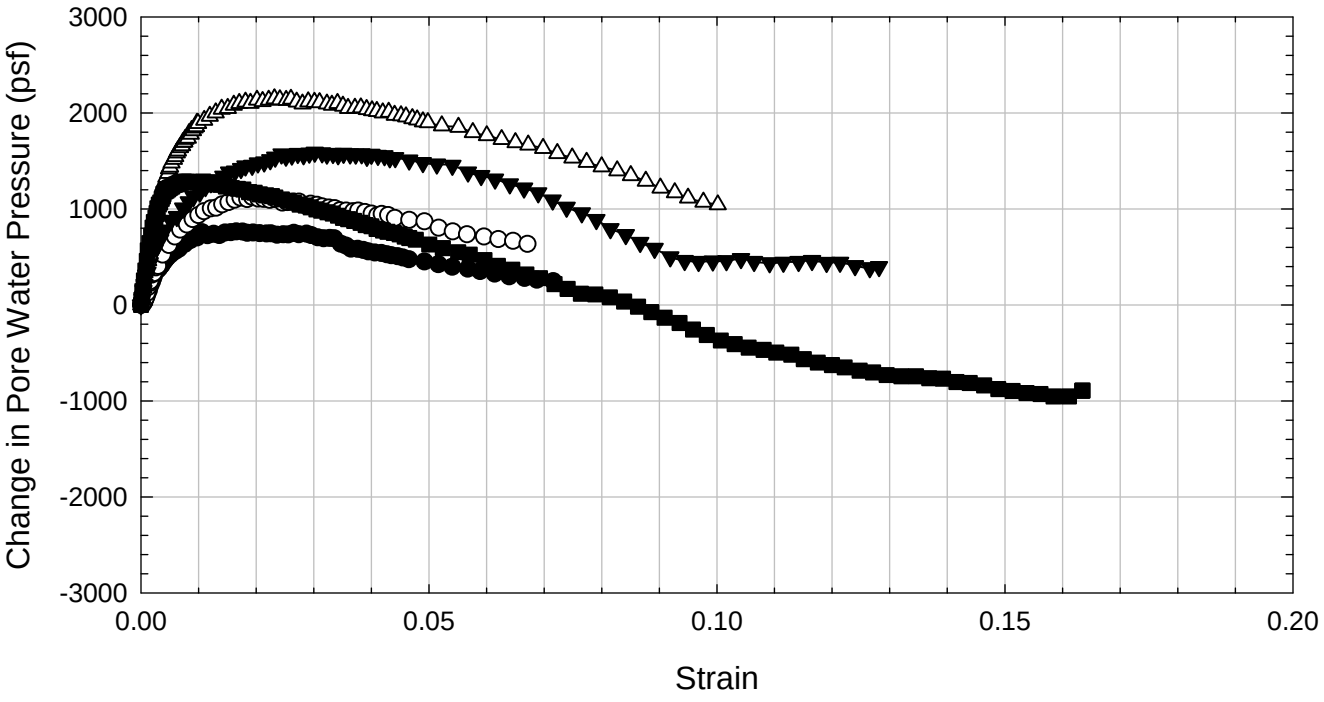

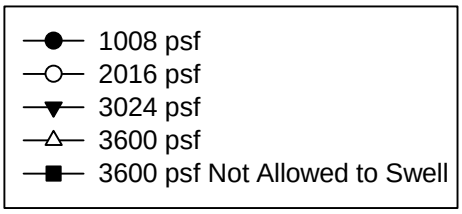

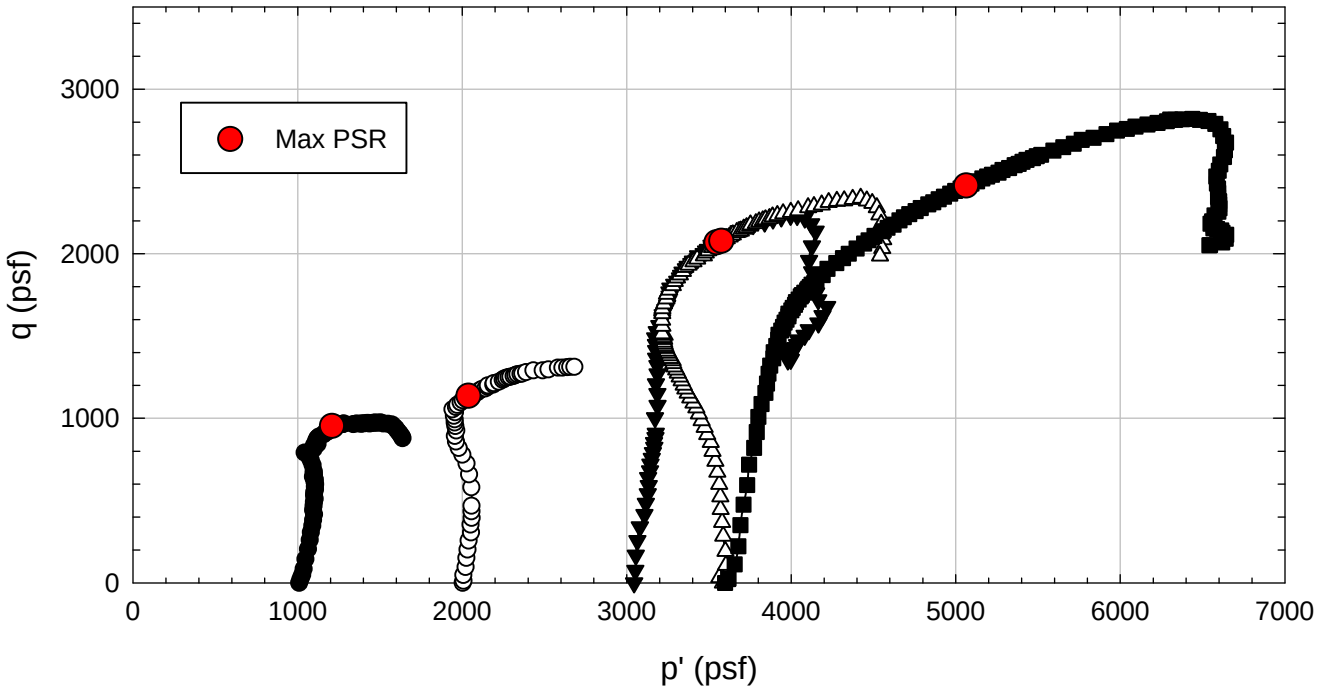

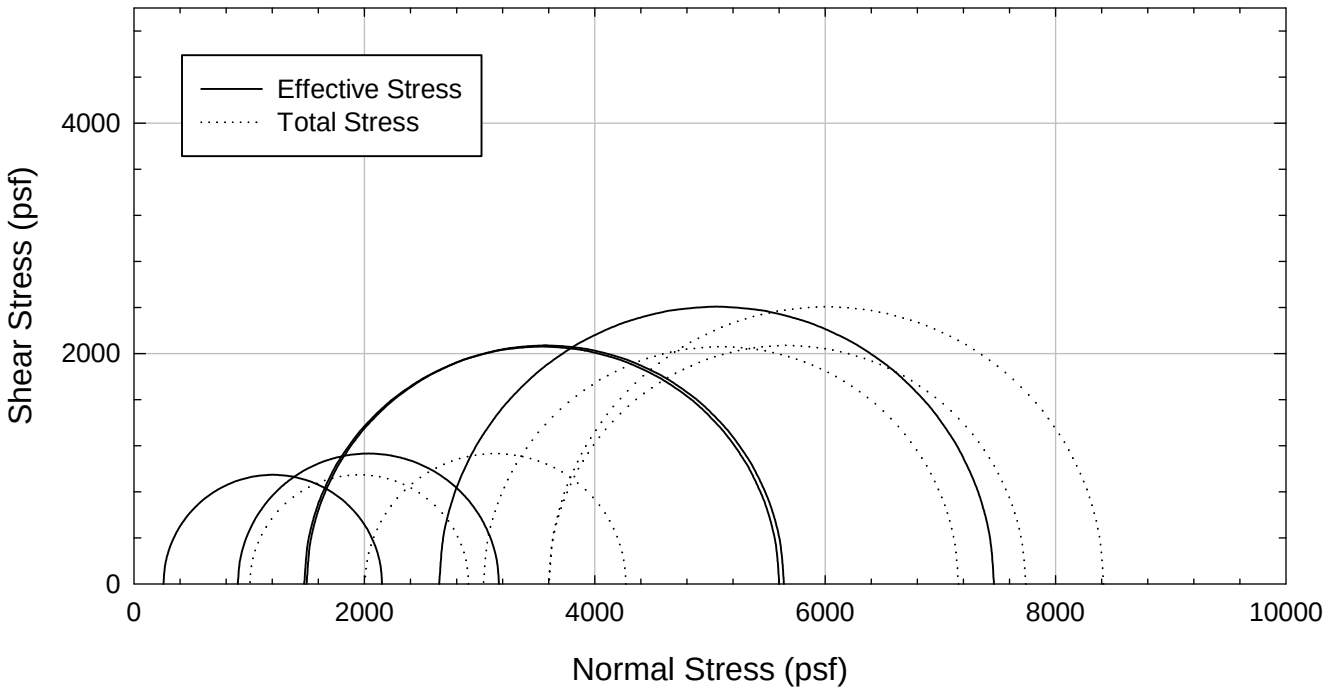
VBC - Compacted - Allowed to Swell
Effective Stress
Total Stress
Shear Stress (psf)
Normal Stress (psf)
0
2000
4000
6000
8000
10000